St. Louis, Cloquet, and Nemadji River Basin Models
Volume 1: Hydrology and Sediment Model Calibration

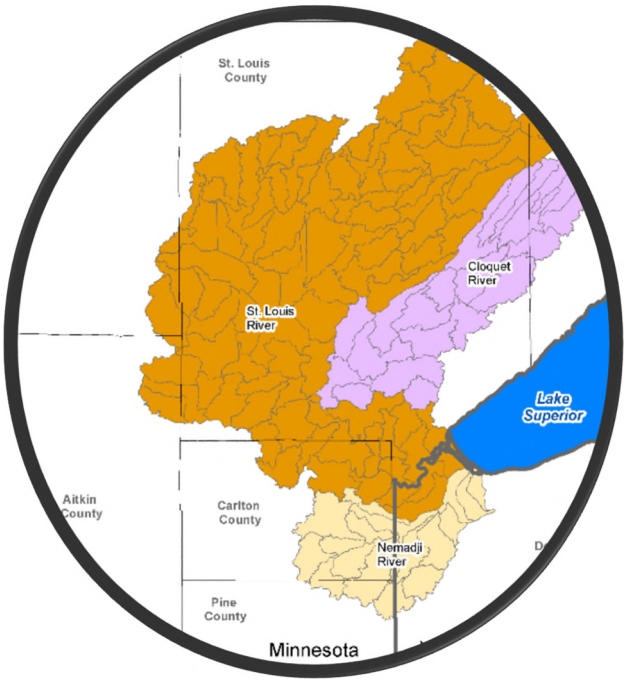

Prepared for

Minnesota Pollution Control Agency

Prepared by

TETRA TECH

One Park Drive, Suite 200 • PO Box 14409
Research Triangle Park, NC 27709

REVISED

February 4, 2016

wq-iw10-06n

(This page left intentionally blank.)

Table of Contents

List of Tables

List of Figures

Snow Depth Calibration

Evapotranspiration Calibration

Flow Calibration

Flow Validation

Detailed Sediment Calibration

1 Introduction

This document is a revised update of St. Louis, Cloquet, and Nemadji River Basins – Hydrology and Sediment Model Calibration, prepared by Tetra Tech for the Minnesota Pollution Control Agency and released on January 16, 2015. The main report has been updated to reflect a variety of small enhancements and corrections made to the basic model structure, point sources, and other features. The revised report now constitutes Volume 1 of a two-volume set, with Volume 2 addressing water quality calibration. The revisions to the model cause only small changes to the hydrology and sediment calibration, so the calibration and validation results for hydrology and sediment have not been updated, with the exception of Rock Creek and Blackhoof River. Changes to the previous version of the document are primarily in Section 2.

This report transmits and describes the development and calibration of 12-digit Hydrologic Unit Code (HUC) scale HSPF watershed models of the adjacent St. Louis, Cloquet, and Nemadji River watersheds. These constitute the 8-digit HUCs St. Louis (04010201), Cloquet (04010202) and a portion of Beartrap-Nemadji (04010301), including the entire Nemadji basin, which includes all of HUC 04010301 lying within Minnesota (Figure 1-1). All three watersheds drain to the western end of Lake Superior at or near Duluth.

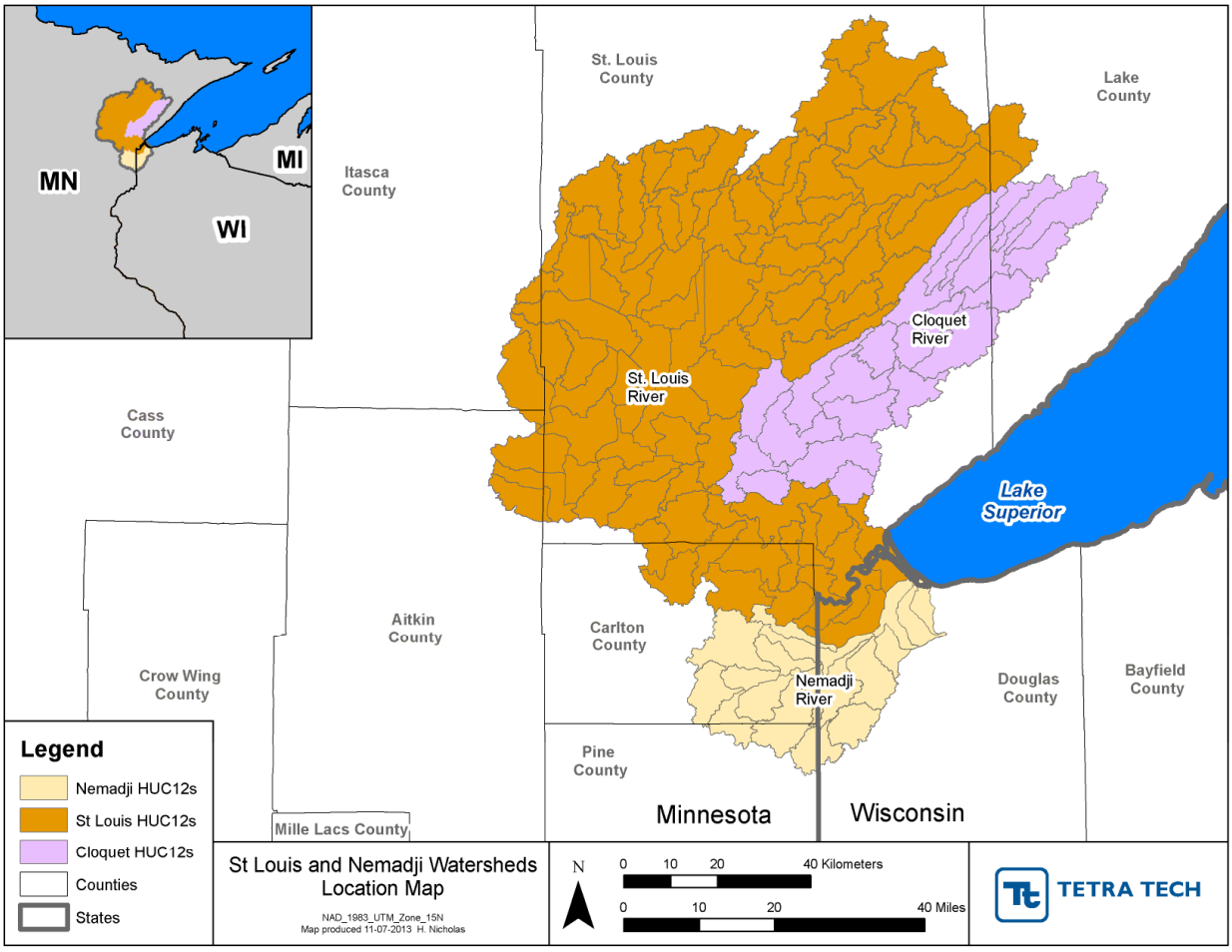

Figure 1-1. Location of the St. Louis, Cloquet, and Nemadji River Watersheds

(This page left intentionally blank.)

2 Watershed Model Development

2.1 UPLAND REPRESENTATION

The HSPF models were set up using a Hydrologic Response Unit (HRU) approach. The HRU concept provides a way to capture landscape variability into discrete units for modeling. In general, the HRU approach holds that landscapes possess an identifiable spatial structure, and that the corresponding patterns of runoff and stream chemistry are strongly influenced by climate, geology, and land use. An HRU is defined as a unit of land with relatively homogenous hydrologic properties determined by its underlying characteristics.

2.1.1 Land Cover and Imperviousness

We investigated several sources of land cover data for the watershed, including the 2006 NLCD, the 2013 Cropland Data Layer (CDL) from USDA, and the 2008 LANDFIRE coverage from the U.S. Forest Service. The NLCD layer is useful in many watersheds, and provides a good spatial distribution of developed, agricultural, and undeveloped land in the watershed (Figure 2-1). The CDL provides additional information on specific crop types, but there is very little cropland in this region and the CDL has the disadvantage of not identifying roads. The LANDFIRE coverage (which is based on the same imagery as the 2006 NLCD) identifies roads and gives additional information on tree canopy type, but does not identify specific agricultural land uses (Figure 2-2). Our examination indicated that LANDFIRE was more accurate than NLCD in differentiating grassland/shrubland and forest data cover. Given the predominance of forest land cover in these watersheds LANDFIRE was adopted as the basis for model land use.

As configured, the model does not contain details on forest age and harvest practices except insofar as forest areas appear as shrub or barren land (due to harvest, storm blow-down, or fire) in the 2006 land use coverage. Representation of land use change over time greatly complicates the modeling effort and an analysis of land use change in the basin suggested that this was not necessary for development of the basin-scale model (see Section 2.1.2).

Effective Imperviousness Area (EIA) associated with each developed land use category was then calculated based on Table 2.5 of '*Modeling Guidance for BASINS/HSPF Applications under the MPCA One Water Program*' (see Table 2-1).

For the model, the pervious and impervious fractions of each developed land use class are separated. The pervious fractions are then lumped together (by hydrologic soil group (HSG)). HSG and HRU development are described further in Section 2.1.4.

Table 2-1. Effective Impervious Area Percentage in Developed Land Use Classes (AQUA TERRA, 2012)

Urban Land Use Category	EIA, %
Developed, Open Space	2
Developed, Low Intensity	10
Developed, Medium and High Intensity	35

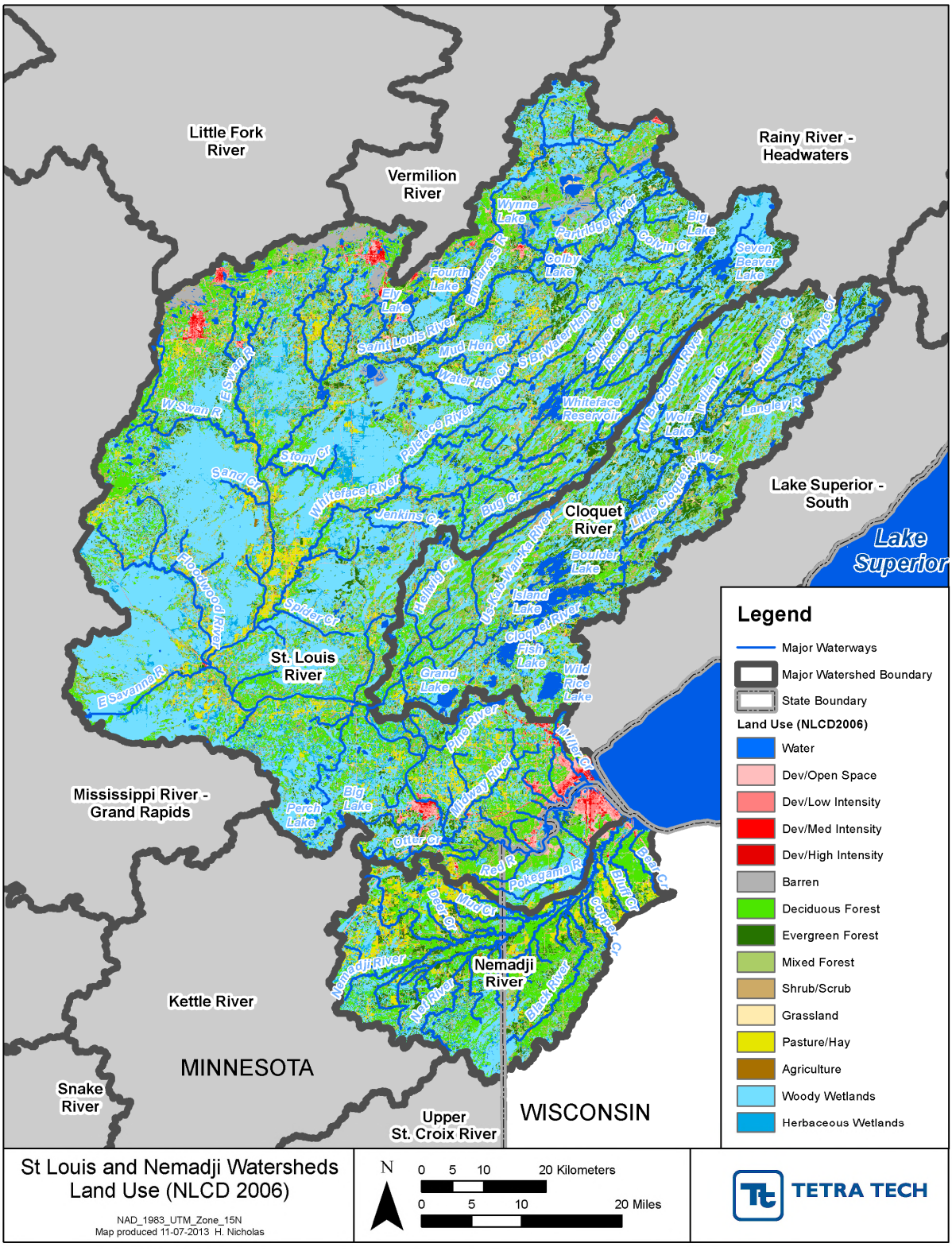

Figure 2-1. NLCD Land Cover (Simplified) in the St. Louis, Cloquet, and Nemadji River Watersheds

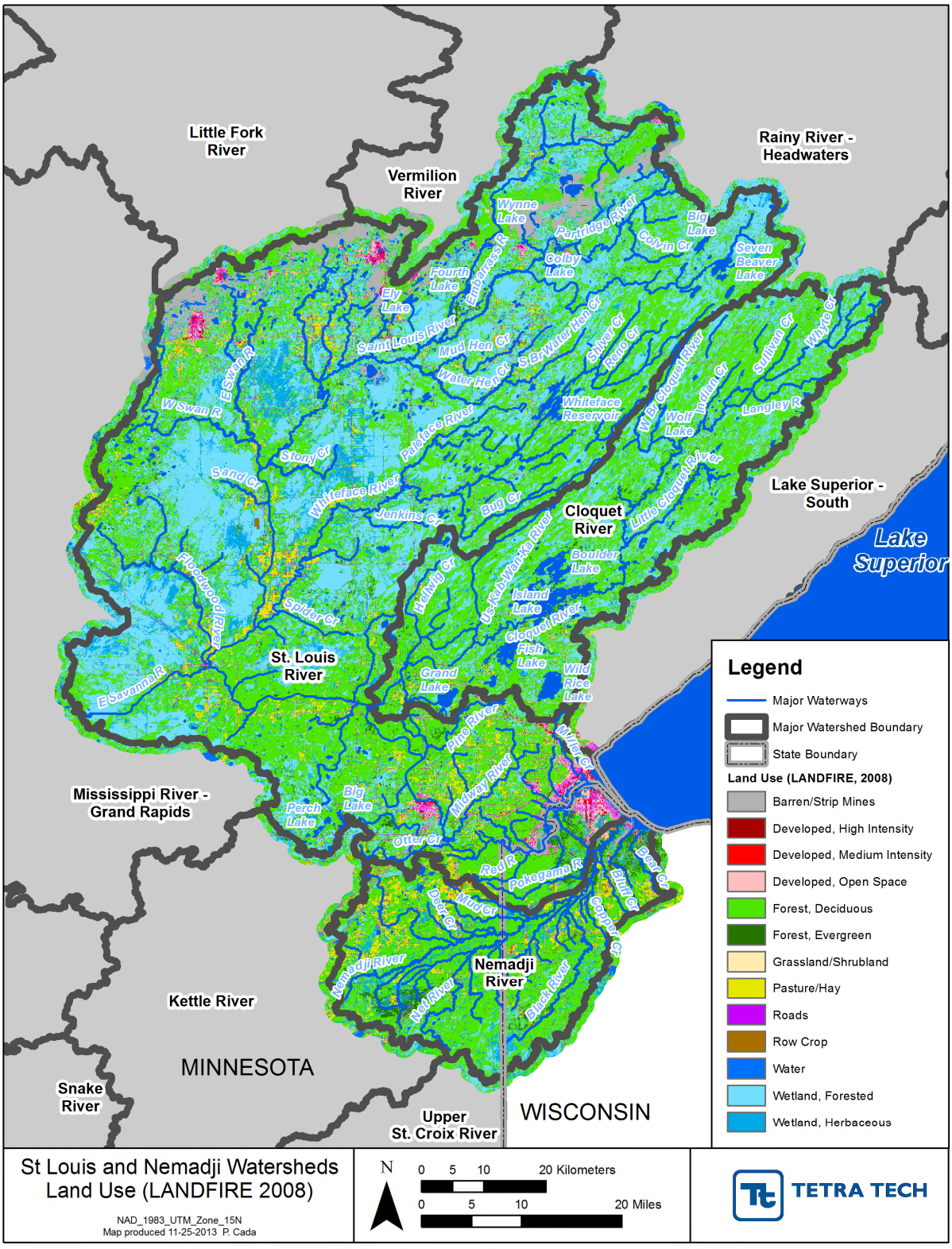

Figure 2-2. LANDFIRE Land Cover (Simplified) in the St. Louis, Cloquet, and Nemadji River Watersheds

2.1.2 Land Use Change Analysis

The HSPF models of the St. Louis, Cloquet, and Nemadji watersheds are constructed using the NLCD and Forest Service LANDFIRE 2006 satellite-based land cover products. The models assume that land cover in these watersheds is approximately steady state over the period of model application (1995-2012). To test the validity of these assumptions we examined differences between the 2001, 2006, and 2011 NLCD coverages of these watersheds. The 2001 and 2006 coverages are directly comparable as they use the same sensors and algorithms; it is less certain whether those from 2011 are fully consistent with 2006 as they are based on different satellite sensors. The distribution of land uses in 2006 is shown in Figure 2-3.

Differences between the coverages may reflect both real land use changes and artifacts relative to the difficulty in defining spectral boundaries between land use classes. In general, a shift from a forested to an urban land classification has a high probability of being correctly identified, while apparent shifts between forest, wetland, and shrub/scrub classes have a higher probability of being artifacts due to uncertainties in interpretation.

Implementing changes in land use over time imposes significant extra burden on the development and run time of HSPF models and should therefore be undertaken only when these changes are significant. Our examination of apparent changes from 2001 to 2006 to 2011 showed first that land use areas in 2011 and 2006 were very similar, and that the trend from 2001 to 2006 was consistent with the changes from 2001 to 2011. More importantly, the median changes in anthropogenic land use categories, such as developed land and crops, is near zero and maximum changes are less than 5 percent of the area of any individual model subbasin, suggesting that the assumption of approximately stable land use is appropriate for models at this scale (Table 2-2). Larger apparent changes in the areas of forest, scrub/shrub, and grass land cover likely in large part reflect difficulties in distinguishing these land covers in satellite imagery, although there may have been some net, although small, loss of forest land use due to pulp and timber harvesting.

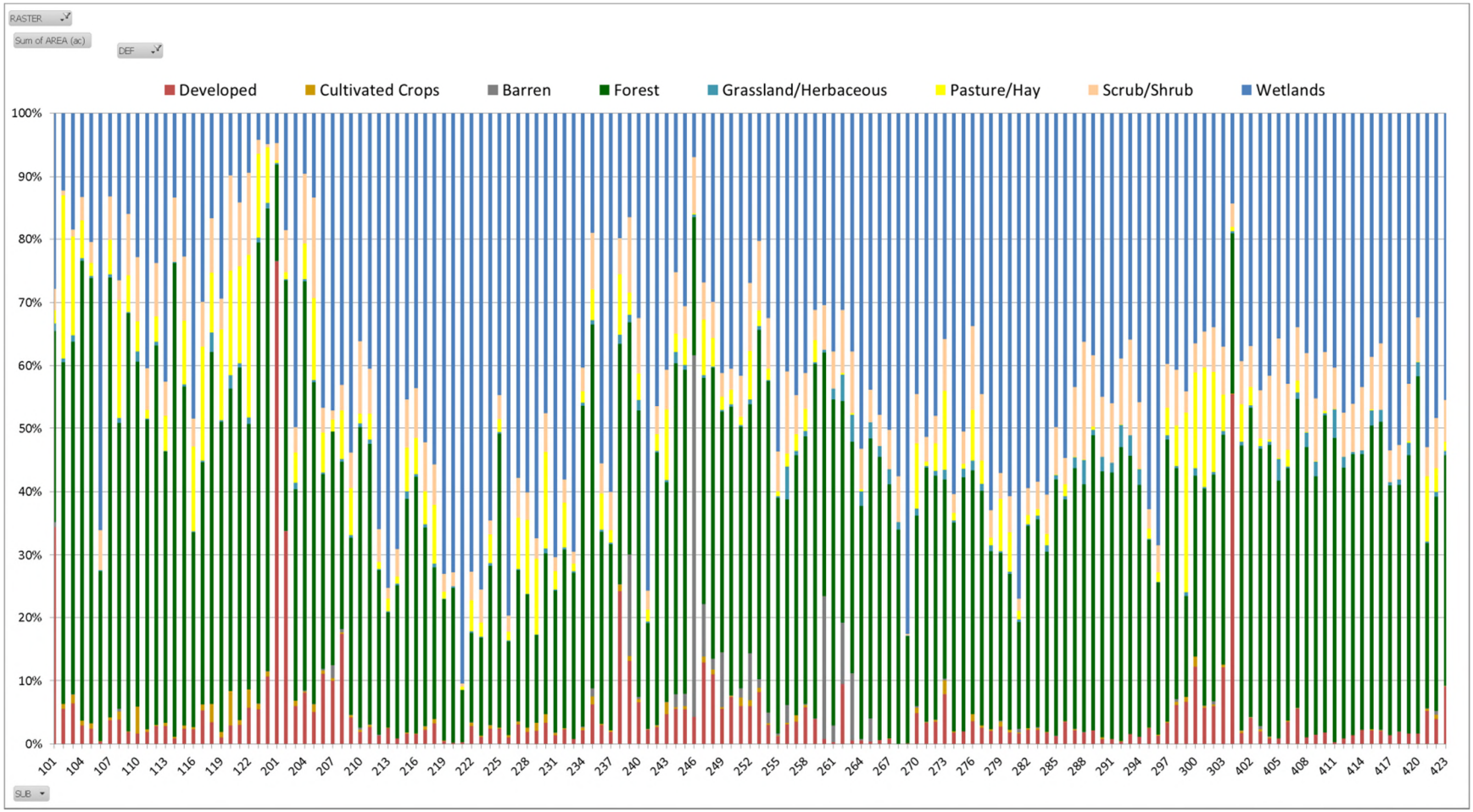

Figure 2-3. Land Use Distribution for 2006 in the St. Louis, Cloquet, and Nemadji HSPF Models

Note: X-axis shows model subbasin number.

Table 2-2. Distribution of Changes in Land Use between 2001 and 2011 NLCD for St. Louis, Cloquet, and Nemadji Watershed Model Subbasins (Percentage of Subbasin Area)

2011-2001	Developed	Cultivated Crops	Barren	Forest	Grass	Pasture/Hay	Scrub/Shrub	Wetlands
median	0.02%	0.00%	0.00%	-1.36%	0.50%	0.00%	0.66%	-0.07%
min	-0.92%	-0.81%	-6.41%	-11.44%	-1.67%	-0.32%	-11.53%	-2.38%
25th	-0.03%	-0.03%	0.00%	-3.08%	0.20%	-0.03%	-0.04%	-0.26%
75th	0.12%	0.00%	0.08%	-0.45%	0.98%	0.05%	1.84%	0.08%
90th	0.32%	0.02%	0.30%	0.77%	2.04%	0.24%	3.60%	0.26%
95th	0.86%	0.04%	0.54%	1.82%	2.75%	0.59%	4.46%	0.38%
99th	2.26%	0.39%	3.54%	7.70%	5.06%	1.50%	6.62%	0.81%
max	4.43%	0.66%	4.31%	11.52%	6.21%	5.49%	8.89%	1.02%

The distribution of changes in land use is displayed graphically in a box and whiskers plot (Figure 2-4). In this figure the "box" shows the inter-quartile range, with a central tic at the median, for all 151 model subbasins. The whiskers are extended beyond the edges of the box by 1.5 times the interquartile range, providing an empirical estimate of 95% confidence intervals. Finally, the three largest outliers outside the range of the whiskers in each direction are plotted as individual points. In general, the interquartile range boxes are very small, indicating that there has been little land use change since 2001, with the exception of the forest, grass, and scrub/shrub categories.

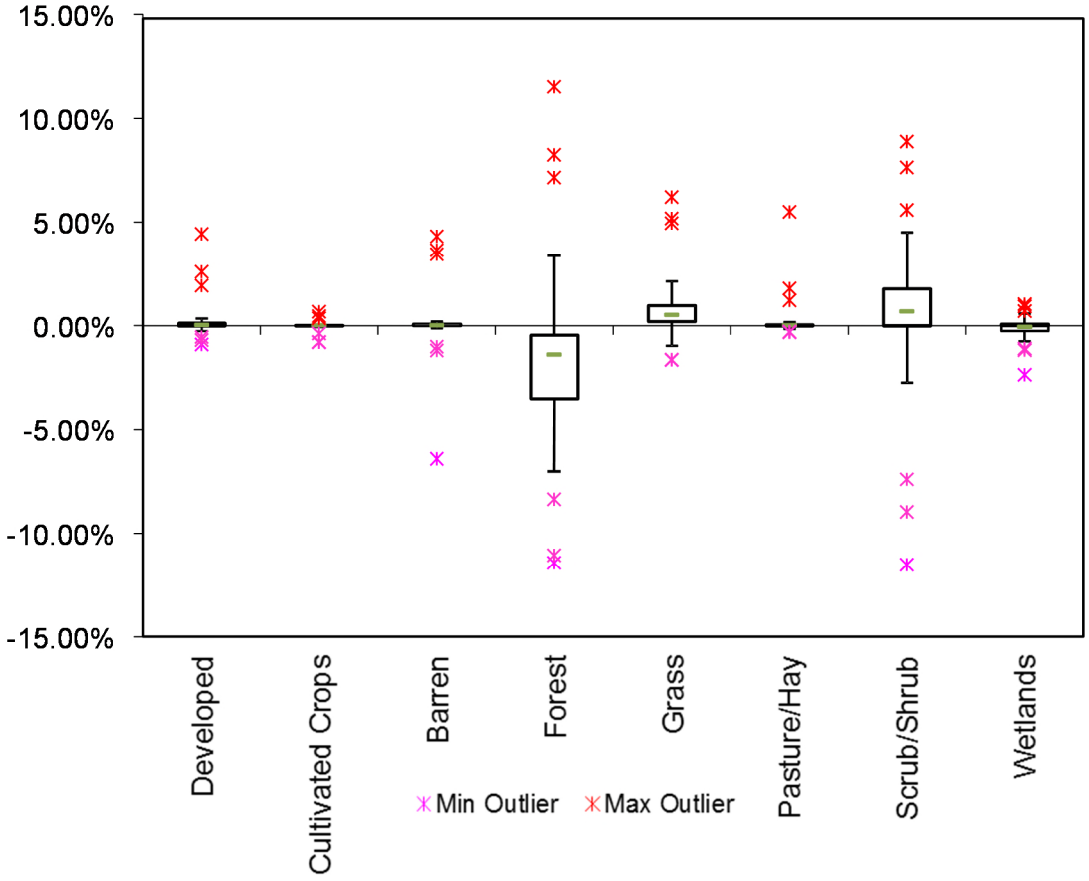

Figure 2-4. Box and Whisker Plots of Land Use Change in the St. Louis, Cloquet, and Nemadji Watersheds 2001-2011 (Percent of Subbasin Area)

For developed land, the interquartile range is only -0.03% to +0.12%; however, there are larger increases in a small number of watersheds. The largest increase in developed land from 2001 to 2011 is 4.43%, in subbasin 304. The only other subbasin with an increase greater than 2 percent is subbasin 300. Both of these modeling subbasins are on the outskirts of Duluth in the lower part of the St. Louis watershed.

As noted above, shifts between forest, grass, and scrub/shrub land covers likely in part reflect uncertainty in distinguishing spectral characteristics of these covers in satellite imagery. The attributed changes in forest do show a consistent downward trend (median change of -0.51% from 2001 to 2006; median change of -1.00% from 2006 to 2011) so there may be some net loss in forest coverage due to harvesting (accompanied by regrowth in previously harvested areas in other subwatersheds). However, the total change is small, except in a few individual watersheds. We therefore conclude that it is sufficient to represent land use in the watershed model using the 2006 NLCD as a static representation. Changes relative to the 2006 NLCD are small, and this coverage also provides an approximate midpoint on net changes between 2001 and 2011 in developed land and forest land covers. Place-specific studies of individual subwatersheds may, however, need to evaluate and account for changes in land use over time.

2.1.3 Geology, Soils, and Slopes

The St. Louis River's source area lies in the area near Hoyt Lakes in the Toimi Drumlin field, a predominantly wooded area of bouldery, coarse-loamy glacial till and outwash deposits. As the river

flows westward across St. Louis County, it passes through forested areas of sand, gravel, and clayey glacial till and outwash deposits. From the town of Floodwood to Thomson, the river continues to pass through very hilly wooded glacial moraine. The soils in this area are coarse-loamy fine sands, loamy mantles, sands, and gravels, interspersed with some fine loam. Valley slopes increase in size and steepness along the river banks. The Cloquet River, another major tributary river, joins just below Brookston. The Cloquet River drains predominantly wooded areas of sand and gravel glacial till deposits. Below the Thomson Dam, the St. Louis River changes abruptly as it flows through the deep narrow gorge of Thomson slates and greywackes of Jay Cooke State Park in lower Carlton County. The final reach of the St. Louis drains through the red clay deposits of Glacial Lake Duluth and enters the St. Louis Bay Estuary (SLRCAC, 1992).

Bedrock in the watershed is largely a variety of Precambrian volcanic, metamorphosed sedimentary and intrusive rocks. The geology of the upper portion of the St. Louis watershed is significant for the entire basin because it is this area where the Iron Range mines are located. The central St. Louis River watershed is fairly flat and the river drains extensive peatlands. As it nears its estuary and Lake Superior in the vicinity of Jay Cooke State Park, the river is surrounding by imposing cliffs and angular outcropping of gray rock (USDA, 2013).

Remnants of glacial activity have impacted the St. Louis River drainage. Past glaciers have left a veneer of sand, gravely tills, and outwash that form the modern landscape. A pattern of glacier advances and retreats created a series of glacial lakes, and as the ice retreated, layers of silt, sandy till, and red clay were deposited. Today, the layering of sandy till and red clay deposits play an important role in stream bank erosion and sedimentation, particularly in the Nemadji River basin (SLRCAC, 1992).

The Nemadji River system starts five miles east of Moose Lake and flows north to the Atkinson area and east through southeastern Carlton County, Minnesota. It then flows northeast into Douglas County, Wisconsin where it enters Superior Bay. The headwaters of its branches and tributaries begin in wooded sand and gravel glacial till and outwash deposits. The Nemadji River System enters the red clay deposits early in its path towards Superior Bay. Red clay deposits make up approximately 30% of its watershed (SLRCAC, 1992). The unique geology and groundwater hydrology of the Nemadji River basin are described further in Section 2.3.4.

The bedrock and surface geologic characteristics of the St. Louis, Cloquet, and Nemadji River watersheds are presented in Figure 2-5 and Figure 2-6.

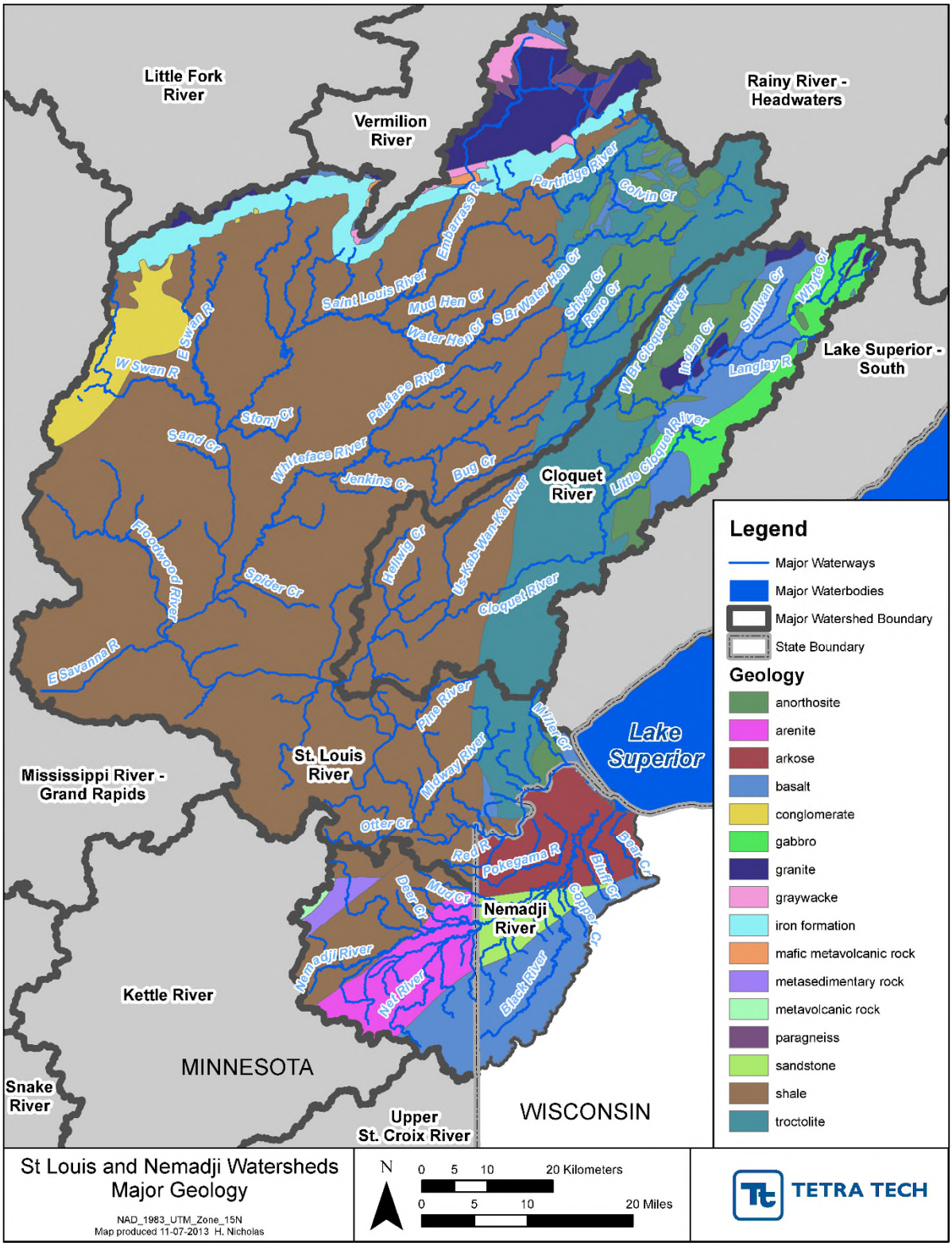

Figure 2-5. Bedrock Geologic Map of the St. Louis, Cloquet, and Nemadji River Watersheds

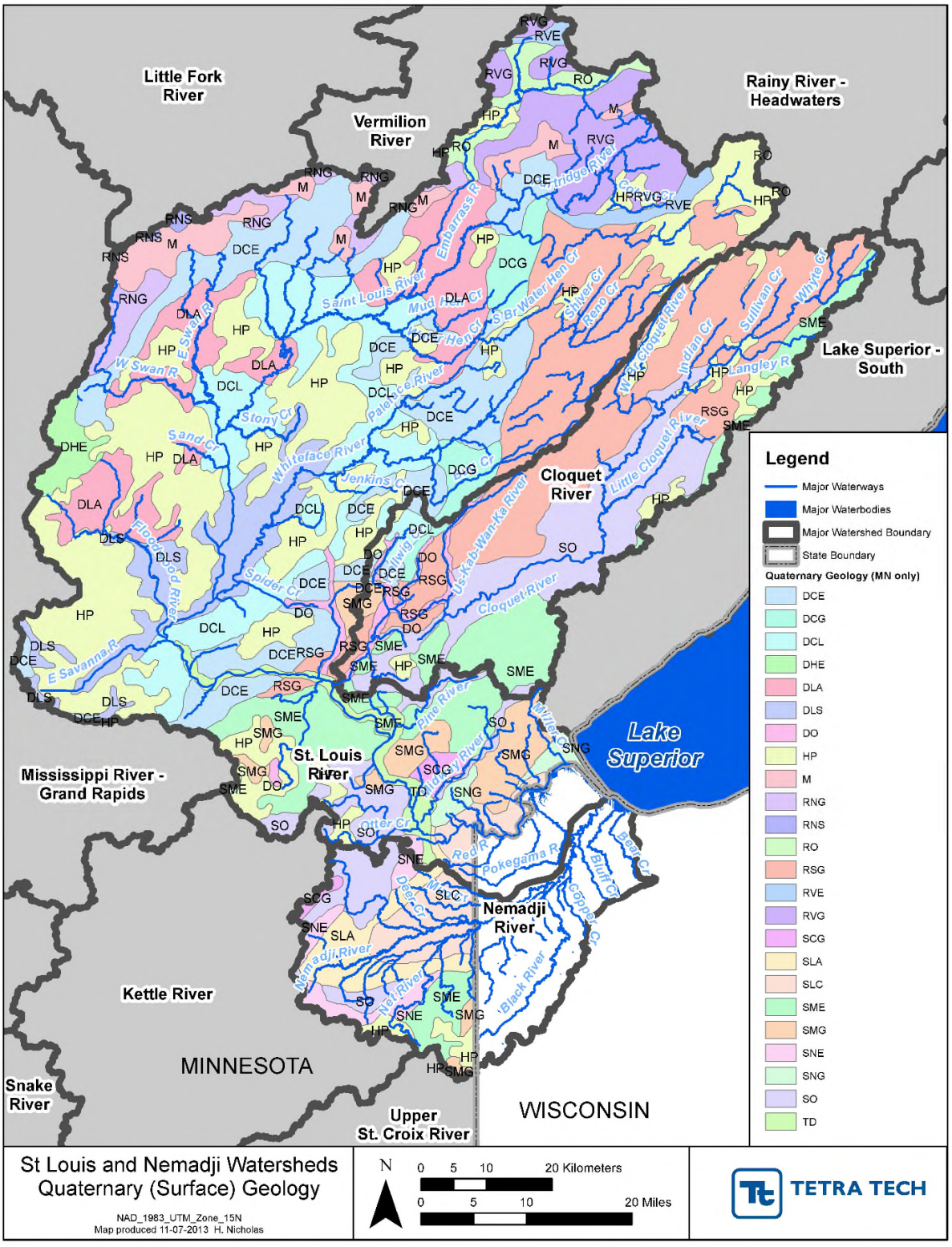

Figure 2-6. Quaternary (Surface) Geology of the St. Louis, Cloquet, and Nemadji Watersheds

Note: See Table 2-3 for Key. Quaternary geology coverage was not readily available for Douglas Co., Wisconsin.

Table 2-3. Key to Quaternary Geologic Units in the Minnesota Portion of the St. Louis, Cloquet, and Nemadji Watersheds

Abbreviation	Quaternary (Surface) Geology
RVG	Ground Moraine (Rainy Lobe--Vermillion Moraine)
SMG	Ground Moraine (Superior Lobe--Mille Lacs-Highland Moraine)
SNG	Ground Moraine (Superior Lobe--Nickerson Moraine)
RVE	End Moraine (Rainy Lobe--Vermillion Moraine)
SME	End Moraine (Superior Lobe--Mille Lacs-Highland Moraine)
RO	Outwash-Undivided as to Moraine Association
RNS	Stagnation Moraine (Rainy Lobe--Nashwauk Moraine)
HP	Peat (Holocene)
M	Mine Pits and Dumps (Holocene)
RSG	Ground Moraine (Rainy Lobe--St. Croix Moraine)
RNG	Ground Moraine (Rainy Lobe--Nashwauk Moraine)
DCE	End Moraine (Des Moines Lobe--Culver Moraine)
DLA	Sand and Gravel (Glacial Lake Sediment--Undivided as to Moraine)
DCG	Ground Moraine (Des Moines Lobe--Culver Moraine)
DCL	Lake-Modified Till (Des Moines Lobe--Culver Moraine)
DHE	End Moraine (Des Moines Lobe--Sugar Hills Moraine)
SO	Outwash-Undivided as to Moraine Association
DLS	Silt & Fine Sand (Glacial Lake Sediment--Undivided as to Moraine)
DO	Outwash-Undivided as to Moraine Association
TD	Terraces (Holocene to Pleistocene)
SCG	Ground Moraine (Superior Lobe--Cloquet Moraine)
SLC	Clay and Clayey Silt (Glacial Lake Sediment)
SLA	Sand and Gravel (Glacial Lake Sediment)
SNE	End Moraine (Superior Lobe--Nickerson Moraine)

The county-level SSURGO soils GIS data were combined into a unified coverage for the entire study area (Figure 2-7). For hydrology, key information from the soils database is provided by the designation of HSG, which provides an index to infiltration capacity. Four HSG classes are defined (Table 2-5) and provide the basis for initial assignment of infiltration rates in the model.

Table 2-4. Description of Hydrologic Soil Groups (USDA, 1986)

Hydrologic Soil Group	Description	Soil Texture
A	Low runoff potential and high infiltration rates even when thoroughly wetted. They consist chiefly of deep, well- to excessively-drained sand or gravel and have a high rate of water transmission (greater than 0.30 in/hr).	Sand, loamy sand, or sandy loam
B	Moderate infiltration rates when thoroughly wetted and consist chiefly of moderately deep to deep, moderately well to well-drained soils with moderately fine to moderately coarse textures. These soils have a moderate rate of water transmission (0.15-0.30 in/hr).	Silt loam or loam
C	Low infiltration rates when thoroughly wetted and consist chiefly of soils with a layer that impedes downward movement of water and soils with moderately fine to fine texture. These soils have a low rate of water transmission (0.05-0.15 in/hr).	Sandy clay loam
D	High runoff potential. They have very low infiltration rates when thoroughly wetted and consist chiefly of clay soils with a high swelling potential, soils with a permanent high water table, soils with a clay pan or clay layer at or near the surface, and shallow soils over nearly impervious material. These soils have a very low rate of water transmission (0-0.05 in/hr).	Clay loam, silty clay loam, sandy clay, silty clay, or clay

The study area contains a substantial proportion of soils with a dual designation (i.e., "B/D" or "C/D"). The two designators represent performance under drained and undrained conditions. During HRU processing, the first (drained) designator was used for cropland, which has drains installed on dual designation soils, and the second (undrained) designator was used for all other land uses. Figure 2-7 shows soils by the drained designation, while hatching indicates areas with an undrained designation of D. Under undrained conditions the majority of the watershed has D soils with high runoff potential.

Slope for model setup was calculated from the 10-meter digital elevation model (DEM) from the National Elevation Dataset. Ground elevations derived from the 10-meter DEM are mapped in Figure 2-8. Detailed LiDAR elevation data are also available for the entire study area; however, the relatively coarse 10-meter DEM is preferable for calculating average slopes. The LiDAR coverage was used in the development of reach cross sections and other fine-scale features.

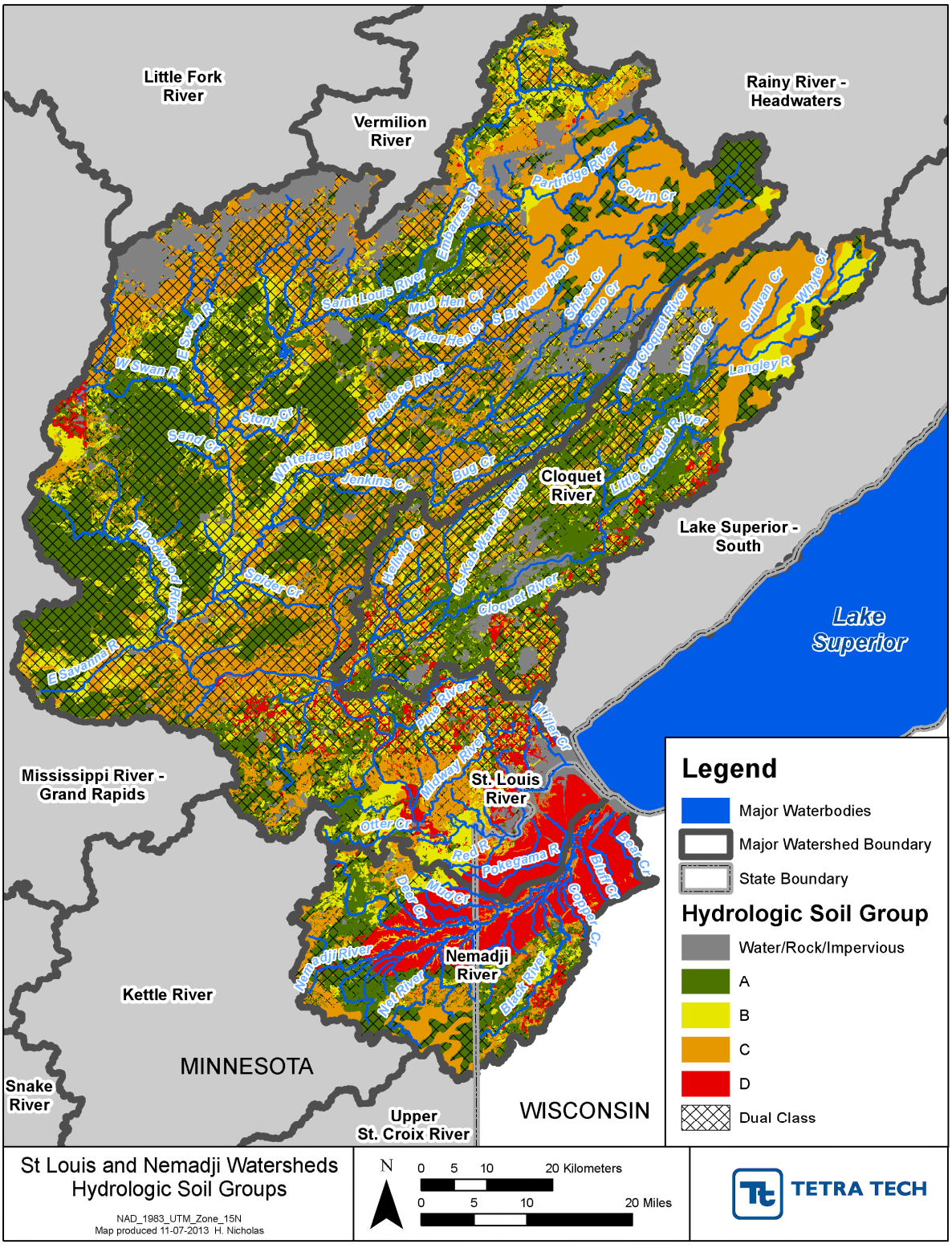

Figure 2-7. Hydrologic Soil Groups in the St. Louis, Cloquet, and Nemadji River Watersheds

Note: Dual class soils have a second, undrained designation of D; the color indicates the drained designation.

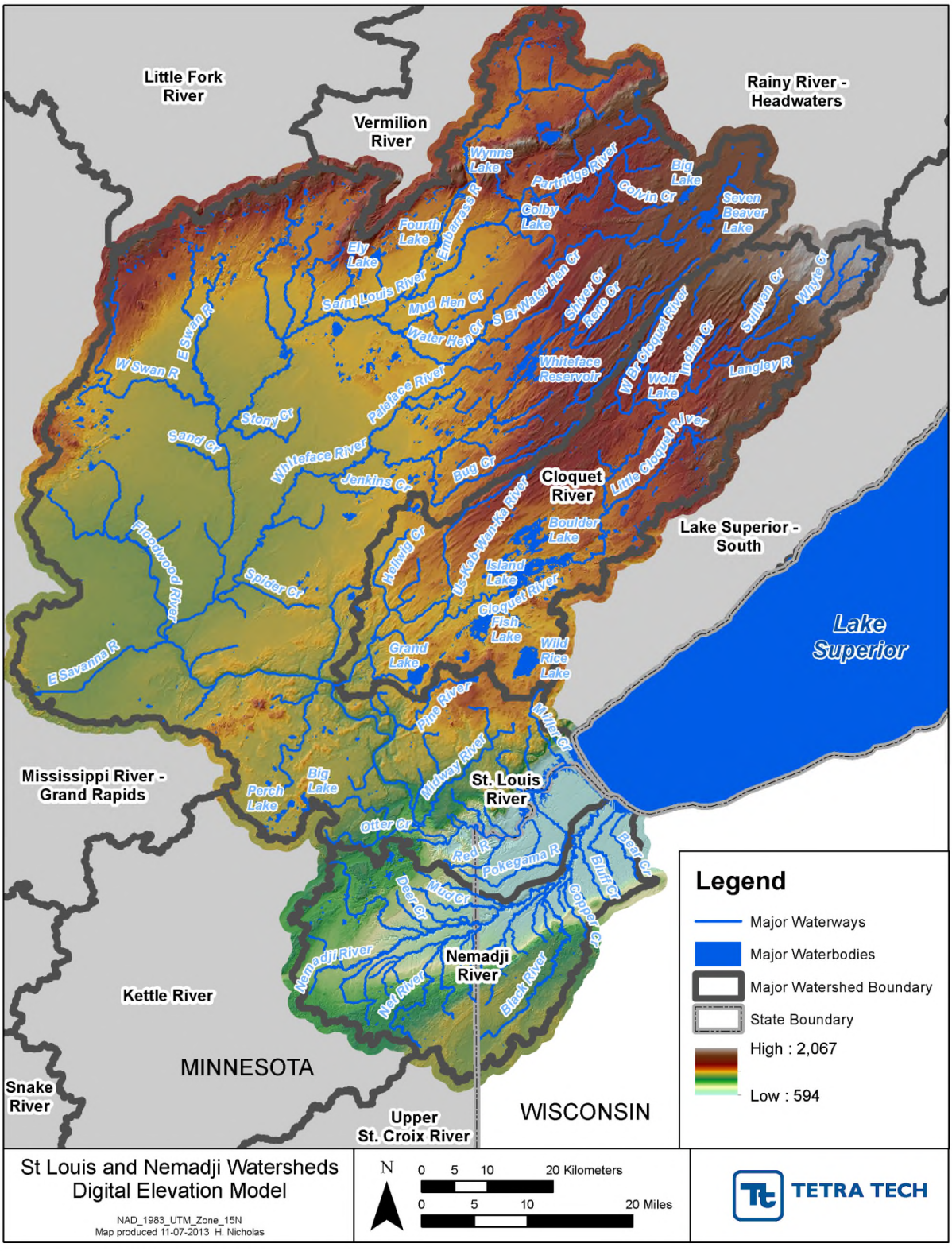

Figure 2-8. Digital Elevation Map of the St. Louis, Cloquet, and Nemadji River Watersheds

2.1.4 Development of HRUs

The basic upland unit of the watershed model is the HRU, which represents a common set of characteristics for land use and soils, along with weather station assignment. HRUs were developed consistent with the methods outlined in '*Modeling Guidance for BASINS/HSPF Applications under the MPCA One Water Program*'. Separation into slope classes was deemed not necessary for these watersheds because the slope information is largely redundant with the land use and soil classes. High resolution is maintained among the forest classes due to their large area in these watersheds.

LANDFIRE land cover and soil HSG were combined in ArcGIS to produce a grid with unique values for each combination. The model was simplified by reducing the number of HSGs represented. In accordance with Modeling Guidance for BASINS/HSPF Applications (Aqua Terra, 2012), group A soils were lumped with group B soils, and group C soils were lumped with group D soils. However, nominal infiltration (INFILT) values were weighted by the proportion of individual HSGs in each subbasin. Fine-grained red clay D soils in the Nemadji basin are represented as a distinct category (by assigning them to a separate nominal weather station group) to allow representation of the unique characteristics of these soils.

For soils with a dual designation (*e.g.*, "B/D"), the two designators represent performance under drained and undrained conditions. The land use processing uses the first (drained) designator for cropland and the second (undrained) designator for all other land uses. Water, barren, developed, and wetland land use/cover are not subdivided by HSG; however, the developed land classes are designated separately as to whether they lie within Municipal Separate Storm Sewer (MS4) permit area.

Each land segment has a three digit numeric code that represents the HRU land use-HSG combination (Table 2-5). The spatial distribution is shown in Figure 2-9. Weather stations are assigned to HRUs by adding a multiple of *50* to the three digit numeric code for each weather station. This enables the land units to be grouped either by land use or weather station, which is useful for parameter entry.

The HRU numbering scheme summarized in Table 2-5 is applied directly to pervious land segments (PERLNDs). The same numbering scheme is also used for impervious land segments (IMPLNDs) associated with each pervious land segment, although the HSG designation is not relevant to impervious land.

The precipitation regions were assigned to model subbasins as discussed in Section 2.2. The HRU grid and subbasins coverage were combined and areas exported for each unique combination of HRU and model subbasin. Because row crop agriculture occupies only a small fraction of the watershed, further post-processing subdivisions of this category to account for tillage practices (as is typically done for models in the Corn Belt region of southern Minnesota) was not pursued.

Table 2-5. Hydrologic Response Units for the St. Louis, Nemadji, and Cloquet River Watershed Models

Land Use	HSG	Base Number	Total area (acres)
Forest, Deciduous	AB	101	229,849
Forest, Deciduous	CD	102	1,058,175
Forest, Evergreen	AB	103	18,068
Forest, Evergreen	CD	104	45,168
Wetlands, Forested	CD	105	786,084
Wetlands, Herbaceous	CD	106	197,632
Grassland/Shrubland	AB	107	2,617
Grassland/Shrubland	CD	108	17,290
Pasture/Hay	AB	109	22,182
Pasture/Hay	CD	110	75,698
Row Crops	AB	111	3,190
Row Crops	CD	112	6,986
Row Crops	Drained	113	4,189
Developed, Open Space (MS4)		114	14,027
Developed, Open Space (non-MS4)		120	14,504
Developed, Medium Intensity (MS4)		115	3,565
Developed, Medium Intensity (non-MS4)		121	1,710
Developed, High Intensity (MS4)		116	1,355
Developed, High Intensity (non-MS4)		122	641
Water	CD	117	82,822
Barren/Strip Mines	CD	118	54,015
Roads (MS4)		119	2,376
Roads (non-MS4)		123	42,431
Total area			***2,684,574***

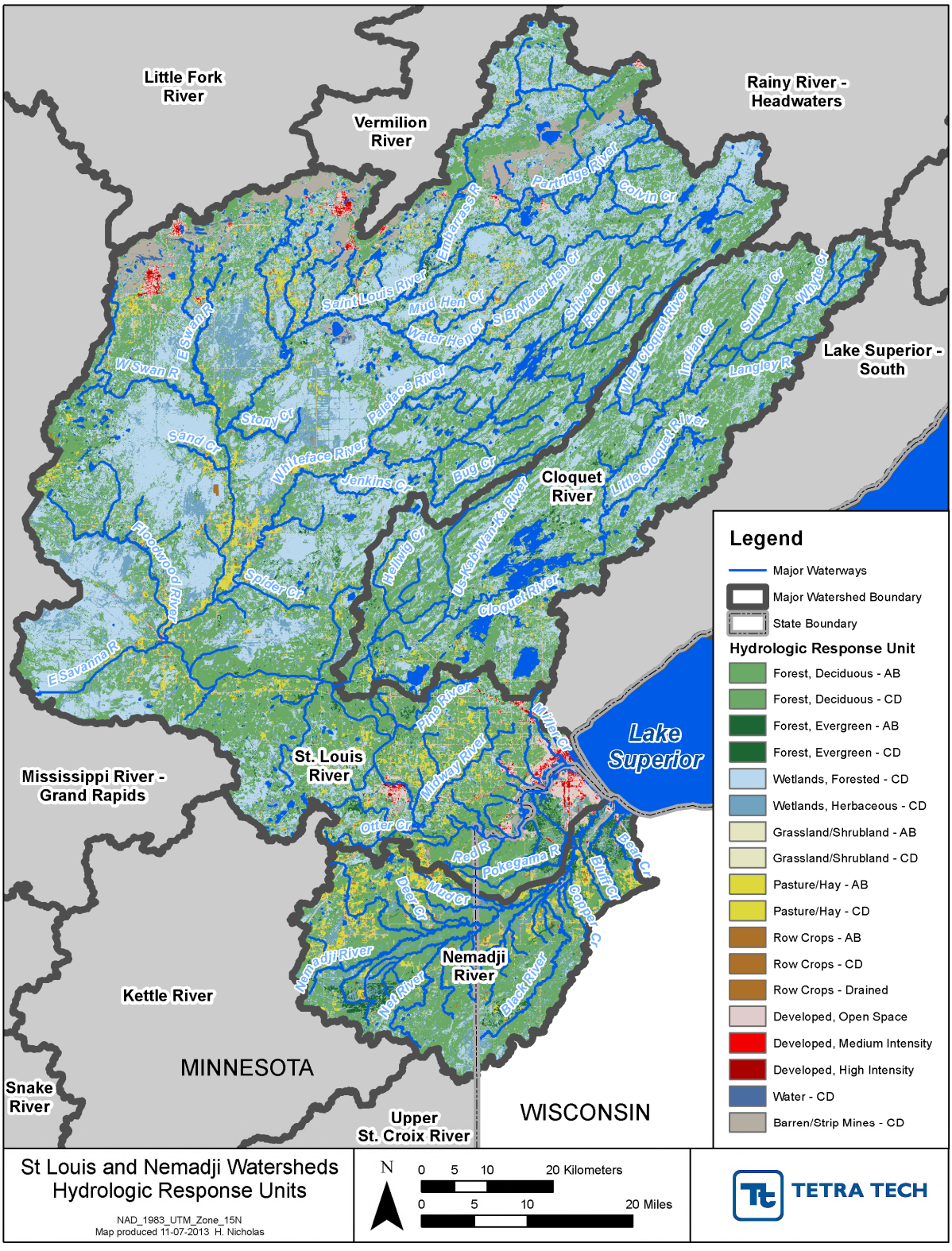

Figure 2-9. HRUs for the St. Louis, Cloquet, and Nemadji River Watersheds

2.1.5 HSPF Representation of Mesabi Range Mining Activities

The northern edge of the St. Louis River watershed corresponds with the Mesabi Range, which contains commercially valuable deposits of iron ore. These iron deposits, like most of the world's iron ore, were formed during the middle Precambrian period when marine algae first began releasing substantial amounts of atmospheric oxygen, causing oxidation and deposition of banded iron formations. Mining in the area began in the late 19th century, and initially focused on high grade hematite ore, which is readily processed into steel. The high grade ore was largely depleted by the 1950s. The industry was rejuvenated by the development of means to extract iron from low grade taconite rock. Most of the taconite formed close to the surface, allowing mining in vast open pits, resulting in large-scale disturbance of the land scape. Locations of some of the major mining facilities in the watershed are shown in Figure 2-10.

Ore is removed from mine pits and transported to a processing plant, where it is crushed to the approximate size of a pea. It is then mixed with water and ground in rotating mills until it is as fine as powder. At this point the iron is separated from the other minerals using magnets. The left over material, including large amounts of silica and pyritic shales, is dumped as a slurry into tailings ponds. The iron powder concentrate is mixed with limestone and baked into balls the size of marbles called taconite pellets, which consist of about 65% iron, and are shipped to steel mills. Producing one ton of taconite pellets requires the processing of 3 tons of ore and results in 2 tons of tailings. Large amounts of waste, non-ore rock are also produced during mining (GLIFWC, 2011).

Taconite mining operations have important impacts on the hydrology and water quality of the upper St. Louis River watershed. Taconite processing requires large volumes of water, while taconite mine pits require dewatering. This results in a complex set of withdrawal, reuse, and discharge flows. Presentations and discussions by Minnesota Department of Natural Resources (MDNR) and MPCA staff provided much enlightening information on taconite mine operations and data availability to represent those operations.

The HSPF model is a large-scale model of the entire St. Louis, Cloquet, and Nemadji watersheds. The typical reach length in the model is around 5 miles – which means that many of the details of hydrology in the mining area occur at a spatial scale that is smaller than can readily be explicitly represented in a whole-watershed model. For instance, in many cases appropriations and discharges occur within the same model subbasin, so explicit routing in the larger scale model is often not needed – although cases where there is a transfer between model subbasins should be represented. It is, however, necessary to represent the aggregate effects on hydrology of active and abandoned mines. The level of detail that can be incorporated for this depends in part on the type and amount of information that is available.

Taconite operations interact with and affect both surface and subsurface hydrology. Some of the larger flows in the system can be internal recycling for process water. Data are available for the surface appropriation and discharge components; however, little data and information are available on subsurface discharges by seepage or incidental subsurface appropriations that occur when groundwater flow is intercepted by taconite pits. A separate, detailed study (Tetra Tech, 2014) was undertaken to evaluate the effects of mining operations on flow in headwater streams in the area, including the development of a steady state groundwater flow model that represents exchanges between the streams and surface aquifer.

Given the complexity of the hydrology of the mining operations, the incompleteness of data on some aspects of flows, and the difference in scale between the HSPF model and mining operations, it is impractical to represent all the details of internal flows in the mining operations. Instead, a mine operation is best represented in the HSPF model as a process box that is characterized in terms of its external interactions with the larger watershed hydrology. The approach to specifying these external interactions is described below for active taconite pits, mining appropriations, taconite processing discharges, and abandoned pits.

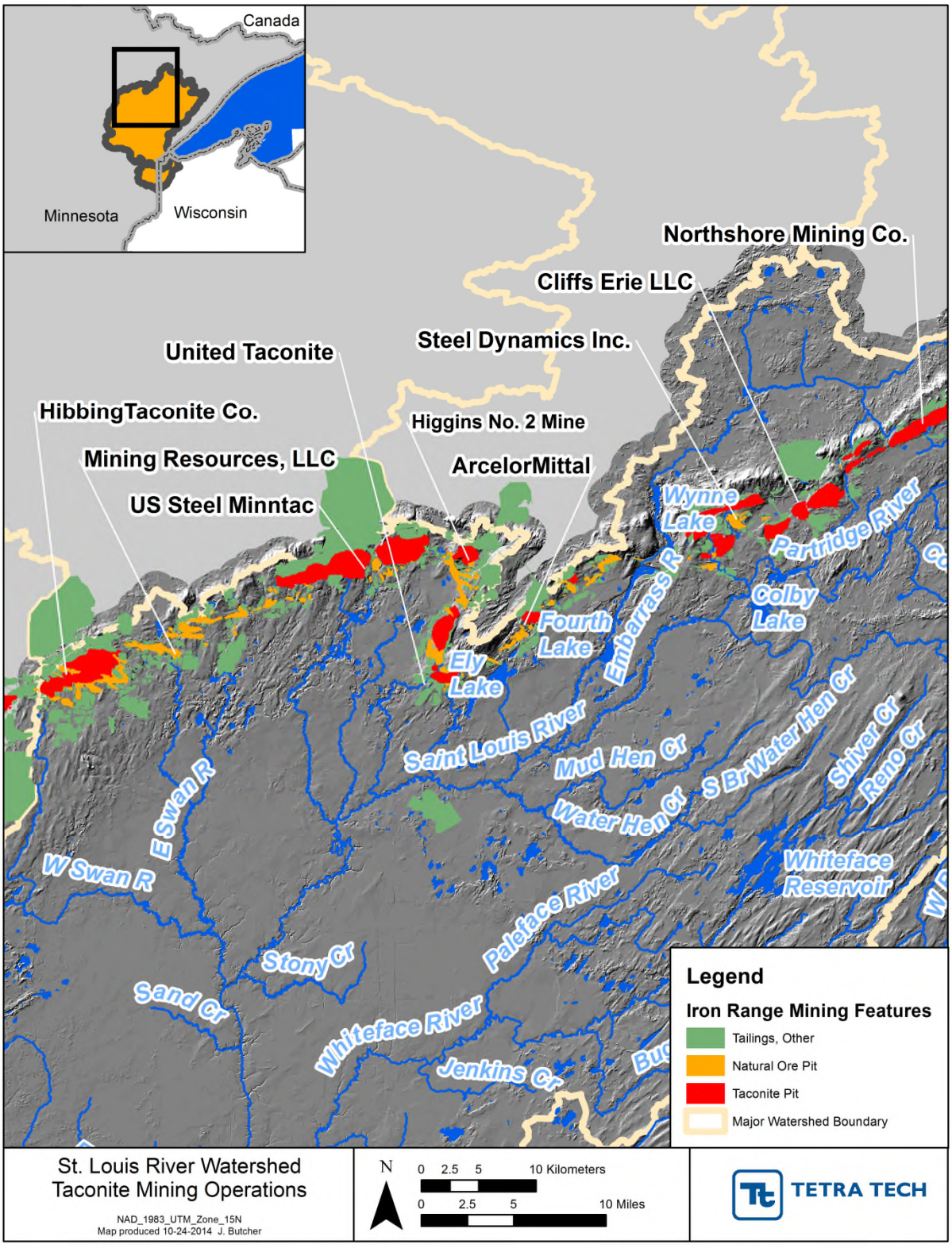

Figure 2-10. Major Taconite Mining Operations in the St. Louis Watershed

Active Taconite Pits

Active taconite pits consistently appear as "barren" in the land use coverage. The pits are typically continuously dewatered throughout the year to allow mining and this dewatering intercepts up-gradient groundwater. The dewatering flows may be discharged or used as mill process makeup water. The following approach was used to represent these areas in the HSPF model:

- Areas of barren land contained in the taconite pit coverage are disconnected from the watershed network because they are internally drained and discharges to the stream network are monitored.
- Dewatering discharges that go to the stream network are represented as point sources based on the DMR data.
- Areas where up-gradient groundwater is intercepted by actively pumped pits were identified through topographic analysis using LiDAR (Tetra Tech, 2014). The subsurface flows from the contributing area are disconnected from the HSPF model.
- The areas where surface flows are intercepted by actively pumped pits are different than the area from which groundwater is intercepted because in certain cases (e.g., Sauntry Creek; see Figure 2-11) the surface channel has been routed along road causeways between adjacent pits. These areas are also disconnected from the model.
- Down-gradient water may also flow back into pumped pits. Analysis with the ground water model GFLOW (Tetra Tech, 2014) demonstrated that this is a minor component of the water balance and so is not incorporated in the larger scale HSPF model.

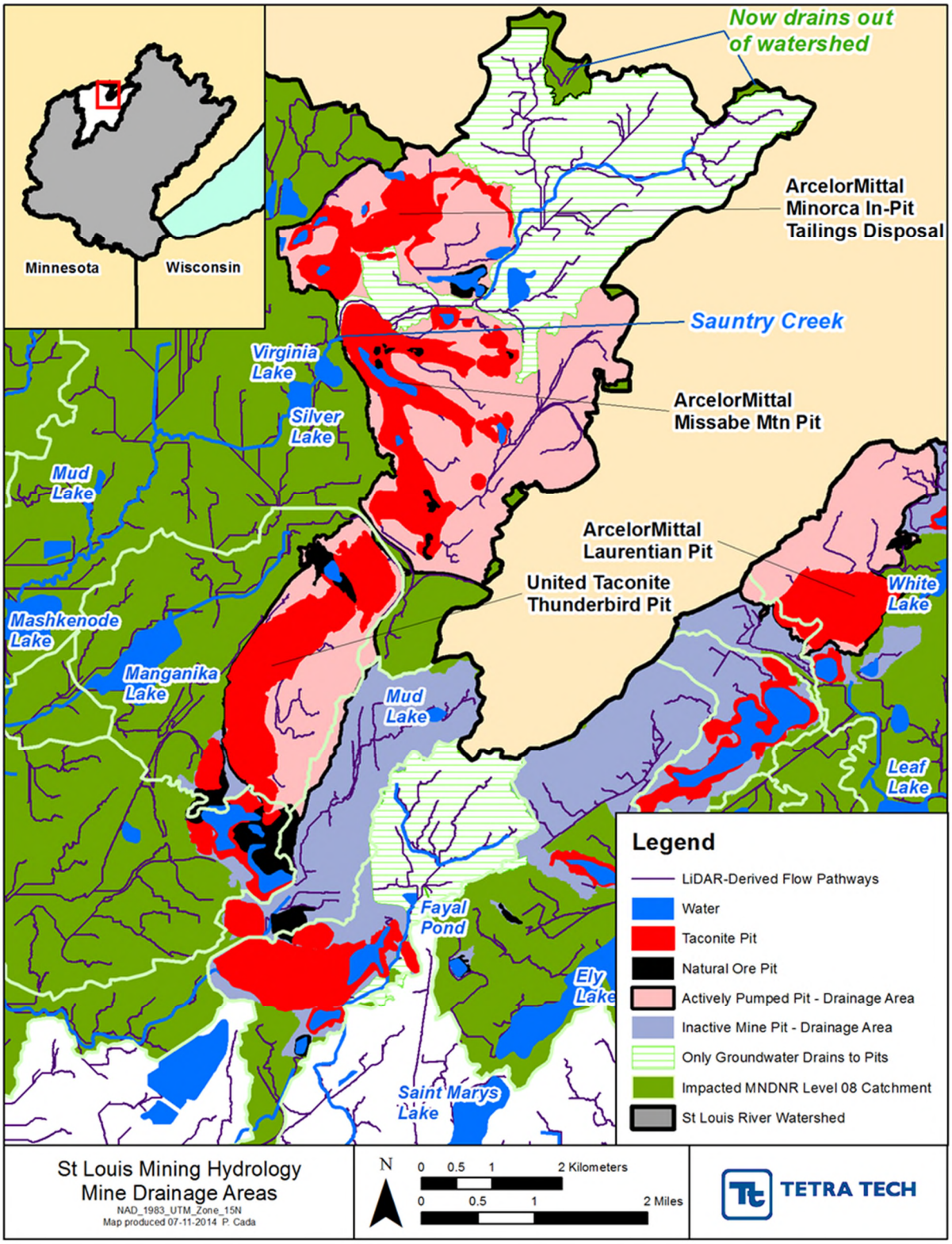

Figure 2-11. Example Analysis of Impacts of Mine Pit Dewatering in the Virginia/Eveleth Area of the St. Louis River Watershed (from Tetra Tech, 2014)

Mining Appropriations

A database of monthly mining process makeup water appropriations was provided by MDNR. Many of these appropriations consist of mine dewatering or withdrawal of water from abandoned mine pits; others come direct from rivers. Explicit appropriations from groundwater via wells are small, but appropriations from mine pits can include intercepted groundwater. The following approach was used to represent mining appropriations:

- The appropriations database is used to specify demand-based withdrawals, but only in the case where these appropriations come from the basin stream network.
- As in the discussion of the active pits, the interception of up-gradient groundwater is represented by disconnecting the contributing area in the HSPF model.

Taconite Processing Discharges

Process water, often mixed with other minor wasteflows from the processing mills, goes to tailings basins. This occurs year round. Most of the processing plants are over the ridgeline in adjacent major watersheds and there is only one major tailings basin currently active within the St. Louis watershed (Fairlane Tailings Basin). A larger tailings basin at Cliffs Erie operated until 2001 and is also included in the model.

A majority of the water discharged to active tailings basins is recycled to the plant. Evaporation rates are high because the discharged water is hot. Surface discharges rarely occur and are monitored and limited by permit to the difference between precipitation and evaporation. The discharges into the tailings basins and the rate of water recycling from the tailings basins are not reported to the state because they are internal process flows.

The tailings basins in the St. Louis watershed are unlined and were constructed by building dikes around flat swampy areas. These areas are underlain by glacial till and the water in the tailings basins establishes a significant hydraulic head, which promotes seepage. Seepage rates are limited by low hydraulic conductivity in fine tailings material, but can be quite high in areas where coarser materials deposit. Some, but not all, surface seeps through the dikes are monitored, but seepage direct to ground water is not measured.

The unmonitored seepage is estimated using mass balance principles on the assumption that the water volume within the tailings basin is approximately constant. Under this assumption, unmonitored seepage is estimated as the sum of process makeup water appropriations to the plant plus direct precipitation on the tailings basin minus evaporation from the tailings basin minus monitored discharges from the tailing basin minus plant process losses minus void lock losses (water that is trapped and retained within fine tailings deposits and not available for seepage).

Measurements are available for each of these components except for the plant process losses and void lock losses. To evaluate the approximate magnitude of these components we relied on a detailed water balance study that was conducted as part of the Environmental Impact Statement for the expansion of the Keetac mine in the Upper Mississippi/Grand Rapids drainage (Liesch, 2009). For Keetac, total losses during processing, including evaporation and water exported within the finished taconite pellets amounted to 9.8 percent of the total water inputs. The total water inputs consist primarily of water recycled (ultimately) from the tailings basins, plus process makeup appropriations and a small amount of additional input in the ore, flux stone, and combustion processes. The total water inputs amount to 4.74 times the makeup appropriation (which is the only portion of the input for which data are available at Fairlane and Cliffs Erie). Therefore, the process losses can be estimated as (0.098 x 4.74) = 0.465 times the appropriations.

Void lock losses in the fine tails are estimated as 11.1% of the plant discharge return water inflow to the tailings basin (see Figure 4 in Liesch, 2009). The return flow is 3.568 times the appropriation. Thus the loss to void lock can be estimated as 0.396 times the appropriations.

Both estimates are only rough approximations; thus, only a long-term average rate is estimated. In addition, the residence time in the aquifer before discharge to the stream may be relatively long. Putting together all the pieces, the unmonitored seepage for active tailings basins is estimated as equal to Precipitation – Evaporation + 0.139 x Appropriations. For the Fairlane tailings basin this yields a seepage discharge of 1.86 cfs. For the Cliffs Erie tailings basin, the average estimated seepage discharge calculated in this way through 2000, while the basin was still in full operation, is 2.64 cfs. However, this estimate may be low because appropriations were much higher prior to 1994, and site specific evaporation and precipitation estimates are not available. The Cliffs-Erie seepage proceeds primarily north toward the Embarrass River, with small amounts seeping to Second Creek, a tributary to the Partridge River.

Cliffs Erie stopped operations in January 2001, but significant seepage discharges have continued. The mill site was sold to LTV Steel and subsequently transferred to PolyMet Mining. PolyMet proposes to develop an open pit mine and to refurbish and modify the former taconite ore processing facility to extract copper metal and precipitates of nickel, cobalt, and precious metals, but the project has not yet been approved. The Draft Environmental Impact Statement (EIS; MDNR, 2009, p. 4.1-7) notes that seepage rates have declined since closure of the tailings basin, but total seepage rates were still estimated at 1,795 gpm (4.0 cfs) as of 2009. Monitored seeps account for 1.7 cfs as an average in the 2001-2012 period.

The PolyMet proposal includes reopening the Cliffs-Erie tailings ponds 1E and 2E. After 20 years of operation the predicted unrecovered seepage is 3,804 gpm (8.5 cfs) based on an appropriation from Colby Lake at an average rate of 3,500 gpm (7.8 cfs), which is much less than the historic appropriations by Cliffs-Erie (14.7 cfs average for 1993-2000); however, the loss rates for the PolyMet operation may be very different from those in a taconite plant. Further, the Cliffs-Erie operation must have had a net seepage loss that was greater than 1990 conditions to account for the mounded groundwater at the site. The EIS also notes that the seepage flux capacity of the local aquifer is only about 155 gpm and that much of the seepage water surfaces and collects in wetlands, where some of it evaporates.

These various estimates of seepage from Cliffs-Erie tailings ponds during operations toward the Embarrass River are not very consistent with one another, and suggest that the method of extrapolation from Keetac may not be appropriate. Given that, the maximum seepage rate predicted for the PolyMet operation (8 cfs) is used as a reasonable estimate of seepage that occurred during Cliffs-Erie operations.

We therefore made the following assumptions:

- The water land use area that represents tailings basins is disconnected from the watershed network.
- Total monitored and unmonitored seepage from the Fairlane tailings basin is estimated as 1.86 cfs.
- Seepage from the Cliffs-Erie tailings basin is approximated as 8 cfs through 2000 and 4 cfs thereafter.

Inactive Mine Pits

There are many inactive mine pits in the watershed, many of them smaller natural ore pits. Many of these abandoned pits reach a hydrologic equilibrium with no surface discharge, but do have subsurface inflows and outflows through the glacial till. In some cases they are sources of small appropriations to public water supplies or taconite plants. One anomalous case is the ArcelorMittal Missabe Mountain Pit. Although this is not an active mine it has large appropriations that supply water to the City of Virginia as well as to the ArcelorMittal taconite plant just over the ridgeline. Because the natural water table is

strongly down by these appropriations, Missabe Mountain is treated as an active pit that intercepts up-gradient flows. The approach for other inactive pits is as follows:

- Remove the area of inactive pits that do not have a surface discharge from the water land use in the model as they will not contribute direct surface flow.
- Do not explicitly model appropriations from abandoned pits as these are likely mostly accounted for in the net difference of precipitation and evaporation.
- Assume that net precipitation minus evaporation in these pits is approximately in balance. Inactive pits are thus in effect represented as transmitting ground water derived from the up-gradient drainage area. The model setup does allow a portion of the groundwater simulated as originating within the subbasin to be lost and not transmitted to the stream network. This could be adjusted to account for residual error associated with appropriations and other adjustments to the water balance in abandoned pits.

2.1.6 Ground Water Simulation of Mining Area

Tetra Tech (2014) provides an analysis of the impacts of mining operations on groundwater hydrology using the GFLOW model. The GFLOW simulations suggest that there are few losing stream reaches outside of the area where drainage is directly intercepted by active mining features, and that losses due to backflow from down-gradient areas into mine pits is relatively small. Therefore, the approach in the larger scale HSPF model of eliminating areas identified as upstream of active mining features (removing all flow or subsurface flow only, as discussed above) is a reasonable approximation. Further, analysis of the HSPF water balance suggests it is compatible with the GFLOW steady state solution. In GFLOW, the groundwater recharge rate is set at 0.0057 m/d or 7.78 in/yr. In HSPF, the independently simulated recharge to the surface groundwater system is output as the variable AGWI. Over the simulated period of water years 1993-2012, the average of AGWI, area-weighted over the portion of the GFLOW study area not intercepted by active mining features and corrected for baseflow evapotranspiration, is 8.58 in/yr, which is within 10 percent of the GFLOW estimate. The two values are thus in good agreement, especially considering that the GFLOW recharge is a long-term steady-state estimate not specific to the period simulated in HSPF.

2.2 METEOROLOGY

Meteorological data available through EPA's BASINS data set 2009 version (documented in USEPA, 2008) and Minnesota State Climatology Database (MSCD) were used to develop weather forcing time-series. The HSPF model of the St. Louis, Cloquet, and Nemadji watersheds operates at an hourly time step. In continuous simulation hydrology models, representation of hydrology is improved considerably by using precipitation data at an hourly, as opposed to daily time scale. The majority of rain-gaging sites in Minnesota are Summary of the Day (SOD) stations that report only daily totals, requiring disaggregation to an hourly scale based on a template which may introduce temporal errors.

Meteorological data required for the HSPF model setup consists of hourly precipitation (PREC), air temperature (ATEM), cloud cover (CLOU), dew point temperature (DEWP), solar radiation (SOLR), wind speed (WIND) and evapotranspiration (PEVT).

2.2.1 Precipitation Stations

Selection of precipitation stations was based upon three factors,

1. Proximity to the watershed: BASINS and state climatology stations within a 15 mile buffer of the watershed were initially selected.
2. Availability of data: Stations lacking data for the modeling period (1/1/1993 to 9/30/2012) were removed from the initial selection.
3. Data gaps: Stations having large data gaps or missing periods were further removed.

The above analysis resulted in a total of 12 BASINS and 8 MSCD stations, three of which were co-located (Figure 2-13 and Table 2-6). These stations were chosen because they were within the watershed boundary and had data for the entire or part of the modeling period. The modeling period was initially directed to be 1/1/1993 to 9/30/2009, but was extended through 9/30/2012 due to the availability of more recent monitoring data. The BASINS data series were extended using data from the National Climatic Data Center.

The BASINS stations are preferred to the state stations because they have already been patched (through 2009); however, the three co-located state climatology stations were also processed for comparison purposes. A total of 17 climate stations are assigned in the model based on proximity. Figure 2-12 shows Thiessen polygons that are used to assign model upland HRUs to meteorological stations based proximity. Figure 2-13 shows the assignment of meteorological stations to water bodies by model subbasin.

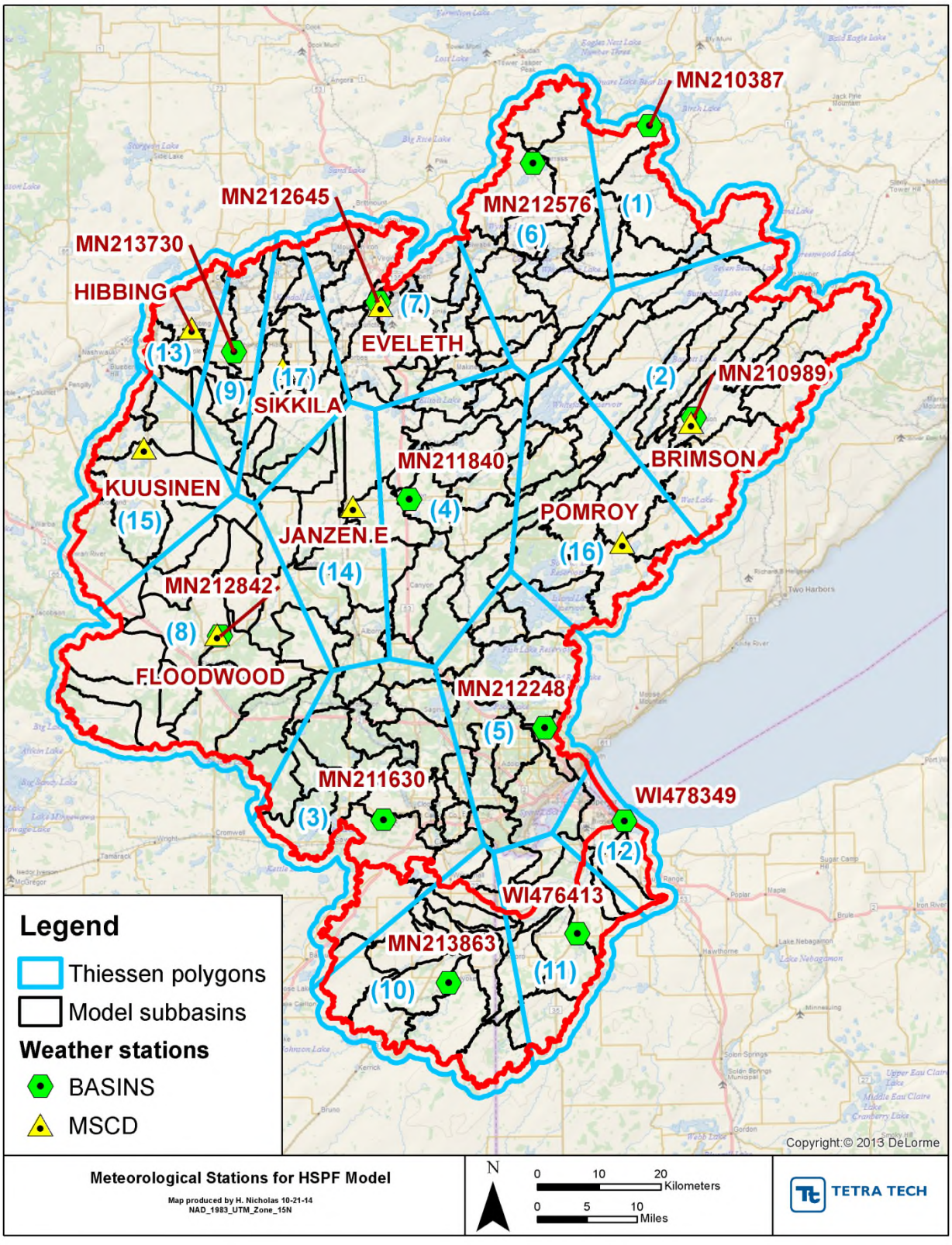

Figure 2-12. Meteorological Stations for the St. Louis, Cloquet, and Nemadji Watersheds: Assignment to Upland Land Segments

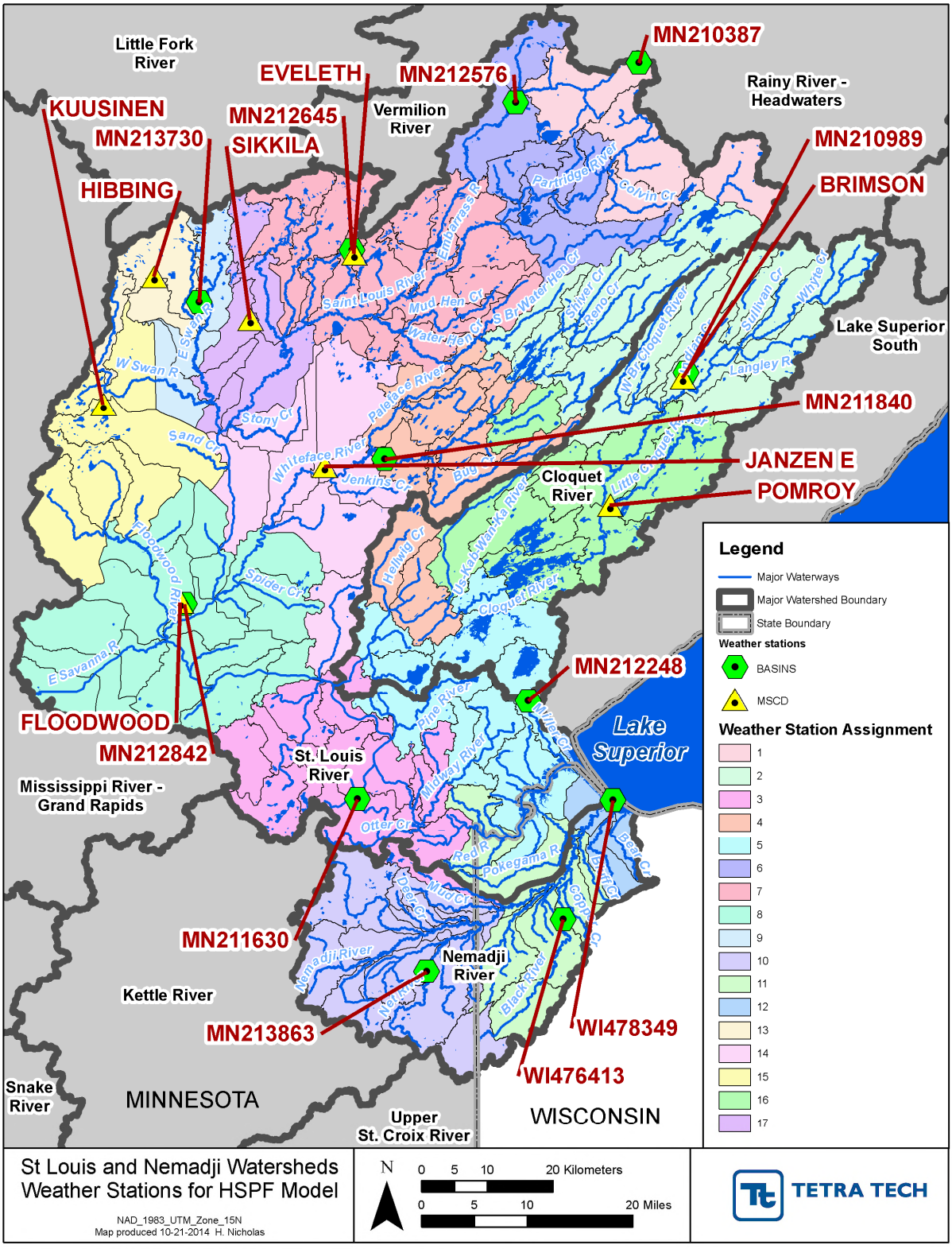

Figure 2-13. Meteorological Stations for the St. Louis, Cloquet, and Nemadji Watersheds: Assignment to Stream Reaches

The regions are identified in Table 2-6, in which the weather base is the starting number for the HRU set shown in Table 2-5. For example, for HRUs associated with Cotton (MN218840), HRU 251 corresponds to the first member of the HRU set, deciduous forest on A/B soils.

Table 2-6. Precipitation Stations

Code	Elevation (ft)	Name	Latitude	Longitude	DSN	Weather Base HRU
MN210387	1492	Babbitt	47.7103	-91.9442	101	101
MN210989	1515	Brimson 1E	47.2847	-91.8581	102	151
MN211630	1265	Cloquet	46.7047	-92.5253	103	201
MN211840	1329	Cotton	47.1700	-92.4667	104	251
MN212248	1422	Duluth International Airport	46.8369	-92.1833	105	301
MN212576	1400	Embarrass	47.6581	-92.1958	106	351
MN212645	1445	Eveleth Waste Water Plant	47.4581	-92.5303	107	401
MN212842	1260	Floodwood 3 NE	46.9728	-92.8700	108	451
MN213730	1347	Hibbing FAA Airport	47.3867	-92.8389	109	501
MN213863	1033	Holyoke	46.4675	-92.3903	110	551
WI476413	1100	Pattison State Park	46.5372	-92.1186	111	601
WI478349	630	Superior	46.7000	-92.0167	112	651
HIBBING	1532	Hibbing	47.4218	-92.9312	113	701
JANZEN E	1329	Janzen E	47.1609	-92.5887	114	751
KUUSINEN	1347	Kuusinen	47.2463	-93.0339	115	801
POMROY	1515	Pomroy	47.1047	-92.0161	116	851
SIKKILA	1347	Sikkila	47.3630	-92.7370	117	901
Supplemental Series used for Patching Only						
EVELETH	1445	Eveleth	47.4529	-92.5265	118	
FLOODWOOD	1260	Floodwood	46.9753	-92.8785	119	
BRIMSON	1515	Brimson	47.2778	-91.8659	120	

2.2.2 Precipitation Data Completeness and Patching

Table 2-7 shows the period of record associated with the BASINS and state climatology stations. BASINS data are available in an hourly format through 2009 with internal missing and accumulated periods addressed. Data for 2009-2012 were checked for outliers and processed to fill gaps and distribute any accumulated records using Tetra Tech's MetAdapt software. Where the period of data for a BASINS station did not extend over the full modeling period of 1993-2012, the record was extended from nearby stations using the normal ratio method.

Table 2-7. Meteorological Stations and Period of Record

#	Location	Source	Start	End	Comment
1	MN210387	BASINS	5/31/1999	12/31/2012	Period prior to 5/31/1999 filled with data from MN212576
2	MN210989	BASINS	7/31/1948	12/31/2012	
3	MN211630	BASINS	3/28/1947	12/31/2012	
4	MN211840	BASINS	8/31/1962	11/29/2002	Period after 11/29/2002 filled with data from Janzen E
5	MN212248	BASINS	8/1/1948	12/31/2012	
6	MN212576	BASINS	10/31/1994	12/31/2012	Period prior to 10/31/1994 filled with data from MN212645
7	MN212645	BASINS	4/1/1991	12/31/2012	
8	MN212842	BASINS	4/1/1991	12/31/2012	
9	MN213730	BASINS	10/31/1962	12/31/2006	Period after 12/31/2006 filled with data from Hibbing
10	MN213863	BASINS	9/1/1948	3/31/2006	Period after 12/31/2006 filled with data from WI476413
11	WI476413	BASINS	4/30/1998	12/31/2012	Period prior to 4/30/1998 filled with data from WI478349
12	WI478349	BASINS	5/31/1948	12/31/2005	Period after 12/31/2005 filled with data from WI476413
13	Kuusinen	MSCD	11/1/1994	12/31/2012	Period prior to 11/1/1994 filled using data from MN213730 and disaggregated using data at MN213730
14	Hibbing	MSCD	1/1/1993	12/31/2012	Disaggregated using data at MN213730
15	Floodwood	MSCD	1/1/1993	12/31/2012	Patching and disaggregation completed using data at MN212842
16	Sikkila	MSCD	7/1/1993	12/31/2012	Disaggregated using data at MN213730
17	Janzen E	MSCD	1/1/1993	12/31/2012	Patching and disaggregation completed using data at MN211840
18	Eveleth	MSCD	1/1/1993	12/31/2012	Patching and disaggregation completed using data at MN212645
19	Pomroy	MSCD	1/1/1993	12/31/2012	Disaggregated using data at MN210989
20	Brimson	MSCD	1/1/1993	12/31/2012	Patching and disaggregation completed using data at MN210989

The state climatology data (MSCD) often has missing and accumulated periods and is available in a daily format. Missing data, if any, were patched using nearby stations and then disaggregated to an hourly format. The patching and disaggregation exercise was carried out using Tetra Tech's MetAdapt weather data processing tool. A quality check on the magnitude and variability of precipitation in comparison with the BASINS data was performed on the final processed state climatology data.

Hourly data for other meteorological were obtained from the BASINS dataset. Table 2-8 shows the stations that were selected and their respective available constituents. Potential evapotranspiration (PEVT) at each of the BASINS station locations was calculated using the Penman Pan method. In the

absence of local CLOU, DEWP, SOLR, or WIND data, nearby stations were used as shown in Table 2-9. PEVT was not calculated for a station if local ATEM was not available; instead, the nearest valid PEVT series was used. For the state climate stations, potential evapotranspiration was assigned based on the nearest BASINS station. Table 2-10 summarizes average annual precipitation, air temperature, and potential evapotranspiration for each meteorological station.

Table 2-8. Meteorological data availability for stations selected for the HSPF model

Location	PREC	ATEM	CLOU	DEWP	SOLR	WIND	PEVT	SNOW
MN210387	X	X					X	X
MN210989	X							X
MN211630	X	X					X	X
MN211840	X	X					X	X
MN212248	X	X	X	X	X	X	X	X
MN212576	X	X					X	X
MN212645	X	X					X	X
MN212842	X	X					X	X
MN213730	X	X	X	X	X	X	X	X
MN213863	X							
WI476413	X	X					X	
WI478349	X	X					X	
Kuusinen	X							
Hibbing	X							
Sikkila	X							
Janzen E	X							
Pomroy	X							

* ATEM was not available for MN210989 at the time of this effort. These data have subsequently been obtained and will be used in the pending update of the modeling period through 2014.

Table 2-9. Data Assignments for PEVT calculation using the Penman Pan method

Location	PREC	ATEM	CLOU	DEWP	SOLR	WIND
MN210387	MN210387	MN210387	MN213730	MN213730	MN213730	MN213730
MN211630	MN211630	MN211630	MN212248	MN212248	MN212248	MN212248
MN211840	MN211840	MN211840	MN213730	MN213730	MN213730	MN213730
MN212248	MN212248	MN212248	MN212248	MN212248	MN212248	MN212248
MN212576	MN212576	MN212576	MN213730	MN213730	MN213730	MN213730
MN212645	MN212645	MN212645	MN213730	MN213730	MN213730	MN213730
MN212842	MN212842	MN212842	MN212248	MN212248	MN212248	MN212248
MN213730	MN213730	MN213730	MN213730	MN213730	MN213730	MN213730
WI476413	WI476413	WI476413	MN212248	MN212248	MN212248	MN212248
WI478349	WI478349	WI478349	MN212248	MN212248	MN212248	MN212248

Note: Red highlighting indicates locations where non-local data were extrapolated.

Table 2-10. Annual Weather Averages by Meteorological Station, 1993-2012

Location	Average Annual PREC (inches)	Average Annual ATEM (°F)	Average Annual PEVT (inches)
MN210387	28.3	36.4	25.4
MN210989	28.0	36.4	25.4
MN211630	31.4	40.9	34.8
MN211840	27.9	38.5	27.7
MN212248	30.6	40.3	33.5
MN212576	27.3	34.5	22.6
MN212645	27.1	38.7	28.3
MN212842	26.1	38.1	30.1
MN213730	25.6	39.1	28.4
MN213863	29.8	40.8	34.5
WI476413	32.2	40.8	34.5
WI478349	29.9	41.3	35.0
Kuusinen	28.4	39.1	28.4
Hibbing	27.5	39.1	28.4
Sikkila	29.5	39.1	28.4
Janzen E	28.1	38.5	27.7
Pomroy	29.9	36.4	25.4

2.3 MODEL SEGMENTATION AND REACH NETWORK

2.3.1 Subbasin Delineation

This section provides an overview of the development of the HSPF watershed model subbasins and reach network. For this project, the subbasins were specified at the HUC-12 scale.

GIS catchment data for the St. Louis, Cloquet, and Nemadji watersheds were obtained from the MDNR GIS website. Level 8 represented the highest level of detail available. The Level 8 catchments were aggregated to the HUC-12 scale using tabular attributes. The general objective is to follow 12-digit HUC boundaries to the extent practical with modifications to address special circumstances. The MDNR HUC-12 boundaries polygon shapefile and MDNR 24k Streams polyline shapefile served as the starting point for model subwatershed delineations.

Further sub-delineations of the MDNR HUC-12 boundaries were made using supplemental spatial data to account for hydrological features such as control by impoundments and water quality monitoring and flow gaging station locations (see Section 2.6). The period of record and currency of HYDSTRA monitoring data were used to select locations to be used for HSPF model development, calibration, and validation. Only those gages with data available during the model simulation period (1993-2012) were selected to include in the HSPF model. Consequently, where needed, new subwatershed boundaries were created to allow easy inclusion of data gathered at these selected locations. New subbasin delineations were created for Cloquet Reservoir and Knife Falls Dam on the St. Louis River mainstem, the recent USGS gage on the upper St. Louis River at Skibo, the upper Blackhoof River above the HYDSTRA gage in the Nemadji basin, and a portion of the Black River of potential interest to Wisconsin Department of

Natural Resources. Other subdivisions were made to delineate the drainage areas of Manganika, Mashkenode, and Ely Lake.

Although the St. Louis Bay Estuary is not modeled as a stream reach in HSPF, the areas draining to the estuary were included to provide potential support for future estuarine modeling. Sub-delineated HUC-12s were divided manually using ESRI ArcGIS Editor and followed the NHDPlus Version 2 Catchments boundaries (http://www.horizon-systems.com/NHDPlus/NHDPlusV2_home.php).

Additionally, three sets of two adjacent MDNR HUC-12s were merged to facilitate model subwatershed creation. One of these was simply merged and not re-divided (reach 217). The other two merged HUC-12s were re-divided to agree with the location of major stream confluences. Figure 2-14 displays the final subbasin routing, consistent with information from NHDPlus, surface elevations, and mine discharge and intake routing provided by MPCA.

The scale of the model segmentation limits the amount of resolution in the stream network. The stream network is essentially fractal in nature, with similar levels of complexity as we go to smaller and smaller scales. We simplify things considerably for a HUC 8-scale model. HSPF allows one defined stream reach per subbasin. For subbasins along the main stem this reach is the main stem reach and we do not simulate smaller tributaries that drain incremental area into the mainstem. This limits the ability of the model to represent certain details, such as the ditches cut into peatlands in the northwestern part of the watershed or diversions of water by road ditches that are not captured by the NHD subbasin delineations. In the iron range there are instances where sub-surface mine shafts provide connections between abandoned pits. These mostly occur within the same model sub-basin, but in some instances cross drainage divides. These details are at too fine a scale to fully incorporate into the whole-basin model, and indeed have little impact on downstream simulations. However, detailed investigations of local areas might benefit from the creation of a finer-scale submodel.

Note that subsequent analyses have demonstrated that the boundaries of the Miller Creek watershed (reach 304) have been altered by stormwater conveyances in the Duluth and Hermantown area and are not correct as specified in the model. Miller Creek and other Duluth local tributaries are being addressed and re-modeled at a finer scale as part of the Duluth WRAPS project.

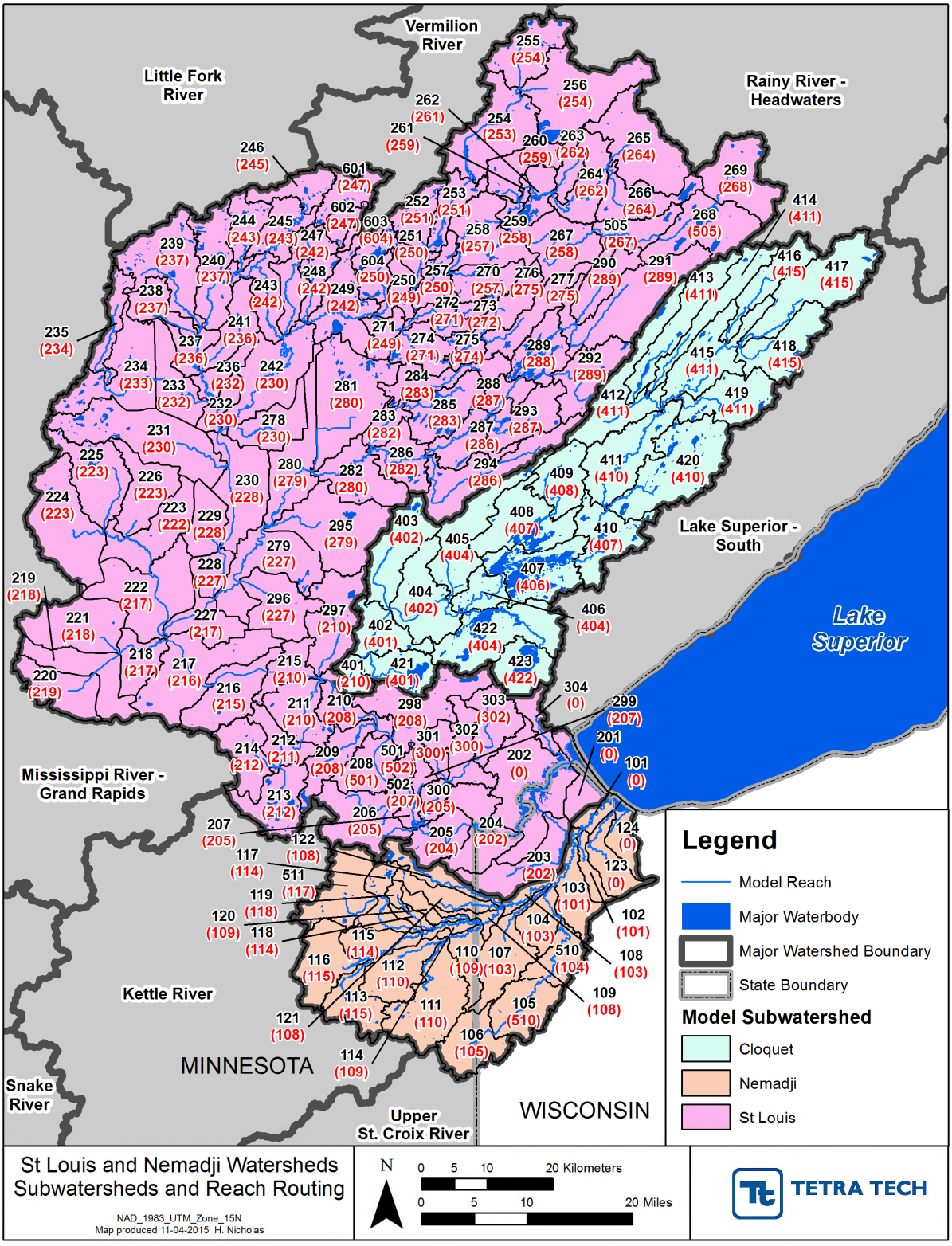

Figure 2-14. Model Subwatershed Delineations and Reach Routing

Note: Downstream reach is shown in (parentheses).

2.3.2 Reach Hydraulics

Movement of sediment in stream networks, including transport, scour, and deposition rates, is determined by flow energy. HSPF does not directly solve hydraulic equations for flow routing, but rather specifies information on the relationship between stage, discharge, and geometry through Functional Tables (FTables). The calculation of boundary shear stress from the FTable information is a key component of the simulation of sediment transport.

HSPF is a water balance (hydrologic) model and not a hydraulic model. HSPF represents stream reaches as one-dimensional fully mixed reactors and, while maintaining mass balance, does not explicitly conserve momentum. To simulate the details of hydrograph response to storm events HSPF relies on Function Tables (FTables) that describe the relationship of reach discharge, depth, and surface area to storage volume. At stable median flow conditions the model results are not particularly sensitive to the details of the FTable specification, as outflow tends to approximate the net inflows; however, the shape of the response to storm event peaks can be highly sensitive to FTable details. Given the interest of MDNR in evaluating the distribution of flows in streams in Minnesota there is an increasing need to refine HSPF basin-scale model FTables.

By default, the BASINS version of HSPF estimates FTables by applying predetermined regressions against drainage area, but this approach does not take into account site-specific characteristics (such as obstructions) and is based on data from sites in ecoregions different from those found in Minnesota. Some local studies on the dependence of stream channel geometry on drainage area have been completed in our area of interest (e.g., Magner and Brooks, 2008 for the Nemadji) and can be used; however, there are a variety of other approaches that are based on inputs ranging from completed hydraulic models to analysis based on individual cross sections. To optimize the models we need to incorporate as much hydraulic information as feasible; however, the scoped level of effort is also limited. For instance, it might be ideal to create detailed HEC-RAS hydraulic models of the entire watershed, but such an effort is not possible within the scope and budget of the HSPF model development task. Therefore, we used a triage approach that seeks to optimize the best information available from a variety of sources at a feasible level of effort. The approaches are listed below in order of priority for application.

Note that the FTables primarily affect the details of the hydrograph shape. If we correctly characterize FTables for most reaches with monitoring the impact of FTable discrepancies in other, unmonitored reaches are likely to be small and can be improved in future iterations of the model without significant disturbance to the calibration.

2.3.2.1 Lakes

Lakes and reservoirs typically have outflows that are determined by dam/weir characteristics or active management. Thus, lake FTables represent a different class of analyses than stream reach FTables, and essentially need to be addressed on a site-specific basis as a first priority. Site-specific FTables are calculated for lakes are discussed below in Section 2.3.3. These are based on specific characteristics of individual lakes/dams and take preference over any other methods.

2.3.2.2 HEC-RAS Models

HEC-RAS is the standard model for Federal Emergency Management Agency (FEMA) flood insurance map studies and typically involves a detailed analysis of stream channel and restricting structure information. HEC-RAS hydraulic models allow for direct calculation of FTables (i.e., by evaluating discharge at HSPF subbasin outflows and summing upstream storage volume and area in the reach), but are available for only limited areas. Where they are available and usable, runs can be made with a variety of flow conditions to directly develop an FTable, usually, by summing and averaging over the cross-sections within an HSPF model reach.

Based on communications with MDNR, several HEC-2 models have been created in connection with FEMA flood studies in the St. Louis watershed. Hydraulic models were located by MDNR for St. Louis County but could not be found for Carlton and Lake Counties. The most recent FEMA Flood Insurance Studies for St. Louis County, as well as the corresponding HEC modeling, were completed in the 1970s and 1980s and have not been recently revised. HEC-2 models appear to be available for small portions of the St. Louis River and tributaries in the cities of Duluth, Floodwood, Hermantown, Hibbing, and Proctor.

In the mid-1990s, HEC-RAS replaced HEC-2 with modernized and more robust hydraulic routines and computational procedures and is the current standard for FEMA flood modeling. For revisions to effective Flood Insurance Studies, FEMA strongly encourages conversion of HEC-2 to HEC-RAS; however, this has not yet been done for St. Louis County, and only the old HEC-2 models are available. We were provided HEC-2 model files for the lower St. Louis below Scanlon Dam, but unfortunately these contain no clear georeferencing and the required file suffixes have been stripped out, rendering the models not immediately usable. In addition, the area covered by this model is largely controlled by dams, and HEC models are not needed for HSPF FTable construction in these reaches. Given the large level of effort that would be required to make these models usable, the likelihood that floods since the 1980s may have reshaped channels, that many structures have likely changed since the 1970s, and the limited spatial coverage, it was decided that the HEC models did not provide sufficient useful information to be viable for FTable construction in this basin.

2.3.2.3 Rating Table with Cross Section

A rating table is used to convert an observed measurement of gage height to an estimate of flow. Rating tables change over time as the channel shape changes in response to storm events. At the basin-scale of modeling, however, the details of elevation and cross-sectional area within individual stream segments are of less importance; rather, we need a reasonable representation of the stage-storage-discharge relationship. This can be obtained from recent rating tables with accompanying cross sections and will remain approximately valid for changing conditions over time (although the base level is likely to change) unless the channel form is extensively reworked. To use rating tables with cross sections, first calculate top width, cross sectional area, and wetted perimeter directly from cross section. Volume and surface area at each rating table depth increment are then calculated by multiplying by length of the reach within the subbasin. This essentially assumes that the gage is located at a point that controls flow within the subbasin or is at least typical of flow in the subbasin. Where the gage does not fall at the subbasin mouth, assume depth and cross-sectional area remain constant over this relatively short distance and use length of entire reach for calculation. We will not use rating tables from the middle of a subbasin if there is a significant proportional increase in drainage area from the gage to the subbasin pour point.

The HYDSTRA cross sections we were able to obtain generally are to the water surface at the date of observation only. These cross sections are extended through use of the LiDAR elevation data flow in May 16 and 17 of 2011. In most cases, the water surface elevation at the date of the cross section is not the same as the water surface elevation in LiDAR. In the case where the cross section does not reach up to the LiDAR elevation the profile was interpolated between the two.

2.3.2.4 Rating Table without Cross Section

In this case a rating table provides a relationship between stream flow and gage height but information on cross section geometry is not available. For these gages we assume that the LiDAR from May 2011 provides the cross-section information above the water level on that date, while the sub-surface cross section is assumed to have a trapezoidal form. The gage height could be rather arbitrarily related to local geometry (e.g., installed in a deep pool or on the side of a bridge) and actual average channel depth. (This circumstance appears to apply to only a few USGS gages in the St. Louis, Cloquet, and Nemadji watersheds.) The USGS rating tables provide on offset value, which represents the elevation that should

be subtracted from the gage height in evaluation of the stage-discharge relationships. The rating tables are thus converted by first adding any shift and then subtracting the offset before proceeding.

In the case of a gage where flow is reported for the date of the LiDAR coverage, back-solve Manning's equation to obtain average depth and top width at the observed flow condition under assumption that side slope of channel, m_c, is equal to 1.5 (see Section 2.3.2.9). The average depth – cross-sectional area – flow relationship up to this flow is calculated by scaling the rating table depths to the calculated average depth at the observed flow. Volume and surface area up to this depth are calculated by multiplying by reach length. Above this level flow as a function of depth increment is taken directly from the rating table, while surface area and incremental volume come from multiplying the LiDAR cross section area and top width (above the level at the LiDAR coverage data) times the reach length (see Section 2.3.2.8). If gaged flow is not available for the LiDAR date, a similar procedure is used except that the flow on the LiDAR date is estimated by comparison to nearby/similar gages as a function of drainage area.

2.3.2.5 Surveyed Cross Section Only (No Rating Table or Gaging)

Where there is information on cross-section geometry, but not a flow rating table, we use Manning's equation, as implemented in WinXSPro (Hardy et al., 2013) for complex cross sections, to develop average depth – cross section area – top width – flow relationships. In many cases the cross section is divided into segments representing channel flow up to bank full and floodplain flow. These segments are assigned separate Manning's coefficients that can reflect site-specific conditions (where known). Default values are 0.04 for the channel and 0.06 for the floodplain. Volume and surface area are calculated by multiplying by reach length.

As the MDNR cross sections typically do not include the overbank profile, these are supplemented by extending into the overbank using the LiDAR data as described in previous sections.

2.3.2.6 Road Culvert

For cases where there is a road culvert either at the subbasin outlet or within the lower third of the subbasin without significant additional tributary inflows, assume that the culvert controls the discharge rate, especially at higher flows. If culvert information is readily available, we can develop stage-discharge relationships based on culvert equations, plus analysis of overtopping of the road, represented as a broad-crested weir.

The Minnesota Department of Transportation provided bridge and culvert information for major stream crossings of state and federal highways. Carlton County also provided a detailed culvert inventory, although few of these are located in the lower third of stream reaches explicitly present in the model. Unfortunately, St. Louis County has only begun the process of assembling culvert information into an electronic database, so readily available information was limited. No culvert databases were identified for the portions of the watershed in Itasca and Lake Counties.

Calculation of flow through a culvert is complicated because culverts are generally a significant constriction to flow and subject to a range of gradually varied and rapidly varied flow types that may be under either outlet control (in which the tailwater elevation has a significant influence) or inlet control (in which the headwater depth at the culvert inlet has a major influence). Culvert design calculations must simultaneously address both possibilities, leading to complex calculations. The Federal Highway Administration program HY8 (http://www.fhwa.dot.gov/engineering/hydraulics/software/hy8/), based on Schall et al., 2012, was used for this purpose.

Design information on most of the culverts was quite limited, so the LiDAR data were used to supplement. The following procedures were implemented:

1. Use the LiDAR to get an approximate estimate of the width of the stream downstream of the culvert (after it widens to a normal width), the length of the road crest (the low portion of the roadway atop the culvert which is the approximate width that will flood if the road is over-topped), road pavement width, length of the culvert, elevation of the water surface upstream and downstream of the culvert, and the water surface grade in the channel downstream of the culvert. Calculate the height (for box culverts) or diameter (for round culverts) as appropriate.
2. Estimate the true bottom elevation of the invert of the partially full culvert. If the culvert top is not discernable in the LiDAR, assume that there is 1.5 ft between the culvert top and the road bed.
3. Use the LiDAR to create a detailed cross-section upstream of the culvert at a location that represents the typical valley cross-section in the area.
4. Open HY-8 and enter culvert information for tailwater data, roadway data, culvert data, and site data. Do the first run with Discharge Method of "Minimum, Design, and Maximum" with arbitrary flows. This yields an estimate of the Overtopping Flow. The model is then run again with the maximum set to a number rounded above the Overtopping Flow, and a third time with the maximum set to 10 times the Overtopping Flow.
5. Combine the two tables from step 4 to establish the upstream head elevation to discharge relationship. Convert elevation to depth, with the bottom of the culvert inlet at zero depth.
6. Use the LiDAR to estimate the upstream cross-sectional area and top width associated with a given elevation/depth.
7. Multiply these results by the reach length to get the volume and surface area associated with a given elevation.

2.3.2.7 Nemadji Unsurveyed Reaches: Regional Regression

In the Nemadji and the adjacent lacustrine core Pokegama and Red River, we use the regional regression equations developed by Dr. Joe Magner to establish depth-cross sectional area-flow relationships for cases where there is not a rating curve or cross section. These equations are available in Magner and Brooks (2008) and accompanying files provided by Tim Larson of MPCA and describe bankfull cross-sectional area A_{bank} (ft^2) and flow Q_{bank} (cfs) as a function of drainage area DA (mi^2).

The following inputs are obtained from GIS.

DA	drainage area	mi^2
L	reach length	ft
W_m	stream width	ft
m_F	floodplain slope (inverse – expressed as run over rise)	
s	reach slope	

We also assume the following based in part on the standard method for FTables in BASINS Technical Note 2 (USEPA, 2007):

$W_F = W_{bank} = W_m$ (i.e., the bankfull width is the same as the observed width and the floodplain side width is assumed equal to the channel width)

$m_C = 1.5$ (channel side slope is assumed 1:1.5 due to somewhat incised nature of many streams in this area)

We then calculate:

A_{bank} (bankfull cross-sectional area in ft^2) = $5.5209 \times DA^{0.7744}$ (Magner 15-sites equation, $R^2 = 0.9744$)

Q_{bank} (bankfull flow in cfs) = $41.913 \times DA^{0.7946}$ (Magner regression, $R^2 = 0.9001$)

Y_c (bankfull depth, ft) = A_{bank}/W_m

$Y_m = Y_c/1.25$ (standard method assumption)

We can use Q_{bank} to back-solve for the channel Manning's coefficient.

P_{bank} (bankfull wetted perimeter) = $W_m - 2\ m_c\ Y_c + 2\ Y_m\ (m_c^2 + 1)^{0.5} = b + 2\ Y_m\ (m_c^2 + 1)^{0.5}$,

$n = A_{bank}/Q_{bank} \times 1.486 \times (A_{bank}/P_{bank})^{2/3} \times s^{0.5}$

The Manning's coefficient derived in this way should be constrained to be greater than or equal to 0.025 to protect against unreasonable solutions. A separate Manning's coefficient is assigned to overbank flow (0.06 in the absence of other information.)

This information obtained in this way can then be used in a modified version of Tetra Tech's FTables_Batch.xlsm, which calculates FTables based on hydraulic geometry.

2.3.2.8 Other Unsurveyed Reaches

A number of reaches do not have any of the information described in preceding sections. For these reaches it is possible to create cross sections using a combination of LiDAR and estimates of the magnitude and depth of flow on the LiDAR date; however, that is a labor intensive process that was beyond the current resources. Therefore, we define three cases. In the first case, the FTable for an adjacent subbasin is likely a good approximation for the candidate subbasin. In the second case, a site-specific analysis using LiDAR can be performed. Finally, for reaches that are of lesser direct interest it is assumed sufficient to retain the default FTable calculation by the BASINS standard method that relates hydraulic geometry to drainage area.

Case 1: In this case the candidate reach is one subbasin upstream or downstream of a gaged reach, the incremental drainage area does not change by more than 25%, and no lake reaches intervene. In such cases, the adjacent FTable is assumed to be applicable with appropriate modifications. Modify the depth-cross sectional area-top width-discharge relationship based on the drainage area ratio. Multiply by reach length to obtain surface area and volume.

Case 2: When Case 1 does not apply, use LiDAR to obtain cross-section (above May 2011 water level) at or near reach outlet. Complete below May 2011 water surface portion of cross section using techniques based on Manning's equation described in Section 2.3.2.4. Then proceed as described in Section 2.3.2.5.

Case 3: We leave FTables for some reaches at BASINS defaults by the standard method, in which bankfull width and depth are estimated by generalized equations such that:

Bankfull Width (m) = 1.29 $DA(km^2)^{0.6}$; Bankfull Depth (m) = 0.13 $DA(km^2)^{0.4}$.

The remainder of the hydraulic geometry and flow relationships are analyzed following the standard method given in USEPA (2007). We modified the default approach to use separate Manning's coefficients for the channel (default 0.04) and floodplain (default 0.06), and assume no friction loss between these two segments, as is done in WinXSPro. This approach is particularly appropriate for minor tributaries with no gaging or monitoring.

2.3.2.9 Back-Solving Manning's Equation

In several situations we will wish to back solve Manning's equation at the depth of flow present in the LiDAR May 2011 data. We assume that streams were at or below bankfull flow on this date to an extent sufficient to assume a single Manning's coefficient appropriate to channel flow for the total flow volume. Manning's equation for flow can be written in the following form (for English units; BASINS Technical Note 2):

$$Q = 1.486/n\ (by + m_c\ y^2)^{5/3} \times [b + 2y\ (m_c^2 + 1)^{0.5}]^{-2/3} \times S^{0.5},$$

where Q is flow in cfs, n is Manning's constant, b is the bottom width, m_c is the side slope of the channel expressed as the ratio of width to depth, y is the average depth, and S is the energy grade. We assume that $m_c = 1.5$ (consistent with the alternative method described in Technical Note 2) and S is approximated by the reach slope, so

$$Q = 1.486/n\ (by + 1.5\ y^2)^{5/3} \times [b + 2y\ (2.5)^{0.5}]^{-2/3} \times S^{0.5}.$$

The channel Manning's coefficient can be specified based on site-specific data where available. A default channel value of 0.04 is used in other cases. The Excel Solver function is then used to estimate b given y.

2.3.2.10 FTable Development Summary

The methods applied to each reach in the current models are summarized in Table 2-11.

Table 2-11. Methods for Establishing Reach FTables

St. Louis River
201: SFP
202: SFP
203: SFP
204: SFP
205: Lake
206: Culvert
207: Lake
208: Lake
209: Adj
210: SFP
211: Adj
212: RTn
213: Adj
214: Adj
215: SFP
216: SFP
217: SFP
218: Culvert
219: SFP
220: SFP
221: SFP
222: Culvert
223: SFP
224: SFP
225: SFP
226: Culvert
227: SFP
228: Adj
229: SFP
230: Adj
231: SFP
232: Adj
233: XS
234: XS
235: Culvert
236: RTC
237: XS
238: Adj
239: XS
240: XS
241: XS
242: Adj
243: SFP
244: SFP
245: Lake
246: SFP
247: SFP
248: SFP
249: RTn
250: Adj
251: Adj
252: SFP
253: Lake
254: Lake
255: SFP
256: SFP
257: Adj
258: RTC
259: RTC
260: RTC
261: Adj
262: Lake
263: SFP
264: RTC
265: Adj
266: Adj
267: Adj
268: Adj
269: Adj
270: SFP
271: SFP
272: SFP
273: SFP
274: SFP
275: Lake
276: SFP
277: SFP
278: SFP
279: RTn
280: Adj
281: SFP
282: Adj
283: Culvert
284: SFP
285: SFP
286: Adj
287: Adj
288: Adj
289: Lake
290: Adj
291: RTn
292: Adj
293: Adj
294: RTn
295: SFP
296: SFP
297: SFP
298: Culvert
299: Culvert
300: SFP
301: SFP
302: SFP
303: Culvert
304: RTC
501: Lake
502: Lake
505: RTn
601 Lake
602 Lake
603 Lake
604 SFP
Cloquet River
401: Adj
402: RTC
403: Culvert
404: Adj
405: SFP
406: Adj
407: Lake
408: Lake
409: SFP
410: SFP
411: SFP
412: Adj
413: Adj
414: Adj
415: Adj
416: Adj
417: RTn
418: Adj
419: Adj
420: SFP
421: SFP
422: Lake
423: Lake
Nemadji River
101: Mag
102: Mag
103: RTn
104: Mag
105: Mag
106: Mag
107: Mag
108: Mag
109: Mag
110: Mag
111: Mag
112: RTC
113: RTC
114: RTC
115: Mag
116: Mag
117: RTC
118: RTC
119: RTC
120: RTC
121: Mag
122: Mag
123: Mag
124: Mag
510: Mag
511: Mag

Key:
Culvert: Culvert analysis with HY8
Adj: Extrapolate from adjacent FTable
Lake: Lake FTable
Mag: Magner hydraulic geometry regression for Nemadji (Magner and Brooks, 2008)
RTC: Rating table with cross section
RTn: Rating table with no cross section
SFP: BASINS standard method with floodplain adjustment
XS: Cross section analysis with WinXSPro

2.3.3 Representation of Lakes and Reservoirs

The St. Louis and Cloquet watersheds contain a large number of reservoirs and smaller ponds. Several of the reservoirs in the St. Louis were originally constructed to provide mine process water. Most of the reservoirs are currently used for hydropower generation, with the majority owned and operated by Minnesota Power.

Lakes and reservoirs can have an important impact on overall basin hydrology and should be included in the model to the extent feasible. On the other hand, data on storage capacity and operations are not readily available for many lakes. We prioritized effort by representing lakes in three ways, in order of descending importance: (1) explicitly represented lakes with defined stage-storage-discharge relationships or operational records, (2) run-of-the-river lakes that are implicitly included within the storage ascribed to a river reach, and (3) smaller lakes off the main channel that are simply represented as a water land use. Lakes off the main channel are typically on smaller streams that are not explicit in the model. This is too fine a scale for representation as reservoirs in the basin-scale model, even though they may behave this way at the local scale. Most of these lakes are represented as a water land use so that their area is accounted for in the mass balance of precipitation and evaporation with parameters assigned in such a way that surface storage and gradual release of water is approximated. This can only be an approximation but is sufficient for representation of the larger scale watershed.

Stage, storage, and outflow data for several reservoirs were supplied to MPCA by Minnesota Power and we explicitly modeled these reservoirs in the HSPF model. In addition, lakes in line with the modeled reaches and at the outlet of a model subbasin were represented using a revised functional table to represent the lake storage. The lakes initially evaluated for inclusion in the model are summarized in Figure 2-15. The final set explicitly represented in the model is shown in Table 2-12 and Figure 2-16.

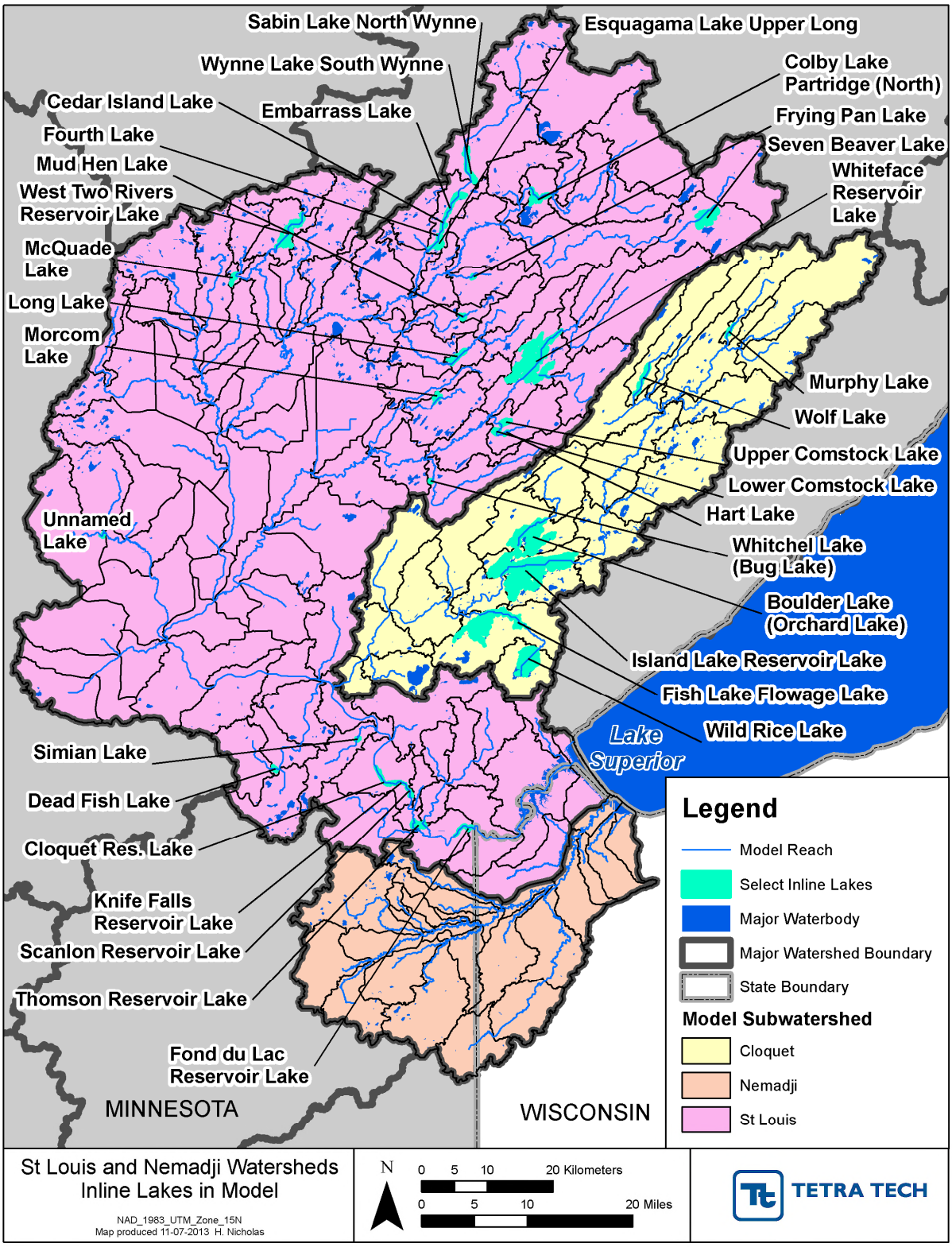

Figure 2-15. Inline Lakes Evaluated in Model Development

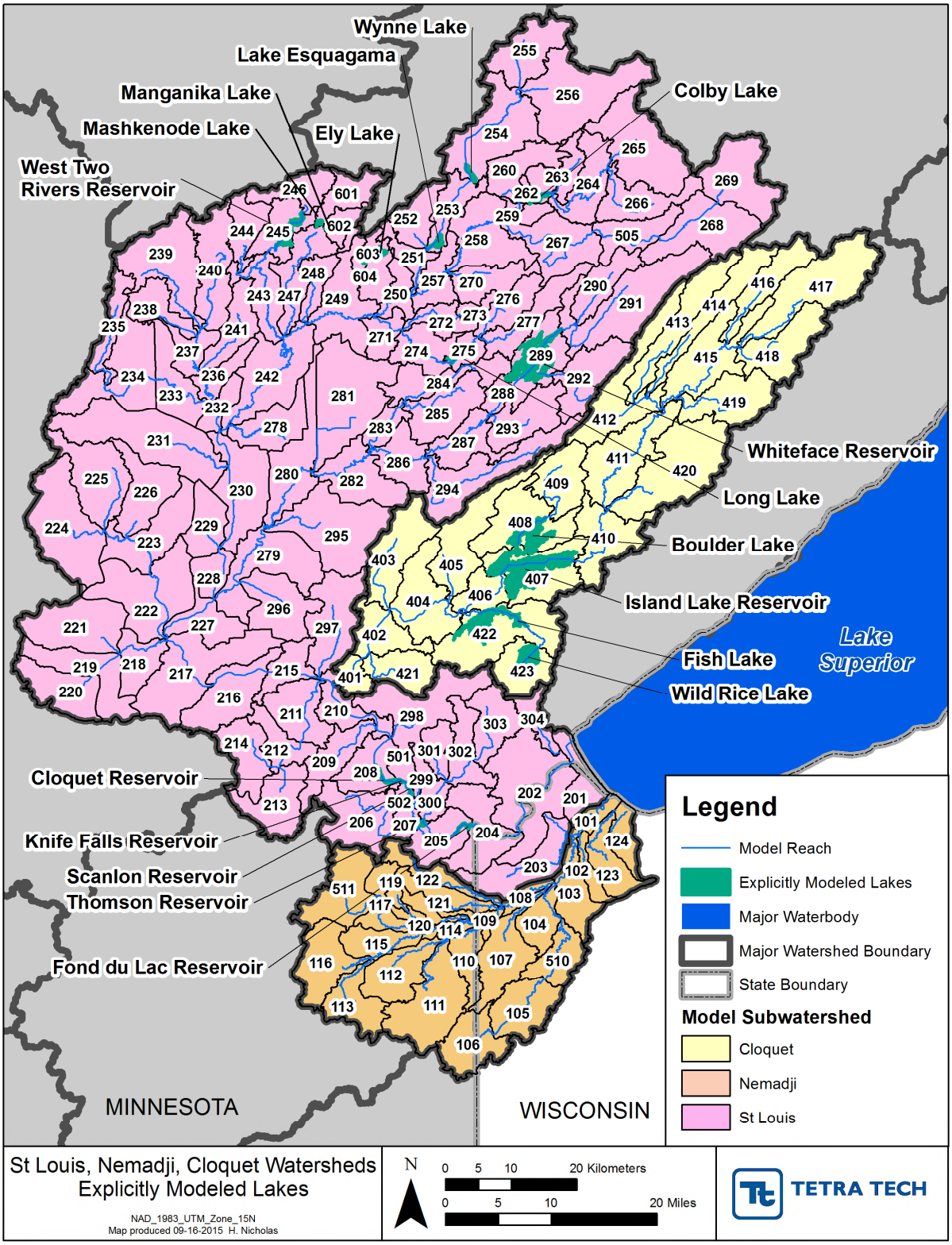

Figure 2-16. Lakes and Reservoirs Explicitly Simulated in the St. Louis, Cloquet, and Nemadji River Models

Table 2-12. Inline Lakes Explicitly Represented in the HSPF Model

Lake Name	Alternate Name	Surface Area (ac)	Time Series Available	Model Reach
Island Lake Reservoir	Orchard Res. (Island)	8,001	Y	407
Whiteface Reservoir		4,567	Y	289
Boulder Lake	Orchard	3,260	Y	408
Fish Lake Flowage	Fish Lake Reservoir	3,259	Y	422
Wild Rice Lake	Rice	2,372	Y	423
Thomson Reservoir	Thompson Reservoir	390	Y	207
Fond du Lac Reservoir		201	Y	205
Scanlon Reservoir		71	Y	502
Knife Falls Reservoir		55	Y	501
Cloquet Reservoir		176		208
West Two River Reservoir		967		245
Colby Lake	Partridge (North)	518		262
Esquagama Lake	Upper Long	453		253
Long Lake		374		275
Wynne Lake	South Wynne	278		254
Mashkenode Lake		130		601
Manganika Lake		170		602
Ely Lake		703		603

In HSPF, the area, volume, and outflow of a reach at different water depths are defined using a functional table (FTable). For the lakes and reservoirs in Table 2-12, the depth, area and volume relationships were determined using the bathymetry contour-line dataset from the MDNR. The area vs. depth relationship was first determined and then the volume using the equation,

$$V_y = \int_0^y \quad .$$

where y = depth of water, V_y = volume at depth y, and A = area as a function of depth y

The outflows associated with various water depths were estimated using a rectangular weir equation. The dimensions of the weir were determined from aerial imagery products.

Daily stage, storage, and outflow data were available for Island, Boulder, Wild Rice, Fish, and Whiteface reservoirs from Minnesota Power. Simulation of the reservoirs uses a combination of volume-based and demand-based flows. Each reservoir is simulated with two exits. Exit 1 is set up to express outflow as the maximum of the volume-based flow from the FTable and the demand flow. The FTable has three discharge series (columns 4 through 6), of which columns 4 and 5 are relevant to Exit 1. Column 4 is a standard depth-discharge relationship, while column 5 is all zeros. A column index (COLIND) time series is used to switch between columns 4 and 5. For periods where there is a non-zero demand outflow,

the COLIND time series points to column 5, as a result of which only the measured outflow is represented for this exit. Outflow for exit 2, which is usually very small, is also volume-based, and is used as a calibration parameter for reservoir storage adjustment.

For Scanlon, Fond du Lac, and Thomson reservoirs on the St. Louis River mainstem, demand-based outflows specified from Minnesota Power records were not used because this tended to result in instabilities with temporary drying of the reservoirs. Instead, these reservoirs are represented by FTables that are based on a statistical analysis of reported information on pool storage and outflow, allowing the discharge to be dynamically simulated. Management related to hydropower operations is implicitly included in this approximation.

2.3.4 Interactions with Regional Groundwater Systems in the Nemadji

The Nemadji River is well known for elevated turbidity and high sediment loads, estimated to be 6.5 times larger than all of Minnesota's North Shore Lake Superior streams combined (Magner and Brooks, 2008). This reflects the Quaternary geology of the basin, which was formed as proglacial lakes retreated to the current elevation of Lake Superior at the end of the last glacial ice advance, leaving basin soils that are dominated by erodible cohesive lacustrine clays. Turbidity problems are further exacerbated by the presence of numerous springs and seeps in the lower Nemadji that yield turbid, clay-rich water. The hydrogeological phenomena that lead to this condition are summarized by Magner and Brooks (2008).

The ridge line at the north and west of the basin is occupied by the Thompson Moraine, which consists of highly permeable sands. In the lower Nemadji, permeable glacial beach sands are overlain by a cap of fine grained clay, resulting in artesian conditions with potentiometric heads 10 m above stream water surfaces (Andrews et al., 1980). Thus, deeper groundwater originating in the Thompson Moraine discharges gradually through fractures in the clay material of the lower portions of the basin. This behavior is evident in the two flow gages operated on Deer Creek, in which flow at the lower gage is substantially greater than flow at the upper gage, with increases more than would be expected due to the incremental drainage area, presumably due to the resurfacing of artesian groundwater.

HSPF simulates shallow ground water, but does not contain a complete groundwater model. A detailed groundwater model of the Nemadji is not available at this time. If such a model was available, the results could be incorporated into the HSPF model with artesian return flow to streams of the lower Nemadji watershed incorporated as external time series. Presumably, percolation to the deep aquifer would be represented as deep losses from shallow groundwater stores in upland units with A or B soils. To provide an approximate representation of this behavior, the model contains a separate version of the Mass-Link table which is used to route subsurface flows originating from A and B soils in the headwaters of the watershed to the next reach downstream, rather than to the local reach. This results in a reasonable fit to the observed gage data, but can undoubtedly be improved once the groundwater model results are released.

2.4 POINT SOURCES

Permitted point sources are present in the St. Louis River watershed and were investigated for inclusion in the HSPF model. None are reported for the Cloquet and Nemadji basins. Within the St. Louis basin there are a variety of municipal and industrial sources – including large discharges associated with the dewatering of taconite mine pits. MPCA researched the locations and discharge monitoring records for all these dischargers, using the Delta system for the more recent records (generally from 1998 or 1999) and the EPA PCS system for earlier records (available from 1/1/1995). A total of 51 point source discharges were quantified, of which five are considered major dischargers and the remaining are considered minor. The locations of permitted point sources are shown in Figure 2-17, and the permit identifier, name, type (major/minor), model subbasin, and average flow are summarized in Table 2-13.

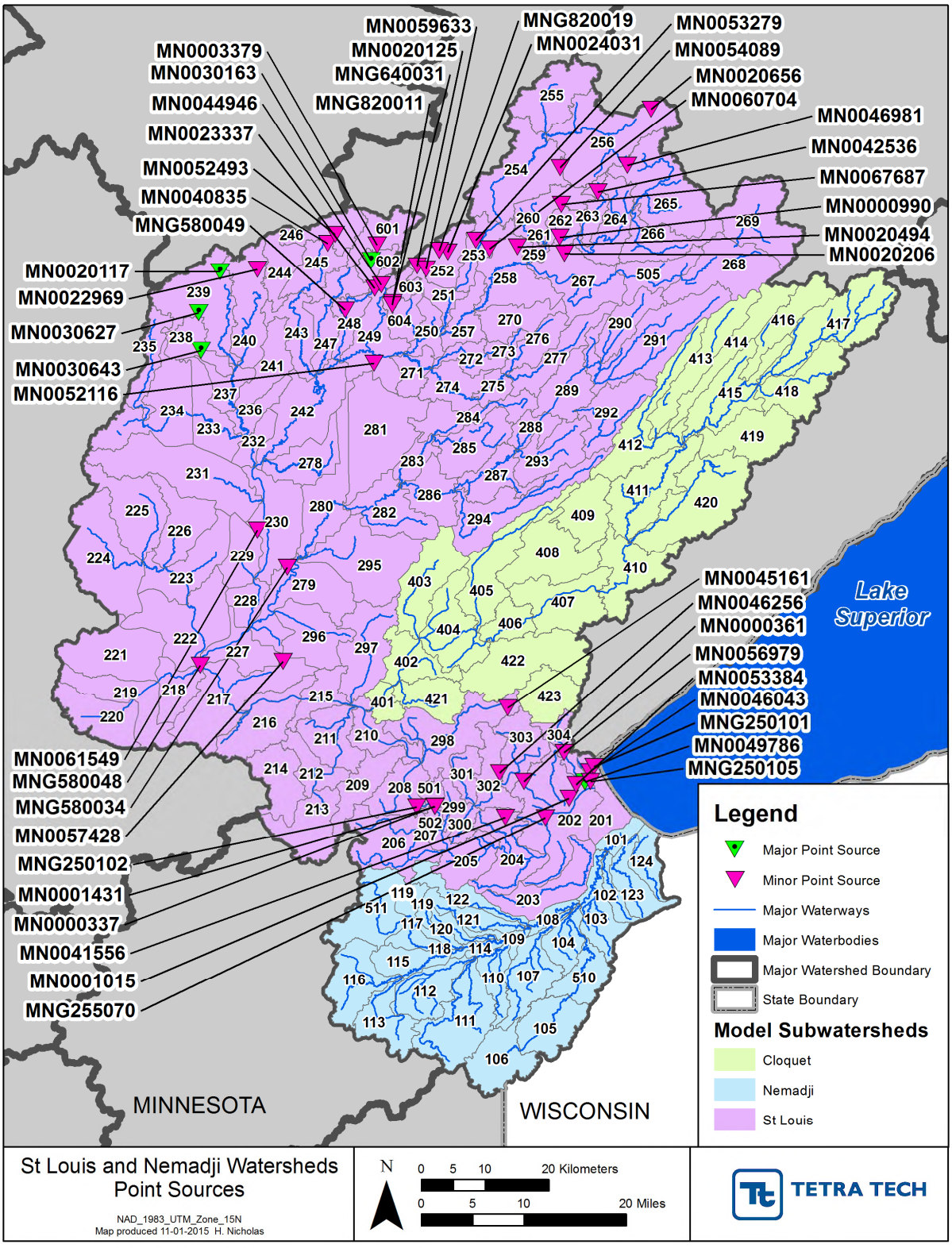

Figure 2-17. Point Sources in the St. Louis, Cloquet, and Nemadji River Watersheds

Table 2-13. Permitted Point Source Discharges in the St. Louis, Cloquet, and Nemadji River Models

NPDES Code	Location Name	Type	Model Subbasin	Avg. Flow (MGD)
MN0020117	Chisholm WWTP	Major	239	0.8180
MN0030627	Hibbing WWTP North Plant	Major	239	0.4840
MN0030643	Hibbing WWTP South Plant	Major	238	1.9860
MN0030163	Virginia WWTP	Major	602	2.0390
MN0049786	WLSSD WWTP	Major	202	38.1990
MN0000337	Jarden Home Brands (discontinued on 10/1/2012)	Minor	208	0.02883
MN0000361	Wisconsin Central Ltd - Proctor Railroad Yard	Minor	202	0.14198
MN0000990	Allete DBA Minnesota Power-Laskin	Minor	262	128.35208
MN0001015	Minnesota Power - Hibbard Renewable Energy Center	Minor	202	21.75619
MN0001431	Sappi Cloquet LLC	Minor	208	0.18887
MN0003379	Virginia Dept. of Public Utilities	Minor	601	15.4819
MN0020125	Gilbert WWTP	Minor	251	0.2904
MN0020206	Hoyt Lakes WWTP	Minor	267	0.2537
MN0020494	Aurora WWTP	Minor	258	0.3458
MN0020656	Babbitt WWTP	Minor	256	0.1910
MN0022969	Buhl Kinney WWTP	Minor	240	0.1133
MN0023337	Eveleth WWTP	Minor	248	0.7038
MN0024031	McKinley WWTP	Minor	252	0.0362
MN0040835	Mountain Iron WWTP	Minor	245, 246	0.2136
MN0041556	Calumet Superior LLC - Duluth Petroleum	Minor	204	0.0498
MN0042536	Cleveland Cliffs LLC	Minor	256, 260, 262, 263	0.2676
MN0044946	United Taconite LLC - Thunderbird Mine	Minor	248, 249, 602	3.531
MN0045161	ISD 704 (discontinued on 2/1/2000)	Minor	298	0.0016
MN0046043	Georgia Pacific Wood Products LLC	Minor	201	0.9891
MN0046256	Minnesota Power - Arrowhead HVDC	Minor	302	0.0018
MN0046981	Northshore Mining Co; Cliffs MN	Minor	265	2.6109
MN0049760	Hibbing Taconite (discontinued 12/1999)	Minor	240	3.9531
MN0052116	United Taconite, LLC	Minor	249	1.9344
MN0052493	US Steel Corp - Minntac	Minor	244, 246	6.4906
MN0053279	Biwabik WWTP	Minor	253	0.8500

NPDES Code	Location Name	Type	Model Subbasin	Avg. Flow (MGD)
MN0053384	Wisconsin Central Ltd - Duluth Ore Dock (discontinued on 8/1/2006)	Minor	202	0.0002
MN0054089	Cliffs Erie, LLC - Hoyt Lakes	Minor	254, 256	0.3226
MN0056979	Miller Hill Mall	Minor	304	0.1576
MN0057428	Conrad Fafard Inc.	Minor	217	1.0423
MN0059633	Arcelor Mittal Minorca Mine Inc. - Laurentian	Minor	252	2.5827
MN0060704	Dyno Nobel Inc.	Minor	253	0.0011
MN0061549	Waupaca NorthWoods LLC	Minor	230	0.0307
MN0067687	Mesabi Nugget Delaware LLC	Minor	260	2.1668
MNG250101	Great Lakes Aquarium at Lake Superior Ct (discontinued on 10/1/2011)	Minor	201	0.4186
MNG250102	USG Interiors LLC - Cloquet	Minor	208	0.1651
MNG250105	Gerdau Ameristeel - Duluth Grinding Ball	Minor	202	0.5711
MNG255070	Tate & Lyle Ingredients Americas LLC	Minor	202	0.5042
MNG580034	Meadowlands WWTP	Minor	279	0.0597
MNG580048	Floodwood WWTP	Minor	218	0.2420
MNG580049	Iron Junction WWTP	Minor	248	0.0250
MNG640031	Eveleth WTP	Minor	250	0.1104
MNG820011	Babbitt WTP	Minor	250	0.0725
MNG820019	McKinley WTP	Minor	252	0.0127

2.5 WATER APPROPRIATIONS

Surface water is withdrawn from rivers and lakes for a variety of purposes, including municipal/domestic supply, industrial processing, and power plant cooling. Monthly or annual records of these appropriations are reported to MDNR. The cooling water uses, while large, result in a relatively small amount of water consumption through evaporation; however, they are important to include in the model because of their impacts on water temperature, which in turn influences water quality kinetics. The municipal/domestic and industrial processing uses are typically paired with records of waste discharges.

As discussed in Section 2.1.5, taconite processing is a major user of water in the basin; however, much of this process water is recycled, reducing impacts on the stream network. The other major industrial use is in pulp and paper processing. Municipal/domestic appropriations are generally small and in most cases are drawn from ground water, abandoned mine pits, or other features not directly connected with the surface stream network.

Table 2-14 summarizes appropriations data in the St. Louis, Cloquet, and Nemadji River basins for permitted users with appropriations from surface water resources (lakes and streams/rivers). Note that appropriations from tailings ponds and mine pits (such as U.S. Steel 1980-2085) are not included per the discussion of representation of taconite mines in Section 2.1.5.

Table 2-14. Permitted Surface Water Appropriations in the St. Louis, Cloquet, and Nemadji River Models

Index	Permit Number	Name	Primary Use	Model Reach	Monthly Avg. Appropriation (MGD)	Period of Operation
1	1949-0135	Minnesota Power & Cliffs Erie LLC	Mine Processing	262	9.49	1993 - 2001
2	1950-0172	Minnesota Power	Steam Power Cooling (once through)	262	128.02	1993 - 2012
3	1954-0036	Hoyt Lakes, City of	Municipal Waterworks	262	0.27	1993 - 2012
4	1963-0691	United Taconite LLC	Mine Processing	249	6.11	1993-2012
5	1975-2162	USG Interiors Inc	Paper/Pulp Processing	208	1.73	1993-2012
6	1975-2165	Sappi Cloquet LLC	Paper/Pulp Processing	208	4.67	1993-2012
7	1962-0182	Aurora, City of	Municipal Waterworks	260	0.23	1993-2012
8	1984-2191	Eveleth, City of	Municipal Waterworks	603	0.61	1993-2012

2.6 FLOW GAGING DATA

There is only one USGS gage currently operating with a relatively long and continuous period of record in the St. Louis watershed, none in the Cloquet, and one in the Nemadji basin. Several other USGS gages provide shorter records. Additional gaging has been conducted at multiple locations in the watershed by MDNR and was retrieved from the HYDSTRA system. The majority of gages operate only on a seasonal basis (generally April through September) due to ice cover, which means that a large portion of the spring runoff may be missed, complicating efforts to fit an overall water balance. The USGS gage on the Nemadji River at South Superior reports results for the full year, but winter flows are estimates based on correlation to other gages as ice jams make direct reading of the gage impossible.

The period of record and currency of HYDSTRA monitoring data was used to select locations to be used for HSPF model development, calibration, and validation. Only those gages with data available during the model simulation period (1993-2012) were selected to include in the HSPF model. Consequently, where needed, new subwatershed boundaries were created to allow easy inclusion of data gathered at these selected locations. HYDSTRA locations selected for use in the model are grouped into three different colors by major watershed in Table 2-15.

Table 2-15. Selected HYDSTRA Flow Gage Locations

HYDSTRA ID	STORET ID	USGS ID	Short Name	Start Date	End Date	Years of Record
03001001	S003-071	04015410	Miller Creek at Duluth	9/1992 10/2004	9/1993 11/2010	1 6
03013001		04021520	Stoney Brook	5/2005	1/2011	6
03084001	S000-641	04020000	Swan R, Toivola 5	10/1952 7/2010	9/1961 12/2012	9 2
03115001	S000-568		St. Louis R -Forbes US53	7/1964 1/2010	3/1990 8/2013	26 3
03138001		04016500	St. Louis R -Aurora	8/1942 9/2010	9/1987 11/2012	45 2
03149002	S007-022		Partridge River	6/2009	6/2012	3
03150001		04015500	Second Crk, Aurora	4/1955	9/2012	57
03174001	S005-089, S000-046, S000-629	04024000	St. Louis R - Scanlon	1/1908	9/2012	104
		04015438	St. Louis R - Skibo	8/2011	12/2012	1
04048001	S003-628, S005-147		Cloquet R near Burnett	9/2008	9/2012	4
05006001	S005-620		Blackhoof R, Pleasant Valley	4/2009	11/2012	3
05008001	S003-250	04024098	Deer Crk nr Holyoke	5/1976	9/2012	36
05008002	S004-929		Deer Crk, CSAH3	6/2008	11/2010	2
05009001	S003-251		Rock Creek	4/2009	10/2010	1
05011001	S000-110	04024095	Nemadji R. nr Pleasant Valley, MN23[1]	4/2008	9/2012	4
05011002	S005-115	04024430	Nemadji R - South Superior	1/1997	9/2012	15
05016001	S005-619		Nemadji River nr Holyoke	4/2009	11/2011	2
05018001	S006-214		S Fork Nemadji River	4/2011	10/2012	2

Notes: 1. USGS refers to this station as Nemadji River nr Holyoke, which is the name given in HYDSTRA to 05016001. The USGS station is, however, at Highway 23 and matches up with HYDSTRA station 05011001.

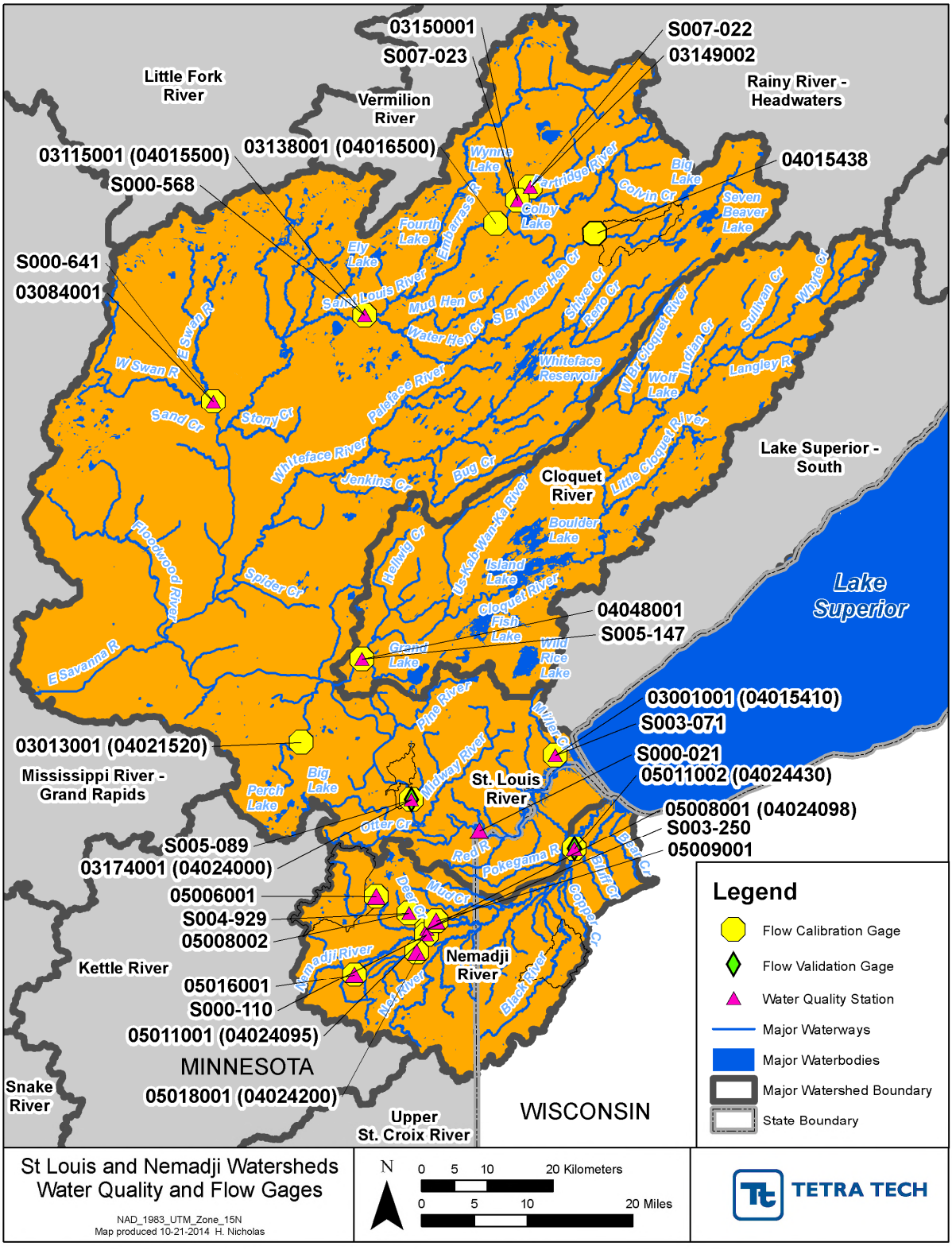

Figure 2-18. Water Quality Monitoring and Flow Gaging Locations

(This page left intentionally blank.)

3 Model Calibration and Validation Approach

3.1 HYDROLOGY CALIBRATION APPROACH

The level of performance and overall quality of hydrologic calibration is evaluated in a weight of evidence approach that includes both visual comparisons and quantitative statistical measures. The calibration proceeds in a sequential manner through (1) general representation of the overall water balance, (2) calibration of snow depth, (3) assurance of consistency with satellite-based estimates of actual ET and soil moisture, and (4) detailed calibration relative to flow gaging for seasonal flows, shape of the flow duration curve, and hydrograph shape.

Key parameters for hydrologic calibration and information on their potential ranges are as described in *BASINS Technical Note 6* (USEPA, 2000). Initial values of key parameters were related to soil and climatological properties where appropriate. Specifically, infiltration rates (INFILT) were initialized (and subsequently varied by) HSG, while initial values of lower zone nominal soil storage capacity (LZSN), upper zone soil storage capacity (UZSN), and interflow inflow (INTFW) were set based on annual average rainfall, consistent with USEPA (2000). Seasonal patterns based on vegetative cover (MON-LZETPARM, MON-INTERCEP, and MON-MANNING) and snow simulations were initialized based on past experience with Minnesota models.

Given the inherent errors in input and observed data and the approximate nature of model formulations, absolute criteria for watershed model acceptance or rejection are not generally considered appropriate by most modeling professionals. And yet, most decision makers want definitive answers to the questions—"How accurate is the model?" and "Is the model good enough for this evaluation?" Consequently, the current state of the art for model evaluation is to express model results in terms of ranges that correspond to "very good", "good", "fair", or "poor" quality of simulation fit to observed behavior. These characterizations inform appropriate uses of the model: for example, where a model achieves a good to very good fit, decision-makers often have greater confidence in having the model assume a strong role in evaluating management options. Conversely, where a model achieves only a fair or poor fit, decision makers may assume a much less prominent role for the model results in the overall weight-of-evidence evaluation of management options.

For HSPF and similar watershed models, a variety of performance targets have been documented in the literature, including Donigian et al. (1984), Lumb et al. (1994), Donigian (2000), and Moriasi et al. (2007). Based on these references and past experience, the HSPF performance targets for simulation of hydrology are summarized in Table 3-1. Model performance is generally deemed fully acceptable where a performance evaluation of "good" or "very good" is attained. It is important to clarify that the tolerance ranges are intended to be applied to mean values, and that individual events or observations may show larger differences and still be acceptable (Donigian, 2000).

The model calibration generally attempts to achieve a good balance between the relative error metrics and the Nash-Sutcliffe coefficient of model fit efficiency (NSE; Nash and Sutcliffe, 1970). Unlike relative error, NSE is a measure of the ability of the model to explain the variance in the observed data. Values may vary from $-\infty$ to 1.0. A value of NSE = 1.0 indicates a perfect fit between modeled and observed data, while values equal to or less than 0 indicate the model's predictions of temporal variability in observed flows are no better than using the average of observed data. The accuracy of a model increases as the value approaches 1.0. Moriasi et al. (2007) suggest that achieving a relative error on total volume of 10 percent or better and an NSE of 0.75 or more on *monthly* flows constitutes a good modeling fit for watershed applications.

It should be noted that many of the available gage records in the St. Louis, Cloquet, and Nemadji watersheds operate only on a seasonal basis, so that full evaluation of seasonal statistics (or, indeed,

evaluation of the total water balance) is not possible. In addition, where winter gaging records are available they are typically imprecise and generally rated poor or fair by USGS due to interference from ice cover.

Table 3-1. Performance Targets for HSPF Hydrologic Simulation (Magnitude of Annual and Seasonal Relative Mean Error (*RE)*; Daily and Monthly NSE)

Model Component	Very Good	Good	Fair	Poor
1. Error in total volume	≤ 5%	5 - 10%	10 - 15%	> 15%
2. Error in 50% lowest flow volumes	≤ 10%	10 - 15%	15 - 25%	> 25%
3. Error in 10% highest flow volumes	≤ 10%	10 - 15%	15 - 25%	> 25%
4. Error in storm volume	≤ 10%	10 - 15%	15 - 25%	> 25%
5. Winter volume error (JFM)	≤ 15%	15 - 30%	30 - 50%	> 50%
6. Spring volume error (AMJ)	≤ 15%	15 - 30%	30 - 50%	> 50%
7. Summer volume error (JAS)	≤ 15%	15 - 30%	30 - 50%	> 50%
8. Fall volume error (OND)	≤ 15%	15 - 30%	30 - 50%	> 50%
9. NSE on daily values	> 0.80	> 0.70	> 0.60	≤ 0.60
10. NSE on monthly values	> 0.85	> 0.75	> 0.65	≤ 0.65

3.2 SEDIMENT CALIBRATION APPROACH

Sediment is one of the more difficult water quality parameters to calibrate in watershed models because observed instream concentrations depend on the net effects of a variety of upland and stream reach processes, only some of which are directly observed. Further, conditions in one stream reach may depend strongly on erosion and deposition patterns in the upstream reaches. Thus mass balance checks need to examine every reach in the model. Sediment calibration for the St. Louis, Cloquet, and Nemadji models was undertaken in accordance with AQUA TERRA (2012) as well as the guidelines BASINS Technical Note 8: *Sediment Parameters and Calibration Guidance for HSPF* (USEPA, 2006). Sediment calibration required an iterative approach. The first step in calibration involves setting channel erosion to values that achieve a reasonable fit to observations when upland erosion is at rates consistent with the literature and soil survey data. The upland simulation is then further tuned. Next, the long-term behavior of sediment in channels is constrained to a reasonable representation in which degradation or aggradation amounts are physically realistic and consistent with available local information. Finally, results from detailed local stream studies (e.g., Deer Creek) are used to further ensure that the model provides a reasonable representation in specific areas.

The upland parameters for sediment were related to soil and topographic properties. HSPF simulates sediment yield to streams in two stages. First, HSPF calculates the detachment rate of sediment by rainfall (in tons/acre) as

$$DET = (1 - COVER) \cdot SMPF \cdot KRER \cdot P^{JRER}$$

where *DET* is the detachment rate (tons/acre), *COVER* is the dimensionless factor accounting for the effects of cover on the detachment of soil particles, *SMPF* is the dimensionless management practice

factor, *KRER* is the coefficient in the soil detachment equation, *JRER* is the exponent in the soil detachment equation, which is recommended to be set to 1.81, and *P* is precipitation depth in inches over the simulation time interval. Direct addition of sediment (e.g., from wind deposition) is also added via the parameter *NVSI*. Actual detached sediment storage available for transport (*DETS*) is a function of accumulation over time and the reincorporation rate, *AFFIX*.

The transport capacity for detached sediment from the land surface (*STCAP*) is represented as a function of overland flow:

$$STCAP = KSER \cdot (SURS + SURO)^{JSER}$$

where *KSER* is the coefficient for transport of detached sediment, *SURS* is surface water storage (inches), *SURO* is surface outflow of water (in/hr), and *JSER* is the exponent for transport of detached sediment.

DET is similar in concept to the Universal Soil Loss Equation (USLE; Wischmeier and Smith, 1978), which predicts sediment detachment as a function of is the rainfall erosivity, *RE*, a soil erodibility factor, *K*, a length-slope factor, *LS*, a cover factor, C, and a practice factor, *P*:

$$DET = RE \cdot K \cdot LS \cdot C \cdot P.$$

USLE predicts sediment loss from one or a series of events at the field scale, and thus incorporates local transport as well as sediment detachment.

There are two approaches that may be pursued from this point. One is to develop a formal approximation between the HSPF *KRER* and the USLE *K* factor as was done in Tetra Tech (2009). The other approach is to simply assume *KRER* = *K*, as is recommended in USEPA (2006). In theory, *KRER* ought to approximate the product of *K* and the *LS* factor, multiplied by a constant. However, slope is also a key factor in determining the depth of surface runoff and storage, and thus transport capacity in HSPF, so the approach of deriving *KRER* from *K* and *LS* may encounter complications in practice. In areas of generally low slopes, such as Minnesota, variation of *KRER* with slope is expected to be small and the relationship will tend toward linear. Therefore, it is sufficient to use the approach recommended in USEPA (2006) and equate *KRER* and *K*, as was done for this model. The major difference between the two approaches is in the practical definition of the reincorporation rate, *AFFIX*, which will assume different values in order to achieve a stable seasonal cycle of *DETS*.

Once *KRER* is established, the primary upland calibration parameter for sediment is *KSER*, which determines the ability of overland flow to transport detached sediment. HSPF can also simulate gully erosion in which sediment generated from the land surface is not constrained by rainfall detachment. There is not strong evidence for extensive gully erosion in these watersheds, so this component, which is difficult to calibrate, was not used.

While upland gully formation was not simulated, there are well-documented issues of channel incision in the lacustrine sediments of the Nemadji watershed. In contrast, much of the St. Louis and Cloquet watersheds appear to have relatively stable channel form. Key parameters controlling channel erosion, deposition, and sediment transport within streams and rivers are as follows (USEPA, 2006):

KSAND: Sand transport is represented with a power function based on average velocity, such that carrying capacity for sand = *KSAND* x AVVEL^{EXPSND}. *KSAND* is set to 0.1 and *EXPSND* to 2 to start calibration and adjusted to improve the comparison between simulated and observed suspended sediment concentrations at flows where cohesive silt and clay sediments do not scour as well as to ensure a reasonable evolution of sand storage over time,.

TAUCD: HSPF calculates bed shear stress (TAU) during each model time step for each individual reach. The critical bed shear stress for deposition (lb/ft^2) represents the energy level below which cohesive sediment (silt and clay) begins to deposit to the bed. Initial values of TAUCD for silt and clay were

estimated by reach by examining the cumulative distribution function of simulated shear stress and setting the parameter to a lower percentile of the distribution in each reach segment, as recommended by USEPA (2006). The 20th percentile was used for clay and the 25th percentile for silt.

TAUCS: The critical bed shear stress for scour (lb/ft^2) represents the energy level above which scour of cohesive sediment begins. Initial values of TAUCS were set, as recommended, at upper percentiles of the distribution of simulated shear stress in each reach (the 90th percentile for clay and the 95th percentile for silt). Values for some individual reaches were subsequently modified during calibration.

M: The erodibility coefficient of the sediment (lb/ft^2-d) determines the maximum rate at which scour of cohesive sediment occurs when shear stress exceeds TAUCS. This coefficient is a calibration parameter. It was initially set to 0.004 for silt, 0.003 for clay, and adjusted during calibration in some reaches.

An example of the distribution of shear stress versus flow for the South Fork Nemadji River is shown in Figure 3-1. The notch that appears in the profile around 170 cfs represents the reduction in cross-section averaged shear stress that occurs when the flow spreads overbank into the flood plain.

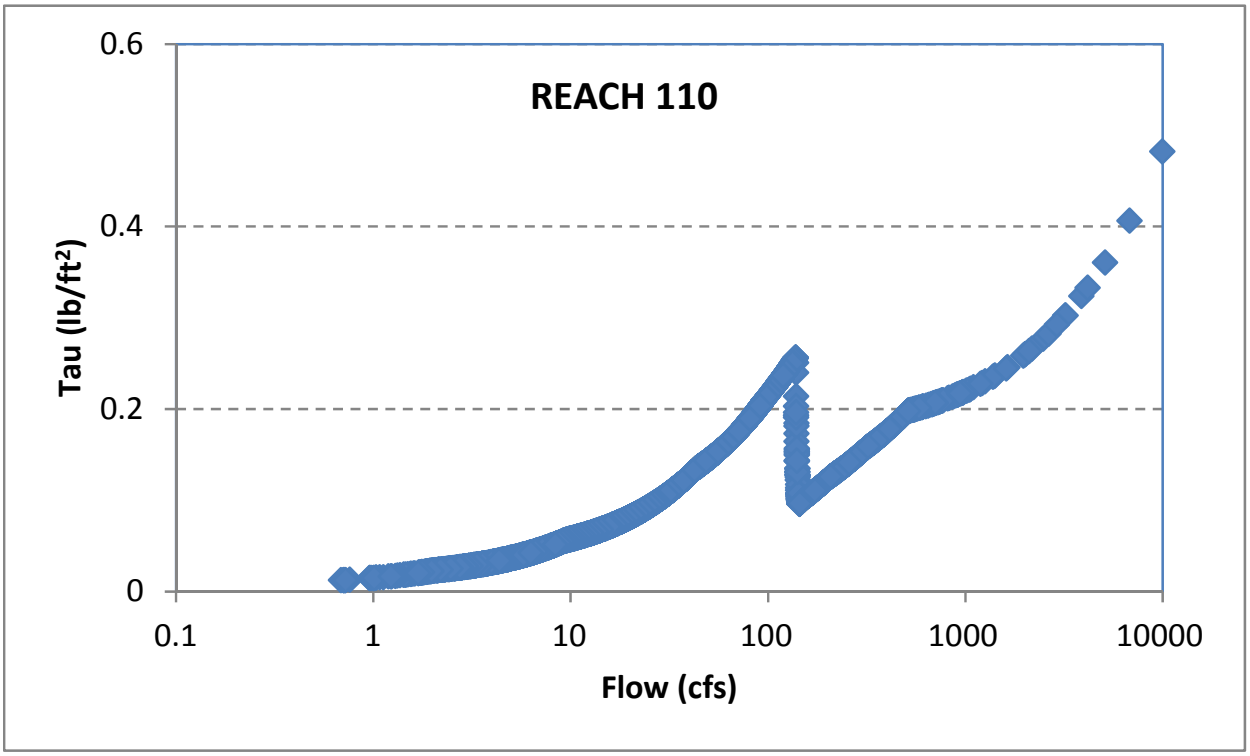

Figure 3-1. Shear Stress Distribution for South Fork Nemadji River (Reach 110)

An important issue for sediment calibration is representing the correct division between sediment derived from uplands and sediment derived from reach scour. In some Minnesota watersheds, radionuclide analysis using ^{210}Pb and ^{10}Be, both of which are derived from the atmosphere and decay over time into more stable forms, has been used to identify the fraction of sediment that derives from upland sources in recent contact with the atmosphere. Such information is not available for the St. Louis, Cloquet, and Nemadji watersheds at this time, but could potentially be used to further refine sediment calibration in the future.

Calibration for sediment and other water quality parameters differs from calibration for hydrology in that pollutant concentrations are in most cases not continuously monitored. Instead, observations typically provide measurements of conditions at a point in time and point in space via a grab sample. The discrete

nature of these samples presents problems for model calibration: A sample that represents a point in time could have been obtained from a system where conditions are changing rapidly over time – for instance, the rising limb of a storm hydrograph. Such samples cannot be expected to be matched by a model prediction of a daily average concentration. On the other hand, there may be large discrepancies between dynamic model predictions of hourly concentrations and data that are a result of small timing errors in the prediction of storm event flow peaks. Spatially, grab samples reflect conditions in one part of a stream reach (which may or may not be composited over the width and depth of a cross section). HSPF model results, in contrast, represent average concentrations over the length of a stream reach which is assumed to be fully mixed. Model predictions and field observations inevitably have some degree of mismatch in space and time and, even in the best models, will not fully match. Accordingly, a statistical best fit approach is needed.

Performance targets for sediment calibration, based on Donigian (2000), are summarized in Table 3-2. These performance targets are evaluated for both concentration and load, where load is estimated from concentration, on paired data, and should only be applied in cases where there are a minimum of 20 observations. Model performance is generally deemed acceptable where a performance evaluation of "good" or "very good" is attained.

Table 3-2. Performance Targets for HSPF Sediment Simulation (Magnitude of Annual and Seasonal Relative Average Error (*RE*) on Daily Values)

Model Component	Very Good	Good	Fair	Poor
1. Suspended Sediment	≤ 20%	20 - 30%	30 - 45%	> 45%

(This page left intentionally blank.)

4 Hydrologic Calibration and Validation Results

4.1 SNOW CALIBRATION

Snow pack is a key component of the water balance of these northern watersheds and is particularly important for calibration when gage data are limited. Daily snow depth as simulated by the HSPF model from 1/1/1995 to 12/31/2012 was compared to observed snow depth at the weather stations selected for the model (see Table 2-7 and Figure 2-13). The fit to snow depth is approximate because depths recorded at specific gage locations may not be representative of averages over the local area. Initial results presented in the Phase 1 report were modified to improve the hydrologic calibration to stream gages at the cost of a slight decline in the statistics for the snow depth calibration.

During the snow depth calibration process values of parameters in the SNOW-PARM1 and SNOW-PARM2 blocks of the HSPF model were configured by weather stations. Slightly different values were optimized for the Nemadji than for the St. Louis and Cloquet watersheds. The calibrated values of these parameters are provided in Table 4-1. Graphical and statistical comparisons were conducted and are provided in detail in Appendix A. Summary statistics of snow depth calibration are provided in Table 4-2. The resulting fit is good with average errors in depth of less than 10 percent.

Table 4-1. HSPF Snow Calibration Parameter Values

Parameter	Description	Calibrated Value	Recommended Range
SHADE	Fraction shaded from solar radiation	0.25 (Deciduous forest)	0 - 0.8
		0.85* (Evergreen forest)	
		0.85* (Forested wetland)	
		0.25 (Herbaceous wetland)	
SNOWCF	Snow gage catch correction factor	1.0 (WST 6)	1.0 - 2.0
		1.17 (WST 1)	
		1.1 (WST 2, 4, 14)	
		1.2 (WST 7)	
		1.3 (WST 11)	
		1.35 (WST 3)	
		1.5 (WST 5, 8, 9, 10, 12, 13, 15, 17)	
		1.6 (WST 16)	
COVIND	Snowfall required to fully cover surface	1.5 – 3.0	0.1 - 10.0
RDCSN	Density of new snow	0.1	0.05 - 0.30
TSNOW	Temperature at which precipitation becomes snow	33.0 - 36.0	30.0 - 40.0
SNOEVP	Snow evaporation factor	0.10 - 0.15	0.0 - 0.5
CCFACT	Condensation/convection melt factor	0.5 – 1.0	0.5 - 8.0
MWATER	Liquid water storage capacity in snowpack	0.05	0.005 - 0.2
MGMELT	Ground heat daily melt rate	0.001 – 0.002	0.0 - 0.1

* The HSPF recommended value of SHADE is the fraction of forest cover that is coniferous or evergreen. For typical HSPF applications, forested land is not segregated into deciduous and evergreen forests. Since evergreen forest is modeled as a separate land use category in this application, the value of SHADE can theoretically be as high as 1.0.

Table 4-2. Summary of Snow Depth Calibration Results

Weather Station	Agency	Period	Error in Total Snow Depth	Daily NSE	Monthly NSE
MN210387 (Babbitt)	NCDC	06/1999 - 12/2012	-7.97%	0.830	0.843
MN210989 (Brimson 1E)	NCDC	01/1995 - 12/2012	-0.05%	0.851	0.859
MN211630 (Cloquet)	NCDC	01/1995 - 12/2012	-4.01%	0.666	0.647
MN211840 (Cotton)	NCDC	01/1995 - 11/2002	3.61%	0.767	0.766
MN212248 (Duluth Intl Ap)	NCDC	01/1995 - 12/2012	-5.57%	0.704	0.698
MN212576 (Embarrass)	NCDC	02/1997 - 12/2012	8.32%	0.774	0.800
MN212645 (Eveleth WWTP)	NCDC	01/1995 - 11/2012	9.98%	0.734	0.782
MN212842 (Floodwood 3 NE)	NCDC	01/1995 - 12/2012	-8.37%	0.741	0.760
MN213730 (Hibbing FAA Ap)	NCDC	01/1995 - 07/2000	-5.86%	0.924	0.944
WI476413 (Pattison State Park)	NCDC	05/1998 – 12/2009	-5.70%	0.577	0.729
WI478349 (Superior)	NCDC	01/1995 – 12/2009	-9.96%	0.577	0.762

4.2 CONSTRAINTS ON SOIL MOISTURE BALANCE AND EVAPOTRANSPIRATION

Evapotranspiration (ET) is the largest component of the water balance and is thus crucial to hydrologic calibration. However, actual ET is often unconstrained in watershed models due to a lack of observed data. For the St. Louis, Cloquet, and Nemadji models this issue was addressed through the use of remotely sensed ET data. The MODIS Global Evapotranspiration Project (MOD16) provides estimates of global terrestrial ET by using satellite remote sensing data at a spatial scale of 1 km^2 grid and at temporal scales of 8-days, months, and yearly totals from 2000 to 2010. The MOD16 datasets are estimated using algorithms of Mu et al. (2011). These data are imprecise, but provide a useful reality check on the model formulation.

Monthly ET estimates for the St. Louis, Cloquet, and Nemadji watersheds were extracted from the global MOD16 dataset. The gridded data were then aggregated to the level of the weather regions used in the model. The aggregated monthly data were compared to actual ET (SAET) simulated by the model and used to inform the pan coefficients used to convert Penman Pan PET to land surface PET in the model (Table 4-3). The pattern of observed monthly evapotranspiration was also used to refine the MON-INTERCEP and MON-LZETPARM blocks in the HSPF model. Table 4-4 provides a summary comparison of simulated ET versus MODIS estimates. Complete details are provided in Appendix B. In general, the model estimated ET is similar to that estimated by MODIS. At all but one station the model provides a somewhat lower total ET estimate. This is primarily due to the winter month, when MODIS

estimates greater ET from snow than does HSPF. It is not clear if this represents systematic over-estimation by MODIS or under-estimation by the HSPF snow sublimation algorithms.

Table 4-3. Penman Pan Coefficient by Weather Station

Weather Station #	Name	Coefficient
1	MN210387 (Babbitt)	0.75
2	MN210989 (Brimson 1E)	0.70
3	MN211630 (Cloquet)	0.65 (Saint Louis/Cloquet) 0.70 (Nemadji)
4	MN211840 (Cotton)	0.75
5	MN212248 (Duluth Intl Ap)	0.60
6	MN212576 (Embarrass)	0.70
7	MN212645 (Eveleth WWTP)	0.70
8	MN212842 (Floodwood 3 NE)	0.70
9	MN213730 (Hibbing FAA Ap)	0.65
10	MN213863 (Holyoke)	0.60
11	WI476413 (Pattison State Park)	0.60
12	WI478349 (Superior)	0.63
13	Hibbing	0.65
14	Janzen E	0.75
15	Kuusinen	0.65
16	Pomroy	0.60
17	Sikkila	0.65

Table 4-4. Summary of Evapotranspiration Calibration Results

Weather Station	Error in Total Evapotranspiration	Monthly NSE
MN210387 (Babbitt) and MN210989 (Brimson 1E)	-6.22%	0.766
MN211630 (Cloquet)	0.08%	0.809
MN211840 (Cotton) and Janzen E	-8.9%	0.774
MN212248 (Duluth Intl Ap) and Pomroy	-2.31%	0.802
MN212576 (Embarrass)	-17.86%	0.782
MN212645 (Eveleth WWTP)	-5.89%	0.763
MN212842 (Floodwood 3 NE)	-6.96%	0.771
MN213730 (Hibbing FAA Ap), Hibbing, Sikkila and Kuusinen	-9.39%	0.809
WI476413 (Pattison State Park)	-5.32%	0.841
WI478349 (Superior)	-5.82%	0.780

4.3 FLOW CALIBRATION

Hydrologic calibration and validation focused on the periods of 2000–2012 and 1993–2000, respectively. Calibration was completed by comparing time-series model results to gaged daily average flow. Key considerations in the hydrology calibration were the overall water balance, the high-flow to low-flow distribution, storm flows, and seasonal variations. The criteria in Table 3-1 are used to evaluate the quality of model fit.

The starting point for hydrologic parameters was provided by previous HSPF model applications in northern Minnesota. These starting values were then modified during calibration to optimize model fit while remaining within ranges recommended by USEPA (2000) and AQUA TERRA (2012)

The St. Louis River has one long-term continuous gage (St. Louis River near Scanlon) and good to very good results were achieved at this gage. In the headwaters, the complex mining operation appropriations and discharges affect the model calibration. The flow calibration for the St. Louis River HSPF models initially focused on the iron-range, then on reservoir operations, and finally on the downstream gages.

The Cloquet River watershed is not influenced by mining operations but has a number of large hydropower reservoirs that affects the hydrology. There is only one active flow gage on the Cloquet River and results are only available for a few years; however, daily reservoir storage information was available for Wild Rice, Fish, Boulder, and Island reservoirs. These storages can be used as subsidiary targets for flow calibration and the HSPF model was parameterized to reasonably represent the observed storage of these reservoirs while also matching downstream gaging results. Reservoir storage calibration was performed for the Whiteface reservoir in the St. Louis River watershed as well. Table 4-5 provides a summary of the reservoir storage calibration.

Table 4-5. Summary of Reservoir Storage Calibration Results

Reservoir	Monitoring Period	Error in Total Storage	Monthly NSE, Storage	Daily NSE, Discharge
Wild Rice	01/1998-10/2002 11/2008-12/2012	-11.99%	0.789	0.709
Fish	01/1998-10/2002 11/2008-12/2012	-3.60%	0.720	1.000
Boulder	01/1998-10/2002 11/2008-12/2012	6.85%	0.529	0.943
Island	01/1998-10/2002 11/2008-12/2012	-0.85%	0.124	0.975
Whiteface	01/1998-10/2002 11/2008-12/2012	-1.60%	0.968	0.794

For the Nemadji River, there is one long-term continuous USGS gage near the outlet, Nemadji River at South Superior, WI (although the records for periods with ice are indirect estimates only), along with numerous shorter-term and partial record gages. Calibration initially focused on the downstream station to get the overall water balance approximately correct. Focus then turned to the two stations on Deer Creek, which span the transition from glacial till and moraine to fine lake sediments. As discussed in Section 2.3.4, there are complex relations between surface water and groundwater in this area, with water that infiltrates the Thompson Moraine resurfacing through artesian seeps in the lower watershed. It is anticipated that a groundwater model will eventually be made available to help quantify these relationships; in the meantime, the observed relationships have been approximated by routing subsurface flows from A/B soils in the uplands to the downstream reach, representing the resurfacing phenomenon. This approach provides a reasonable, but imprecise approximation.

Following work on the Deer Creek stations, we cycled back to simultaneous calibration of all gage stations in the Nemadji watershed. The quality of model fit appears to be constrained by the representativeness of precipitation data from station MN213863, which drives the response in the southern portion of the basin. This weather station ceased operation on 3/31/2006 and subsequent years are filled from WI476413. Some of the earlier records also appear to be reported at low precision (tenths rather than hundredths of inches). Both factors may degrade the quality of model fit.

Detailed results of the hydrologic calibration are provided in Appendix C and summarized in Table 4-6. Calibration results are ranked against the performance targets shown in Table 3-1. While there are many gages in the watershed, the majority have only operated for a few years, and most report data only seasonally. Rating curves are also imprecise for many of these stations due to continual shifting of bed forms. This lends considerable uncertainty to the calibration. The short operational period of most gages also means that there are limited data for temporal validation.

Model fit was good to very good for the continuous gage record for the St. Louis River near Scanlon. The complicated hydrology of the iron range in the St. Louis River watershed is captured reasonably by the model. The MDNR HYDSTRA gages in the region are mostly seasonal and have been operating only for a few years. Given these limitations the model was able to meet the total flow criteria at all these partial record gages, but often did not meet the high flow, low flow, seasonal and storm flow volume criteria. For the NSE criteria, the monthly results for the St. Louis gages ranged from “Fair” to “Very Good,” while the daily results tend to vary from “Poor” to “Very Good.” In addition to the mining areas,

relatively poor performance was observed for the gage on Lower Miller Creek. It was later determined that the drainage area above this gage has been substantially modified by stormwater conveyances. This station will be re-modeled in a finer-scale model application for the Duluth area WRAPS project.

For the Nemadji River, the results at the long term continuous gage, Nemadji River near South Superior, are ranked very good for total flow volume, error in 50% low flows, and error in 10% high flows; however, the daily NSE is only fair, likely reflecting the uncertainty introduced by estimation of flows during winter ice jam conditions as well as the complex groundwater interconnections in this basin. Relatively large errors are present for low flows in several of the short-record gages on small drainage areas in the Nemadji Basin. In addition to limited data, rating curves are likely to be highly uncertain in actively degrading channels.

Table 4-6. Summary of Hydrologic Calibration Results

Gage*	Agency	Model Reach	Waterbody	Period	Error in Total Flow Volume	Error in 50% Low Flows	Error in 10% High Flows	Daily NSE	Monthly NSE
03174001 (04024000)	**HYDSTRA /USGS**	**502**	**St. Louis River nr Scanlon**	**10/2000 09/2012**	**4.55%**	**6.63%**	**5.23%**	**0.876**	**0.928**
03149002	HYDSTRA	262	Partridge River	06/2009 06/2012	9.69%	-9.30%	5.45%	0.523	0.650
03150001	HYDSTRA	260	Second Creek	05/2008 09/2012	-2.79%	3.24%	-1.65%	0.141	0.755
(04015438)	USGS	505	St. Louis River nr Skibo	08/2011 12/2012	-1.00%	366%	-15.32	0.746	0.879
03138001 (04016500)	HYDSTRA /USGS	259+ 267	St. Louis River nr Aurora	04/2010 09/2012	-12.1%	8.79%	-28.8%	0.750	0.777
03115001 (04015500)	HYDSTRA /USGS	249	St. Louis River nr Forbes	03/2010 09/2012	-2.07%	-21.6%	-11.3%	0.724	0.841
03084001 (04020000)	HYDSTRA /USGS	250+ 271	Swan River	07/2010 09/2012	-6.23%	-0.14%	-16.8%	0.707	0.760
04048001	HYDSTRA	233+ 236	Cloquet River	09/2008 09/2012	-4.18%	-3.91%	-9.72%	0.859	0.830
03013001 (04021520)	HYDSTRA /USGS	402+ 421	Stoney Brook	05/2005 09/2012	4.75%	3.21%	7.55%	0.367	0.658
03001001	HYDSTRA	304	Miller Creek	04/2005 10/2010	0.42%	38.6%	-17.8%	0.43	0.612
05011002 (04024430)	**HYDSTRA /USGS**	**103**	**Nemadji River nr S. Superior**	**10/2000 09/2012**	**-0.32%**	**-4.98%**	**-8.03%**	**0.663**	**0.800**
05011001 (04024095)	HYDSTRA /USGS	115+ 117	Nemadji River nr Pleasant Valley, MN23	04/2003 09/2012	-8.68%	3.59%	-14.9%	0.655	0.750

Gage*	Agency	Model Reach	Waterbody	Period	Error in Total Flow Volume	Error in 50% Low Flows	Error in 10% High Flows	Daily NSE	Monthly NSE
05006001	HYDSTRA	511	Blackhoof River nr Pleasant Valley	04/2009 11/2012	6.22%	-3.44%	15.0%	0.698	0.627
05008001 (04024098)	HYDSTRA /USGS	118	Deer Creek nr Holyoke	10/2000 09/2012	-0.06%	-32.9%	-9.77%	0.606	0.773
05008002	HYDSTRA	119	Deer Creek nr Pleasant Valley	06/2008 10/2010	8.57%	7.61%	-3.36%	0.315	0.371
05009001	HYDSTRA	120+	Rock Creek	04/2009 10/2010	10.1%	377%	-12.6%	0.436	0.950
05016001	HYDSTRA	113	Nemadji River nr Holyoke, CSAH8	04/2009 11/2011	4.48%	1.33%	-0.32%	0.382	0.510
05018001	HYDSTRA	112+	South Fork Nemadji River	04/2011 10/2012	-0.75%	-36.4%	2.17%	0.671	0.709

Notes:
* USGS gage number shown in parenthesis.
+ Subbasin flow pro-rated to gage location within the subbasin.

4.4 FLOW VALIDATION

Only the two long-term gages, one on the St. Louis and one on the Nemadji River, had long enough periods of record to undertake separate validation tests. Results for the validation period are summarized in Table 4-7 and generally confirm the calibration results. Full results are provided in Appendix D.

Table 4-7. Summary of Hydrologic Validation Results

Gage*	Agency	Waterbody	Period	Error in Total Flow Volume	Error in 50% Low Flows	Error in 10% High Flows	Daily NSE	Monthly NSE
03174001 (04024000)	HYDSTRA /USGS	St. Louis River	10/1995 09/2000	3.48%	-2.57%	2.18%	0.766	0.864
05011002 (04024430)	HYDSTRA /USGS	Nemadji River	01/1993 09/2000	-4.43%	-13.92%	-7.73%	0.234	0.707

4.5 PEATLAND HYDROLOGY

Significant areas of the St. Louis watershed are occupied by peatlands, especially in the Swan River and parts of the Embarrass River drainage. Peatlands have unique hydrologic characteristics and a number of experiments were undertaken to attempt to match hydrologic behavior of the model to detailed studies of peatland hydrology reported from the Marcell Experimental Forest (e.g., Bay, 1969; Nichols and Verry, 2001; Verry and Kolka, 2003), located east of the study watershed near Grand Rapids. These studies

suggest that in watersheds in the Marcell consisting of glacial moraine upland forest surrounding peatlands the peatland components contribute most of the direct flow, as saturation excess, while the uplands contribute most of the groundwater discharge. Both components convert approximately 65 percent of precipitation to ET, and most of the flow (about 66 percent according to Bay, 1969) originates from snowmelt runoff in the spring and early summer.

Several problems were encountered in converting findings from the Marcell to the St. Louis watershed. Peatlands are generally classified as forested wetlands in the model, but are not uniquely identified, although they should generally match up with black spruce and tamarack vegetation in LANDFIRE. Contributions from uplands surrounding peatlands are likely different in the St. Louis watershed than in the Marcell Experimental Forest due to confining clay layers, as most of the soils in this part of the St. Louis have a dual; (B/D) hydrologic soil group classification, likely limiting the deep groundwater contribution. The vegetation coverages also do not clearly distinguish between the two main types of peatlands: bogs (or ombrotrophic peatlands), which are hydrologically isolated from regional groundwater, and fens (or minerotrophic peatlands), which are connected to regional groundwater and exhibit different streamflow responses with more stable baseflow (Brooks, 1988). Finally, there are not flow gages that isolate peatland runoff in the watershed. Of the available flow gages, the short record for the Swan River at Toivola is most dominated by peatland runoff.

An experimental version of the model for the Swan River that replicated the Marcell Experimental Forest findings of significant direct runoff and no direct recharge from peatlands (by reducing soil storage and percolation rates) failed to fit gaged results for the Swan River at Toivola and resulted in a significant degradation in model fit. We also tested HSPF's high water table options, but did not achieve improvement. Therefore, the model was reverted to a more standard representation of forested wetland hydrology. This representation still matches several of the findings reported above, including an approximately 65% rate of conversion of precipitation to evapotranspiration, and generation of about 65% of runoff. It is likely the case that the forested wetland representation is but a crude approximation of peatland hydrology, and the model could likely be improved at the local watershed scale by incorporation of detailed monitoring of peatland and other wetland runoff if and when such monitoring data become available.

4.6 WATER BALANCE SUMMARY

An additional check on the hydrologic calibration is provided in terms of an aggregated water balance for the combined land segments in the 8-digit HUC watershed. For the modeling period of record, the volume of precipitation on the watershed is compared to the sum of actual (simulated) ET, surface runoff, interflow, and active groundwater flow.

The St. Louis (HUC 04010201) and Cloquet (HUC 04010202) watersheds are summarized together, as they have a common outlet, while the Nemadji (HUC 04010102) is summarized separately (Table 4-8). The results are area-weighted across all hydrologic response units and weather stations. The St. Louis and Cloquet watersheds are covered primarily by forests and wetlands on low gradients. Not surprisingly, evapotranspiration (TAET) and active groundwater outflow (AGWO) dominate the hydrology. The Nemadji has greater average slopes and large areas of poorly permeable lacustrine clay deposits, and thus converts a larger proportion of precipitation into surface runoff. Both basins are simulated with small losses to deep groundwater, which occurs only in limited areas of permeable sands.

Table 4-8. Aggregated Water Balance for the St. Louis, Cloquet, and Nemadji River Watersheds (in/yr), based on 1993-2012 Simulations

	Precipitation (SUPY)	Surface Runoff (SURO)	Interflow (IFWO)	Active Ground Water Outflow (AGWO)	Loss to Deep Ground Water (IGWI)	Total Actual Evapo-transpiration (TAET)	Sum of Outputs	Storage Change
St. Louis/ Cloquet	30.43	0.76	0.58	8.96	0.34	19.71	30.34	0.08
Nemadji	32.98	2.67	1.47	6.92	0.25	21.60	32.91	0.07

The percentage distributions for the aggregated water balance are shown in Figure 4-1 and Figure 4-2. In both watersheds about 34% of precipitation is converted to runoff; however, the direct surface (SURO) and interflow (IFWO) fraction is much greater, and the groundwater discharge baseflow (AGWO) component smaller, in the Nemadji watershed consistent with the soils and the findings of Riedel et al. (2005). Estimates of actual ET for 1993-2012 are slightly higher than reported by Sanford and Selnick (2013) based on climate and land use regression equations, who suggest that the fraction of precipitation converted to ET is in the range of 50 to 59 percent in St. Louis and Carlton Counties based on 1971-2000 meteorology. The greater percentage predicted in this study may reflect gradual trends of increasing temperature and precipitation in the model period of 1995-2012 relative to the earlier period reported by Sanford and Selnick.

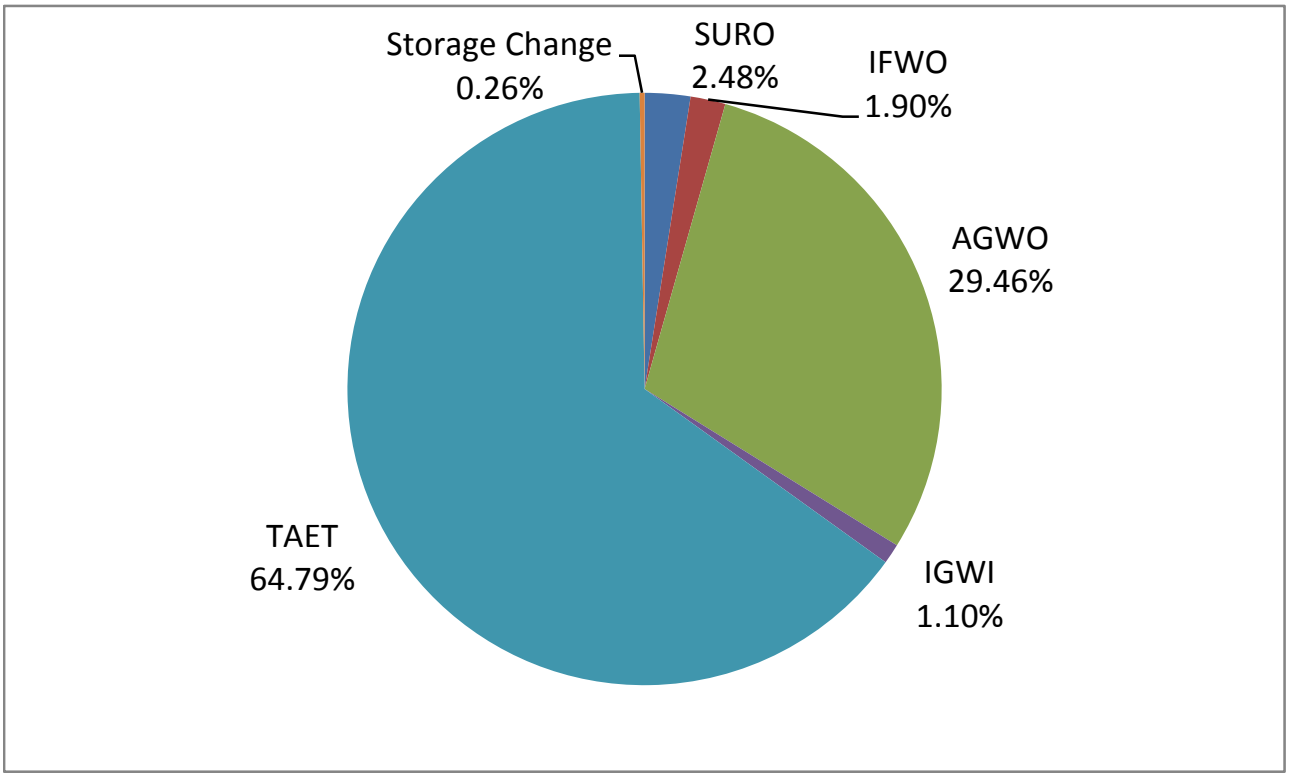

Figure 4-1. Water Balance Distribution for the St. Louis and Cloquet River Watersheds

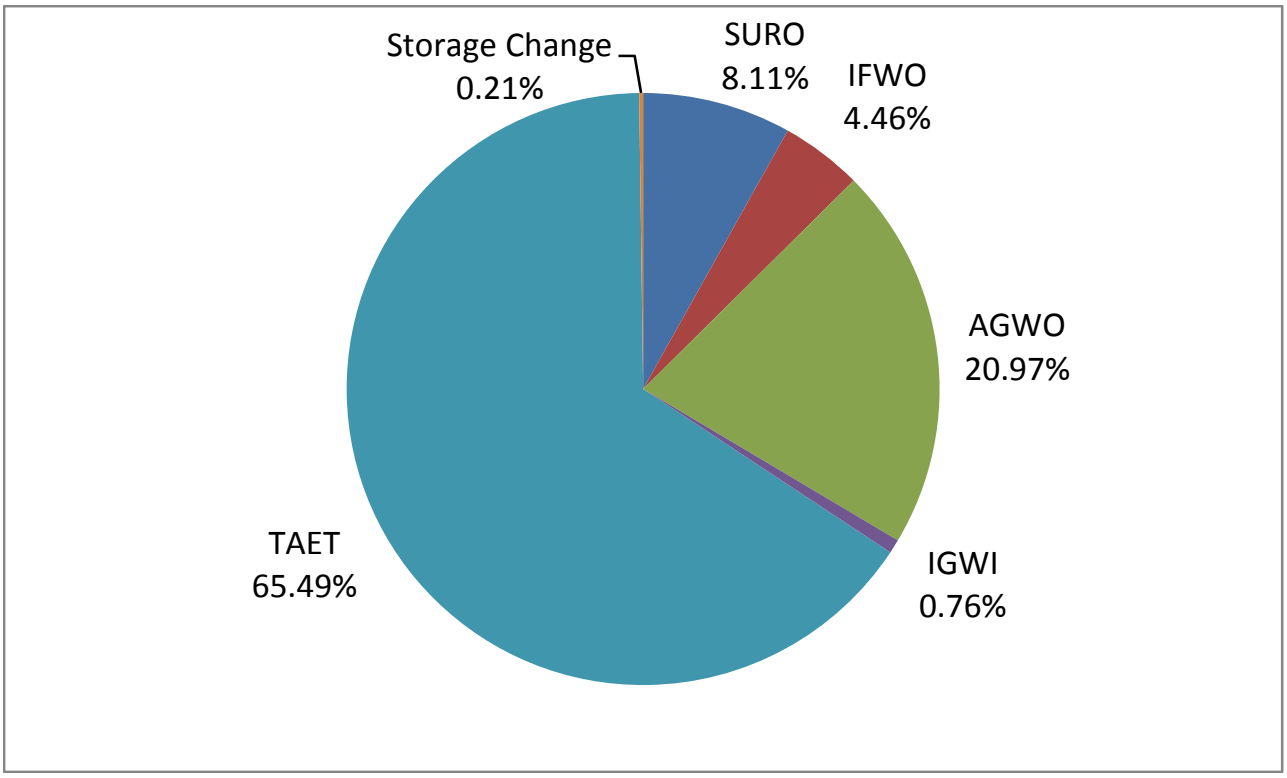

Figure 4-2. Water Balance Distribution for the Nemadji River Watershed

5 Sediment Calibration

Sediment calibration follows the sequential procedure outlined in Section 3. The observed data sets for calibration are generally small and typically cover limited time periods (refer to Figure 2-18 for locations). More stations are available for the Nemadji than for the much larger St. Louis and Cloquet watersheds, although data were collected at many of these only briefly. There are insufficient data for a temporal validation exercise. Instead, all available data are used for calibration. The calibrated parameters yield reasonable representations of suspended sediment at multiple stations, including downstream stations that integrate across the upstream watershed, so the models are reasonable.

Sediment erosion and transport is of particular concern in the Nemadji watershed, which has been identified as the largest source of sediment load to Lake Superior (Stortz and Sydor, 1976), transporting an average of 120,000 tons of sediment per year (NRCS, 1998). The high sediment load is associated with steep slopes and highly erodible lacustrine clay deposits. Riedel et al. (2005) discuss the erosional response of the Nemadji and show that it is in part due to the combination of active glacial rebound and lowering of the base level in Lake Superior, which causes steep channel slopes in the Nemadji, but that naturally high erosion rates have been more than doubled by human activities. These include forest harvesting in the 1850s, major forest fires in 1894 and 1918, and agricultural expansion on the uplands in the 1930s and 1950s. The harvest of the native mature white pine and red pine forest was of particular importance as it not only removed cover but also resulted in increased water yield and bankfull discharge (Riedel et al., 2005). This was exacerbated by direct impacts on channel geomorphology. As was common practice in the industry, the river channel was used to float logs downstream, a process which was enhanced by removing snags, straightening river meanders, and pulsing of flow through creation and subsequent dynamiting of temporary dams, setting off a chain reaction of geomorphological instability (NRCS, 1998).

The detailed study by NRCS (1998) concluded that the majority of sediment exported from the Nemadji is generated from mass wasting processes due to slumps of valley walls as the streams downcut into erodible lacustrine sediment (Magner and Brooks, 2008). Stream reaches with mass wasting are present throughout the watershed except on the relatively flat terrain of the headwaters area and the fraction of stream channel length exhibiting mass wasting increases with the bankfull discharge ratio to watershed area and decreases with the fraction of watershed area as wetlands.

Mass wasting is also enhanced by artesian pressure and groundwater discharges into the stream (see discussion in Section 2.3.4). In some locations, direct seepage into the stream is associated with mud "volcanos" that actively pump fine sediment into suspension as artesian groundwater discharges through the stream bed (Mooers and Wattrus, 2005; Emmons & Olivier Resources, 2014).

It appears that the extraordinarily high sediment loads in the Nemadji are in large part due to channel incision and mass wasting (i.e., bank collapse) events. These processes are by their very nature in part random events. This creates a significant challenge to modeling sediment in the Nemadji and suggests that a good model can simulate average response over time but is unlikely to be able to predict individual high loading events.

5.1 Detached Sediment Storage

Time series of detached sediment storage (DETS) were checked for reasonableness, defined as exhibiting a quasi-stationary equilibrium with seasonal changes from wet to dry periods. Example series from the southwestern part of the Nemadji watershed are shown in Figure 5-1.

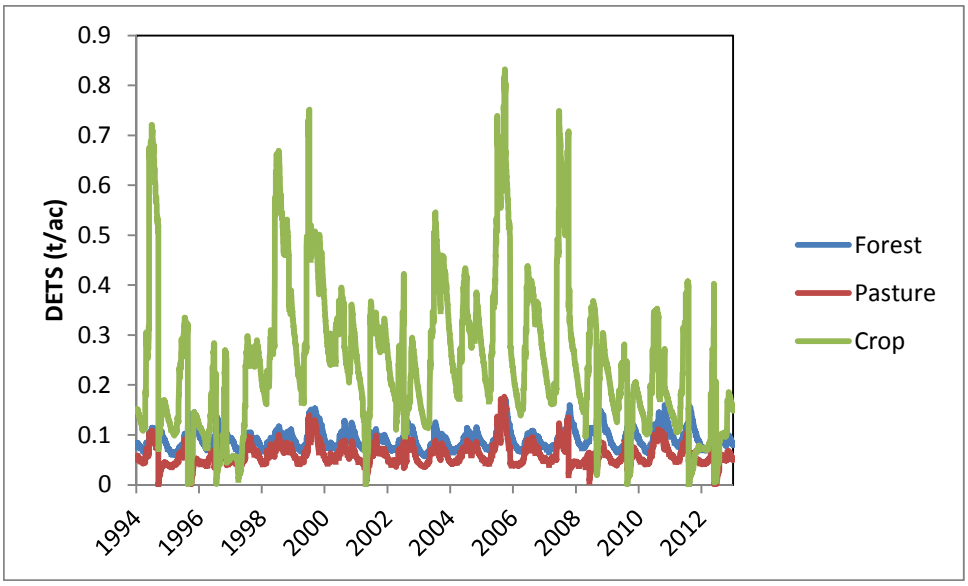

Figure 5-1. Example Detached Sediment Storage (DETS) Series for Southwestern Nemadji Watershed

5.2 Upland Sediment Loading Rates

The St. Louis/Cloquet and Nemadji watershed models were calibrated separately for sediment. They also have rather different soil and slope characteristics, and thus different sediment loading rates. Land use in both watersheds is dominated by forest and wetlands, with more pasture and agricultural land use in the Nemadji. Average upland sediment loading rates by land use (Table 5-1) show generally higher rates for the Nemadji than for the St. Louis and Cloquet watersheds, as was expected due to slopes and sediment characteristics.

Table 5-1. Average Upland Sediment Loading Rates (1994-2012) for St. Louis, Cloquet, and Nemadji Watershed Models

Landuse	St. Louis and Cloquet (t/ac/yr)	Nemadji (t/ac/yr)
Forest	0.016	0.031
Wetland	0.003	0.045
Shrub	0.194	0.339
Pasture	0.075	0.133
Crop	0.274	0.665
Developed	0.200	0.208
Water	0.000	0.000
Barren	0.492	0.554
Roads	0.104	0.135

Few estimates of typical upland sediment loading rates in these watersheds are available in the literature. In general, loads from undisturbed forest lands are expected to be low, but the combination of erosive soils and steep slopes results in higher loads in the Nemadji (Jaako Poyry Consulting, 1992), although the majority of loads in the Nemadji likely derive from mass wasting and channel degradation (Riedel et al., 2005). The upland loading rates shown in Table 5-1 for forestry are lower than the typical range of 0.05 – 0.4 tons/ac/yr cited in Donigian and Love (2003) and Packer (1967), likely because harvested areas (represented as barren or shrub land) and roads, which contribute much of the forest upland sediment load, as well as channel erosion sources, are accounted for separately in our model. For comparison, Ellison et al. (2014) reported total sediment yield in the range of 0.04 – 0.08 tons/ac/yr for two largely forested northern Minnesota watersheds (Knife River and Little Fork River).

Loading rates for pasture and crop are also relatively low compared to national typical ranges cited in USEPA (2006); however, these low rates are needed to match instream sediment concentrations

5.3 REACH SEDIMENT MASS BALANCE

Sediment scour and deposition was analyzed through tabulation on a reach by reach basis with the aim of insuring that significant amounts of scour and deposition occur only in areas where reasonably expected. Summary analysis in terms of stream depth for the St. Louis and Cloquet watersheds is shown in Figure 5-2. The majority of stream reaches have a simulated change in depth of less than plus or minus 0.25 feet over the 20-year period of simulation, corresponding to trapping rates in the range of ±20% or less. A majority of reaches are slightly degradational. Larger amounts of deposition are simulated for six reaches, all of which correspond to major lakes. A few reaches have larger amounts of degradation simulated. These are Reach 204 (St. Louis River downstream of Fond du Lac Reservoir, Reach 208 (Cloquet Reservoir), and Reach 236 (Swan River near Toivola). Degradation in Reach 204 makes sense. The other two reaches require some net loss of sand to match up with downstream total suspended sediment concentrations, but it is not known if this representation is reasonable. For most reaches, the bulk of degradation is associated with large flow events in 1997, 1999, and 2012.

In contrast to the St. Louis, the Nemadji River is known to have extensive areas with headcuts and bank sloughing. Accordingly, many of the stream reaches in the lacustrine core are simulated as having significant bed degradation (Figure 5-3). The amount of degradation corresponds well to the reaches identified as having high delivery rates to Lake Superior in NRCS (1998).

Over the entirety of the St. Louis and Cloquet watersheds channel scour is a relatively small portion of the total sediment balance. The net effect of trapping in the many reservoirs is an overall loss of total sediment load to deposition; in the non-lake reaches, sediment erosion is estimated to contribute a net of about 0.024 t/ac/yr when averaged over the entire watershed area. In contrast, channel erosion processes in the Nemadji are estimated to contribute 0.21 t/ac/yr (again as an average over the entire drainage area), which is the same order of magnitude as the upland loading rates shown in Table 5-1.

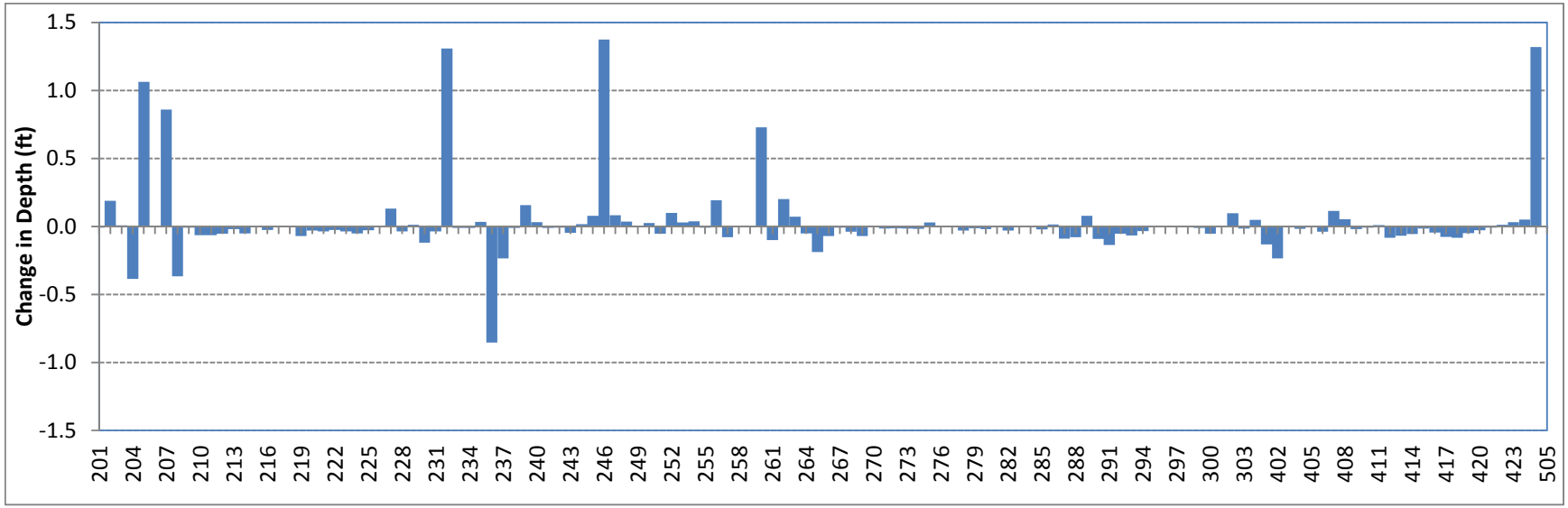

Figure 5-2. Reach Sediment Balance, St. Louis and Cloquet River Models, 1994-2012

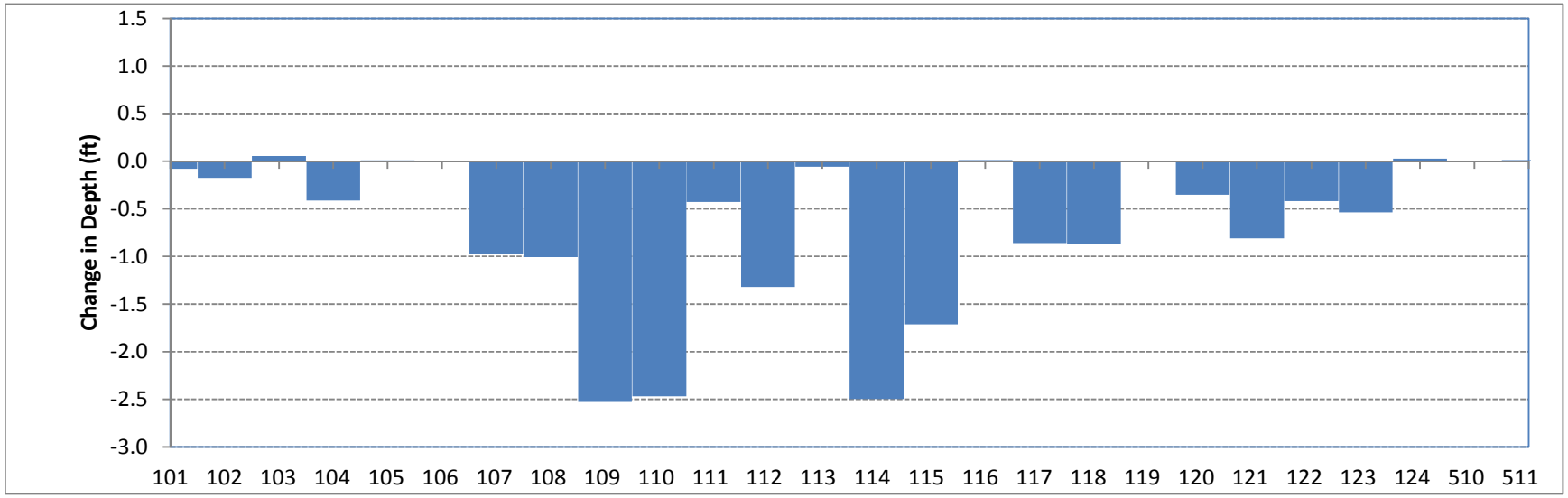

Figure 5-3. Reach Sediment Balance, Nemadji River Watershed Model, 1994-2012

5.4 CALIBRATION TO OBSERVED SUSPENDED SOLIDS DATA

Suspended sediment calibration took place at thirteen stations and used both visual and statistical approaches. Available observations are reported as total suspended solids (TSS) and not suspended sediment concentration (SSC). The two analytical methods can produce different results: TSS is a small sample method requires drawing a subsample, while SSC processes (through filtration and drying) the entire sample, and it has long been observed that the two methods can produce rather different results (Gray et al., 2000). The most common problem is for TSS to under-estimate the sand fraction and TSS is often, but not always, biased low relative to SSC. Recently, Ellison et al. (2014) demonstrated that TSS tends to under-estimate SSC in many Minnesota streams. All sampling methods may encounter problems associated with obtaining representative samples of larger particles that move near the sediment bed, but most TSS samples are obtained as a single grab whereas SSC samples are depth and width integrated, introducing further discrepancies.

The HSPF model simulates sand, silt, and clay-sized fractions of sediment separately, and sums these values to provide an estimate for comparison to the TSS data. The calibration process may thus under-estimate the movement of larger, non-cohesive sediment particles. Unfortunately, little information on particle size distribution of suspended solids is available for the St. Louis, Cloquet, and Nemadji systems. Obtaining such information in future may of great assistance in improving the quality of the sediment simulation.

We attempted to replicate the observed time series while at the same time minimizing relative errors associated with both concentration and load (as inferred from concentration and flow). Attention was paid to matching observed and simulated relationships between load and flow through the use of power plots, while also examining the distribution of error terms relative to both season and flow. It is not uncommon for relative error to be strongly leveraged by one or more outliers (especially for load, which tends to be determined by concentrations at high flows); therefore, the median error (which is not sensitive to outliers) is reported as well as the average error.

The detailed calibration process is shown here by example for the Nemadji River at South Superior, WI monitoring station, while a complete set of graphical and statistical results is provided in Appendix E. Four years of observations are available at this station. The model appears to track the observed data fairly well, although several very high observations are under-estimated (Figure 5-4). The average and median relative errors on concentration are very good (-2.4% and 0.5%, respectively), while the average and median relative errors on load are 28.3% and 0.03%, suggesting some over-estimation at higher flows. A log-log power plot (Figure 5-5) shows that the observed and simulated loads have a similar distribution relative to flow; however, the simulation has a “kink” in the middle flow range which deviates from the observed pattern. This is due to the simulation of channel erosion processes and may be a result of uncertainty in the representation of channel dimensions in upstream reaches of the model. The distribution of prediction errors versus flow (Figure 5-6) also reveals this discrepancy in the region around flow of 500 cfs. Finally, several high concentration outliers are noticeable at high flows, leading to the inflated relative average error on load.

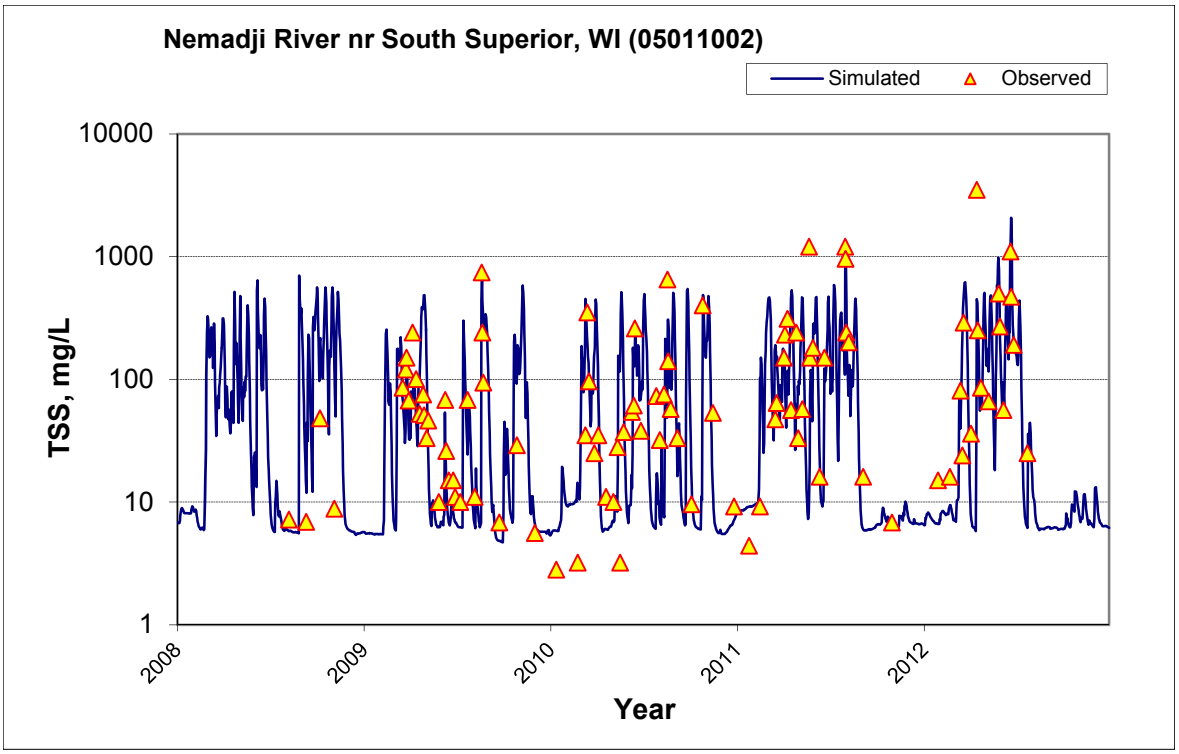

Figure 5-4. Time Series Plot for Total Suspended Sediment, Nemadji River at South Superior, WI

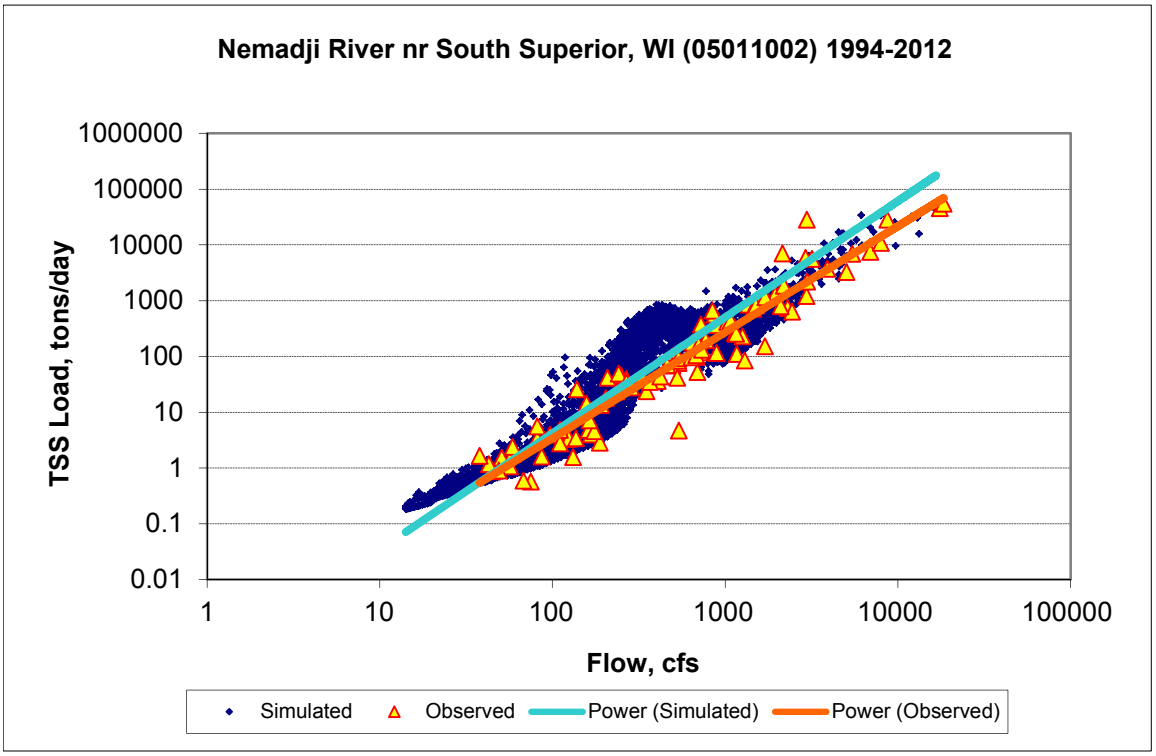

Figure 5-5. Log-log Power Plot of Simulated Total Suspended Sediment Load and Load Inferred from Observed Concentration, Nemadji River at South Superior, WI

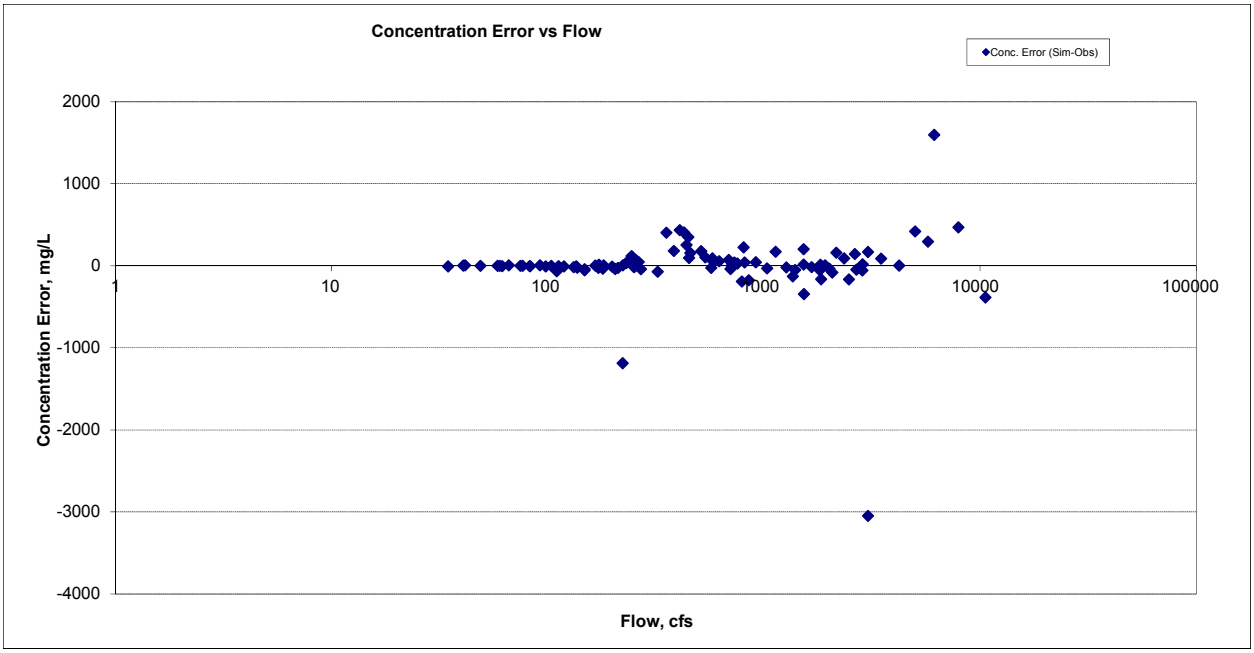

Figure 5-6. Distribution of Concentration Error for Total Suspended Sediment, Nemadji River at South Superior, WI

Sediment calibration statistics for all stations are provided in Table 5-2 (the accompanying graphics are in Appendix E). The fit for concentration is within the target range (±25%) for the major stations that have longer periods of record and integrate over larger drainage areas (highlighted in the table). These same stations also show a good fit to paired estimates of load, except that the estimated average load error for Nemadji River at South Superior is -28%. This appears to be due to a few outliers at high flows, as was discussed above. Several of the other stations show larger errors, which may be in part an artifact of short periods of record. Some specific comments are provided following Table 5-2.

Table 5-2. Summary of Sediment Calibration Results

Station	Dates	Relative Error on Concentration		Relative Error on Load	
		Average	Median	Average	Median
03115001: St Louis River at Forbes	2002-2009	18.24%	-12.88%	-0.07%	-2.93%
03084001: Swan River near Toivola	2012	5.54%	-13.53%	-12.30%	-2.83%
04048001: Cloquet River near Burnett	2008-2012	-14.03%	-5.09%	16.72%	-3.70%
03174001: St. Louis River at Scanlon	2009-2012	5.98%	-4.60%	22.51%	-0.17%
S00-021: St Louis River at Fond du Lac	2002-2009	-6.28%	-7.71%	-3.10%	-3.56%
03001001: Miller Creek at Duluth	1999, 2006-2008	3.92%	-4.98%	-59.85%	-3.90%
05006001: Blackhoof River nr Pleasant Valley	2008-2012	42.46%	-3.87%	274.29%	-0.43%
05008001: Deer Creek nr Pleasant Valley, MN23	2001-2005	-86.00%	-56.07%	-49.63%	-14.96%
05008001: Deer Creek nr Pleasant Valley, MN23	2007-2010	11.55%	13.03%	-8.74%	0.37%
05008002: Deer Creek nr Pleasant Valley, CSAH3	2007-2010	-18.51%	-8.37%	129.89%	-0.48%
05009001; Rock Creek nr Pleasant Valley	2002-2005, 2008-2011	15.52%	-8.45%	240.22%	-0.05%
05016001: Nemadji River nr Holyoke	2008-2012	-35.62%	-4.58%	14.97%	0.05%
05011001: Nemadji River nr Pleasant Valley	2008-2011	-15.06%	-1.77%	-11.68%	-0.10%
05011002: Nemadji River nr South Superior	1997-1998, 2007-2012	3.05%	-0.20%	-28.20%	0.00%

Notes regarding individual monitoring stations:

Miller Creek at Duluth: This station was monitored in 1999 and again in 2006-2008. These two brief periods exhibit different behavior, with higher concentrations in the earlier period (see Figures E-27 and E-29). The average relative error on load is associated with a few outliers from the earlier period (see Figure E-30). As noted above, the model showed relatively poor performance for hydrology on Lower

Miller Creek. It was later determined that the drainage area above this gage has been substantially modified by stormwater conveyances. This station will be re-modeled in a finer-scale model application for the Duluth area WRAPS project.

Blackhoof River near Pleasant Valley: This station drains a flat area with low stream density. Observed total suspended sediment concentrations tend to be very low (average of 7 mg/L) and the absolute magnitude of the average error is small (about 3 mg/L). The apparent over-estimation of loads is associated with two outliers at higher flows (see Figure E-34). Given the small drainage area and short time of concentration, those observations could well be unrepresentative of the daily average.

Deer Creek near Pleasant Valley, MN 23: This is the downstream station on Deer Creek, an area of extensive bank failure and channel incision. Intensive monitoring occurred in two different periods, 2001-2005 and 2007-2010. These periods have very different characteristics, with much higher total suspended sediment concentrations in the earlier period (see Figures E-37 and E-38). Accordingly, the statistics for the two periods are presented separately in Table 5-2. The model fits well for the latter period, but under-estimates the high concentrations observed during the earlier period. A detailed investigation of excess sediment problems in Deer Creek conducted in 2005 (Mooers and Wattrus, 2005) sheds light on the causes of this discrepancy. Based on local landowner comments, significant groundwater seeps and accompanying mud "volcanos" began about the time that beavers built a dam on the creek. On July 4, 1999 rainfall from a large storm caused the beaver dam to overtop and the impoundment subsequently washed out. In 2001 MDNR dynamited and removed another beaver dam that was impounding water further upstream, resulting in rapid drainage of the impoundment. Neither dam was rebuilt at the time of the Mooers investigation. In 2005 there were at least eight seeps along the edges of the former beaver pond and significant sediment loading due to rotational slumps. As a result, many observations in 2004 had total suspended sediment concentrations greater than 1,000 mg/L and as high as 3,740 mg/L. These anomalous events are not easily captured by a model of this sort; however, the model does a reasonable job of representing observed total suspended sediment from 2007 on, when conditions were presumably more stable.

Rock Creek: Rock Creek is a small drainage immediately north of Deer Creek, and, like Deer Creek, appears to have cycles of greater and lesser stability. The model segmentation does not line up with the monitoring point, which is well upstream from the mouth, so the model-data comparison may not be fully valid. Further, the fit to observed flow in Rock Creek appears poor (see Section 4.3 and Appendix C). Currently, observations are over-predicted at high flows, leading to the large apparent error in average loads (Figure E-49).

Nemadji River near Holyoke: This is the upstream station on the Nemadji River, with a small drainage area and thus a flashy response that makes comparison to point in time measurements difficult. The model fits the central tendency of the data, but has poor precision, leading to an under-estimate of the average concentration (e.g., Figure E-63). Attempts to further tune model performance at this station tended to degrade model fit for the station downstream at Nemadji River near Pleasant Valley.

5.5 COMPARISON TO FLUX LOAD ESTIMATES

The final check on the sediment calibration is comparison of simulated loads to loads estimated from observed flow and concentration data. As with the calibration to observed TSS concentrations, there is a potential issue in that the HSPF model estimate of sediment load is based on the sum of sand, silt, and clay, whereas observed TSS data are likely to under-estimate the sand fraction. The calibration process is likely to result in a potential low bias for sand, as noted in Section 5.4, but sufficient data are not available to test this hypothesis.

The "observed" loads can be estimated only where there is both flow and concentration monitoring, and requires interpolation against sparse monitoring data. This interpolation is done with the Corps of Engineers' FLUX32 model (Walker, 1986).

Only a few locations in the St. Louis, Cloquet, and Nemadji watersheds have records of both flow and water quality that are sufficient for estimation of long-term mass loading rates. Results are shown in Table 5-3. For each of these stations, the simulated load is similar to the FLUX-estimated load and well within the FLUX 95% confidence limits on the mean, thus confirming the calibration.

Table 5-3. Comparison of Simulated and FLUX-Estimated Sediment Loads

Station	Date Range	Simulated Load (t/yr)	FLUX Load
04048001: Cloquet River near Burnett	8/2008-10/2012	3,025	2,790 (2,215 – 3,364)
03174001: St. Louis River at Scanlon	8/2008 – 10/2012	52,138	63,470 (32,370 - 94,570)
05011001: Nemadji River nr Pleasant Valley	4/2003-10/2012	31,433	38,800 (28,914 - 48,686)
05011002: Nemadji River nr South Superior	1/1997-9/2012	76,025	85,021 (51,692 – 118,349)

Note: FLUX estimates show mean with 95% confidence intervals in parentheses.

6 References

Andrews, S.C., R.G. Christensen, and C.D. Wilson. 1980. Impact of Nonpoint Pollution Control on Western Lake Superior: Red Clay Project Final Report, Part III. EPA-905/9-76-002. U.S. Environmental Protection Agency, Washington, DC.

AQUA TERRA Consultants. 2012. Modeling Guidance for BASINS/HSPF Applications under the MPCA One Water Program.

Bay, R.R. 1969. Runoff from small peatland watersheds. *Journal of Hydrology*, 9: 90-102.

Brooks, K.N. 1988. Hydrologic impacts of peat mining. Pp. 160-169 in *Ecology and Management of Wetlands, Vol. 2: Management, Use and Value of Wetlands*. Croom Helm, London.

Donigian, A.S., Jr. 2000. HSPF Training Workshop Handbook and CD. Lecture #19. Calibration and Verification Issues. Prepared for and presented to the U.S. Environmental Protection Agency, Office of Water, Office of Science and Technology, Washington, DC.

Donigian, A.S., Jr., J.C. Imhoff, B.R. Bicknell, and J.L. Kittle, Jr. 1984. Application Guide for Hydrological Simulation Program – FORTRAN (HSPF). EPA-600/3-84-965. U.S. Environmental Protection Agency, Environmental Research Laboratory, Athens, GA.

Ellison, C.A., B.E. Savage, and G.D. Johnson. 2014. Suspended-Sediment Concentrations, Loads, Total Suspended Solids, Turbidity, and Particle-Size Fractions for Selected Rivers in Minnesota, 2007 through 2011. Scientific Investigations Report 2013–5205. U.S. Geological Survey, Reston, VA. http://dx.doi.org/10.3133/sir20135205

Emmons & Oliver Resources. 2014. Nemadji River Watershed Stressor ID Report, Hydrologic Change in Relation to IBI Impairment.

GLIFWC. 2011. Iron Mining in the Lake Superior Basin. Project Report 11-1. Great Lakes Indian Fish & Wildlife Commission, Environmental Section, Odanah, WI.

Gray, J.R., G.D. Glysson, L.M. Turcios, and G.E. Schwarz. 2000. Comparability of Suspended-Sediment Concentration and Total Suspended Solids Data. Water-Resources Investigations Report 00-4191. U.S. Geological Survey, Reston, VA.

Hardy, T., P. Panja, and D. Mathias. 2005. WinXSPRO, A Channel Cross-Section Analyzer, User's Manual, Version 3.0. Gen. Tech. Rep. RMRS-GTR-147.. USDA Forest Service Rocky Mountain Research Station, Stream Systems Technology Center, Fort Collins, CO. http://www.fs.fed.us/rm/pubs/rmrs_gtr147.pdf.

Jaakko Pöyry Consulting, Inc. 1992. Generic Environmental Impact Statement on Timber Harvesting and Forest Management in Minnesota. Prepared for Minnesota Water Quality Board by Jaakko Pöyry Consulting, Tarrytown, NY.

Liesch. 2009. Water Balance/Mine Yield Study, Keetac Expansion Project. Prepared for United States Steel Corporation, Keewatin Taconite Operations by Liesch Associates, Inc., Minneapolis, MN.

Lumb, A.M., R.B. McCammon, and J.L. Kittle, Jr. 1994. Users Manual for an Expert System (HSPEXP) for Calibration of the Hydrological Simulation Program – FORTRAN. Water-Resources Investigation Report 94-4168. U.S. Geological Survey, Reston, VA.

Magner, J.A., and K.N. Brooks. 2008. Predicting stream channel erosion in the lacustrine core of the upper Nemadji River, Minnesota (USA) using stream geomorphology metrics. *Environmental Geology*, 54:1424-1434, doi:10.1007/s00254-007-0923-3.

McCuen, R.H., Z. Knight, and A.G. Cutter. 2006. Evaluation of the Nash-Sutcliffe efficiency index. *Journal of Hydrologic Engineering*, 11(6): 597-602.

MDNR. 2009. Draft Environmental Impact Statement, NorthMet Project, PolyMet Mining, Inc. Prepared by Minnesota Dept. of Natural Resources and U.S. Army Corps of Engineers, St. Paul District. http://www.dnr.state.mn.us/input/environmentalreview/polymet/index.html.

Mooers, H., and N. Wattrus. 2005. Results of Deer Creek Groundwater Seepage Investigation. Report to Carlton County Planning and Zoning. Dept. of Geological Sciences, University of Minnesota, Duluth, MN.

Moriasi, D.N., J.G. Arnold, M.W. Van Liew, R.L. Bingner, R.D. Harmel, and T.L. Veith. 2007. Model evaluation guidelines for systematic quantification of accuracy in watershed simulations. *Transactions of the ASABE*, 50(3): 885-900.

Nash, J. E., and J. V. Sutcliffe. 1970. River flow forecasting through conceptual models: Part 1: A discussion of principles. *Journal of Hydrology*, 10(3): 282-290.

Nichols, D.S., and E.S. Verry. 2001. Stream flow and ground water recharge from small forested watersheds in north central Minnesota. *Journal of Hydrology*, 245: 89-103.

NRCS. 1998. Nemadji River Basin Project Report. Natural Resources Conservation Service, St. Paul, MN.

Packer, P. E. 1967. Forest Treatment Effects on Water Quality. In *Forest Hydrology*, eds. W. E. Sopper and H. W. Lull. Pergamon Press, New York.

Riedel, M.S., E.S. Verry, and K.N. Brooks. 2005. Impacts of land use conversion on bankfull discharge and mass wasting. *Journal of Environmental Management*, 76: 326-337.

Sanford, W.E., and D.L. Selnick. 2013. Estimation of evapotranspiration across the conterminous United States using a regression with climate and land-cover data. *Journal of the American Water Resources Association*, 49(1): 217-230.

Schall, J.D., P.L. Thompson, S.M. Zerges, R.T. Kilgore, and J.L. Morris. 2012. Hydraulic Design of Highway Culverts, Third Edition. Hydraulic Design Series # 5, FHWA-NHI-12-029. Federal Highway Administration, Washington, DC.

SLRCAC. 1992. The St. Louis River System Remedial Action Plan (RAP), Stage 1 – April 1992. St. Louis River Citizens Action Committee, Duluth, MN. URL: http://www.stlouisriver.org/rap.html; accessed 12/1/2013.

Stortz, K.R., and C.M. Sydor. 1976. Turbidity sources in Lake Superior. *Journal of Great Lakes Research*, 2(2): 393-401.

USDA. [2013?]. Rapid Watershed Assessment: St. Louis River (MN) HUC: 04010201. Accessed November 2013. United States Department of Agriculture, Natural Resources Conservation Service, Conservation Engineering Division, Washington, DC. URL: http://www.nrcs.usda.gov/wps/portal/nrcs/detail/mn/technical/?cid=nrcs142p2_023579

USDA. 1986. Urban Hydrology for Small Watersheds, TR-55. United States Department of Agriculture, Natural Resources Conservation Service, Conservation Engineering Division, Washington, DC.

USEPA. 2000. Estimating Hydrology and Hydraulic Parameters for HSPF. BASINS Technical Note 6, EPA-823-R00-012. Office of Water, U.S. Environmental Protection Agency, Washington, DC.

USEPA. 2007. Two Automated Methods for Creating Hydraulic Function Tables (FTABLES). BASINS Technical Note 2. Office of Water, U.S. Environmental Protection Agency, Washington, DC.

USEPA. 2008. Using the BASINS Meteorological Database—Version 2006. BASINS Technical Note 10. Office of Water, U.S. Environmental Protection Agency, Washington, DC. Available online at http://water.epa.gov/scitech/datait/models/basins/upload/2009_04_13_BASINSs_tecnote10.pdf.

Verry, E.S., and R.K. Kolka. 2003. Importance of wetlands to streamflow generation. Pp. 126-132 *in* Renard, K. G.,et al., eds. 1st Interagency Conference on Research in the Watersheds; 2003 October 27-30; Benson, AZ. U.S. Department of Agriculture, Agricultural Research Service.

Walker, W. W. 1986. Empirical Methods for Predicting Eutrophication in Impoundments; Report 3, Phase III: Applications Manual. Technical Report E-81-9. U.S. Army Engineer Waterways Experiment Station, Vicksburg, MS.

(This page left intentionally blank.)

Appendix A. Detailed Snow Calibration Results

MN210387 (Babbitt)

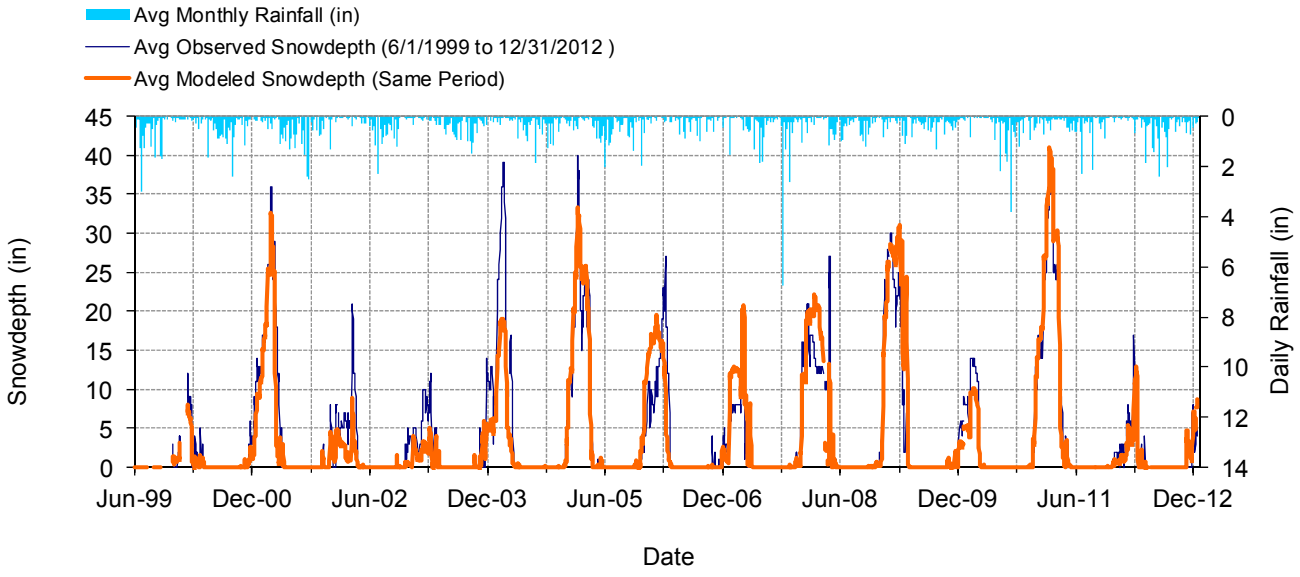

Figure A-1. Mean daily snow depth at MN210387 (Babbitt)

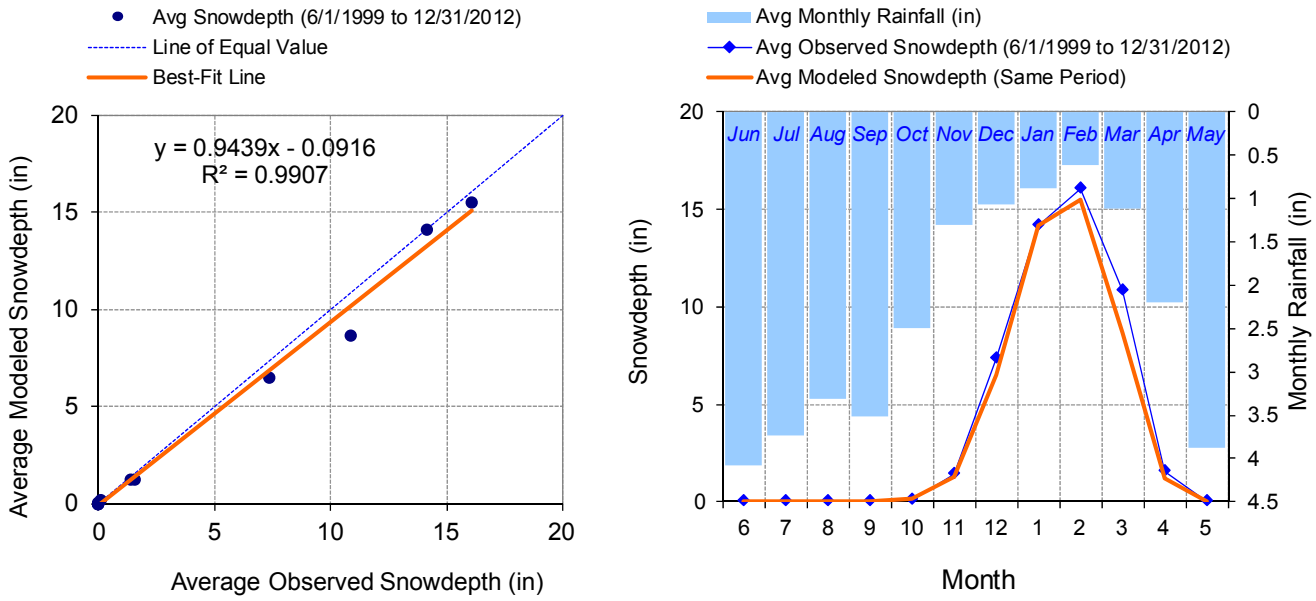

Figure A-2. Seasonal regression and temporal aggregate at MN210387 (Babbitt)

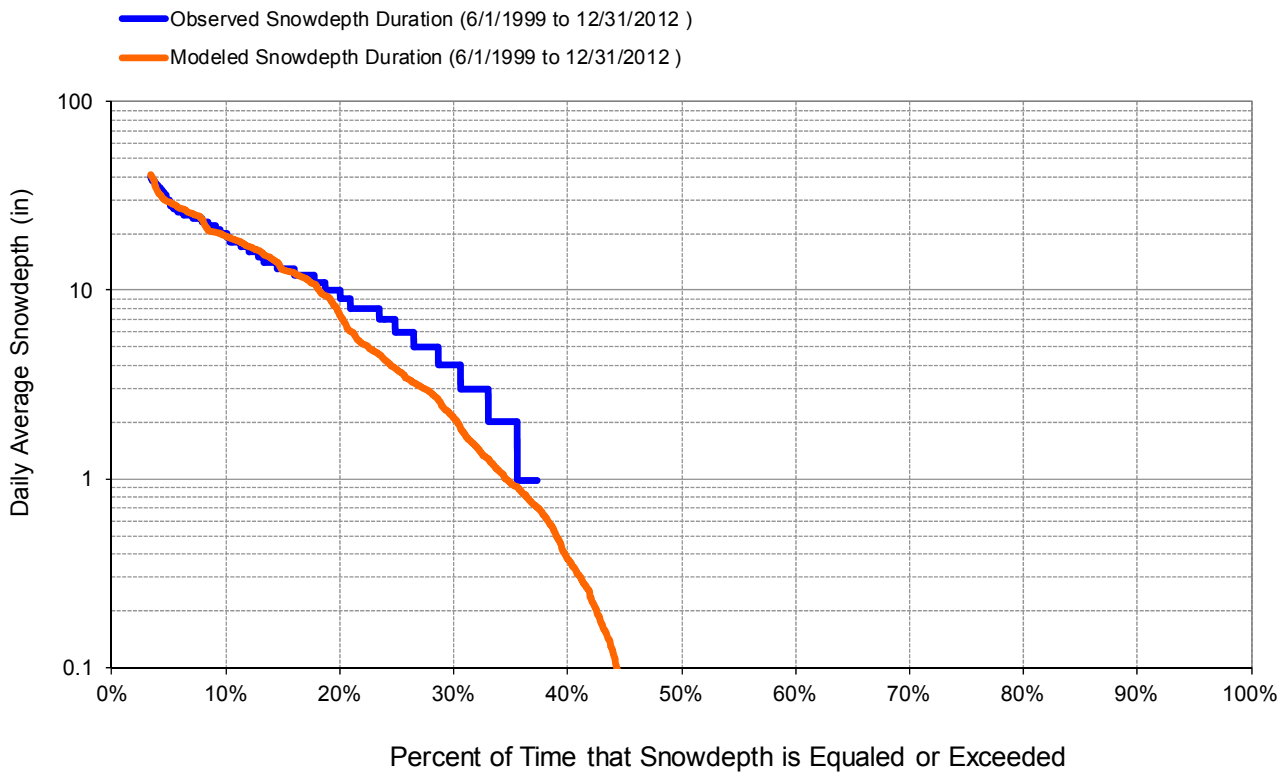

Figure A-3. Snow depth exceedance at MN210387 (Babbitt)

Table A-1. Summary statistics at MN210387 (Babbitt)

HSPF Simulated Snowdepth		Observed Precipitation Gage	
REACH OUTFLOW FROM DSN 1 13.59-Year Analysis Period: 6/1/1999 - 12/31/2012 Flow volumes are (inches/year) for upstream drainage area		MN210387 (Babbitt)	
Total Simulated Snowdepth:	**1321.62**	Total Observed Snowdepth:	**1436.02**
Simulated Summer Snowdepth (months 7-9):	**0.05**	Observed Summer Snowdepth (7-9):	**0.00**
Simulated Fall Snowdepth (months 10-12):	**238.73**	Observed Fall Snowdepth (10-12):	**266.03**
Simulated Winter Snowdepth (months 1-3):	**1046.95**	Observed Winter Snowdepth (1-3):	**1126.00**
Simulated Spring Snowdepth (months 4-6):	**35.89**	Observed Spring Snowdepth (4-6):	**44.00**
Errors (Simulated-Observed)	*Error Statistics*	*Recommended Criteria*	
Error in total snowdepth:	-7.97	10	
Nash-Sutcliffe Coefficient of Efficiency, E:	0.830	Model accuracy increases as E or E' approaches 1.0	
Baseline adjusted coefficient (Garrick), E':	0.742		
Monthly NSE	0.843		

MN210989 (Brimson 1E)

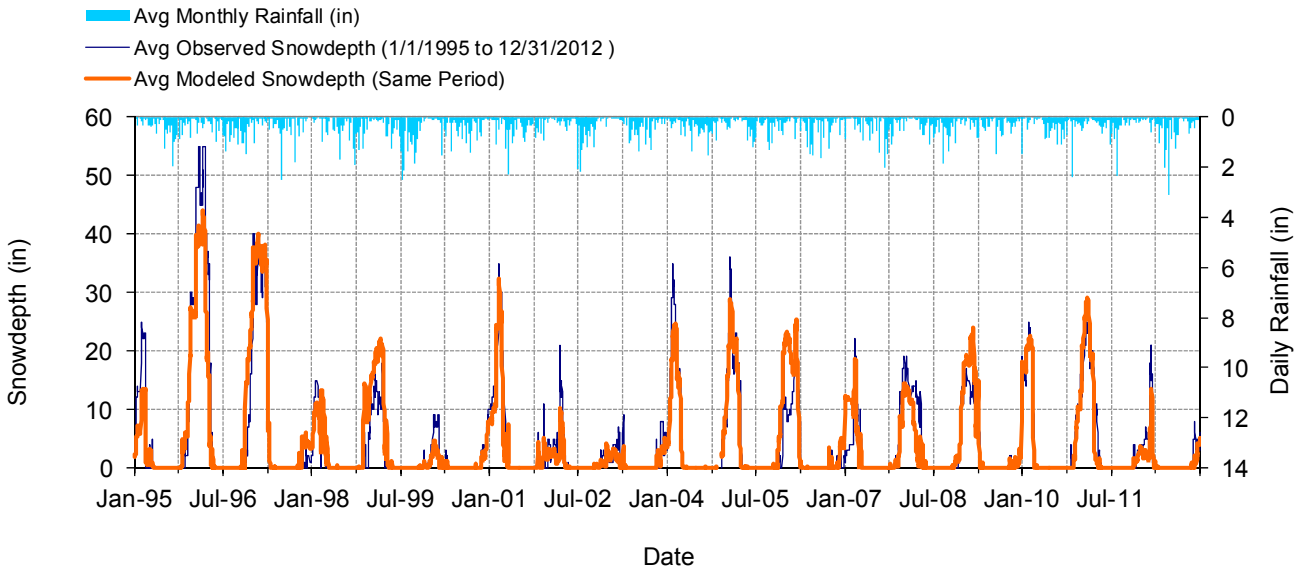

Figure A-4. Mean daily snow depth at MN210989 (Brimson 1E)

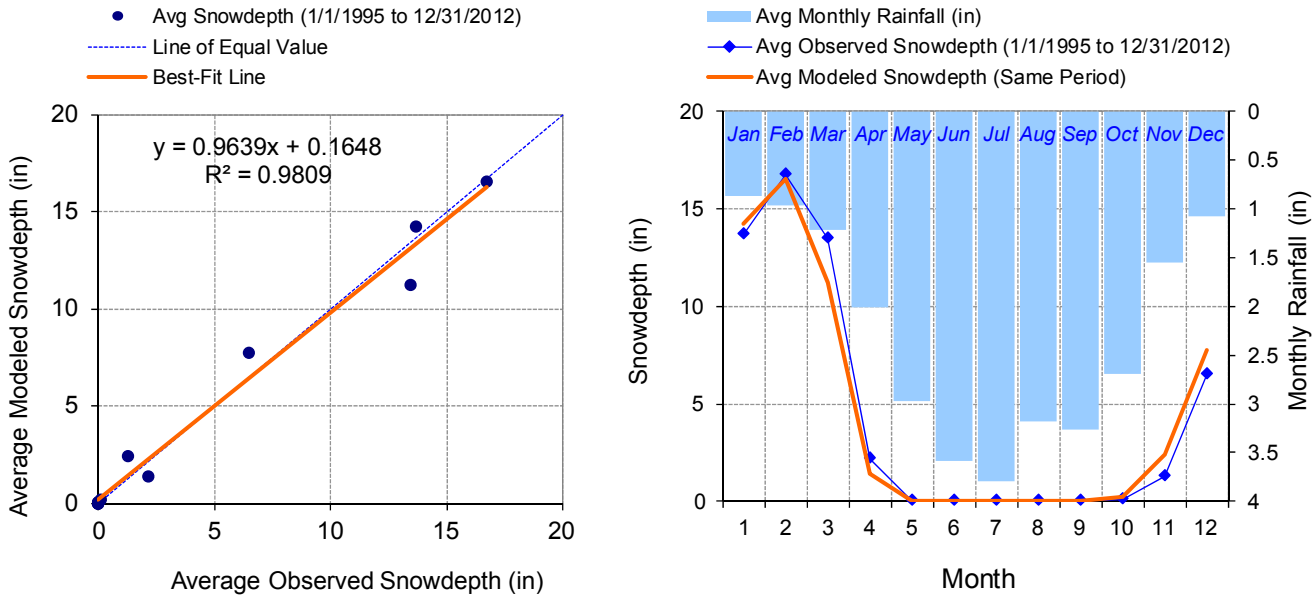

Figure A-5. Seasonal regression and temporal aggregate at MN210989 (Brimson 1E)

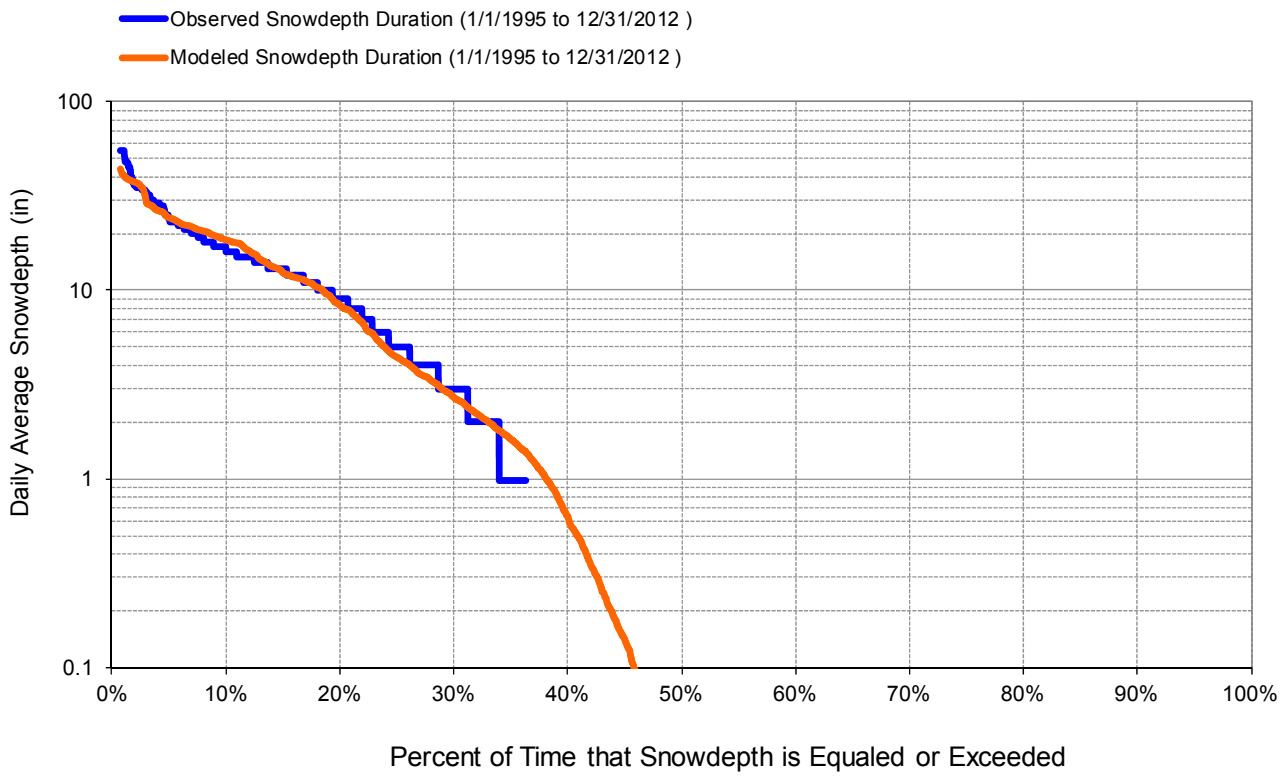

Figure A-6. Snow depth exceedance at MN210989 (Brimson 1E)

Table A-2. Summary statistics at MN210989 (Brimson 1E)

HSPF Simulated Snowdepth		Observed Precipitation Gage	
REACH OUTFLOW FROM DSN 2 18-Year Analysis Period: 1/1/1995 - 12/31/2012 Flow volumes are (inches/year) for upstream drainage area		MN210989 (Brimson 1E)	
Total Simulated Snowdepth:	**1614.75**	Total Observed Snowdepth:	**1615.49**
Simulated Summer Snowdepth (months 7-9):	**0.28**	Observed Summer Snowdepth (7-9):	**0.00**
Simulated Fall Snowdepth (months 10-12):	**314.86**	Observed Fall Snowdepth (10-12):	**238.46**
Simulated Winter Snowdepth (months 1-3):	**1257.61**	Observed Winter Snowdepth (1-3):	**1312.55**
Simulated Spring Snowdepth (months 4-6):	**42.00**	Observed Spring Snowdepth (4-6):	**64.48**
Errors (Simulated-Observed)	*Error Statistics*	*Recommended Criteria*	
Error in total snowdepth:	-0.05	10	
Nash-Sutcliffe Coefficient of Efficiency, E:	0.851	Model accuracy increases as E or E' approaches 1.0	
Baseline adjusted coefficient (Garrick), E':	0.738		
Monthly NSE	0.859		

MN211630 (Cloquet)

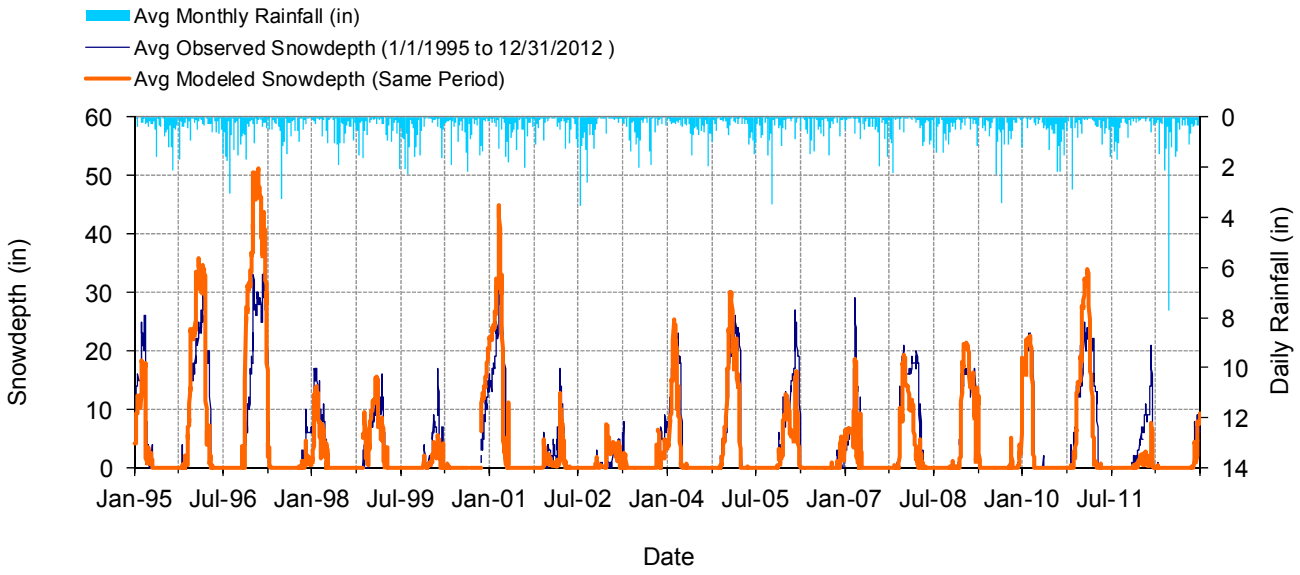

Figure A-7. Mean daily snow depth at MN211630 (Cloquet)

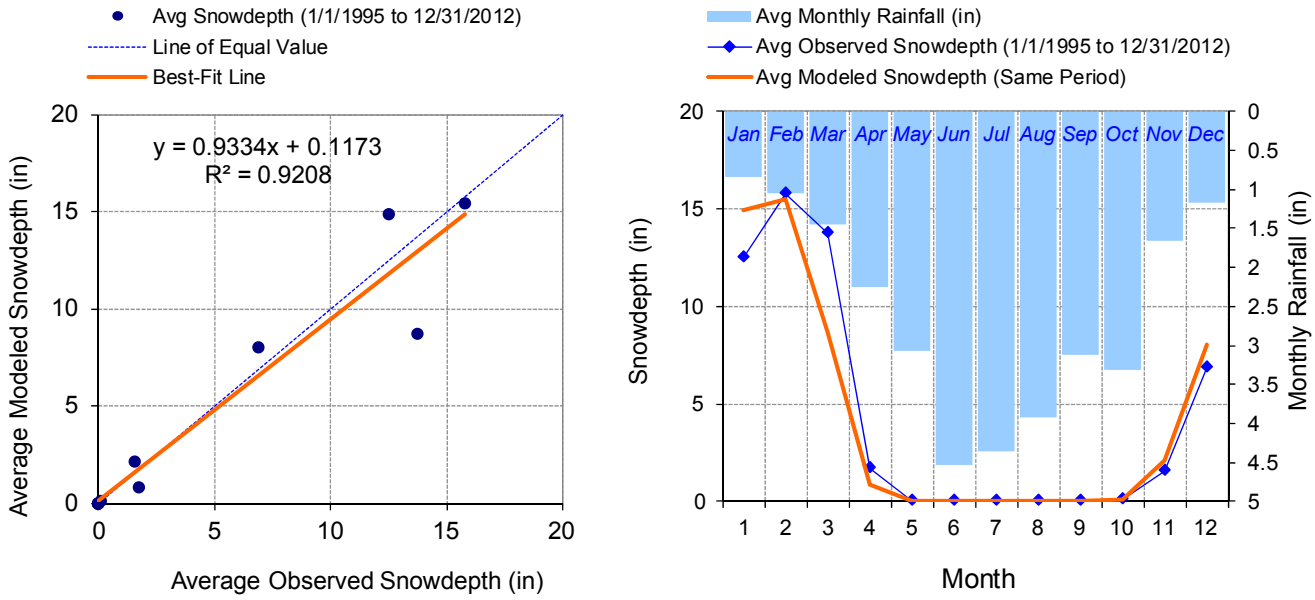

Figure A-8. Seasonal regression and temporal aggregate at MN211630 (Cloquet)

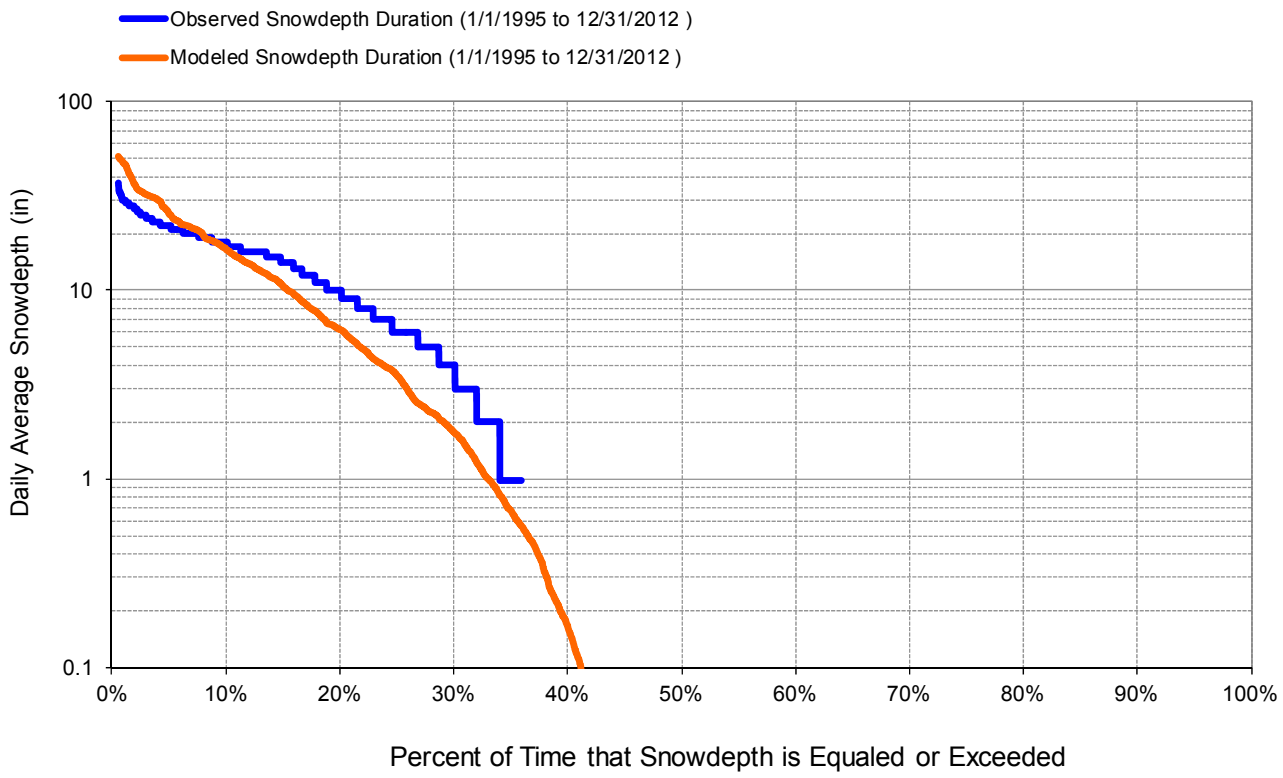

Figure A-9. Snow depth exceedance at MN211630 (Cloquet)

Table A-3. Summary statistics at MN211630 (Cloquet)

HSPF Simulated Snowdepth		**Observed Precipitation Gage**	
REACH OUTFLOW FROM DSN 3 18-Year Analysis Period: 1/1/1995 - 12/31/2012 Flow volumes are (inches/year) for upstream drainage area		MN211630 (Coquet)	
Total Simulated Snowdepth:	**1500.93**	Total Observed Snowdepth:	**1563.69**
Simulated Summer Snowdepth (months 7-9):	**0.00**	Observed Summer Snowdepth (7-9):	**0.00**
Simulated Fall Snowdepth (months 10-12):	**314.12**	Observed Fall Snowdepth (10-12):	**259.79**
Simulated Winter Snowdepth (months 1-3):	**1162.10**	Observed Winter Snowdepth (1-3):	**1252.48**
Simulated Spring Snowdepth (months 4-6):	**24.70**	Observed Spring Snowdepth (4-6):	**51.43**
Errors (Simulated-Observed)	*Error Statistics*	*Recommended Criteria*	
Error in total snowdepth:	-4.01	10	
Nash-Sutcliffe Coefficient of Efficiency, E:	0.666	Model accuracy increases as E or E' approaches 1.0	
Baseline adjusted coefficient (Garrick), E':	0.667		
Monthly NSE	0.647		

MN211840 (Cotton)

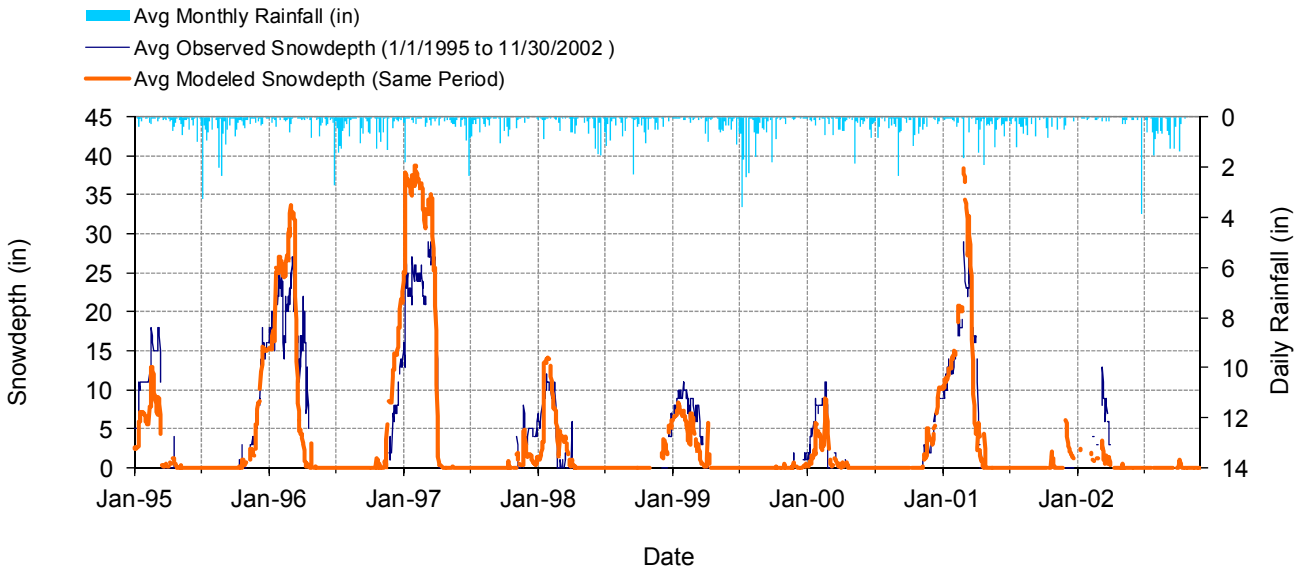

Figure A-10. Mean daily snow depth at MN211840 (Cotton)

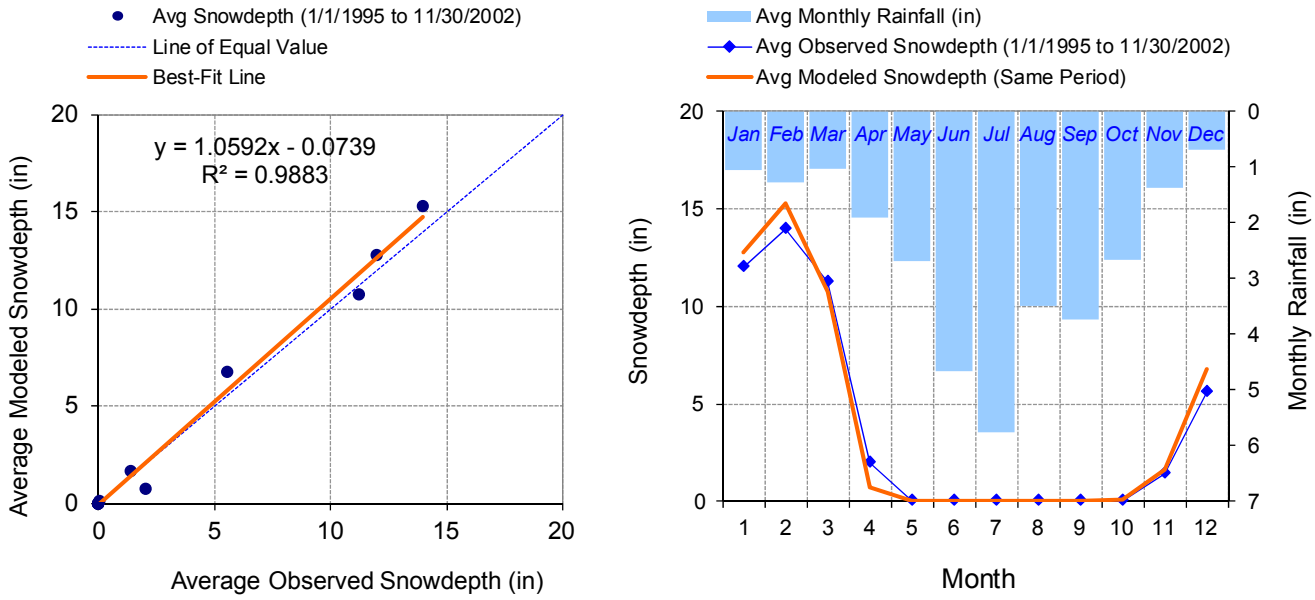

Figure A-11. Seasonal regression and temporal aggregate at MN211840 (Cotton)

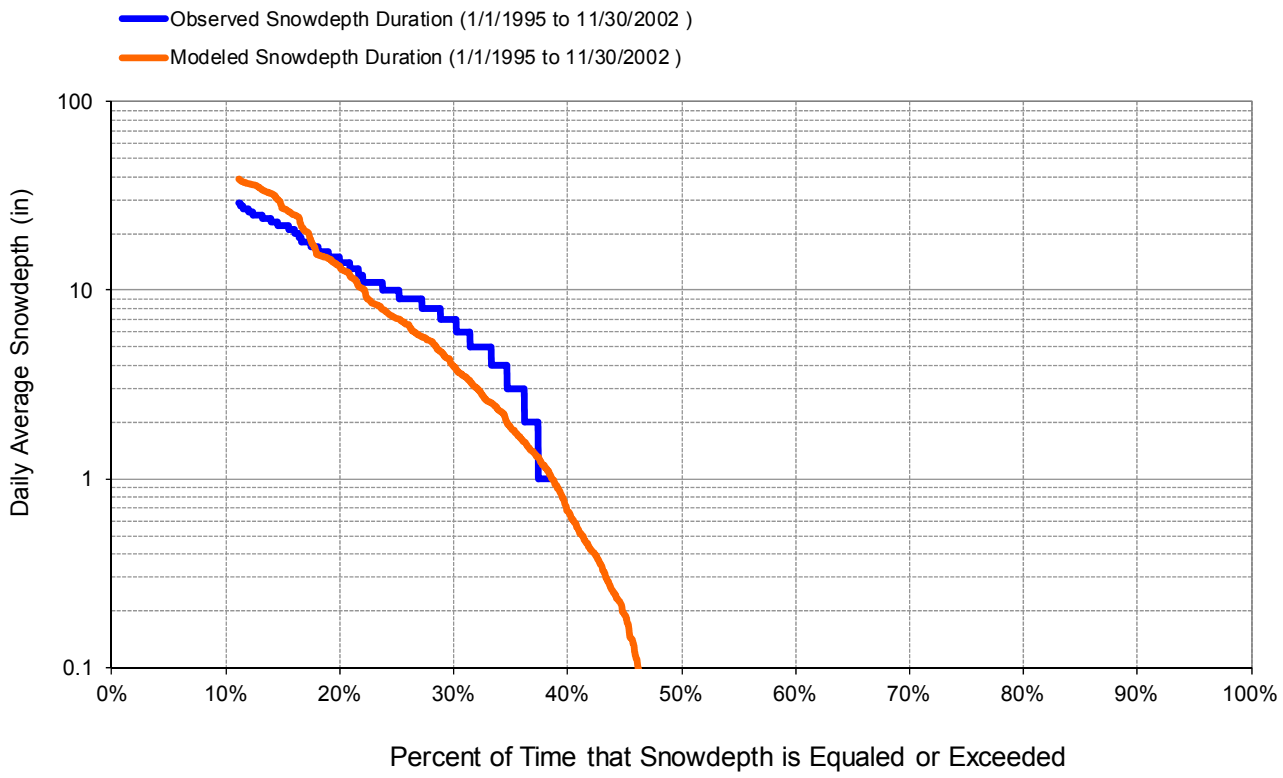

Figure A-12. Snow depth exceedance at MN211840 (Cotton)

Table A-4. Summary statistics at MN211840 (Cotton)

HSPF Simulated Snowdepth		Observed Precipitation Gage	
REACH OUTFLOW FROM DSN 4 7.92-Year Analysis Period: 1/1/1995 - 11/30/2002 Flow volumes are (inches/year) for upstream drainage area		MN211840 (Cotton)	
Total Simulated Snowdepth:	**1198.61**	Total Observed Snowdepth:	**1156.90**
Simulated Summer Snowdepth (months 7-9):	**0.03**	Observed Summer Snowdepth (7-9):	**0.00**
Simulated Fall Snowdepth (months 10-12):	**190.89**	Observed Fall Snowdepth (10-12):	**156.03**
Simulated Winter Snowdepth (months 1-3):	**989.22**	Observed Winter Snowdepth (1-3):	**951.22**
Simulated Spring Snowdepth (months 4-6):	**18.47**	Observed Spring Snowdepth (4-6):	**49.65**
Errors (Simulated-Observed)	*Error Statistics*	*Recommended Criteria*	
Error in total snowdepth:	3.61	10	
Nash-Sutcliffe Coefficient of Efficiency, E:	0.767	Model accuracy increases as E or E' approaches 1.0	
Baseline adjusted coefficient (Garrick), E':	0.710		
Monthly NSE	0.766		

MN212248 (Duluth Intl Ap)

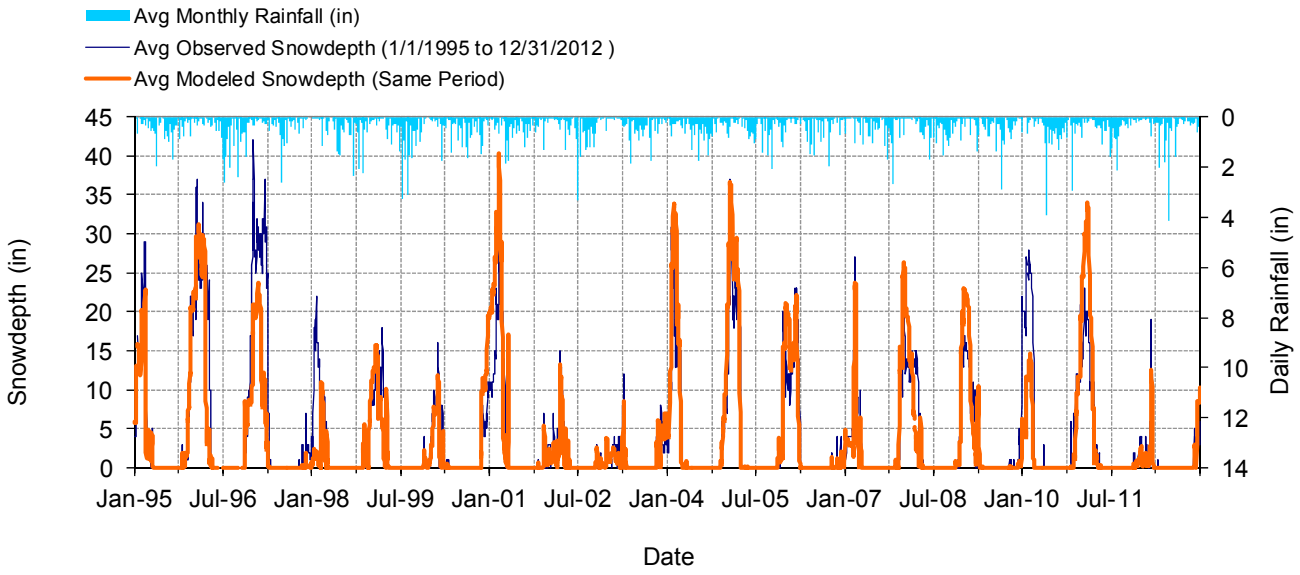

Figure A-13. Mean daily snow depth at MN212248 (Duluth Intl Ap)

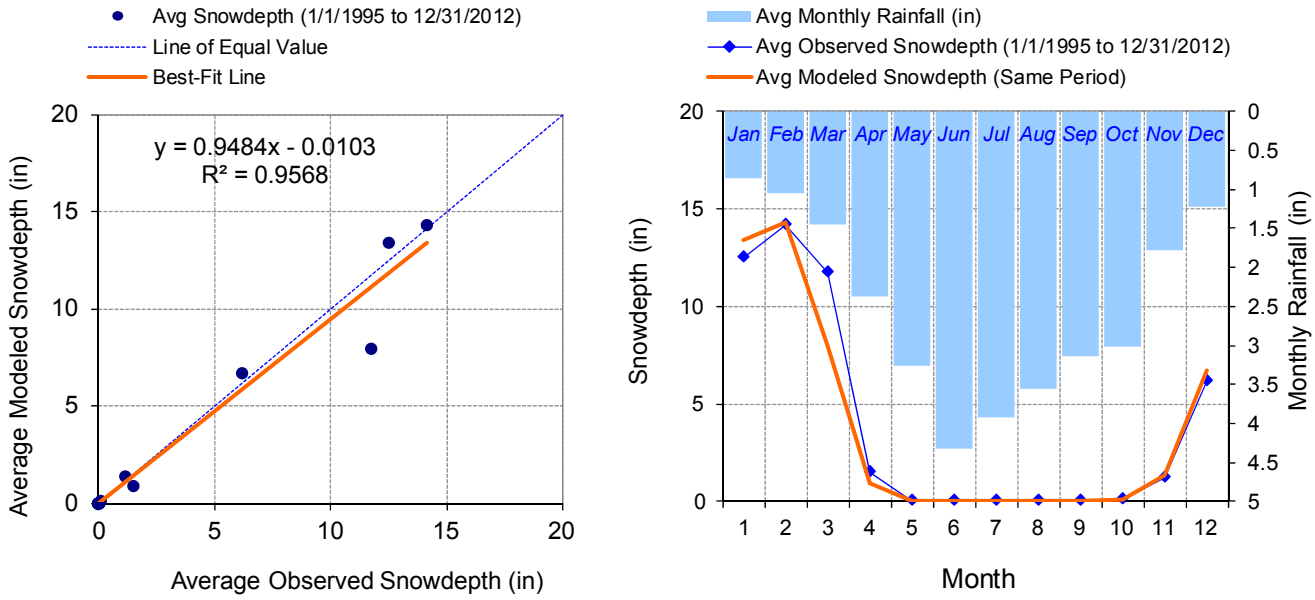

Figure A-14. Seasonal regression and temporal aggregate at MN212248 (Duluth Intl Ap)

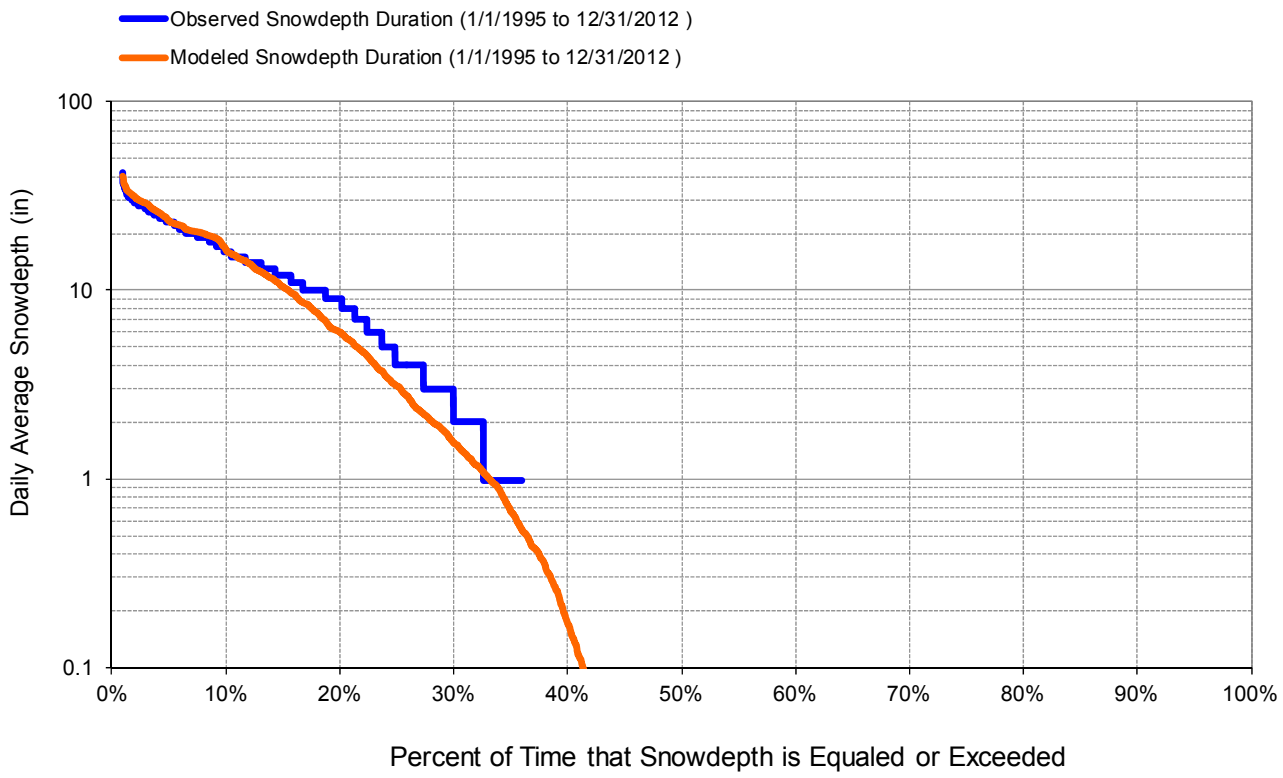

Figure A-15. Snow depth exceedance at MN212248 (Duluth Intl Ap)

Table A-5. Summary statistics at MN212248 (Duluth Intl Ap)

HSPF Simulated Snowdepth		Observed Precipitation Gage	
REACH OUTFLOW FROM DSN 5 18-Year Analysis Period: 1/1/1995 - 12/31/2012 Flow volumes are (inches/year) for upstream drainage area		MN212248 (Duluth Int Ap)	
Total Simulated Snowdepth:	**1343.12**	Total Observed Snowdepth:	**1422.36**
Simulated Summer Snowdepth (months 7-9):	**0.00**	Observed Summer Snowdepth (7-9):	**0.00**
Simulated Fall Snowdepth (months 10-12):	**252.41**	Observed Fall Snowdepth (10-12):	**229.23**
Simulated Winter Snowdepth (months 1-3):	**1063.29**	Observed Winter Snowdepth (1-3):	**1147.44**
Simulated Spring Snowdepth (months 4-6):	**27.42**	Observed Spring Snowdepth (4-6):	**45.68**
Errors (Simulated-Observed)	*Error Statistics*	*Recommended Criteria*	
Error in total snowdepth:	-5.57	10	
Nash-Sutcliffe Coefficient of Efficiency, E:	0.704	Model accuracy increases as E or E' approaches 1.0	
Baseline adjusted coefficient (Garrick), E':	0.686		
Monthly NSE	0.698		

MN212576 (Embarrass)

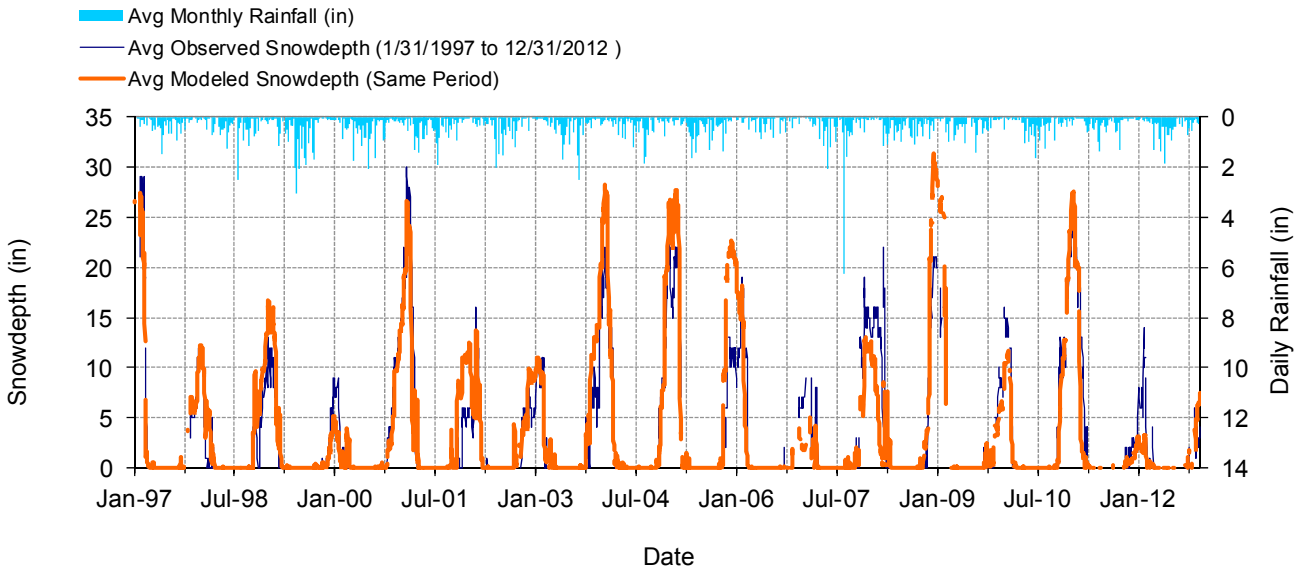

Figure A-16. Mean daily snow depth at MN212576 (Embarrass)

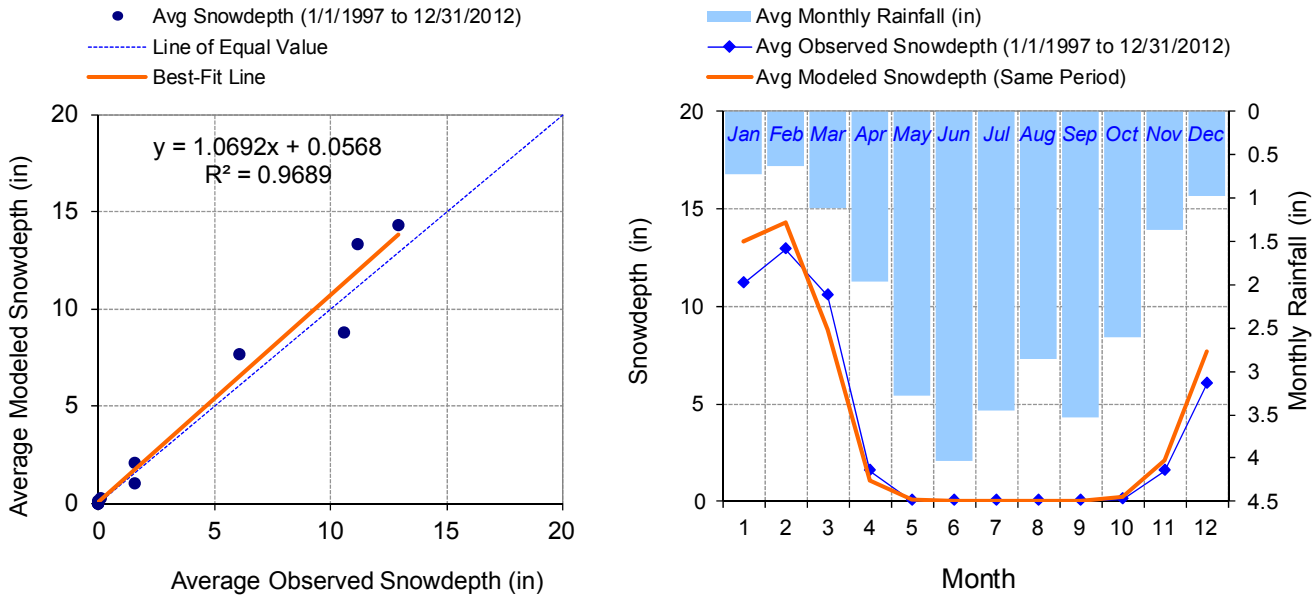

Figure A-17. Seasonal regression and temporal aggregate at MN212576 (Embarrass)

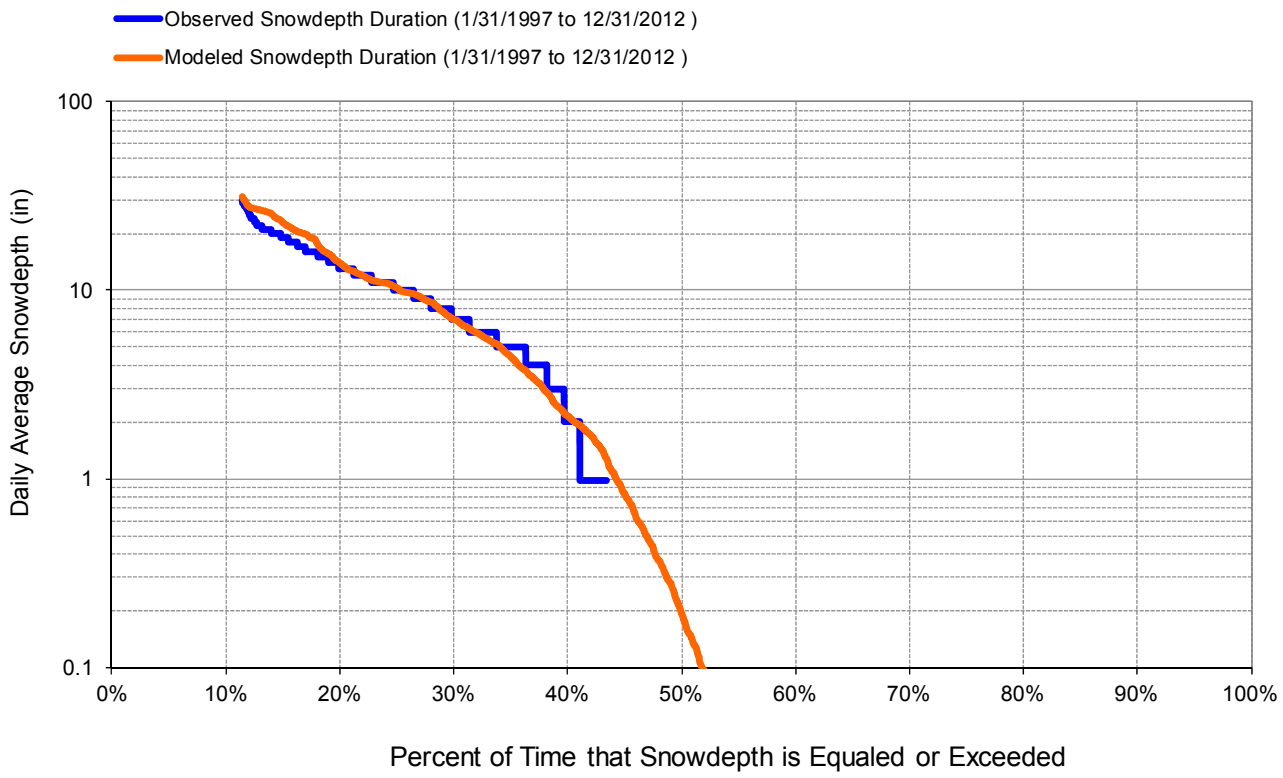

Figure A-18. Snow depth exceedance at MN212576 (Embarrass)

Table A-6. Summary statistics at MN212576 (Embarrass)

HSPF Simulated Snowdepth		Observed Precipitation Gage	
REACH OUTFLOW FROM DSN 6 15.92-Year Analysis Period: 1/1/1997 - 12/31/2012 Flow volumes are (inches/year) for upstream drainage area		MN212576 (Embarrass)	
Total Simulated Snowdepth:	**1256.77**	Total Observed Snowdepth:	**1160.28**
Simulated Summer Snowdepth (months 7-9):	**0.25**	Observed Summer Snowdepth (7-9):	**0.00**
Simulated Fall Snowdepth (months 10-12):	**267.04**	Observed Fall Snowdepth (10-12):	**205.13**
Simulated Winter Snowdepth (months 1-3):	**959.94**	Observed Winter Snowdepth (1-3):	**915.59**
Simulated Spring Snowdepth (months 4-6):	**29.54**	Observed Spring Snowdepth (4-6):	**39.56**
Errors (Simulated-Observed)	*Error Statistics*	*Recommended Criteria*	
Error in total snowdepth:	8.32	10	
Nash-Sutcliffe Coefficient of Efficiency, E:	0.774	Model accuracy increases as E or E' approaches 1.0	
Baseline adjusted coefficient (Garrick), E':	0.700		
Monthly NSE	0.800		

MN212645 (Eveleth WWTP)

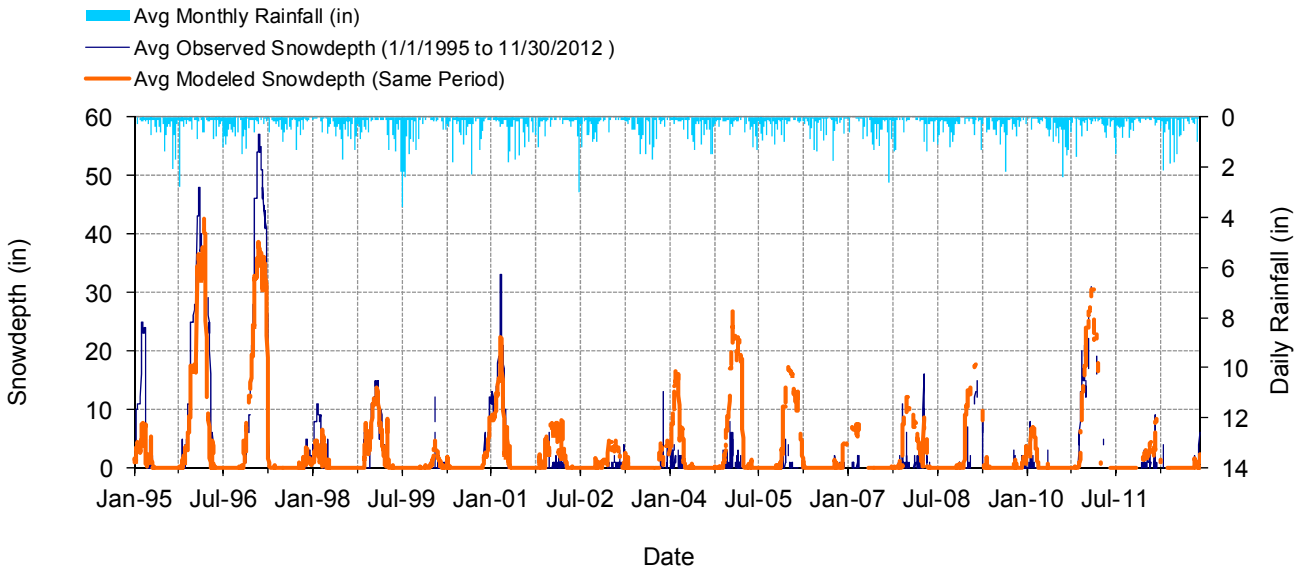

Figure A-19. Mean daily snow depth at MN212645 (Eveleth WWTP)

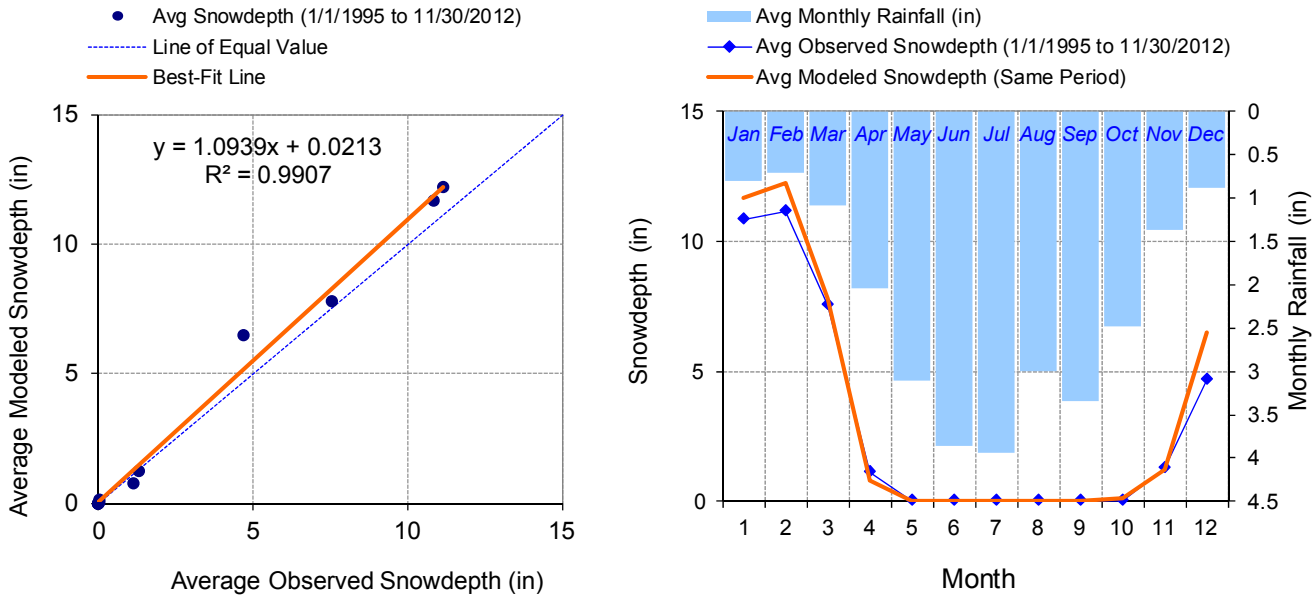

Figure A-20. Seasonal regression and temporal aggregate at MN212645 (Eveleth WWTP)

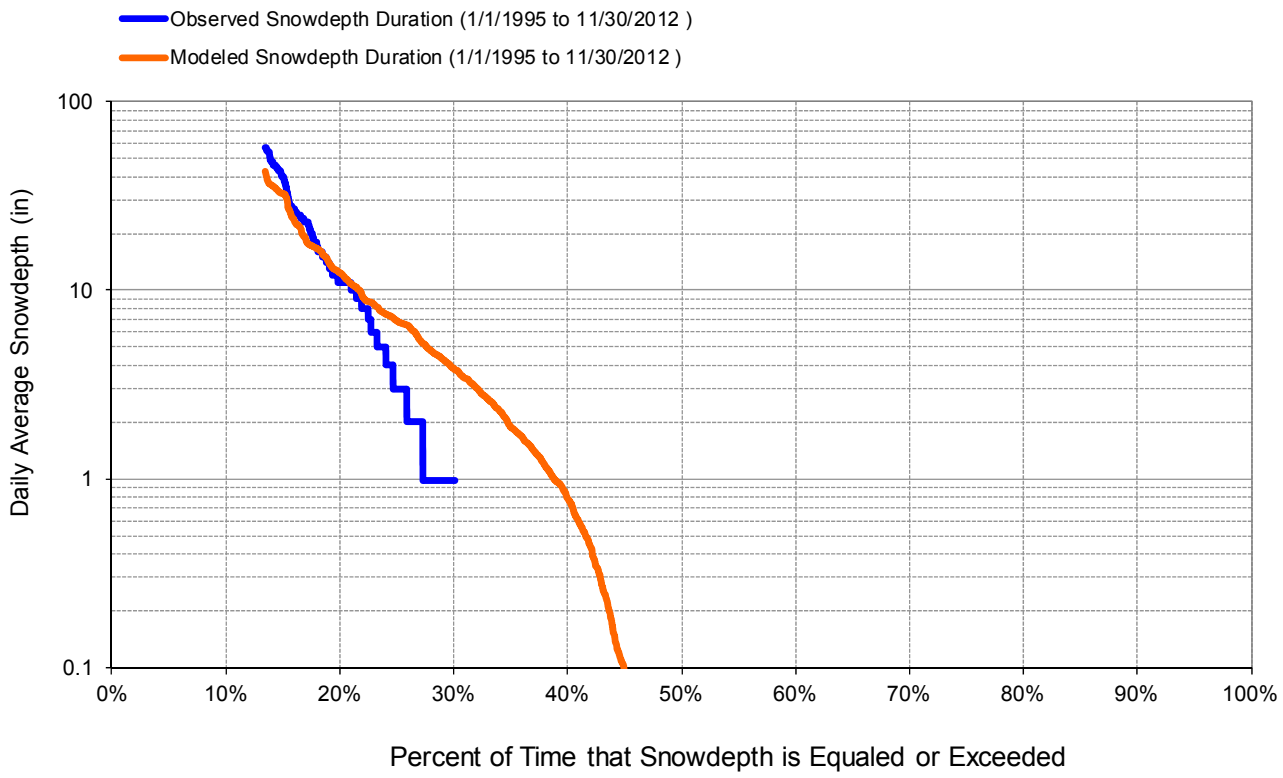

Figure A-21. Snow depth exceedance at MN212645 (Eveleth WWTP)

Table A-7. Summary statistics at MN212645 (Eveleth WWTP)

HSPF Simulated Snowdepth		Observed Precipitation Gage	
REACH OUTFLOW FROM DSN 7 17.92-Year Analysis Period: 1/1/1995 - 11/30/2012 Flow volumes are (inches/year) for upstream drainage area		MN212645 (Eveleth Waste Water Plant)	
Total Simulated Snowdepth:	**896.94**	Total Observed Snowdepth:	**815.51**
Simulated Summer Snowdepth (months 7-9):	**0.03**	Observed Summer Snowdepth (7-9):	**0.00**
Simulated Fall Snowdepth (months 10-12):	**174.97**	Observed Fall Snowdepth (10-12):	**134.01**
Simulated Winter Snowdepth (months 1-3):	**703.72**	Observed Winter Snowdepth (1-3):	**655.49**
Simulated Spring Snowdepth (months 4-6):	**18.22**	Observed Spring Snowdepth (4-6):	**26.00**
Errors (Simulated-Observed)	*Error Statistics*	*Recommended Criteria*	
Error in total snowdepth:	9.98	10	
Nash-Sutcliffe Coefficient of Efficiency, E:	0.734	Model accuracy increases as E or E' approaches 1.0	
Baseline adjusted coefficient (Garrick), E':	0.593		
Monthly NSE	0.782		

MN212842 (Floodwood 3 NE)

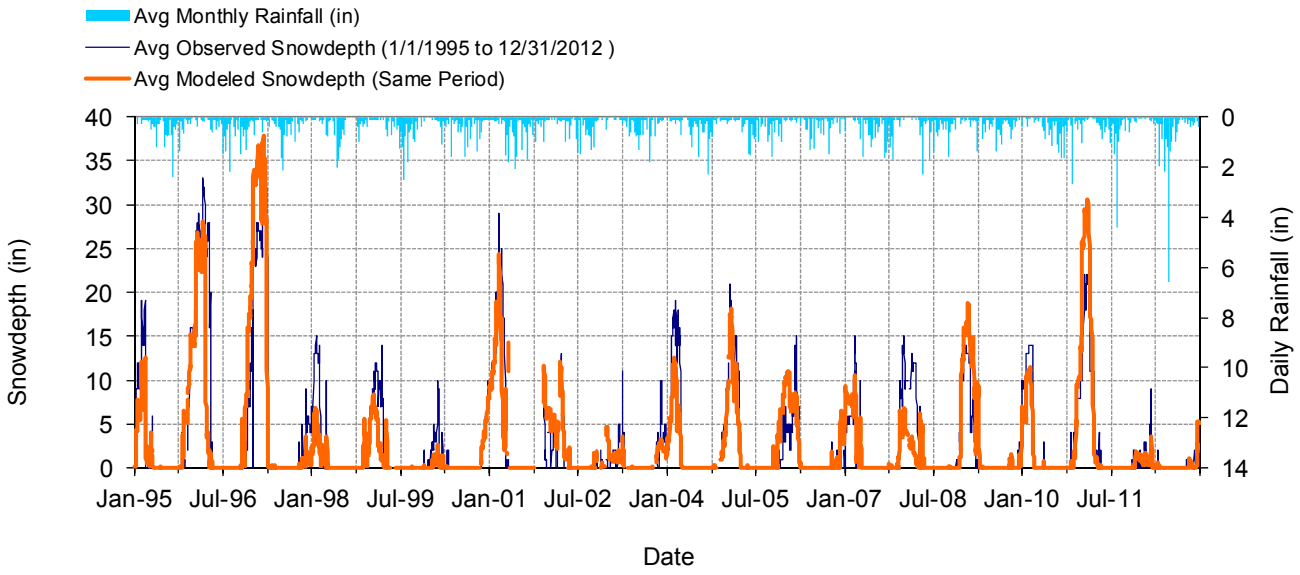

Figure A-22. Mean daily snow depth at MN212842 (Floodwood 3 NE)

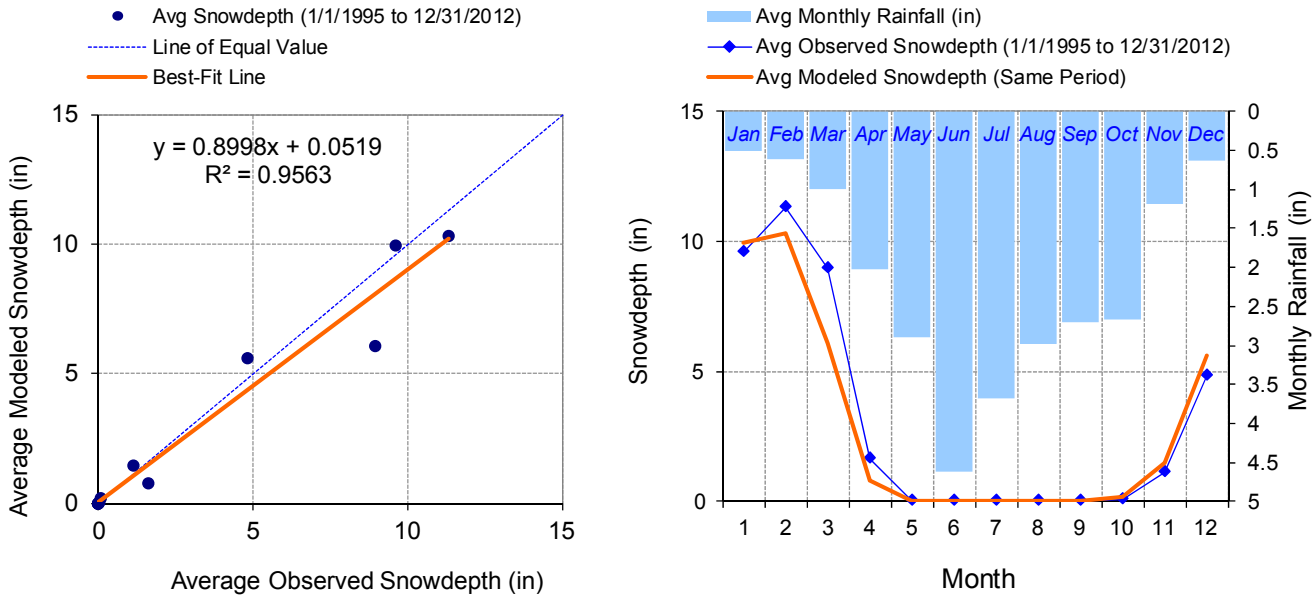

Figure A-23. Seasonal regression and temporal aggregate at MN212842 (Floodwood 3 NE)

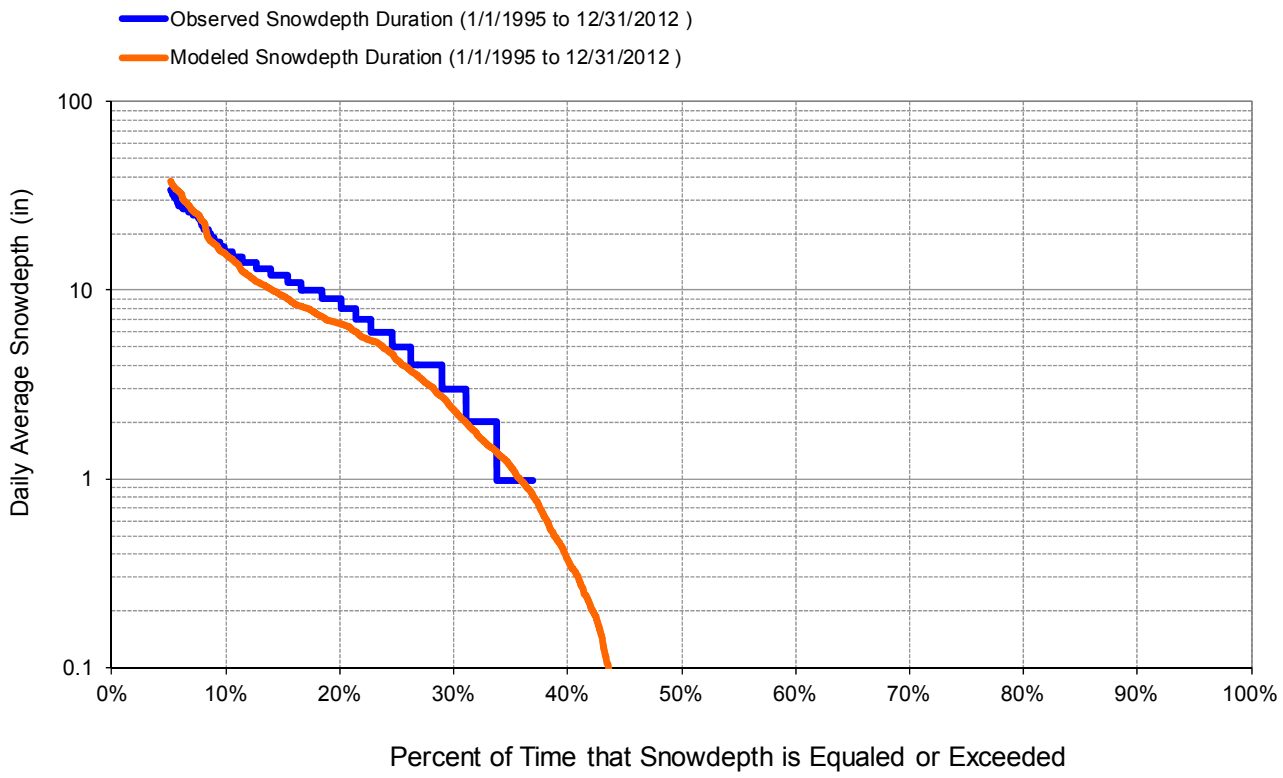

Figure A-24. Snow depth exceedance at MN212842 (Floodwood 3 NE)

Table A-8. Summary statistics at MN212842 (Floodwood 3 NE)

HSPF Simulated Snowdepth		**Observed Precipitation Gage**	
REACH OUTFLOW FROM DSN 8 18-Year Analysis Period: 1/1/1995 - 12/31/2012 Flow volumes are (inches/year) for upstream drainage area		MN212842 (Floodwood 3 NE)	
Total Simulated Snowdepth:	**1004.22**	Total Observed Snowdepth:	**1096.00**
Simulated Summer Snowdepth (months 7-9):	**0.06**	Observed Summer Snowdepth (7-9):	**0.00**
Simulated Fall Snowdepth (months 10-12):	**205.30**	Observed Fall Snowdepth (10-12):	**171.93**
Simulated Winter Snowdepth (months 1-3):	**777.78**	Observed Winter Snowdepth (1-3):	**880.97**
Simulated Spring Snowdepth (months 4-6):	**21.08**	Observed Spring Snowdepth (4-6):	**43.10**
Errors (Simulated-Observed)	*Error Statistics*	*Recommended Criteria*	
Error in total snowdepth:	-8.37	10	
Nash-Sutcliffe Coefficient of Efficiency, E:	0.741	Model accuracy increases as E or E' approaches 1.0	
Baseline adjusted coefficient (Garrick), E':	0.680		
Monthly NSE	0.760		

MN213730 (Hibbing FAA Ap)

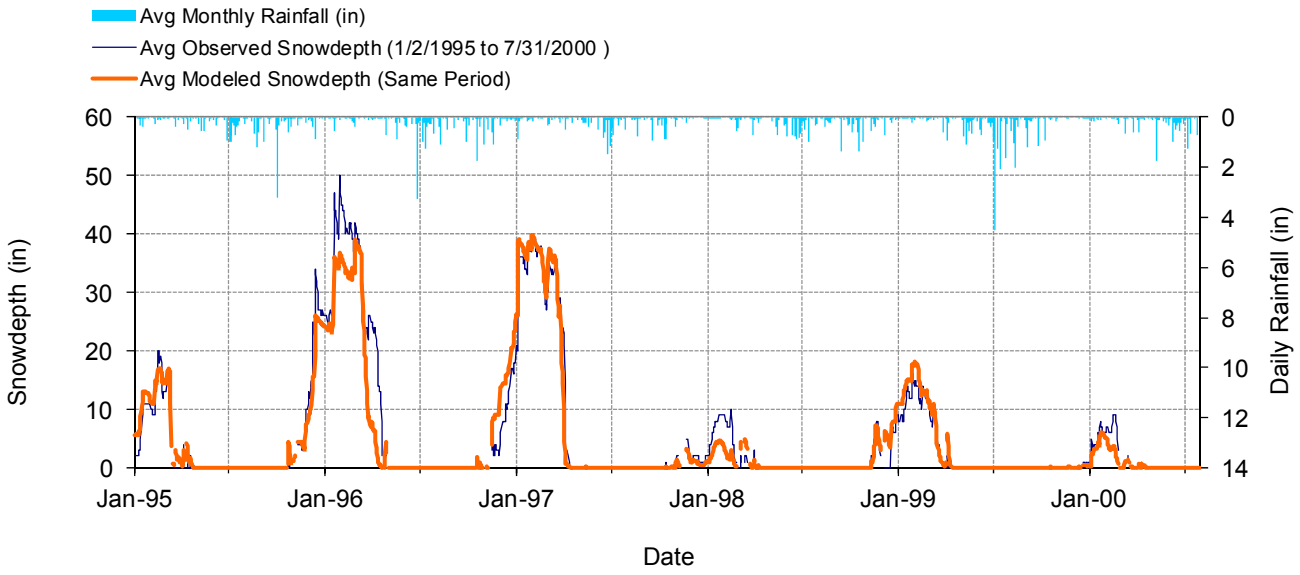

Figure A-25. Mean daily snow depth at MN213730 (Hibbing FAA Ap)

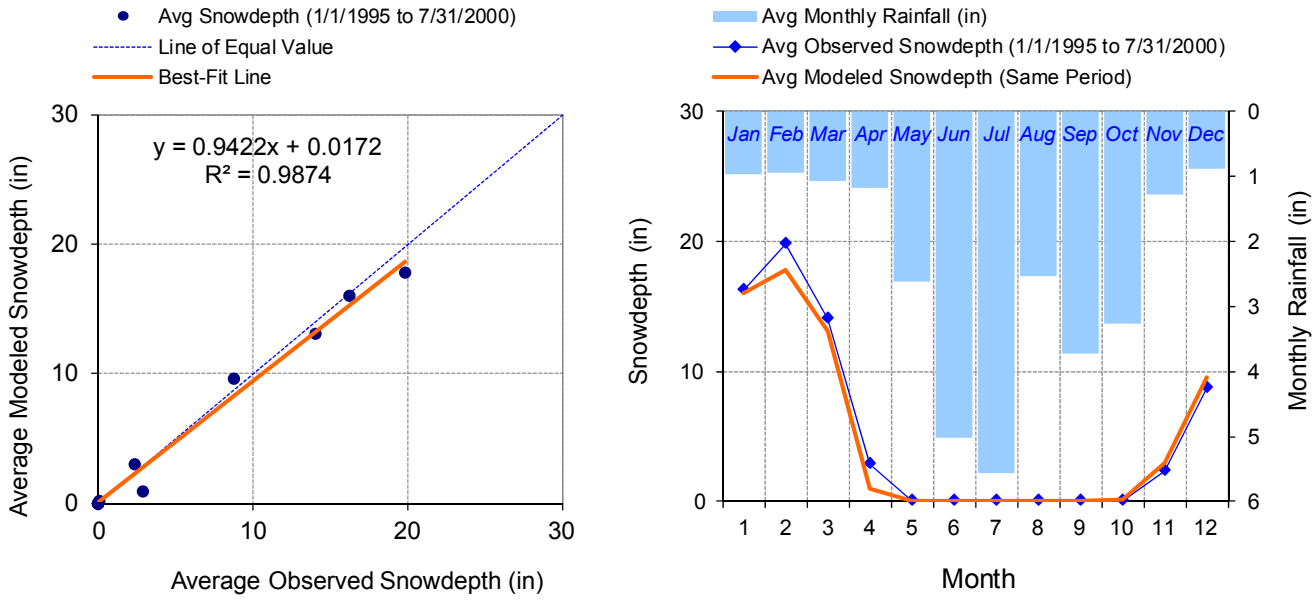

Figure A-26. Seasonal regression and temporal aggregate at MN213730 (Hibbing FAA Ap)

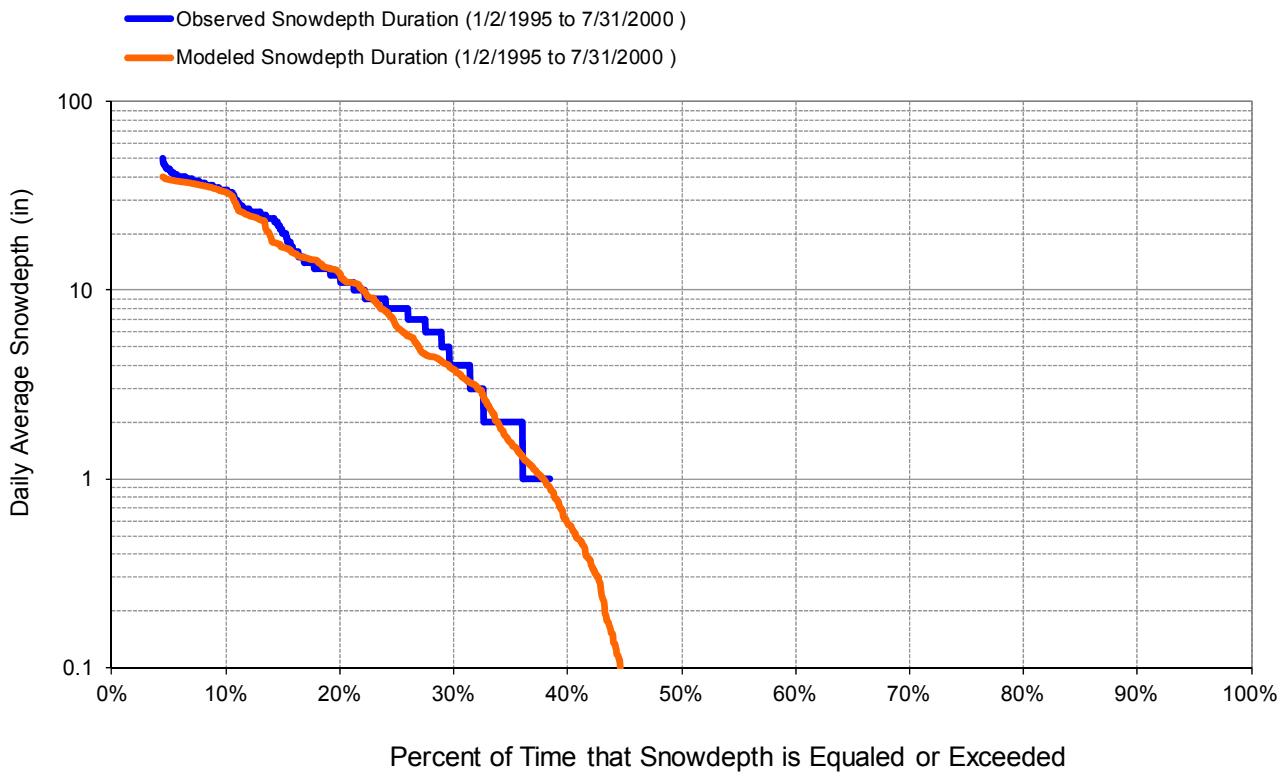

Figure A-27. Snow depth exceedance at MN213730 (Hibbing FAA Ap)

Table A-9. Summary statistics at MN213730 (Hibbing FAA Ap)

HSPF Simulated Snowdepth		**Observed Precipitation Gage**	
REACH OUTFLOW FROM DSN 9 5.58-Year Analysis Period: 1/1/1995 - 7/31/2000 Flow volumes are (inches/year) for upstream drainage area		MN213730 (Hibbing FAA Airport)	
Total Simulated Snowdepth:	**1780.38**	Total Observed Snowdepth:	**1891.13**
Simulated Summer Snowdepth (months 7-9):	**0.00**	Observed Summer Snowdepth (7-9):	**0.00**
Simulated Fall Snowdepth (months 10-12):	**318.83**	Observed Fall Snowdepth (10-12):	**279.94**
Simulated Winter Snowdepth (months 1-3):	**1434.06**	Observed Winter Snowdepth (1-3):	**1528.21**
Simulated Spring Snowdepth (months 4-6):	**27.49**	Observed Spring Snowdepth (4-6):	**82.98**
Errors (Simulated-Observed)	*Error Statistics*	*Recommended Criteria*	
Error in total snowdepth:	-5.86	10	
Nash-Sutcliffe Coefficient of Efficiency, E:	0.924	Model accuracy increases as E or E' approaches 1.0	
Baseline adjusted coefficient (Garrick), E':	0.836		
Monthly NSE	0.944		

WI476413 (Pattison State Park)

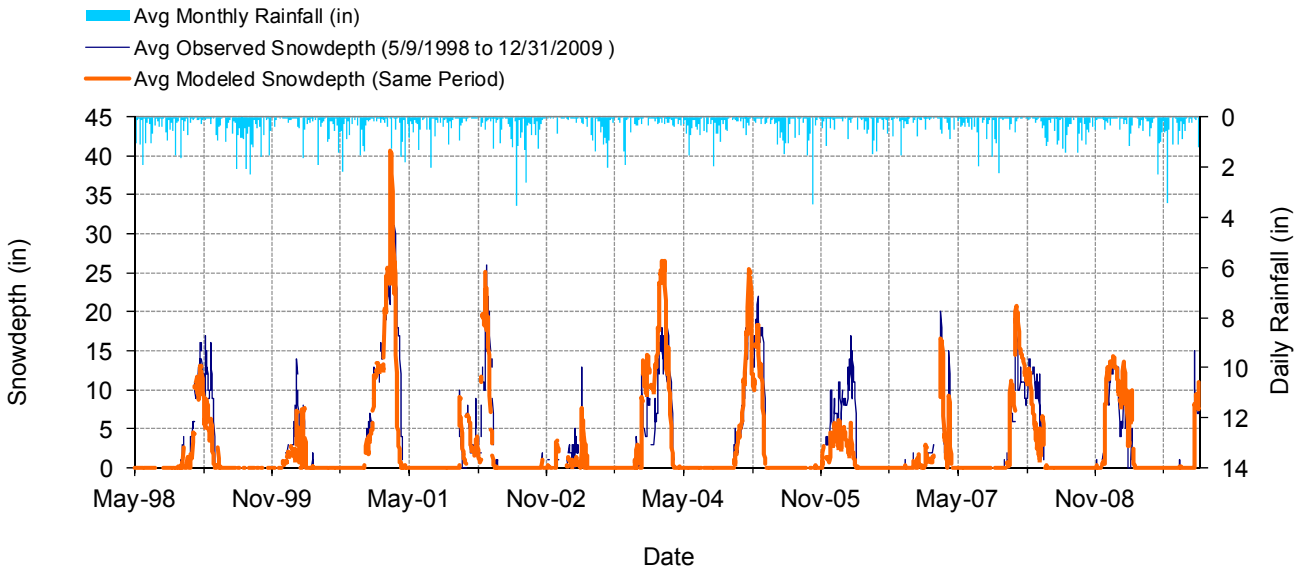

Figure A-28. Mean daily snow depth at WI476413 (Pattison State Park)

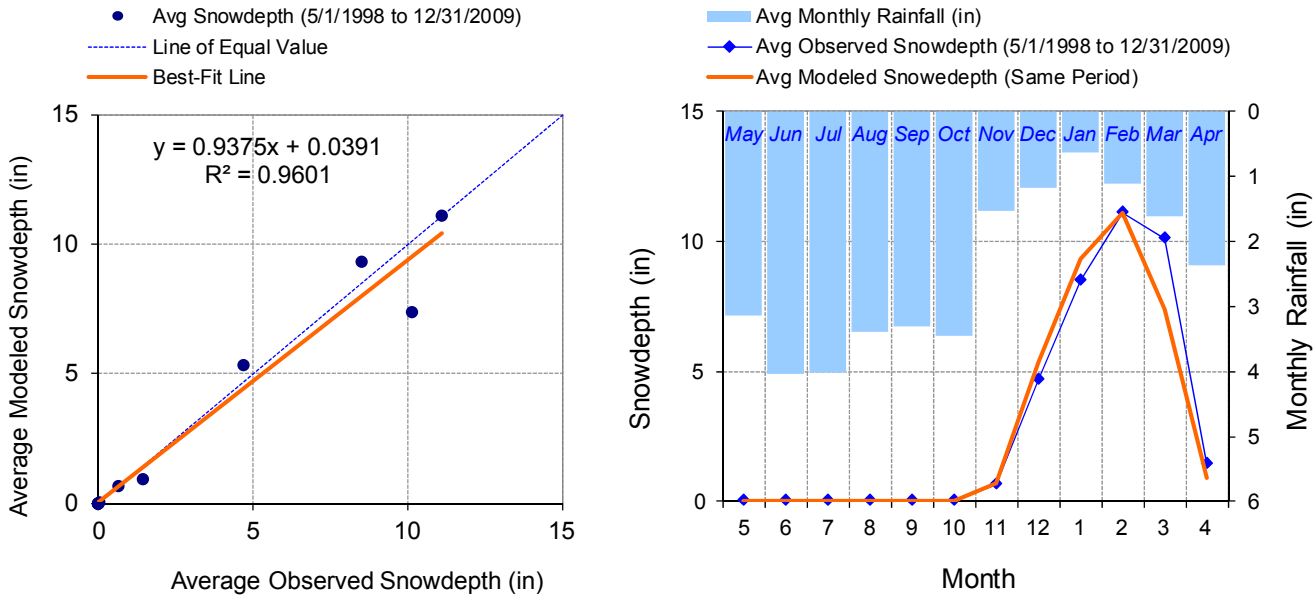

Figure A-29. Seasonal regression and temporal aggregate at WI476413 (Pattison State Park)

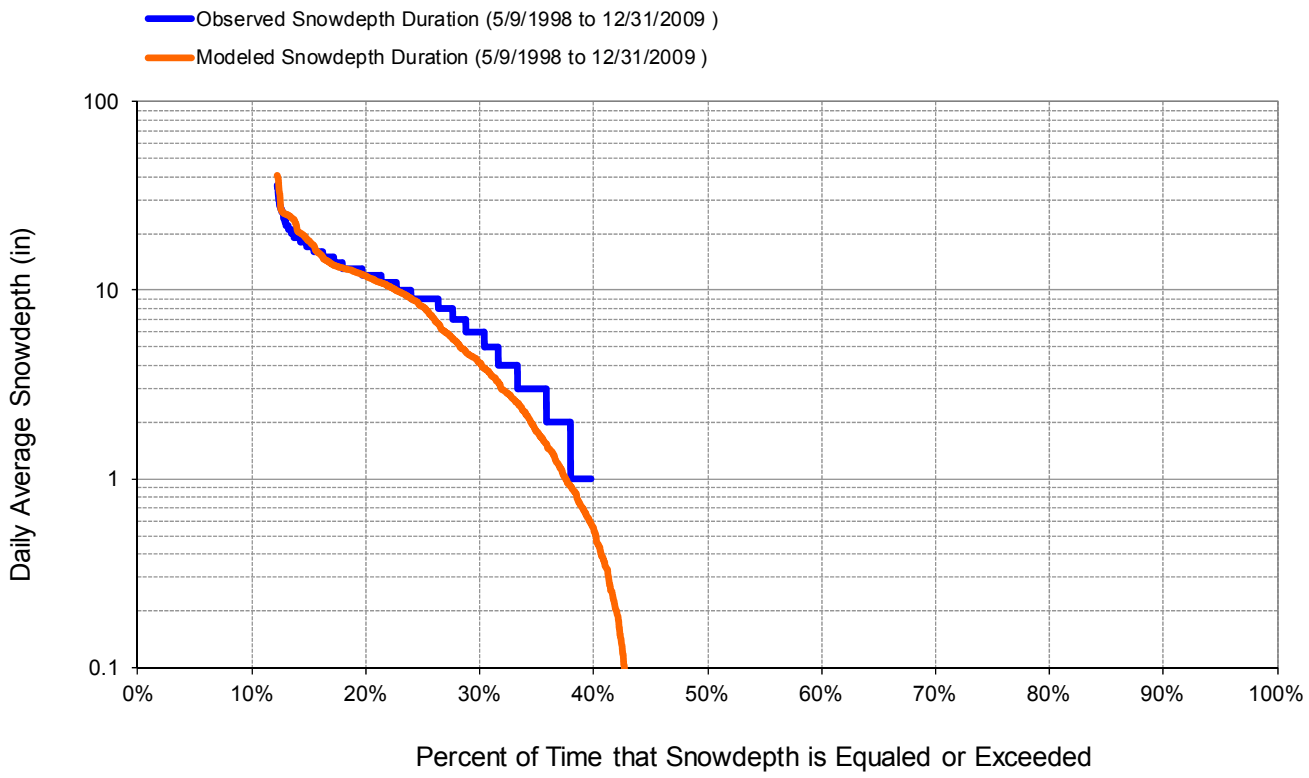

Figure A-30. Snow depth exceedance at WI476413 (Pattison State Park)

Table A-10. Summary statistics at WI476413 (Pattison State Park)

HSPF Simulated Snowdepth		Observed Precipitation Gage	
REACH OUTFLOW FROM DSN 11 11.65-Year Analysis Period: 5/1/1998 - 12/31/2009 Flow volumes are (inches/year) for upstream drainage area		WI476413 Manually Entered Data Drainage Area (sq-mi): 3430	
Total Simulated Snowdepth:	**865.14**	Total Observed Snowdepth:	**917.46**
Simulated Summer Snowdepth (months 7-9):	**0.00**	Observed Summer Snowdepth (7-9):	**0.00**
Simulated Fall Snowdepth (months 10-12):	**155.31**	Observed Fall Snowdepth (10-12):	**138.37**
Simulated Winter Snowdepth (months 1-3):	**687.38**	Observed Winter Snowdepth (1-3):	**743.63**
Simulated Spring Snowdepth (months 4-6):	**22.45**	Observed Spring Snowdepth (4-6):	**35.45**
Errors (Simulated-Observed)	*Error Statistics*	*Recommended Criteria*	
Error in total snowdepth:	-5.70	10	
Nash-Sutcliffe Coefficient of Efficiency, E:	0.577	Model accuracy increases	
Baseline adjusted coefficient (Garrick), E':	0.582	as E or E' approaches 1.0	
Monthly NSE	0.729		

WI478349 (Superior)

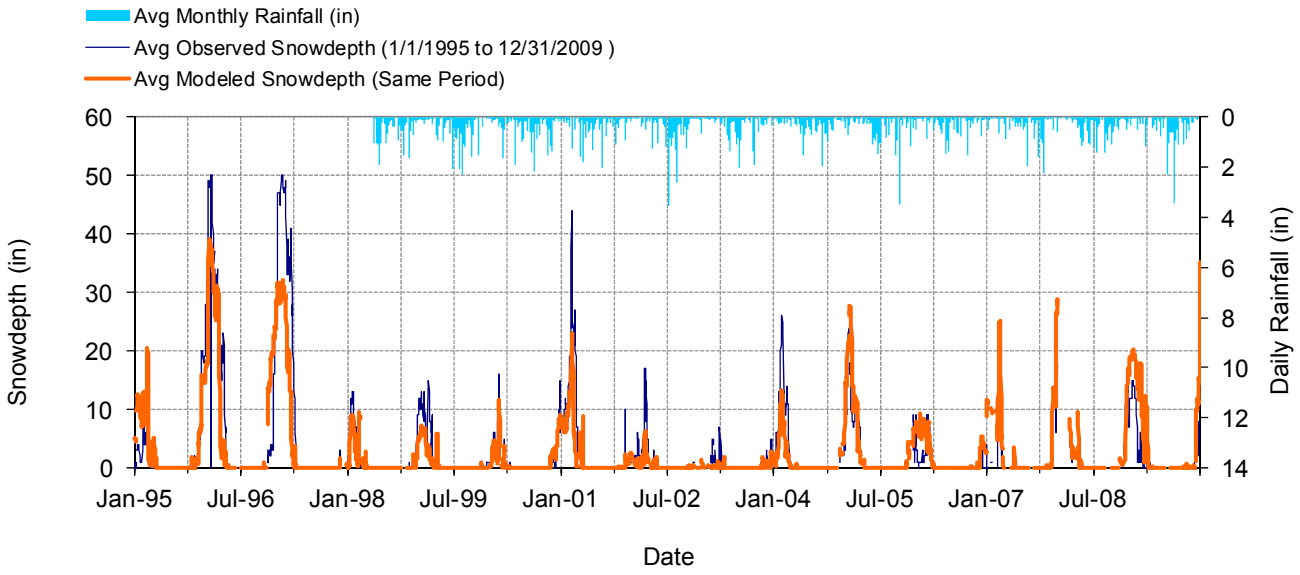

Figure A-31. Mean daily snow depth at WI478349 (Superior)

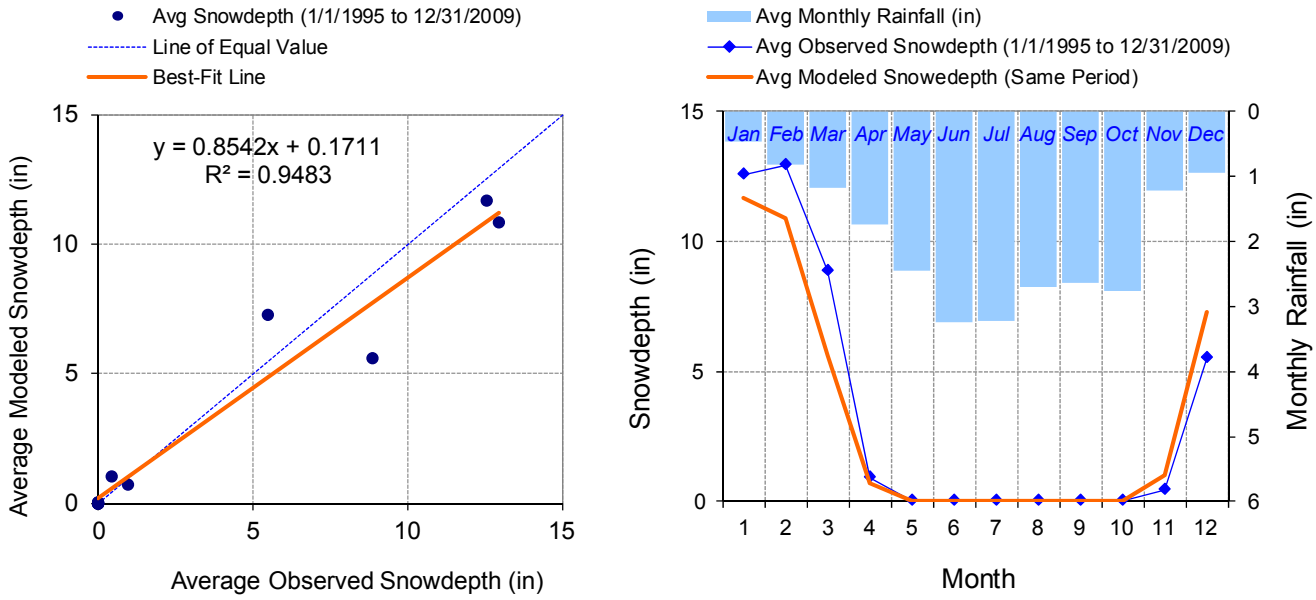

Figure A-32. Seasonal regression and temporal aggregate at WI478349 (Superior)

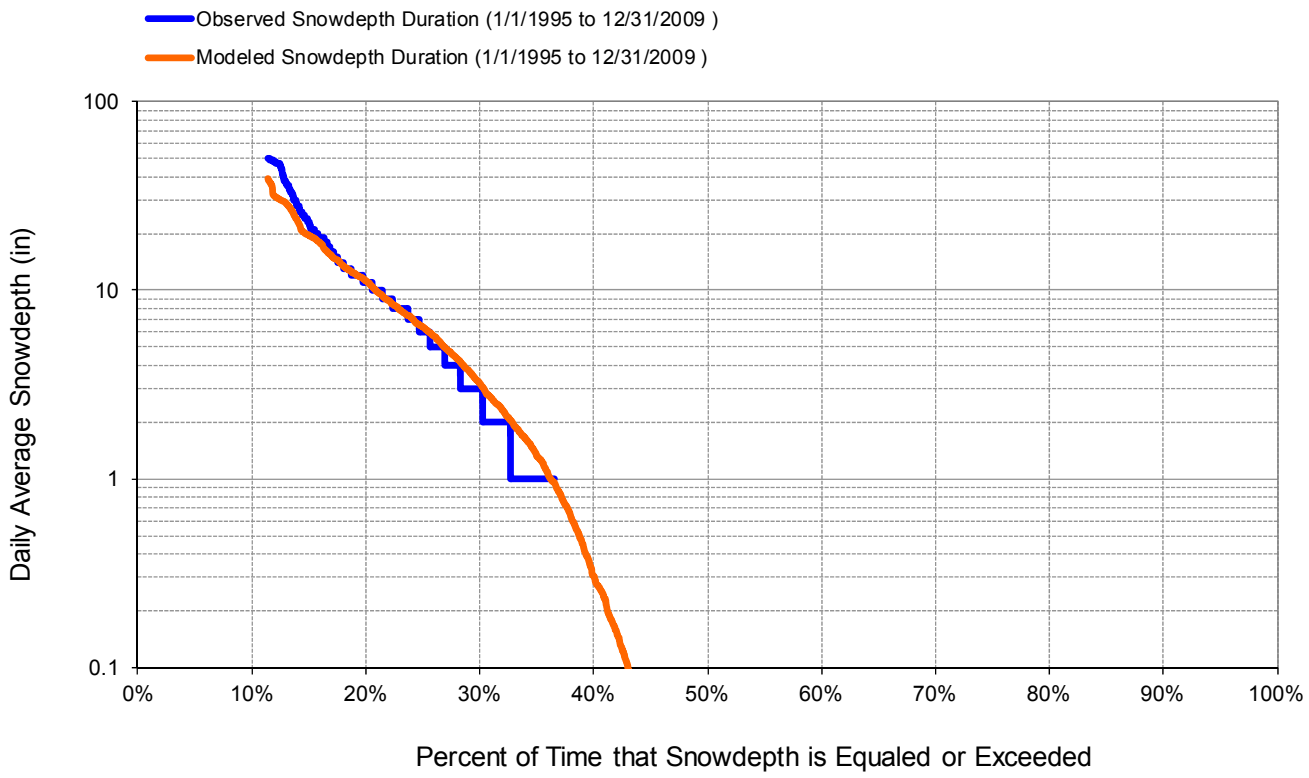

Figure A-33. Snow depth exceedance at WI478349 (Superior)

Table A-11. Summary statistics at WI478349 (Superior)

HSPF Simulated Snowdepth		Observed Precipitation Gage	
REACH OUTFLOW FROM DSN 12 15-Year Analysis Period: 1/1/1995 - 12/31/2009 Flow volumes are (inches/year) for upstream drainage area		WI478349 Manually Entered Data Drainage Area (sq-mi): 3430	
Total Simulated Snowdepth:	**927.34**	Total Observed Snowdepth:	**1029.95**
Simulated Summer Snowdepth (months 7-9):	**0.00**	Observed Summer Snowdepth (7-9):	**0.00**
Simulated Fall Snowdepth (months 10-12):	**206.72**	Observed Fall Snowdepth (10-12):	**146.19**
Simulated Winter Snowdepth (months 1-3):	**702.42**	Observed Winter Snowdepth (1-3):	**860.43**
Simulated Spring Snowdepth (months 4-6):	**18.20**	Observed Spring Snowdepth (4-6):	**23.33**
Errors (Simulated-Observed)	*Error Statistics*	*Recommended Criteria*	
Error in total snowdepth:	-9.96	10	
Nash-Sutcliffe Coefficient of Efficiency, E:	0.577	Model accuracy increases	
Baseline adjusted coefficient (Garrick), E':	0.582	as E or E' approaches 1.0	
Monthly NSE	0.762		

Appendix B. Detailed Evapotranspiration Calibration Results

MN210387 (Babbitt) and MN210989 (Brimson 1E)

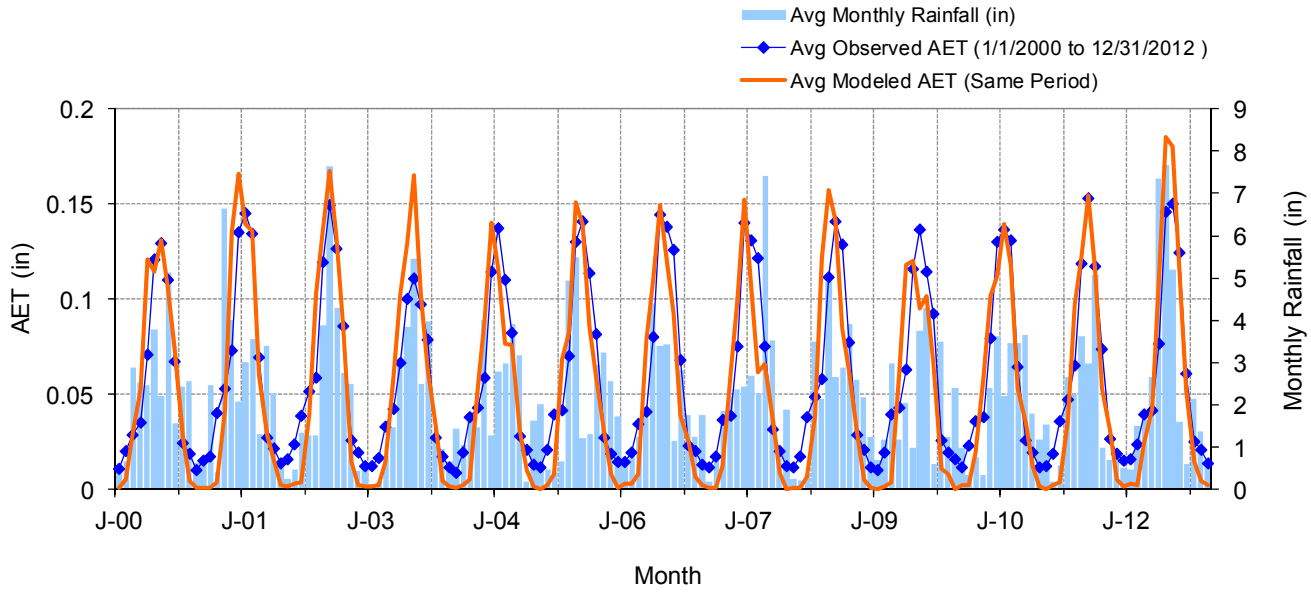

Figure B-1. Mean monthly AET at MN210387 (Babbitt) and MN210989 (Brimson 1E)

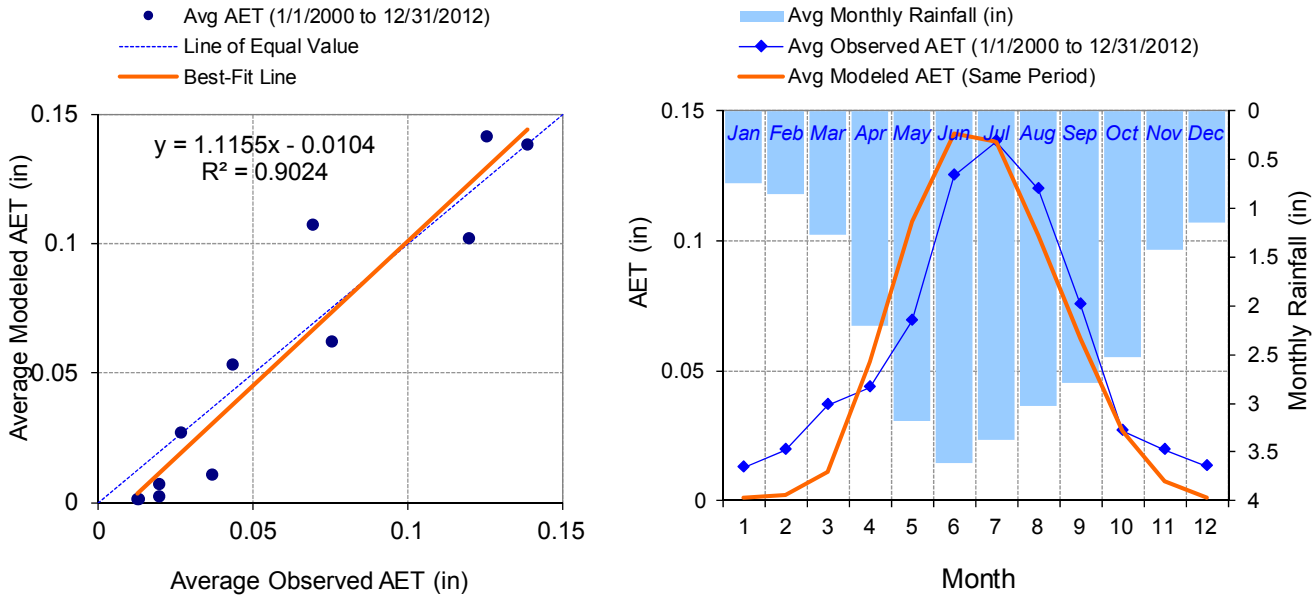

Figure B-2. Seasonal regression and temporal aggregate at MN210387 (Babbitt) and MN210989 (Brimson 1E)

Table B-1. Summary statistics at MN210387 (Babbitt) and MN210989 (Brimson 1E)

HSPF Simulated AET		Observed Precipitation Gage		
REACH OUTFLOW FROM DSN 101 13-Year Analysis Period: 1/1/2000 - 12/31/2012 Flow volumes are (inches/year) for upstream drainage area		MN210387 (Babbitt) and MN210989 (Brimson 1E) Manually Entered Data		
Total Simulated AET:	**20.04**	Total Observed AET:		**21.37**
Simulated Summer AET (months 7-9):	**9.32**	Observed Summer AET (7-9):		**10.26**
Simulated Fall AET (months 10-12):	**1.10**	Observed Fall AET (10-12):		**1.82**
Simulated Winter AET (months 1-3):	**0.45**	Observed Winter AET (1-3):		**2.09**
Simulated Spring AET (months 4-6):	**9.17**	Observed Spring AET (4-6):		**7.20**
Errors (Simulated-Observed)	*Error Statistics*	*Recommended Criteria*		
Error in total AET:	-6.22	10		
Monthly NSE	0.766			

MN211630 (Cloquet)

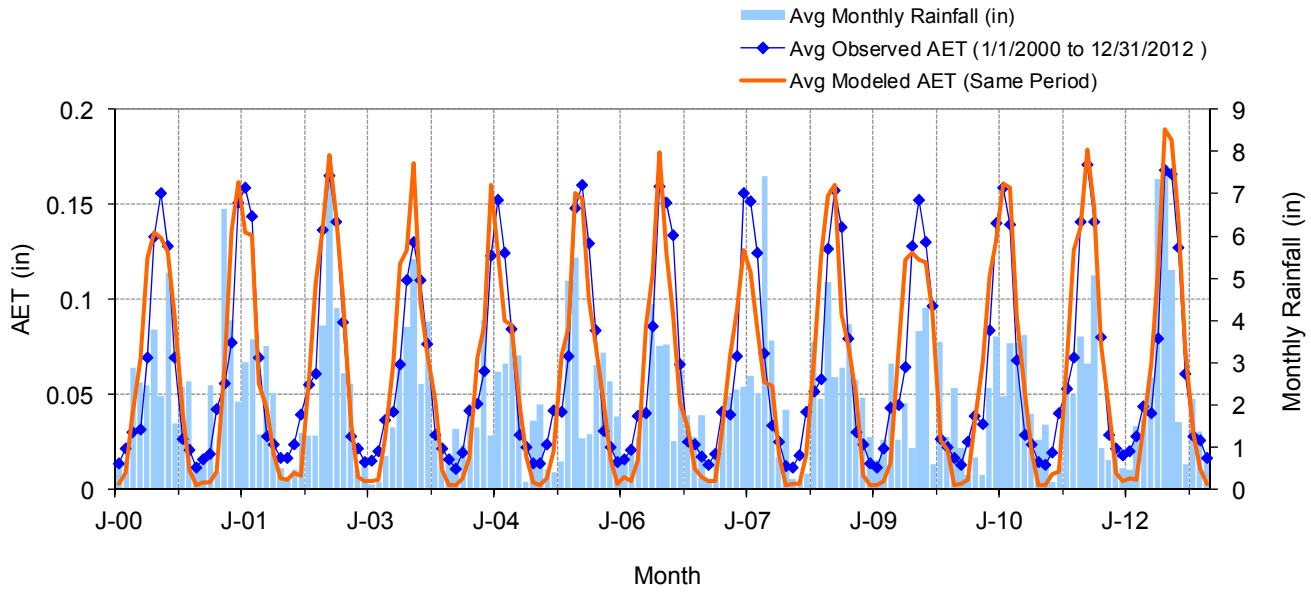

Figure B-3. Mean monthly AET at MN211630 (Cloquet)

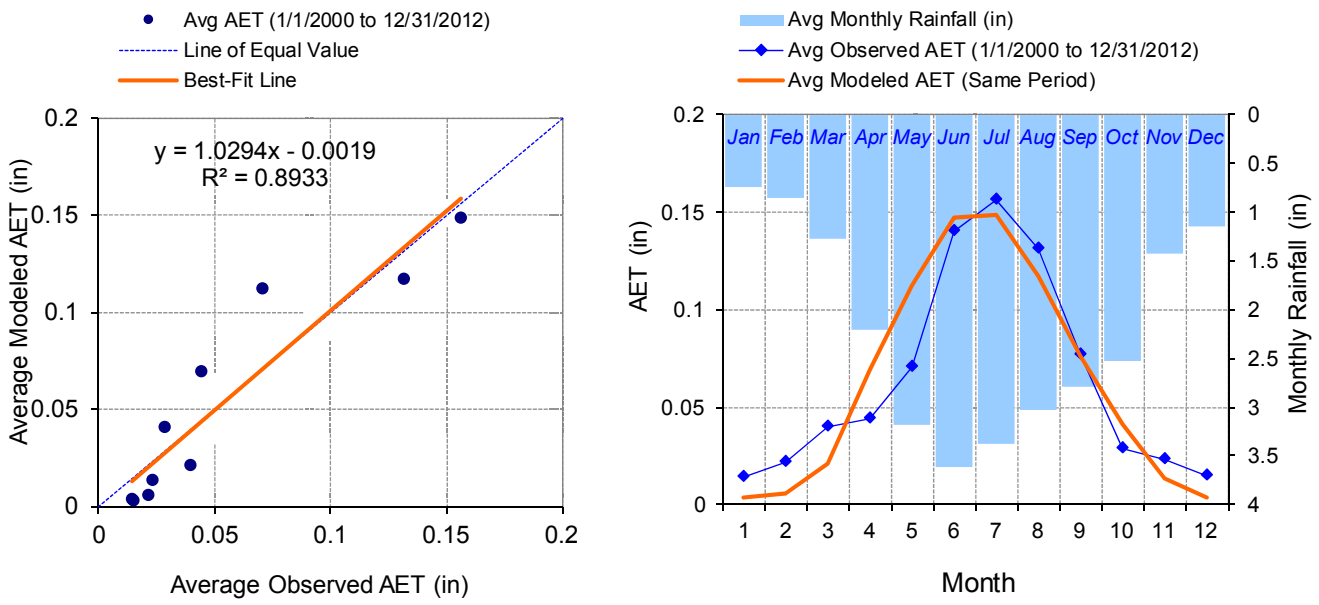

Figure B-4. Seasonal regression and temporal aggregate at MN211630 (Cloquet)

Table B-2. Summary statistics at MN211630 (Cloquet)

HSPF Simulated AET		**Observed Precipitation Gage**		
REACH OUTFLOW FROM DSN 103 13-Year Analysis Period: 1/1/2000 - 12/31/2012 Flow volumes are (inches/year) for upstream drainage area		MN211630 (Cloquet) Manually Entered Data		
Total Simulated AET:	**23.28**	Total Observed AET:		**23.26**
Simulated Summer AET (months 7-9):	**10.56**	Observed Summer AET (7-9):		**11.21**
Simulated Fall AET (months 10-12):	**1.79**	Observed Fall AET (10-12):		**2.05**
Simulated Winter AET (months 1-3):	**0.94**	Observed Winter AET (1-3):		**2.28**
Simulated Spring AET (months 4-6):	**9.99**	Observed Spring AET (4-6):		**7.71**
Errors (Simulated-Observed)	*Error Statistics*	*Recommended Criteria*		
Error in total AET:	0.08	10		
Monthly NSE	0.809			

MN211840 (Cotton) and Janzen E

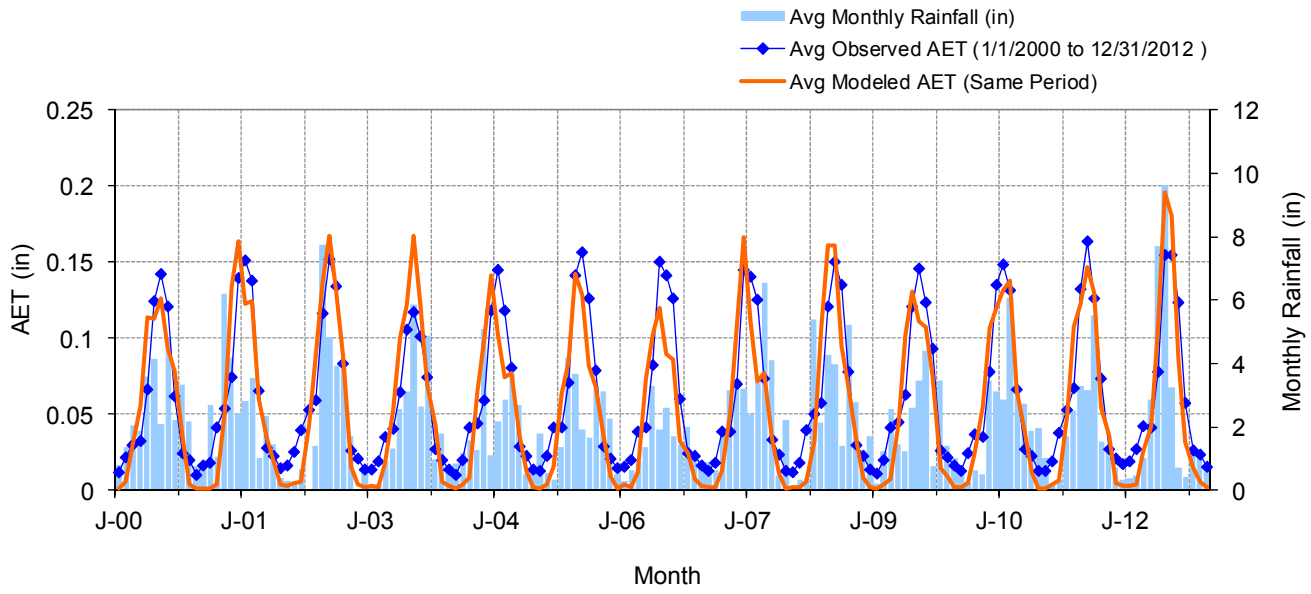

Figure B-5. Mean monthly AET at MN211840 (Cotton) and Janzen E

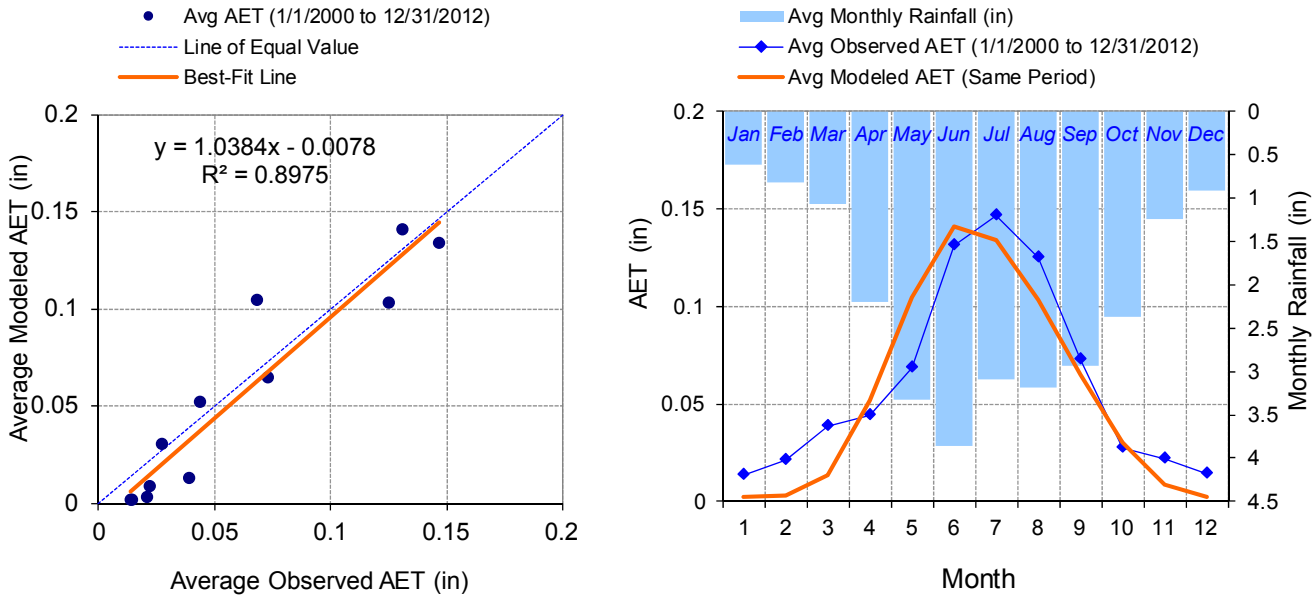

Figure B-6. Seasonal regression and temporal aggregate at MN211840 (Cotton) and Janzen E

Table B-3. Summary statistics at MN211840 (Cotton) and Janzen E

HSPF Simulated AET		Observed Precipitation Gage		
REACH OUTFLOW FROM DSN 104 13-Year Analysis Period: 1/1/2000 - 12/31/2012 Flow volumes are (inches/year) for upstream drainage area		MN211840 (Cotton) and Janzen E Manually Entered Data		
Total Simulated AET:	**20.17**	Total Observed AET:		**22.14**
Simulated Summer AET (months 7-9):	**9.31**	Observed Summer AET (7-9):		**10.61**
Simulated Fall AET (months 10-12):	**1.26**	Observed Fall AET (10-12):		**1.94**
Simulated Winter AET (months 1-3):	**0.57**	Observed Winter AET (1-3):		**2.22**
Simulated Spring AET (months 4-6):	**9.03**	Observed Spring AET (4-6):		**7.37**
Errors (Simulated-Observed)	*Error Statistics*	*Recommended Criteria*		
Error in total AET:	-8.90	10		
Monthly NSE	0.774			

MN212248 (Duluth Intl Ap) and Pomroy

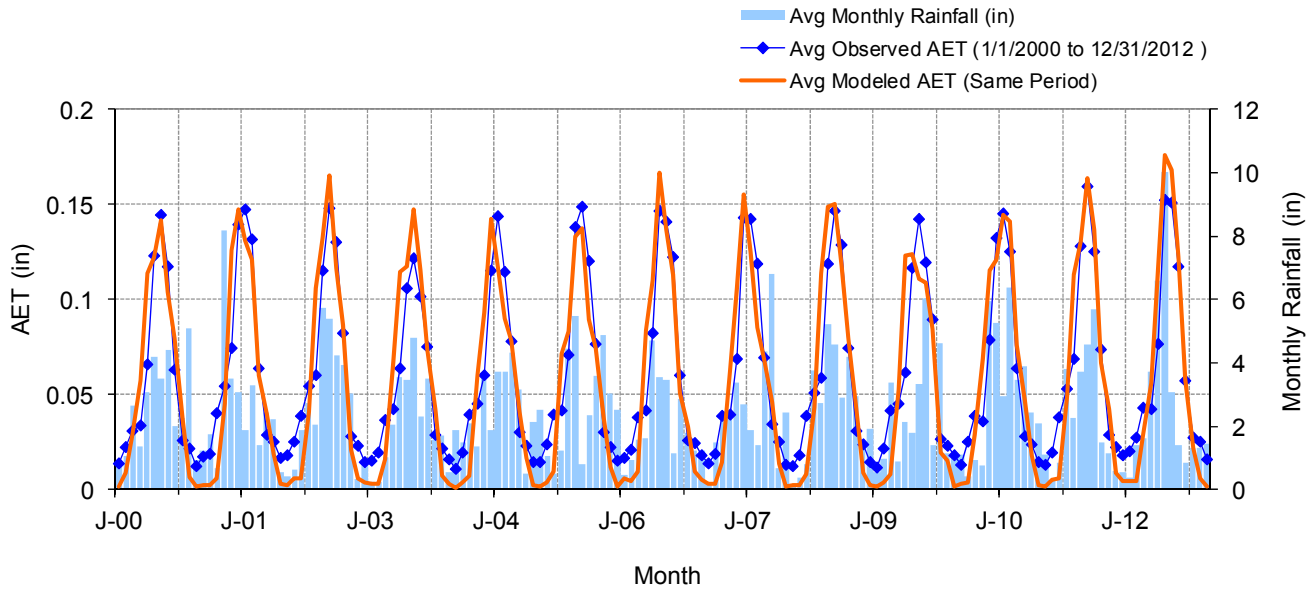

Figure B-7. Mean monthly AET at MN212248 (Duluth Intl Ap) and Pomroy

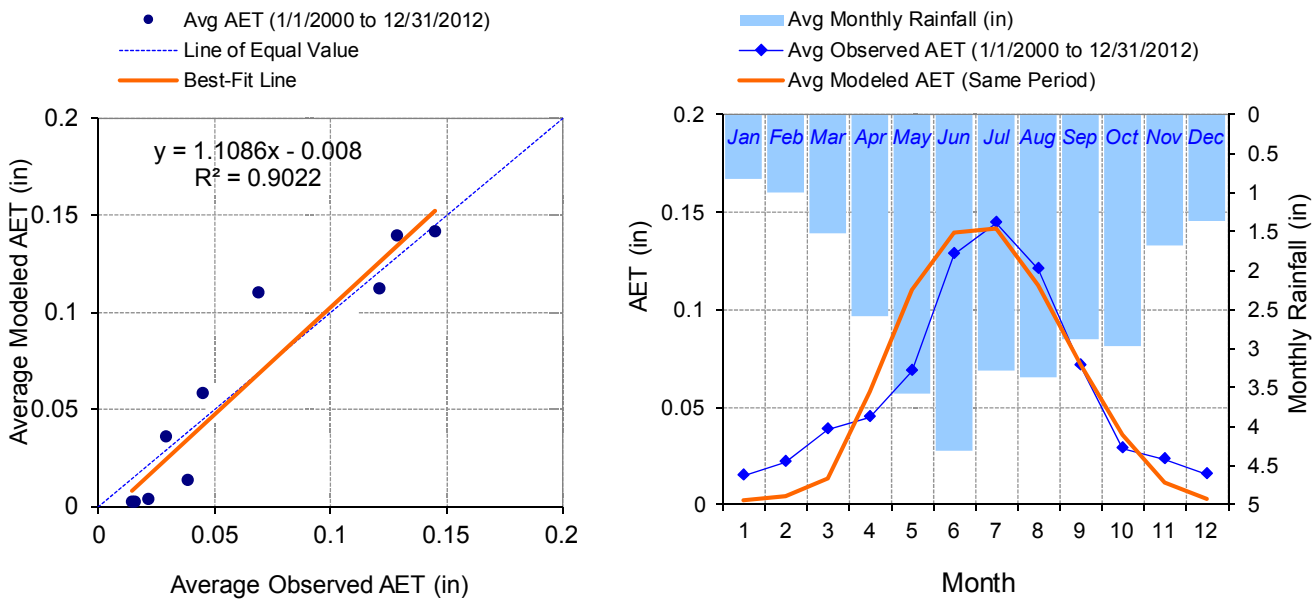

Figure B-8. Seasonal regression and temporal aggregate at MN212248 (Duluth Intl Ap) and Pomroy

Table B-4. Summary statistics at MN212248 (Duluth Intl Ap) and Pomroy

HSPF Simulated AET		Observed Precipitation Gage	
REACH OUTFLOW FROM DSN 105 13-Year Analysis Period: 1/1/2000 - 12/31/2012 Flow volumes are (inches/year) for upstream drainage area		MN212248 (Duluth Int Ap) and Pomroy Manually Entered Data	
Total Simulated AET:	**21.54**	Total Observed AET:	**22.04**
Simulated Summer AET (months 7-9):	**10.03**	Observed Summer AET (7-9):	**10.38**
Simulated Fall AET (months 10-12):	**1.54**	Observed Fall AET (10-12):	**2.08**
Simulated Winter AET (months 1-3):	**0.62**	Observed Winter AET (1-3):	**2.26**
Simulated Spring AET (months 4-6):	**9.35**	Observed Spring AET (4-6):	**7.33**
Errors (Simulated-Observed)	*Error Statistics*	*Recommended Criteria*	
Error in total AET:	-2.31	10	
Monthly NSE	0.802		

MN212576 (Embarrass)

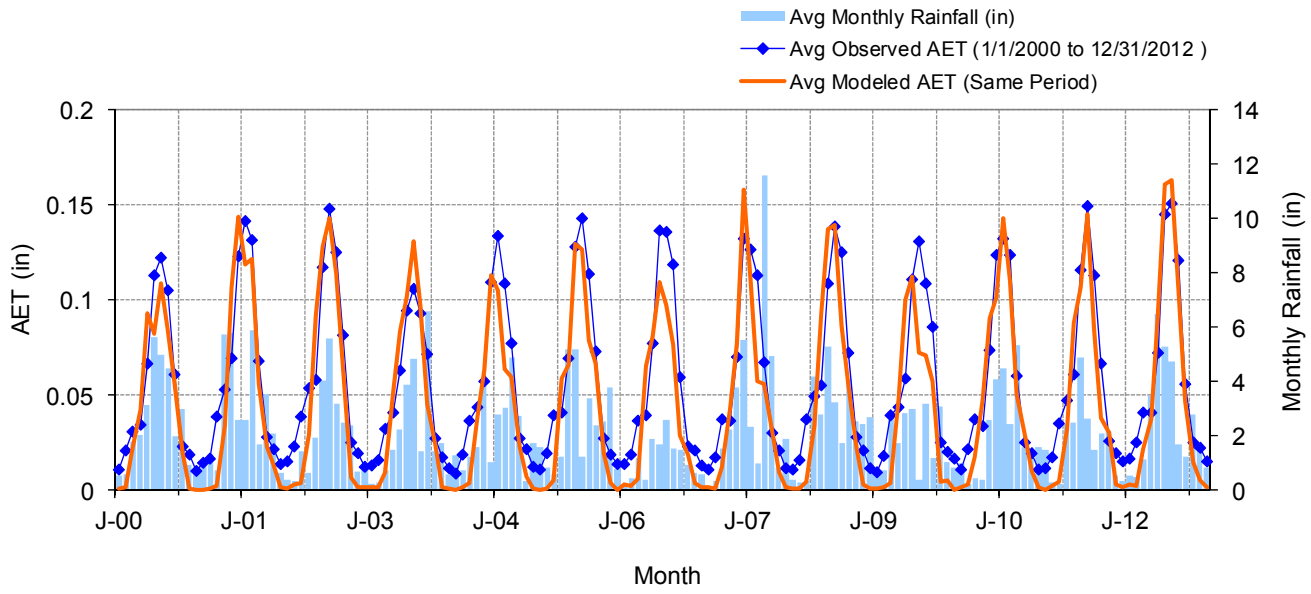

Figure B-9. Mean monthly AET at MN212576 (Embarrass)

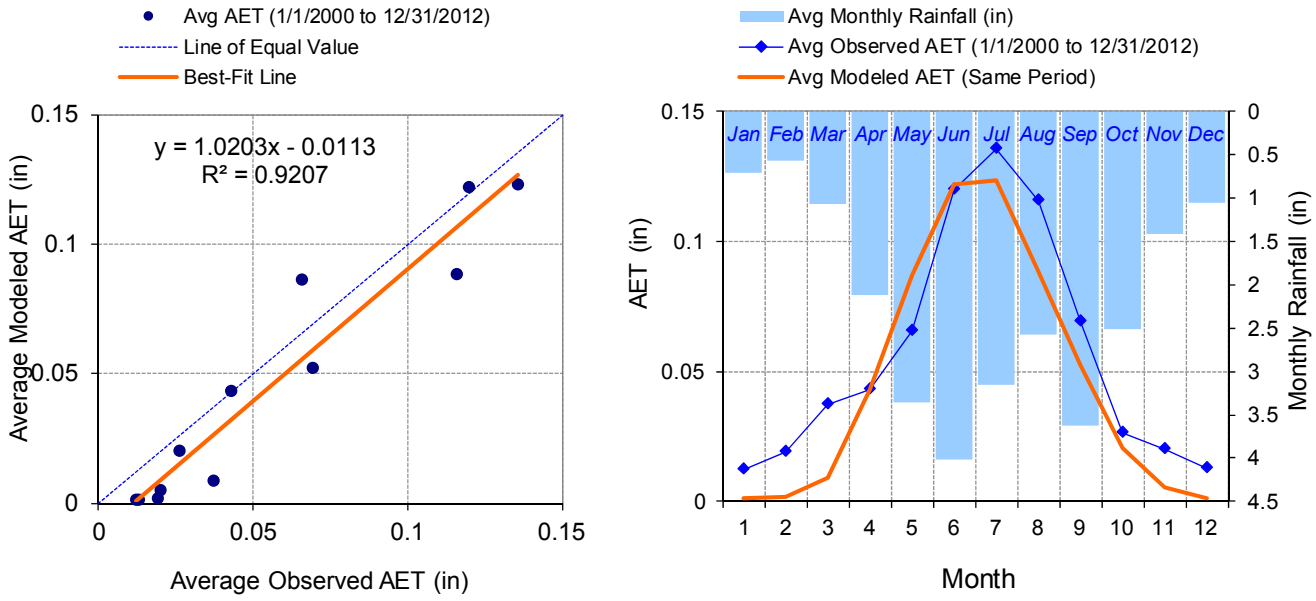

Figure B-10. Seasonal regression and temporal aggregate at MN212576 (Embarrass)

Table B-5. Summary statistics at MN212576 (Embarrass)

HSPF Simulated AET		Observed Precipitation Gage		
REACH OUTFLOW FROM DSN 106 13-Year Analysis Period: 1/1/2000 - 12/31/2012 Flow volumes are (inches/year) for upstream drainage area		MN212576 (Embarrass) Manually Entered Data		
Total Simulated AET:	**16.97**	Total Observed AET:		**20.67**
Simulated Summer AET (months 7-9):	**8.14**	Observed Summer AET (7-9):		**9.86**
Simulated Fall AET (months 10-12):	**0.83**	Observed Fall AET (10-12):		**1.82**
Simulated Winter AET (months 1-3):	**0.37**	Observed Winter AET (1-3):		**2.07**
Simulated Spring AET (months 4-6):	**7.64**	Observed Spring AET (4-6):		**6.92**
Errors (Simulated-Observed)	*Error Statistics*	*Recommended Criteria*		
Error in total AET:	-17.86	10		
Monthly NSE	0.782			

MN212645 (Eveleth WWTP)

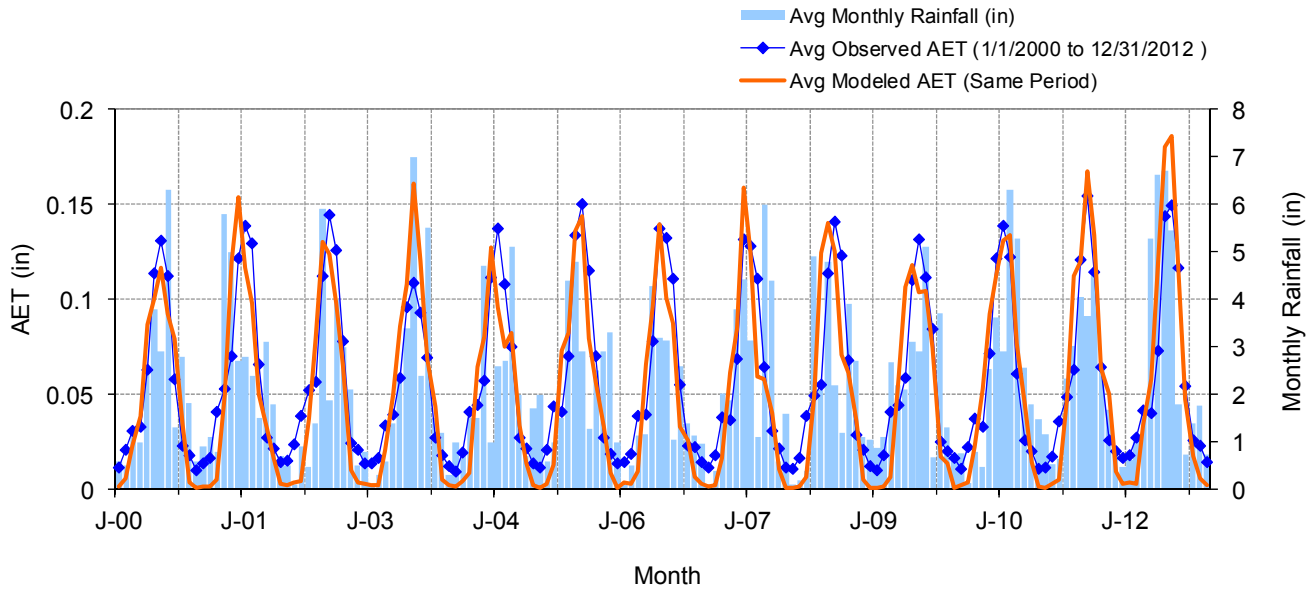

Figure B-11. Mean monthly AET at MN212645 (Eveleth WWTP)

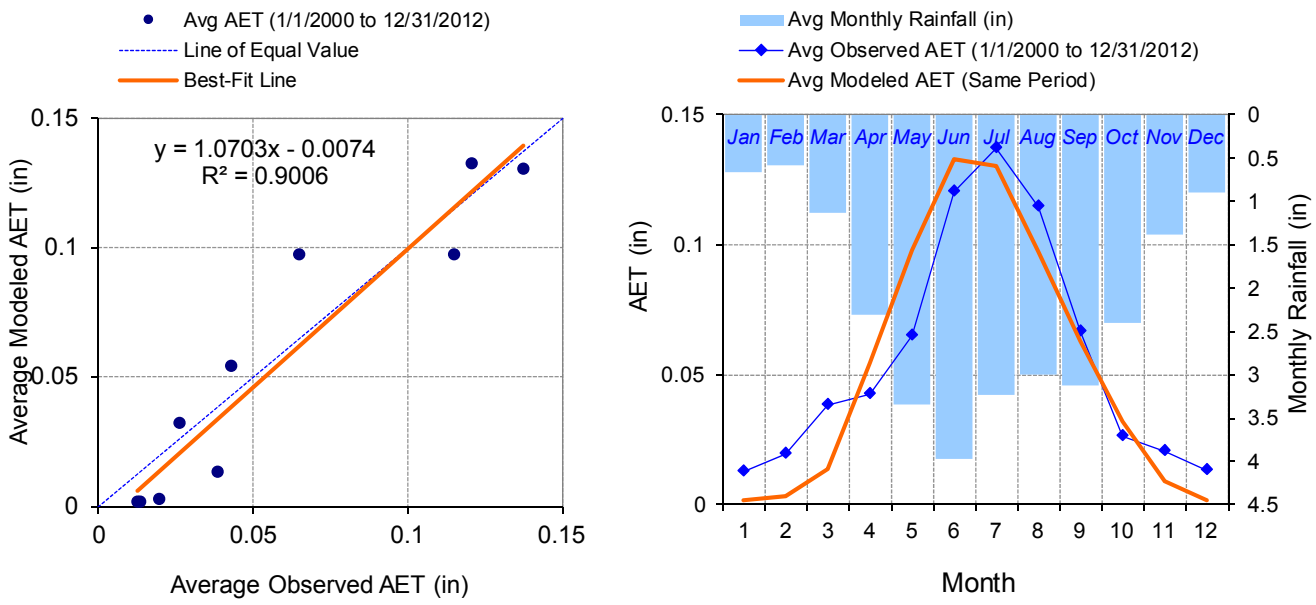

Figure B-12. Seasonal regression and temporal aggregate at MN212645 (Eveleth WWTP)

Table B-6. Summary statistics at MN212645 (Eveleth WWTP)

HSPF Simulated AET		**Observed Precipitation Gage**		
REACH OUTFLOW FROM DSN 107 13-Year Analysis Period: 1/1/2000 - 12/31/2012 Flow volumes are (inches/year) for upstream drainage area		MN212645 (Eveleth WWTP) Manually Entered Data		
Total Simulated AET:	**19.50**	Total Observed AET:		**20.72**
Simulated Summer AET (months 7-9):	**8.95**	Observed Summer AET (7-9):		**9.82**
Simulated Fall AET (months 10-12):	**1.33**	Observed Fall AET (10-12):		**1.85**
Simulated Winter AET (months 1-3):	**0.57**	Observed Winter AET (1-3):		**2.14**
Simulated Spring AET (months 4-6):	**8.65**	Observed Spring AET (4-6):		**6.91**
Errors (Simulated-Observed)	*Error Statistics*	*Recommended Criteria*		
Error in total AET:	-5.89	10		
Monthly NSE	0.763			

MN212842 (Floodwood 3 NE)

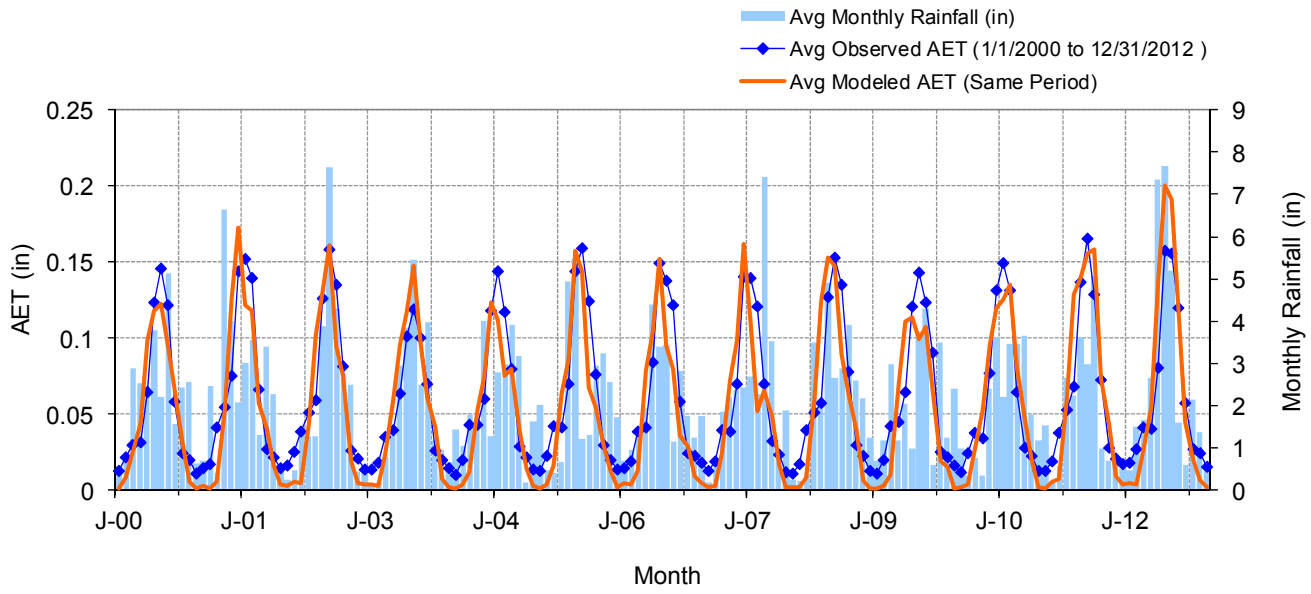

Figure B-13. Mean monthly AET at MN212842 (Floodwood 3 NE)

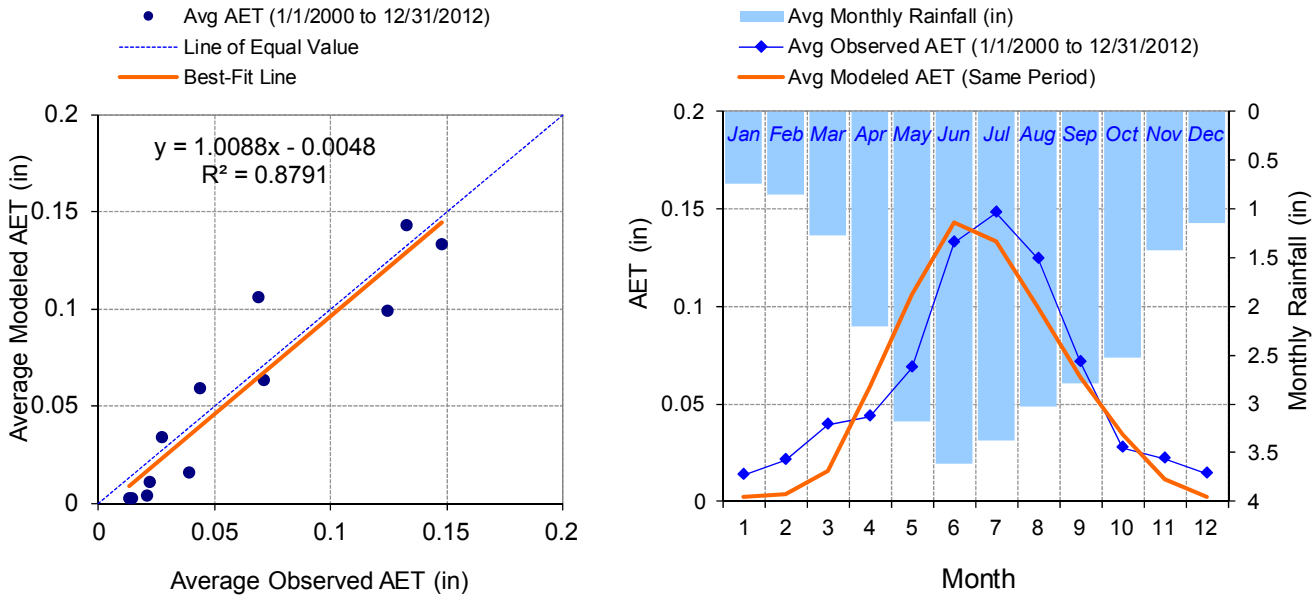

Figure B-14. Seasonal regression and temporal aggregate at MN212842 (Floodwood 3 NE)

Table B-7. Summary statistics at MN212842 (Floodwood 3 NE)

HSPF Simulated AET		Observed Precipitation Gage	
REACH OUTFLOW FROM DSN 108 13-Year Analysis Period: 1/1/2000 - 12/31/2012 Flow volumes are (inches/year) for upstream drainage area		MN212842 (Floodwood 3 NE) Manually Entered Data	
Total Simulated AET:	**20.60**	Total Observed AET:	**22.14**
Simulated Summer AET (months 7-9):	**9.11**	Observed Summer AET (7-9):	**10.58**
Simulated Fall AET (months 10-12):	**1.47**	Observed Fall AET (10-12):	**1.94**
Simulated Winter AET (months 1-3):	**0.67**	Observed Winter AET (1-3):	**2.21**
Simulated Spring AET (months 4-6):	**9.35**	Observed Spring AET (4-6):	**7.41**
Errors (Simulated-Observed)	*Error Statistics*	*Recommended Criteria*	
Error in total AET:	-6.96	10	
Monthly NSE	0.771		

MN213730 (Hibbing FAA Ap), Hibbing, Sikkila and Kuusinen

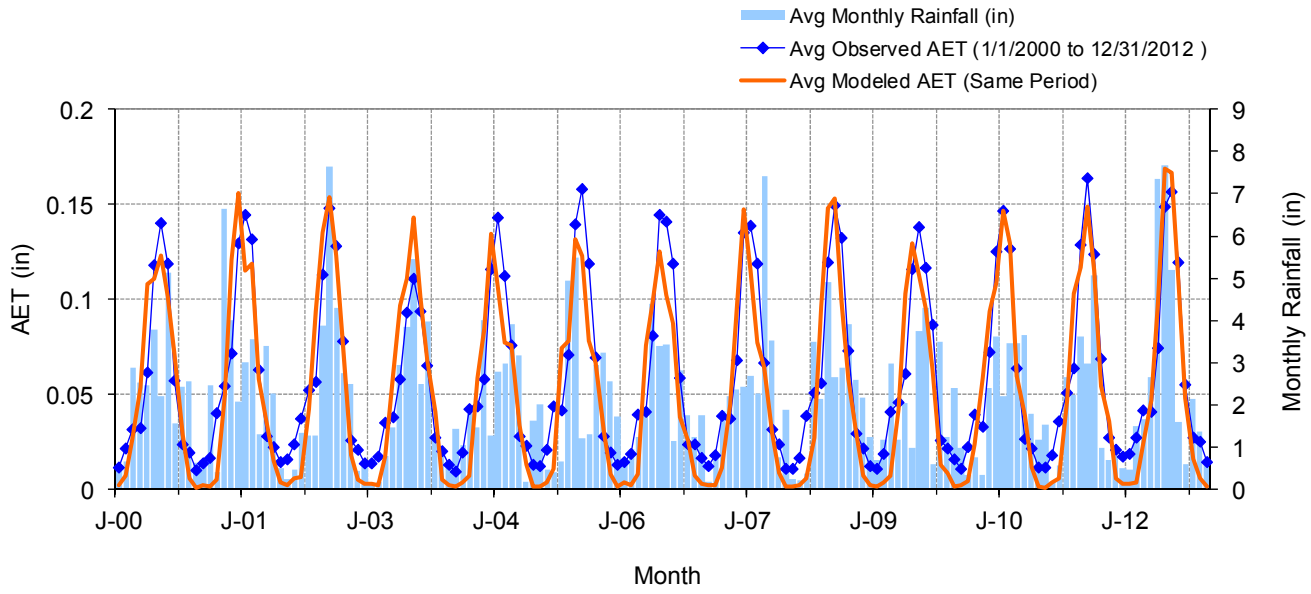

Figure B-15. Mean monthly AET at MN213730 (Hibbing FAA Ap), Hibbing, Sikkila and Kuusinen

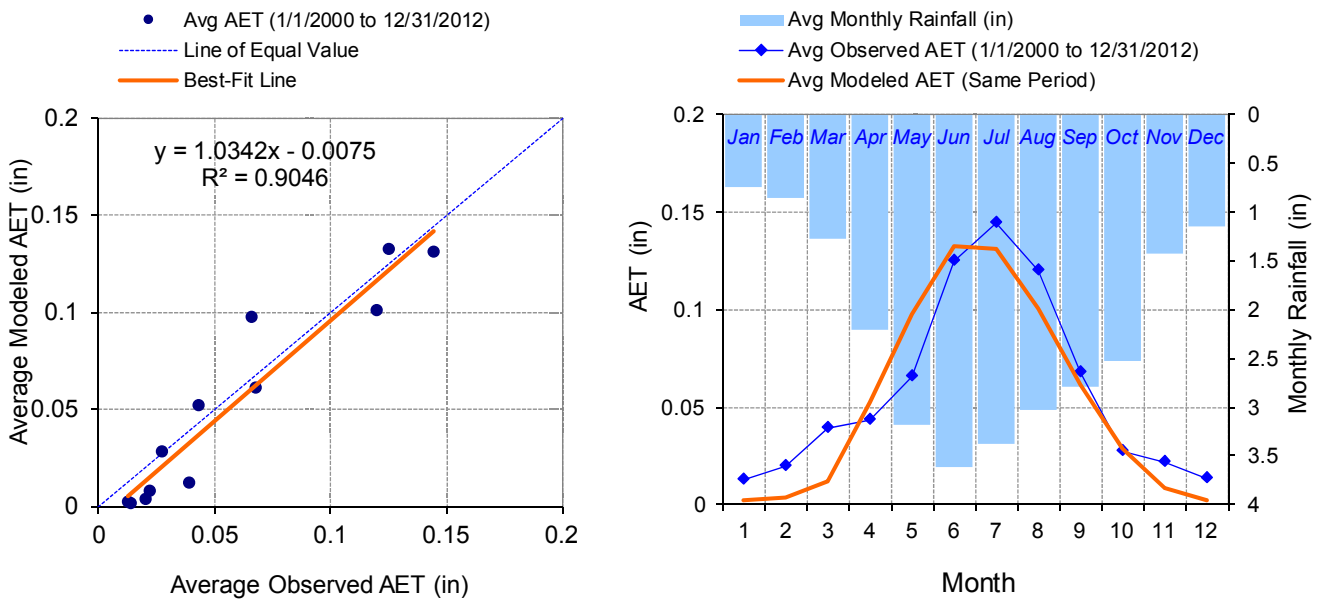

Figure B-16. Seasonal regression and temporal aggregate at MN213730 (Hibbing FAA Ap), Hibbing, Sikkila and Kuusinen

Table B-8. Summary statistics at MN213730 (Hibbing FAA Ap), Hibbing, Sikkila and Kuusinen

HSPF Simulated AET		**Observed Precipitation Gage**	
REACH OUTFLOW FROM DSN 109 13-Year Analysis Period: 1/1/2000 - 12/31/2012 Flow volumes are (inches/year) for upstream drainage area		MN213730 (Hibbing FAA Ap), Hibbing, Sikkila and Kuusinen Manually Entered Data	
Total Simulated AET:	**19.39**	Total Observed AET:	**21.40**
Simulated Summer AET (months 7-9):	**9.05**	Observed Summer AET (7-9):	**10.23**
Simulated Fall AET (months 10-12):	**1.21**	Observed Fall AET (10-12):	**1.92**
Simulated Winter AET (months 1-3):	**0.55**	Observed Winter AET (1-3):	**2.17**
Simulated Spring AET (months 4-6):	**8.58**	Observed Spring AET (4-6):	**7.08**
Errors (Simulated-Observed)	*Error Statistics*	*Recommended Criteria*	
Error in total AET:	-9.39	10	
Monthly NSE	0.809		

WI476413 (Pattison State Park)

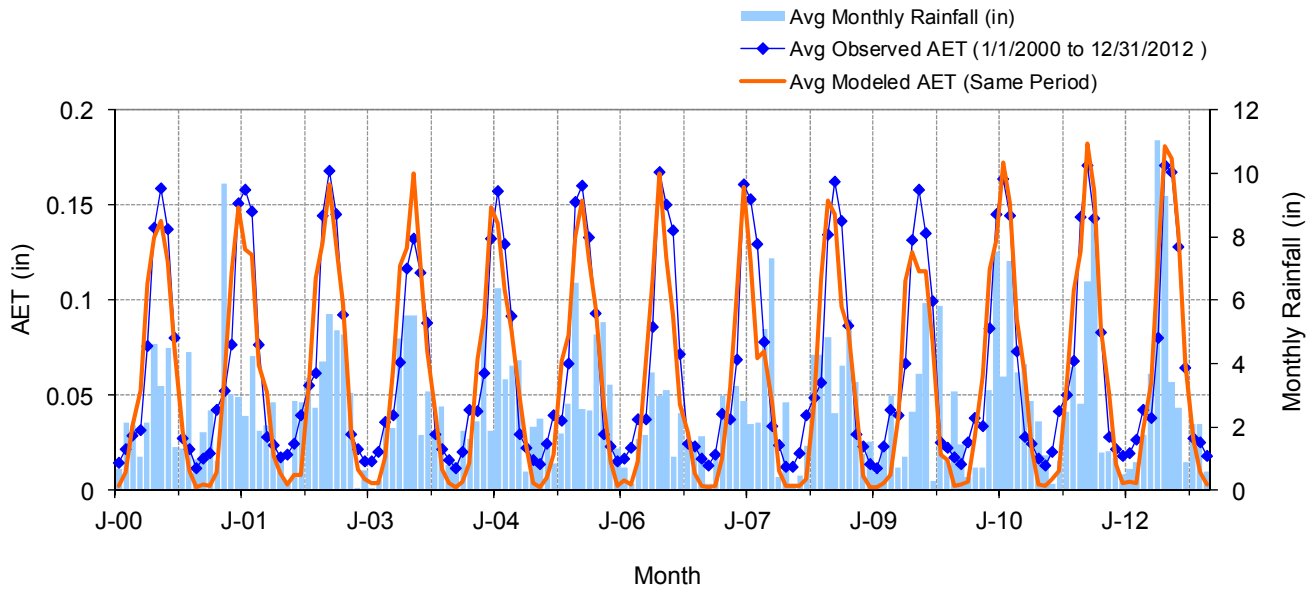

Figure B-17. Mean monthly AET at WI476413 (Pattison State Park)

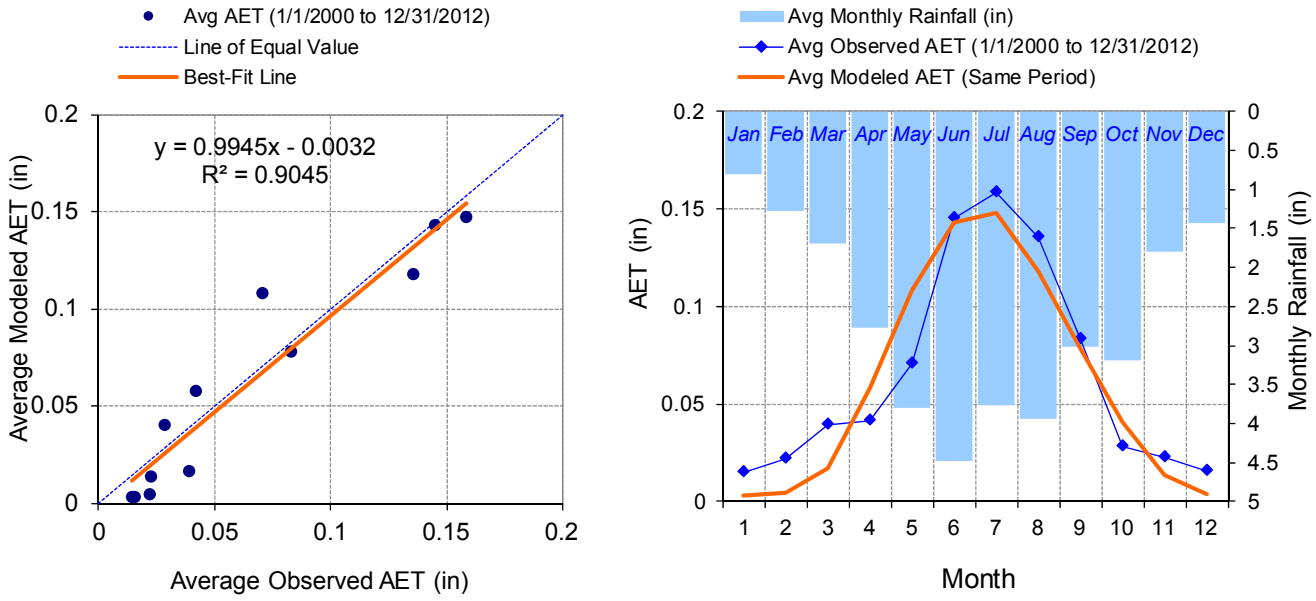

Figure B-18. Seasonal regression and temporal aggregate at WI476413 (Pattison State Park)

Table B-9. Summary statistics at WI476413 (Pattison State Park)

HSPF Simulated AET		Observed Precipitation Gage		
REACH OUTFLOW FROM DSN 110 13-Year Analysis Period: 1/1/2000 - 12/31/2012 Flow volumes are (inches/year) for upstream drainage area		WI476413 (Pattison State Park) Manually Entered Data		
Total Simulated AET:	**22.48**	Total Observed AET:		**23.75**
Simulated Summer AET (months 7-9):	**10.58**	Observed Summer AET (7-9):		**11.60**
Simulated Fall AET (months 10-12):	**1.77**	Observed Fall AET (10-12):		**2.05**
Simulated Winter AET (months 1-3):	**0.74**	Observed Winter AET (1-3):		**2.29**
Simulated Spring AET (months 4-6):	**9.40**	Observed Spring AET (4-6):		**7.80**
Errors (Simulated-Observed)	*Error Statistics*	*Recommended Criteria*		
Error in total AET:	-5.32	10		
Monthly NSE	0.841			

WI478349 (Superior)

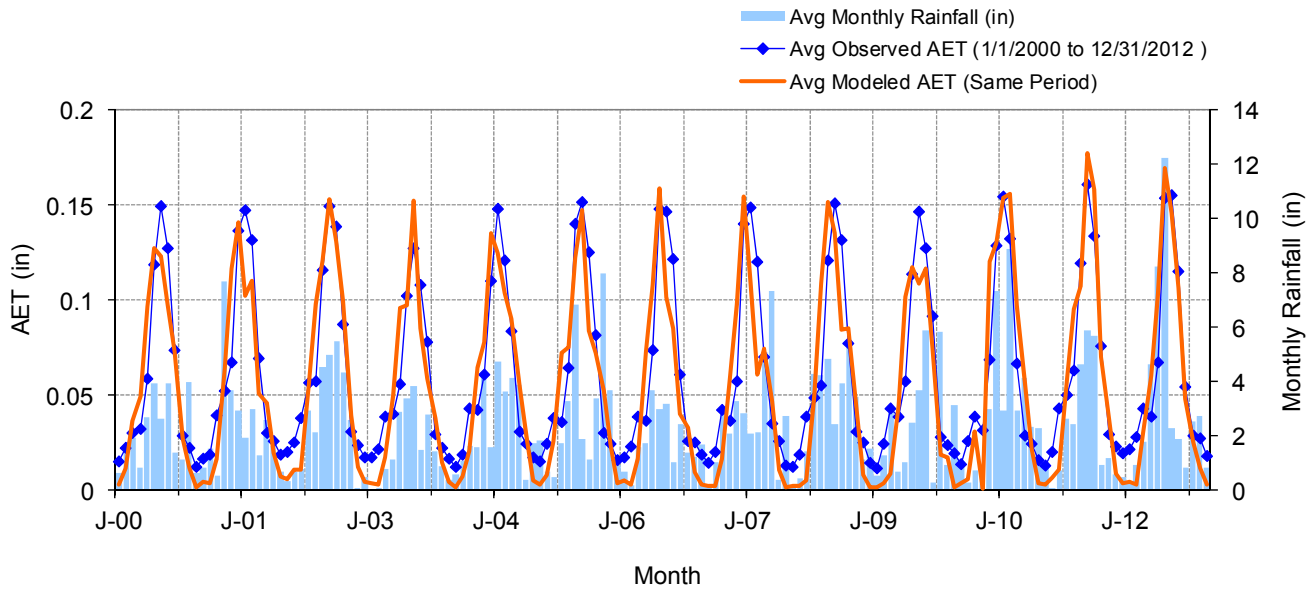

Figure B-19. Mean monthly AET at WI478349 (Superior)

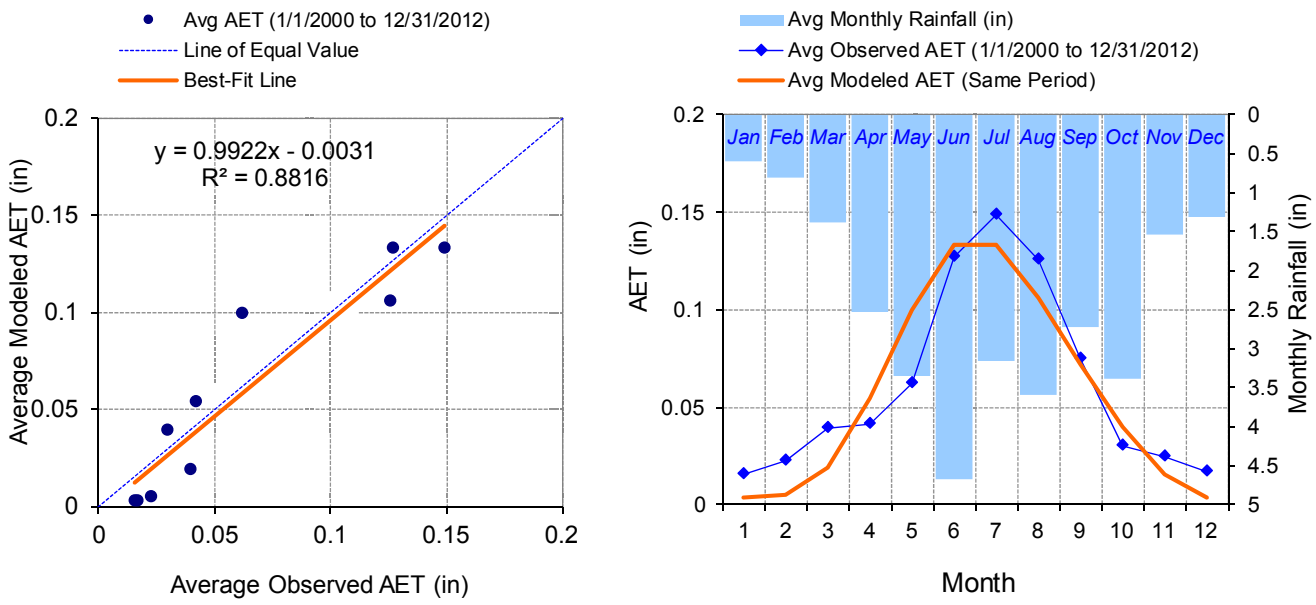

Figure B-20. Seasonal regression and temporal aggregate at WI478349 (Superior)

Table B-10. Summary statistics at WI478349 (Superior)

HSPF Simulated AET		**Observed Precipitation Gage**		
REACH OUTFLOW FROM DSN 120 13-Year Analysis Period: 1/1/2000 - 12/31/2012 Flow volumes are (inches/year) for upstream drainage area		WI478349 (Superior) Manually Entered Data		
Total Simulated AET:	**20.96**	Total Observed AET:		**22.25**
Simulated Summer AET (months 7-9):	**9.59**	Observed Summer AET (7-9):		**10.75**
Simulated Fall AET (months 10-12):	**1.80**	Observed Fall AET (10-12):		**2.18**
Simulated Winter AET (months 1-3):	**0.85**	Observed Winter AET (1-3):		**2.34**
Simulated Spring AET (months 4-6):	**8.72**	Observed Spring AET (4-6):		**6.98**
Errors (Simulated-Observed)	*Error Statistics*	*Recommended Criteria*		
Error in total AET:	-5.82	10		
Monthly NSE	0.780			

(This page left intentionally blank.)

Appendix C. Detailed Hydrology Calibration Results

HYDSTRA 03149002 Partridge River near Hoyt Lakes

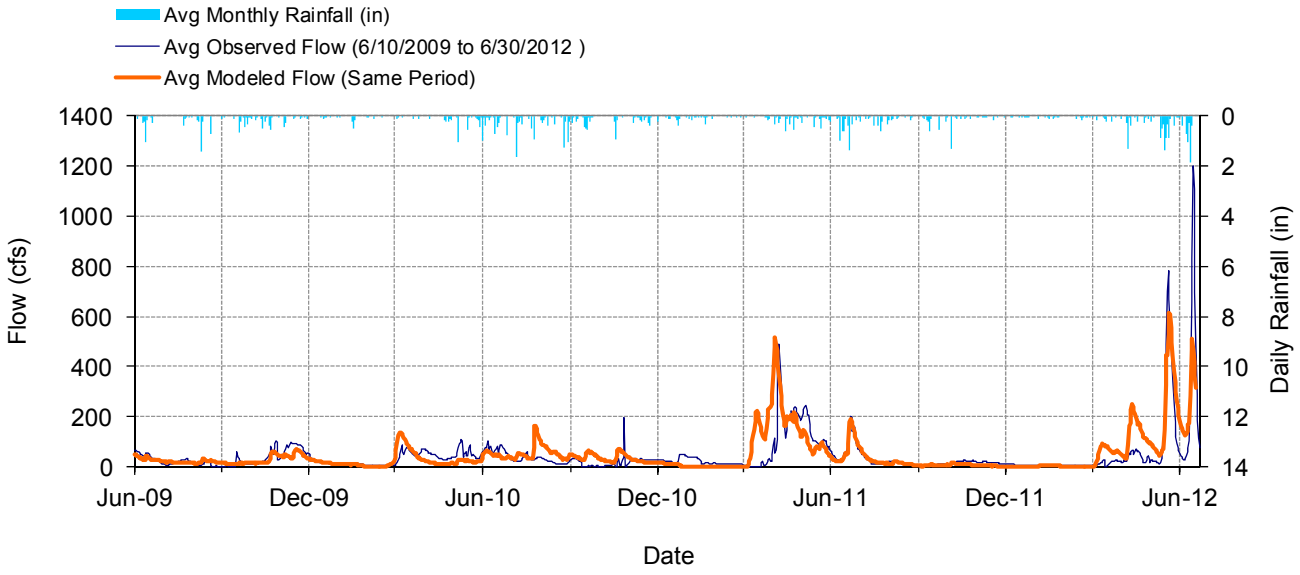

Figure C-1. Mean daily flow at HYDSTRA 03149002 Partridge River near Hoyt Lakes

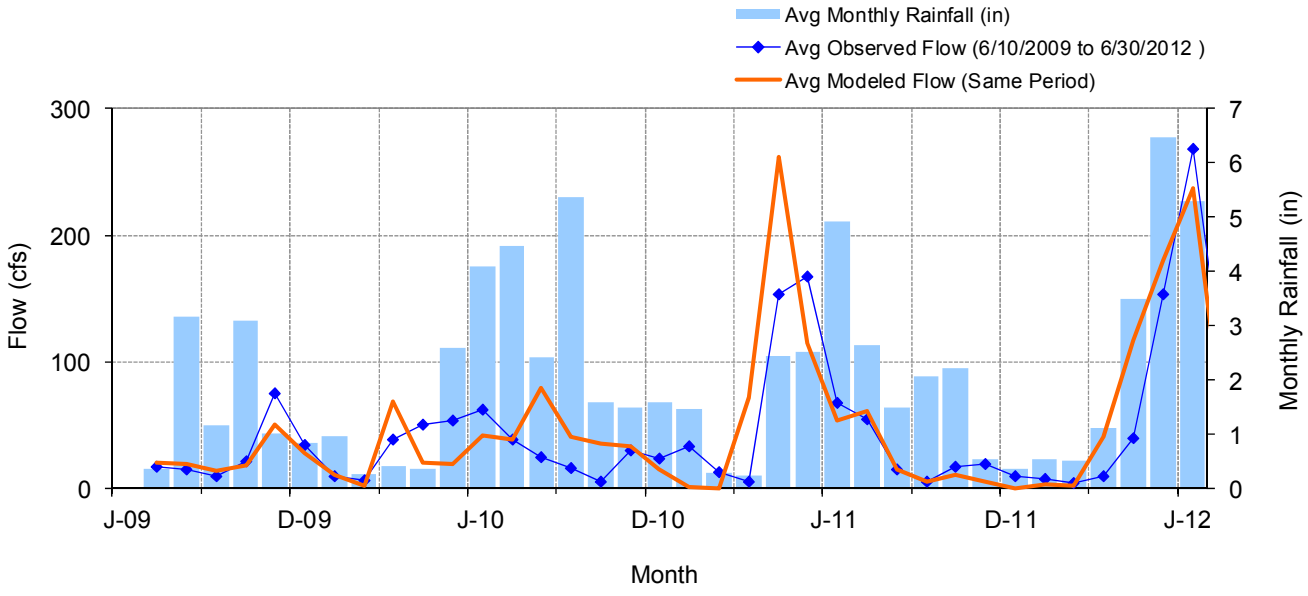

Figure C-2. Mean monthly flow at HYDSTRA 03149002 Partridge River near Hoyt Lakes

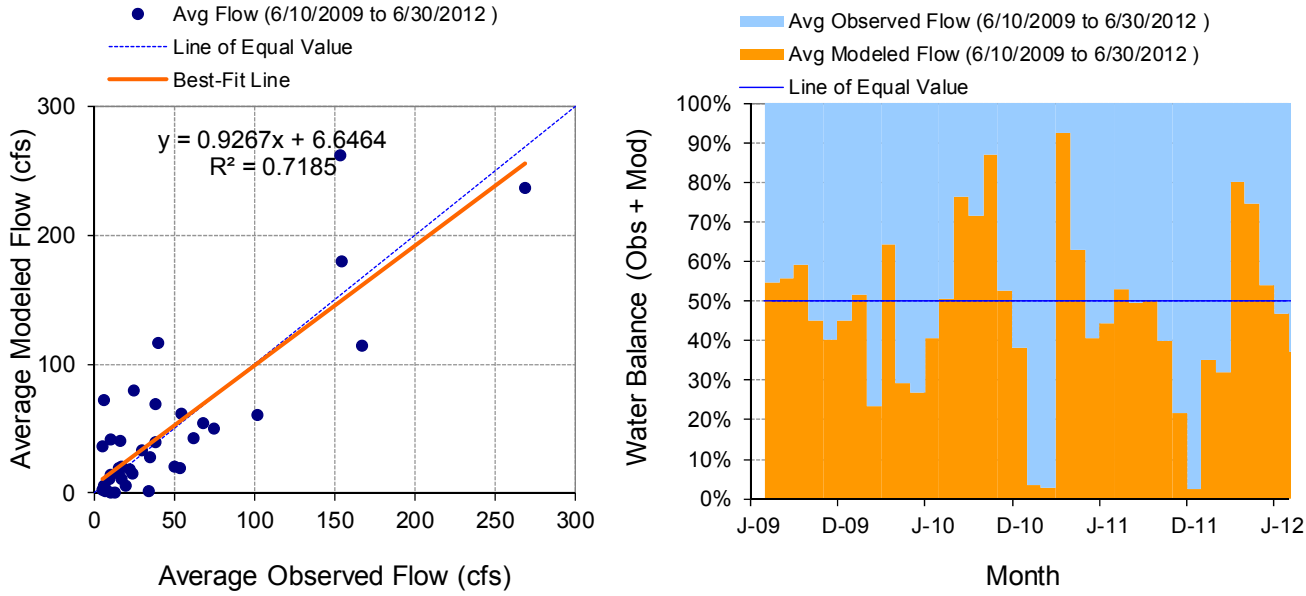

Figure C-3. Monthly flow regression and temporal variation at HYDSTRA 03149002 Partridge River near Hoyt Lakes

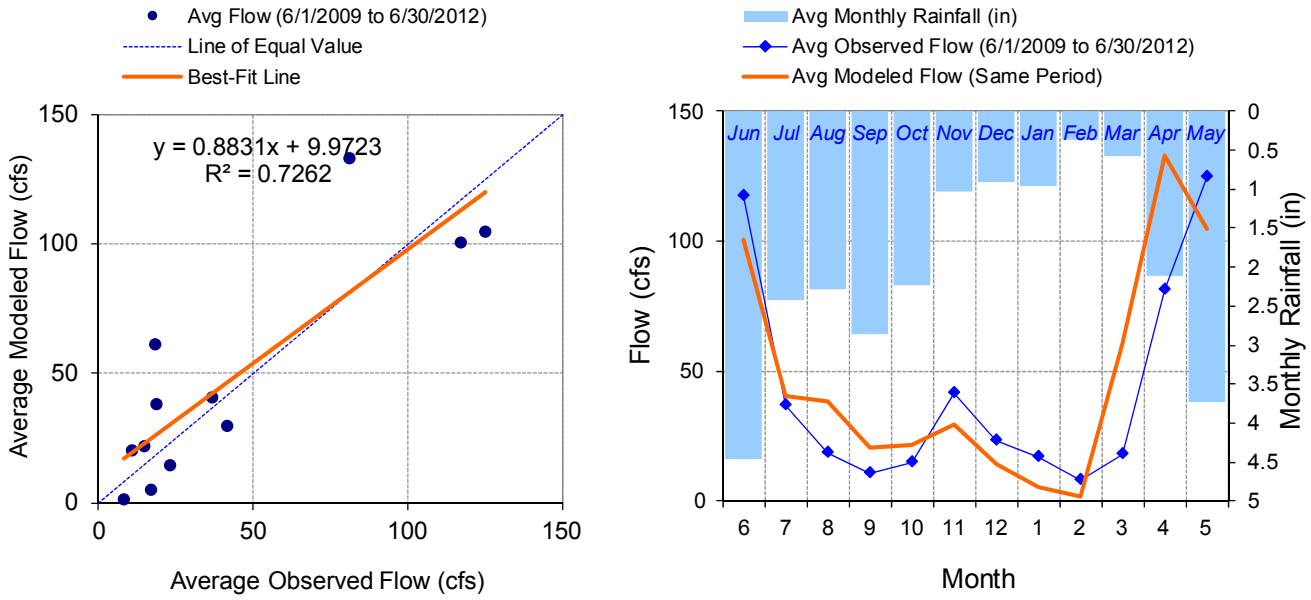

Figure C-4. Seasonal regression and temporal aggregate at HYDSTRA 03149002 Partridge River near Hoyt Lakes

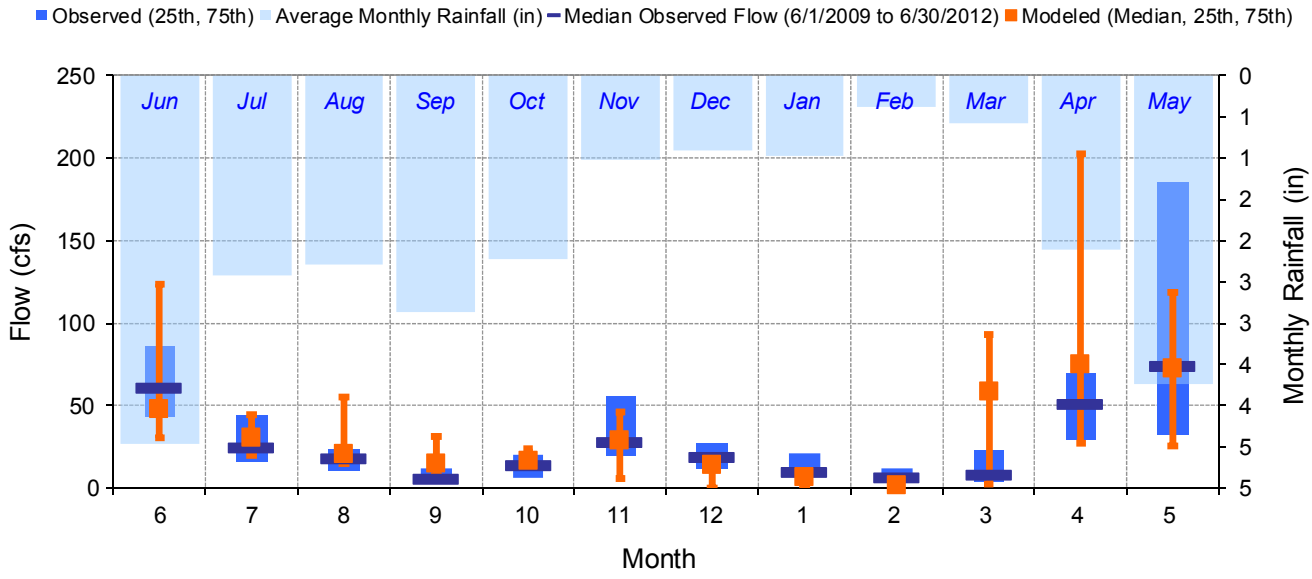

Figure C-5. Seasonal medians and ranges at HYDSTRA 03149002 Partridge River near Hoyt Lakes

Table C-1. Seasonal summary at HYDSTRA 03149002 Partridge River near Hoyt Lakes

MONTH	OBSERVED FLOW (CFS)				MODELED FLOW (CFS)			
	MEAN	MEDIAN	25TH	75TH	MEAN	MEDIAN	25TH	75TH
Jun	117.18	61.00	43.66	86.00	100.61	47.63	30.43	123.63
Jul	36.72	25.00	16.00	44.00	40.52	30.52	20.01	44.25
Aug	18.51	18.00	10.68	24.00	38.09	20.51	14.80	55.24
Sep	10.75	5.67	3.00	11.75	20.46	14.54	7.59	31.24
Oct	14.88	14.00	5.90	20.00	21.82	16.87	13.44	23.69
Nov	41.47	28.00	19.40	56.00	29.65	29.18	6.18	46.59
Dec	22.95	19.00	11.76	28.00	14.53	14.38	0.14	19.10
Jan	16.99	9.90	7.60	21.00	5.26	6.36	0.35	9.25
Feb	8.06	6.50	5.02	11.79	1.59	1.60	0.35	2.13
Mar	18.15	8.60	4.16	22.38	60.98	58.28	2.66	93.56
Apr	81.10	50.84	29.00	69.67	133.18	74.74	27.27	202.62
May	124.82	74.00	33.00	185.50	104.72	72.40	25.74	118.40

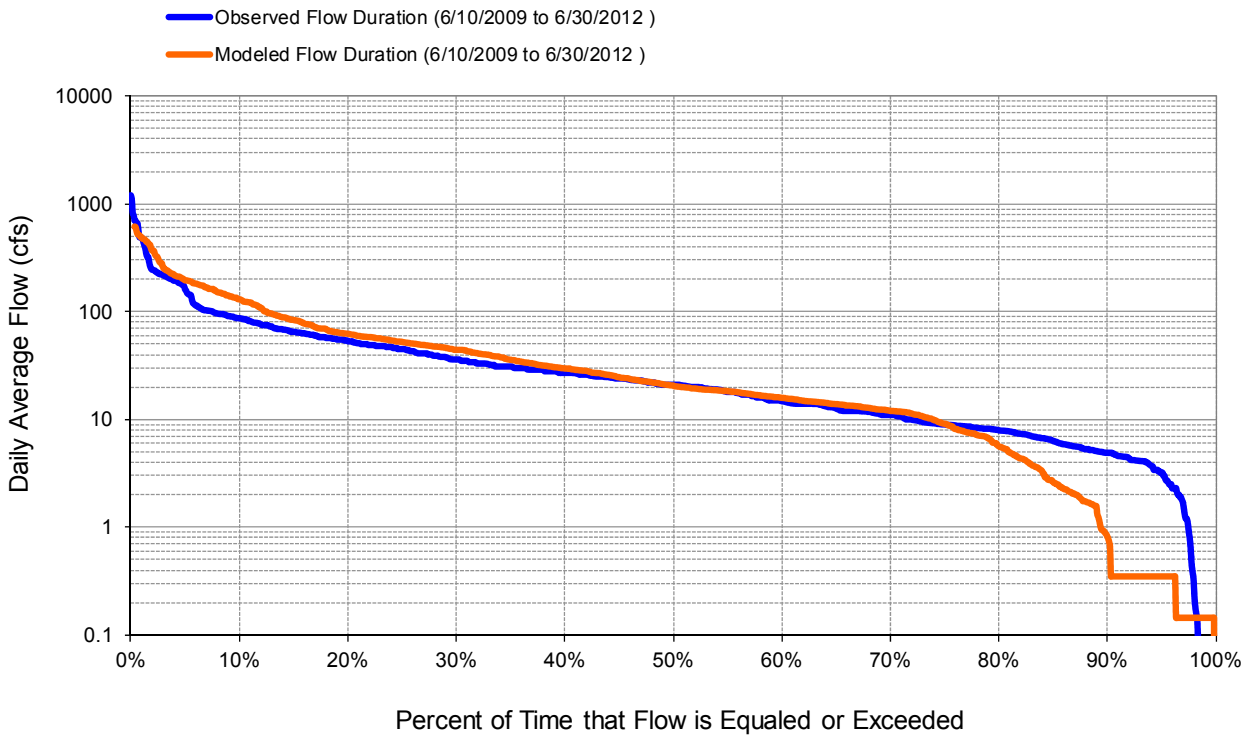

Figure C-6. Flow exceedance at HYDSTRA 03149002 Partridge River near Hoyt Lakes

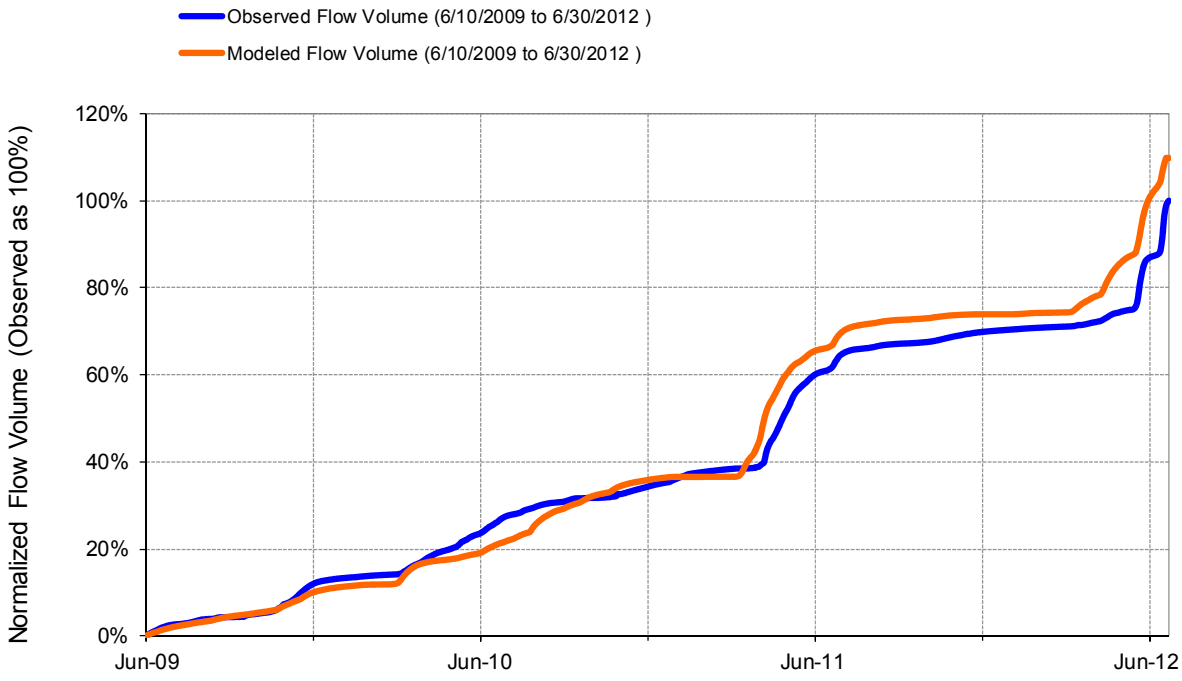

Figure C-7. Flow accumulation at HYDSTRA 03149002 Partridge River near Hoyt Lakes

Table C-2. Summary statistics at HYDSTRA 03149002 Partridge River near Hoyt Lakes

HSPF Simulated Flow		Observed Flow Gage	
REACH OUTFLOW FROM DSN 262 3.06-Year Analysis Period: 6/1/2009 - 6/30/2012 Flow volumes are (inches/year) for upstream drainage area		HYDSTRA 03149002 Partridge River nr Hoyt Lakes Manually Entered Data Drainage Area (sq-mi): 128	
Total Simulated In-stream Flow:	**5.13**	Total Observed In-stream Flow:	**4.68**
Total of simulated highest 10% flows:	**2.53**	Total of Observed highest 10% flows:	**2.40**
Total of Simulated lowest 50% flows:	**0.47**	Total of Observed Lowest 50% flows:	**0.52**
Simulated Summer Flow Volume (months 7-9):	**0.87**	Observed Summer Flow Volume (7-9):	**0.58**
Simulated Fall Flow Volume (months 10-12):	**0.57**	Observed Fall Flow Volume (10-12):	**0.69**
Simulated Winter Flow Volume (months 1-3):	**0.60**	Observed Winter Flow Volume (1-3):	**0.38**
Simulated Spring Flow Volume (months 4-6):	**3.09**	Observed Spring Flow Volume (4-6):	**3.03**
Total Simulated Storm Volume:	**0.92**	Total Observed Storm Volume:	**1.31**
Simulated Summer Storm Volume (7-9):	**0.13**	Observed Summer Storm Volume (7-9):	**0.12**
Errors (Simulated-Observed)	*Error Statistics*	*Recommended Criteria*	
Error in total volume:	9.69	10	
Error in 50% lowest flows:	-9.30	10	
Error in 10% highest flows:	5.45	15	
Seasonal volume error - Summer:	49.96	30	
Seasonal volume error - Fall:	-16.57	30	
Seasonal volume error - Winter:	59.30	30	
Seasonal volume error - Spring:	1.81	30	
Error in storm volumes:	-29.60	20	
Error in summer storm volumes:	6.71	50	
Nash-Sutcliffe Coefficient of Efficiency, E:	0.523		
Baseline adjusted coefficient (Garrick), E':	0.282	Model accuracy increases	
Monthly NSE	0.650		

>> Clear

HYDSTRA 03150001 Second Creek near Aurora

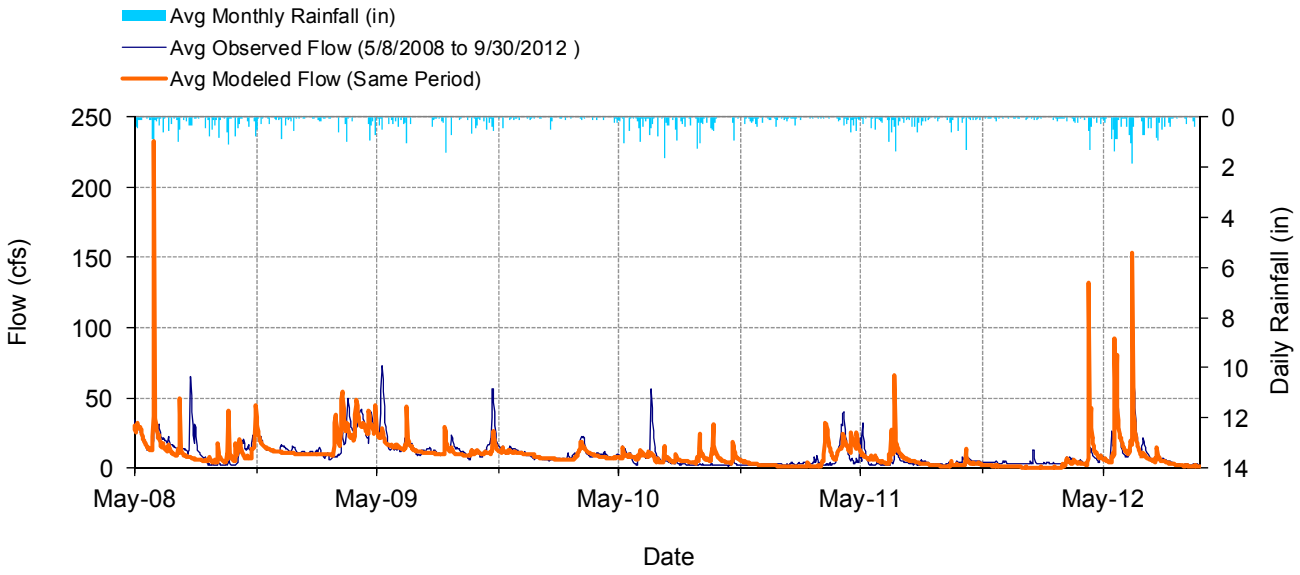

Figure C-8. Mean daily flow at HYDSTRA 03150001 Second Creek near Aurora

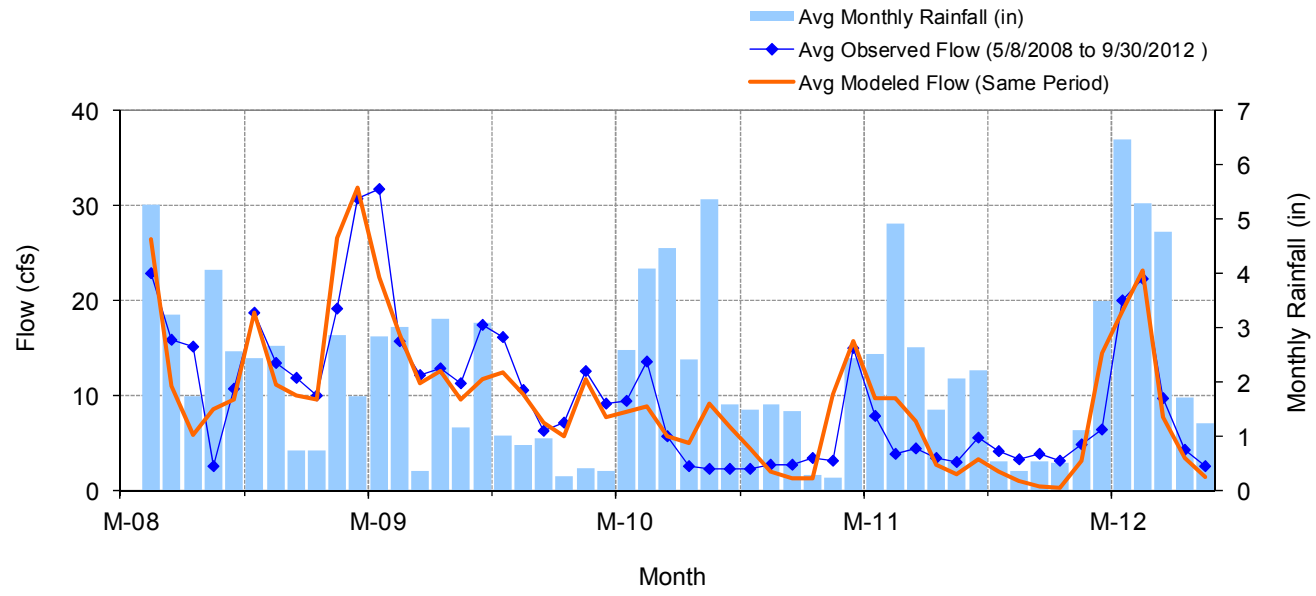

Figure C-9. Mean monthly flow at HYDSTRA 03150001 Second Creek near Aurora

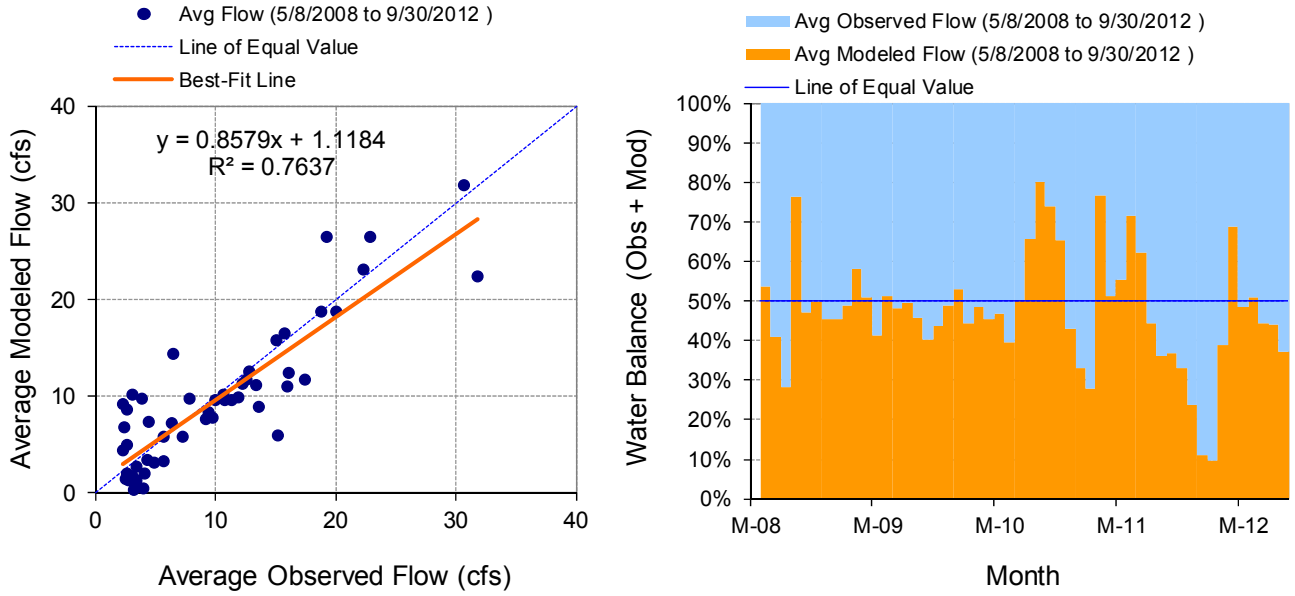

Figure C-10. Monthly flow regression and temporal variation at HYDSTRA 03150001 Second Creek near Aurora

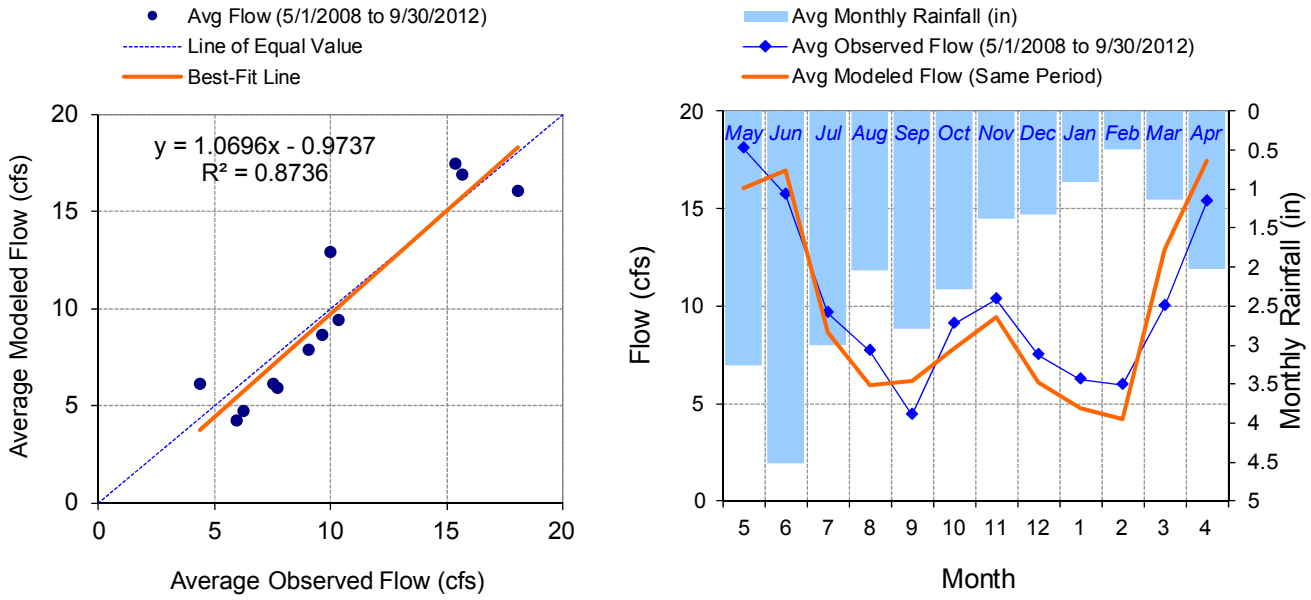

Figure C-11. Seasonal regression and temporal aggregate at HYDSTRA 03150001 Second Creek near Aurora

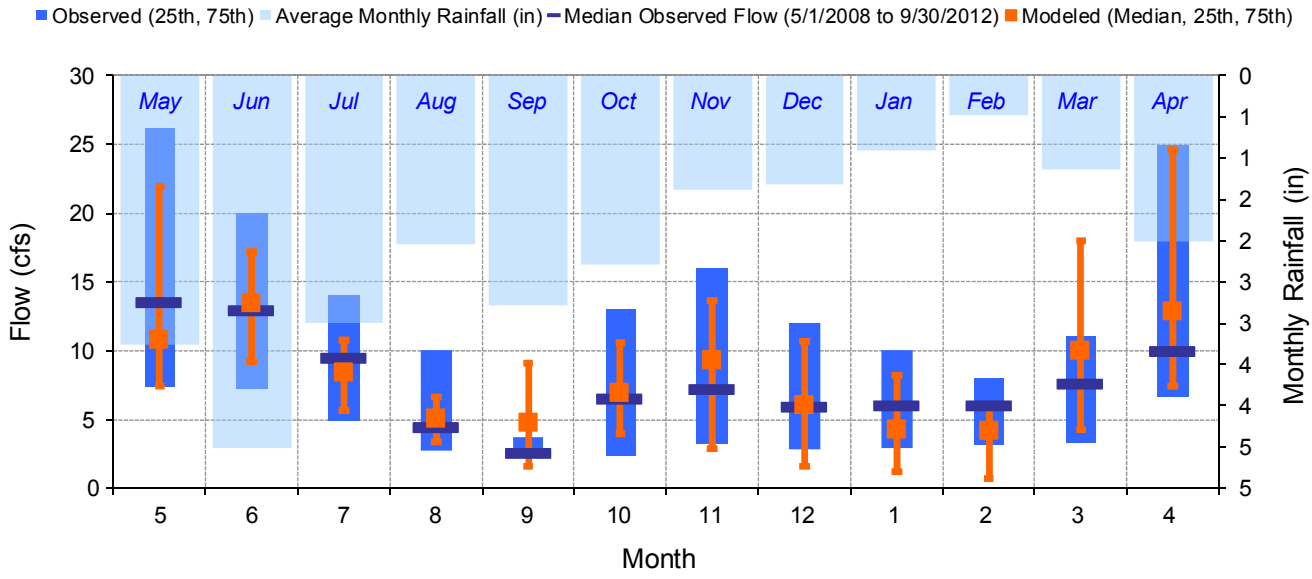

Figure C-12. Seasonal medians and ranges at HYDSTRA 03150001 Second Creek near Aurora

Table C-3. Seasonal summary at HYDSTRA 03150001 Second Creek near Aurora

MONTH	OBSERVED FLOW (CFS)				MODELED FLOW (CFS)			
	MEAN	MEDIAN	25TH	75TH	MEAN	MEDIAN	25TH	75TH
May	18.04	13.50	7.35	26.11	16.08	10.78	7.38	21.90
Jun	15.69	13.00	7.30	20.00	16.95	13.47	9.16	17.19
Jul	9.63	9.50	4.90	14.00	8.68	8.41	5.69	10.77
Aug	7.70	4.44	2.69	10.00	5.95	5.03	3.36	6.59
Sep	4.39	2.58	2.30	3.75	6.13	4.75	1.59	9.15
Oct	9.06	6.54	2.30	13.00	7.86	6.88	3.94	10.61
Nov	10.35	7.22	3.26	16.00	9.42	9.30	2.90	13.62
Dec	7.51	5.92	2.85	12.00	6.12	6.02	1.58	10.67
Jan	6.24	6.00	2.90	10.00	4.75	4.24	1.17	8.17
Feb	5.95	6.00	3.16	8.00	4.23	4.15	0.73	5.97
Mar	9.97	7.58	3.33	11.00	12.93	9.96	4.22	17.95
Apr	15.36	10.00	6.70	25.00	17.46	12.88	7.44	24.64

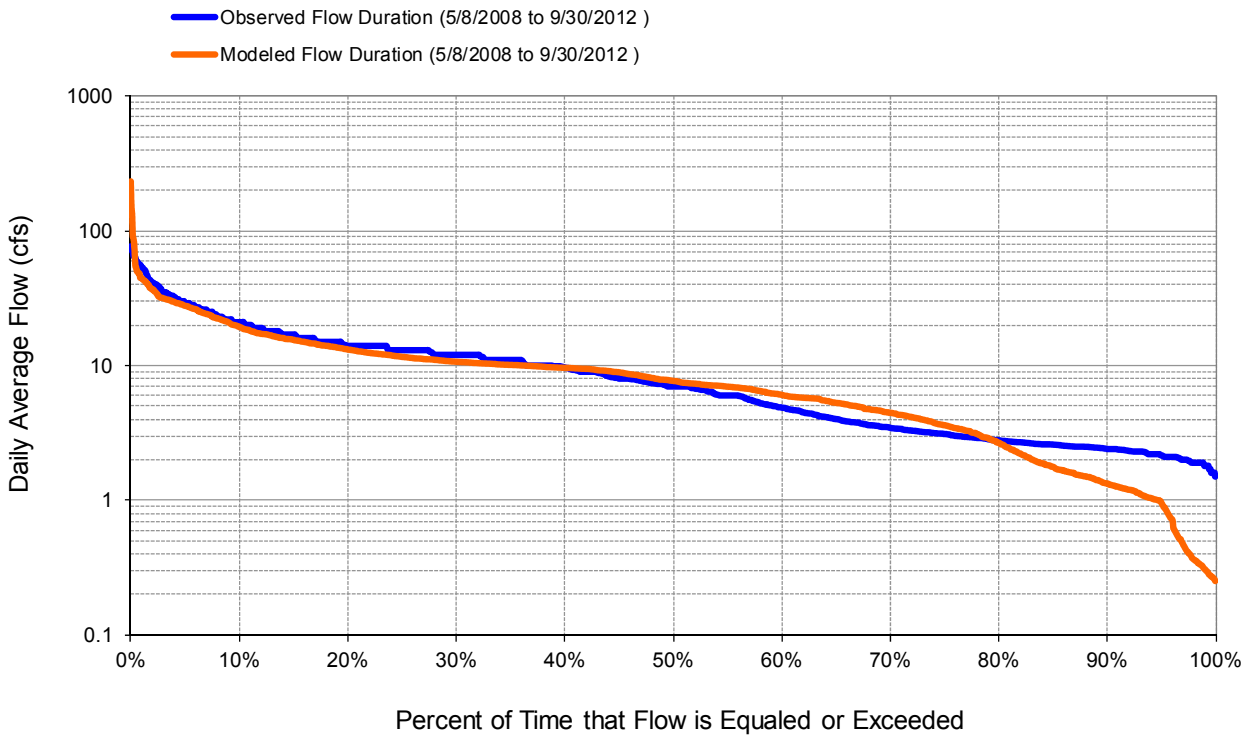

Figure C-13. Flow exceedance at HYDSTRA 03150001 Second Creek near Aurora

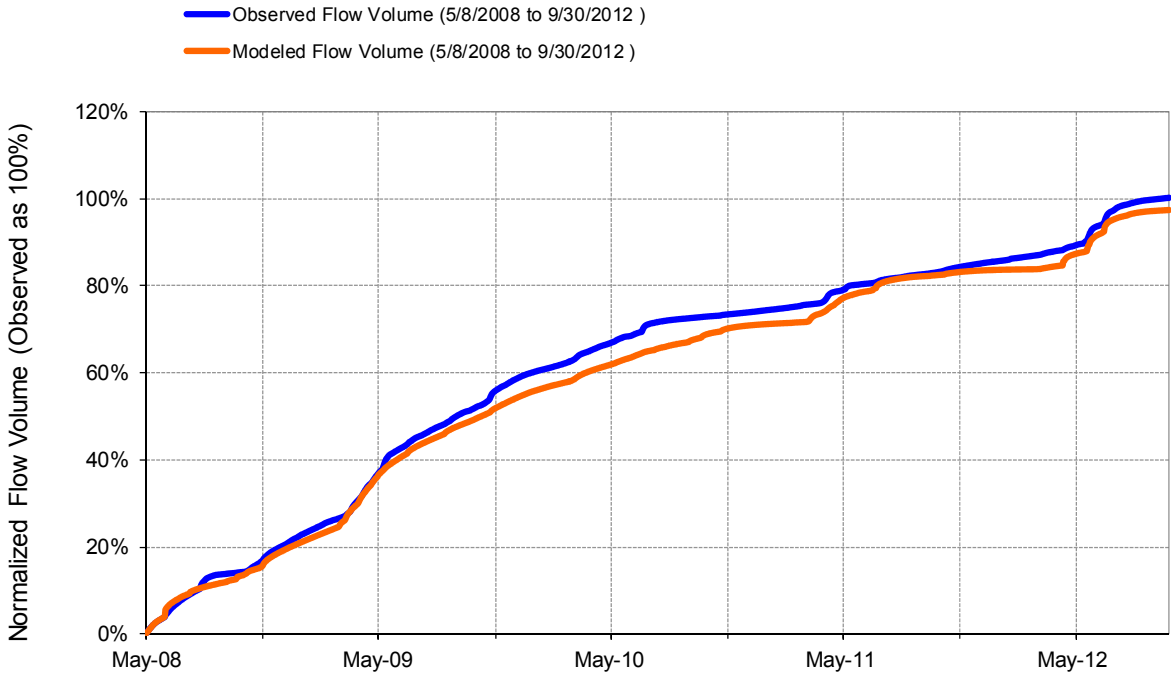

Figure C-14. Flow accumulation at HYDSTRA 03150001 Second Creek near Aurora

Table C-4. Summary statistics at HYDSTRA 03150001 Second Creek near Aurora

HSPF Simulated Flow			Observed Flow Gage		
REACH OUTFLOW FROM DSN 260 4.4-Year Analysis Period: 5/1/2008 - 9/30/2012 Flow volumes are (inches/year) for upstream drainage area			Second Creek nr Aurora Manually Entered Data Drainage Area (sq-mi): 22		
Total Simulated In-stream Flow:	**6.05**		Total Observed In-stream Flow:		**6.22**
Total of simulated highest 10% flows:	**2.06**		Total of Observed highest 10% flows:		**2.09**
Total of Simulated lowest 50% flows:	**1.15**		Total of Observed Lowest 50% flows:		**1.11**
Simulated Summer Flow Volume (months 7-9):	**1.22**		Observed Summer Flow Volume (7-9):		**1.29**
Simulated Fall Flow Volume (months 10-12):	**1.10**		Observed Fall Flow Volume (10-12):		**1.27**
Simulated Winter Flow Volume (months 1-3):	**1.03**		Observed Winter Flow Volume (1-3):		**1.03**
Simulated Spring Flow Volume (months 4-6):	**2.70**		Observed Spring Flow Volume (4-6):		**2.64**
Total Simulated Storm Volume:	**0.83**		Total Observed Storm Volume:		**0.71**
Simulated Summer Storm Volume (7-9):	**0.15**		Observed Summer Storm Volume (7-9):		**0.14**
Errors (Simulated-Observed)	*Error Statistics*	*Recommended Criteria*			
Error in total volume:	-2.79	10			
Error in 50% lowest flows:	3.24	10			
Error in 10% highest flows:	-1.65	15			
Seasonal volume error - Summer:	-4.71	30			
Seasonal volume error - Fall:	-13.12	30	>>	Clear	
Seasonal volume error - Winter:	-0.46	30			
Seasonal volume error - Spring:	2.19	30			
Error in storm volumes:	15.99	20			
Error in summer storm volumes:	5.13	50			
Nash-Sutcliffe Coefficient of Efficiency, E:	0.141	Model accuracy increases			
Baseline adjusted coefficient (Garrick), E':	0.379				
Monthly NSE	0.755				

HYDSTRA 03138001 St. Louis River near Aurora

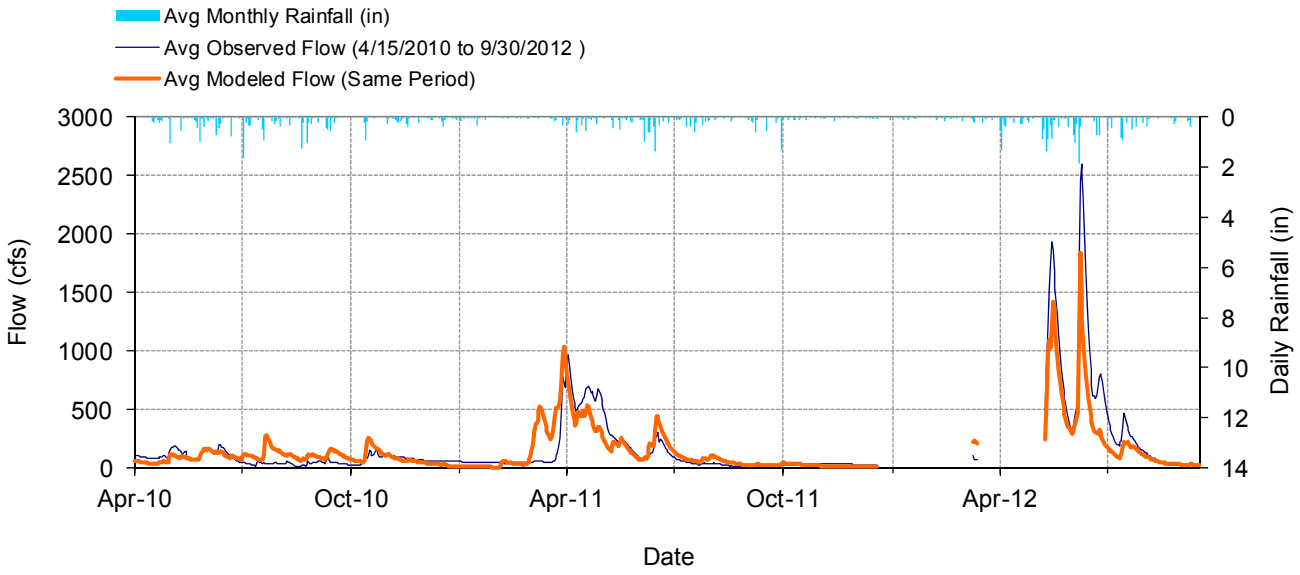

Figure C-15. Mean daily flow at HYDSTRA 03138001 St. Louis River near Aurora

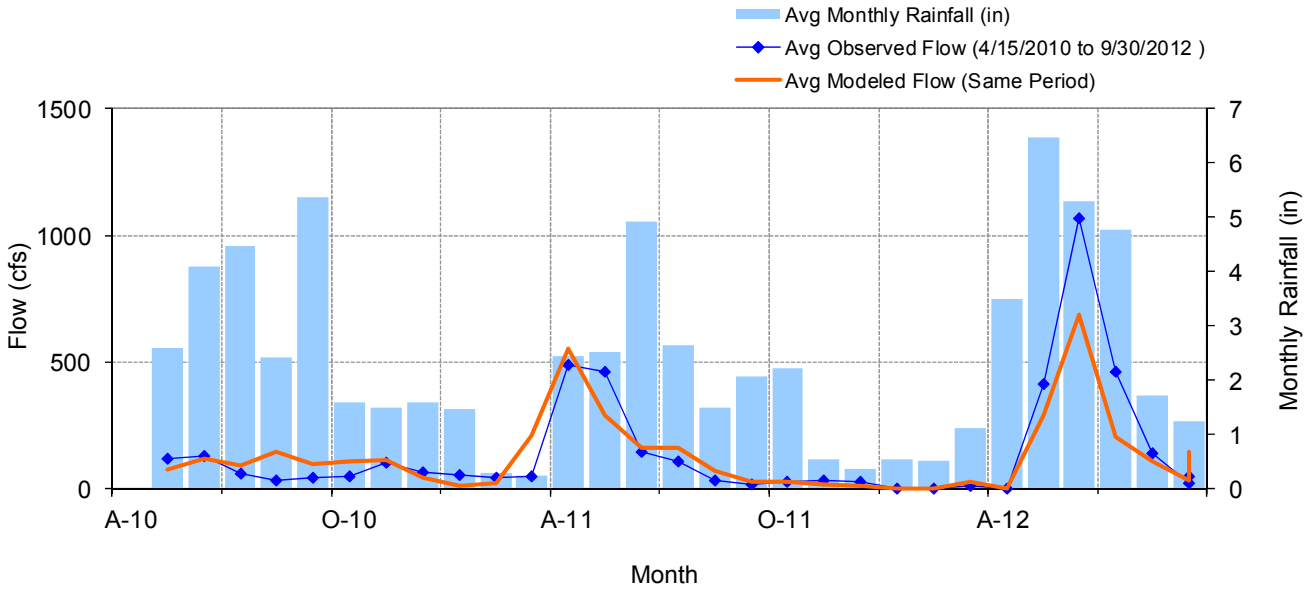

Figure C-16. Mean monthly flow at HYDSTRA 03138001 St. Louis River near Aurora

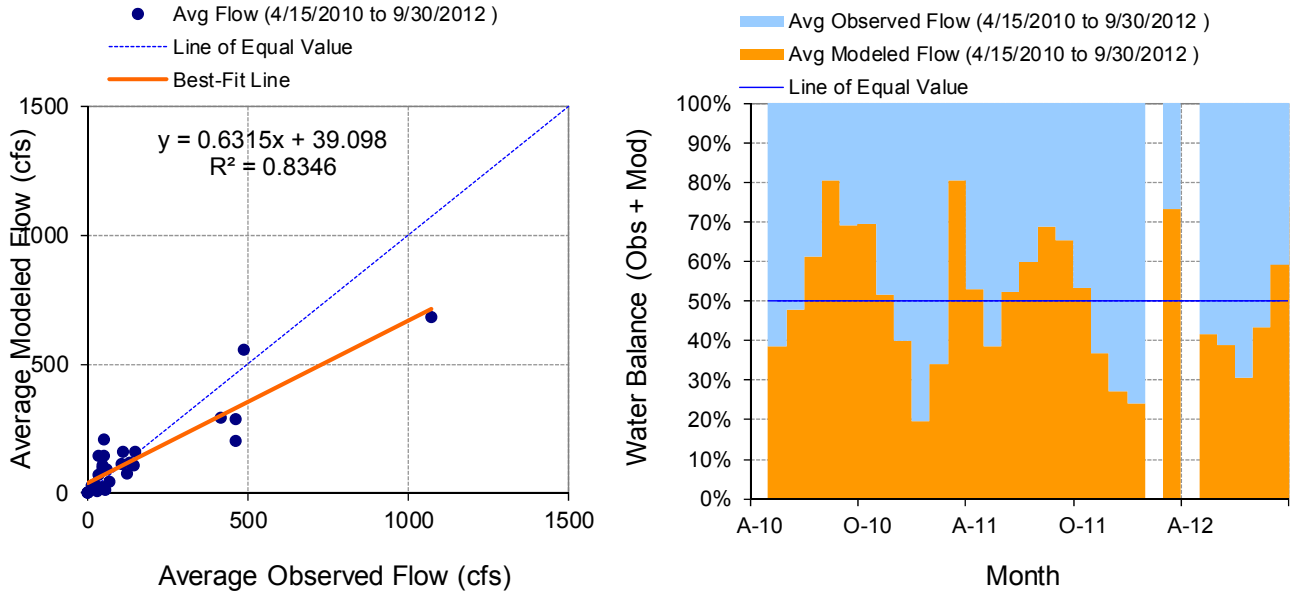

Figure C-17. Monthly flow regression and temporal variation at HYDSTRA 03138001 St. Louis River near Aurora

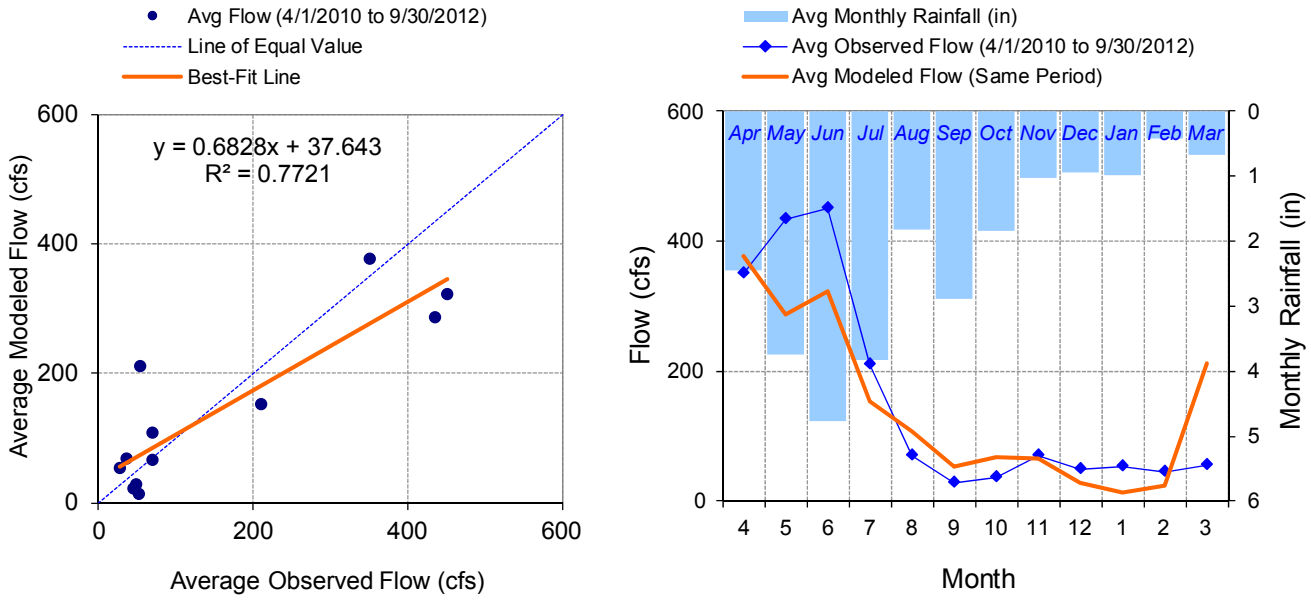

Figure C-18. Seasonal regression and temporal aggregate at HYDSTRA 03138001 St. Louis River near Aurora

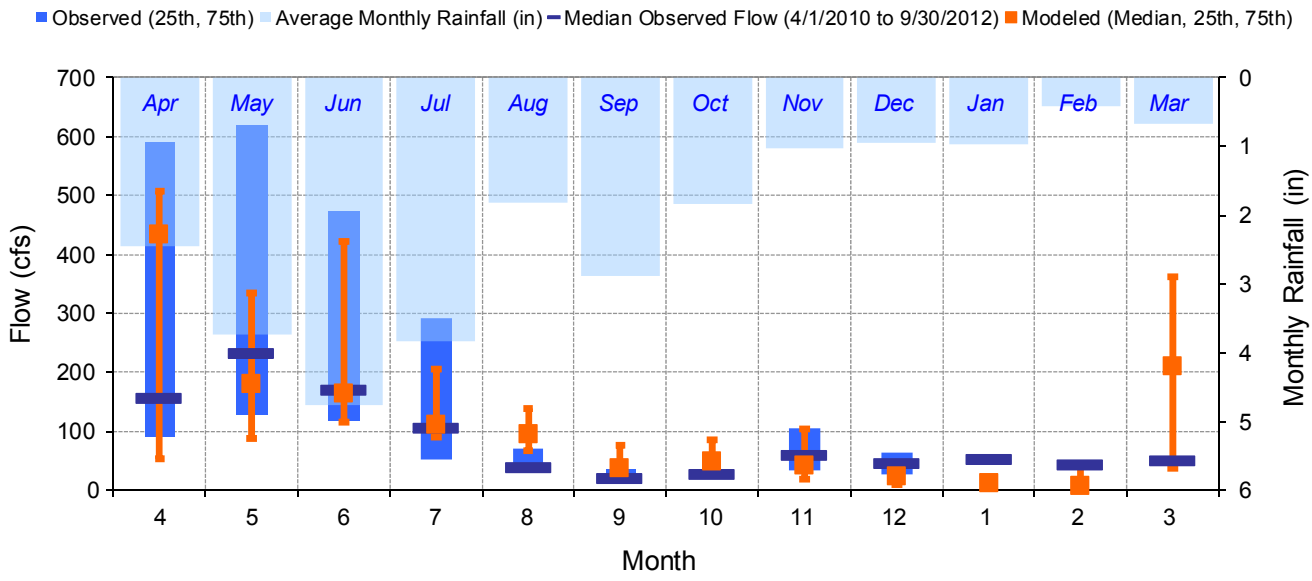

Figure C-19. Seasonal medians and ranges at HYDSTRA 03138001 St. Louis River near Aurora

Table C-5. Seasonal summary at HYDSTRA 03138001 St. Louis River near Aurora

MONTH	OBSERVED FLOW (CFS)				MODELED FLOW (CFS)			
	MEAN	MEDIAN	25TH	75TH	MEAN	MEDIAN	25TH	75TH
Apr	350.41	157.95	91.75	592.50	377.48	433.69	52.93	508.57
May	434.10	234.00	128.00	619.50	287.79	180.94	87.66	334.69
Jun	449.96	170.00	119.50	473.50	322.68	163.86	114.95	421.57
Jul	209.63	106.00	52.00	293.00	153.24	110.11	89.88	206.05
Aug	69.83	39.00	33.00	71.00	108.12	94.10	67.69	139.48
Sep	27.48	20.50	16.25	37.00	53.81	36.30	27.97	76.29
Oct	36.67	29.05	27.00	33.00	68.59	49.34	31.18	84.58
Nov	70.05	60.73	34.33	104.13	66.24	42.93	18.39	104.48
Dec	47.90	47.24	26.25	63.87	27.85	23.52	10.14	41.60
Jan	52.67	53.09	50.05	57.35	13.01	11.64	9.62	13.41
Feb	44.30	44.25	41.75	46.68	22.92	7.97	6.94	45.17
Mar	54.51	51.27	47.86	55.58	211.53	210.37	36.92	362.12

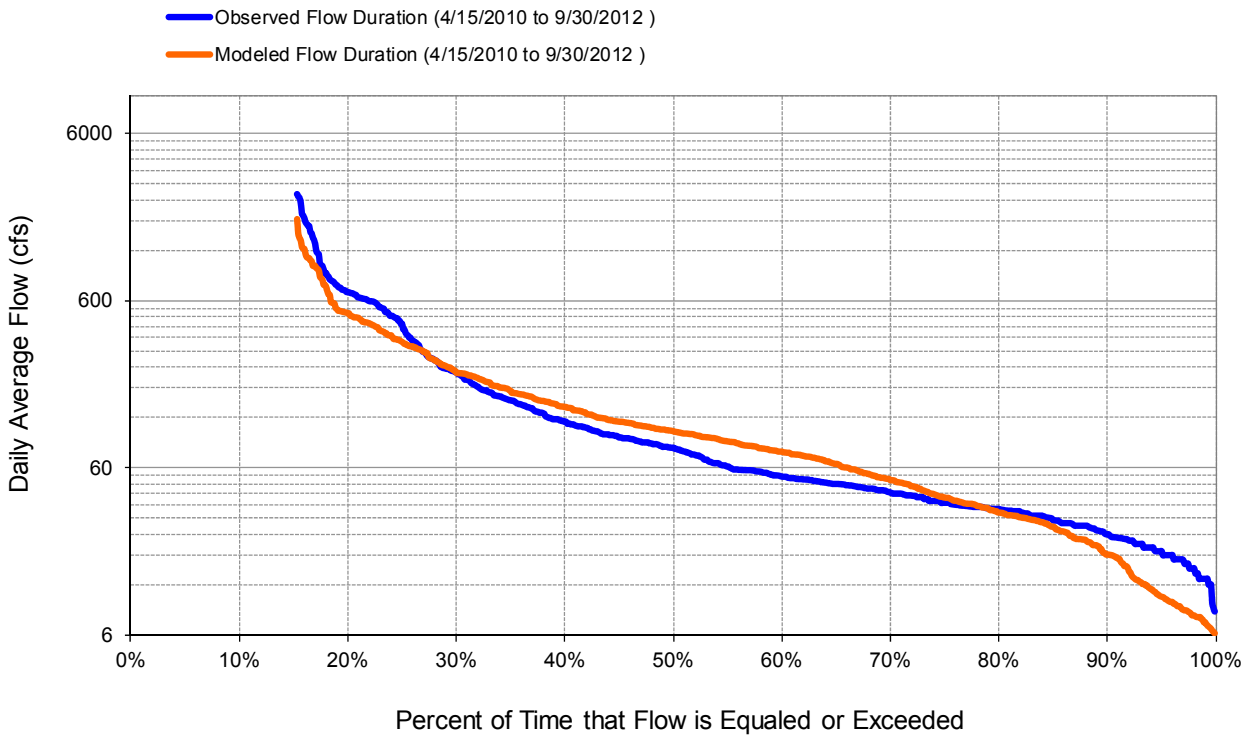

Figure C-20. Flow exceedance at HYDSTRA 03138001 St. Louis River near Aurora

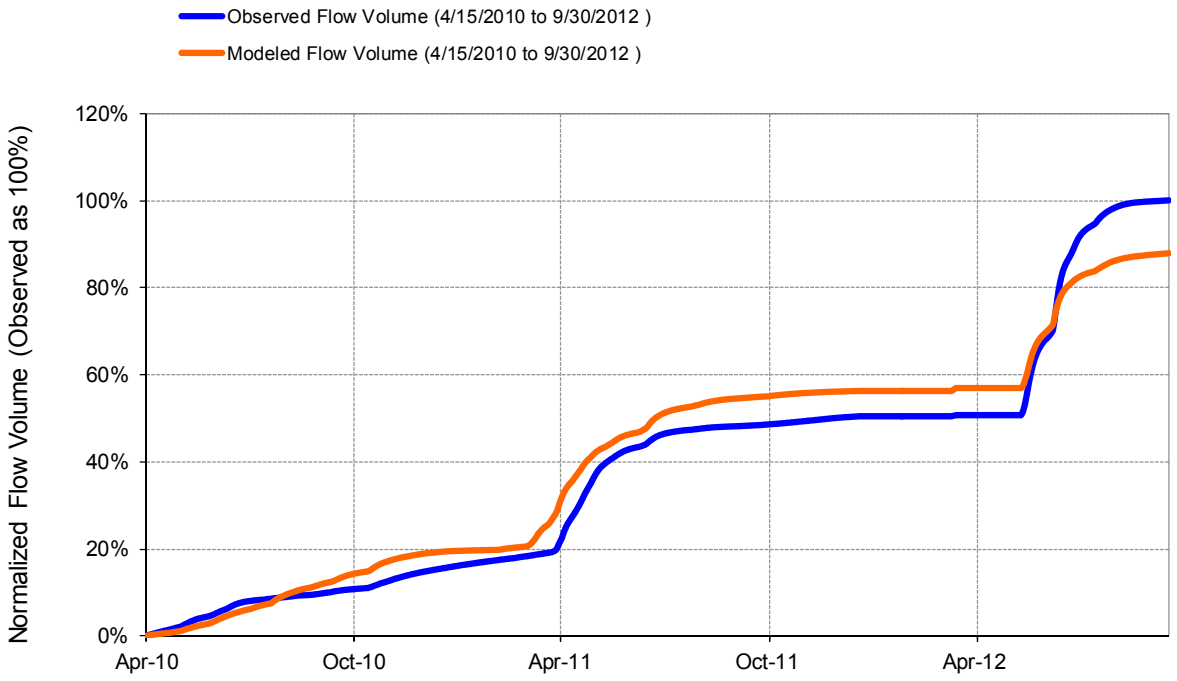

Figure C-21. Flow accumulation at HYDSTRA 03138001 St. Louis River near Aurora

Table C-6. Summary statistics at HYDSTRA 03138001 St. Louis River near Aurora

HSPF Simulated Flow			Observed Flow Gage		
REACH OUTFLOW FROM DSN 258 2.46-Year Analysis Period: 4/1/2010 - 9/30/2012 Flow volumes are (inches/year) for upstream drainage area			HYDSTRA 03138001 St. Louis River nr Aurora Manually Entered Data Drainage Area (sq-mi): 277		
Total Simulated In-stream Flow:	**6.23**		Total Observed In-stream Flow:		**7.09**
Total of simulated highest 10% flows:	**2.80**		Total of Observed highest 10% flows:		**3.93**
Total of Simulated lowest 50% flows:	**0.78**		Total of Observed Lowest 50% flows:		**0.72**
Simulated Summer Flow Volume (months 7-9):	**1.59**		Observed Summer Flow Volume (7-9):		**1.55**
Simulated Fall Flow Volume (months 10-12):	**0.54**		Observed Fall Flow Volume (10-12):		**0.51**
Simulated Winter Flow Volume (months 1-3):	**0.46**		Observed Winter Flow Volume (1-3):		**0.26**
Simulated Spring Flow Volume (months 4-6):	**3.64**		Observed Spring Flow Volume (4-6):		**4.76**
Total Simulated Storm Volume:	**1.59**		Total Observed Storm Volume:		**1.85**
Simulated Summer Storm Volume (7-9):	**0.29**		Observed Summer Storm Volume (7-9):		**0.32**
Errors (Simulated-Observed)	*Error Statistics*	*Recommended Criteria*			
Error in total volume:	-12.12	10			
Error in 50% lowest flows:	8.79	10			
Error in 10% highest flows:	-28.83	15			
Seasonal volume error - Summer:	2.41	30			
Seasonal volume error - Fall:	5.37	30			
Seasonal volume error - Winter:	75.06	30			
Seasonal volume error - Spring:	-23.56	30			
Error in storm volumes:	-14.47	20			
Error in summer storm volumes:	-10.41	50			
Nash-Sutcliffe Coefficient of Efficiency, E:	0.750	Model accuracy increases			
Baseline adjusted coefficient (Garrick), E':	0.545				
Monthly NSE	0.777				

>> Clear

HYDSTRA 03115001 St. Louis River near Forbes

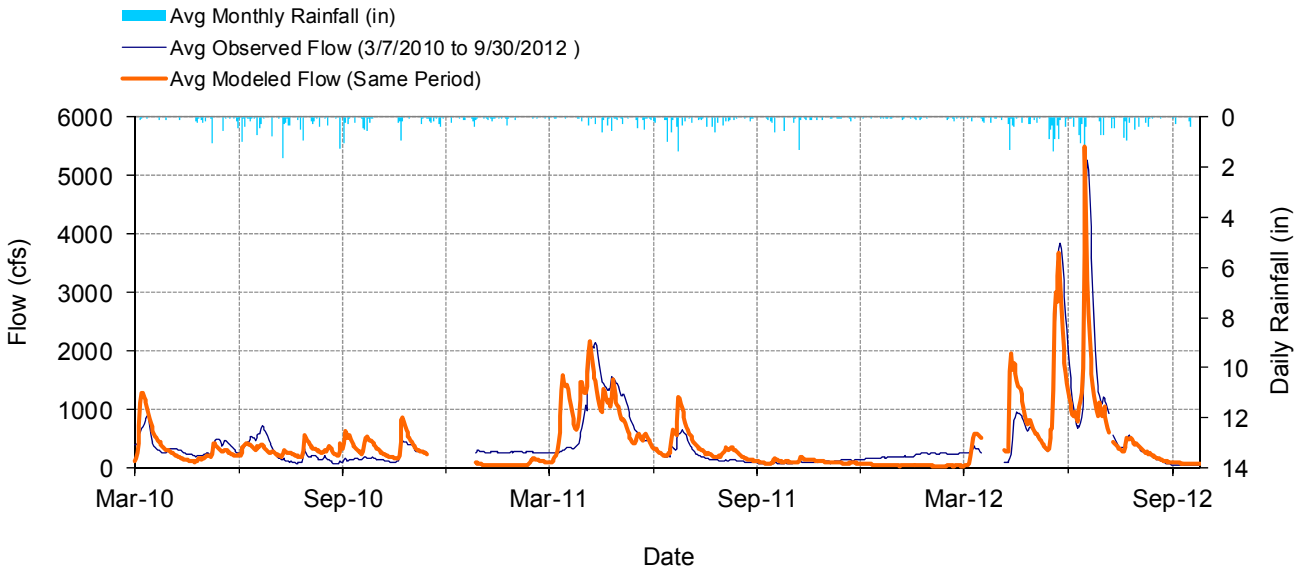

Figure C-22. Mean daily flow at HYDSTRA 03115001 St. Louis River near Forbes

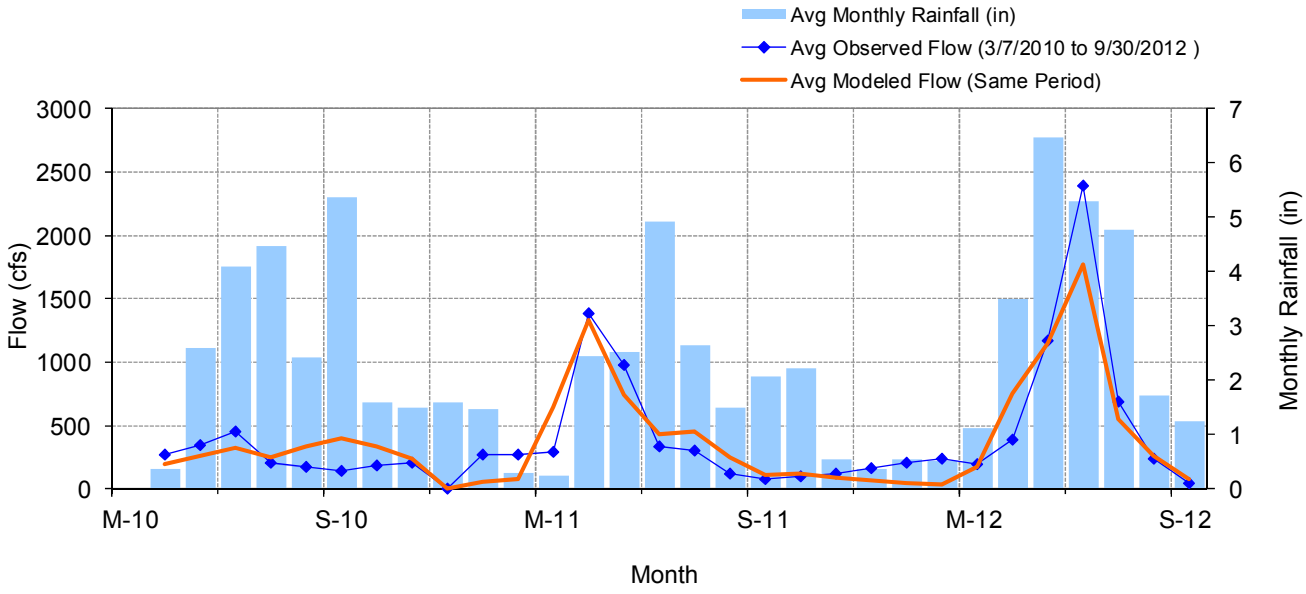

Figure C-23. Mean monthly flow at HYDSTRA 03115001 St. Louis River near Forbes

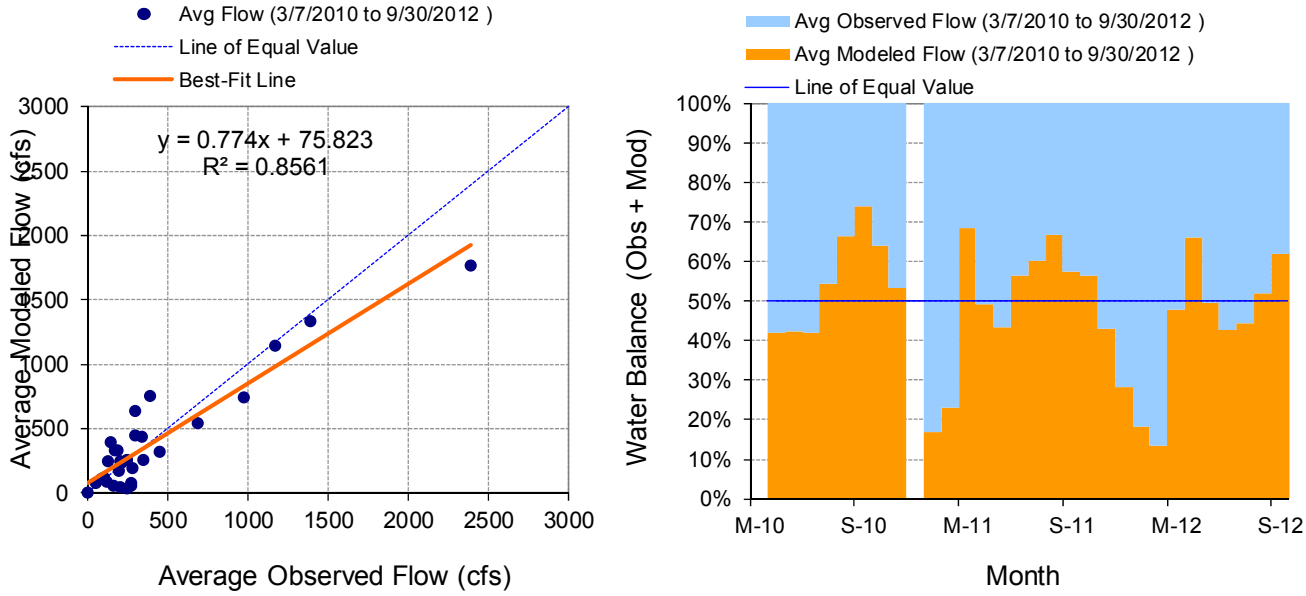

Figure C-24. Monthly flow regression and temporal variation at HYDSTRA 03115001 St. Louis River near Forbes

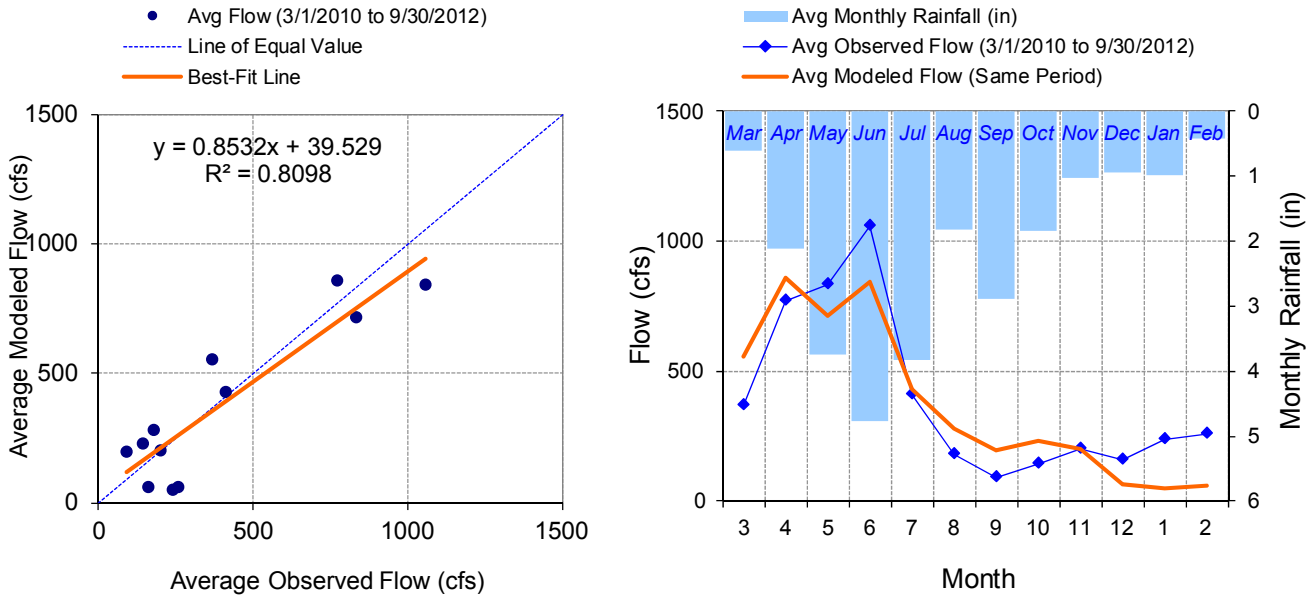

Figure C-25. Seasonal regression and temporal aggregate at HYDSTRA 03115001 St. Louis River near Forbes

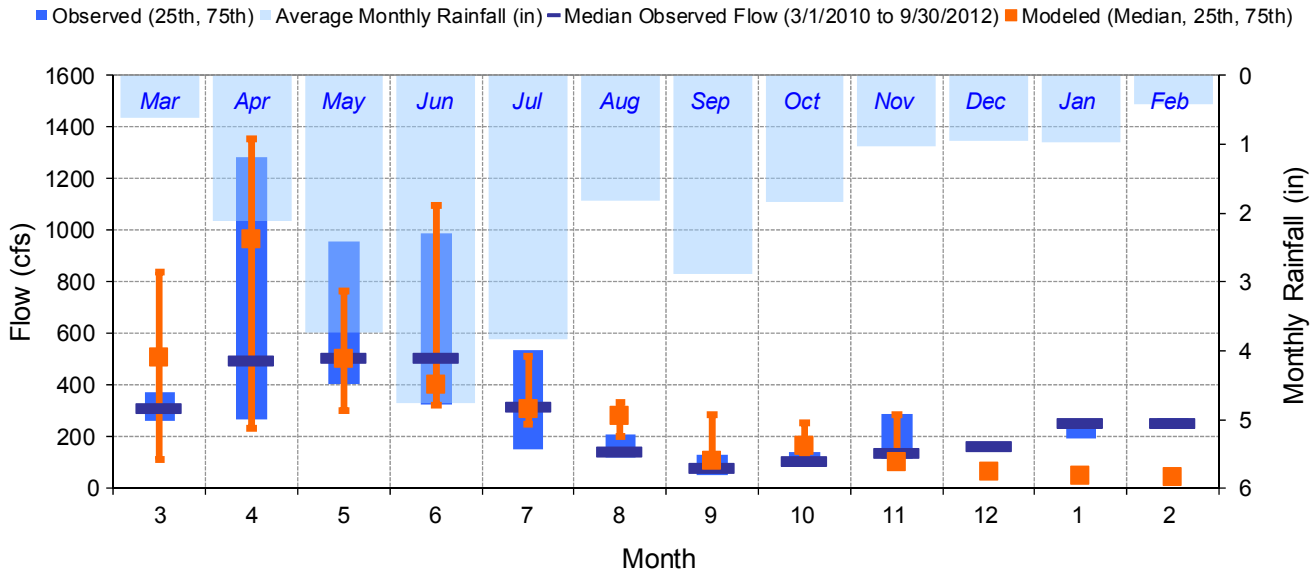

Figure C-26. Seasonal medians and ranges at HYDSTRA 03115001 St. Louis River near Forbes

Table C-7. Seasonal summary at HYDSTRA 03115001 St. Louis River near Forbes

MONTH	OBSERVED FLOW (CFS)				MODELED FLOW (CFS)			
	MEAN	MEDIAN	25TH	75TH	MEAN	MEDIAN	25TH	75TH
Mar	365.19	310.00	262.30	369.74	556.19	507.53	111.93	840.77
Apr	769.17	493.83	264.50	1285.80	859.02	965.00	235.02	1354.63
May	830.59	505.83	402.00	957.95	715.23	501.27	303.17	765.81
Jun	1058.41	504.00	322.29	989.38	842.60	401.88	321.33	1094.67
Jul	410.01	318.25	152.60	534.59	429.26	304.71	247.10	514.37
Aug	177.53	143.00	121.44	209.00	280.65	278.19	198.53	334.16
Sep	90.49	77.47	53.39	128.75	197.04	106.86	81.87	287.77
Oct	142.85	106.48	97.18	138.75	229.95	166.53	126.56	252.64
Nov	201.35	136.37	113.87	287.00	201.88	102.50	87.94	286.47
Dec	160.38	161.96	146.44	171.31	63.01	61.63	53.36	70.39
Jan	237.81	252.12	191.44	269.20	50.55	48.63	45.37	52.65
Feb	255.65	254.68	246.32	270.15	58.52	40.76	36.86	45.46

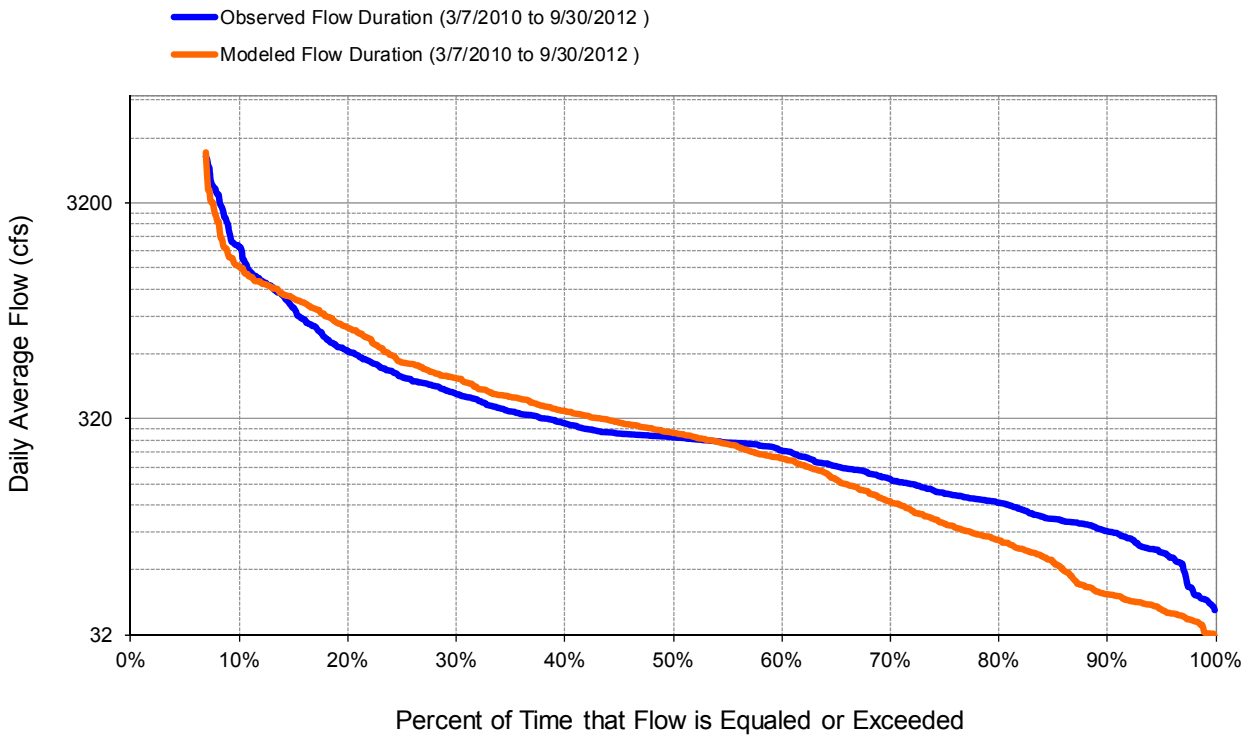

Figure C-27. Flow exceedance at HYDSTRA 03115001 St. Louis River near Forbes

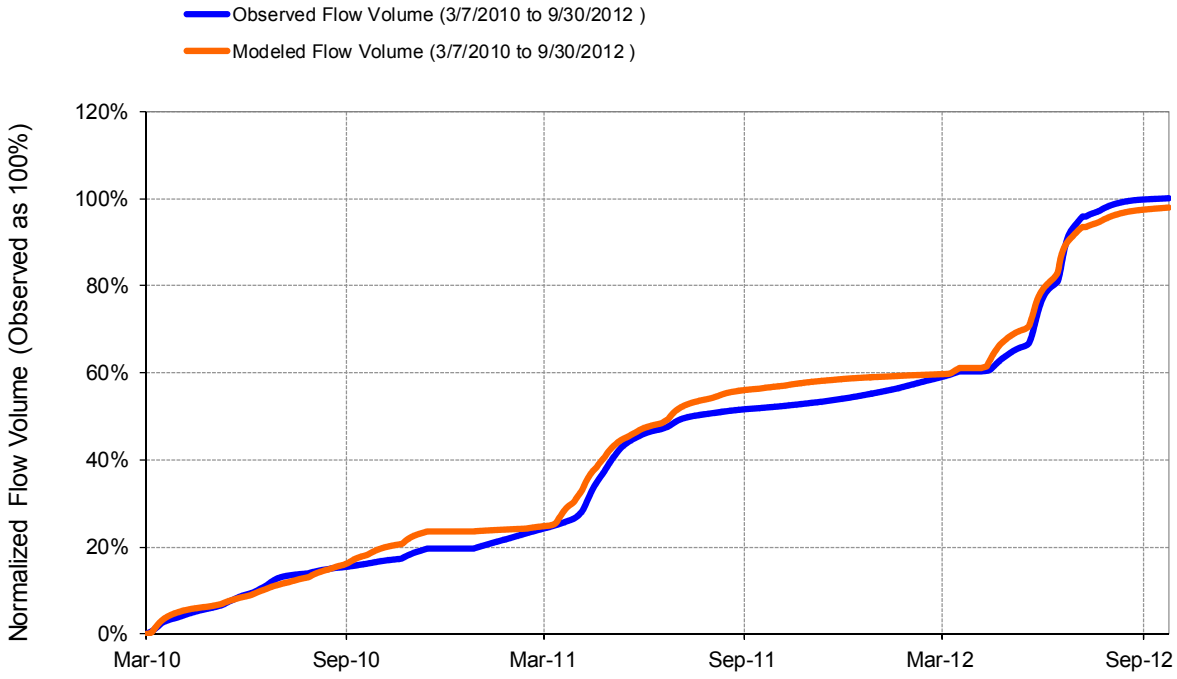

Figure C-28. Flow accumulation at HYDSTRA 03115001 St. Louis River near Forbes

Table C-8. Summary statistics at HYDSTRA 03115001 St. Louis River near Forbes

HSPF Simulated Flow		Observed Flow Gage		
REACH OUTFLOW FROM DSN 249 2.57-Year Analysis Period: 3/1/2010 - 9/30/2012 Flow volumes are (inches/year) for upstream drainage area		HYDSTRA 03115001 St. Louis River nr Forbes Manually Entered Data Drainage Area (sq-mi): 692		
Total Simulated In-stream Flow:	**7.71**	Total Observed In-stream Flow:		**7.88**
Total of simulated highest 10% flows:	**3.13**	Total of Observed highest 10% flows:		**3.53**
Total of Simulated lowest 50% flows:	**1.06**	Total of Observed Lowest 50% flows:		**1.36**
Simulated Summer Flow Volume (months 7-9):	**1.72**	Observed Summer Flow Volume (7-9):		**1.29**
Simulated Fall Flow Volume (months 10-12):	**0.55**	Observed Fall Flow Volume (10-12):		**0.50**
Simulated Winter Flow Volume (months 1-3):	**1.03**	Observed Winter Flow Volume (1-3):		**1.20**
Simulated Spring Flow Volume (months 4-6):	**4.41**	Observed Spring Flow Volume (4-6):		**4.89**
Total Simulated Storm Volume:	**1.96**	Total Observed Storm Volume:		**1.66**
Simulated Summer Storm Volume (7-9):	**0.27**	Observed Summer Storm Volume (7-9):		**0.17**
Errors (Simulated-Observed)	*Error Statistics*	*Recommended Criteria*		
Error in total volume:	-2.07	10		
Error in 50% lowest flows:	-21.65	10		
Error in 10% highest flows:	-11.32	15		
Seasonal volume error - Summer:	33.97	30		
Seasonal volume error - Fall:	10.16	30		
Seasonal volume error - Winter:	-14.17	30		
Seasonal volume error - Spring:	-9.81	30		
Error in storm volumes:	17.59	20		
Error in summer storm volumes:	59.78	50		
Nash-Sutcliffe Coefficient of Efficiency, E:	0.724			
Baseline adjusted coefficient (Garrick), E':	0.450	Model accuracy increases		
Monthly NSE	0.841		0.837	

>> Clear

HYDSTRA 03084001 Swan River near Toivola

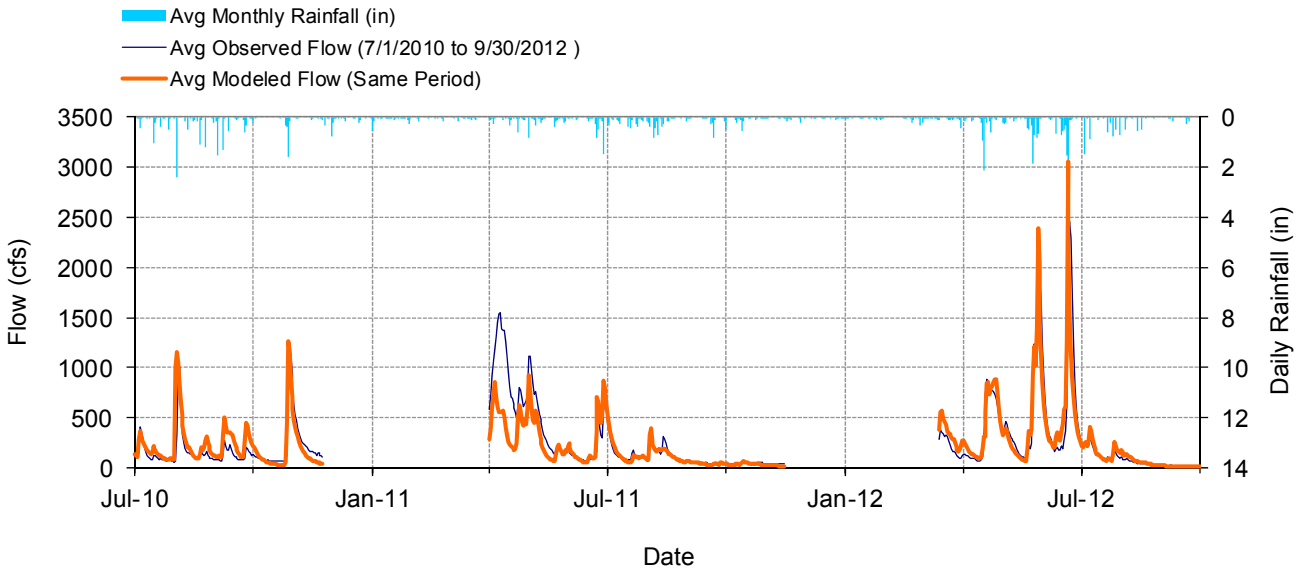

Figure C-29. Mean daily flow at HYDSTRA 03084001 Swan River near Toivola

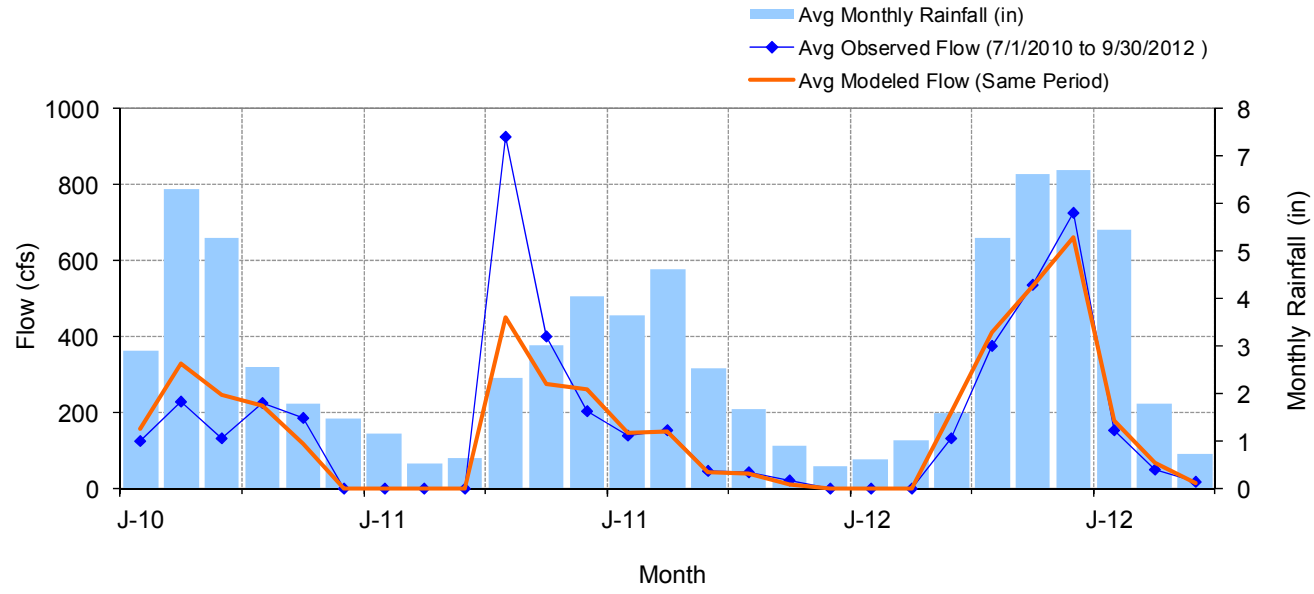

Figure C-30. Mean monthly flow at HYDSTRA 03084001 Swan River near Toivola

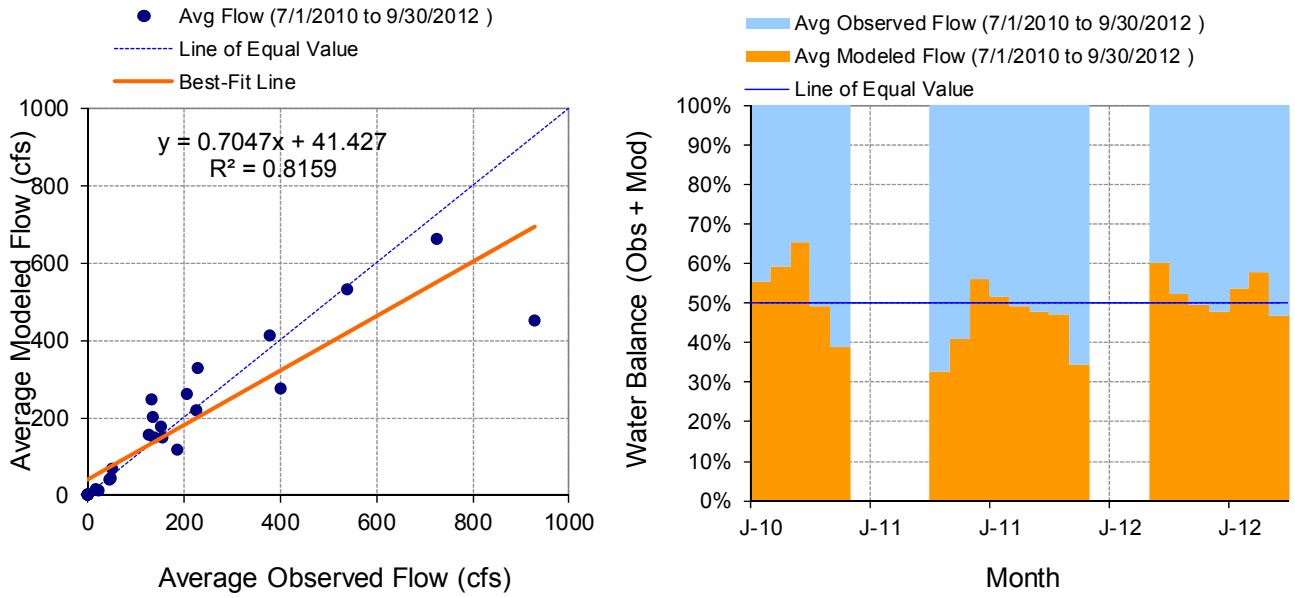

Figure C-31. Monthly flow regression and temporal variation at HYDSTRA 03084001 Swan River near Toivola

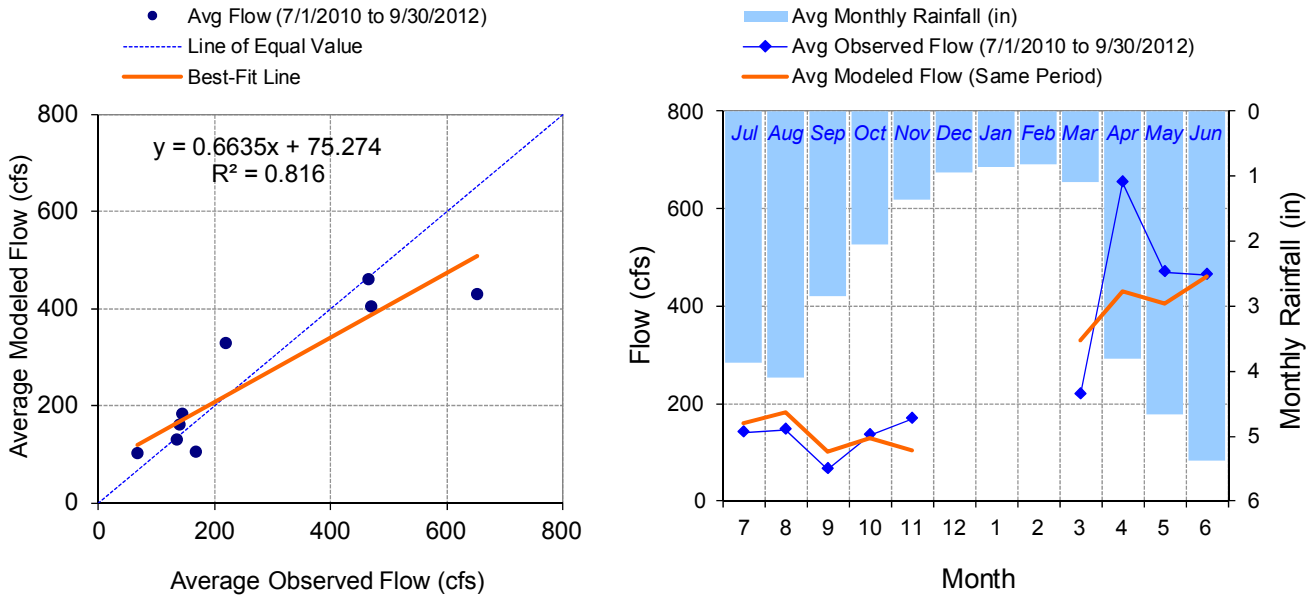

Figure C-32. Seasonal regression and temporal aggregate at HYDSTRA 03084001 Swan River near Toivola

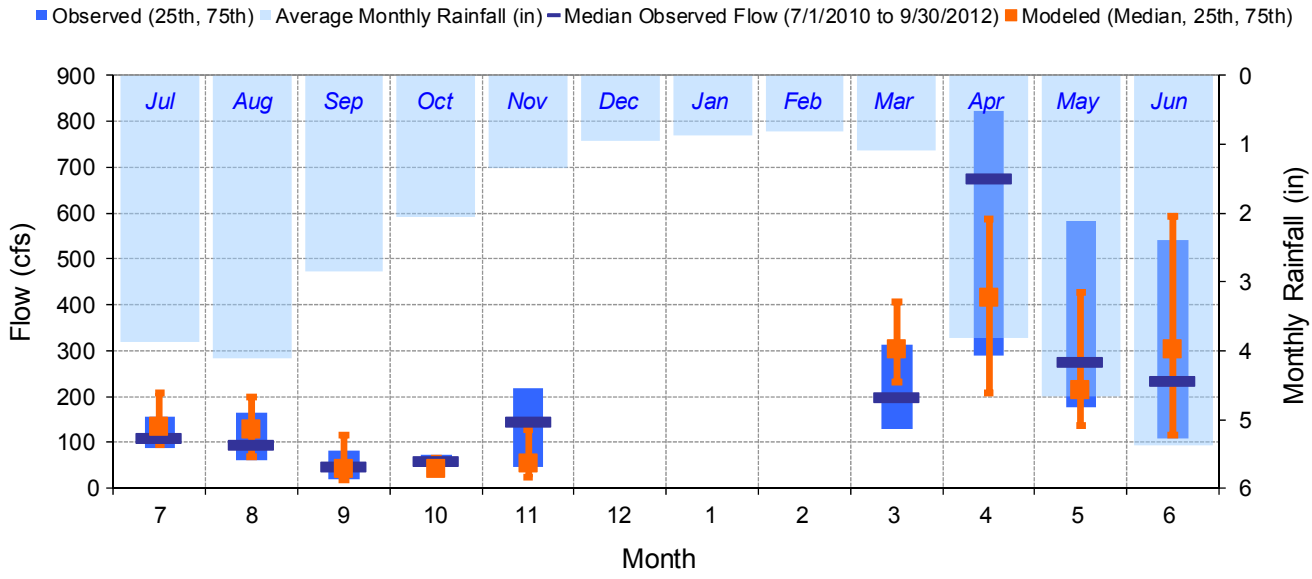

Figure C-33. Seasonal medians and ranges at HYDSTRA 03084001 Swan River near Toivola

Table C-9. Seasonal summary at HYDSTRA 03084001 Swan River near Toivola

MONTH	OBSERVED FLOW (CFS)				MODELED FLOW (CFS)			
	MEAN	MEDIAN	25TH	75TH	MEAN	MEDIAN	25TH	75TH
Jul	139.41	109.00	87.00	157.00	160.94	132.92	96.38	208.55
Aug	144.55	96.00	62.00	164.00	182.85	129.16	67.48	197.94
Sep	65.86	48.00	19.00	83.00	102.19	42.12	19.42	116.72
Oct	135.03	59.50	46.00	74.00	129.60	43.32	34.09	65.22
Nov	168.38	145.00	46.00	217.00	105.04	53.80	25.67	127.54
Dec	0.00	0.00	0.00	0.00	0.00	0.00	0.00	0.00
Jan	0.00	0.00	0.00	0.00	0.00	0.00	0.00	0.00
Feb	0.00	0.00	0.00	0.00	0.00	0.00	0.00	0.00
Mar	219.21	198.00	129.50	314.50	330.26	302.97	232.73	405.65
Apr	652.12	675.00	290.25	824.25	431.61	415.57	206.95	588.24
May	469.63	275.50	177.50	583.00	404.50	213.01	135.84	427.35
Jun	464.98	234.50	109.50	541.75	462.12	303.21	116.90	594.32

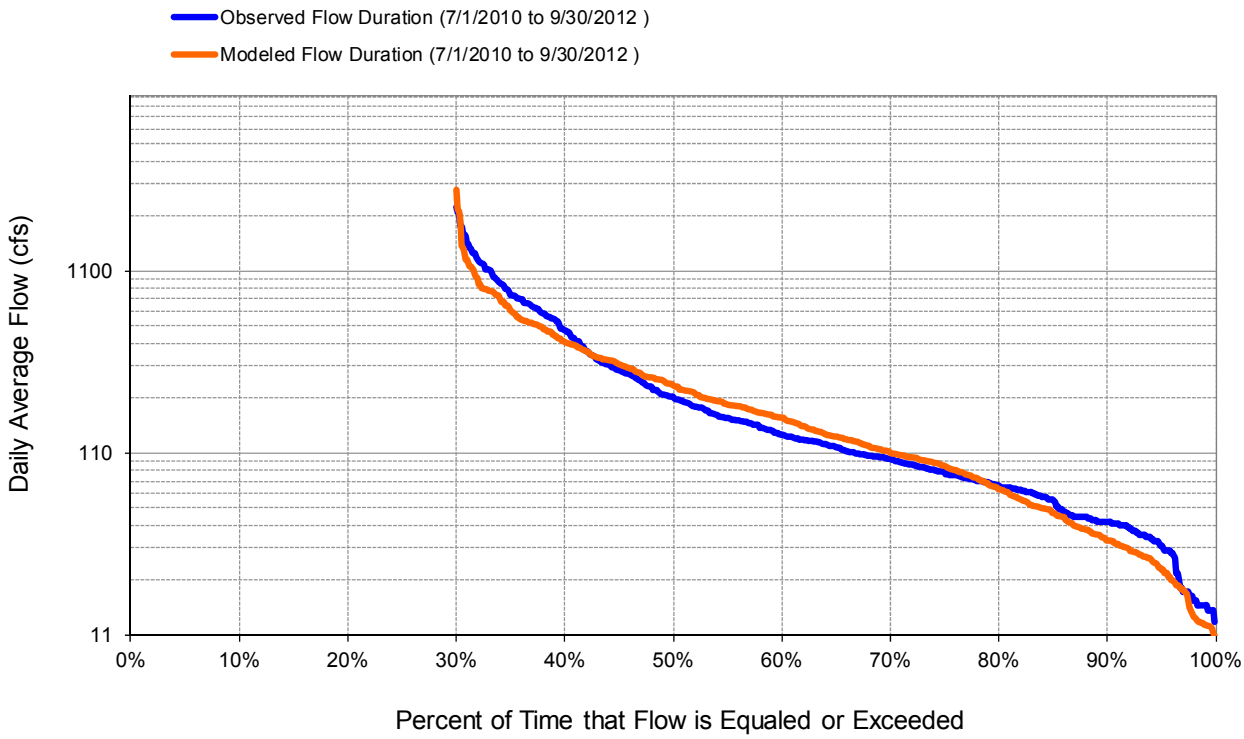

Figure C-34. Flow exceedance at HYDSTRA 03084001 Swan River near Toivola

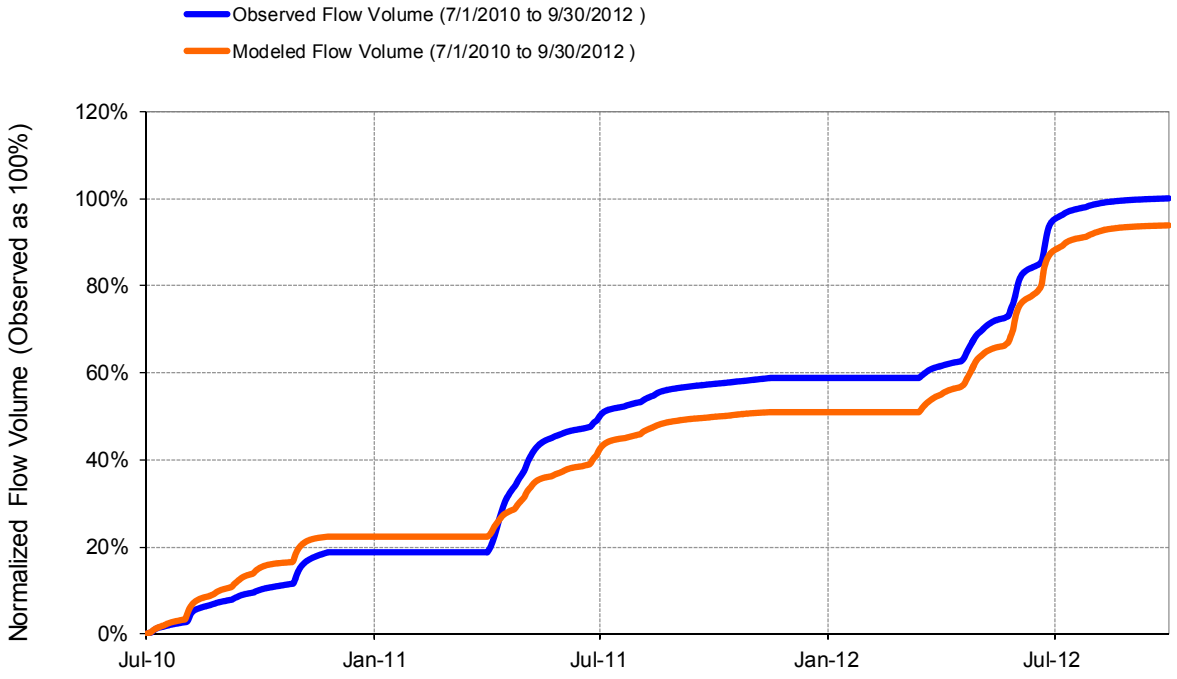

Figure C-35. Flow accumulation at HYDSTRA 03084001 Swan River near Toivola

Table C-10. Summary statistics at HYDSTRA 03084001 Swan River near Toivola

HSPF Simulated Flow			Observed Flow Gage		
REACH OUTFLOW FROM DSN 232 2.25-Year Analysis Period: 7/1/2010 - 9/30/2012 Flow volumes are (inches/year) for upstream drainage area			HYDSTRA 03084001 Swan River nr Toivola Manually Entered Data Drainage Area (sq-mi): 239		
Total Simulated In-stream Flow:	**9.53**		Total Observed In-stream Flow:		**10.17**
Total of simulated highest 10% flows:	**3.86**		Total of Observed highest 10% flows:		**4.64**
Total of Simulated lowest 50% flows:	**1.31**		Total of Observed Lowest 50% flows:		**1.32**
Simulated Summer Flow Volume (months 7-9):	**2.84**		Observed Summer Flow Volume (7-9):		**2.23**
Simulated Fall Flow Volume (months 10-12):	**0.82**		Observed Fall Flow Volume (10-12):		**1.01**
Simulated Winter Flow Volume (months 1-3):	**0.43**		Observed Winter Flow Volume (1-3):		**0.29**
Simulated Spring Flow Volume (months 4-6):	**5.44**		Observed Spring Flow Volume (4-6):		**6.64**
Total Simulated Storm Volume:	**3.02**		Total Observed Storm Volume:		**2.86**
Simulated Summer Storm Volume (7-9):	**0.80**		Observed Summer Storm Volume (7-9):		**0.61**
Errors (Simulated-Observed)	*Error Statistics*		*Recommended Criteria*		
Error in total volume:	-6.23		10		
Error in 50% lowest flows:	-0.14		10		
Error in 10% highest flows:	-16.85		15		
Seasonal volume error - Summer:	27.32		30		
Seasonal volume error - Fall:	-18.35	>>	30	Clear	
Seasonal volume error - Winter:	50.66		30		
Seasonal volume error - Spring:	-18.14		30		
Error in storm volumes:	5.67		20		
Error in summer storm volumes:	31.72		50		
Nash-Sutcliffe Coefficient of Efficiency, E:	0.707		Model accuracy increases		
Baseline adjusted coefficient (Garrick), E':	0.598				
Monthly NSE	0.760				

USGS 04021520 Stoney Brook at Pine Drive near Brookston

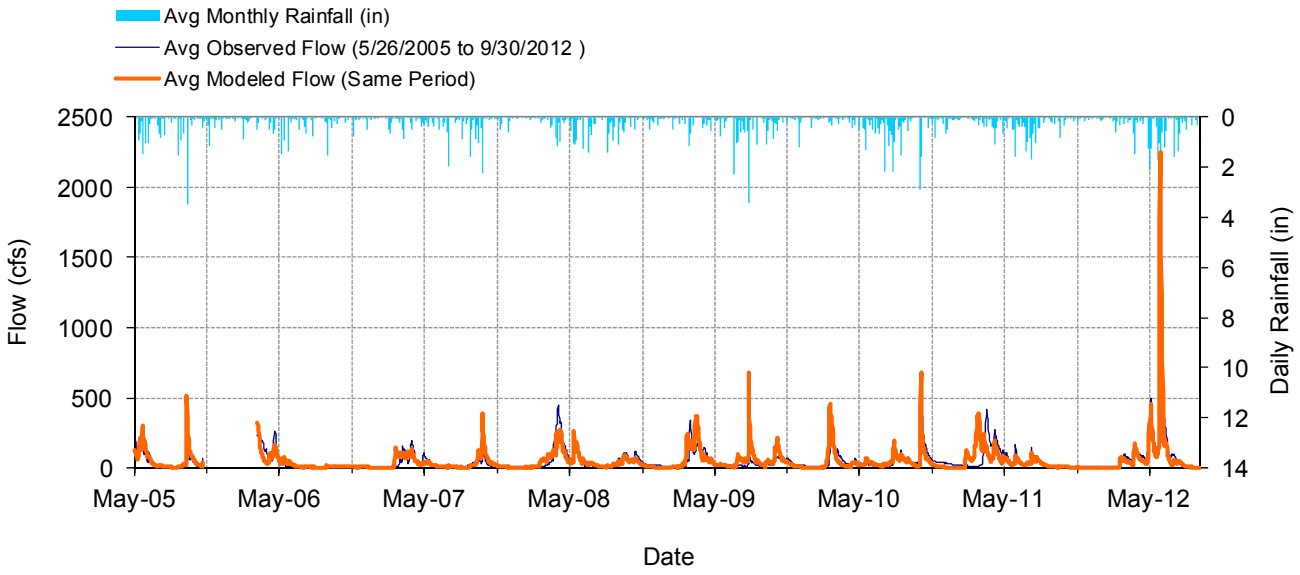

Figure C-36. Mean daily flow at USGS 04021520 Stoney Brook at Pine Drive near Brookston

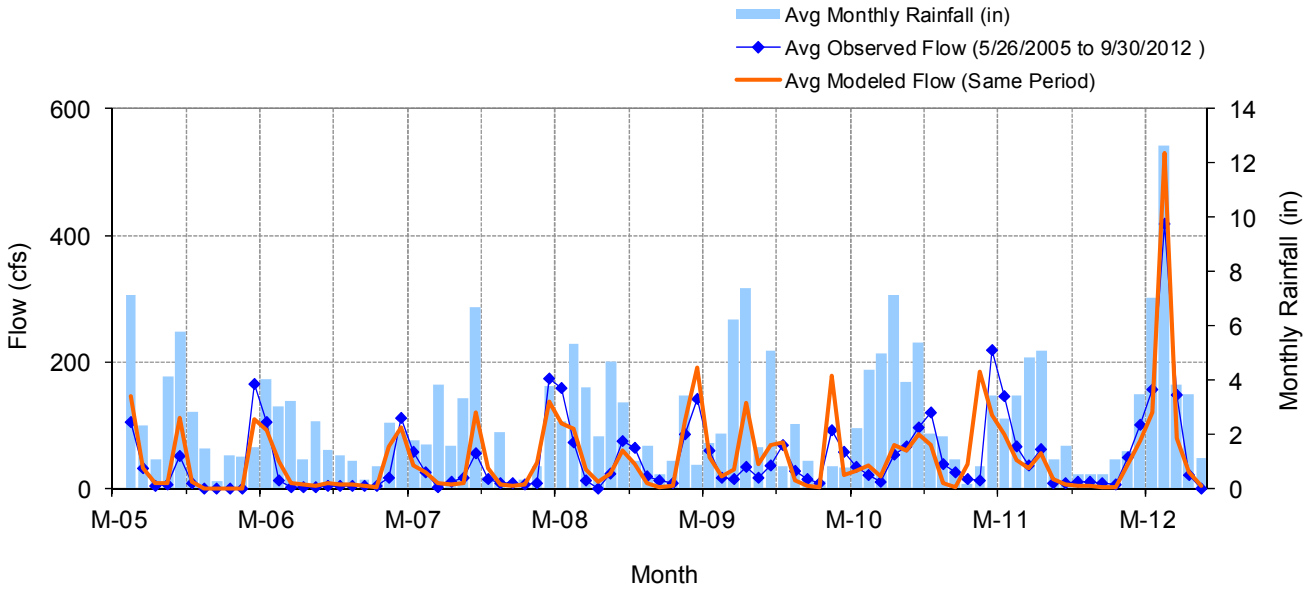

Figure C-37. Mean monthly flow at USGS 04021520 Stoney Brook at Pine Drive near Brookston

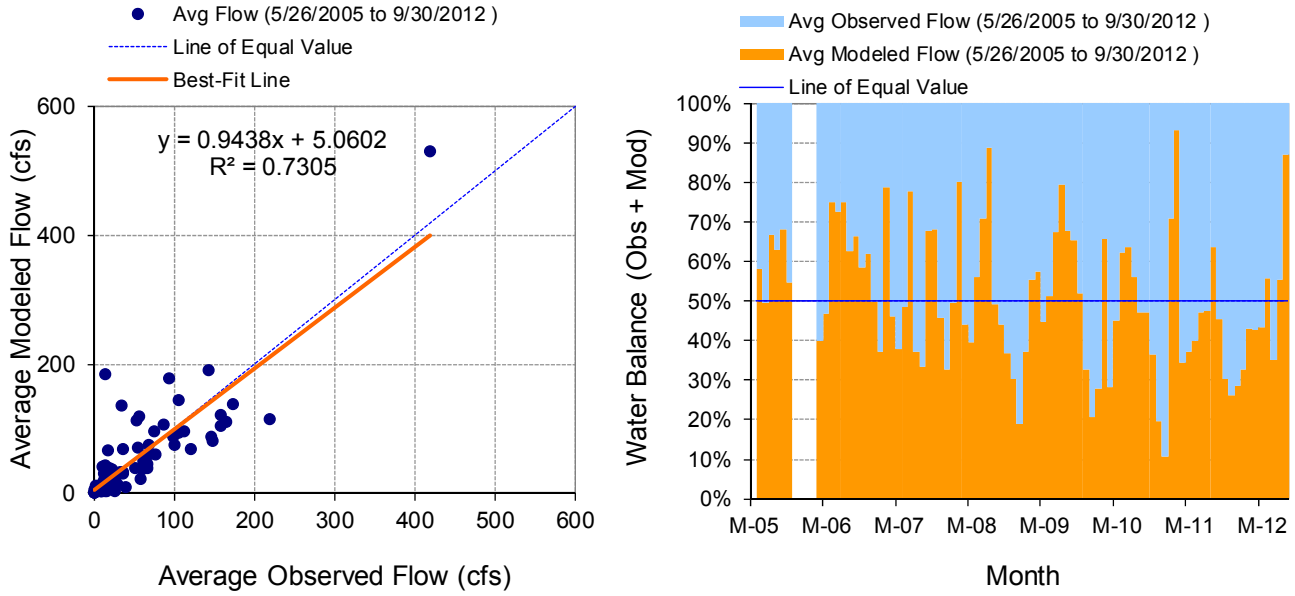

Figure C-38. Monthly flow regression and temporal variation at USGS 04021520 Stoney Brook at Pine Drive near Brookston

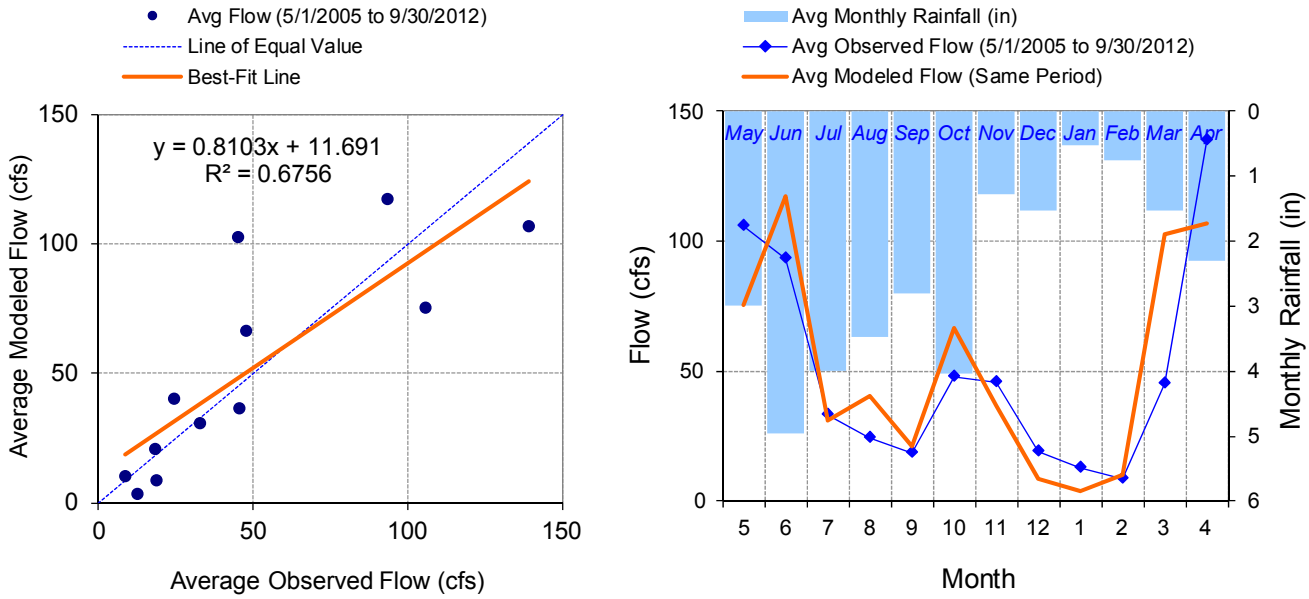

Figure C-39. Seasonal regression and temporal aggregate at USGS 04021520 Stoney Brook at Pine Drive near Brookston

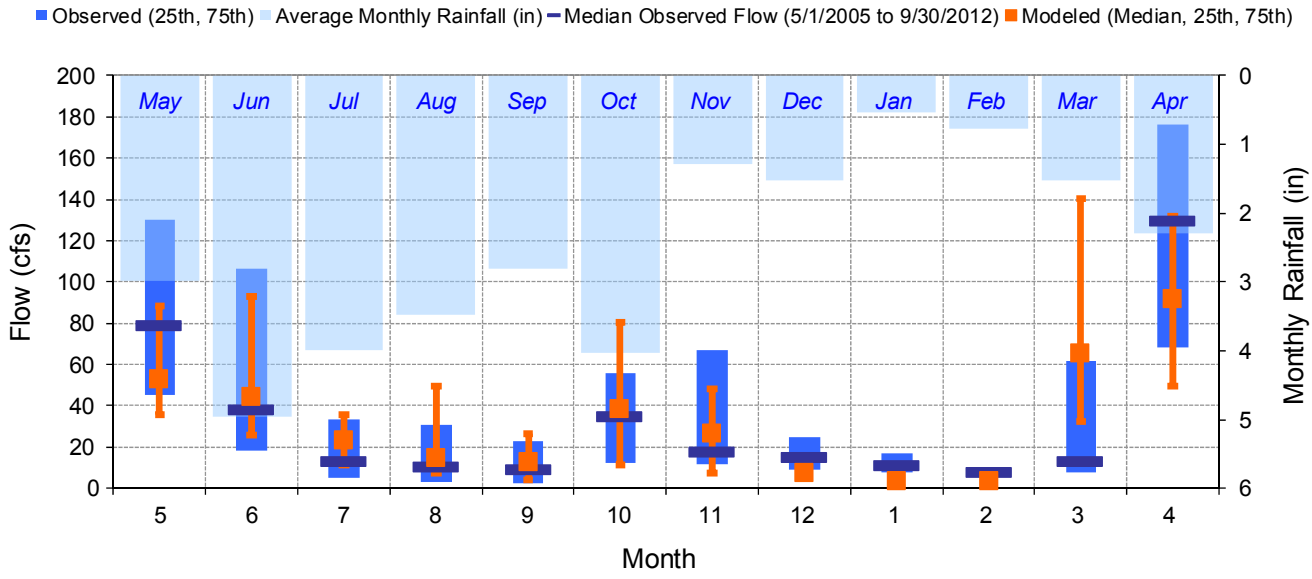

Figure C-40. Seasonal medians and ranges at USGS 04021520 Stoney Brook at Pine Drive near Brookston

Table C-11. Seasonal summary at USGS 04021520 Stoney Brook at Pine Drive near Brookston

MONTH	OBSERVED FLOW (CFS)				MODELED FLOW (CFS)			
	MEAN	MEDIAN	25TH	75TH	MEAN	MEDIAN	25TH	75TH
May	105.52	79.00	45.00	130.00	75.22	52.57	35.36	88.42
Jun	93.25	38.50	18.00	106.25	117.43	44.50	25.69	92.82
Jul	32.87	13.00	4.80	33.25	30.79	22.85	11.25	35.40
Aug	24.27	10.50	2.80	30.75	40.49	14.84	7.13	49.21
Sep	18.46	9.55	2.60	22.50	20.91	12.95	4.23	26.39
Oct	47.81	35.00	12.00	56.00	66.50	38.16	11.21	80.73
Nov	45.65	18.00	11.50	67.00	36.59	26.59	7.48	48.09
Dec	18.88	15.00	8.80	25.00	8.65	7.44	5.33	10.65
Jan	12.68	11.00	7.80	16.75	3.69	3.59	2.98	4.25
Feb	8.58	7.70	6.23	9.58	10.08	3.31	2.31	5.86
Mar	45.26	13.00	7.50	62.00	102.70	65.14	32.38	140.48
Apr	138.82	130.00	68.50	176.00	106.98	91.38	49.62	131.58

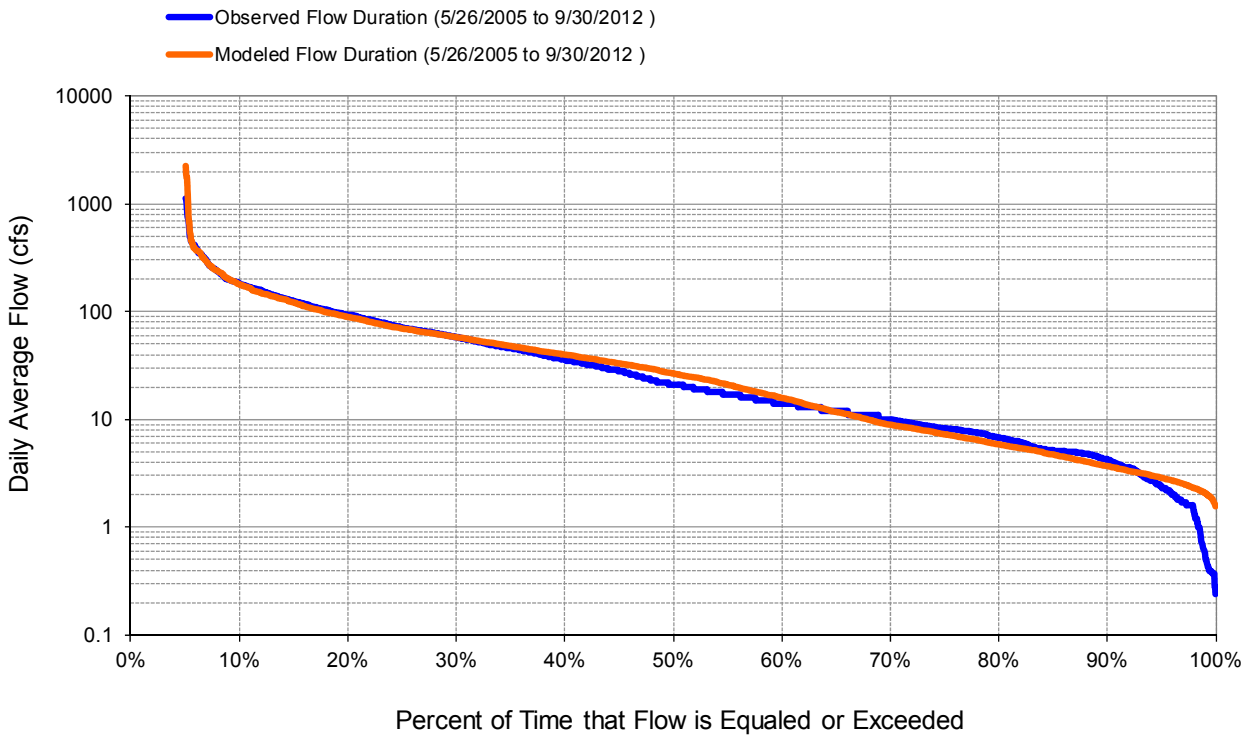

Figure C-41. Flow exceedance at USGS 04021520 Stoney Brook at Pine Drive near Brookston

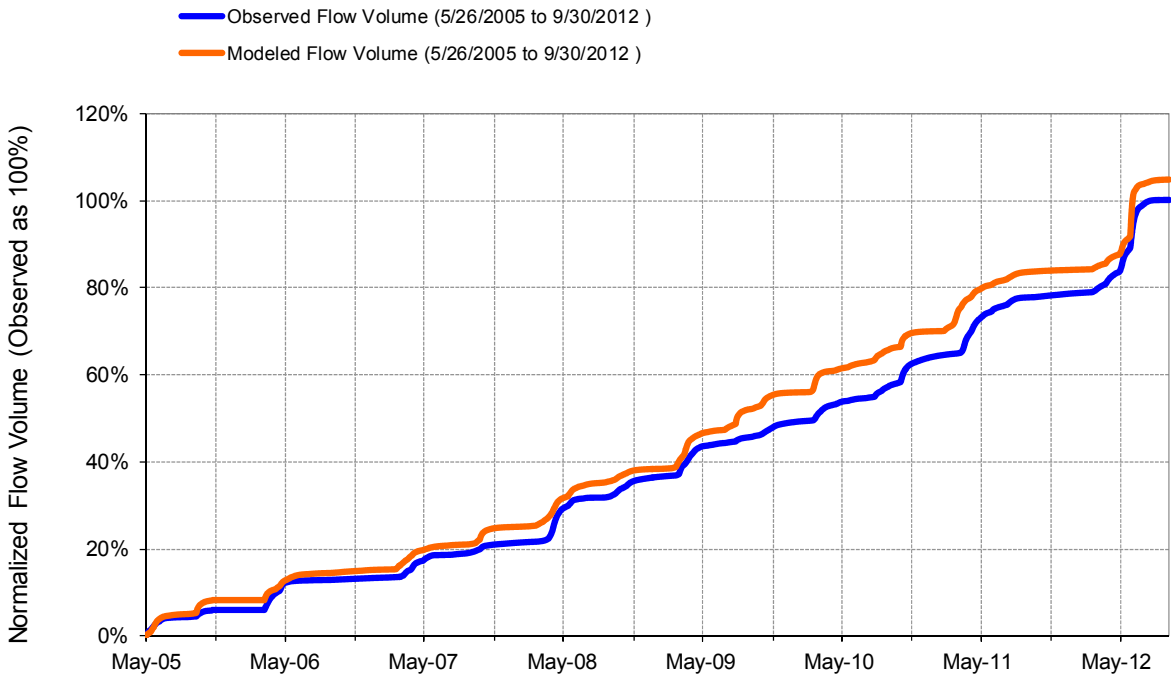

Figure C-42. Flow accumulation at USGS 04021520 Stoney Brook at Pine Drive near Brookston

Table C-12. Summary statistics at USGS 04021520 Stoney Brook at Pine Drive near Brookston

HSPF Simulated Flow		Observed Flow Gage		
REACH OUTFLOW FROM DSN 212 7.35-Year Analysis Period: 5/1/2005 - 9/30/2012 Flow volumes are (inches/year) for upstream drainage area		USGS 04021520 Stoney Br at Pine Dr nr Brookston, MN Manually Entered Data Drainage Area (sq-mi): 74		
Total Simulated In-stream Flow:	**9.22**	Total Observed In-stream Flow:		**8.80**
Total of simulated highest 10% flows:	**4.49**	Total of Observed highest 10% flows:		**4.17**
Total of Simulated lowest 50% flows:	**0.77**	Total of Observed Lowest 50% flows:		**0.74**
Simulated Summer Flow Volume (months 7-9):	**1.55**	Observed Summer Flow Volume (7-9):		**1.27**
Simulated Fall Flow Volume (months 10-12):	**1.58**	Observed Fall Flow Volume (10-12):		**1.56**
Simulated Winter Flow Volume (months 1-3):	**1.47**	Observed Winter Flow Volume (1-3):		**0.84**
Simulated Spring Flow Volume (months 4-6):	**4.61**	Observed Spring Flow Volume (4-6):		**5.13**
Total Simulated Storm Volume:	**2.36**	Total Observed Storm Volume:		**1.70**
Simulated Summer Storm Volume (7-9):	**0.35**	Observed Summer Storm Volume (7-9):		**0.26**
Errors (Simulated-Observed)	*Error Statistics*	*Recommended Criteria*		
Error in total volume:	4.75	10		
Error in 50% lowest flows:	3.21	10		
Error in 10% highest flows:	7.55	15		
Seasonal volume error - Summer:	22.02	30		
Seasonal volume error - Fall:	1.70	30		
Seasonal volume error - Winter:	75.73	30		
Seasonal volume error - Spring:	-10.18	30		
Error in storm volumes:	38.20	20		
Error in summer storm volumes:	36.35	50		
Nash-Sutcliffe Coefficient of Efficiency, E:	0.367			
Baseline adjusted coefficient (Garrick), E':	0.403	Model accuracy increases		
Monthly NSE	0.658		0.657	

>> Clear

USGS 04048001 Cloquet River near Burnett

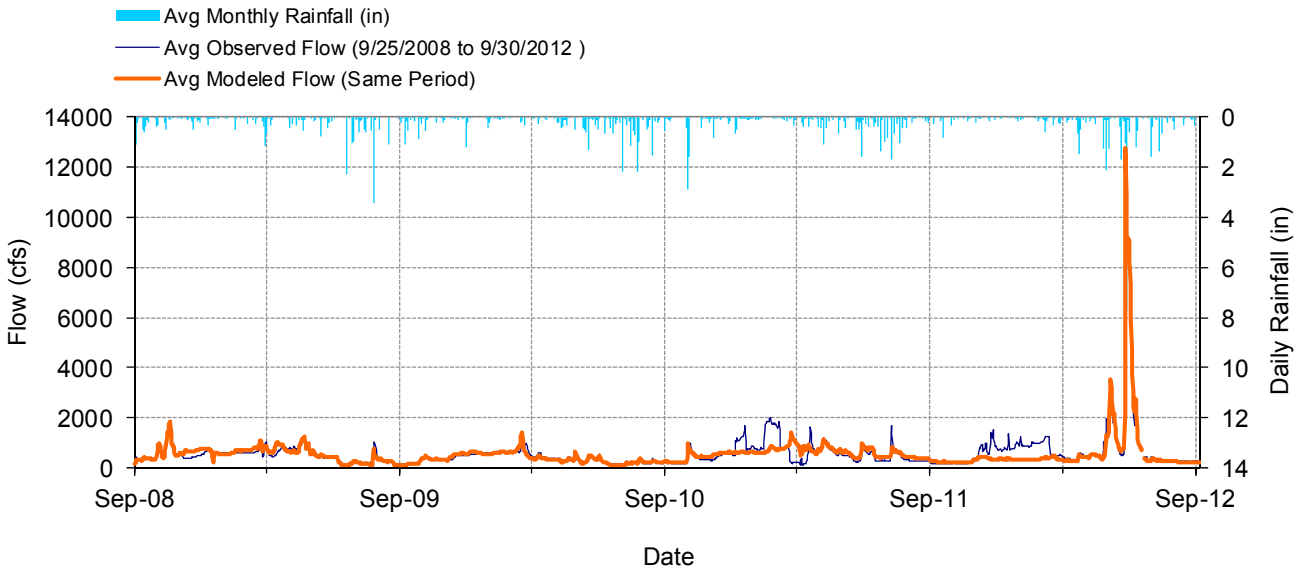

Figure C-43. Mean daily flow at USGS 04048001 Cloquet River near Burnett

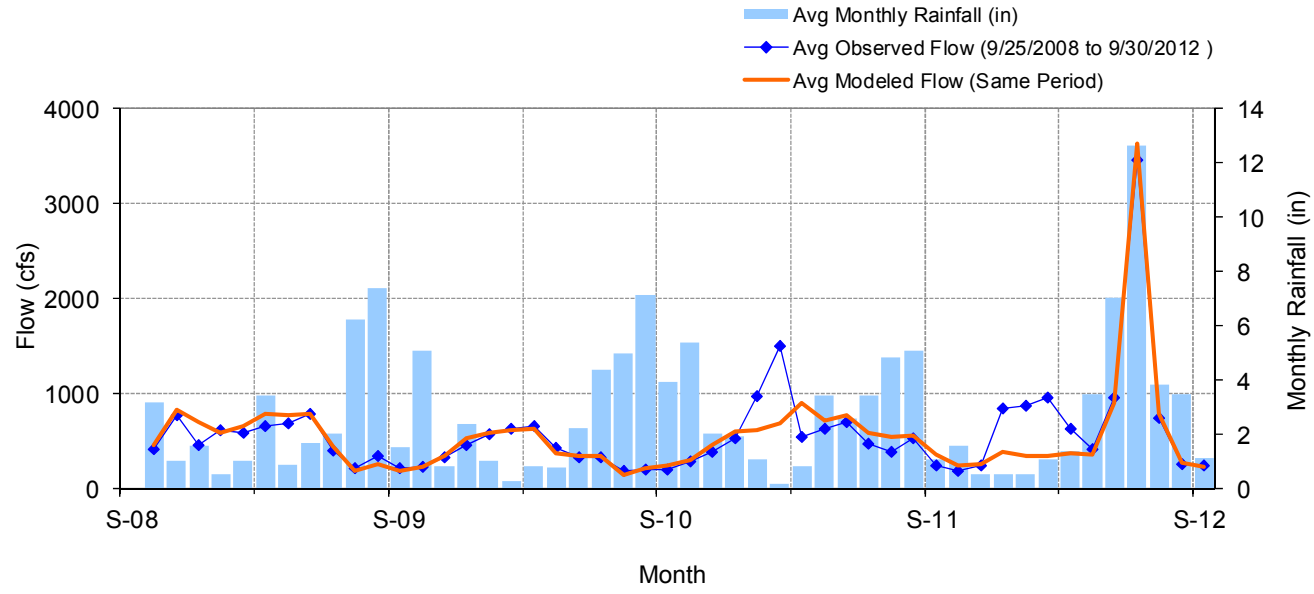

Figure C-44. Mean monthly flow at USGS 04048001 Cloquet River near Burnett

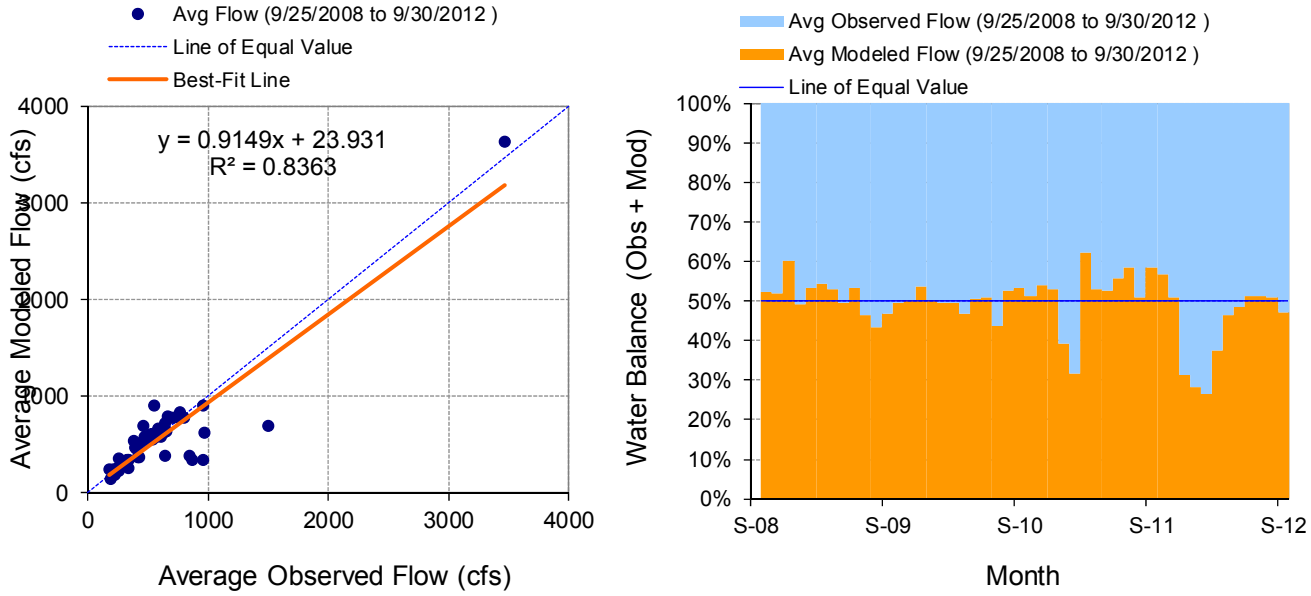

Figure C-45. Monthly flow regression and temporal variation at USGS 04048001 Cloquet River near Burnett

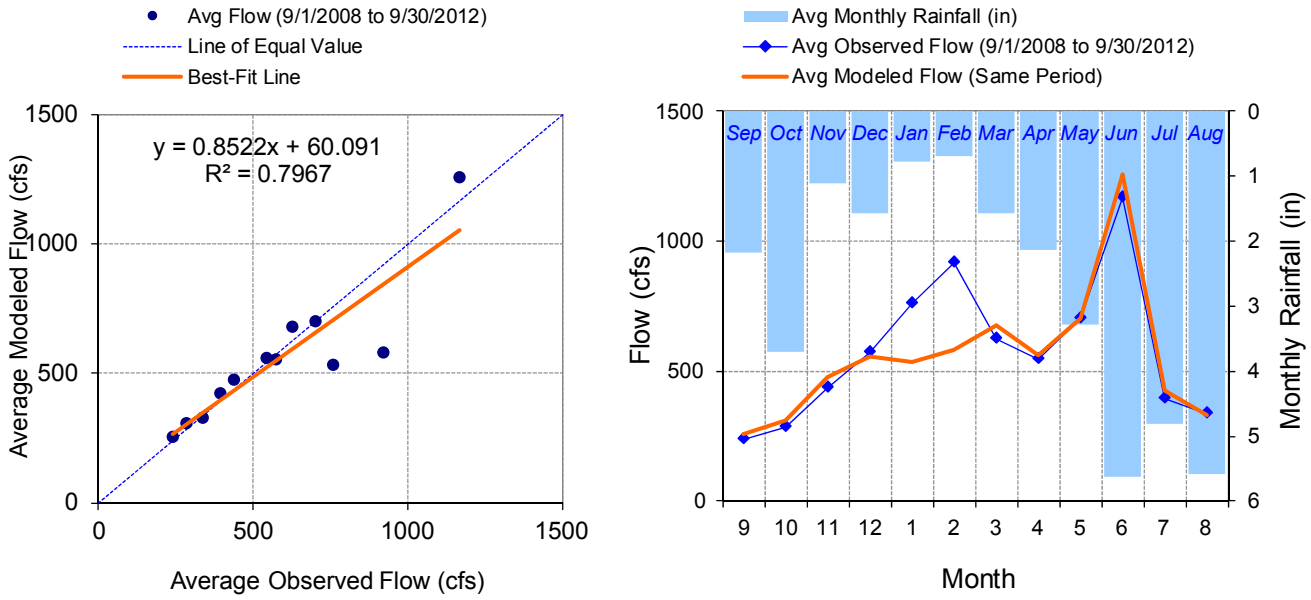

Figure C-46. Seasonal regression and temporal aggregate at USGS 04048001 Cloquet River near Burnett

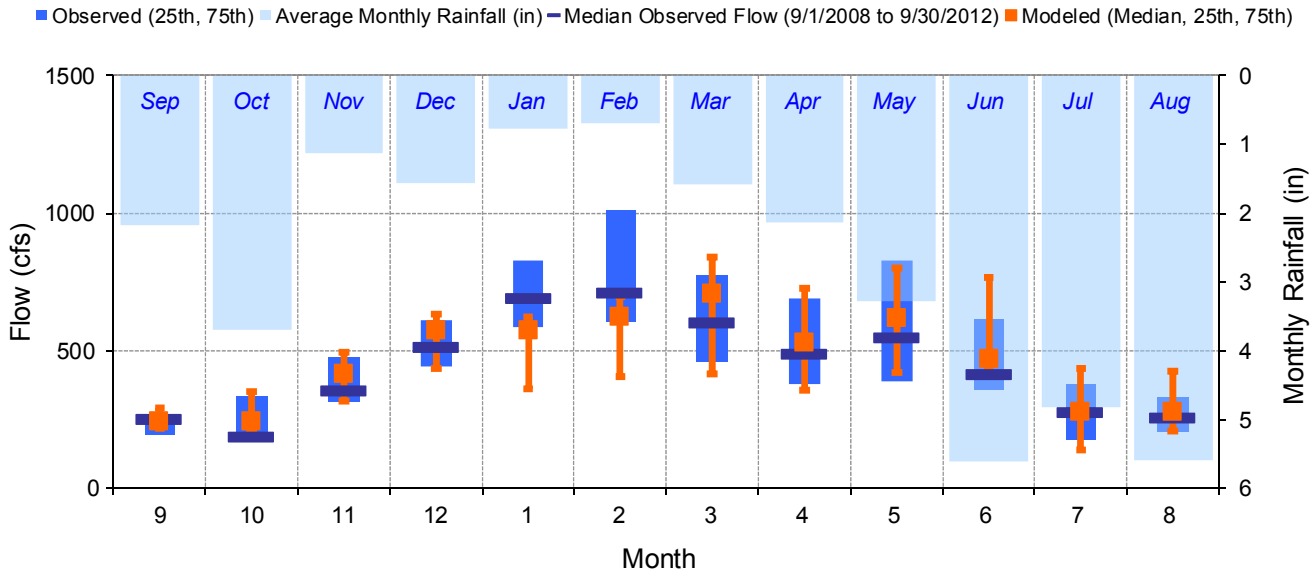

Figure C-47. Seasonal medians and ranges at USGS 04048001 Cloquet River near Burnett

Table C-13. Seasonal summary at USGS 04048001 Cloquet River near Burnett

MONTH	OBSERVED FLOW (CFS)				MODELED FLOW (CFS)			
	MEAN	MEDIAN	25TH	75TH	MEAN	MEDIAN	25TH	75TH
Sep	239.14	252.66	196.00	270.03	256.60	242.39	218.50	291.49
Oct	281.50	186.76	174.17	332.25	308.40	241.81	213.84	351.76
Nov	437.93	354.50	316.25	478.48	474.86	414.90	318.31	492.48
Dec	573.94	513.90	442.40	608.40	556.10	573.74	435.34	633.56
Jan	757.86	693.17	587.35	829.58	535.24	575.62	361.42	621.80
Feb	919.10	713.36	608.00	1009.46	580.66	621.42	404.91	697.32
Mar	626.37	605.50	459.61	775.78	678.10	705.69	413.30	839.51
Apr	544.29	488.50	380.50	689.63	561.95	530.26	356.21	726.24
May	699.81	550.20	389.19	825.75	702.75	617.70	418.80	799.95
Jun	1164.96	413.50	360.75	613.78	1255.69	467.64	423.30	767.87
Jul	392.93	276.71	178.00	377.83	424.78	276.87	140.01	436.10
Aug	337.20	257.62	205.50	330.45	329.96	277.94	205.81	424.54

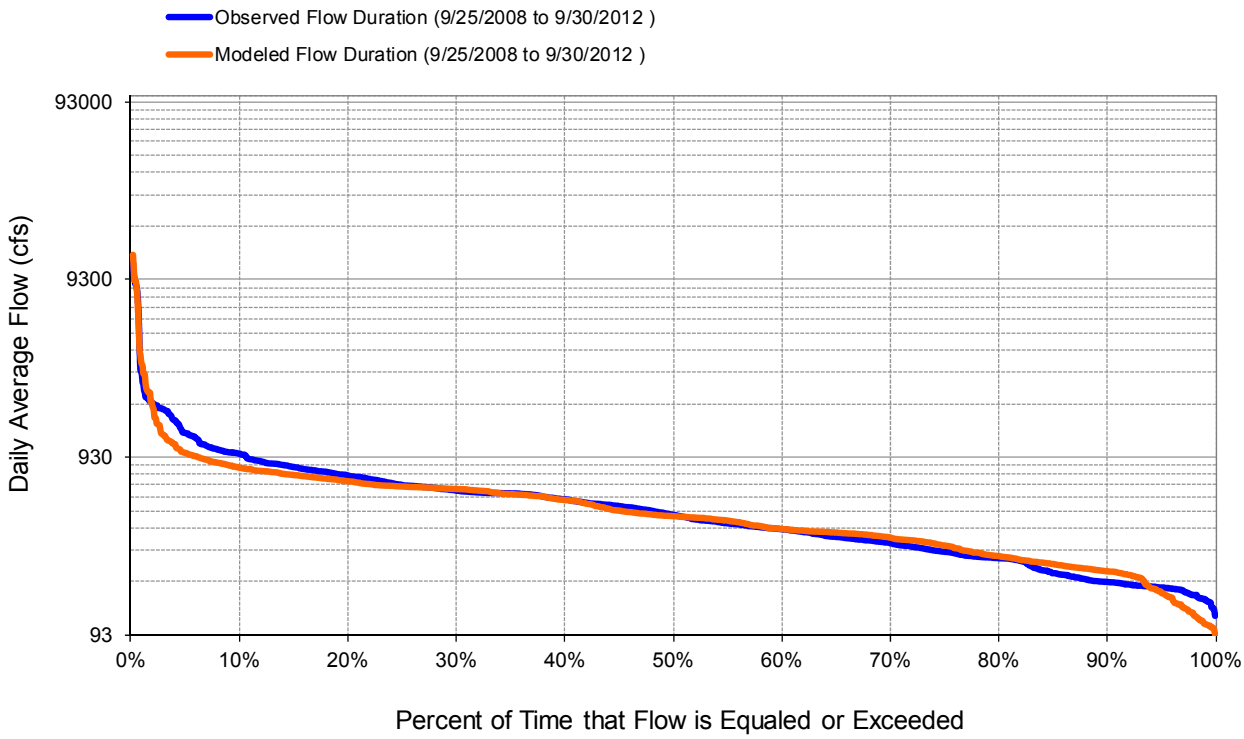

Figure C-48. Flow exceedance at USGS 04048001 Cloquet River near Burnett

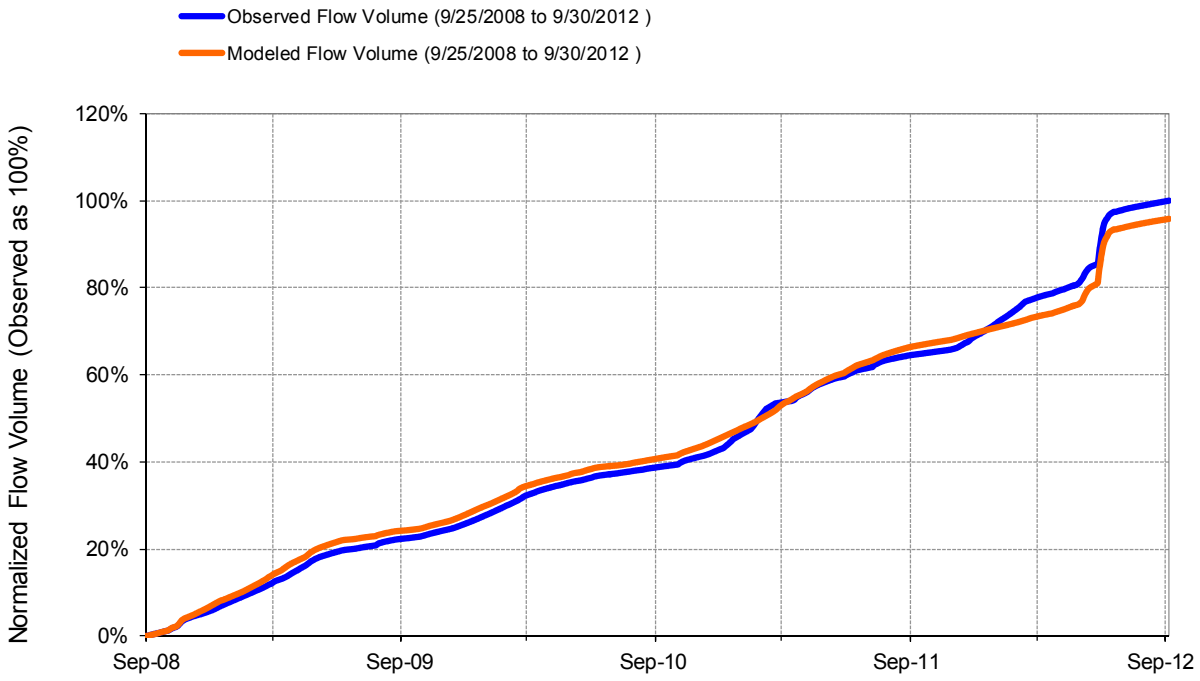

Figure C-49. Flow accumulation at USGS 04048001 Cloquet River near Burnett

Table C-14. Summary statistics at USGS 04048001 Cloquet River near Burnett

HSPF Simulated Flow			Observed Flow Gage		
REACH OUTFLOW FROM DSN 401 4.02-Year Analysis Period: 9/1/2008 - 9/30/2012 Flow volumes are (inches/year) for upstream drainage area			HYDSTRA 04048001 Cloquet River nr Burnett Manually Entered Data Drainage Area (sq-mi): 783		
Total Simulated In-stream Flow:	**9.58**		Total Observed In-stream Flow:		**10.00**
Total of simulated highest 10% flows:	**2.88**		Total of Observed highest 10% flows:		**3.19**
Total of Simulated lowest 50% flows:	**2.50**		Total of Observed Lowest 50% flows:		**2.41**
Simulated Summer Flow Volume (months 7-9):	**1.47**		Observed Summer Flow Volume (7-9):		**1.41**
Simulated Fall Flow Volume (months 10-12):	**1.94**		Observed Fall Flow Volume (10-12):		**1.88**
Simulated Winter Flow Volume (months 1-3):	**2.56**		Observed Winter Flow Volume (1-3):		**3.26**
Simulated Spring Flow Volume (months 4-6):	**3.61**		Observed Spring Flow Volume (4-6):		**3.45**
Total Simulated Storm Volume:	**1.70**		Total Observed Storm Volume:		**1.95**
Simulated Summer Storm Volume (7-9):	**0.20**		Observed Summer Storm Volume (7-9):		**0.22**
Errors (Simulated-Observed)	*Error Statistics*		*Recommended Criteria*		
Error in total volume:	-4.18		10		
Error in 50% lowest flows:	3.91		10		
Error in 10% highest flows:	-9.72		15		
Seasonal volume error - Summer:	4.32		30		
Seasonal volume error - Fall:	3.50	>>	30	Clear	
Seasonal volume error - Winter:	-21.57		30		
Seasonal volume error - Spring:	4.58		30		
Error in storm volumes:	-12.95		20		
Error in summer storm volumes:	-9.56		50		
Nash-Sutcliffe Coefficient of Efficiency, E:	0.859		Model accuracy increases		
Baseline adjusted coefficient (Garrick), E':	0.528				
Monthly NSE	0.830				

HYDSTRA 03001001 Miller Creek at Duluth

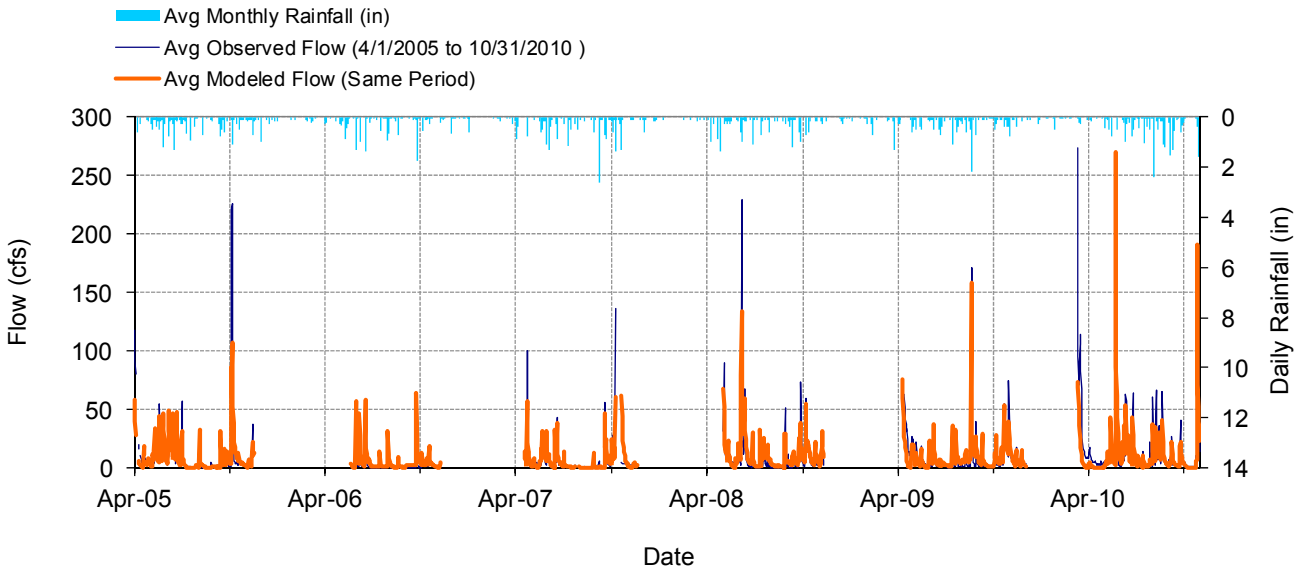

Figure C-50. Mean daily flow at HYDSTRA 03001001 Miller Creek at Duluth

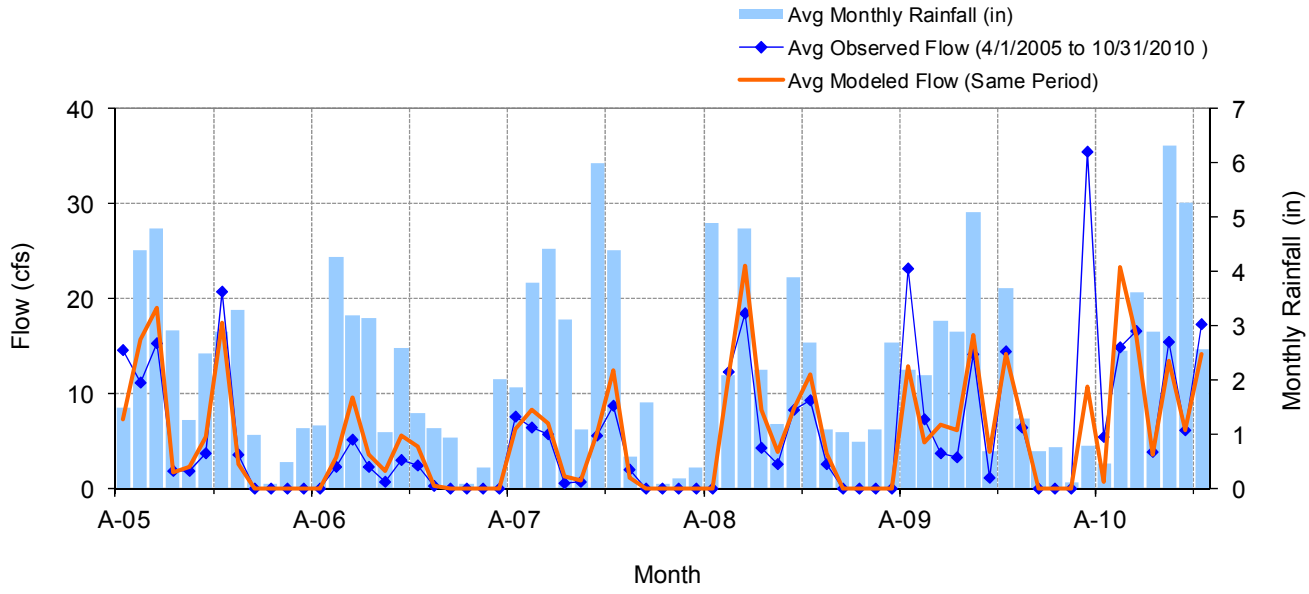

Figure C-51. Mean monthly flow at HYDSTRA 03001001 Miller Creek at Duluth

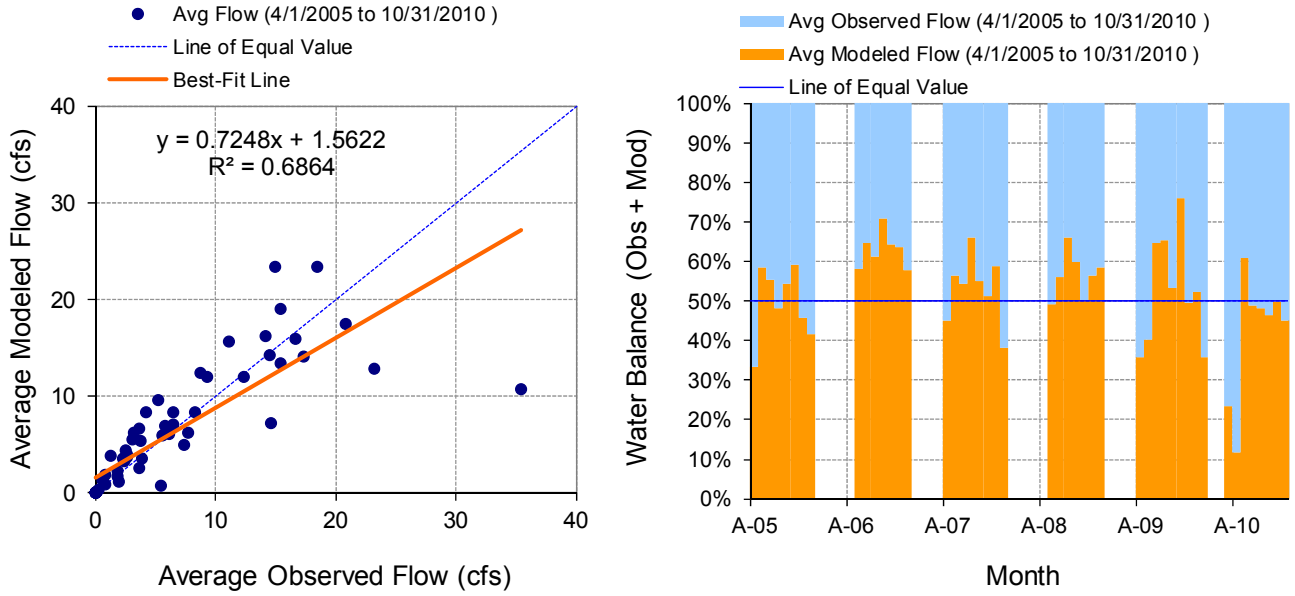

Figure C-52. Monthly flow regression and temporal variation at HYDSTRA 03001001 Miller Creek at Duluth

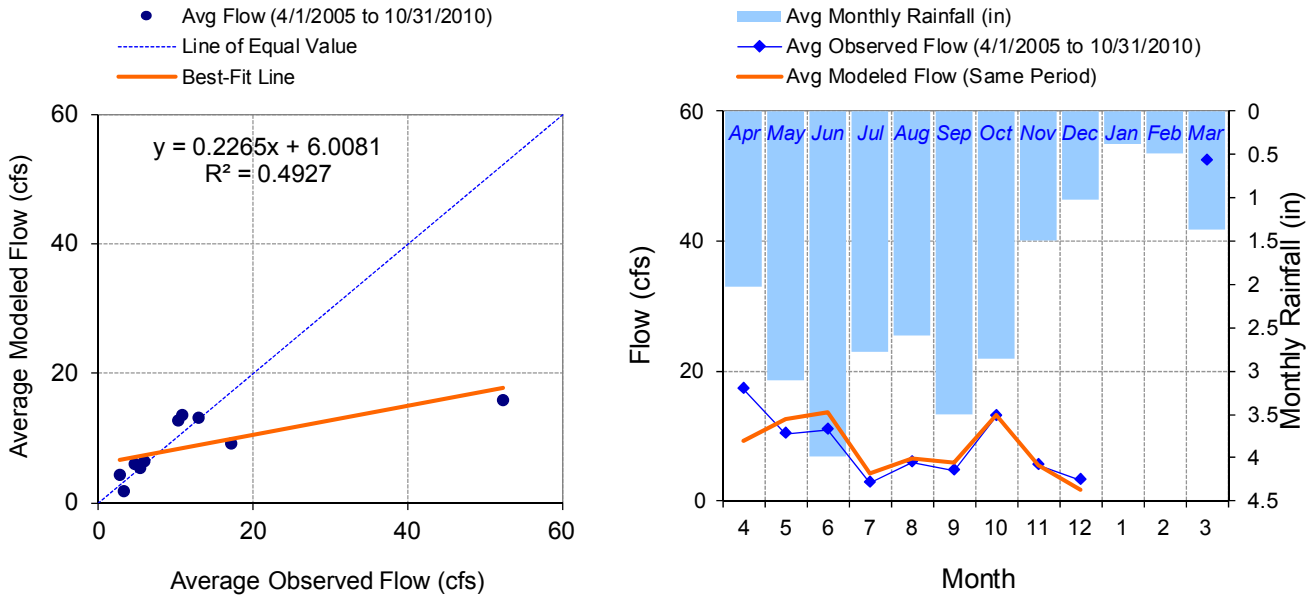

Figure C-53. Seasonal regression and temporal aggregate at HYDSTRA 03001001 Miller Creek at Duluth

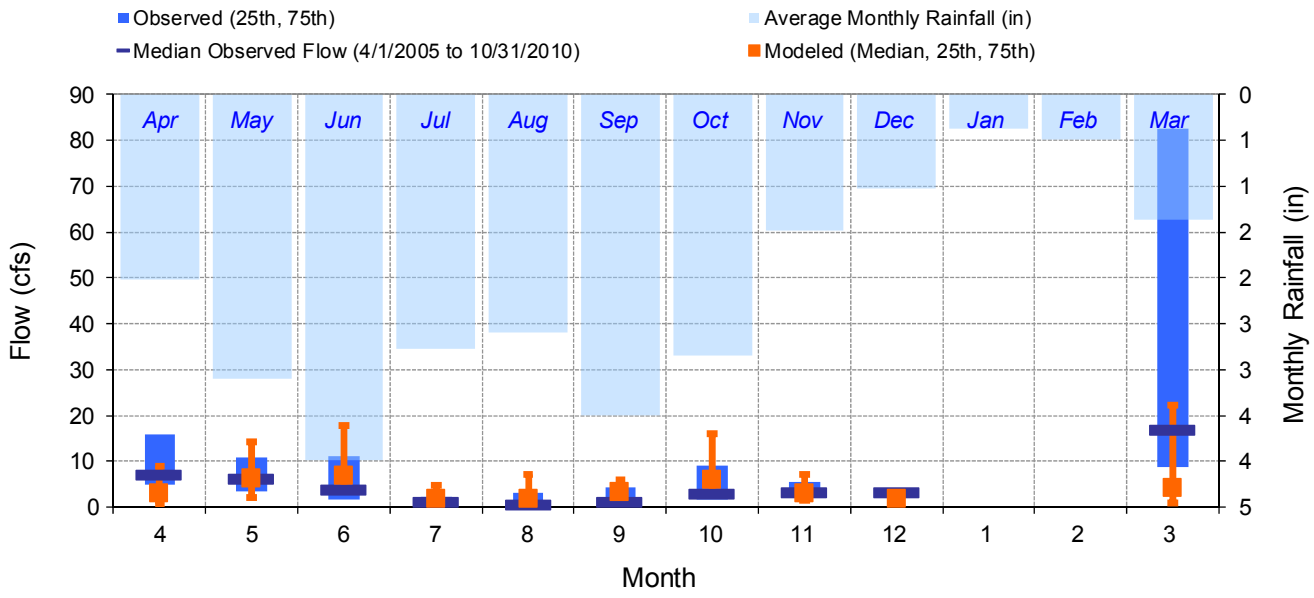

Figure C-54. Seasonal medians and ranges at HYDSTRA 03001001 Miller Creek at Duluth

Table C-15. Seasonal summary at HYDSTRA 03001001 Miller Creek at Duluth

MONTH	OBSERVED FLOW (CFS)				MODELED FLOW (CFS)			
	MEAN	MEDIAN	25TH	75TH	MEAN	MEDIAN	25TH	75TH
Apr	17.21	7.30	4.85	16.00	9.20	2.96	0.62	9.03
May	10.22	6.30	3.33	11.00	12.64	6.23	2.20	14.35
Jun	10.85	3.80	1.60	11.25	13.61	6.90	3.92	17.74
Jul	2.82	1.10	0.46	2.28	4.32	1.80	0.92	4.80
Aug	5.96	0.55	0.23	3.26	6.46	1.96	0.60	7.09
Sep	4.69	1.30	0.54	4.31	5.91	3.32	1.54	5.86
Oct	12.95	3.10	1.70	9.05	13.23	6.03	3.05	16.03
Nov	5.44	3.40	2.90	5.65	5.44	3.14	1.52	7.23
Dec	3.20	3.20	3.20	3.20	1.79	1.79	1.79	1.79
Jan	0.00	0.00	0.00	0.00	0.00	0.00	0.00	0.00
Feb	0.00	0.00	0.00	0.00	0.00	0.00	0.00	0.00
Mar	52.33	16.97	8.89	82.64	15.94	4.11	0.84	22.28

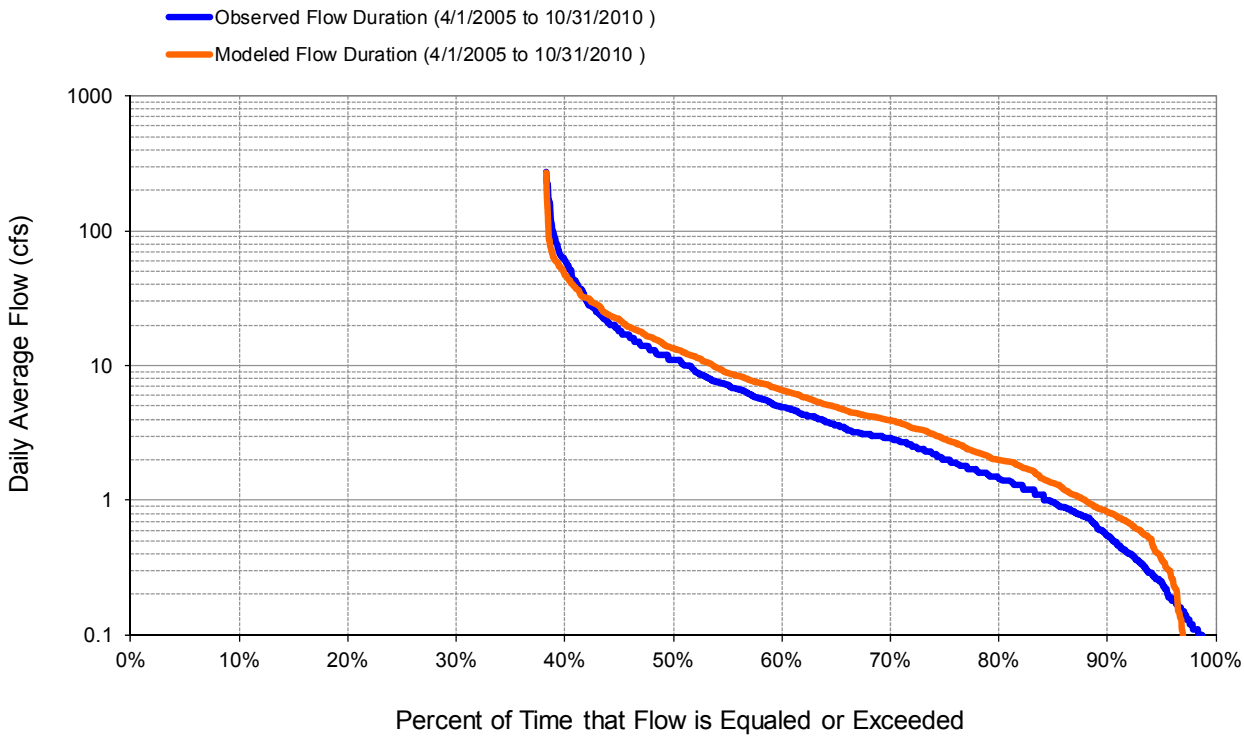

Figure C-55. Flow exceedance at HYDSTRA 03001001 Miller Creek at Duluth

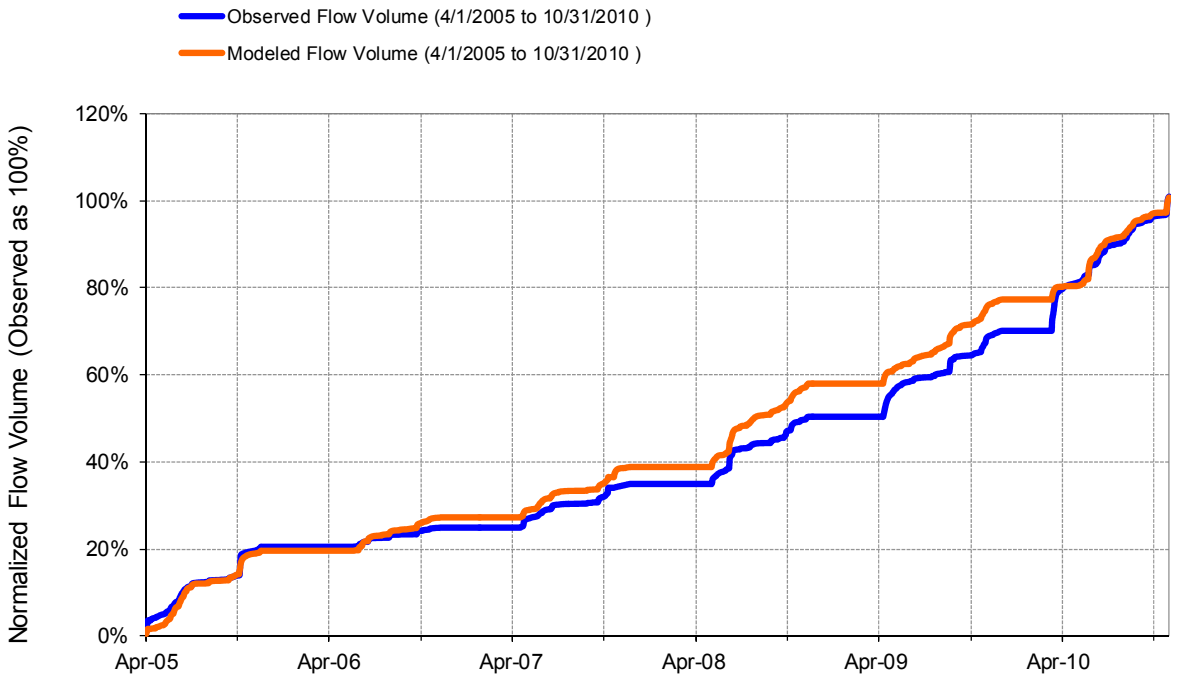

Figure C-56. Flow accumulation at HYDSTRA 03001001 Miller Creek at Duluth

Table C-16. Summary statistics at HYDSTRA 03001001 Miller Creek at Duluth

HSPF Simulated Flow		Observed Flow Gage		
REACH OUTFLOW FROM DSN 304 5.59-Year Analysis Period: 4/1/2005 - 10/31/2010 Flow volumes are (inches/year) for upstream drainage area		USGS 04155410 Miller Cr at Duluth Manually Entered Data Drainage Area (sq-mi): 9.9		
Total Simulated In-stream Flow:	**7.74**	Total Observed In-stream Flow:		**7.71**
Total of simulated highest 10% flows:	**3.80**	Total of Observed highest 10% flows:		**4.62**
Total of Simulated lowest 50% flows:	**0.69**	Total of Observed Lowest 50% flows:		**0.50**
Simulated Summer Flow Volume (months 7-9):	**2.04**	Observed Summer Flow Volume (7-9):		**1.65**
Simulated Fall Flow Volume (months 10-12):	**1.86**	Observed Fall Flow Volume (10-12):		**1.83**
Simulated Winter Flow Volume (months 1-3):	**0.23**	Observed Winter Flow Volume (1-3):		**0.74**
Simulated Spring Flow Volume (months 4-6):	**3.61**	Observed Spring Flow Volume (4-6):		**3.49**
Total Simulated Storm Volume:	**3.29**	Total Observed Storm Volume:		**3.83**
Simulated Summer Storm Volume (7-9):	**0.90**	Observed Summer Storm Volume (7-9):		**1.09**
Errors (Simulated-Observed)	*Error Statistics*	*Recommended Criteria*		
Error in total volume:	0.42	10		
Error in 50% lowest flows:	38.60	10		
Error in 10% highest flows:	-17.79	15		
Seasonal volume error - Summer:	23.59	30		
Seasonal volume error - Fall:	1.71	30		
Seasonal volume error - Winter:		30		
Seasonal volume error - Spring:	3.59	30		
Error in storm volumes:	-14.06	20		
Error in summer storm volumes:	-17.73	50		
Nash-Sutcliffe Coefficient of Efficiency, E:	0.430			
Baseline adjusted coefficient (Garrick), E':	0.423			
Monthly NSE	0.612		0.637	

>> Clear

USGS 04024000 St Louis River near Scanlon

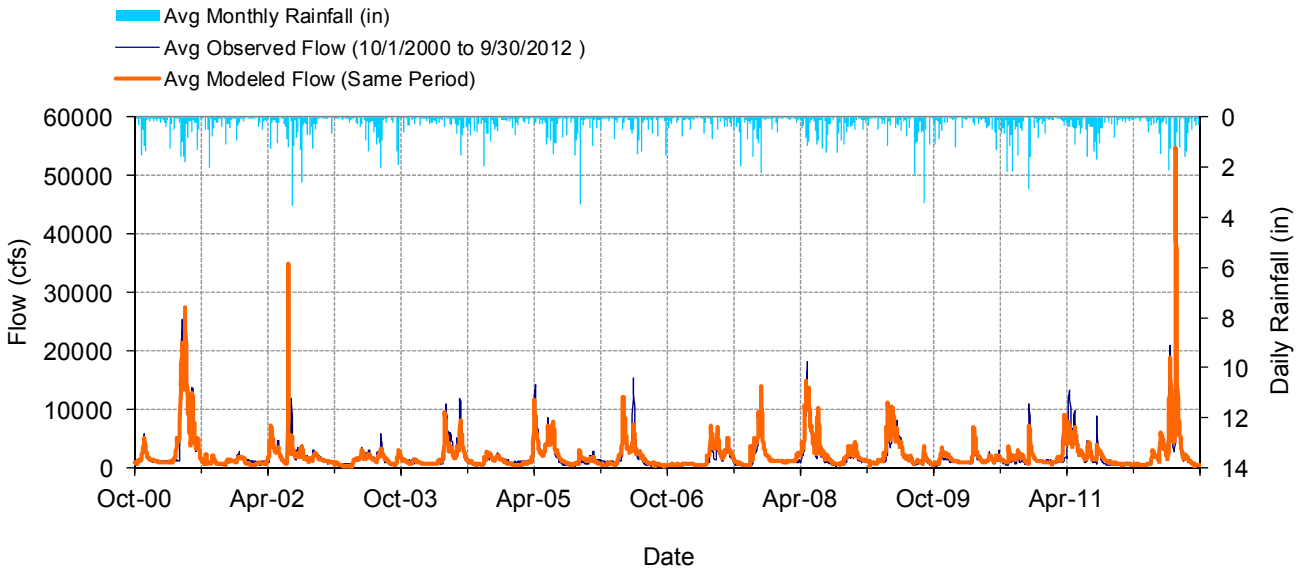

Figure C-57. Mean daily flow at USGS 04024000 St Louis River near Scanlon

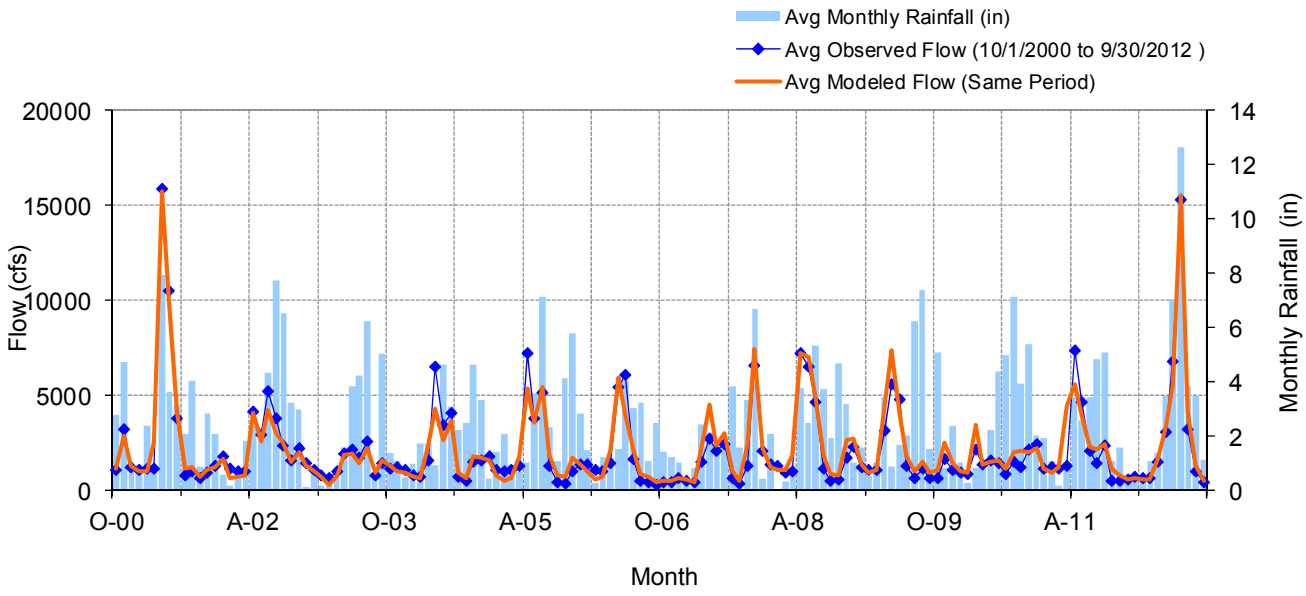

Figure C-58. Mean monthly flow at USGS 04024000 St Louis River near Scanlon

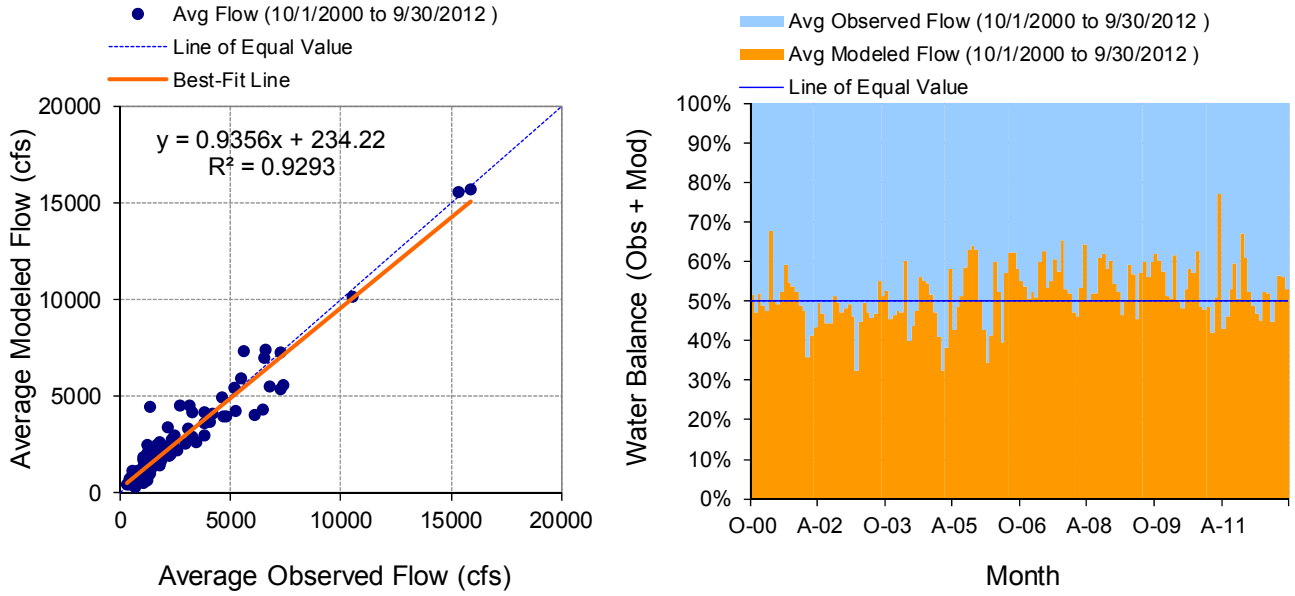

Figure C-59. Monthly flow regression and temporal variation at USGS 04024000 St Louis River near Scanlon

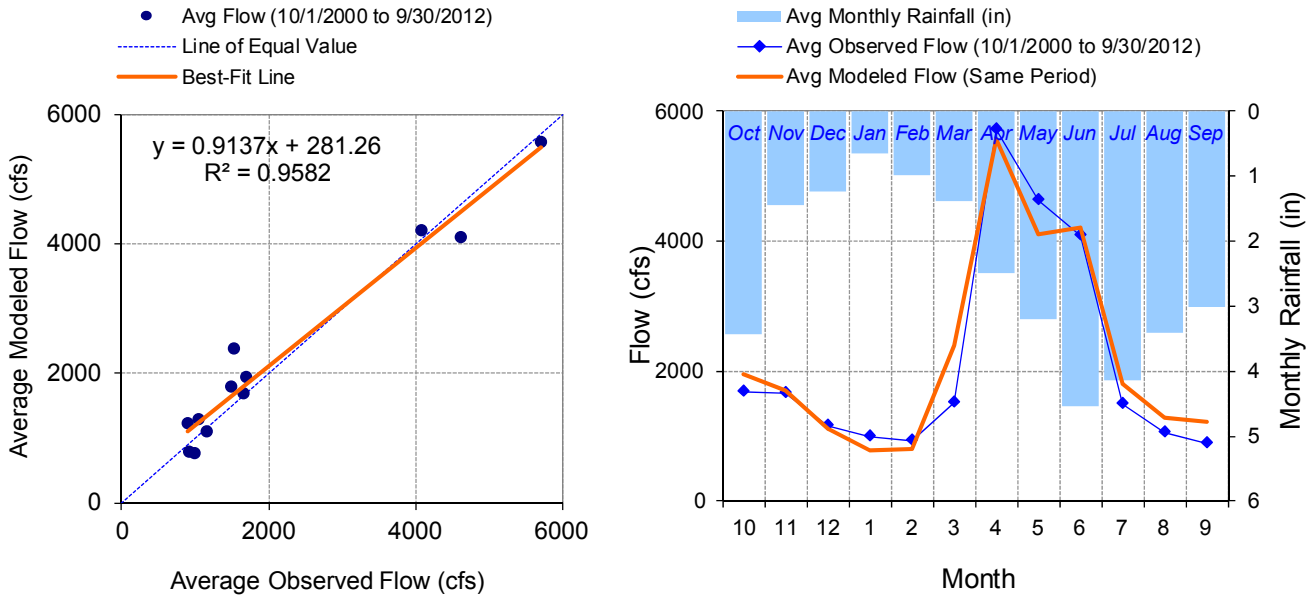

Figure C-60. Seasonal regression and temporal aggregate at USGS 04024000 St Louis River near Scanlon

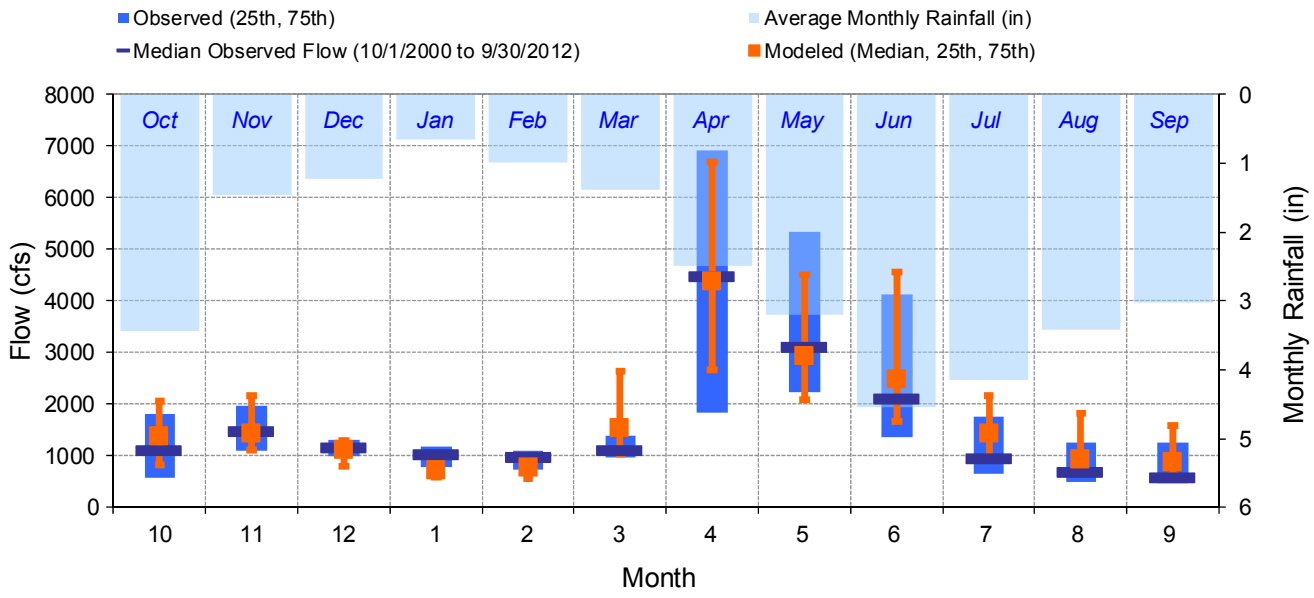

Figure C-61. Seasonal medians and ranges at USGS 04024000 St Louis River near Scanlon

Table C-17. Seasonal summary at USGS 04024000 St Louis River near Scanlon

MONTH	OBSERVED FLOW (CFS)				MODELED FLOW (CFS)			
	MEAN	MEDIAN	25TH	75TH	MEAN	MEDIAN	25TH	75TH
Oct	1686.25	1110.00	580.50	1802.50	1953.65	1370.01	824.92	2046.54
Nov	1653.57	1490.00	1090.00	1970.00	1694.85	1439.58	1116.30	2174.68
Dec	1164.60	1160.00	992.75	1320.00	1106.14	1119.14	800.74	1304.49
Jan	985.80	1025.00	769.00	1170.00	777.06	727.68	592.06	1000.21
Feb	917.27	970.00	739.50	1090.00	796.85	763.64	566.09	990.84
Mar	1519.28	1120.00	959.75	1400.00	2386.50	1538.30	1033.27	2646.64
Apr	5708.89	4475.00	1847.50	6925.00	5574.50	4377.05	2653.12	6691.80
May	4618.95	3110.00	2240.00	5337.50	4109.30	2940.34	2096.08	4517.99
Jun	4078.99	2100.00	1350.00	4122.50	4203.56	2474.73	1659.72	4574.05
Jul	1488.60	945.50	656.00	1760.00	1797.40	1438.30	957.10	2173.00
Aug	1053.27	700.00	488.25	1250.00	1290.56	931.35	698.27	1821.47
Sep	892.22	578.00	453.75	1242.50	1229.13	864.90	600.39	1586.61

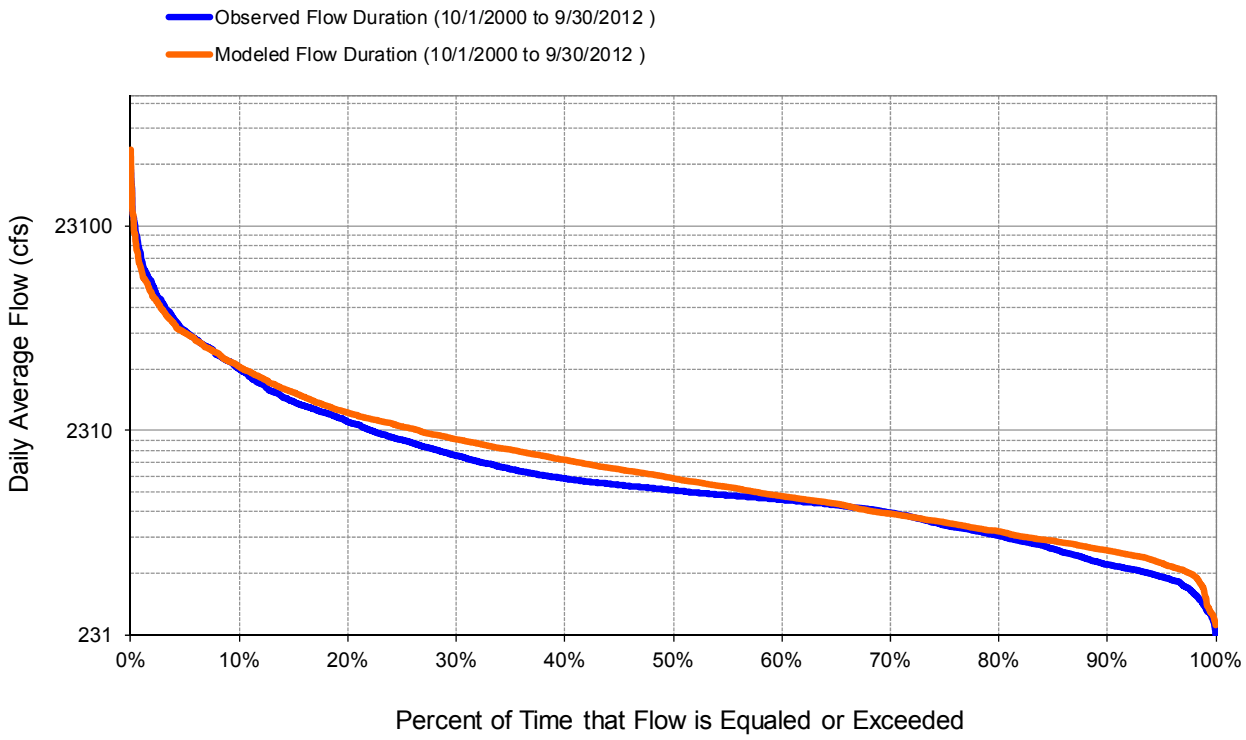

Figure C-62. Flow exceedance at USGS 04024000 St Louis River near Scanlon

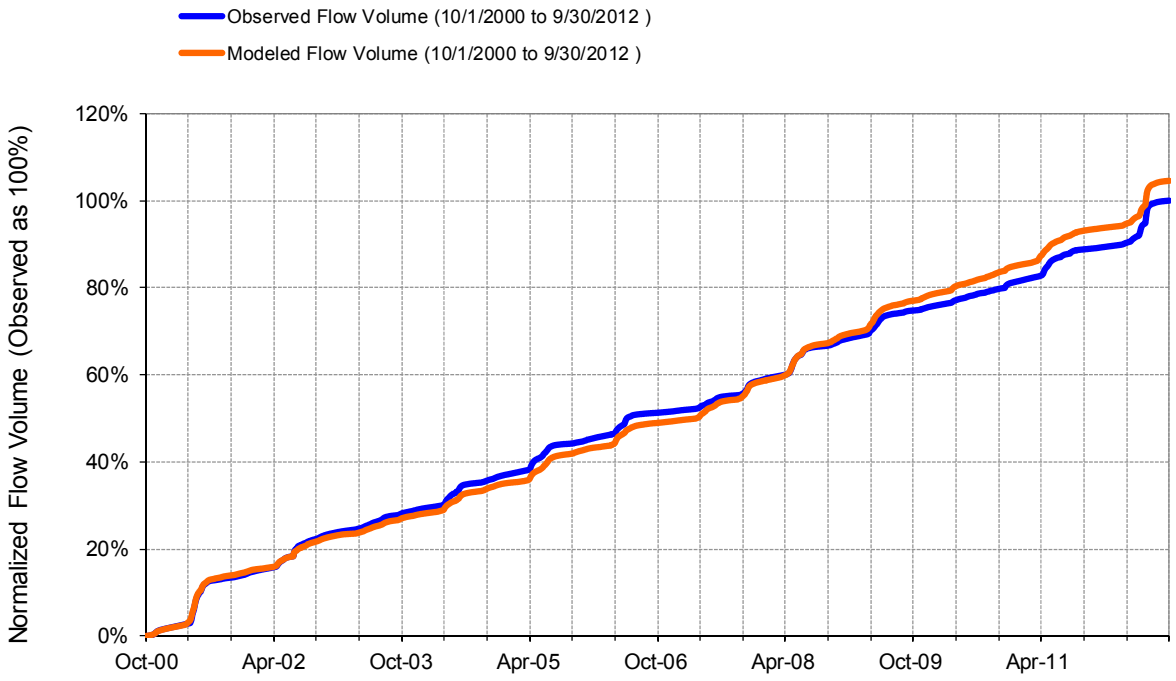

Figure C-63. Flow accumulation at USGS 04024000 St Louis River near Scanlon

Table C-18. Summary statistics at USGS 04024000 St Louis River near Scanlon

HSPF Simulated Flow		Observed Flow Gage		
REACH OUTFLOW FROM DSN 208 12-Year Analysis Period: 10/1/2000 - 9/30/2012 Flow volumes are (inches/year) for upstream drainage area		St. Louis River near Scanlon, MN Manually Entered Data Drainage Area (sq-mi): 3430		
Total Simulated In-stream Flow:	**8.89**	Total Observed In-stream Flow:		**8.50**
Total of simulated highest 10% flows:	**3.49**	Total of Observed highest 10% flows:		**3.69**
Total of Simulated lowest 50% flows:	**1.67**	Total of Observed Lowest 50% flows:		**1.57**
Simulated Summer Flow Volume (months 7-9):	**1.44**	Observed Summer Flow Volume (7-9):		**1.14**
Simulated Fall Flow Volume (months 10-12):	**1.58**	Observed Fall Flow Volume (10-12):		**1.50**
Simulated Winter Flow Volume (months 1-3):	**1.31**	Observed Winter Flow Volume (1-3):		**1.12**
Simulated Spring Flow Volume (months 4-6):	**4.56**	Observed Spring Flow Volume (4-6):		**4.74**
Total Simulated Storm Volume:	**2.46**	Total Observed Storm Volume:		**2.80**
Simulated Summer Storm Volume (7-9):	**0.32**	Observed Summer Storm Volume (7-9):		**0.34**
Errors (Simulated-Observed)	*Error Statistics*	*Recommended Criteria*		
Error in total volume:	4.55	10		
Error in 50% lowest flows:	6.63	10		
Error in 10% highest flows:	-5.23	15		
Seasonal volume error - Summer:	25.61	30		
Seasonal volume error - Fall:	5.59	30		
Seasonal volume error - Winter:	16.42	30		
Seasonal volume error - Spring:	-3.68	30		
Error in storm volumes:	-12.04	20		
Error in summer storm volumes:	-6.38	50		
Nash-Sutcliffe Coefficient of Efficiency, E:	0.876	Model accuracy increases as E or E' approaches 1.0		
Baseline adjusted coefficient (Garrick), E':	0.667			
Monthly NSE	0.928		0.928	0.93

>> Clear

USGS 04015438 St. Louis River near Skibo, MN

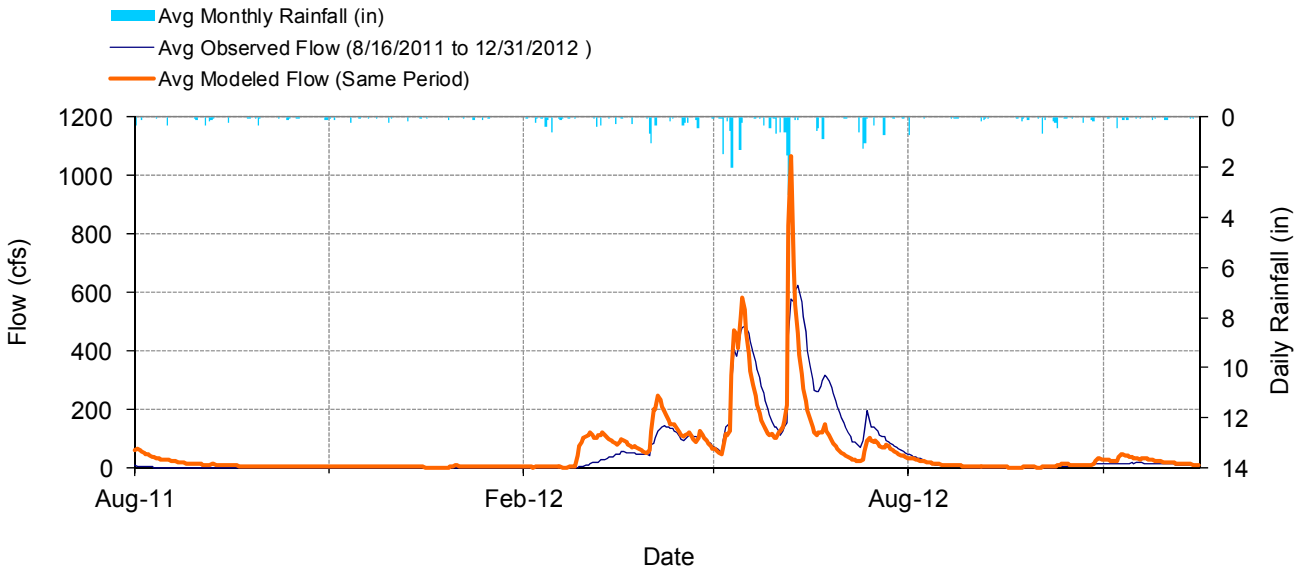

Figure C-64. Mean daily flow at USGS 04015438 St. Louis River near Skibo, MN

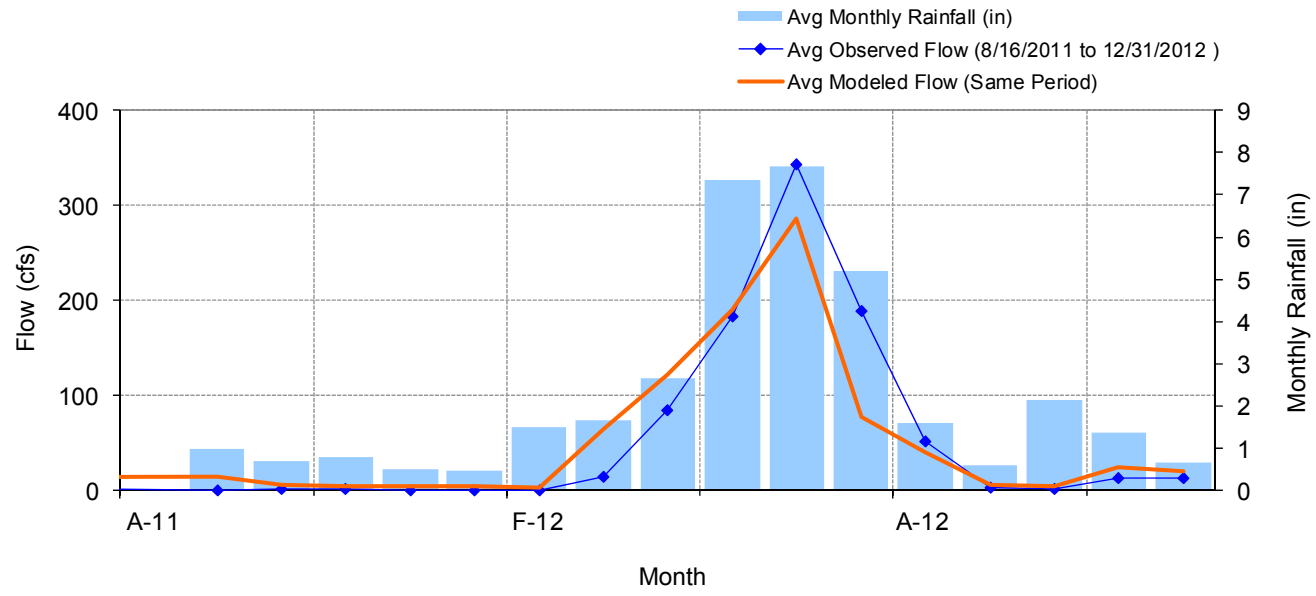

Figure C-65. Mean monthly flow at USGS 04015438 St. Louis River near Skibo, MN

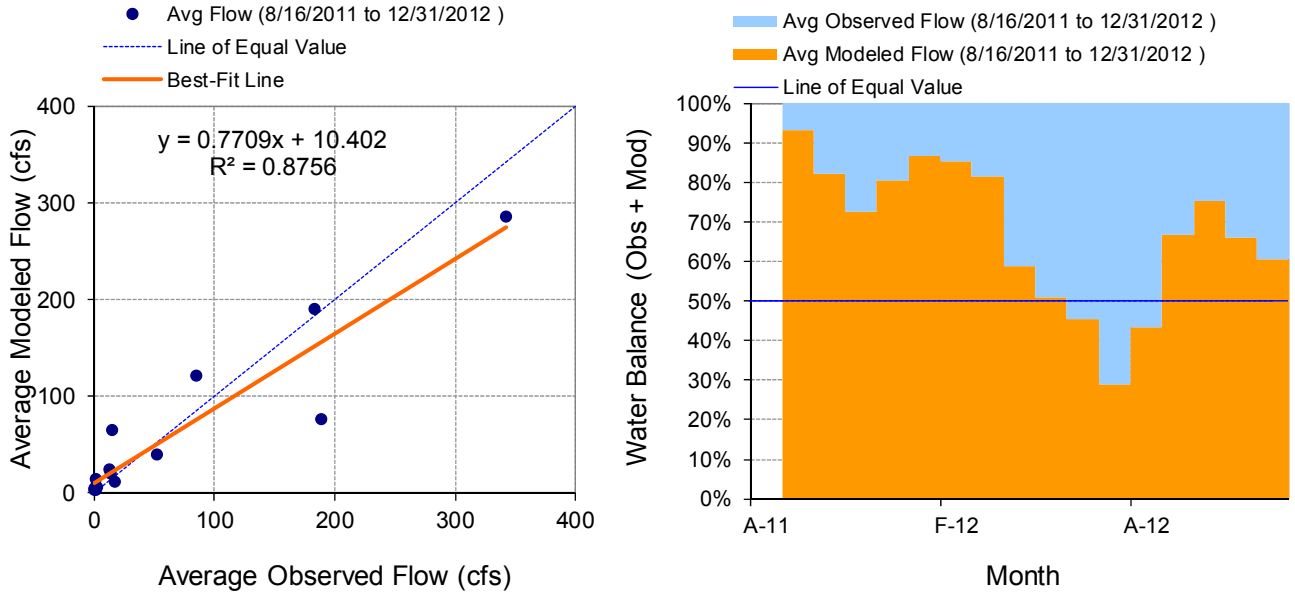

Figure C-66. Monthly flow regression and temporal variation at USGS 04015438 St. Louis River near Skibo, MN

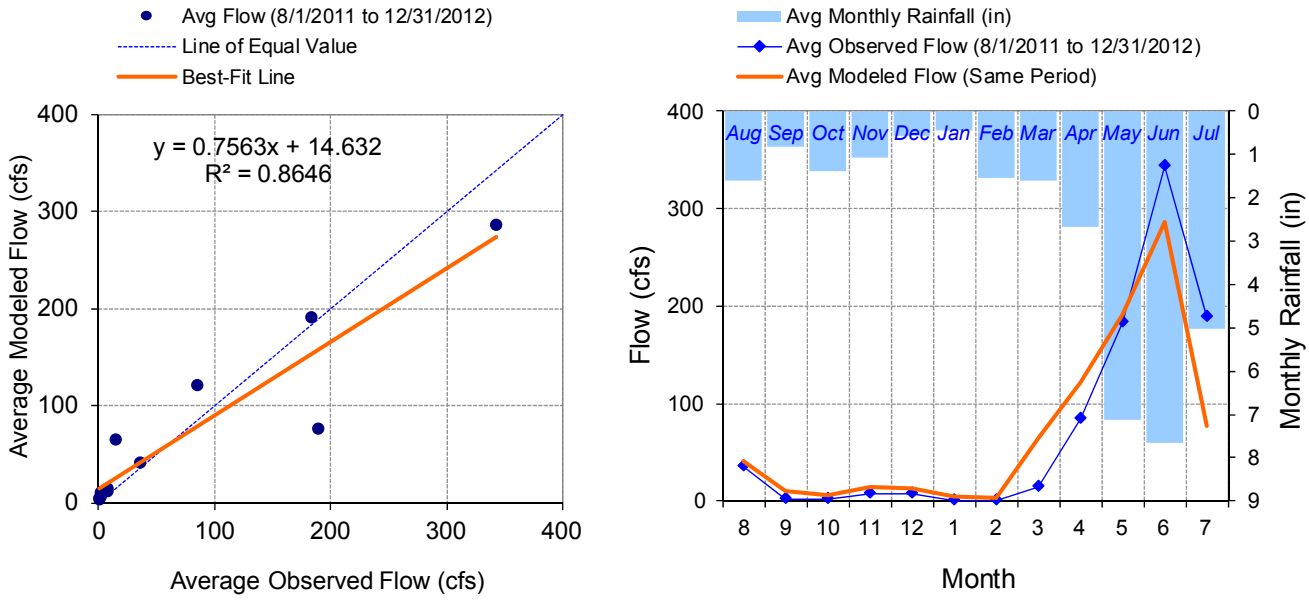

Figure C-67. Seasonal regression and temporal aggregate at USGS 04015438 St. Louis River near Skibo, MN

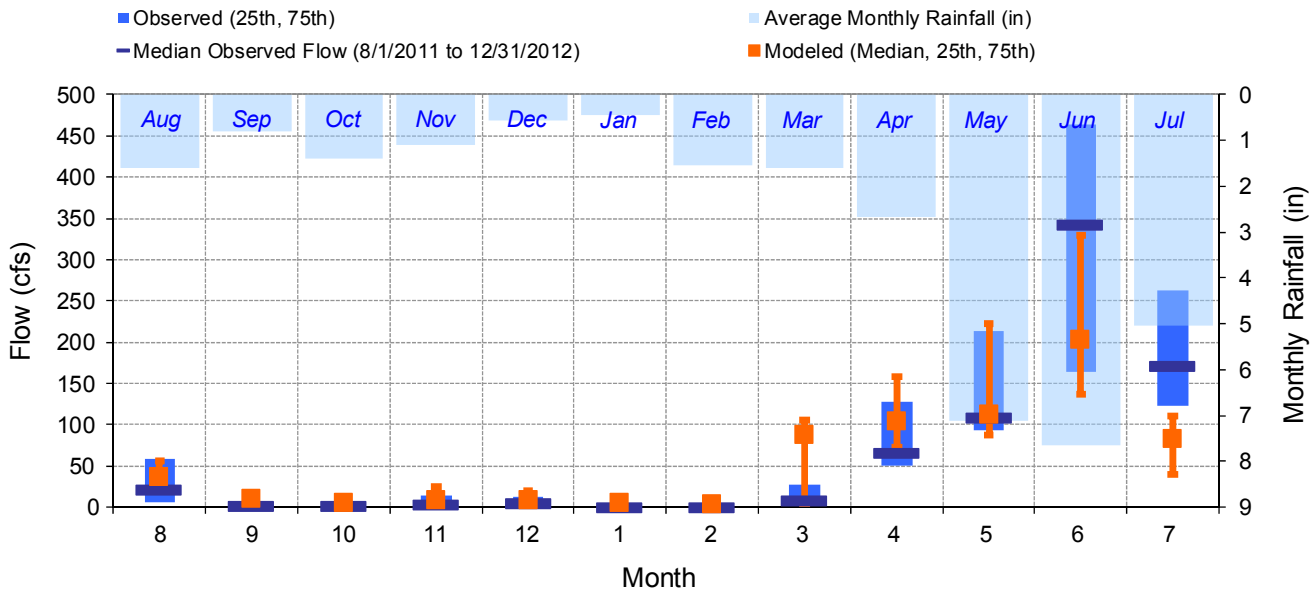

Figure C-68. Seasonal medians and ranges at USGS 04015438 St. Louis River near Skibo, MN

Table C-19. Seasonal summary at USGS 04015438 St. Louis River near Skibo, MN

MONTH	OBSERVED FLOW (CFS)				MODELED FLOW (CFS)			
	MEAN	MEDIAN	25TH	75TH	MEAN	MEDIAN	25TH	75TH
Aug	35.84	21.39	5.23	58.61	41.10	36.20	26.44	56.73
Sep	2.04	1.19	1.03	1.60	10.33	9.56	5.19	12.39
Oct	1.57	1.47	0.95	1.66	5.86	5.72	3.03	6.81
Nov	7.19	3.13	1.74	14.26	14.66	8.05	4.36	25.52
Dec	7.19	5.78	0.95	13.27	12.38	8.27	4.02	19.43
Jan	0.74	0.67	0.43	1.03	4.74	5.19	2.45	6.33
Feb	0.59	0.59	0.55	0.63	3.42	3.28	3.12	3.66
Mar	14.83	8.71	0.66	27.33	65.02	86.79	4.17	104.99
Apr	84.78	66.14	49.70	127.33	121.62	104.37	72.56	158.78
May	183.10	109.31	93.07	213.86	190.77	112.12	86.97	222.39
Jun	342.73	343.37	164.55	463.17	286.10	203.33	136.17	329.96
Jul	188.69	171.88	123.56	263.37	77.02	83.20	39.64	111.19

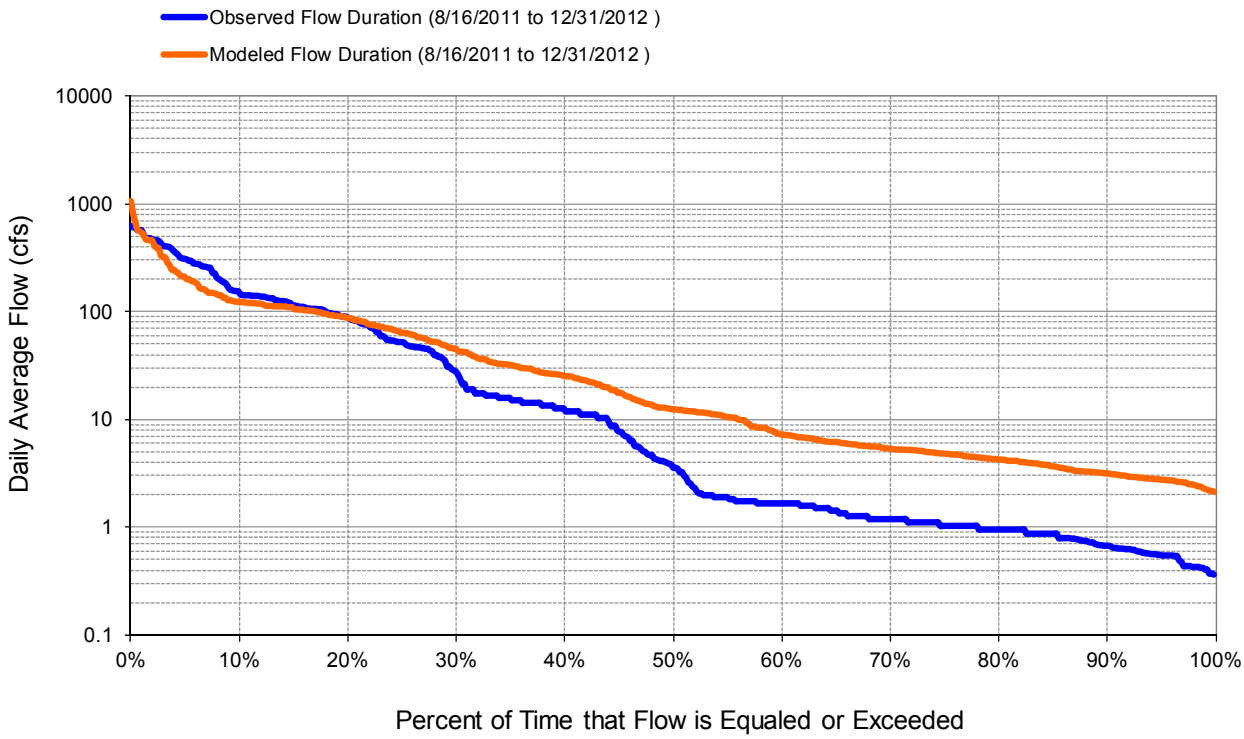

Figure C-69. Flow exceedance at USGS 04015438 St. Louis River near Skibo, MN

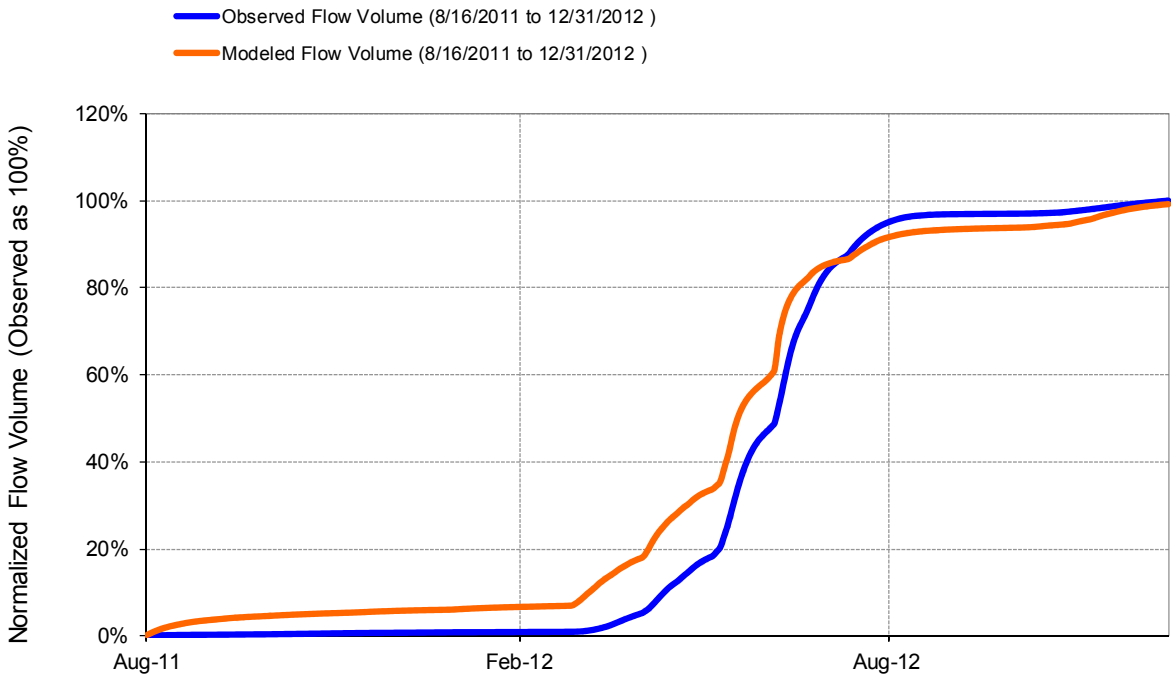

Figure C-70. Flow accumulation at USGS 04015438 St. Louis River near Skibo, MN

Table C-20. Summary statistics at USGS 04015438 St. Louis River near Skibo, MN

HSPF Simulated Flow			Observed Flow Gage		
REACH OUTFLOW FROM DSN 268 1.38-Year Analysis Period: 8/1/2011 - 12/31/2012 Flow volumes are (inches/year) for upstream drainage area			St. Louis River nr Skibo, MN Manually Entered Data Drainage Area (sq-mi): 80		
Total Simulated In-stream Flow:	**9.22**		Total Observed In-stream Flow:		**9.31**
Total of simulated highest 10% flows:	**4.98**		Total of Observed highest 10% flows:		**5.88**
Total of Simulated lowest 50% flows:	**0.47**		Total of Observed Lowest 50% flows:		**0.10**
Simulated Summer Flow Volume (months 7-9):	**1.66**		Observed Summer Flow Volume (7-9):		**2.58**
Simulated Fall Flow Volume (months 10-12):	**0.68**		Observed Fall Flow Volume (10-12):		**0.33**
Simulated Winter Flow Volume (months 1-3):	**0.76**		Observed Winter Flow Volume (1-3):		**0.17**
Simulated Spring Flow Volume (months 4-6):	**6.11**		Observed Spring Flow Volume (4-6):		**6.23**
Total Simulated Storm Volume:	**2.30**		Total Observed Storm Volume:		**1.68**
Simulated Summer Storm Volume (7-9):	**0.25**		Observed Summer Storm Volume (7-9):		**0.38**
Errors (Simulated-Observed)	*Error Statistics*		*Recommended Criteria*		
Error in total volume:	-1.00		10		
Error in 50% lowest flows:	366.87		10		
Error in 10% highest flows:	-15.32		15		
Seasonal volume error - Summer:	-35.49		30		
Seasonal volume error - Fall:	106.25	>>	30	Clear	
Seasonal volume error - Winter:	352.61		30		
Seasonal volume error - Spring:	-1.92		30		
Error in storm volumes:	37.12		20		
Error in summer storm volumes:	-32.26		50		
Nash-Sutcliffe Coefficient of Efficiency, E:	0.746		Model accuracy increases		
Baseline adjusted coefficient (Garrick), E':	0.630				
Monthly NSE	0.879				

HYDSTRA 05011001 Nemadji River near Pleasant Valley, MN23

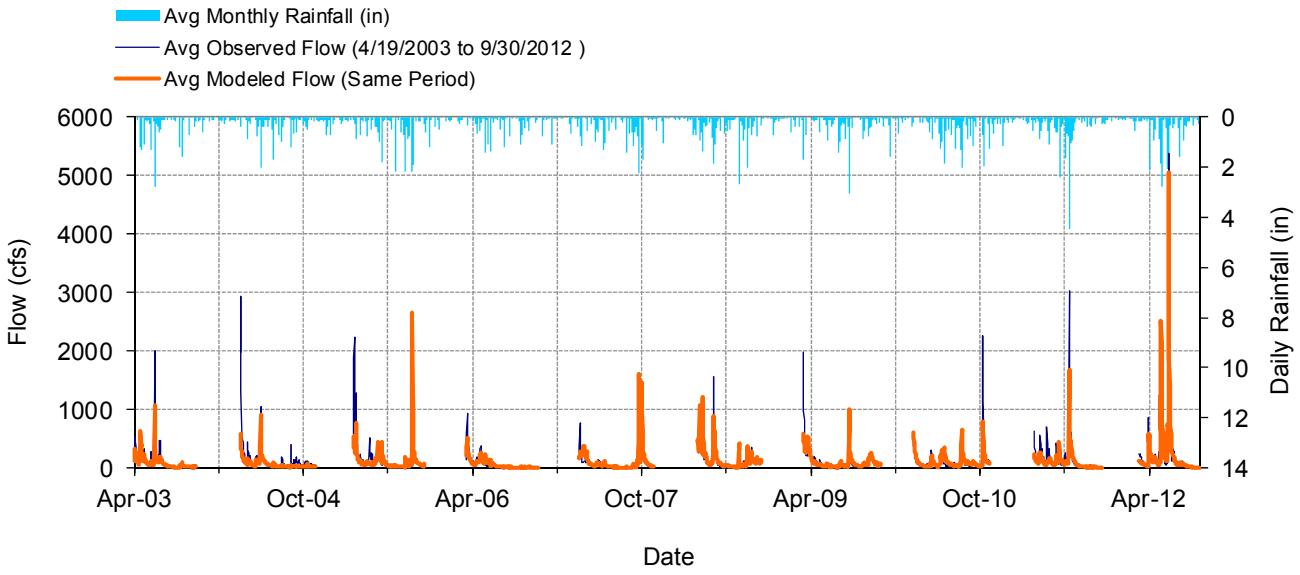

Figure C-71. Mean daily flow at HYDSTRA 05011001 Nemadji River near Pleasant Valley, MN23

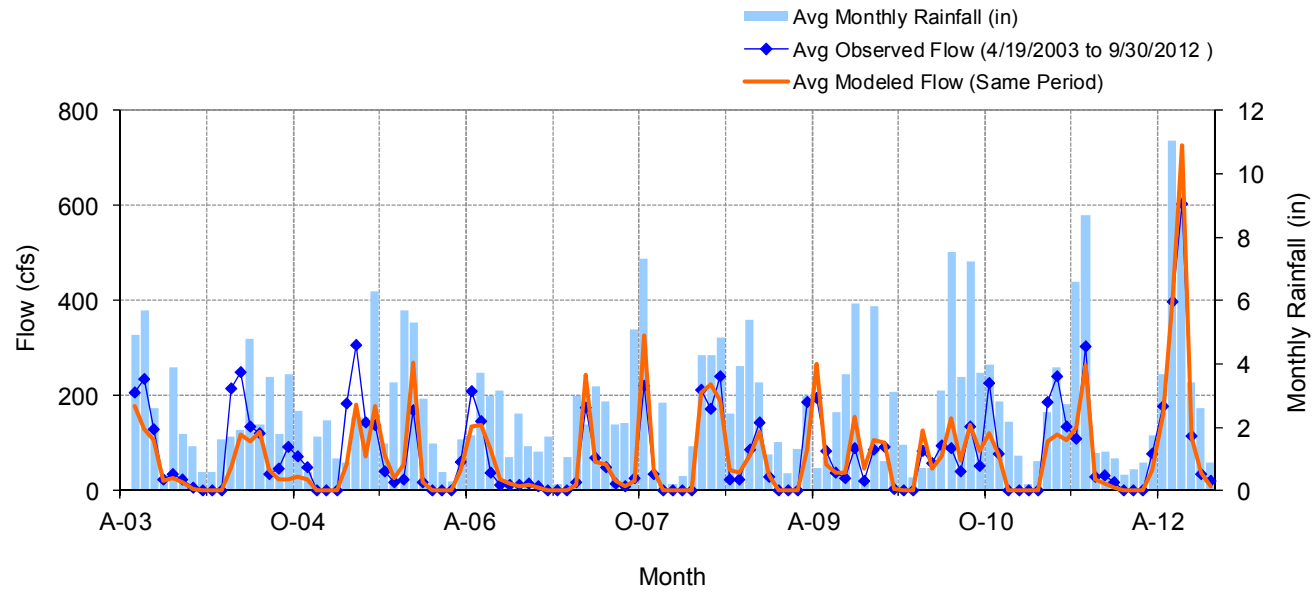

Figure C-72. Mean monthly flow at HYDSTRA 05011001 Nemadji River near Pleasant Valley, MN23

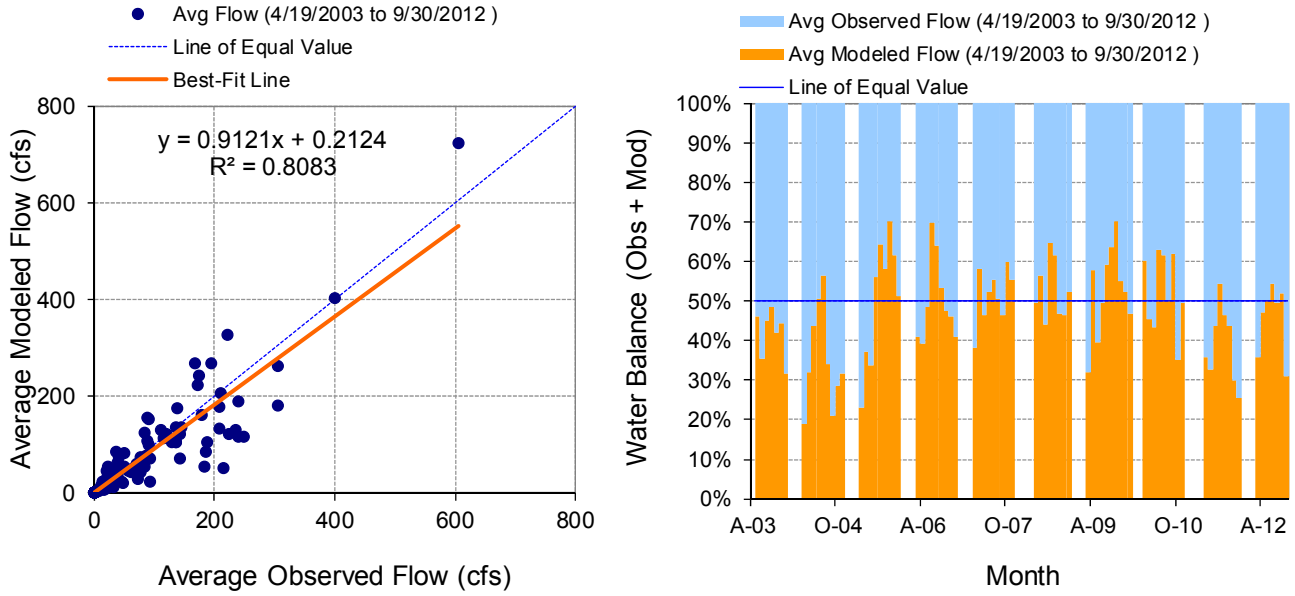

Figure C-73. Monthly flow regression and temporal variation at HYDSTRA 05011001 Nemadji River near Pleasant Valley, MN23

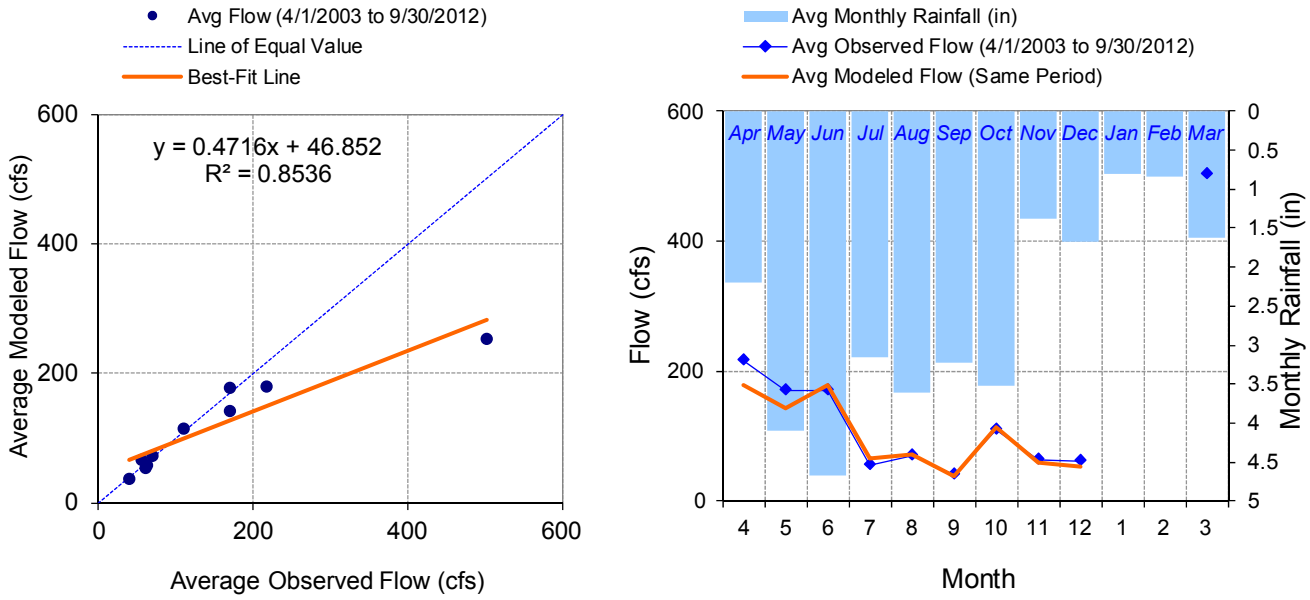

Figure C-74. Seasonal regression and temporal aggregate at HYDSTRA 05011001 Nemadji River near Pleasant Valley, MN23

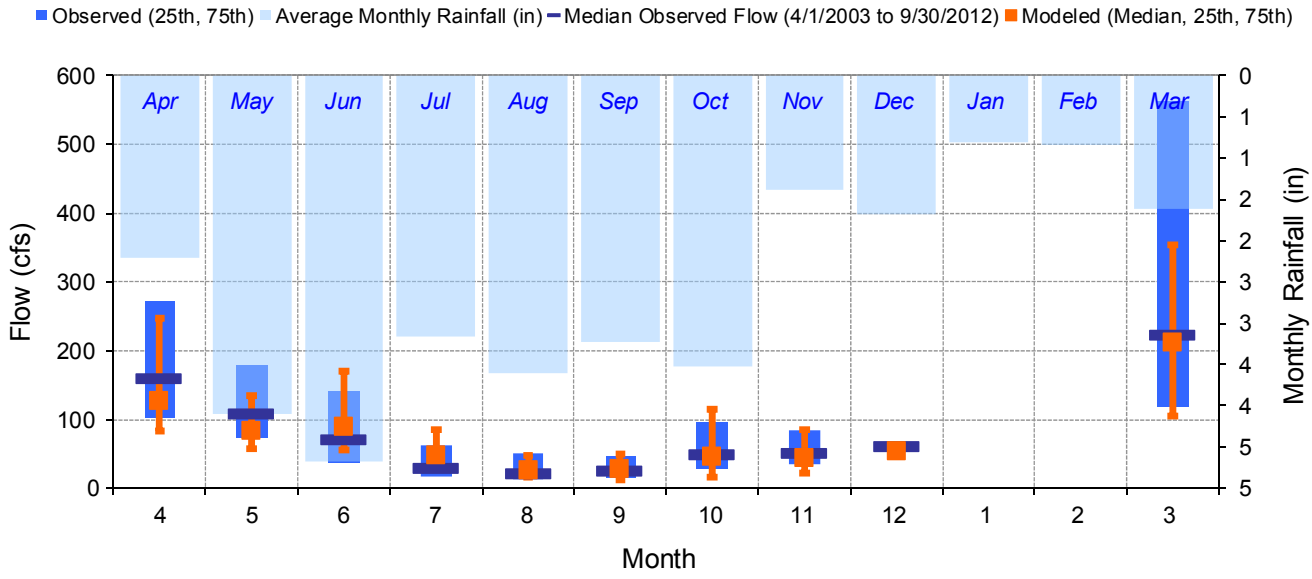

Figure C-75. Seasonal medians and ranges at HYDSTRA 05011001 Nemadji River near Pleasant Valley, MN23

Table C-21. Seasonal summary at HYDSTRA 05011001 Nemadji River near Pleasant Valley, MN23

MONTH	OBSERVED FLOW (CFS)				MODELED FLOW (CFS)			
	MEAN	MEDIAN	25TH	75TH	MEAN	MEDIAN	25TH	75TH
Apr	216.72	160.00	102.00	271.00	178.89	127.74	83.77	247.58
May	169.11	108.00	75.00	179.00	142.38	83.66	58.15	135.08
Jun	169.14	70.50	37.00	142.00	178.13	89.62	56.46	169.76
Jul	55.04	30.50	18.00	63.00	65.87	47.38	30.31	84.99
Aug	69.82	22.00	14.00	49.75	72.82	25.80	15.78	48.19
Sep	39.63	26.00	16.00	47.25	37.57	27.14	11.92	49.90
Oct	109.90	49.00	29.00	97.00	113.72	46.06	16.82	114.00
Nov	62.86	51.00	35.00	84.50	58.43	42.93	21.45	84.64
Dec	61.00	61.00	60.50	61.50	53.37	53.37	52.61	54.14
Jan	0.00	0.00	0.00	0.00	0.00	0.00	0.00	0.00
Feb	0.00	0.00	0.00	0.00	0.00	0.00	0.00	0.00
Mar	501.65	224.00	118.00	562.50	253.48	211.96	104.96	354.01

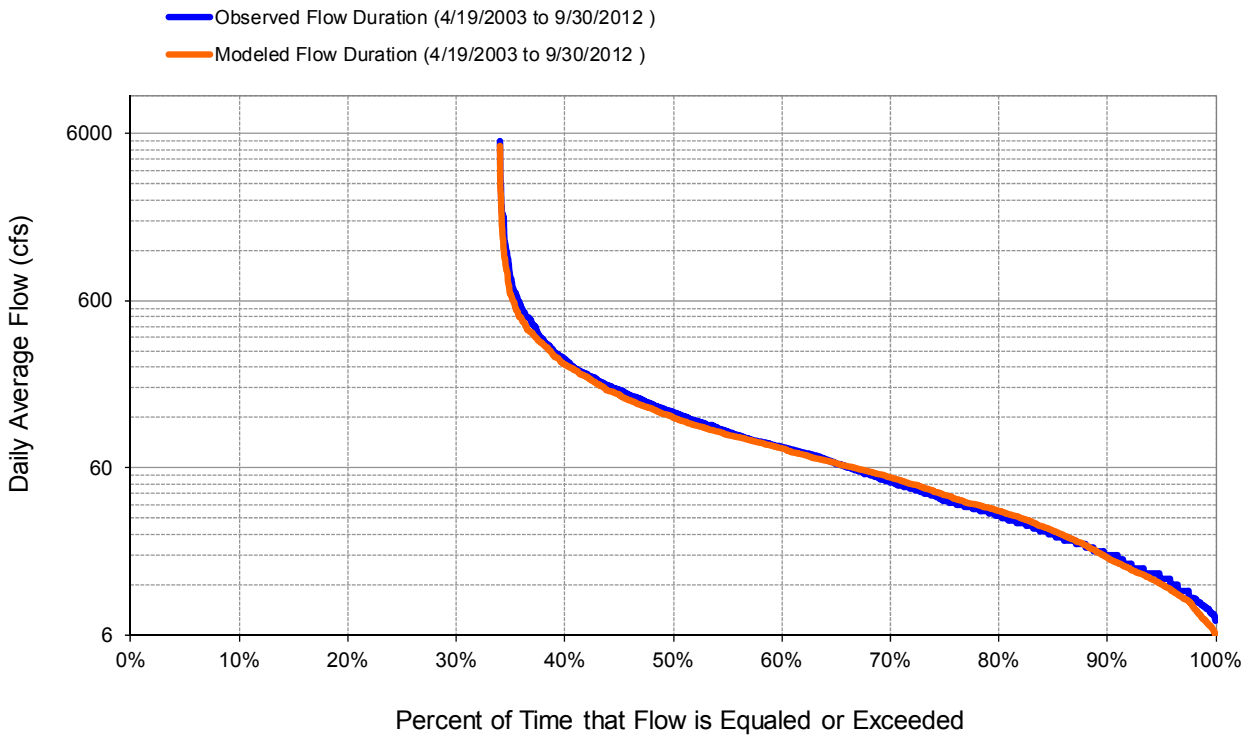

Figure C-76. Flow exceedance at HYDSTRA 05011001 Nemadji River near Pleasant Valley, MN23

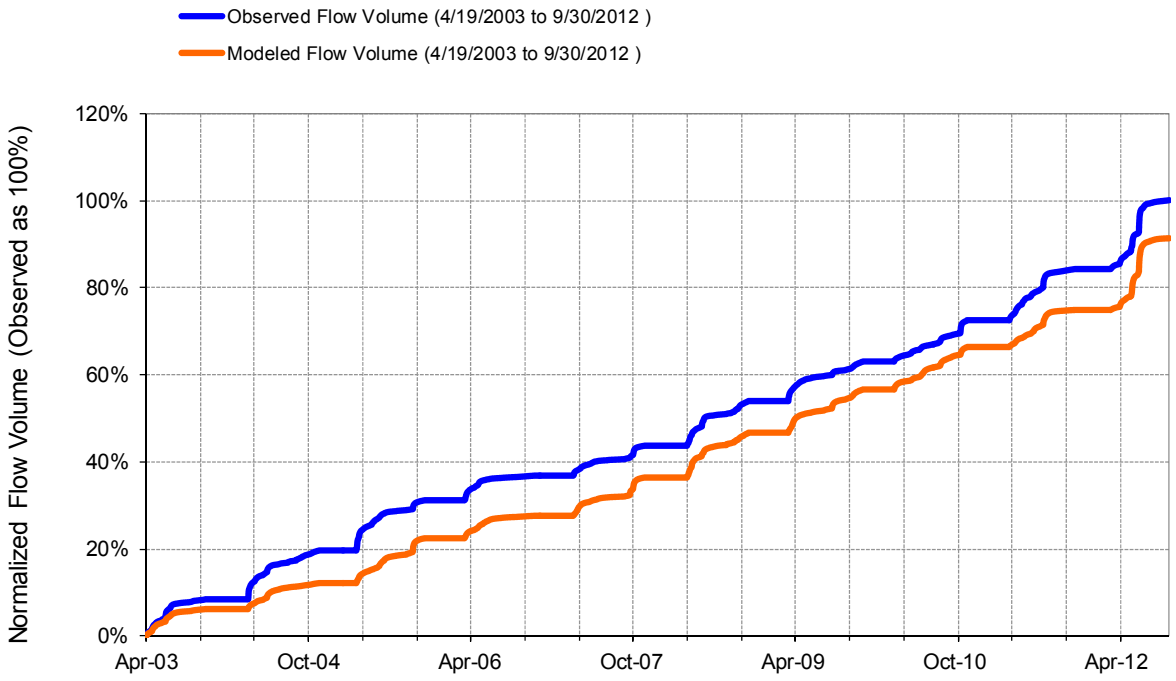

Figure C-77. Flow accumulation at HYDSTRA 05011001 Nemadji River near Pleasant Valley, MN23

Table C-22. Summary statistics at HYDSTRA 05011001 Nemadji River near Pleasant Valley, MN23

HSPF Simulated Flow		Observed Flow Gage		
REACH OUTFLOW FROM DSN 13 9.45-Year Analysis Period: 4/1/2003 - 9/30/2012 Flow volumes are normalized, with total observed as 100		H05011001 Nemadji River near Pleasant Valley, MN 23 Manually Entered Data Drainage Area (sq-mi): 127		
Total Simulated In-stream Flow:	**91.32**	Total Observed In-stream Flow:		**100.00**
Total of simulated highest 10% flows:	**41.96**	Total of Observed highest 10% flows:		**49.30**
Total of Simulated lowest 50% flows:	**12.01**	Total of Observed Lowest 50% flows:		**11.59**
Simulated Summer Flow Volume (months 7-9):	**19.67**	Observed Summer Flow Volume (7-9):		**18.34**
Simulated Fall Flow Volume (months 10-12):	**14.91**	Observed Fall Flow Volume (10-12):		**14.78**
Simulated Winter Flow Volume (months 1-3):	**4.69**	Observed Winter Flow Volume (1-3):		**9.28**
Simulated Spring Flow Volume (months 4-6):	**52.05**	Observed Spring Flow Volume (4-6):		**57.60**
Total Simulated Storm Volume:	**20.44**	Total Observed Storm Volume:		**27.18**
Simulated Summer Storm Volume (7-9):	**3.90**	Observed Summer Storm Volume (7-9):		**4.70**
Errors (Simulated-Observed)	*Error Statistics*	*Recommended Criteria*	*Run (n-1)*	*Run (n-2)*
Error in total volume:	-8.68	10	-8.66	0.32
Error in 50% lowest flows:	3.59	10	3.65	16.48
Error in 10% highest flows:	-14.89	15	-14.91	-5.43
Seasonal volume error - Summer:	7.25	30	7.27	26.27
Seasonal volume error - Fall:	0.85	30	0.86	7.18
Seasonal volume error - Winter:	**-49.47**	**30**	**-49.47**	**ND**
Seasonal volume error - Spring:	-9.64	30	-9.61	-3.64
Error in storm volumes:	**-24.79**	**20**	**-25.01**	**-5.20**
Error in summer storm volumes:	-16.99	50	-17.06	31.69
Nash-Sutcliffe Coefficient of Efficiency, E:	0.655	Model accuracy increases	0.656	0.624
Baseline adjusted coefficient (Garrick), E':	0.525	as E or E' approaches 1.0	0.525	0.522
Monthly NSE	0.750			

>>
>>
Clear

USGS 04024098 Deer Creek near Holyoke, MN

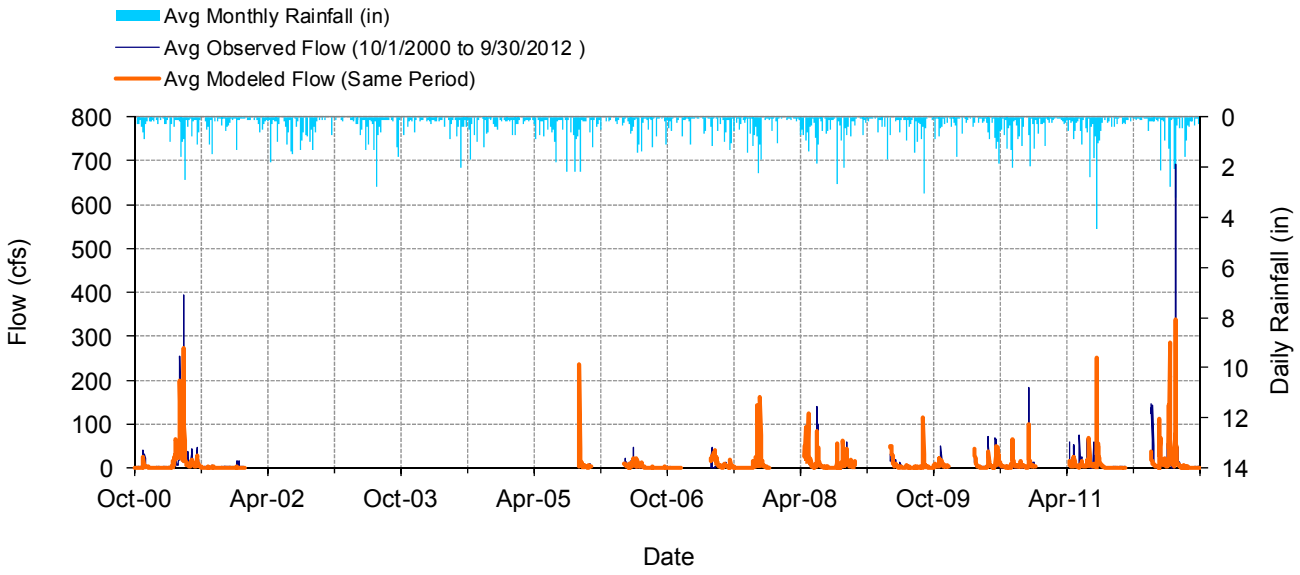

Figure C-78. Mean daily flow at USGS 04024098 Deer Creek near Holyoke, MN

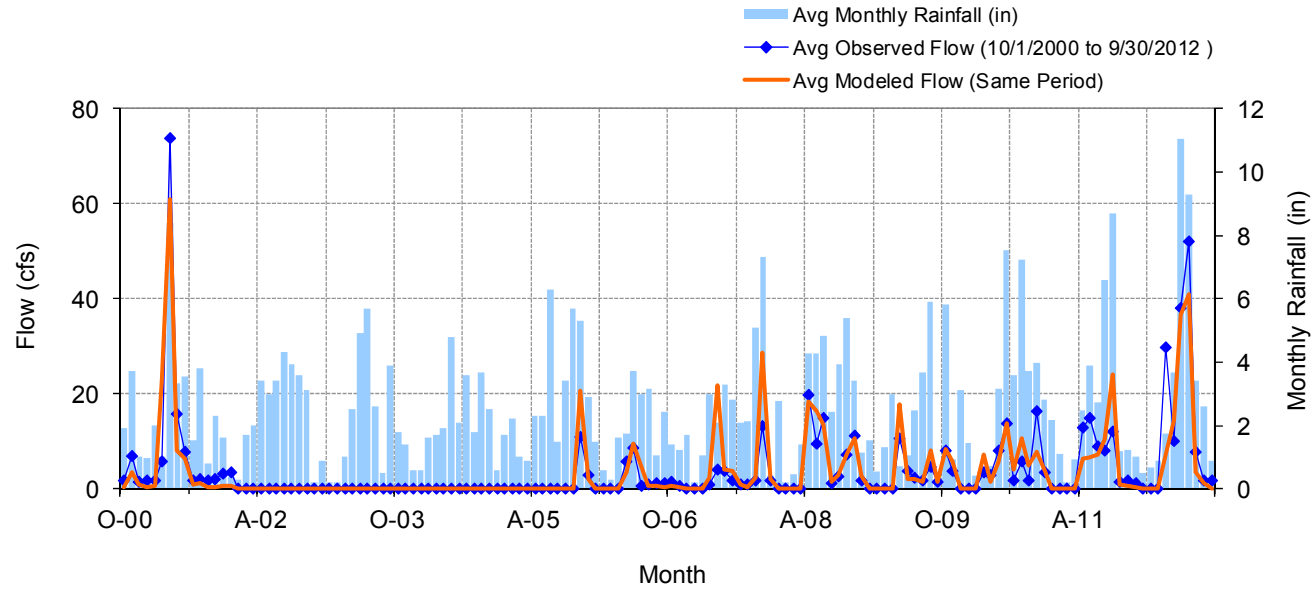

Figure C-79. Mean monthly flow at USGS 04024098 Deer Creek near Holyoke, MN

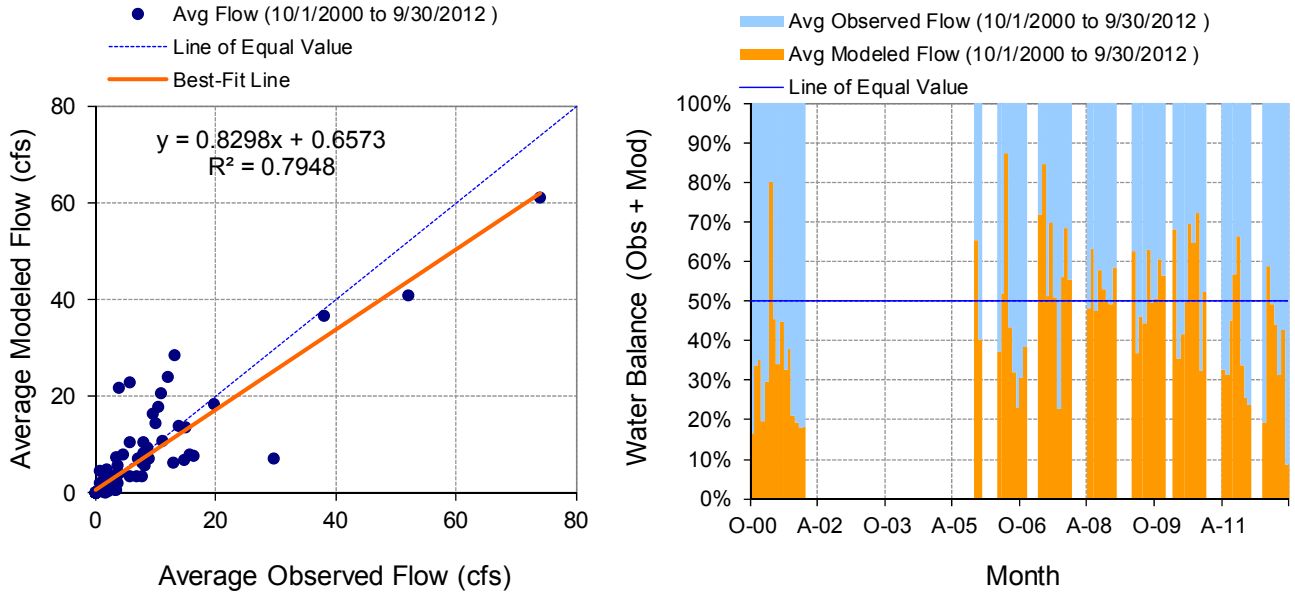

Figure C-80. Monthly flow regression and temporal variation at USGS 04024098 Deer Creek near Holyoke, MN

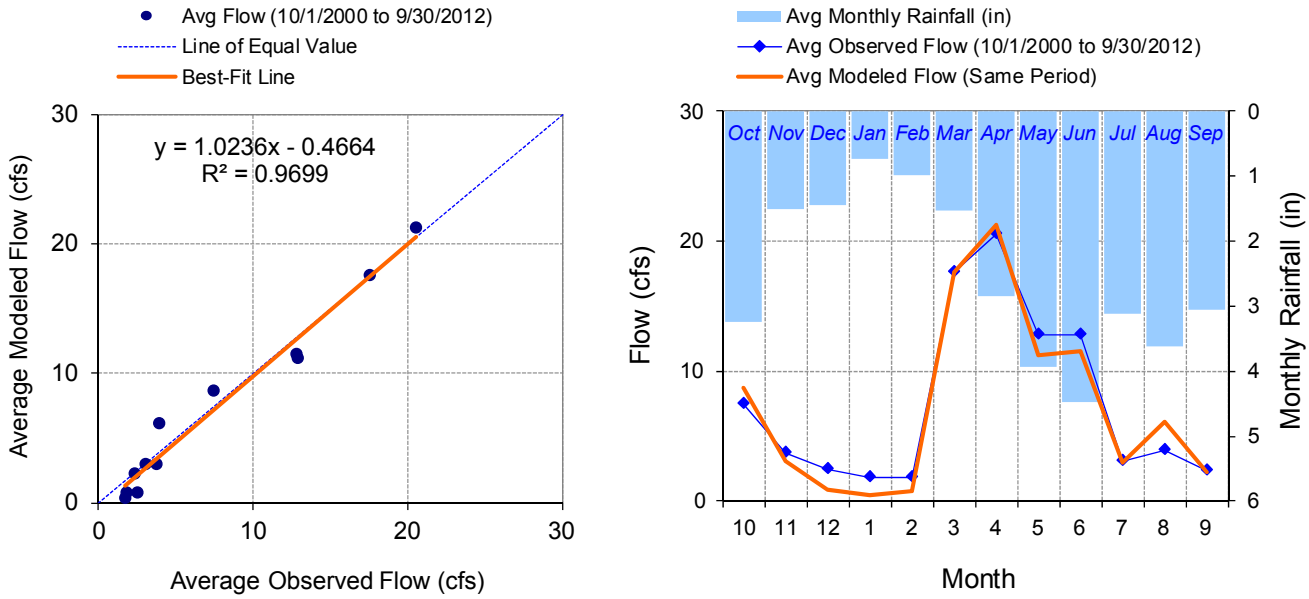

Figure C-81. Seasonal regression and temporal aggregate at USGS 04024098 Deer Creek near Holyoke, MN

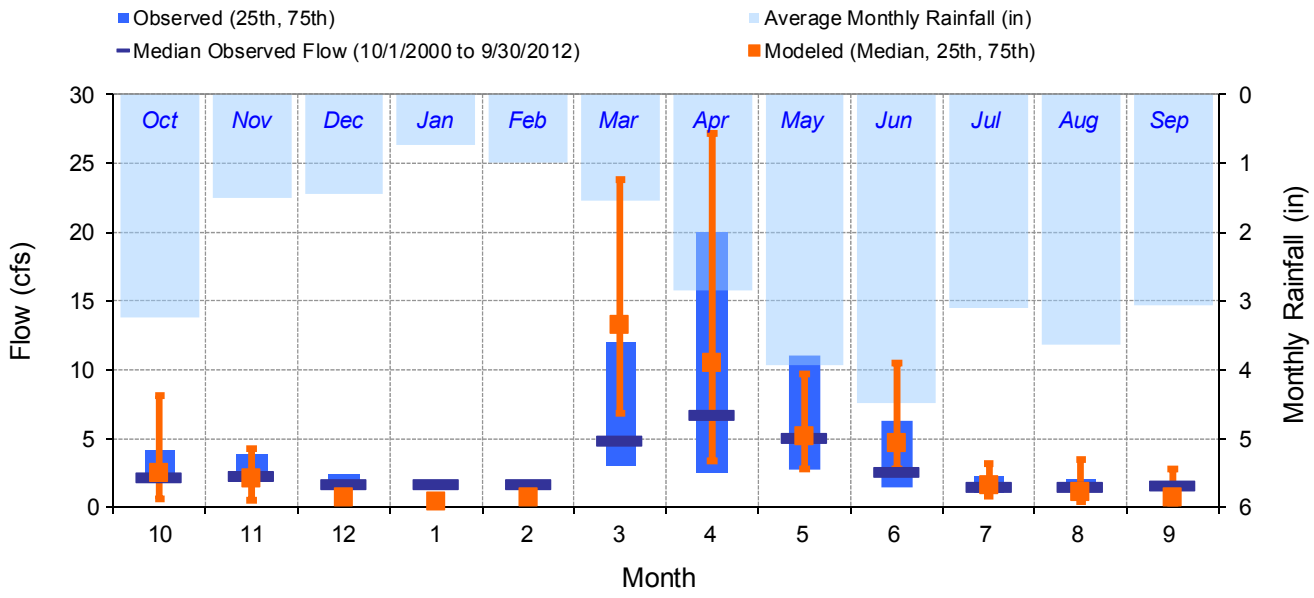

Figure C-82. Seasonal medians and ranges at USGS 04024098 Deer Creek near Holyoke, MN

Table C-23. Seasonal summary at USGS 04024098 Deer Creek near Holyoke, MN

MONTH	OBSERVED FLOW (CFS)				MODELED FLOW (CFS)			
	MEAN	MEDIAN	25TH	75TH	MEAN	MEDIAN	25TH	75TH
Oct	7.45	2.20	1.80	4.10	8.68	2.44	0.57	8.08
Nov	3.70	2.30	1.80	3.83	3.04	2.11	0.53	4.29
Dec	2.49	1.70	1.60	2.45	0.84	0.76	0.58	1.02
Jan	1.76	1.70	1.60	1.90	0.43	0.41	0.37	0.48
Feb	1.77	1.70	1.60	1.90	0.75	0.75	0.71	0.81
Mar	17.55	4.90	3.03	12.00	17.59	13.25	6.85	23.82
Apr	20.50	6.70	2.50	20.00	21.23	10.48	3.33	27.23
May	12.84	5.05	2.70	11.00	11.19	5.11	2.74	9.67
Jun	12.77	2.60	1.48	6.25	11.55	4.70	2.80	10.52
Jul	3.02	1.50	1.08	2.20	2.96	1.55	0.81	3.13
Aug	3.90	1.50	1.18	2.00	6.14	1.13	0.44	3.43
Sep	2.35	1.60	1.40	1.80	2.22	0.67	0.28	2.76

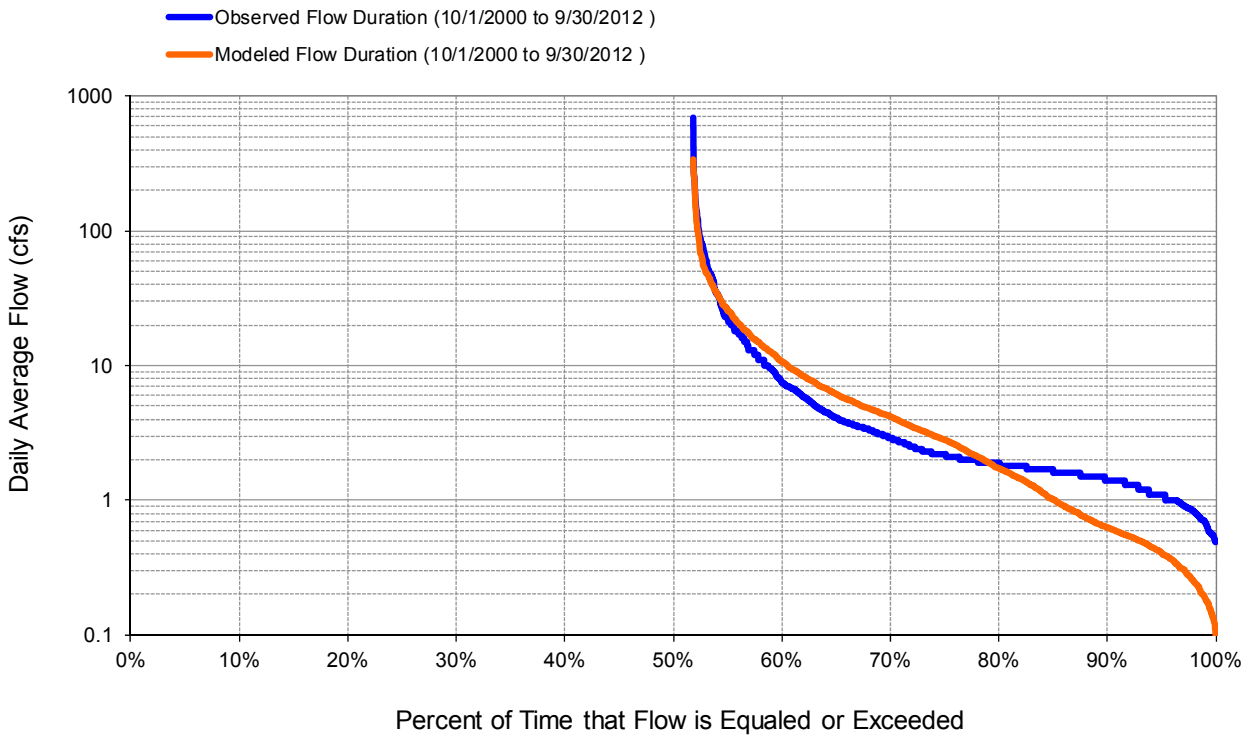

Figure C-83. Flow exceedance at USGS 04024098 Deer Creek near Holyoke, MN

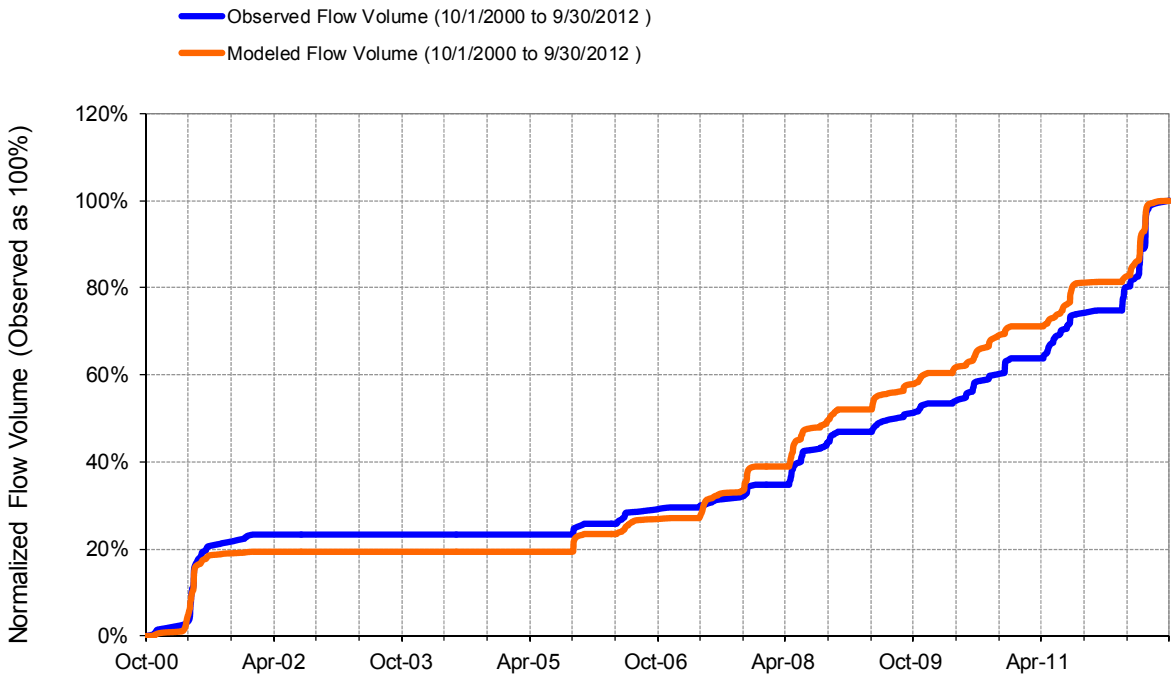

Figure C-84. Flow accumulation at USGS 04024098 Deer Creek near Holyoke, MN

Table C-24. Summary statistics at USGS 04024098 Deer Creek near Holyoke, MN

HSPF Simulated Flow		Observed Flow Gage	
REACH OUTFLOW FROM DSN 118 12-Year Analysis Period: 10/1/2000 - 9/30/2012 Flow volumes are (inches/year) for upstream drainage area		Deer Creek near Holyoke, MN Manually Entered Data Drainage Area (sq-mi): 7.64	
Total Simulated In-stream Flow:	**6.93**	Total Observed In-stream Flow:	**6.93**
Total of simulated highest 10% flows:	**4.16**	Total of Observed highest 10% flows:	**4.61**
Total of Simulated lowest 50% flows:	**0.42**	Total of Observed Lowest 50% flows:	**0.62**
Simulated Summer Flow Volume (months 7-9):	**1.13**	Observed Summer Flow Volume (7-9):	**0.92**
Simulated Fall Flow Volume (months 10-12):	**1.27**	Observed Fall Flow Volume (10-12):	**1.23**
Simulated Winter Flow Volume (months 1-3):	**0.51**	Observed Winter Flow Volume (1-3):	**0.54**
Simulated Spring Flow Volume (months 4-6):	**4.02**	Observed Spring Flow Volume (4-6):	**4.24**
Total Simulated Storm Volume:	**2.45**	Total Observed Storm Volume:	**3.18**
Simulated Summer Storm Volume (7-9):	**0.43**	Observed Summer Storm Volume (7-9):	**0.40**

Errors (Simulated-Observed)	*Error Statistics*	*Recommended Criteria*
Error in total volume:	-0.06	10
Error in 50% lowest flows:	-32.86	10
Error in 10% highest flows:	-9.77	15
Seasonal volume error - Summer:	22.47	30
Seasonal volume error - Fall:	3.31	30
Seasonal volume error - Winter:		30
Seasonal volume error - Spring:	-5.30	30
Error in storm volumes:	-22.97	20
Error in summer storm volumes:	7.39	50
Nash-Sutcliffe Coefficient of Efficiency, E:	0.606	Model accuracy increases
Baseline adjusted coefficient (Garrick), E':	0.408	as E or E' approaches 1.0
Monthly NSE	0.773	

>> Clear

USGS 04024430 Nemadji River near South Superior, WI

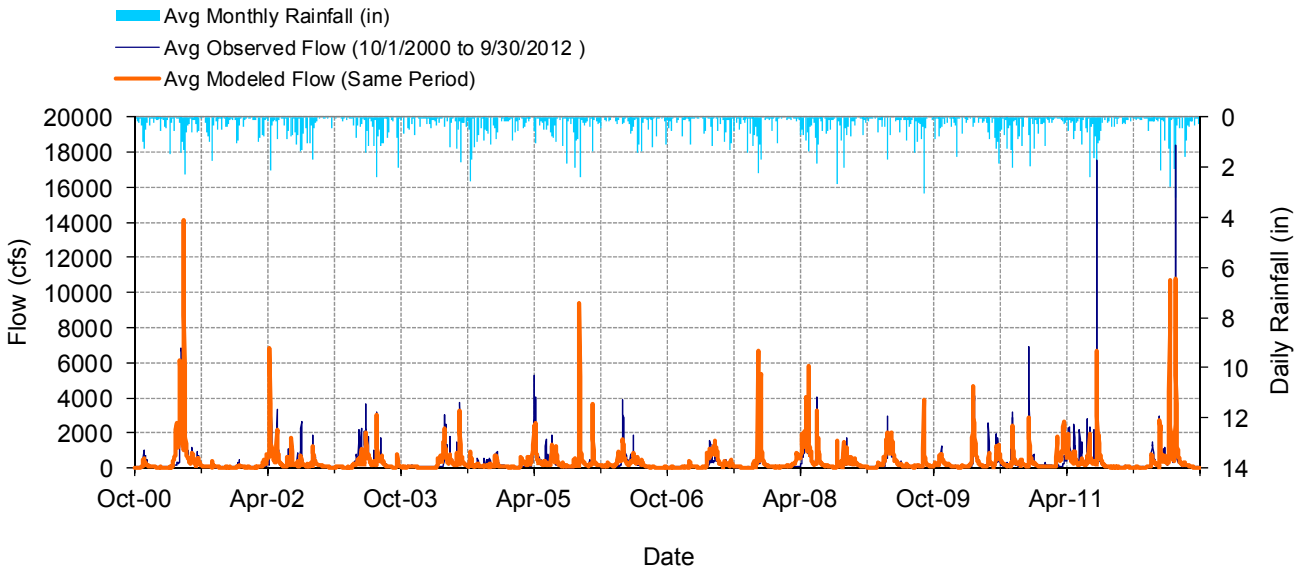

Figure C-85. Mean daily flow at USGS 04024430 Nemadji River near South Superior, WI

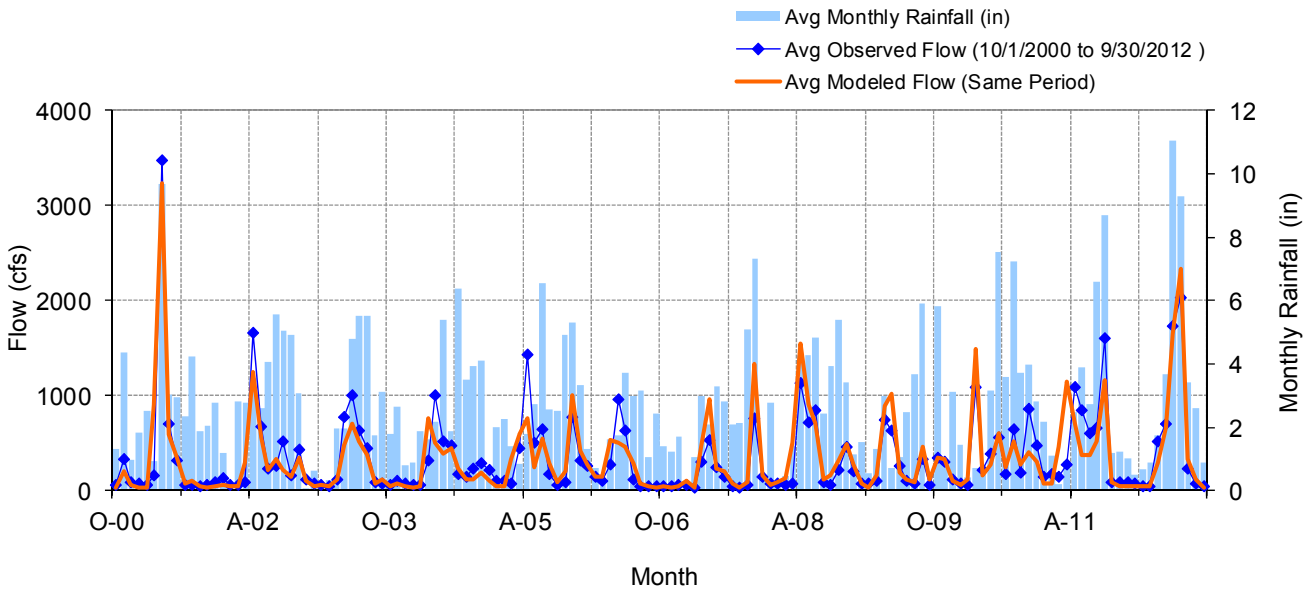

Figure C-86. Mean monthly flow at USGS 04024430 Nemadji River near South Superior, WI

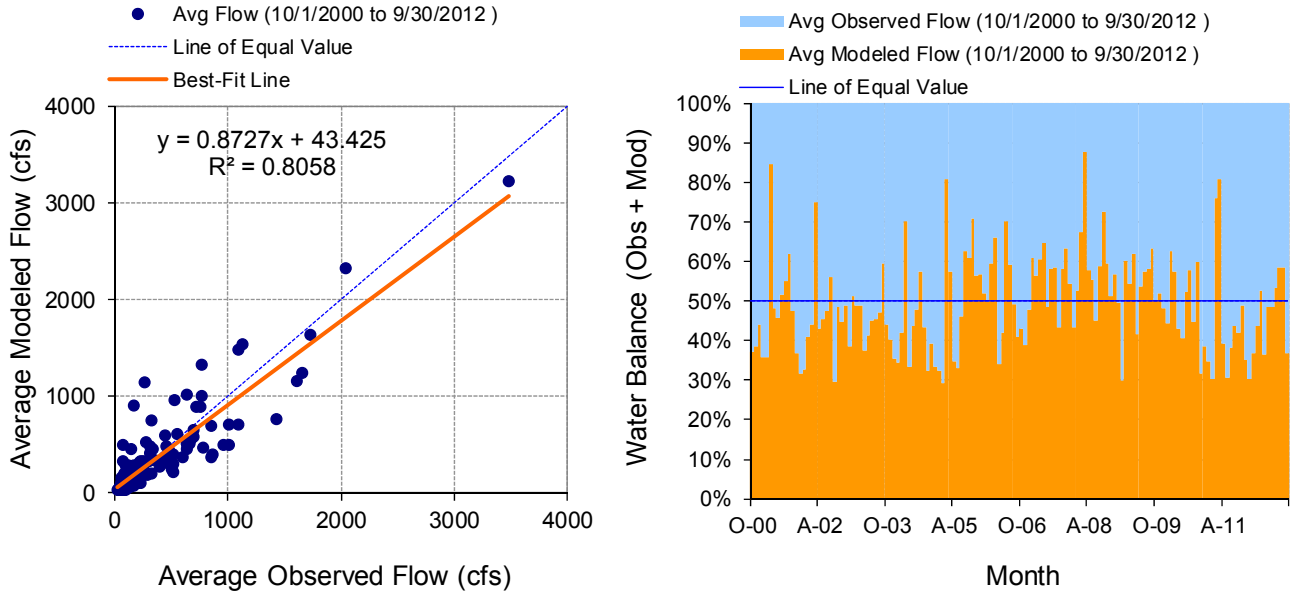

Figure C-87. Monthly flow regression and temporal variation at USGS 04024430 Nemadji River near South Superior, WI

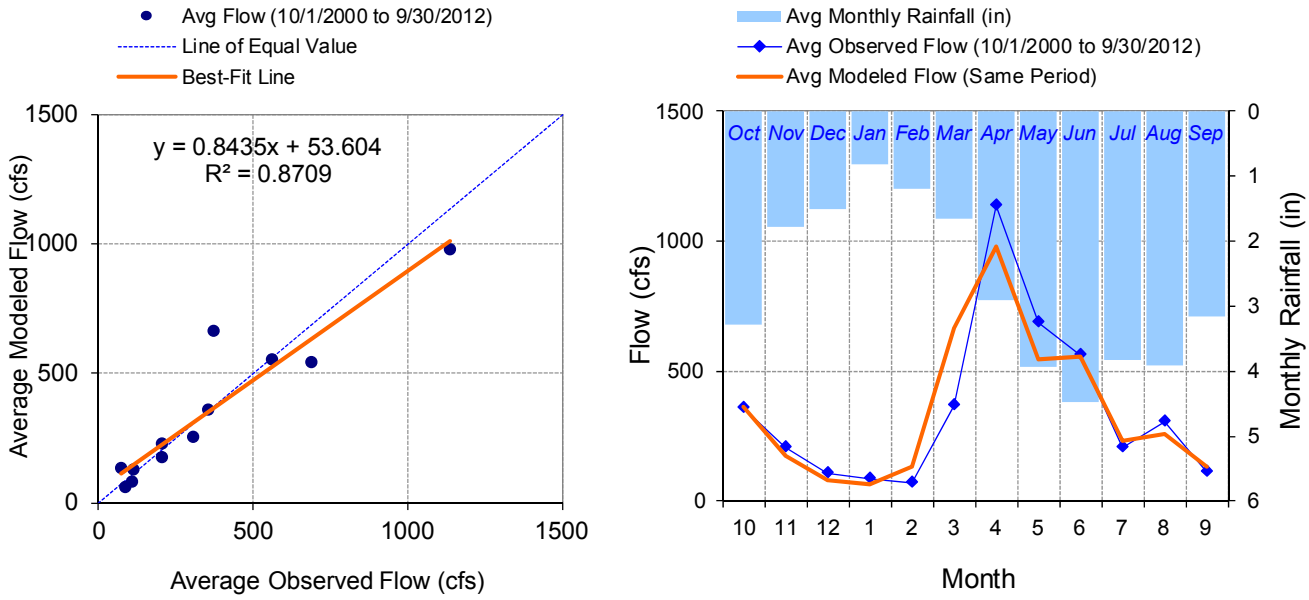

Figure C-88. Seasonal regression and temporal aggregate at USGS 04024430 Nemadji River near South Superior, WI

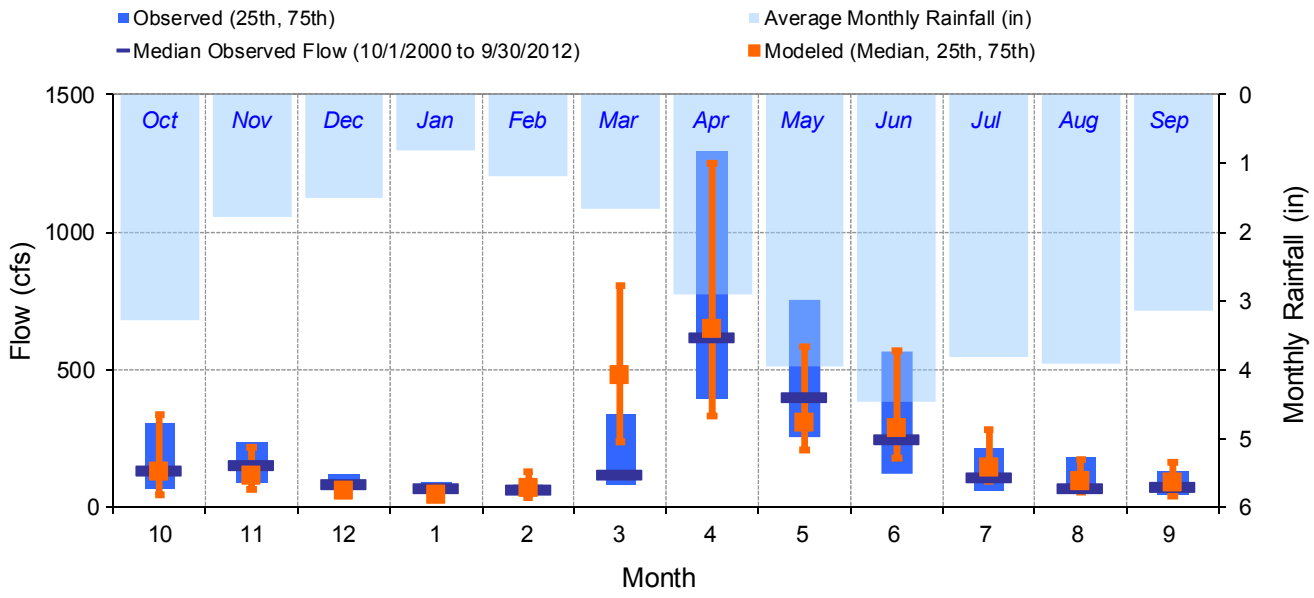

Figure C-89. Seasonal medians and ranges at USGS 04024430 Nemadji River near South Superior, WI

Table C-25. Seasonal summary at USGS 04024430 Nemadji River near South Superior, WI

MONTH	OBSERVED FLOW (CFS)				MODELED FLOW (CFS)			
	MEAN	MEDIAN	25TH	75TH	MEAN	MEDIAN	25TH	75TH
Oct	355.42	133.00	66.75	304.50	360.02	131.48	45.30	339.02
Nov	204.25	152.50	86.00	234.25	174.83	115.97	64.26	219.17
Dec	107.43	83.00	74.00	120.00	80.73	58.14	45.24	81.47
Jan	84.27	72.00	59.00	92.00	62.75	46.41	35.60	76.51
Feb	71.38	66.00	51.00	80.00	132.35	67.72	35.96	129.89
Mar	369.62	119.50	84.00	340.25	667.07	477.89	237.94	803.68
Apr	1134.69	620.00	391.75	1290.00	981.10	647.16	331.38	1249.99
May	685.56	402.50	255.00	755.50	546.67	308.09	210.42	584.49
Jun	560.39	246.50	121.00	566.75	556.29	287.37	178.35	566.97
Jul	203.79	109.50	62.00	214.50	229.58	144.67	93.09	280.92
Aug	306.80	71.50	47.00	179.00	257.83	94.25	55.72	172.53
Sep	110.41	74.00	48.00	132.50	131.55	91.61	39.22	165.56

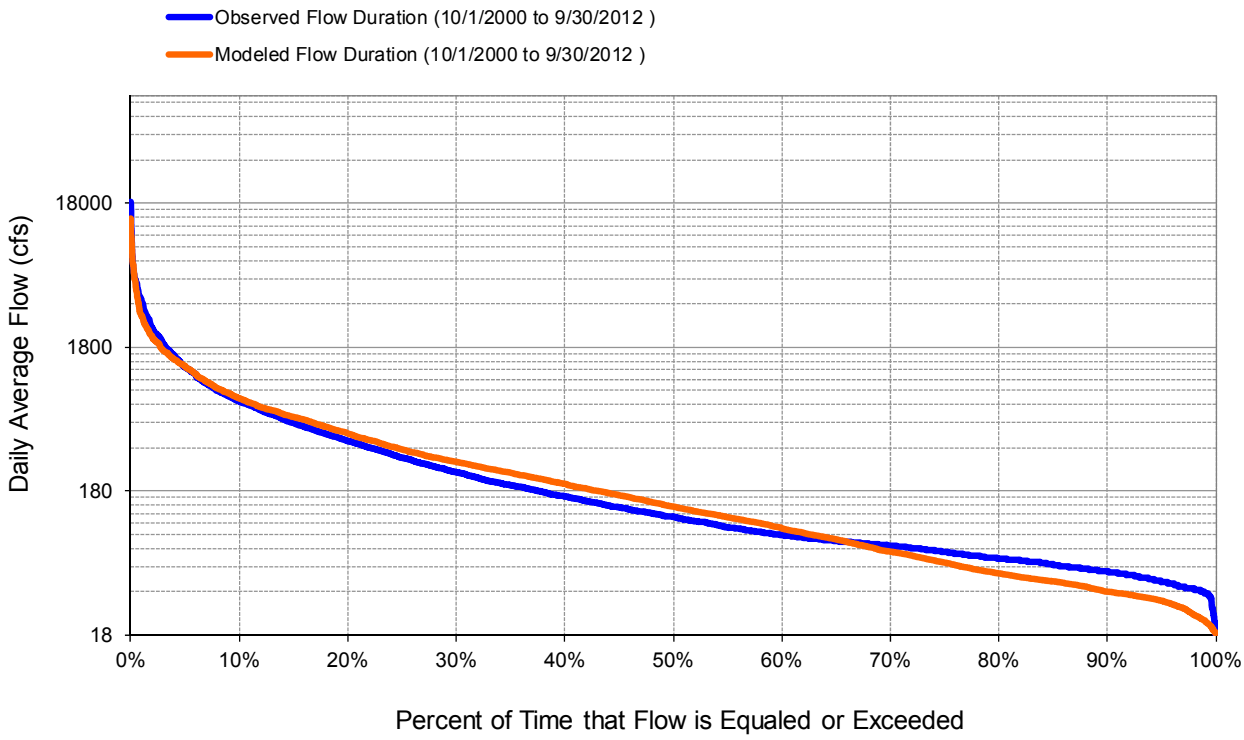

Figure C-90. Flow exceedance at USGS 04024430 Nemadji River near South Superior, WI

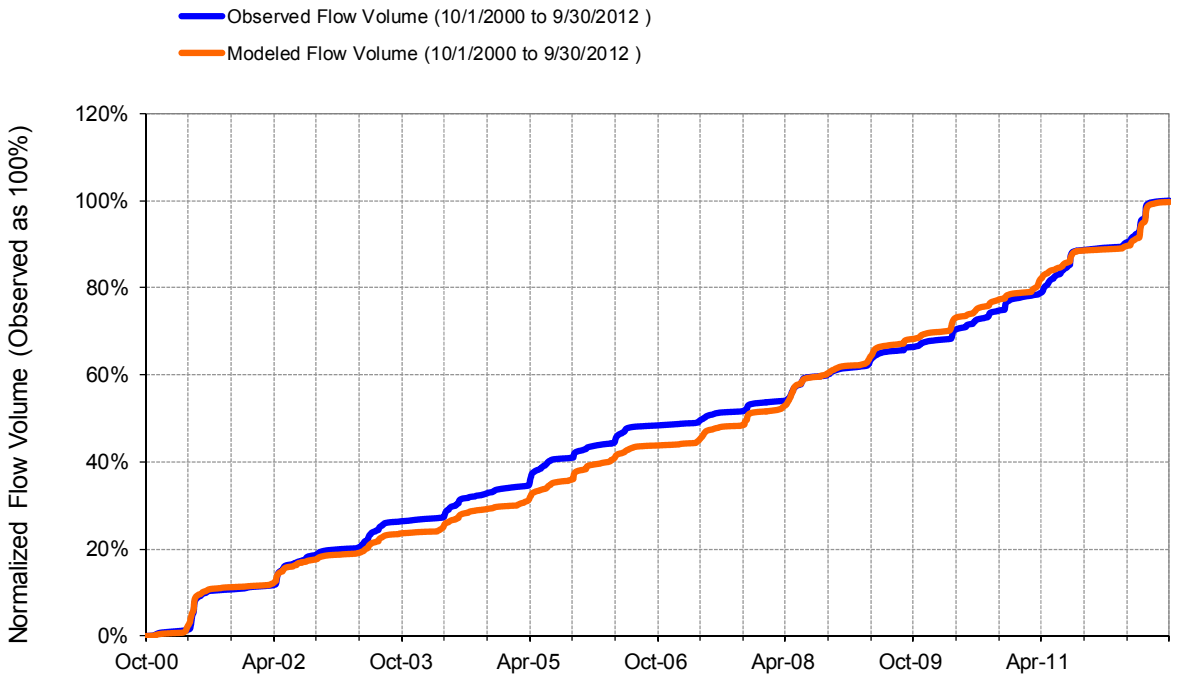

Figure C-91. Flow accumulation at USGS 04024430 Nemadji River near South Superior, WI

Table C-26. Summary statistics at USGS 04024430 Nemadji River near South Superior, WI

HSPF Simulated Flow		Observed Flow Gage		
REACH OUTFLOW FROM DSN 103 12-Year Analysis Period: 10/1/2000 - 9/30/2012 Flow volumes are (inches/year) for upstream drainage area		Nemadji River near South Superior, WI Manually Entered Data Drainage Area (sq-mi): 420		
Total Simulated In-stream Flow:	**11.28**	Total Observed In-stream Flow:		**11.32**
Total of simulated highest 10% flows:	**5.79**	Total of Observed highest 10% flows:		**6.29**
Total of Simulated lowest 50% flows:	**1.07**	Total of Observed Lowest 50% flows:		**1.13**
Simulated Summer Flow Volume (months 7-9):	**1.69**	Observed Summer Flow Volume (7-9):		**1.69**
Simulated Fall Flow Volume (months 10-12):	**1.67**	Observed Fall Flow Volume (10-12):		**1.81**
Simulated Winter Flow Volume (months 1-3):	**2.33**	Observed Winter Flow Volume (1-3):		**1.42**
Simulated Spring Flow Volume (months 4-6):	**5.58**	Observed Spring Flow Volume (4-6):		**6.38**
Total Simulated Storm Volume:	**4.43**	Total Observed Storm Volume:		**5.23**
Simulated Summer Storm Volume (7-9):	**0.65**	Observed Summer Storm Volume (7-9):		**0.83**
Errors (Simulated-Observed)	*Error Statistics*	*Recommended Criteria*		
Error in total volume:	-0.32	10		
Error in 50% lowest flows:	-4.98	10		
Error in 10% highest flows:	-8.03	15		
Seasonal volume error - Summer:	-0.44	30		
Seasonal volume error - Fall:	-7.66	30		
Seasonal volume error - Winter:	63.88	30		
Seasonal volume error - Spring:	-12.53	30		
Error in storm volumes:	-15.38	20		
Error in summer storm volumes:	-21.98	50		
Nash-Sutcliffe Coefficient of Efficiency, E:	0.663	Model accuracy increases		
Baseline adjusted coefficient (Garrick), E':	0.514	as E or E' approaches 1.0		
Monthly NSE	0.800			

>>

Clear

HYDSTRA 05006001 Blackhoof River near Pleasant Valley, MN

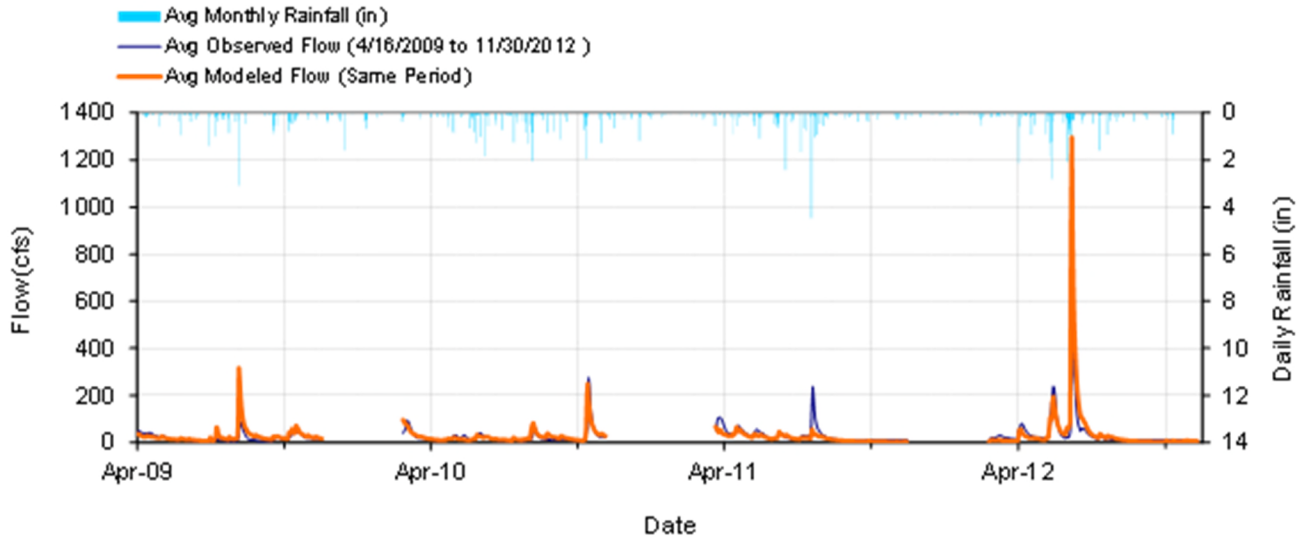

Figure C-92. Mean daily flow at HYDSTRA 05006001 Blackhoof River near Pleasant Valley

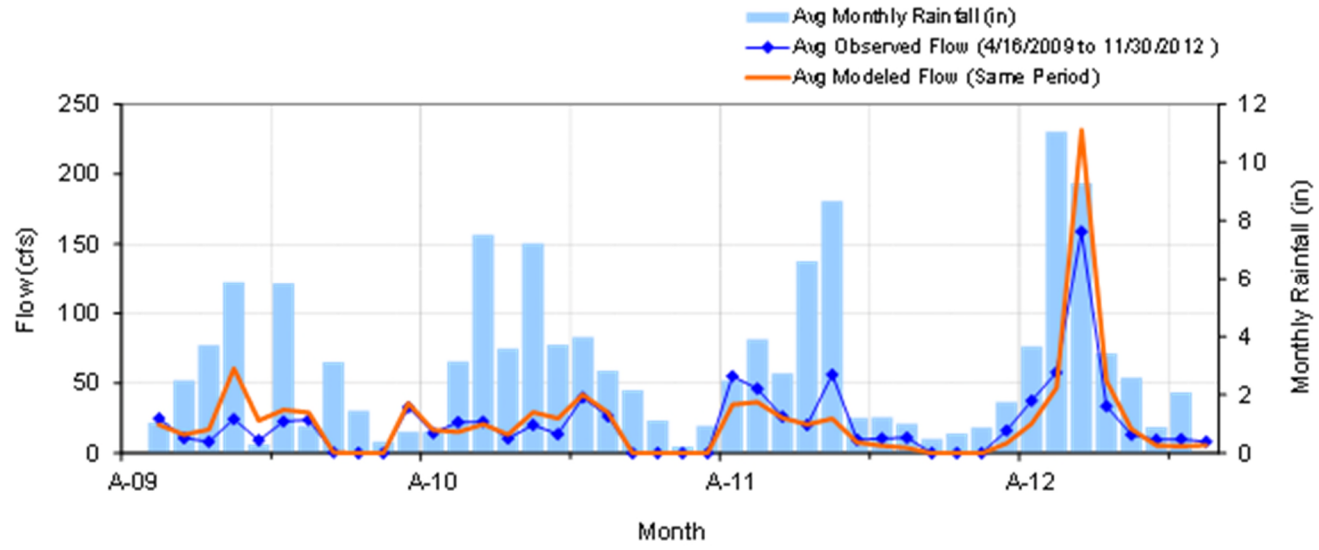

Figure C-93. Mean monthly flow at HYDSTRA 05006001 Blackhoof River near Pleasant Valley

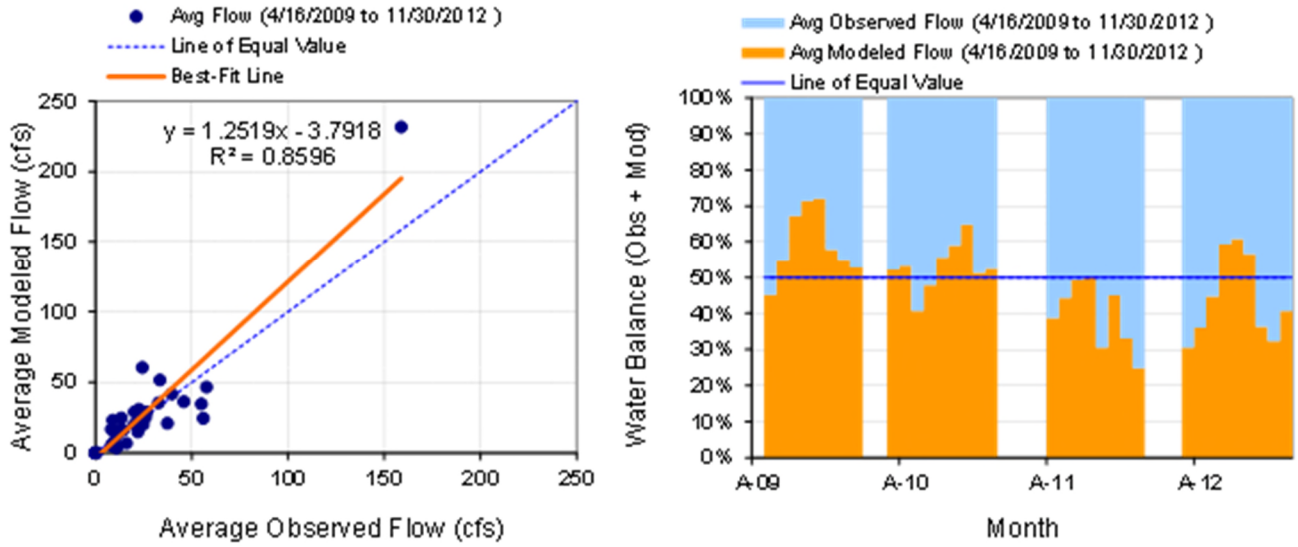

Figure C-94. Monthly flow regression and temporal variation at HYDSTRA 05006001 Blackhoof River near Pleasant Valley

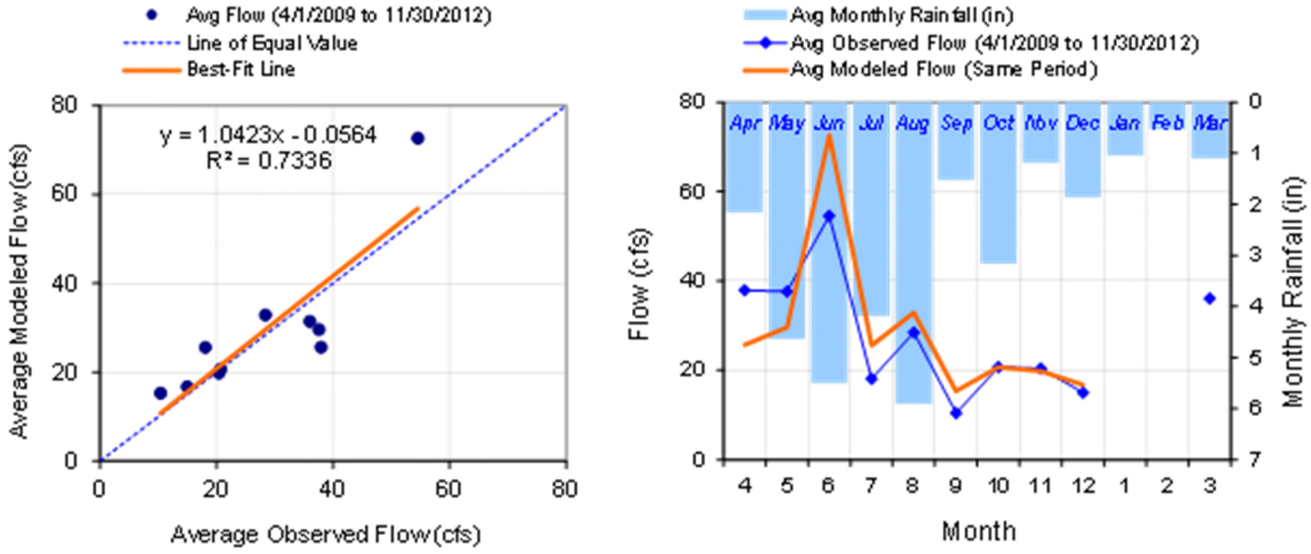

Figure C-95. Seasonal regression and temporal aggregate at HYDSTRA 05006001 Blackhoof River near Pleasant Valley

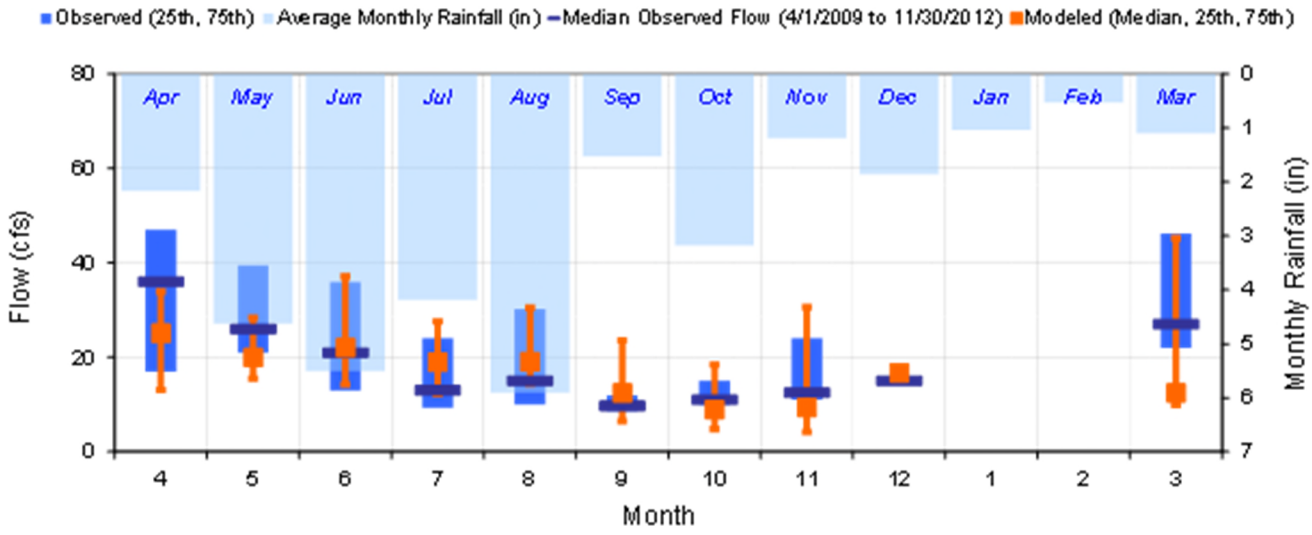

Figure C-96. Seasonal medians and ranges at HYDSTRA 05006001 Blackhoof River near Pleasant Valley

Table C-27. Seasonal summary at HYDSTRA 05006001 Blackhoof River near Pleasant Valley

MONTH	OBSERVED FLOW (CFS)				MODELED FLOW (CFS)			
	MEAN	MEDIAN	25TH	75TH	MEAN	MEDIAN	25TH	75TH
Apr	37.92	36.00	17.00	47.00	25.67	25.16	13.09	33.92
May	37.59	26.00	21.00	39.50	29.60	20.03	15.49	28.36
Jun	54.55	21.00	13.00	36.00	72.64	22.08	14.25	37.16
Jul	18.10	13.00	9.30	24.00	25.57	19.01	12.16	27.59
Aug	28.42	15.00	10.00	30.25	32.86	19.08	14.40	30.49
Sep	10.40	9.70	8.60	12.00	15.34	12.49	6.44	23.60
Oct	20.69	11.00	10.00	15.00	20.68	8.97	4.81	18.48
Nov	20.39	12.50	11.00	24.00	19.77	9.45	4.17	30.62
Dec	15.00	15.00	15.00	15.00	16.75	16.75	16.75	16.75
Jan	0.00	0.00	0.00	0.00	0.00	0.00	0.00	0.00
Feb	0.00	0.00	0.00	0.00	0.00	0.00	0.00	0.00
Mar	36.03	27.00	22.00	46.25	31.46	12.49	9.88	45.22

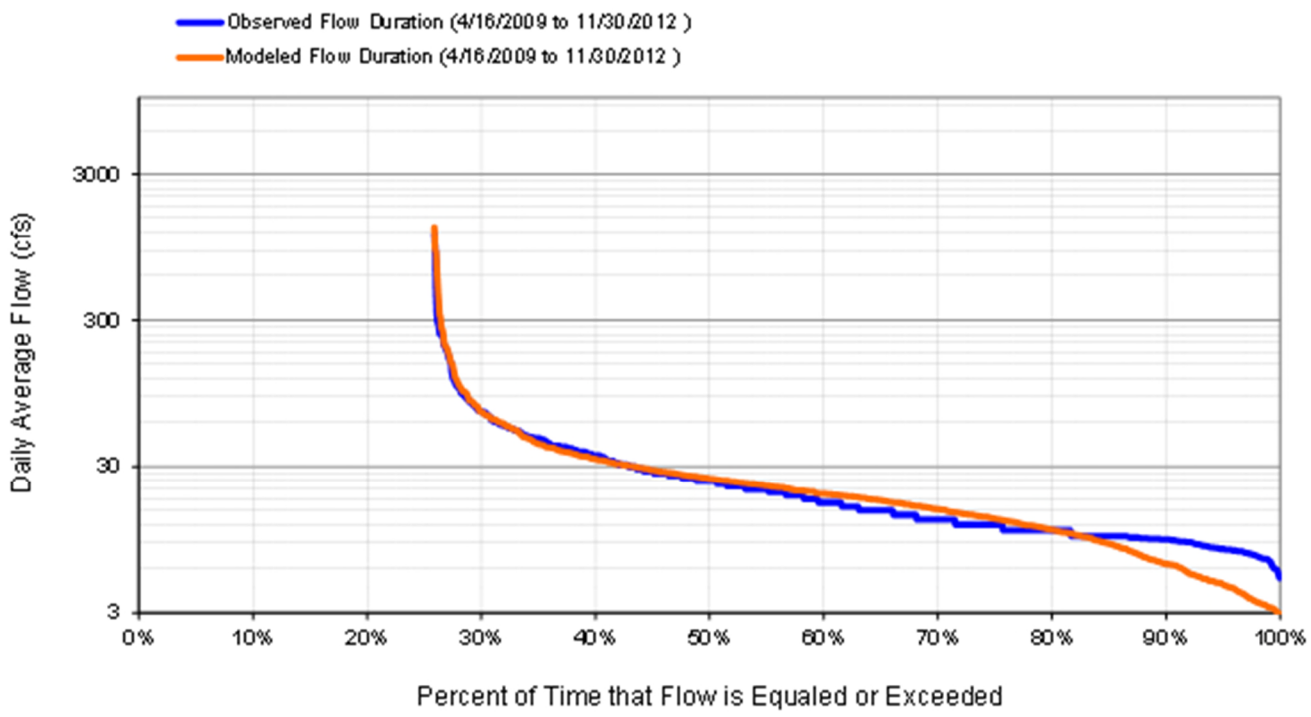

Figure C-97. Flow exceedance at HYDSTRA 05006001 Blackhoof River near Pleasant Valley

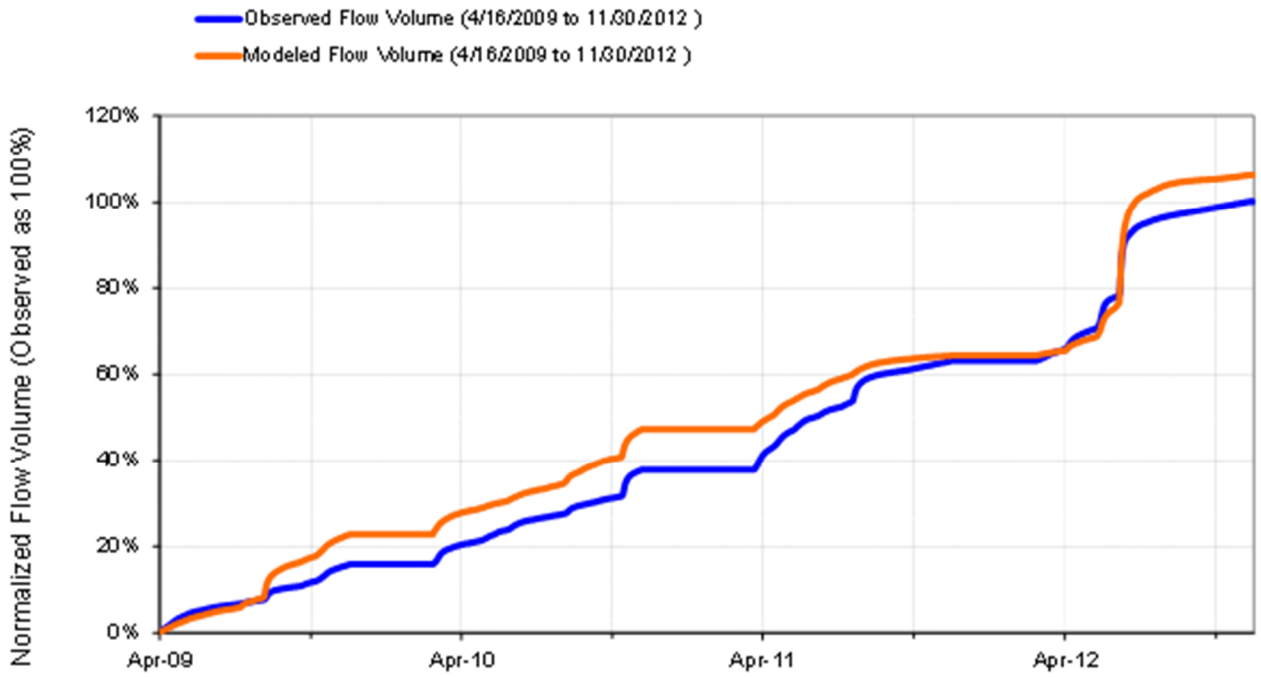

Figure C-98. Flow accumulation at HYDSTRA 05006001 Blackhoof River near Pleasant Valley

Table C-28. Summary statistics at HYDSTRA 05006001 Blackhoof River near Pleasant Valley

HSPF Simulated Flow		Observed Flow Gage	
REACH OUTFLOW FROM DSN 511 363-Year Analysis Period: 4/1/2009 - 11/30/2012 Flow volumes are (inches/year) for upstream drainage area		H05006001 Blackhoof Pleasant Manually Entered Data Drainage Area (sq-mi): 3.43	
Total Simulated In-stream Flow:	8.54	Total Observed In-stream Flow:	8.04
Total of simulated highest 10% flows:	3.94	Total of Observed highest 10% flows:	3.43
Total of Simulated lowest 50% flows:	1.46	Total of Observed Lowest 50% flows:	1.51
Simulated Summer Flow Volume (months 7-9):	2.59	Observed Summer Flow Volume (7-9):	2.00
Simulated Fall Flow Volume (months 10-12):	1.31	Observed Fall Flow Volume (10-12):	1.33
Simulated Winter Flow Volume (months 1-3):	0.38	Observed Winter Flow Volume (1-3):	0.43
Simulated Spring Flow Volume (months 4-6):	4.27	Observed Spring Flow Volume (4-6):	4.28
Total Simulated Storm Volume:	2.38	Total Observed Storm Volume:	2.19
Simulated Summer Storm Volume (7-9):	0.59	Observed Summer Storm Volume (7-9):	0.44

Errors (Simulated-Observed)	*Error Statistics*		*Recommended Criteria*	*Run (n-1)*	*Run (n-2)*
Error in total volume:	6.22		10	6.02	
Error in 50% lowest flows:	-3.44		10	-3.74	
Error in 10% highest flows:	14.96		15	13.93	
Seasonal volume error - Summer:	29.49		30	29.22	
Seasonal volume error - Fall:	-1.36	>>	30	-1.96	Clear
Seasonal volume error - Winter:	-12.69	>>	30	-12.19	
Seasonal volume error - Spring:	-0.38		30	-0.50	
Error in storm volumes:	8.69		20	7.80	
Error in summer storm volumes:	33.07		50	31.85	
Nash-Sutcliffe Coefficient of Efficiency, E:	0.698		Model accuracy increases as E or E' approaches 1.0	0.714	
Baseline adjusted coefficient (Garrick), E':	0.433			0.442	
Monthly NSE	0.627				

HYDSTRA 05008002 Deer Creek near Pleasant Valley, MN

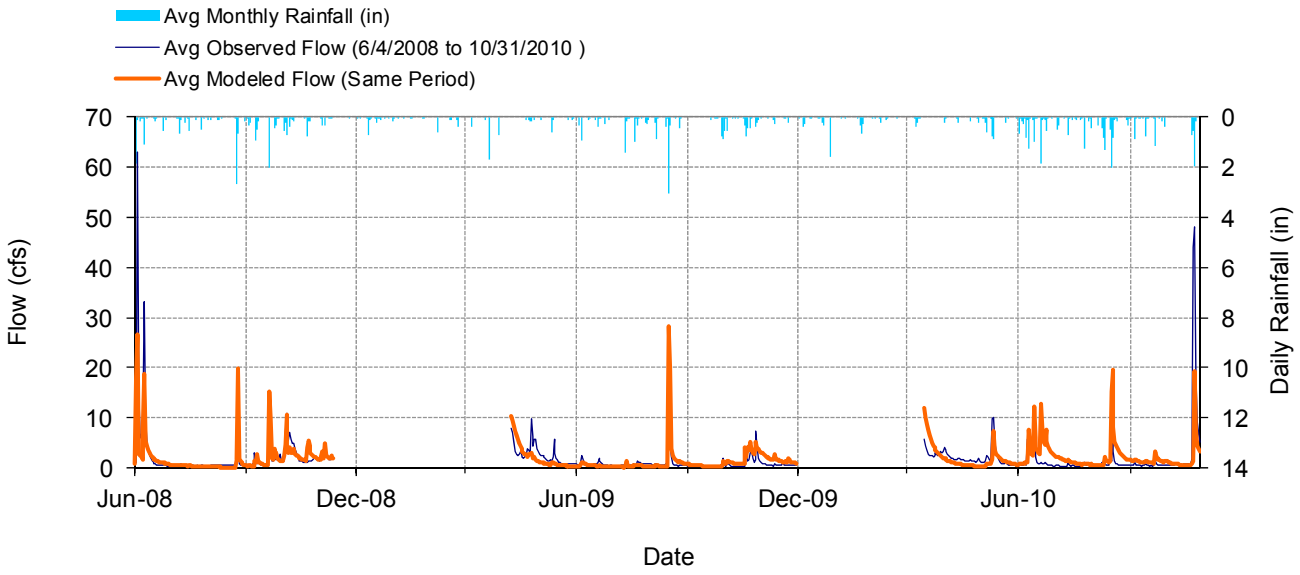

Figure C-99. Mean daily flow at HYDSTRA 05008002 Deer Creek near Pleasant Valley, MN

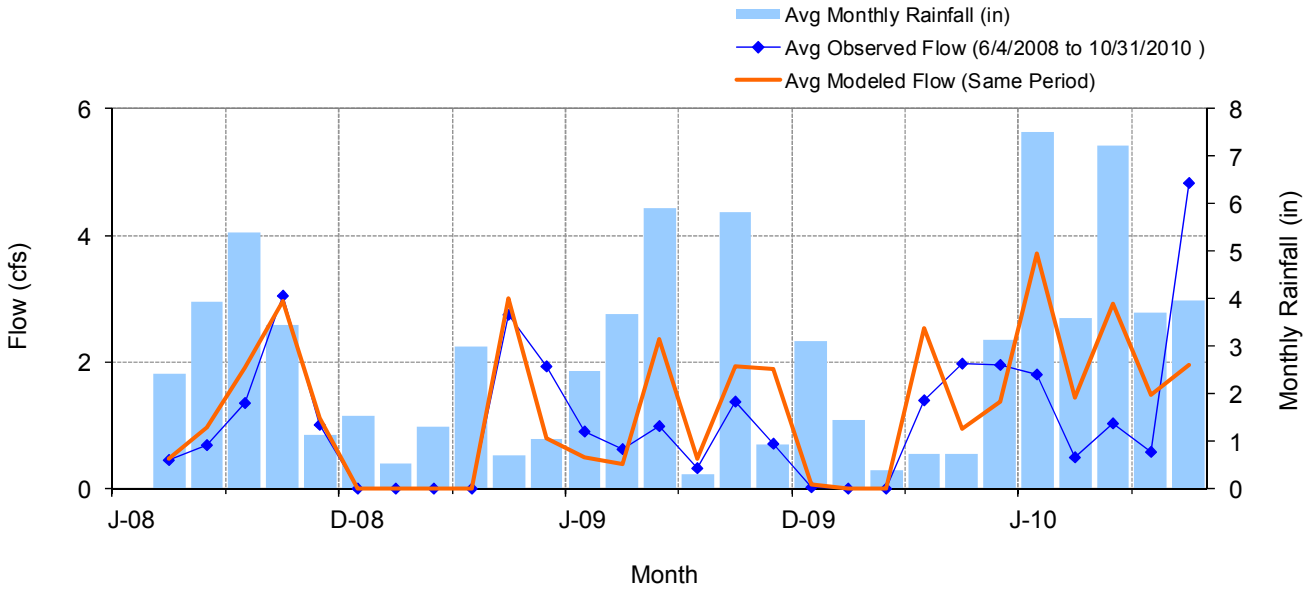

Figure C-100. Mean monthly flow at HYDSTRA 05008002 Deer Creek near Pleasant Valley, MN

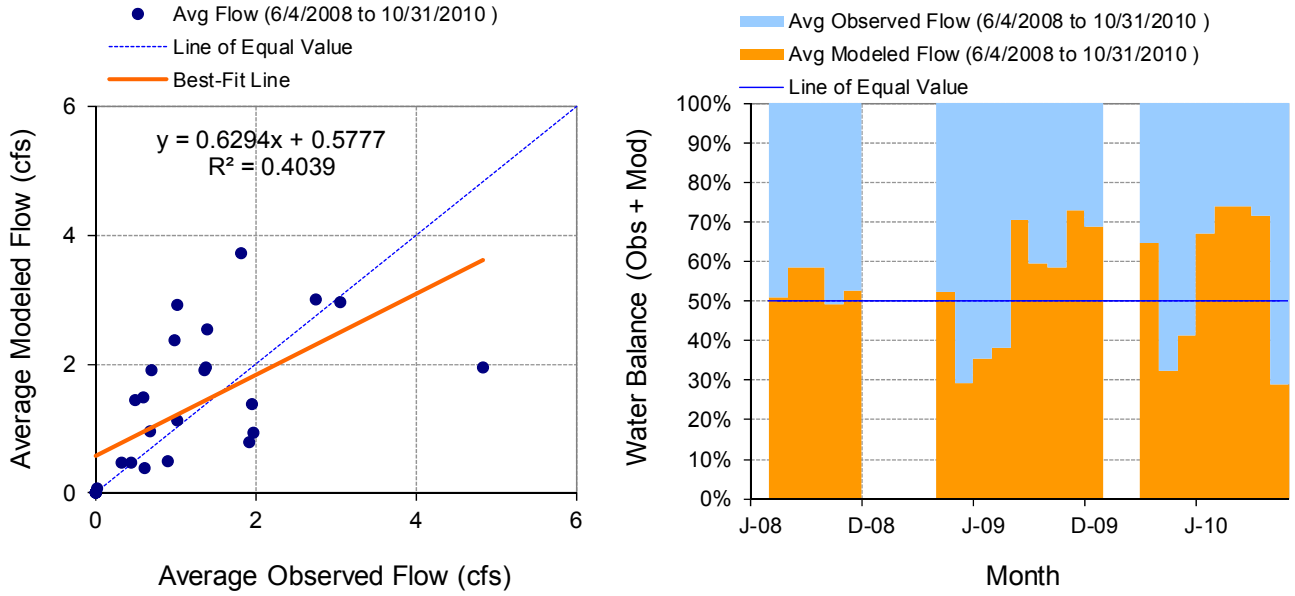

Figure C-101. Monthly flow regression and temporal variation at HYDSTRA 05008002 Deer Creek near Pleasant Valley, MN

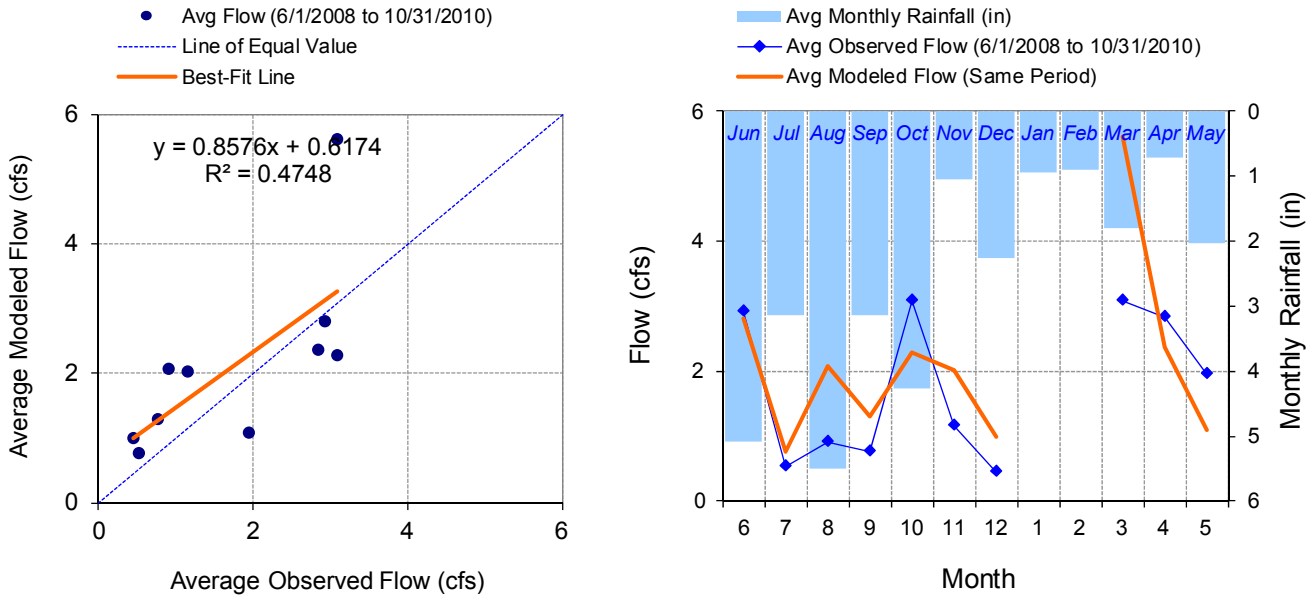

Figure C-102. Seasonal regression and temporal aggregate at HYDSTRA 05008002 Deer Creek near Pleasant Valley, MN

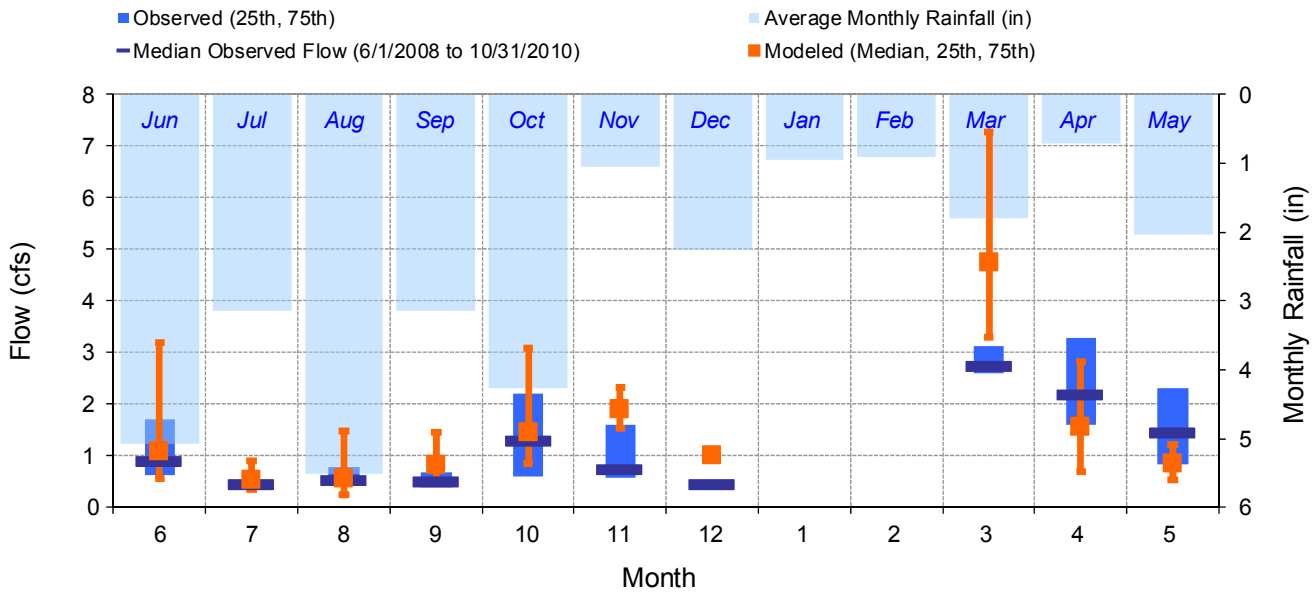

Figure C-103. Seasonal medians and ranges at HYDSTRA 05008002 Deer Creek near Pleasant Valley, MN

Table C-29. Seasonal summary at HYDSTRA 05008002 Deer Creek near Pleasant Valley, MN

MONTH	OBSERVED FLOW (CFS)				MODELED FLOW (CFS)			
	MEAN	MEDIAN	25TH	75TH	MEAN	MEDIAN	25TH	75TH
Jun	2.92	0.90	0.63	1.70	2.80	1.10	0.55	3.19
Jul	0.53	0.45	0.40	0.53	0.77	0.52	0.36	0.90
Aug	0.90	0.53	0.47	0.77	2.08	0.56	0.24	1.48
Sep	0.76	0.51	0.38	0.68	1.29	0.82	0.48	1.45
Oct	3.09	1.30	0.61	2.20	2.29	1.46	0.86	3.09
Nov	1.15	0.75	0.56	1.60	2.02	1.89	1.53	2.32
Dec	0.46	0.46	0.45	0.46	1.00	1.00	0.98	1.01
Jan	0.00	0.00	0.00	0.00	0.00	0.00	0.00	0.00
Feb	0.00	0.00	0.00	0.00	0.00	0.00	0.00	0.00
Mar	3.08	2.75	2.60	3.13	5.62	4.76	3.30	7.29
Apr	2.83	2.20	1.60	3.28	2.37	1.56	0.69	2.81
May	1.94	1.45	0.83	2.30	1.09	0.85	0.53	1.22

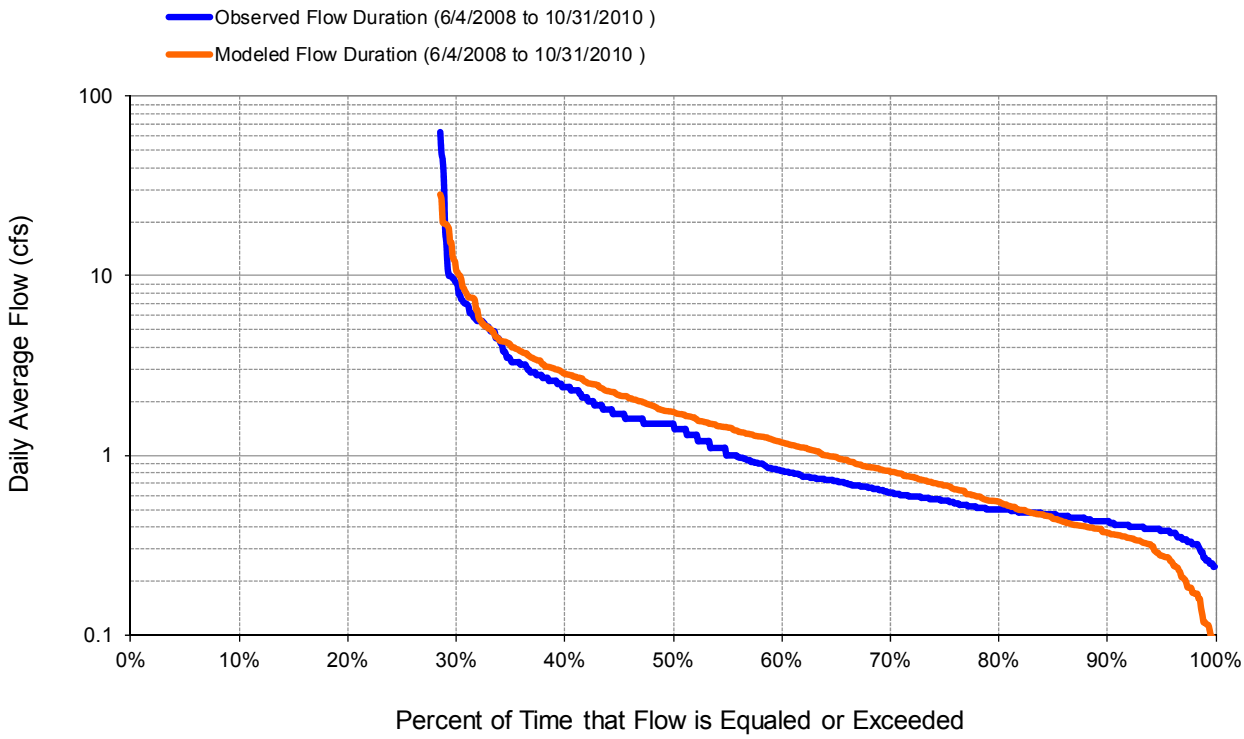

Figure C-104. Flow exceedance at HYDSTRA 05008002 Deer Creek near Pleasant Valley, MN

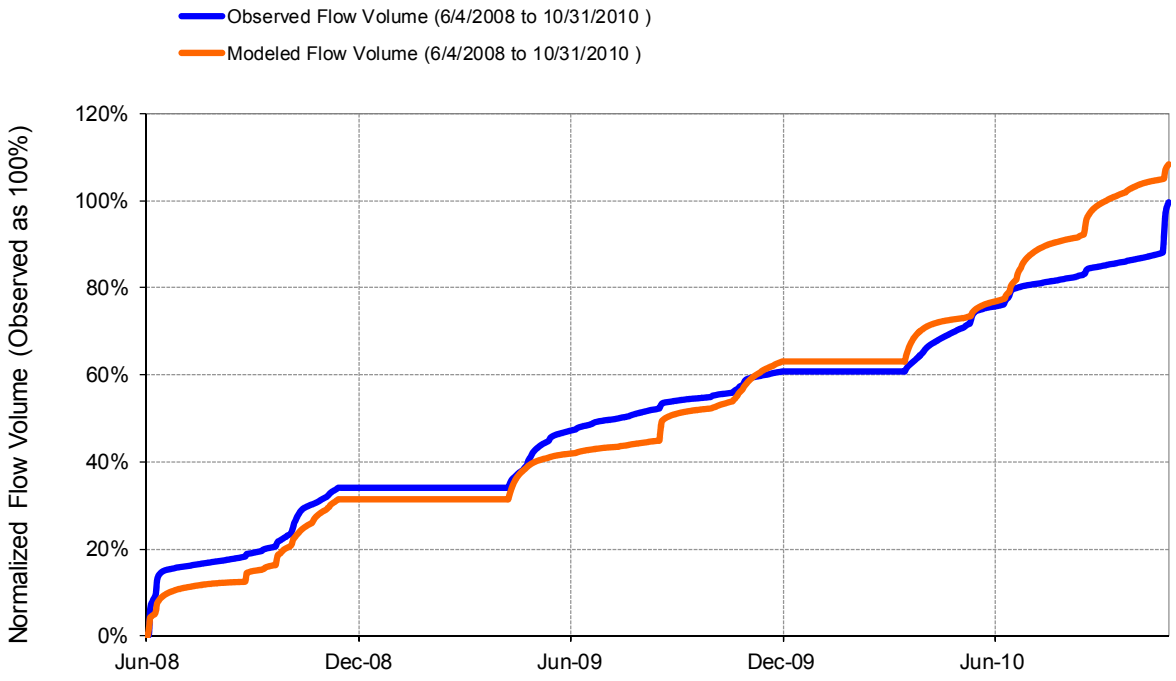

Figure C-105. Flow accumulation at HYDSTRA 05008002 Deer Creek near Pleasant Valley, MN

Table C-30. Summary statistics at HYDSTRA 05008002 Deer Creek near Pleasant Valley, MN

HSPF Simulated Flow		Observed Flow Gage		
REACH OUTFLOW FROM DSN 119 2.41-Year Analysis Period: 6/1/2008 - 10/31/2010 Flow volumes are (inches/year) for upstream drainage area		Deer Creek near Pleasant Valley, MN Manually Entered Data Drainage Area (sq-mi): 3.43		
Total Simulated In-stream Flow:	**5.38**	Total Observed In-stream Flow:		**4.95**
Total of simulated highest 10% flows:	**2.44**	Total of Observed highest 10% flows:		**2.52**
Total of Simulated lowest 50% flows:	**0.76**	Total of Observed Lowest 50% flows:		**0.70**
Simulated Summer Flow Volume (months 7-9):	**1.72**	Observed Summer Flow Volume (7-9):		**0.90**
Simulated Fall Flow Volume (months 10-12):	**1.38**	Observed Fall Flow Volume (10-12):		**1.53**
Simulated Winter Flow Volume (months 1-3):	**0.35**	Observed Winter Flow Volume (1-3):		**0.19**
Simulated Spring Flow Volume (months 4-6):	**1.93**	Observed Spring Flow Volume (4-6):		**2.32**
Total Simulated Storm Volume:	**1.54**	Total Observed Storm Volume:		**1.77**
Simulated Summer Storm Volume (7-9):	**0.66**	Observed Summer Storm Volume (7-9):		**0.25**
Errors (Simulated-Observed)	*Error Statistics*	*Recommended Criteria*		
Error in total volume:	8.57	10		
Error in 50% lowest flows:	7.61	10		
Error in 10% highest flows:	-3.35	15		
Seasonal volume error - Summer:	89.64	30		
Seasonal volume error - Fall:	-10.14	30		
Seasonal volume error - Winter:	>>	30	Clear	
Seasonal volume error - Spring:	-16.80	30		
Error in storm volumes:	-13.18	20		
Error in summer storm volumes:	157.83	50		
Nash-Sutcliffe Coefficient of Efficiency, E:	0.315	Model accuracy increases		
Baseline adjusted coefficient (Garrick), E':	0.171	as E or E' approaches 1.0		
Monthly NSE	0.371			

HYDSTRA 05009001 Rock Creek

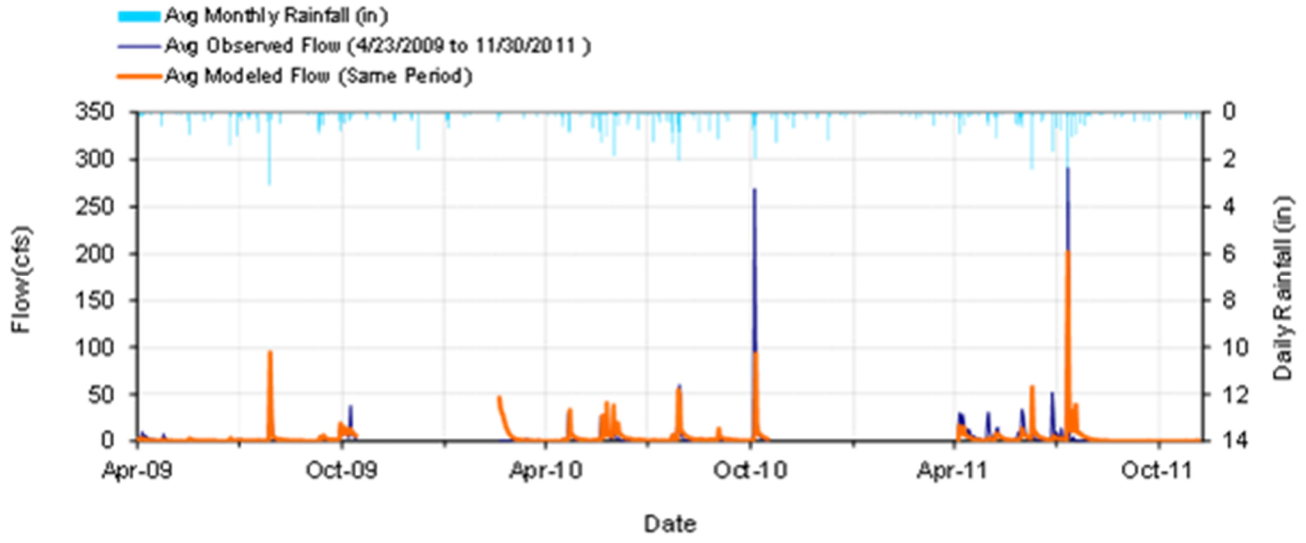

Figure C-106. Mean daily flow at HYDSTRA 05009001 Rock Creek

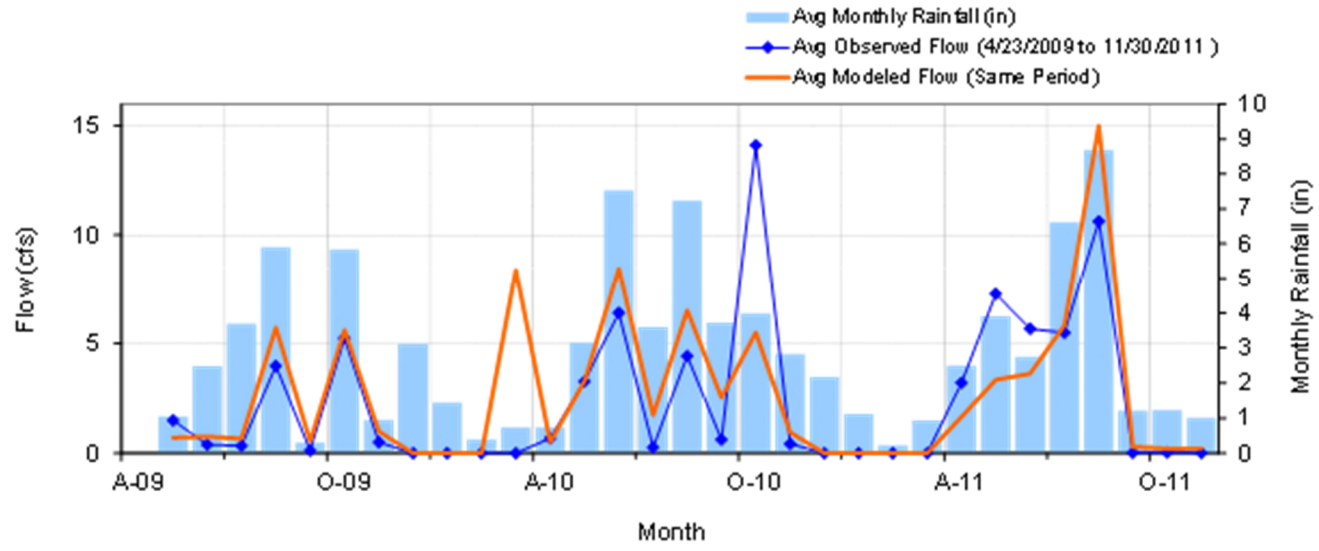

Figure C-107. Mean monthly flow at HYDSTRA 05009001 Rock Creek

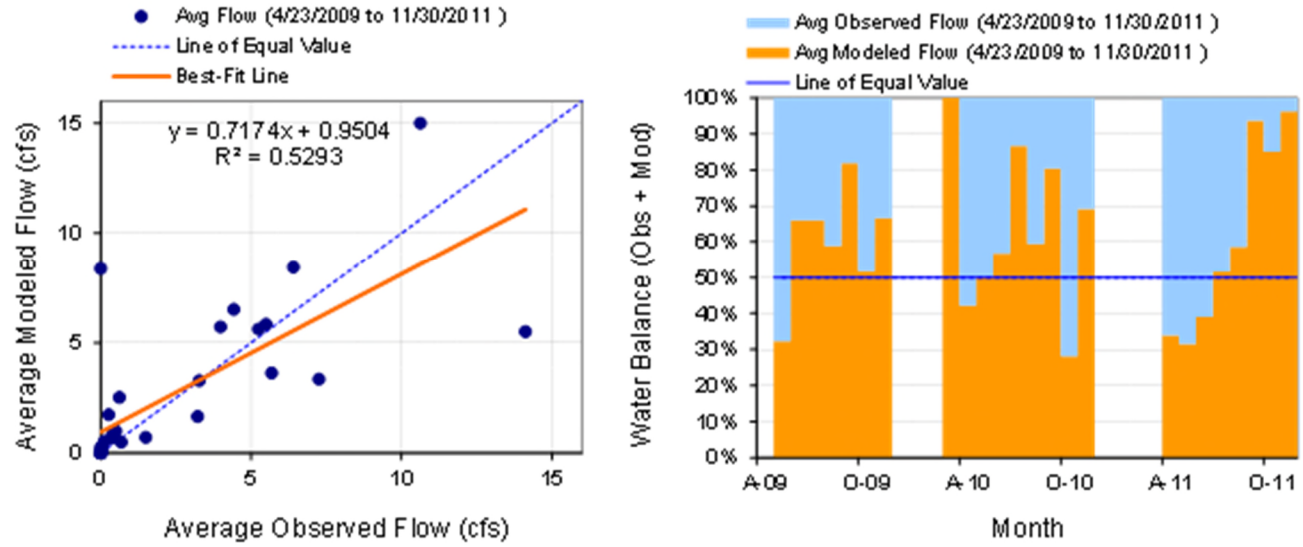

Figure C-108. Monthly flow regression and temporal variation at HYDSTRA 05009001 Rock Creek

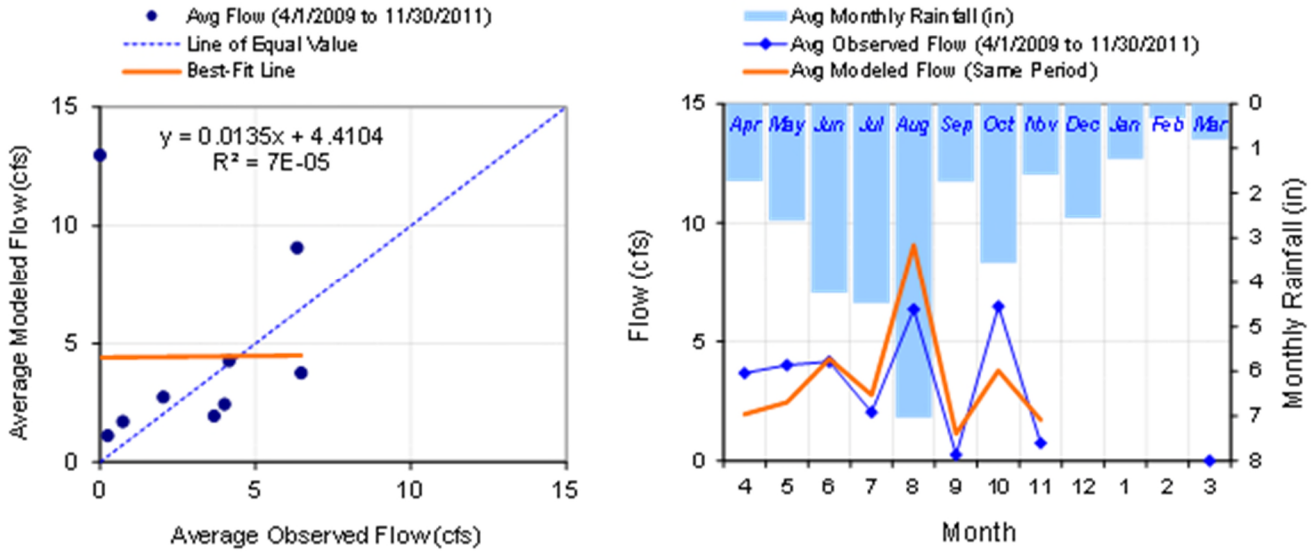

Figure C-109. Seasonal regression and temporal aggregate at HYDSTRA 05009001 Rock Creek

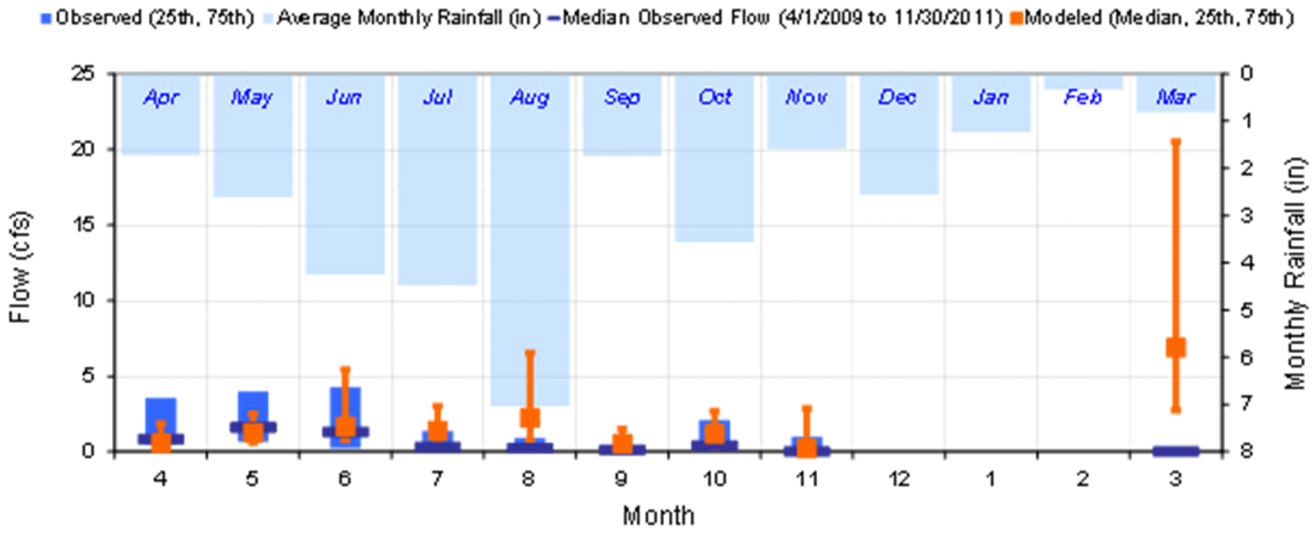

Figure C-110. Seasonal medians and ranges at HYDSTRA 05009001 Rock Creek

Table C-31. Seasonal summary at HYDSTRA 05009001 Rock Creek

MONTH	OBSERVED FLOW (CFS)				MODELED FLOW (CFS)			
	MEAN	MEDIAN	25TH	75TH	MEAN	MEDIAN	25TH	75TH
Apr	3.68	0.84	0.45	3.55	1.95	0.58	0.33	1.88
May	4.01	1.60	0.66	4.00	2.45	1.27	0.60	2.53
Jun	4.16	1.30	0.26	4.28	4.27	1.68	0.76	5.45
Jul	2.03	0.30	0.10	1.40	2.75	1.42	0.67	3.02
Aug	6.34	0.22	0.09	0.92	9.08	2.26	0.69	6.56
Sep	0.25	0.11	0.03	0.20	1.12	0.55	0.25	1.52
Oct	6.47	0.41	0.04	2.10	3.77	1.18	0.23	2.70
Nov	0.74	0.00	0.00	1.00	1.71	0.23	0.14	2.86
Dec	0.00	0.00	0.00	0.00	0.00	0.00	0.00	0.00
Jan	0.00	0.00	0.00	0.00	0.00	0.00	0.00	0.00
Feb	0.00	0.00	0.00	0.00	0.00	0.00	0.00	0.00
Mar	0.00	0.00	0.00	0.00	12.97	6.89	2.76	20.52

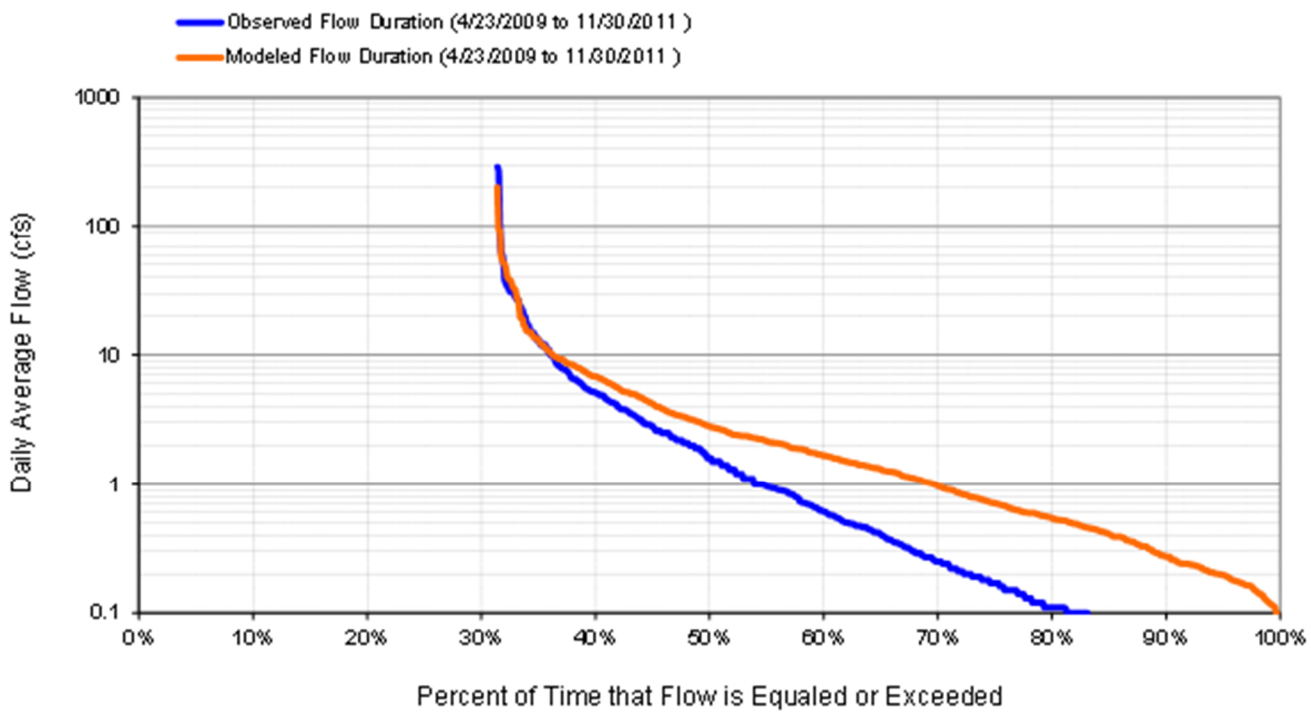

Figure C-111. Flow exceedance at HYDSTRA 05009001 Rock Creek

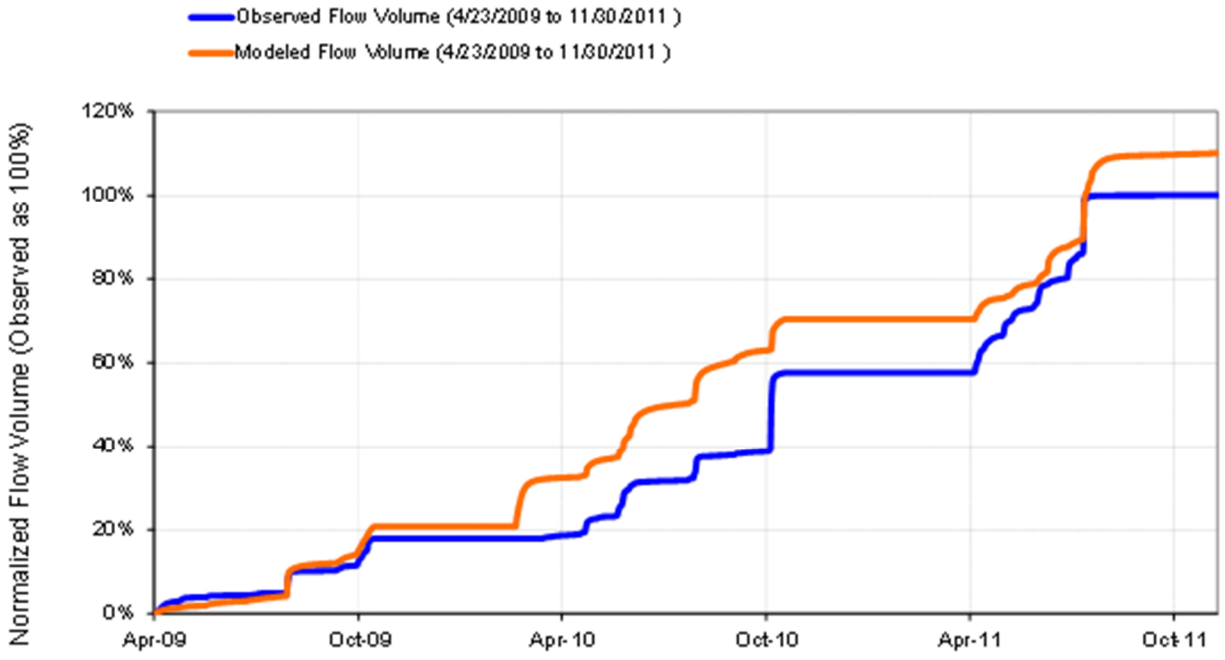

Figure C-112. Flow accumulation at HYDSTRA 05009001 Rock Creek

Table C-32. Summary statistics at HYDSTRA 05009001 Rock Creek

HSPF Simulated Flow		Observed Flow Gage	
REACH OUTFLOW FROM DSN 1120 261-Year Analysis Period: 4/1/2009 - 11/30/2011 Flow volumes are (inches/year) for upstream drainage area		H05009001 Rock Creek Manually Entered Data Drainage Area (sq-mi): 3.43	
Total Simulated In-stream Flow:	7.34	Total Observed In-stream Flow:	6.67
Total of simulated highest 10% flows:	4.49	Total of Observed highest 10% flows:	5.13
Total of Simulated lowest 50% flows:	0.49	Total of Observed Lowest 50% flows:	0.10
Simulated Summer Flow Volume (months 7-9):	3.43	Observed Summer Flow Volume (7-9):	2.29
Simulated Fall Flow Volume (months 10-12):	1.19	Observed Fall Flow Volume (10-12):	1.80
Simulated Winter Flow Volume (months 1-3):	0.74	Observed Winter Flow Volume (1-3):	ND
Simulated Spring Flow Volume (months 4-6):	1.99	Observed Spring Flow Volume (4-6):	2.58
Total Simulated Storm Volume:	3.23	Total Observed Storm Volume:	4.49
Simulated Summer Storm Volume (7-9):	1.88	Observed Summer Storm Volume (7-9):	1.85

Errors (Simulated-Observed)	*Error Statistics*	*Recommended Criteria*		
Error in total volume:	10.08	10		
Error in 50% lowest flows:	377.21	10		
Error in 10% highest flows:	-12.57	15		
Seasonal volume error - Summer:	49.69	30		
Seasonal volume error - Fall:	-33.93	30	>>	Clear
Seasonal volume error - Winter:	ND	30	>>	
Seasonal volume error - Spring:	-23.08	30		
Error in storm volumes:	-28.14	20		
Error in summer storm volumes:	1.55	50		
Nash-Sutcliffe Coefficient of Efficiency, E:	0.436	Model accuracy increases as E or E' approaches 1.0		
Baseline adjusted coefficient (Garrick), E':	0.329			
Monthly NSE	0.950			

HYDSTRA 05016001 Nemadji River near Holyoke, CSAH8

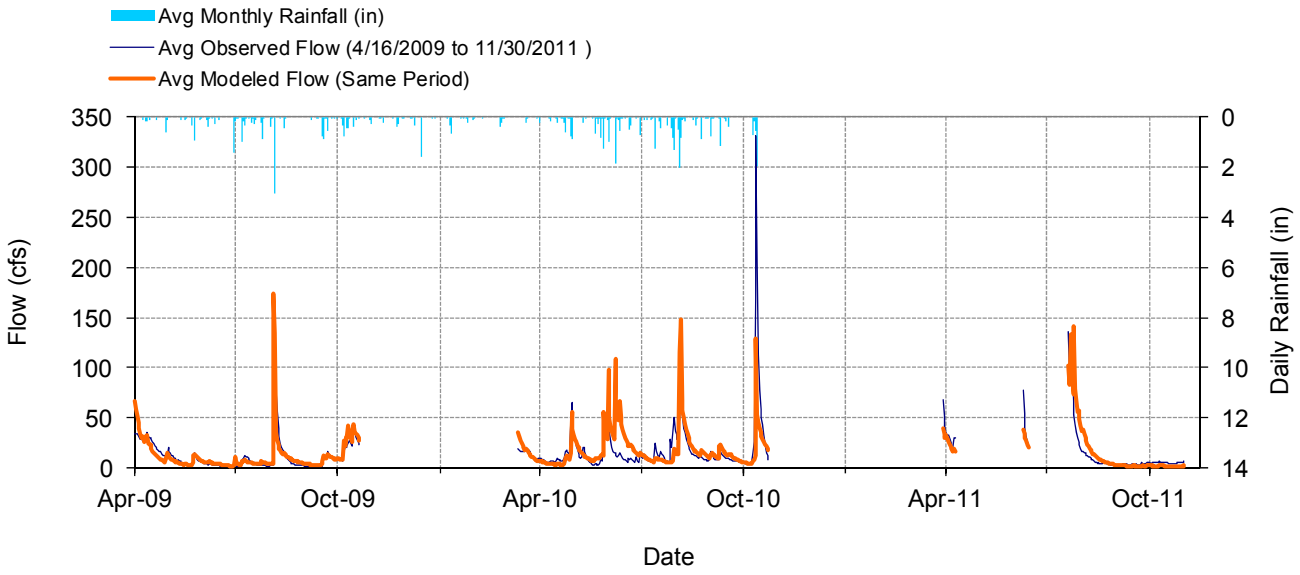

Figure C-113. Mean daily flow at HYDSTRA 05016001 Nemadji River near Holyoke, CSAH8

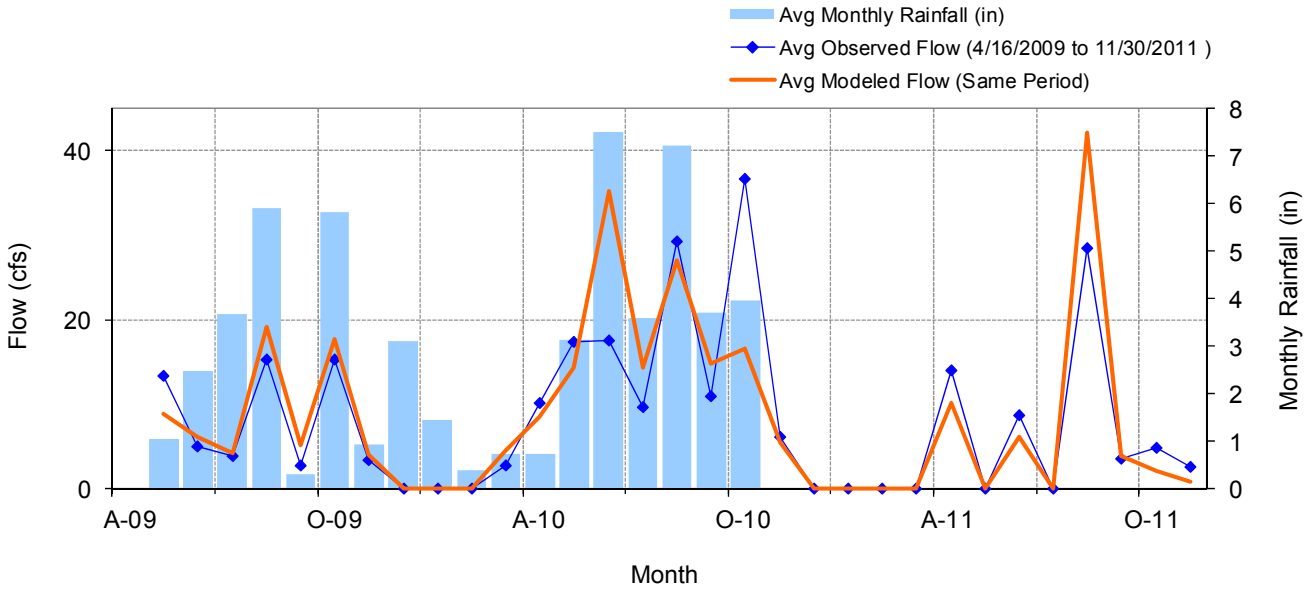

Figure C-114. Mean monthly flow at HYDSTRA 05016001 Nemadji River near Holyoke, CSAH8

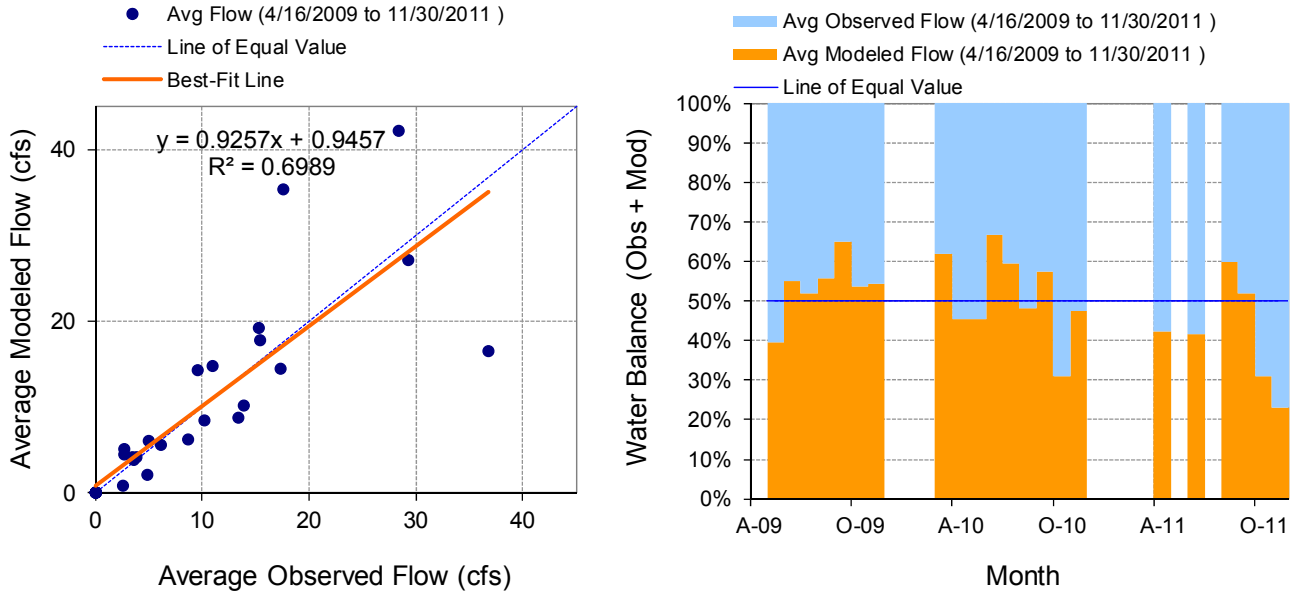

Figure C-115. Monthly flow regression and temporal variation at HYDSTRA 05016001 Nemadji River near Holyoke, CSAH8

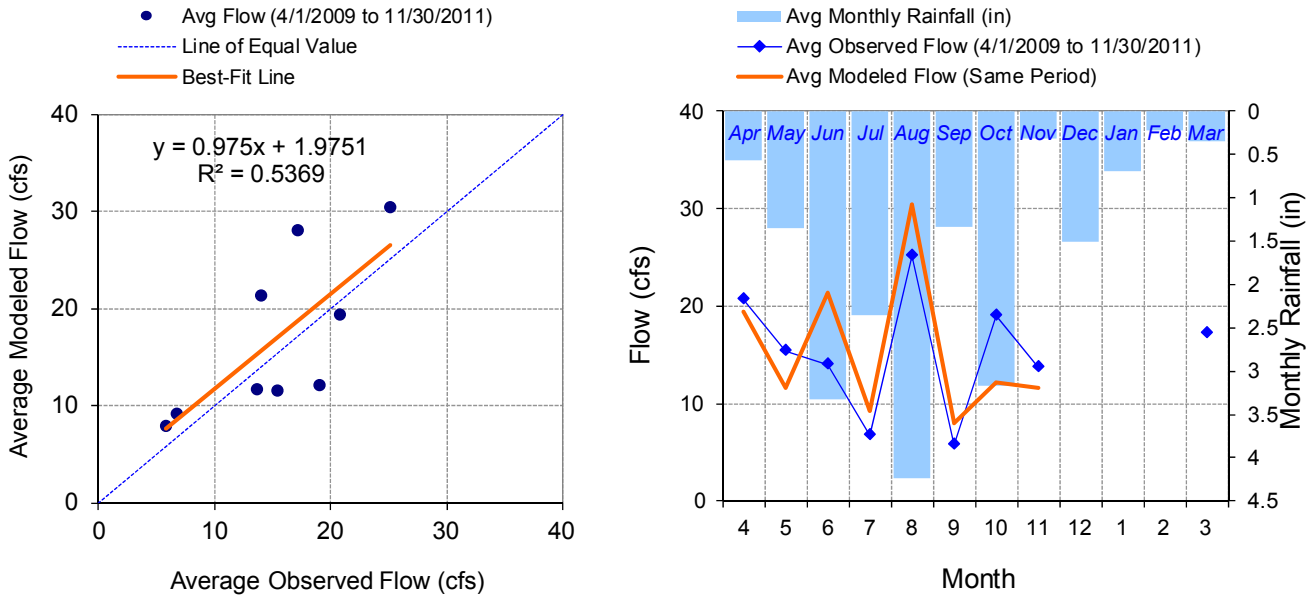

Figure C-116. Seasonal regression and temporal aggregate at HYDSTRA 05016001 Nemadji River near Holyoke, CSAH8

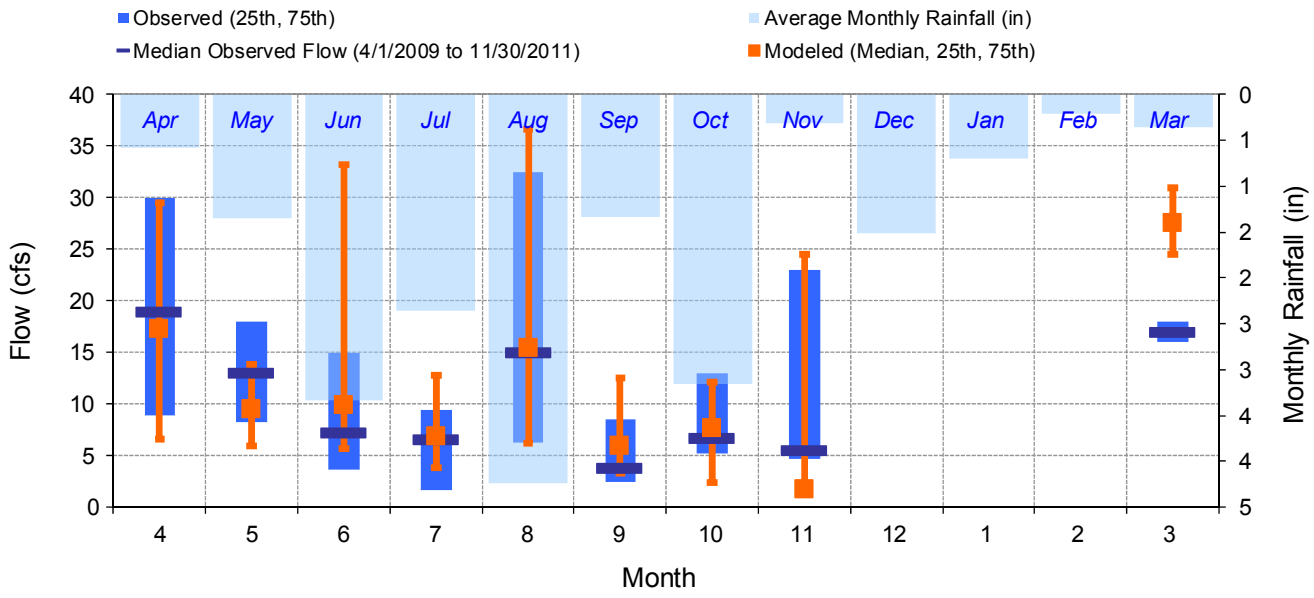

Figure C-117. Seasonal medians and ranges at HYDSTRA 05016001 Nemadji River near Holyoke, CSAH8

Table C-33. Seasonal summary at HYDSTRA 05016001 Nemadji River near Holyoke, CSAH8

MONTH	OBSERVED FLOW (CFS)				MODELED FLOW (CFS)			
	MEAN	MEDIAN	25TH	75TH	MEAN	MEDIAN	25TH	75TH
Apr	20.74	19.00	8.90	30.00	19.48	17.24	6.64	29.58
May	15.40	13.00	8.20	18.00	11.63	9.51	5.98	13.82
Jun	13.98	7.20	3.70	15.00	21.32	9.93	5.62	33.21
Jul	6.78	6.65	1.73	9.40	9.25	6.85	3.84	12.76
Aug	25.14	15.00	6.33	32.50	30.48	15.41	6.19	36.61
Sep	5.76	3.80	2.50	8.55	7.95	5.93	3.27	12.50
Oct	19.00	6.70	5.20	13.00	12.15	7.61	2.39	12.14
Nov	13.69	5.50	4.75	23.00	11.67	1.71	1.38	24.49
Dec	0.00	0.00	0.00	0.00	0.00	0.00	0.00	0.00
Jan	0.00	0.00	0.00	0.00	0.00	0.00	0.00	0.00
Feb	0.00	0.00	0.00	0.00	0.00	0.00	0.00	0.00
Mar	17.20	17.00	16.00	18.00	28.08	27.53	24.54	30.97

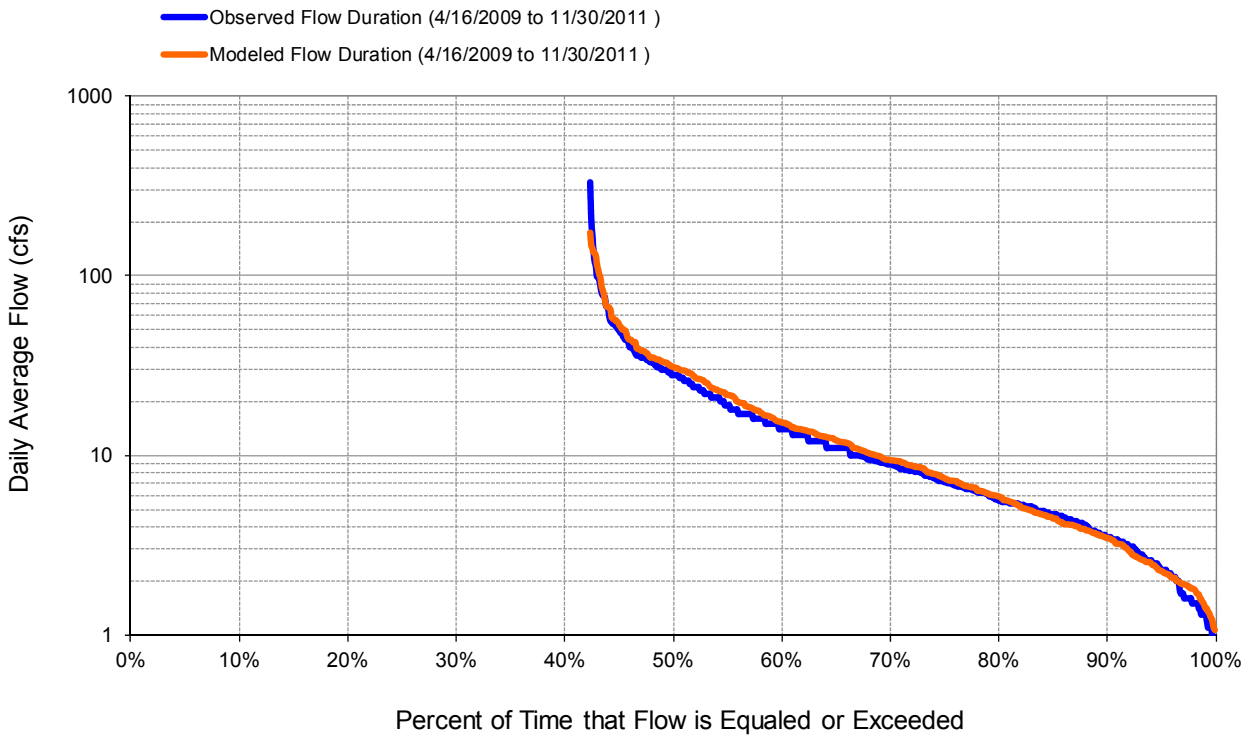

Figure C-118. Flow exceedance at HYDSTRA 05016001 Nemadji River near Holyoke, CSAH8

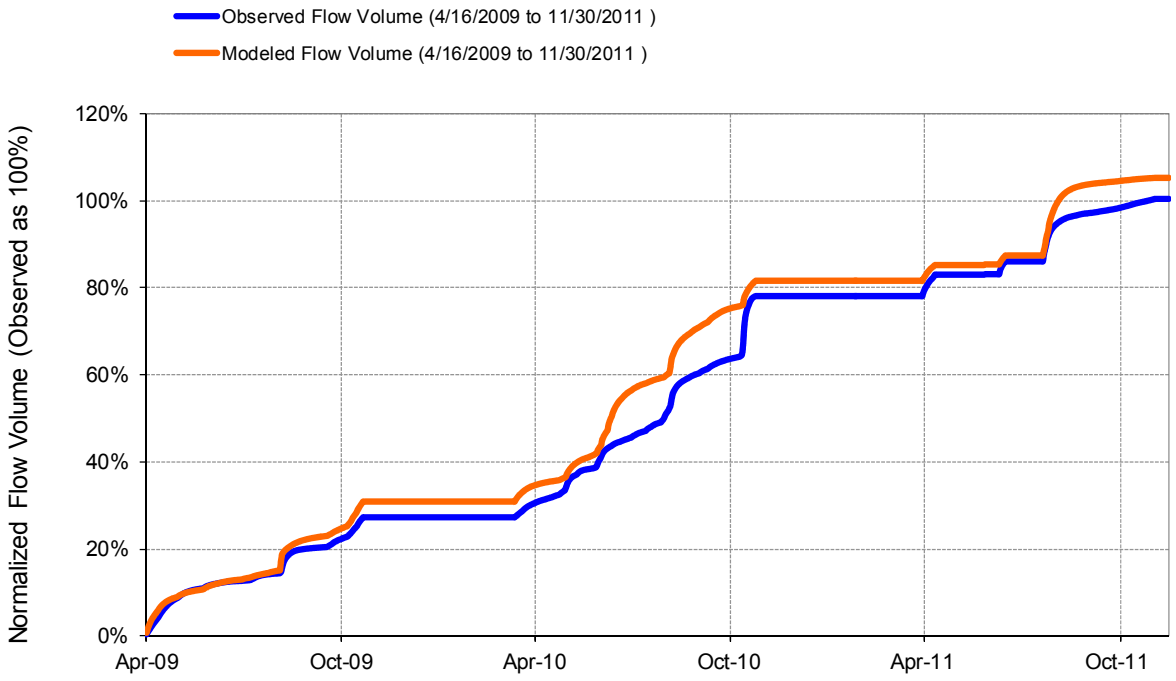

Figure C-119. Flow accumulation at HYDSTRA 05016001 Nemadji River near Holyoke, CSAH8

Table C-34. Summary statistics at HYDSTRA 05016001 Nemadji River near Holyoke, CSAH8

HSPF Simulated Flow		Observed Flow Gage		
REACH OUTFLOW FROM DSN 113 2.63-Year Analysis Period: 4/1/2009 - 11/30/2011 Flow volumes are (inches/year) for upstream drainage area		H05016001 Nemadji River near Holyoke, CSAH8 Manually Entered Data Drainage Area (sq-mi): 3.43		
Total Simulated In-stream Flow:	**5.99**	Total Observed In-stream Flow:		**5.73**
Total of simulated highest 10% flows:	**2.43**	Total of Observed highest 10% flows:		**2.44**
Total of Simulated lowest 50% flows:	**0.87**	Total of Observed Lowest 50% flows:		**0.86**
Simulated Summer Flow Volume (months 7-9):	**2.72**	Observed Summer Flow Volume (7-9):		**2.16**
Simulated Fall Flow Volume (months 10-12):	**0.97**	Observed Fall Flow Volume (10-12):		**1.44**
Simulated Winter Flow Volume (months 1-3):	**0.09**	Observed Winter Flow Volume (1-3):		**0.06**
Simulated Spring Flow Volume (months 4-6):	**2.20**	Observed Spring Flow Volume (4-6):		**2.07**
Total Simulated Storm Volume:	**1.18**	Total Observed Storm Volume:		**1.21**
Simulated Summer Storm Volume (7-9):	**0.54**	Observed Summer Storm Volume (7-9):		**0.38**
Errors (Simulated-Observed)	*Error Statistics*	*Recommended Criteria*	*Run (n-1)*	*Run (n-2)*
Error in total volume:	4.48	10	6.17	
Error in 50% lowest flows:	1.33	10	1.80	
Error in 10% highest flows:	-0.32	15	1.34	
Seasonal volume error - Summer:	25.98	30	25.82	
Seasonal volume error - Fall:	**-32.38** >>	**30**	**-32.49**	Clear
Seasonal volume error - Winter:	**63.25** >>	**30**	**77.32**	
Seasonal volume error - Spring:	6.07	30	10.60	
Error in storm volumes:	-2.63	20	-1.62	
Error in summer storm volumes:	42.95	50	42.56	
Nash-Sutcliffe Coefficient of Efficiency, E:	0.382	Model accuracy increases	0.377	
Baseline adjusted coefficient (Garrick), E':	0.380	as E or E' approaches 1.0	0.380	
Monthly NSE	0.510			

HYDSTRA 05018001 South Fork Nemadji at MN23

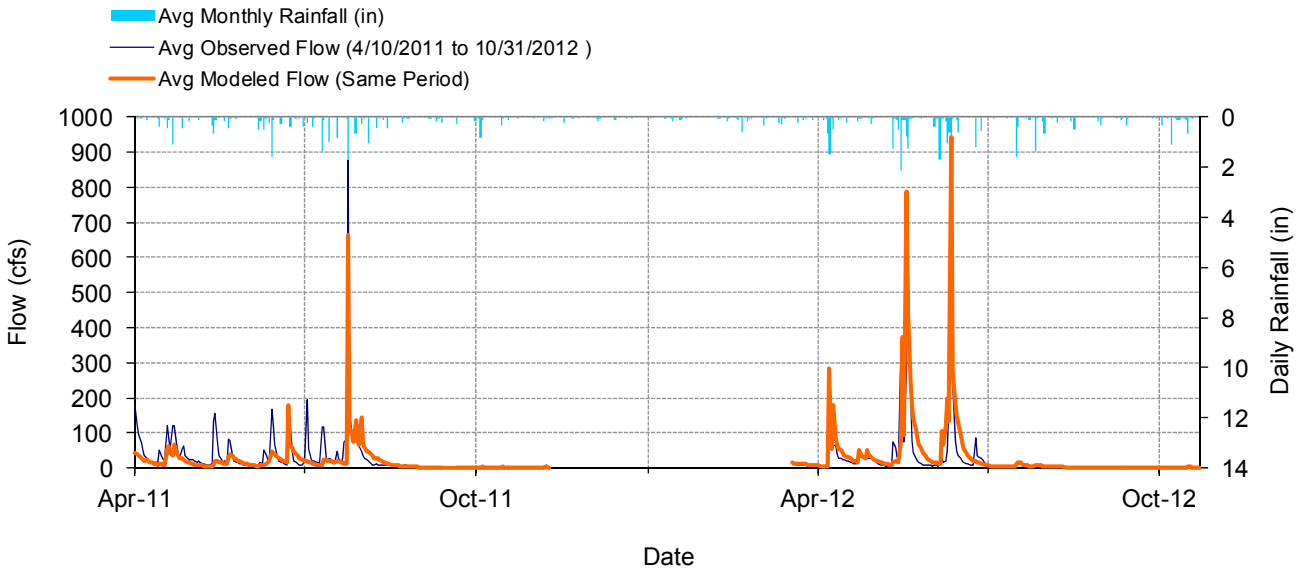

Figure C-120. Mean daily flow at HYDSTRA 05018001 South Fork Nemadji at MN23

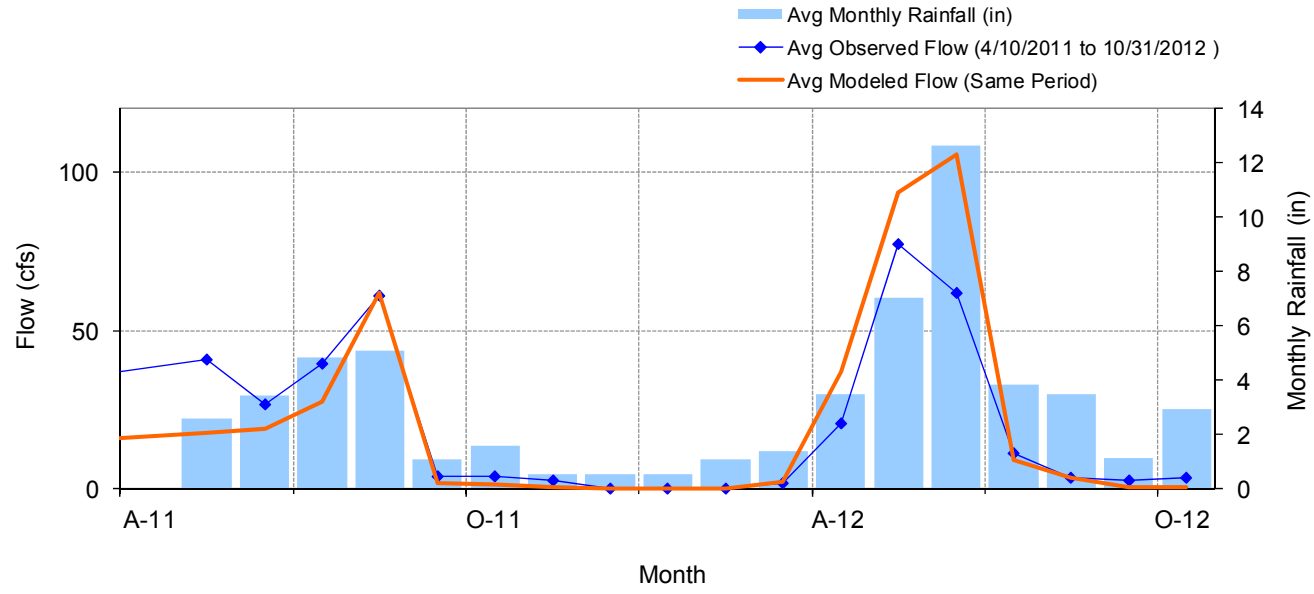

Figure C-121. Mean monthly flow at HYDSTRA 05018001 South Fork Nemadji at MN23

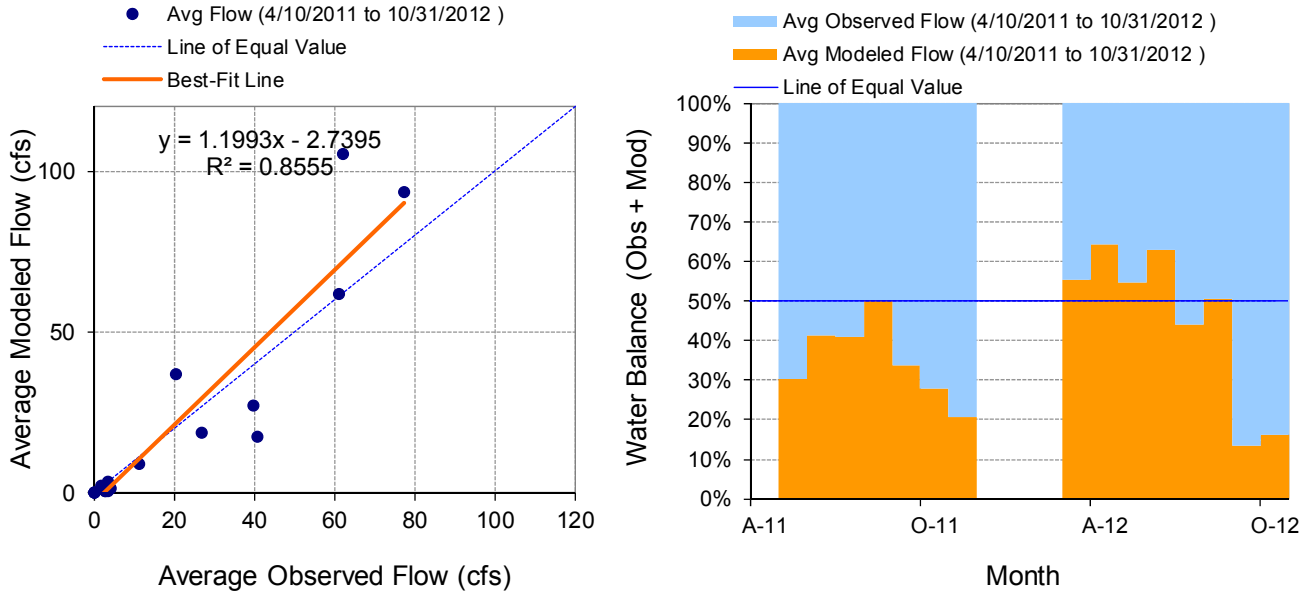

Figure C-122. Monthly flow regression and temporal variation at HYDSTRA 05018001 South Fork Nemadji at MN23

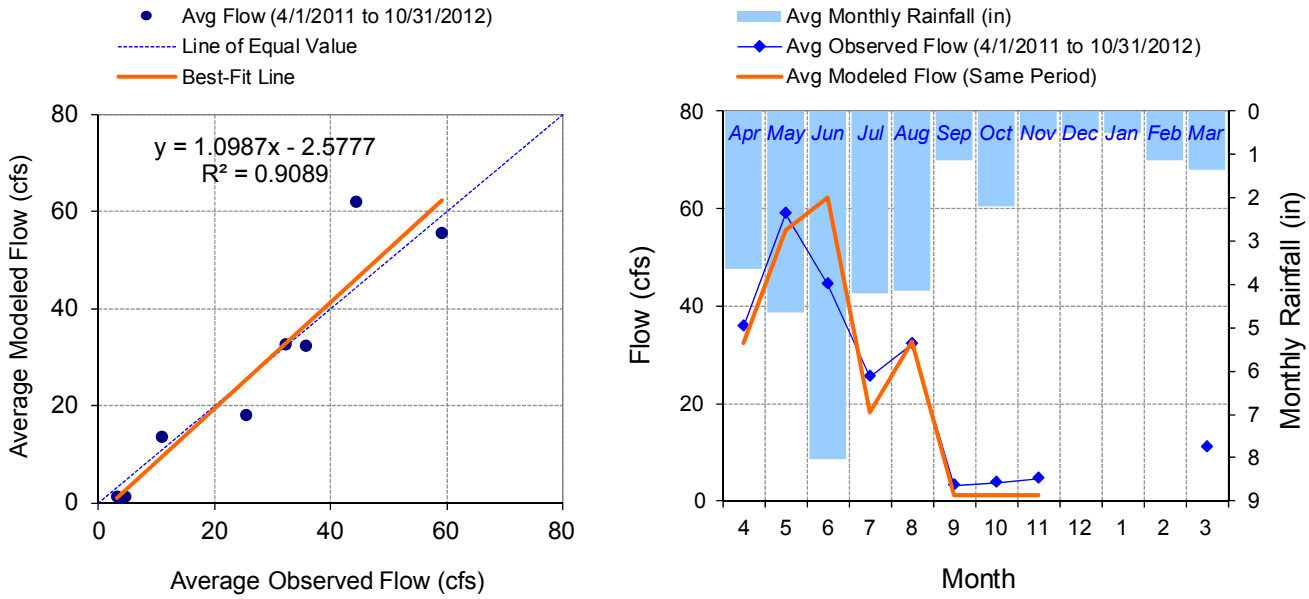

Figure C-123. Seasonal regression and temporal aggregate at HYDSTRA 05018001 South Fork Nemadji at MN23

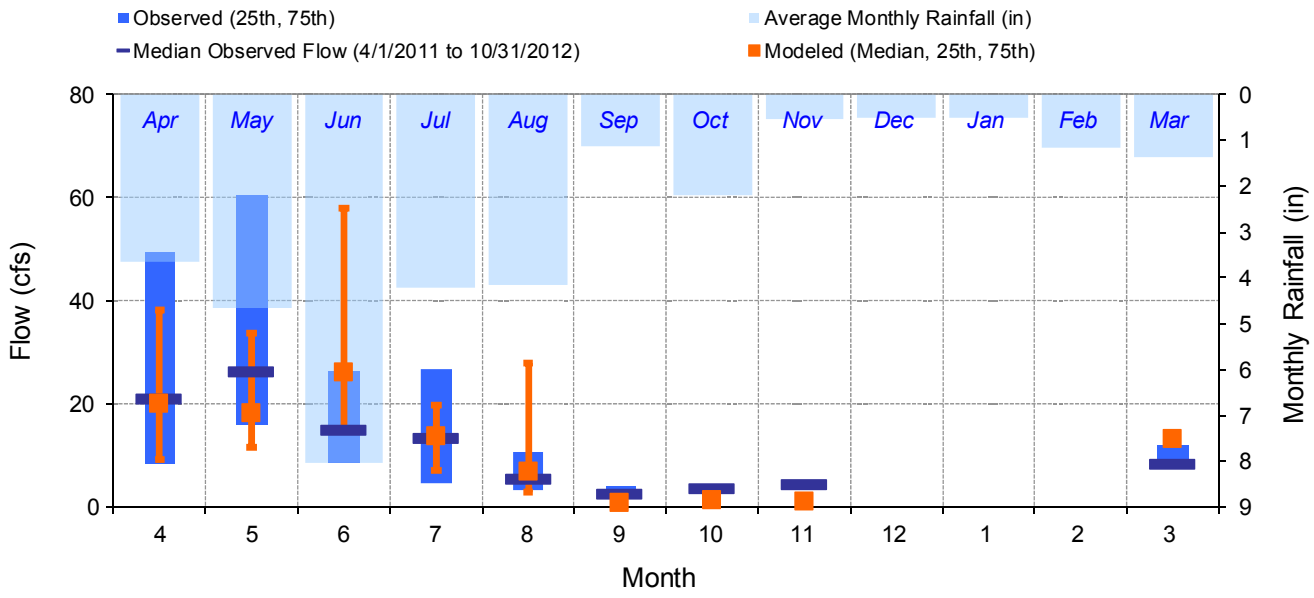

Figure C-124. Seasonal medians and ranges at HYDSTRA 05018001 South Fork Nemadji at MN23

Table C-35. Seasonal summary at HYDSTRA 05018001 South Fork Nemadji at MN23

MONTH	OBSERVED FLOW (CFS)				MODELED FLOW (CFS)			
	MEAN	MEDIAN	25TH	75TH	MEAN	MEDIAN	25TH	75TH
Apr	35.72	21.00	8.45	49.50	32.34	20.04	9.17	38.31
May	59.05	26.50	16.00	60.50	55.50	18.32	11.65	33.80
Jun	44.39	15.00	8.48	26.25	62.13	26.10	14.67	57.91
Jul	25.48	13.50	4.73	26.75	18.15	13.80	7.08	19.74
Aug	32.22	5.60	3.30	10.75	32.69	6.88	3.04	28.10
Sep	3.27	2.80	2.60	4.10	1.18	0.71	0.39	1.54
Oct	3.80	3.85	3.33	4.30	1.14	1.31	0.24	1.61
Nov	4.62	4.40	4.40	4.48	1.20	1.04	0.89	1.26
Dec	0.00	0.00	0.00	0.00	0.00	0.00	0.00	0.00
Jan	0.00	0.00	0.00	0.00	0.00	0.00	0.00	0.00
Feb	0.00	0.00	0.00	0.00	0.00	0.00	0.00	0.00
Mar	10.92	8.60	8.50	12.00	13.63	13.10	13.09	13.88

Figure C-125. Flow exceedance at HYDSTRA 05018001 South Fork Nemadji at MN23

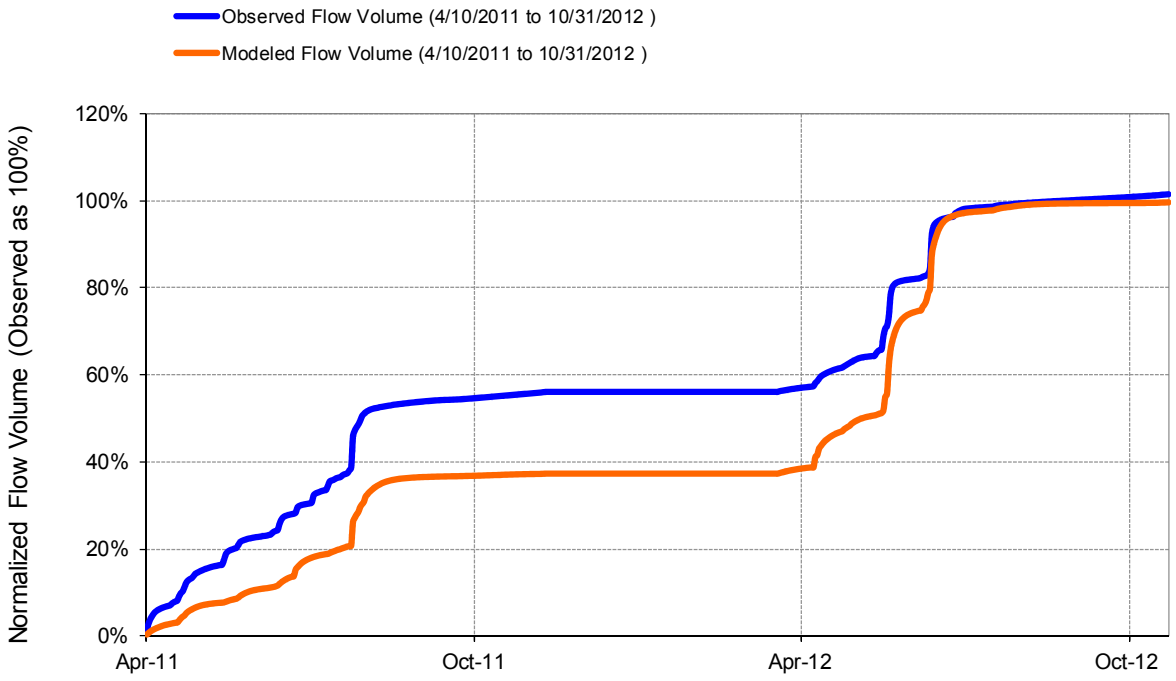

Figure C-126. Flow accumulation at HYDSTRA 05018001 South Fork Nemadji at MN23

Table C-36. Summary statistics at HYDSTRA 05018001 South Fork Nemadji at MN23

HSPF Simulated Flow		Observed Flow Gage	
REACH OUTFLOW FROM DSN 104 1.56-Year Analysis Period: 4/1/2011 - 10/31/2012 Flow volumes are (inches/year) for upstream drainage area		H05018001 South Fork Nemadji at MN23 Manually Entered Data Drainage Area (sq-mi): 3.43	
Total Simulated In-stream Flow:	**14.51**	Total Observed In-stream Flow:	**14.62**
Total of simulated highest 10% flows:	**9.27**	Total of Observed highest 10% flows:	**9.08**
Total of Simulated lowest 50% flows:	**0.68**	Total of Observed Lowest 50% flows:	**1.07**
Simulated Summer Flow Volume (months 7-9):	**3.83**	Observed Summer Flow Volume (7-9):	**4.49**
Simulated Fall Flow Volume (months 10-12):	**0.11**	Observed Fall Flow Volume (10-12):	**0.38**
Simulated Winter Flow Volume (months 1-3):	**0.08**	Observed Winter Flow Volume (1-3):	**0.06**
Simulated Spring Flow Volume (months 4-6):	**10.49**	Observed Spring Flow Volume (4-6):	**9.69**
Total Simulated Storm Volume:	**5.90**	Total Observed Storm Volume:	**7.12**
Simulated Summer Storm Volume (7-9):	**1.47**	Observed Summer Storm Volume (7-9):	**2.27**
Errors (Simulated-Observed)	*Error Statistics*	*Recommended Criteria*	
Error in total volume:	-0.75	10	
Error in 50% lowest flows:	-36.39	10	
Error in 10% highest flows:	2.17	15	
Seasonal volume error - Summer:	-14.60	30	
Seasonal volume error - Fall:	-71.07	30	
Seasonal volume error - Winter:	24.78	30	
Seasonal volume error - Spring:	8.25	30	
Error in storm volumes:	-17.06	20	
Error in summer storm volumes:	-35.16	50	
Nash-Sutcliffe Coefficient of Efficiency, E:	0.671	Model accuracy increases	
Baseline adjusted coefficient (Garrick), E':	0.446	as E or E' approaches 1.0	
Monthly NSE	0.709		

>>
>>
Clear

Appendix D. Detailed Hydrology Validation Results

USGS 04024000 St Louis River near Scanlon

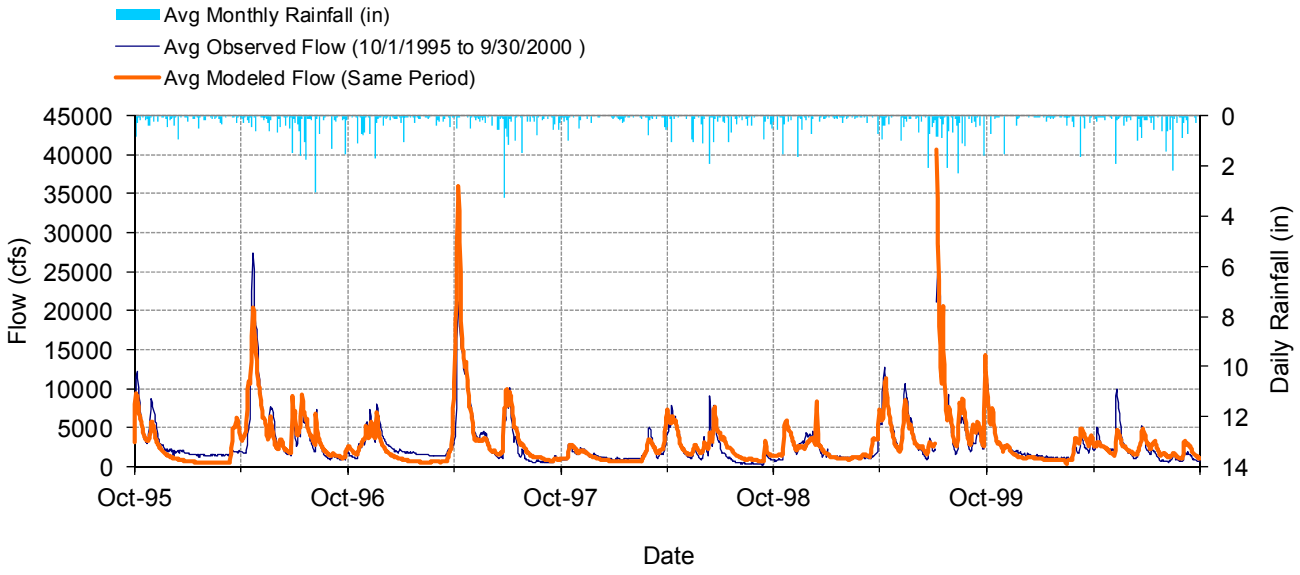

Figure D-1. Mean daily flow at USGS 04024000 St Louis River near Scanlon

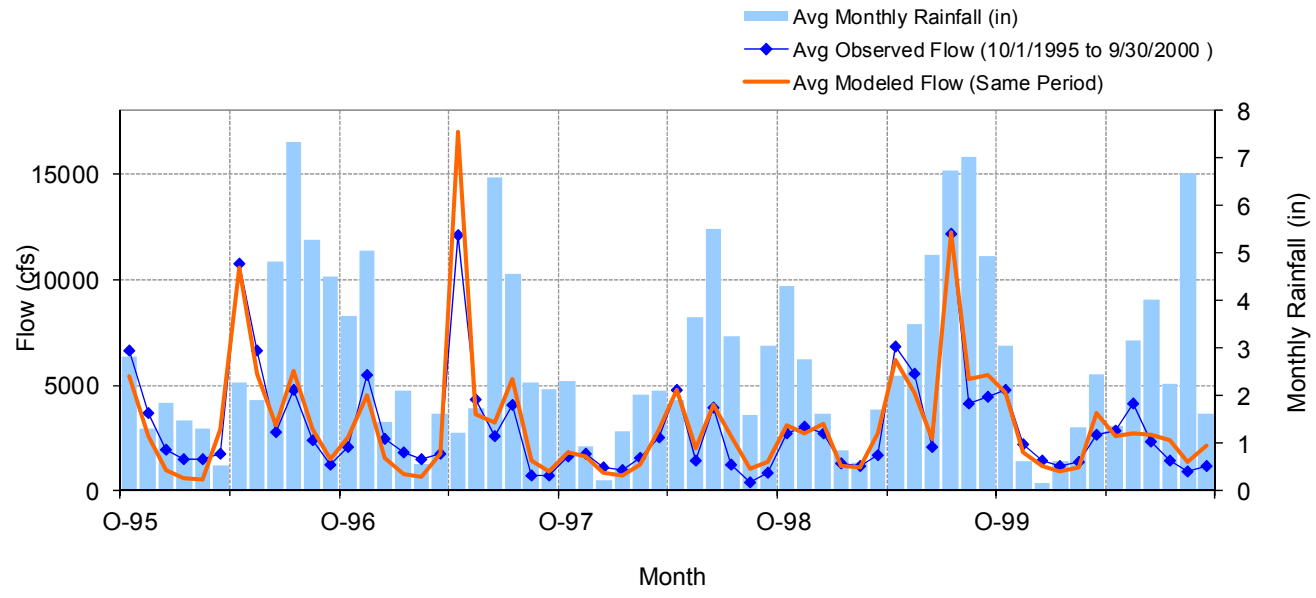

Figure D-2. Mean monthly flow at USGS 04024000 St Louis River near Scanlon

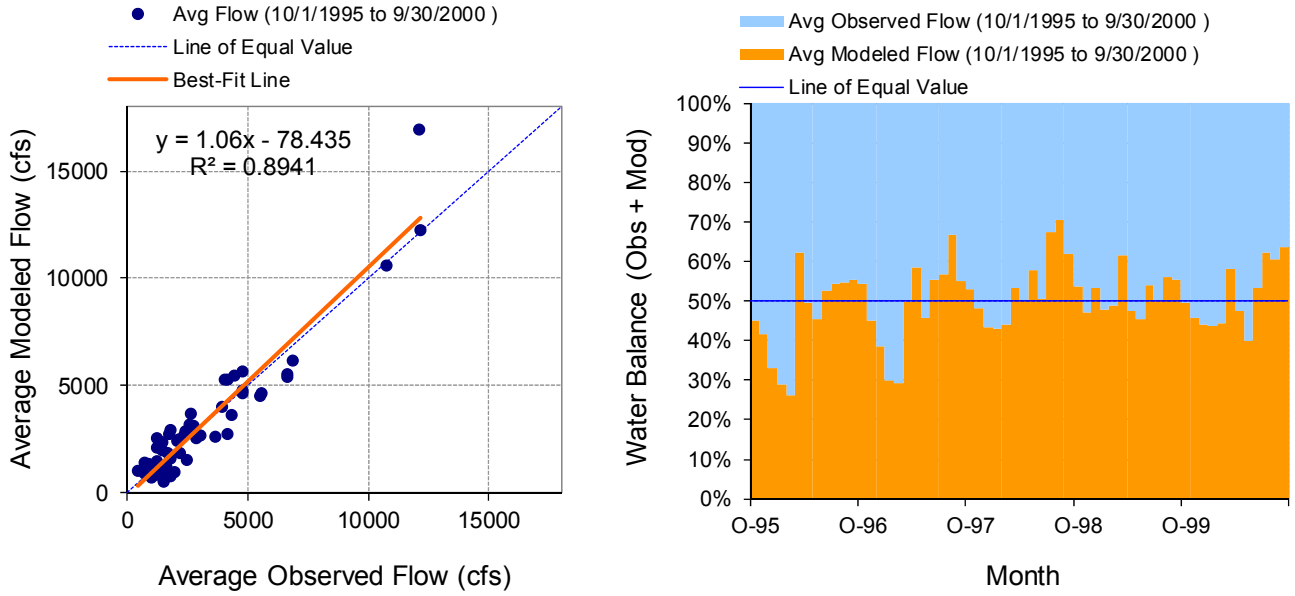

Figure D-3. Monthly flow regression and temporal variation at USGS 04024000 St Louis River near Scanlon

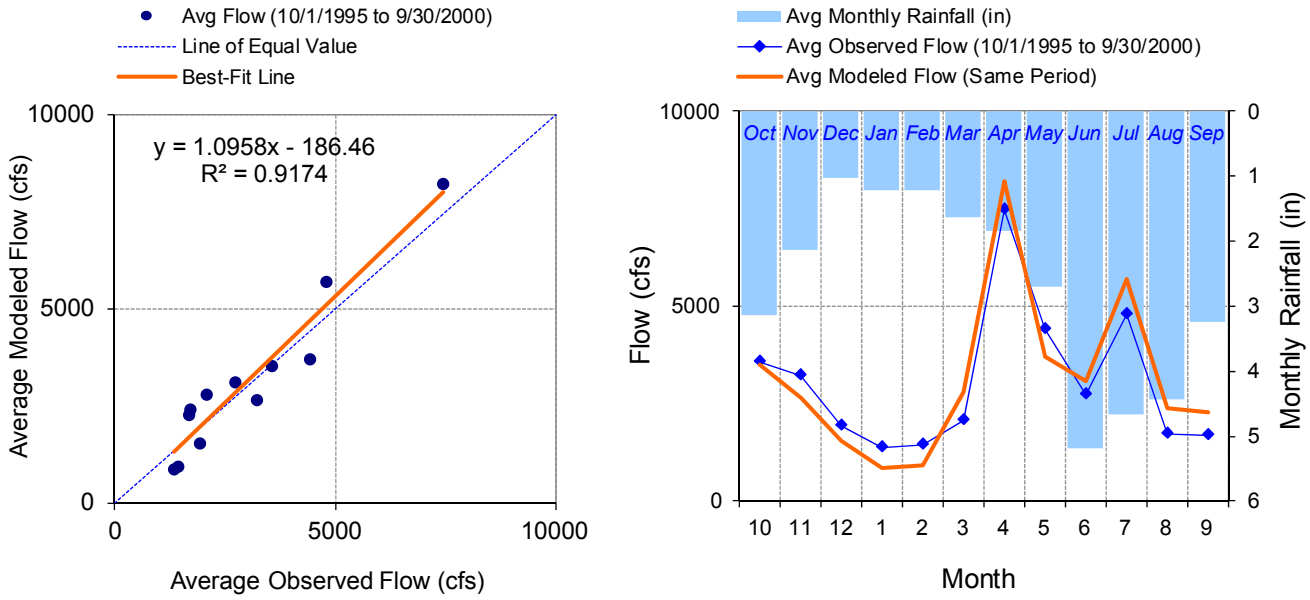

Figure D-4. Seasonal regression and temporal aggregate at USGS 04024000 St Louis River near Scanlon

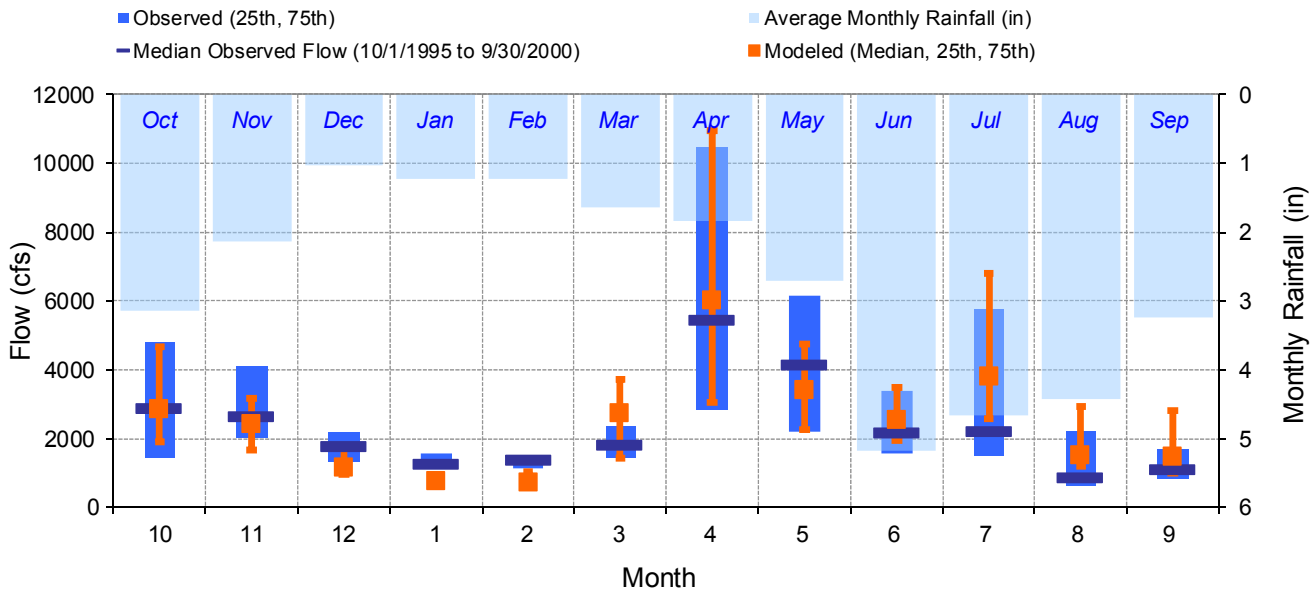

Figure D-5. Seasonal medians and ranges at USGS 04024000 St Louis River near Scanlon

Table D-1. Seasonal summary at USGS 04024000 St Louis River near Scanlon

MONTH	OBSERVED FLOW (CFS)				MODELED FLOW (CFS)			
	MEAN	MEDIAN	25TH	75TH	MEAN	MEDIAN	25TH	75TH
Oct	3559.26	2910.00	1445.00	4820.00	3505.57	2833.52	1907.11	4658.26
Nov	3230.27	2640.00	2012.50	4100.00	2659.80	2418.59	1647.69	3165.58
Dec	1941.50	1800.00	1335.00	2200.00	1530.03	1145.47	943.73	1702.70
Jan	1358.17	1280.00	1125.00	1580.00	847.44	767.00	690.88	959.63
Feb	1425.61	1370.00	1142.50	1507.50	923.44	734.56	591.59	1026.93
Mar	2082.65	1830.00	1445.00	2375.00	2804.07	2713.95	1420.77	3703.05
Apr	7458.20	5455.00	2817.50	10450.00	8213.08	6017.39	3035.69	10950.97
May	4417.90	4140.00	2200.00	6170.00	3712.55	3389.29	2239.82	4730.60
Jun	2744.89	2170.00	1552.50	3367.50	3095.29	2518.23	1951.60	3489.47
Jul	4792.41	2230.00	1480.00	5770.00	5700.66	3793.26	2576.31	6801.17
Aug	1712.92	867.00	618.50	2185.00	2392.84	1494.81	1193.03	2937.99
Sep	1684.27	1095.00	800.50	1700.00	2273.47	1466.85	1007.34	2802.45

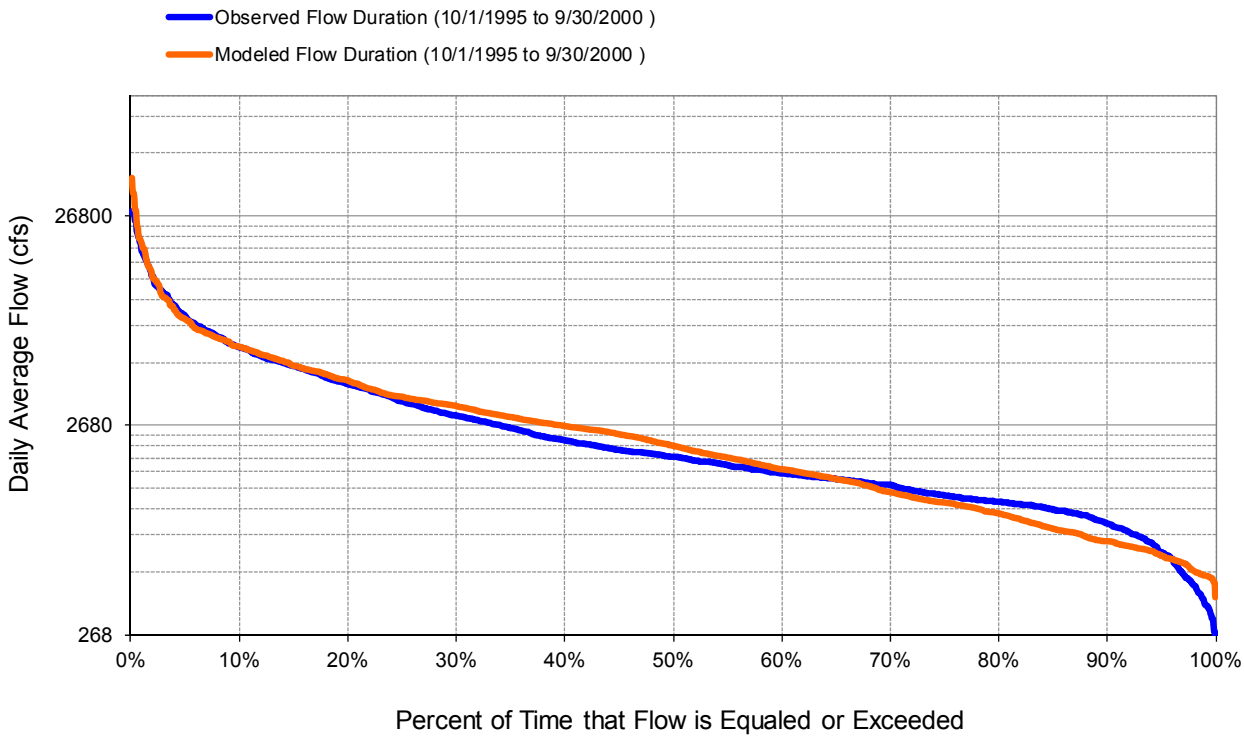

Figure D-6. Flow exceedance at USGS 04024000 St Louis River near Scanlon

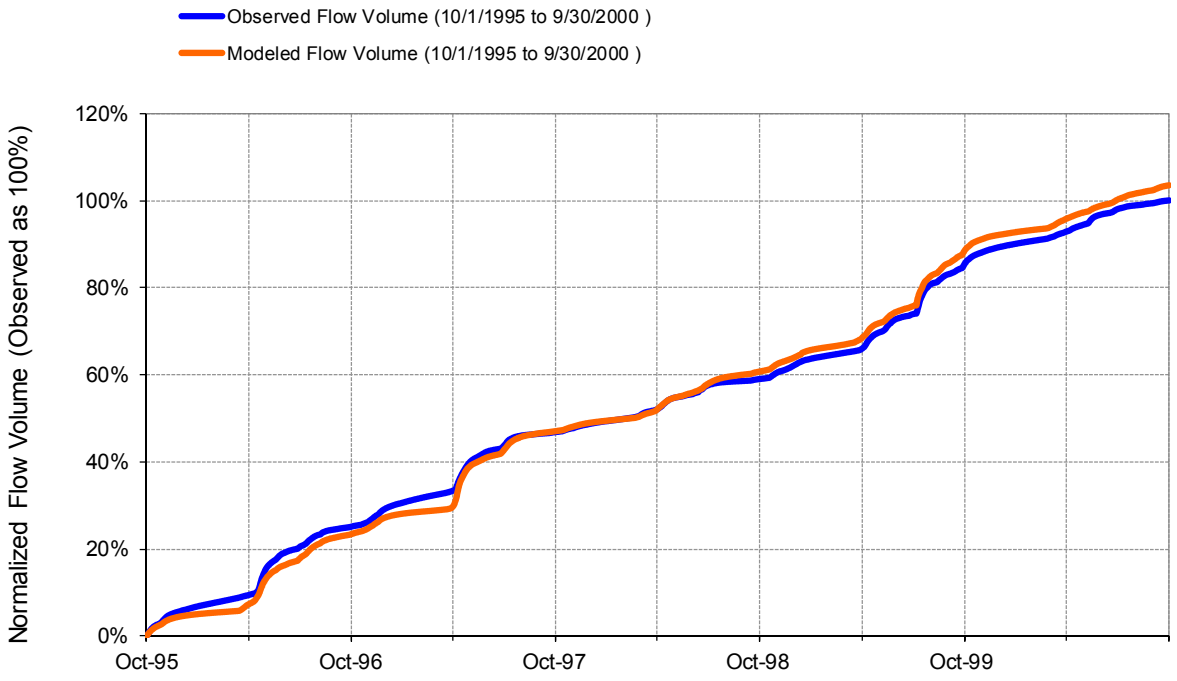

Figure D-7. Flow accumulation at USGS 04024000 St Louis River near Scanlon

Table D-2. Summary statistics at USGS 04024000 St Louis River near Scanlon

HSPF Simulated Flow		Observed Flow Gage		
REACH OUTFLOW FROM DSN 208 5-Year Analysis Period: 10/1/1995 - 9/30/2000 Flow volumes are (inches/year) for upstream drainage area		St. Louis River near Scanlon, MN Manually Entered Data Drainage Area (sq-mi): 3430		
Total Simulated In-stream Flow:	**12.43**	Total Observed In-stream Flow:		**12.01**
Total of simulated highest 10% flows:	**4.37**	Total of Observed highest 10% flows:		**4.28**
Total of Simulated lowest 50% flows:	**2.38**	Total of Observed Lowest 50% flows:		**2.45**
Simulated Summer Flow Volume (months 7-9):	**3.43**	Observed Summer Flow Volume (7-9):		**2.71**
Simulated Fall Flow Volume (months 10-12):	**2.56**	Observed Fall Flow Volume (10-12):		**2.90**
Simulated Winter Flow Volume (months 1-3):	**1.51**	Observed Winter Flow Volume (1-3):		**1.59**
Simulated Spring Flow Volume (months 4-6):	**4.92**	Observed Spring Flow Volume (4-6):		**4.80**
Total Simulated Storm Volume:	**3.60**	Total Observed Storm Volume:		**3.86**
Simulated Summer Storm Volume (7-9):	**1.12**	Observed Summer Storm Volume (7-9):		**1.06**
Errors (Simulated-Observed)	*Error Statistics*	*Recommended Criteria*		
Error in total volume:	3.48	10		
Error in 50% lowest flows:	-2.57	10		
Error in 10% highest flows:	2.18	15		
Seasonal volume error - Summer:	26.59	30		
Seasonal volume error - Fall:	-11.79	30		
Seasonal volume error - Winter:	-5.25	30		
Seasonal volume error - Spring:	2.55	30		
Error in storm volumes:	-6.80	20		
Error in summer storm volumes:	5.57	50		
Nash-Sutcliffe Coefficient of Efficiency, E:	0.766	Model accuracy increases		
Baseline adjusted coefficient (Garrick), E':	0.573	as E or E' approaches 1.0		
Monthly NSE	0.864		0.814	

USGS 04024430 Nemadji River near South Superior, WI

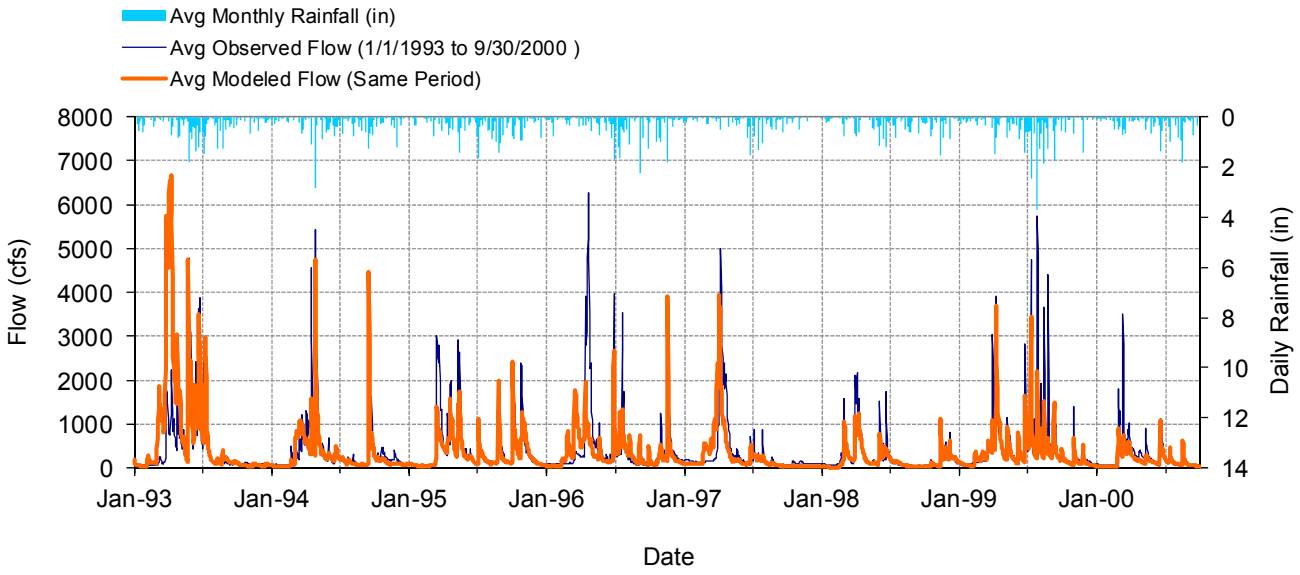

Figure D-8. Mean daily flow at USGS 04024430 Nemadji River near South Superior, WI

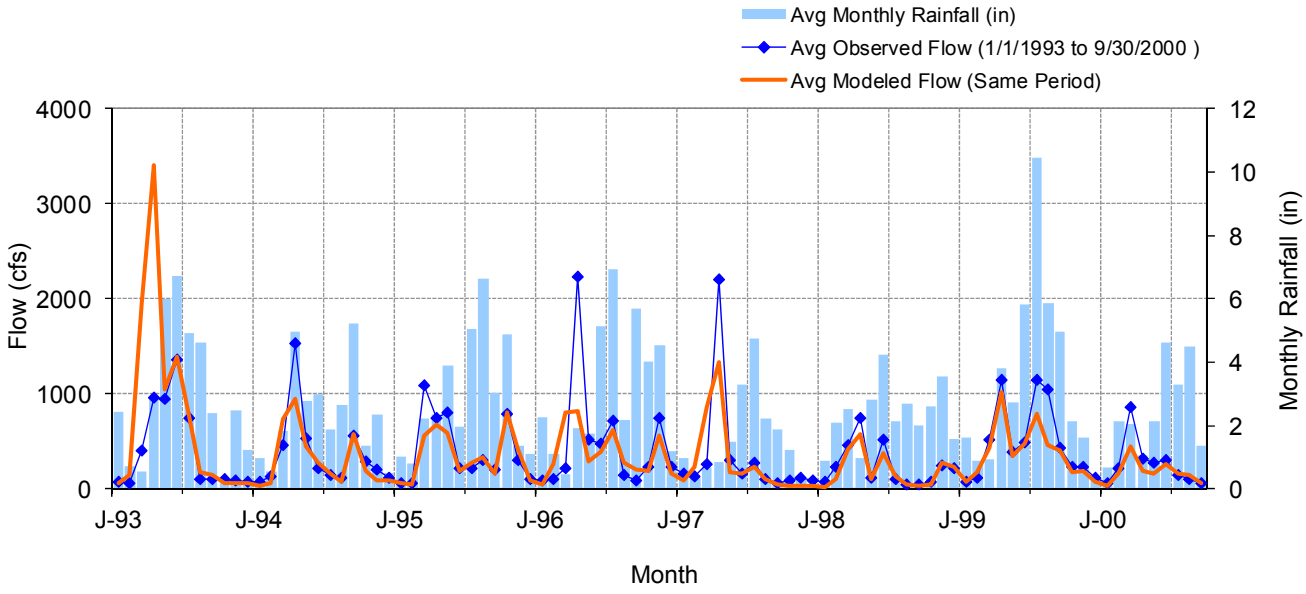

Figure D-9. Mean monthly flow at USGS 04024430 Nemadji River near South Superior, WI

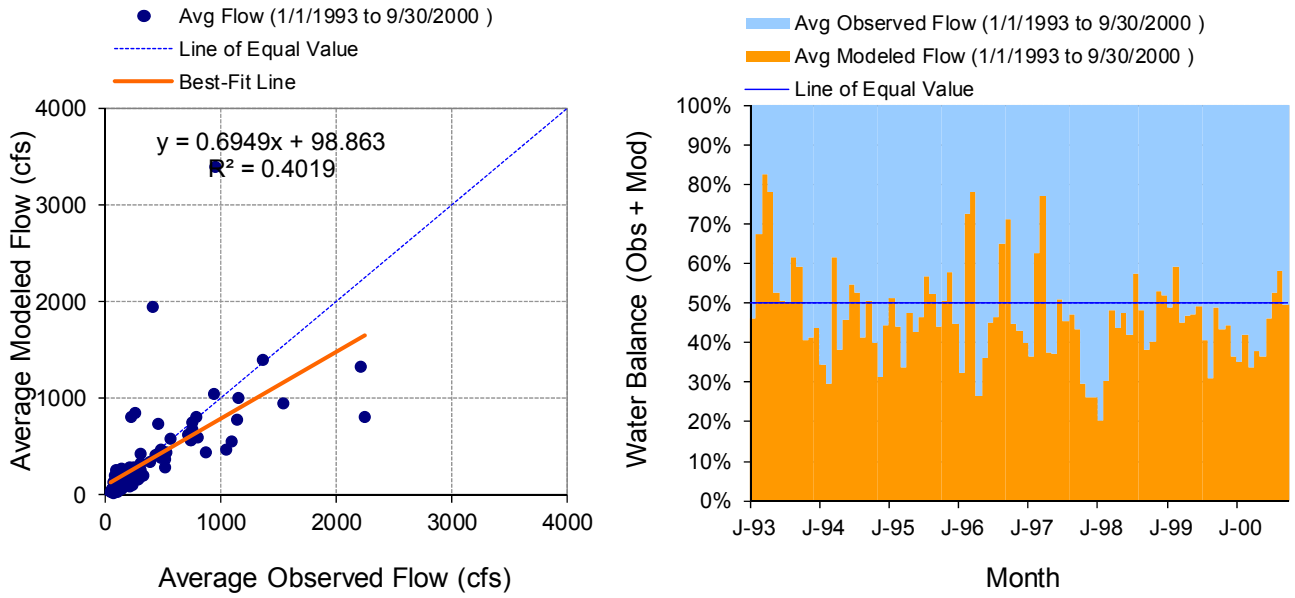

Figure D-10. Monthly flow regression and temporal variation at USGS 04024430 Nemadji River near South Superior, WI

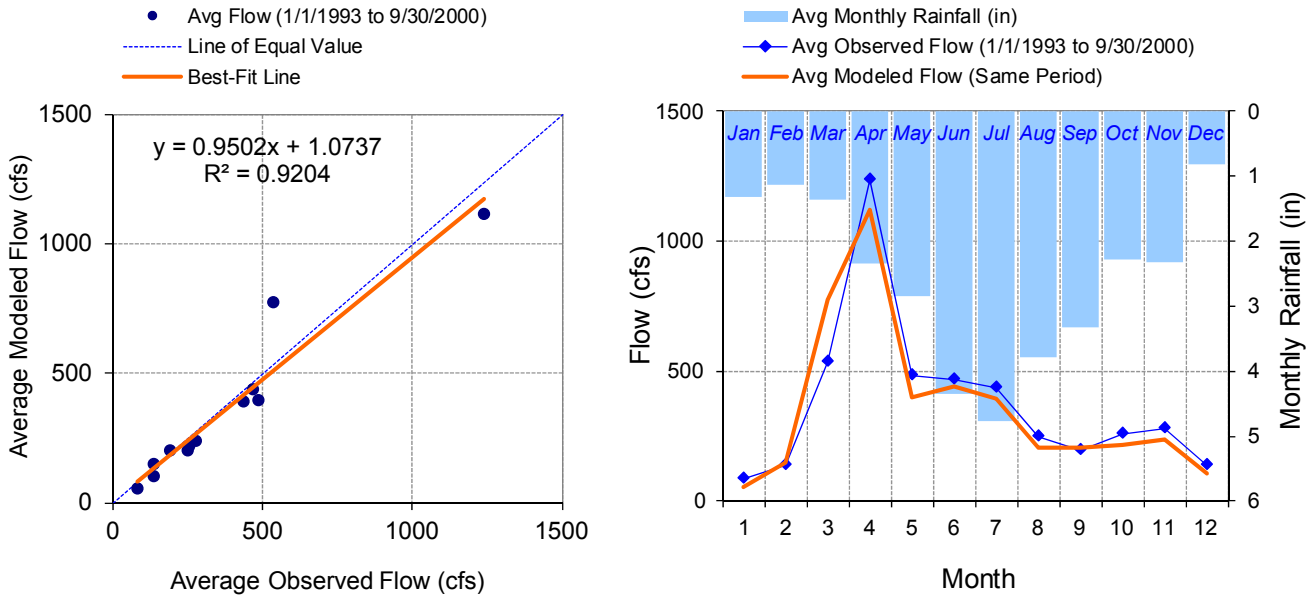

Figure D-11. Seasonal regression and temporal aggregate at USGS 04024430 Nemadji River near South Superior, WI

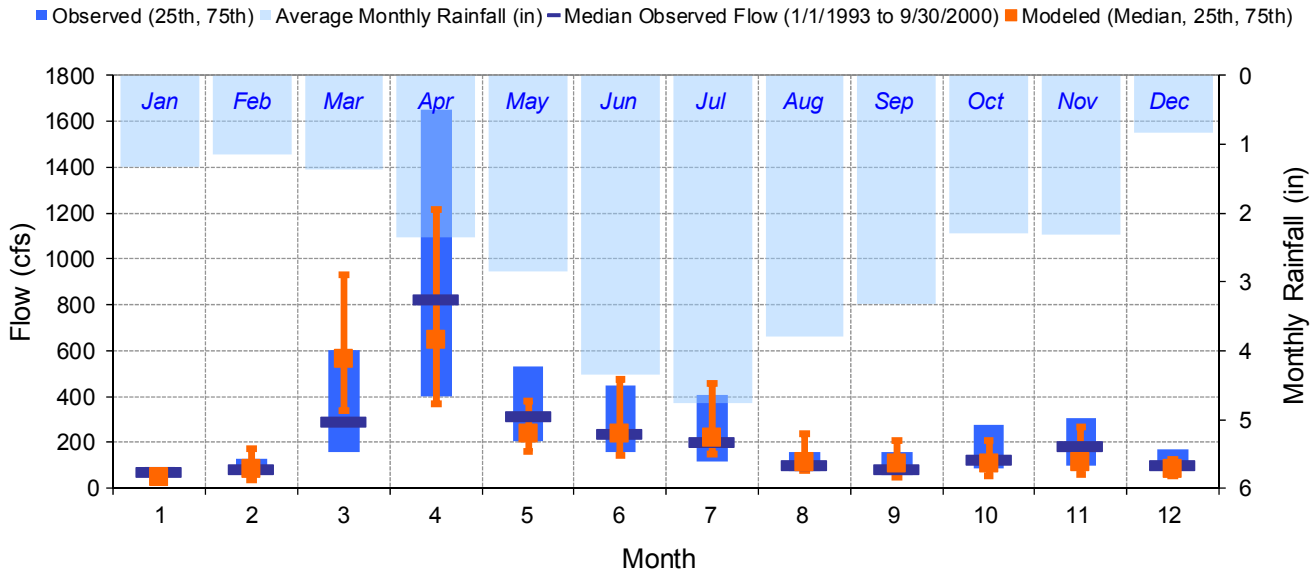

Figure D-12. Seasonal medians and ranges at USGS 04024430 Nemadji River near South Superior, WI

Table D-3. Seasonal summary at USGS 04024430 Nemadji River near South Superior, WI

MONTH	OBSERVED FLOW (CFS)				MODELED FLOW (CFS)			
	MEAN	MEDIAN	25TH	75TH	MEAN	MEDIAN	25TH	75TH
Jan	84.24	74.00	66.00	90.00	53.47	45.72	34.76	71.46
Feb	135.42	86.00	64.00	130.00	147.70	84.98	36.39	172.07
Mar	534.95	290.00	160.00	600.00	773.43	565.99	341.54	932.09
Apr	1237.21	827.00	401.50	1650.00	1118.39	646.46	369.87	1217.91
May	484.05	313.50	206.50	534.25	396.40	235.33	158.39	382.23
Jun	467.11	241.00	156.50	448.50	438.91	238.57	143.93	472.66
Jul	437.06	202.50	117.75	405.00	391.58	220.39	146.44	455.28
Aug	249.64	103.50	74.75	160.00	203.78	116.23	79.67	237.83
Sep	193.56	81.50	60.00	155.25	204.35	109.37	50.24	207.97
Oct	256.78	127.00	85.00	277.00	216.32	105.67	52.04	208.61
Nov	279.34	183.50	98.50	304.75	236.99	112.66	59.28	264.94
Dec	137.51	100.00	88.00	170.00	104.70	86.60	52.66	127.13

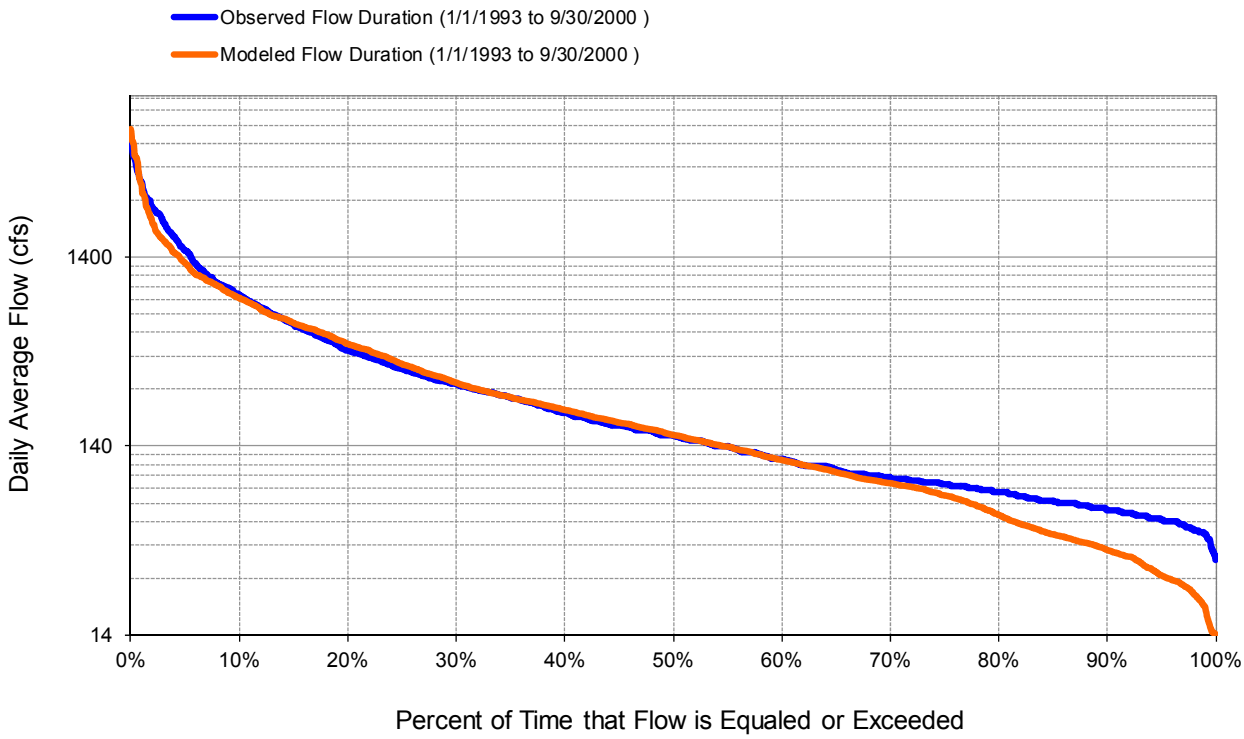

Figure D-13. Flow exceedance at USGS 04024430 Nemadji River near South Superior, WI

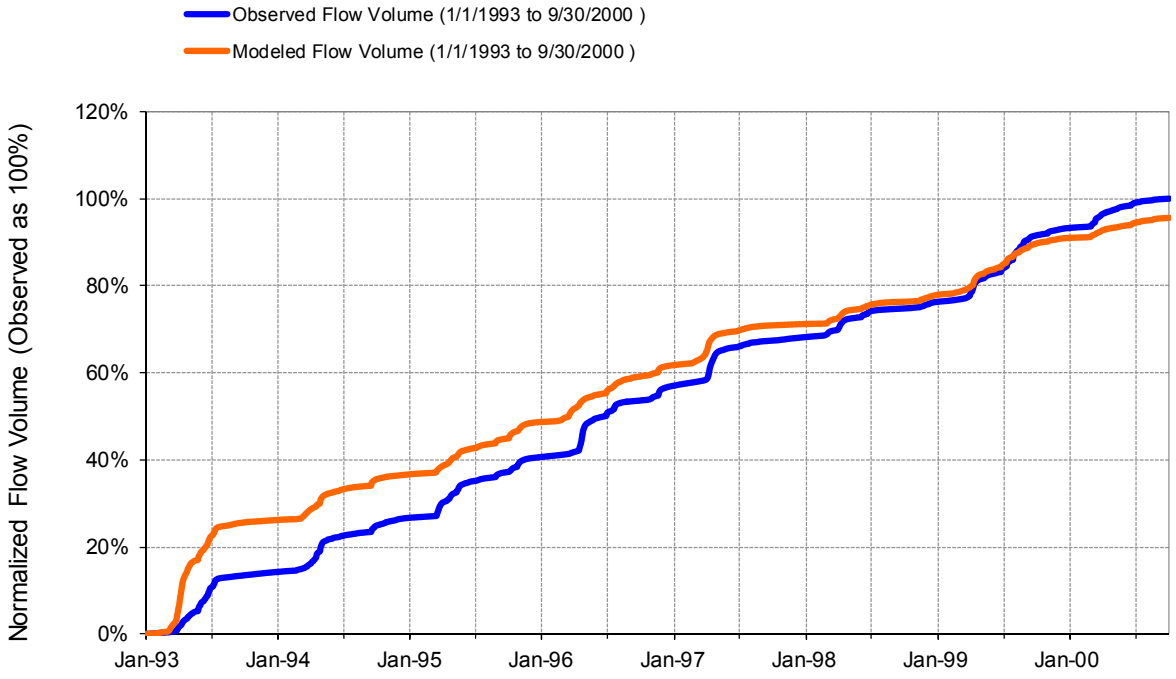

Figure D-14. Flow accumulation at USGS 04024430 Nemadji River near South Superior, WI

Table D-4. Summary statistics at USGS 04024430 Nemadji River near South Superior, WI

HSPF Simulated Flow		Observed Flow Gage	
REACH OUTFLOW FROM DSN 103 7.75-Year Analysis Period: 1/1/1993 - 9/30/2000 Flow volumes are (inches/year) for upstream drainage area		Nemadji River near South Superior, WI Manually Entered Data Drainage Area (sq-mi): 420	
Total Simulated In-stream Flow:	**11.73**	Total Observed In-stream Flow:	**12.28**
Total of simulated highest 10% flows:	**5.69**	Total of Observed highest 10% flows:	**6.16**
Total of Simulated lowest 50% flows:	**1.28**	Total of Observed Lowest 50% flows:	**1.49**
Simulated Summer Flow Volume (months 7-9):	**2.25**	Observed Summer Flow Volume (7-9):	**2.48**
Simulated Fall Flow Volume (months 10-12):	**1.36**	Observed Fall Flow Volume (10-12):	**1.65**
Simulated Winter Flow Volume (months 1-3):	**2.73**	Observed Winter Flow Volume (1-3):	**2.10**
Simulated Spring Flow Volume (months 4-6):	**5.39**	Observed Spring Flow Volume (4-6):	**6.05**
Total Simulated Storm Volume:	**3.98**	Total Observed Storm Volume:	**4.98**
Simulated Summer Storm Volume (7-9):	**0.86**	Observed Summer Storm Volume (7-9):	**1.19**

Errors (Simulated-Observed)	*Error Statistics*	*Recommended Criteria*
Error in total volume:	-4.43	10
Error in 50% lowest flows:	-13.92	10
Error in 10% highest flows:	-7.73	15
Seasonal volume error - Summer:	-9.26	30
Seasonal volume error - Fall:	-17.19	30
Seasonal volume error - Winter:	29.48	30
Seasonal volume error - Spring:	-10.78	30
Error in storm volumes:	-20.12	20
Error in summer storm volumes:	-27.90	50
Nash-Sutcliffe Coefficient of Efficiency, E:	0.234	Model accuracy increases
Baseline adjusted coefficient (Garrick), E':	0.418	as E or E' approaches 1.0
Monthly NSE	0.707	

>> Clear

Appendix E. Detailed Sediment Calibration Results

This section provides graphical comparisons for the sediment calibration summarized in the main text, Section 5. The following plots are provided for each station: (1) a power plot of observed and simulated load versus flow; (2-4) time series plots of simulated and observed concentrations over the period 1994-2012, broken into three separate segments, and (5) a plot of discrepancies (simulated minus observed) versus simulated flow.

St Louis River at CSAH-7, 0.5 mi S of Forbes

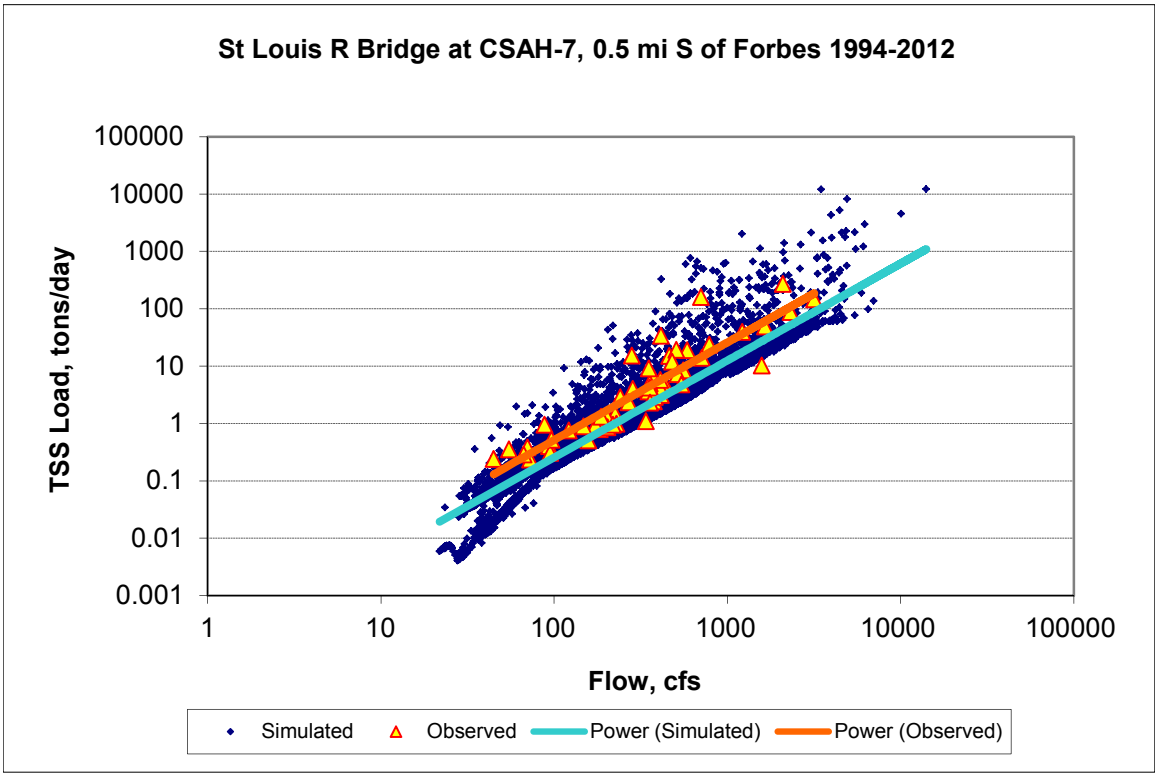

Figure E-1. TSS Load Power Plot, St Louis R Bridge at CSAH-7, 0.5 mi S of Forbes

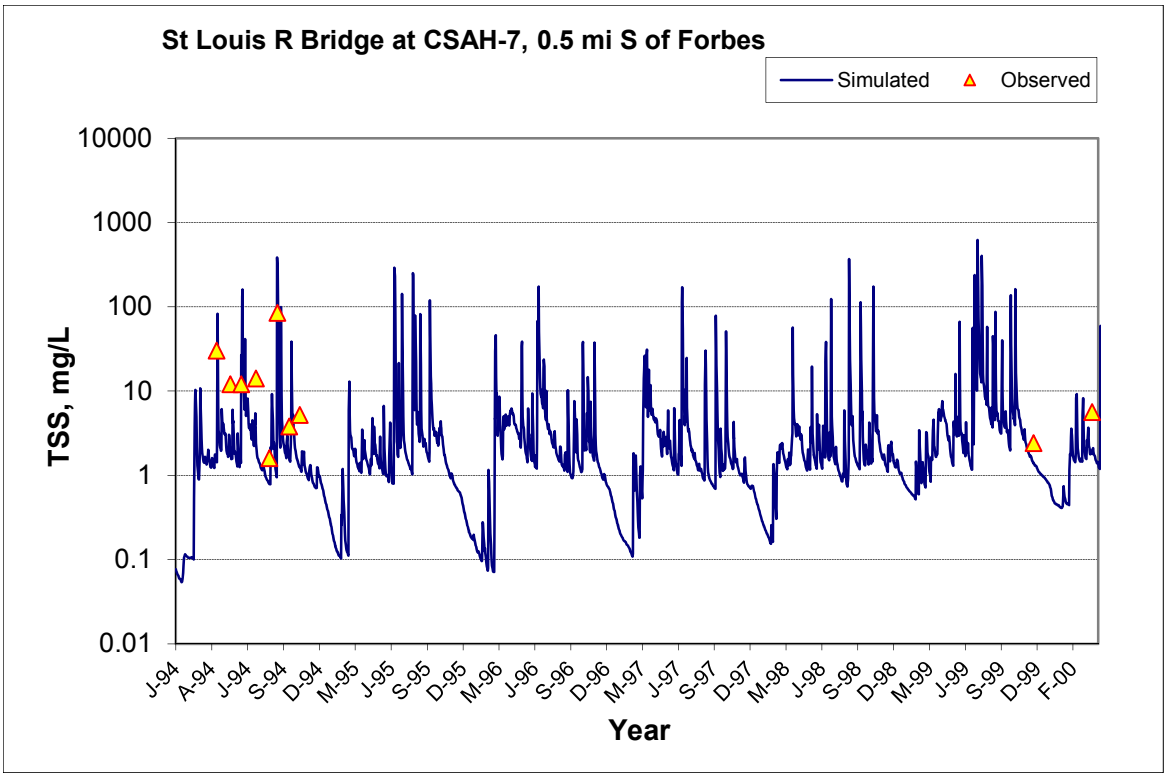

Figure E-2. TSS Concentration Time Series, St Louis R Bridge at CSAH-7, 0.5 mi S of Forbes, 1994-2000

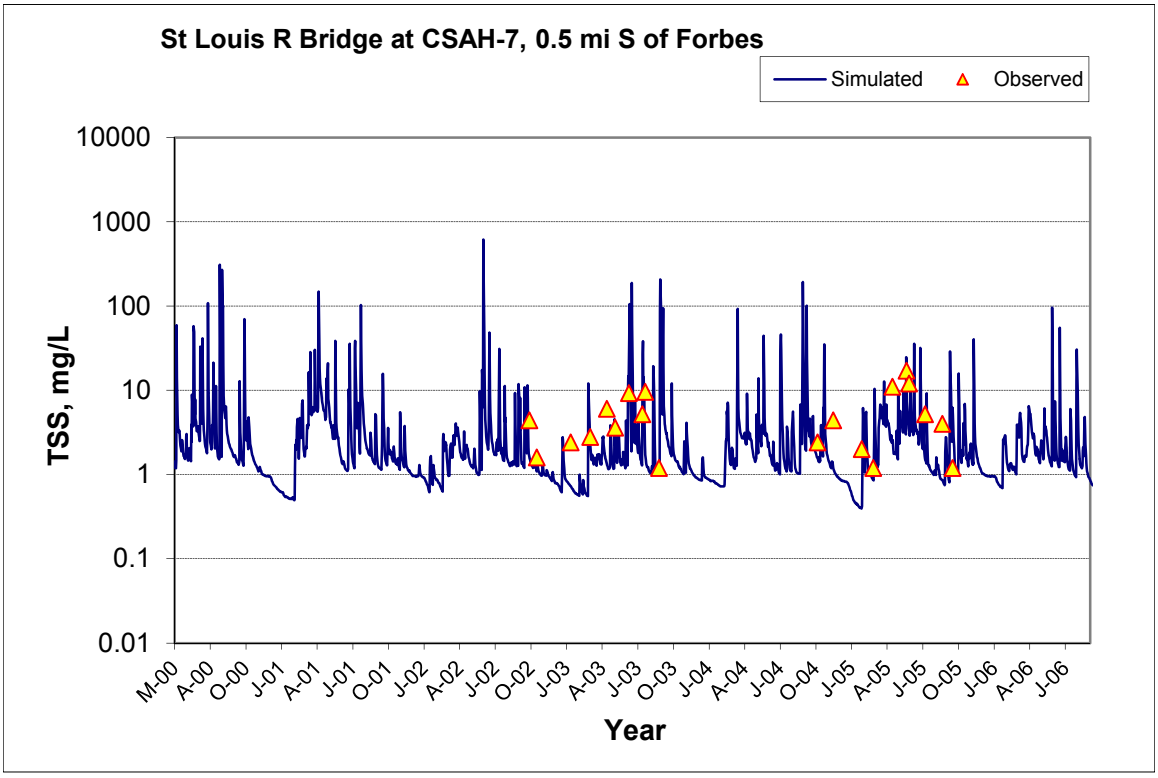

Figure E-3. TSS Concentration Time Series, St Louis R Bridge at CSAH-7, 0.5 mi S of Forbes, 2000-2006

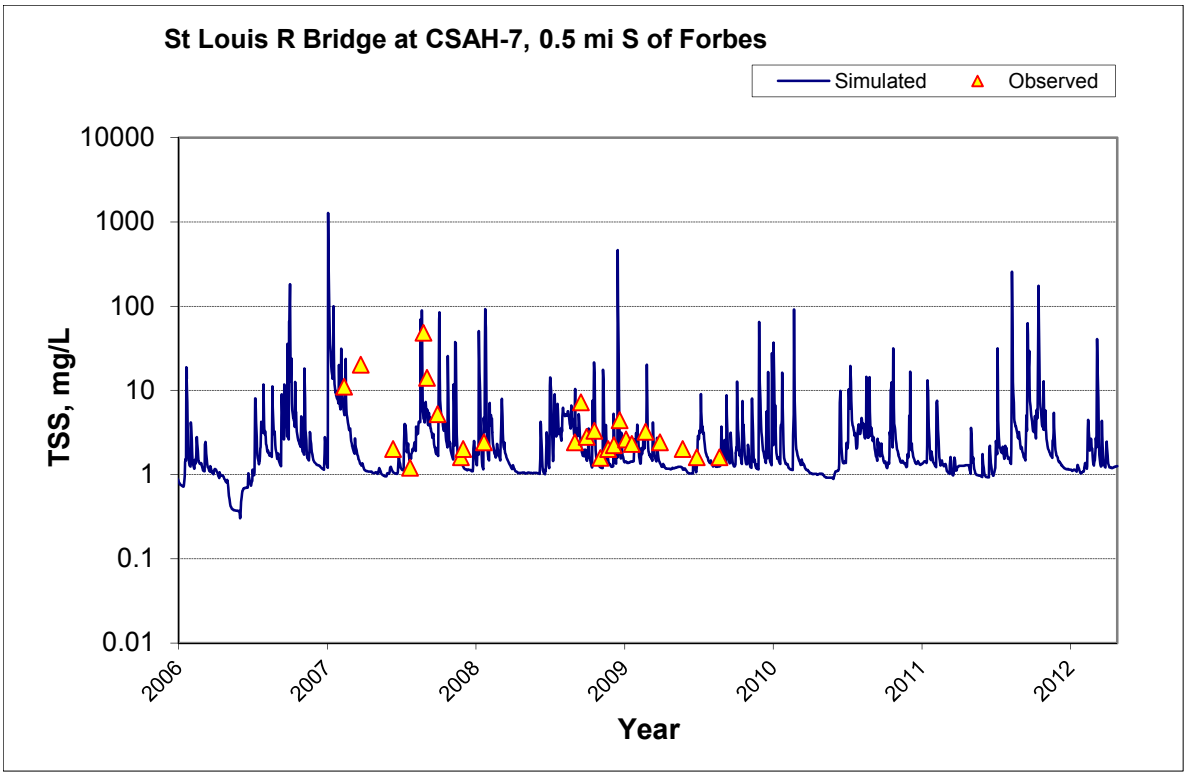

Figure E-4. TSS Concentration Time Series, St Louis R Bridge at CSAH-7, 0.5 mi S of Forbes, 2006-2012

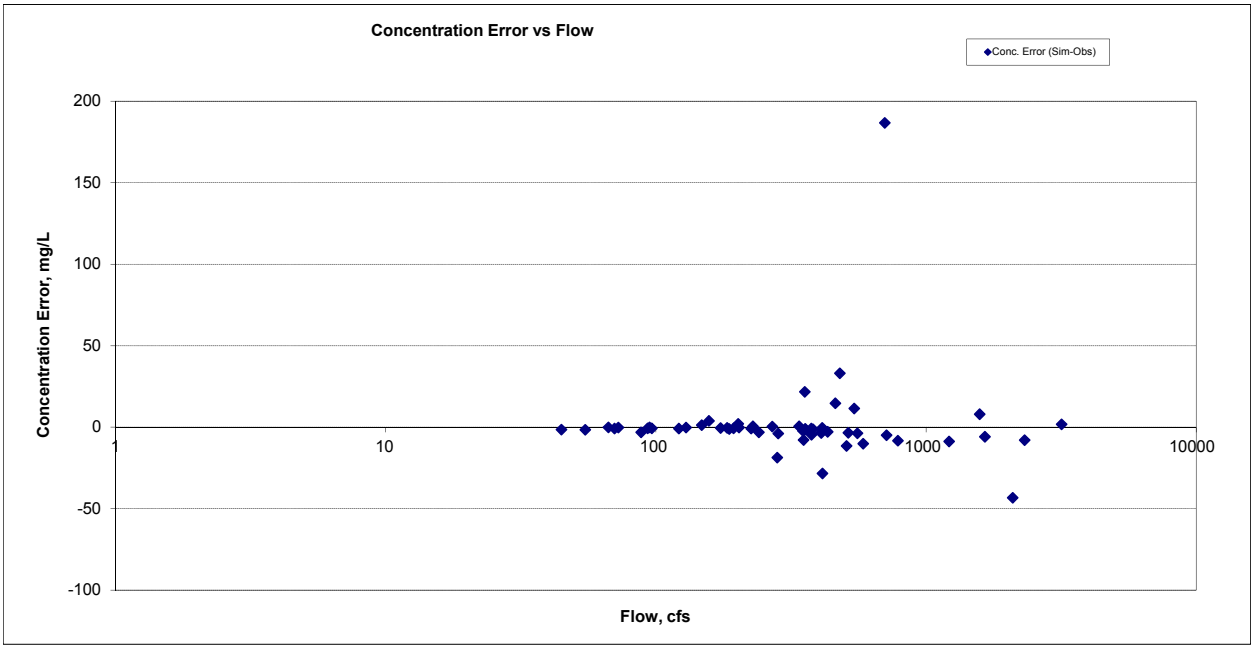

Figure E-5. TSS Concentration, Residual vs. Flow, St Louis R Bridge at CSAH-7, 0.5 mi S of Forbes

Swan River nr Toivola (03084001)

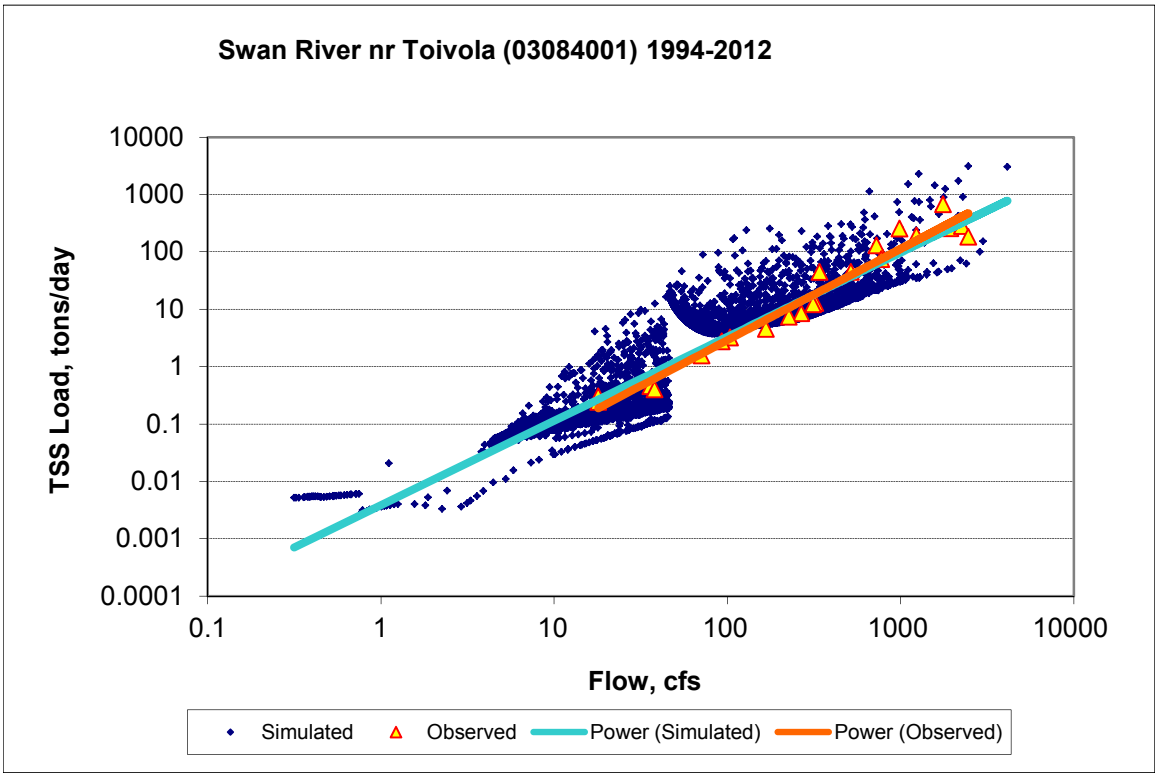

Figure E-6. TSS Load Power Plot, Swan River nr Toivola (03084001)

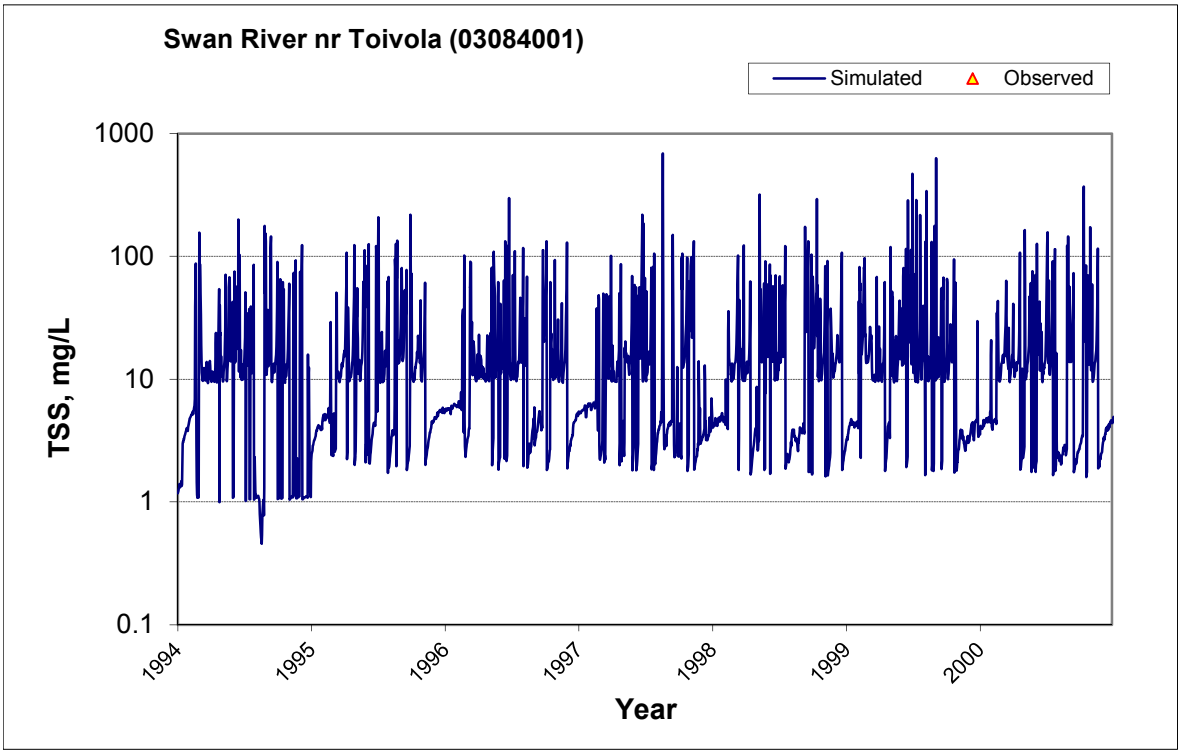

Figure E-7. TSS Concentration Time Series, Swan River nr Toivola (03084001), 1994-2000

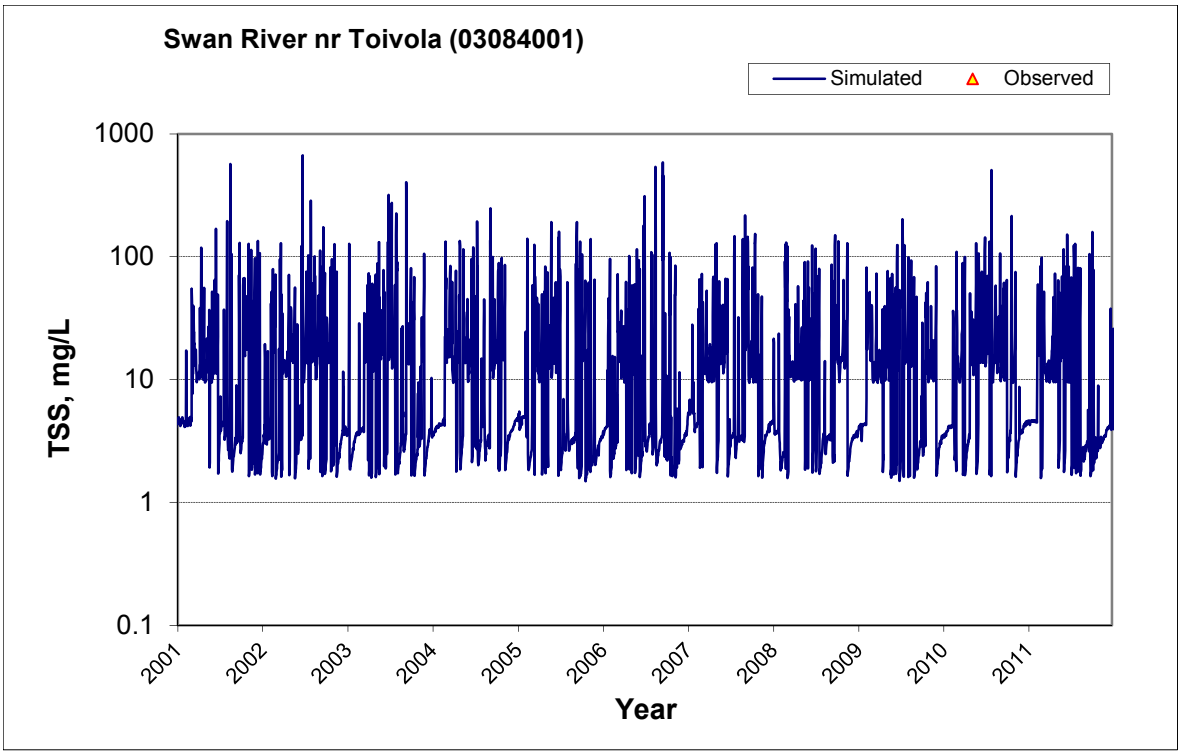

Figure E-8. TSS Concentration Time Series, Swan River nr Toivola (03084001), 2001-2011

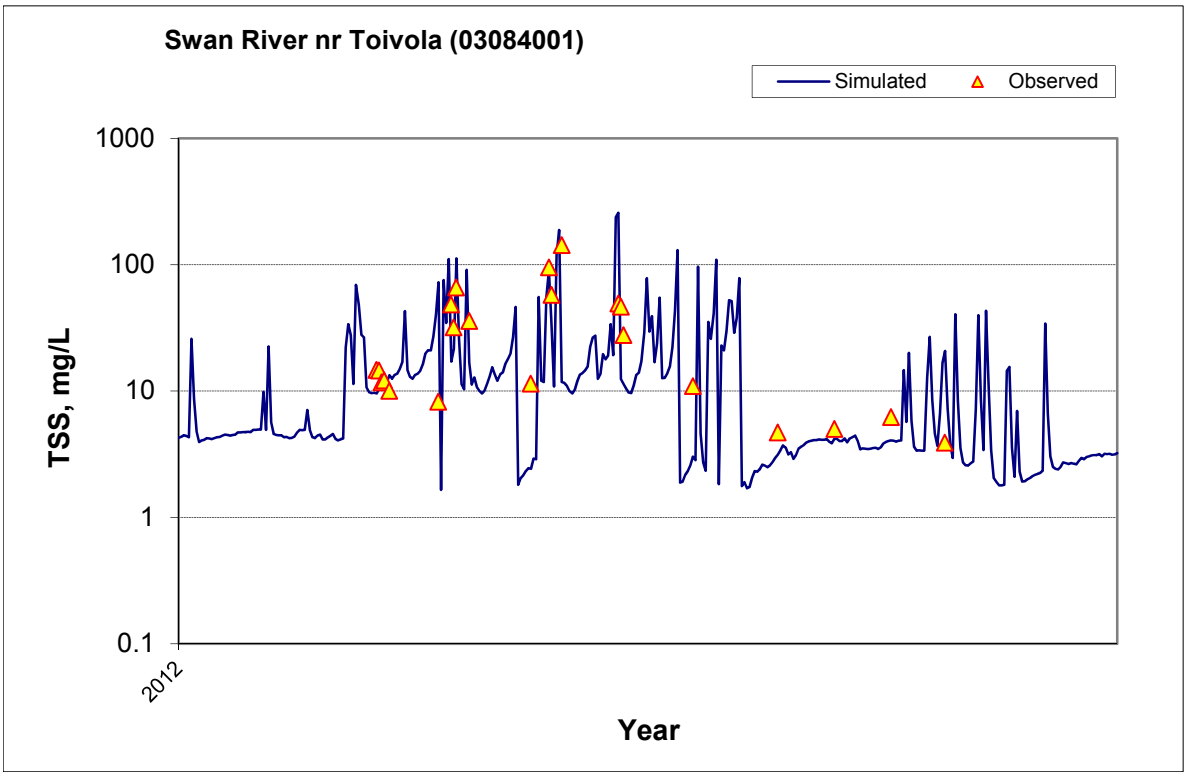

Figure E-9. TSS Concentration Time Series, Swan River nr Toivola (03084001), 2012

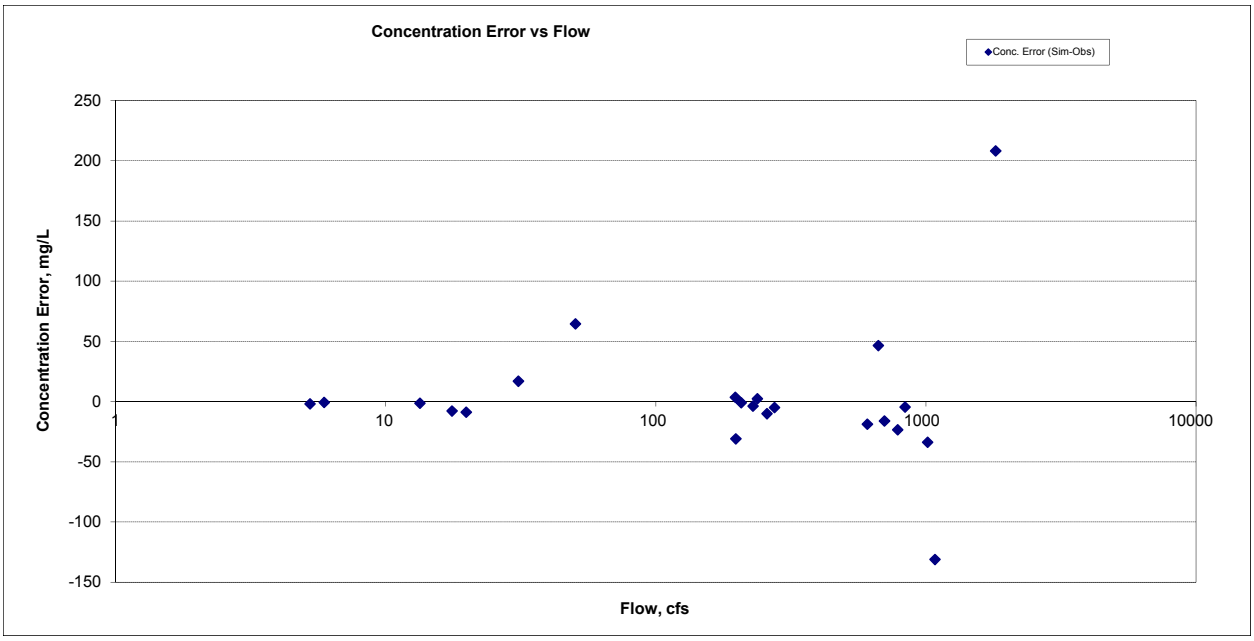

Figure E-10. TSS Concentration, Residual vs. Flow, Swan River nr Toivola (03084001)

Cloquet River nr Burnett (04048001)

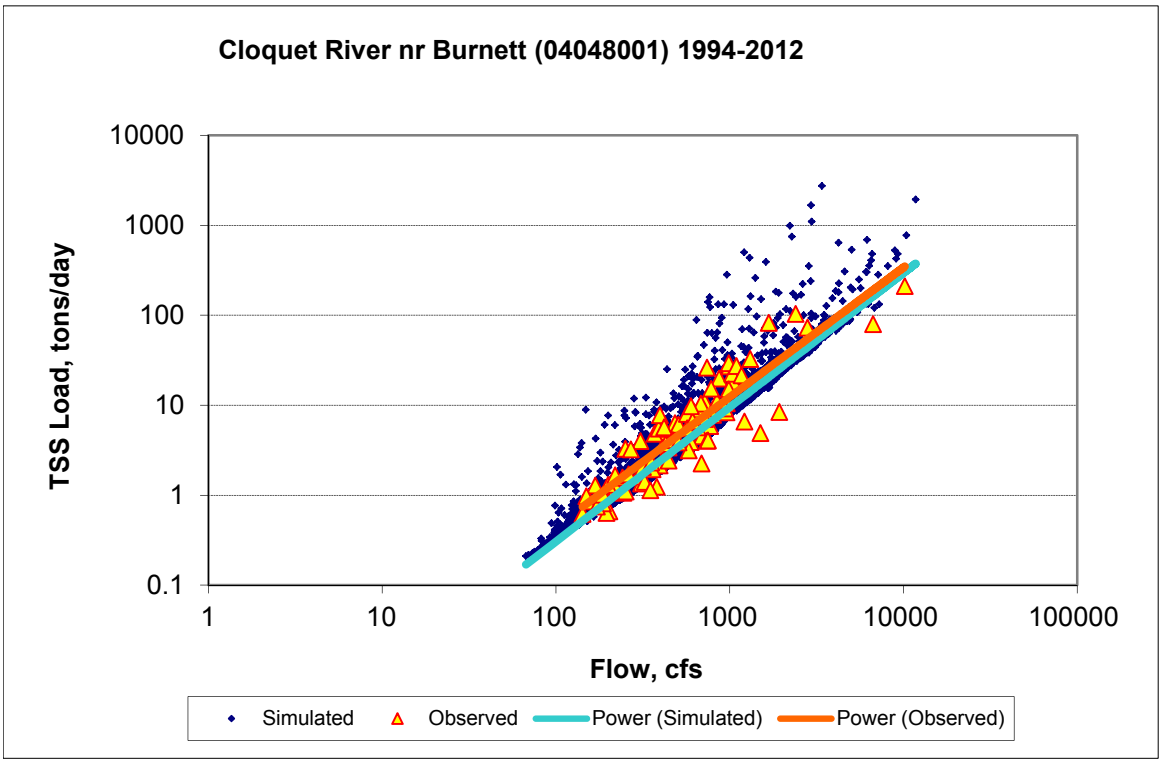

Figure E-11. TSS Load Power Plot, Cloquet River nr Burnett (04048001)

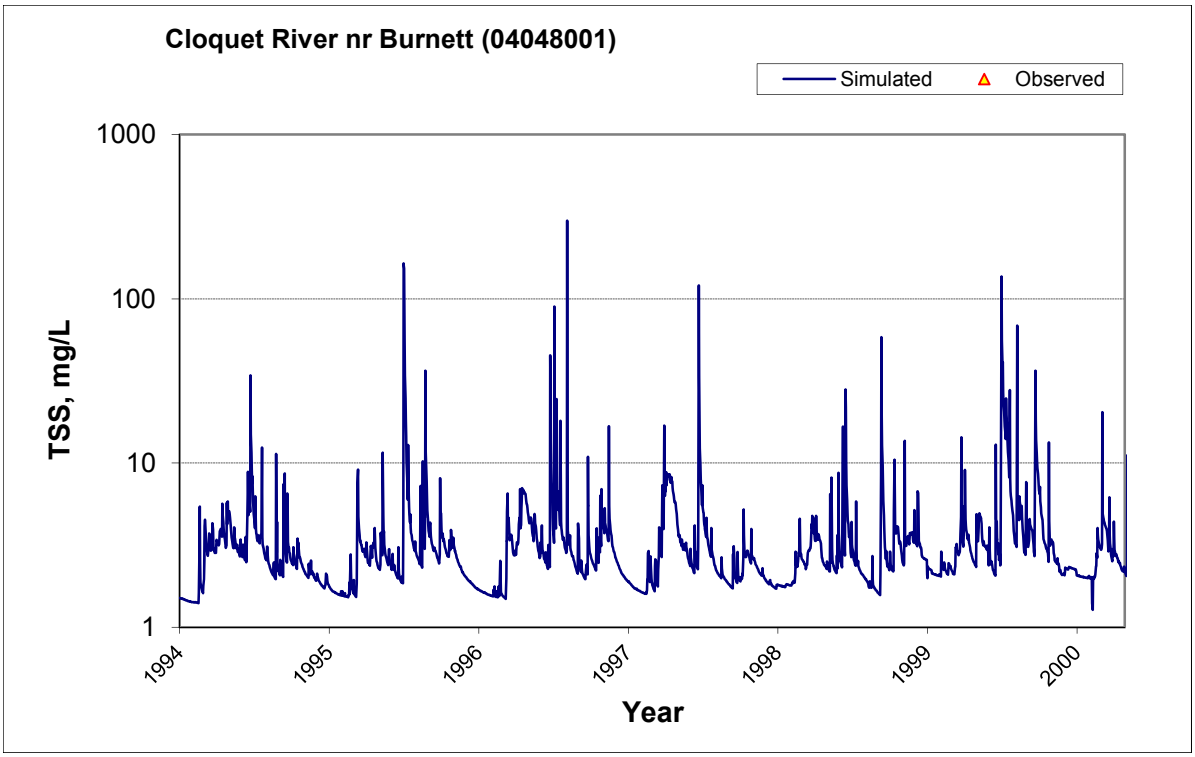

Figure E-12. TSS Concentration Time Series, Cloquet River nr Burnett (04048001), 1994-2000

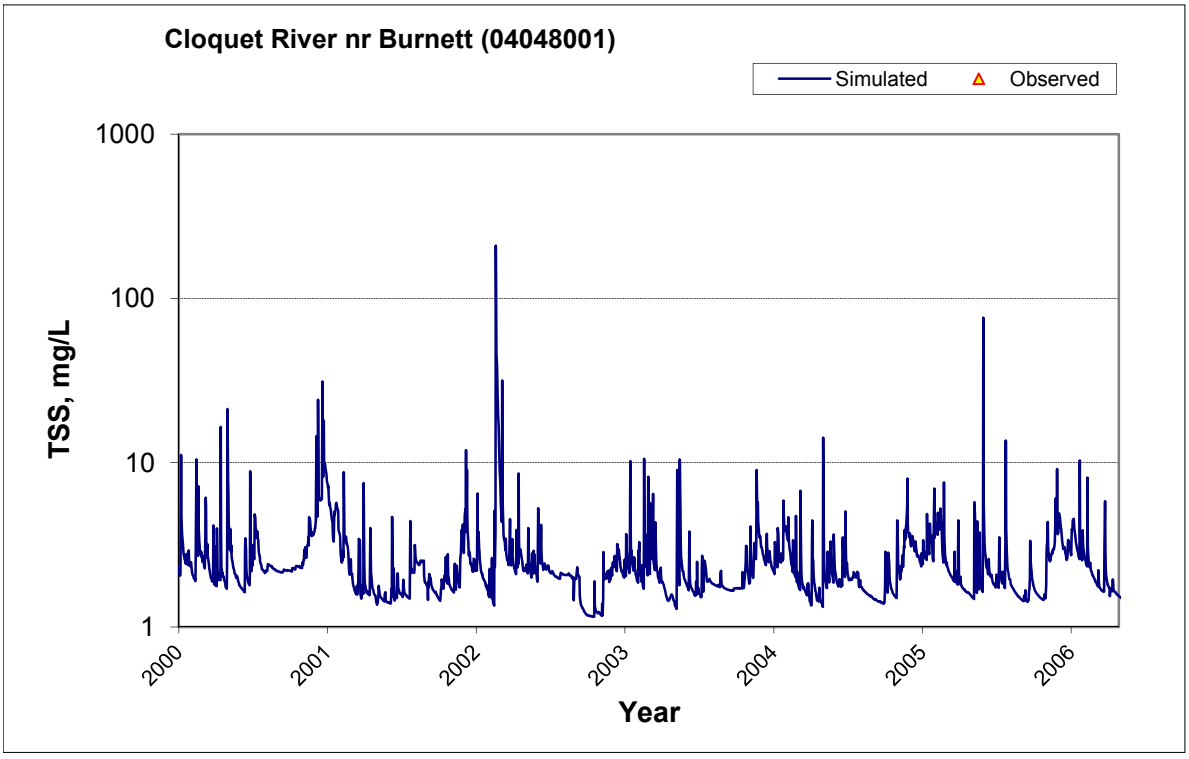

Figure E-13. TSS Concentration Time Series, Cloquet River nr Burnett (04048001), 2000-2006

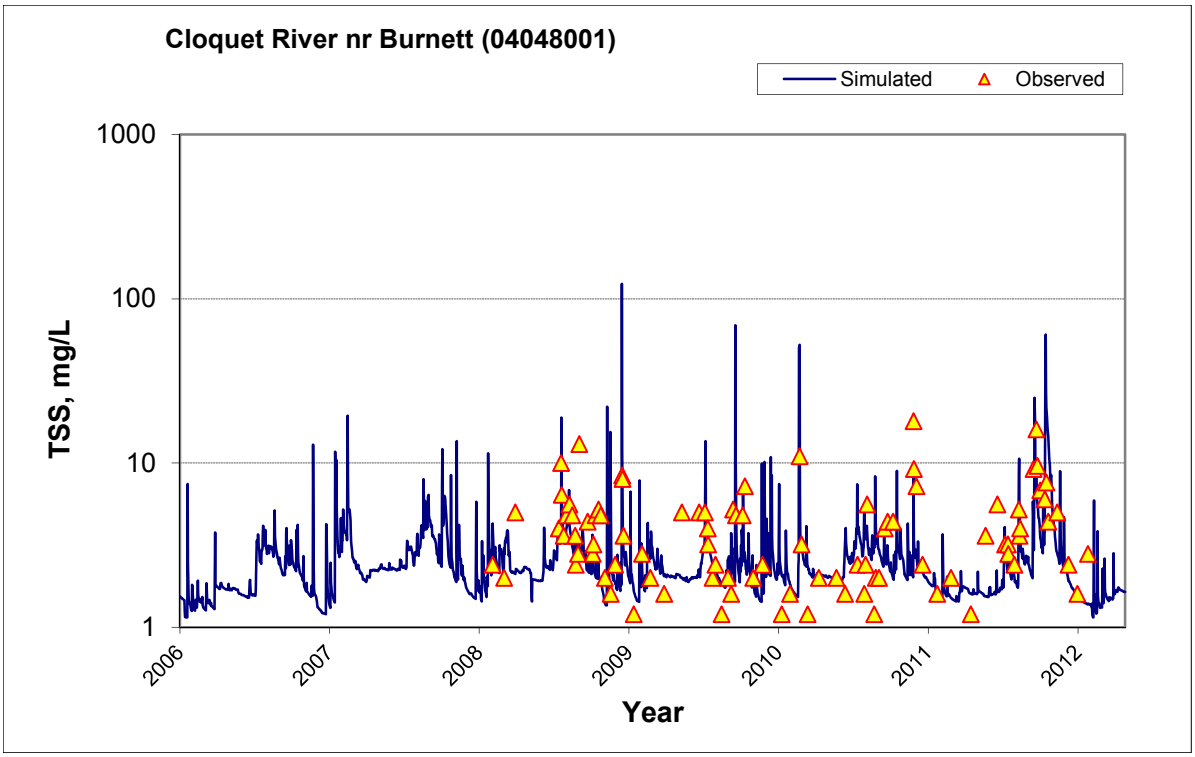

Figure E-14. TSS Concentration Time Series, Cloquet River nr Burnett (04048001), 2006-2012

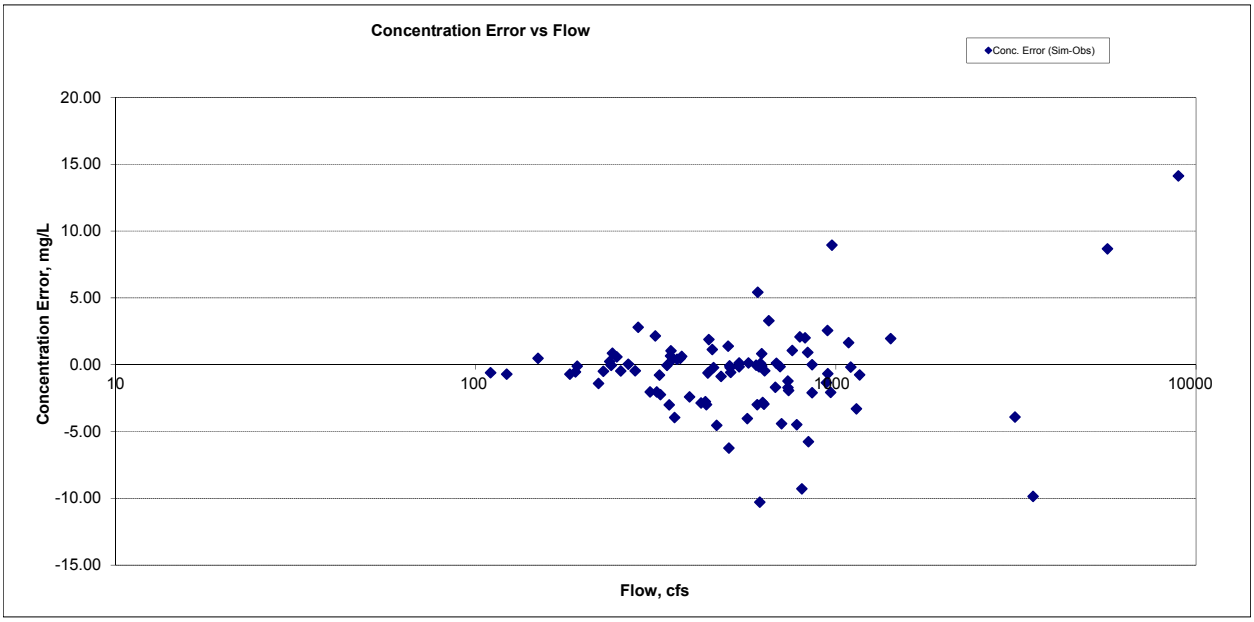

Figure E-15. TSS Concentration, Residual vs. Flow, Cloquet River nr Burnett (04048001)

St. Louis River at Scanlon, MN (03174001)

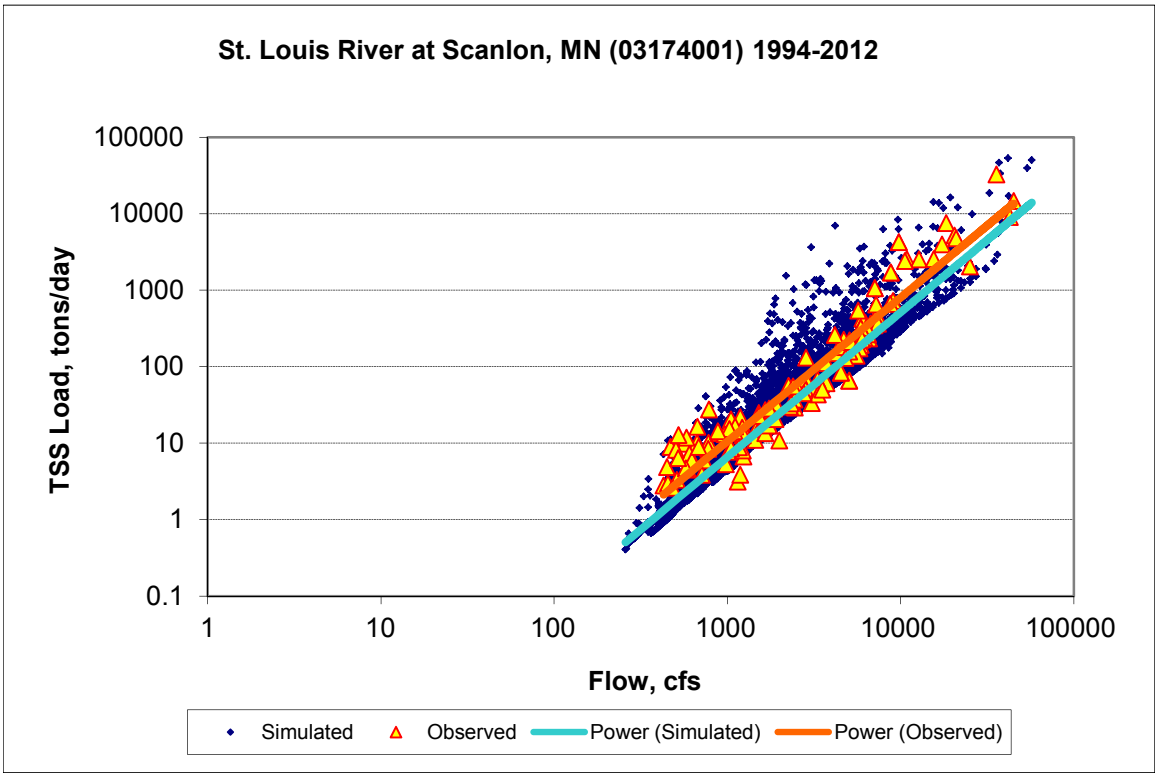

Figure E-16. TSS Load Power Plot, St. Louis River at Scanlon, MN (03174001)

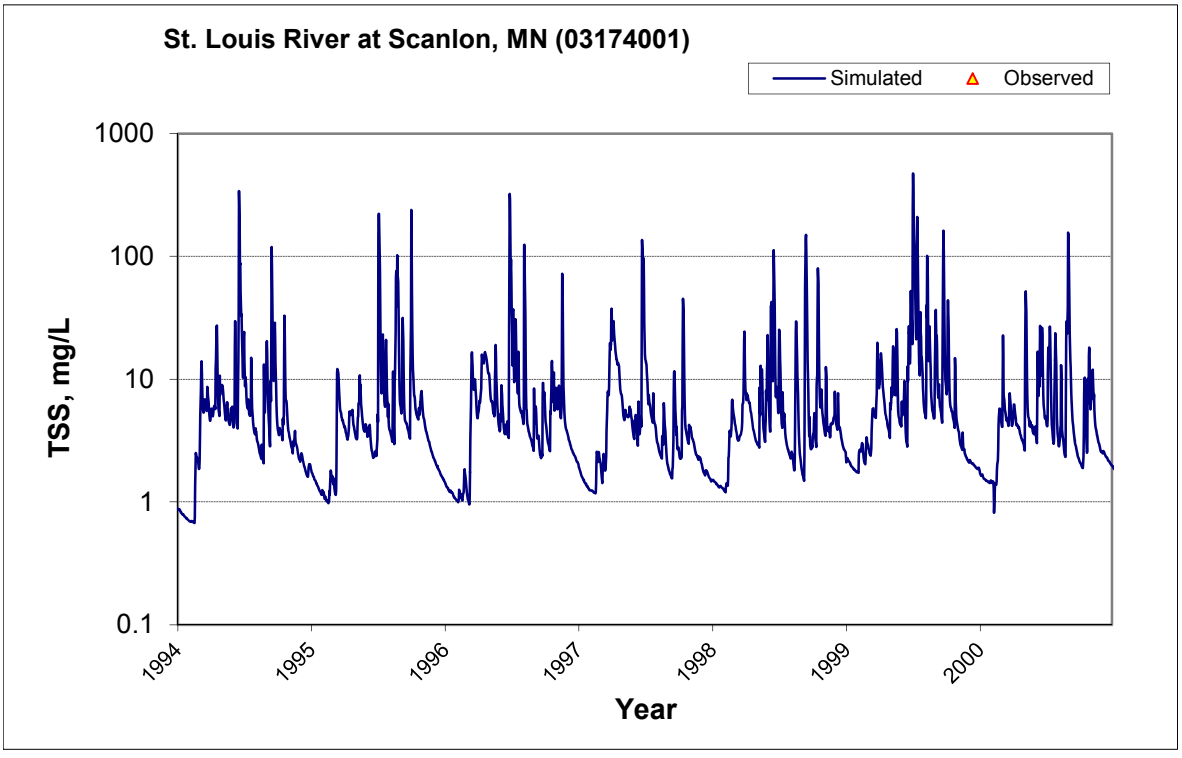

Figure E-17. TSS Concentration Time Series, St. Louis River at Scanlon, MN (03174001), 1994-2000

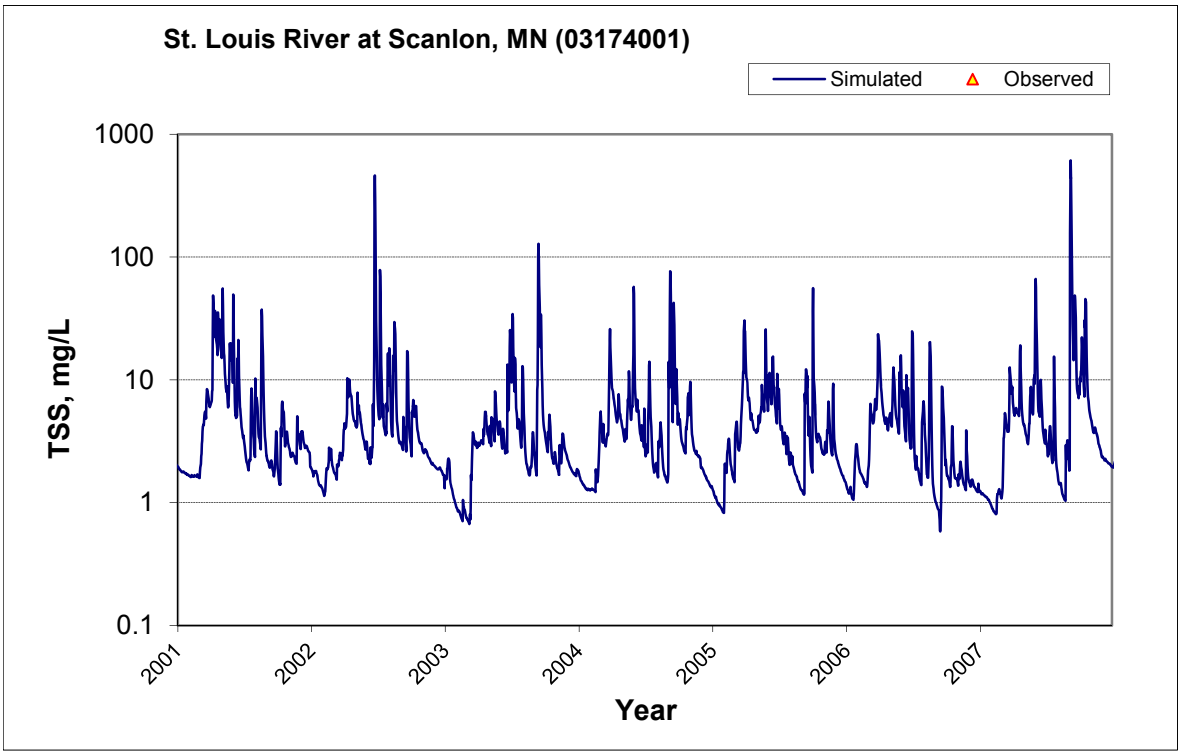

Figure E-18. TSS Concentration Time Series, St. Louis River at Scanlon, MN (03174001), 2001-2007

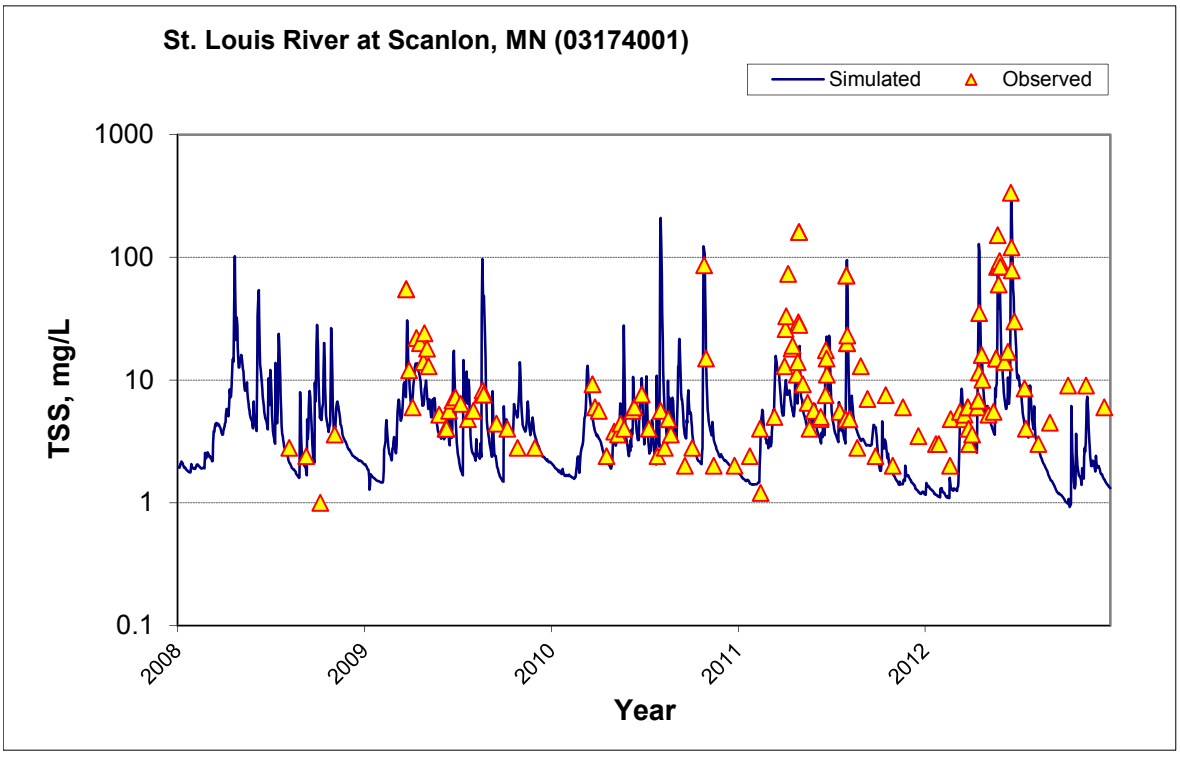

Figure E-19. TSS Concentration Time Series, St. Louis River at Scanlon, MN (03174001), 2008-2012

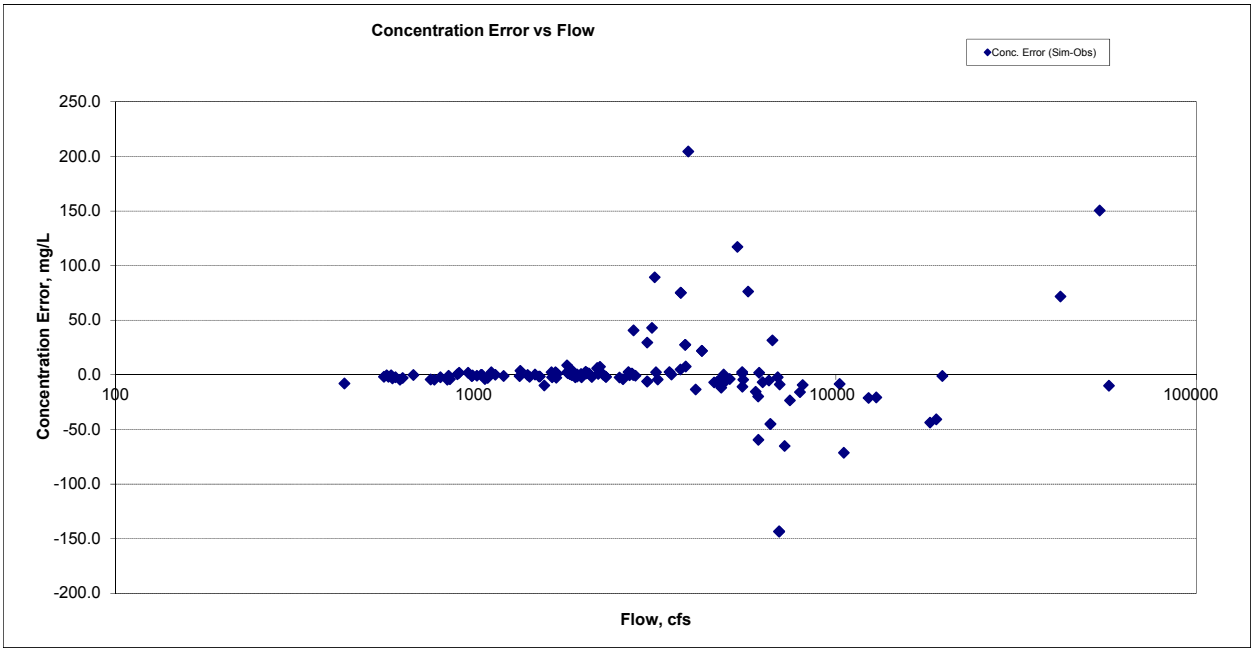

Figure E-20. TSS Concentration, Residual vs. Flow, St. Louis River at Scanlon, MN (03174001)

St Louis River at Bridge on MN-23 at Fond du Lac

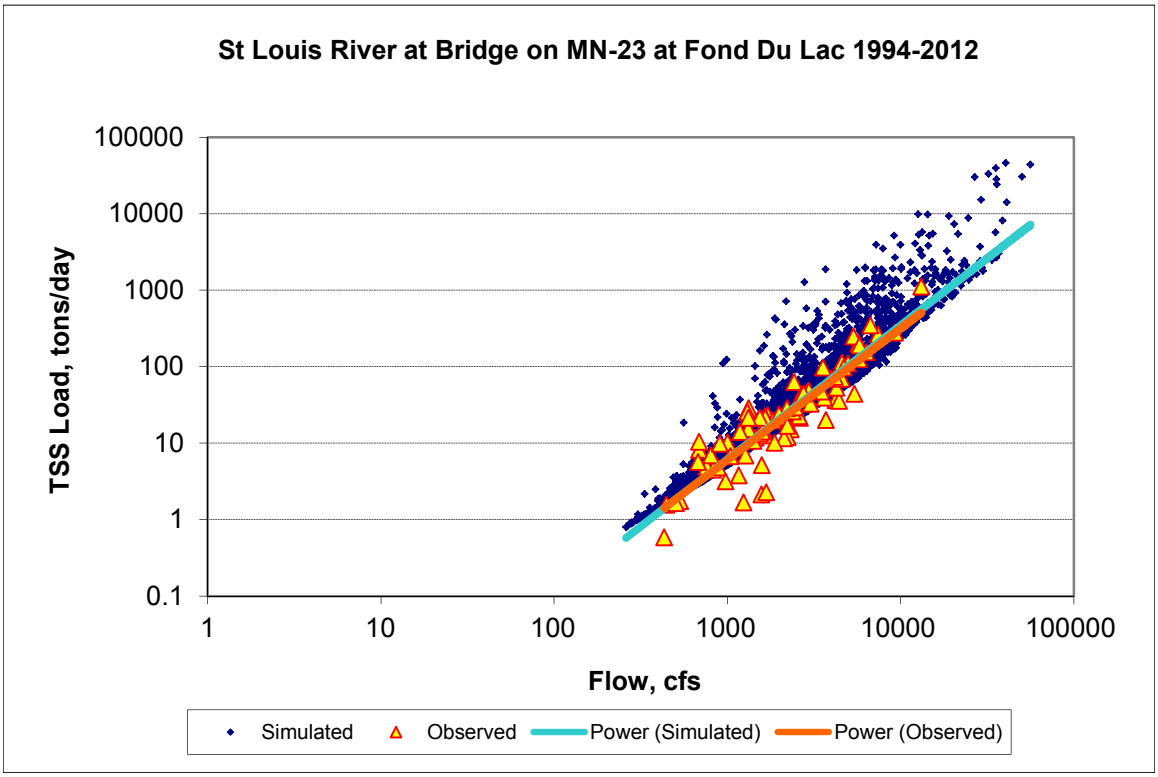

Figure E-21. TSS Load Power Plot, St Louis River at Bridge on MN-23 at Fond du Lac

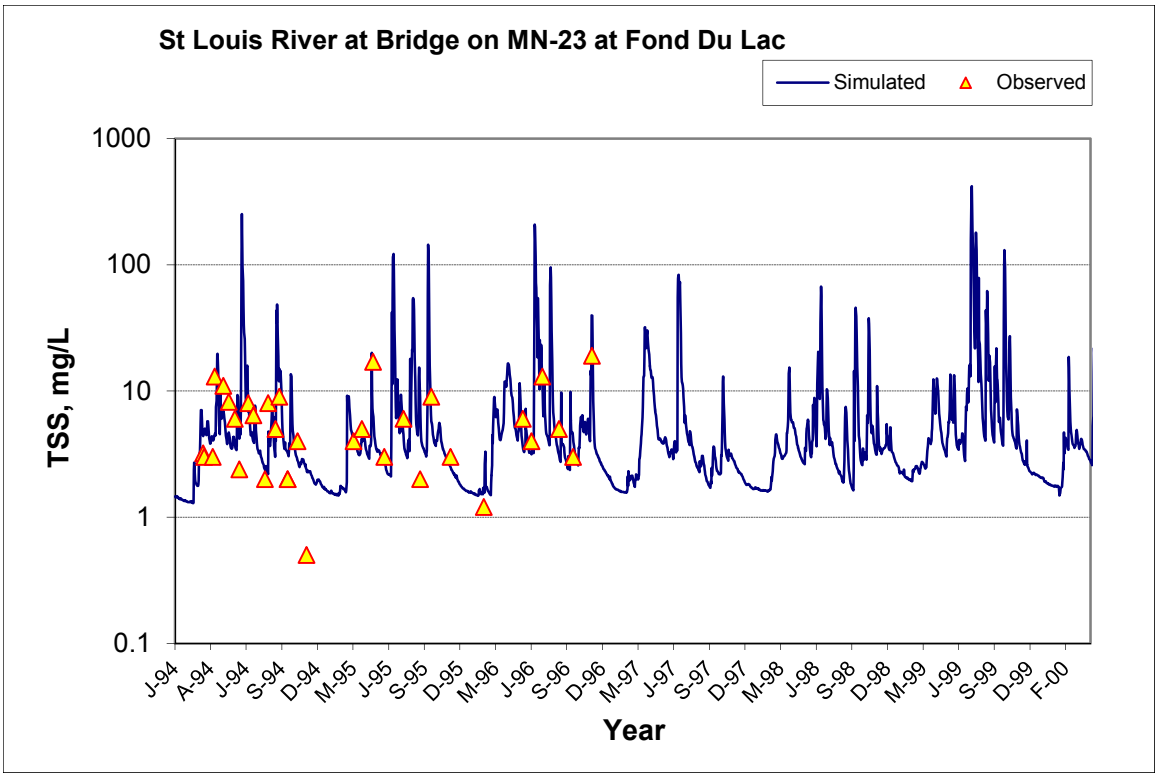

Figure E-22. TSS Concentration Time Series, St Louis River at Bridge on MN-23 at Fond du Lac, 1994-2000

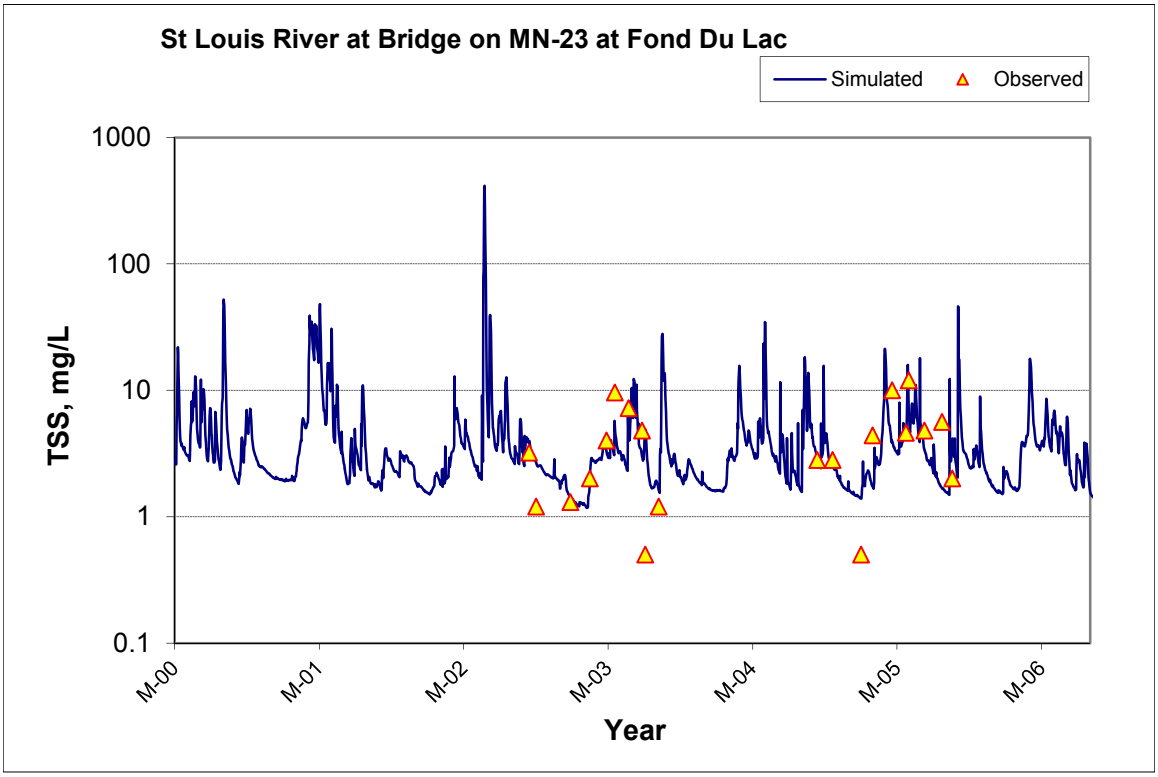

Figure E-23. TSS Concentration Time Series, St Louis River at Bridge on MN-23 at Fond du Lac, 2000-2006

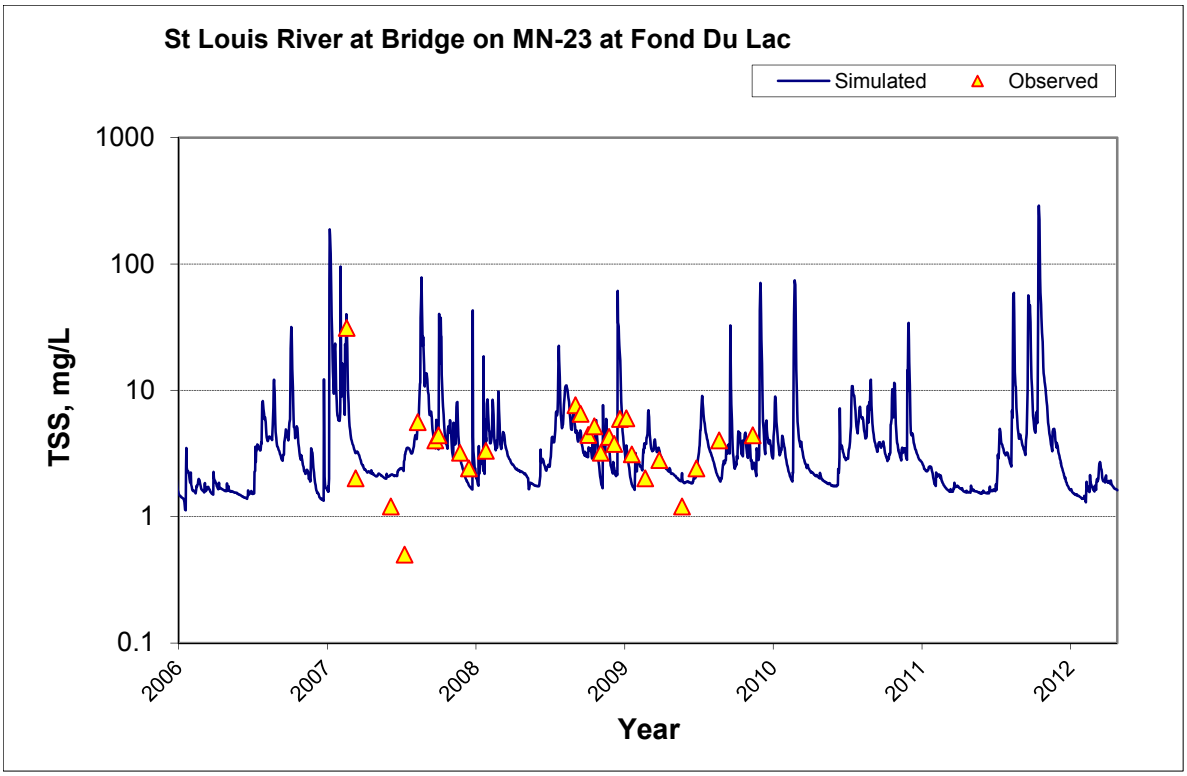

Figure E-24. TSS Concentration Time Series, St Louis River at Bridge on MN-23 at Fond du Lac, 2006-2012

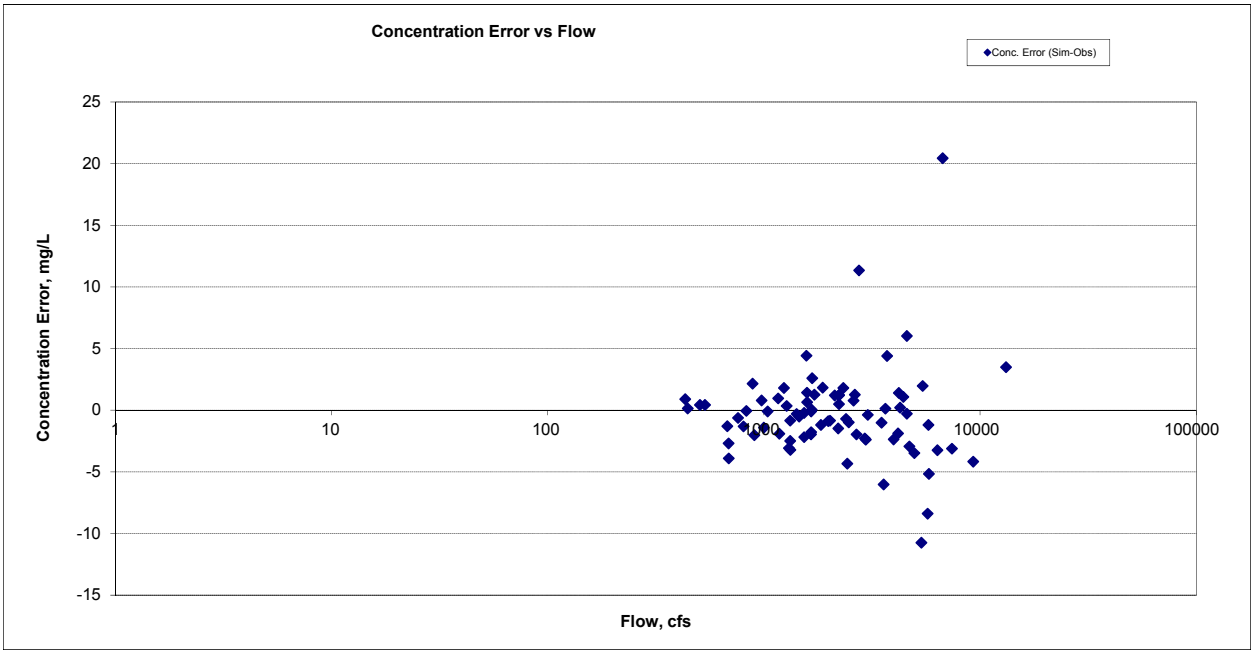

Figure E-25. TSS Concentration, Residual vs. Flow, St Louis River at Bridge on MN-23 at Fond du Lac

Miller Creek at Duluth (03001001)

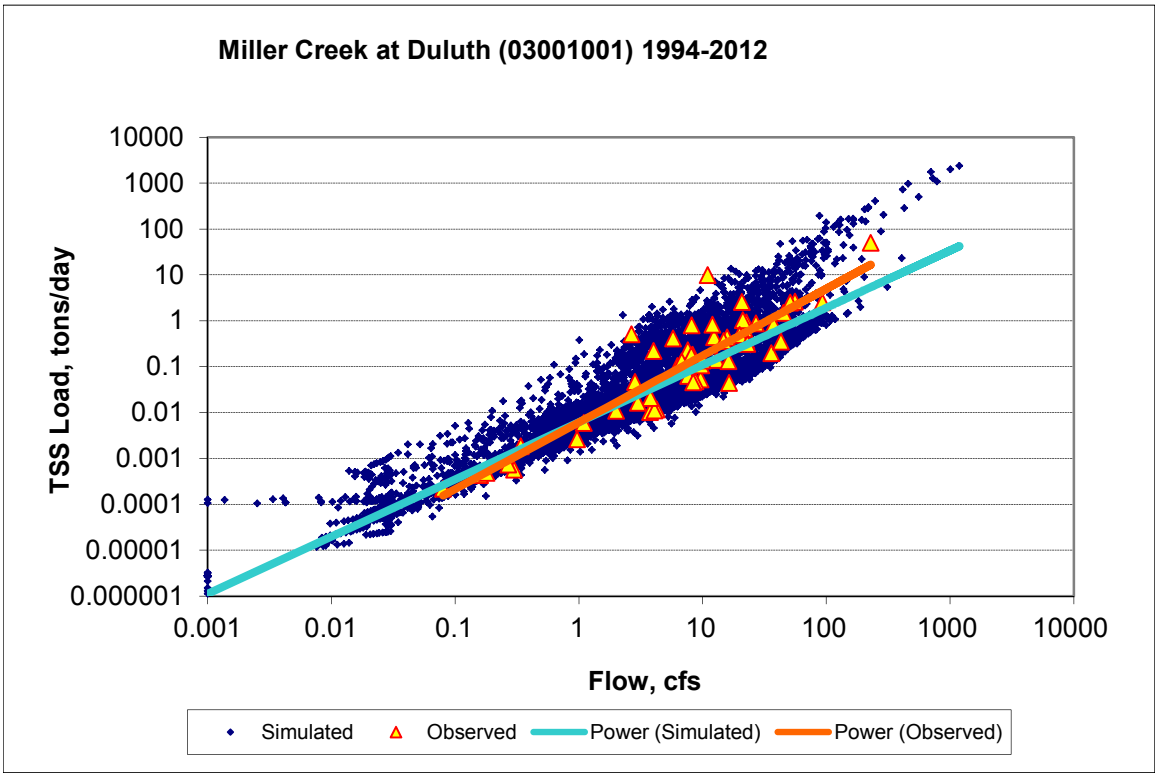

Figure E-26. TSS Load Power Plot, Miller Creek at Duluth (03001001)

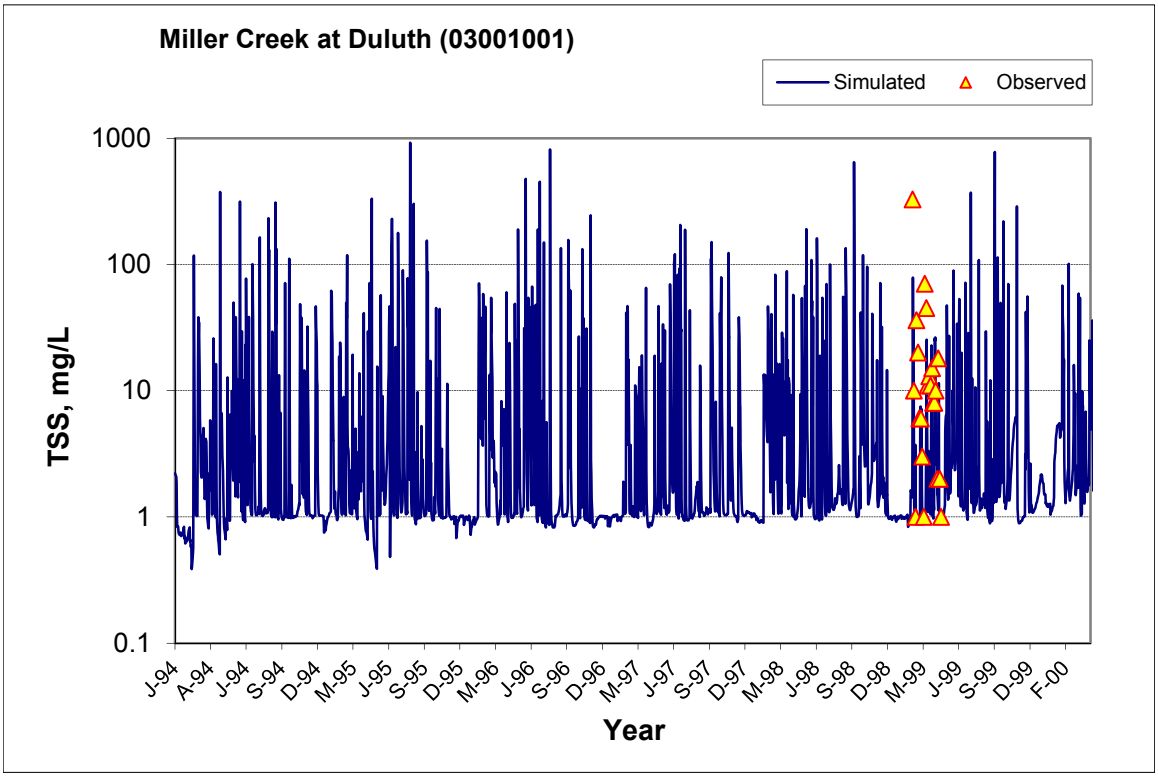

Figure E-27. TSS Concentration Time Series, Miller Creek at Duluth (03001001), 1994-2000

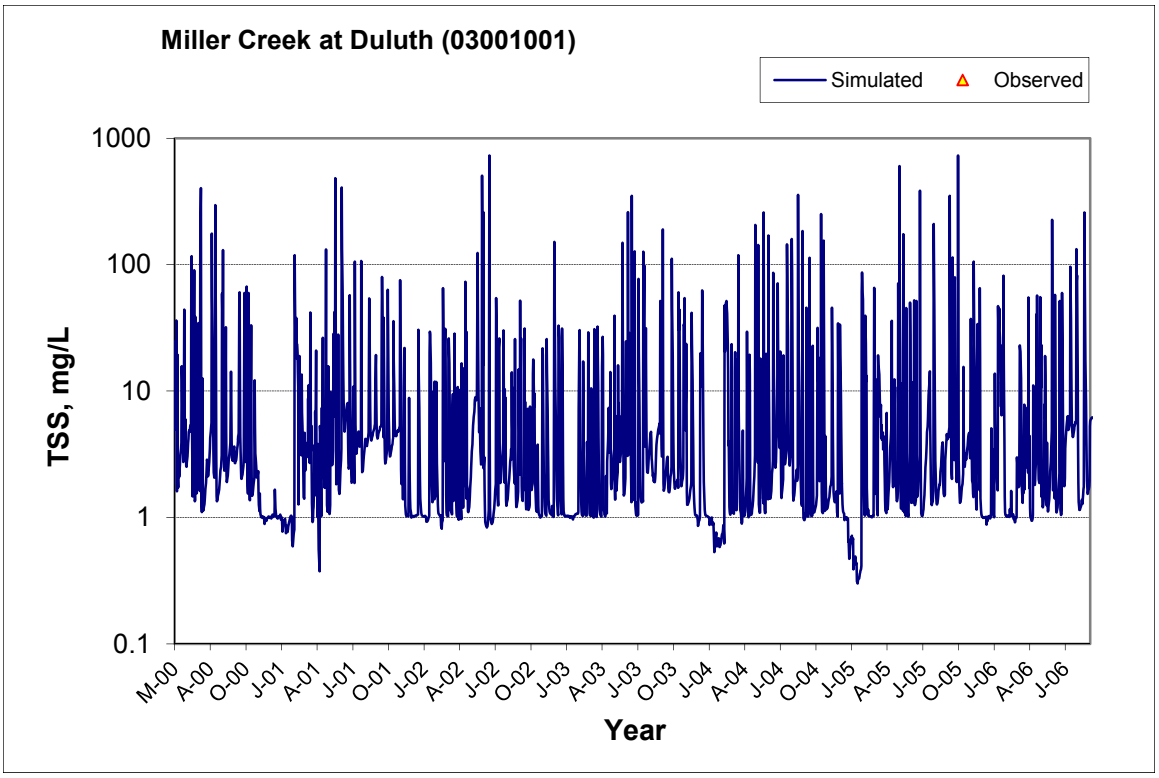

Figure E-28. TSS Concentration Time Series, Miller Creek at Duluth (03001001), 2000-2006

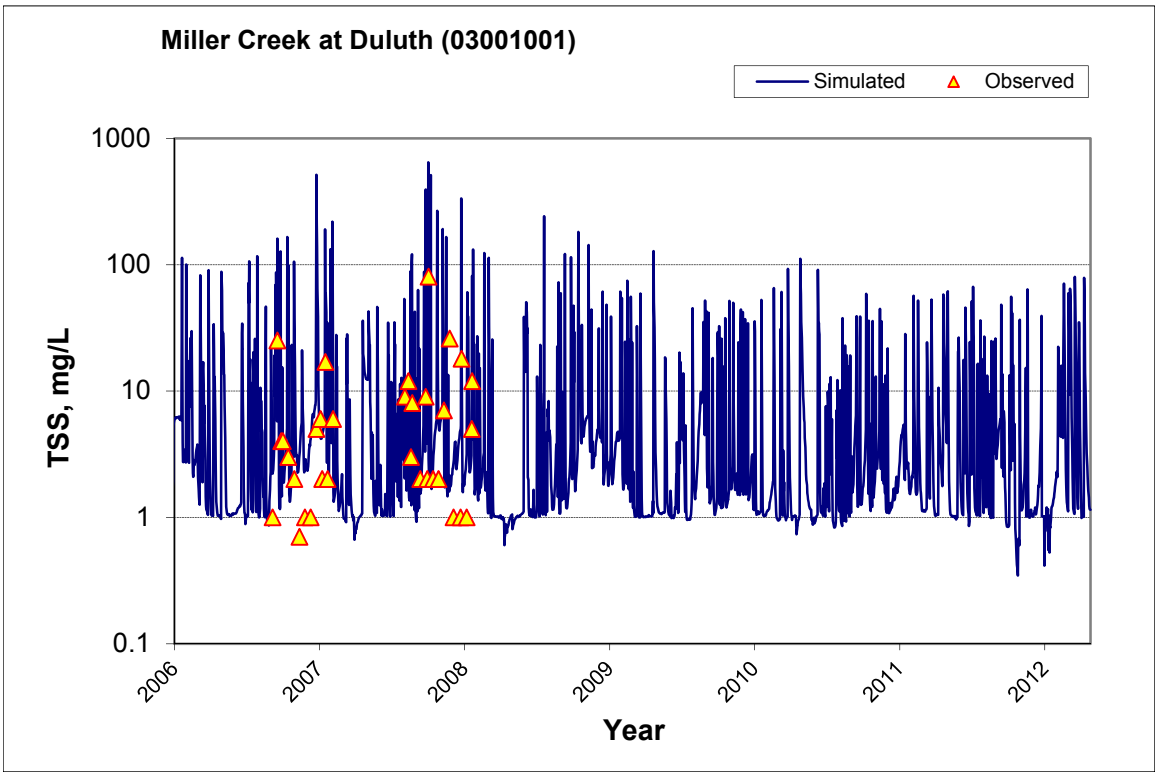

Figure E-29. TSS Concentration Time Series, Miller Creek at Duluth (03001001), 2006-2012

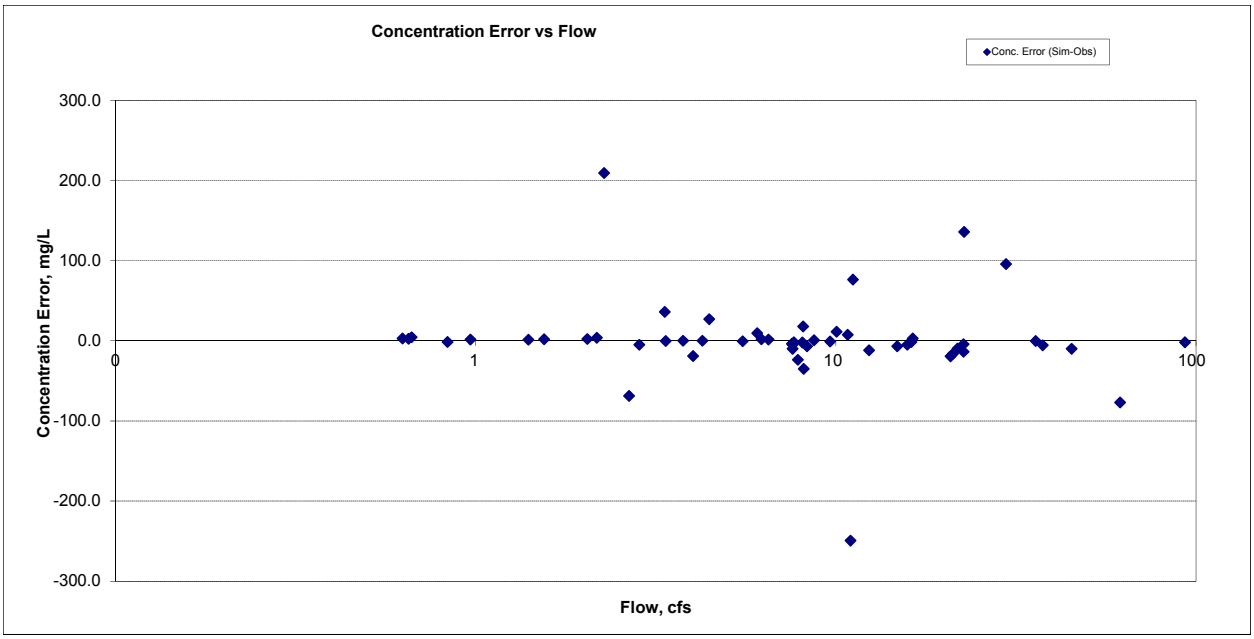

Figure E-30. TSS Concentration, Residual vs. Flow, Miller Creek at Duluth (03001001)

Blackhoof River nr Pleasant Valley (05006001)

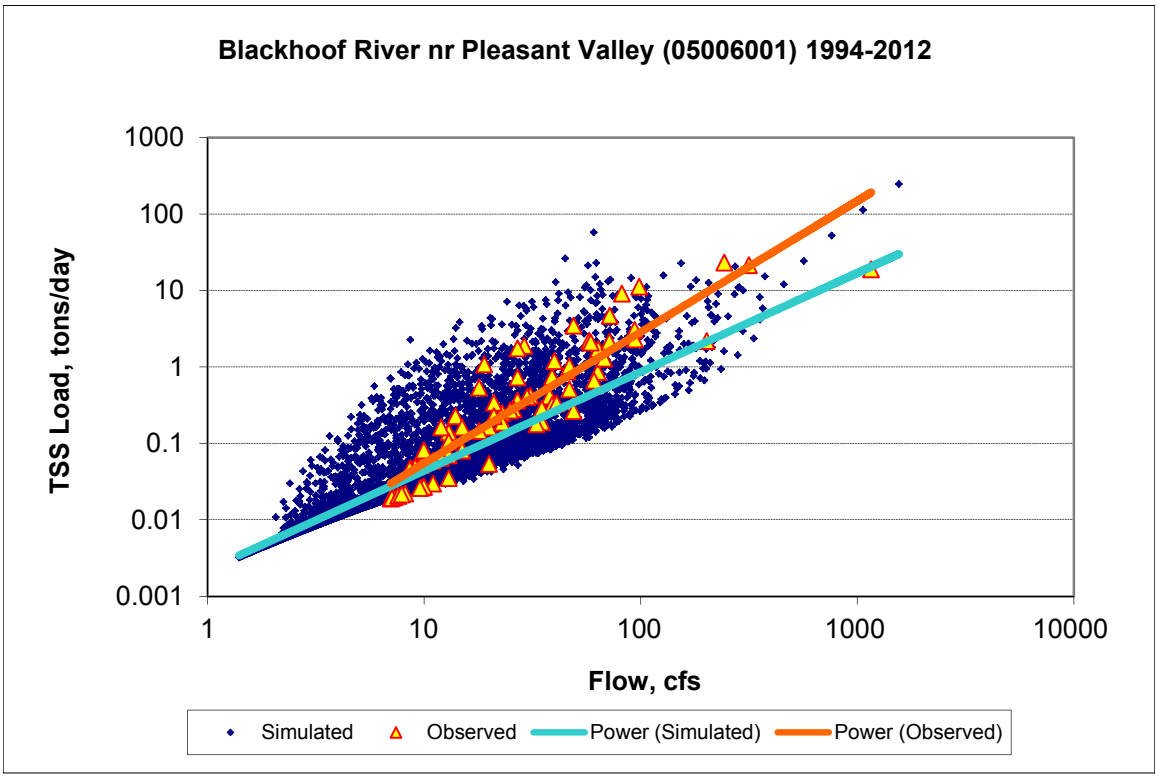

TSS Load Power Plot, Blackhoof River nr Pleasant Valley (05006001)

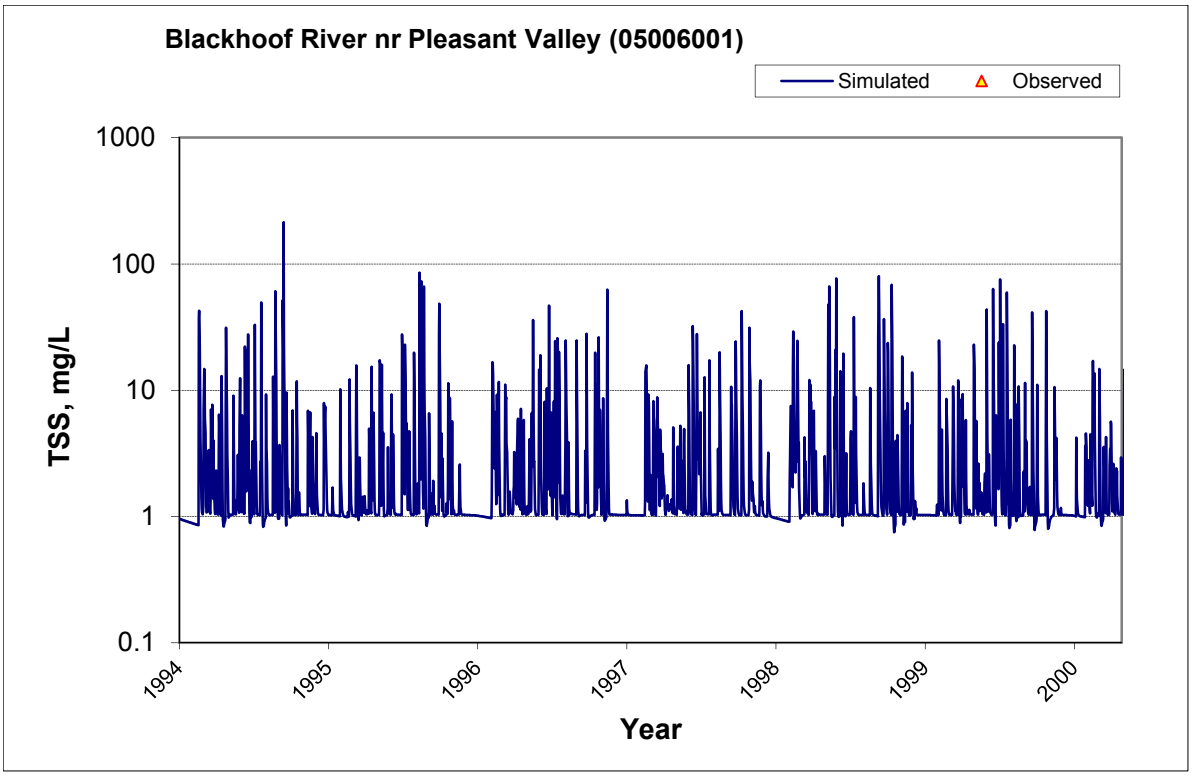

Figure E-31. TSS Concentration Time Series, Blackhoof River nr Pleasant Valley (05006001), 1994-2000

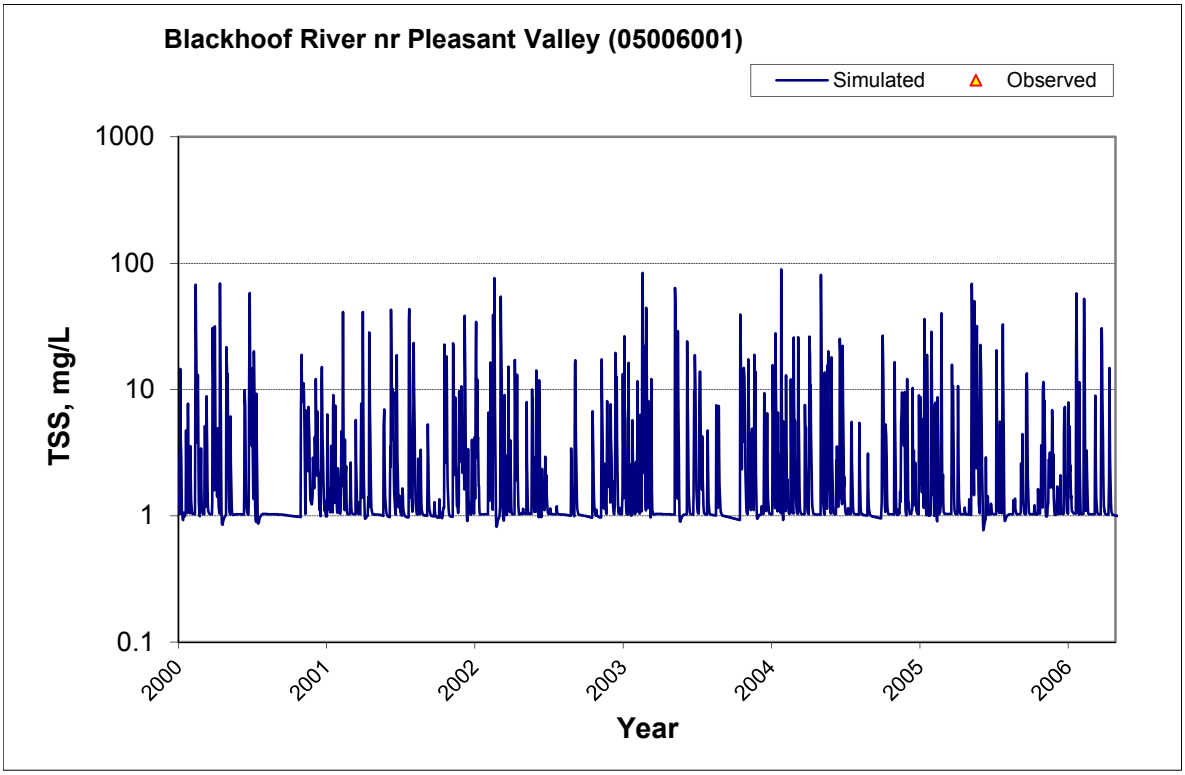

Figure E-32. TSS Concentration Time Series, Blackhoof River nr Pleasant Valley (05006001), 2000-2006

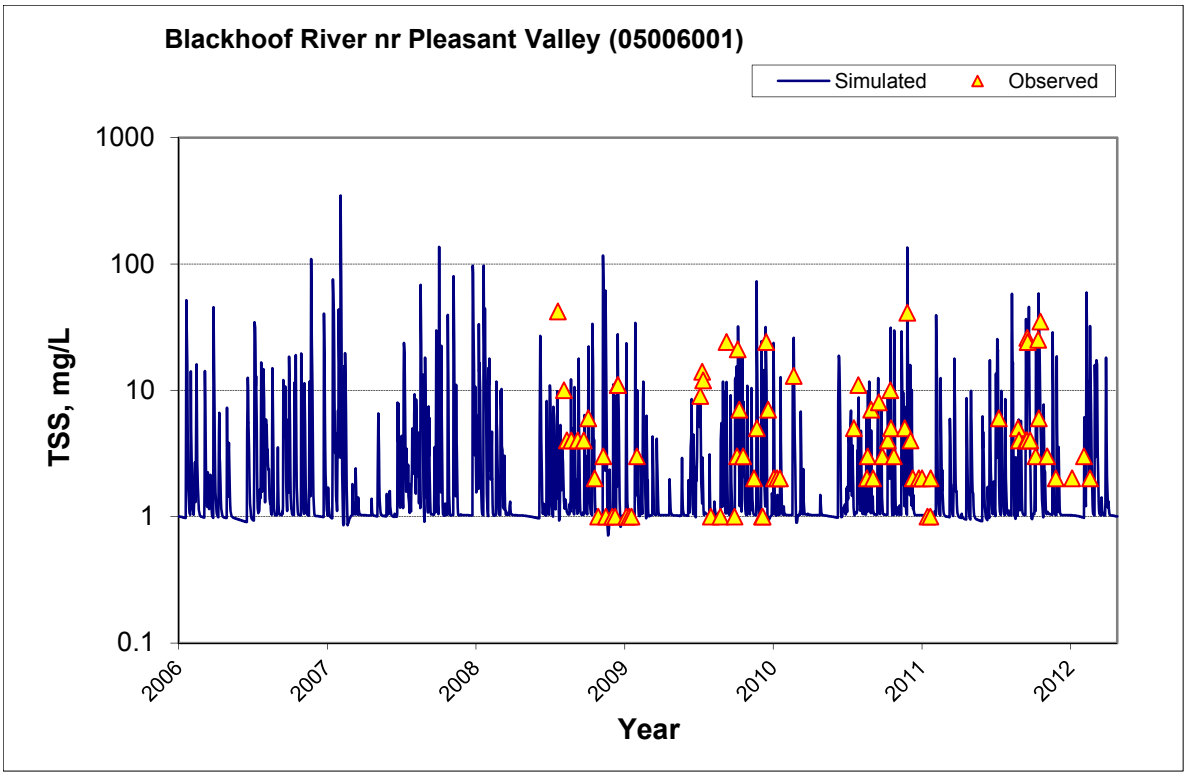

Figure E-33. TSS Concentration Time Series, Blackhoof River nr Pleasant Valley (05006001), 2006-2012

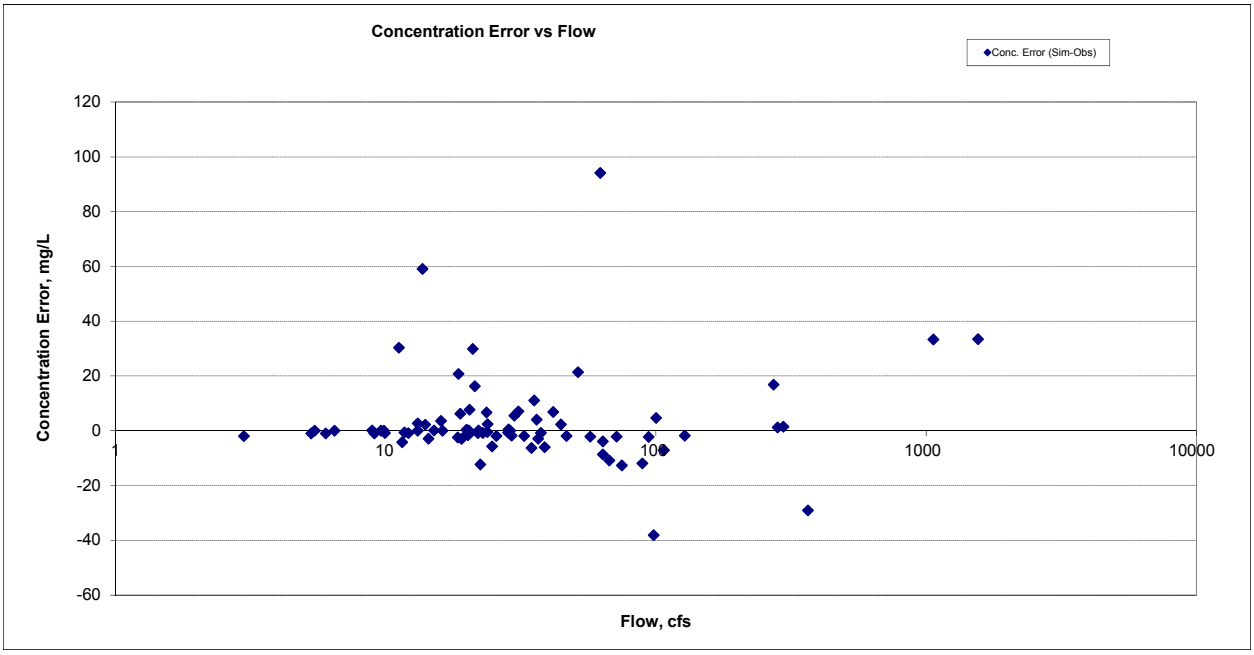

Figure E-34. TSS Concentration, Residual vs. Flow, Blackhoof River nr Pleasant Valley (05006001)

Deer Creek nr Pleasant Valley, MN23 (05008001)

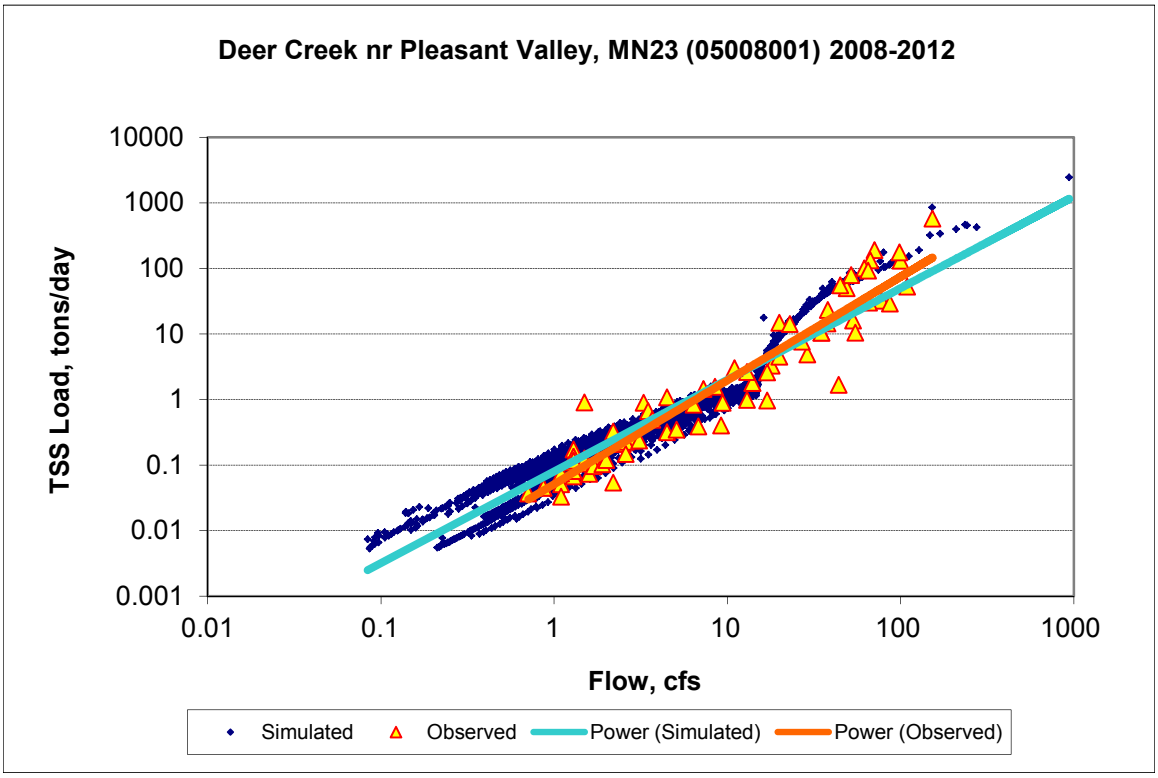

Figure E-35. TSS Load Power Plot, Deer Creek nr Pleasant Valley, MN23 (05008001)

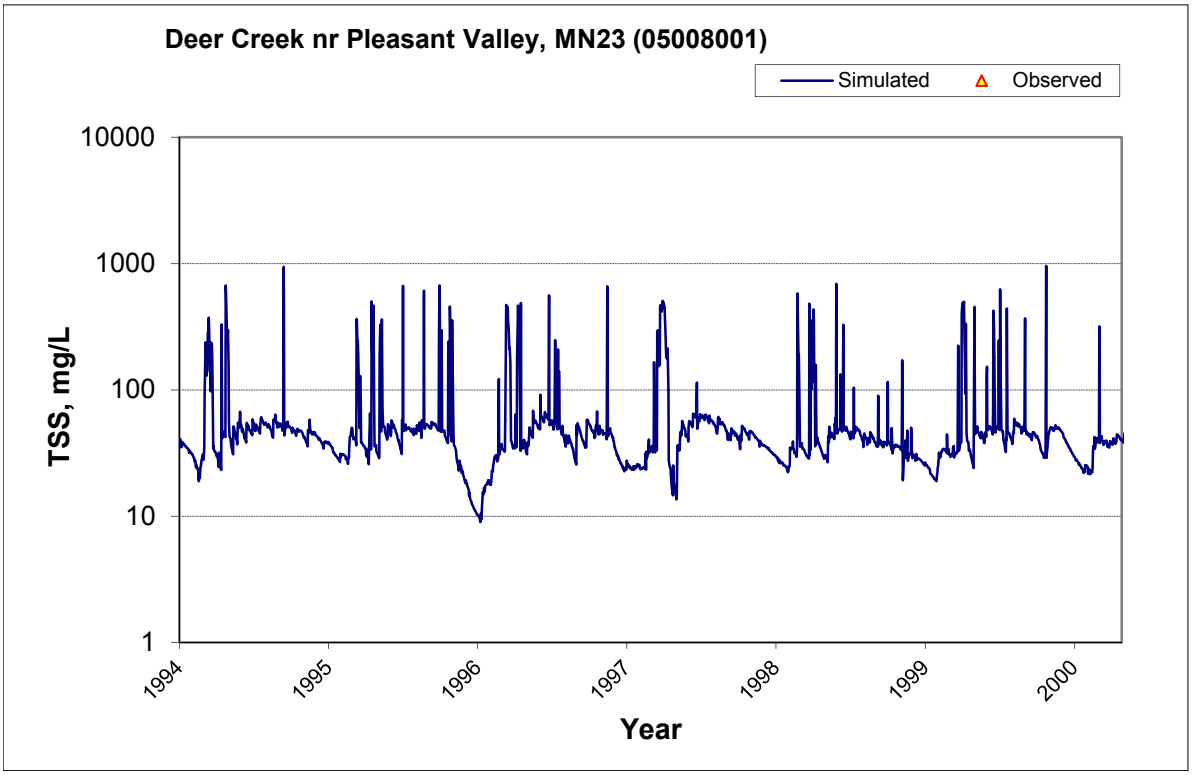

Figure E-36. TSS Concentration Time Series, Deer Creek nr Pleasant Valley, MN23 (05008001), 1994-2000

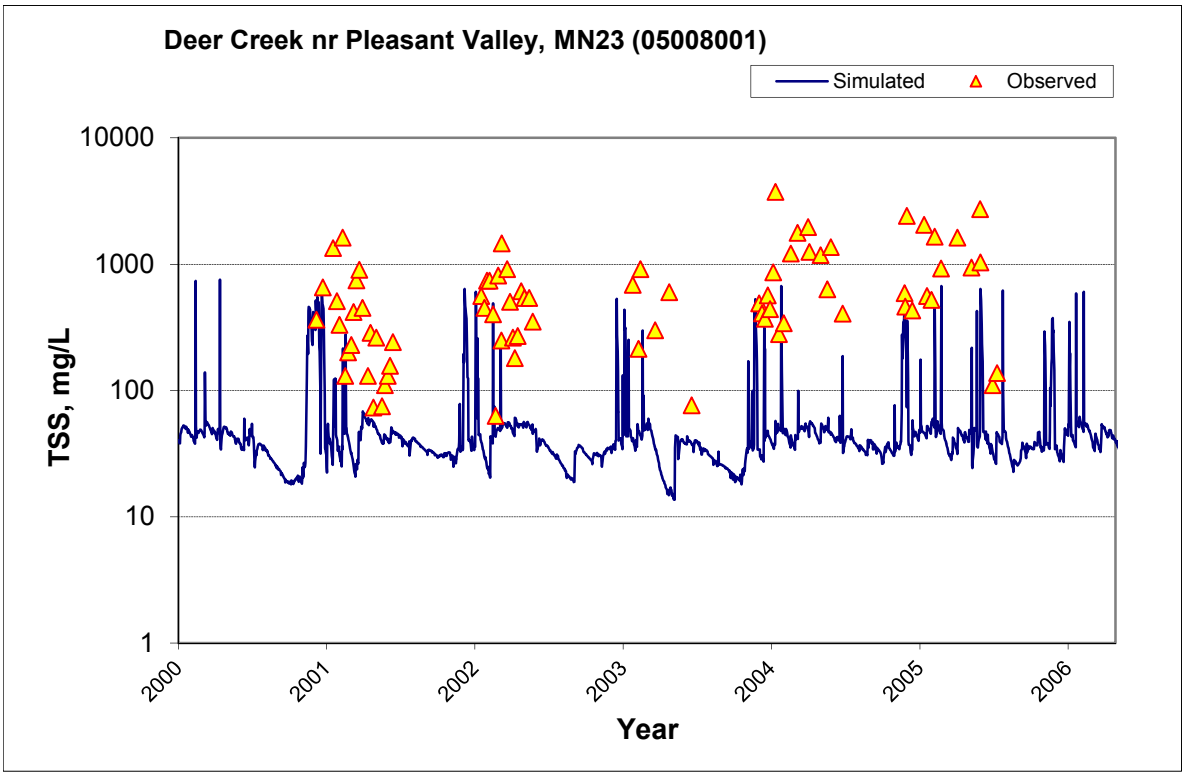

Figure E-37. TSS Concentration Time Series, Deer Creek nr Pleasant Valley, MN23 (05008001), 2000-2006

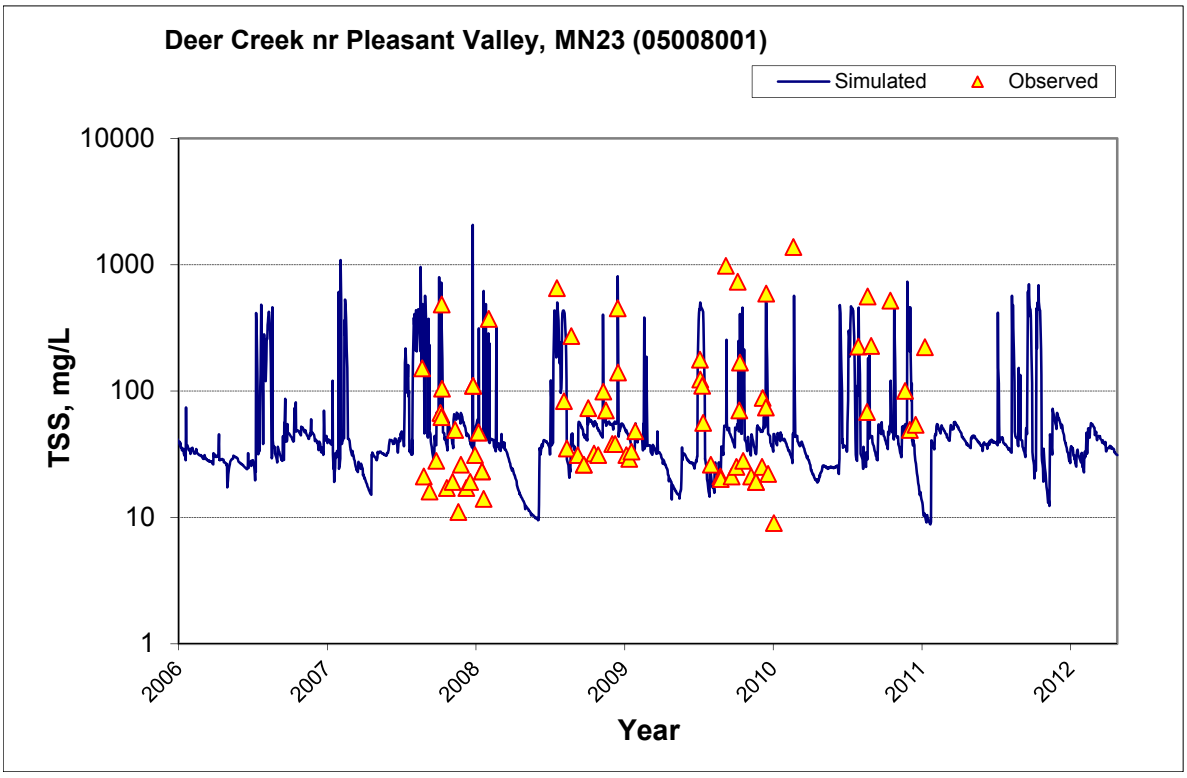

Figure E-38. TSS Concentration Time Series, Deer Creek nr Pleasant Valley, MN23 (05008001), 2006-2012

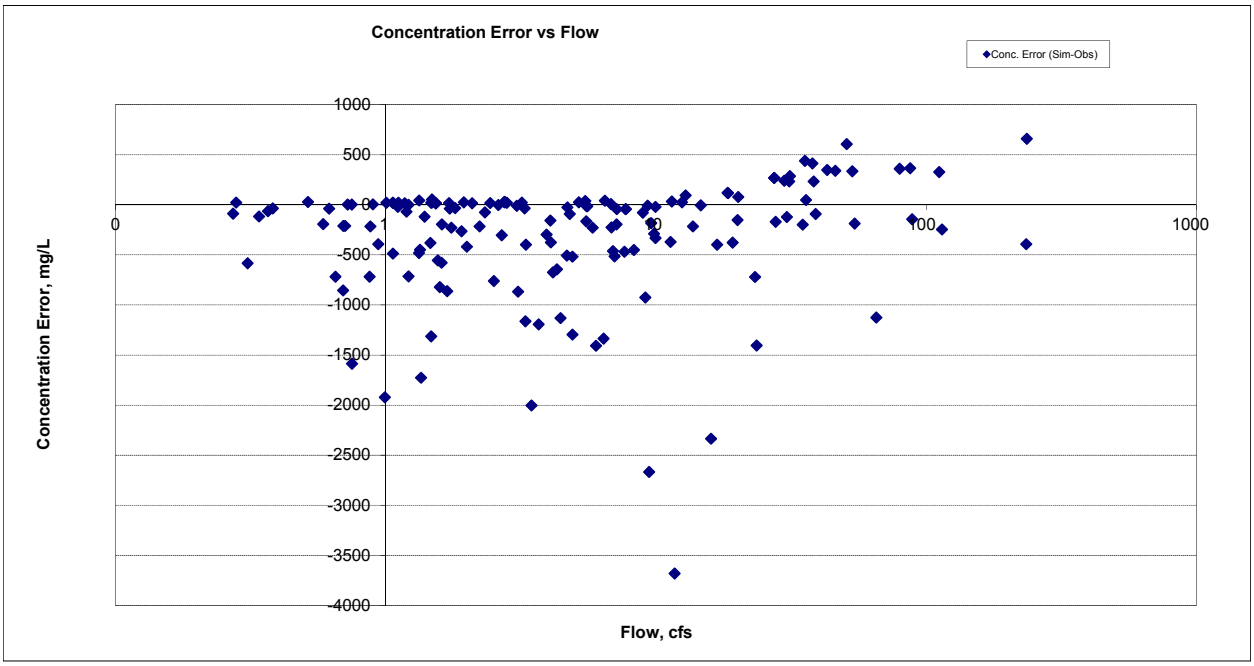

Figure E-39. TSS Concentration, Residual vs. Flow, Deer Creek nr Pleasant Valley, MN23 (05008001)

Deer Creek nr Pleasant Valley, CSAH3 (05008002)

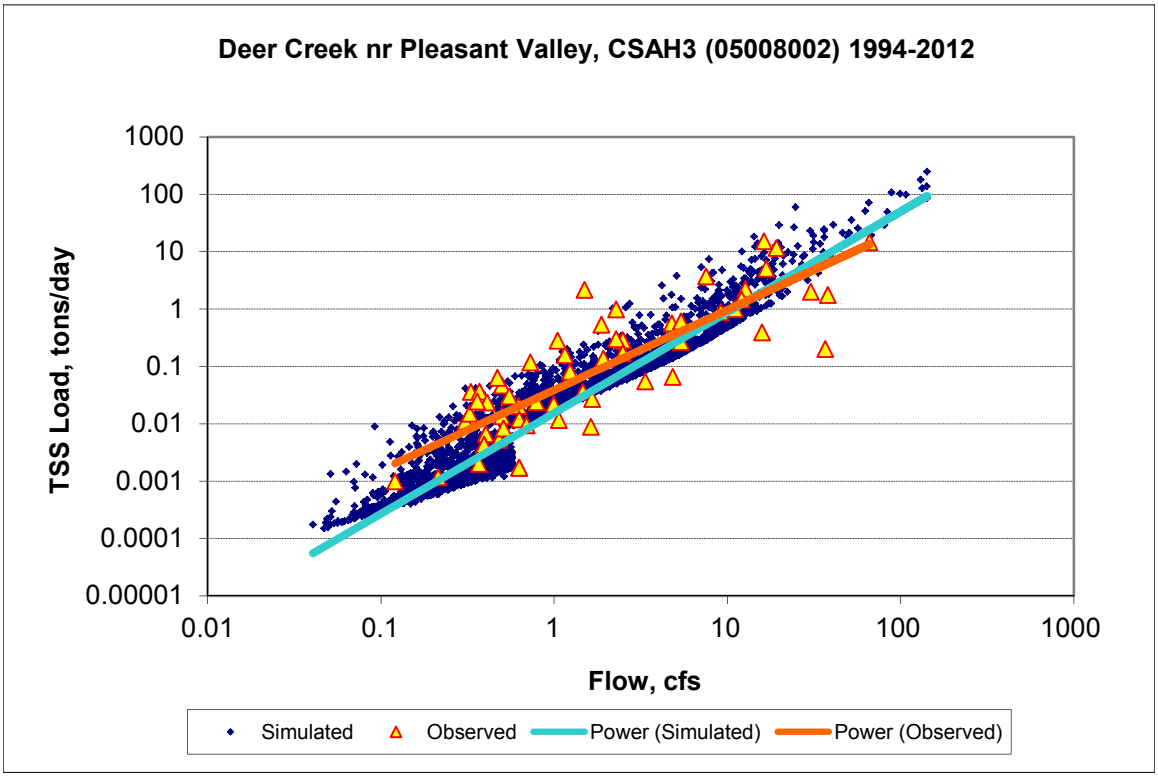

Figure E-40. TSS Load Power Plot, Deer Creek nr Pleasant Valley, CSAH3 (05008002)

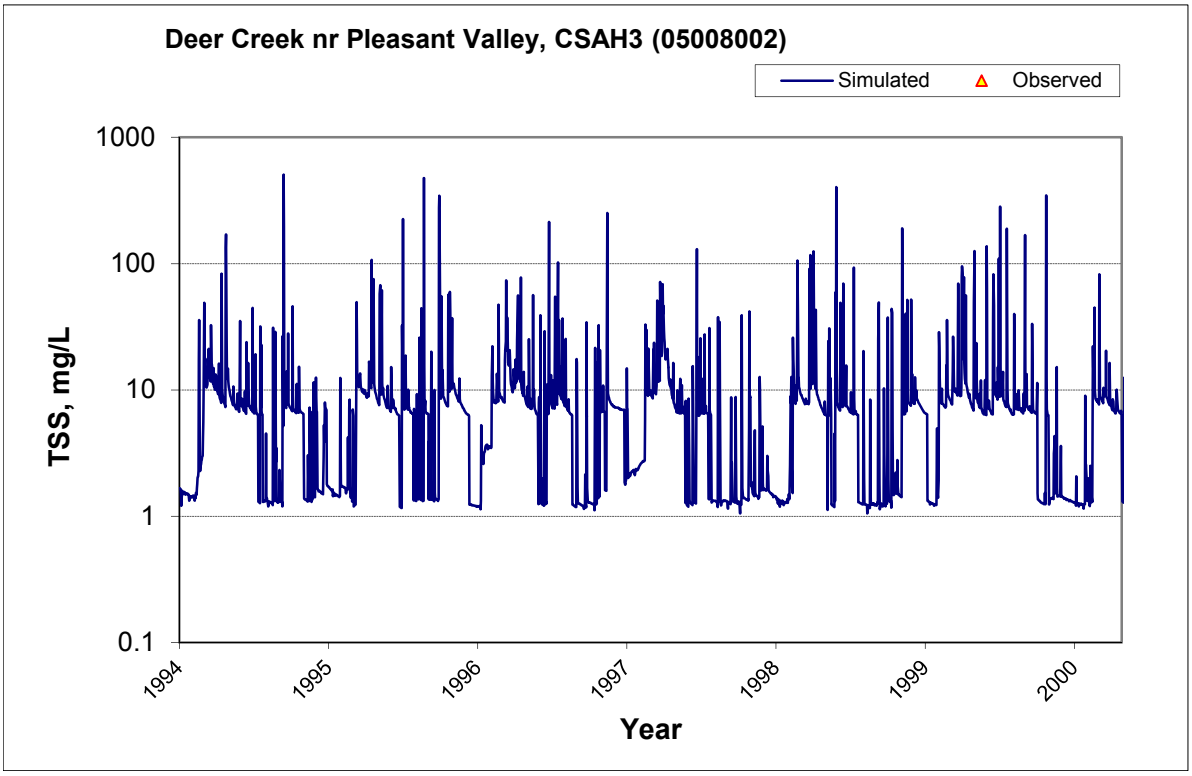

Figure E-41. TSS Concentration Time Series, Deer Creek nr Pleasant Valley, CSAH3 (05008002), 1994-2000

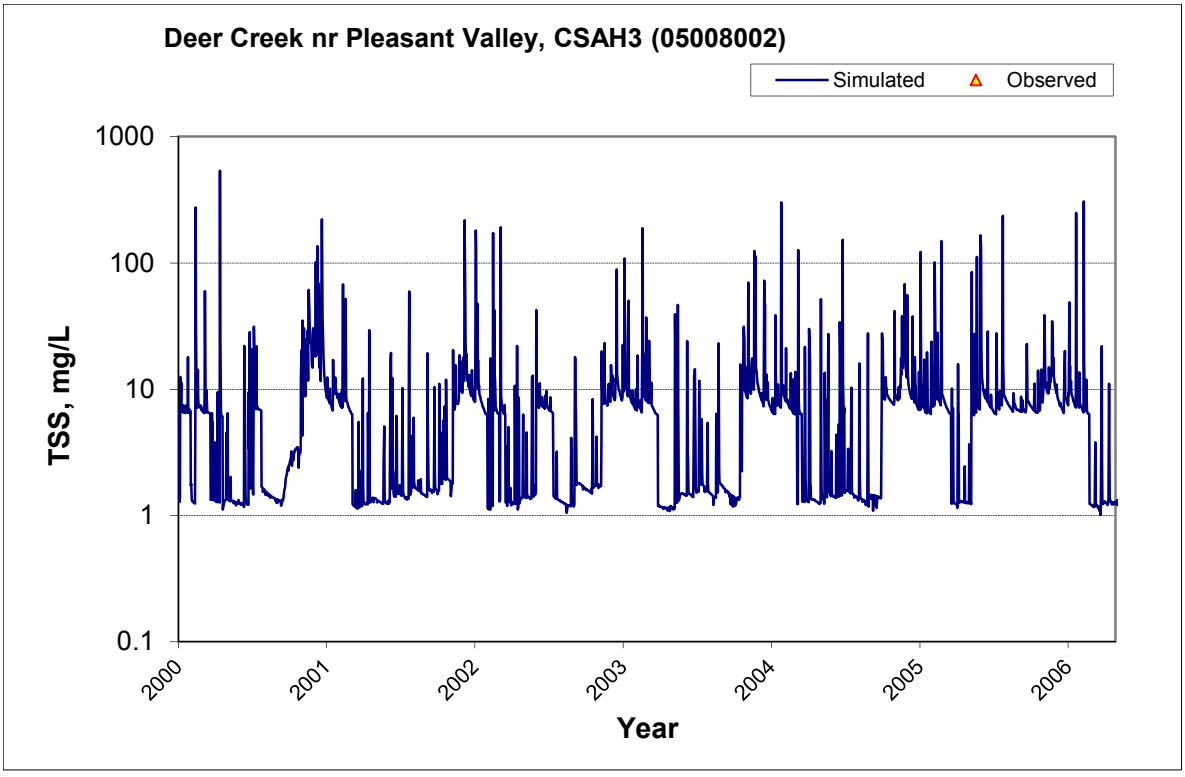

Figure E-42. TSS Concentration Time Series, Deer Creek nr Pleasant Valley, CSAH3 (05008002), 2000-2006

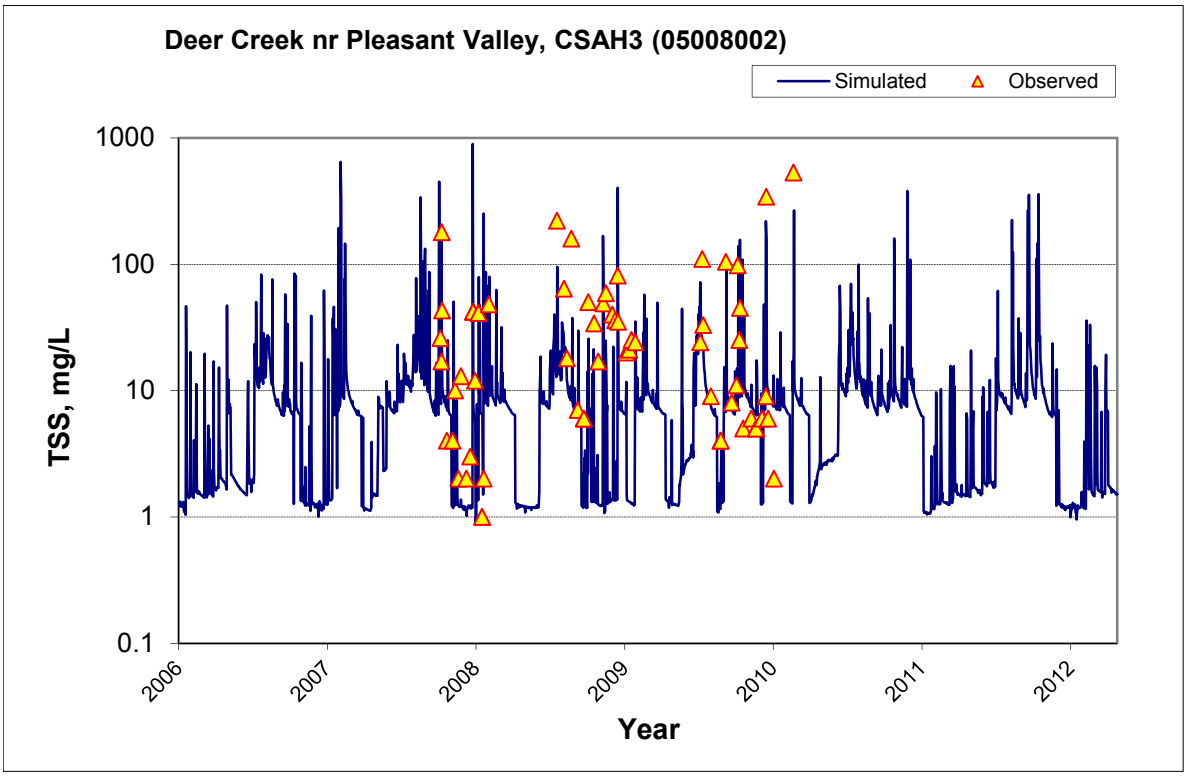

Figure E-43. TSS Concentration Time Series, Deer Creek nr Pleasant Valley, CSAH3 (05008002), 2006-2012

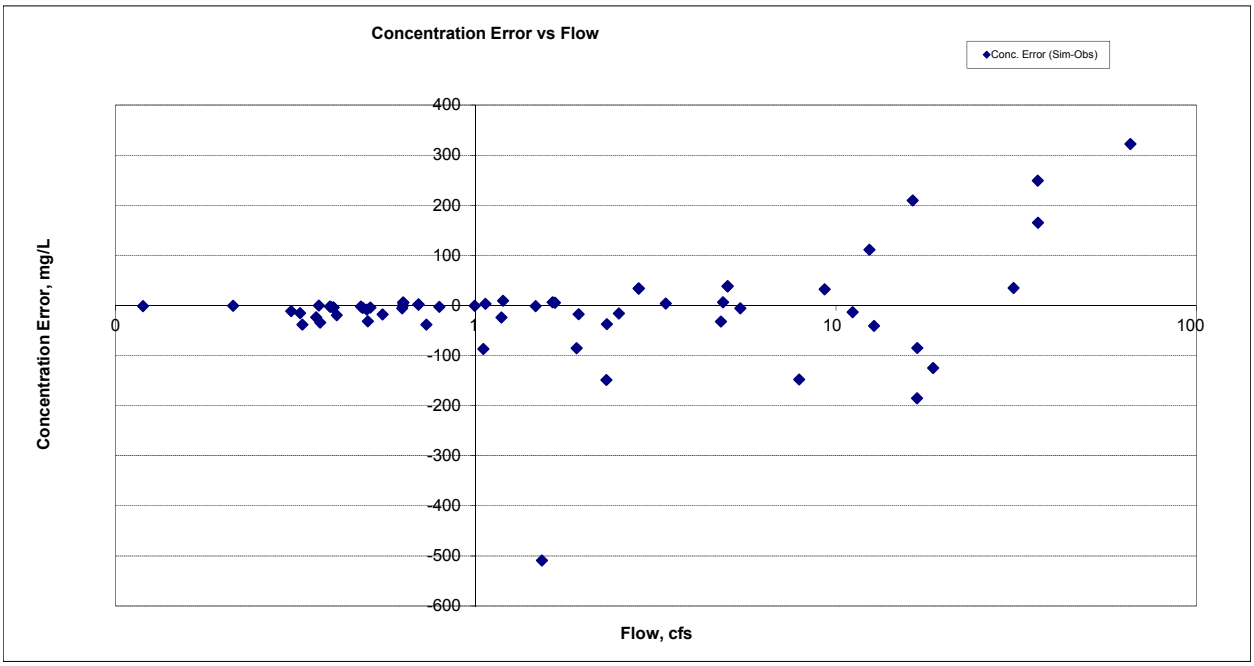

Figure E-44. TSS Concentration, Residual vs. Flow, Deer Creek nr Pleasant Valley, CSAH3 (05008002)

Rock Creek nr Pleasant Valley (05009001)

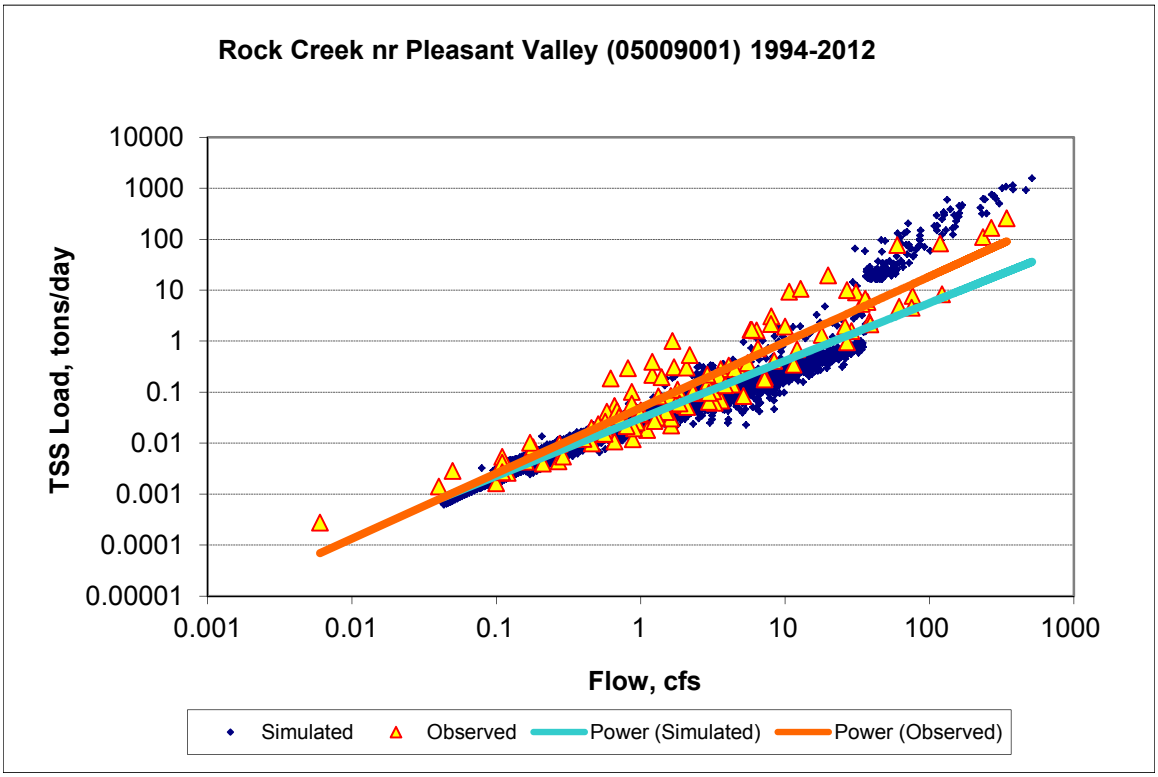

Figure E-45. TSS Load Power Plot, Rock Creek nr Pleasant Valley (05009001)

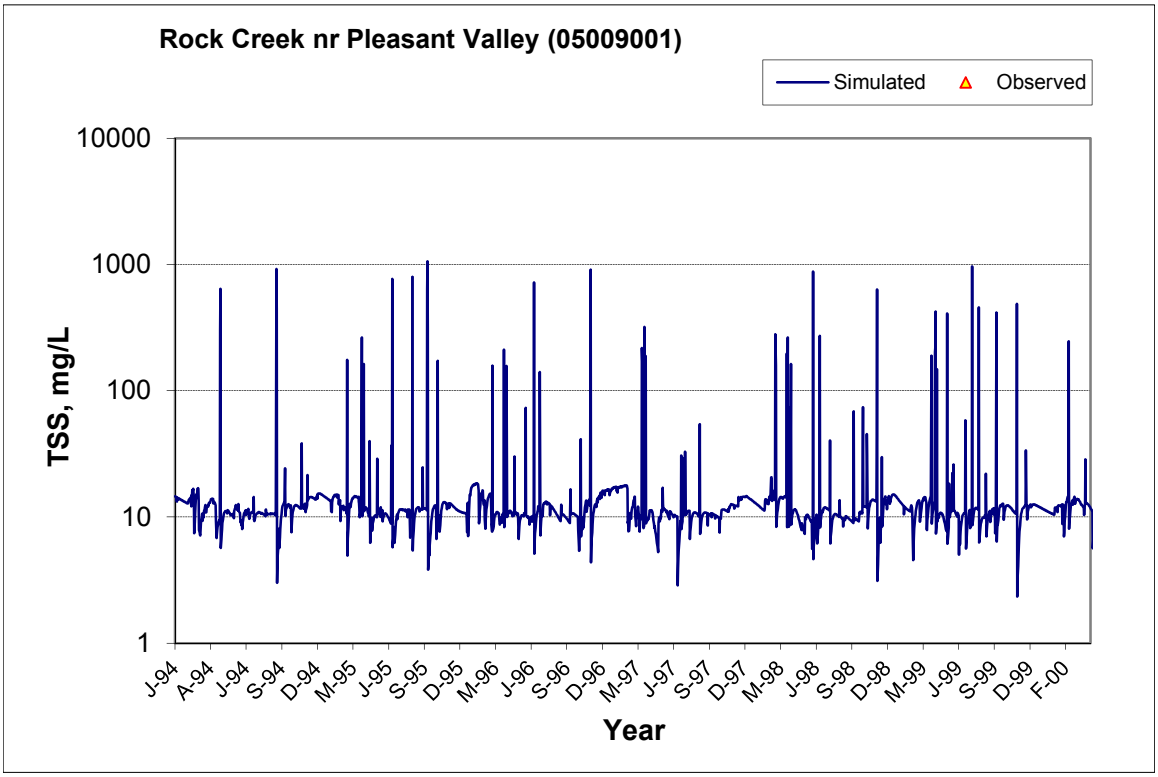

Figure E-46. TSS Concentration Time Series, Rock Creek nr Pleasant Valley (05009001), 1994-2000

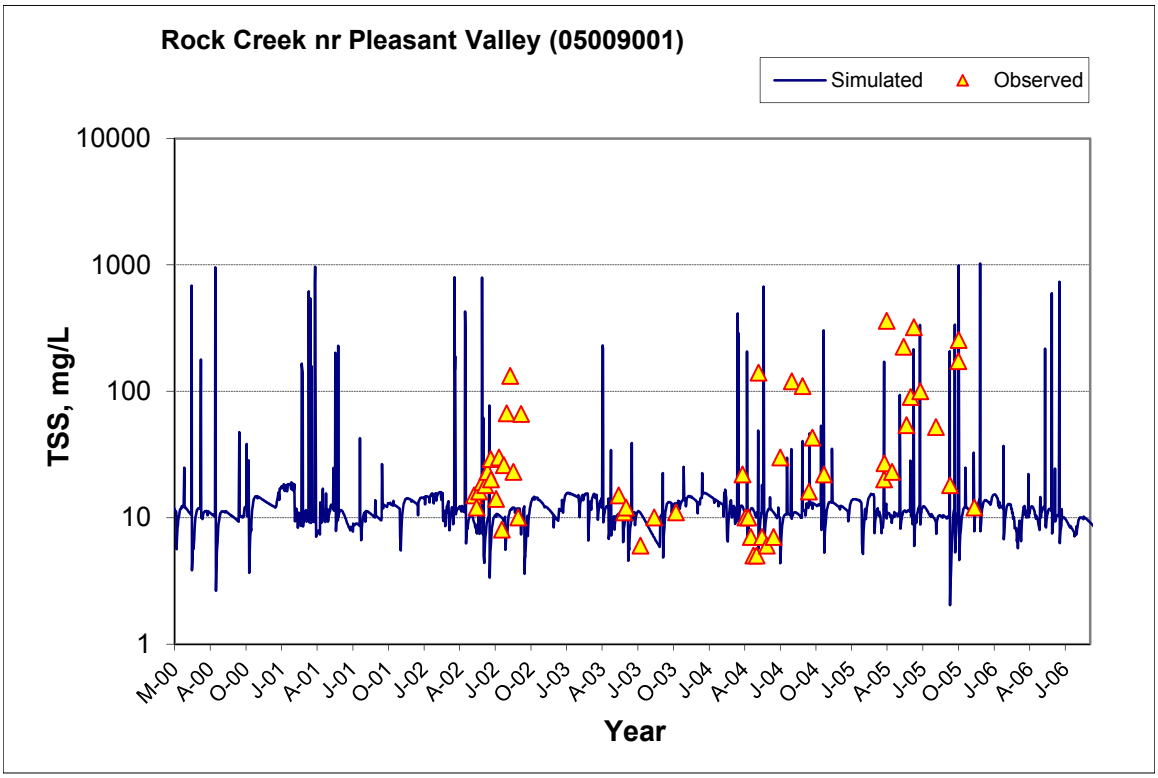

Figure E-47. TSS Concentration Time Series, Rock Creek nr Pleasant Valley (05009001), 2000-2006

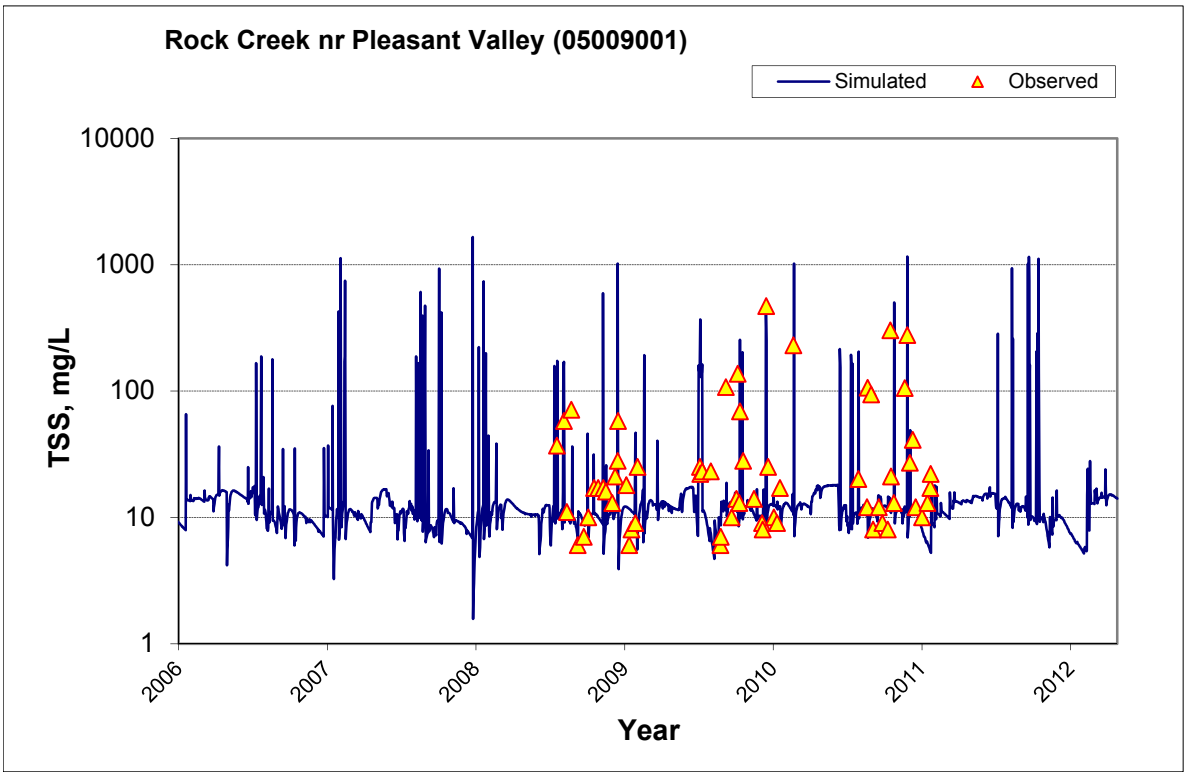

Figure E-48. TSS Concentration Time Series, Rock Creek nr Pleasant Valley (05009001), 2006-2012

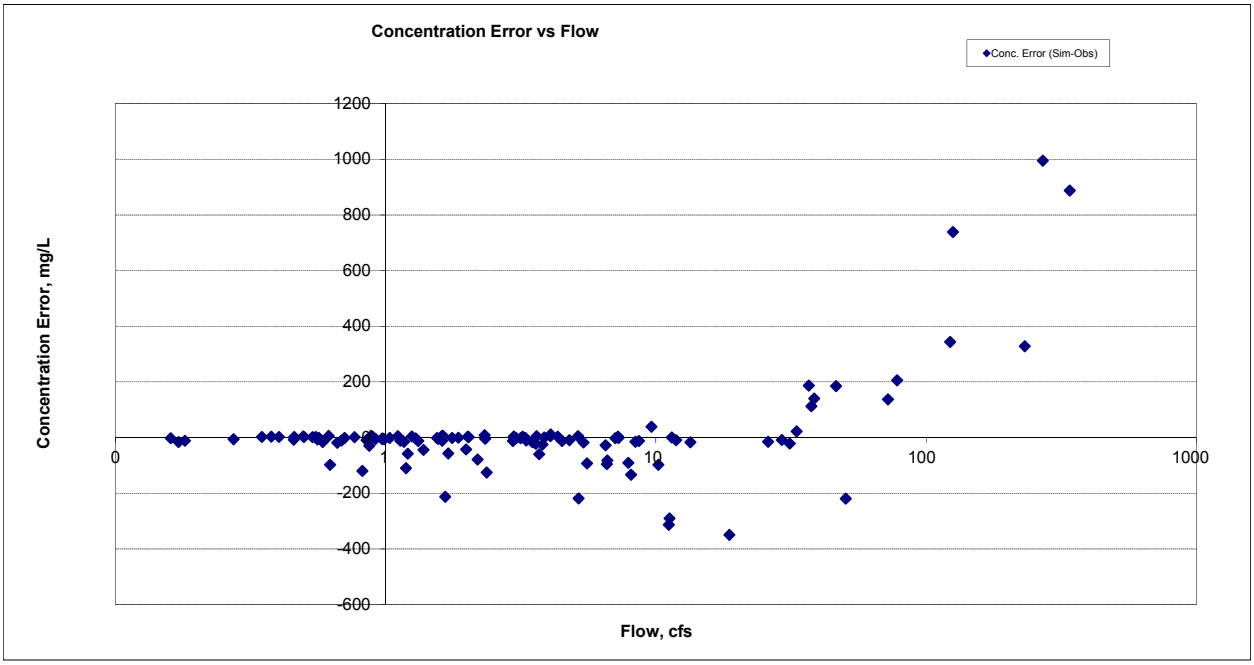

Figure E-49. TSS Concentration, Residual vs. Flow, Rock Creek nr Pleasant Valley (05009001)

Nemadji River nr Pleasant Valley (05011001)

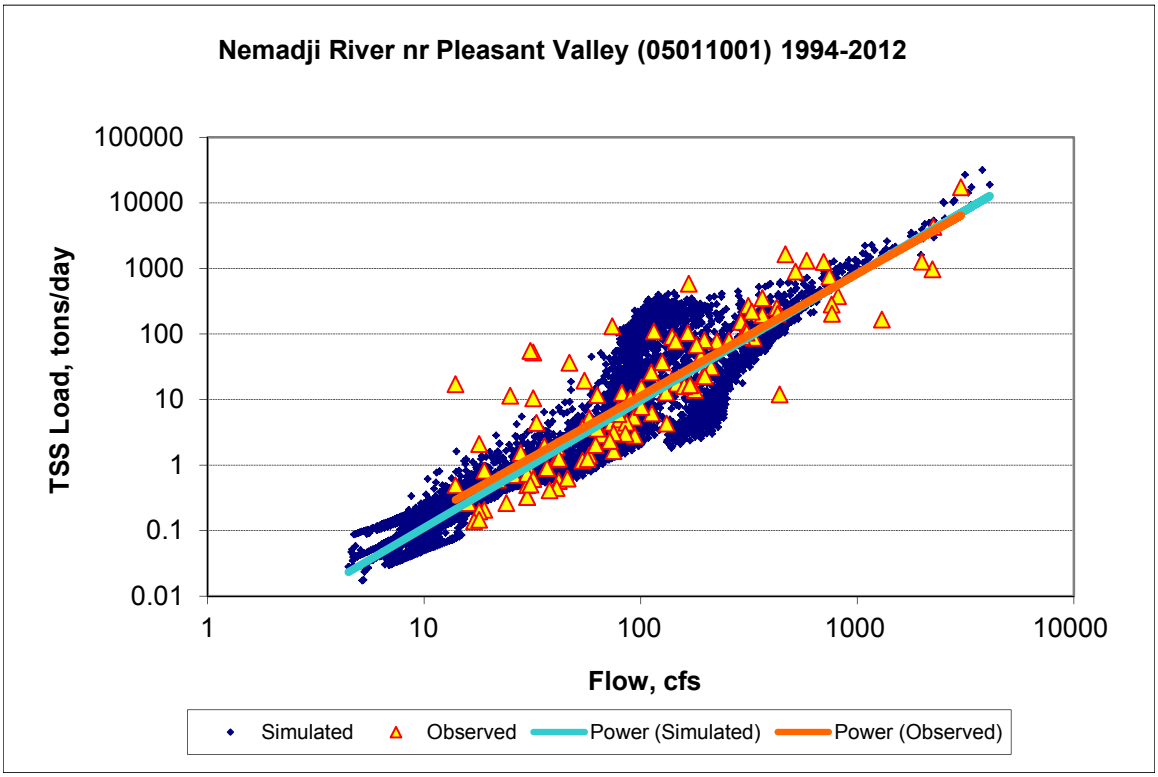

Figure E-50. TSS Load Power Plot, Nemadji River nr Pleasant Valley (05011001)

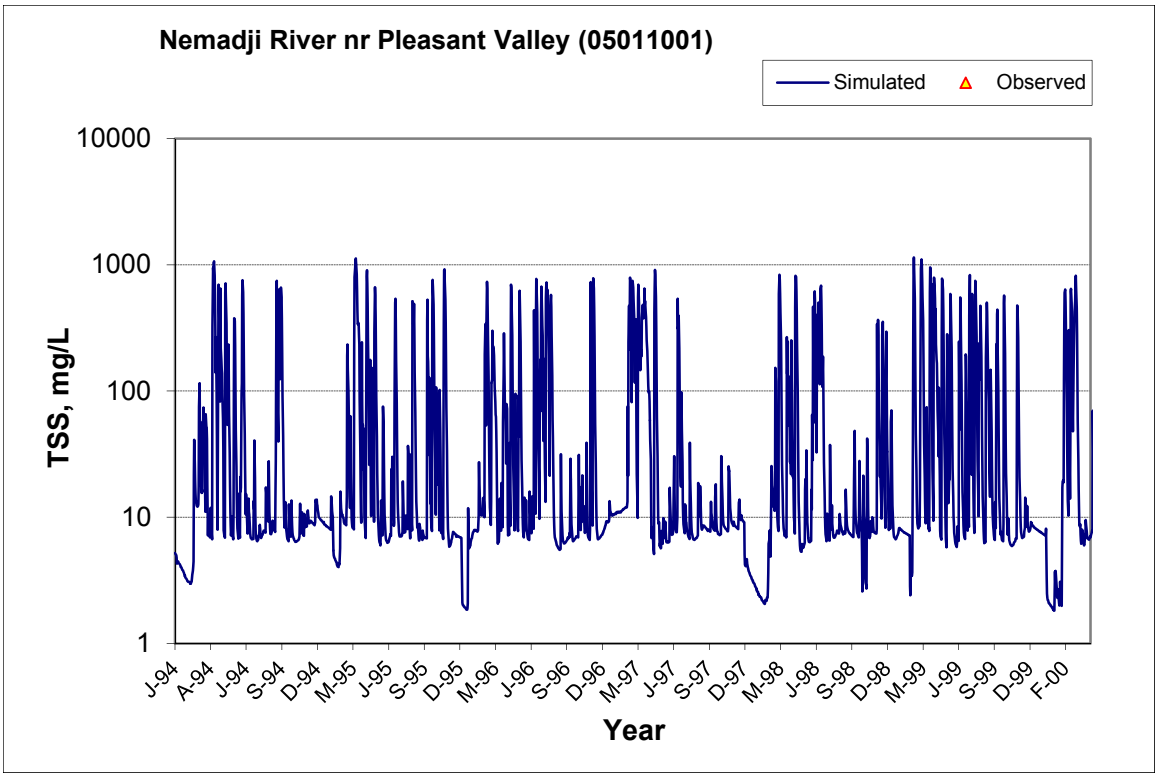

Figure E-51. TSS Concentration Time Series, Nemadji River nr Pleasant Valley (05011001), 1994-2000

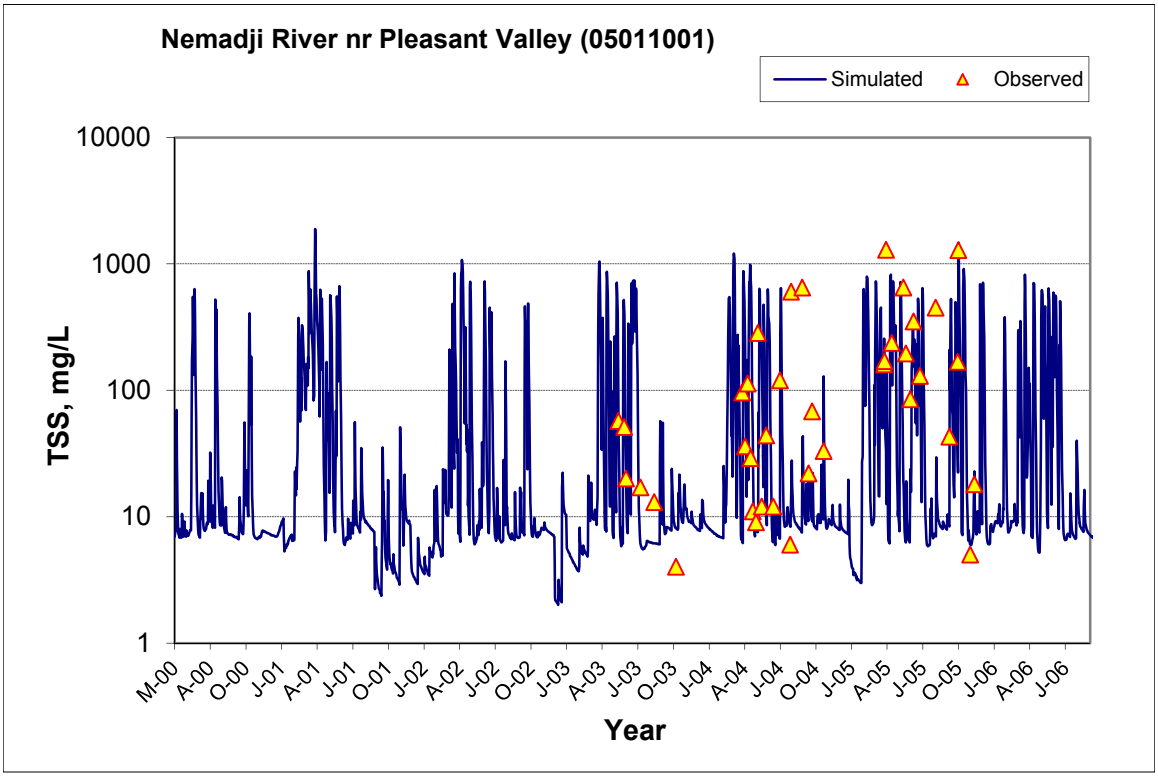

Figure E-52. TSS Concentration Time Series, Nemadji River nr Pleasant Valley (05011001), 2000-2006

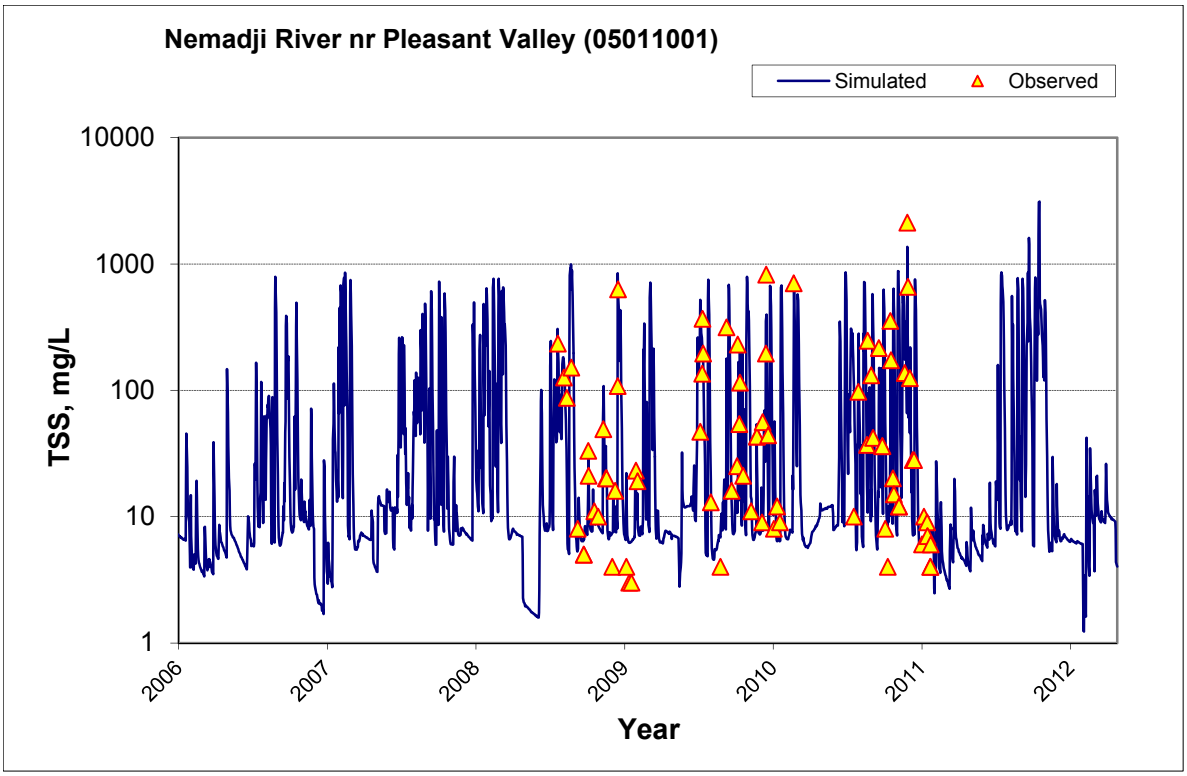

Figure E-53. TSS Concentration Time Series, Nemadji River nr Pleasant Valley (05011001), 2006-2012

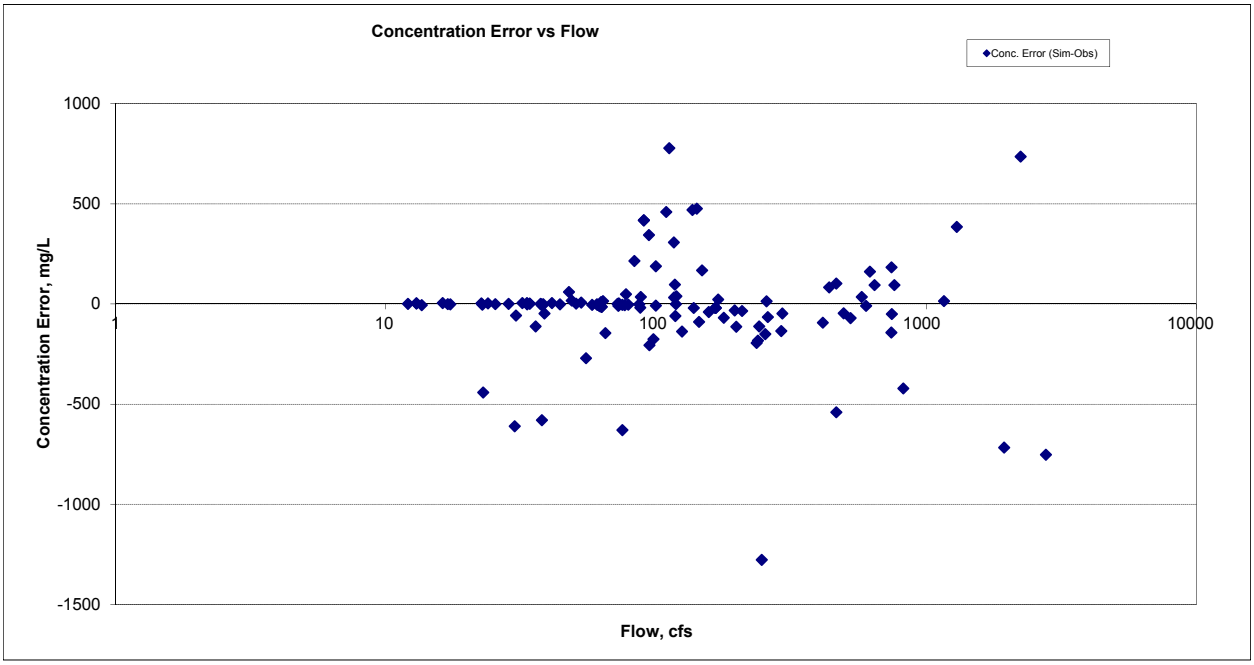

Figure E-54. TSS Concentration, Residual vs. Flow, Nemadji River nr Pleasant Valley (05011001)

Nemadji River nr South Superior, WI (05011002)

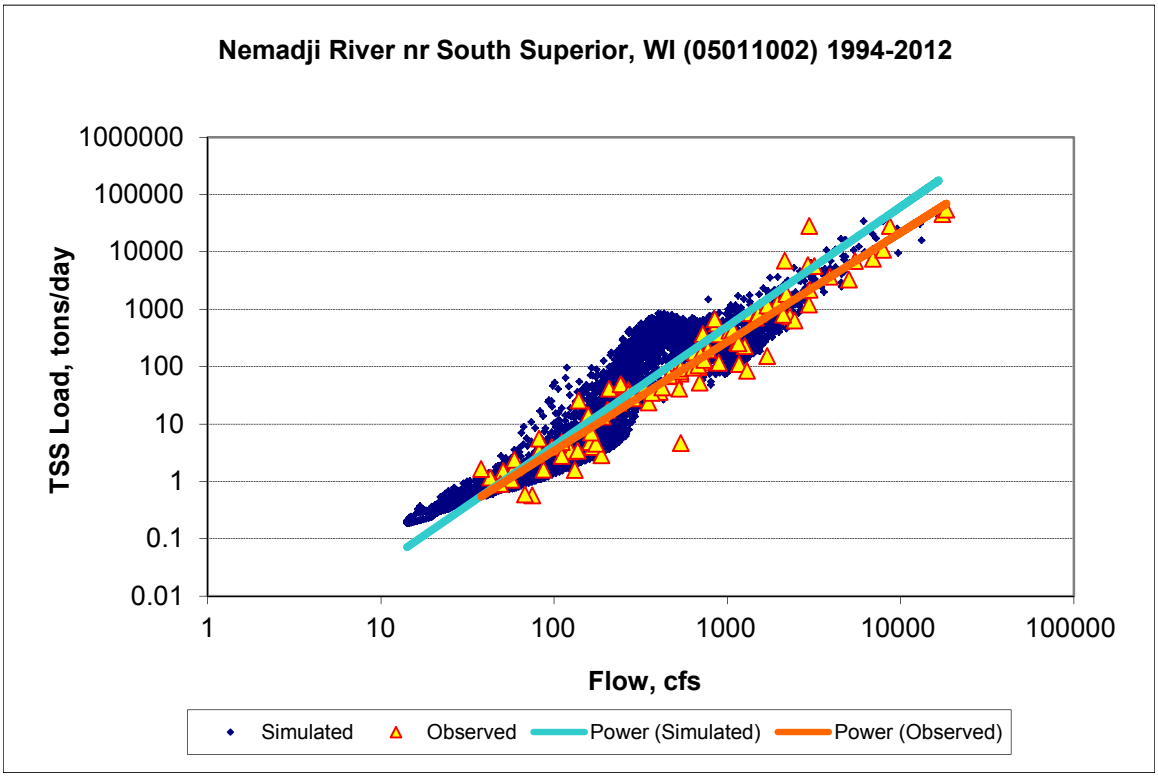

Figure E-55. TSS Load Power Plot, Nemadji River nr South Superior, WI (05011002)

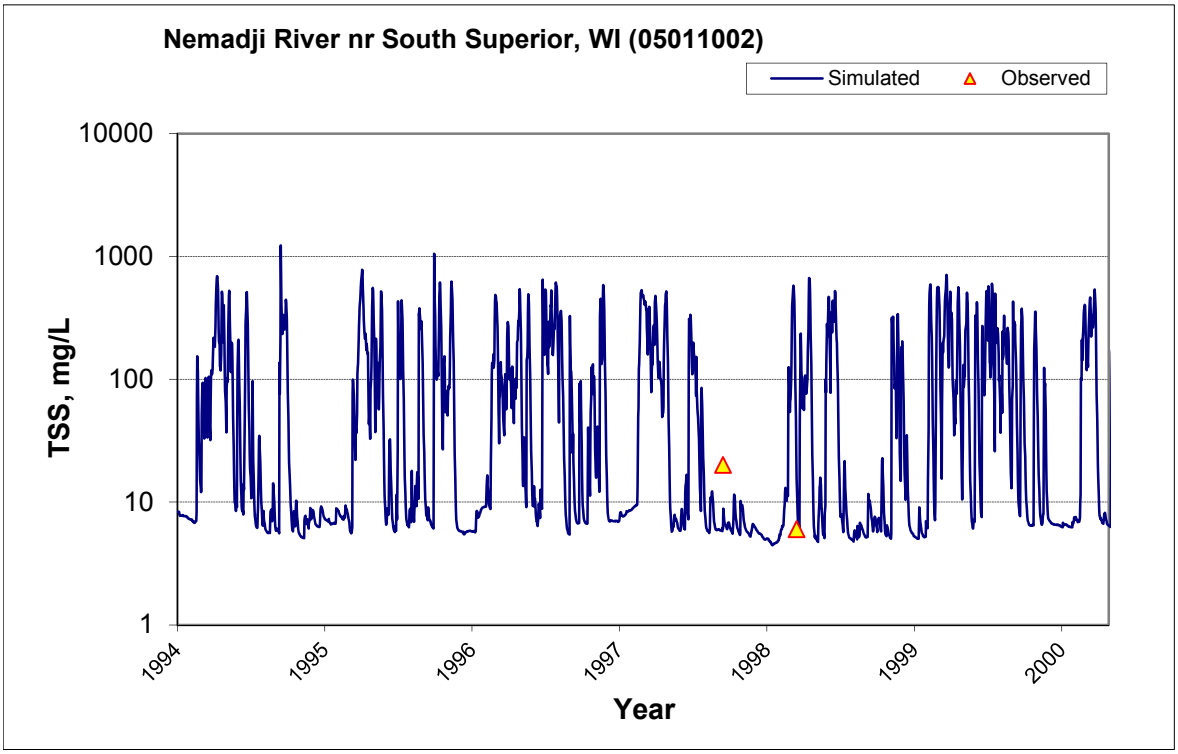

Figure E-56. TSS Concentration Time Series, Nemadji River nr South Superior, WI (05011002), 1994-2000

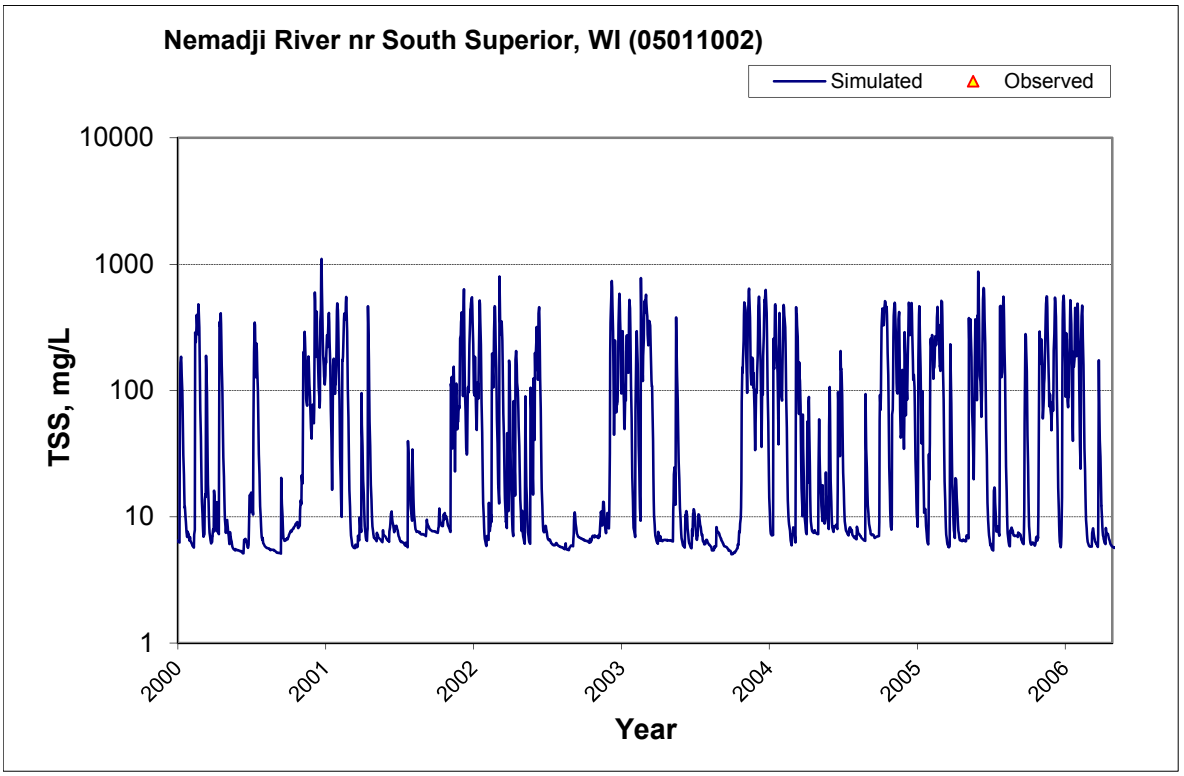

Figure E-57. TSS Concentration Time Series, Nemadji River nr South Superior, WI (05011002), 1994-2006

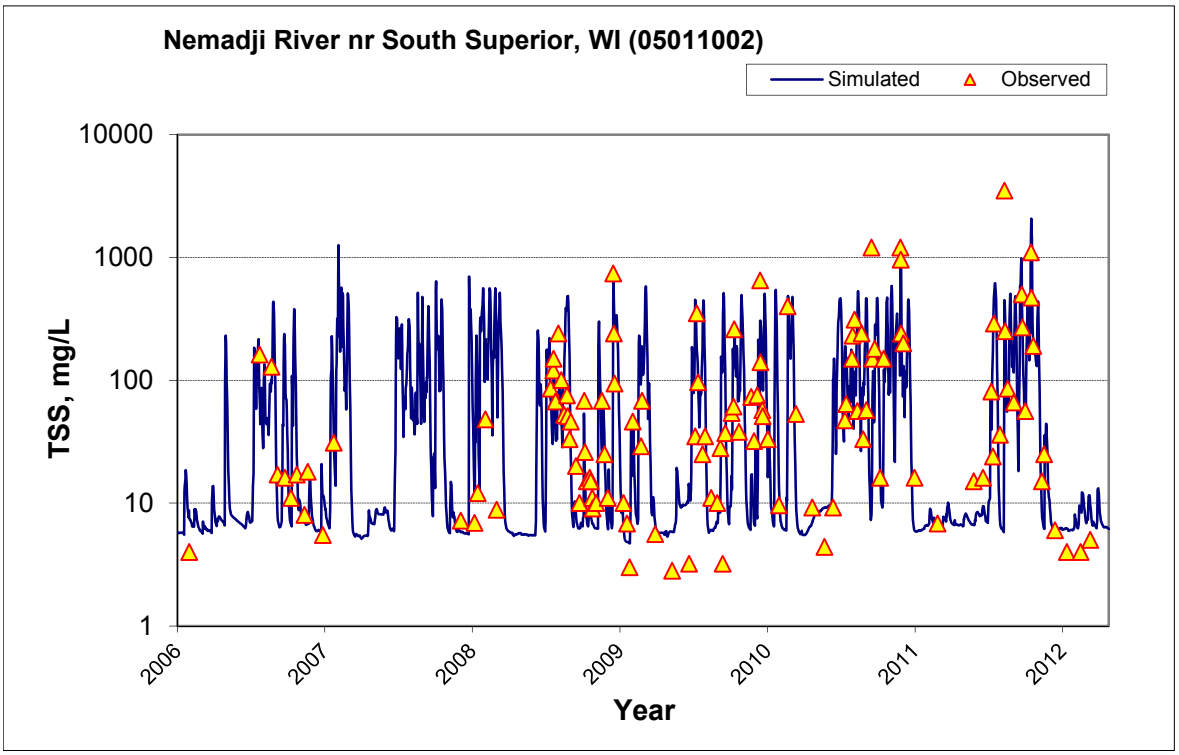

Figure E-58. TSS Concentration Time Series, Nemadji River nr South Superior, WI (05011002), 2006-2012

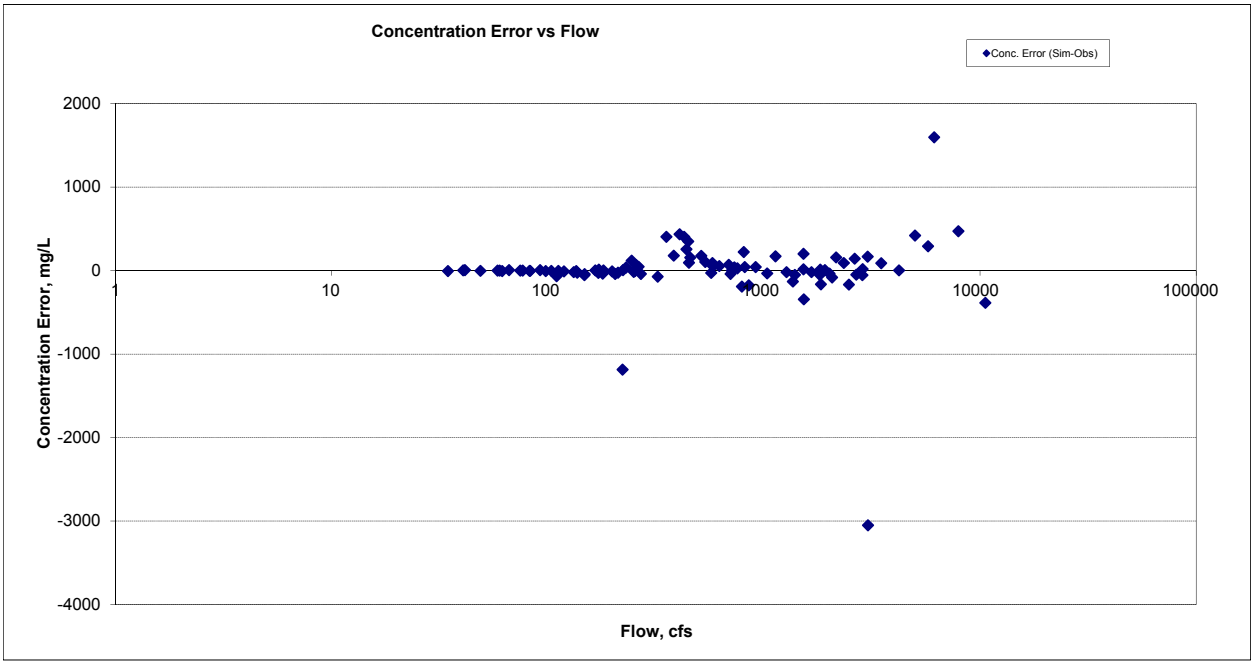

Figure E-59. TSS Concentration, Residual vs. Flow, Nemadji River nr South Superior, WI (05011002)

Nemadji River nr Holyoke (05016001)

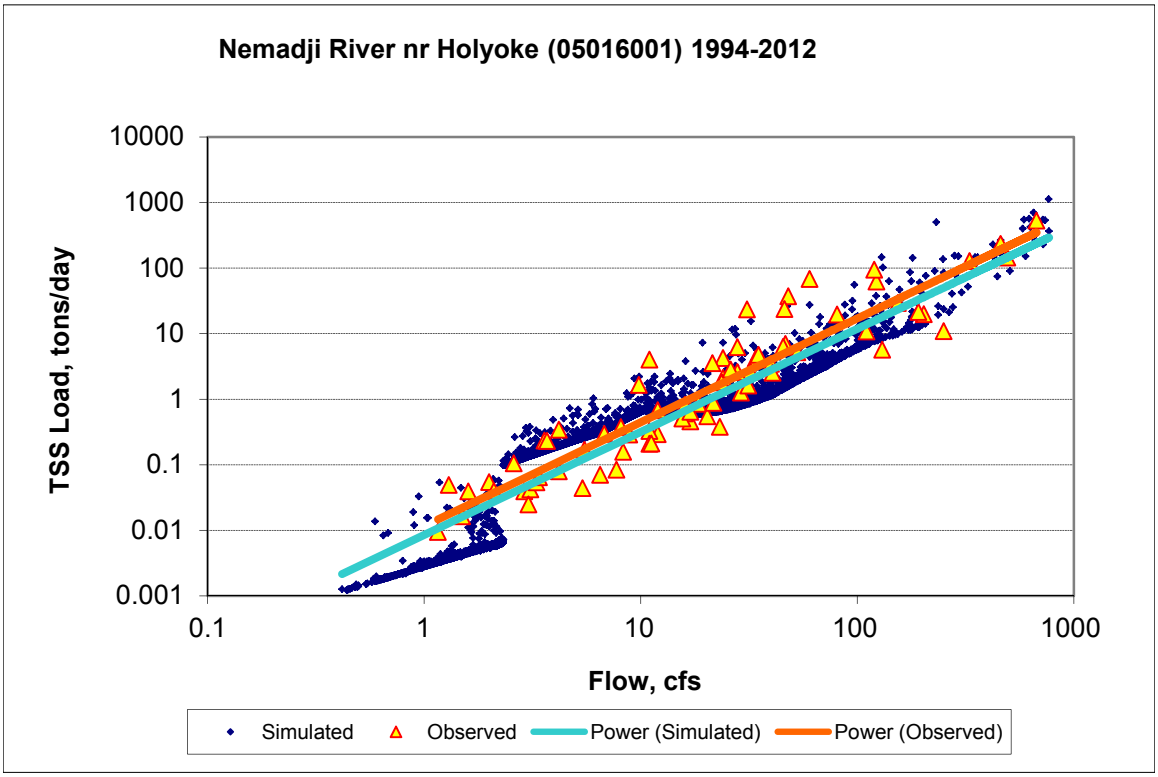

Figure E-60. TSS Load Power Plot, Nemadji River nr Holyoke (05016001)

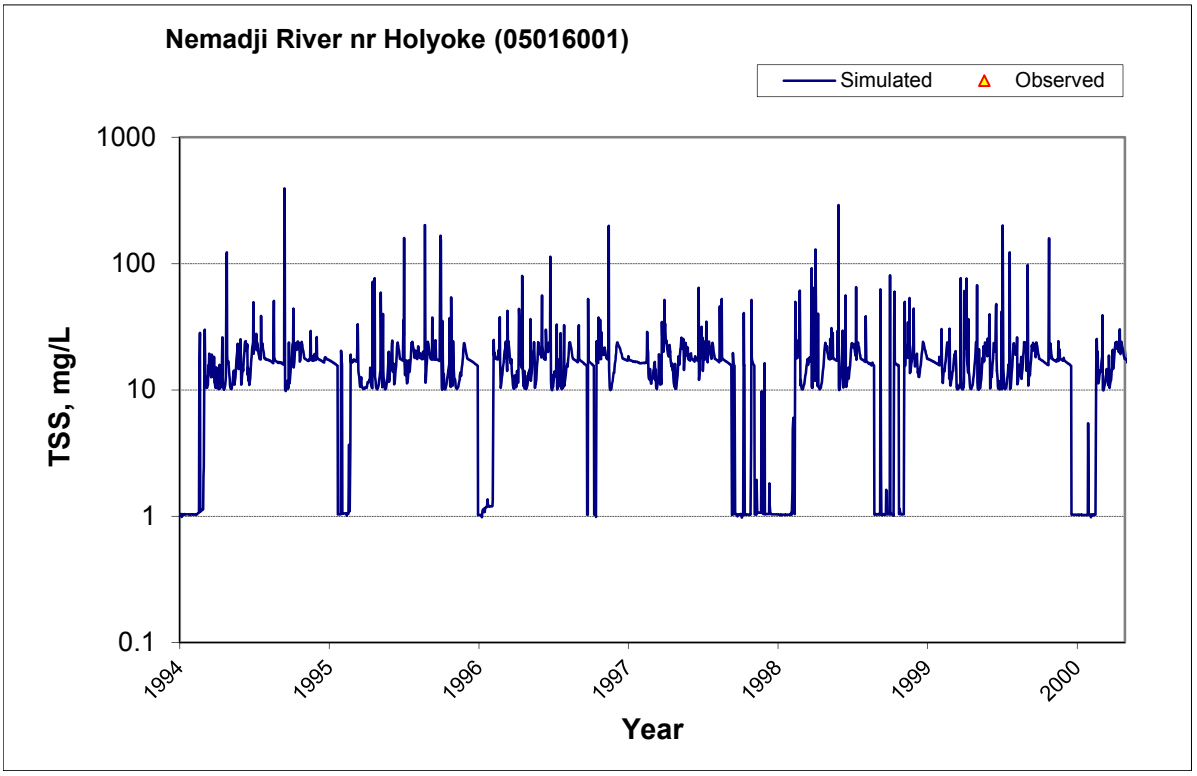

Figure E-61. TSS Concentration Time Series, Nemadji River nr Holyoke (05016001), 1994-2000

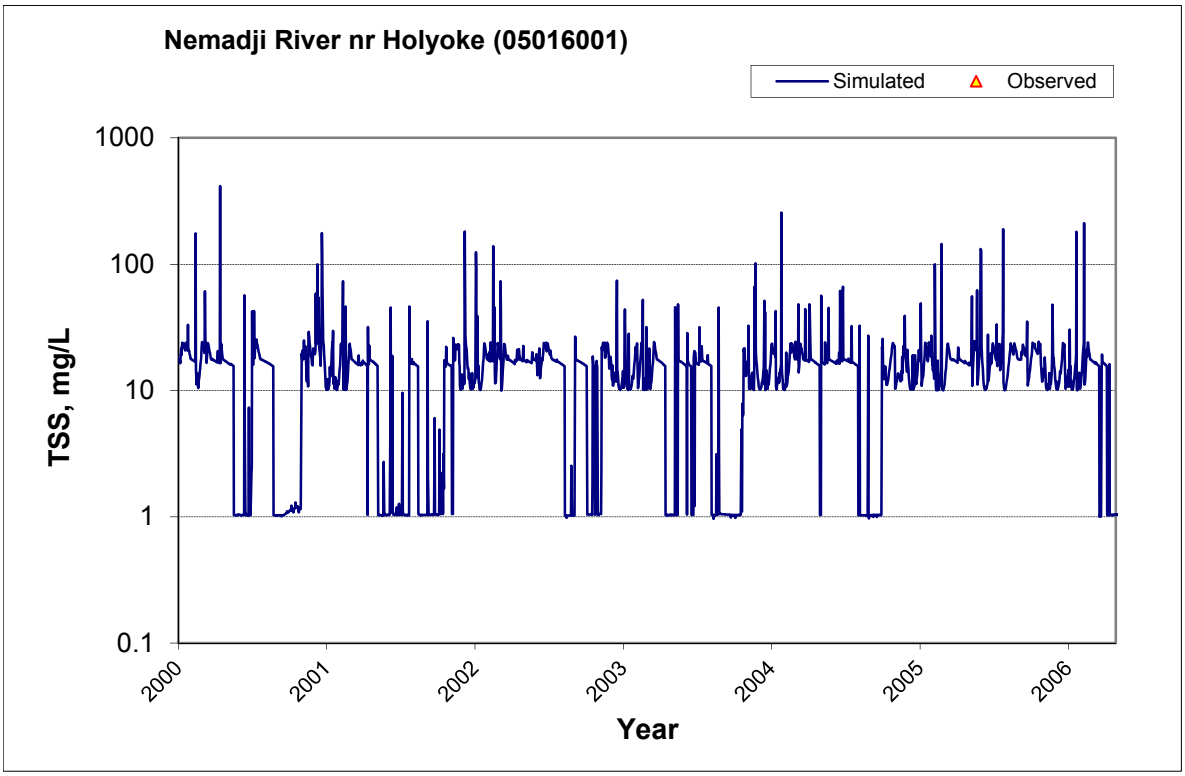

Figure E-62. TSS Concentration Time Series, Nemadji River nr Holyoke (05016001), 2000-2006

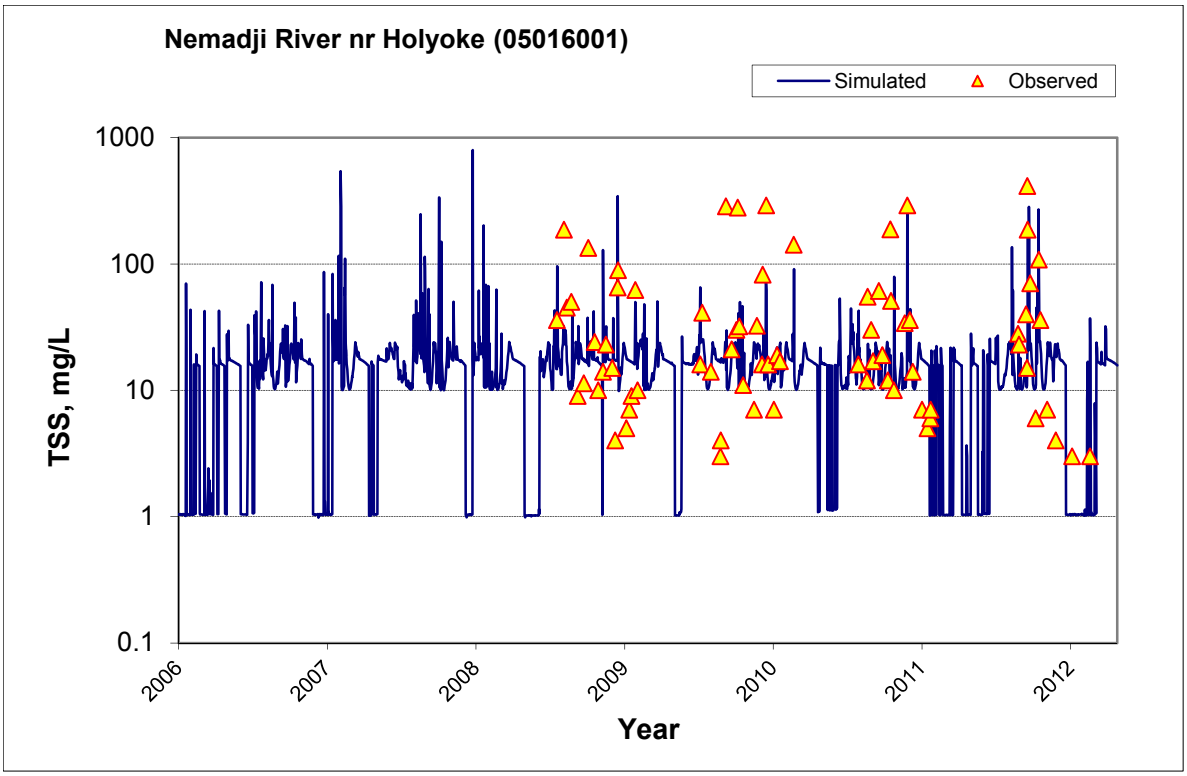

Figure E-63. TSS Concentration Time Series, Nemadji River nr Holyoke (05016001), 2006-2012

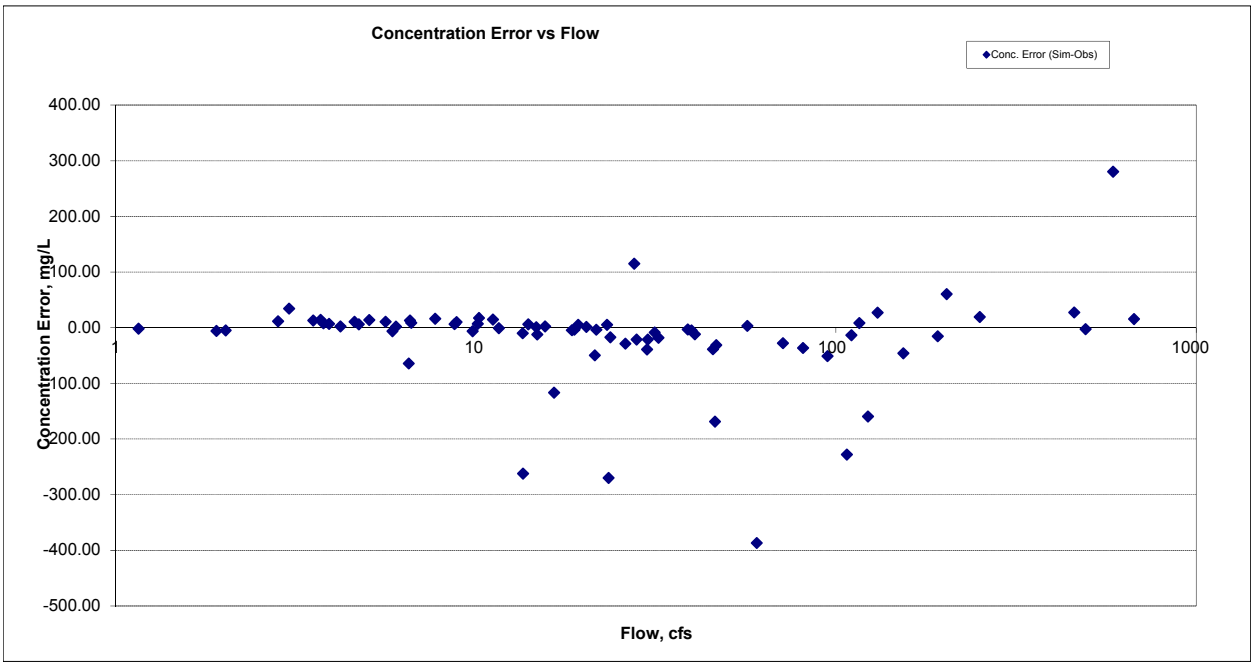

Figure E-64. TSS Concentration, Residual vs. Flow, Nemadji River nr Holyoke (05016001)

(This page left intentionally blank.)

St. Louis, Cloquet, and Nemadji River Basin Models

Volume 2
Water Quality Calibration

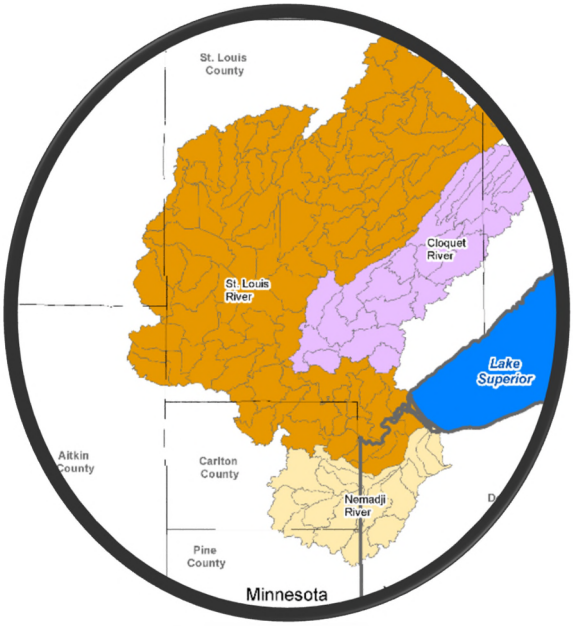

Prepared for

Minnesota Pollution Control Agency

Prepared by

TETRA TECH

One Park Drive, Suite 200 • PO Box 14409
Research Triangle Park, NC 27709

REVIEW DRAFT

January 18, 2016

(This page left intentionally blank.)

Table of Contents

List of Tables

List of Figures

(This page left intentionally blank.)

1 Introduction

This report is presented as Volume 2 in a set of reports that document the calibration and validation of watershed hydrology and water quality simulation models for three major watersheds in northeastern Minnesota – The St. Louis, Cloquet, and Nemadji River watersheds. Volume 1 addressed model setup and the calibration for hydrology and sediment transport. That report was initially released in 2014, but is being updated to reflect several changes in the model, including corrections to mining discharges and additional sub-basin discretization to represent some individual lakes of interest. This report (Volume II) documents the water quality calibration and validation.

The work described in this report is consistent with the objectives of Minnesota's One Water program, which seeks to develop operational hydrology and water quality simulation models of all major watershed (8-digit hydrologic unit code [HUC] watersheds) within the state. These are basin-scale models, with sub-basin resolution resolved down to the approximately 12-digit HUC level. Models at this scale are most useful for addressing basin-scale management questions, such as the impacts of land use change within the basin on loadings of sediment and nutrients to Duluth Harbor and Lake Superior. Local-scale issues, such as headcuts in stream segments in the Nemadji River basin or streams with locally depressed dissolved oxygen in the St. Louis River basin are addressed in the model through relatively broad-scale approximations; however, development of models at finer spatial scales may needed to correctly address localized environmental problems.

The simulation model is implemented, developed, and calibrated for the period of 1995 – 2012. Unfortunately, monitoring data are somewhat limited for this period. For various parts of the St. Louis River watershed there was intensive water quality monitoring during the 1970s and 1980s that was subsequently discontinued. For both the St. Louis and Nemadji watersheds where has been extensive data collection during the 2012 to present period in support of stressor identification and development of a Watershed Restoration and Protection Strategy (WRAPS) for these basins. Concurrent with this work, Minnesota Department of Natural Resources (MDNR) has funded an effort to extend the St. Louis, Cloquet, and Nemadji models through the end of 2014. This requires updating of meteorology input files as well as records of waste discharges, water appropriations, atmospheric deposition, and managed releases from reservoirs. Once this effort is completed the model can be compared against additional monitoring data and the water quality calibration improved.

(This page left intentionally blank.)

2 Water Quality Calibration Approach

Water quality simulation depends on the simulation of hydrology and sediment transport. Those aspects of the model are documented in detail in Volume 1 of this set. This section addresses the calibration and validation of the model simulation of water temperature, dissolved oxygen, nutrients, and algae.

Although not a primary focus of the modeling effort, water temperature simulation is important in the watershed model for several reasons: water temperature affects many biologically mediated processes that influence water quality in the streams, and the temperature of the water determines how it will mix when it enters the lake.

Daily average water temperature in shallow flowing streams is largely controlled by air temperature. Temperature cycles within the day, however, may be strongly affected by heat gain from incoming solar radiation and heat loss due to longwave back radiation. Both of these effects are controlled by the extent of cover and shading on the stream in addition to meteorological variables such as solar radiation and cloud cover.

A detailed diel simulation of stream water temperature is a complex undertaking. The timing and magnitude of heat fluxes are controlled by a variety of factors such as stream orientation and vegetative and topographic shading angles that cannot be fully represented in a basin-scale HSPF model. For example, a stream oriented east-west is likely to be exposed to unshaded solar radiation for a longer part of the day than a stream oriented north-south. Stream shading varies over the course of the year as canopy density changes, and may also change over time as trees grow, are cut, fall due to ice and wind storms, or due to fire. HSPF approximates all these complex details through the assignment of a temporally constant "surface exposed" (CFSAEX) factor that represents the average fraction of tree-top solar radiation reaching the water surface. Given these issues, the stream temperature calibration was checked for reasonableness, but not constrained to achieve specific statistical targets.

Loading of nutrients that may support excess algal growth is an important concern. The major nutrients controlling algal growth are phosphorus and nitrogen. Both are simulated in detail in the model. Minor nutrients (e.g., silica, iron) may also play a role in determining algal response but are not simulated in the watershed model. (Iron may play an important role in inorganic phosphorus cycling, but is not a direct limiting factor on algal growth in this watershed). The first step in a sequential process for nutrient calibration is to verify that unit area loading rates were reasonable compared to literature values. Next, calibration to instream observations is carried out to refine the simulation. Plant growth has an important effect on nutrient balances during low flow conditions and serves to convert inorganic nutrients into organic forms; therefore, nitrogen and phosphorus species must be calibrated simultaneously with algae.

In forested watersheds, much of the nutrient load moves as a constituent of organic matter (including leaf litter, other debris, and dissolved organic compounds, such as humic acids), while stream concentrations of inorganic nutrients remain low in these watersheds. In contrast, agriculture and fertilized lawns may export significant amounts of nutrients in inorganic forms. Point source discharges can contain a mix of organic and inorganic nutrient forms dependent on the treatment process.

The approach taken is to simulate three components in loading from the land surface as general quality constituents (GQUALs): inorganic nitrogen (nitrate, nitrite, and ammonia), inorganic phosphorus (total orthophosphate), and organic matter. Each of these constituents is then partitioned at the point of entry into the stream network:

- Inorganic nitrogen is partitioned into dissolved nitrate, dissolved ammonium, and sorbed ammonium. Fractions of the dissolved constituents are set to reproduce observed data, while sorption of ammonium is simulated using equilibrium partitioning assumptions (the model connects inorganic N from the land surface to dissolved N in the stream reach, but equilibrium

partitioning to the sorbed form occurs instantaneously). Assignment of total inorganic nitrogen from the land surface to nitrate and ammonium at the point of entry to the stream is represented by a constant ratio throughout the model, but differs for agricultural land and impervious surfaces. Partitioning of ammonium between dissolved and sorbed forms depends on local suspended sediment concentrations. A small portion of the inorganic N is routed directly to organic N to represent uptake by heterotrophic organisms in low order streams (a process not explicitly simulated by the model).

- Inorganic phosphorus is partitioned into dissolved and sorbed fractions using equilibrium partitioning assumptions. As with ammonium, the fraction that becomes sorbed depends on the local suspended sediment concentration,
- Organic matter (biomass) is partitioned into labile and refractory organic carbon, organic nitrogen, and organic phosphorus components. Initial specifications were based on expected stoichiometry of forest litter, and then revised during calibration to achieve agreement with observed concentrations.

All three upland components (inorganic nitrogen, inorganic phosphorus, and organic matter) may be loaded through either surface flow or subsurface flow (interflow and groundwater discharge). The HSPF GQUAL algorithms do not maintain a full mass balance of subsurface constituents (which would require a groundwater quality model); rather, the user specifies concentration values, which may vary monthly, for interflow and groundwater. Surface washoff loading is considered from both pervious and impervious surfaces.

Inorganic phosphorus loading from pervious surfaces is simulated as a sediment-associated process because of the strong affinity of orthophosphate for soil particles. Surface loading of inorganic phosphorus is thus determined by a potency factor applied to sediment load, which may vary on a monthly basis to reflect changes in surface soil concentration associated with the annual growth cycle. (While this reflects the physical basis of surface loading of inorganic phosphorus, it does mean that any errors in the simulation of sediment loading will also affect estimates of inorganic phosphorus loading.) Subsurface flow pathways are assumed to primarily load small amounts of dissolved inorganic phosphorus. Organic matter is also simulated as a sediment-associated load from pervious surfaces, as this primarily represents the erosion of humus, leaf litter, and other detritus.

In contrast to phosphorus, inorganic nitrogen is highly soluble, and loading in surface runoff may occur independent of sediment movement (particularly where fertilizer is applied). Further, much of the nitrate load in surface runoff represents input from atmospheric deposition. Therefore, inorganic nitrogen loading from pervious surfaces is represented via a buildup-washoff process in which the user specifies a rate of accumulation, an accumulation limit, and a flow rate sufficient to remove 90 percent of the accumulated material.

As noted above, representation of plant growth is a necessary part of the nutrient calibration process. HSPF contains routines for simulating planktonic (floating) and benthic (attached) algae. Growth, respiration, and death processes are affected and potentially limited by the availability of light, availability of inorganic nutrients, water depth, and water temperature. Because HSPF represents stream segments as one-dimensional, fully-mixed reactors, the predictions of algal response are averages throughout the stream segment volume. Planktonic and benthic algae simulations differ primarily in the way that the attenuation of light availability is calculated. For plankton light availability is calculated as the average over the euphotic depth, such that all phytoplankton are assumed to be mid-depth in the reach or the middle of the euphotic zone, whichever is smaller, then adjusted to the full volume of the reach. Benthic algae are assumed to be at the average depth of the reach. These simplifying assumptions can distort the actual response in some situations. For deeper reaches, especially lakes, the phytoplankton simulation results are an average over the reach volume, which does not match well with chlorophyll *a*

observations collected from the photic zone. When the average depth is large relative to the light extinction rate benthic algal growth will be simulated as minimal, whereas significant growth may actually occur in the shallower edges of the lake or stream. The scheme does not include a representation of floating or emergent rooted macrophytes. While these can sometimes be successfully approximated with the benthic algae routines, the light availability calculations for benthic algae are not appropriate to these types of macrophytes and the program does not consider that floating/rooted macrophytes can exchange gases with the atmosphere and obtain nutrients from the sediment.

The dissolved oxygen simulation considers reaeration, the decay of organic matter (carbonaceous biochemical oxygen demand), oxidation of ammonia and nitrite N, sediment oxygen demand, and algal photosynthesis and respiration. In the slow-moving, swampy areas of the upper St. Louis, Cloquet, and Nemadji watersheds, the DO balance is largely a factor of the interplay of algal growth and sediment oxygen demand exerted by the decay of settled organic matter. The model is not designed to simulate the oxidation of reduced iron and sulfur, which could play an important role in and downstream of the Iron Range.

For most water quality constituents, it is unreasonable to propose that the model predict all temporal variations in concentration and load. The model should, however, provide an accurate representation of long-term and seasonal trends in concentration and load, and correctly represent the relationship between flow and load. To ensure this, it is important to use statistical tests of equivalence between observed and simulated concentrations, rather than relying on a pre-specified model tolerance on difference in concentrations.

Ideally, average errors and average absolute errors should both be low, reflecting a lack of bias and high degree of precision, respectively. In many cases, the average error statistics will be inflated by a few highly discrepant outliers. It is therefore also useful to compare the median error statistics.

General performance targets for water quality simulation with HSPF are also provided by Duda et al. (2012) and are shown in Table 1-1. These are calculated from observed and simulated daily concentrations, and should only be applied in cases where there are a minimum of 20 observations.

Table 2-1. Performance Targets for HSPF Water Quality Simulation (Magnitude of Annual and Seasonal Relative Average Error (*RE*) on Daily Values)

Model Component	Very Good	Good	Fair	Poor
Temperature	≤ 7%	8 - 12%	13 - 18%	> 18%
Water Quality/Nutrients	≤ 15%	15 - 25%	25 - 35%	> 35%

Evaluation of water quality simulations presents a number of challenges because, unlike flow, water quality is generally not monitored continuously. Grab samples at a point in space and time may not be representative of average conditions in a model reach on a given day due to either spatial or temporal uncertainty (i.e., an instantaneous measurement in time may deviate from the daily average, especially during storm events, while a point in space may not be representative of average conditions across an entire model reach). Where constituent concentrations are near reporting levels, relative uncertainty in reported results is naturally high. Accurate information on daily variability in point source loads is also rarely available.

Evaluation of relative average error is recommended, but averages are prone to biasing by one or a few extreme outliers. Therefore, it is also useful to examine median relative errors, which are less influenced by outliers.

The performance targets for water quality simulation may be applied to either concentrations or loads. Concentrations provide the most natural metric, but error magnitude may be unduly influenced by variability at low flow conditions that has little effect on cumulative loading downstream. Loads are more meaningful for impacts in downstream lakes, harbors, and estuaries but are not directly observed and need to be estimated from flow and concentration – both uncertain. Tests on loads are performed in two ways: on paired data (observed and simulated daily average concentration multiplied by flow) and on complete time series of monthly loads. For the latter approach, "observed" monthly loads are estimated using the USACE FLUX32 program (a Windows-based update of the FLUX program developed by Walker, 1996; available at https://www.pca.state.mn.us/water/watershed-pollutant-load-monitoring-network#flux32-8f1620f5), and are themselves subject to significant uncertainty.

Additional statistical tests are also applied as part of a weight-of-evidence examination of the water quality calibration. Two-sample *t*-tests are reported on the differences in mean concentration and mean load, with higher probability values indicating less chance that the measures are systematically different. A problem with the *t*-test is that the test is on a null hypothesis that the mean difference is exactly equal to zero, not whether the difference is physically meaningful. Therefore, a low value on the *t*-test (rejection of the null hypothesis) is generally considered of practical significance only when the mean difference is greater than 10 percent. Additional graphical tests are also performed to ensure that errors in the prediction of load and concentration do not exhibit strong correlations relative to flow magnitude and season.

3 Nitrogen and Phosphorus Calibration

3.1 NUTRIENT MODEL SETUP

The nutrient simulation follows the same general approach used in other Minnesota HSPF models and recommended by AQUA TERRA (2012). Ammonia, nitrate nitrogen, orthophosphate, and generalized organic matter are simulated on the land surface, with the first two being represented by buildup-washoff processes and the second two simulated as sediment-associated using potency factors for pervious land (with a buildup-washoff approach for impervious land). Representation of point source loads of nutrients are described in Section 3.1.2. Full nutrient kinetics are represented instream, including the decay of organic matter, uptake by and release from planktonic and benthic algae, nitrification, denitrification, exchanges with the sediment bed, and sorption to sediment of ammonium and ortho-phosphate.

3.1.1 Nonpoint Sources

As described in Section 1, the nutrient simulation for the uplands represents inorganic nitrogen, inorganic phosphorus, and organic matter as three distinct constituents. Inorganic phosphorus and organic matter on pervious surfaces are simulated using a sediment potency approach, while inorganic nitrogen on pervious surfaces and all three constituents on impervious surfaces are represented as a buildup/washoff process. Concentrations associated with subsurface flows are also included.

Within the stream reaches the model represents individual nutrient species (ammonia, nitrate, nitrite, organic nitrogen, orthophosphate, organic phosphorus, and organic carbon/BOD). The stream reach module is implemented with full nutrient simulation, including uptake by and release from plankton and benthic algae, decay of organic matter, oxidation of ammonium to nitrite and nitrite to nitrate nitrogen, bed exchanges of dissolved and sorbed nutrients, and ammonia volatilization.

The key parameters controlling the upland nutrient simulation are listed below:

MON-ACCUM: The monthly varying assignment of the build-up or accumulation of a constituent on a particular surface (lb/ac-d).

MON-SQOLIM: The monthly varying upper limit value beyond which a constituent can no longer accumulate on a surface (lb/ac).

MON-IFLW-CONC and **MON-GRND-CONC**: These parameters are used to assign the interflow and groundwater constituent concentrations on a monthly basis. The values for these parameters were estimated from the observed data with consideration of flow regime and then calibrated as necessary.

MON-POTFW: The monthly varying specification of constituent mass per sediment mass (lb/ton). For organic matter the assigned values were around 10^0 to 10^1. The seasonal assignment for organic matter reflects the annual cycle of growth and then litter.

The sediment potency, build-up/washoff, and subsurface flow parameters were initialized for the St. Louis, Cloquet, and Nemadji watershed models based on past experience. A literature review was conducted to establish appropriate ranges for unit-area loading rates of the diverse land use categories found in the watersheds (Table 3-1). The simulated unit-area loading rates were compared to the literature-based ranges and the surface and subsurface flow parameters were revised until reasonable loading estimates were established for TN and TP. Results for the St. Louis and Cloquet watersheds were aggregated and are provided in Figure 3-1 and Figure 3-2. Results for the Nemadji watershed are shown in Figure 3-3 and Figure 3-4.

The mean simulated TN unit loading rate for forest land segments in the St. Louis and Cloquet River watersheds is 2.9 lb-N/ac/yr, which is in the center of the reported range in Table 3-1. The developed

pervious and impervious mean simulated values are 4.2 lb-N/ac/yr and 12.5 lb-N/ac/yr, respectively. These results are similar to the values reported by the Minnesota Pollution Control Agency, which range from 2-17 lb-N/ac/yr for mixed developed land use (MPCA, 2013a). The mean simulated TN unit loading rate for wetlands is 5.3 lb-N/ac/year and this is slightly higher than the literature supported range of 0.5 – 5 lb-N/ac/yr (MPCA, 2004); this can be attributed to the fact that the literature values are largely based on surface runoff whereas the model results include nitrogen loading from subsurface waters. The cropland unit loading rate is near the lower limit of the reference range at 7.6 lb-N/ac/yr. The simulated unit loading rate for croplands, however, is comparable to the average loading rate of 17 watersheds in Wisconsin, 7.5 lb-N/ac/yr (Clesceri et al, 1986).

Reference TP unit loading rates for forest are as low as 0.05 lb-P/ac/yr (MPCA, 2004) and as high as 0.5 lb-P/ac/yr (Loehr et al, 1989). The simulated TP unit loading rate for forest in the St. Louis and Cloquet watersheds aligns with the reference values at 0.17 lb-P/ac/yr. The TP unit loading rate from wetlands are higher than reference values because subsurface flows contribute to the simulated load but generally are not considered in the literature-based values. The mean simulated TP unit loading rate for croplands, 0.60 lb-P/ac/yr, aligns well with other studies that recommend use of 0.11-1.7 lb-P/ac/yr (Dodd et al, 1992; Loehr et al, 1989).

Table 3-1. Reference Ranges for the Nutrient Loading Rates of Diverse Land Use Categories

Land Use	TN (lb-N/ac/yr)	TP (lb-P/ac/yr)	Source
Forest	1.97 – 4.2	0.05 – 5	Clesceri et al, 1986; Loehr et al, 1989; MPCA, 2013a, MPCA, 2004; Reckhow et al, 1980
Wetland	0.5 – 5	0	MPCA, 2013a; MPCA, 2004
Pasture	6.1 – 23	0.11 – 0.43	Clesceri et al, 1986; McFarland and Hauck, 2001; MPCA, 2013a; MPCA 2004
Crop	7.5 – 23	0.11 – 1.7	Dodd et al, 1992; Clesceri et al, 1986; Loehr et al, 1989, MPCA, 2013a; MPCA 2004
Developed (pervious)	2 – 17	0.8 – 1.02	Loehr et al, 1989; MPCA, 2013a; MPCA, 2004; Reckhow et al, 1980
Developed (impervious)	2 – 17	0.8 -1.02	Loehr et al, 1989; MPCA, 2013a; MPCA, 2004; Reckhow et al, 1980
Barren	0.5 - 5	ND	MPCA, 2013a
Shrub	0.5 - 5	0.05 – 0.12	MPCA, 2013a; MPCA, 2004

The Nemadji watershed model was calibrated separately and results differ somewhat from the St. Louis and Cloquet model. This is in part due to the calibration data not strongly constraining exact results for individual land uses, but also may reflect some systematic differences between the watersheds. Total N loading rates are generally lower in the Nemadji, possibly reflecting greater denitrification potential in this basin's clay soils. Total P loading rates are generally higher because phosphorus is sediment-associated and erosion rates are higher in the Nemadji, on average, than in the St. Louis basin. Note, however, that the averages depend on the mix of different HRU characteristics associated with a given land use and there is a wide range of loading rates among different HRUs in a single land use class, reflecting differences in erosion rates and runoff potential.

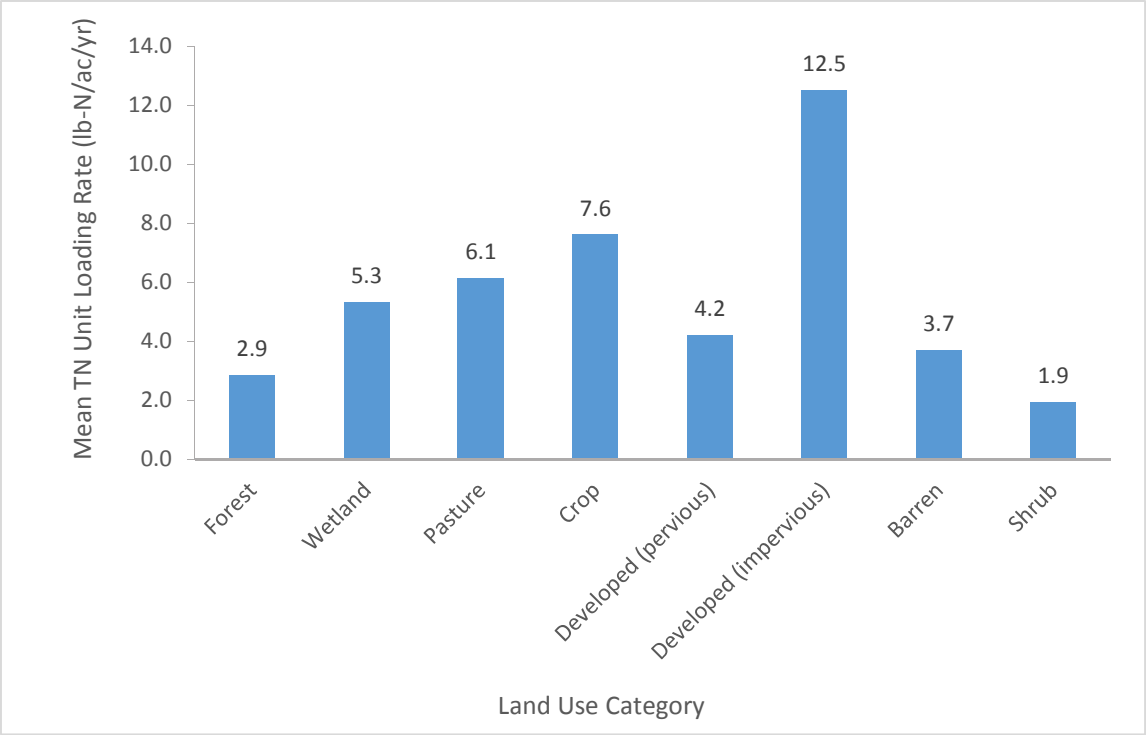

Figure 3-1. Mean Simulated Total Nitrogen (TN) Unit Loading Rates for Land Use Categories in the St. Louis and Cloquet Watersheds

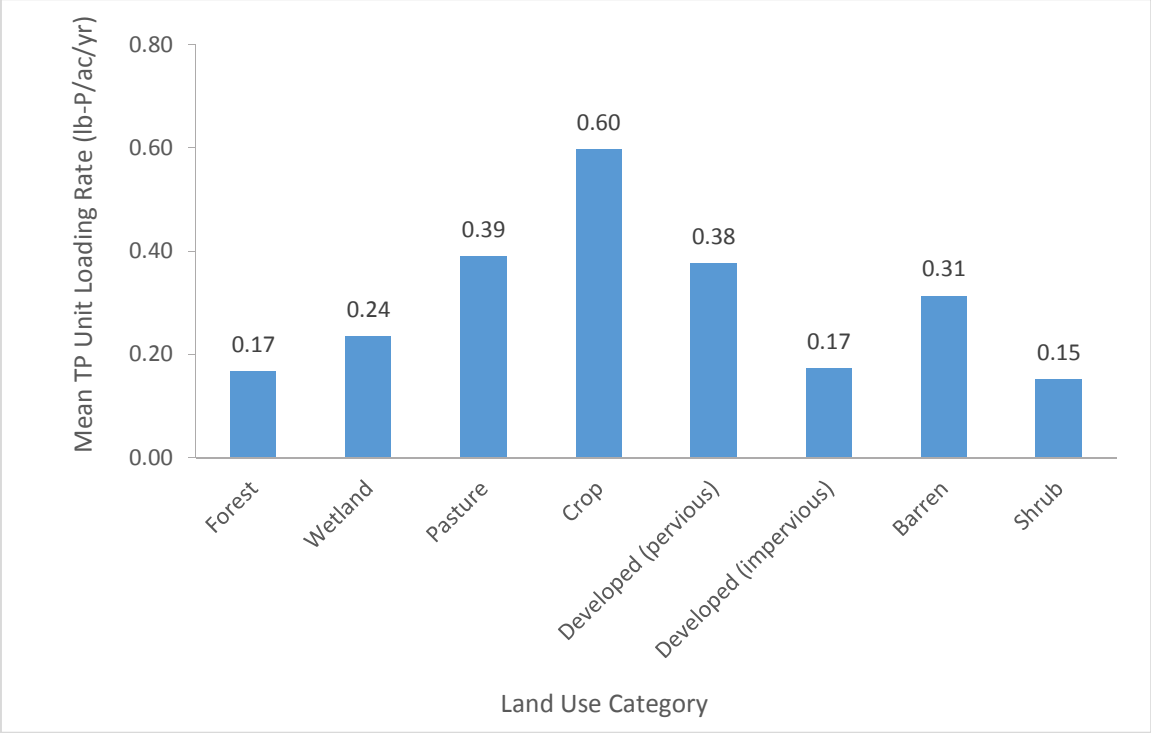

Figure 3-2. Mean Simulated Total Phosphorus (TP) Unit Loading Rates for Land Use Categories in the St. Louis and Cloquet Watersheds

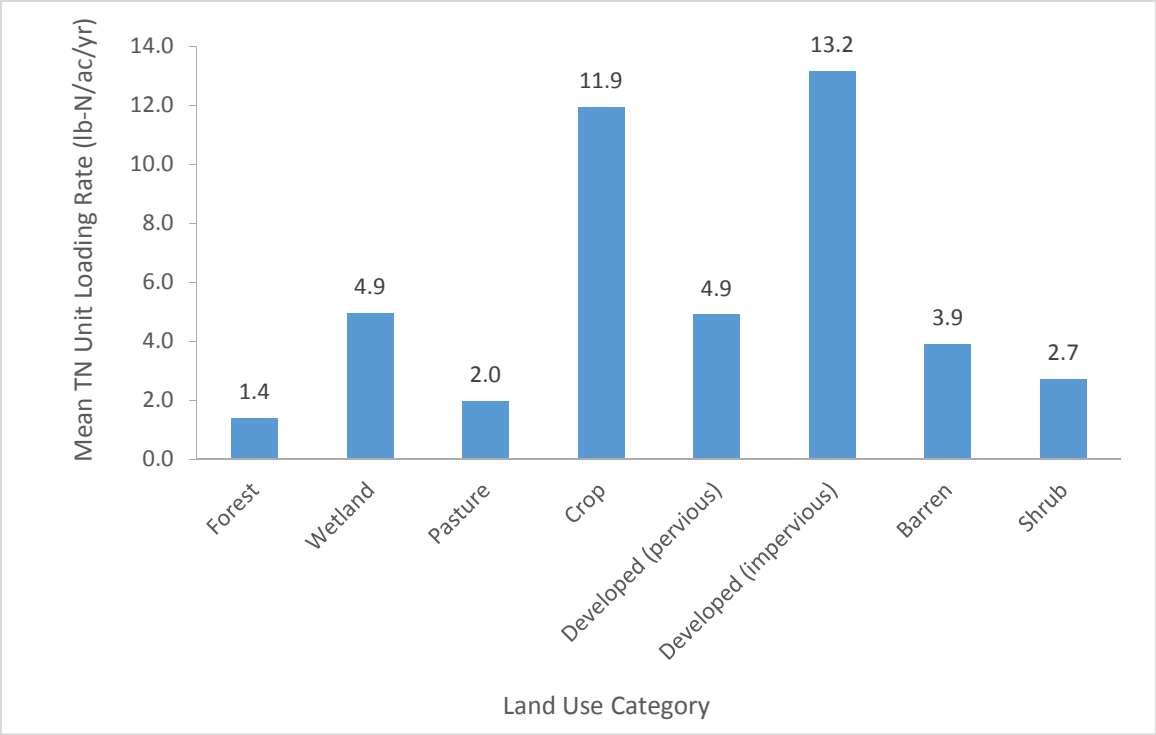

Figure 3-3. Mean Simulated Total Nitrogen (TN) Unit Loading Rates for Land Use Categories in the Nemadji Watershed

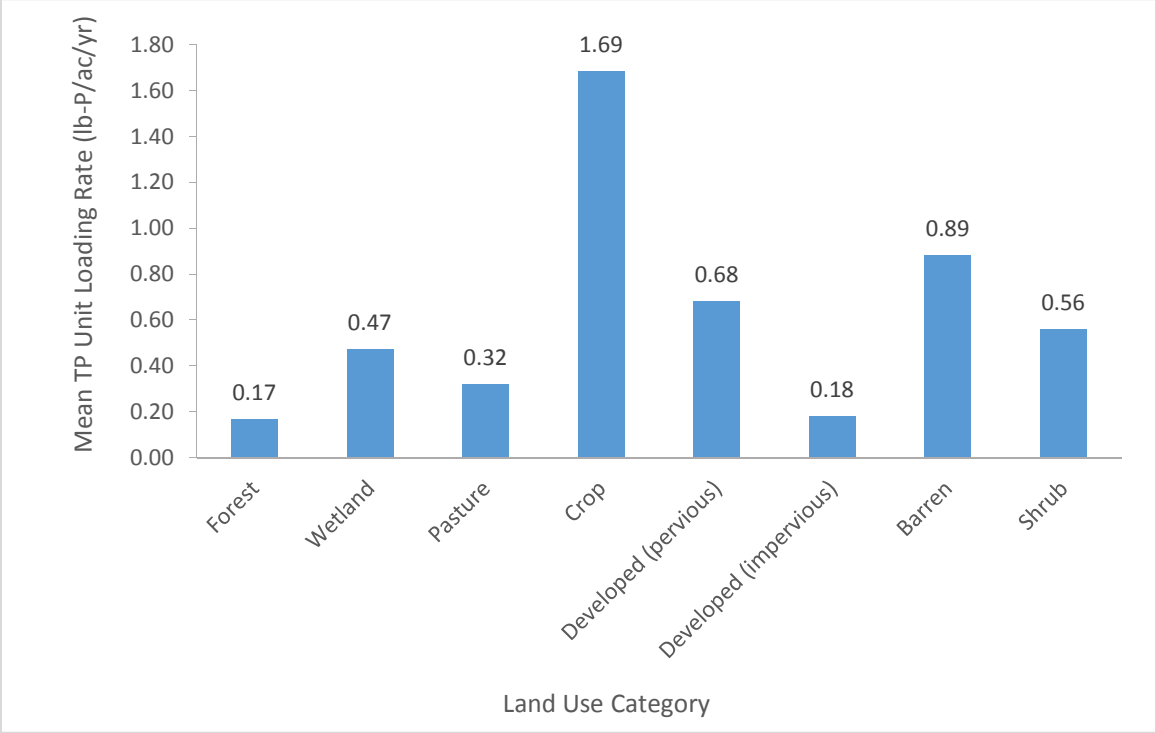

Figure 3-4. Mean Simulated Total Phosphorus (TP) Unit Loading Rates for Land Use Categories in the Nemadji Watershed

3.1.2 Point Sources

Point sources that have discharge permits in the St. Louis watershed are included in the modeling framework. Permitted point sources are not present in the Cloquet and Nemadji watersheds and, therefore, are not represented. The St. Louis-Cloquet model incorporates five major WWTP discharges and forty-nine minor point sources. The minor point sources include a variety of industrial, mining, and smaller municipal wastewater dischargers. Although classified as "minor" they include some very large discharges of non-contact cooling water and mine pit dewatering flows. The point sources included in the model are documented in Section 2.4 of Volume I of this report. The locations of the discharges are recapped in Figure 3-5. Note that the majority of the point sources are located either in the northern part of the watershed along the Iron Range or downstream in the Duluth area.

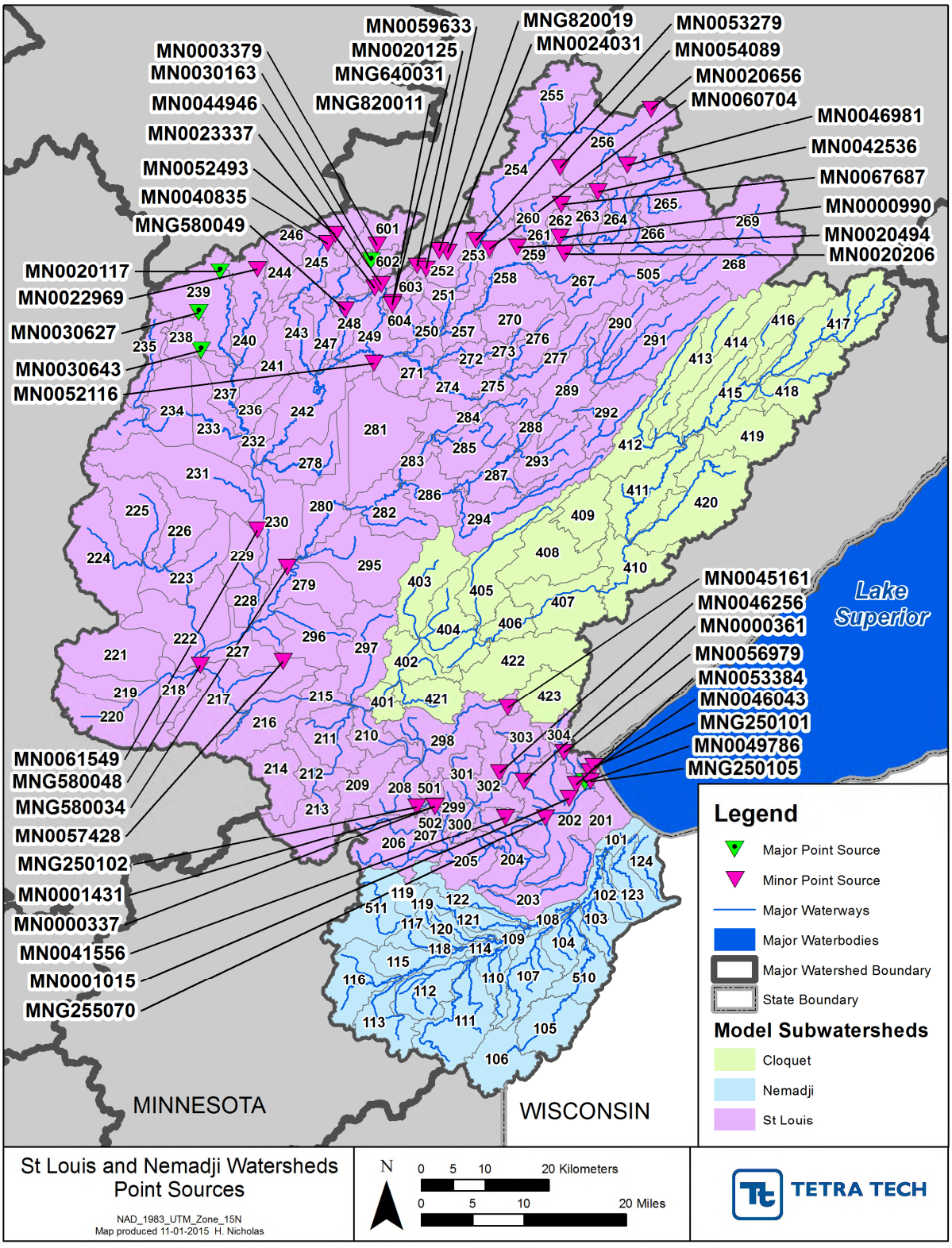

Figure 3-5. Point Source Discharges Included in the Model

Daily effluent flows are available for the major point sources and were used to create daily nutrient load series. Minor point sources rely on monthly flow and load series. Wastewater treatment plant discharges generally have monitored and reported effluent total phosphorus and ammonia concentrations in the Discharge Monitoring Reports (DMRs) commencing in 1995. These were assembled and provided by MPCA. Effluent nitrite + nitrate (NO_2 +NO_3-N), organic nitrogen, and phosphorus species were generally not reported. Discharge concentrations of these nutrients were established according to observations at upstream and downstream water quality stations and based on the type of discharger being represented (e.g. small municipal, industrial, mining). Large non-contact cooling water discharges that draw from and discharge back to the same reach, such as the 128 MGD discharge from the Laskin Power Plant, are simulated as having no net effect on nutrient loads. Mean nutrient concentrations simulated for the point sources are provided in Table 3-2. Phosphorus and ammonia discharge concentrations are generally low relative to concentrations observed in other parts of Minnesota. This likely reflects the influence of elevated levels of iron and sulfate in the surface and ground water supply sources of the St. Louis watershed, which in turn, respectively, may enhance complexation and removal of ortho-phosphorus and ammonia nitrogen in the wastewater systems.

Table 3-2. Mean Modeled Discharge Concentrations (mg/L) for Point Sources in the St. Louis River Watershed, 1995-2012

Discharge (Major Source or Minor Type)	NH_4-N	NO_2 +NO_3-N	Organic N	TP	PO_4-P	Organic P	CBOD
Chisholm-Mech.	3.53	7	2	0.42	0.23	0.2	3.62
Hibbing WWTP North Plant	0.64	10	4	0.31	0.17	0.14	2.87
Hibbing WWTP South Plant	0.56	10	4	0.35	0.19	0.16	2.84
Virginia WWTP	3	10	4	0.52	0.38	0.14	4.68
WLSSD WWTP	3.05	10	4	0.42	0.31	0.12	6.24
Minor Municipal WWTPs	1 - 4	3 - 10	2.36	0.12 – 0.85	0.09 – 0.61	0.03 – 024	12
Minor Industrial	2	1	1	0.12	0.1	0.02	0.5
Iron Range Industrial Discharges	0	0.25	0	0.02	0.02	0	0.5

Notes: Total phosphorus (TP) concentrations for WWTPs are based on monitoring reports, while the split between phosphorus species is based on fixed ratio assumptions. Iron Range Industrial Discharges are primarily mine dewatering flows which are expected to have low nutrient concentrations due to the presence of reduced iron and sulfur species. Nitrate plus nitrite N concentrations for minor municipal WWTPs are not monitored and are based on MPCA summaries by source type, ranging from Class D municipal discharges to ponds (3 mg/L) to Class B medium size mechanical plants (10 mg/L). Ammonia (NH_4-N) and carbonaceous biochemical oxygen demand (CBOD) are also based on MPCA summaries.

3.1.3 Channel Sources

Nutrients can be gained or lost through exchanges with the sediment bed – either through releases in the dissolved form or by scour or deposition of nutrients that sorb to sediment. HSPF simulates ortho-phosphate and ammonia as sorbing to sediment and also represents release of dissolved ortho-phosphate, ammonia, and labile organic matter (as BOD, with associated nutrients) from the sediment.

Based on past experience, sorption coefficients were set for ortho-phosphate as 1,000 ml/g relative to silt and clay and 600 ml/g relative to sand; the corresponding numbers for total ammonia N were 100 and 10 ml/g. Default background sediment bed concentrations for ortho-phosphate are set at 250 mg/kg for silt and clay and 100 mg/kg for sand, and, for total ammonia N, 100 mg/kg for silt and clay and 10 mg/kg for sand. Higher bed concentrations are used in the red clay portions of the Nemadji River (2,000 mg/kg of clay for ortho-phosphate and 600 mg/kg total ammonia N). Those higher concentrations are based on calibration to observed data from the Nemadji River at South Superior monitoring station, and are also qualitatively consistent with the clay sediment leaching experiments reported by Bahnick et al. (1979), who reported that "The Nemadji River particulate sample gave the largest [soluble] orthophosphate release."[1]

For the Nemadji River, comparison of monitoring data to observations suggest that there is also a significant amount of organic phosphorus that is associated with channel bank erosion. HSPF does not directly provide for this source, but it was implemented using GENER statements that associate a refractory organic phosphorus load with scoured sediment, with potency factors ranging from 8 to 20 lb/ton.

The waters of these basins tend to contain ample amounts of iron, which can enhance the deposition of phosphorus in complexes with iron hydroxide under oxidized conditions. In anaerobic sediment this complexed phosphorus can be re-released in dissolved form. This is hypothesized as likely to be a significant process in lakes of the region that develop summer stratification and oxygen depletion in the hypolimnion, and also possibly in some slower-moving stream segments. The model is therefore set up to simulate releases of orthophosphate and ammonia N from sediment in lake segments as well as the most downstream reaches of the Nemadji. These releases are somewhat speculative and could be refined with detailed mass balance studies of individual lakes.

3.1.4 Atmospheric Deposition

The model simulates wet and dry deposition of ammonia-N and nitrate-N to pervious surfaces, impervious surfaces, and water bodies. In addition, both dry and wet deposition of phosphorus to phosphorus is simulated. Atmospheric deposition of phosphorus to the uplands is not simulated because it is assumed to be implicit in the sediment potency representation of pervious land loading and the buildup/washoff representation of impervious land loading of phosphorus.

Direct phosphorus deposition to surface water is represented in the model. The phosphorus deposition rate specified is the average estimated for the Lake Superior basin in the 2007 update to *Detailed Assessment of Phosphorus Sources to Minnesota Watersheds - Atmospheric Deposition* (Twaroski, et al. 2007) of 0.115 kg/ha/yr. The wet deposition concentration for phosphorus is set at the average concentration for Fond du Lac of 10.7 µg/L given in the same resource.

Wet deposition concentrations of ammonia and nitrate N (as mg/L) are taken from seasonal data recorded at NADP station MN16 (Marcell Experimental Forest) because other NADP stations within the watershed either did not become operational until 1997 or ended prior to 2012 and thus do not cover the full time span of the model. Dry deposition rates of ammonia and nitrate N (as lb/ac) are taken from CASTNET

[1] The sediment potency assigned in the model is much higher than the total P content of sediment reported in two sediment cores from the lower channel of the Nemadji by Bahnick et al. of 17.1 ppm (=mg/kg); however, these core samples were only about 20% clay and are stated to represent original glacial lacustrine depositional material that is largely unimpacted by human activities. Desorption experiments reported by Bahnick et al. released about 150 mg of dissolved orthophosphate per kg of clay from suspended particulate material from the Nemadji, but the total P concentration of these sediment samples is not reported. The average ratio of total P to TSS from monitoring samples in the Nemadji River at South Superior is about 2,300 mg/kg, consistent with the concentrations applied in the model, and assignment of higher bed sediment concentrations in the lower Nemadji mainstem provide a good fit to observed total P in the water column. Material eroded and suspended during high flows in the lower Nemadji may be enriched in phosphorus due to human activities over the last 150 years, but further understanding of phosphorus exchanges between the water column and sediment in the Nemadji is needed.

monitoring. There are not CASTNET stations within or particularly close to the watersheds studied here, so we use the station at Voyageurs National Park (VOY413) for the period after 1996, filling in earlier dates with monitoring from Perkinstown, WI (PRK134). In all cases, reported data were converted from molar units to mass or mass-based concentration as N.

3.2 NUTRIENT CALIBRATION

Nutrients from point and nonpoint sources are loaded to the stream reaches. Within the stream reaches the model represents the following nutrient species: ammonia, nitrite, nitrate, organic nitrogen, orthophosphate, organic phosphorus, and organic carbon/BOD. The stream reach module simulates instream biogeochemical processes including nutrient uptake and release by plankton and benthic algae, decay of organic matter, nitrification/denitrification, absorption/desorption of nutrients on suspended sediment, and deposition and scour of sediment-stored nutrients.

3.2.1 Calibration Data and Locations

Water quality data have been collected at many locations within the St. Louis, Cloquet, and Nemadji watersheds. Most of these data are available in EQUIS, and MPCA provided a full download of all stations. Despite the volume of data, stations that have collected significant amounts of nutrient data over a time period coincident with the model simulation period are few and an even smaller number are at or near flow gaging stations. The model segmentation was designed to line up with available flow gage locations and monitoring sites known to have large amounts of water quality data; however, some stations with small to moderate amounts of monitoring data were not usable for calibration because a major tributary or point source discharge enters the model segment between the monitoring station and the downstream end of the segment, or because they were on tributaries or lakes that were too small for explicit inclusion in the basin-scale models. In other cases, multiple closely located EQUIS stations were combined for use in model calibration.

Ultimately, 13 locations (represented by 17 EQUIS stations) were selected as primary model calibration locations in the St. Louis, Cloquet, and Nemadji watersheds. These locations are summarized in Table 3-3 and displayed in Figure 3-6 (St. Louis and Cloquet) and Figure 3-7 (Nemadji). For the St. Louis watershed, comparison to Figure 3-5 reveals that all these stations are affected to some extent by point sources, and most are downstream of major WWTP discharges in the Iron Range. For the sparsely populated Cloquet watershed, only one station (Cloquet River near Burnett) met the screening criteria. This station has a reasonable quantity of observations, but is downstream of Island Lake and observations will be affected by in-lake processes in this large reservoir. For the Nemadji watershed a number of EQUIS stations are on reaches too small to be explicitly simulated in the model, leaving a total of six stations with significant amounts of data. The downstream station at South Superior was augmented by observations supplied by Wisconsin DNR.

Calibration is not presented here for Miller Creek or other Duluth-area monitoring stations on small streams. These are being addressed separately in a finer-scale HSPF model of the Duluth area that accounts for managed stormwater drainage. It should also be noted that significant amounts of additional data have been collected throughout these watersheds since 2012. When the model is updated to run through more recent years, additional calibration could be undertaken with more recent monitoring.

Table 3-3. Water Quality Calibration Locations

Location	Model Reach	EQUIS Station(s)
Partridge River near Hoyt Lakes	262	S007-022
Swan River near Toivola	232	S000-641
St. Louis River at CSAH 7 nr Forbes	249	S000-119
St. Louis River below Cloquet R	210	S000-023
St. Louis River at Scanlon	501	S005-089, S000-629, S000-046
St. Louis River near Fond du Lac	205	S000-021, S003-972
Cloquet River near Burnett	402	S003-968, S005-147
Deer Creek near Pleasant Valley MN 23*	118	S003-250
Rock Creek near Pleasant Valley	120	S003-251
Blackhoof R nr Pleasant Valley	511	S005-620
Nemadji River nr Holyoke	113	S005-619
Nemadji River near Pleasant Valley	115	S000-110
Nemadji River near South Superior	103	S005-115

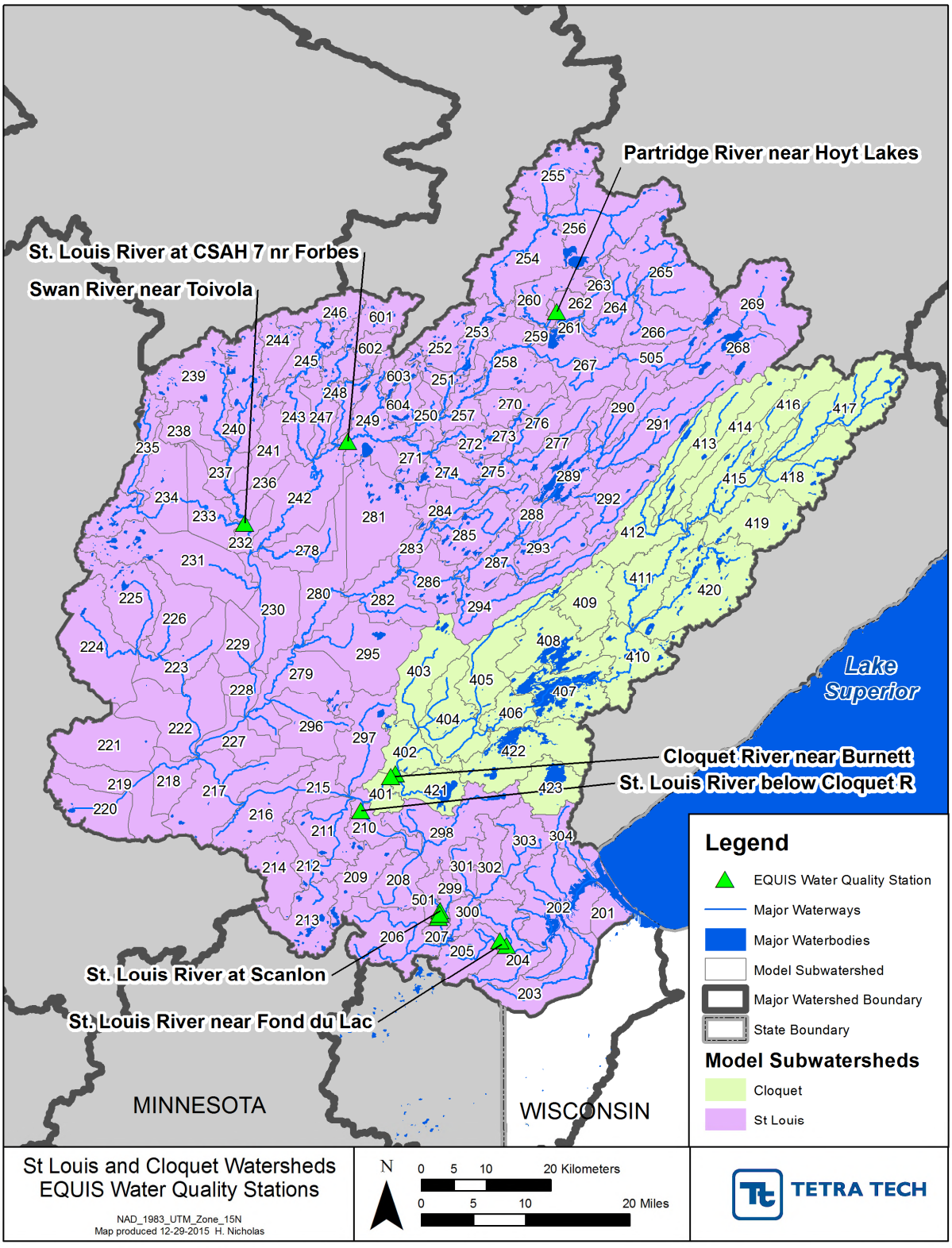

Figure 3-6. Water Quality Calibration Locations in the St. Louis and Cloquet Watersheds

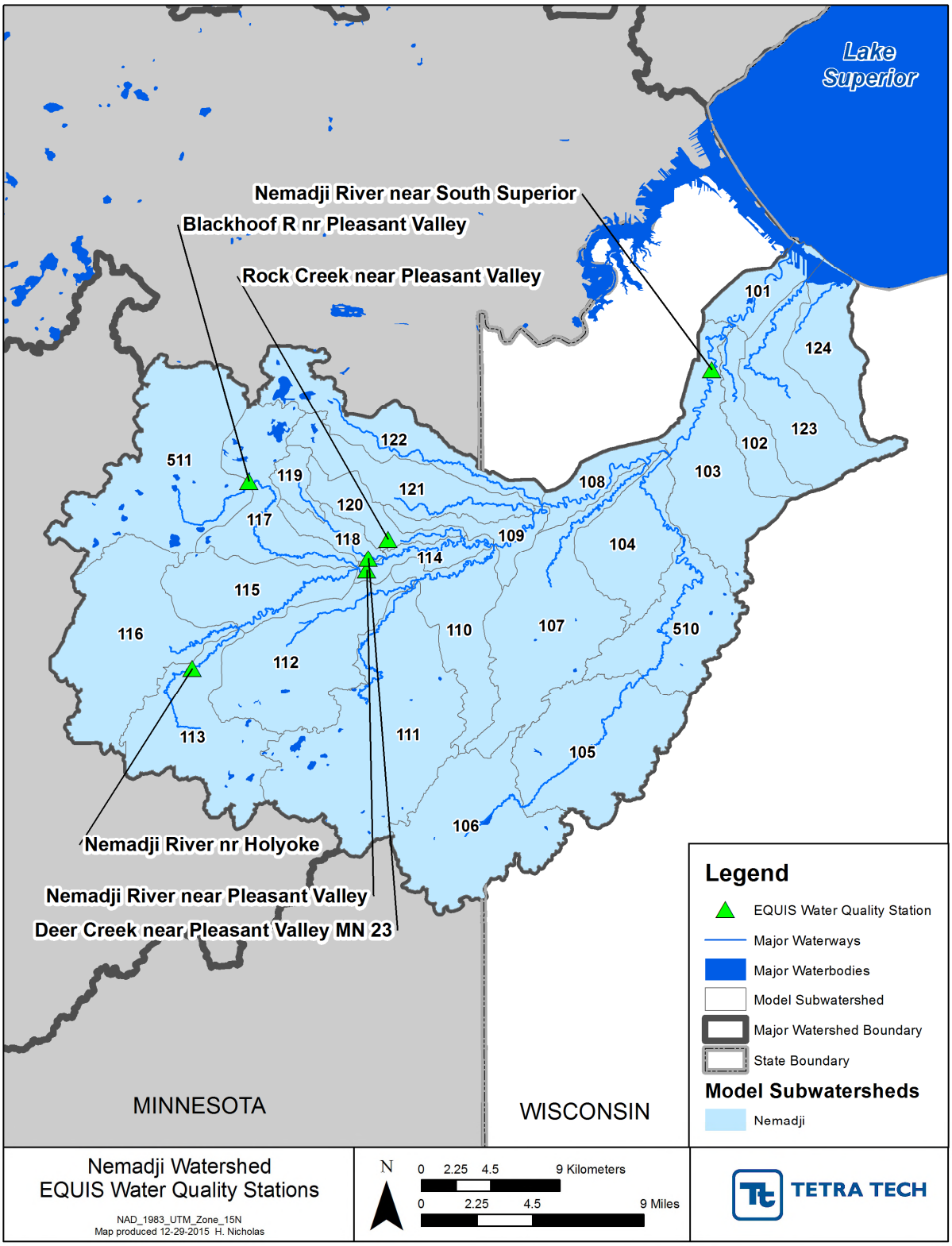

Figure 3-7. Water Quality Calibration Locations in the Nemadji Watershed

During the early stages of the calibration process efforts focused on accurately portraying nutrient concentrations at the stations located on the mainstems. In the St. Louis watershed this included the stations on the St. Louis River near Scanlon, Forbes, and Fond du Lac. Much of the St. Louis, Cloquet, and Nemadji watersheds are dominated by wetlands and hardwood forests, and the upland dynamics in the wetlands and forests complicate the modeling effort. A literature review was completed to support the selection of parameters appropriate for northern, wetland and hardwood forest dominated watersheds (see Table 3-1). The water quality calibration consisted of refining parameters that control nutrient stoichiometry (P:C, and P:N), phytoplankton and benthic algae population dynamics, nutrient transport, deposition, and scour, and nitrogen transformations (e.g. ammonification rate).

The water quality stations that are located on tributary streams had diverse location-based effects to consider; the water quality at the Swan River near Toivola station, for example, is highly influenced by major point source discharges. The water quality at the Partridge River near Hoyt Lakes and Cloquet River near Burnett are subjective to upstream lake dynamics. Specialized parameters were assigned to subbasins that have nutrient dynamics that differ from the rest of the basin.

Water quality was consistently monitored during the calibration and validation periods at the St. Louis River near Scanlon water quality station and, therefore, this site was selected to characterize the results of the water quality calibration. Similarly, the Nemadji River near South Superior was selected to showcase the water quality calibration for the HSPF model of the Nemadji watershed. Nitrogen and phosphorus were calibrated simultaneously but are summarized independently in the following sections.

3.2.2 Calibration and Validation

The nutrient calibration and validation relies on a weight of evidence approach. Upland loading rates are constrained to be in general agreement with literature values (as described in Section 3.1.1), while point source discharges are based on monitoring or recommended assumptions for unmonitored parameters provided by MPCA. Model calibration then adjusts parameters to optimize the fit between model predictions and observations at multiple stations throughout the watershed and the robustness of the fit is checked with validation tests on a different time period. Model performance is then checked against other sources of information, including information developed by MPCA on delivered loads and lake phosphorus balances.

3.2.2.1 Comparison of Model to Observations

Comparisons between model predictions and sample observations are made in terms of both concentration and inferred load (concentration times simulated or observed flow). Complete graphical and tabular statistical results for each station are provided in Appendix A (St. Louis and Cloquet River) and Appendix B (Nemadji River). Figure 3-8 provides an example of the primary types of calibration plots provided for each monitored nutrient parameter at each site, in this case showing the total phosphorus calibration for the Nemadji River at South Superior. The four panels in Figure 3-8 are:

a. Standard time series plot, showing the observations and continuous model predictions of daily average concentrations. This shows general agreement, but can obscure biases in the simulation.

b. A power plot comparing the relationship of observed and simulated loads versus flow. The objective here is that the relationship to flow (summarized by the power regression lines) should be similar for the model and observations. While generally true in this case, it will be noted that the simulated loads have a “hump” in the mid-range of flows. This in turn reflects the simulated relationship of flow and channel scour, derived from the channel form assumptions, which indicate a reduction in shear stress as flow spreads out onto the floodplain (see discussion in Volume I).

c. A scatterplot of simulated versus observed concentrations shows the degree of spread or uncertainty about the 1:1 line.

d. A plot of the residuals against flow is used to diagnose bias relative to the flow regime. In this case there is a fair balance between over and under-prediction across the range of flows, but some indication of a tendency to under-predict concentrations at the highest flows. A similar plot of residuals versus month is used to diagnose potential seasonal biases.

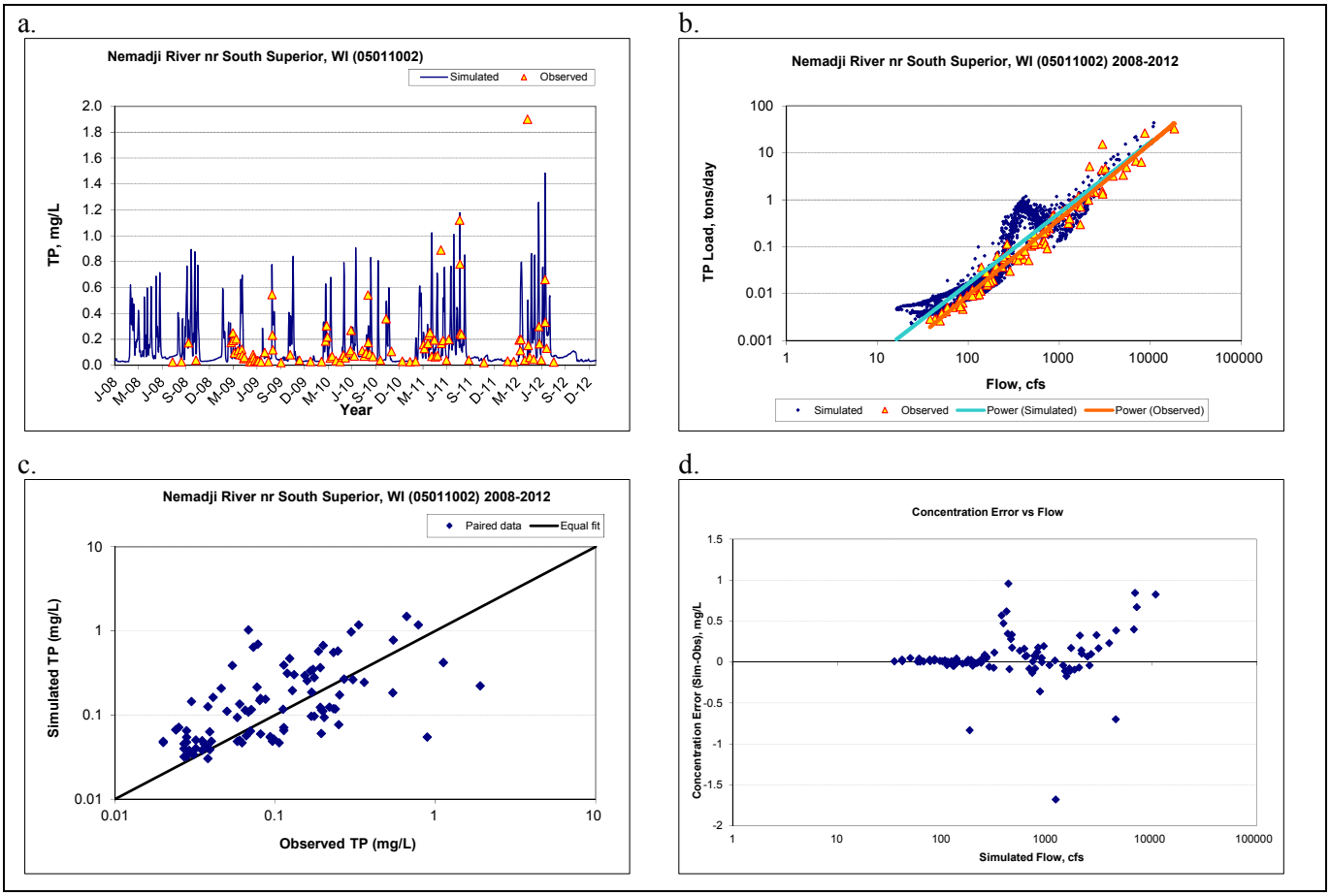

Figure 3-8. Example Calibration Plots for Total Phosphorus, Nemadji River near South Superior, WI

This section first provides an overview of the results with a focus on total phosphorus, total nitrogen, and nitrate nitrogen (nitrate nitrogen is included in the overview because it is often the predominant form of nitrogen and the number of observations for total nitrogen is limited at many stations). Results for individual nutrient species are then summarized, with full results provided in the appendices.

Summary statistics for the calibration and validation of total phosphorus, total nitrogen, and nitrate nitrogen at all stations are provided in Table 3-4, Table 3-5, and Table 3-6, respectively. Discussion by watershed and parameter follows the tables. Note that the number of samples available is relatively small, except for a few select stations.

Table 3-4. Summary Statistics for Total Phosphorus Calibration and Validation

Station	Calibration (2002-2012)*						Validation (1994-2001)*					
	Count	Average Concentration (mg/L)	Concentration Average Relative Error (%)	Concentration Median Relative Error (%)	Paired Load Average Relative Error (%)	Paired Load Median Relative Error (%)	Count	Average Concentration (mg/L)	Concentration Average Relative Error (%)	Concentration Median Relative Error (%)	Paired Load Average Relative Error (%)	Paired Load Median Relative Error (%)
Partridge River near Hoyt Lakes	18	0.025	33%	19%	31%	17%	0					
Swan River near Toivola	22	0.080	17%	-4%	-42%	-8%	0					
St. Louis River at CSAH 7 nr Forbes	50	0.029	20%	20%	5%	12%	10	0.042	6%	6%	-1%	7%
St. Louis River below Cloquet R	39	0.042	-18%	3%	-4%	1%	9	0.038	1%	11%	-2%	7%
St. Louis River at Scanlon	125	0.053	-10%	13%	-53%	3%	41	0.035	27%	22%	4%	15%
St. Louis River near Fond du Lac	50	0.036	15%	22%	7%	8%	38	0.039	13%	7%	4%	5%
Cloquet River near Burnett	80	0.033	6%	32%	-1%	18%	29	0.027	19%	34%	21%	24%
Deer Creek near Pleasant Valley MN 23*	35	0.31	-38%	1%	-79%	0%	79	0.78	-84%	-52%	-58%	-13%
Rock Creek near Pleasant Valley	63	0.12	27%	41%	53%	86%	0					
Blackhoof R nr Pleasant Valley	17	0.042	41%	53%	86%	20%	0					
Nemadji River nr Holyoke	15	0.080	16%	8%	-1%	1%	0					
Nemadji River near Pleasant Valley	100	0.20	-8%	1%	-35%	0%	22	0.12	59%	11%	35%	1%
Nemadji River near South Superior	97	0.17	31%	11%	-5%	0%	0					

Note:

* For Deer Creek the calibration period is 2008-2012 and the validation period is 1994-2006.

Table 3-5. Summary Statistics for Total Nitrogen Calibration and Validation

Station	Calibration (2002-2012)*						Validation (1994-2001)*					
	Count	Average Concentration (mg/L)	Concentration Average Relative Error (%)	Concentration Median Relative Error (%)	Paired Load Average Relative Error (%)	Paired Load Median Relative Error (%)	Count	Average Concentration (mg/L)	Concentration Average Relative Error (%)	Concentration Median Relative Error (%)	Paired Load Average Relative Error (%)	Paired Load Median Relative Error (%)
Partridge River near Hoyt Lakes	0						0					
Swan River near Toivola	0						0					
St. Louis River at CSAH 7 nr Forbes	7	0.74	1%	0%	20%	28%	6	0.92	-5%	1%	0%	0%
St. Louis River below Cloquet R	6	0.98	10%	8%	5%	4%	7	0.75	41%	33%	45%	36%
St. Louis River at Scanlon	127	1.19	-6%	-1%	-11%	2%	8	0.69	38%	37%	39%	34%
St. Louis River near Fond du Lac	7	1.08	0%	-1%	-1%	-2%	7	0.86	29%	27%	28%	10%
Cloquet River near Burnett	94	0.82	12%	18%	-10%	4%	0					
Deer Creek near Pleasant Valley MN 23*	17	0.84	17%	12%	-59%	0%	5	1.09	-30%	-38%	-23%	-16%
Rock Creek near Pleasant Valley	5	0.93	49%	47%	13%	8%	0					
Blackhoof R nr Pleasant Valley	17	0.91	-22%	-26%	26%	0%	0					
Nemadji River nr Holyoke	15	0.85	6%	-14%	5%	-6%	0					
Nemadji River near Pleasant Valley	31	1.04	11%	-17%	-4%	0%	0					
Nemadji River near South Superior	100	1.16	-1%	-5%	-23%	-1%	0					

Note:

* For Deer Creek the calibration period is 2008-2012 and the validation period is 1994-2006.

Table 3-6. Summary Statistics for Total Nitrate+Nitrite-N Calibration and Validation

Station	Calibration (2002-2012)*						Validation (1994-2001)*					
	Count	Average Concentration (mg/L)	Concentration Average Relative Error (%)	Concentration Median Relative Error (%)	Paired Load Average Relative Error (%)	Paired Load Median Relative Error (%)	Count	Average Concentration (mg/L)	Concentration Average Relative Error (%)	Concentration Median Relative Error (%)	Paired Load Average Relative Error (%)	Paired Load Median Relative Error (%)
Partridge River near Hoyt Lakes	18	0.16	-18%	-42%	-33%	-3%	0					
Swan River near Toivola	22	0.73	-2%	-10%	-57%	-49%	0					
St. Louis River at CSAH 7 nr Forbes	48	0.092	44%	55%	5%	32%	35	0.13	-34%	-26%	-41%	-11%
St. Louis River below Cloquet R	38	0.093	45%	45%	16%	25%	36	0.09	2%	14%	-8%	13%
St. Louis River at Scanlon	140	0.20	-28%	2%	-4%	1%	8	0.046	135%	120%	19%	40%
St. Louis River near Fond du Lac	49	0.10	30%	23%	5%	16%	36	0.12	0%	7%	-5%	5%
Cloquet River near Burnett	94	0.081	34%	46%	3%	18%	0					
Deer Creek near Pleasant Valley MN 23*	35	0.11	-19%	7%	-28%	0%	5	0.009	178%	63%	219%	64%
Rock Creek near Pleasant Valley	14	0.032	361%	262%	38%	12%	0					
Blackhoof R nr Pleasant Valley	17	0.19	-28%	12%	356%	-1%	0					
Nemadji River nr Holyoke	15	0.019	438%	71%	245%	20%	0					
Nemadji River near Pleasant Valley	48	0.12	-32%	-24%	-3%	-5%	0					
Nemadji River near South Superior	100	0.087	-7%	-9%	30%	-3%	0					

Note: Statistics calculated with non-detects set to one-half the detection limit.

* For Deer Creek the calibration period is 2008-2012 and the validation period is 1994-2006.

St. Louis Watershed

Ambient phosphorus concentrations in the St. Louis tend to be relatively low, with most stations having an average concentration less than 0.05 mg/L, despite the presence of point source discharges. For the calibration period, the average relative errors on concentration fall into the "Very Good" category (≤15%) of "Good" category (15-25%) for five out of six locations, while the average relative error on load falls into these categories on three out of six locations. Results are rated only "Fair" for Partridge River, but the sample size is small. Of greater concern are the paired load relative errors for Swan River and especially Saint Louis River at Scanlon, both of which are rated as "Poor" – although the median relative errors are very good.

For Swan River near Toivola there is only a single year of monitoring data coincident with the model (2012). Concentrations appear to be under-estimated at higher flows. Nitrate nitrogen is also under-estimated at this station. The location is downstream of two major WWTPs (Hibbing and Chisolm), both of which discharge to complexes of small streams and wetlands. It seems possible that there may be historic storage of nutrients in the wetland areas near the WWTPs that is flushed out during high flows, which may bear further investigation.

The apparent load under-estimation at Scanlon is more difficult to interpret. This station is only a short distance downstream of the monitoring station for St. Louis River below Cloquet River, where the fit for load is "Very Good". In between these monitoring stations are a series of impoundments (Cloquet Reservoir, Knife Falls, Scanlon Dam), and the monitoring point is downstream of the hydropower station at Scanlon Dam. As shown in Figure 3-9, the apparent underestimation of load is due to a small number of observations at high flow where the observed concentration is greater than the simulated concentration – such as the observation of 6/20/12 when a total phosphorus concentration of 0.344 mg/L (predominantly in non-soluble form) was reported on a flow of 35,900 cfs – versus a modeled concentration of 0.087 mg/L. Possibly this sample could represent stored material washed out of the bottom of Scanlon Reservoir by hydropower releases on the rising limb of a flood flow.

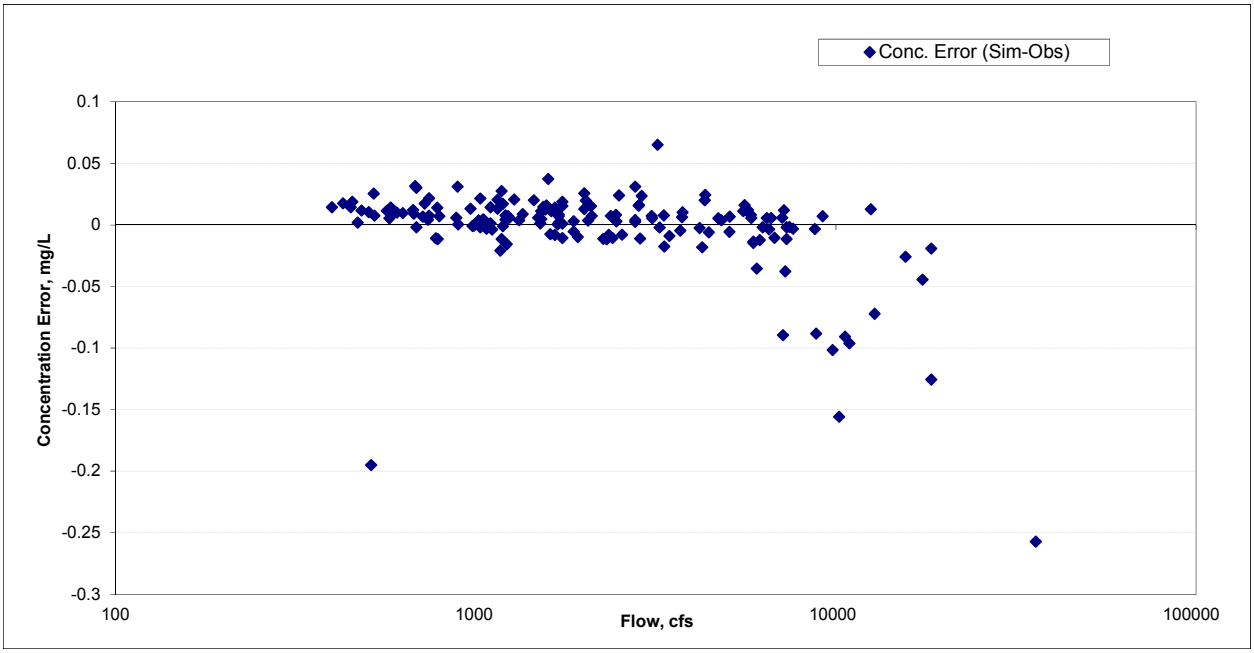

Figure 3-9. Concentration Error versus Flow for Total Phosphorus, St. Louis River at Scanlon

It was not found to be possible to simulate the reported phosphorus concentration for this or a few other similar events. It appears, however, that these may be anomalies as the model and FLUX estimates of

total load (not just paired loads) are in near perfect agreement (see Section 3.2.2.2). Further, phosphorus load at this station during the validation period is fit well. Indeed, all validation statistics for the St. Louis River stations are rated as "Good" or "Very Good."

For total nitrogen, the average relative errors for the St. Louis stations are all in the "Good" or "Very Good" range, although sample sizes are small except for the St. Louis River at Scanlon. On the other hand, validation results (for a very small sample size) are less promising, with over-estimation by the model by similar amounts at both St. Louis River below Cloquet River and St. Louis River at Scanlon. This could be associated with the representation of point sources, for which nitrogen releases (other than ammonia) are based on generalized estimates of concentration, not measurements. Observations of nitrate N are more numerous and are fit well at Scanlon during the calibration period, but show considerable variability in results at other stations. In addition to the uncertain nitrogen loads from point sources, the model representation of kinetic transformations among nitrogen species is suspect. In particular, the amount of different inorganic species is highly sensitive to the specification of the algal preference ratio for nitrate versus ammonia nitrogen. This is a fixed ratio in HSPF, but in reality may vary over the seasons as different planktonic and benthic algae/macrophytes predominate.

Cloquet Watershed

Only one station has a significant number of observations in this watershed and it is located downstream of Island Lake, a large and deep reservoir. Processes within Island Lake and the other large impoundments in this watershed likely have a significant impact on results. For example, HSPF, as a one-dimensional model, cannot represent the impacts of seasonal stratification on nutrient loads leaving this lake.

For total phosphorus, the model achieves very good calibration statistics for average relative error, but larger median relative errors – indicating that the average is balanced out by a few observations with larger negative errors. Average relative errors during the validation period are only of "Fair" quality. Note, however, that the average concentration is only 0.027 mg/L so that an error of only 0.01 mg/L is equal to a deviation of 37 percent.

For total nitrogen, the model achieves good statistics during the calibration period, but no older validation data are available. Nitrate tends to be over-estimated, likely due to algal dynamics within the lakes.

Nemadji Watershed

Average total phosphorus concentrations at several of the monitoring stations in the Nemadji watershed are nearly an order of magnitude greater than those observed in the St. Louis River watershed. The exceptions are the Blackhoof River and Nemadji River near Holyoke stations, both of which have watersheds wholly or largely outside of the lacustrine red clay area. Thus, the higher concentrations of total phosphorus at downstream stations appear to be associated with the high erosion rates in the red clay area. This also means that the accuracy of the phosphorus simulation will be closely tied to the accuracy of the channel sediment simulation – which, as seen in Volume I, presents challenges in this dynamic basin.

Phosphorus simulation results for the downstream station, Nemadji River near South Superior, were provided above as an example of the calibration graphs used in model fitting (Figure 3-8). Average relative error statistics at this station rate as "Very Good" for load, but only "Fair" for concentration. For smaller streams, the model appears to over-predict phosphorus concentrations and loads in Rock Creek and Blackhoof River, while under-predicting in Deer Creek. This largely reflects difficulties in the sediment calibration (Volume I), where it was noted that the stream response appeared very different in the later period after 2008 as opposed to the earlier intensive monitoring of 2001-2005, which had much higher sediment concentrations. The sediment model was intentionally fit to the later period. This in turn affects the phosphorus simulation, where the model systematically under-predicts observed phosphorus in

the earlier period. It provides a much better visual fit in the later period, but average relative errors are still much less than zero due to the presence of a few outliers. For both Deer Creek and Rock Creek the excess observed phosphorus appears to be largely organic phosphorus (and indeed ortho-phosphorus is fit well in Rock Creek and acceptably in Deer Creek). Evidently there are differences in condition between these two neighboring creeks that result in higher organic phosphorus loads associated with channel erosion in Deer Creek for reasons that are not fully understood.

For Nemadji River near Pleasant Valley the model appears to under-predict total phosphorus loads based on the average relative error for paired observations and predictions. This may be misleading, however: Tetra Tech conducted a FLUX analysis of load at this station that interpolates loads as a stratified regression against flow. For the period of data collection (2003-2012) the model simulation and FLUX produce results that are within 1 percent of each other.

Statistics for total nitrogen are in the "Very Good" to "Good" range for the downstream stations on the Nemadji River (Pleasant Valley and South Superior), but the results are more variable in the smaller streams. Large relative errors are seen for nitrate plus nitrite-N at some of these stations, primarily where total nitrogen is dominated by the organic fraction. For instance, in Blackhoof River observed total nitrogen concentrations average just under 1 mg/L, but the average nitrate concentration is only about 0.2 mg/L. As with total phosphorus, the model and FLUX estimates of nitrate-N load for the monitored and gaged station Nemadji River near South Superior are close to one another, differing by only 2 percent.

3.2.2.2 Comparison of Model to FLUX Estimates of Delivered Load

MPCA's Watershed Pollutant Load Monitoring Network (WPLMN) is designed to obtain spatial and temporal pollutant load information from Minnesota's rivers and streams and track water quality trends. As part of this program, MPCA releases estimates of annual pollutant loads for each 8-digit hydrologic unit code basin developed using the FLUX program, as described in Section 2. MPCA estimates at the downstream gage station on the St. Louis River (St. Louis River at Scanlon), Cloquet River (at Burnett), and Nemadji River (at South Superior) are currently available for calendar years 2009 – 2011. (Most early years were judged to have insufficient data and flow gaging on the Cloquet did not commence until Water Year 2009.) Comparisons between the MPCA FLUX estimates and model simulated results are shown in Figure 3-10 through Figure 3-12 and Table 3-7.

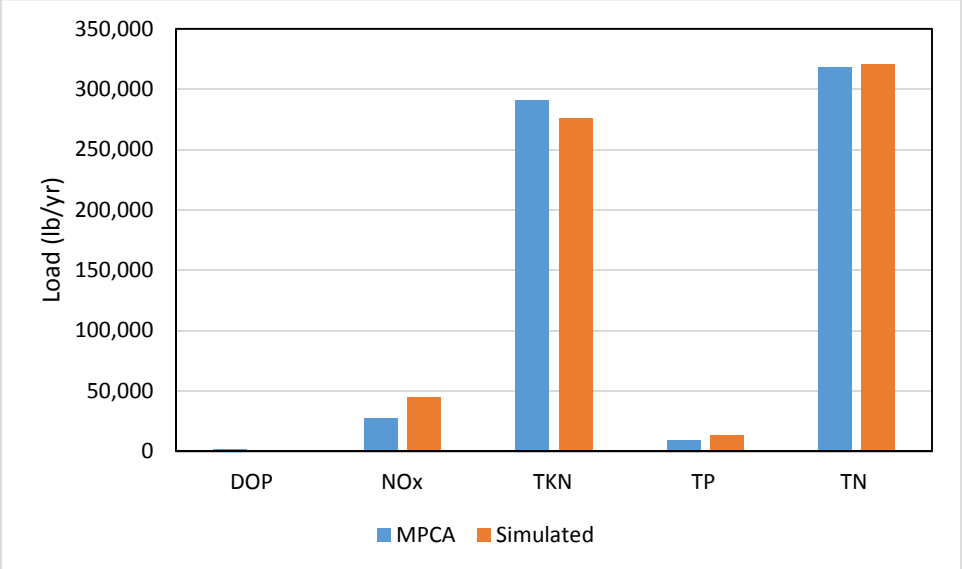

Figure 3-10. Comparison of Model to MPCA FLUX Estimates of Pollutant Load, Calendar Years 2009-2011, Cloquet River near Burnett

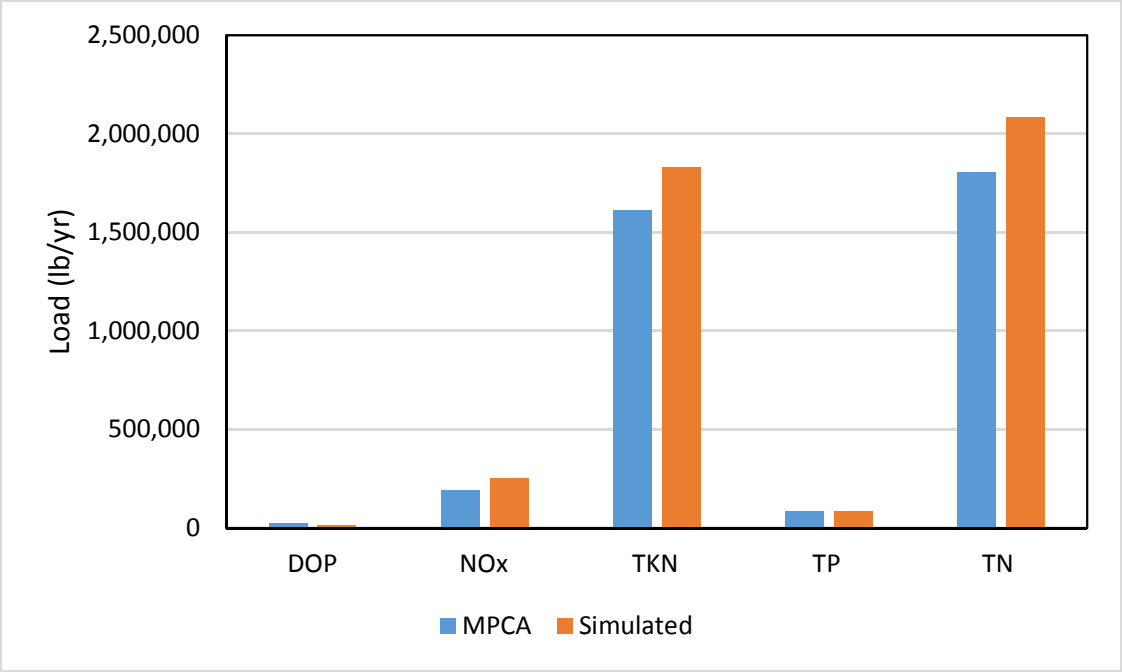

Figure 3-11. Comparison of Model to MPCA FLUX Estimates of Pollutant Load, Calendar Years 2009-2011, St. Louis River at Scanlon

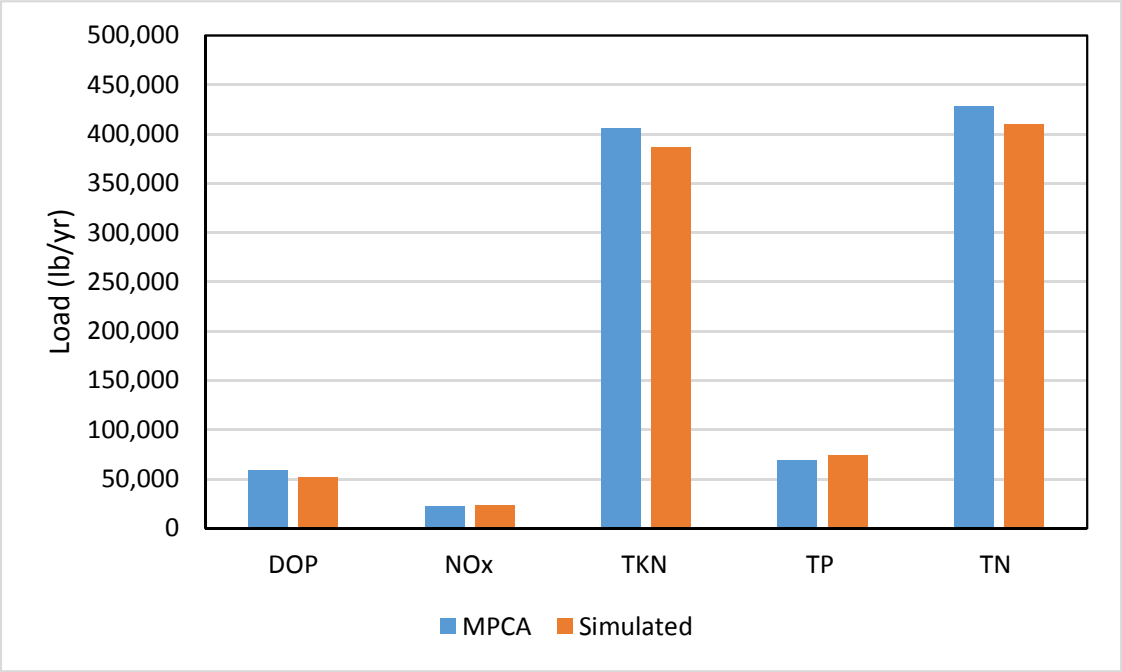

Figure 3-12. Comparison of Model to MPCA FLUX Estimates of Pollutant Load, Calendar Years 2009-2011, Nemadji River near South Superior, WI

Table 3-7. MPCA FLUX Estimates and Model Simulated Annual Nutrient Loads, Calendar Years 2009-2011

Station		Total N	Total P	Total Kjeldahl N	Nitrate + Nitrite N	Dissolved Ortho-P
Cloquet River nr Burnett	MPCA FLUX	318,431	9,374	290,598	27,834	1,920
	Simulated	320,531	12,922	275,839	44,692	1,074
	Difference	0.7%	37.9%	-5.1%	60.6%	-44.0%
St. Louis River at Scanlon	MPCA FLUX	1,801,717	84,517	1,609,440	192,277	24,597
	Simulated	2,080,380	85,720	1,830,385	249,995	13,786
	Difference	15.5%	1.4%	13.7%	30.0%	-44.0%
Nemadji River nr South Superior, WI	MPCA FLUX	428,683	68,615	405,594	23,089	58,981
	Simulated	410,495	74,571	386,865	23,630	52,031
	Difference	-4.2%	8.7%	-4.6%	2.3%	-11.8%

For total nitrogen, the match between FLUX and model simulations is rated "Very Good" or "Good" for all three basins, as is total phosphorus for the St. Louis and Nemadji River basins. The model does appear to over-predict total phosphorus load in the Cloquet River (although the total load is small). Improving this would likely require a better understanding and representation of processes within Island Lake and the other large impoundments in this basin, perhaps using a two-dimensional lake model.

Model performance is also "Very Good" for total Kjeldahl nitrogen, which is the dominant fraction of nitrogen load (primarily as organic nitrogen). The match is not as good for nitrate + nitrite nitrogen or dissolved ortho-phosphorus. Both of these constituents are very sensitive to plant/algal uptake of inorganic nutrients and release of organic nutrients, much of which occurs in wetlands. HSPF does not provide detailed simulation of kinetic processes in emergent wetlands. In addition, results for the St. Louis are sensitive to the specification of point source discharges, for which complete nitrogen species are generally not monitored, and only total phosphorus is available for most permits.

Tetra Tech used FLUX to estimate long-term loads for 1995-2012 at the two stations (Saint Louis River at Scanlon and Nemadji River near South Superior, WI) that have consistent continuous flow gaging for this period. Results have greater uncertainty than the MPCA analyses presented above because monitoring was relatively scarce in the earlier period. These results show the model slightly under-estimating nutrient loads of total P, nitrate + nitrite-N, and total Kjeldahl N for the St. Louis River at Scanlon (Figure 3-13), which is the opposite of the comparison to MDNR analyses of the 2008-2011 period. The difference for total nitrogen is -11% (within the "Very Good") range, while that for total phosphorus is -25% (at the border between "Good" and "Fair"). The longer-term FLUX results suggest that the model may produce some under-estimation of total phosphorus and total nitrogen load in the St. Louis River, although the FLUX estimates for periods prior to 2008 are highly uncertain due to the lack of contemporaneous water quality monitoring data and limited information on some point source discharges. Similar results are provided for the Nemadji River in Figure 3-13. For the Nemadji, the differences in long-term total nitrogen loads (-14%) and total phosphorus loads (+11%) are both within the "Very Good" range.

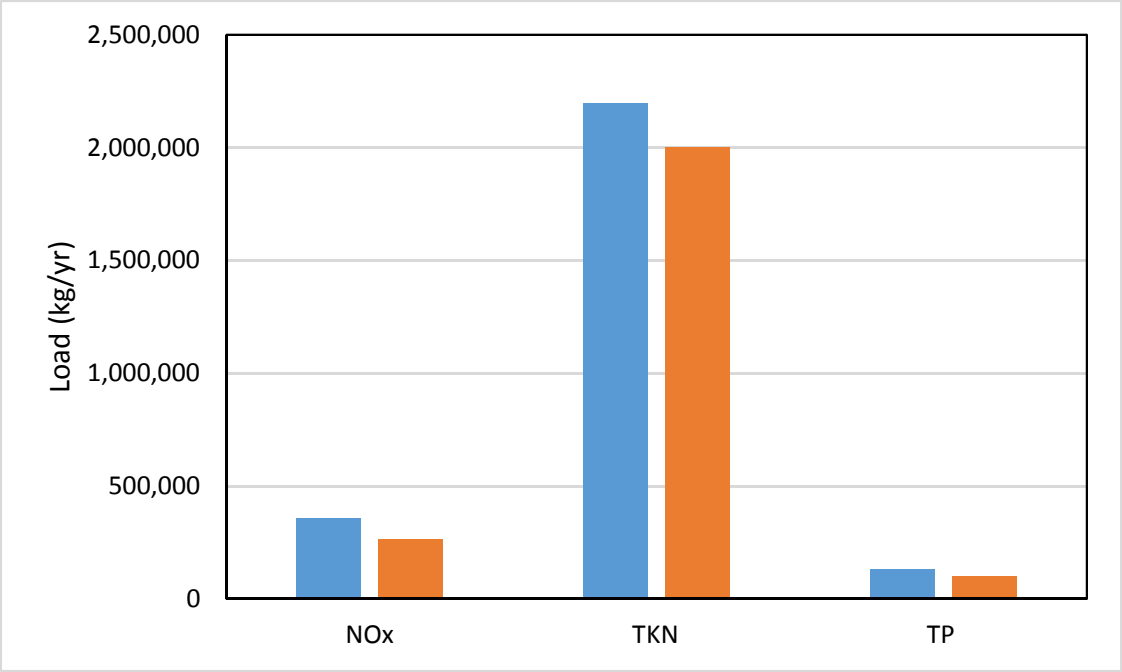

Figure 3-13. Comparison of Model to FLUX Estimates of Annual Nutrient Load, St. Louis River at Scanlon, 1995 – 2012

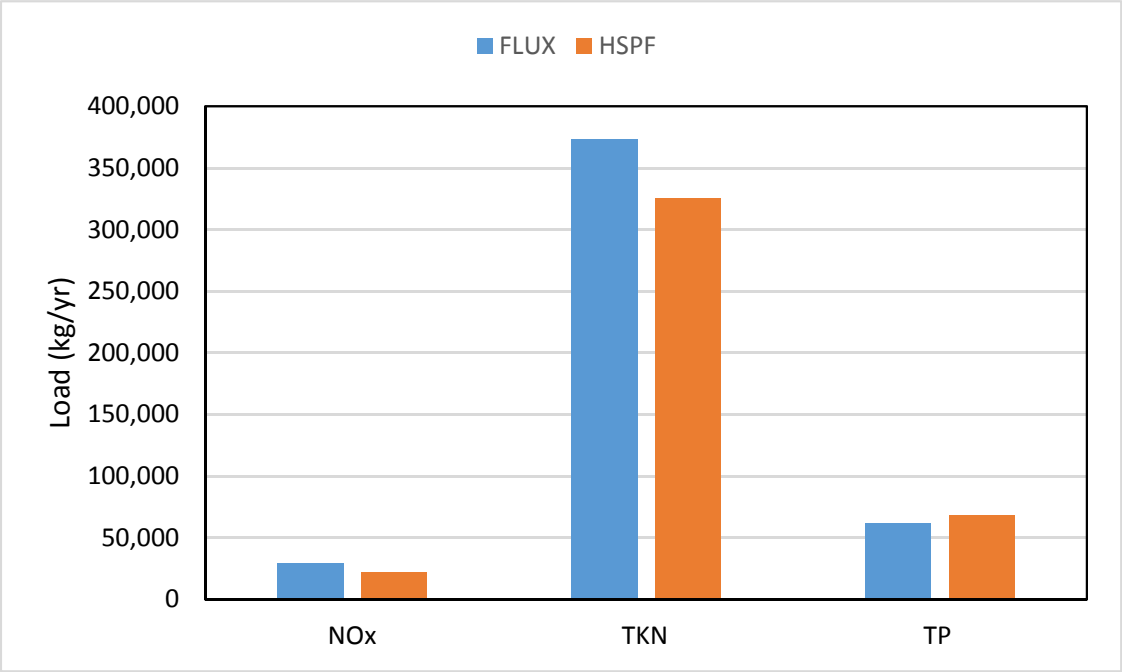

Figure 3-14. Comparison of Model to FLUX Estimates of Annual Nutrient Load, Nemadji River at South Superior, 1995 – 2012

3.2.2.3 Consistency with Lake Analyses

The St. Louis and Cloquet watersheds have a large number of lakes. In contrast, the Nemadji watershed has only a few lakes with small watersheds. Detailed nutrient balance studies are not available for most,

if any, of these lakes. MPCA has, however, conducted screening analyses of many of these lakes using the MINLEAP protocol (Wilson and Walker, 1989: MPCA, 2005). MINLEAP is designed to predict eutrophication in Minnesota lakes based on watershed area, lake depth, and ecoregional phosphorus concentrations. It is a scoping tool designed to estimate lake condition based on minimal data that calculates water and phosphorus balance and in-lake predicted phosphorus and chlorophyll *a* concentrations, which are compared to observed concentrations.

Because MINLEAP is a scoping-level tool that is not calibrated to individual lakes it does not provide a direct basis for comparison to the basin-scale HSPF model. However, it is somewhat informative to examine the deviations between MINLEAP predictions and observed lake conditions and to interpret these relative to the HSPF model predictions.

The St. Louis, Cloquet, and Nemadji watersheds are in the Northern Lakes and Forests ecoregion, for which MINLEAP assigns a stream phosphorus concentration of 55 µg/L. This is somewhat higher than the total phosphorus concentrations observed in most of the St. Louis and Cloquet monitoring stations, although lower than observed at most monitoring locations in the Nemadji (refer to Table 3-4 above).

For the St. Louis River watershed, MINLEAP analyses of 25 lakes (MPCA, 2013b, Appendix 12) tended to over-estimate in-lake phosphorus concentrations where concentrations were less than about 30 µg/L and under-estimate in-lake phosphorus concentrations where observed concentrations were greater than about 50 µg/L. Most of the assessed lakes are smaller waterbodies that are not explicitly represented in the basin-scale HSPF model. Results for five lakes that are explicit in HSPF, but for which the model was not calibrated, are compared in Table 3-8. HSPF results are shown for 2003 – 2012 as the average for the May – September growing season, along with the range of monthly averages. The observations fall within the range of predicted monthly concentrations for three of the five lakes, but appear to predict concentrations that are too high in Long and Esquagama

Table 3-8. Comparison of Observed, MINLEAP, and HSPF Projections of Growing Season Average Total Phosphorus Concentrations, 2003-2012

Lake	Model Reach	Observed Total P (µg/L)	MINLEAP Total P (µg/L)	HSPF Total P (Growing Season Average, µg/L)	
				Average	Monthly Range
Esquagama	253	16	34	37	(25 - 58)
Long (64-0495)	275	51	40	25	(13 - 77)
Manganika	602	308	166	67	(46 - 336)
West Two River	245	42	31	25	(13 - 77)
Whiteface	289	26	30	18	(12 - 30)

Note: MINLEAP and observed results from MPCA (2013b), except that Esquagama has been recalculated by Tetra Tech using MINLEAP standard assumptions. MPCA (2013b) adjusted the inflow concentration to Esquagama based on local monitoring to achieve a predicted in-lake concentration of 12 µg/L. Phosphorus loading to Manganika Lake used in the MINLEAP analysis in MPCA (2013b) is based on wastewater discharges and not regional assumptions. HSPF results are based on May – September monthly averages for the years 2003 – 2012.

We analyzed average annual phosphorus loading rates to a subset of the assessed lakes (using the land use distribution in the drainage area of the lake where the lake was not explicitly delineated for the basin-scale HSPF model) and determined that the HSPF-predicted total average phosphorus load per year was generally greater than the MINLEAP prediction. The combination of higher watershed loads but lower

predicted in-lake concentrations for the lakes that appear in both Table 3-8 and Table 3-9 occurs because (1) the MINLEAP equations estimate a lower fraction of runoff relative to precipitation, (2) the MINLEAP analyses assume a flow-weighted concentration that applies across all flows, and (3) HSPF predicts greater deposition and retention in these lakes than the MINLEAP default calculations.

Table 3-9. Comparison of MINLEAP Total Phosphorus Loads to HSPF Simulated Phosphorus Load for Assessed Lakes in the St. Louis River Basin, 2003-2012

	HSPF Upland Load (lb/ac/yr)	HSPF Average Annual Load (kg/yr)	MINLEAP Average Load (kg/yr)
Dinham	0.175	358	224
Esquagama	0.124	5,542	4,933
Long (69-0495)	0.158	2,262	266
Manganika	0.160	373	162
McQuade	0.232	1,254	606
Mudhen	0.141	236	174
Strand	0.184	240	144
West Two Rivers	0.153	844	979
Whiteface	0.119	3,340	4,197

Note: MINLEAP results from MPCA (2013b), except that Esquagama has been recalculated using MINLEAP standard assumptions. MPCA (2013b) adjusted the inflow concentration to Esquagama based on local monitoring to achieve a predicted annual load of 1,443 kg/yr. HSPF Loads are summarized for 2003 – 2012.

For the Nemadji River watershed, MINLEAP results are given in Appendix 9 of MPCA (2014). These are compared to HSPF loads in Table 3-10. For seven of these eight lakes the HSPF-predicted watershed loads are again higher than MINLEAP. None of these small lakes are explicitly simulated in the basin-scale HSPF model.

Table 3-10. Comparison of MINLEAP Total Phosphorus Loads to HSPF Simulated Phosphorus Load for Assessed Lakes in the Nemadji River Basin, 2003-2012

	HSPF Upland Load (lb/ac/yr)	HSPF Average Annual Load (kg/yr)	MINLEAP Average Load (kg/yr)
Bear	0.153	159	55
Chub	0.143	162	117
Hay	0.156	163	113
Lac La Belle	0.232	246	25
Net	0.238	120	324
Sand	0.223	45	24
Spring	0.226	17	14
Venoah	0.258	930	130

Note: MINLEAP results from MPCA (2014).

4 Water Temperature Calibration

Instream temperature is an important parameter for simulating biochemical transformations. The HSPF modules used to represent water temperature include PSTEMP (soil temperature) and HTRCH (heat exchange and water temperature).

Simulation of soil temperature is accomplished by using three layers: surface, upper subsurface, and groundwater subsurface. The surface layer is the portion of the land segment that determines the overland flow water temperature. The upper subsurface layer determines interflow temperature while the groundwater subsurface layer determines groundwater temperature. Surface and upper subsurface layer temperatures are estimated by applying a regression equation relative to measured air temperature. The groundwater subsurface temperatures are supplied a temperature which reflects the average subsoil temperature for the region. Initial parameters for the St. Louis, Cloquet, and Nemadji models are based on recommendations in the Long Prairie example file provided as part of MPCA's HSPF modeling guidance (AQUA TERRA, 2012).

Soil temperature is only used to determine the water temperature of the three different flow paths (surface outflow, upper subsurface/interflow outflow, lower subsurface/groundwater outflow) as the water is contributing to stream flow. Once the water is in the stream, the temperature is impacted by mechanisms that can increase or decrease the heat content of the water. Mechanisms that can increase the heat content of the water are absorption of solar radiation, absorption of long-wave radiation, and conduction-convection. Mechanisms that decrease the heat content are emission of long-wave radiation, conduction-convection, and evaporation. Heat exchanges between the water and stream bed are also simulated.

Stream temperature follows diel cycles and is strongly affected by the pattern of shading over the course of the day and the local microclimate, as well as specific locations of groundwater discharges to streams. Local-scale variations in hydraulics can also influence temperature readings: for instance, temperatures are likely to be different in a part of a reach impounded by a beaver dam than in a free-flowing riffle. A watershed-scale HSPF model can typically match daily average water temperature but is limited in its ability to simulate the daily cycles of water temperature at specific locations. This is because HSPF represents stream segments as one-dimensional, fully-mixed reactors. These segments are typically in the range of 3 to 15 miles in length in models built at a HUC12 scale, as is the case here and variations within the segment are averaged out. For instance, a single average value represents shading over the whole stream segment and the model does not consider the orientation or aspect of the stream segment relative to the position of the sun. HSPF, as a one-dimensional model, also does not address vertical variation in temperature, which is especially important in deeper lakes and reservoirs. In contrast, a detailed water temperature model for a stream reach (e.g., the QUAL2K model) would typically specify segments with lengths on the order of a tenth of a mile and include a detailed analysis of shading from vegetation and topography in relation to solar position throughout the day and year. For the HSPF application we used an empirical approximation fit during calibration in which the shading factor (i.e., CFSAEX, the fraction of light not shaded out) is scaled relative to the fraction of forest cover in a subwatershed as $1 - 0.73 \cdot$ fraction forest.

While water temperature is measured along with most water quality observations, scattered point in time measurements are of limited use for adjusting the temperature calibration due to strong diel patterns. Fortunately, there are two sources of continuous data: continuous summer data collected by MDNR at a variety of locations, mostly on smaller streams, and continuous monitoring at the USGS gage at Scanlon. The MDNR records available for this project for the St. Louis and Cloquet are from the 1999-2005 period, while those for the Nemadji run from 2000 - 2011. More recent temperature monitoring was collected in the St. Louis watershed beginning in 2011 as part of the recent stressor identification project but was not supplied in time for use in the temperature calibration of the model.

A typical comparison between the simulation and MDNR temperature probe monitoring (for Otter Creek, a tributary to the St. Louis River) is shown in Figure 2-1. HSPF captures the general trend in average temperature, but is imprecise and does not exactly represent the daily minimum and maximum. Average discrepancies by time of day (Figure 2-2) show that the model tends to over-predict during mid-day and under-predict at night, likely related to the diel pattern of shading near the observation site. In addition, the 2000 simulation suggests that peak temperature is under-estimated during August and over-estimated during an early October cold snap. These discrepancies are likely associated with differences between local and meteorological station air temperature and humidity.

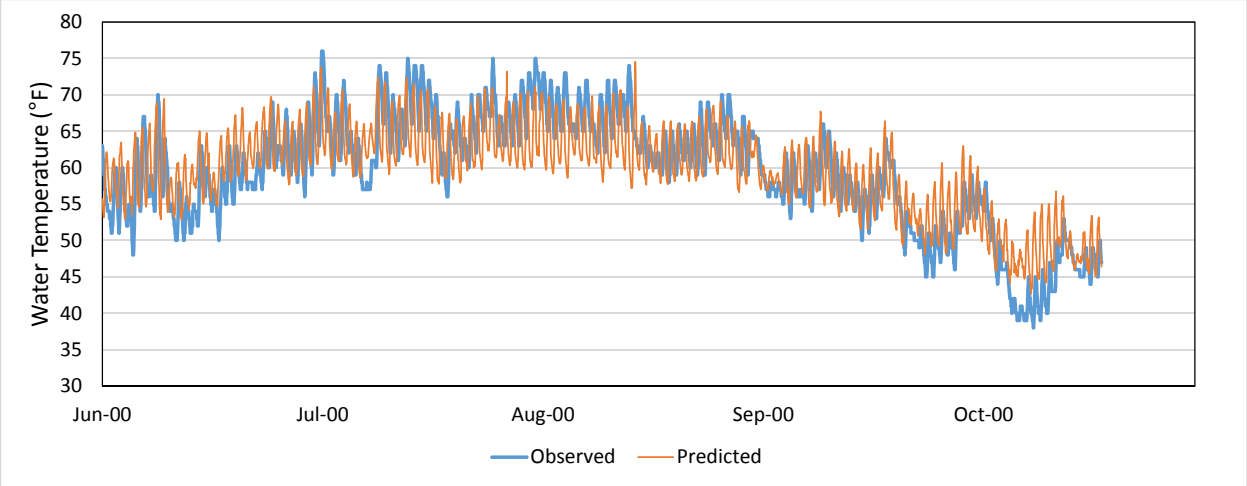

Figure 4-1. Water Temperature Calibration for Otter Creek (Reach 206)

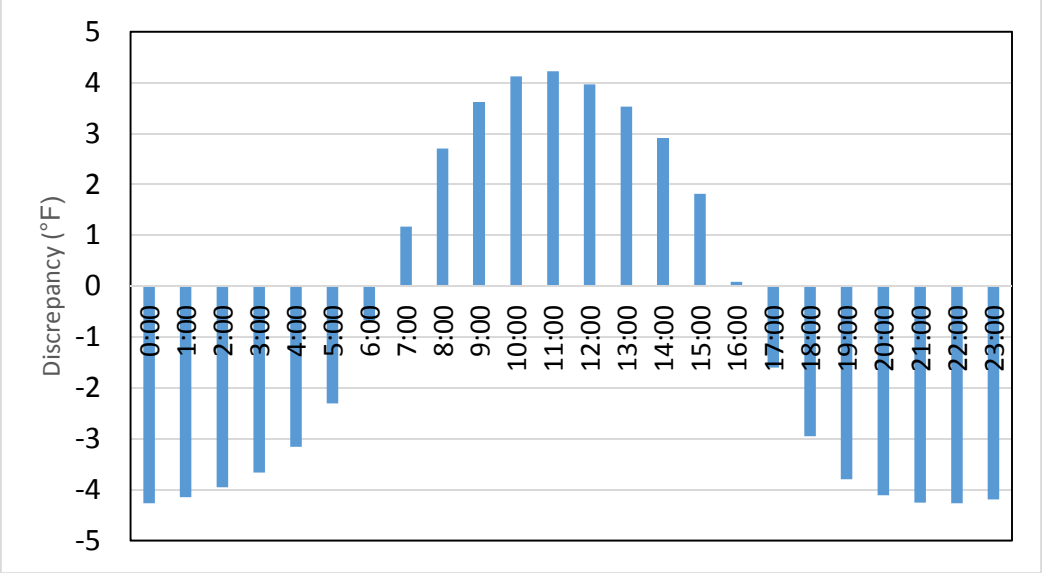

Figure 4-2. Average Water Temperature Discrepancy (Simulated minus Observed) by Time of Day for Otter Creek (Reach 206), 1999-2001

Temperature records were supplied for a large number of stations, with varying periods of record, completeness, and notes regarding quality. We selected a representative set of stations that are (1) near the downstream end of a reach that is simulated in the HSPF model, and (2) have relatively complete, longer periods of record. Results are summarized in Table 2-1. Relative average errors (a measure of bias) range between -4.85 and 2.56 percent; relative absolute errors (a measure of precision) range from

0.62 to 5.73 percent. Duda et al. (2012) state that average percent differences of less than 7 percent should be considered to represent "Very Good" model fit in HSPF – despite the fact that the model does not represent all the observed precipitation extremes. Note that the relative absolute errors are somewhat higher for the Nemadji River watershed stations. In part this is due to the fact that HSPF turns off simulation of water temperature dynamics when water depth falls below 3 inches, resulting in brief periods in which the water temperature simulation is not re-equilibrating with atmospheric temperature.

Table 4-1. Continuous Water Temperature Calibration Statistics

Station	Monitoring Period (seasonal)	Model Reach	Average Error (F)	Relative Average Error	Average Absolute Error (F)	Relative Absolute Error
Otter Creek at mouth	1999-2001	St. Louis 206	-0.80	-1.31%	1.17	1.92%
Stony Brook	2000-2002	St. Louis 211	1.50	2.56%	1.22	2.09%
Stoney Creek @ Hwy 3	2000	St. Louis 278	0.00	0.00%	0.37	0.62%
Cloquet R @ Bear Trap Cr	2003-2004	Cloquet 402	-0.66	-1.05%	1.13	1.81%
Hellwig Cr.	2002-2004	Cloquet 403	1.35	2.18%	1.92	3.12%
UsKabWanKa @ mouth	2002-2003	Cloquet 405	-1.11	-1.78%	0.87	1.40%
Cloquet R @ UsKabWanKa	2003-2004	Cloquet 406	-3.11	-4.85%	0.90	1.40%
Blackhoof R @ Hwy 104	2001-2011	Nemadji 511	0.99	1.62%	3.04	4.99%
SF Nemadji @ Hwy 23	2007-2009	Nemadji 112	1.47	2.45%	3.42	5.73%
Net River @ Hwy 8	2000-2009	Nemadji 111	-0.65	-1.06%	2.74	4.45%
Skunk Creek	2006-2008	Nemadji 115	0.09	0.15%	2.82	4.60%

Since April 2011, USGS has monitored water temperature at the Saint Louis River at Scanlon flow gage (04024000), reporting the daily mean, minimum, and maximum on the NWIS system. Interpretation of water temperature at this station is somewhat problematic, as it is located just downstream of Scanlon Dam and affected by hydropower releases from that dam, plus the Knife Falls Dam just upstream. At this station, the average error is -1.33 °F (-2.52%) and the average absolute error is 3.84 °F (7.29%). Comparison of the time series of daily means shows discrepancies in the summer, when the model under-predicts observed temperatures. This may be due to vertical variation in temperature in the reservoirs in which the surface water flowing over the dams is warmer than the vertically averaged water temperature simulated by HSPF. There are also discrepancies during winter ice conditions as HSPF predicts short-term responses to weather variability where none are observed because the presence of ice is not explicitly simulated.

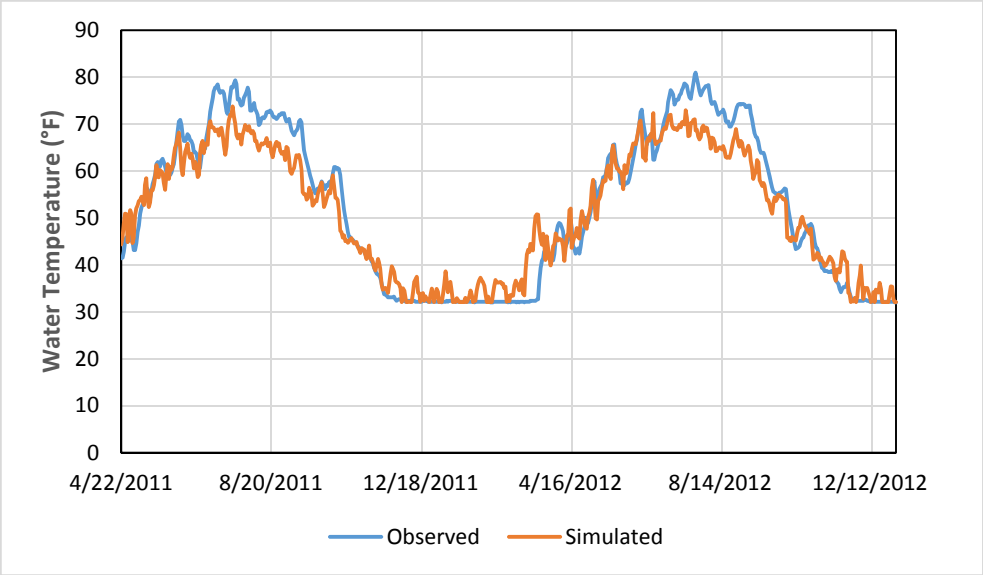

Figure 4-3. Observed and Simulated Daily Average Water Temperature, Saint Louis River at Scanlon

5 Algae and Dissolved Oxygen Calibration

Dissolved oxygen (DO) concentration in streams results from a complex interaction of reaeration rate (a function of turbulence), the oxygen concentration of inflowing water, the saturation concentration of oxygen (which depends on temperature and salinity), consumption of oxygen by bacterial breakdown of carbonaceous and nitrogenous material in the water column (biochemical oxygen demand) and at the water-sediment interface (sediment oxygen demand), production of oxygen during photosynthesis by algae and macrophytes, and consumption of oxygen during nighttime algal/macrophytes respiration. The impact of plant photosynthesis/respiration and diel cycles of water temperature result in a situation where grab sample measures of DO are not very informative for model calibration. Further, the influence of algae/macrophytes on DO means that DO and algae must be calibrated simultaneously.

5.1 ALGAE

Unfortunately, only very limited data are available on algae and macrophytes in flowing streams and wetlands of the St. Louis, Cloquet, and Nemadji watersheds. Observations of chlorophyll *a*, the primary photosynthetic pigment in most algae, are available for many lakes and serve as an indicator of planktonic algae density – but do not provide information on benthic algae and macrophytes. However, many of the monitored lakes are of small size and not explicitly simulated in the basin-scale model. Given the relative paucity of information on algal density, model calibration focused on ensuring that planktonic chlorophyll *a* concentrations were in a reasonable range.

Chlorophyll *a* is not routinely monitored at most stream stations. Four samples from St. Louis River downstream of CR 7, 1 mile south of Forbes (S000-119) show samples ranging from 1.5 to 3.1 µg/L. Average growing season simulated concentrations from streams in the St. Louis River watershed are around 2.5 µg/L.

For the St. Louis River basin the assessed lakes subject to MINLEAP modeling by MPCA (2013) had average observed (growing season) chlorophyll *a* concentrations ranging from 0.2 to 21 µg/L, with the exception of impaired Manganika Lake, which had a mean concentration of 67 µg/L and a median concentration in intensive 2004-2006 monitoring reported in EQUIS of 39 µg/L. Most of the lakes that do not have large point source inputs of nutrients fall between 2 and 12 µg/L.

While more data are available for lakes than streams, chlorophyll *a* data are not known to be available for some of the largest lakes, such as Island Lake, which controls the outflow from the Cloquet basin. In addition, much of the available data are from periods outside the model simulation period (1993-2012). Chlorophyll *a* predictions in 18 explicitly simulated lakes in the St. Louis and Cloquet models are compared to available observations for 1995 – 2012 in Table 5-1. Given the small sample sizes, the model and observations are reasonably in agreement for most of the monitored lakes. The model does appear to over-predict chlorophyll *a* in Esquagama, but, as seen in Section 3.2.2.3, phosphorus concentrations are also over-predicted in this lake. The model under-predicts observations in Long and Wild Rice lakes. Both of these lakes are very shallow with substantial rooted macrophyte growth that is not directly addressed by the HSPF code.

Table 5-1. Chlorophyll *a* Concentrations in Explicitly Simulated Lakes of the St. Louis and Nemadji River Watersheds

Lake	Model Reach	# Samples, 1995-2012	Monitored Average and Range	Simulated Average and Monthly Max
Fond du Lac Reservoir	205	ND		4.7 (8.6)
Thomson Reservoir	207	9	3.5 (1.1 - 5.7)	4.4 (6.9)
Cloquet Reservoir	208	ND		2.8 (6.6)
West Two River Res.	245	10	15.2 (4.3 - 28.6)	3.1 (36.6)
Esquagama	253	9	3.0 (1.8 – 5.0)	8.2 (17.5)
Wynne	254	5	3.1 (1.1 – 7.4)	9.4 (18.5)
Colby	262	10	2.5 (1.0 – 3.8)	10.9 (18.8)
Long (69-0495)	275	22	7.2 (0.05 – 39.8)	0.8 (7.3)
Whiteface	289	19	6.9 (1.1 -14.9)	5.2 (10.7)
Island	407	ND		0.4 (11.6)
Boulder	408	ND		0.2 (2.9)
Fish Lake Flowage	422	ND		0.1 (1.7)
Wild Rice	423	2	15 (13.3 - 16.7)	4.5 (8.7)
Knife Falls	501	ND		3.3 (6.6)
Scanlon Reservoir	502	6	4.8 (3.2 – 9.2)	3.6 (6.5)
Mashkenode	601	ND	4.8 (3.2 – 9.2)	3.2 (20.5)
Manganika	602	30	21.8 (0 – 42.7)	16.1 (38.2)
Ely	603	5	1.2 (1.0 -2.0)	2.3 (28.1)

The current version of the model does not explicitly represented any of the lakes in the Nemadji watershed due to their small size and small drainage areas. Seven of eight assessed lakes had average observed chlorophyll *a* concentrations between 2.8 and 11.2 µg/L, while Lac La Belle had an average of 43.4 µg/L (MPCA, 2014). MINLEAP screening failed to predict the high chlorophyll *a* in Lac La Belle, but HSPF predicts substantially higher phosphorus loading to this lake than would be expected from MINLEAP regional average loading rates (Section 3.2.2.3).

5.2 DISSOLVED OXYGEN

Simulation of dissolved oxygen (DO) in the stream depends on a complex interaction between reaeration, algal production and respiration, and biochemical oxygen demand (Figure 5-1). Many of these processes

also affect nutrient balances, so the DO calibration must be achieved consistent with the nutrient calibration. The oxygen balance is also strongly dependent on water temperature simulation, which affects reaction rates and determines the saturation DO concentration.

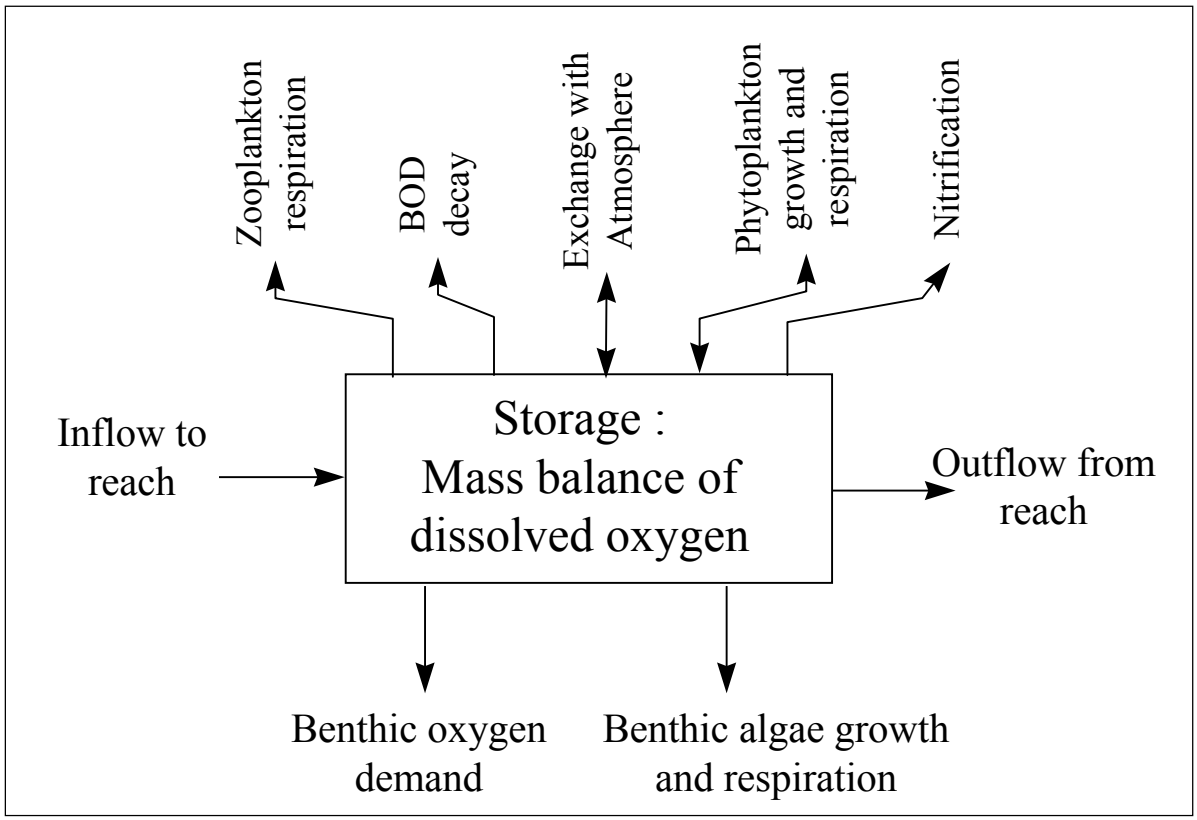

Figure 5-1. Process Diagram for Oxygen Mass Balance in HSPF

Many of the components of the oxygen mass balance in the St. Louis, Cloquet, and Nemadji watersheds have little or no available monitoring data. Specifically, there are no known monitoring data for reaeration rates, benthic oxygen demand, or benthic algal or zooplankton densities. As noted in Section 5.1, monitoring for planktonic algae in streams is very limited. While biochemical oxygen demand (BOD) data exist for many locations, the majority of observations are for 5-day total BOD, whereas HSPF uses ultimate carbonaceous BOD. Total BOD includes the nitrogenous component and may also be affected by the presence of reduced iron. As a result, the model parameters must be specified based on best professional judgment and experience with other, similar sites. The model can then be tested on its ability to reproduce observed DO concentrations.

Reaeration: When oxygen concentrations are reduced below saturation, oxygen tends to move from the atmosphere to the water, a process known as reaeration. The rapidity of reaeration depends on how well the water is mixed and the turbulence present at the water surface. HSPF provides several options for simulating stream reaeration. For the St. Louis, Cloquet, and Nemadji models the Tsivoglou energy dissipation method (Tsivoglou and Wallace, 1972) is used (with default parameters) for stream segments, while reaeration in lake segments is a function of wind speed and surface area (Bicknell et al., 2014).

Biochemical Oxygen Demand: HSPF simulates nitrogenous and carbonaceous components of biochemical oxygen demand separately, with the nitrogenous component being determined by concentrations of reduced inorganic nitrogen species (ammonium and nitrite). Carbonaceous biochemical

oxygen demand (CBOD) loading from the watershed is simulated as the labile fraction of total organic carbon, as described in Section 3.1. As the decay of CBOD results in the conversion of labile organic matter to inorganic nutrients, the representation of CBOD is largely constrained by the nutrient calibration.

The CBOD decay rate (k_d) is expected to be relatively low due both to the nature of organic carbon derived from forest and wetland vegetation, except immediately downstream of point sources. A k_d value of 0.0035 per hour (0.084 per day) appears to provide reasonable results. This is near the low end of the range of values reported nationally for streams without untreated waste input (USEPA, 1997). A higher rate of 0.01 per hour (0.24 per day) is used for segments near major WWTP discharges.

Benthic Interactions. Organic soils and sediment associated with northern wetlands affect the oxygen balance. These may both release BOD into the stream and exert a sediment oxygen demand (SOD) at the sediment-water interface. No direct measurements of SOD were identified, and these components are at this time a calibration adjustment factor. Note that in parts of the watershed the oxidation of reduced iron or sulfide could exert a significant oxygen demand. As HSPF does not explicitly address these components in the oxygen balance they are treated as part of the SOD.

Algal Dynamics: The activities of floating (planktonic) and attached (benthic) algae also affect the oxygen balance in streams. Algae produce oxygen as a byproduct of photosynthesis during sunlight hours, but are net consumers of oxygen through respiration at night. Algae can also die off, contributing to the biochemical oxygen demand.

Average CBOD concentrations predicted by the model are in the range of 1 to 2 mg/L in areas without large wastewater inputs. In stations downstream of significant wastewater discharges the predicted instream concentrations are largely a result of the BOD concentrations reported for the discharges. Comparison of simulated and observed average and maximum BOD is provided in Table 5-2. No observations are available for the Cloquet watershed, and only one stream station is available for the Nemadji. The BOD results are in reasonably good agreement, given the discrepancy between observations of 5-day BOD and model simulation of ultimate carbonaceous BOD (CBODu). Much higher concentrations (up to 30 mg/L) were observed in the 1960s and 1970s prior to modern wastewater treatment plant improvements.

Table 5-2. Comparison of Simulated and Observed Biochemical Oxygen Demand (mg/L)

Location	EQUIS Station	Count	Observed Average (and Maximum) BOD-5	Simulated Average (and Maximum) CBODu
St. Louis River at CSAH 7 nr Forbes	S000-119	22	1.4 (2.4)	2.3 (6.6)
St. Louis River below Cloquet R.	S000-023	22	1.2 (1.8)	2.7 (4.9)
St. Louis River at Scanlon	S000-629	33	1.6 (5)	2.7 (4.9)
St. Louis River nr Fond du Lac	S000-021	48	1.4 (2.4)	2.2 (4.6)
Nemadji River nr Pleasant Valley	S000-110	38	1.8 (9)	2.0 (11.9)

Calibration for dissolved oxygen presents some of the same challenges as the temperature calibration as there is likely to be significant diel variability due to the influence of algal photosynthesis and respiration that limits the information value of scattered grab samples. There may also be significant spatial

variability at scales smaller than the reaches in the basin-scale model due to local changes in light availability, substrate composition, and reaeration capacity.

Two sources of data were used for dissolved oxygen calibration. Relatively short periods of continuous DO data were collected throughout the St. Louis watershed from 2012 – 2014 as part of MPCA's Stressor Identification process. Draft data from this effort were provided by Jeff Jasperson of MPCA. We selected stations that were located near the lower end of reaches explicitly simulated in the model and that had good quality ratings assigned to the data. Continuous data are best for DO calibration, but these monitoring efforts typically encompass only a few weeks. We also identified several EQUIS water quality monitoring stations that had frequent, but not continuous DO data. The selected stations for the St. Louis watershed are shown in Table 5-3. Similar data were not available for the Cloquet and Nemadji watersheds.

Table 5-3. Locations and Sources of DO Calibration Data

HSPF Reach	Waterbody	source
205	St. Louis River @ Fond du Lac, S000-021 and S003-972	EQUIS
206	Otter Crk at Carlton, 4th St. N.	Stressor ID
210	St. Louis River below Cloquet River, S000-023	EQUIS
226	Vaara Crk near Wawina, MN 73	Stressor ID
229	Skunk Crk near Meadowlands, CR 196	Stressor ID
231	Sand Crk near Toivola, CR 743	Stressor ID
236	Swan R, S000-641	EQUIS
238	East Swan Crk, Koivu Rd.	Stressor ID
241	Little Swan Crk, CR 444	Stressor ID
244	McQuade Crk near Buhl, CR 592	Stressor ID
248	Elbow Crk, CR 310	Stressor ID
249	St. Louis River at Forbes, S000-568 and S000-119	EQUIS
254	Embarrass River at Embarrass	Stressor ID
256	Embarrass River, Mattson Rd.	Stressor ID
262	Partridge River, S007-022	EQUIS
263	Wyman Crk at Hoyt Lakes, CR 666	Stressor ID
272	Mud Hen Crk near Makinen, CSAH 93	Stressor ID
274	Water Hen Crk near Makinen, CSAH 93	Stressor ID
276	Water Hen Crk near Markhamm, CR 340	Stressor ID
278	Stony Crk near Toivola, CSAH 83	Stressor ID
285	Paleface Crk at Melrude, TWP 6630	Stressor ID
402	Cloquet R @ Burnett, S003-968 and S005-147	EQUIS
502	St. Louis River @ Scanlon, S005-089, S000-639, and S000-146	EQUIS
604	Ely Crk, CSAH 95	Stressor ID

Note: Stations shown as “Stressor ID” are short-term continuous DO records collected to support the draft St. Louis River Stressor Identification Report and provided by Jeff Jasperson of MDNR. Stations shown as “EQUIS” are sets of non-continuous grab samples stored in the MPCA EQUIS System.

Neither type of data is ideal for comprehensive calibration: the Stressor ID data cover too short a period, while the EQUIS data likely do not sample the full diel range of DO. Further, like temperature, the DO response may reflect conditions at a specific point in the stream that are not representative of the reach-averaged DO results produced by HSPF. Therefore, the calibration approach was semi-quantitative, and focused on obtaining reasonable agreement to the summer mean and minimum DO concentrations revealed by the available data.

Some streams showed a rather typical summer DO pattern with a daily average concentration that reflects temperature and the balance between reaeration and instream oxygen demand with a diel sinusoidal pattern superimposed that is a function of algal photosynthesis and respiration cycles. A good example is provided by Sand Creek near Toivola (Figure 5-2).

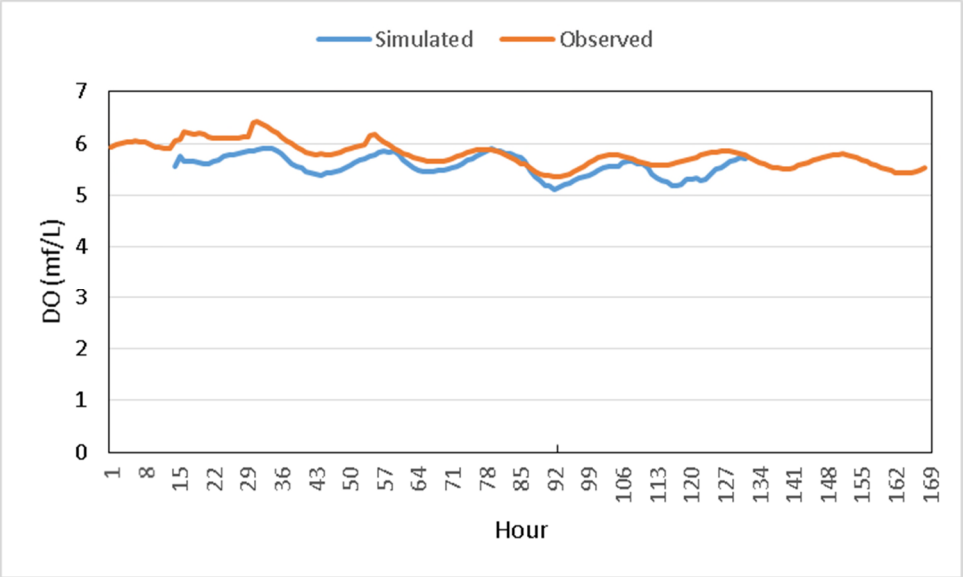

Figure 5-2. Dissolved Oxygen Calibration, Sand Creek near Toivola at CR 231, July 13 – July 18, 2012

In a series of other stream stations, especially those near the Sax Zim bog and Paleface and Mud Hen creeks, monitored DO concentrations remained near zero, with little diel variability imposed by algal photosynthesis. Assuming the data are correct, this is only possible if there is a strong source of oxygen demand within the stream that overwhelms reaeration. An example is shown for Paleface Creek in Figure 5-3. Results for this type of stream (even with an assumption of minimal DO in flow out of adjoining wetlands) could only be matched by assigning a very high SOD of 1,000 mg/m^2/hr. This is higher than the SOD rates measured using *in situ* chambers and reported in USEPA (1997), which range up to a maximum of 780 mg/m^2/hr, but may be enhanced by a chemical oxygen demand from the oxidation of reduced iron seeping into the stream. Oxidation of ferrous iron generally occurs quite rapidly in the presence of oxygen (c.f. Stumm and Morgan, 1996) and the discharge of reduced iron likely a contributor to the low DO and high DO deficit in these streams.

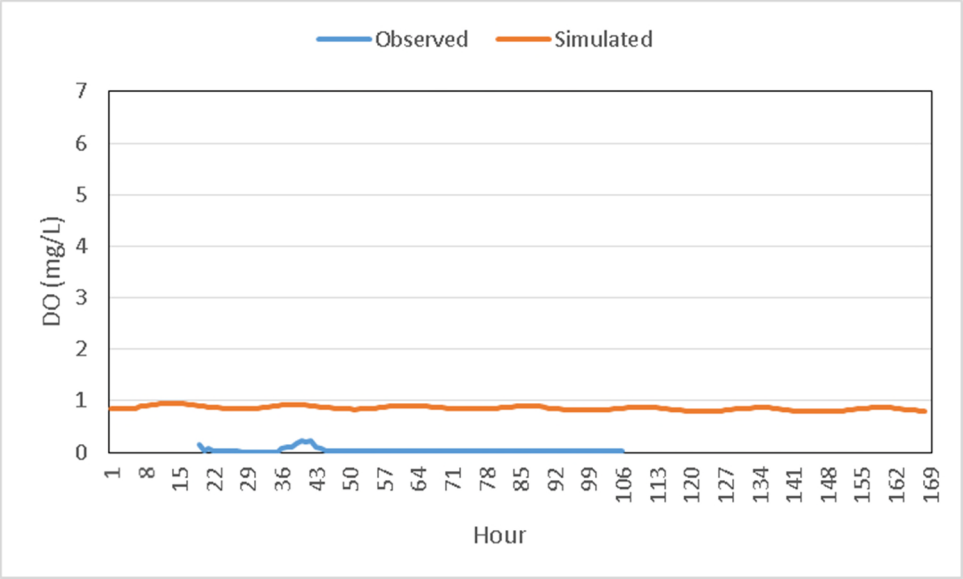

Figure 5-3. Dissolved Oxygen Calibration, Paleface Creek at Melrude TWP 6630, August 23 – August 27, 2012

The St. Louis River HSPF model does a reasonable job of representing observed astronomical summer (June 20 – September 20) mean DO concentrations in monitored reaches, with some exceptions (Figure 5-4), while also predicting minimum concentrations that are generally equal to or less than observed minima. For the mean concentrations the average difference between model and observations is -0.43 mg/L and the average absolute difference is 1.59 mg/L. One notable exception to the relatively good fit is reach 502, which is the EQUIS station just downstream of Scanlon Dam and hydropower station. There, the observed mean of 16.5 mg/L appears likely to represent supersaturated conditions due to air entrainment in the hydropower turbines. This mechanism is not incorporated into the HSPF reaeration equations, but could be described as a point source addition of oxygen mass.

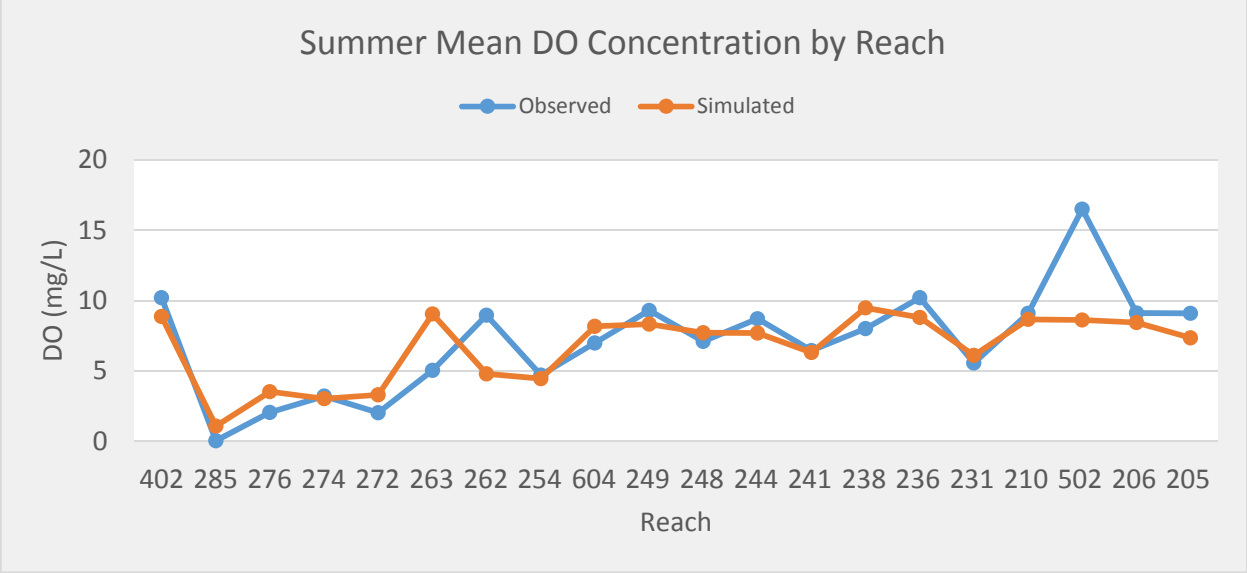

Figure 5-4. Dissolved Oxygen Calibration, Summer Daily Mean Concentration

DO calibration was not possible for the Cloquet and Nemadji watersheds at this time due to lack of monitoring data – for both DO and algae in streams. The calibrated DO parameters from the St. Louis model were transferred to these watersheds; however, benthic oxygen demand was set to the relatively low value of 100 $mg/m^2/hr$ for all reaches. These assumptions will need to be revisited as additional data become available.

(This page left intentionally blank.)

6 Potential Model Enhancements

The model calibrations presented in this report are based on model simulations through the end of 2012. Substantial amounts of data have been collected since 2012. MDNR is currently funding extension of all the model forcing time series (meteorology, point source discharges, appropriations, lake operational discharges, and atmospheric deposition) through the end of 2014. Once completed, this will open the possibility of revising model calibration with substantially more data for comparison – which is likely to result in some adjustments in calibration.

During the completion of this work it has become evident that many issues of interest to stakeholders – such as channel instability in the Nemadji or localized temperature and DO excursions in parts of the St. Louis watershed – may require analysis at finer spatial scales. Further, additional refinements to model segmentation may be needed to make use of data collected on smaller tributaries or at locations in the stream network not currently demarcated in the model. The basin-scale (HUC12-scale) models described here could be further segmented to a finer scale. Alternatively, the basin-scale model provides a framework that could be used for setting boundary conditions for more detailed local models (nested within the basin-scale model) to investigate and simulate specific areas of interest.

As is often the case in watershed models, monitoring data are not sufficient to constrain the simulation to a unique solution relative to individual source areas and processes. In the St. Louis watershed the stations with long periods of monitoring data are mostly downstream of point sources, while in both the St. Louis and Cloquet most stations with nutrient data are downstream of and affected by processes in lakes. Both factors limit our ability to calibrate source loads from individual land uses.

One area in which additional attention may be needed is the representation of wetlands and bogs. Few monitoring or flow gaging data are available to directly evaluate the representation of these land forms. Bog and wetland hydrology simulation may need to be re-evaluated when further information is available. For instance, the impacts of ditches on the hydrologic and water quality response of wetlands is potentially important but is not explicitly addressed in the model at this time.

Water chemistry in the St. Louis watershed is strongly affected by the unique geology of the Iron Range, which provides distinctive ionic signatures for surface and subsurface flows associated with mine dewatering sources and mine tailings. Sulfate and isotope work has proved valuable for identifying and validating flow pathways (e.g., Kelly et al., 2014). Ongoing work by MDNR is evaluating the ionic chemistry of the watershed in comparison to the attribution of surface and subsurface sources of flow in the model. This work may provide important evidence for refinements and enhancements to the model representation of the water balance and flow pathways. Elevated sulfate levels associated with Iron Range geochemistry are of particular interest in the St. Louis watershed due to deleterious impacts on wild rice. Sulfate chemistry is also closely tied to mercury cycling in the watershed (Berndt and Bavin, 2012). The basin-scale HSPF model could be modified in future (e.g., using the geochemical representation of the Mining Data Analysis System [MDAS; Tetra Tech, 2012]).

Surface water interactions with regional groundwater could also be enhanced. In the northern part of the St. Louis watershed the surface water hydrology is impacted by mining operations and mine pit dewatering. An initial exploration of the water balance in this area was carried out using a steady state ground water - surface water simulation model (Tetra Tech, 2014). Future development of a dynamic groundwater model for the region would further enhance representation of these processes. In the Nemadji River watershed, regional groundwater flow and the presence of clay aquitards result in artesian pressure in parts of the watershed (e.g., Deer Creek) that causes surface seeps and sediment "volcanos" that increase sediment and nutrient loads. A preliminary groundwater model application helps understanding of the water balance in this region (Barr, 2013), but awaits further improvement to better inform the surface water modeling.

(This page left intentionally blank.)

7 References

AQUA TERRA. 2012. Modeling Guidance for BASINS/HSPF Applications under the MPCA One Water Program. Prepared for Minnesota Pollution Control Agency by AQUA TERRA Consultants, Mountain View, CA.

Bahnick, D.A., T.P. Markee, and R.K. Roubal. 1979. Chemical Effects of Red Clays on Western Lake Superior. EPA-905/9-7-003. Great Lakes National Program, U.S. Environmental Protection Agency, Region V, Chicago, IL.

Barr. 2013. Appendix A: Deer Creek Watershed and Groundwater Modeling. Prepared in support of the Deer Creek Watershed Total Maximum Daily Load Implementation Plan. Barr, Minneapolis, MN.

Berndt, M.E., and T.K. Bavin. 2012. On the Cycling of Sulfur and Mercury in the St. Louis River Watershed. An Environmental and Natural Resources Trust Fund Final Report. Minnesota Department of Natural Resources, St. Paul, MN.

Bicknell, B.R., J.C. Imhoff, J.L. Kittle, Jr., T.H. Jobes, P.B. Duda, and A.S. Donigian, Jr. 2014. HSPF Version 12.4 User's Manual. National Exposure Research Laboratory, Office of Research and Development, U.S. Environmental Protection Agency, Athens, GA.

Clesceri, N.L., S.J. Curran, and R.I. Sedlak. 1986. Nutrient loads to Wisconsin lakes: Part I. Nitrogen and phosphorus export coefficients. *Water Resources Bulletin,* 22(6), 983-989.

Duda, P.B., P.R. Hummel, A.S. Donigian, Jr., and J.C. Imhoff. 2012. BASINS/HSPF: Model use, calibration, and validation. *Transactions of the ASABE*, 55(4): 1523-1547.

Kelly, M., M. Berndt, and T. Bavin. 2014. Use of Sulfate and Water Isotopes to Improve Water and Chemical Balance Estimates for Water Seeping from Tailings Basins (Focus on US Steel's Minntac Basin). An MWRAP 2 Final Report. Minnesota Department of Natural Resources, St. Paul, MN

Loehr, R. C., S.O. Ryding, and W.C. Sonzogni. 1989. Estimating the nutrient load to a waterbody. *The Control of Eutrophication of Lakes and Reservoirs, Volume I, Man and the Biosphere Series,* S. O. Ryding and W. Rast, ed., Parthenon Publishing Group, 115-146.

McFarland, A. M. S., and Hauck, L. M. 2001. Determining nutrient export coefficients and source loading uncertainty using in stream monitoring data. *Journal of the American Water Resources Association,* 37(1), 223-236.

Minnesota Pollution Control Agency (MPCA). 2004. Detailed Assessment of Phosphorus Sources to Minnesota Watersheds. Minnesota Pollution Control Agency, St. Paul, MN.

Minnesota Pollution Control Agency (MPCA). 2005. Minnesota Lake Water Quality Assessment Report: Developing Nutrient Criteria (Third Edition). Minnesota Pollution Control Agency, St. Paul, MN.

Minnesota Pollution Control Agency (MPCA). 2013a. Nitrogen in Minnesota Surface Waters: Conditions, Trends, Sources, and Reductions. Minnesota Pollution Control Agency, St. Paul, MN.

Minnesota Pollution Control Agency (MPCA). 2013b. St. Louis River Watershed Monitoring and Assessment Report. Minnesota Pollution Control Agency, St. Paul, MN.

Minnesota Pollution Control Agency (MPCA). 2014. Nemadji River Watershed Monitoring and Assessment Report. Minnesota Pollution Control Agency, St. Paul, MN.

Reckhow, K.H., M.N. Beaulac, and J.T. Simpson. 1980. Modeling Phosphorus Loading and Lake Response under Uncertainty: A Manual and Compilation of Export Coefficients. EPA-440/5-80-011. Office of Water Regulations, Criteria and Standards Division, U.S. Environmental Protection Agency, Washington, DC.

Stumm, W., and Morgan, J. J. 1996. *Aquatic Chemistry, Chemical Equilibria, and Rates in Natural Waters*, third edition. Wiley-Interscience, NY.

Tetra Tech. 2012. Updated MDAS Model Capabilities within the LSPC Modeling Framework. Tetra Tech, Inc., Fairfax, VA.

Tetra Tech. 2014. Upper St. Louis River Watershed Mining Area Hydrology. Prepared for Minnesota Pollution Control Agency by Tetra Tech, Inc., Research Triangle Park, NC.

Tsivoglou, E.C., and J.R. Wallace. 1972. Characterization of Stream Reaeration Capacity. EPA-R3-72-012. U.S. Environmental Protection Agency, Washington, DC.

Twaroski, C., N. Czoschke, and T. Anderson. 2007. Detailed Assessment of Phosphorus Sources to Minnesota Watersheds – Atmospheric Deposition: 2007 Update. Prepared for Minnesota Pollution Control Agency by Barr Engineering, Minneapolis, MN.

USEPA. 1997. Technical Guidance Manual for Developing Total Maximum Daily Loads, Book II: Streams and Rivers, Part 1: Biochemical Oxygen Demand / Dissolved Oxygen and Nutrients / Eutrophication. EPA 823-B-97-002. Office of Science and Technology, U.S. Environmental Protection Agency, Washington, DC.

Walker, W.W. 1996. Simplified Procedures for Eutrophication Assessment and Prediction: User Manual. Instruction Report W-96-2. U.S. Army Engineer Waterways Experiment Station, Vicksburg, MS.

Wilson, C.B., and W.W. Walker, Jr. 1989. Development of lake assessment methods based upon the aquatic ecoregion concept. *Lake and Reservoir Management*, 5(2): 11-22.

Appendix A. Detailed Calibration and Validation Results for Water Quality Simulation in the St. Louis and Cloquet River Watersheds

(See separate file.)

(This page left intentionally blank.)

Appendix B. Detailed Calibration and Validation Results for Water Quality Simulation in the Nemadji River Watershed

(See separate file.)

(This page left intentionally blank.)

Appendix A. Water Quality Calibration Details for St. Louis and Cloquet River Watersheds

A.1 PARTRIDGE R NR HOYT LAKES (S007-022)

A.1.1 Ammonia Nitrogen (NH3)

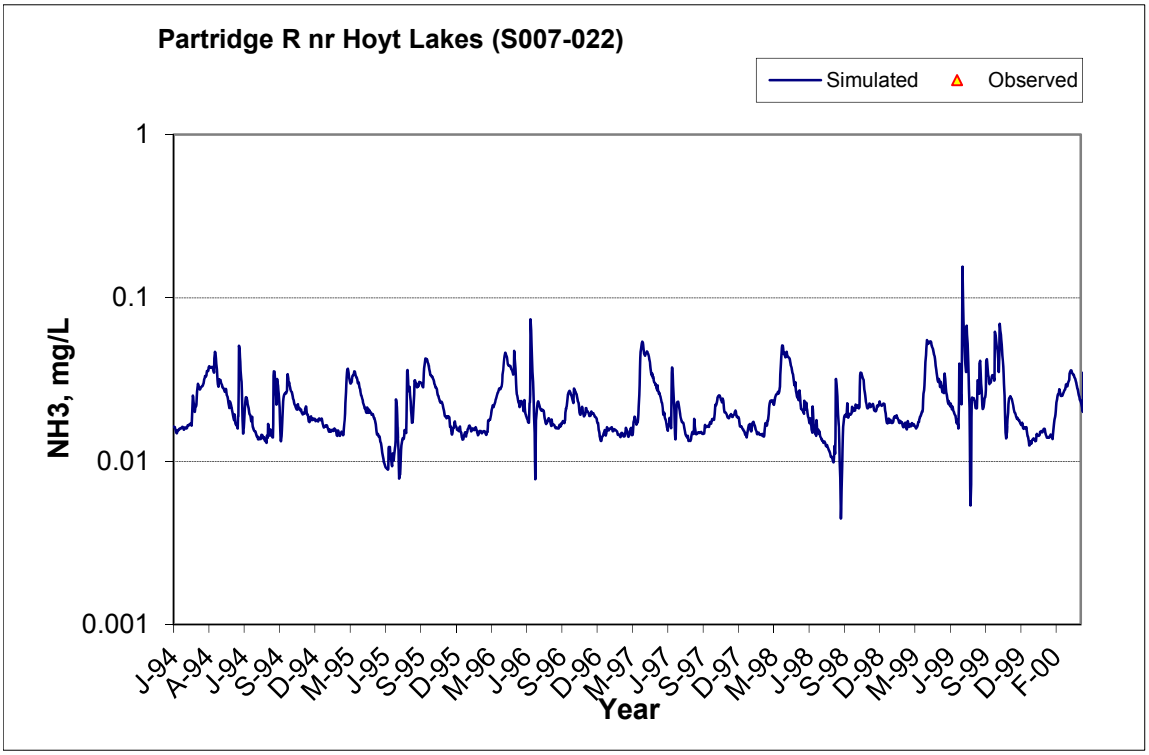

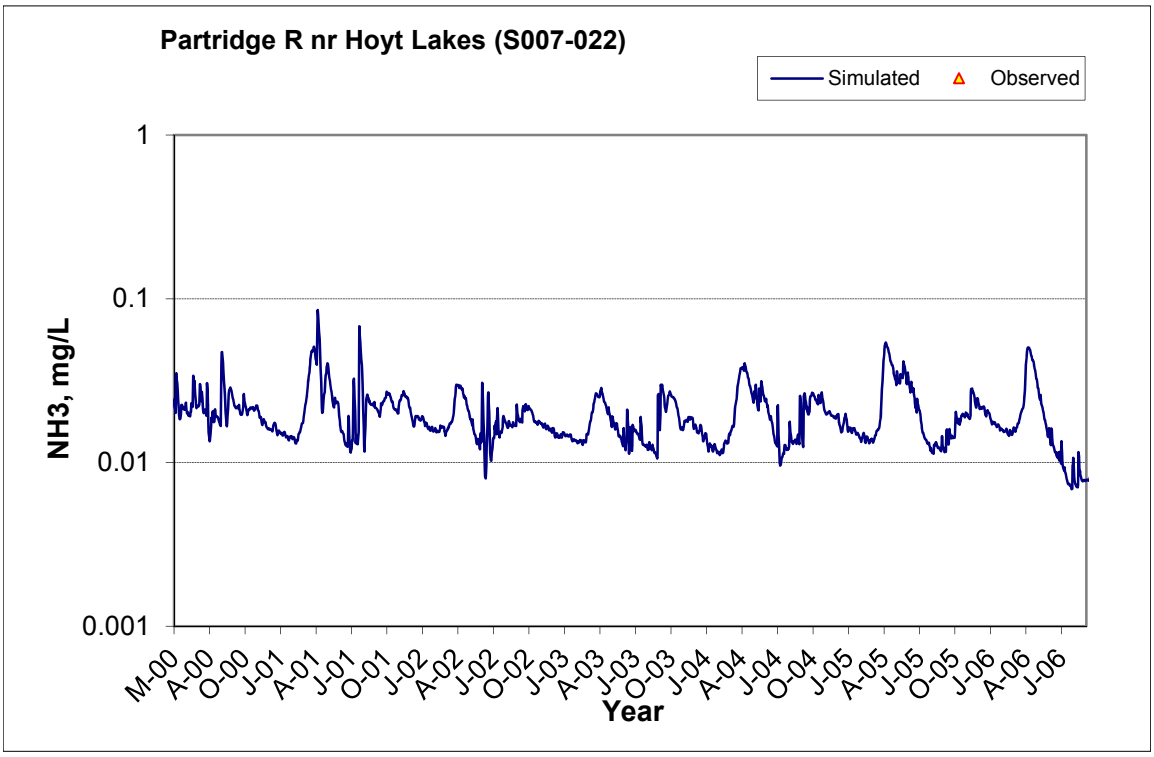

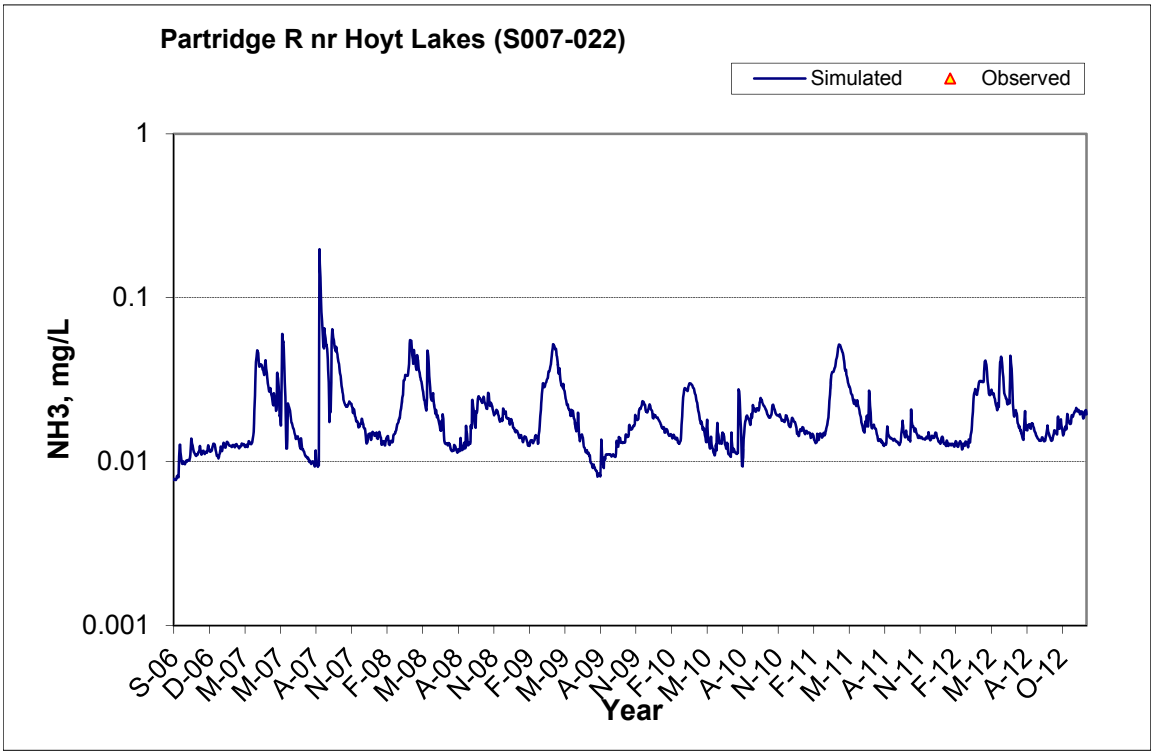

Figure A-1. Time series of observed and simulated Ammonia Nitrogen (NH3) concentration at Partridge R nr Hoyt Lakes (S007-022)

A.1.2 Organic Nitrogen (OrgN)

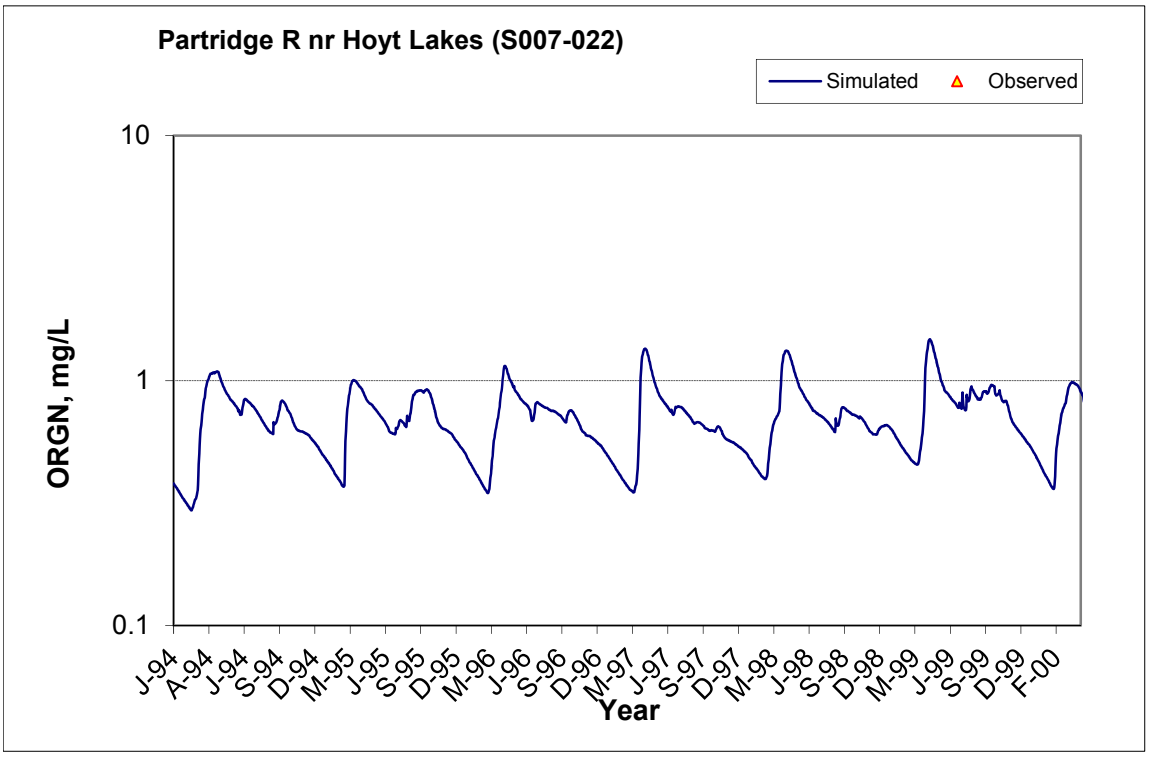

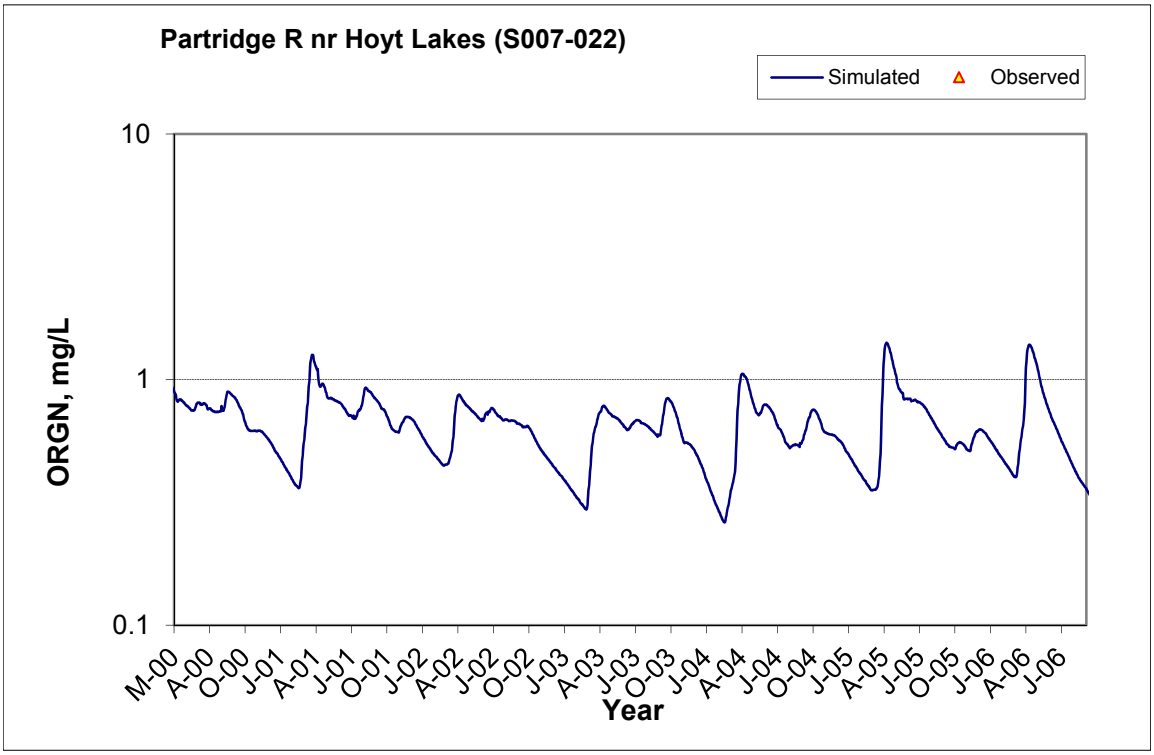

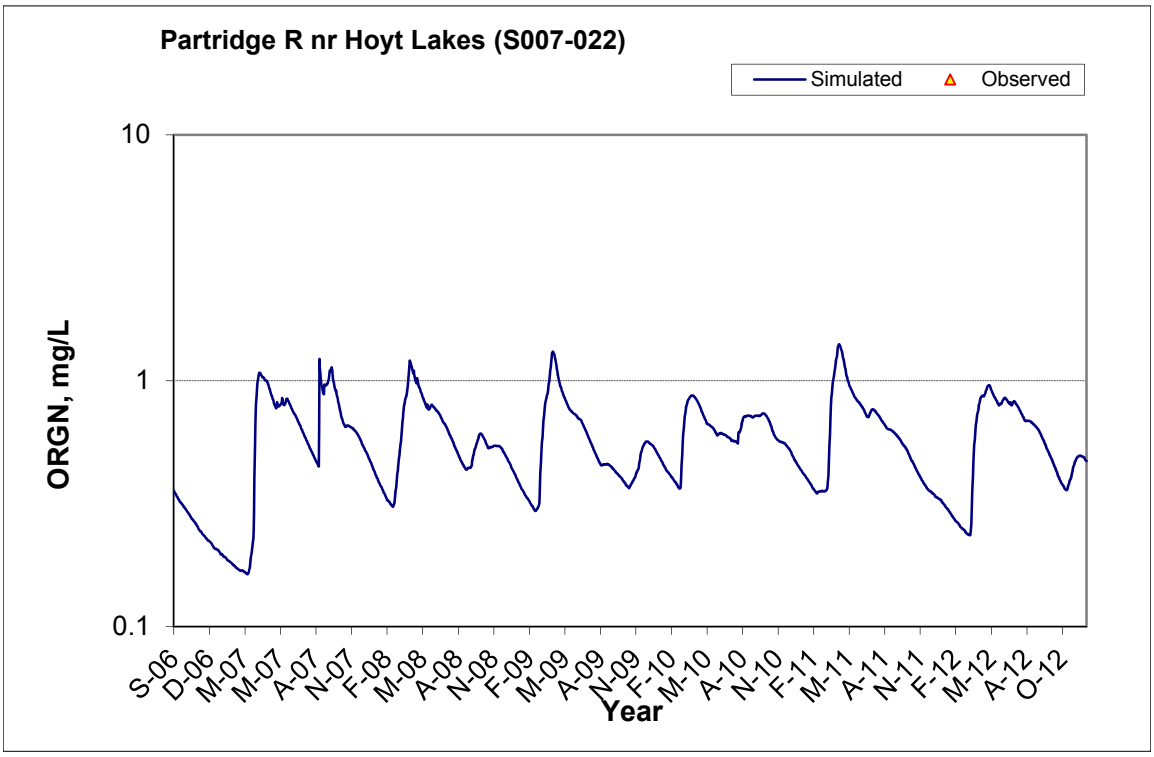

Figure A-2. Time series of observed and simulated Organic Nitrogen (OrgN) concentration at Partridge R nr Hoyt Lakes (S007-022)

A.1.3 Total Kjeldahl Nitrogen (TKN)

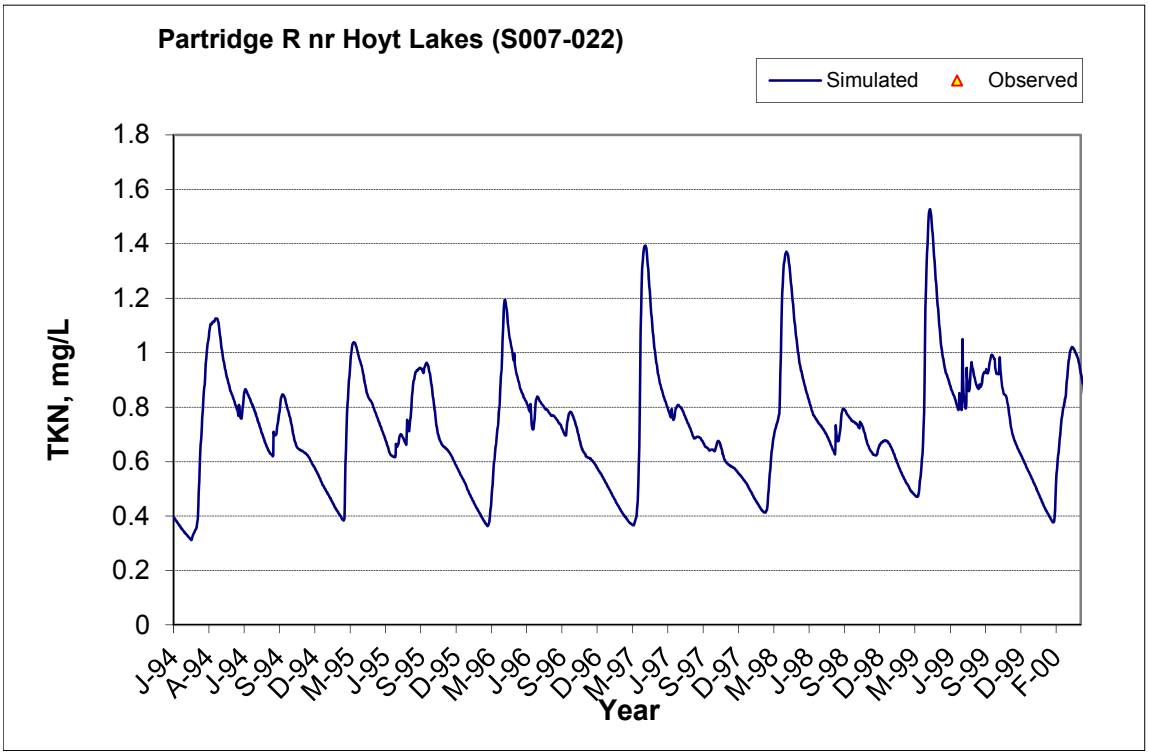

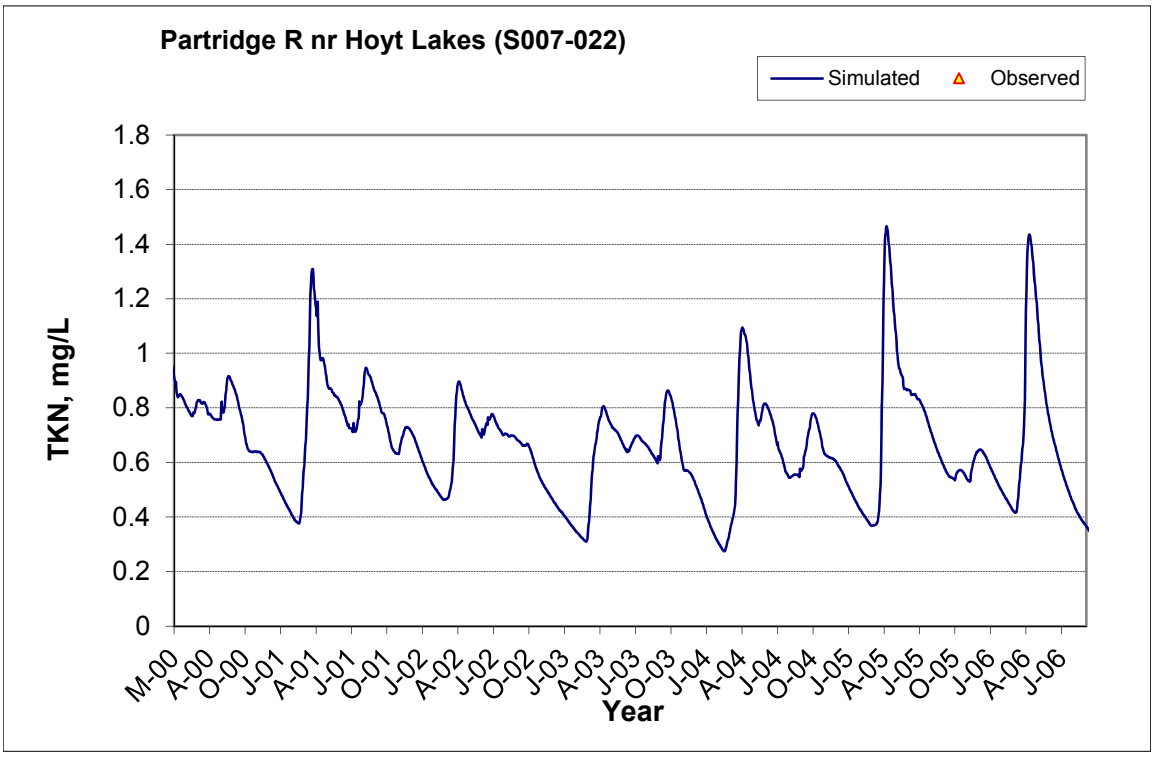

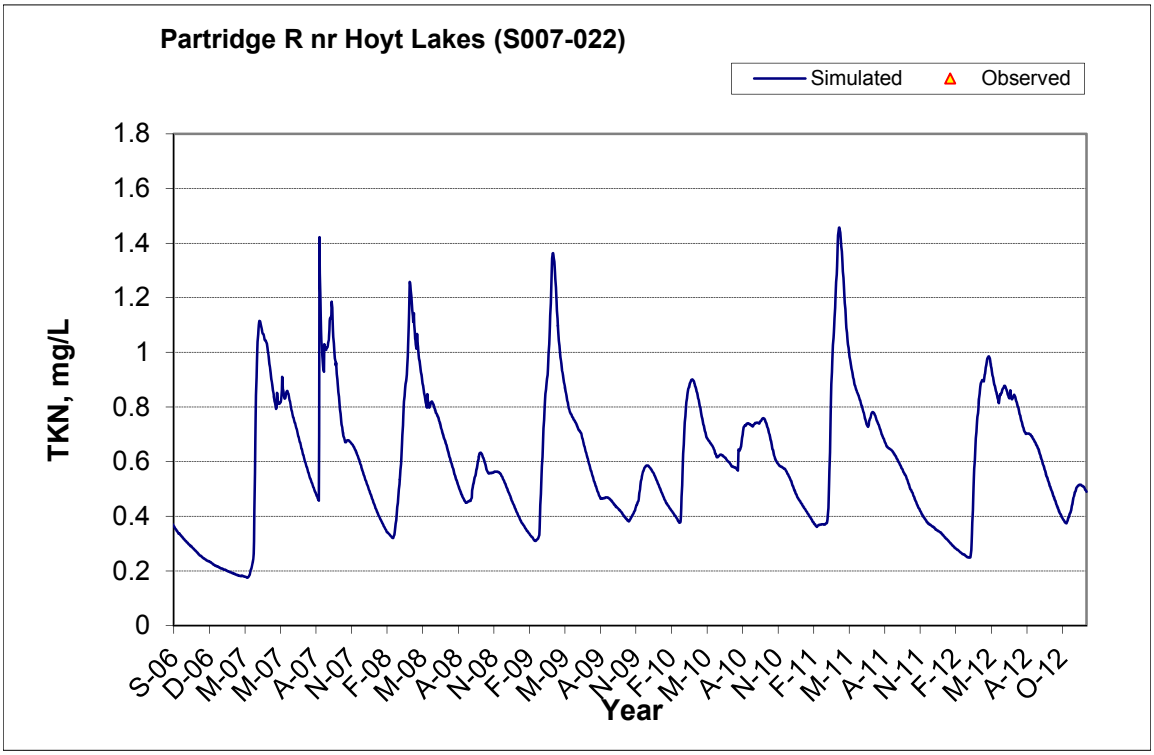

Figure A-3. Time series of observed and simulated Total Kjeldahl Nitrogen (TKN) concentration at Partridge R nr Hoyt Lakes (S007-022)

A.1.4 Nitrite+ Nitrate Nitrogen (NOx)

Table A-1. Nitrite+ Nitrate Nitrogen (NOx) statistics

Period	1994-1993	1994-2012
Count	ND	18
Concentration Average Error		-18.97%
Concentration Median Error		-41.85%
Load Average Error		-33.08%
Load Median Error		-3.21%
Paired t conc		0.54
Paired t load		0.31

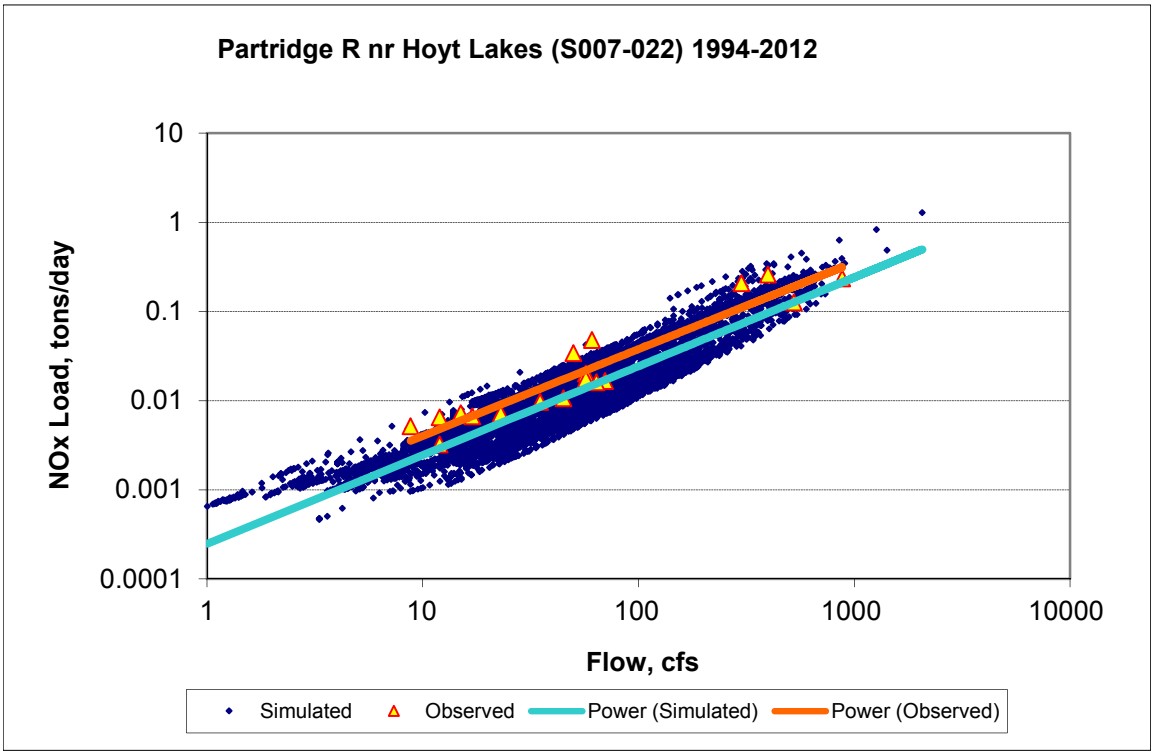

Figure A-4. Power plot of simulated and observed Nitrite+ Nitrate Nitrogen (NOx) load vs flow at Partridge R nr Hoyt Lakes (S007-022) (calibration period)

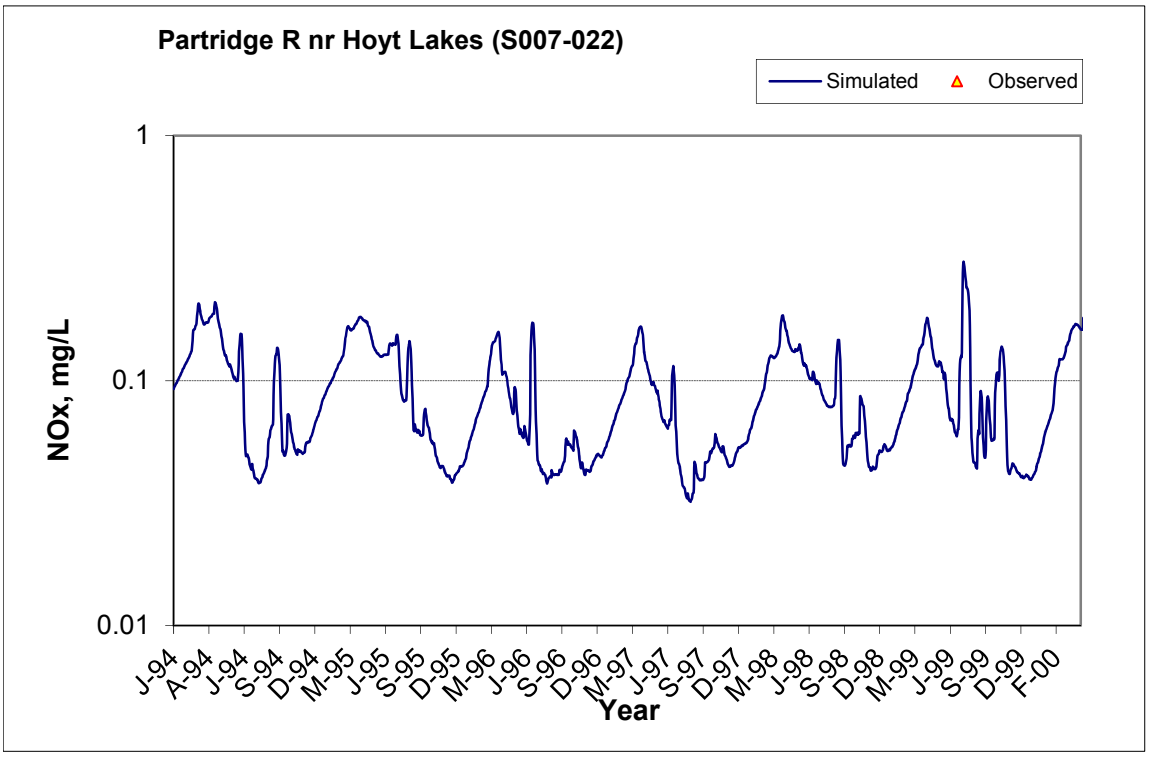
Partridge R nr Hoyt Lakes (S007-022)
Simulated
Observed
NOx, mg/L
1
0.1
0.01
J-94 A-94 J-94 S-94 D-94 M-95 J-95 S-95 D-95 M-96 J-96 S-96 D-96 M-97 J-97 S-97 D-97 M-98 J-98 S-98 D-98 M-99 J-99 S-99 D-99 F-00
Year

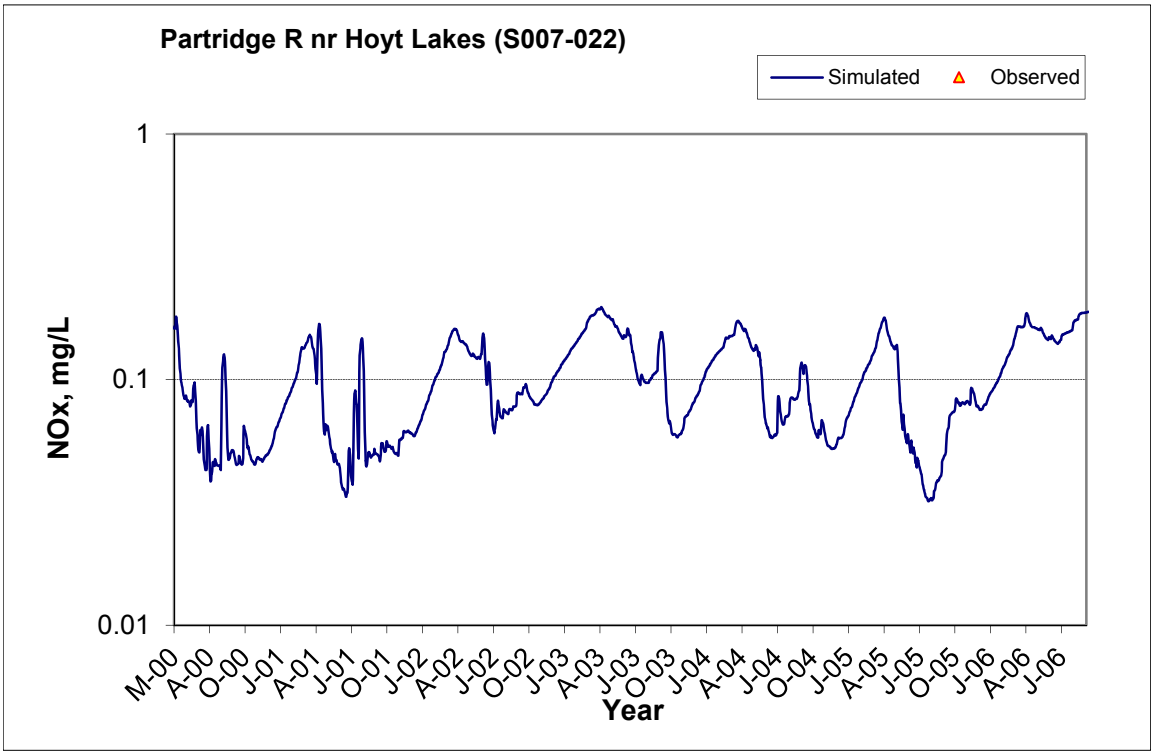
Partridge R nr Hoyt Lakes (S007-022)
Simulated
Observed
NOx, mg/L
1
0.1
0.01
M-00 A-00 O-00 J-01 A-01 J-01 O-01 J-02 A-02 J-02 O-02 J-03 A-03 J-03 O-03 J-04 A-04 J-04 O-04 J-05 A-05 J-05 O-05 J-06 A-06 J-06
Year

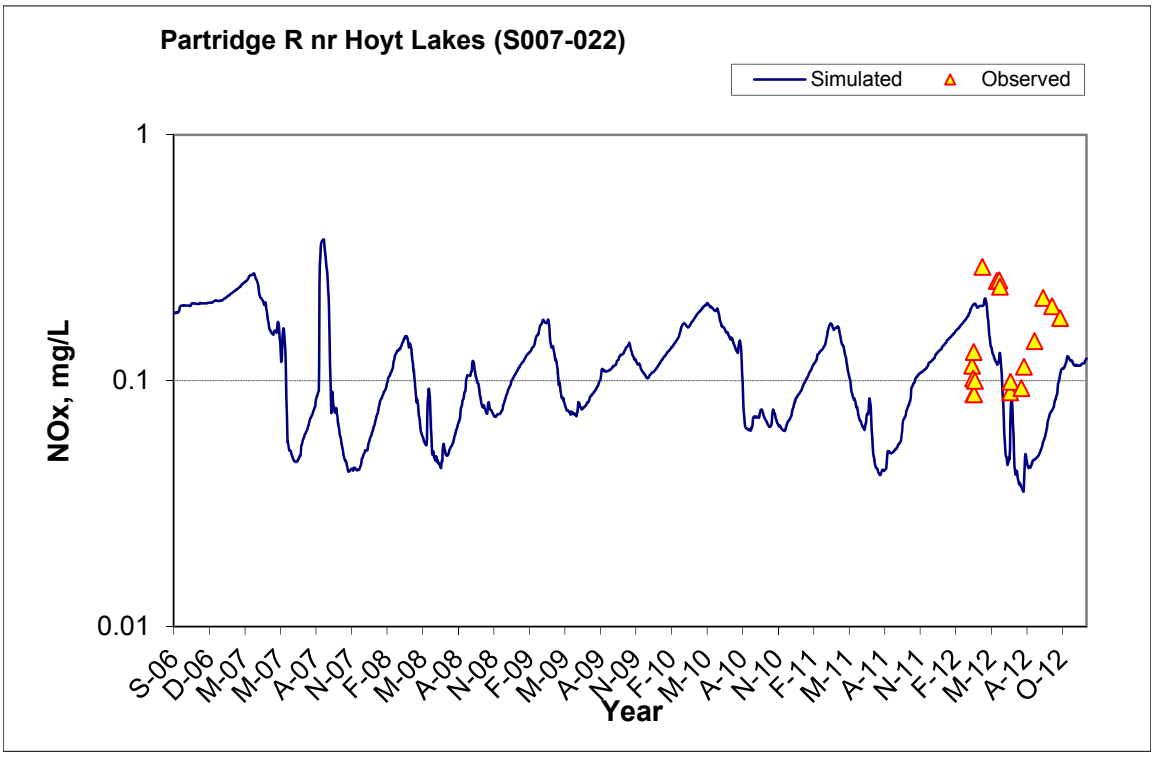

Figure A-5. Time series of observed and simulated Nitrite+ Nitrate Nitrogen (NOx) concentration at Partridge R nr Hoyt Lakes (S007-022)

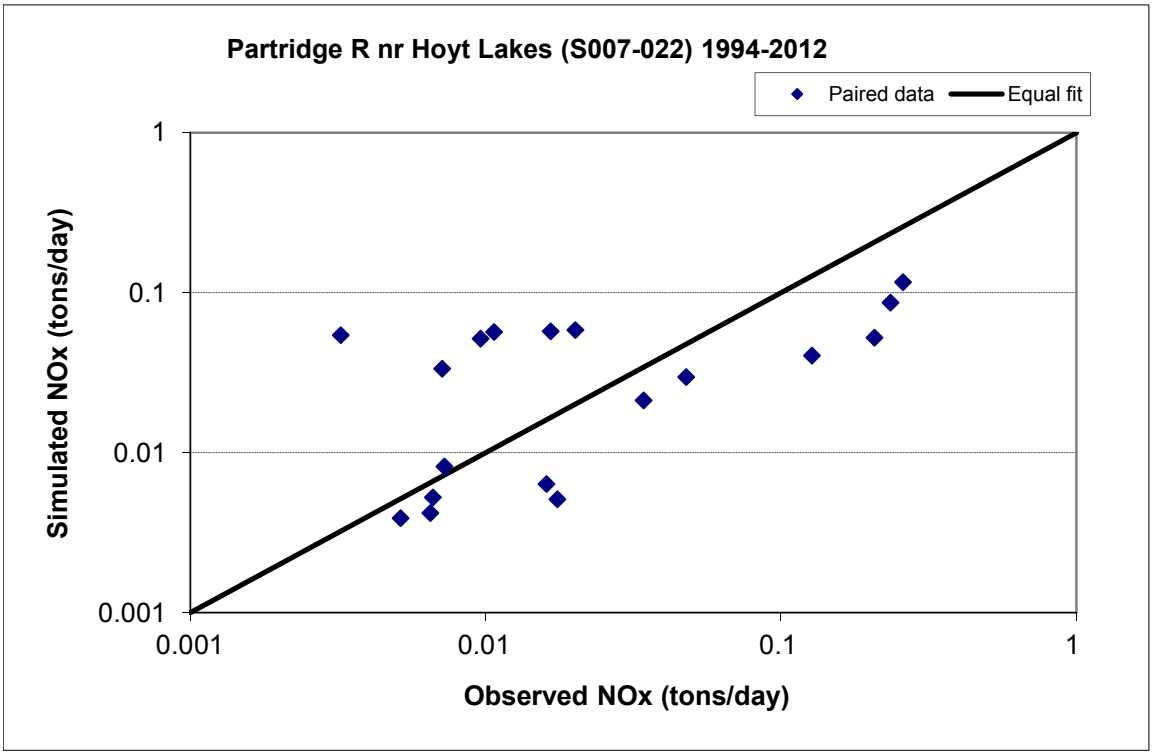

Figure A-6. Paired simulated vs. observed Nitrite+ Nitrate Nitrogen (NOx) load at Partridge R nr Hoyt Lakes (S007-022) (calibration period)

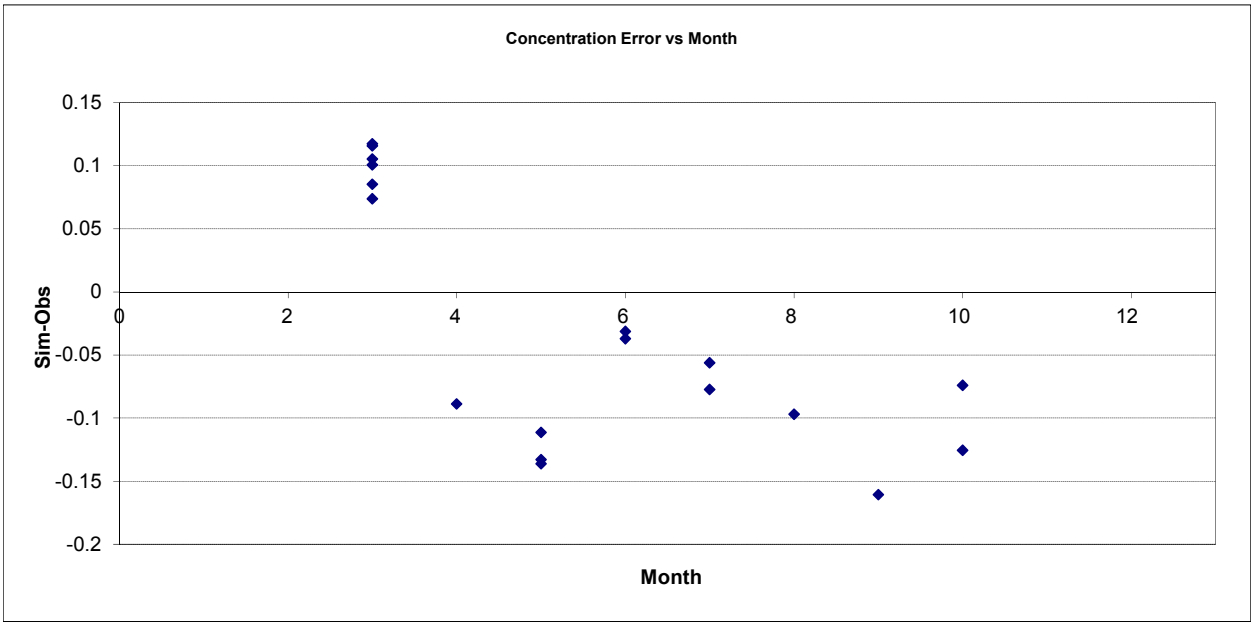

Figure A-7. Residual (Simulated - Observed) vs. Month Nitrite+ Nitrate Nitrogen (NOx) at Partridge R nr Hoyt Lakes (S007-022)

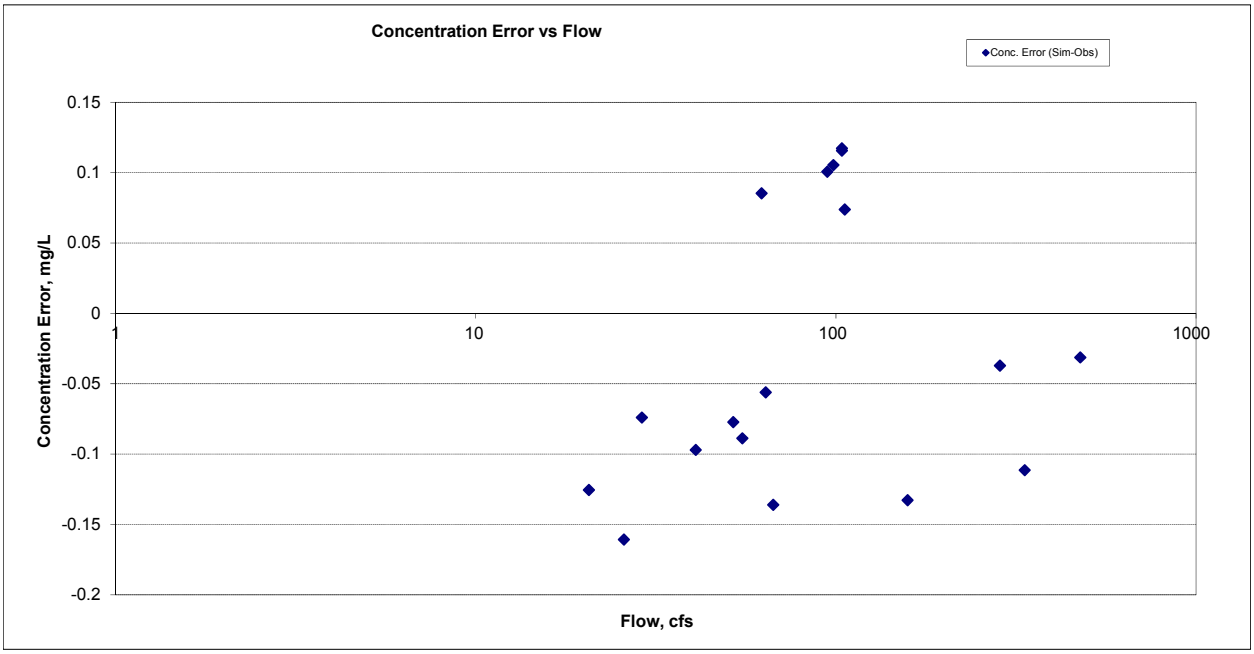

Figure A-8. Residual (Simulated - Observed) vs. Flow Nitrite+ Nitrate Nitrogen (NOx) at Partridge R nr Hoyt Lakes (S007-022)

A.1.5 Total Nitrogen (TN)

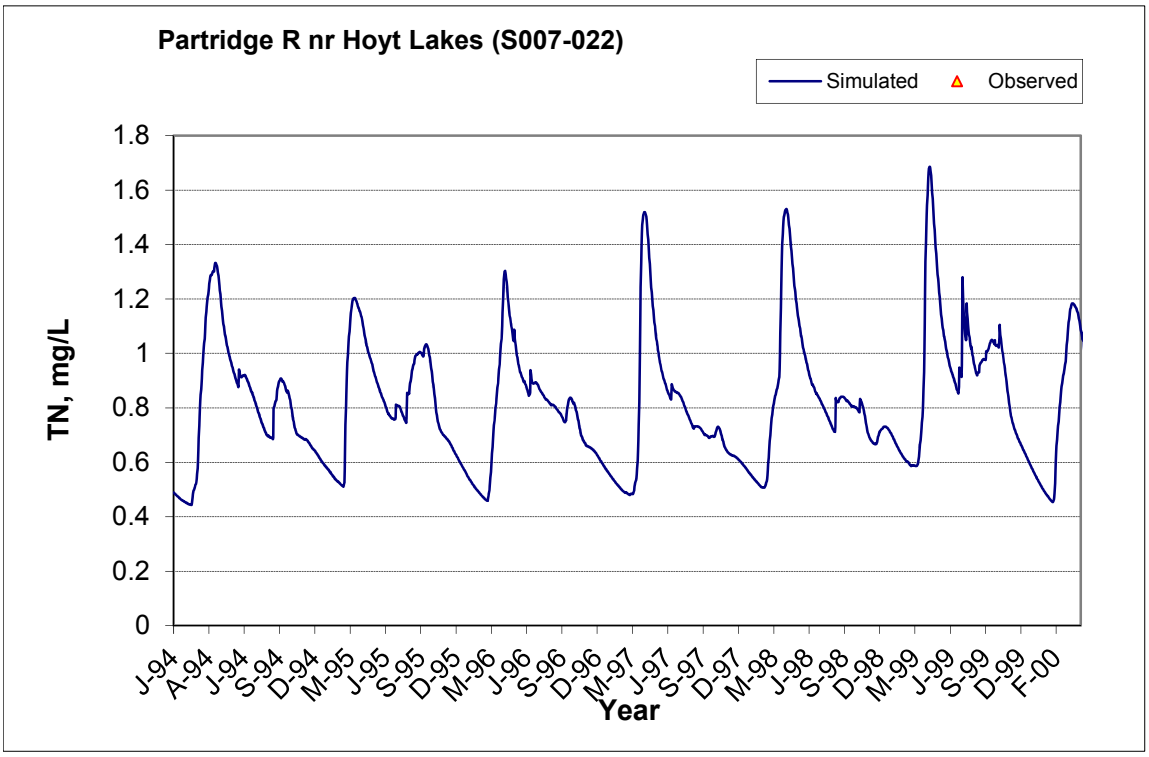

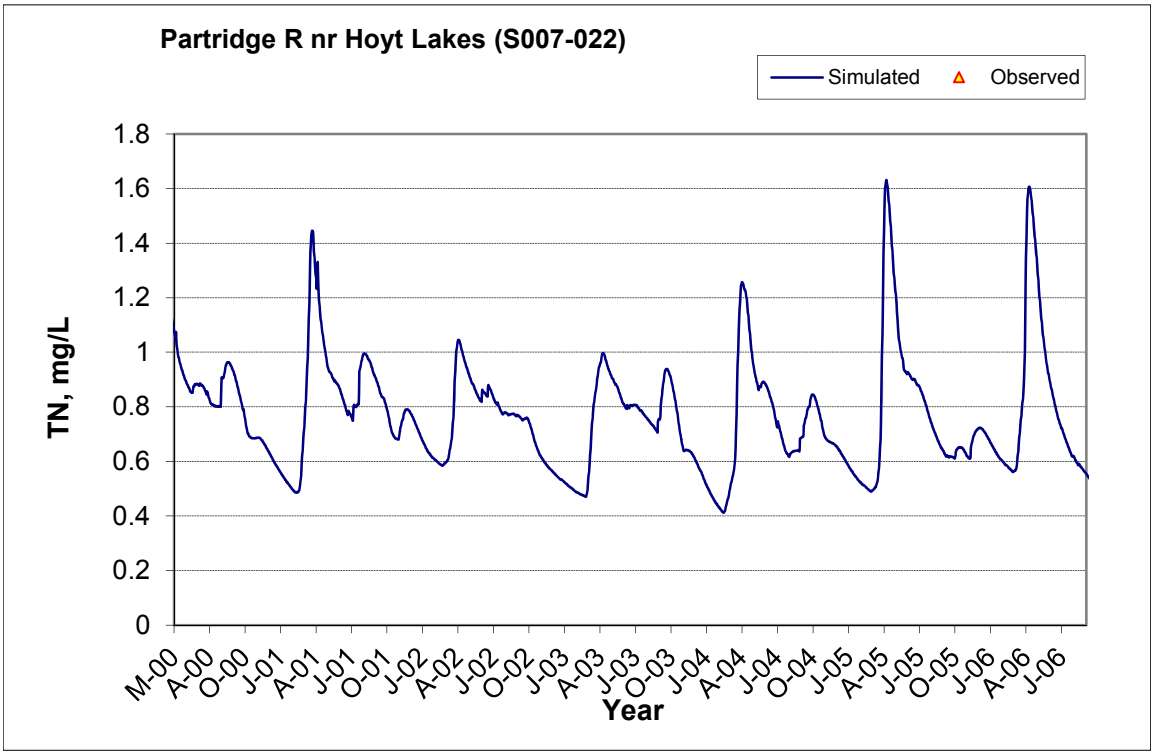

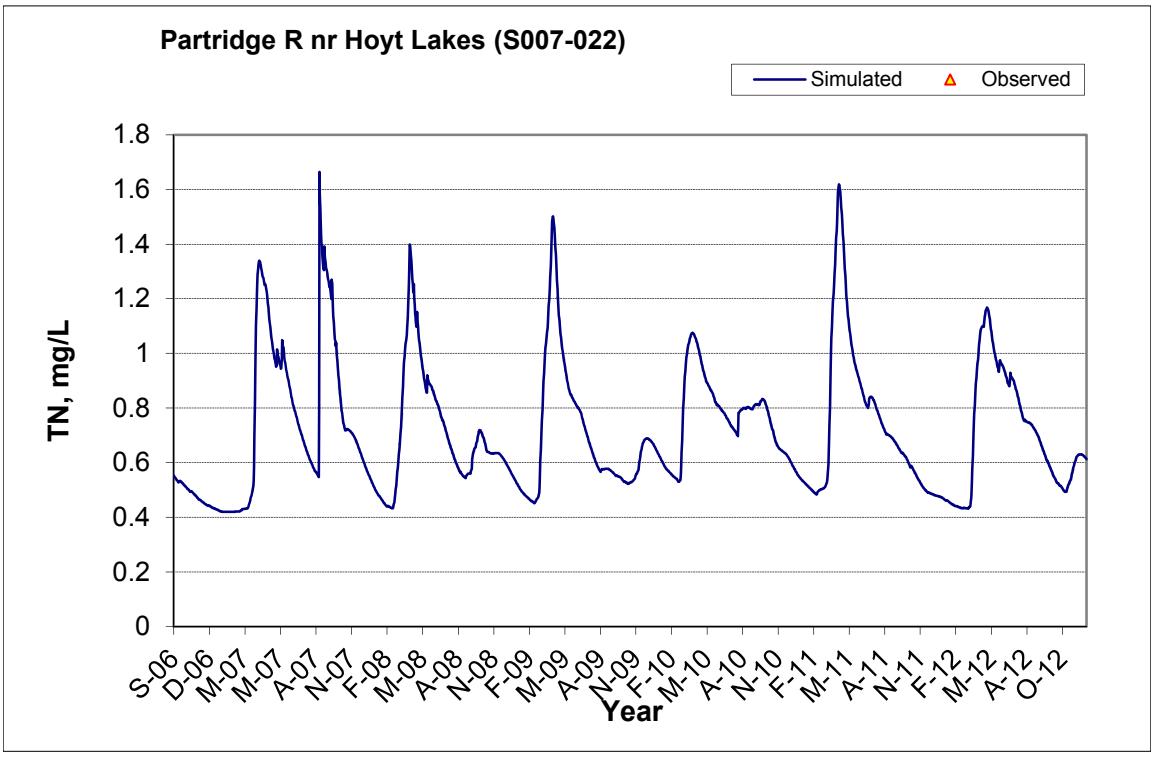

Figure A-9. Time series of observed and simulated Total Nitrogen (TN) concentration at Partridge R nr Hoyt Lakes (S007-022)

A.1.6 Soluble Reactive Phosphorus (SRP)

Table A-2. Soluble Reactive Phosphorus (SRP) statistics

Period	1994-1993	1994-2012
Count	ND	18
Concentration Average Error		-32.36%
Concentration Median Error		-24.18%
Load Average Error		13.85%
Load Median Error		-3.00%
Paired t conc		0.15
Paired t load		0.55

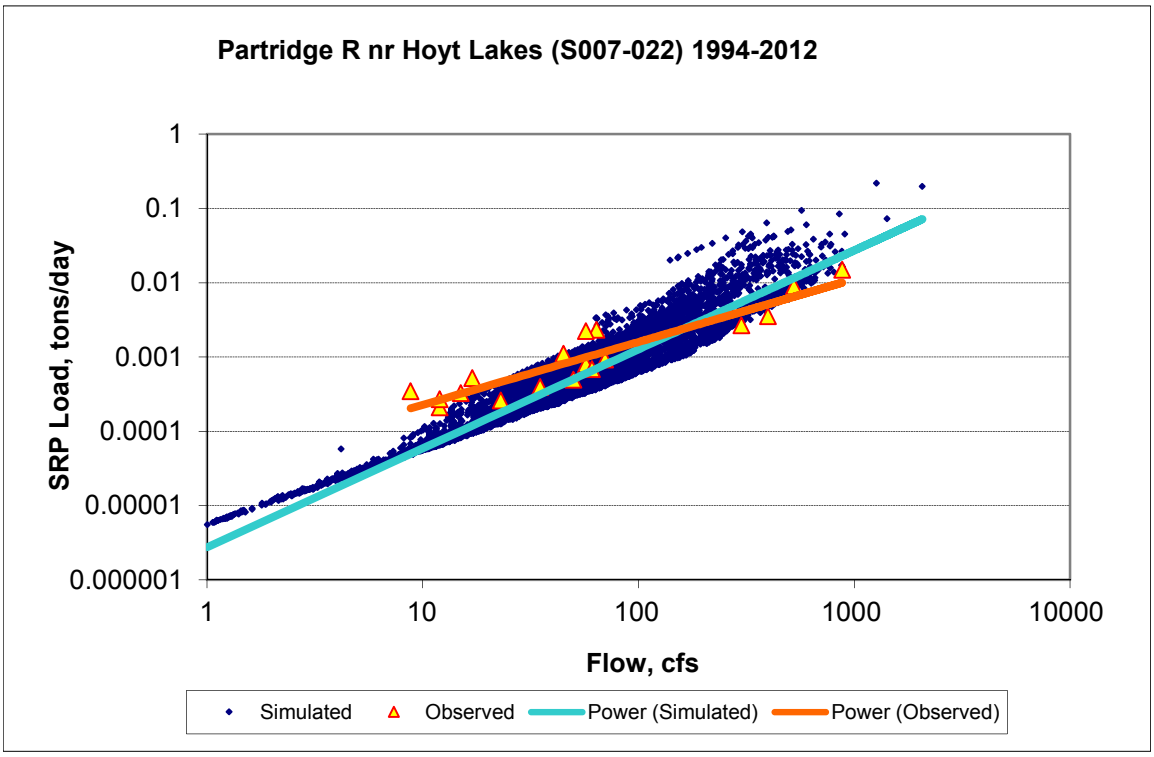

Figure A-10. Power plot of simulated and observed Soluble Reactive Phosphorus (SRP) load vs flow at Partridge R nr Hoyt Lakes (S007-022) (calibration period)

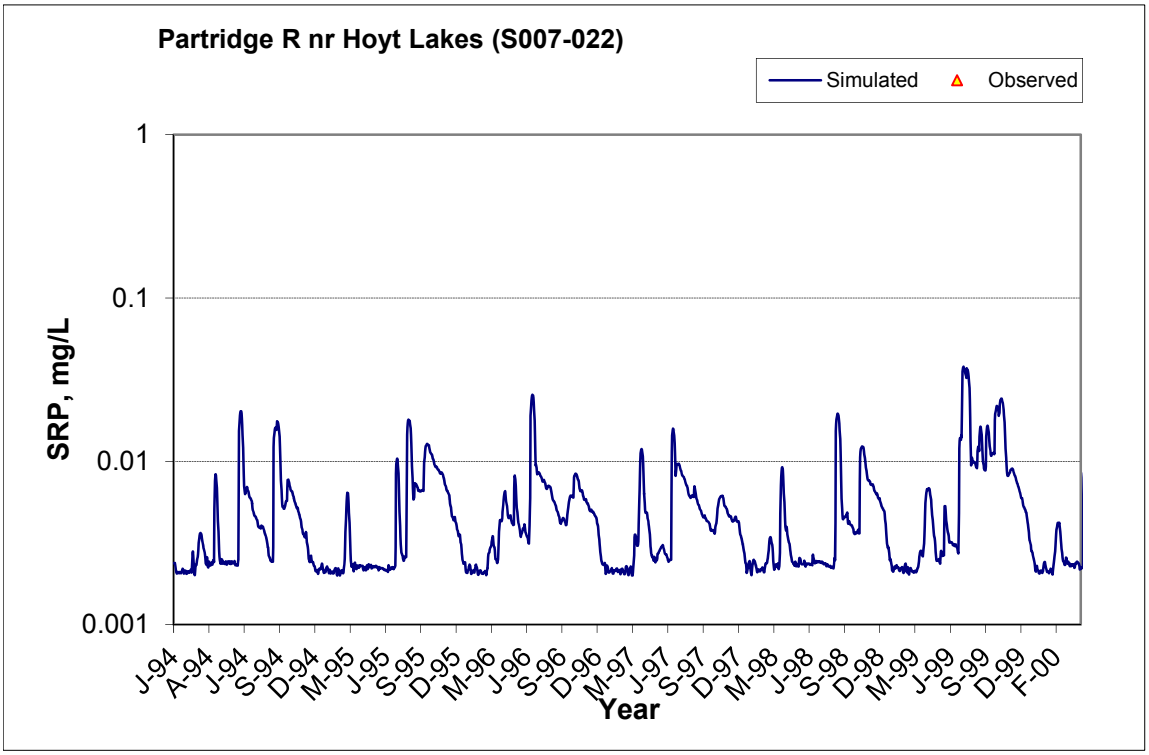

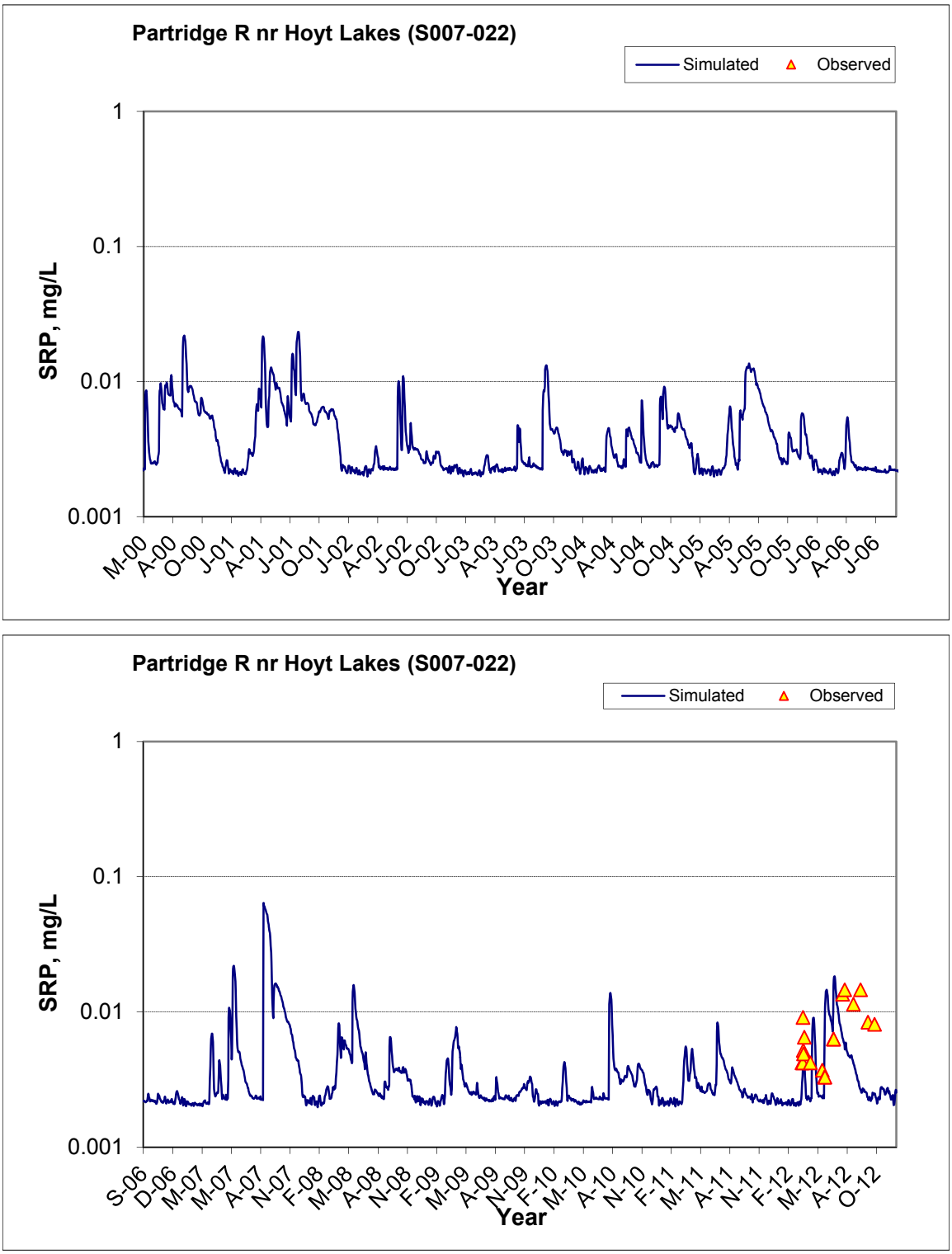

Figure A-11. Time series of observed and simulated Soluble Reactive Phosphorus (SRP) concentration at Partridge R nr Hoyt Lakes (S007-022)

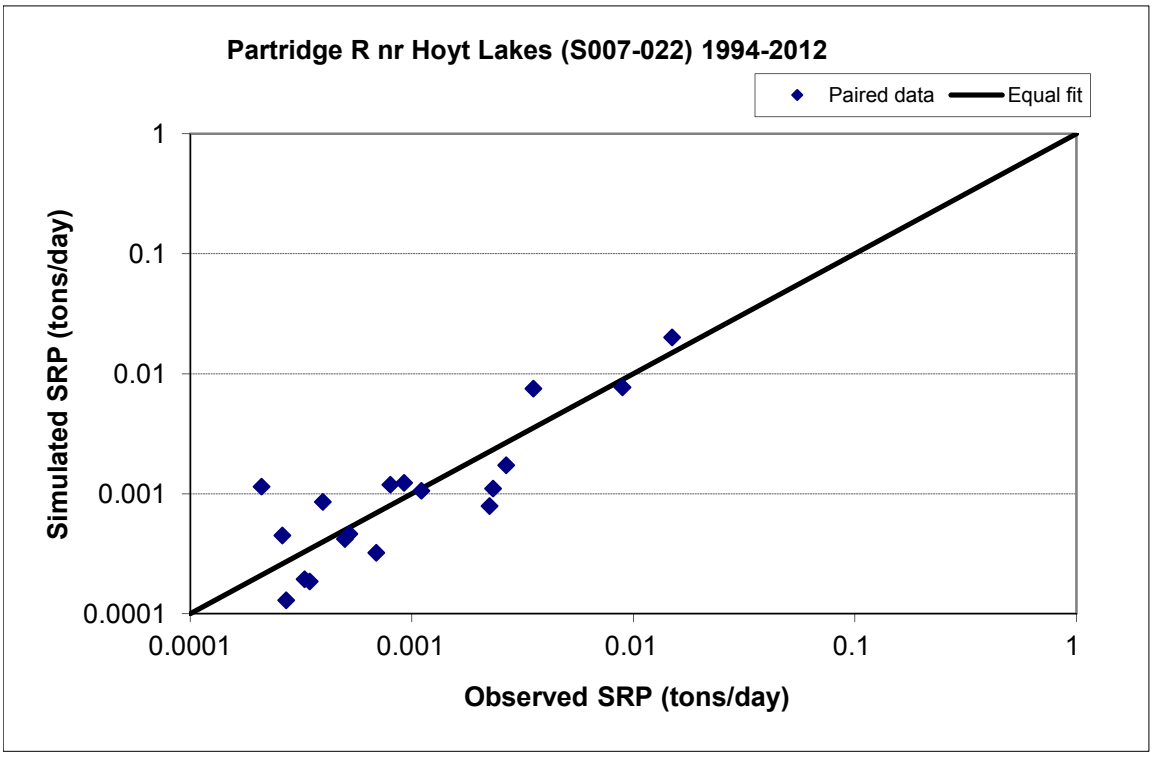

Figure A-12. Paired simulated vs. observed Soluble Reactive Phosphorus (SRP) load at Partridge R nr Hoyt Lakes (S007-022) (calibration period)

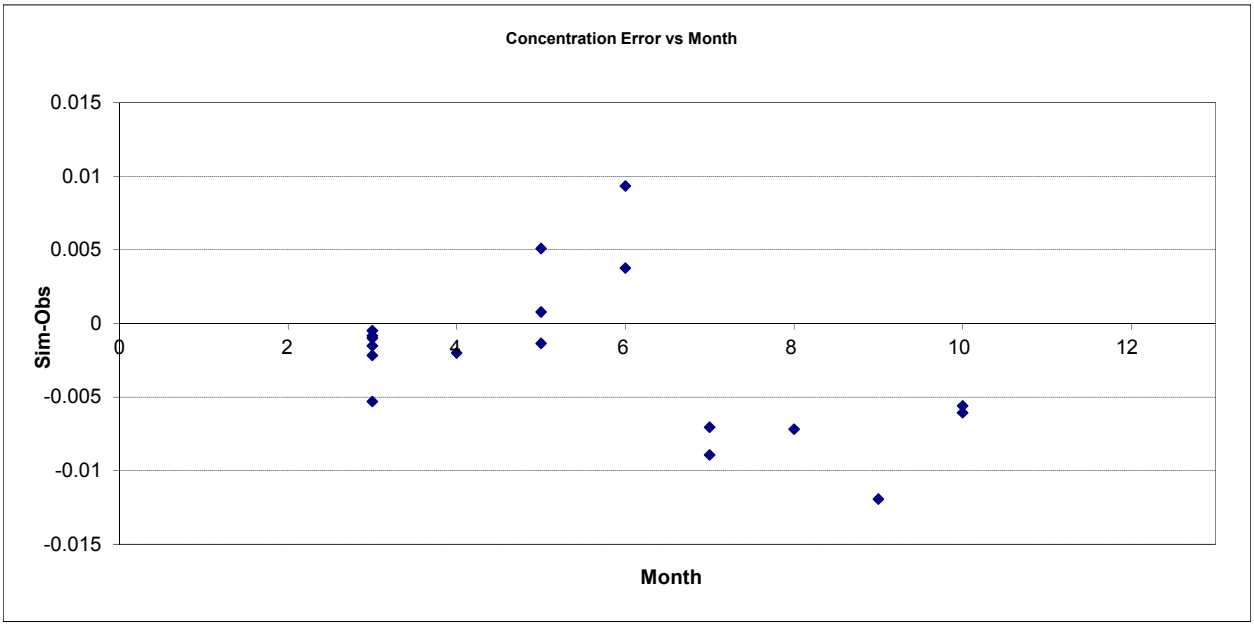

Figure A-13. Residual (Simulated - Observed) vs. Month Soluble Reactive Phosphorus (SRP) at Partridge R nr Hoyt Lakes (S007-022)

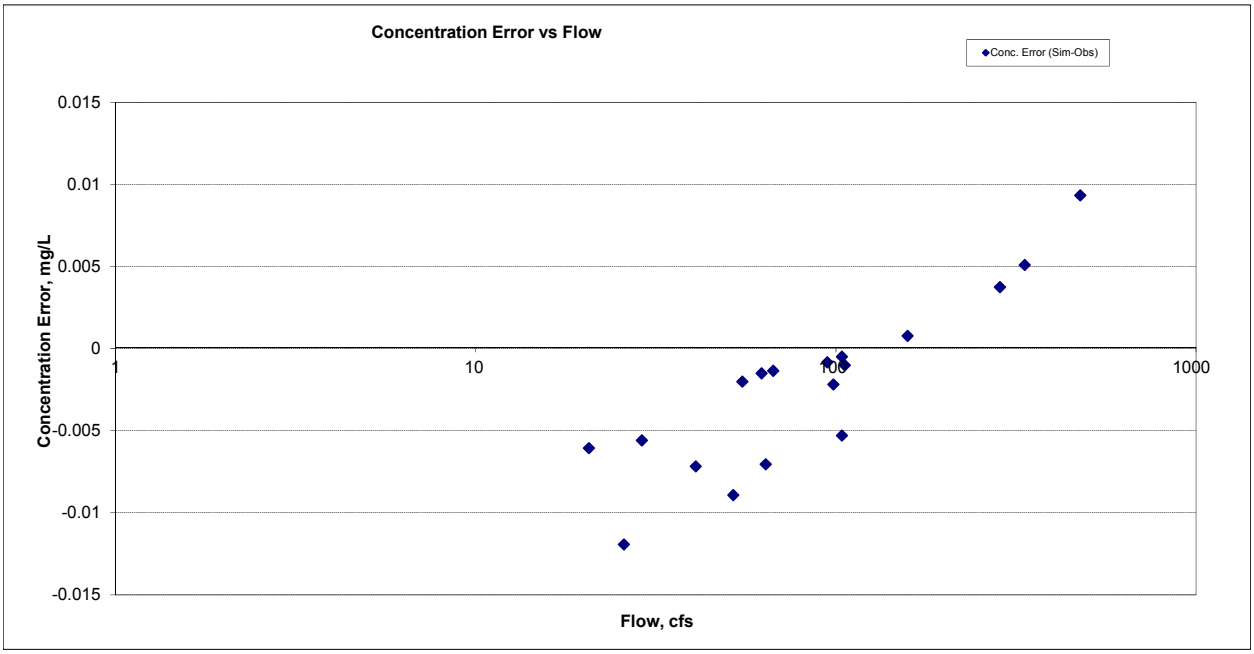

Figure A-14. Residual (Simulated - Observed) vs. Flow Soluble Reactive Phosphorus (SRP) at Partridge R nr Hoyt Lakes (S007-022)

A.1.7 Organic Phosphorus (OrgP)

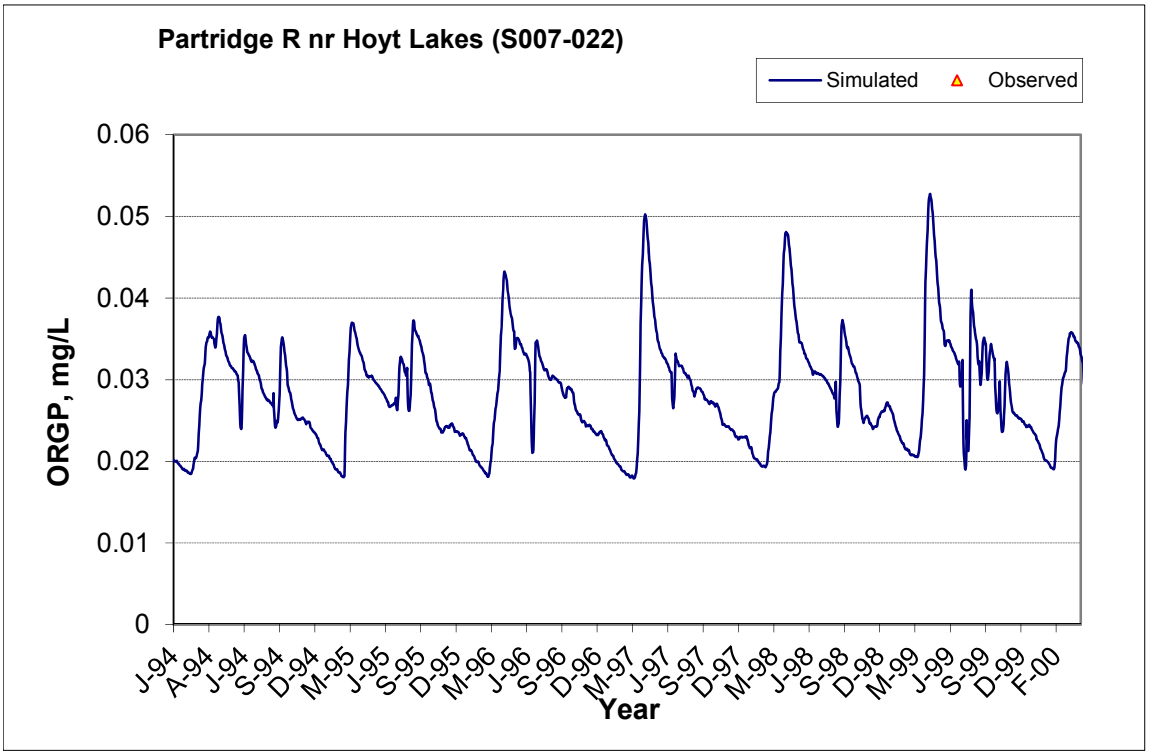

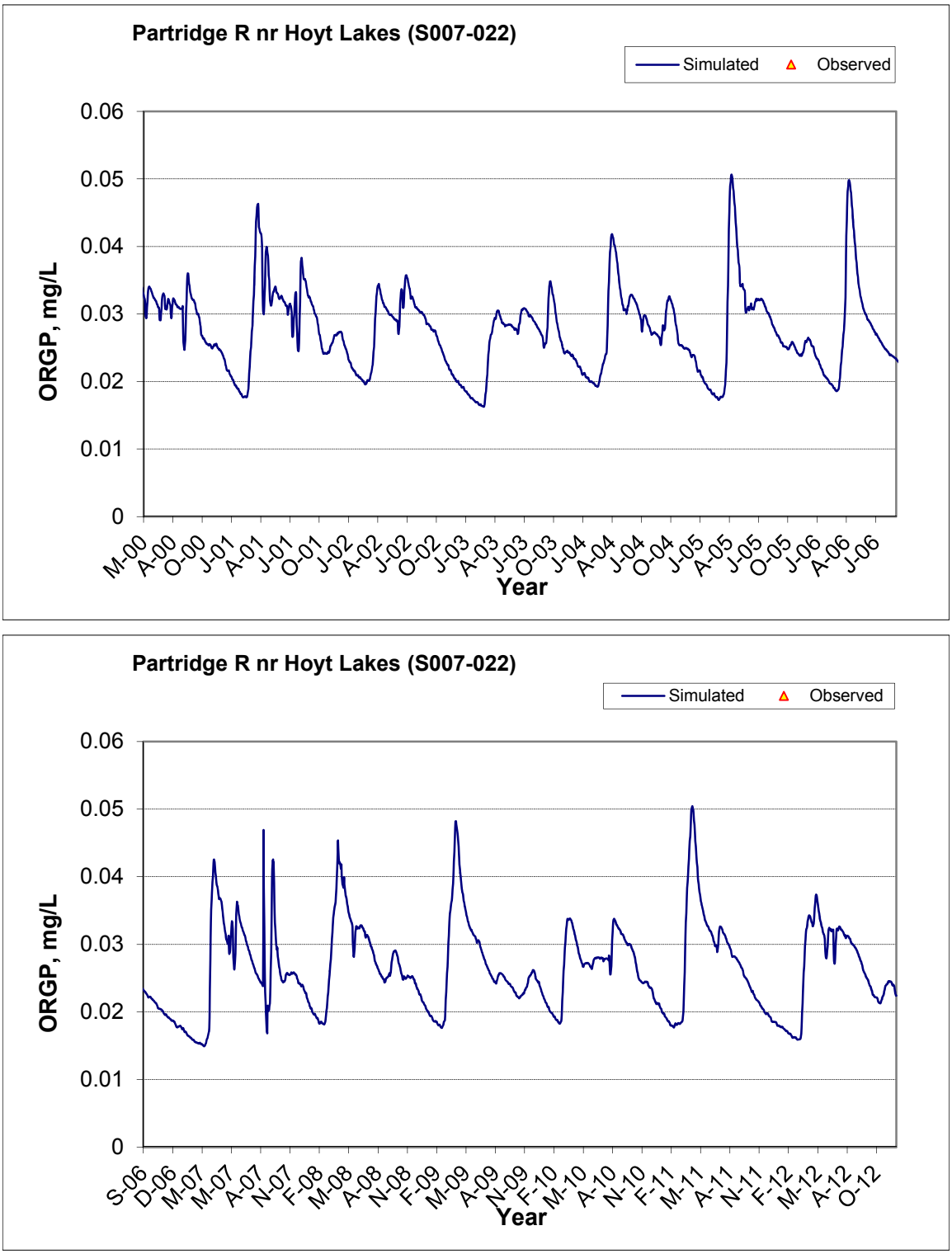

Figure A-15. Time series of observed and simulated Organic Phosphorus (OrgP) concentration at Partridge R nr Hoyt Lakes (S007-022)

A.1.8 Total Phosphorus (TP)

Table A-3. Total Phosphorus (TP) statistics

Period	1994-1993	1994-2012
Count	ND	18
Concentration Average Error		32.62%
Concentration Median Error		40.48%
Load Average Error		30.75%
Load Median Error		24.81%
Paired t conc		0.06
Paired t load		0.39

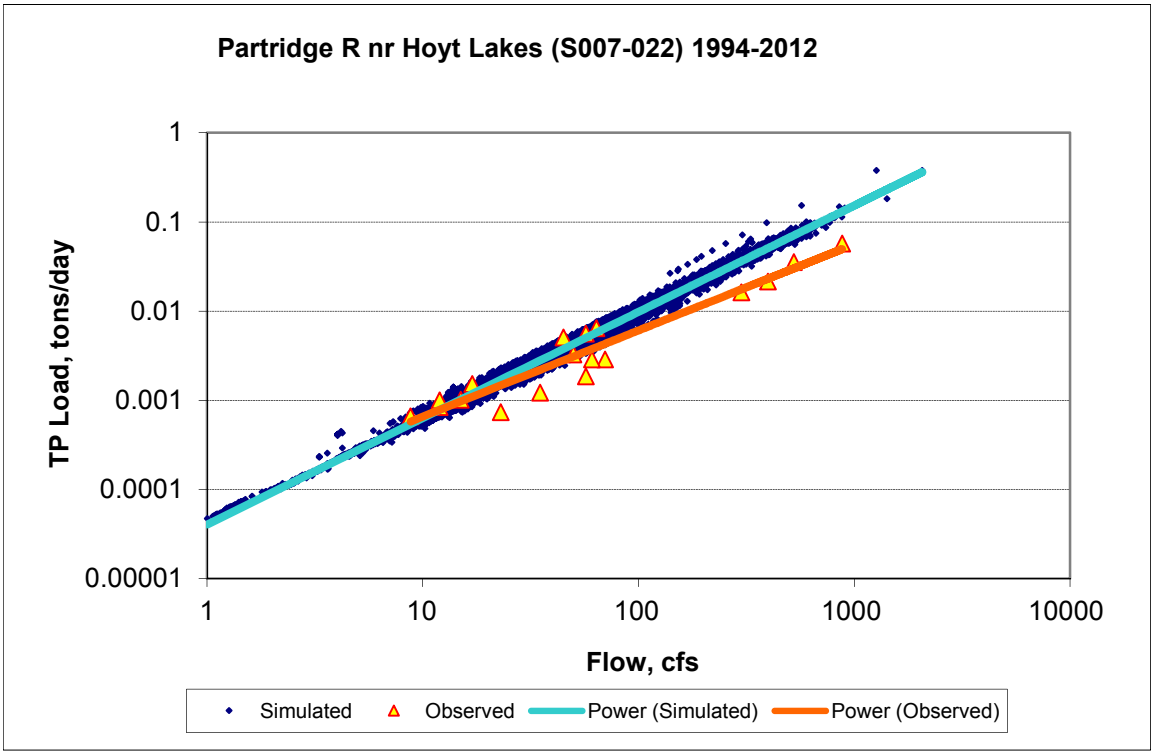

Figure A-16. Power plot of simulated and observed Total Phosphorus (TP) load vs flow at Partridge R nr Hoyt Lakes (S007-022) (calibration period)

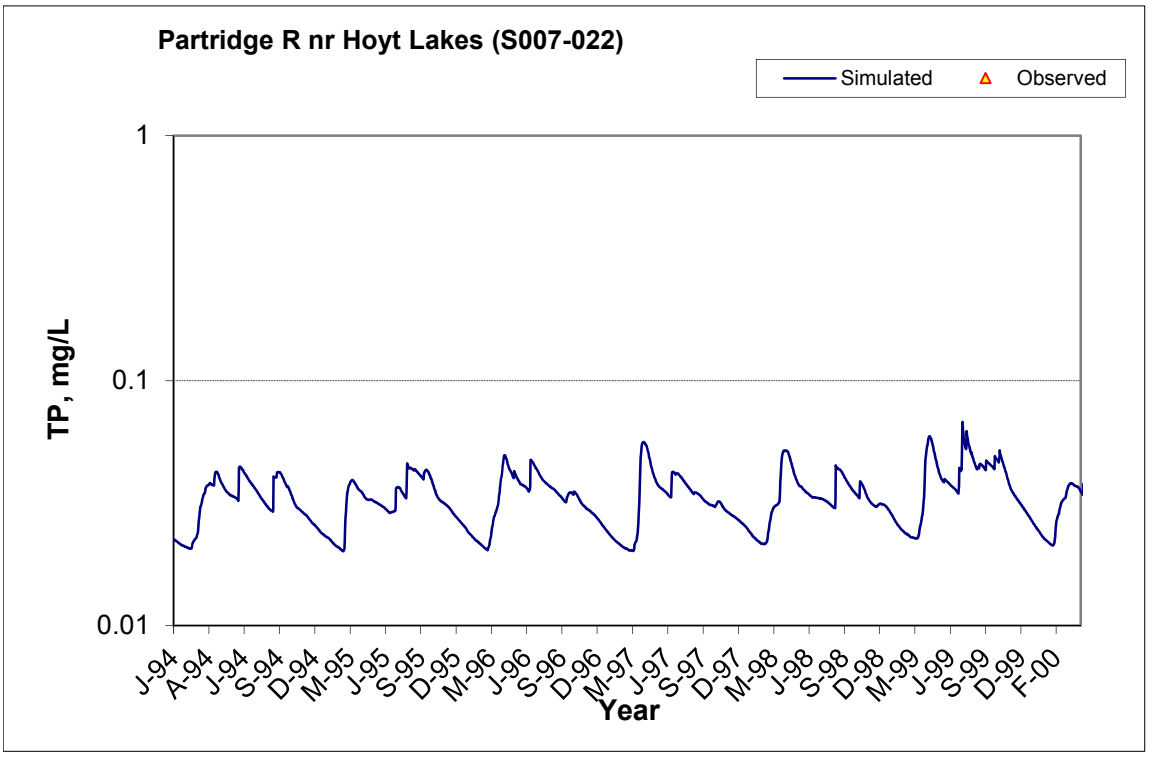
Partridge R nr Hoyt Lakes (S007-022)
Simulated
Observed
TP, mg/L
1
0.1
0.01
J-94 A-94 J-94 S-94 D-94 M-95 J-95 S-95 D-95 M-96 J-96 S-96 D-96 M-97 J-97 S-97 D-97 M-98 J-98 S-98 D-98 M-99 J-99 S-99 D-99 F-00
Year

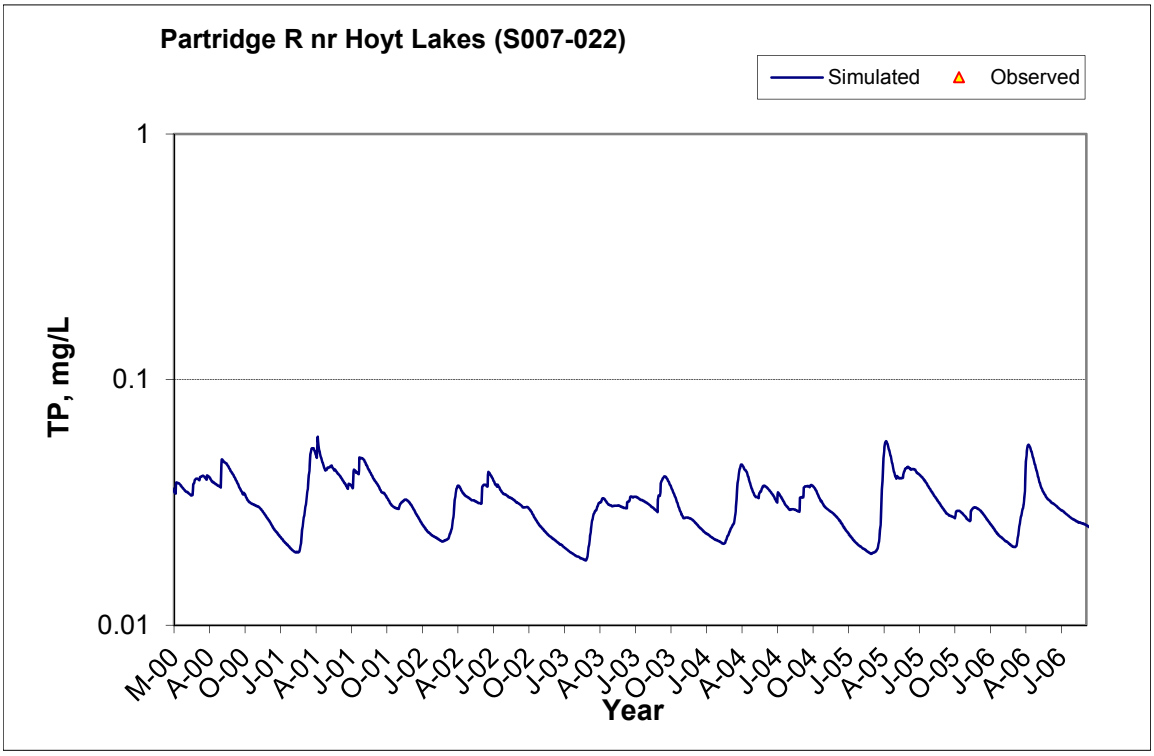
Partridge R nr Hoyt Lakes (S007-022)
Simulated
Observed
TP, mg/L
1
0.1
0.01
M-00 A-00 O-00 J-01 A-01 J-01 O-01 J-02 A-02 J-02 O-02 J-03 A-03 J-03 O-03 J-04 A-04 J-04 O-04 J-05 A-05 J-05 O-05 J-06 A-06 J-06
Year

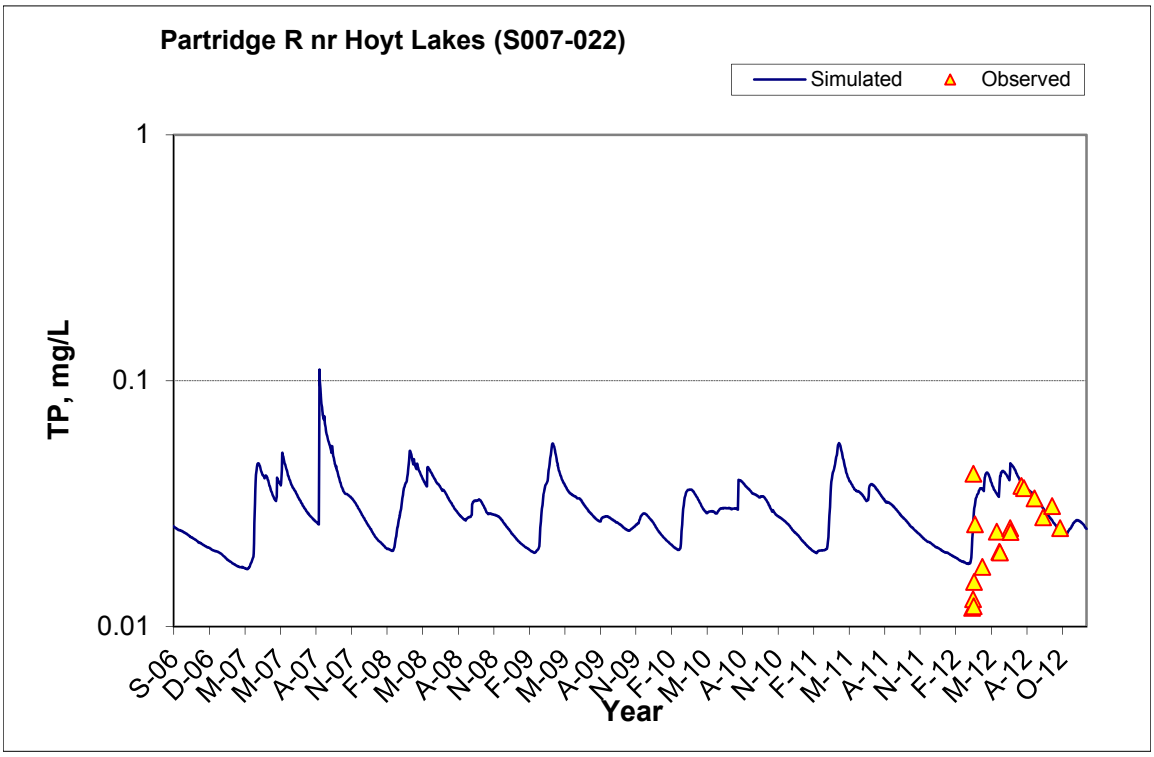

Figure A-17. Time series of observed and simulated Total Phosphorus (TP) concentration at Partridge R nr Hoyt Lakes (S007-022)

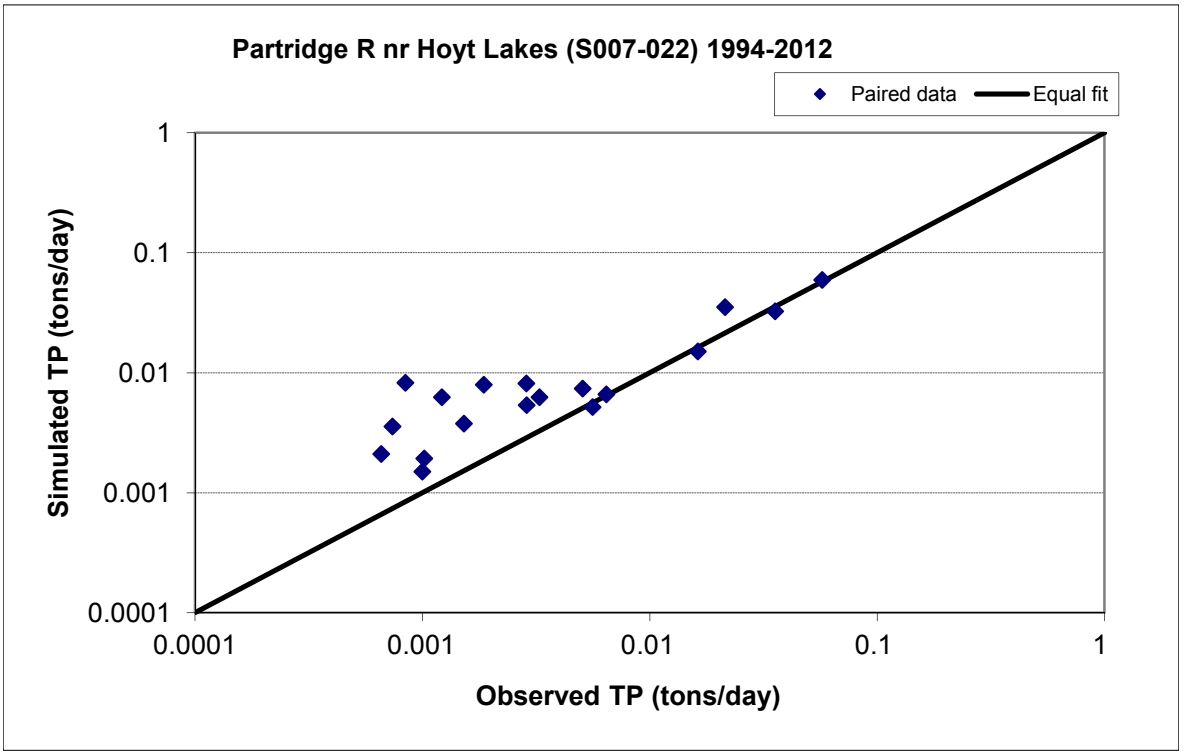

Figure A-18. Paired simulated vs. observed Total Phosphorus (TP) load at Partridge R nr Hoyt Lakes (S007-022) (calibration period)

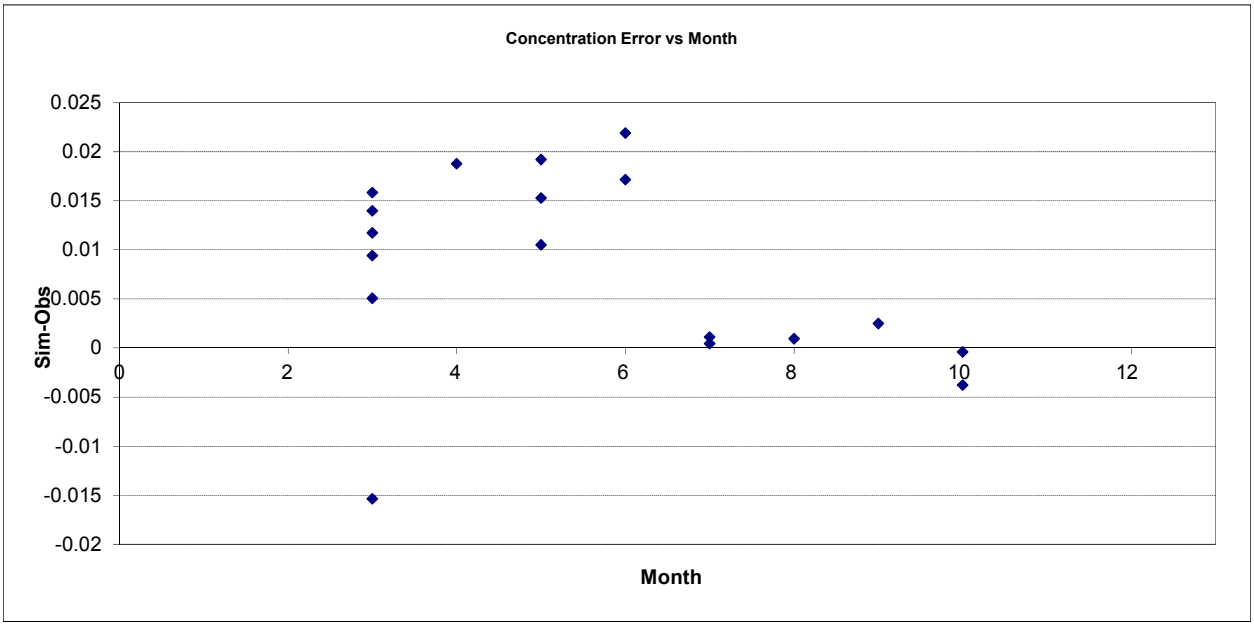

Figure A-19. Residual (Simulated - Observed) vs. Month Total Phosphorus (TP) at Partridge R nr Hoyt Lakes (S007-022)

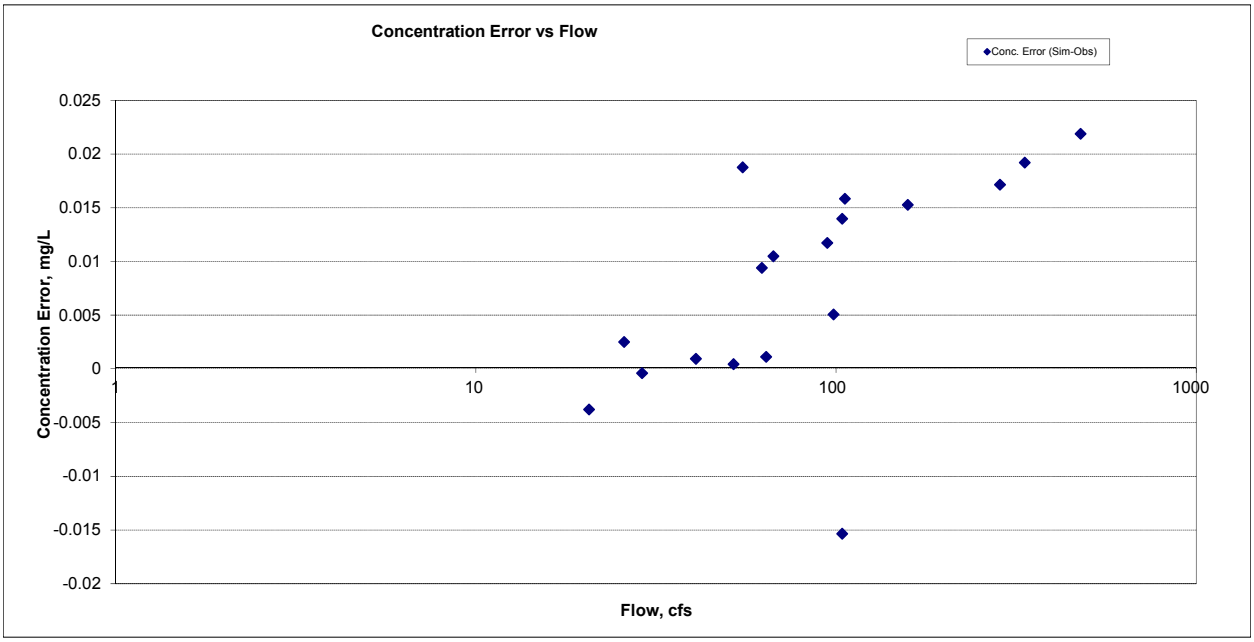

Figure A-20. Residual (Simulated - Observed) vs. Flow Total Phosphorus (TP) at Partridge R nr Hoyt Lakes (S007-022)

A.2 SWAN RIVER NR TOIVOLA (03084001)

A.2.1 Ammonia Nitrogen (NH3)

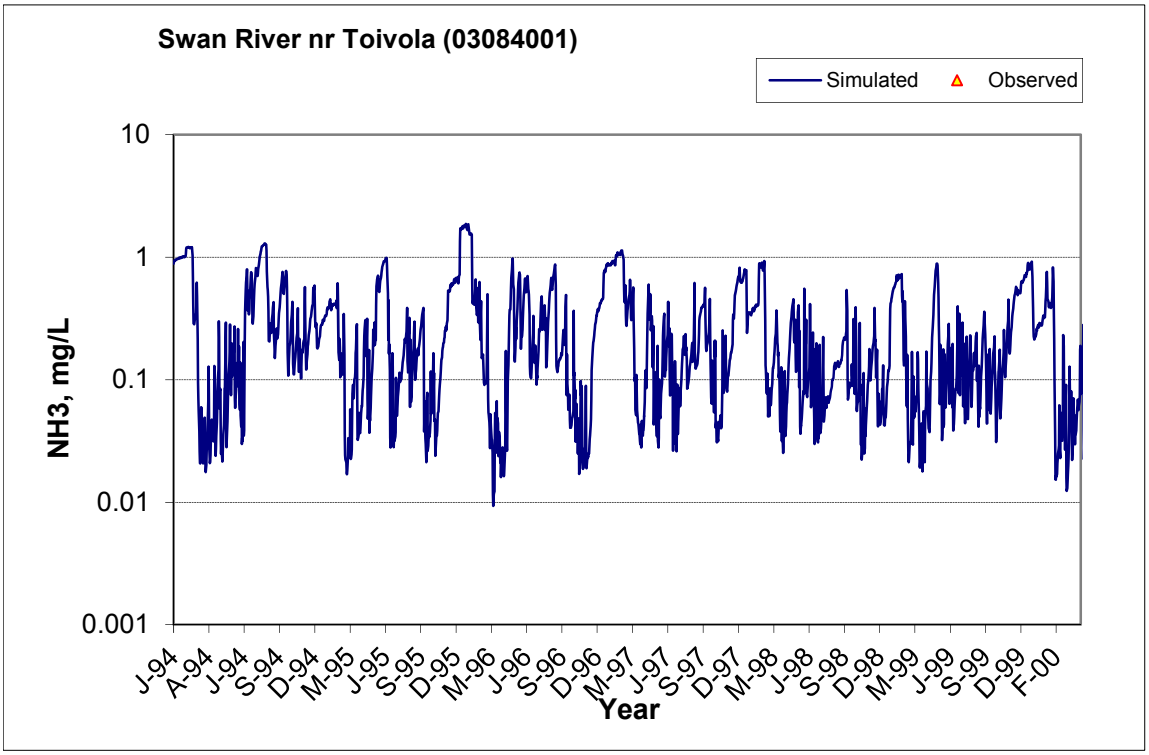

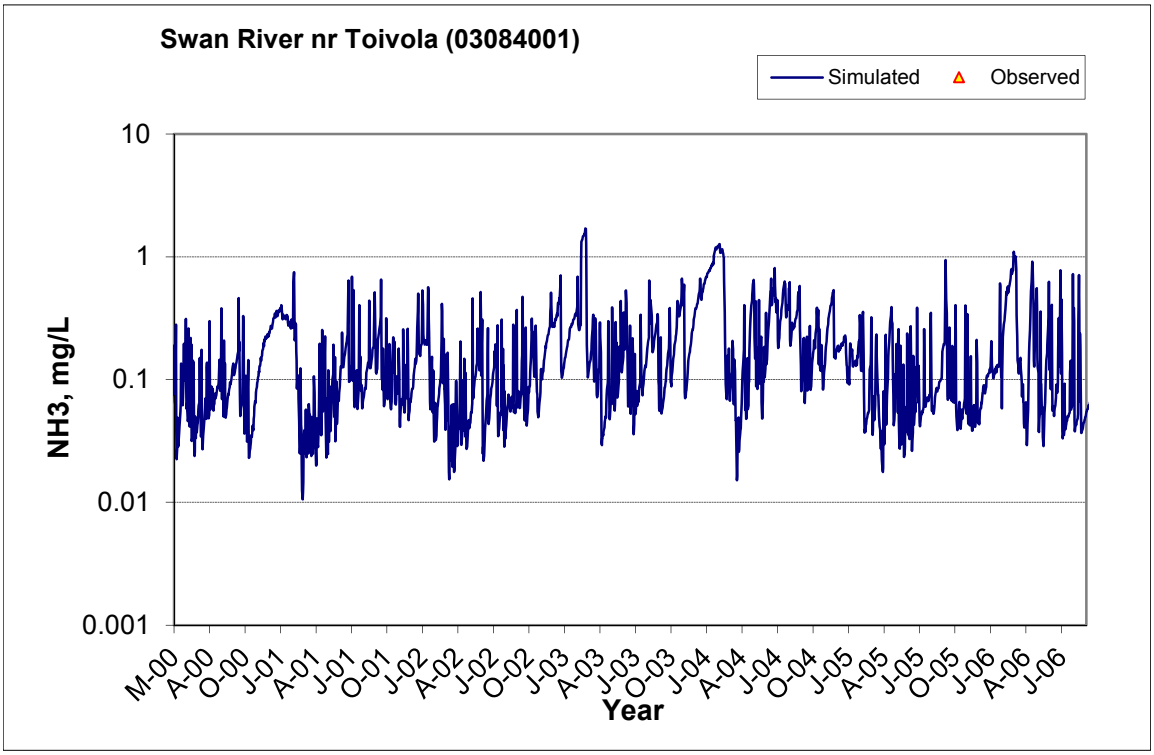

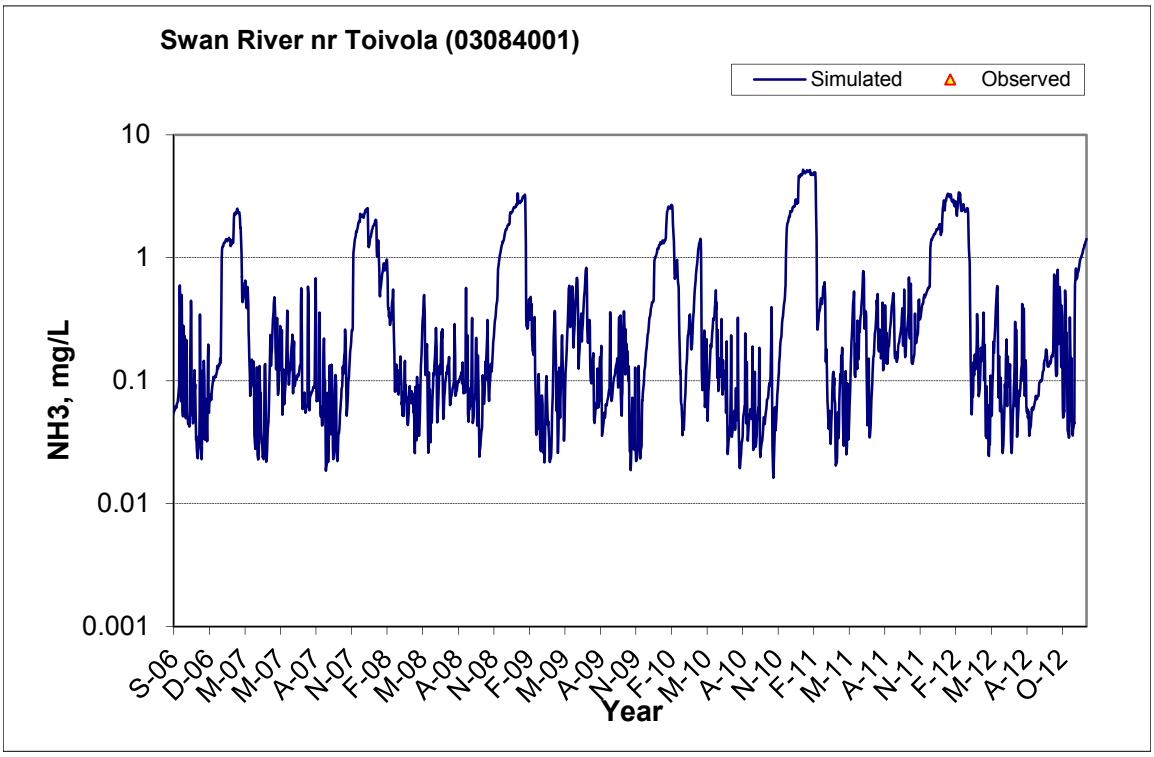

Figure A-21. Time series of observed and simulated Ammonia Nitrogen (NH3) concentration at Swan River nr Toivola (03084001)

A.2.2 Organic Nitrogen (OrgN)

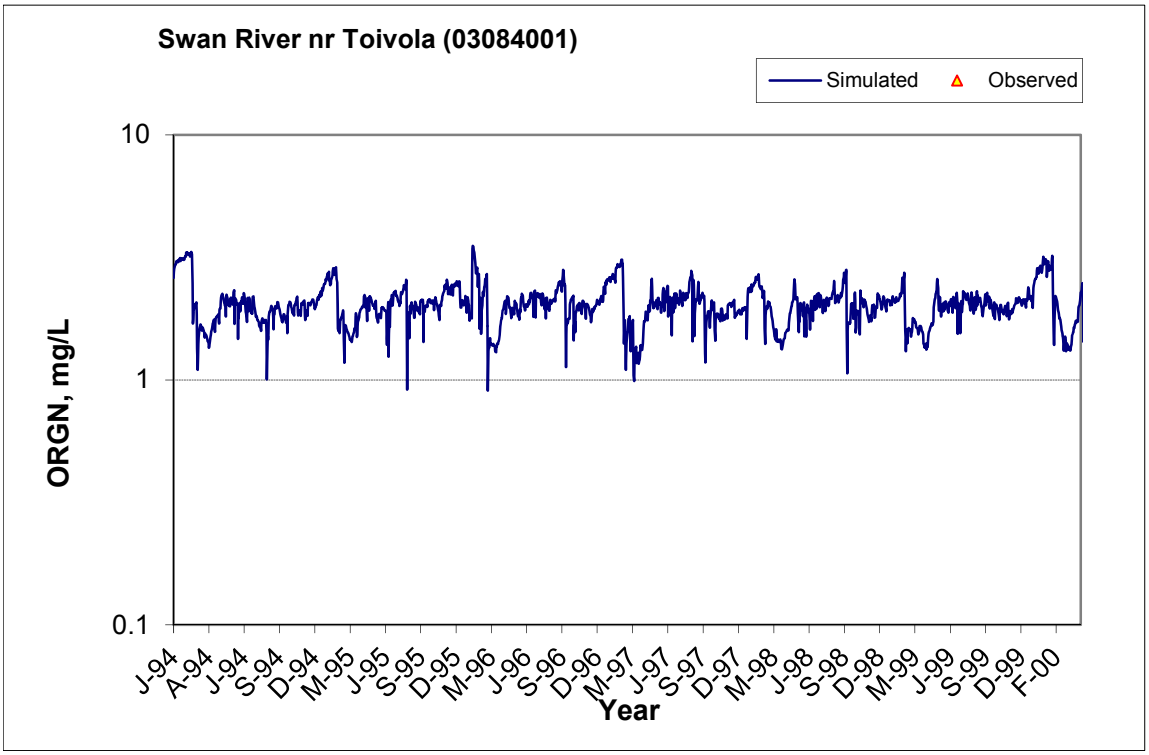

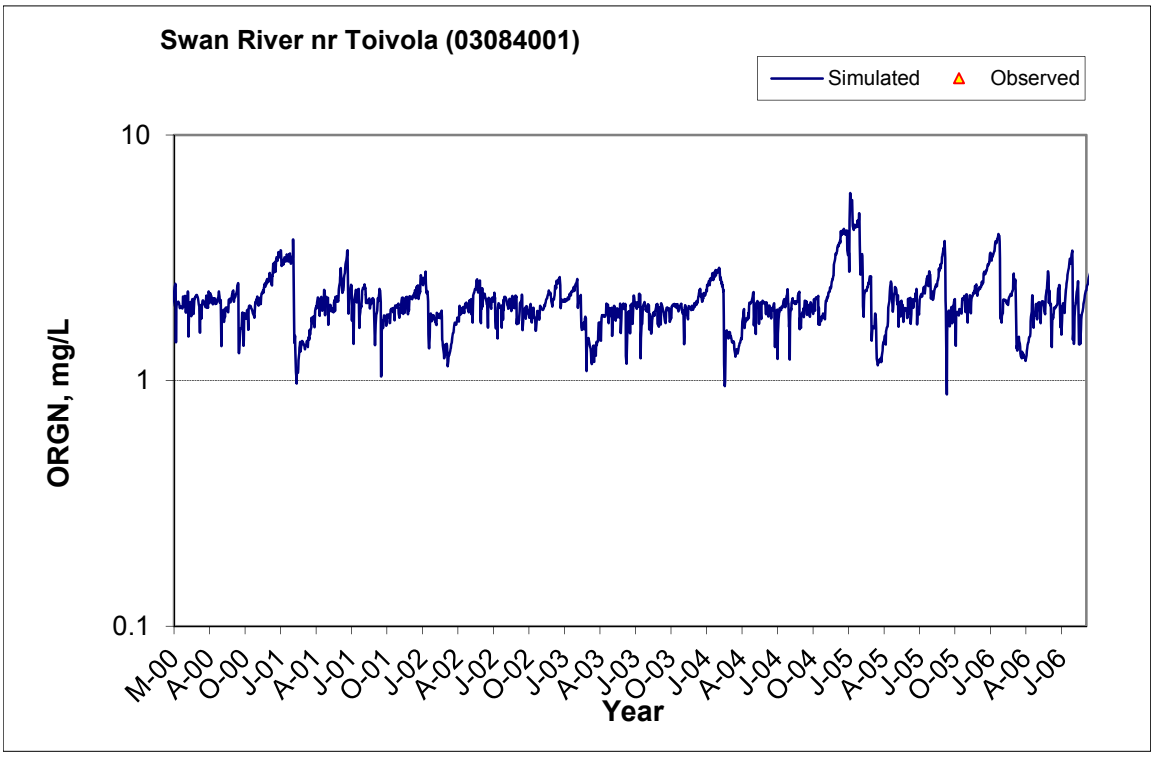

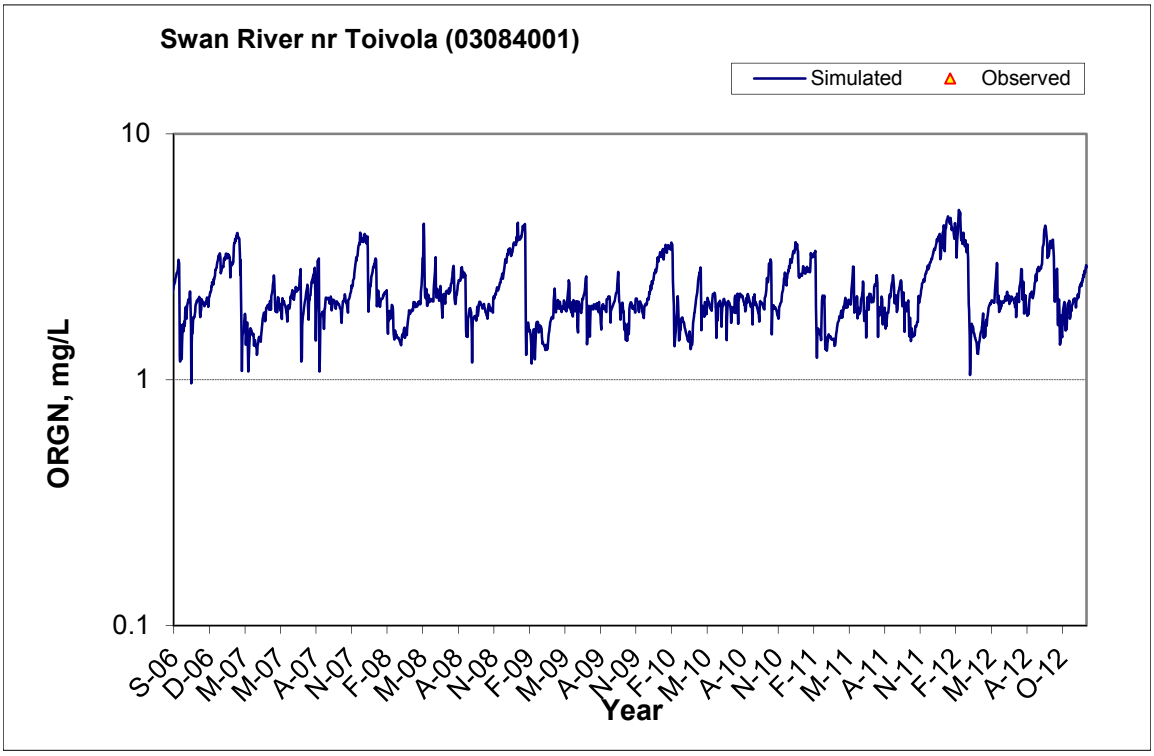

Figure A-22. Time series of observed and simulated Organic Nitrogen (OrgN) concentration at Swan River nr Toivola (03084001)

A.2.3 Total Kjeldahl Nitrogen (TKN)

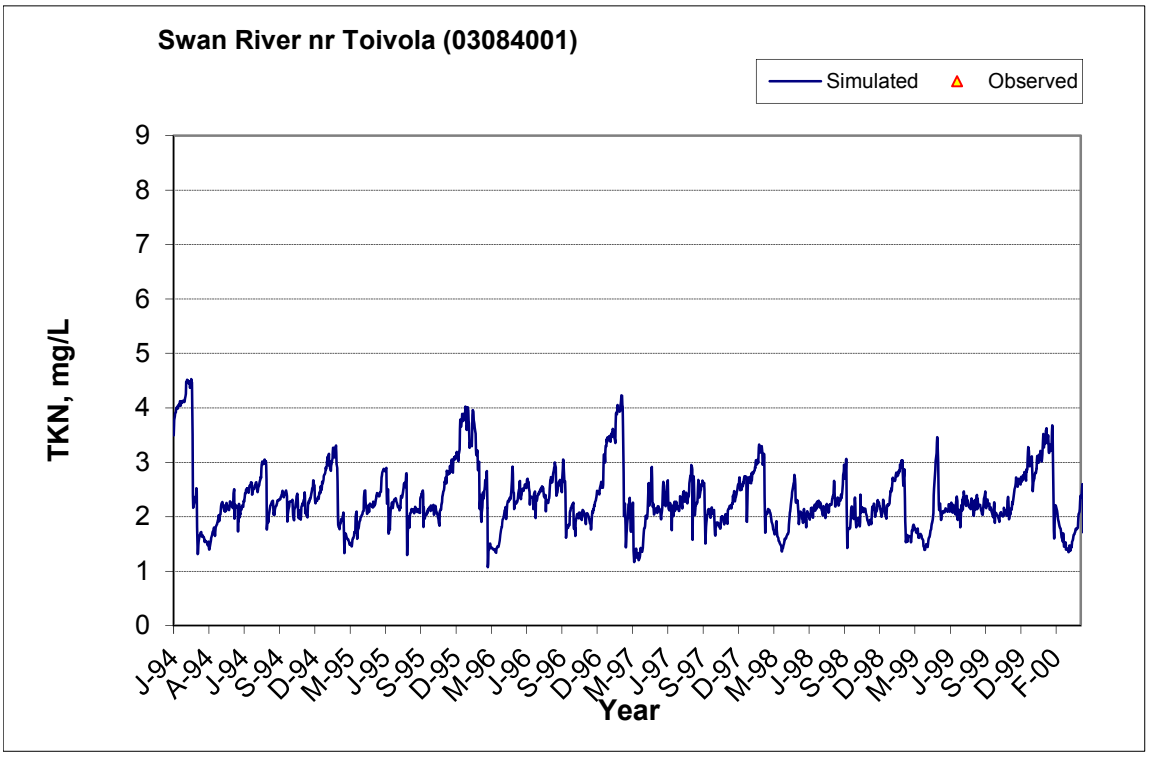

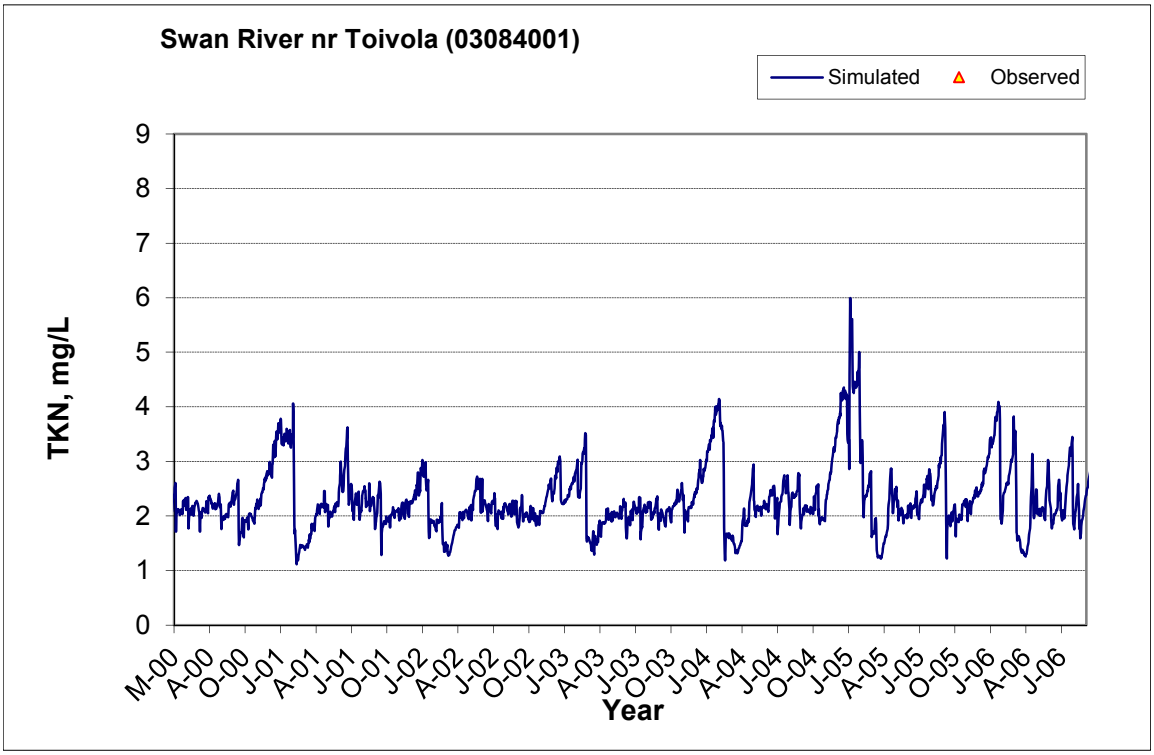

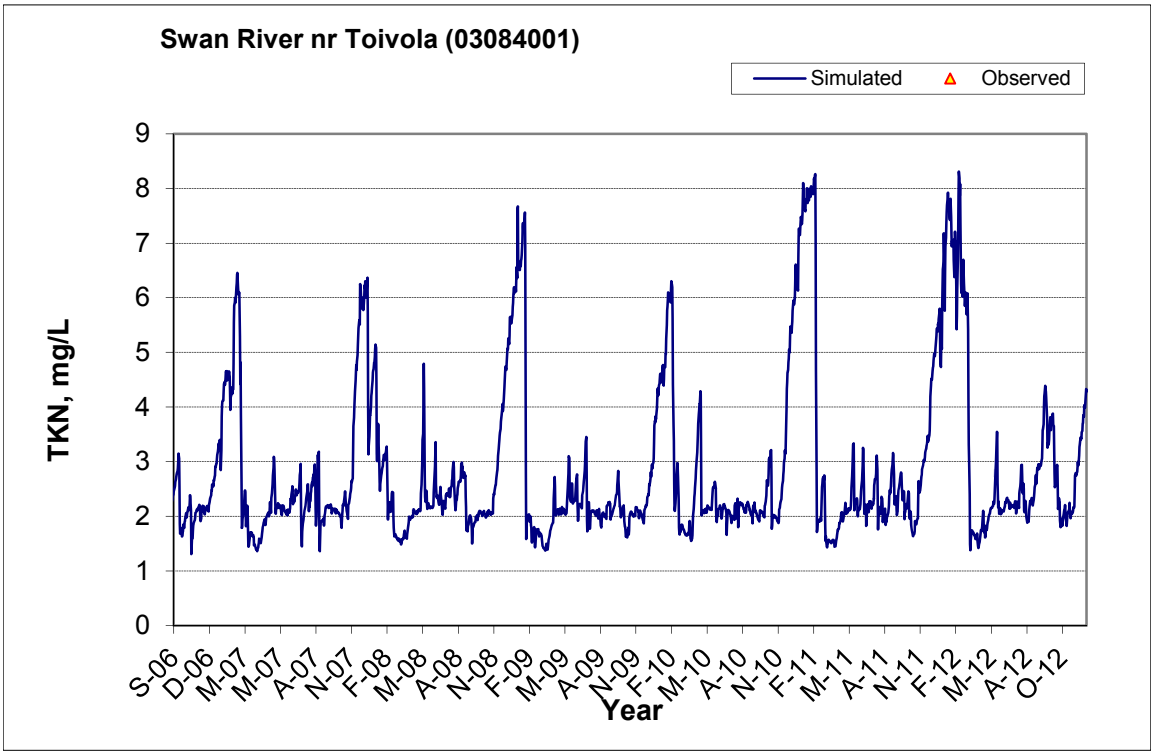

Figure A-23. Time series of observed and simulated Total Kjeldahl Nitrogen (TKN) concentration at Swan River nr Toivola (03084001)

A.2.4 Nitrite+ Nitrate Nitrogen (NOx)

Table A-4. Nitrite+ Nitrate Nitrogen (NOx) statistics

Period	1994-2001	2002-2012
Count	ND	22
Concentration Average Error		2.23%
Concentration Median Error		-7.35%
Load Average Error		-55.24%
Load Median Error		-48.10%
Paired t conc		0.78
Paired t load		0.00

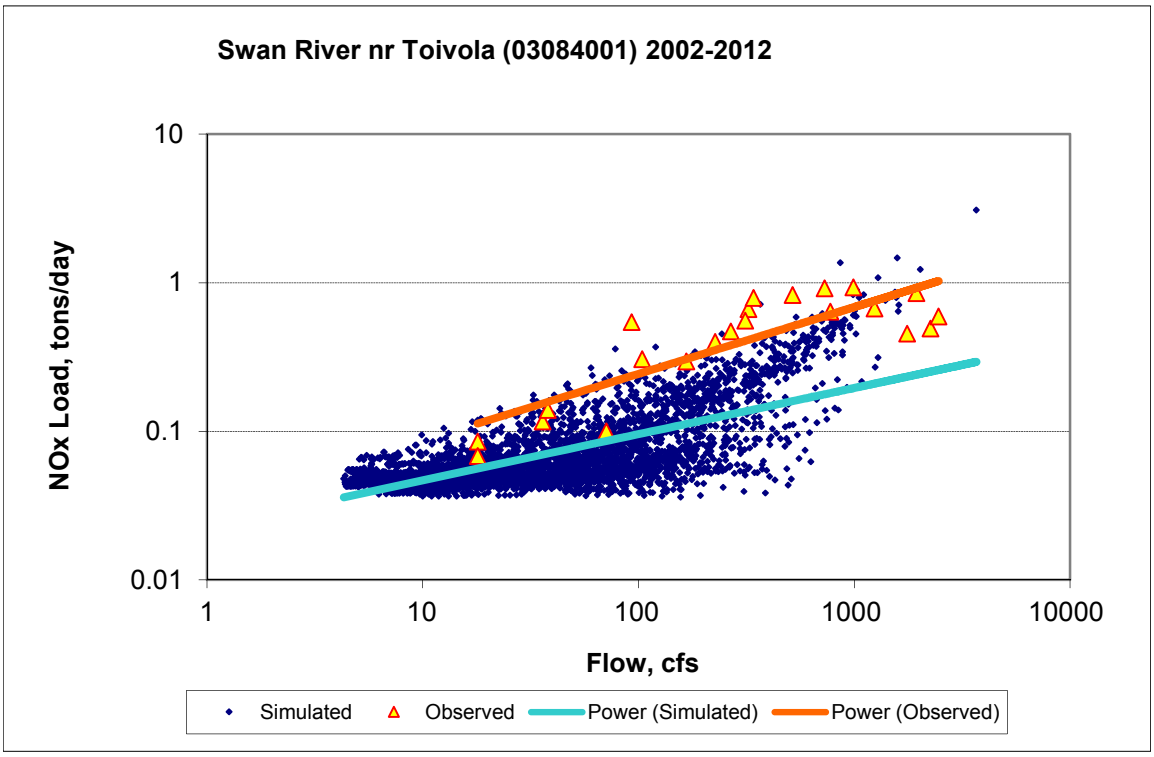

Figure A-24. Power plot of simulated and observed Nitrite+ Nitrate Nitrogen (NOx) load vs flow at Swan River nr Toivola (03084001) (calibration period)

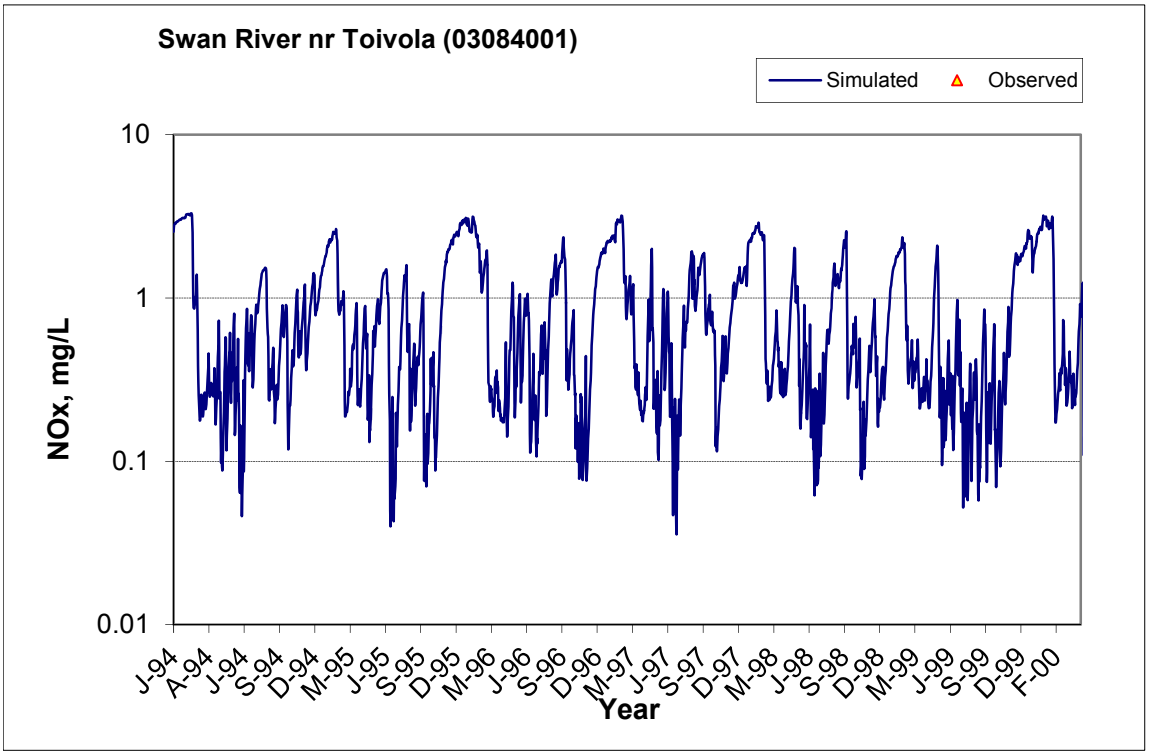

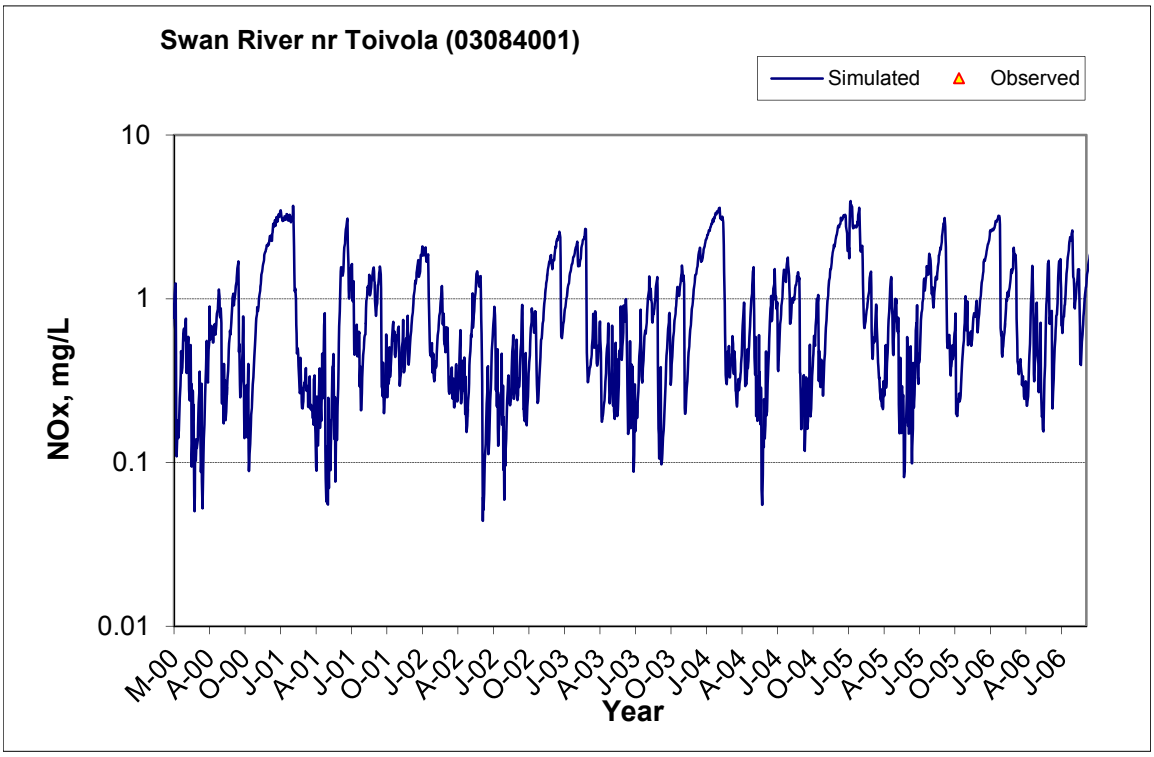

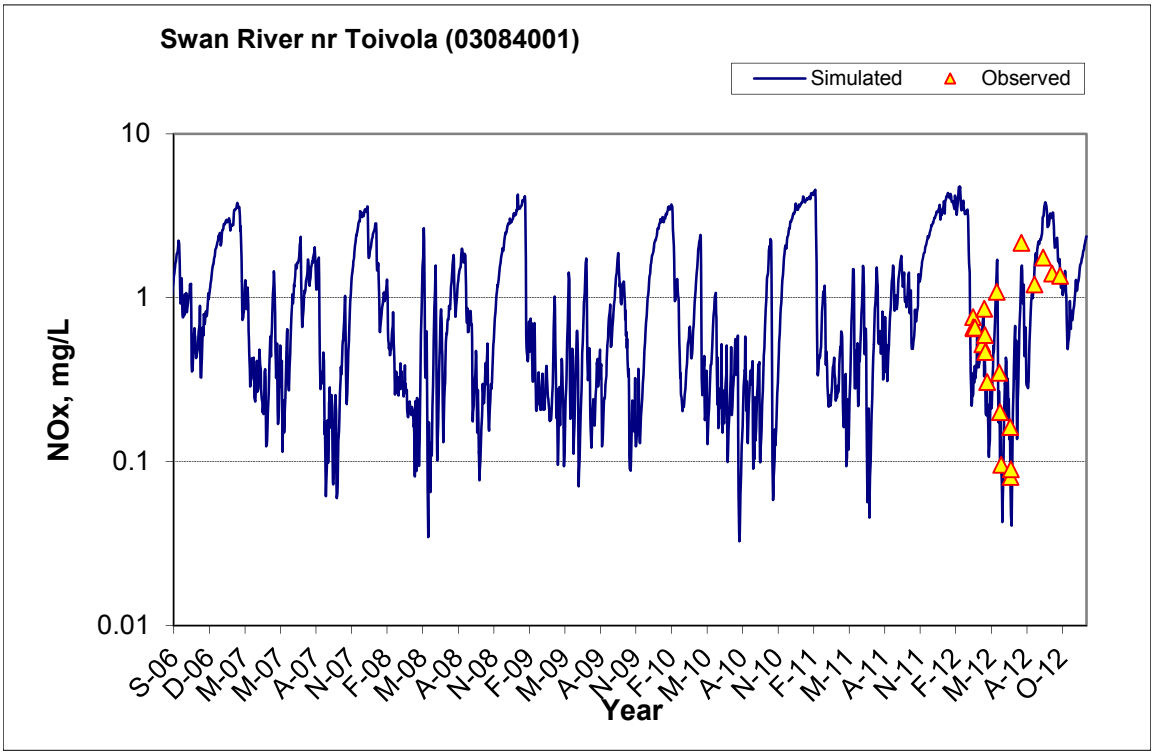

Figure A-25. Time series of observed and simulated Nitrite+ Nitrate Nitrogen (NOx) concentration at Swan River nr Toivola (03084001)

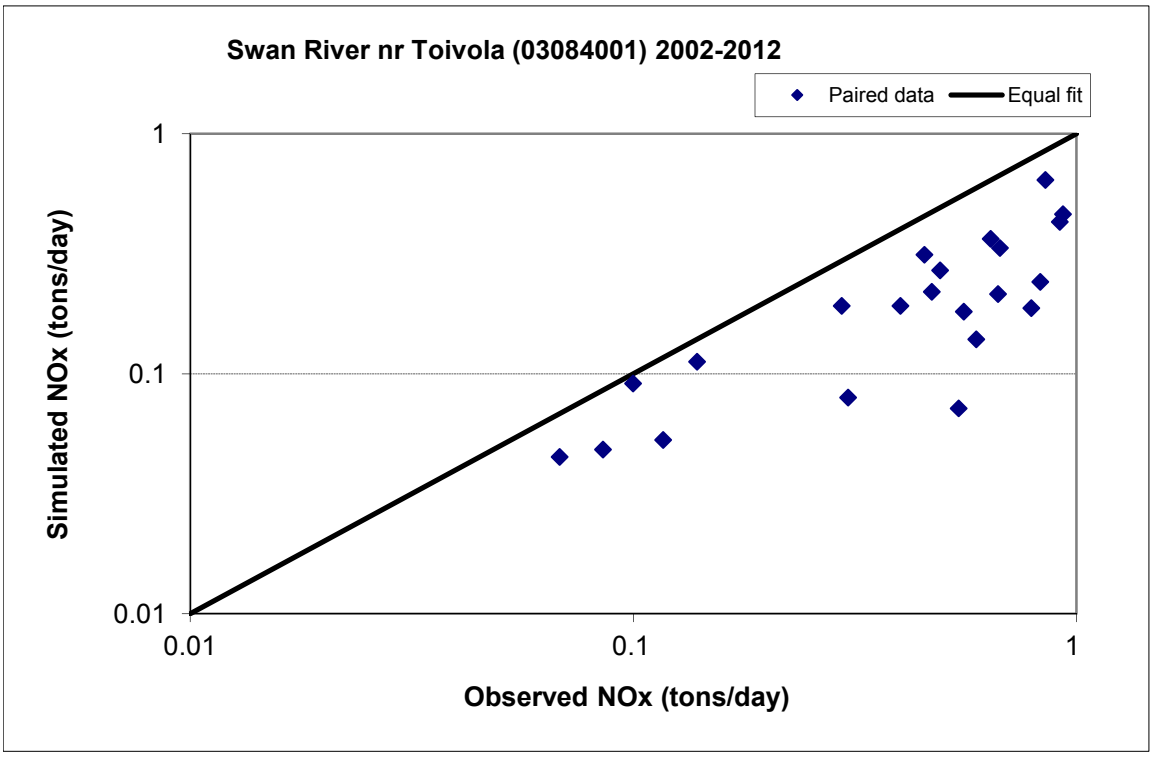

Figure A-26. Paired simulated vs. observed Nitrite+ Nitrate Nitrogen (NOx) load at Swan River nr Toivola (03084001) (calibration period)

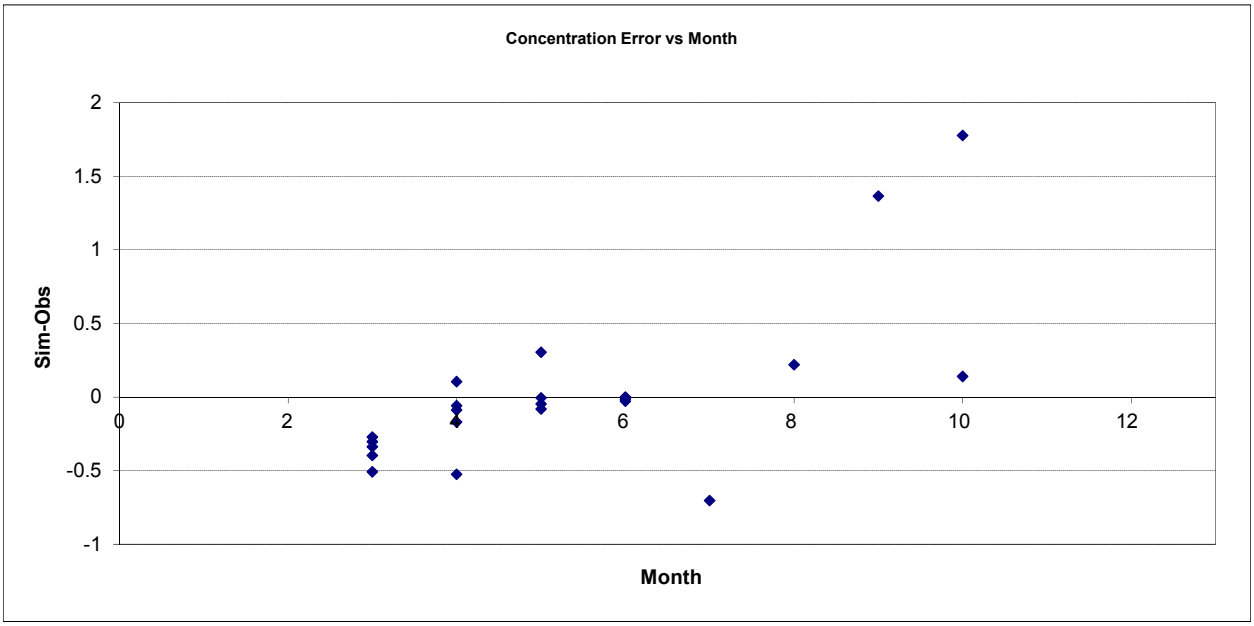

Figure A-27. Residual (Simulated - Observed) vs. Month Nitrite+ Nitrate Nitrogen (NOx) at Swan River nr Toivola (03084001)

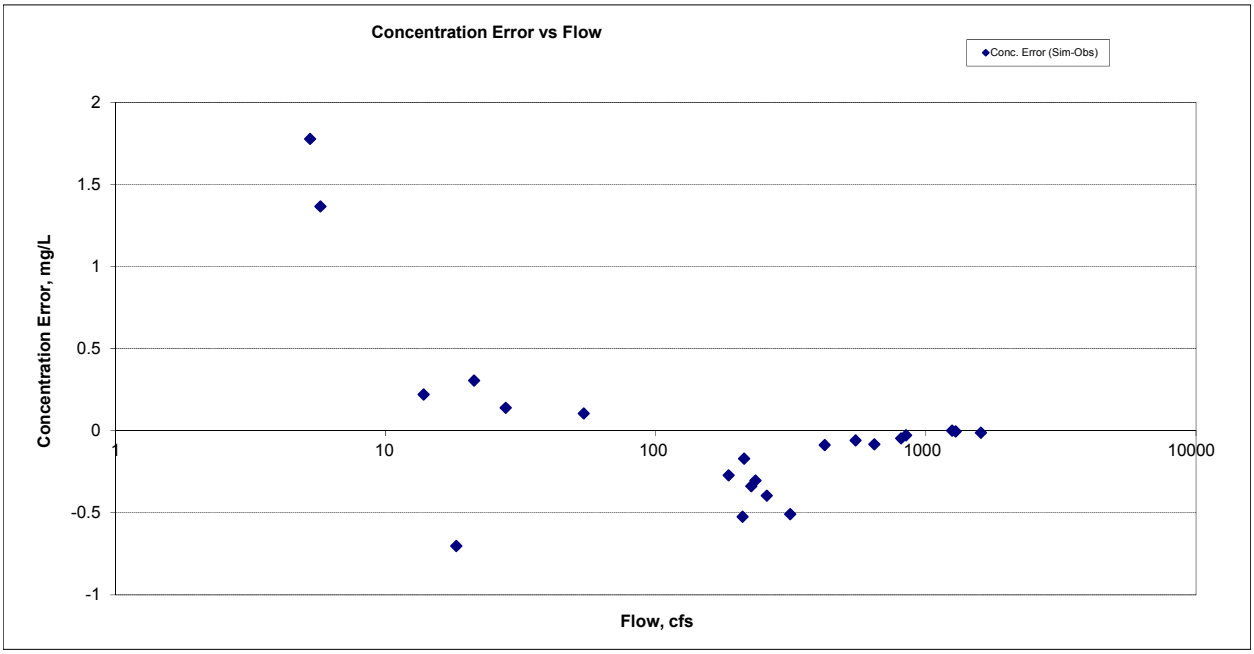

Figure A-28. Residual (Simulated - Observed) vs. Flow Nitrite+ Nitrate Nitrogen (NOx) at Swan River nr Toivola (03084001)

A.2.5 Total Nitrogen (TN)

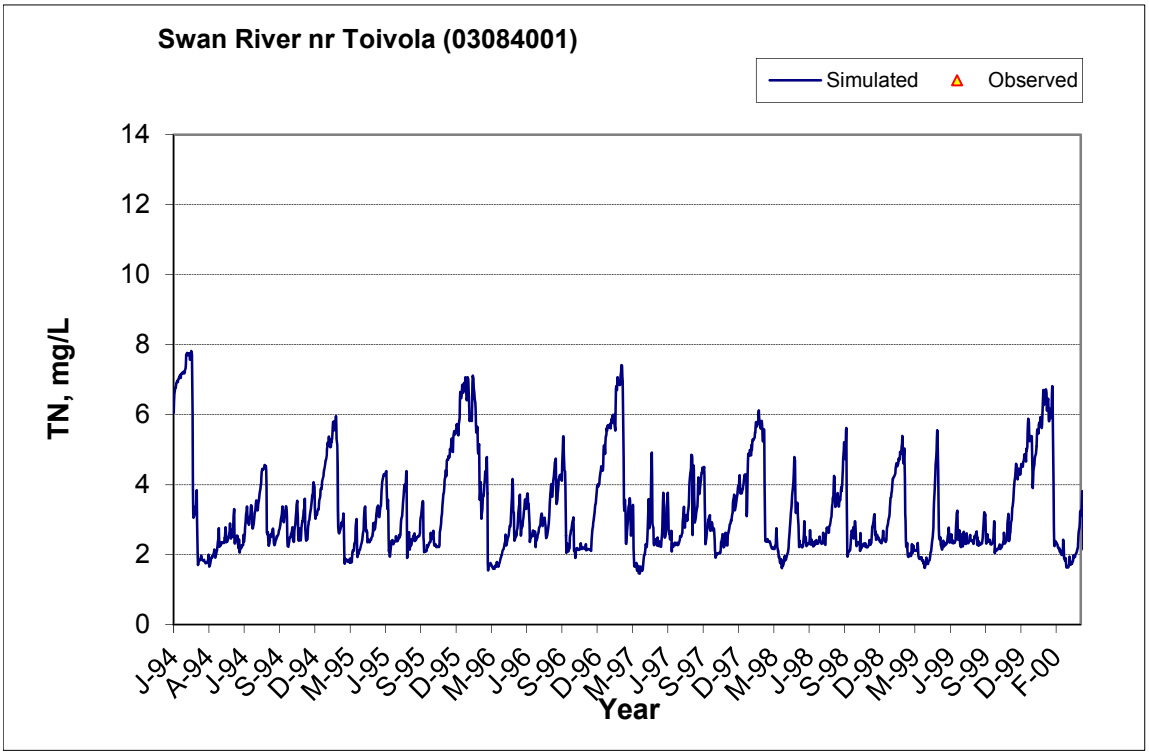

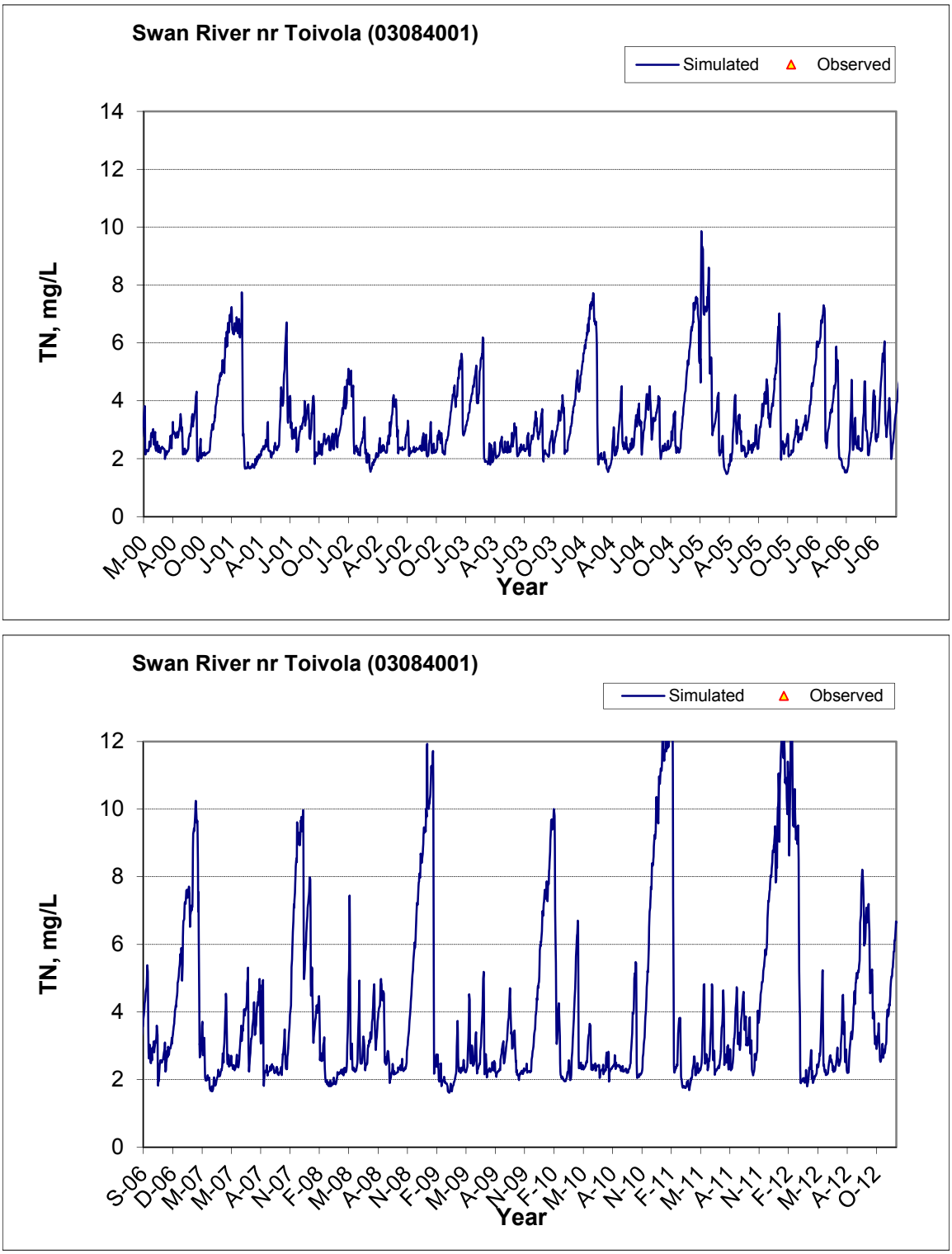

Figure A-29. Time series of observed and simulated Total Nitrogen (TN) concentration at Swan River nr Toivola (03084001)

A.2.6 Soluble Reactive Phosphorus (SRP)

Table A-5. Soluble Reactive Phosphorus (SRP) statistics

Period	1994-2001	2002-2012
Count	ND	22
Concentration Average Error		50.97%
Concentration Median Error		38.04%
Load Average Error		12.25%
Load Median Error		-6.51%
Paired t conc		0.07
Paired t load		0.57

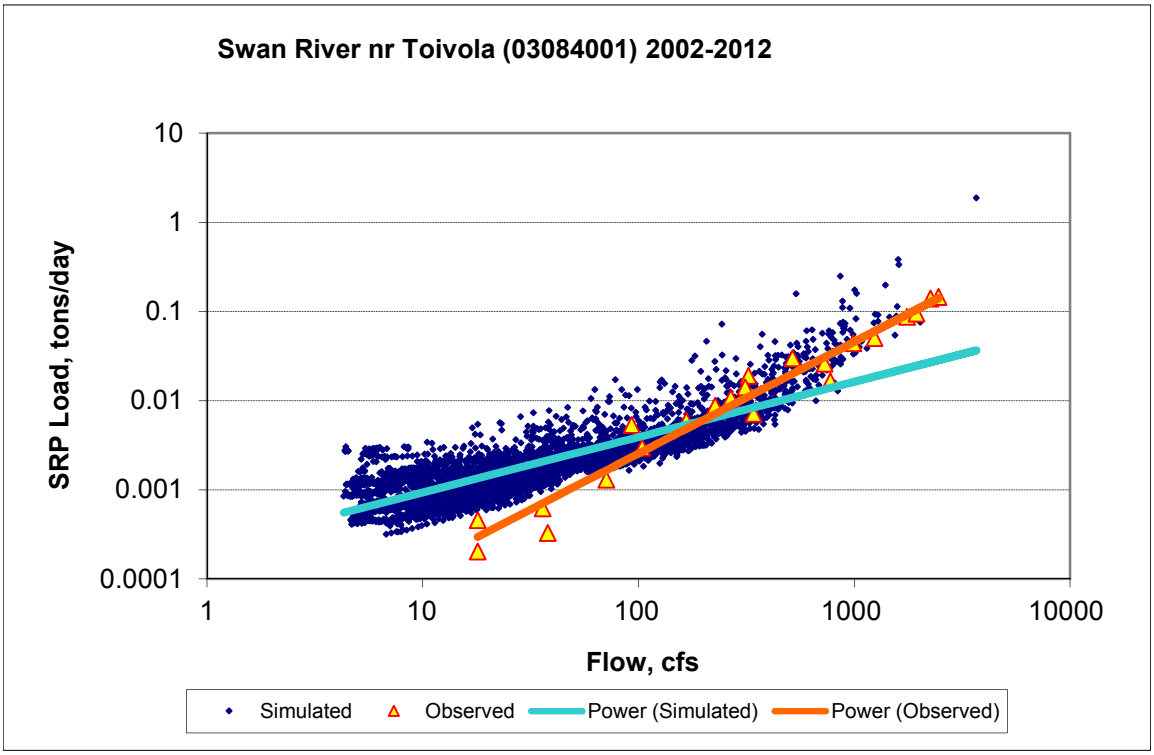

Figure A-30. Power plot of simulated and observed Soluble Reactive Phosphorus (SRP) load vs flow at Swan River nr Toivola (03084001) (calibration period)

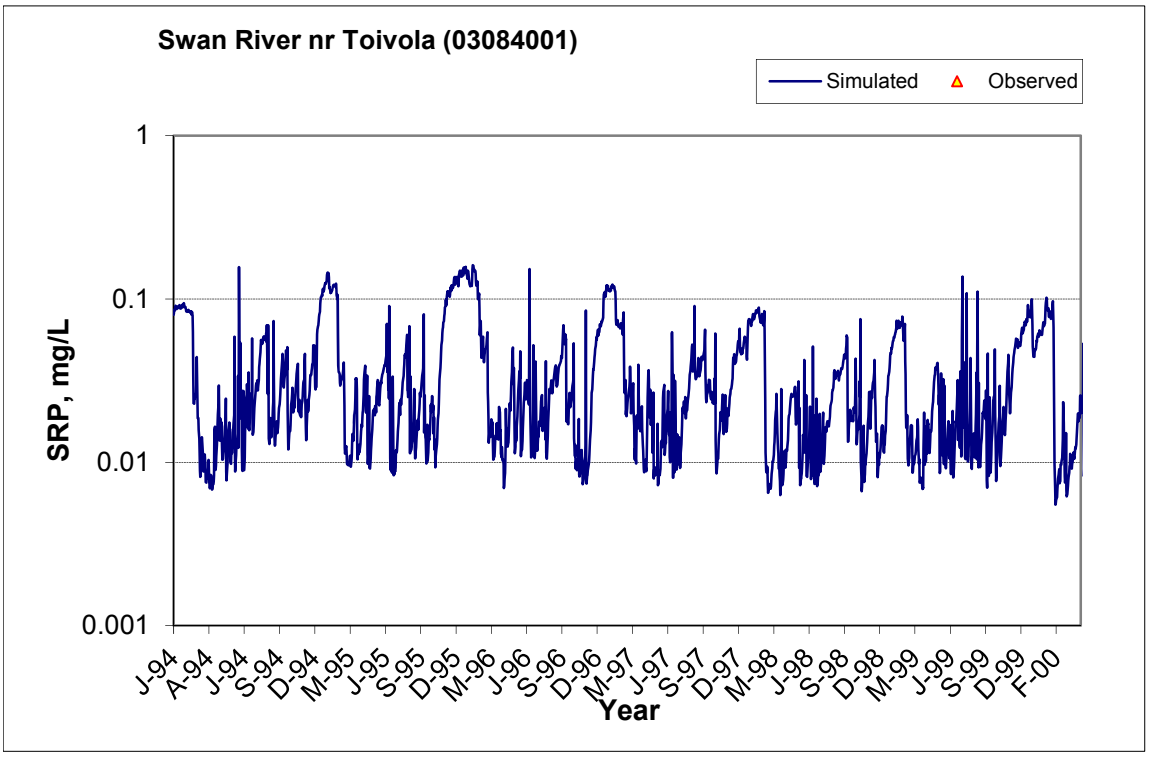
Swan River nr Toivola (03084001)
Simulated
Observed
SRP, mg/L
1
0.1
0.01
0.001
J-94 A-94 J-94 S-94 D-94 M-95 J-95 S-95 D-95 M-96 J-96 S-96 D-96 M-97 J-97 S-97 D-97 M-98 J-98 S-98 D-98 M-99 J-99 S-99 D-99 F-00
Year

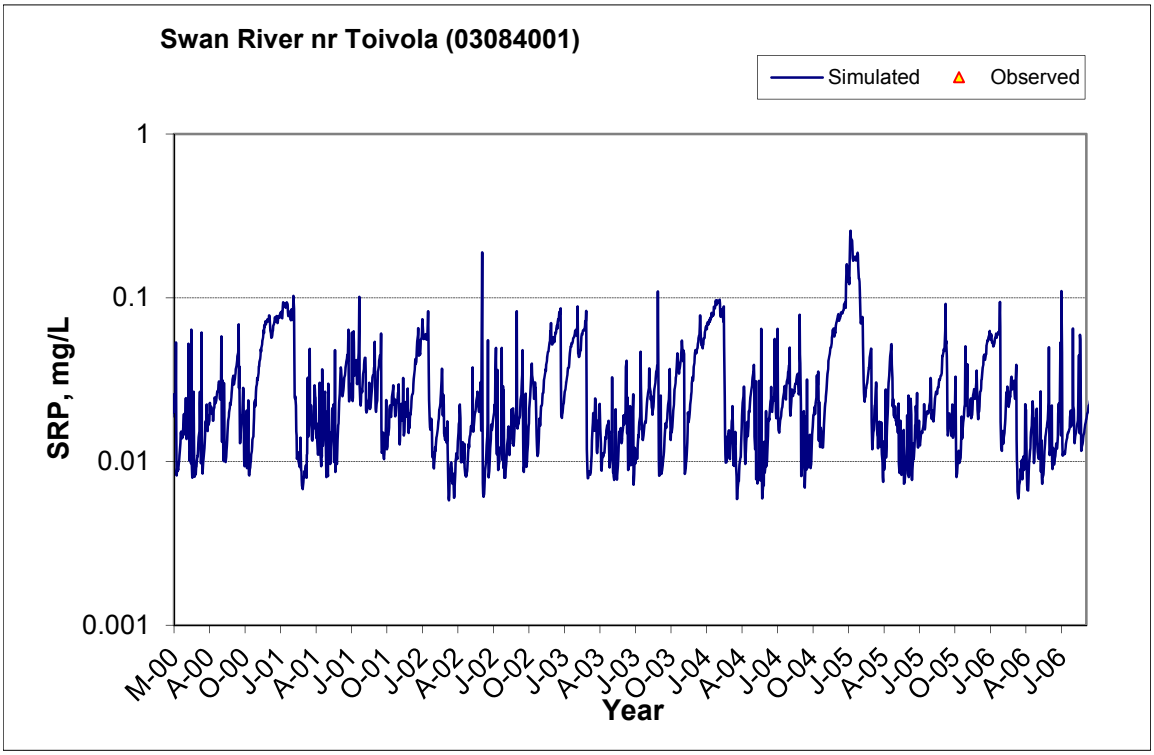
Swan River nr Toivola (03084001)
Simulated
Observed
SRP, mg/L
1
0.1
0.01
0.001
M-00 A-00 O-00 J-01 A-01 J-01 O-01 J-02 A-02 J-02 O-02 J-03 A-03 J-03 O-03 J-04 A-04 J-04 O-04 J-05 A-05 J-05 O-05 J-06 A-06 J-06
Year

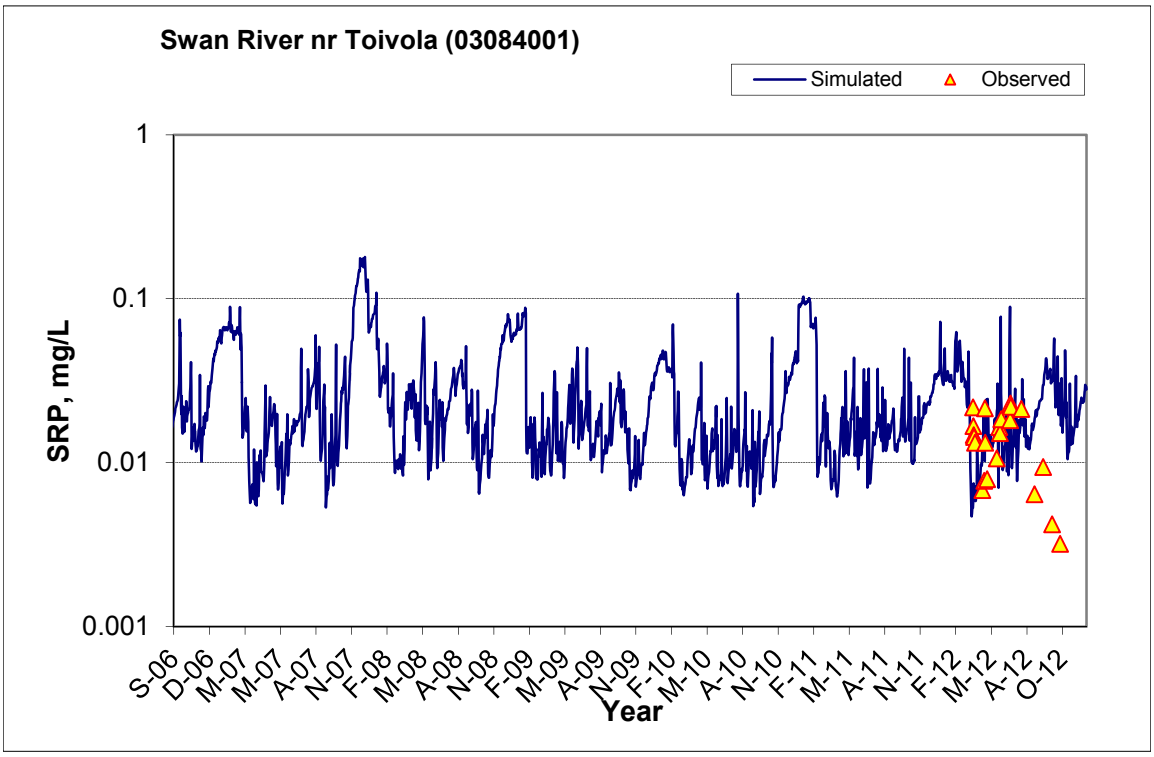

Figure A-31. Time series of observed and simulated Soluble Reactive Phosphorus (SRP) concentration at Swan River nr Toivola (03084001)

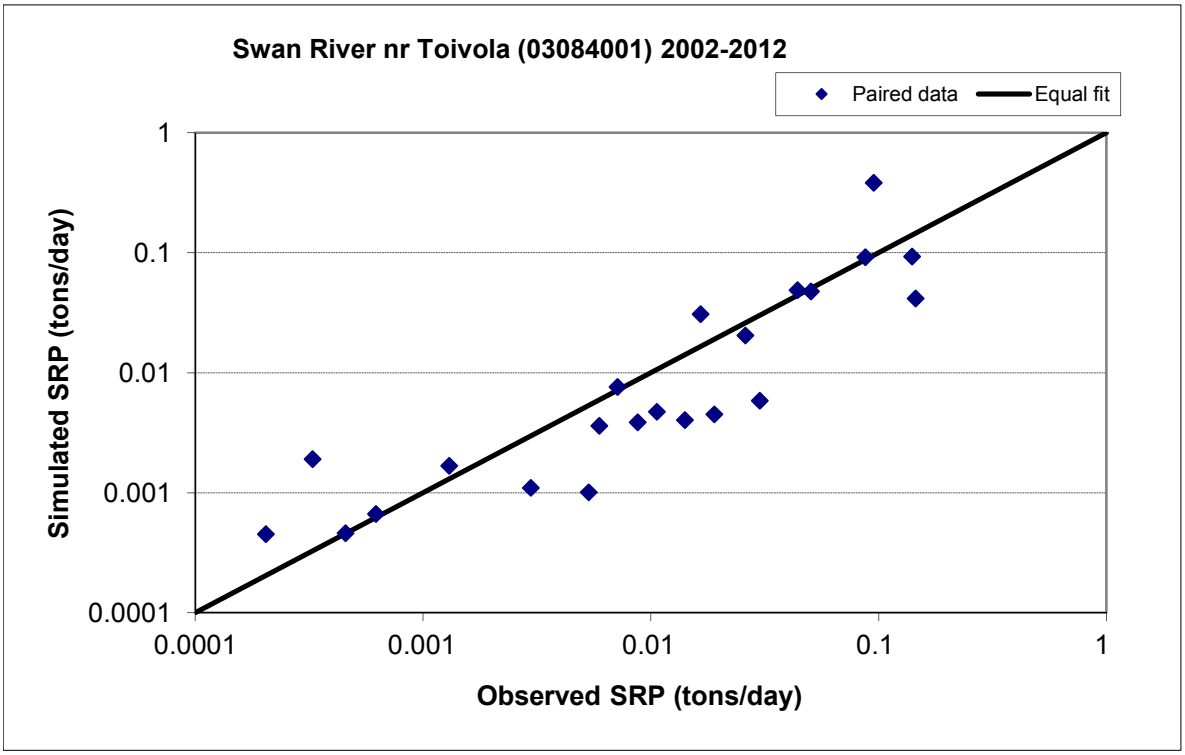

Figure A-32. Paired simulated vs. observed Soluble Reactive Phosphorus (SRP) load at Swan River nr Toivola (03084001) (calibration period)

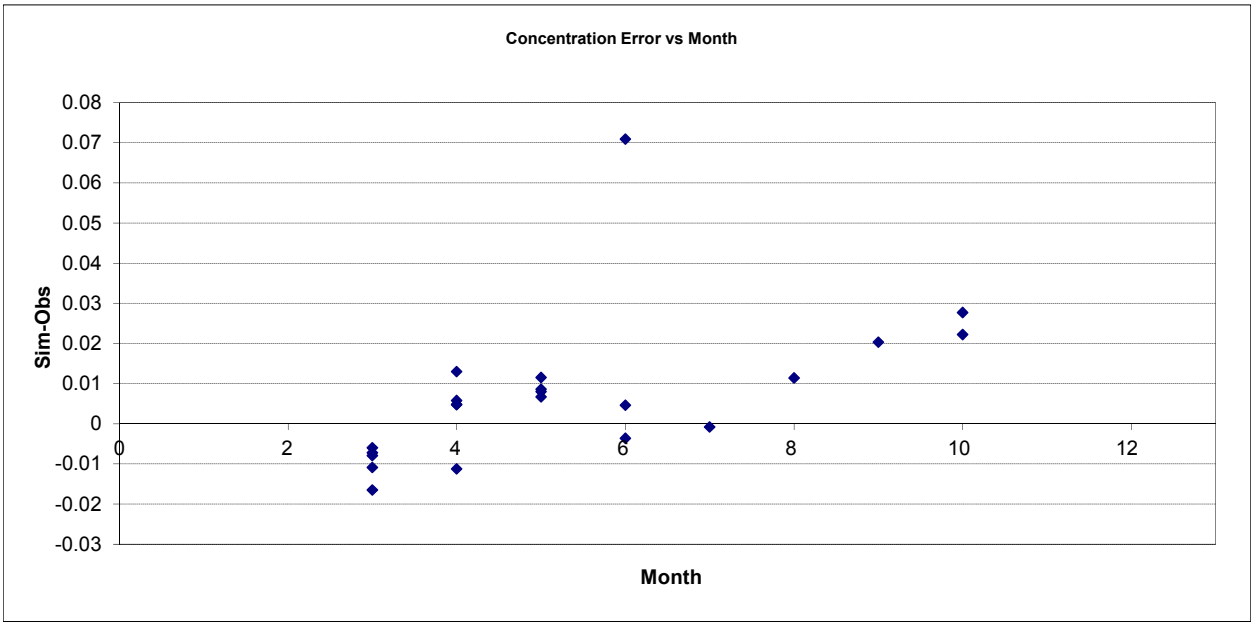

Figure A-33. Residual (Simulated - Observed) vs. Month Soluble Reactive Phosphorus (SRP) at Swan River nr Toivola (03084001)

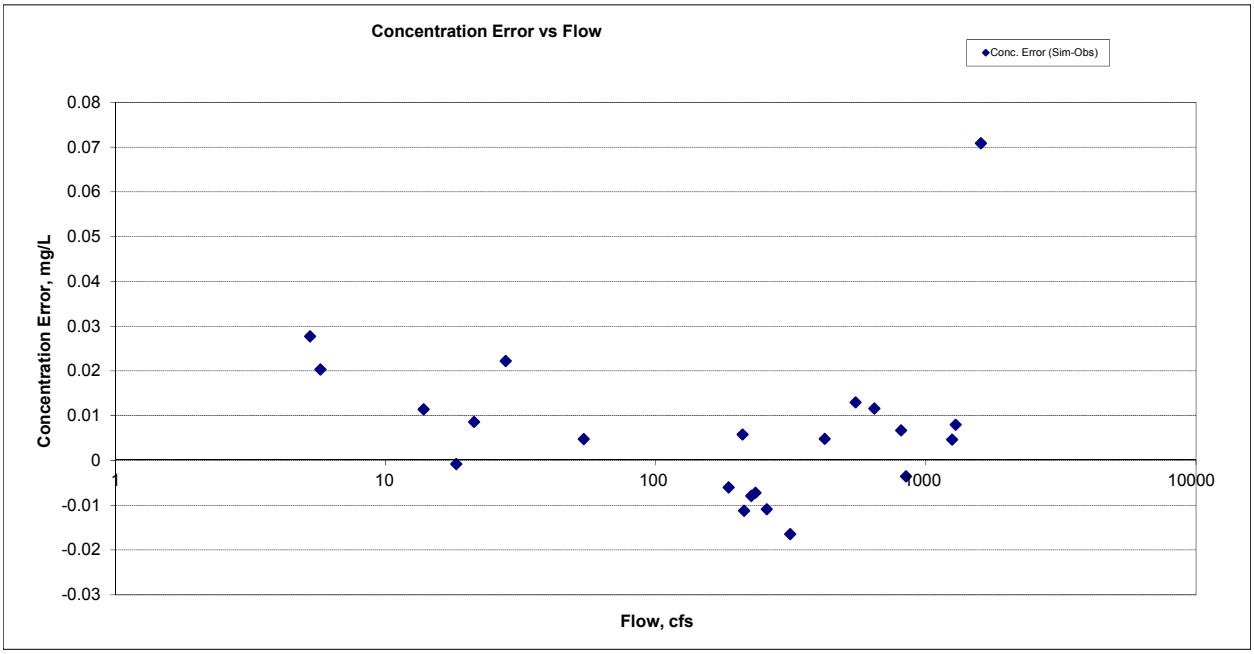

Figure A-34. Residual (Simulated - Observed) vs. Flow Soluble Reactive Phosphorus (SRP) at Swan River nr Toivola (03084001)

A.2.7 Organic Phosphorus (OrgP)

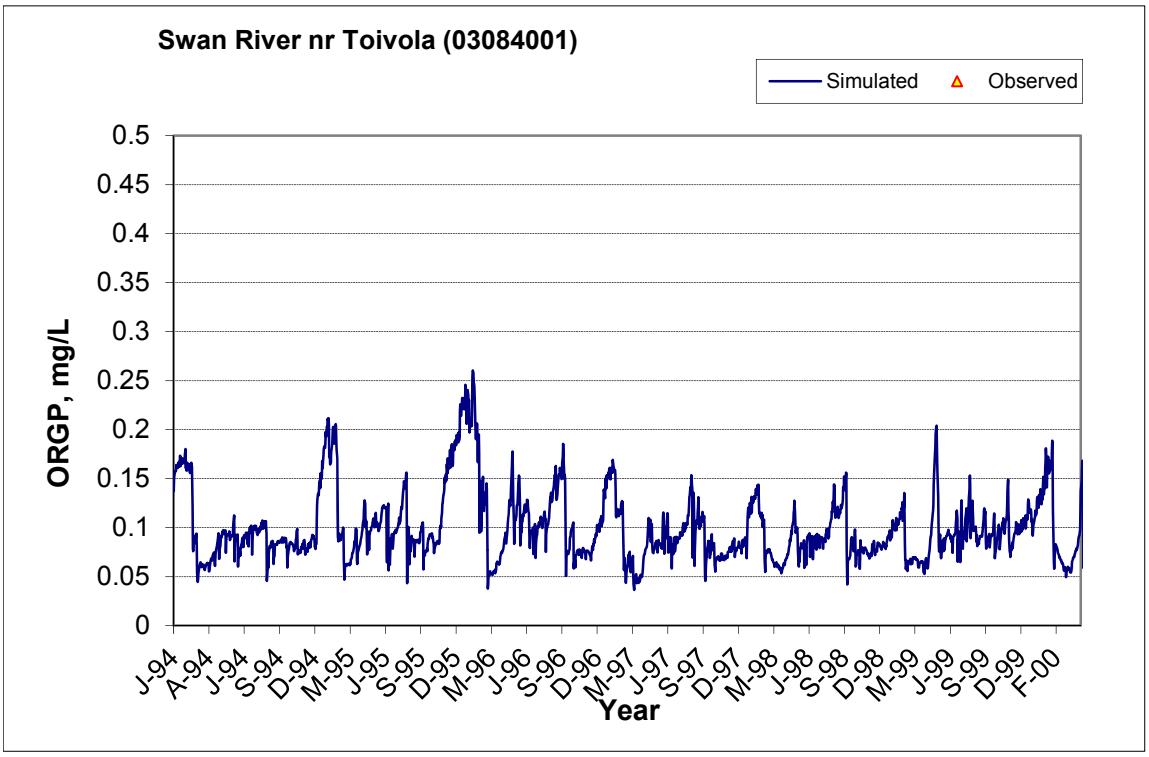

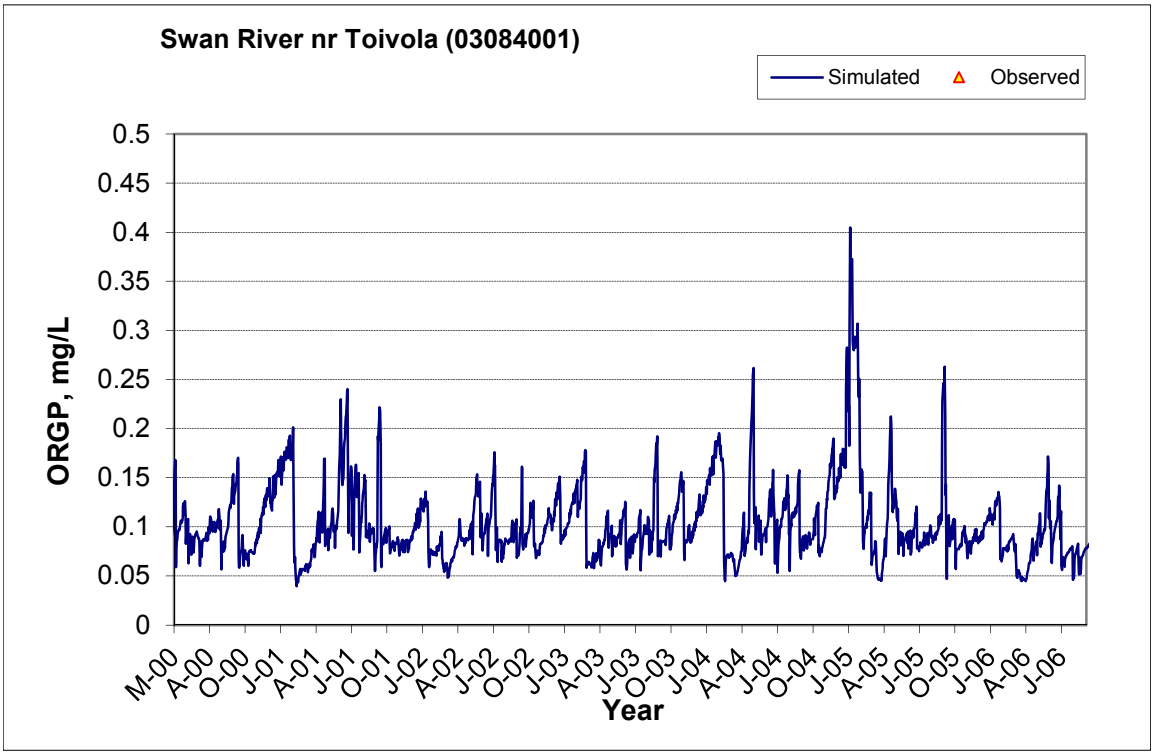

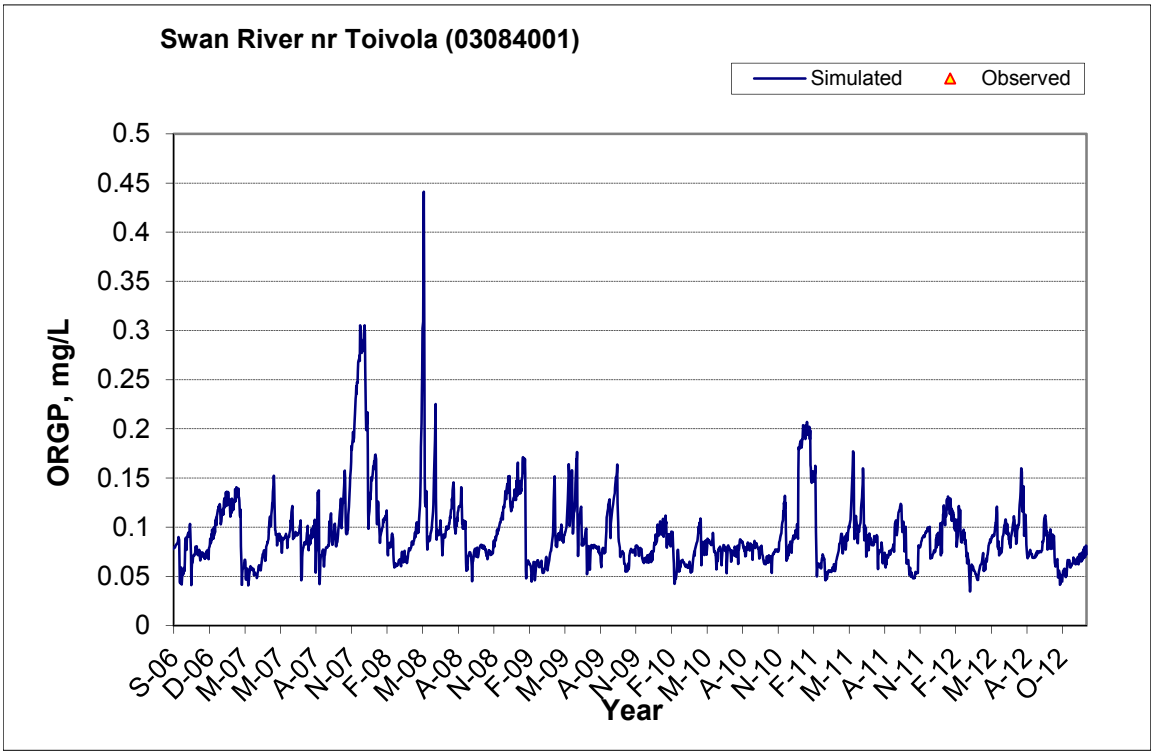

Figure A-35. Time series of observed and simulated Organic Phosphorus (OrgP) concentration at Swan River nr Toivola (03084001)

A.2.8 Total Phosphorus (TP)

Table A-6. Total Phosphorus (TP) statistics

Period	1994-2001	2002-2012
Count	ND	22
Concentration Average Error		18.07%
Concentration Median Error		-4.18%
Load Average Error		-41.22%
Load Median Error		-6.41%
Paired t conc		0.58
Paired t load		0.19

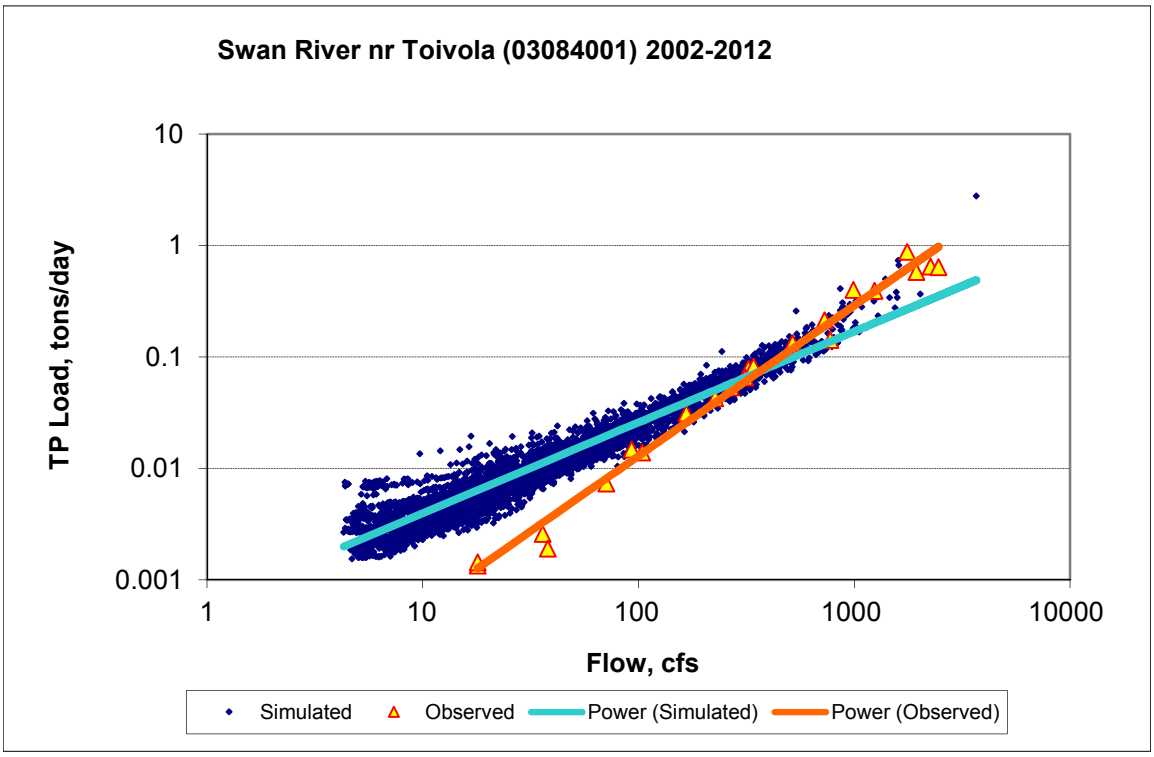

Figure A-36. Power plot of simulated and observed Total Phosphorus (TP) load vs flow at Swan River nr Toivola (03084001) (calibration period)

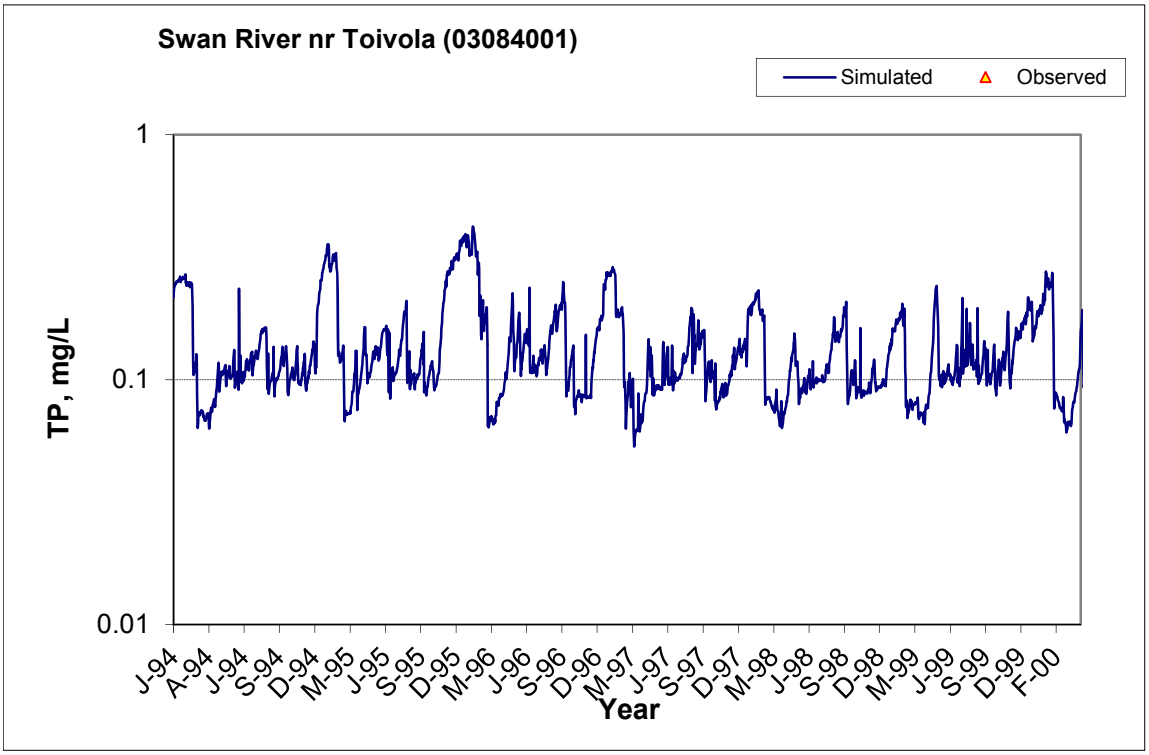

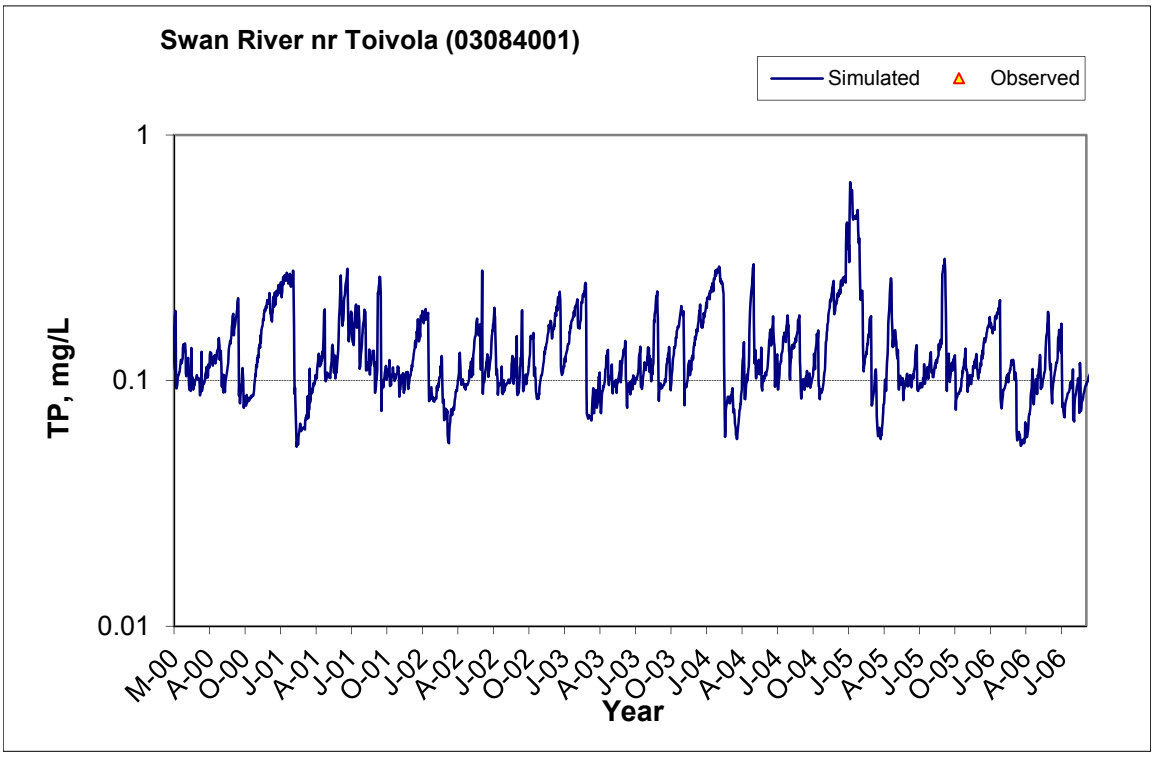

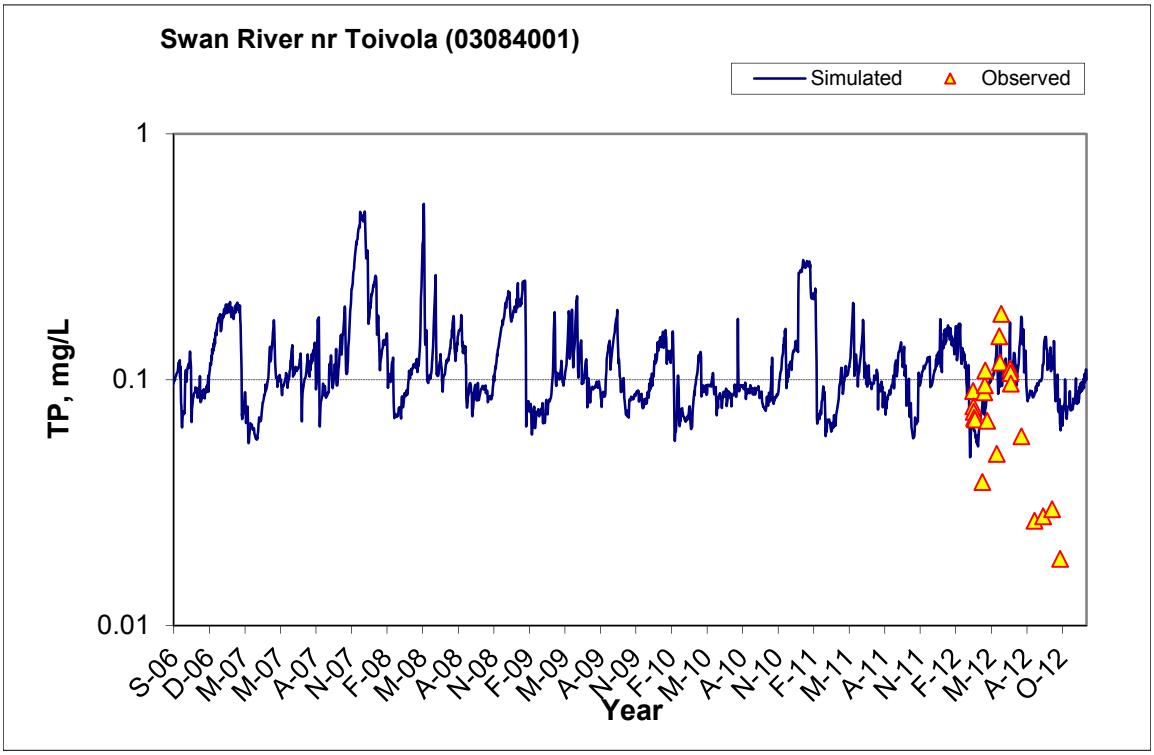

Figure A-37. Time series of observed and simulated Total Phosphorus (TP) concentration at Swan River nr Toivola (03084001)

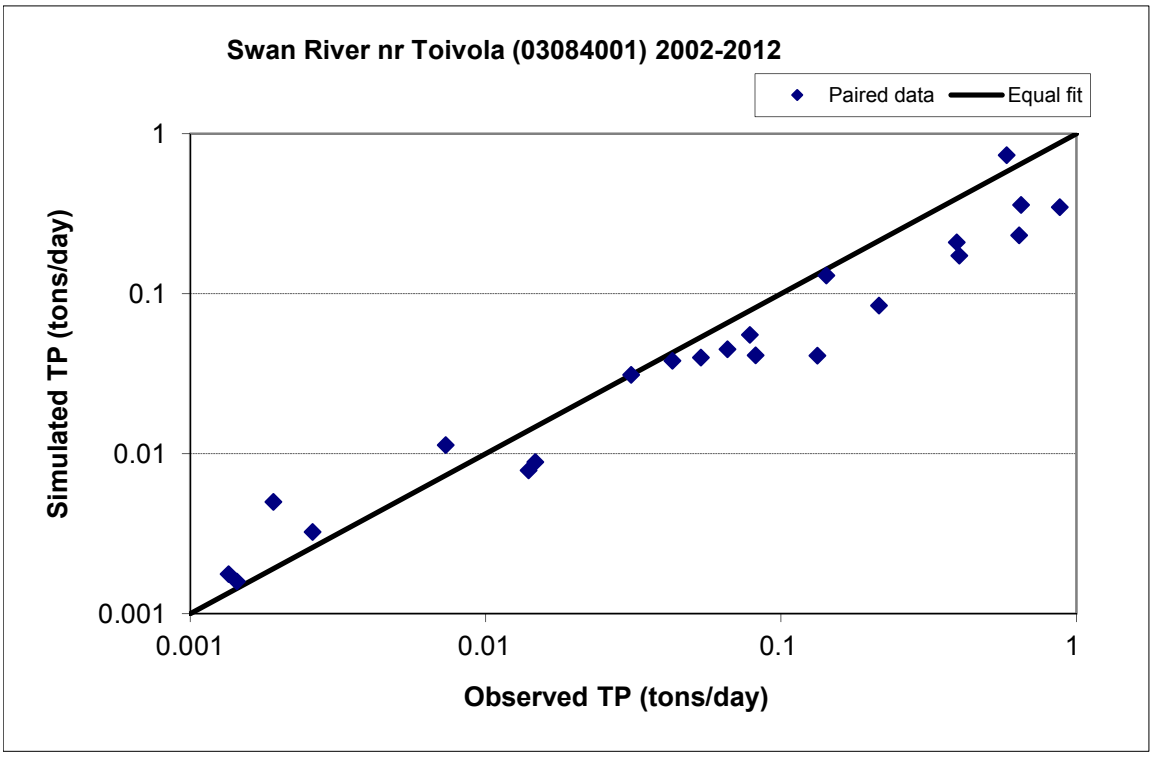

Figure A-38. Paired simulated vs. observed Total Phosphorus (TP) load at Swan River nr Toivola (03084001) (calibration period)

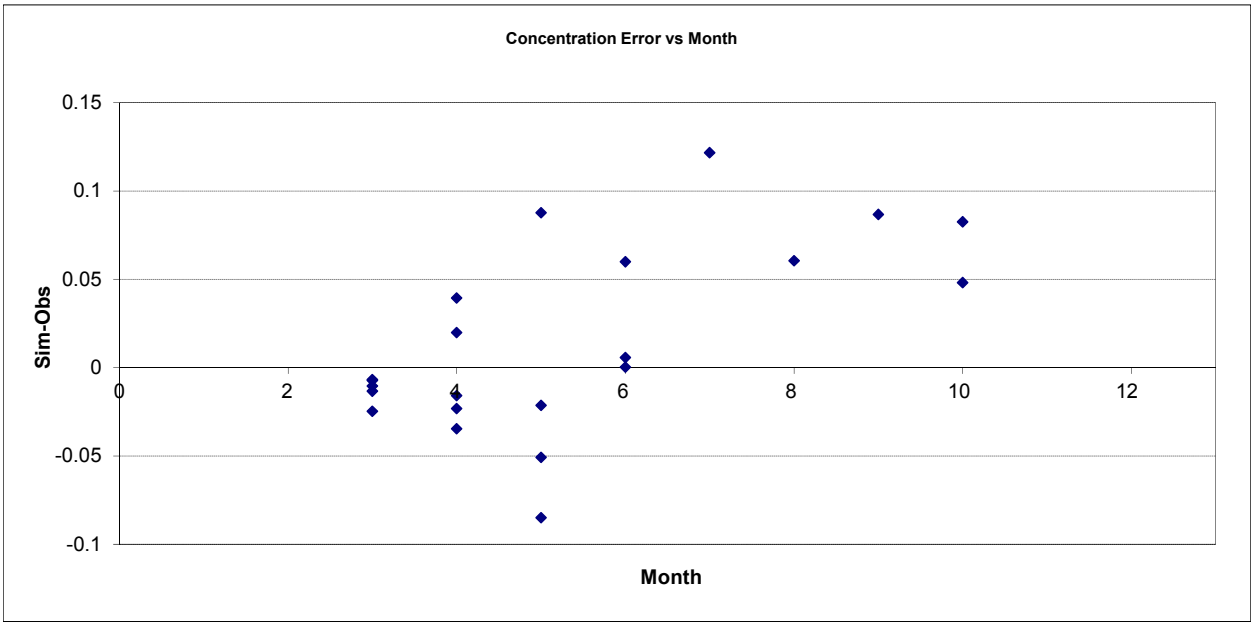

Figure A-39. Residual (Simulated - Observed) vs. Month Total Phosphorus (TP) at Swan River nr Toivola (03084001)

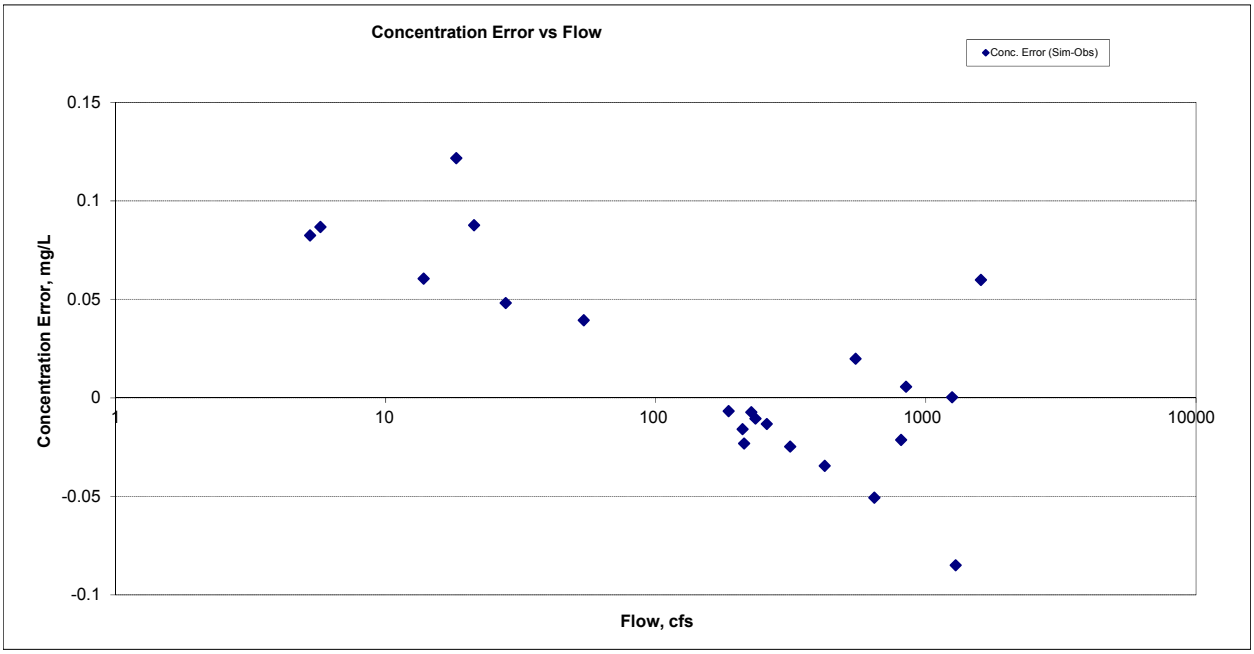

Figure A-40. Residual (Simulated - Observed) vs. Flow Total Phosphorus (TP) at Swan River nr Toivola (03084001)

A.3 ST LOUIS R BRIDGE AT CSAH-7, 0.5 MI S OF FORBES

A.3.1 Ammonia Nitrogen (NH3)

Table A-7. Ammonia Nitrogen (NH3) statistics

Period	1994-2001	2002-2012
Count	35	49
Concentration Average Error	136.20%	76.77%
Concentration Median Error	143.18%	97.38%
Load Average Error	120.54%	72.25%
Load Median Error	115.13%	65.99%
Paired t conc	0.00	0.00
Paired t load	0.00	0.03

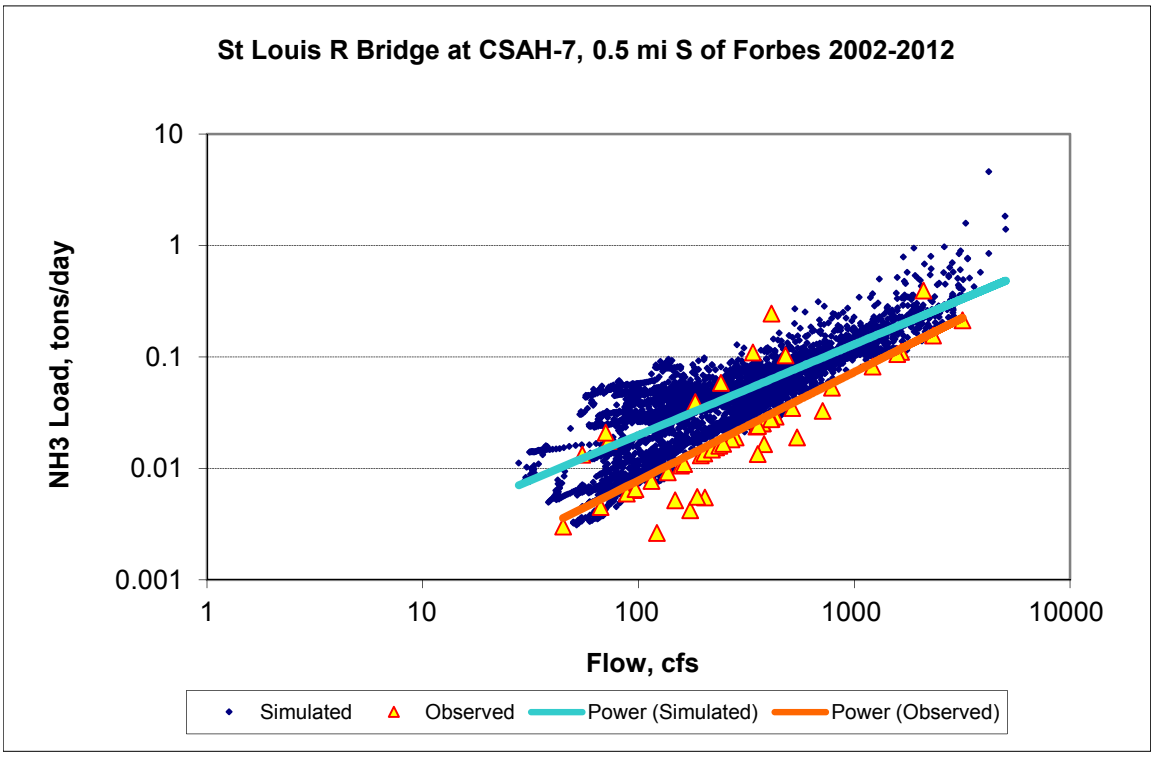

Figure A-41. Power plot of simulated and observed Ammonia Nitrogen (NH3) load vs flow at St Louis R Bridge at CSAH-7, 0.5 mi S of Forbes (calibration period)

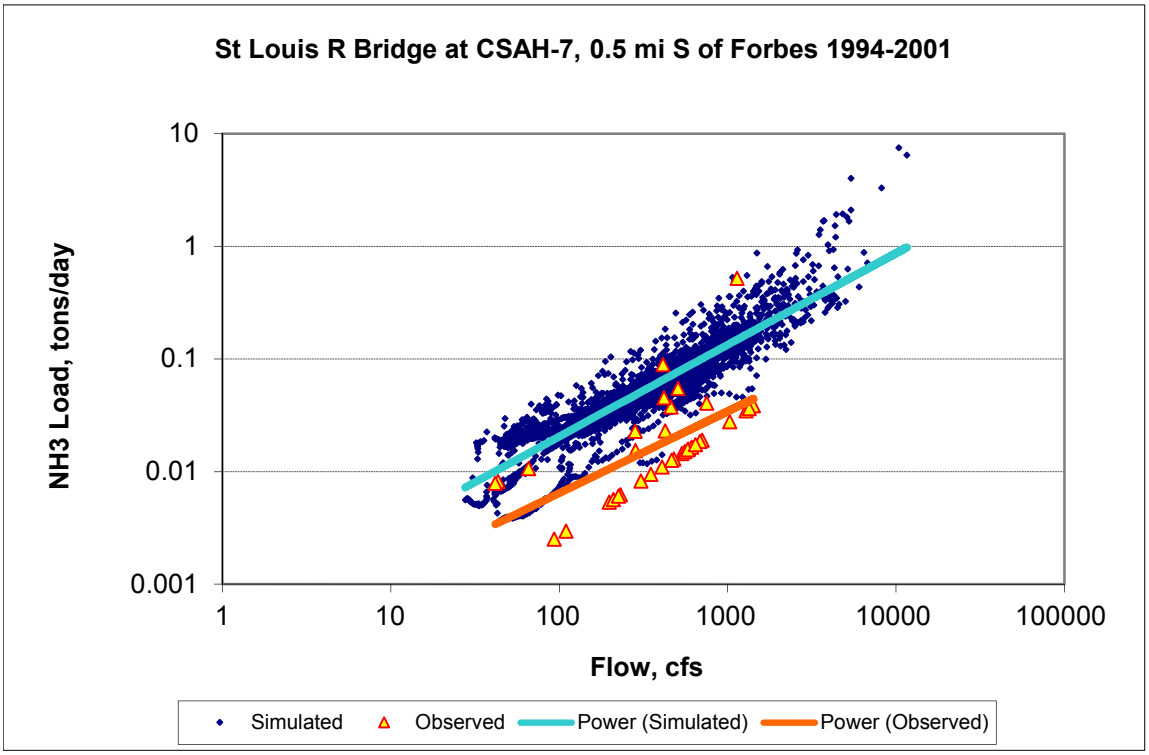

Figure A-42. Power plot of simulated and observed Ammonia Nitrogen (NH3) load vs flow at St Louis R Bridge at CSAH-7, 0.5 mi S of Forbes (validation period)

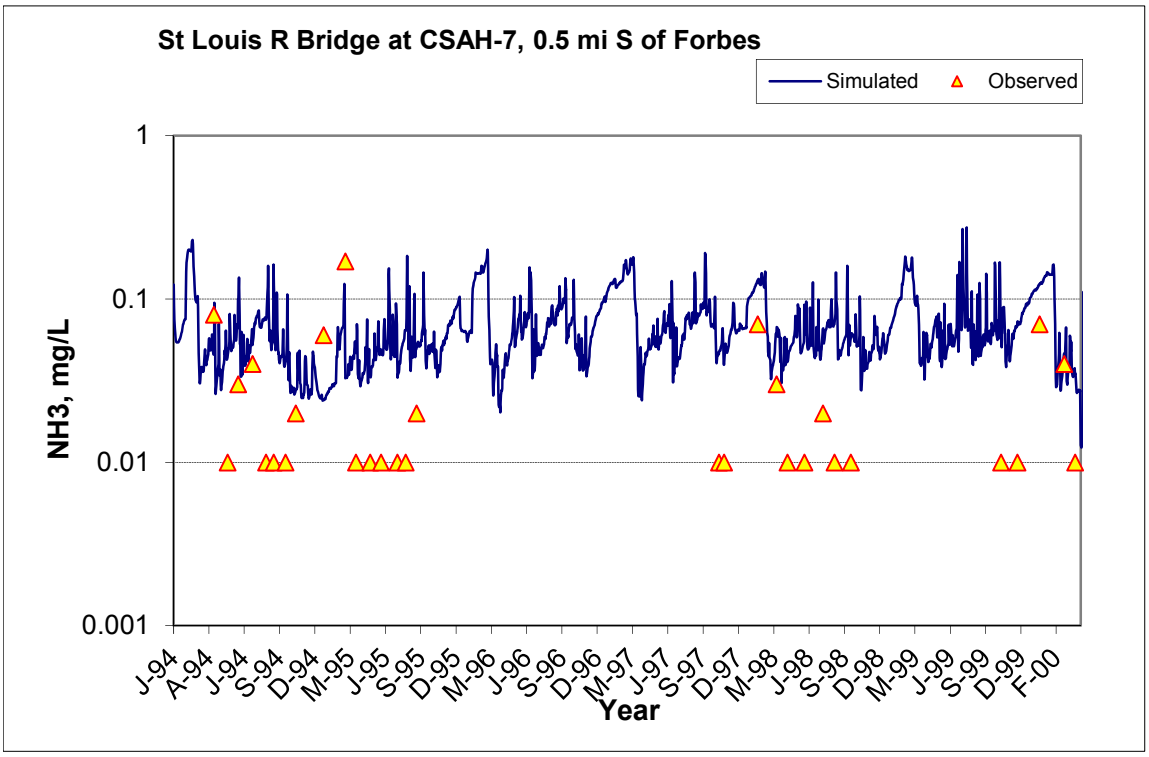
St Louis R Bridge at CSAH-7, 0.5 mi S of Forbes
Simulated
Observed
NH3, mg/L
1
0.1
0.01
0.001
J-94 A-94 J-94 S-94 D-94 M-95 J-95 S-95 D-95 M-96 J-96 S-96 D-96 M-97 J-97 S-97 D-97 M-98 J-98 S-98 D-98 M-99 J-99 S-99 D-99 F-00
Year

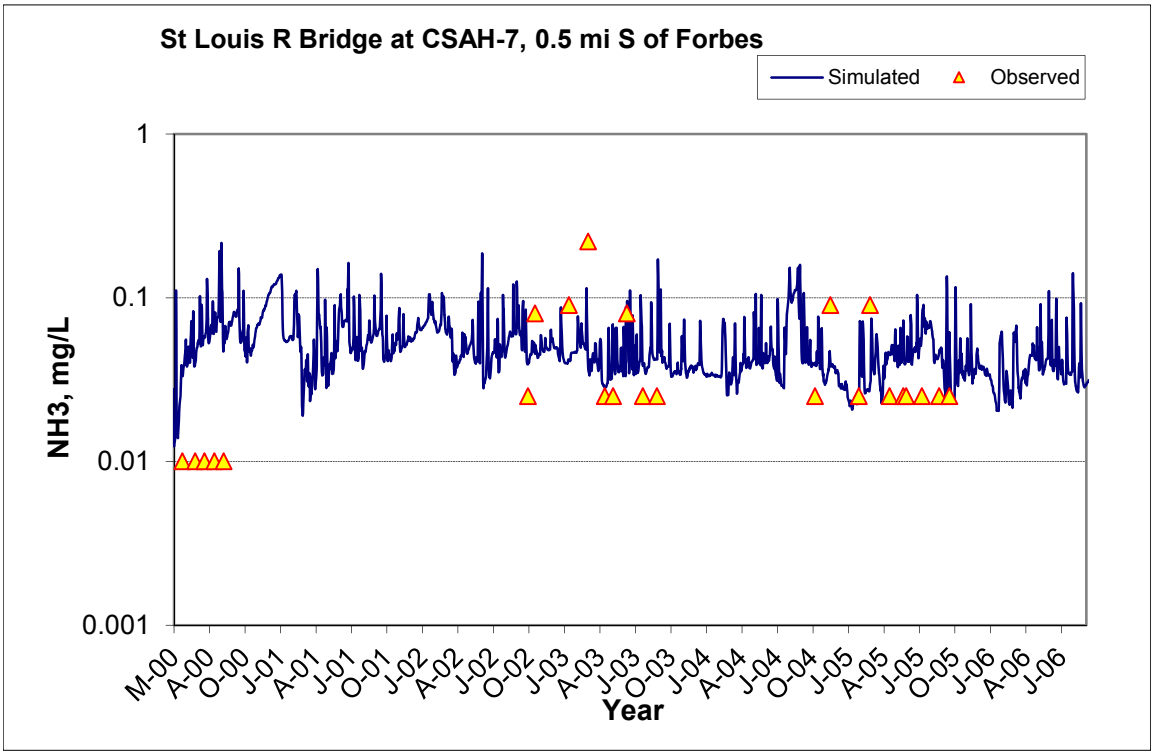
St Louis R Bridge at CSAH-7, 0.5 mi S of Forbes
Simulated
Observed
NH3, mg/L
1
0.1
0.01
0.001
M-00 A-00 O-00 J-01 A-01 J-01 O-01 J-02 A-02 J-02 O-02 J-03 A-03 J-03 O-03 J-04 A-04 J-04 O-04 J-05 A-05 J-05 O-05 J-06 A-06 J-06
Year

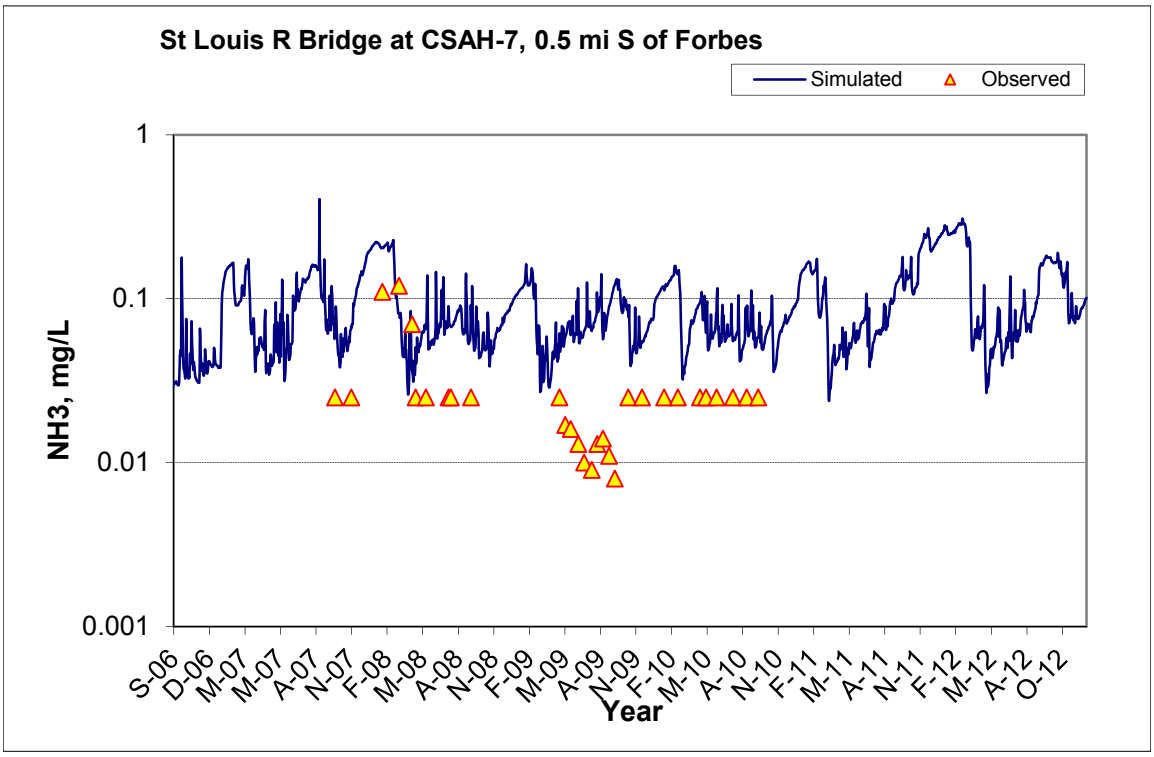

Figure A-43. Time series of observed and simulated Ammonia Nitrogen (NH3) concentration at St Louis R Bridge at CSAH-7, 0.5 mi S of Forbes

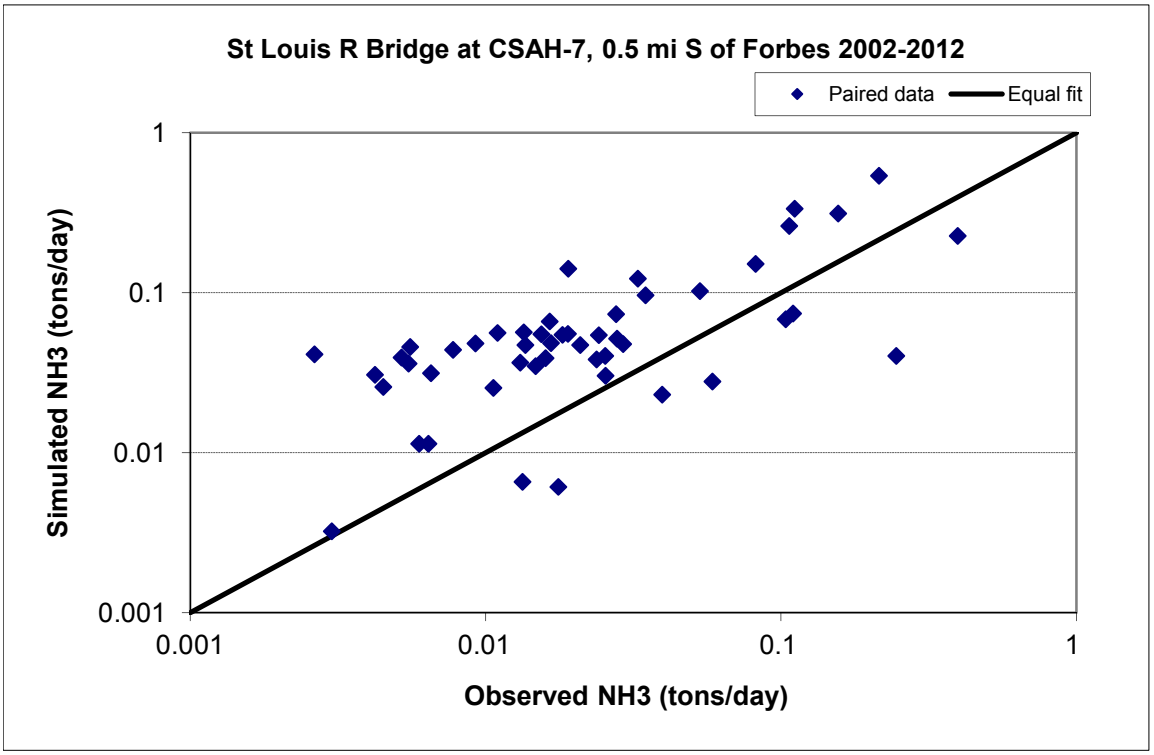

Figure A-44. Paired simulated vs. observed Ammonia Nitrogen (NH3) load at St Louis R Bridge at CSAH-7, 0.5 mi S of Forbes (calibration period)

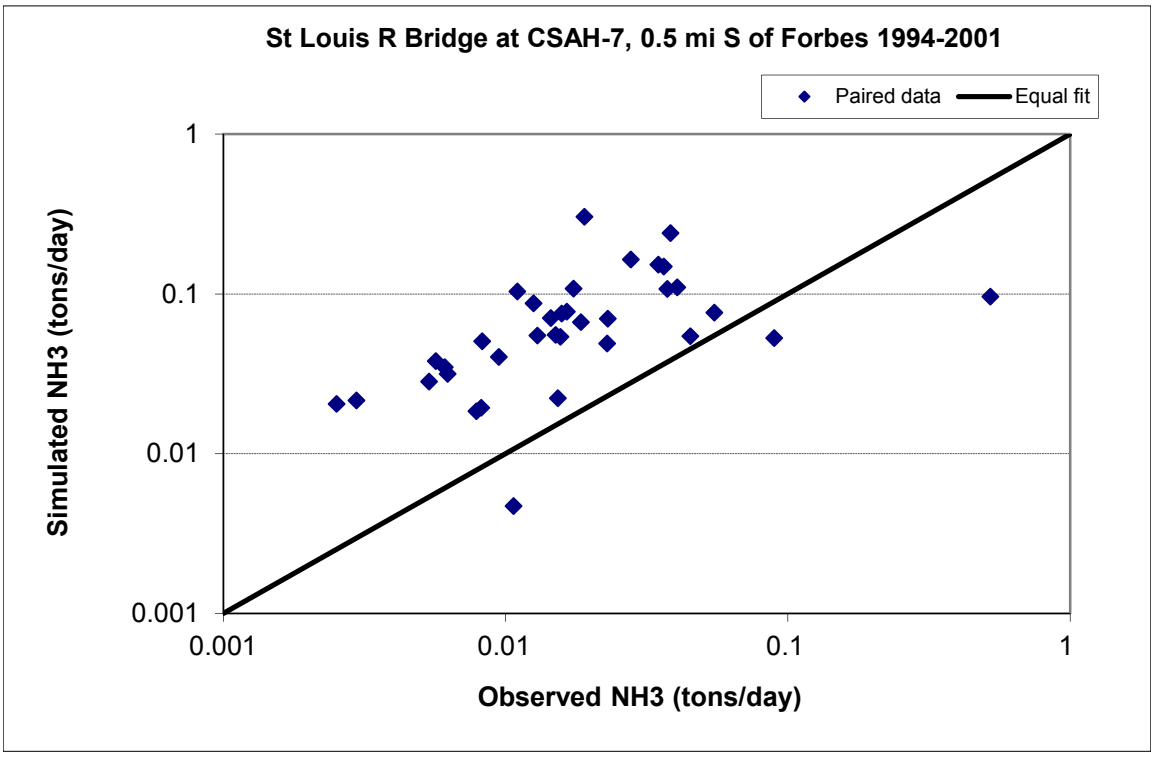

Figure A-45. Paired simulated vs. observed Ammonia Nitrogen (NH3) load at St Louis R Bridge at CSAH-7, 0.5 mi S of Forbes (validation period)

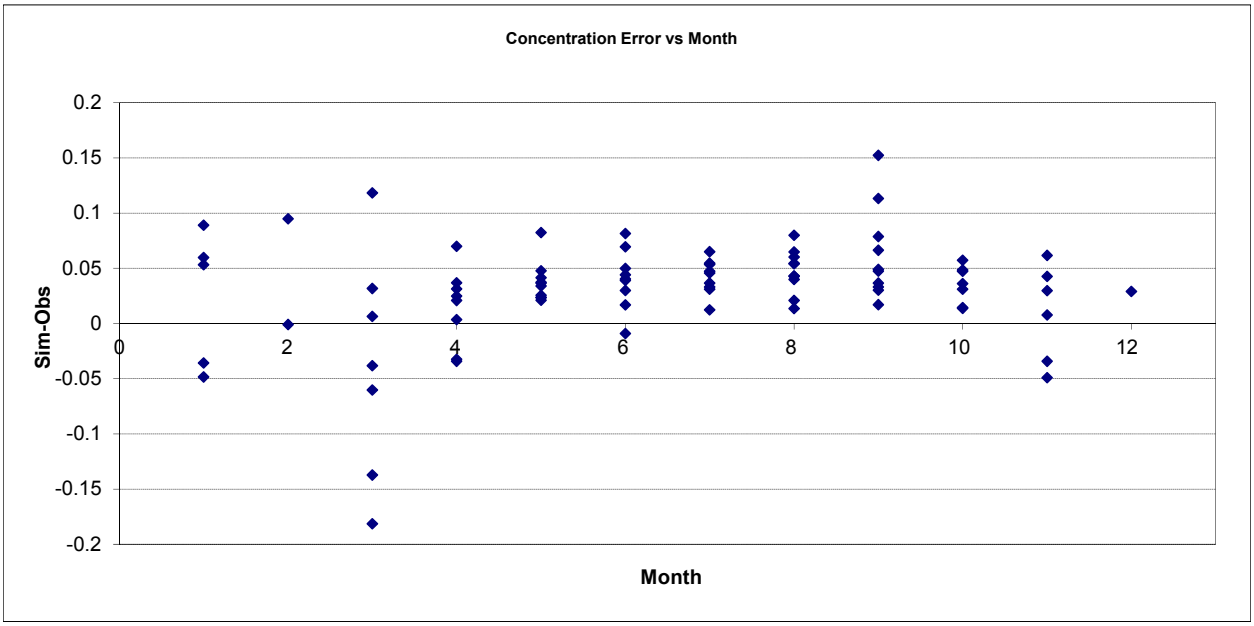

Figure A-46. Residual (Simulated - Observed) vs. Month Ammonia Nitrogen (NH3) at St Louis R Bridge at CSAH-7, 0.5 mi S of Forbes

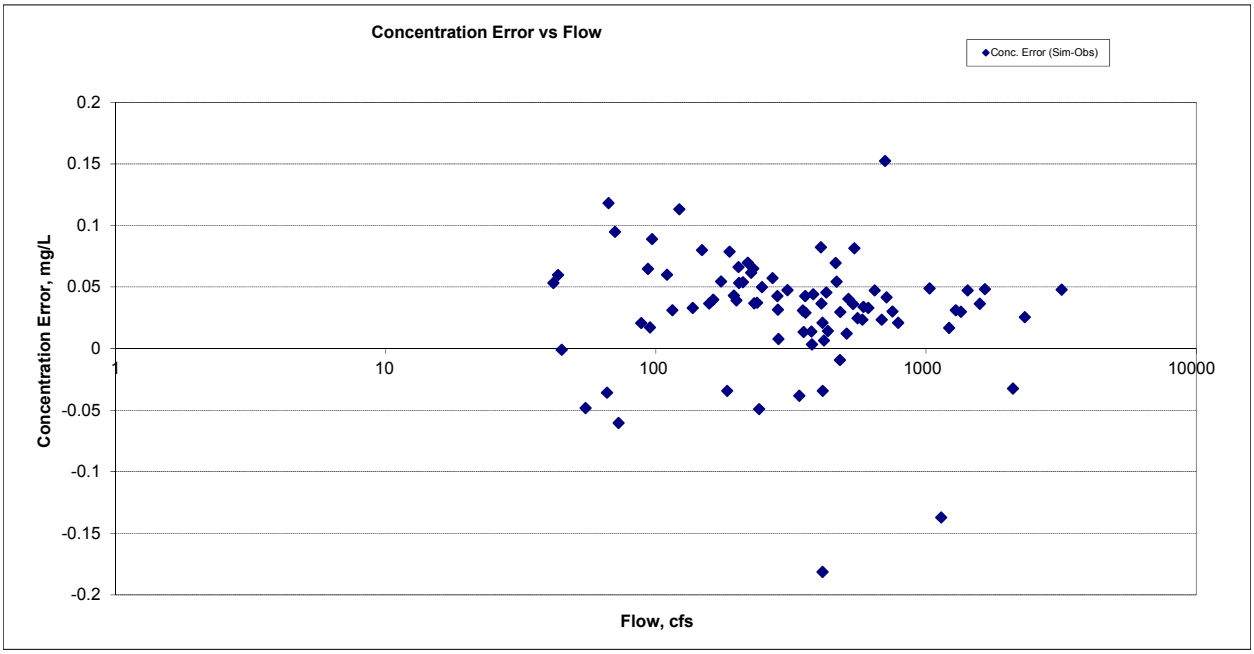

Figure A-47. Residual (Simulated - Observed) vs. Flow Ammonia Nitrogen (NH3) at St Louis R Bridge at CSAH-7, 0.5 mi S of Forbes

A.3.2 Organic Nitrogen (OrgN)

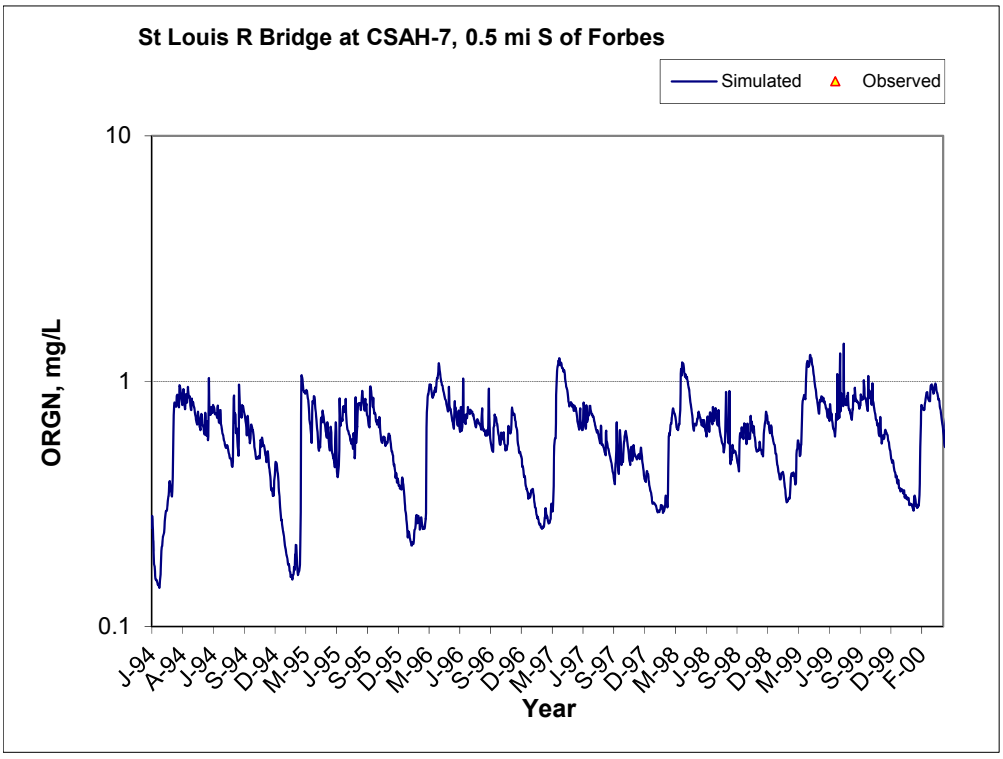

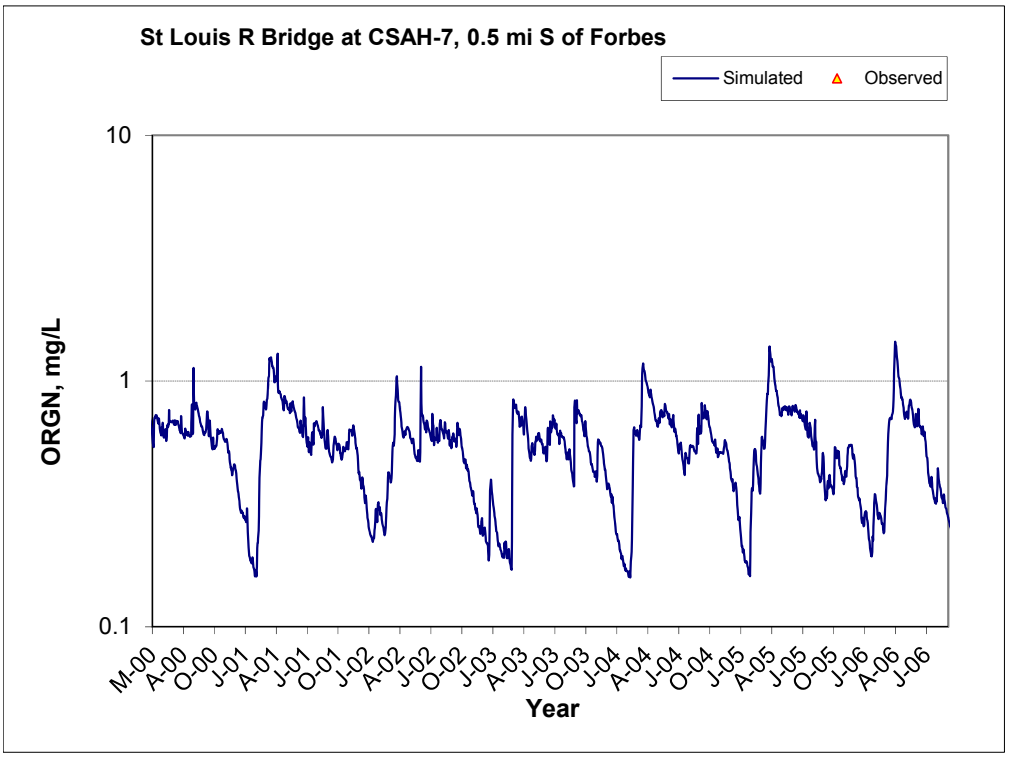

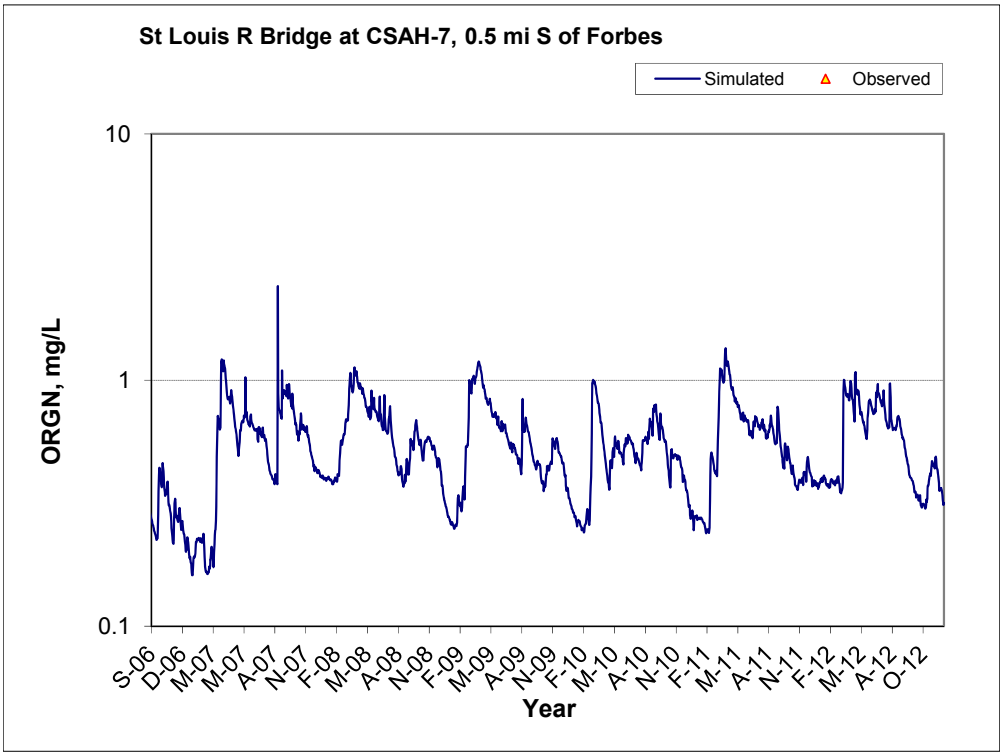

Figure A-48. Time series of observed and simulated Organic Nitrogen (OrgN) concentration at St Louis R Bridge at CSAH-7, 0.5 mi S of Forbes

A.3.3 Total Kjeldahl Nitrogen (TKN)

Table A-8. Total Kjeldahl Nitrogen (TKN) statistics

Period	1994-2001	2002-2012
Count	6	7
Concentration Average Error	-7.54%	-11.94%
Concentration Median Error	-2.63%	-22.38%
Load Average Error	-3.55%	12.63%
Load Median Error	-3.12%	22.32%
Paired t conc	0.86	0.85
Paired t load	0.73	0.55

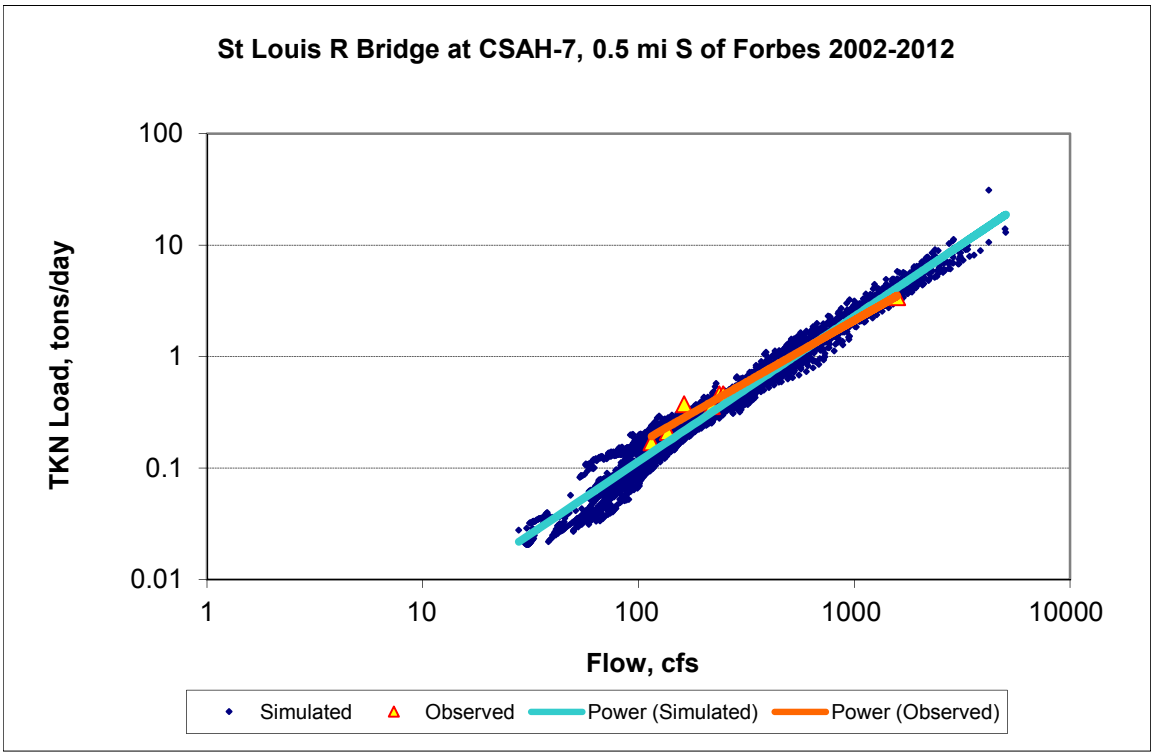

Figure A-49. Power plot of simulated and observed Total Kjeldahl Nitrogen (TKN) load vs flow at St Louis R Bridge at CSAH-7, 0.5 mi S of Forbes (calibration period)

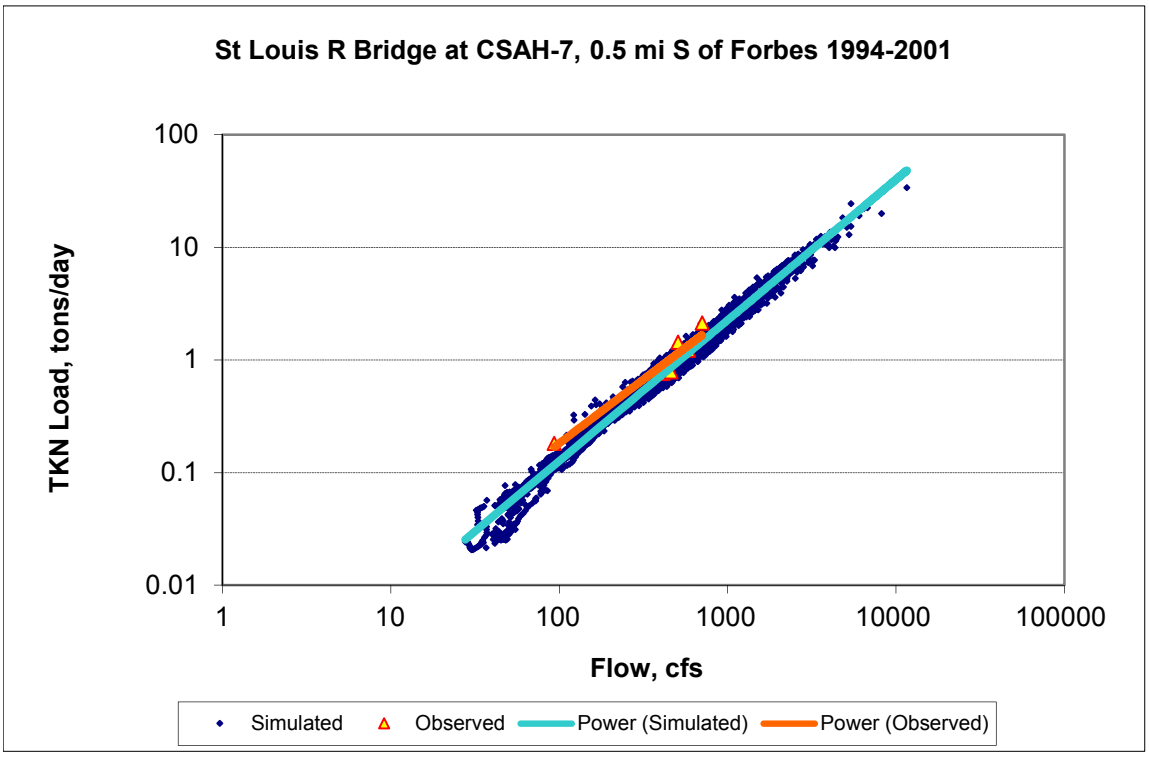

Figure A-50. Power plot of simulated and observed Total Kjeldahl Nitrogen (TKN) load vs flow at St Louis R Bridge at CSAH-7, 0.5 mi S of Forbes (validation period)

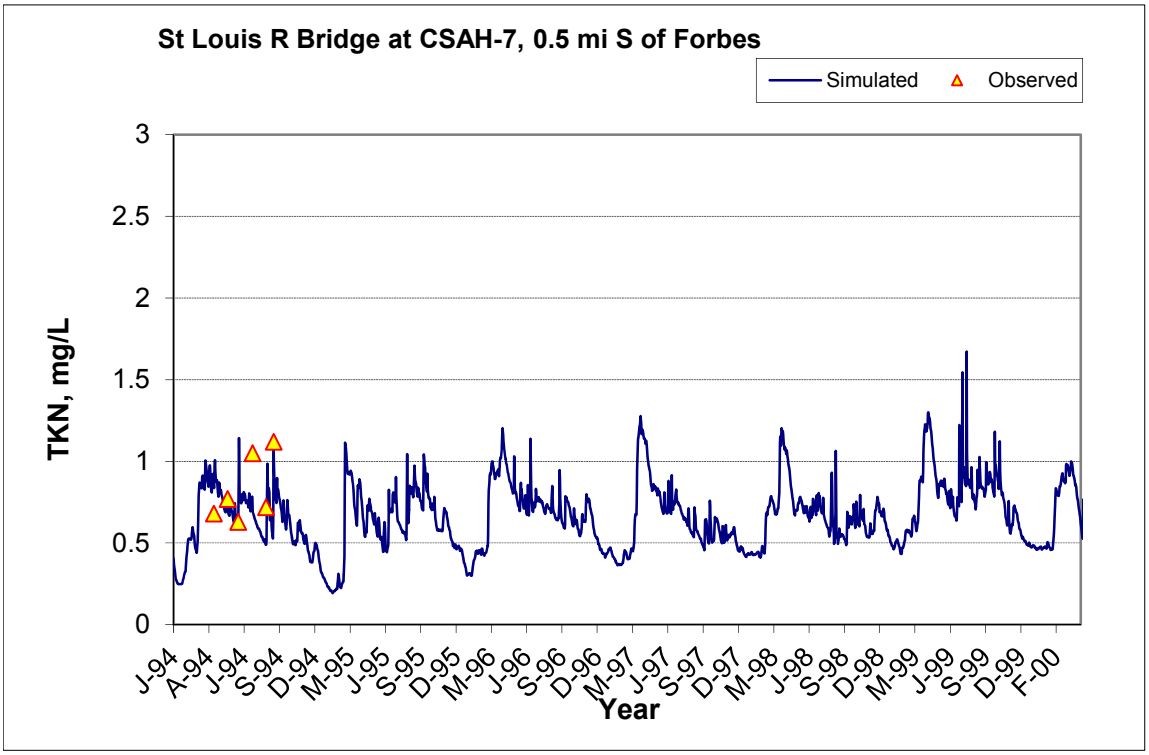

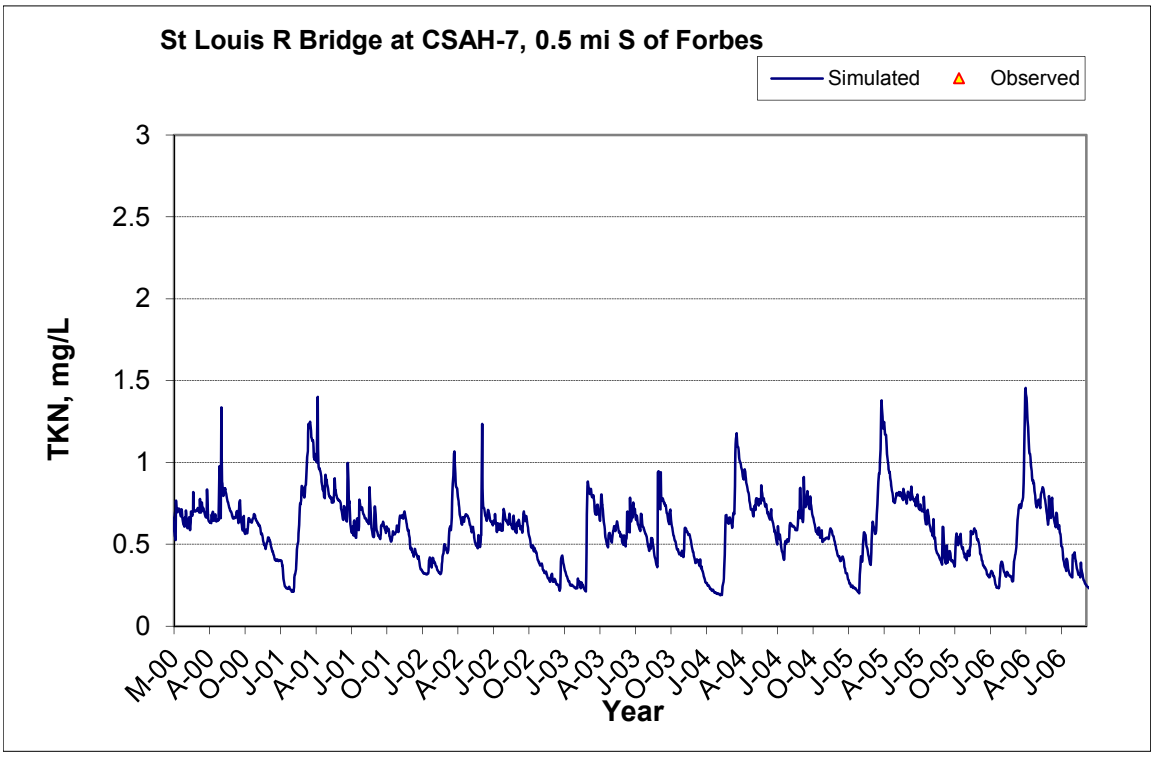

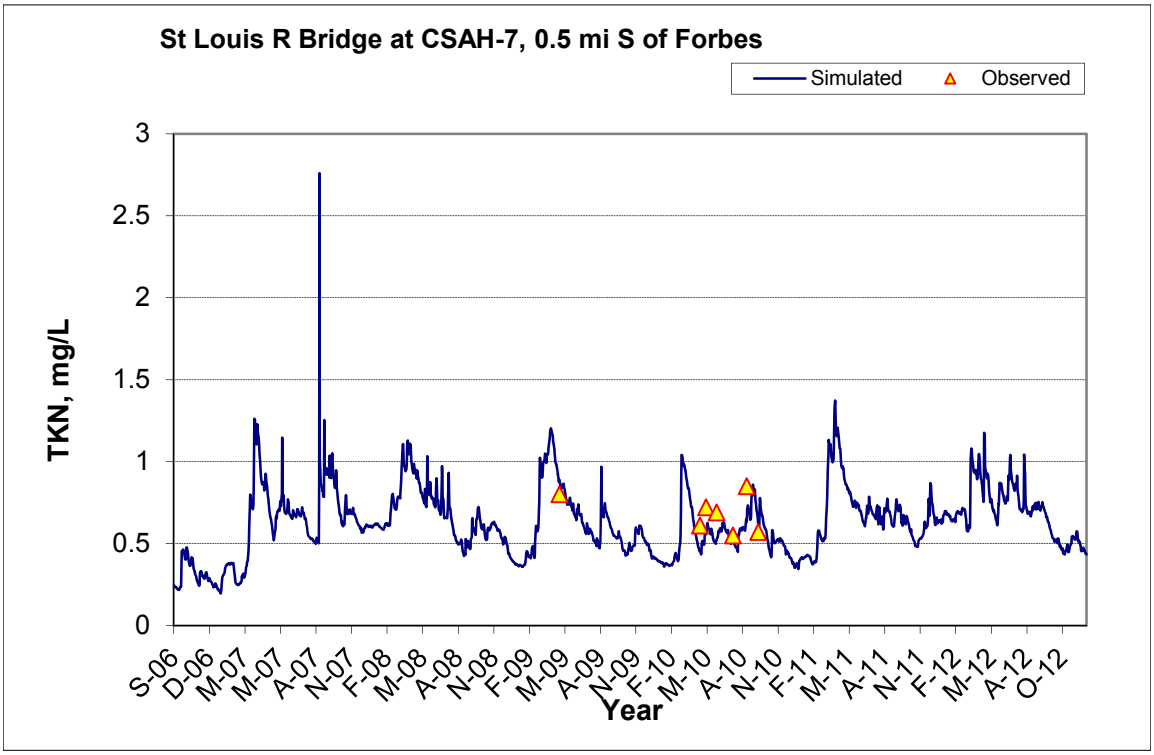

Figure A-51. Time series of observed and simulated Total Kjeldahl Nitrogen (TKN) concentration at St Louis R Bridge at CSAH-7, 0.5 mi S of Forbes

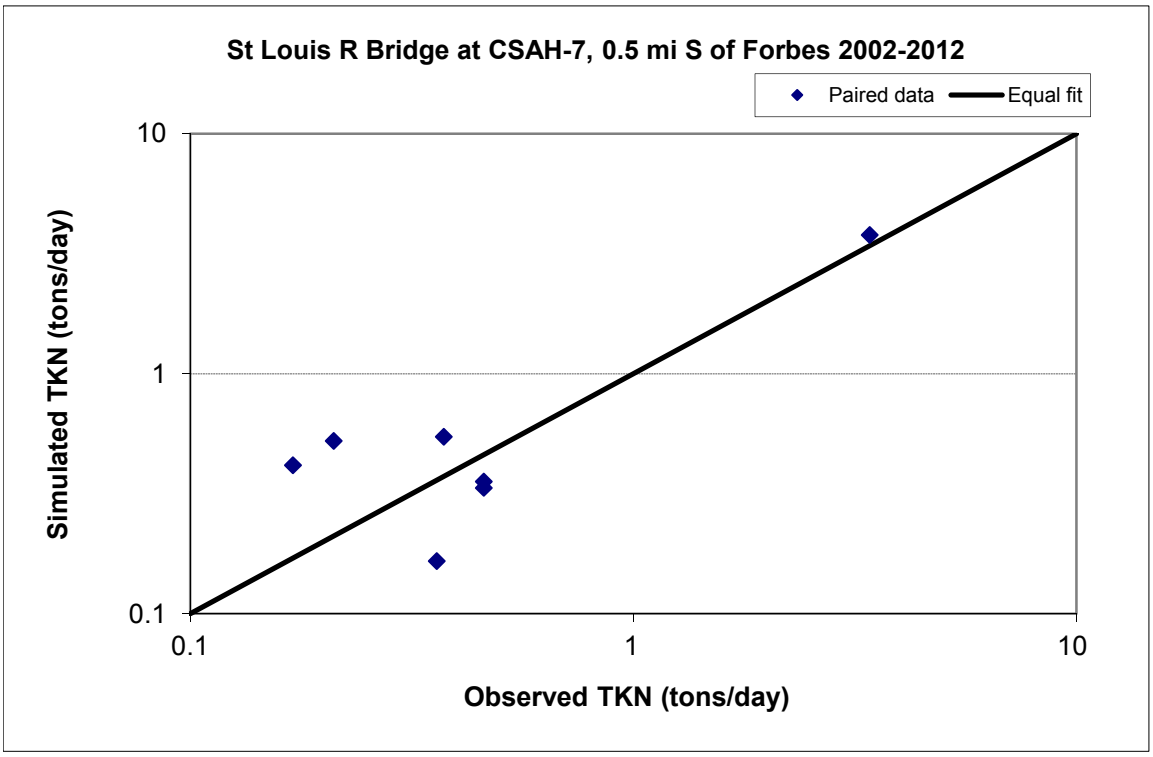

Figure A-52. Paired simulated vs. observed Total Kjeldahl Nitrogen (TKN) load at St Louis R Bridge at CSAH-7, 0.5 mi S of Forbes (calibration period)

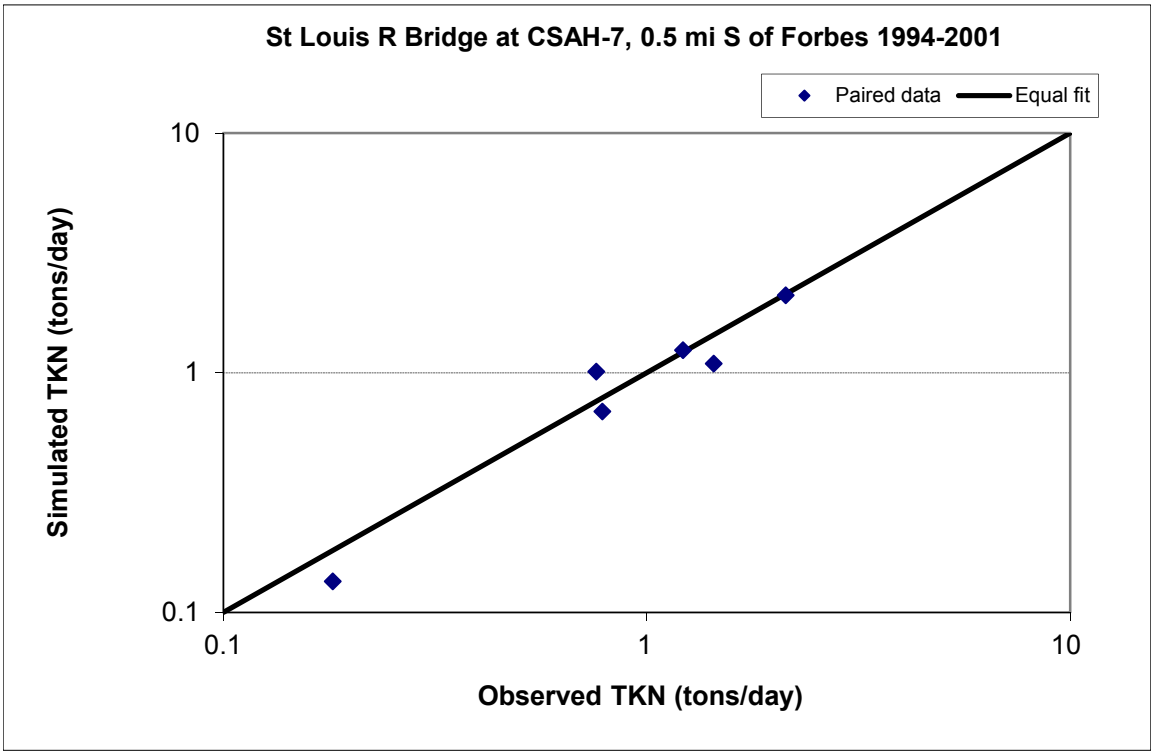

Figure A-53. Paired simulated vs. observed Total Kjeldahl Nitrogen (TKN) load at St Louis R Bridge at CSAH-7, 0.5 mi S of Forbes (validation period)

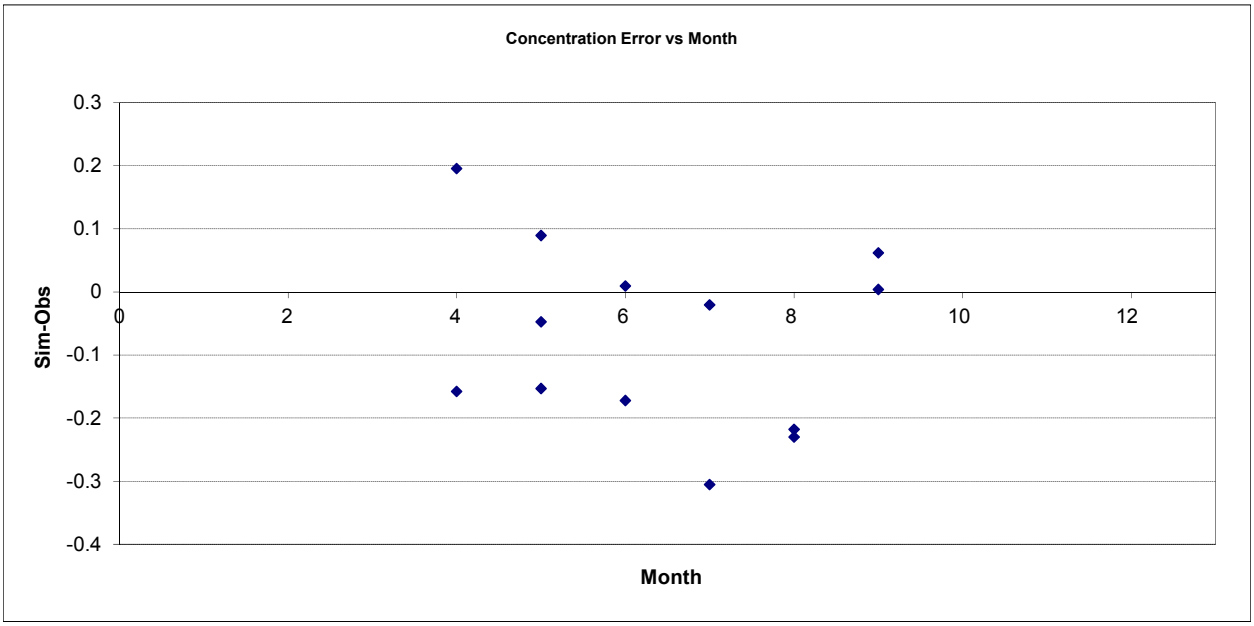

Figure A-54. Residual (Simulated - Observed) vs. Month Total Kjeldahl Nitrogen (TKN) at St Louis R Bridge at CSAH-7, 0.5 mi S of Forbes

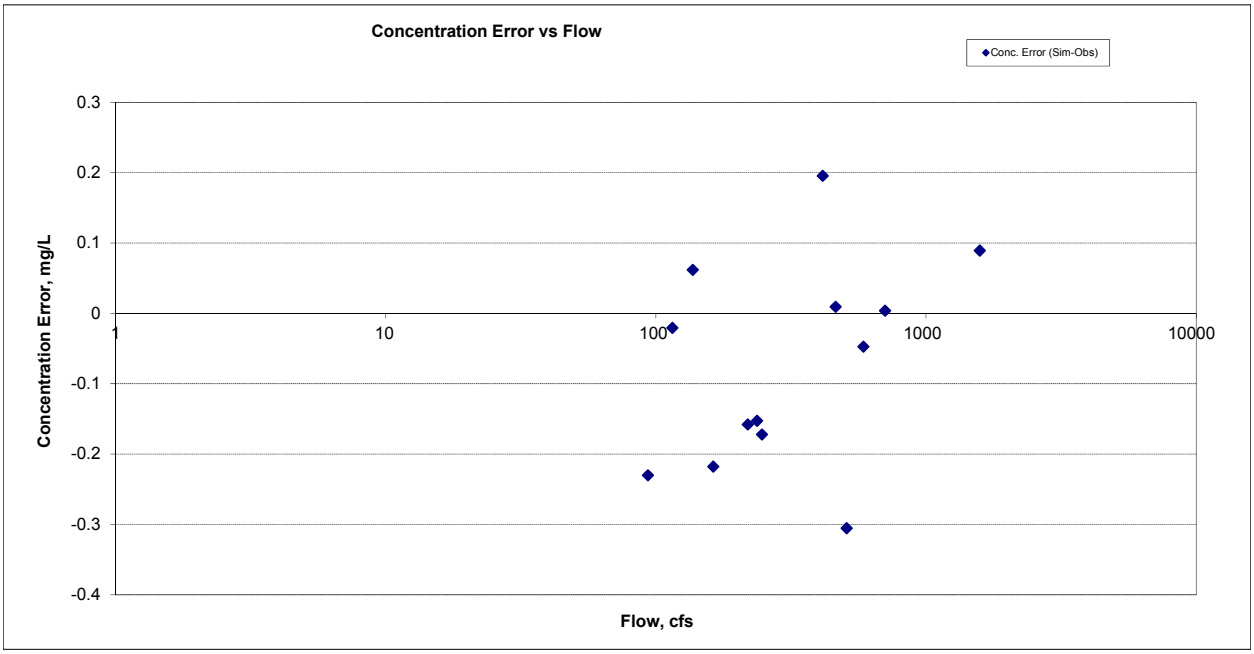

Figure A-55. Residual (Simulated - Observed) vs. Flow Total Kjeldahl Nitrogen (TKN) at St Louis R Bridge at CSAH-7, 0.5 mi S of Forbes

A.3.4 Nitrite+ Nitrate Nitrogen (NOx)

Table A-9. Nitrite+ Nitrate Nitrogen (NOx) statistics

Period	1994-2001	2002-2012
Count	35	48
Concentration Average Error	-33.89%	43.87%
Concentration Median Error	-25.84%	54.81%
Load Average Error	-40.97%	5.09%
Load Median Error	-11.20%	31.97%
Paired t conc	0.11	0.02
Paired t load	0.16	0.74

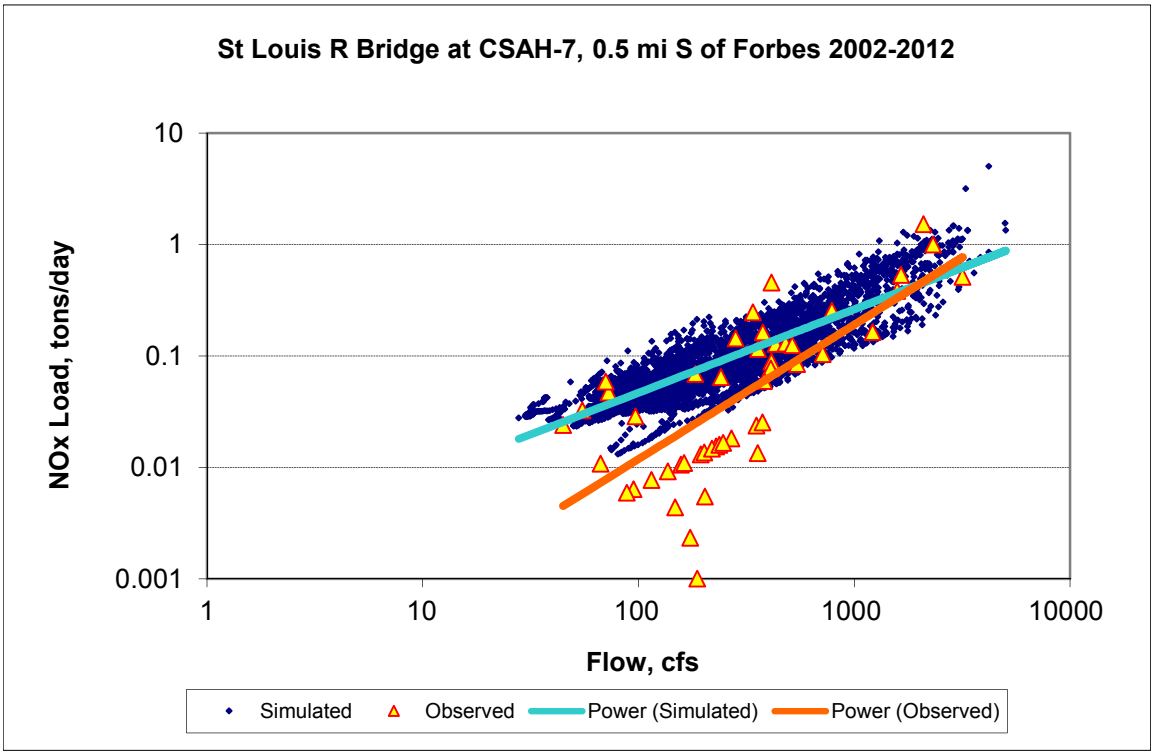

Figure A-56. Power plot of simulated and observed Nitrite+ Nitrate Nitrogen (NOx) load vs flow at St Louis R Bridge at CSAH-7, 0.5 mi S of Forbes (calibration period)

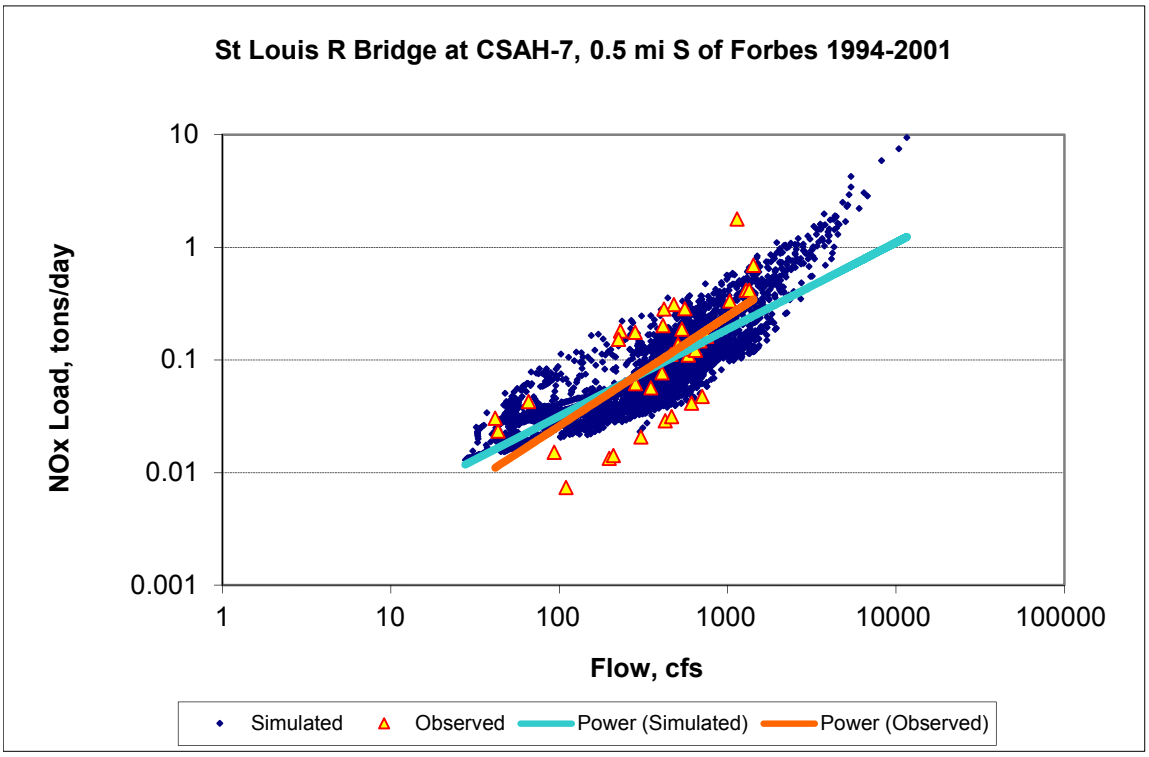

Figure A-57. Power plot of simulated and observed Nitrite+ Nitrate Nitrogen (NOx) load vs flow at St Louis R Bridge at CSAH-7, 0.5 mi S of Forbes (validation period)

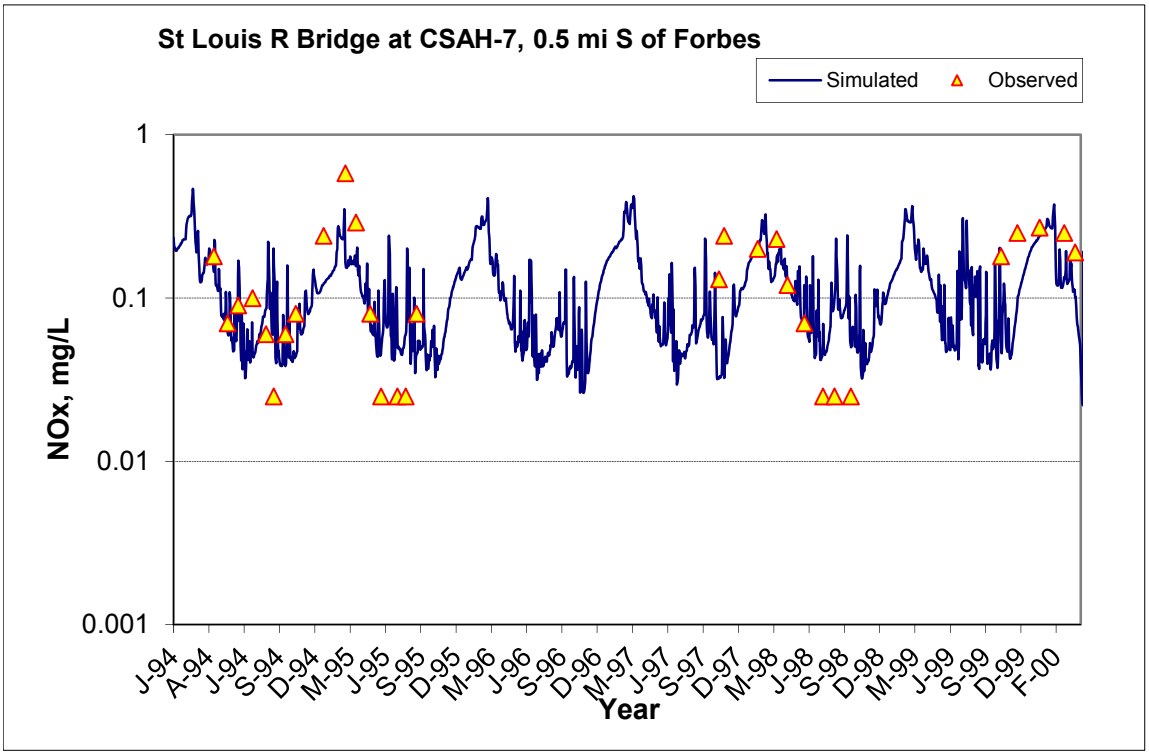

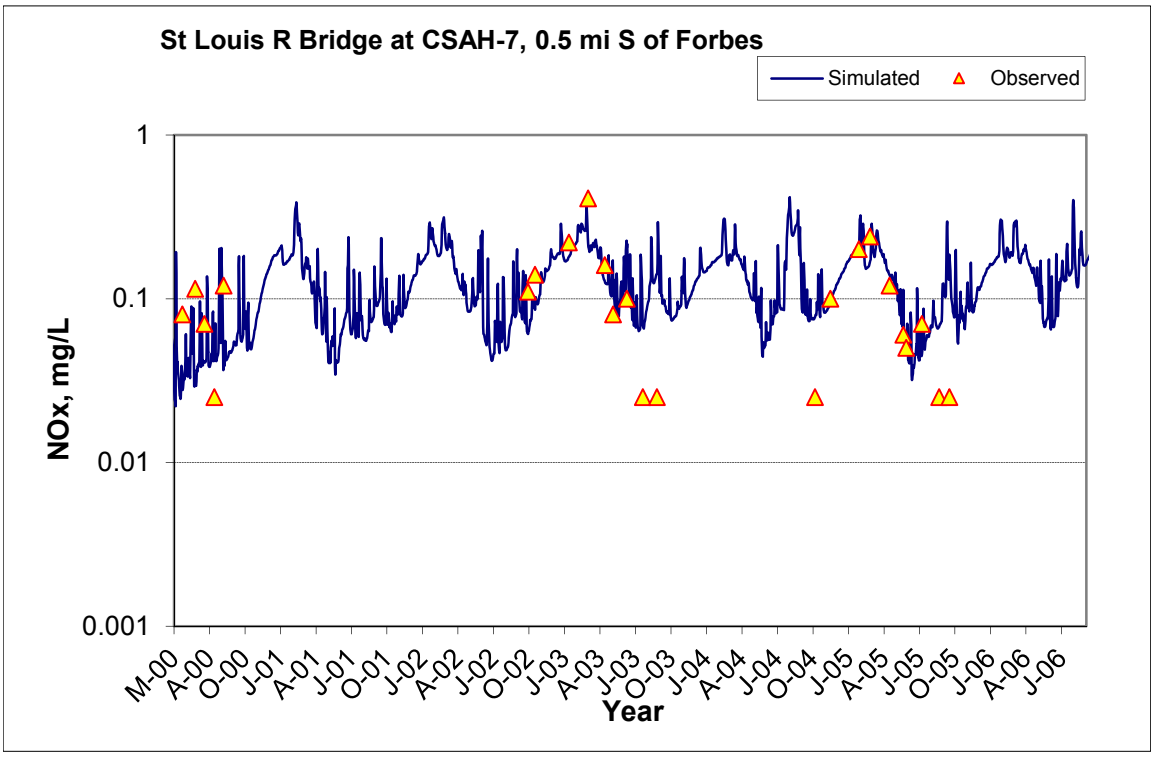

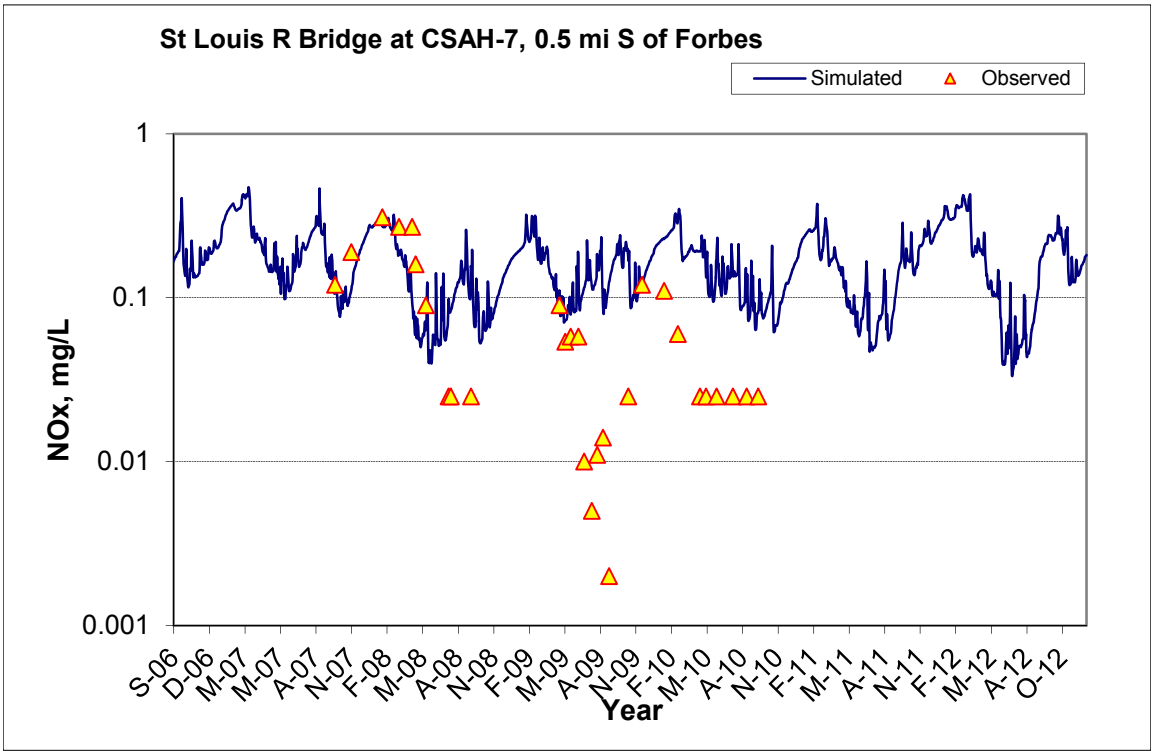

Figure A-58. Time series of observed and simulated Nitrite+ Nitrate Nitrogen (NOx) concentration at St Louis R Bridge at CSAH-7, 0.5 mi S of Forbes

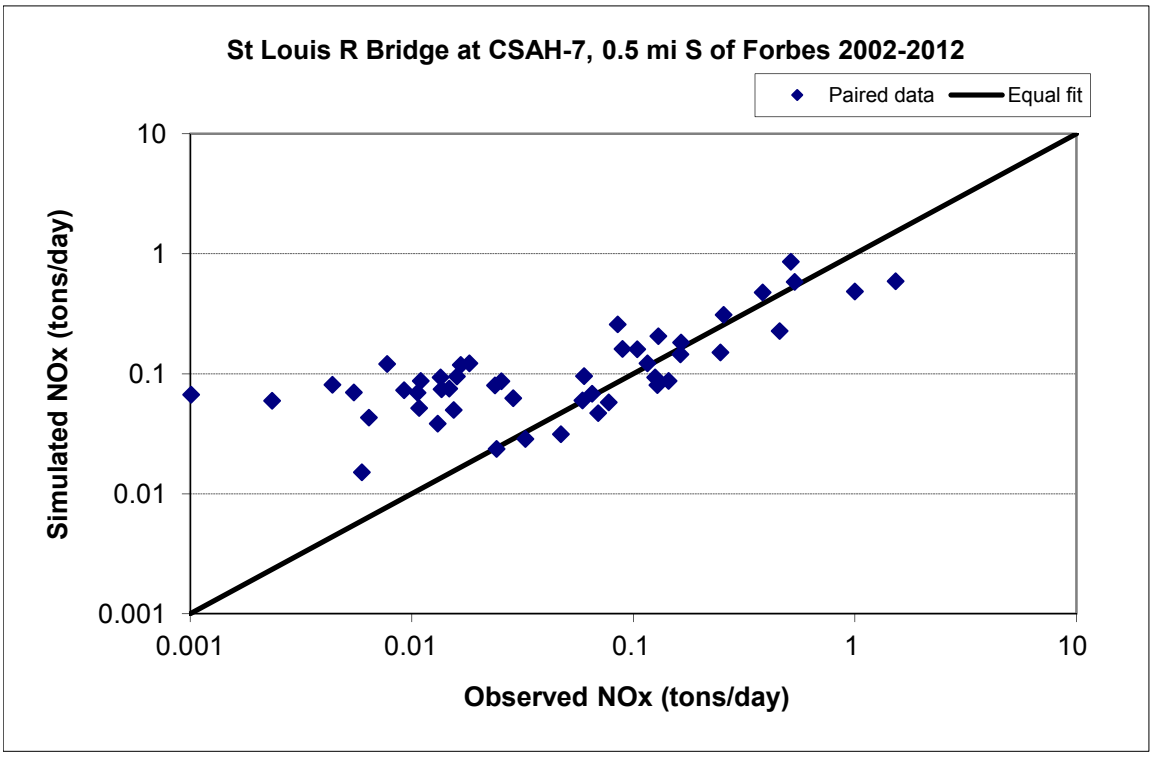

Figure A-59. Paired simulated vs. observed Nitrite+ Nitrate Nitrogen (NOx) load at St Louis R Bridge at CSAH-7, 0.5 mi S of Forbes (calibration period)

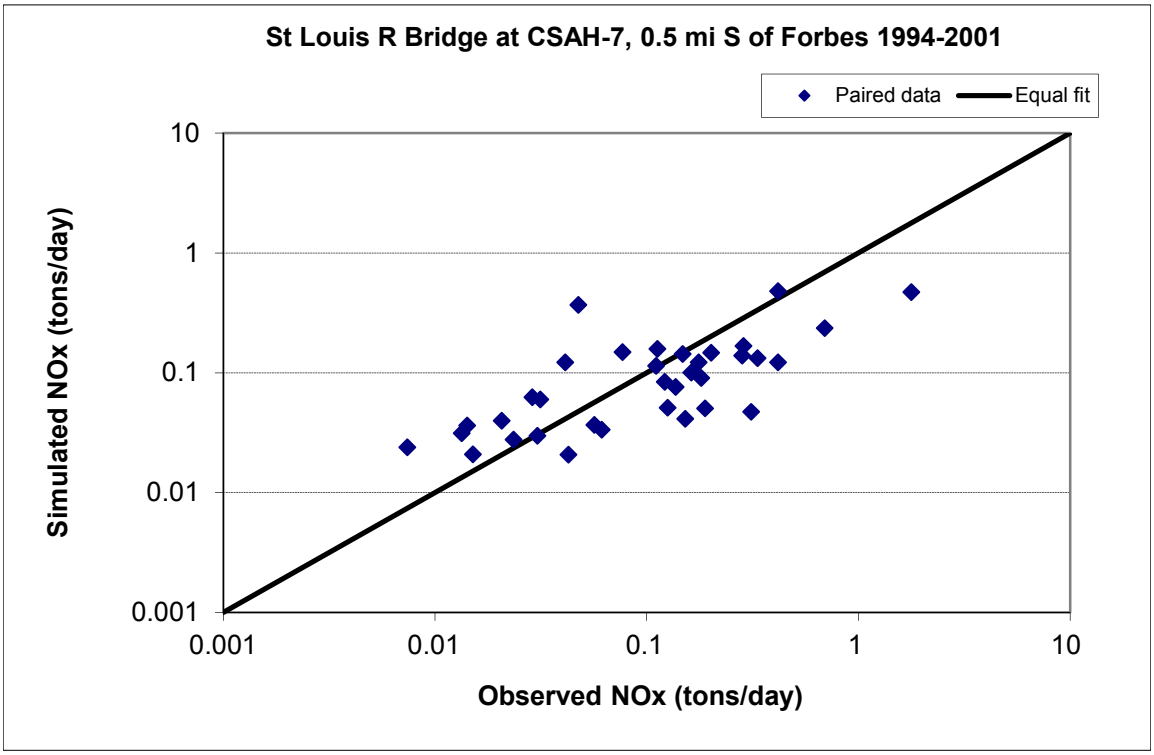

Figure A-60. Paired simulated vs. observed Nitrite+ Nitrate Nitrogen (NOx) load at St Louis R Bridge at CSAH-7, 0.5 mi S of Forbes (validation period)

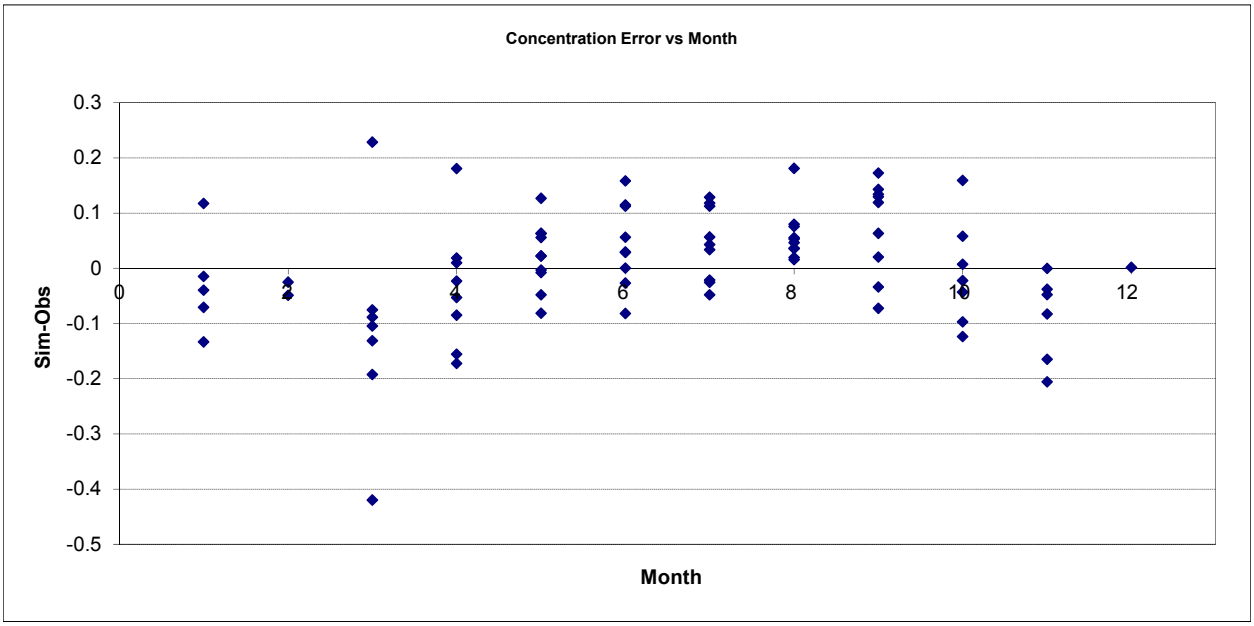

Figure A-61. Residual (Simulated - Observed) vs. Month Nitrite+ Nitrate Nitrogen (NOx) at St Louis R Bridge at CSAH-7, 0.5 mi S of Forbes

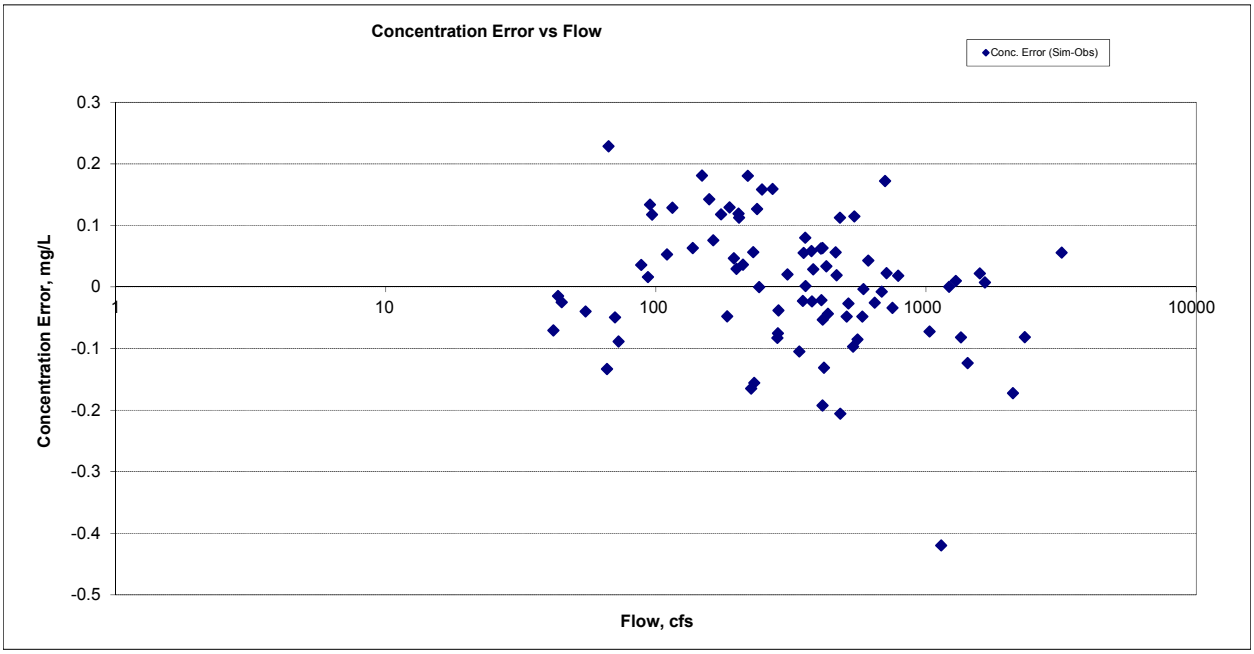

Figure A-62. Residual (Simulated - Observed) vs. Flow Nitrite+ Nitrate Nitrogen (NOx) at St Louis R Bridge at CSAH-7, 0.5 mi S of Forbes

A.3.5 Total Nitrogen (TN)

Table A-10. Total Nitrogen (TN) statistics

Period	1994-2001	2002-2012
Count	6	7
Concentration Average Error	-4.73%	0.63%
Concentration Median Error	0.78%	-0.37%
Load Average Error	-0.24%	20.07%
Load Median Error	-0.48%	27.95%
Paired t conc	0.90	0.99
Paired t load	0.77	0.50

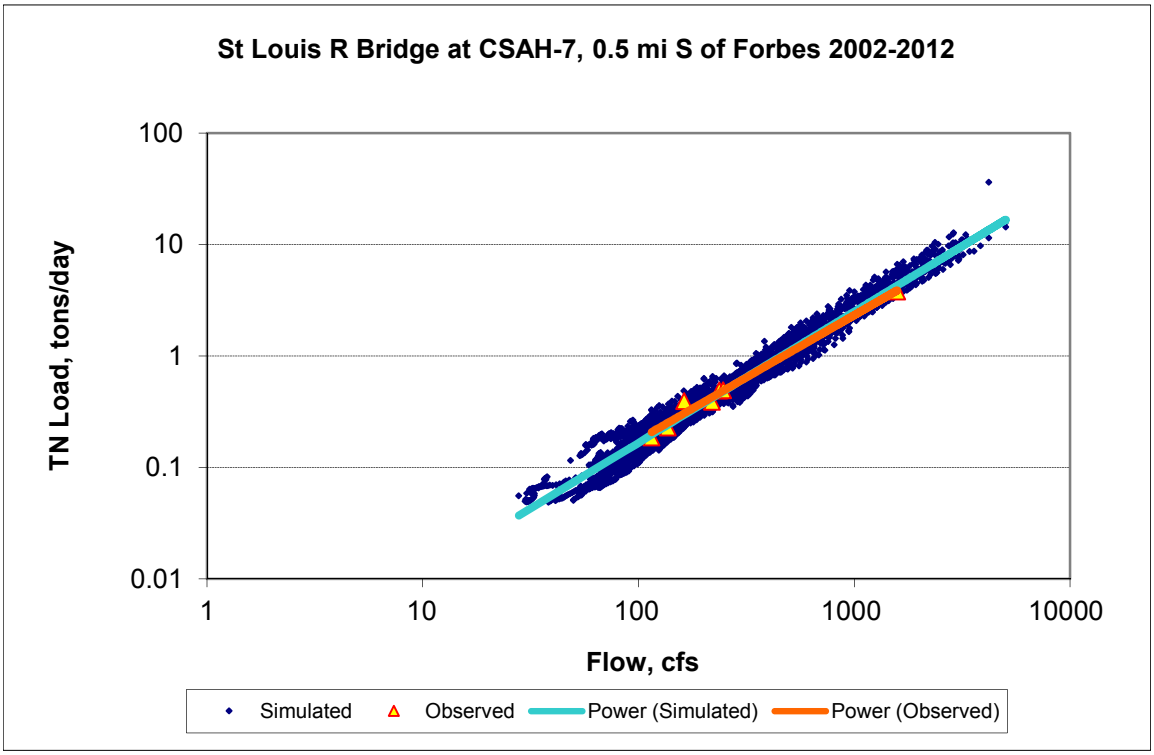

Figure A-63. Power plot of simulated and observed Total Nitrogen (TN) load vs flow at St Louis R Bridge at CSAH-7, 0.5 mi S of Forbes (calibration period)

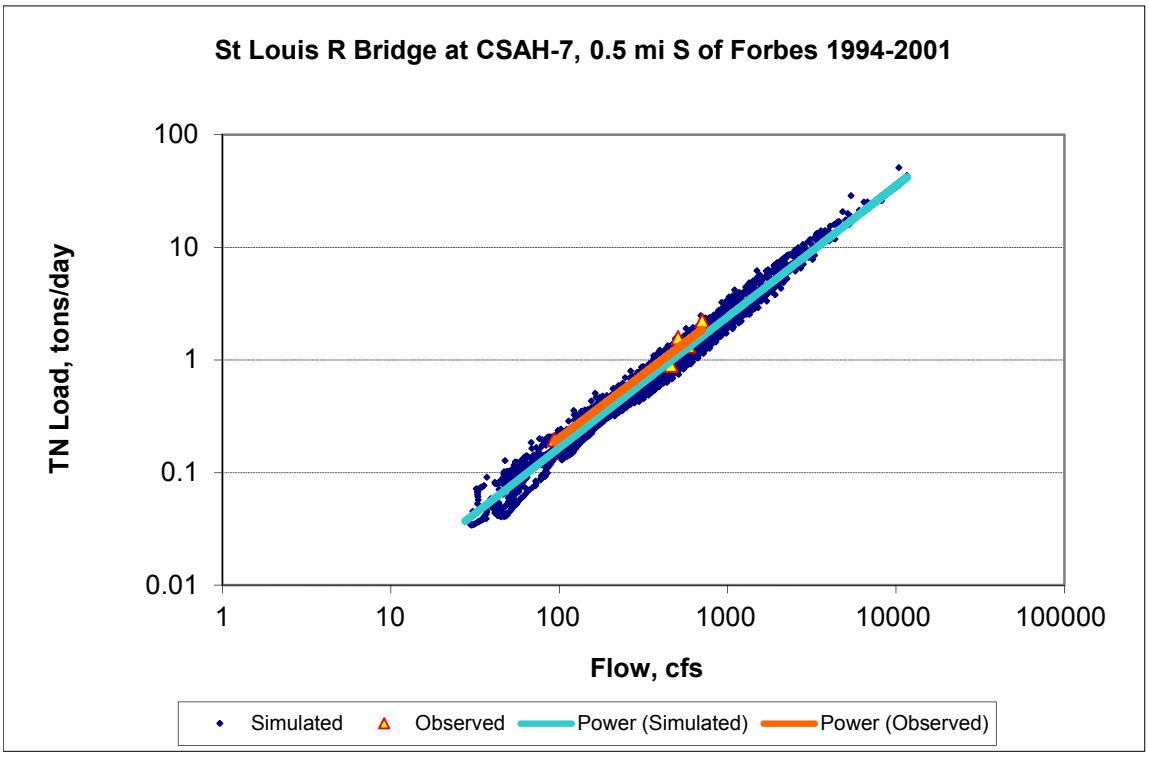

Figure A-64. Power plot of simulated and observed Total Nitrogen (TN) load vs flow at St Louis R Bridge at CSAH-7, 0.5 mi S of Forbes (validation period)

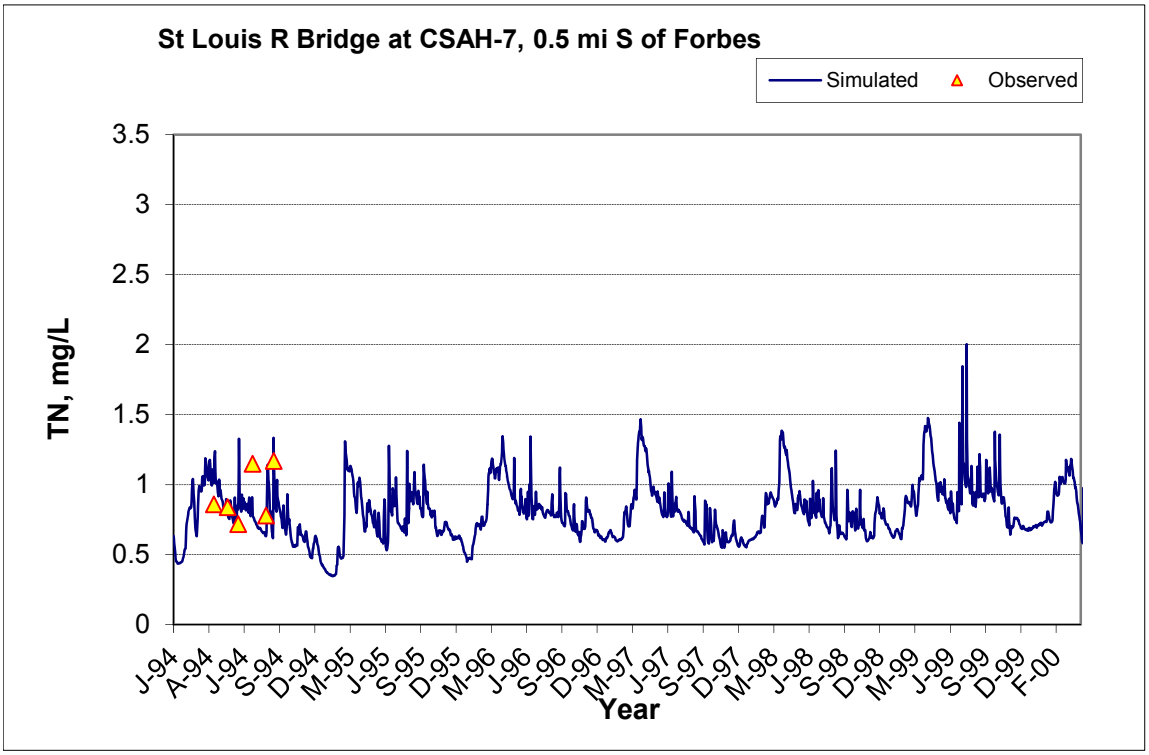

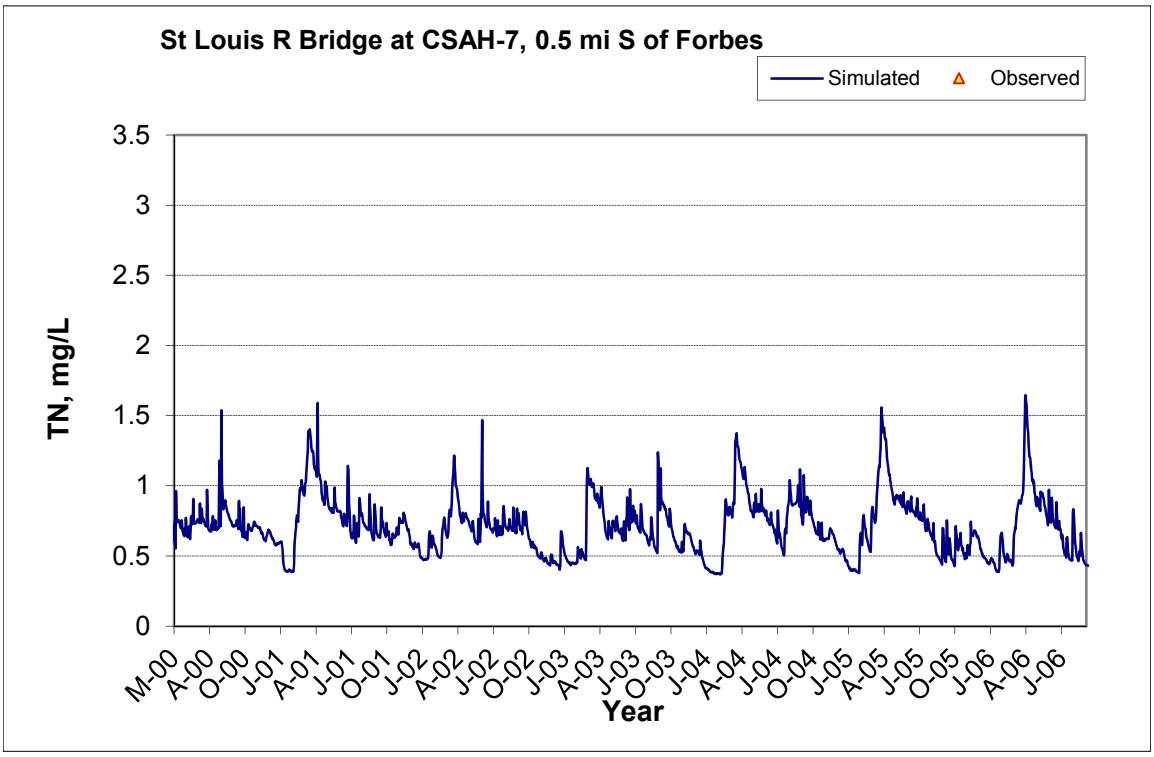

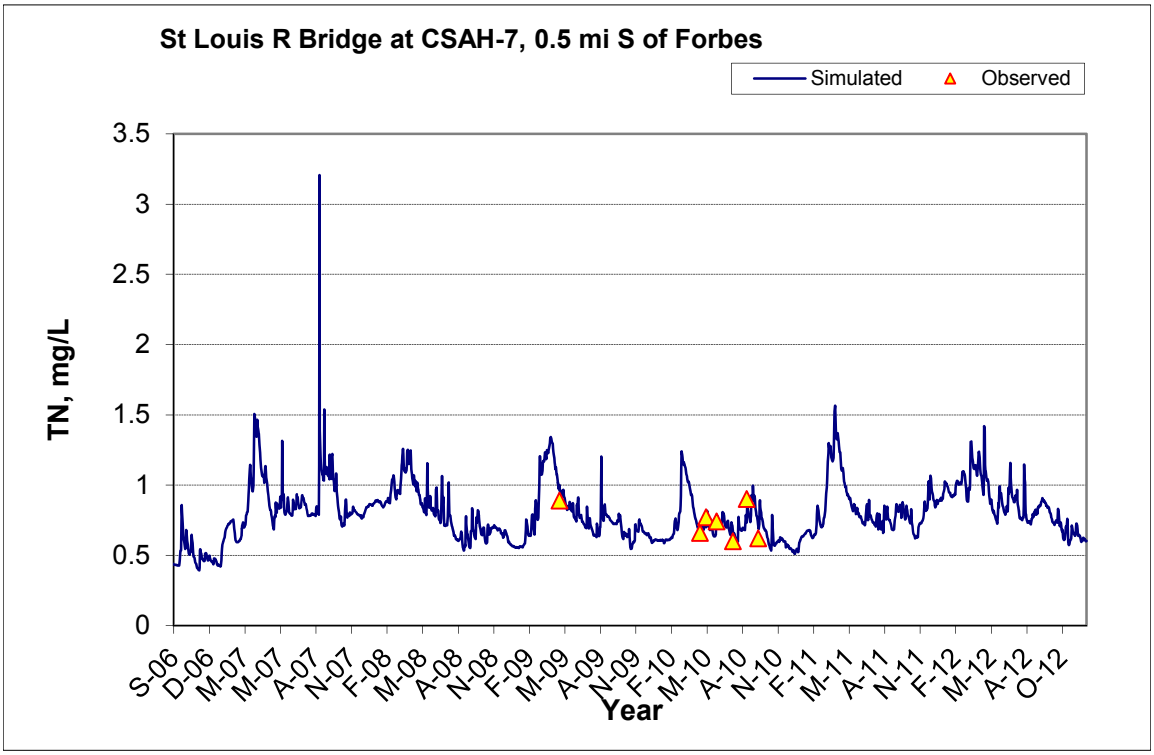

Figure A-65. Time series of observed and simulated Total Nitrogen (TN) concentration at St Louis R Bridge at CSAH-7, 0.5 mi S of Forbes

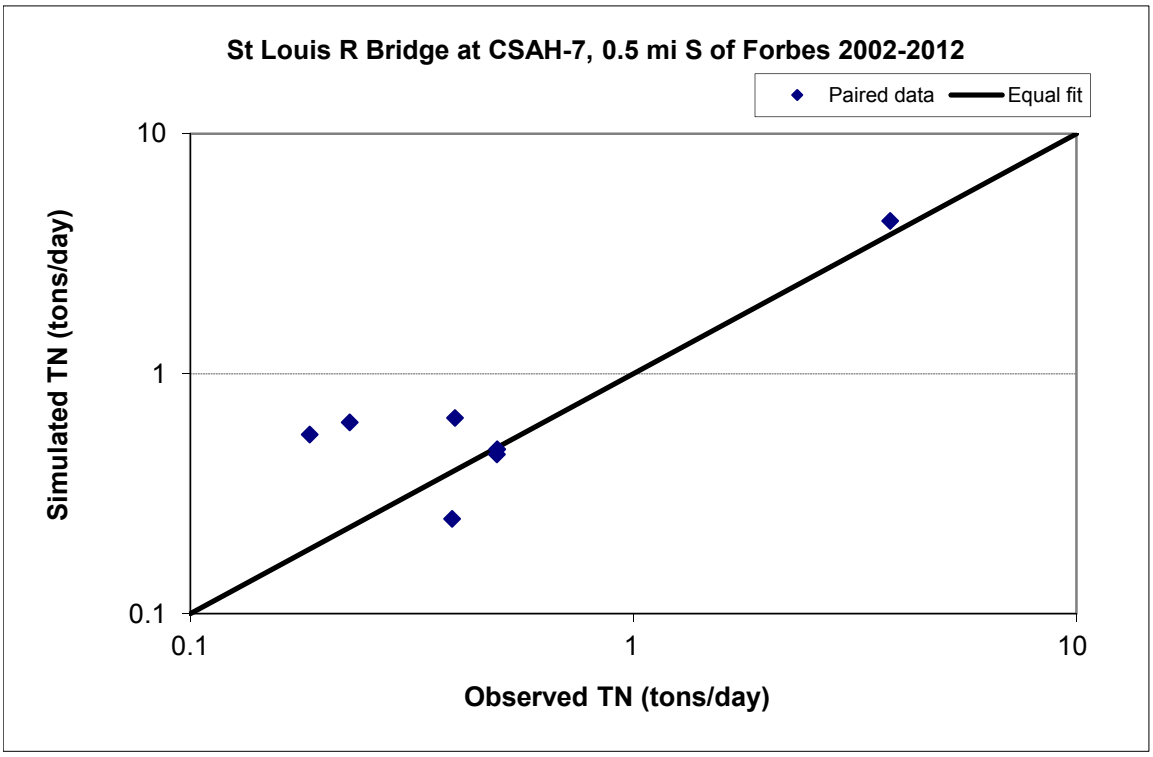

Figure A-66. Paired simulated vs. observed Total Nitrogen (TN) load at St Louis R Bridge at CSAH-7, 0.5 mi S of Forbes (calibration period)

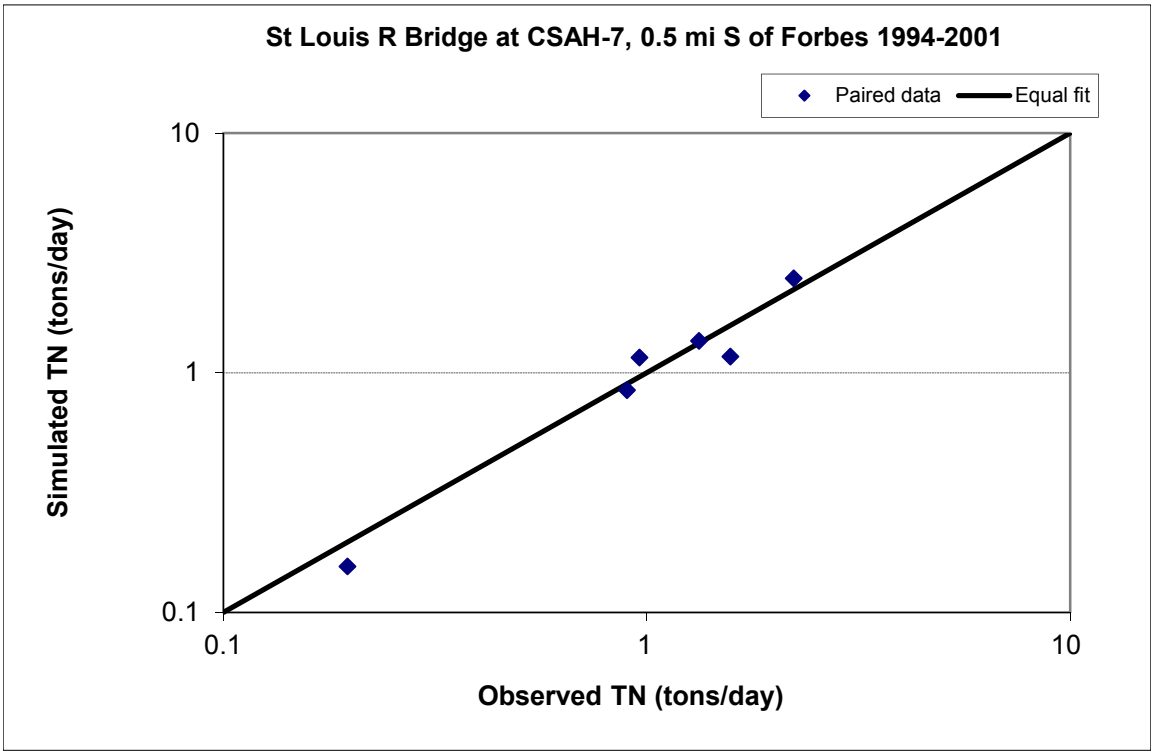

Figure A-67. Paired simulated vs. observed Total Nitrogen (TN) load at St Louis R Bridge at CSAH-7, 0.5 mi S of Forbes (validation period)

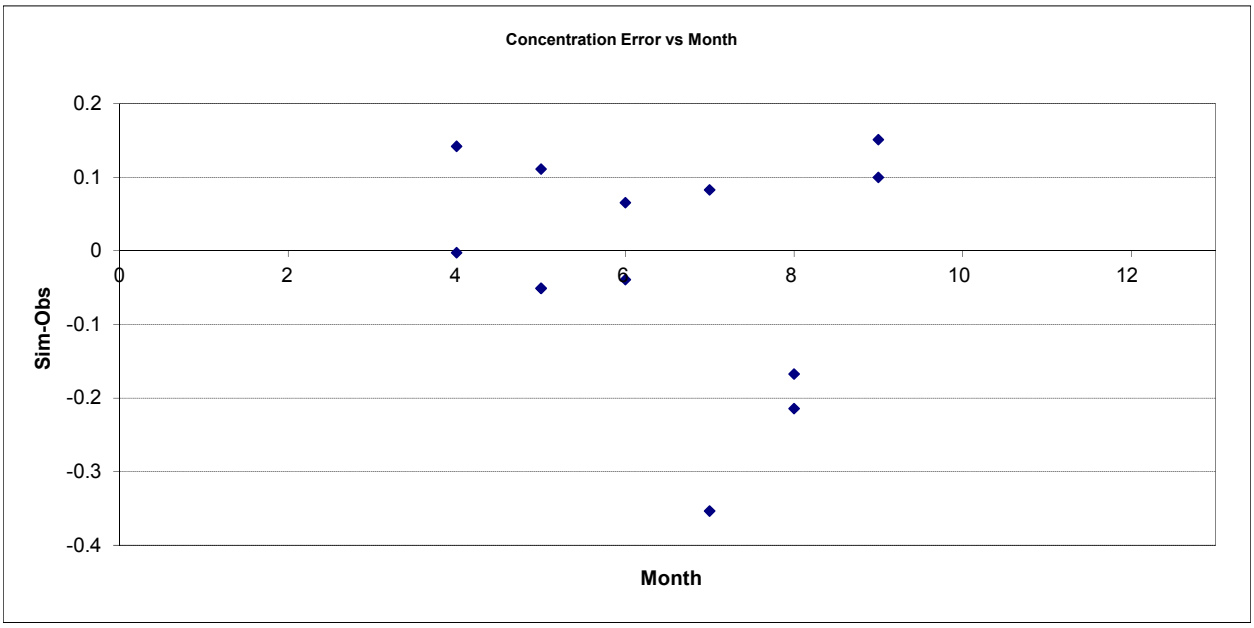

Figure A-68. Residual (Simulated - Observed) vs. Month Total Nitrogen (TN) at St Louis R Bridge at CSAH-7, 0.5 mi S of Forbes

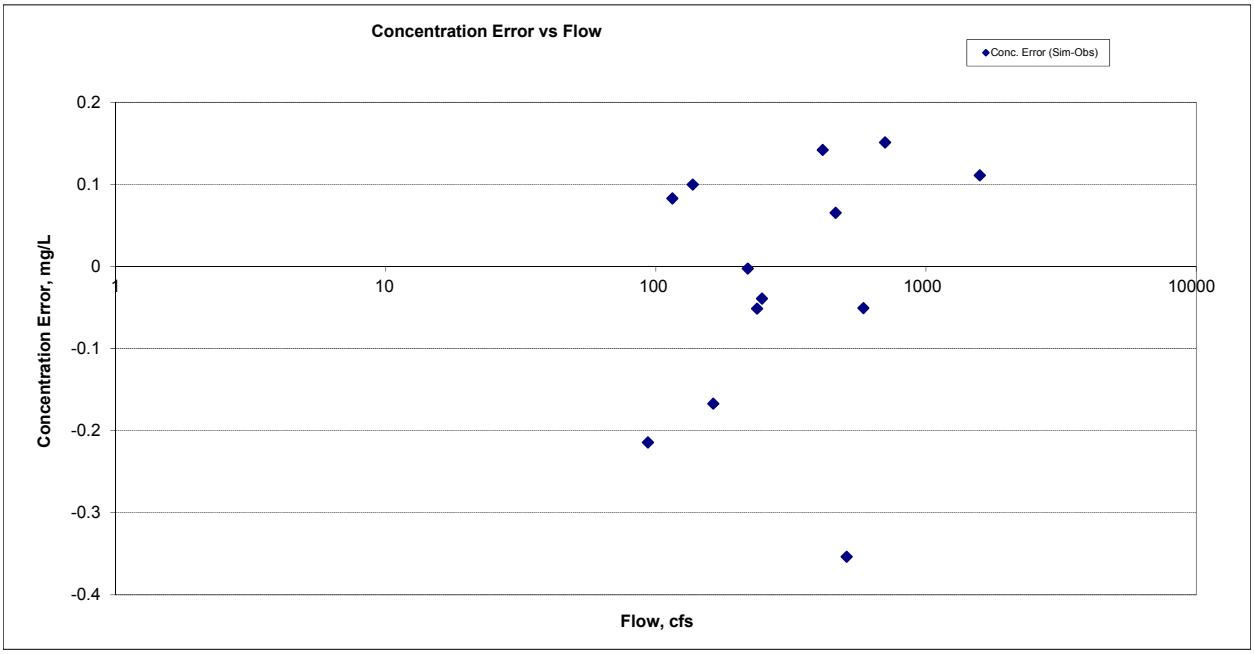

Figure A-69. Residual (Simulated - Observed) vs. Flow Total Nitrogen (TN) at St Louis R Bridge at CSAH-7, 0.5 mi S of Forbes

A.3.6 Soluble Reactive Phosphorus (SRP)

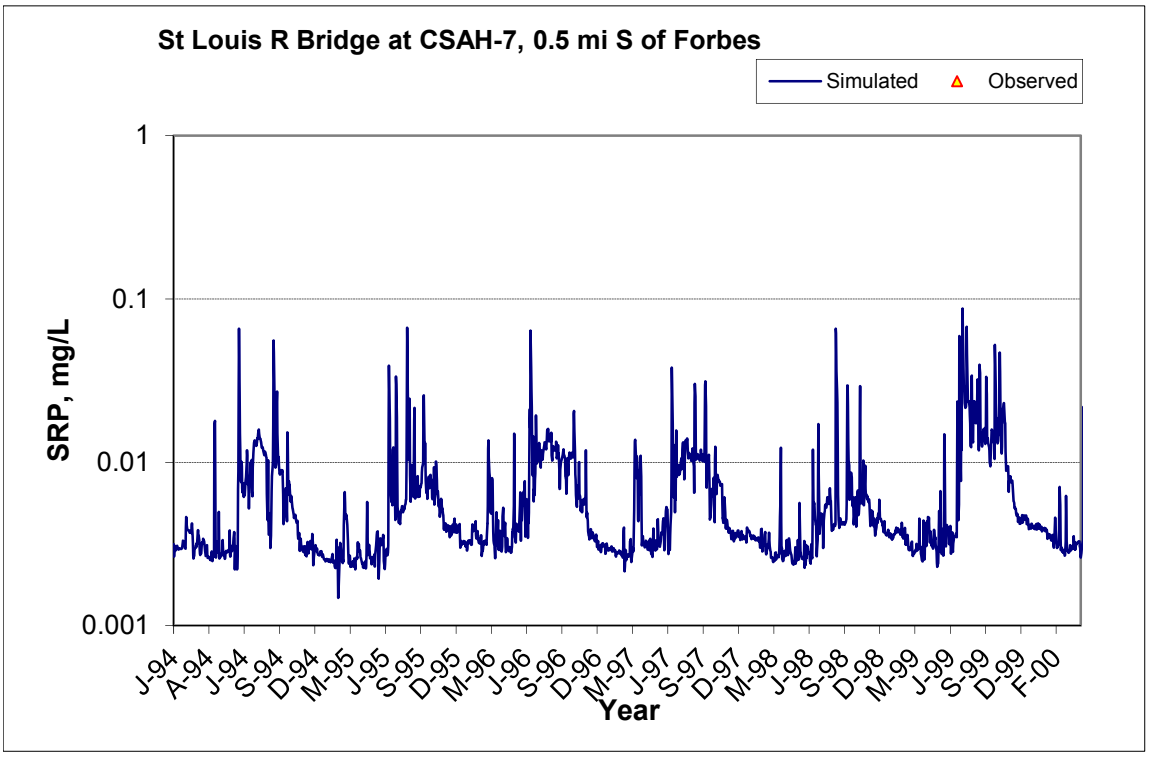

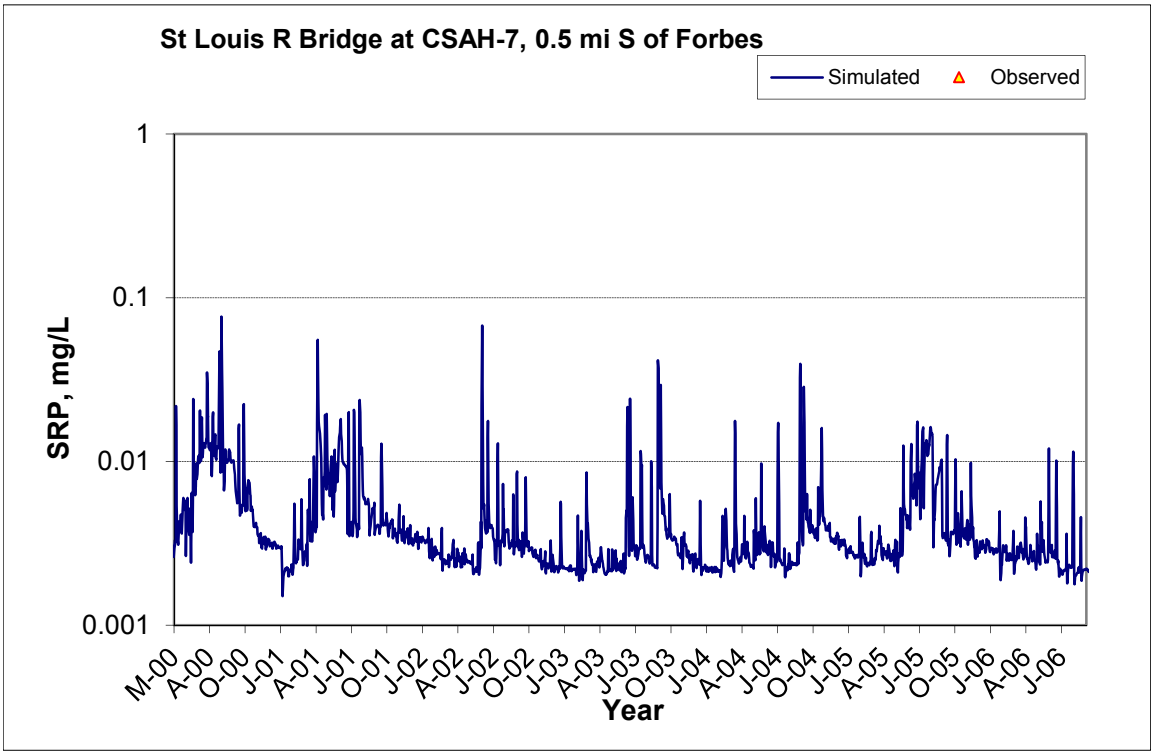

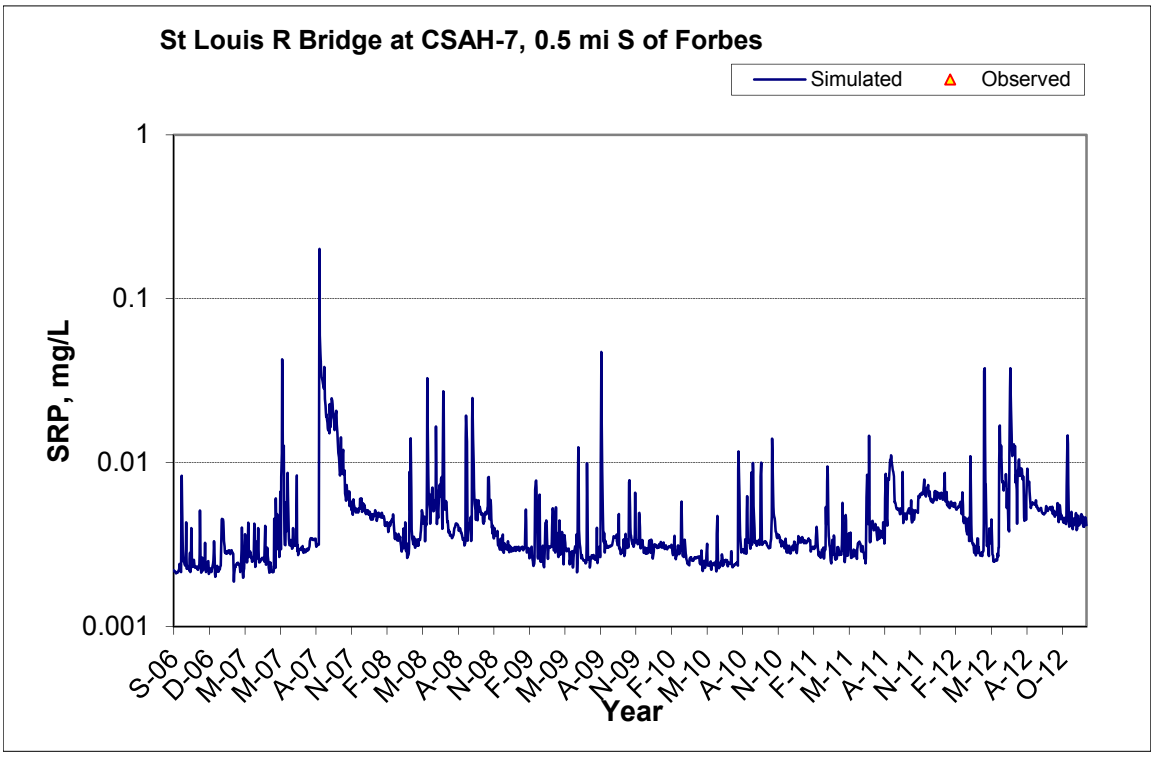

Figure A-70. Time series of observed and simulated Soluble Reactive Phosphorus (SRP) concentration at St Louis R Bridge at CSAH-7, 0.5 mi S of Forbes

A.3.7 Organic Phosphorus (OrgP)

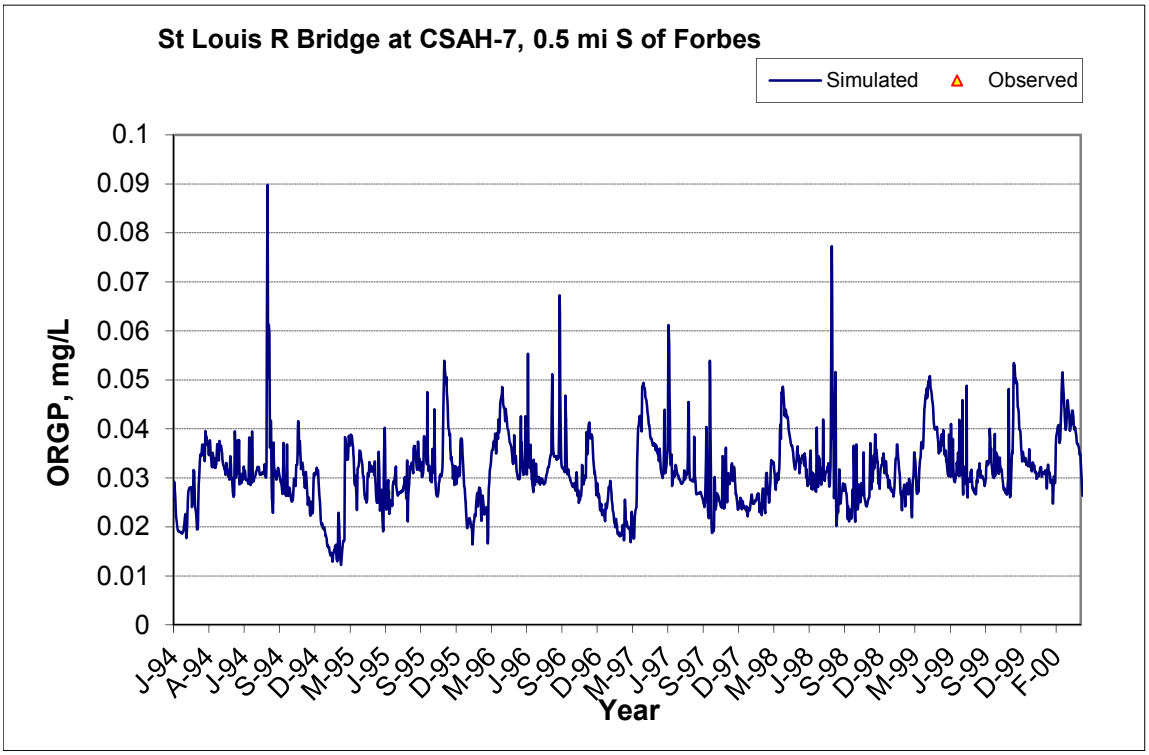

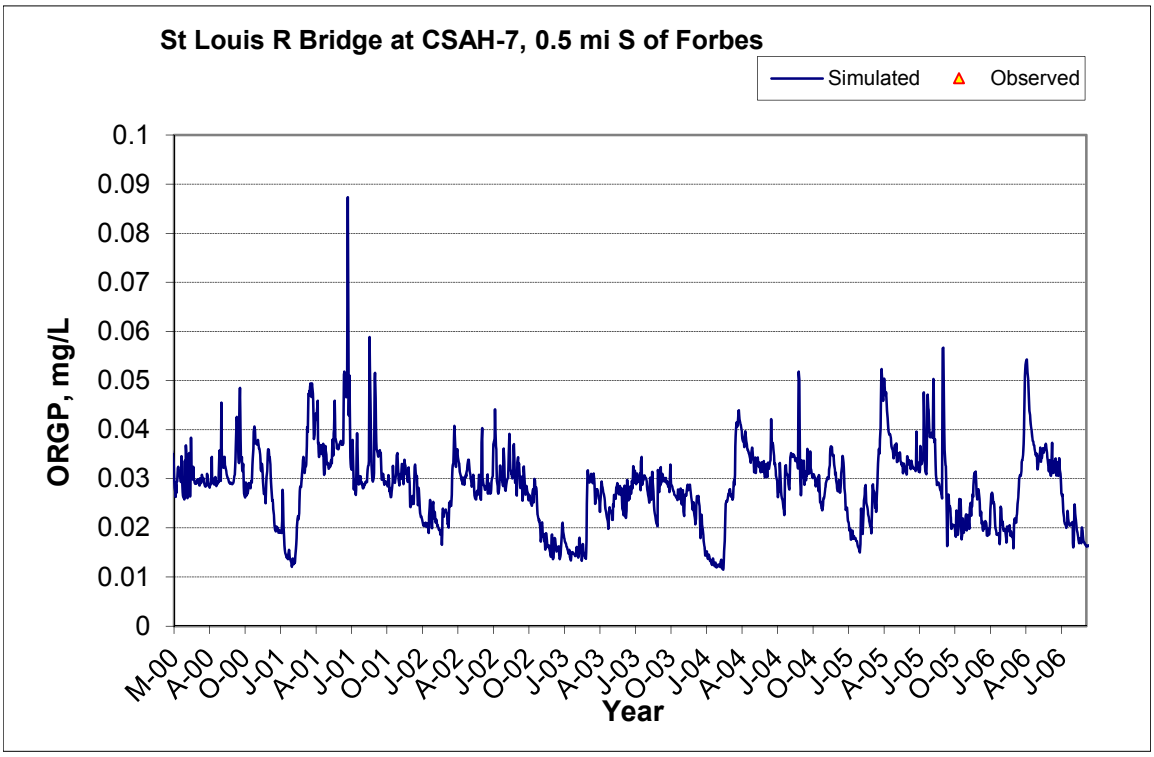

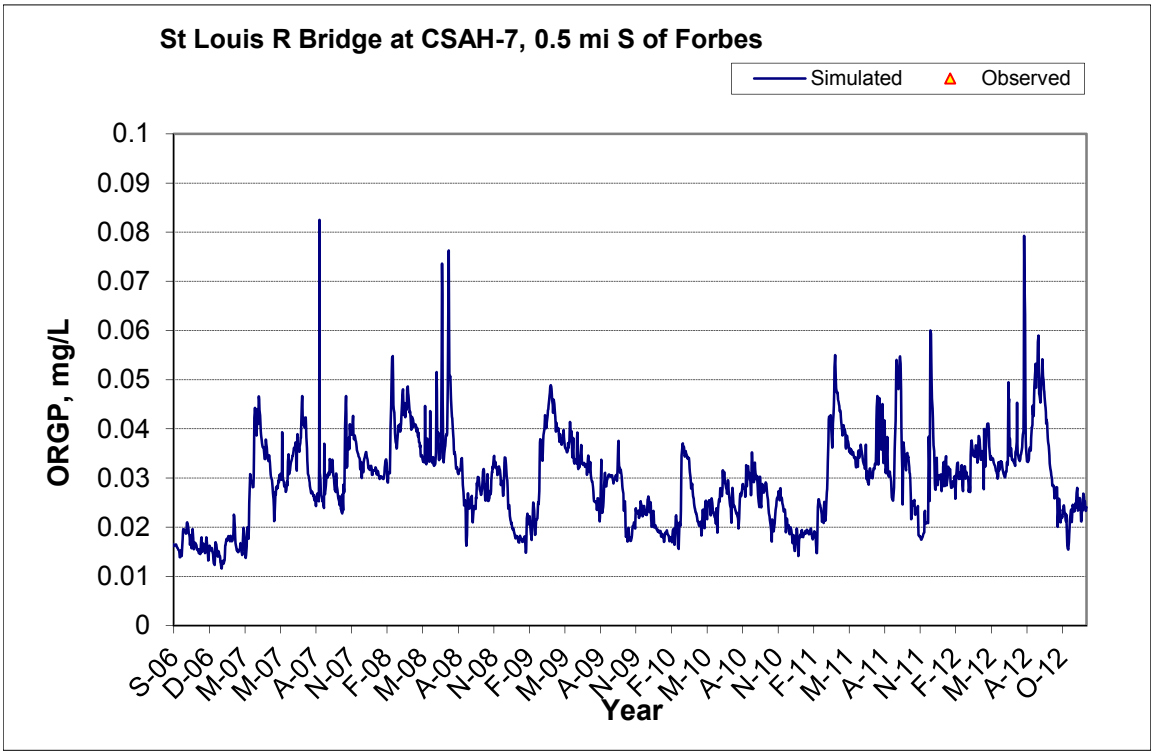

Figure A-71. Time series of observed and simulated Organic Phosphorus (OrgP) concentration at St Louis R Bridge at CSAH-7, 0.5 mi S of Forbes

A.3.8 Total Phosphorus (TP)

Table A-11. Total Phosphorus (TP) statistics

Period	1994-2001	2002-2012
Count	10	50
Concentration Average Error	6.03%	20.00%
Concentration Median Error	6.42%	20.47%
Load Average Error	-0.77%	4.92%
Load Median Error	7.11%	12.32%
Paired t conc	0.77	0.50
Paired t load	0.73	0.73

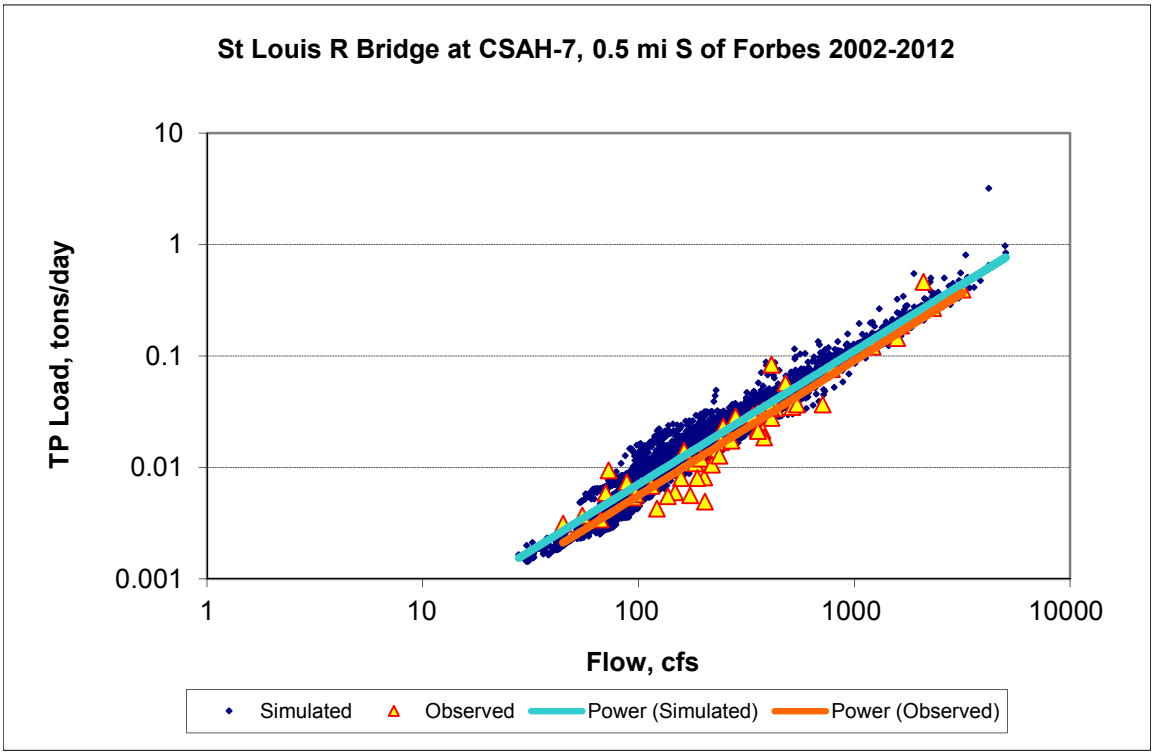

Figure A-72. Power plot of simulated and observed Total Phosphorus (TP) load vs flow at St Louis R Bridge at CSAH-7, 0.5 mi S of Forbes (calibration period)

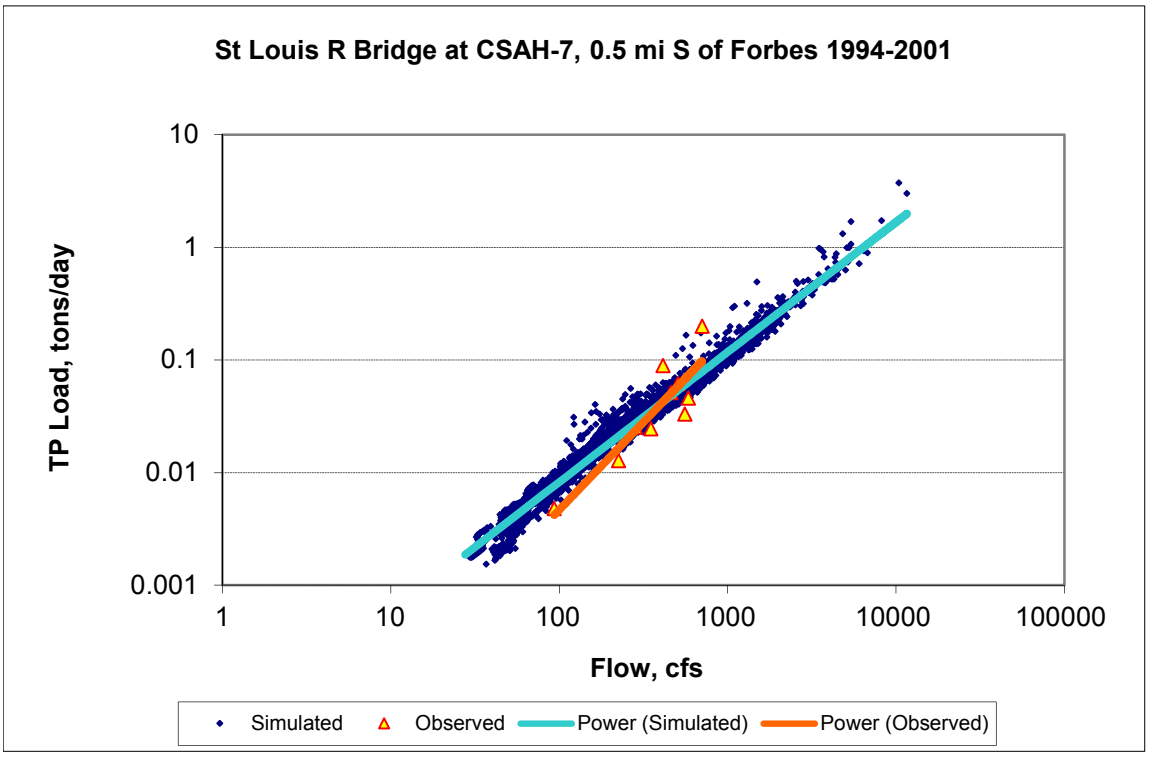

Figure A-73. Power plot of simulated and observed Total Phosphorus (TP) load vs flow at St Louis R Bridge at CSAH-7, 0.5 mi S of Forbes (validation period)

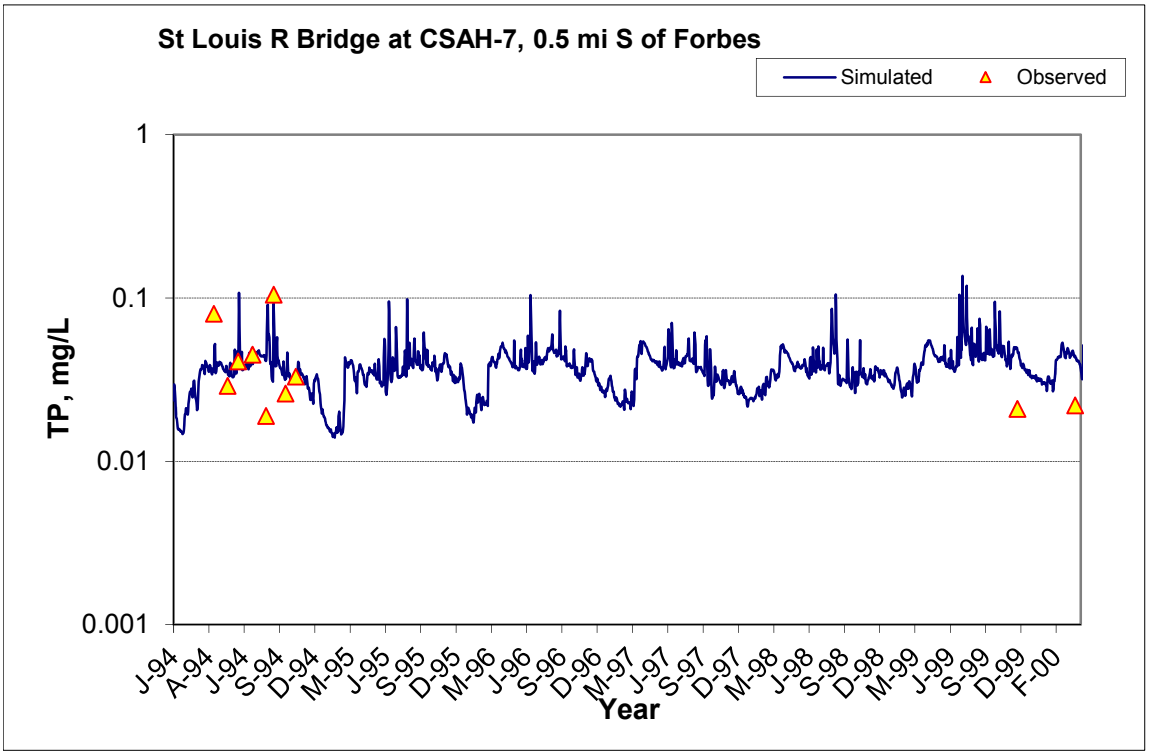

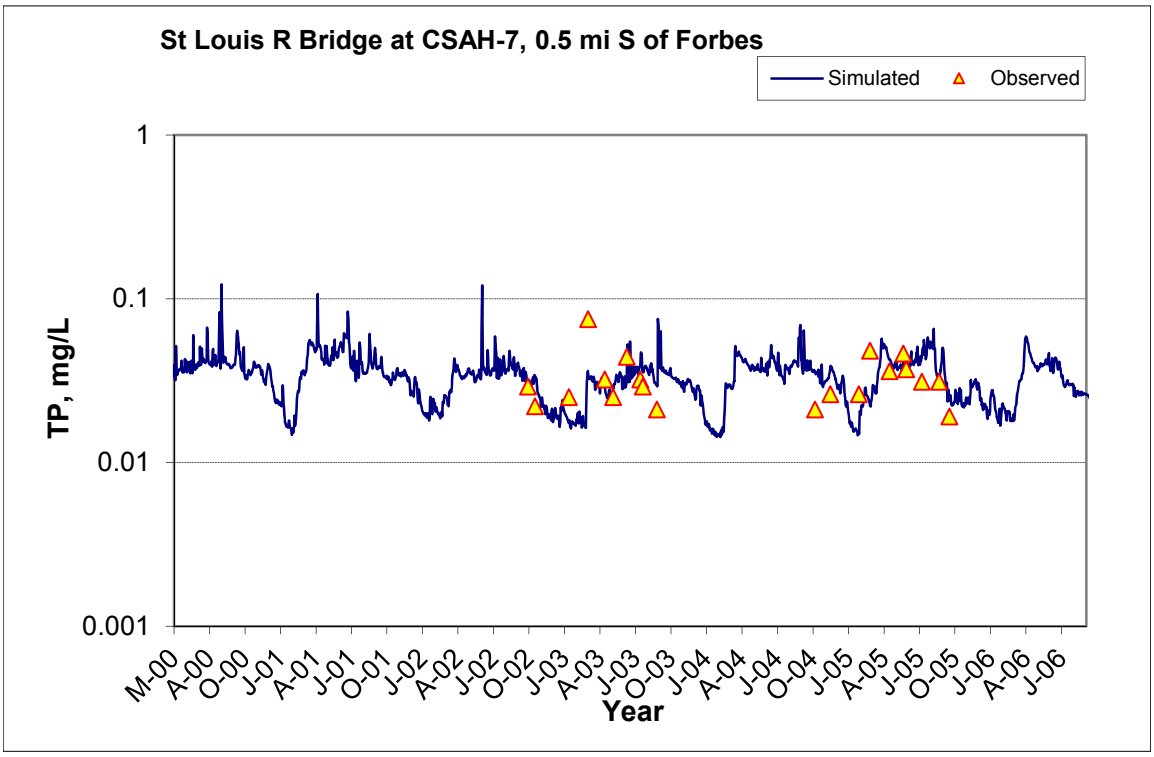

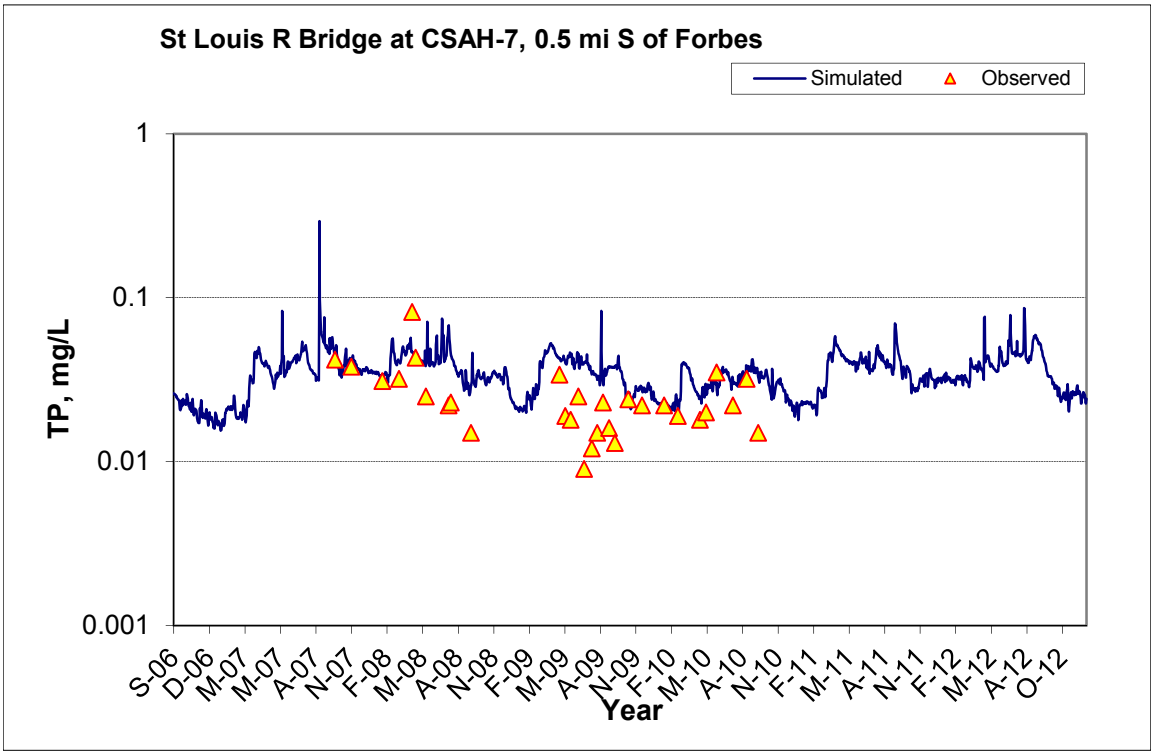

Figure A-74. Time series of observed and simulated Total Phosphorus (TP) concentration at St Louis R Bridge at CSAH-7, 0.5 mi S of Forbes

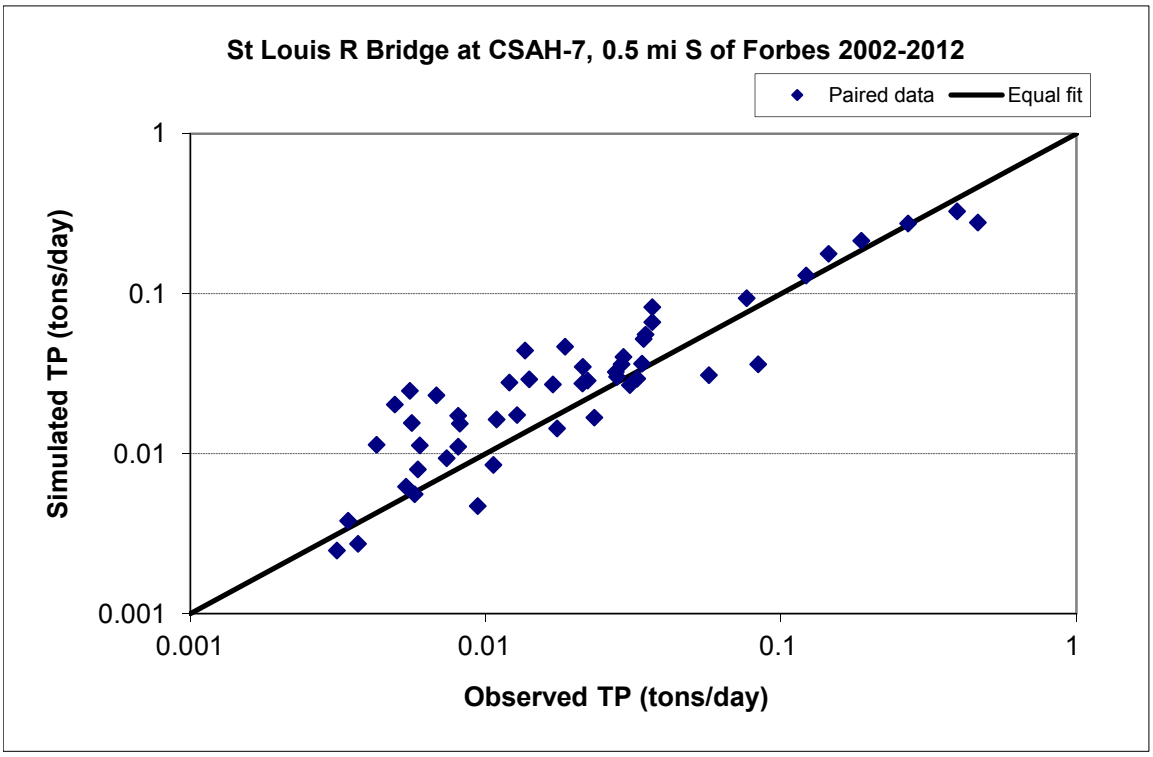

Figure A-75. Paired simulated vs. observed Total Phosphorus (TP) load at St Louis R Bridge at CSAH-7, 0.5 mi S of Forbes (calibration period)

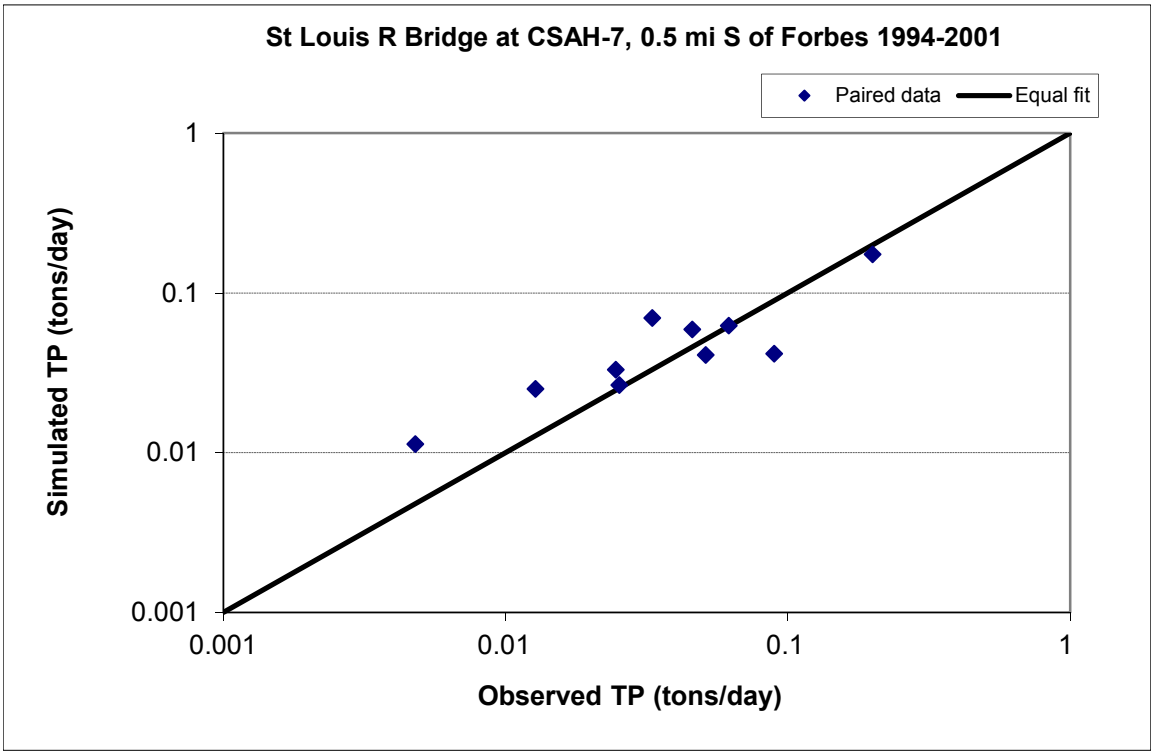

Figure A-76. Paired simulated vs. observed Total Phosphorus (TP) load at St Louis R Bridge at CSAH-7, 0.5 mi S of Forbes (validation period)

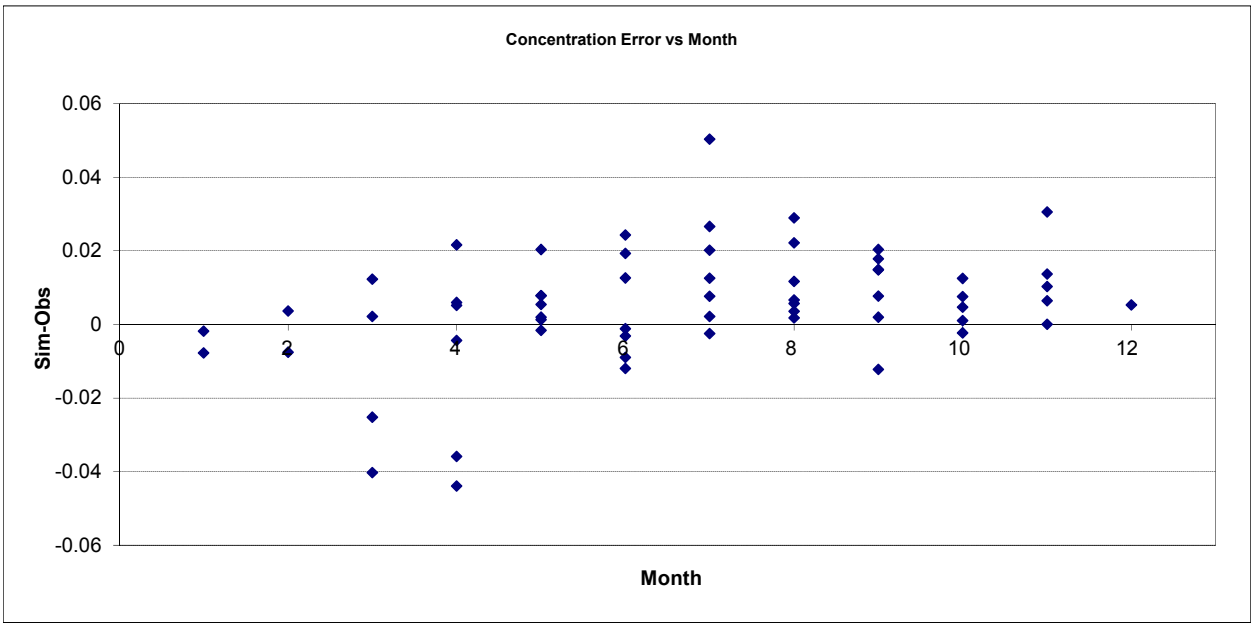

Figure A-77. Residual (Simulated - Observed) vs. Month Total Phosphorus (TP) at St Louis R Bridge at CSAH-7, 0.5 mi S of Forbes

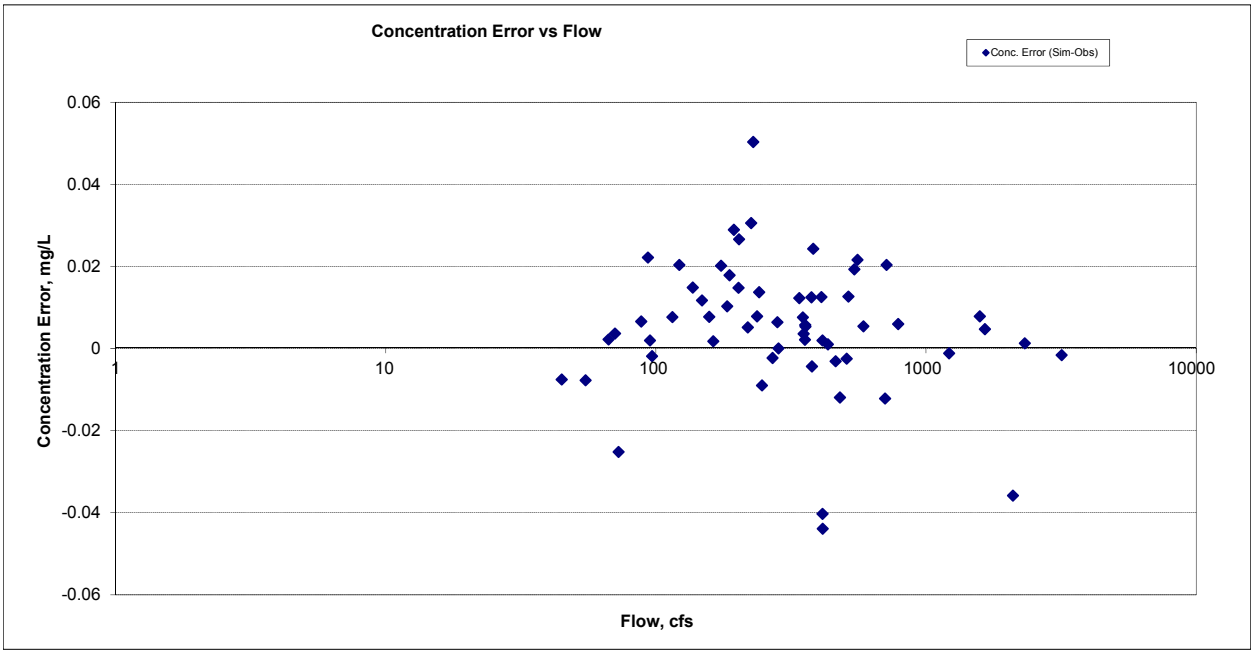

Figure A-78. Residual (Simulated - Observed) vs. Flow Total Phosphorus (TP) at St Louis R Bridge at CSAH-7, 0.5 mi S of Forbes

A.4 ST. LOUIS R BLW CLOQUET R (S000-023)

A.4.1 Ammonia Nitrogen (NH3)

Table A-12. Ammonia Nitrogen (NH3) statistics

Period	1994-2001	2002-2012
Count	36	38
Concentration Average Error	92.81%	16.55%
Concentration Median Error	105.61%	18.49%
Load Average Error	77.19%	7.75%
Load Median Error	77.60%	18.56%
Paired t conc	0.00	0.66
Paired t load	0.03	0.78

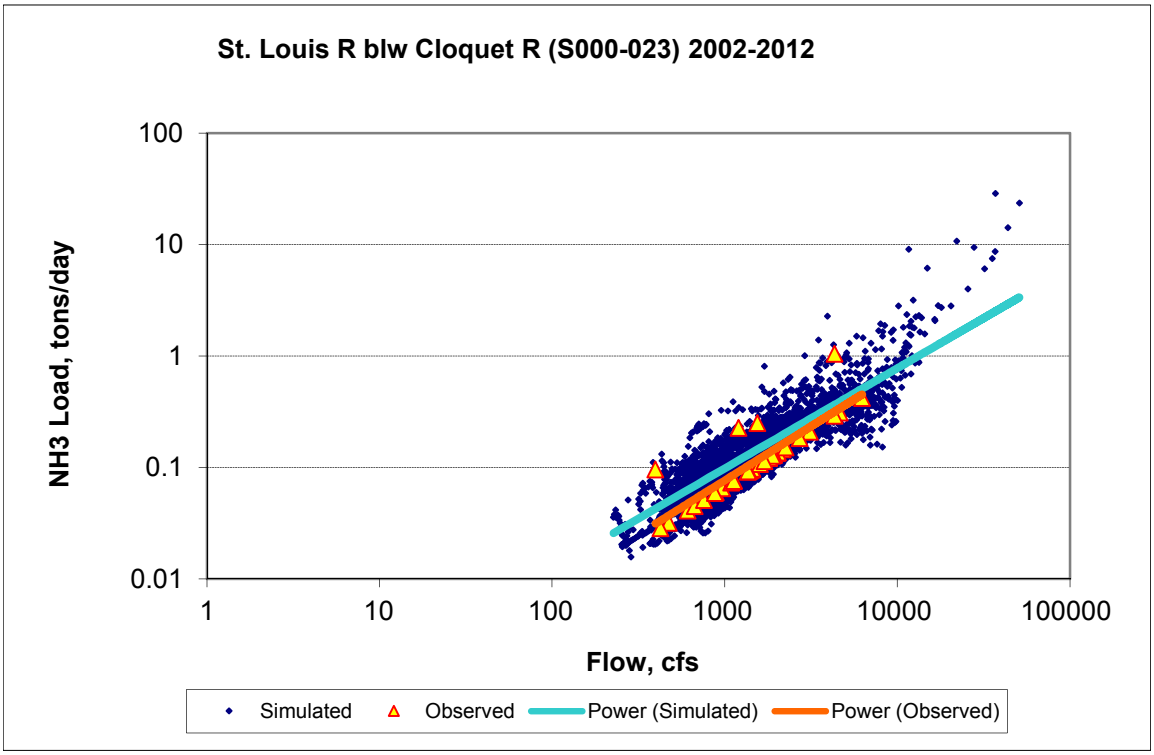

Figure A-79. Power plot of simulated and observed Ammonia Nitrogen (NH3) load vs flow at St. Louis R blw Cloquet R (S000-023) (calibration period)

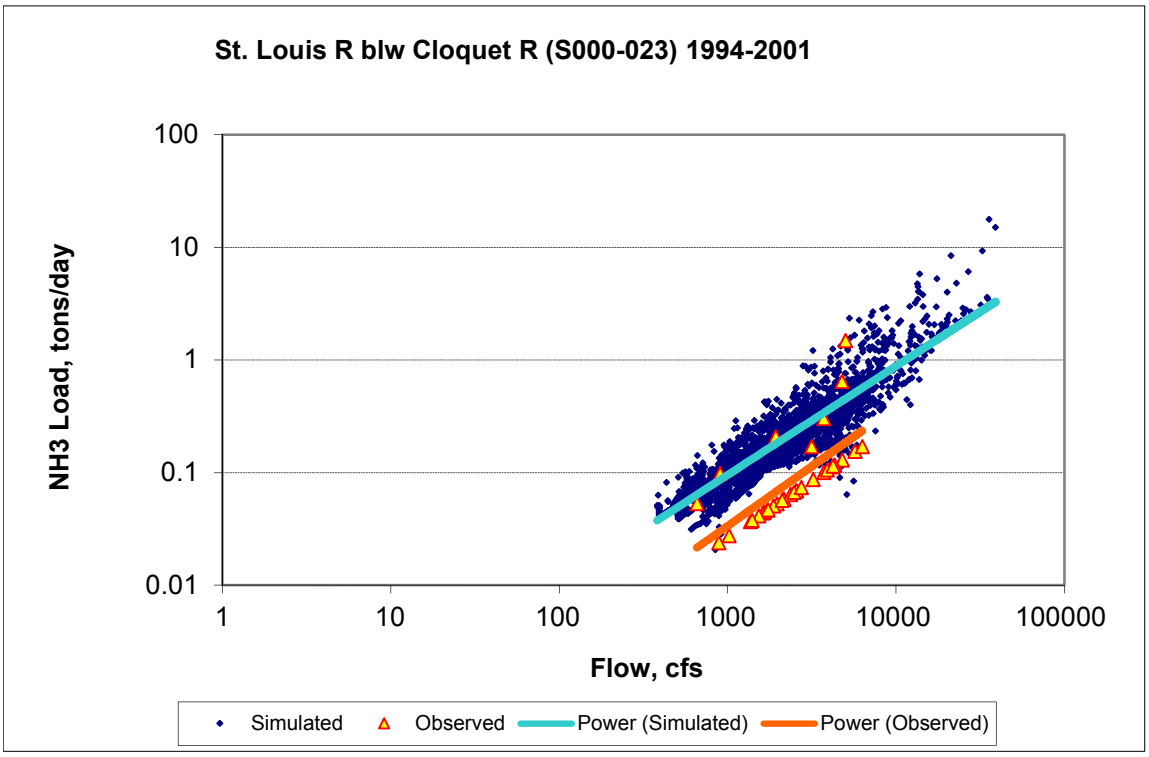

Figure A-80. Power plot of simulated and observed Ammonia Nitrogen (NH3) load vs flow at St. Louis R blw Cloquet R (S000-023) (validation period)

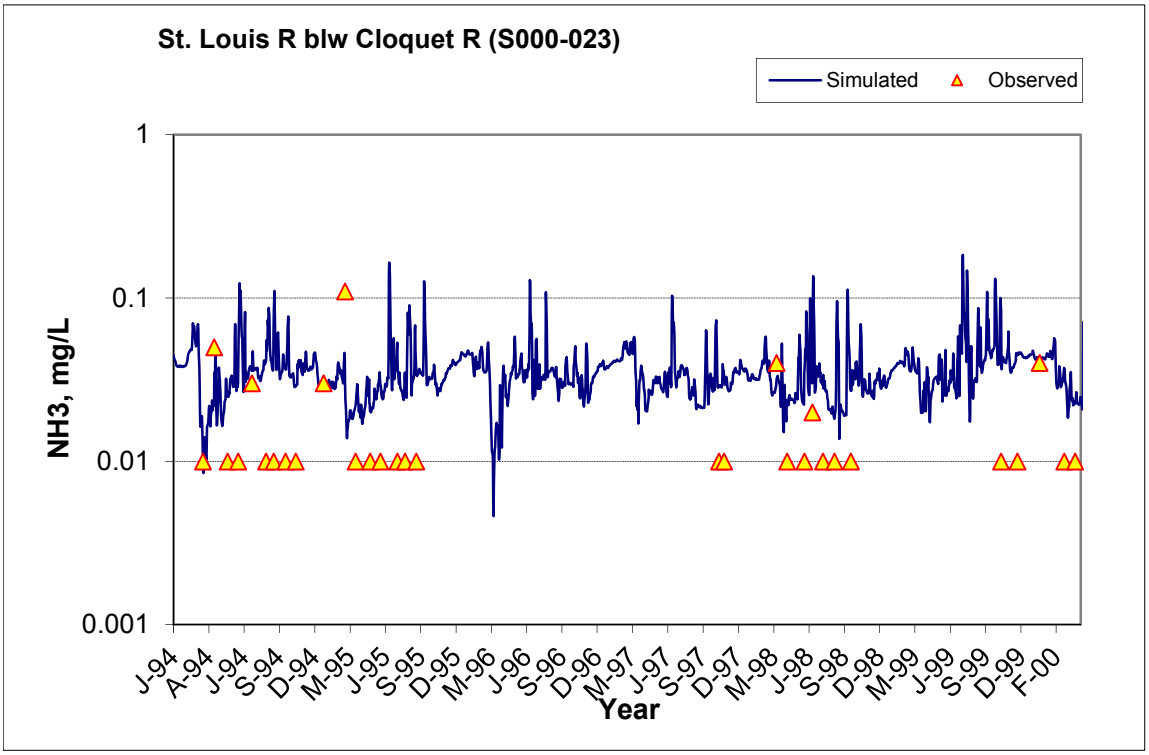

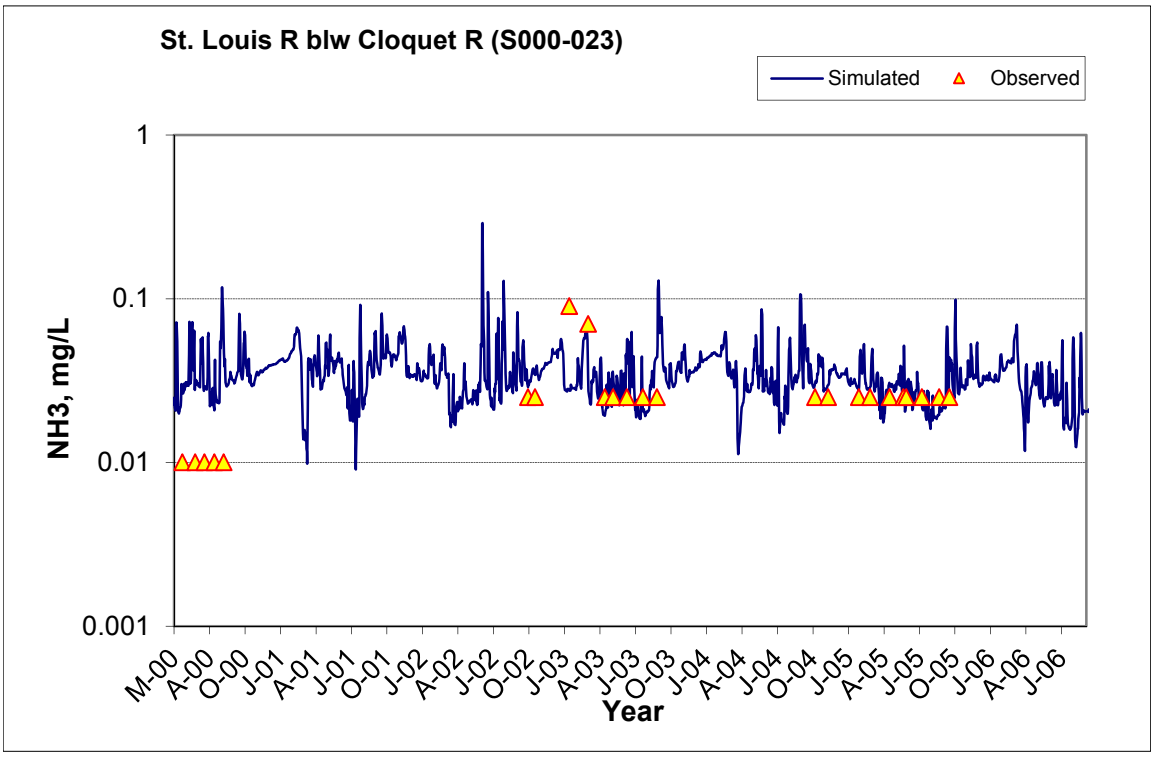

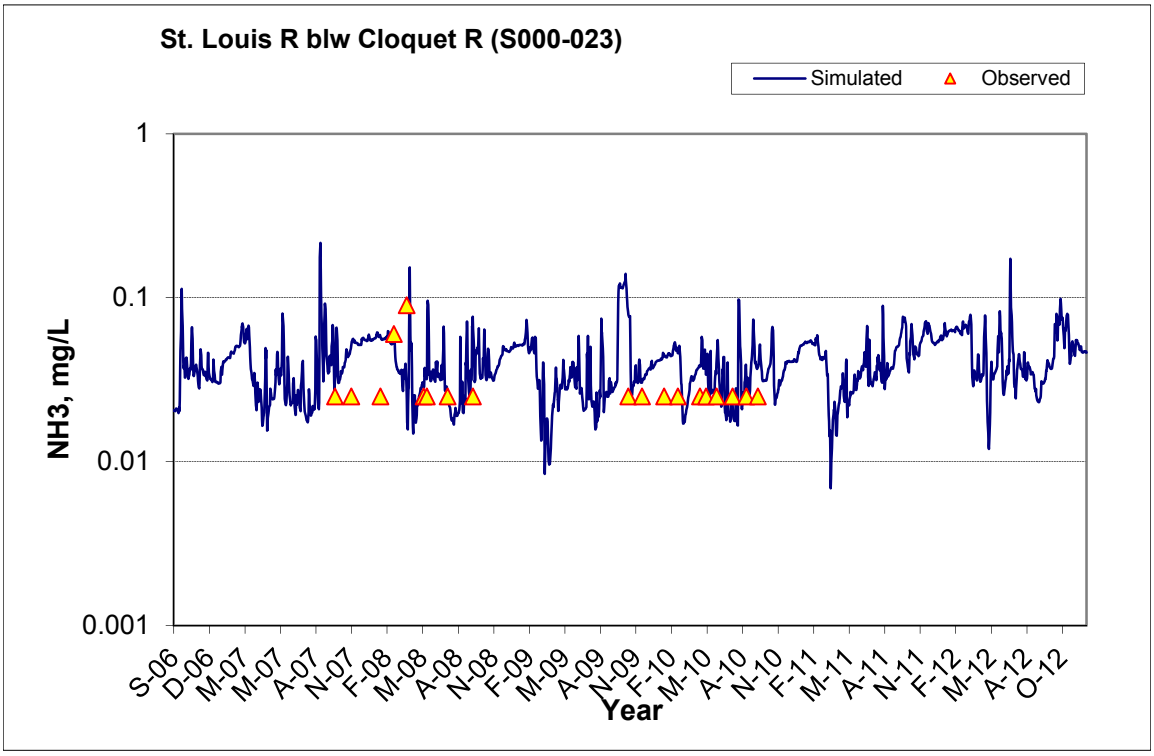

Figure A-81. Time series of observed and simulated Ammonia Nitrogen (NH3) concentration at St. Louis R blw Cloquet R (S000-023)

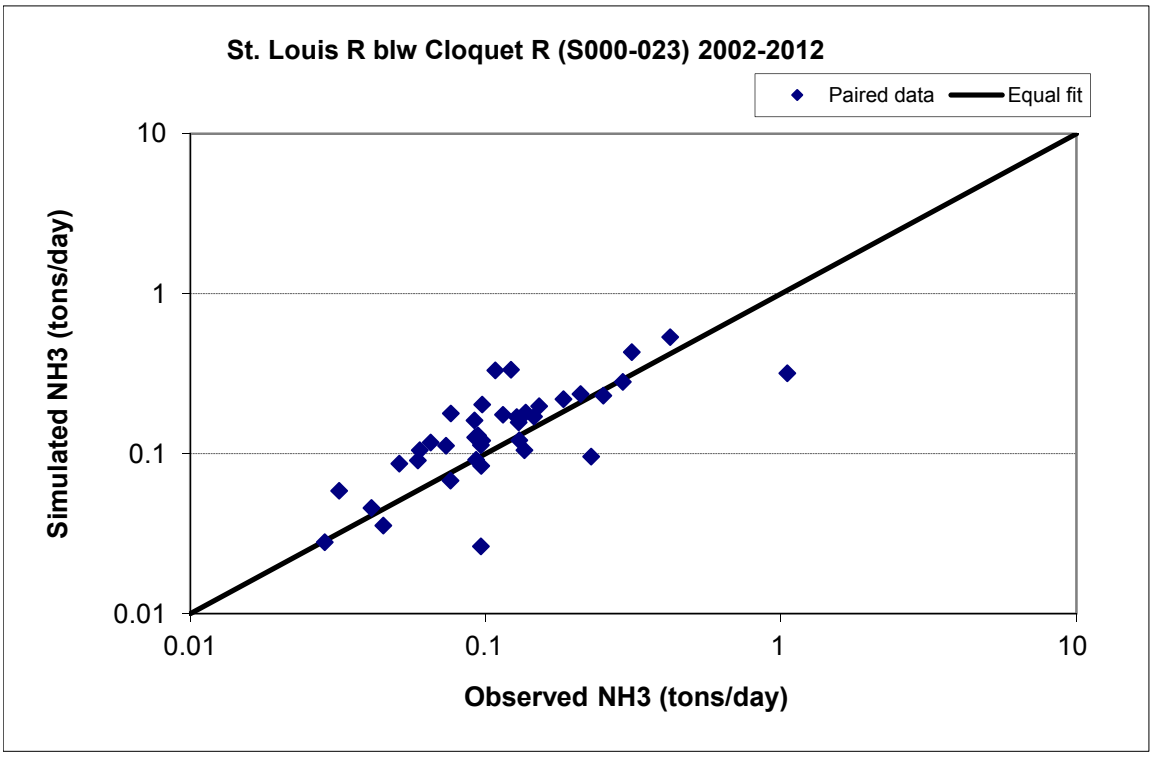

Figure A-82. Paired simulated vs. observed Ammonia Nitrogen (NH3) load at St. Louis R blw Cloquet R (S000-023) (calibration period)

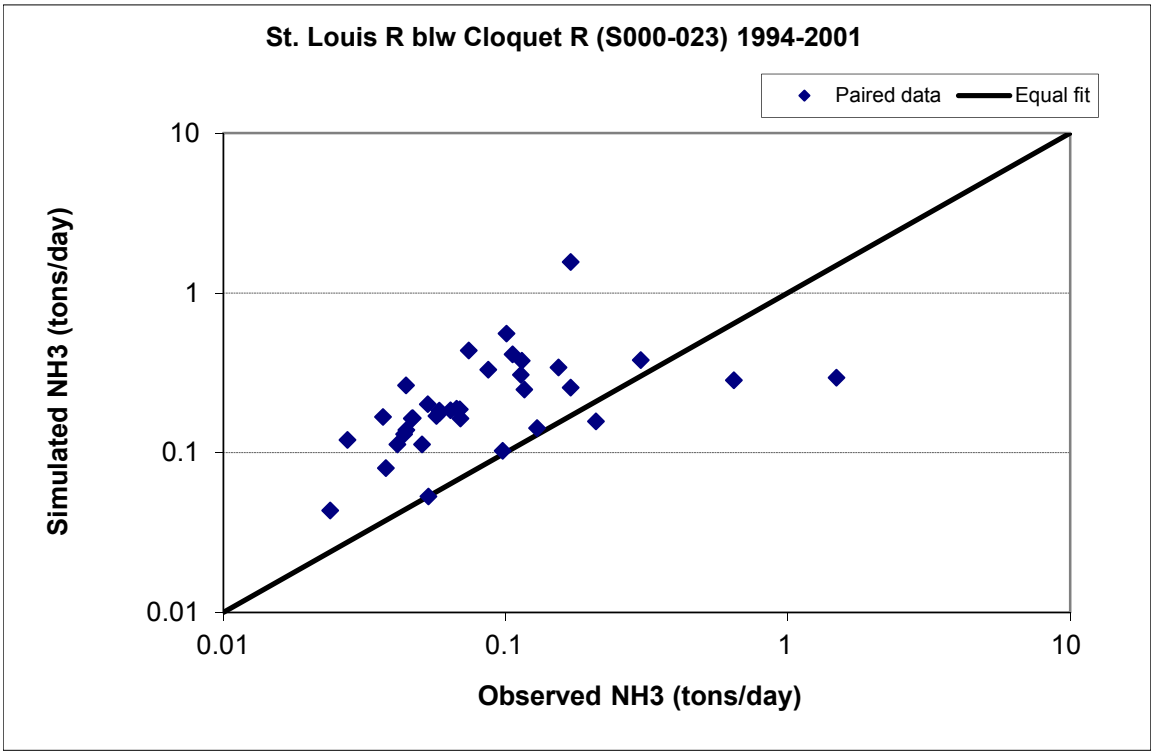

Figure A-83. Paired simulated vs. observed Ammonia Nitrogen (NH3) load at St. Louis R blw Cloquet R (S000-023) (validation period)

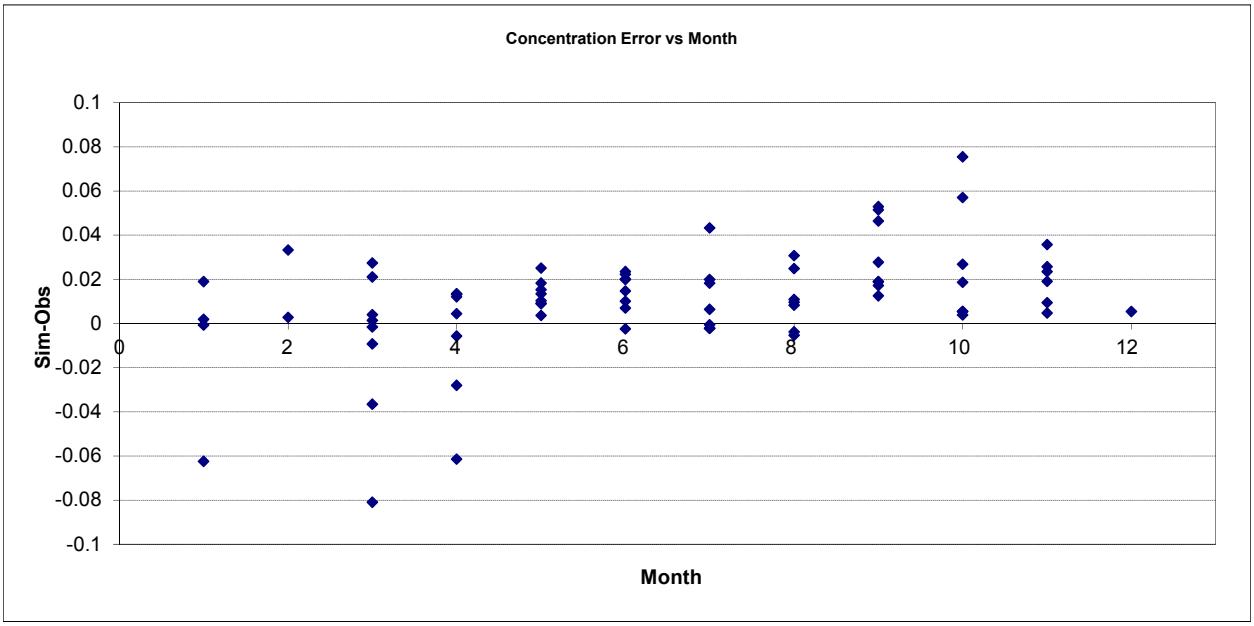

Figure A-84. Residual (Simulated - Observed) vs. Month Ammonia Nitrogen (NH3) at St. Louis R blw Cloquet R (S000-023)

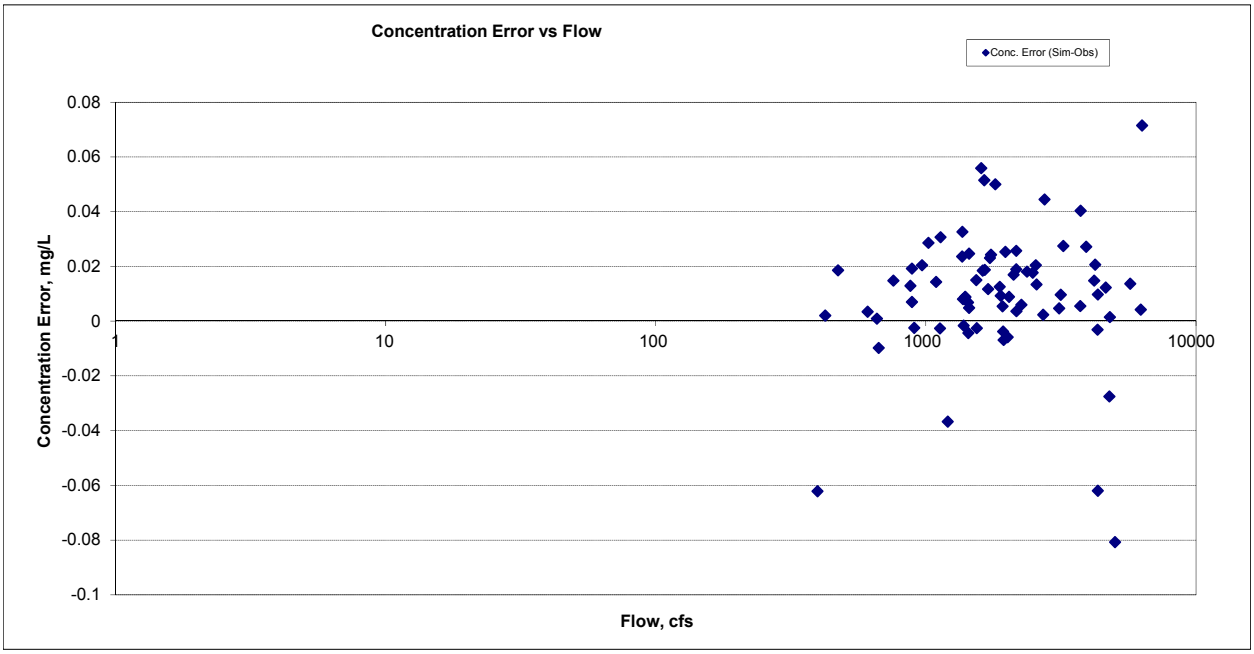

Figure A-85. Residual (Simulated - Observed) vs. Flow Ammonia Nitrogen (NH3) at St. Louis R blw Cloquet R (S000-023)

A.4.2 Organic Nitrogen (OrgN)

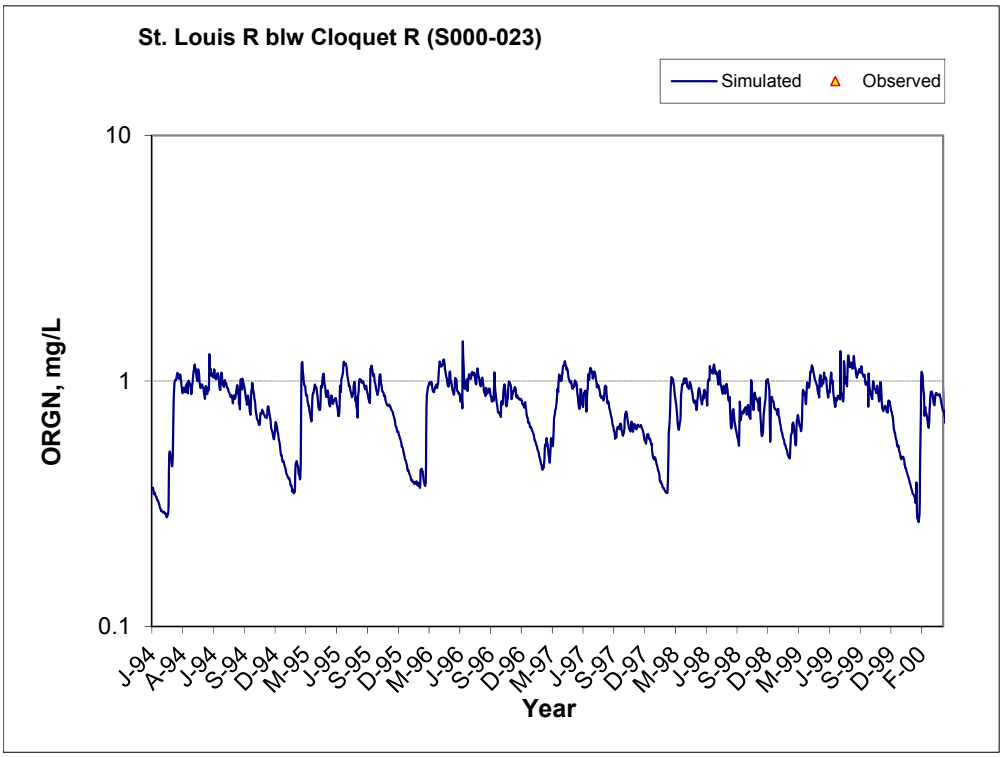

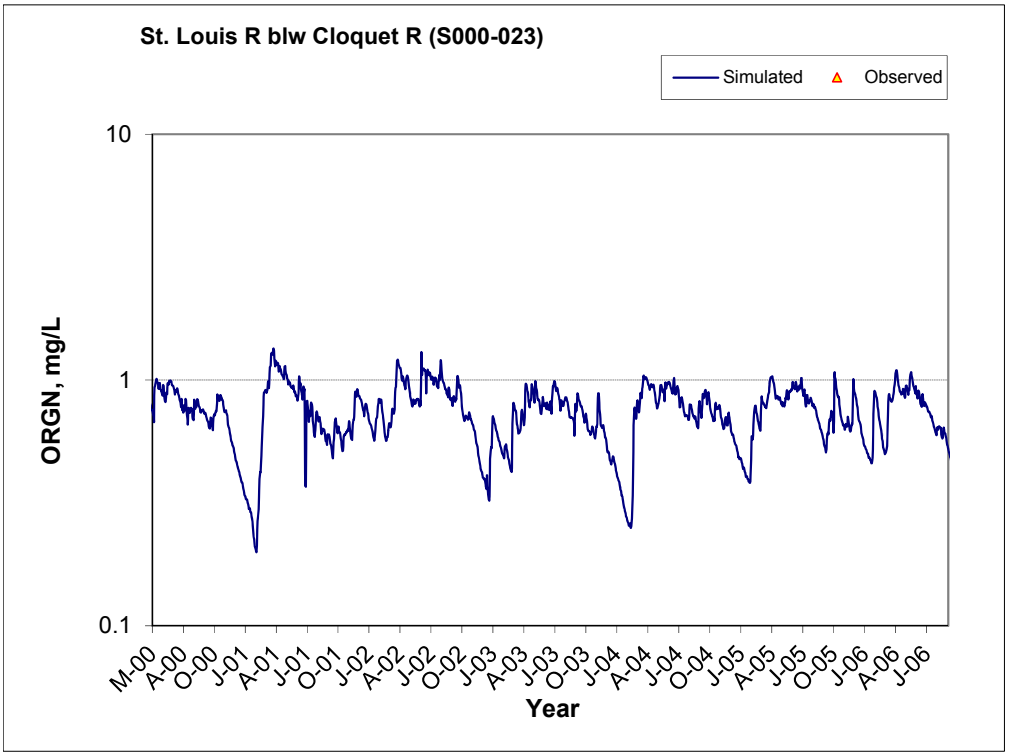

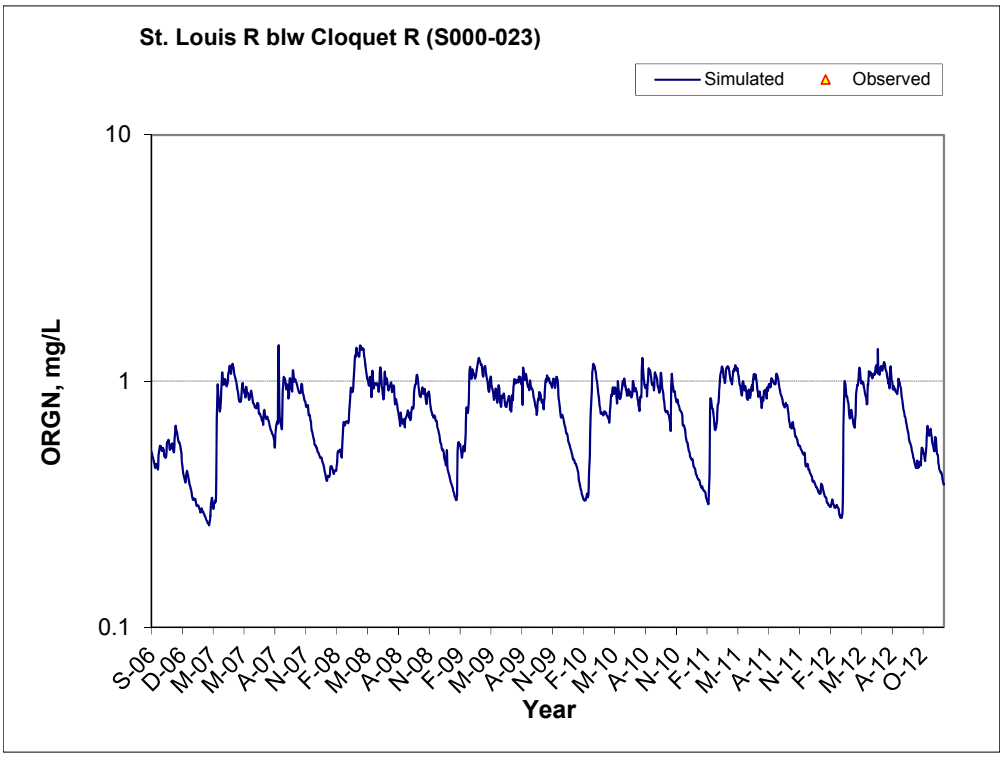

Figure A-86. Time series of observed and simulated Organic Nitrogen (OrgN) concentration at St. Louis R blw Cloquet R (S000-023)

A.4.3 Total Kjeldahl Nitrogen (TKN)

Table A-13. Total Kjeldahl Nitrogen (TKN) statistics

Period	1994-2001	2002-2012
Count	7	6
Concentration Average Error	44.41%	4.20%
Concentration Median Error	34.32%	1.49%
Load Average Error	52.50%	0.65%
Load Median Error	43.01%	-0.64%
Paired t conc	0.00	0.93
Paired t load	0.13	0.82

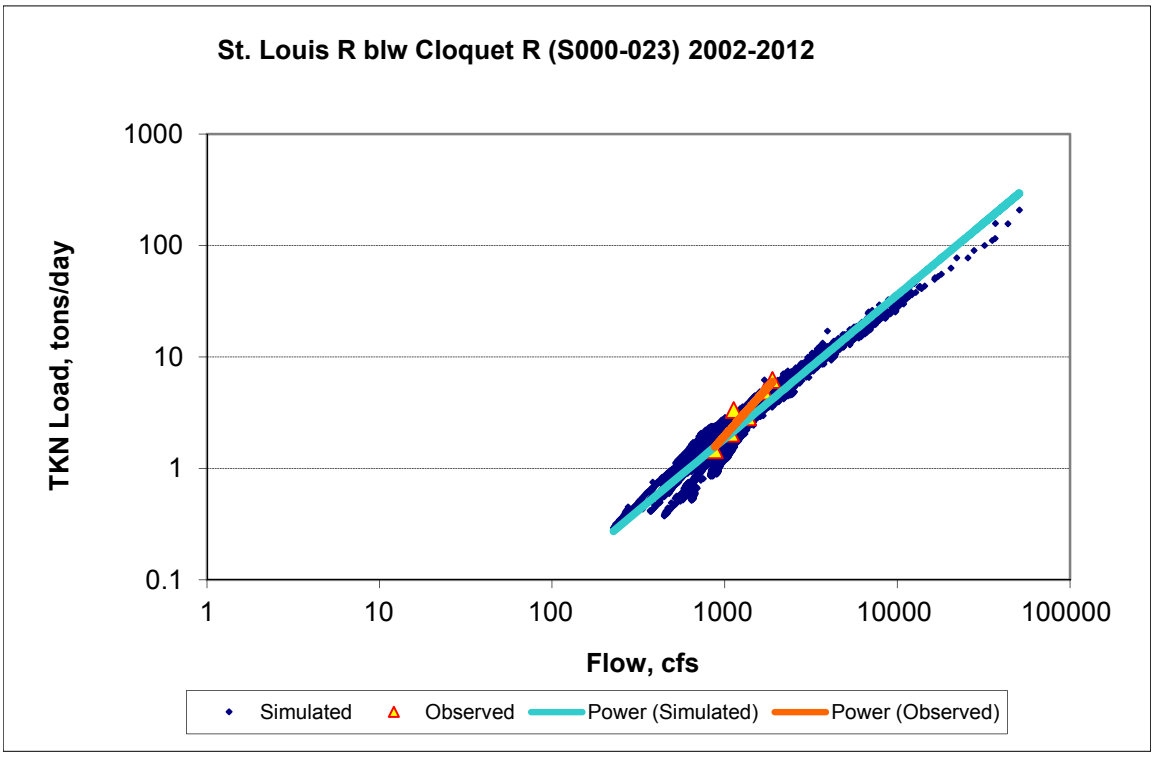

Figure A-87. Power plot of simulated and observed Total Kjeldahl Nitrogen (TKN) load vs flow at St. Louis R blw Cloquet R (S000-023) (calibration period)

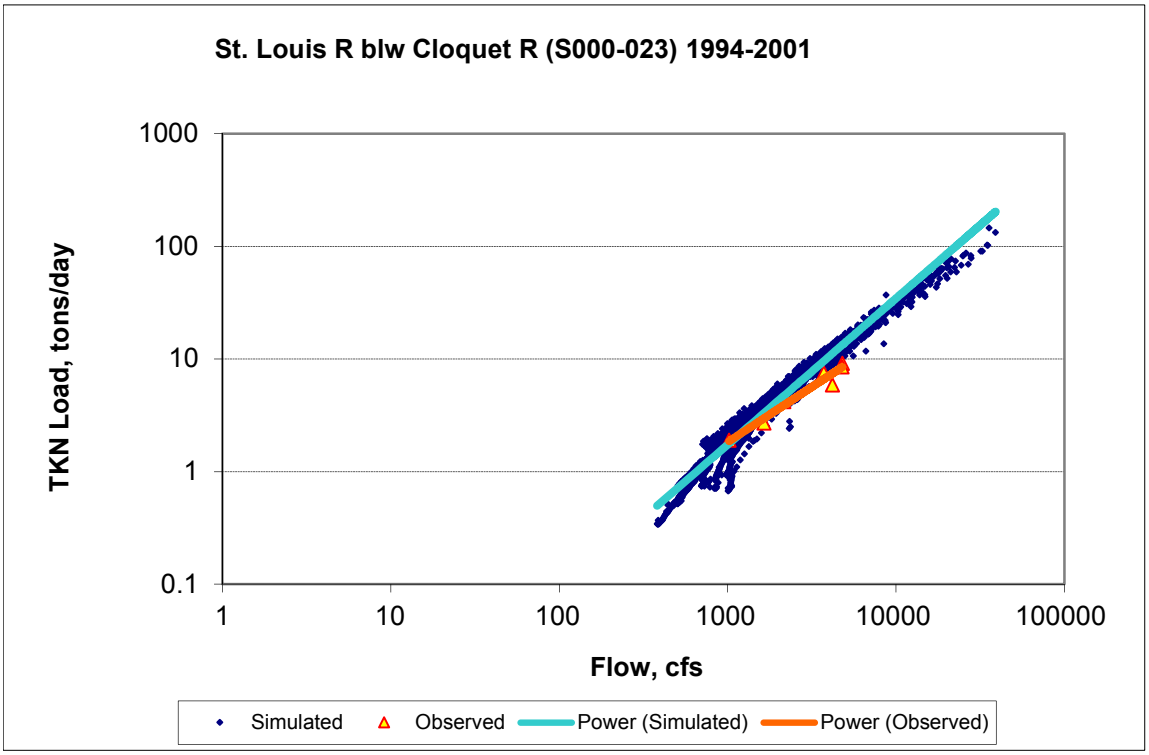

Figure A-88. Power plot of simulated and observed Total Kjeldahl Nitrogen (TKN) load vs flow at St. Louis R blw Cloquet R (S000-023) (validation period)

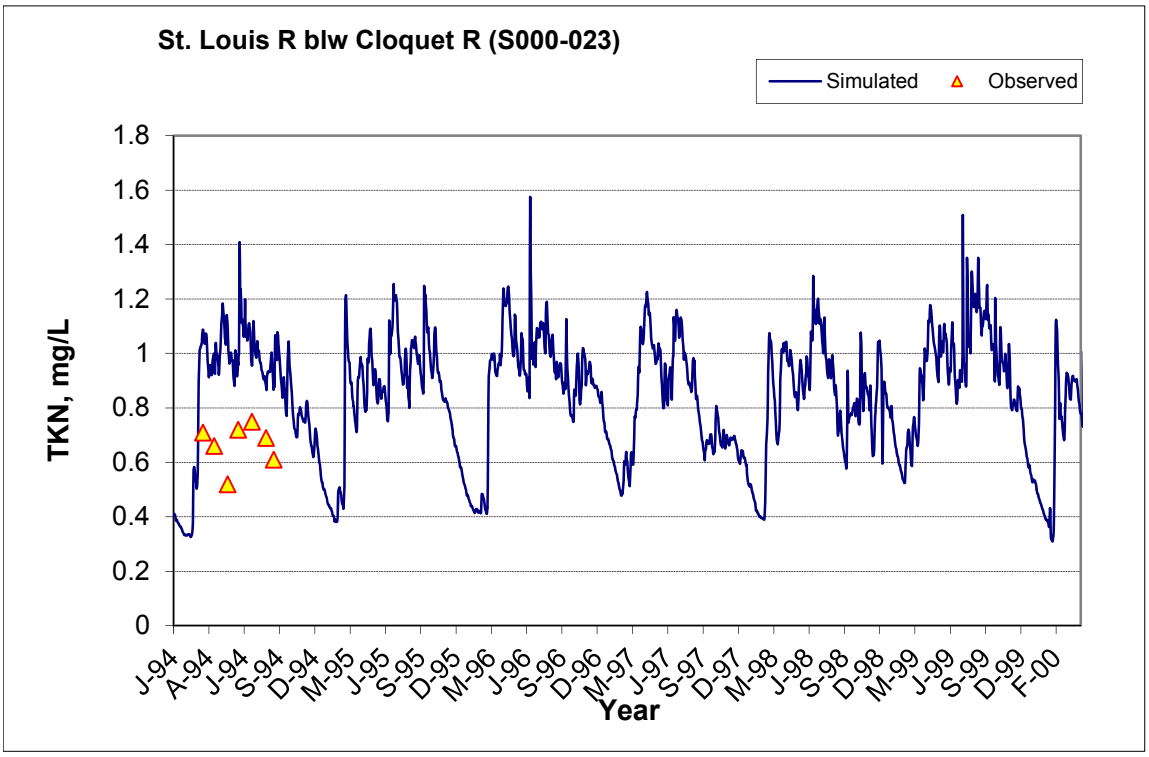
St. Louis R blw Cloquet R (S000-023)
Simulated
Observed
TKN, mg/L
1.8
1.6
1.4
1.2
1
0.8
0.6
0.4
0.2
0
J-94 A-94 J-94 S-94 D-94 M-95 J-95 S-95 D-95 M-96 J-96 S-96 D-96 M-97 J-97 S-97 D-97 M-98 J-98 S-98 D-98 M-99 J-99 S-99 D-99 F-00
Year

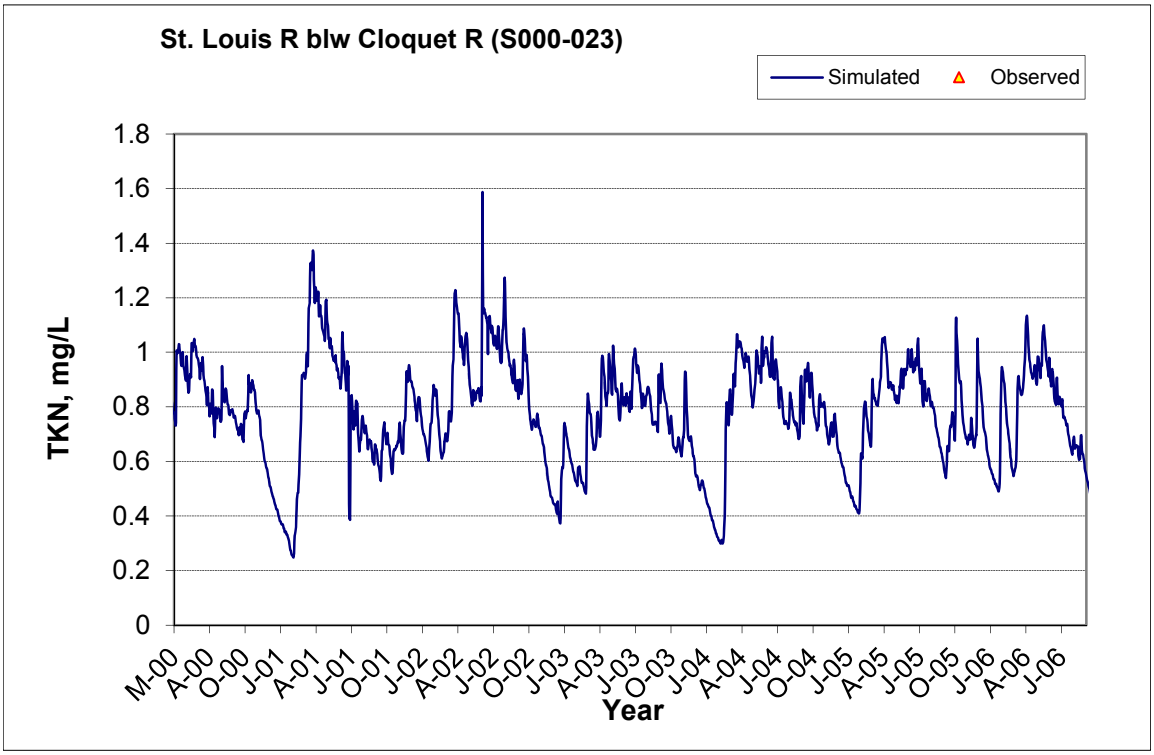
St. Louis R blw Cloquet R (S000-023)
Simulated
Observed
TKN, mg/L
1.8
1.6
1.4
1.2
1
0.8
0.6
0.4
0.2
0
M-00 A-00 O-00 J-01 A-01 J-01 O-01 J-02 A-02 J-02 O-02 J-03 A-03 J-03 O-03 J-04 A-04 J-04 O-04 J-05 A-05 J-05 O-05 J-06 A-06 J-06
Year

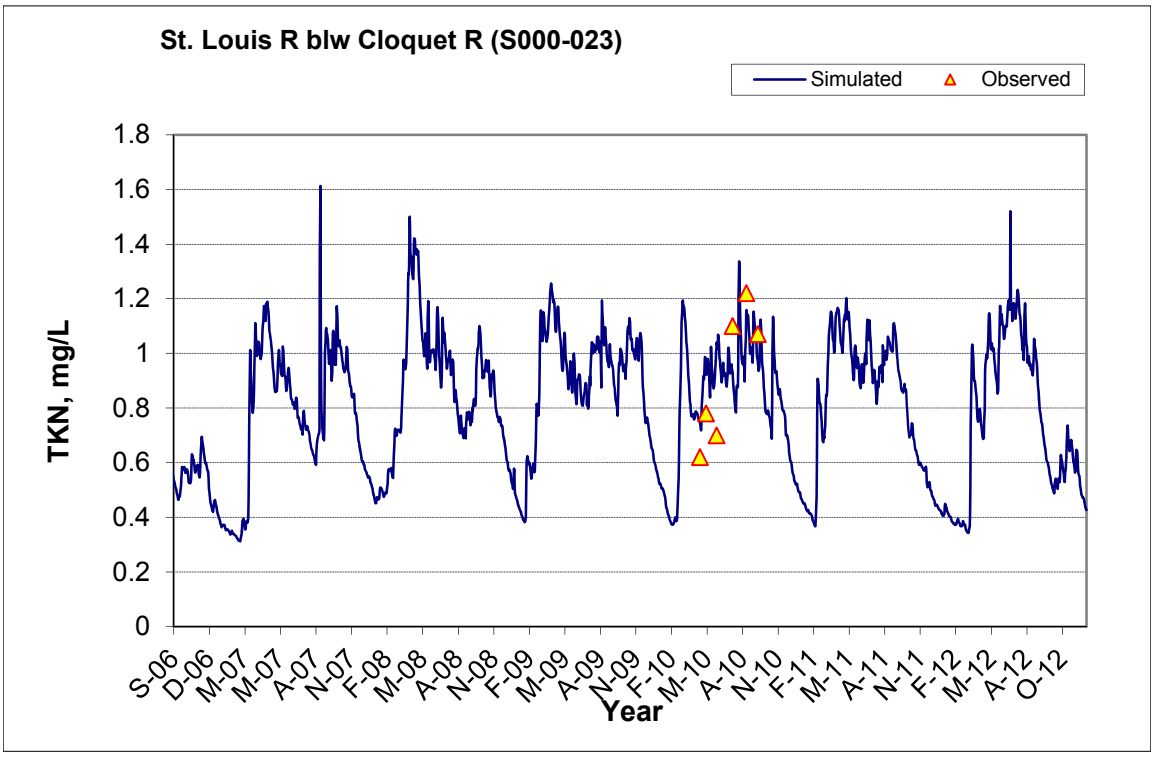

Figure A-89. Time series of observed and simulated Total Kjeldahl Nitrogen (TKN) concentration at St. Louis R blw Cloquet R (S000-023)

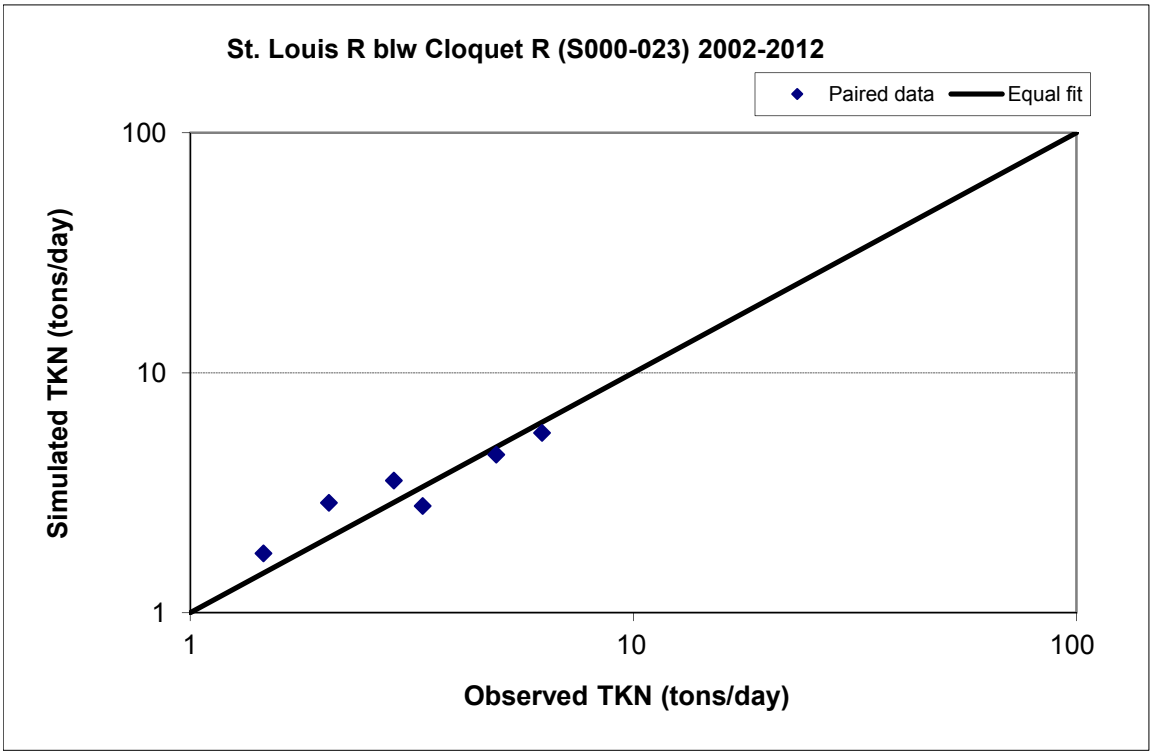

Figure A-90. Paired simulated vs. observed Total Kjeldahl Nitrogen (TKN) load at St. Louis R blw Cloquet R (S000-023) (calibration period)

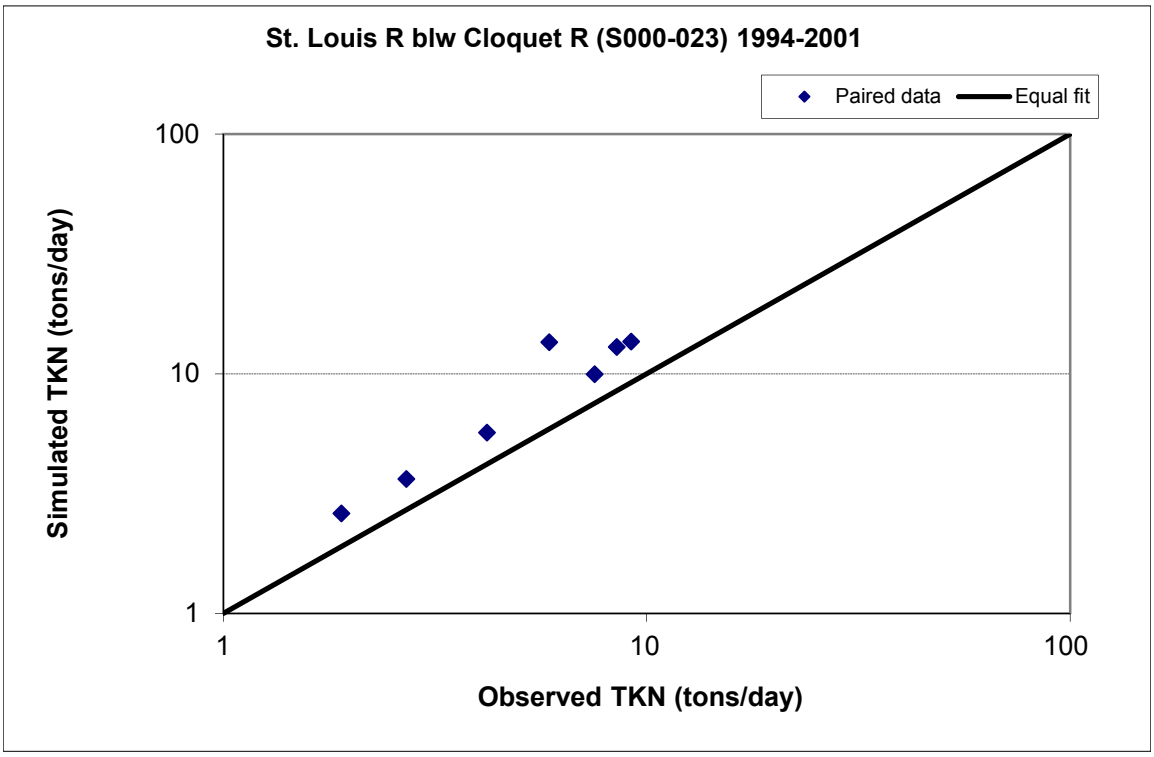

Figure A-91. Paired simulated vs. observed Total Kjeldahl Nitrogen (TKN) load at St. Louis R blw Cloquet R (S000-023) (validation period)

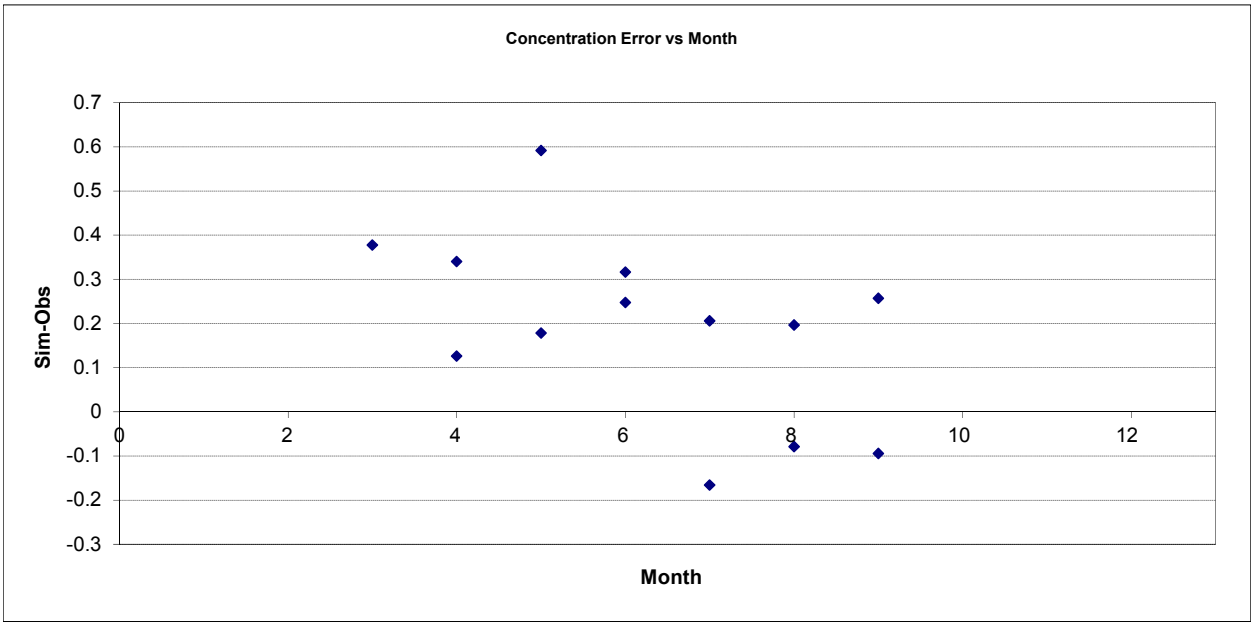

Figure A-92. Residual (Simulated - Observed) vs. Month Total Kjeldahl Nitrogen (TKN) at St. Louis R blw Cloquet R (S000-023)

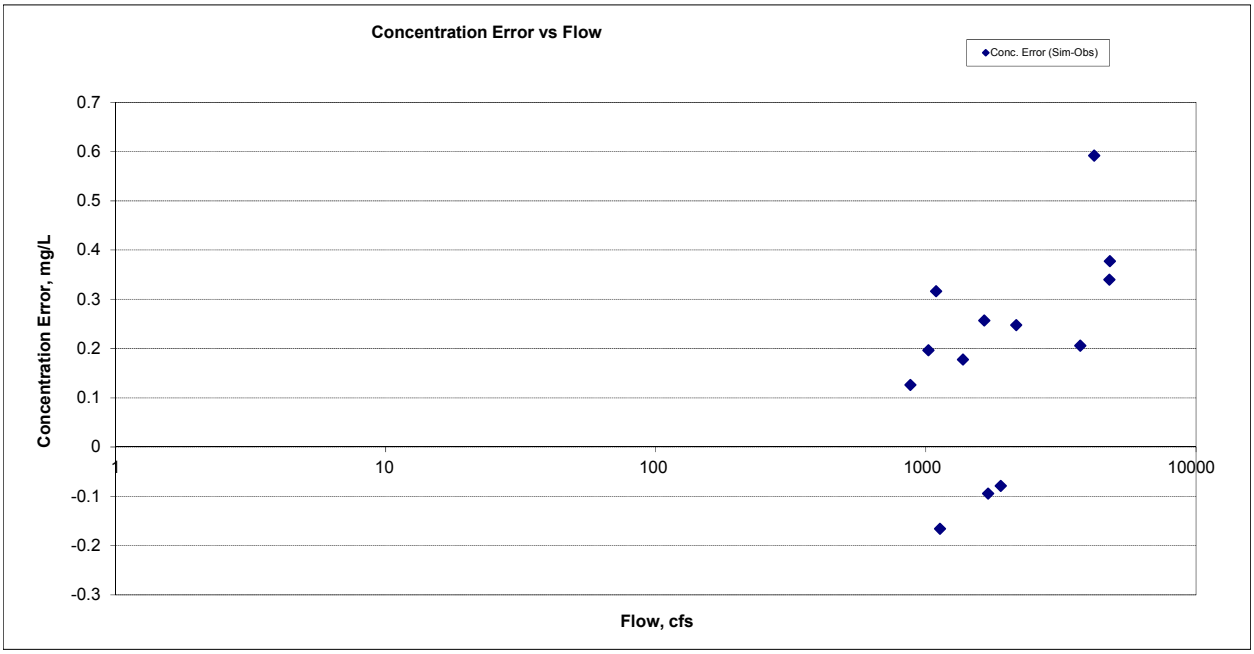

Figure A-93. Residual (Simulated - Observed) vs. Flow Total Kjeldahl Nitrogen (TKN) at St. Louis R blw Cloquet R (S000-023)

A.4.4 Nitrite+ Nitrate Nitrogen (NOx)

Table A-14. Nitrite+ Nitrate Nitrogen (NOx) statistics

Period	1994-2001	2002-2012
Count	36	38
Concentration Average Error	2.19%	45.49%
Concentration Median Error	13.72%	45.20%
Load Average Error	-8.05%	15.81%
Load Median Error	13.08%	24.58%
Paired t conc	0.90	0.02
Paired t load	0.71	0.59

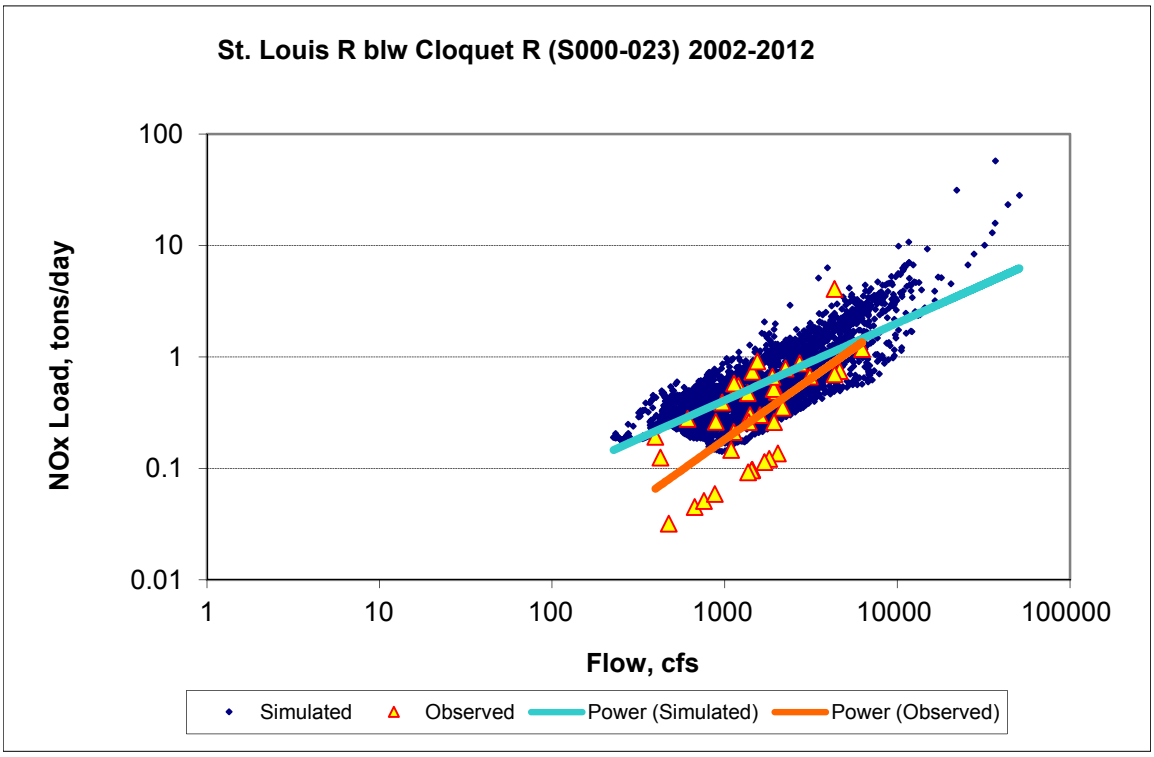

Figure A-94. Power plot of simulated and observed Nitrite+ Nitrate Nitrogen (NOx) load vs flow at St. Louis R blw Cloquet R (S000-023) (calibration period)

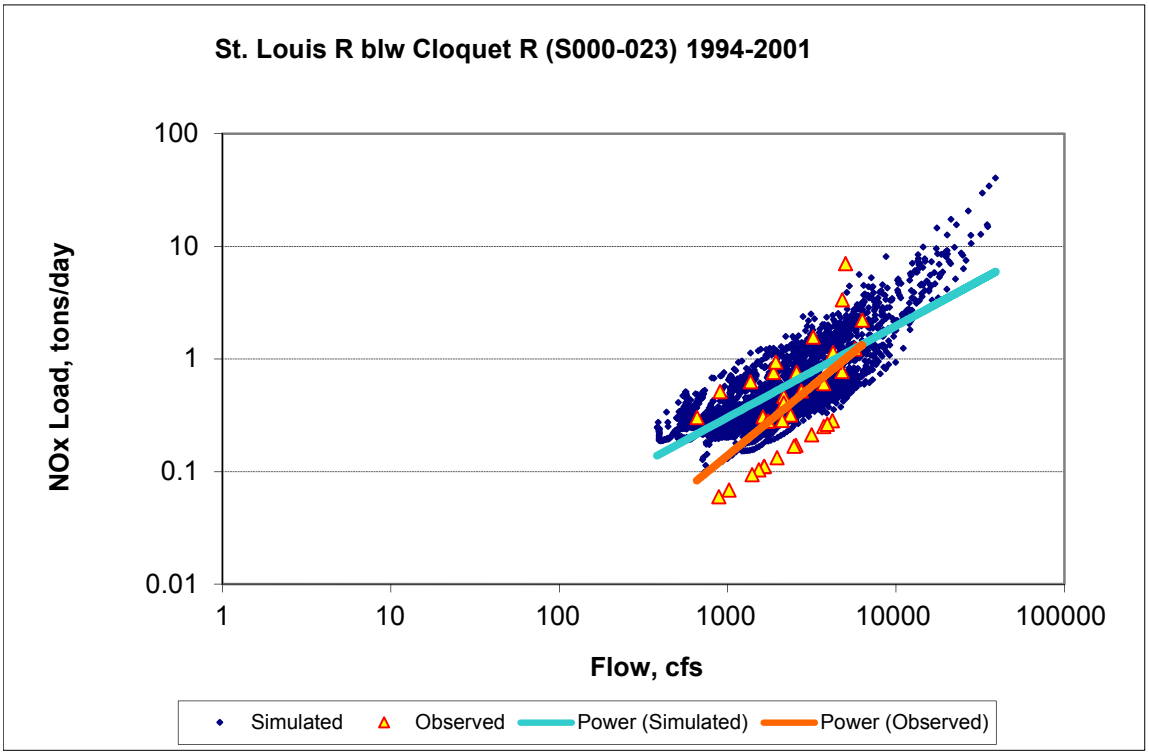

Figure A-95. Power plot of simulated and observed Nitrite+ Nitrate Nitrogen (NOx) load vs flow at St. Louis R blw Cloquet R (S000-023) (validation period)

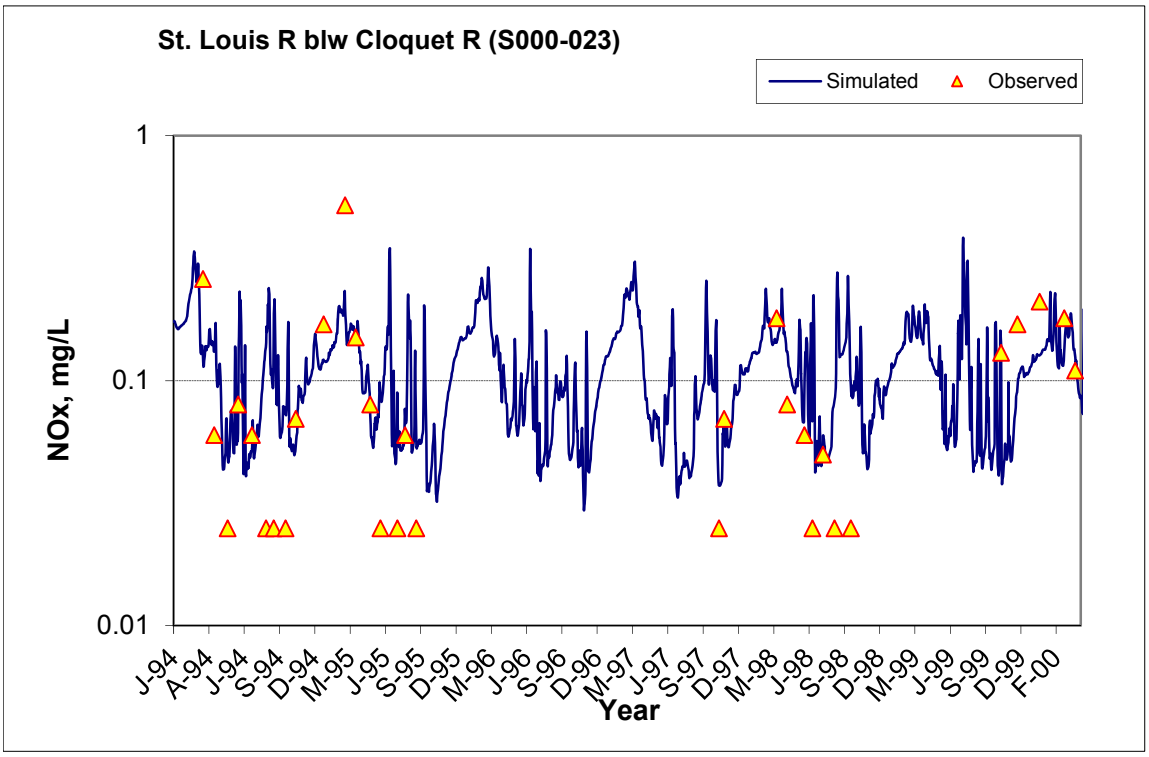
St. Louis R blw Cloquet R (S000-023)
Simulated
Observed
NOx, mg/L
1
0.1
0.01
J-94 A-94 J-94 S-94 D-94 M-95 J-95 S-95 D-95 M-96 J-96 S-96 D-96 M-97 J-97 S-97 D-97 M-98 J-98 S-98 D-98 M-99 J-99 S-99 D-99 F-00
Year

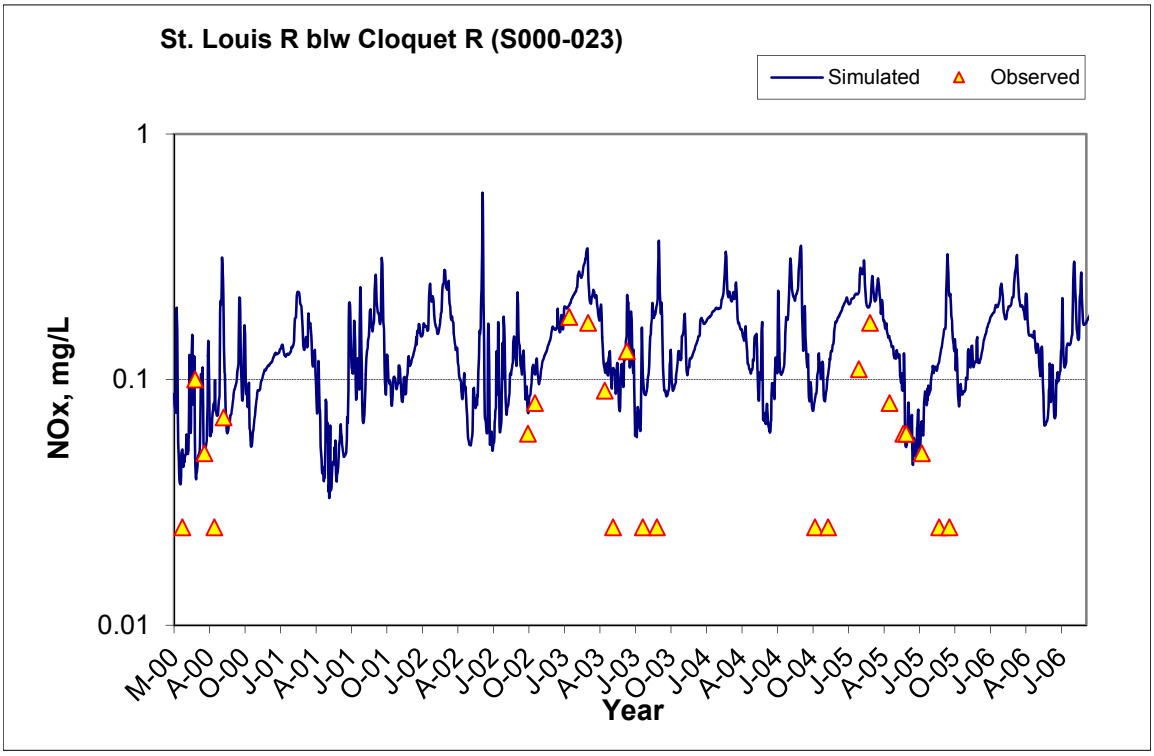
St. Louis R blw Cloquet R (S000-023)
Simulated
Observed
NOx, mg/L
1
0.1
0.01
M-00 A-00 O-00 J-01 A-01 J-01 O-01 J-02 A-02 J-02 O-02 J-03 A-03 J-03 O-03 J-04 A-04 J-04 O-04 J-05 A-05 J-05 O-05 J-06 A-06 J-06
Year

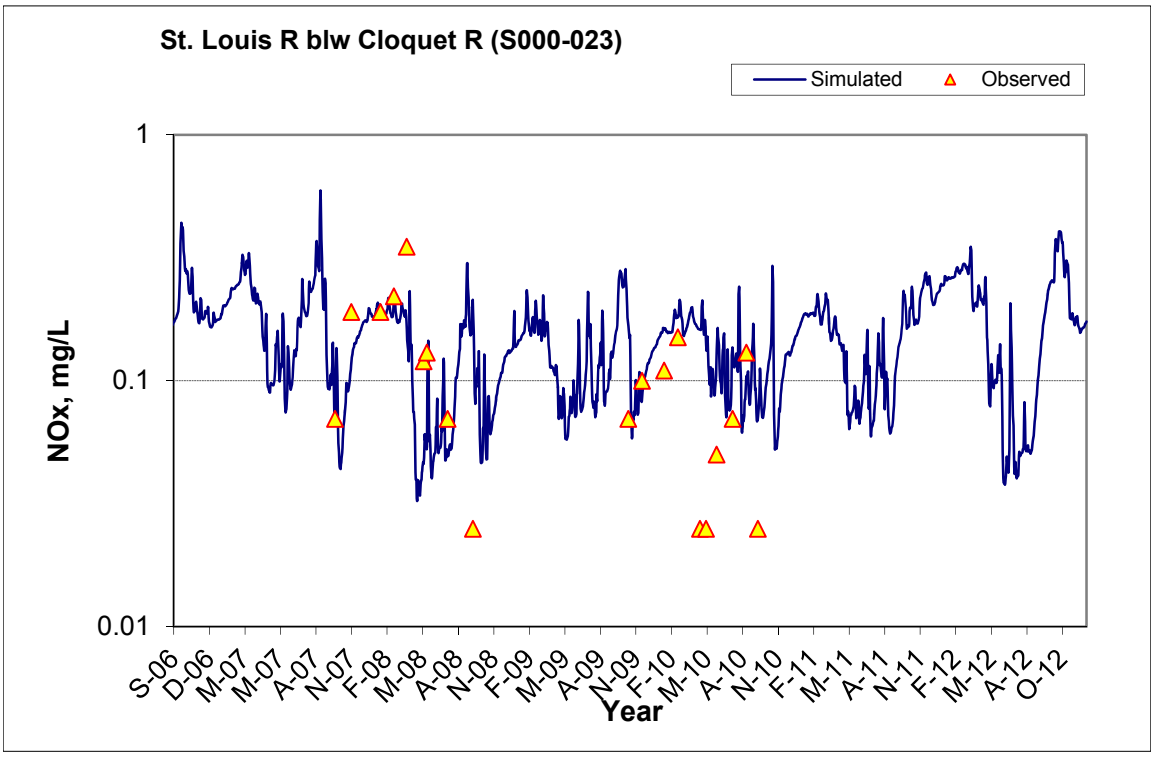

Figure A-96. Time series of observed and simulated Nitrite+ Nitrate Nitrogen (NOx) concentration at St. Louis R blw Cloquet R (S000-023)

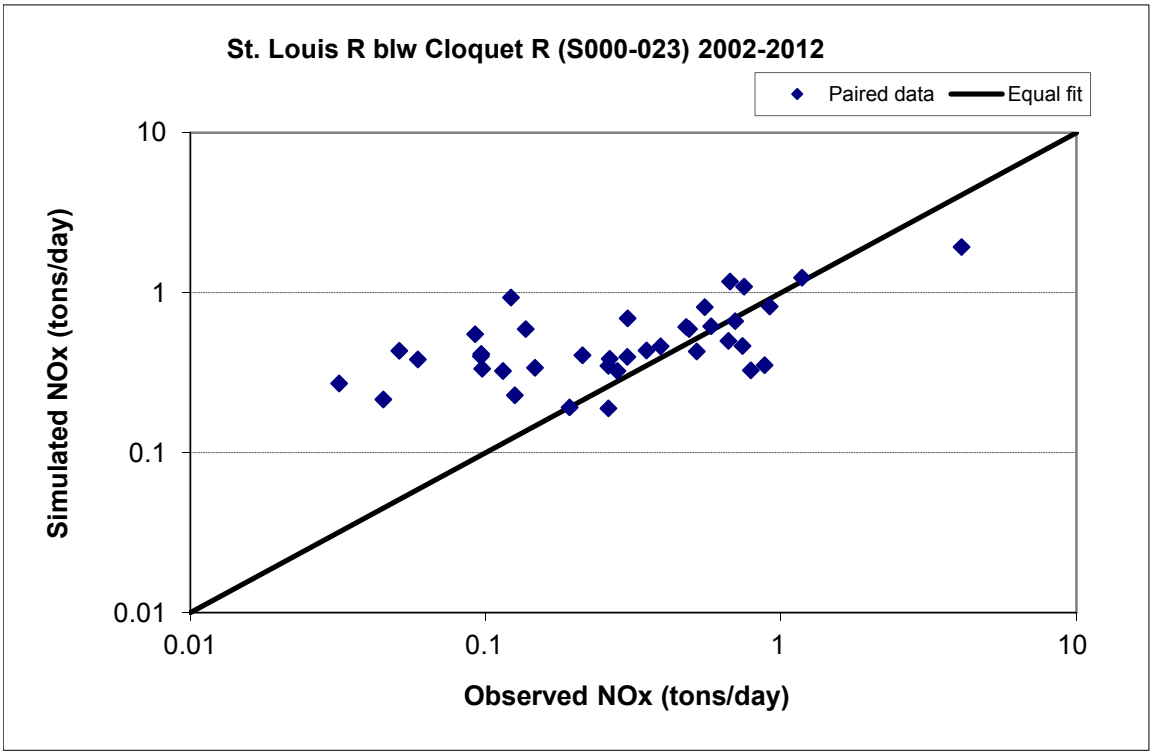

Figure A-97. Paired simulated vs. observed Nitrite+ Nitrate Nitrogen (NOx) load at St. Louis R blw Cloquet R (S000-023) (calibration period)

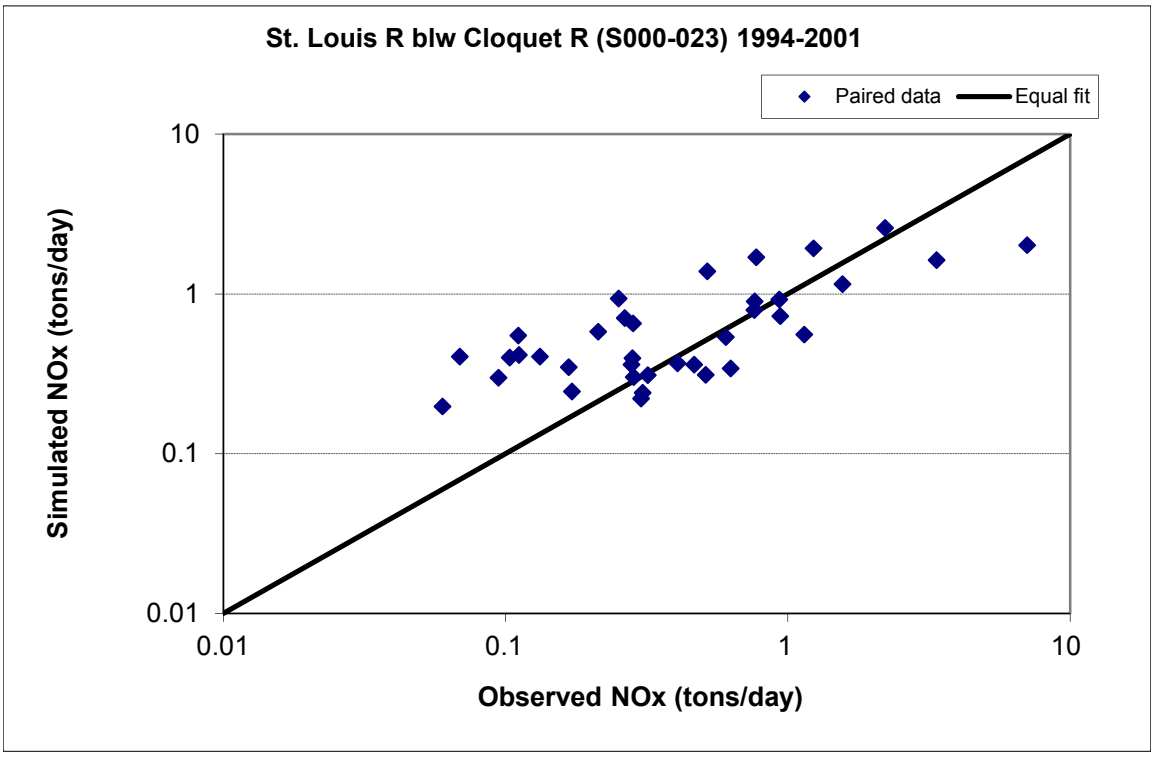

Figure A-98. Paired simulated vs. observed Nitrite+ Nitrate Nitrogen (NOx) load at St. Louis R blw Cloquet R (S000-023) (validation period)

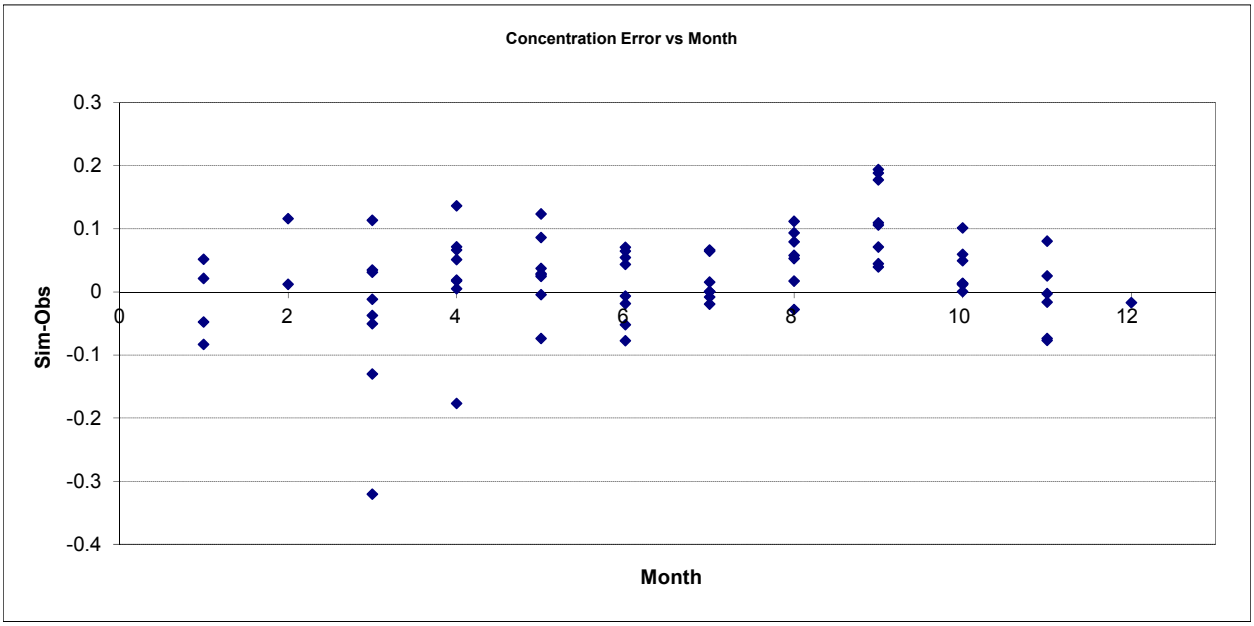

Figure A-99. Residual (Simulated - Observed) vs. Month Nitrite+ Nitrate Nitrogen (NOx) at St. Louis R blw Cloquet R (S000-023)

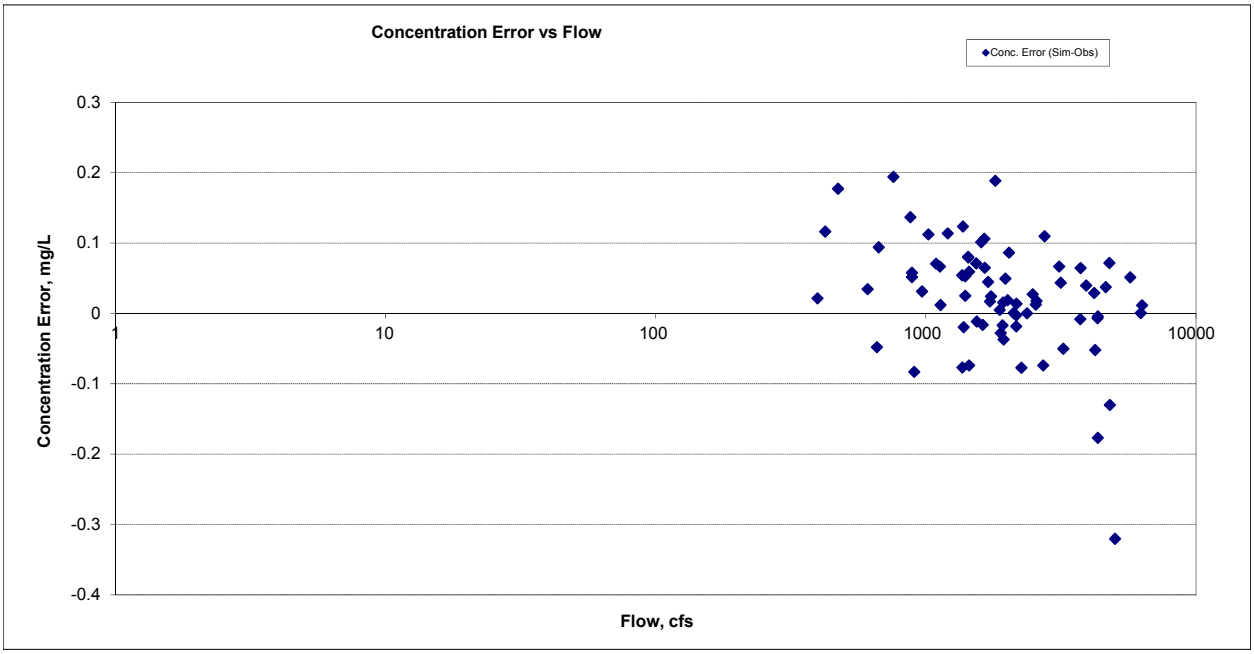

Figure A-100. Residual (Simulated - Observed) vs. Flow Nitrite+ Nitrate Nitrogen (NOx) at St. Louis R blw Cloquet R (S000-023)

A.4.5 Total Nitrogen (TN)

Table A-15. Total Nitrogen (TN) statistics

Period	1994-2001	2002-2012
Count	40.74%	9.84%
Concentration Average Error	33.42%	7.81%
Concentration Median Error	44.68%	5.01%
Load Average Error	36.15%	4.38%
Load Median Error	0.00	0.85
Paired t conc	0.19	0.77
Paired t load	40.74%	9.84%

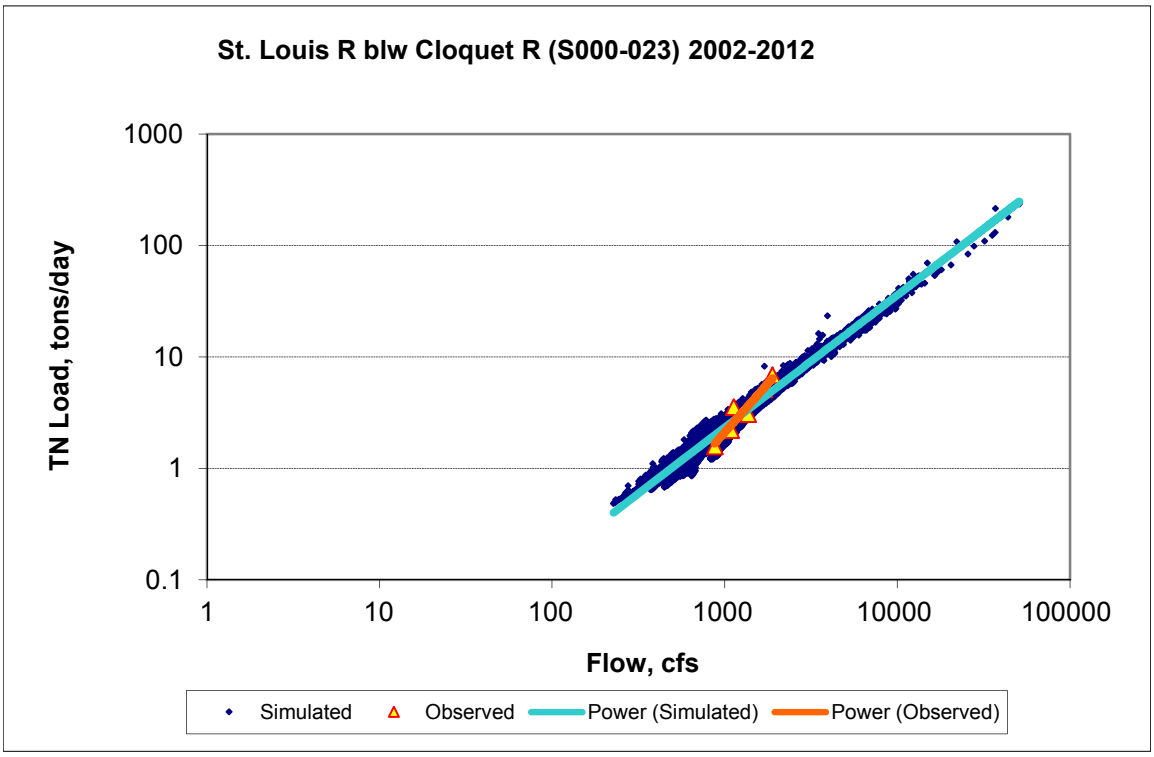

Figure A-101. Power plot of simulated and observed Total Nitrogen (TN) load vs flow at St. Louis R blw Cloquet R (S000-023) (calibration period)

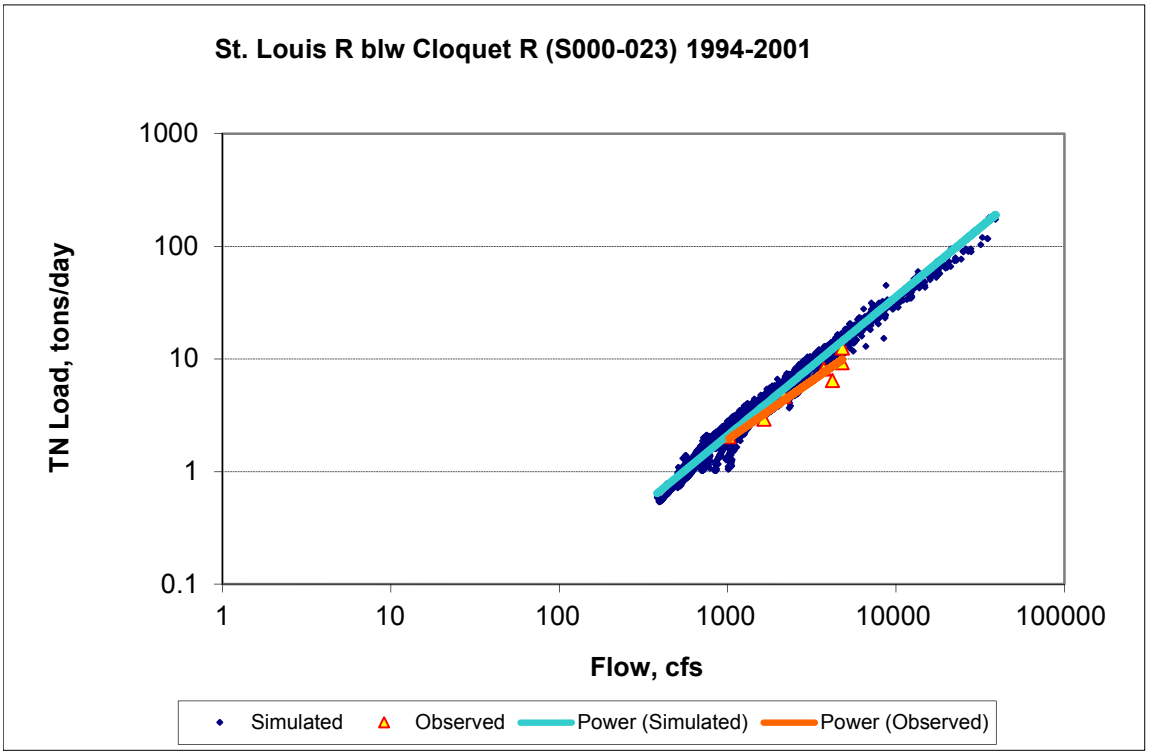

Figure A-102. Power plot of simulated and observed Total Nitrogen (TN) load vs flow at St. Louis R blw Cloquet R (S000-023) (validation period)

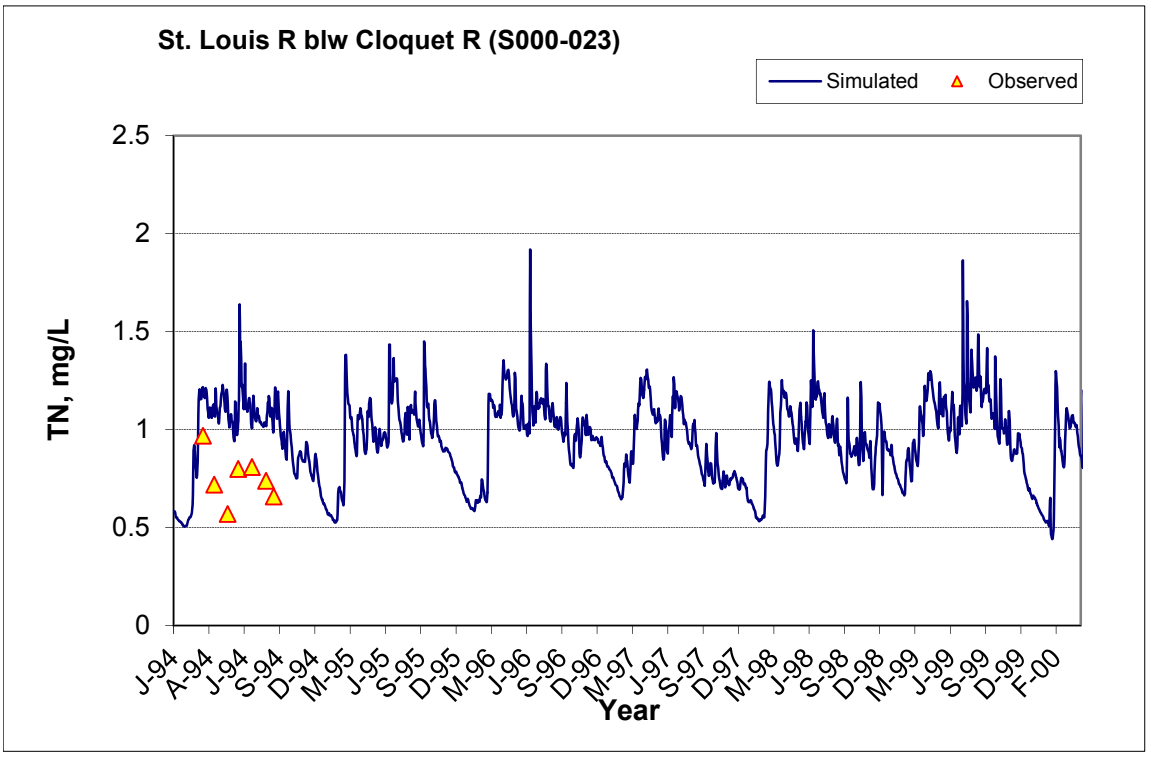
St. Louis R blw Cloquet R (S000-023)
Simulated
Observed
TN, mg/L
2.5
2
1.5
1
0.5
0
J-94 A-94 J-94 S-94 D-94 M-95 J-95 S-95 D-95 M-96 J-96 S-96 D-96 M-97 J-97 S-97 D-97 M-98 J-98 S-98 D-98 M-99 J-99 S-99 D-99 F-00
Year

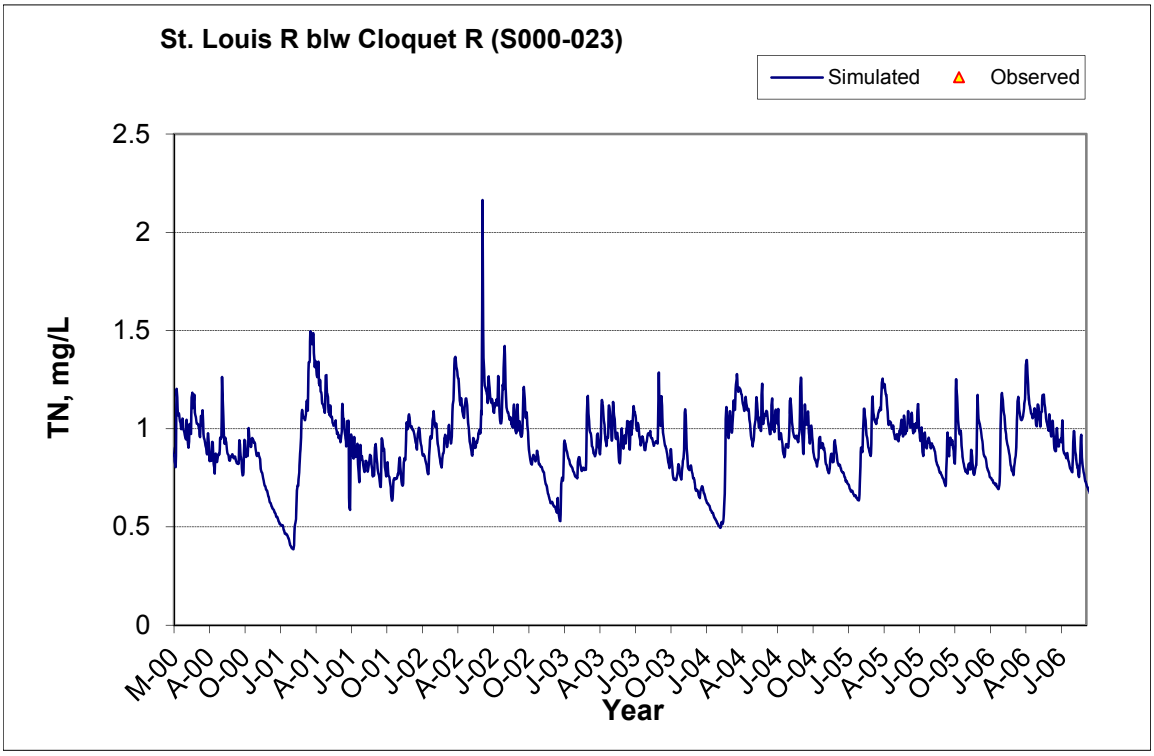
St. Louis R blw Cloquet R (S000-023)
Simulated
Observed
TN, mg/L
2.5
2
1.5
1
0.5
0
M-00 A-00 O-00 J-01 A-01 J-01 O-01 J-02 A-02 J-02 O-02 J-03 A-03 J-03 O-03 J-04 A-04 J-04 O-04 J-05 A-05 J-05 O-05 J-06 A-06 J-06
Year

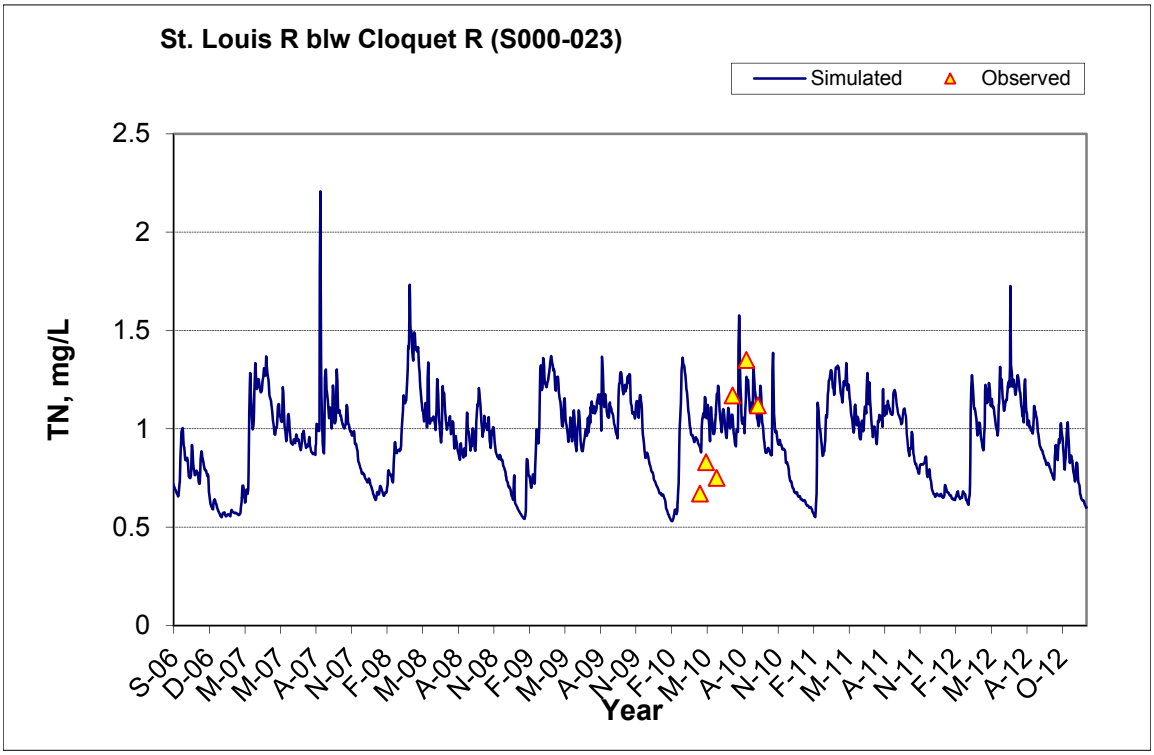

Figure A-103. Time series of observed and simulated Total Nitrogen (TN) concentration at St. Louis R blw Cloquet R (S000-023)

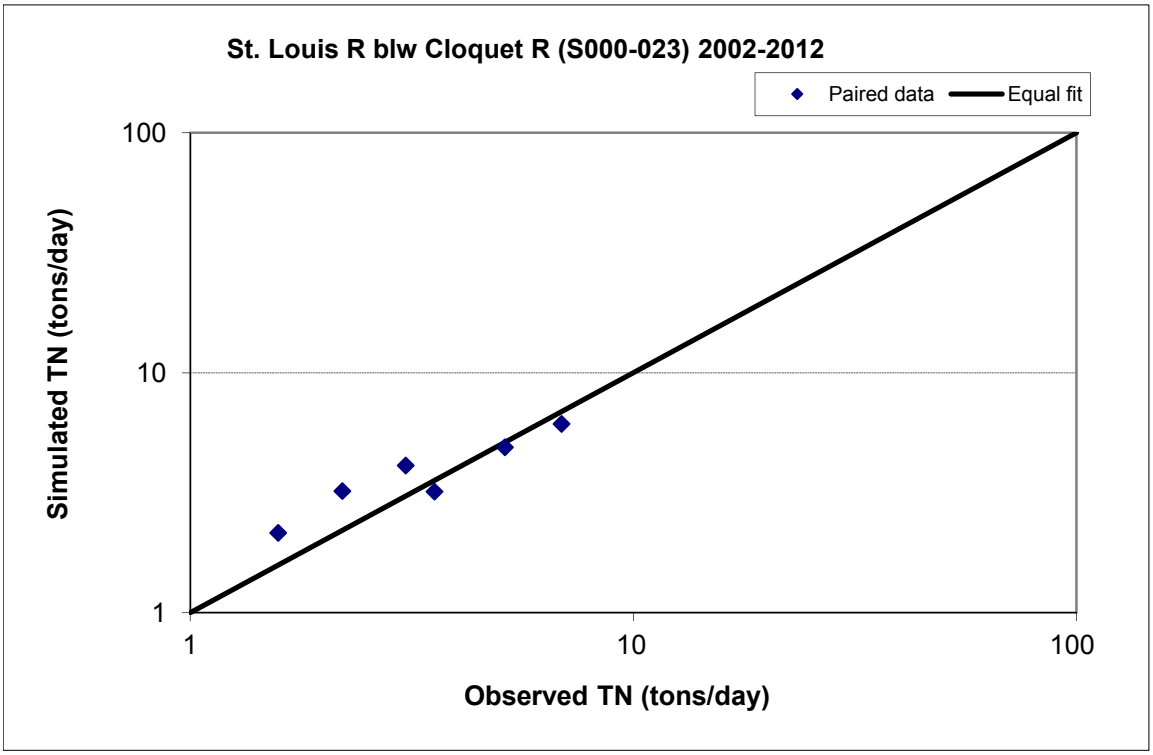

Figure A-104. Paired simulated vs. observed Total Nitrogen (TN) load at St. Louis R blw Cloquet R (S000-023) (calibration period)

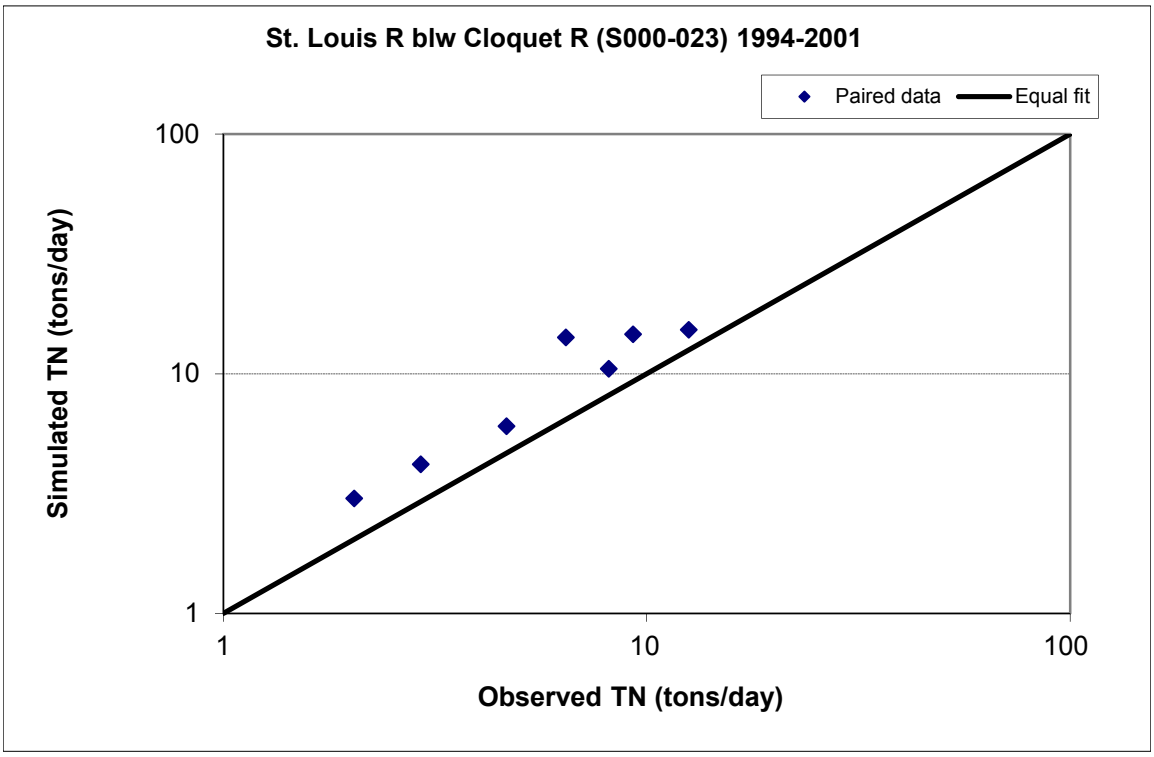

Figure A-105. Paired simulated vs. observed Total Nitrogen (TN) load at St. Louis R blw Cloquet R (S000-023) (validation period)

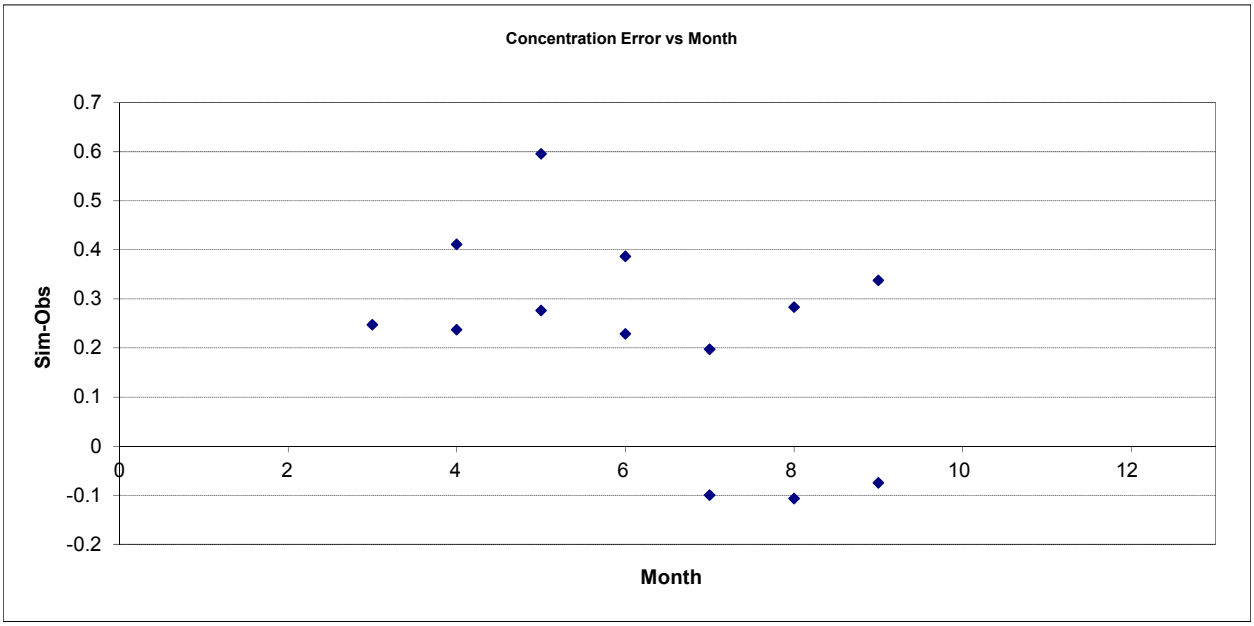

Figure A-106. Residual (Simulated - Observed) vs. Month Total Nitrogen (TN) at St. Louis R blw Cloquet R (S000-023)

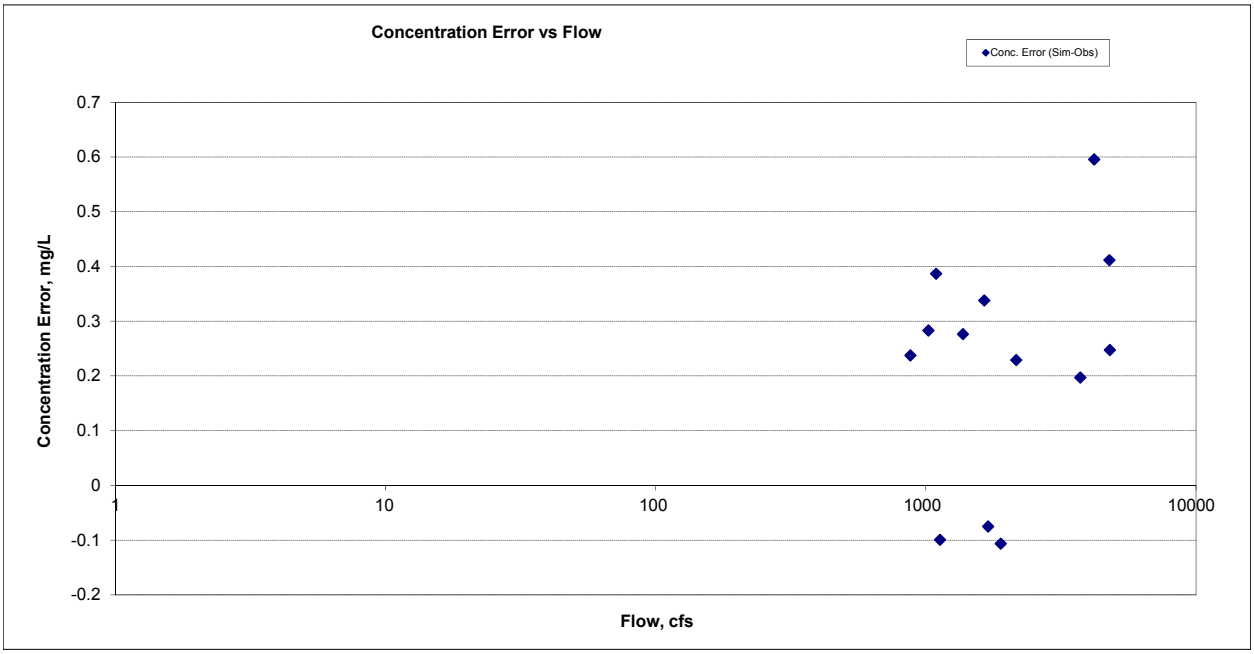

Figure A-107. Residual (Simulated - Observed) vs. Flow Total Nitrogen (TN) at St. Louis R blw Cloquet R (S000-023)

A.4.6 Soluble Reactive Phosphorus (SRP)

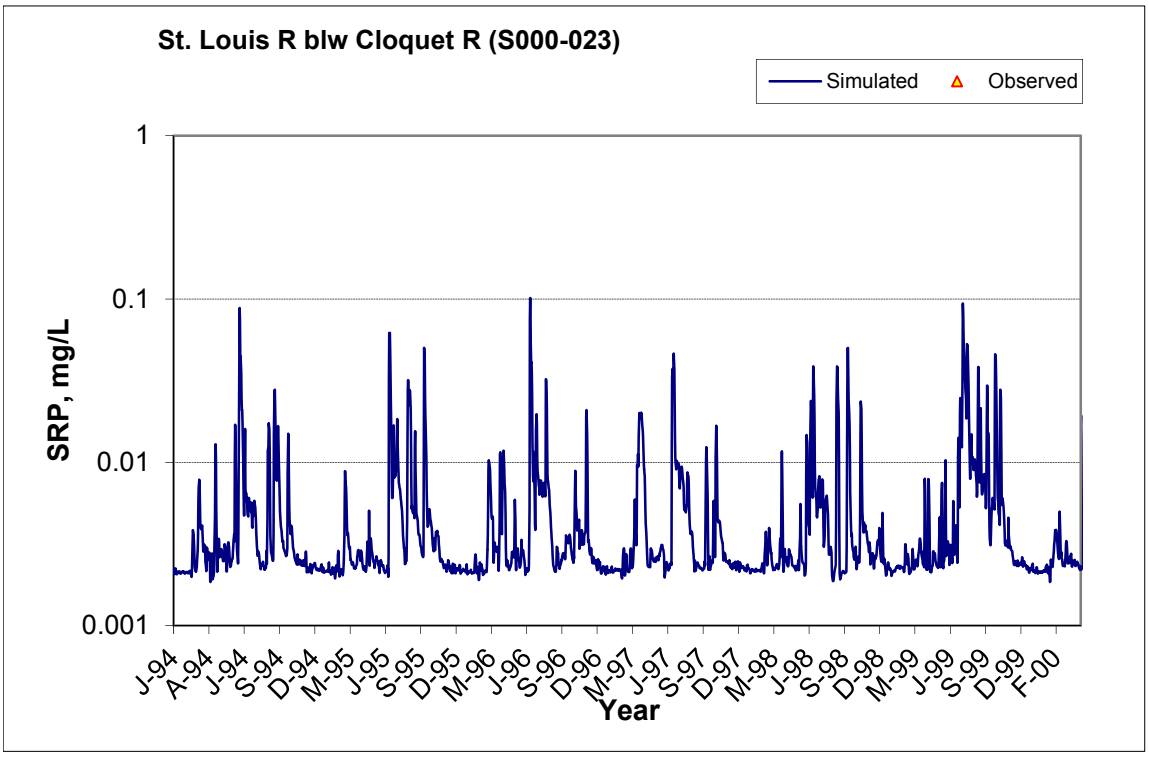

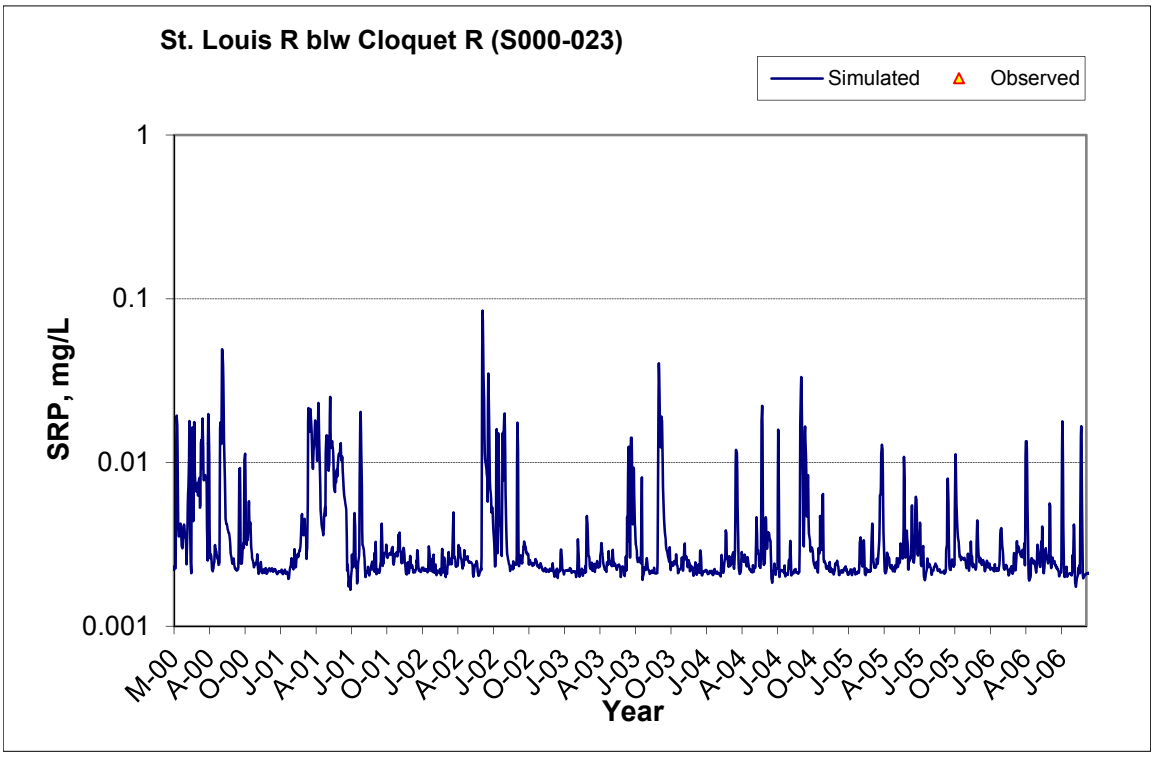

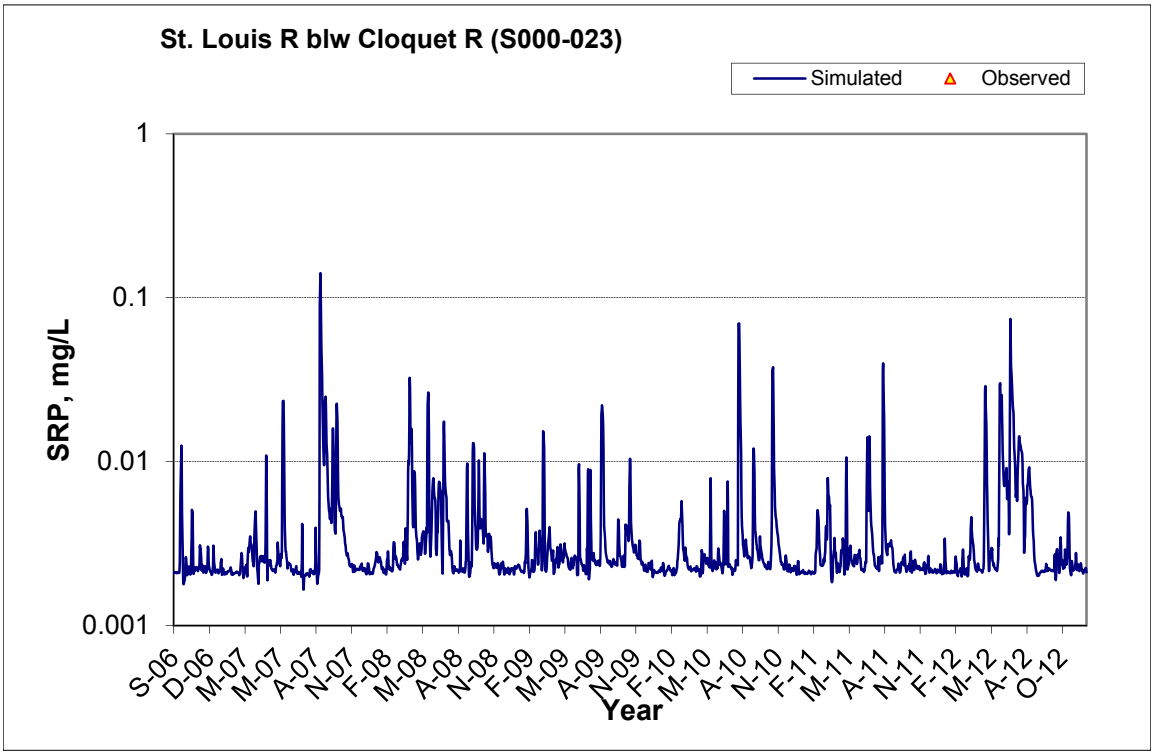

Figure A-108. Time series of observed and simulated Soluble Reactive Phosphorus (SRP) concentration at St. Louis R blw Cloquet R (S000-023)

A.4.7 Organic Phosphorus (OrgP)

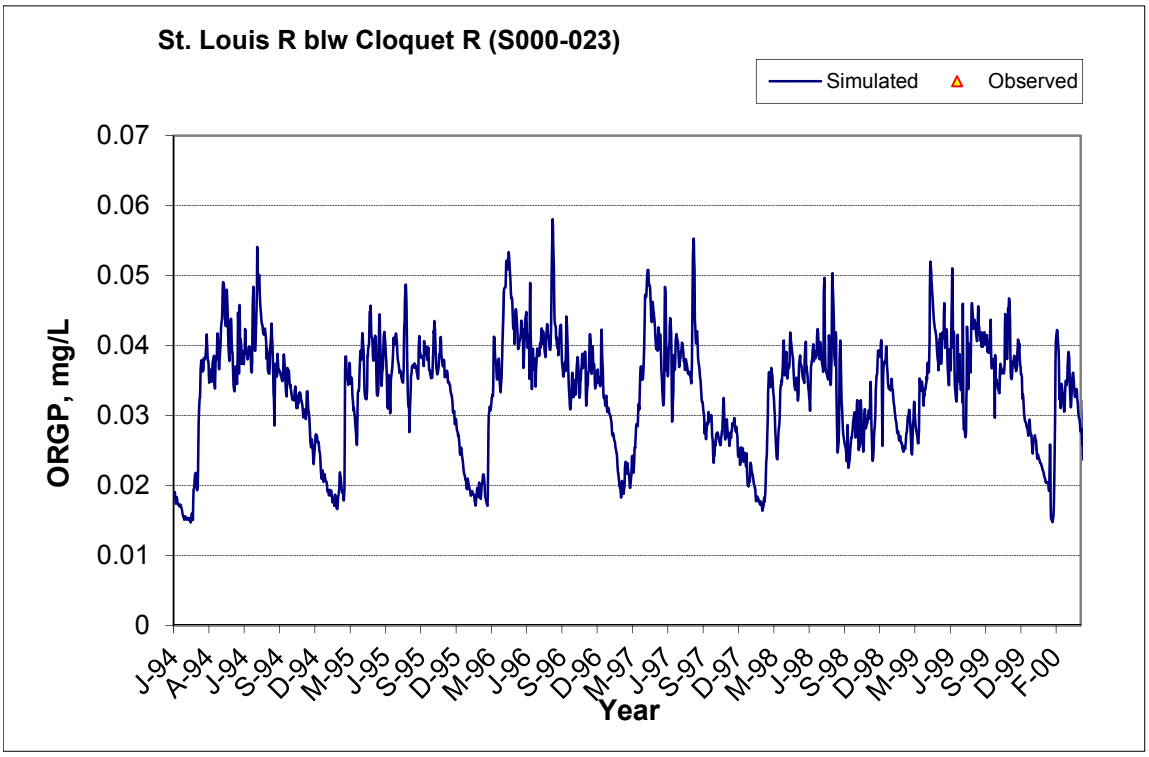

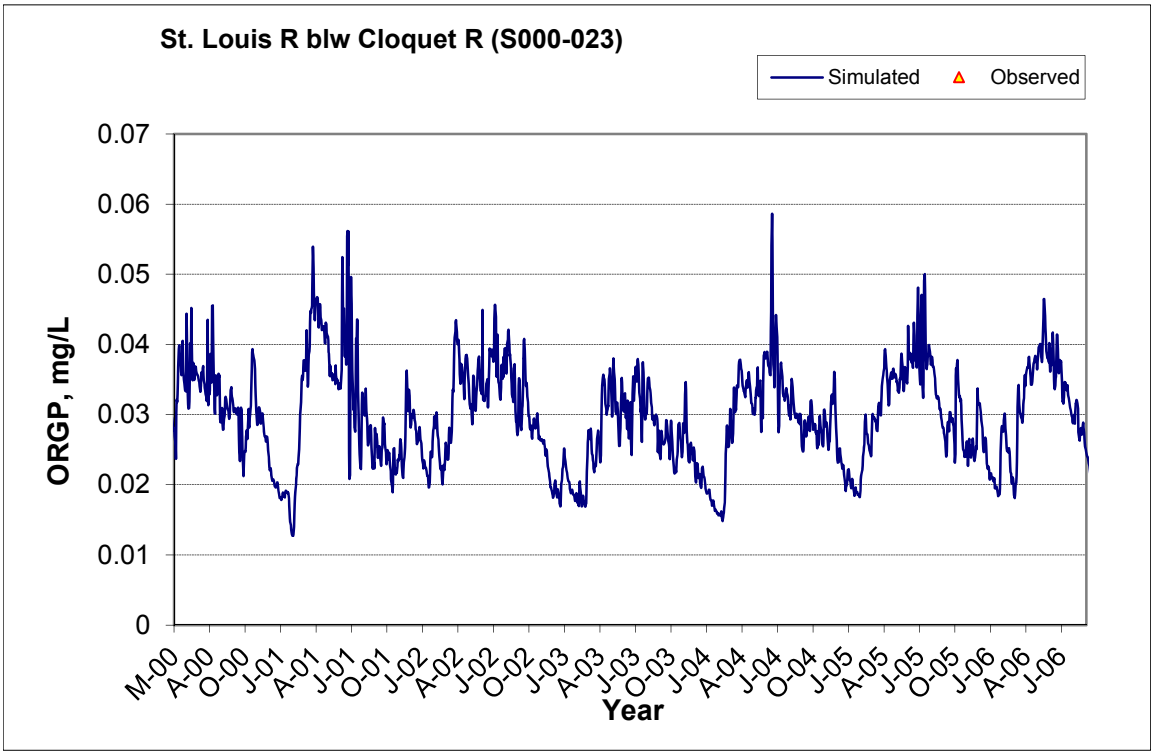

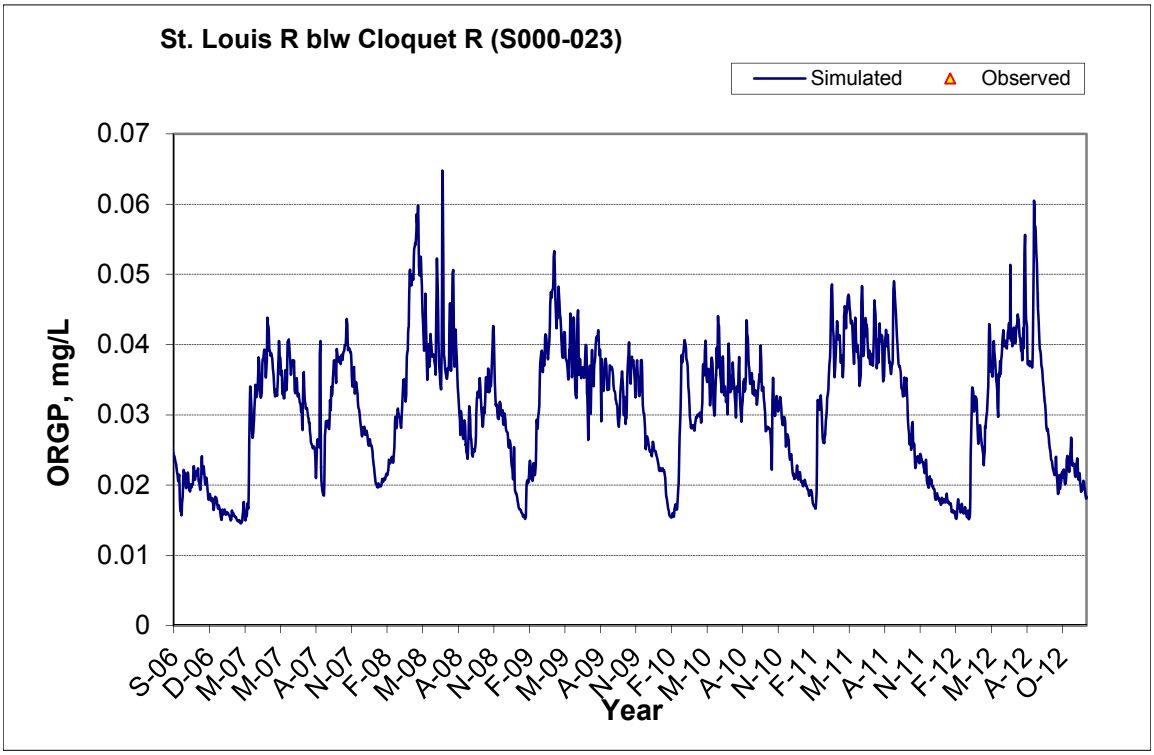

Figure A-109. Time series of observed and simulated Organic Phosphorus (OrgP) concentration at St. Louis R blw Cloquet R (S000-023)

A.4.8 Total Phosphorus (TP)

Table A-16. Total Phosphorus (TP) statistics

Period	1994-2001	2002-2012
Count	9	39
Concentration Average Error	0.91%	-17.68%
Concentration Median Error	10.54%	2.81%
Load Average Error	-3.29%	-4.43%
Load Median Error	6.72%	1.30%
Paired t conc	0.97	0.63
Paired t load	0.77	0.90

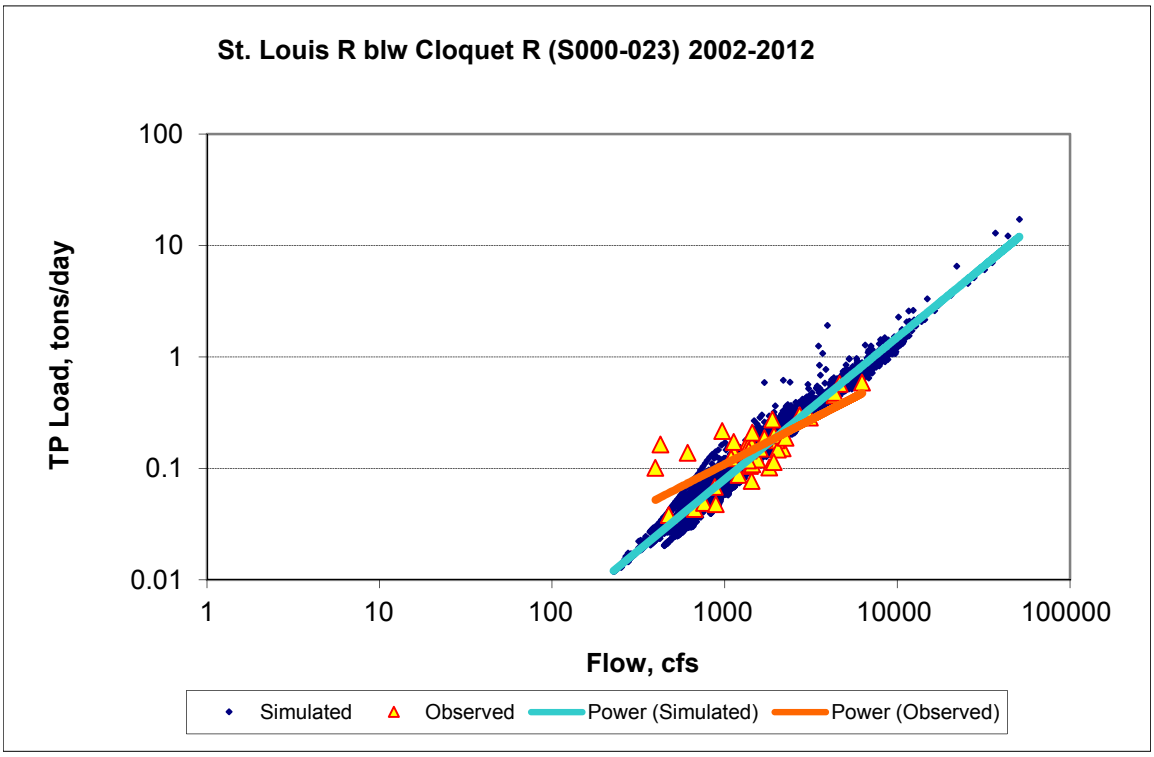

Figure A-110. Power plot of simulated and observed Total Phosphorus (TP) load vs flow at St. Louis R blw Cloquet R (S000-023) (calibration period)

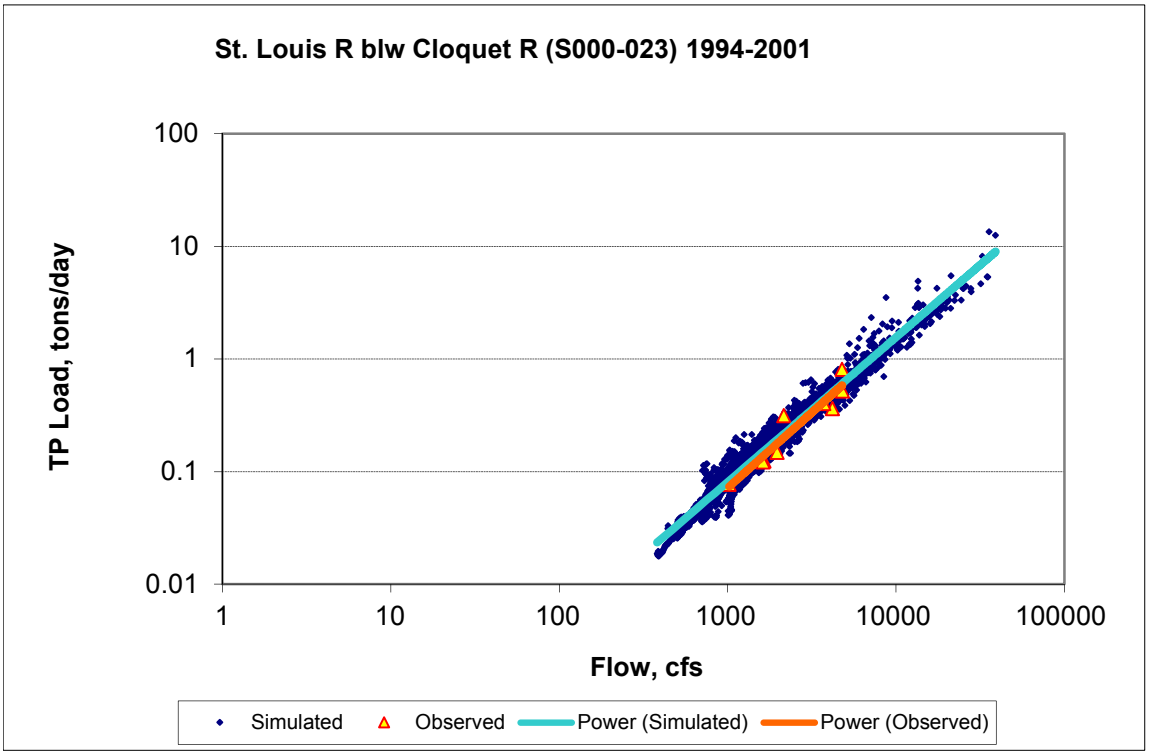

Figure A-111. Power plot of simulated and observed Total Phosphorus (TP) load vs flow at St. Louis R blw Cloquet R (S000-023) (validation period)

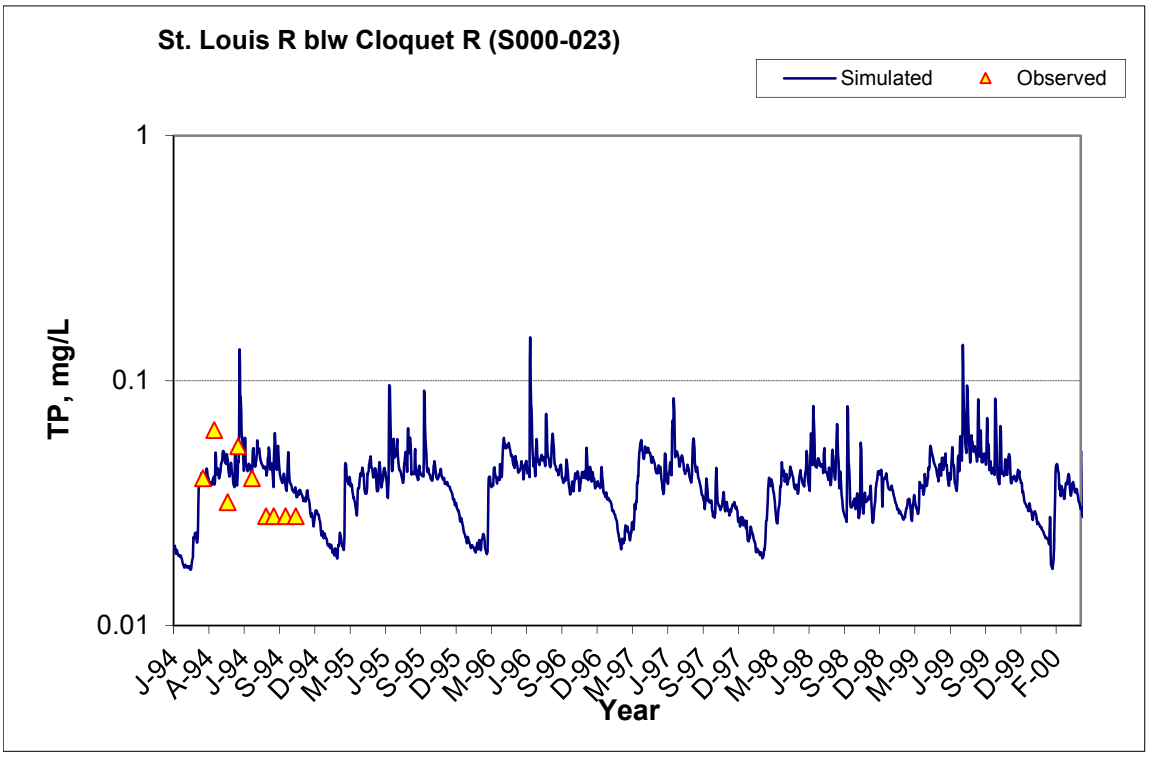
St. Louis R blw Cloquet R (S000-023)
Simulated
Observed
TP, mg/L
1
0.1
0.01
J-94 A-94 J-94 S-94 D-94 M-95 J-95 S-95 D-95 M-96 J-96 S-96 D-96 M-97 J-97 S-97 D-97 M-98 J-98 S-98 D-98 M-99 J-99 S-99 D-99 F-00
Year

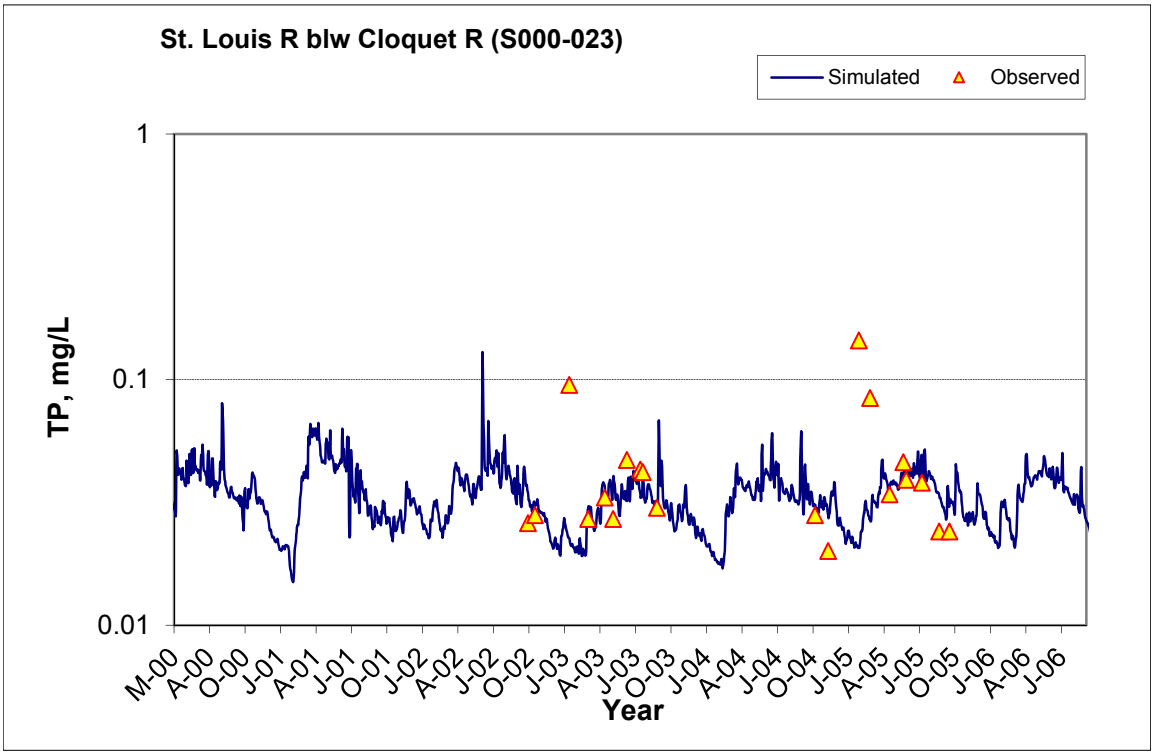
St. Louis R blw Cloquet R (S000-023)
Simulated
Observed
TP, mg/L
1
0.1
0.01
M-00 A-00 O-00 J-01 A-01 J-01 O-01 J-02 A-02 J-02 O-02 J-03 A-03 J-03 O-03 J-04 A-04 J-04 O-04 J-05 A-05 J-05 O-05 J-06 A-06 J-06
Year

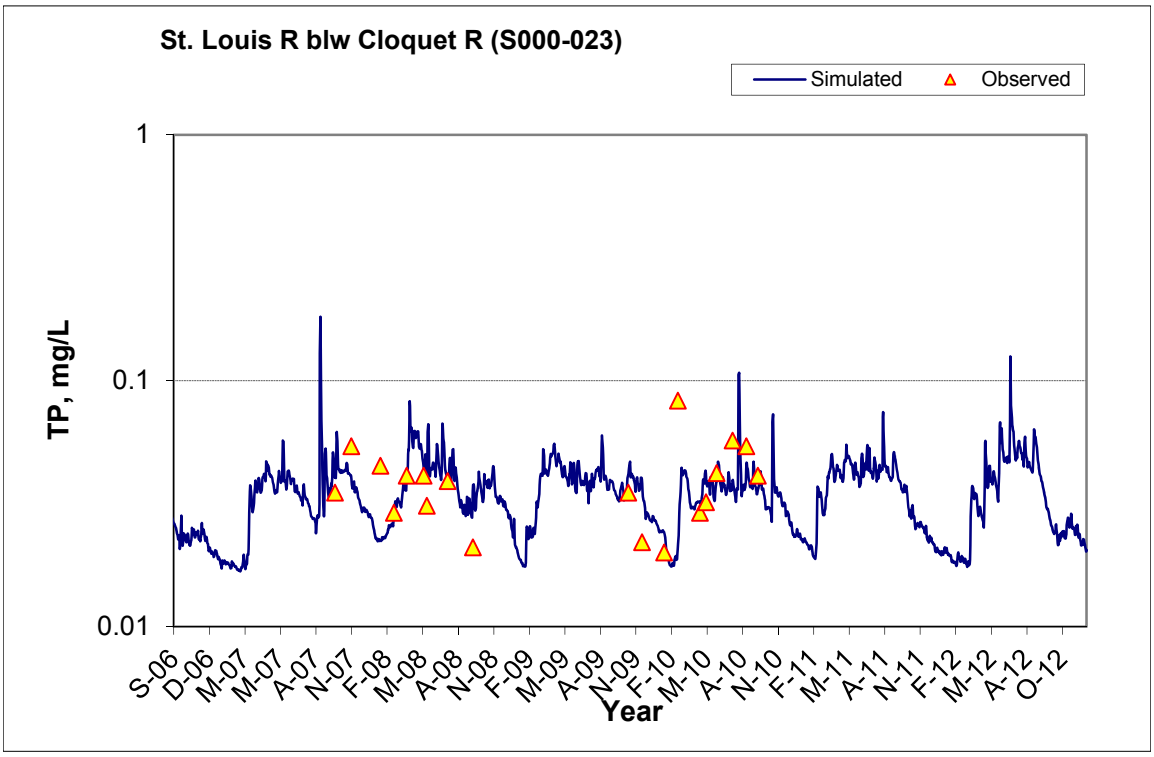

Figure A-112. Time series of observed and simulated Total Phosphorus (TP) concentration at St. Louis R blw Cloquet R (S000-023)

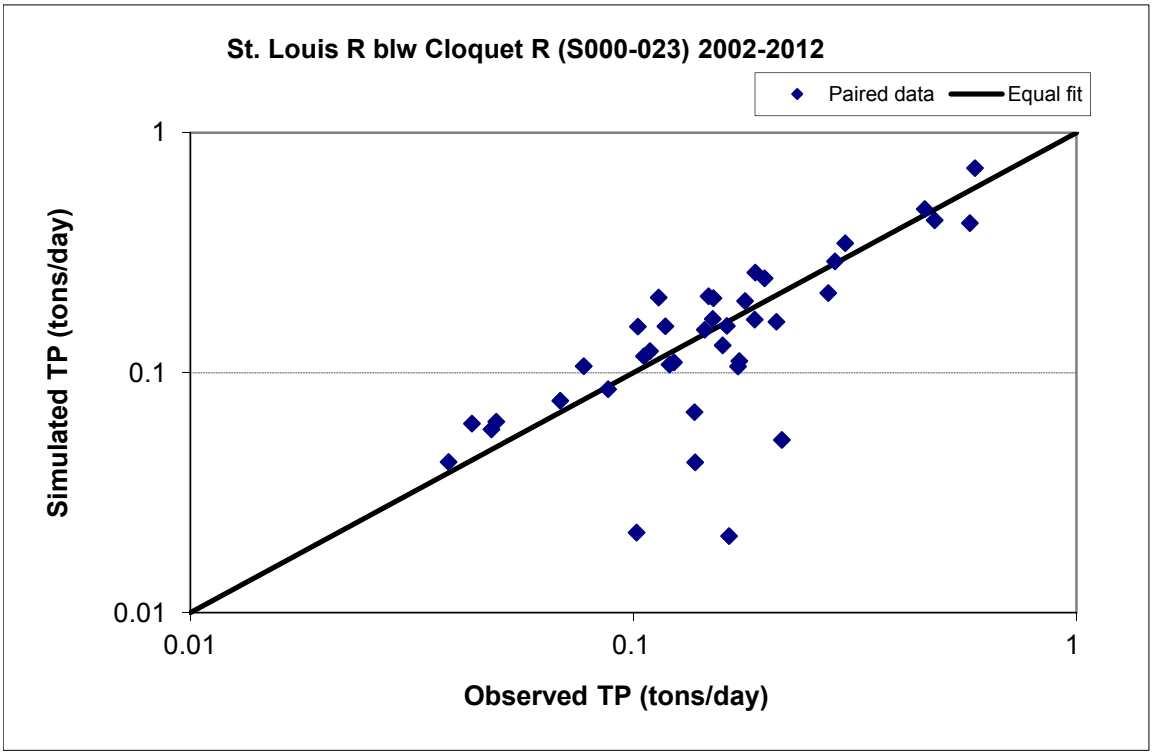

Figure A-113. Paired simulated vs. observed Total Phosphorus (TP) load at St. Louis R blw Cloquet R (S000-023) (calibration period)

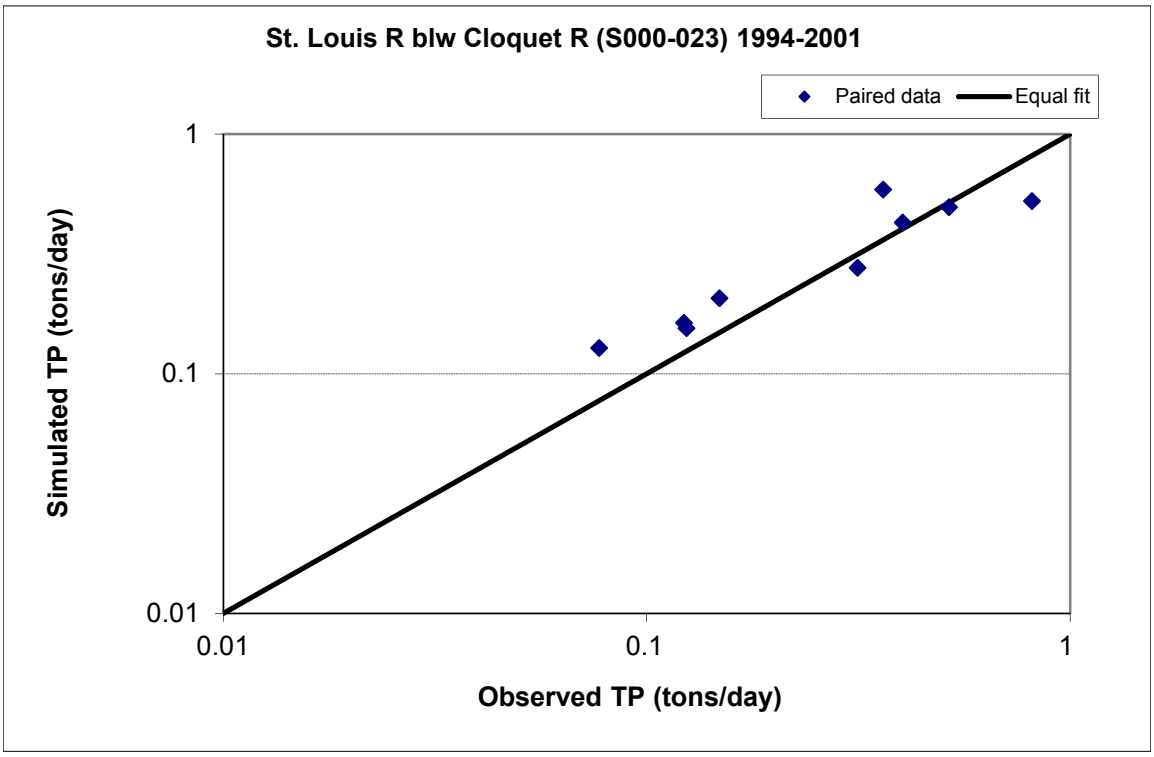

Figure A-114. Paired simulated vs. observed Total Phosphorus (TP) load at St. Louis R blw Cloquet R (S000-023) (validation period)

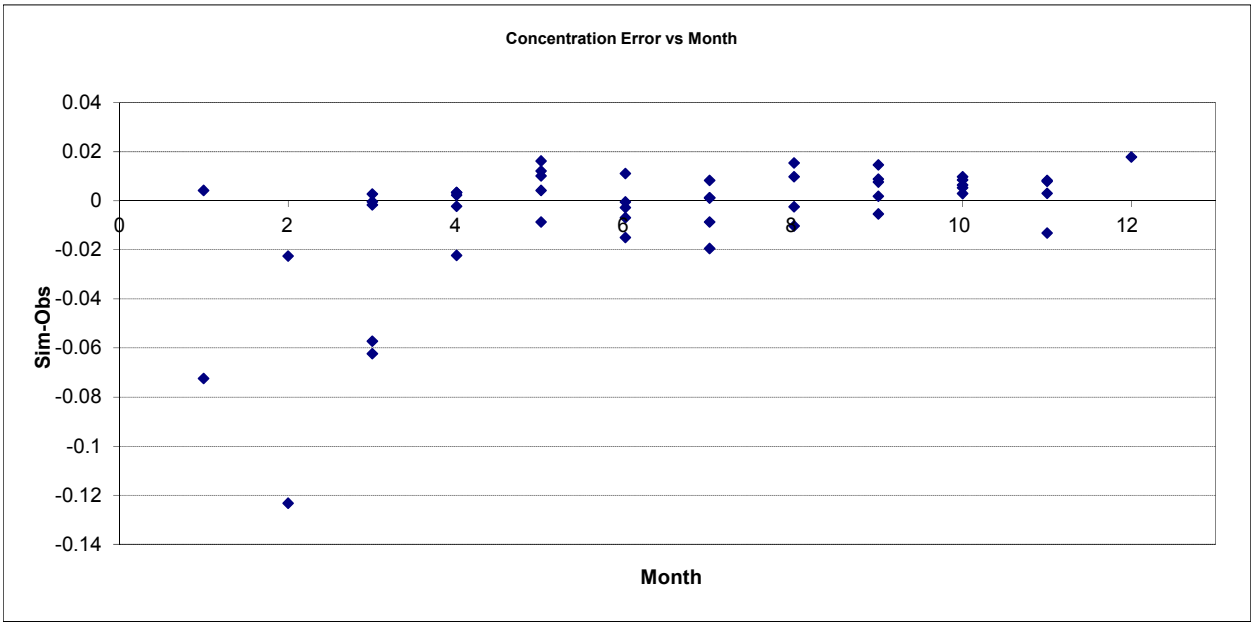

Figure A-115. Residual (Simulated - Observed) vs. Month Total Phosphorus (TP) at St. Louis R blw Cloquet R (S000-023)

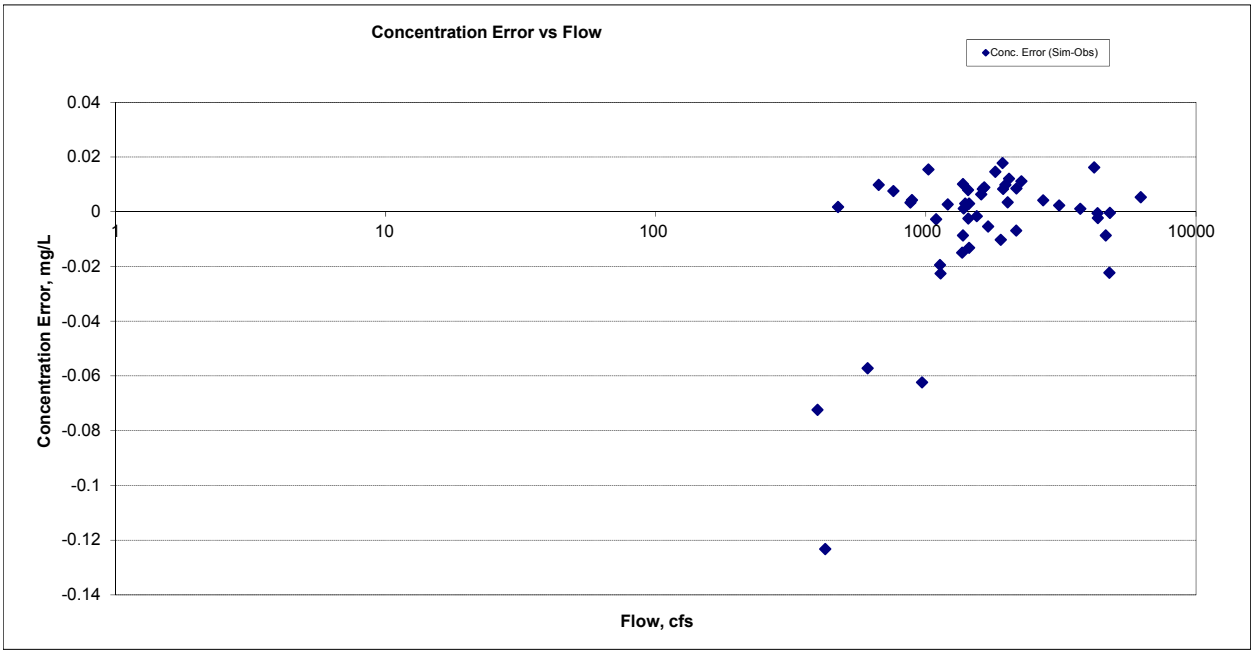

Figure A-116. Residual (Simulated - Observed) vs. Flow Total Phosphorus (TP) at St. Louis R blw Cloquet R (S000-023)

A.5 ST. LOUIS RIVER AT SCANLON, MN (03174001)

A.5.1 Ammonia Nitrogen (NH3)

Table A-17. Ammonia Nitrogen (NH3) statistics

Period	1994-2001	2002-2012
Count	17	66
Concentration Average Error	-69.31%	12.30%
Concentration Median Error	-65.21%	25.74%
Load Average Error	-74.22%	10.40%
Load Median Error	-32.56%	13.94%
Paired t conc	0.00	0.77
Paired t load	0.00	0.64

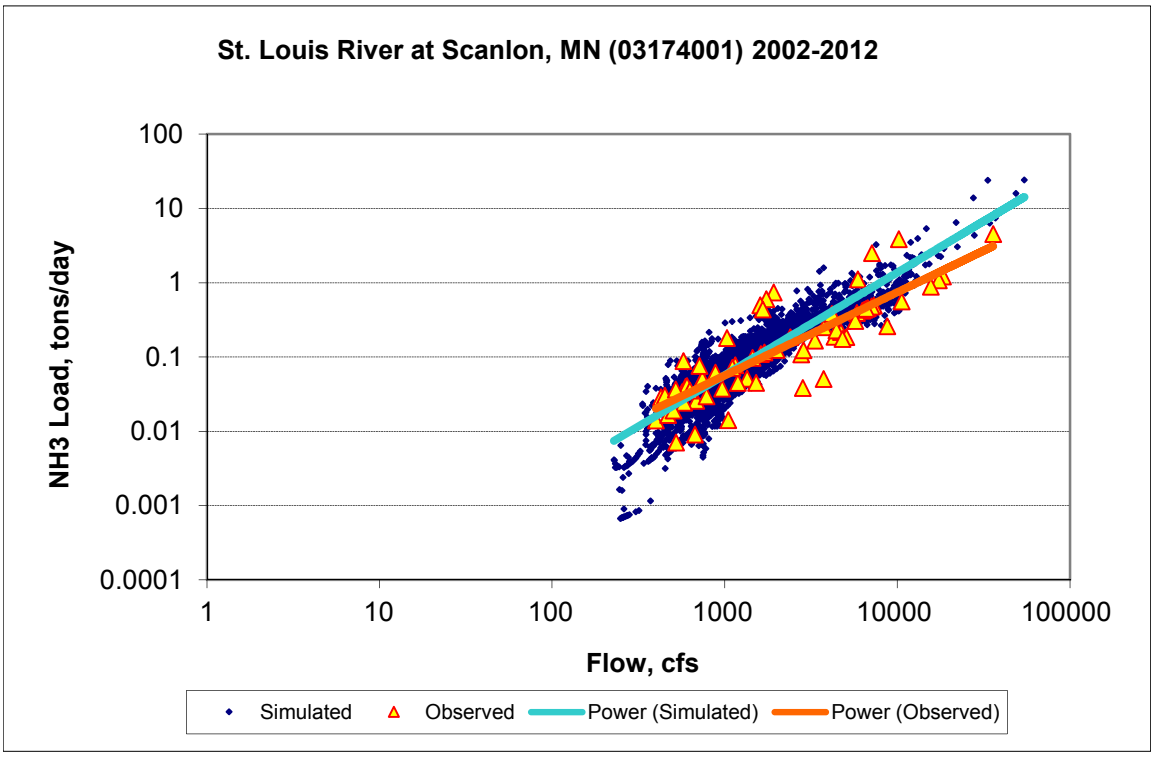

Figure A-117. Power plot of simulated and observed Ammonia Nitrogen (NH3) load vs flow at St. Louis River at Scanlon, MN (03174001) (calibration period)

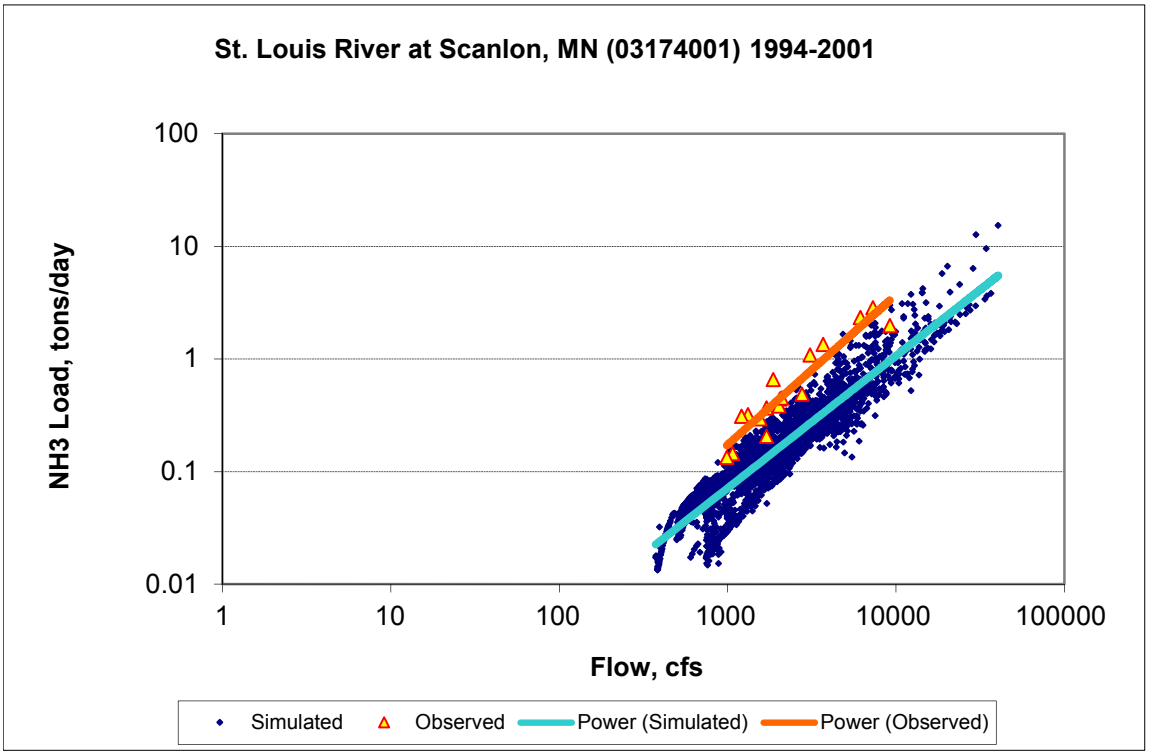

Figure A-118. Power plot of simulated and observed Ammonia Nitrogen (NH3) load vs flow at St. Louis River at Scanlon, MN (03174001) (validation period)

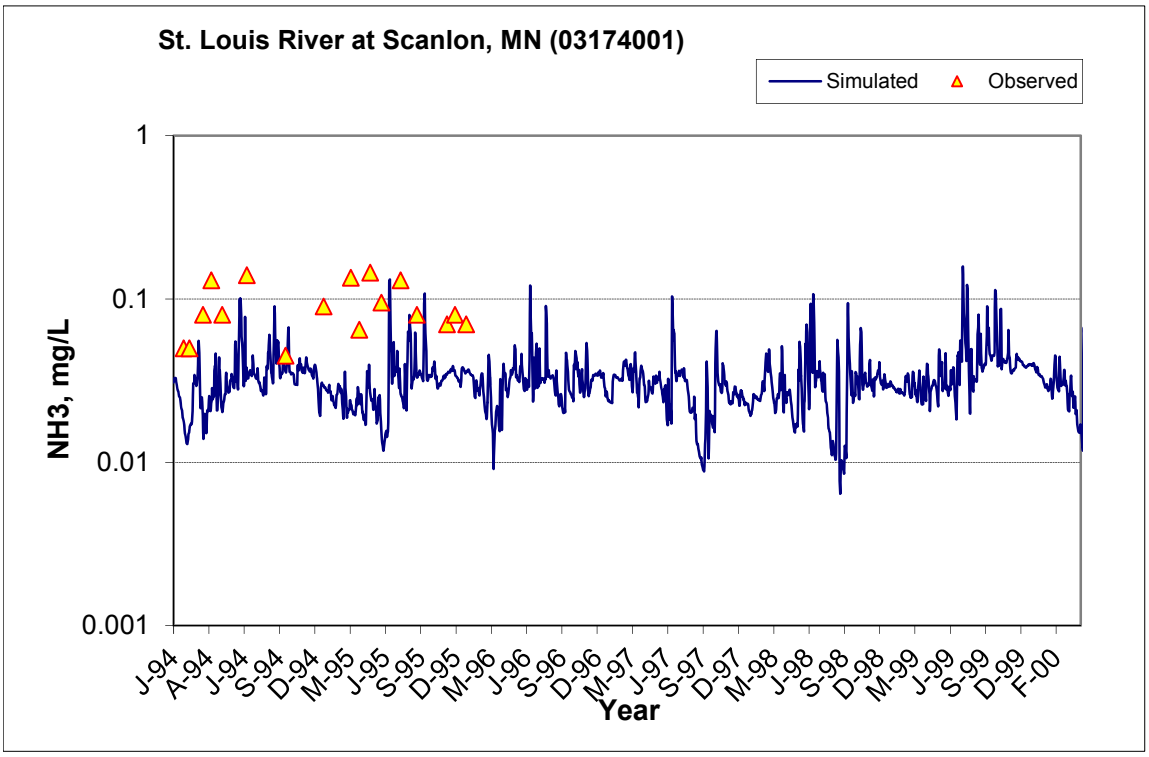
St. Louis River at Scanlon, MN (03174001)
Simulated
Observed
NH3, mg/L
1
0.1
0.01
0.001
J-94 A-94 J-94 S-94 D-94 M-95 J-95 S-95 D-95 M-96 J-96 S-96 D-96 M-97 J-97 S-97 D-97 M-98 J-98 S-98 D-98 M-99 J-99 S-99 D-99 F-00
Year

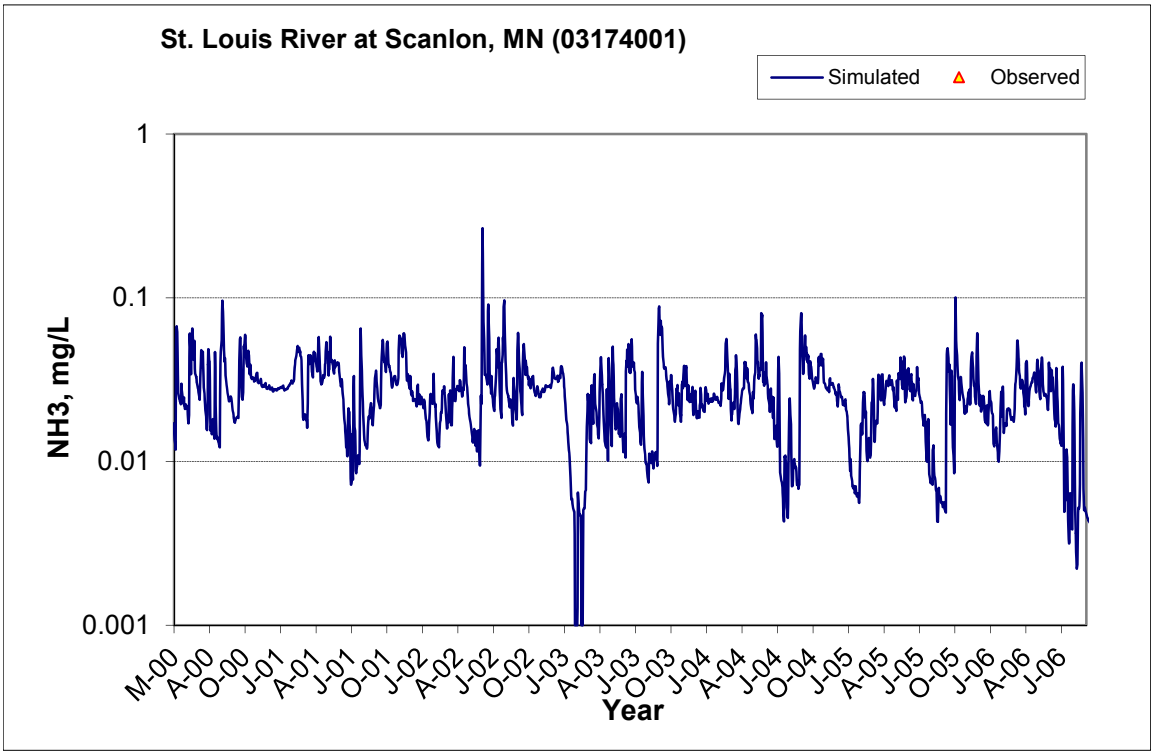
St. Louis River at Scanlon, MN (03174001)
Simulated
Observed
NH3, mg/L
1
0.1
0.01
0.001
M-00 A-00 O-00 J-01 A-01 J-01 O-01 J-02 A-02 J-02 O-02 J-03 A-03 J-03 O-03 J-04 A-04 J-04 O-04 J-05 A-05 J-05 O-05 J-06 A-06 J-06
Year

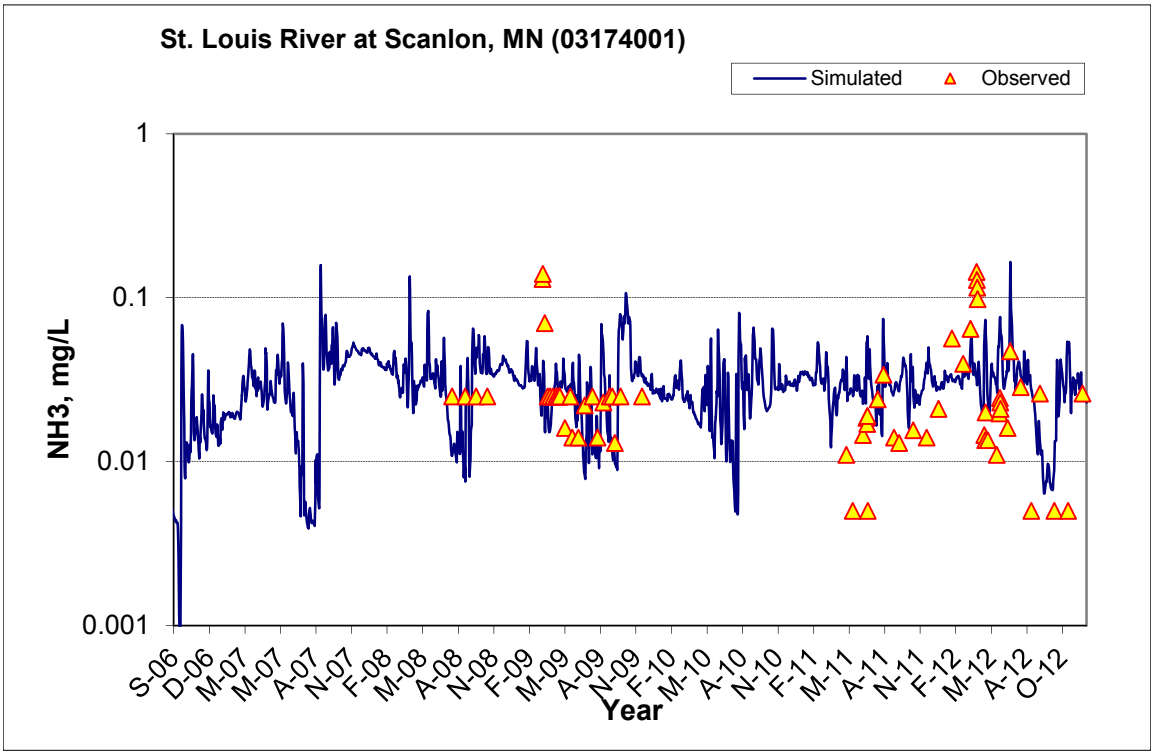

Figure A-119. Time series of observed and simulated Ammonia Nitrogen (NH3) concentration at St. Louis River at Scanlon, MN (03174001)

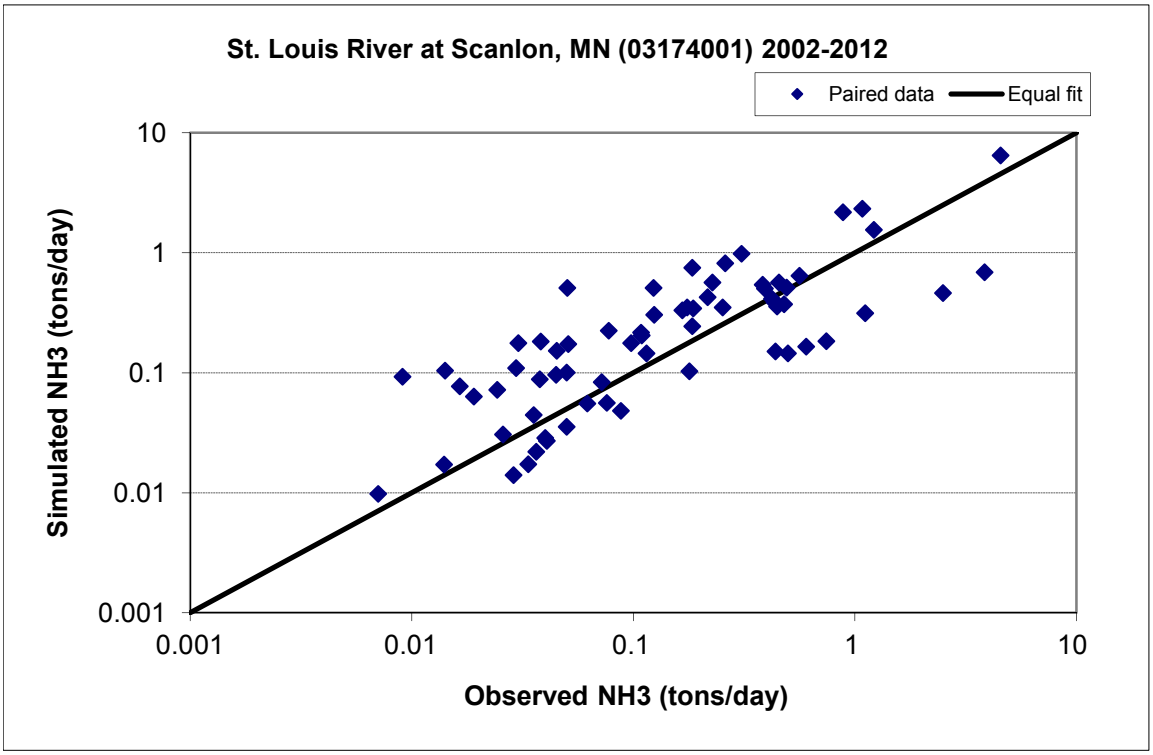

Figure A-120. Paired simulated vs. observed Ammonia Nitrogen (NH3) load at St. Louis River at Scanlon, MN (03174001) (calibration period)

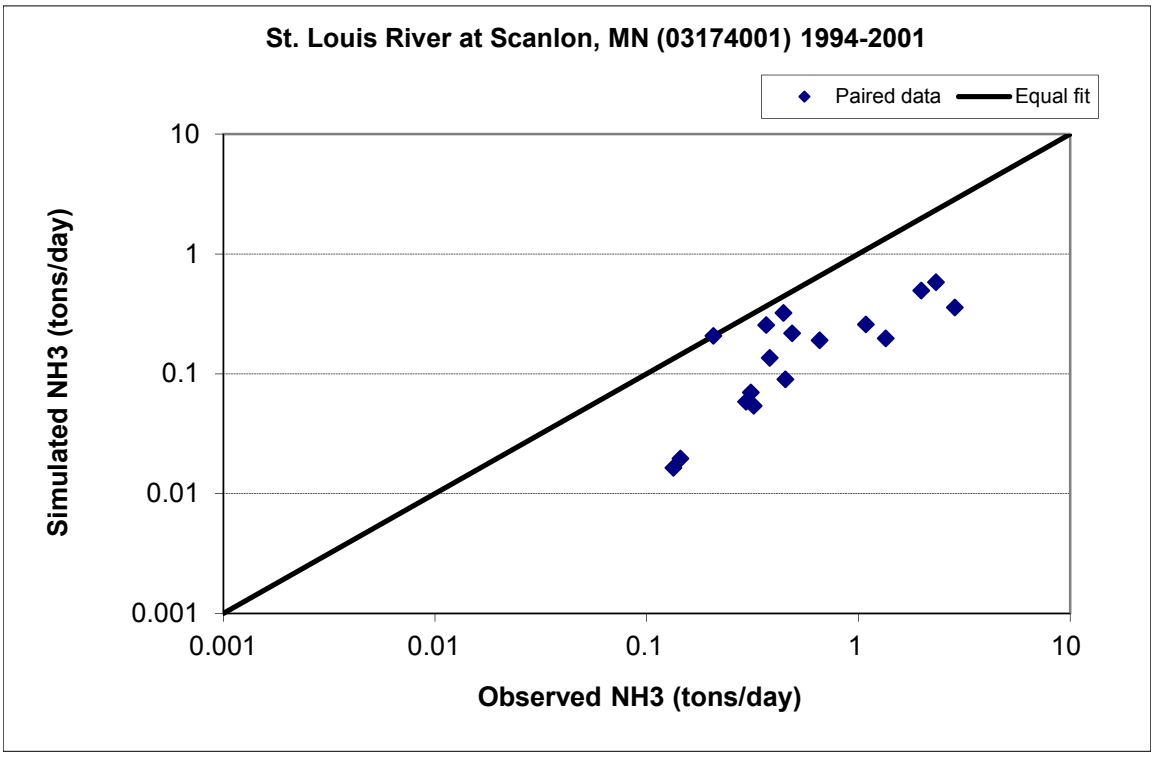

Figure A-121. Paired simulated vs. observed Ammonia Nitrogen (NH3) load at St. Louis River at Scanlon, MN (03174001) (validation period)

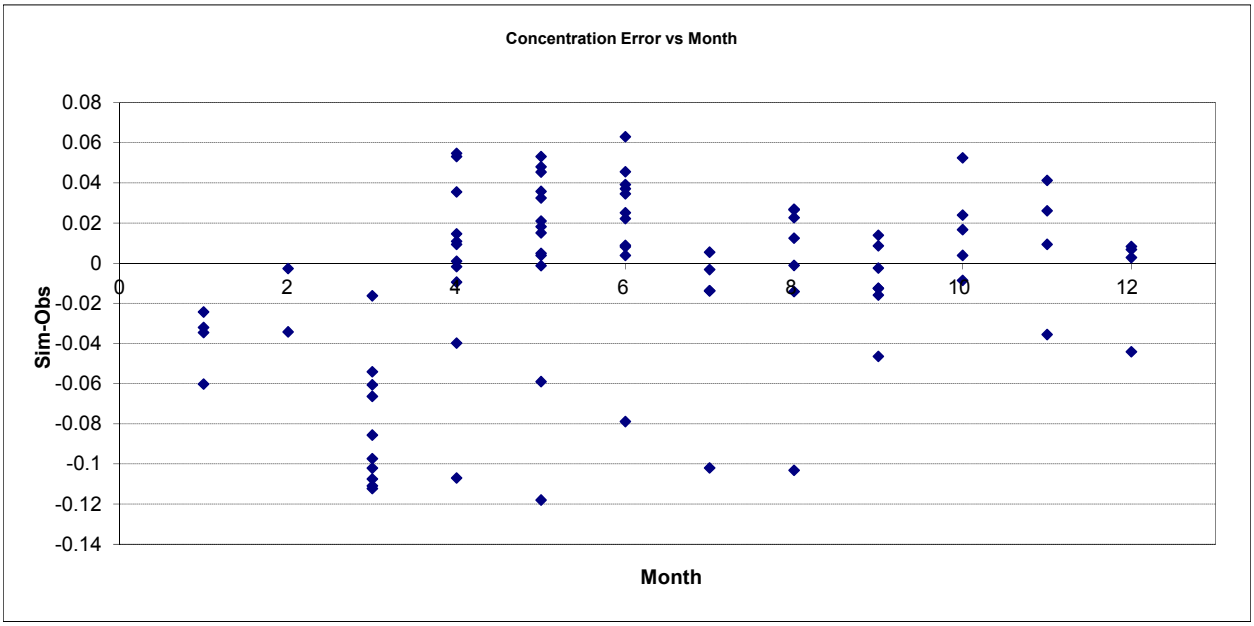

Figure A-122. Residual (Simulated - Observed) vs. Month Ammonia Nitrogen (NH3) at St. Louis River at Scanlon, MN (03174001)

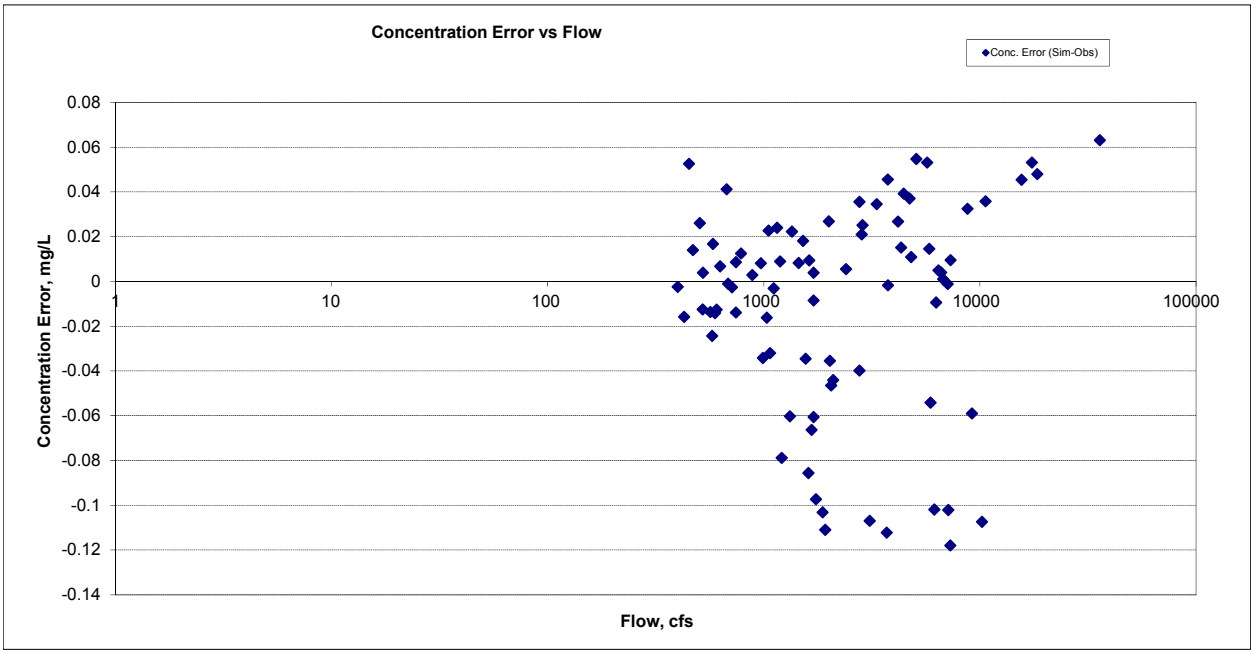

Figure A-123. Residual (Simulated - Observed) vs. Flow Ammonia Nitrogen (NH3) at St. Louis River at Scanlon, MN (03174001)

A.5.2 Organic Nitrogen (OrgN)

Table A-18. Organic Nitrogen (OrgN) statistics

Period	1994-2001	2002-2012
Count	ND	38
Concentration Average Error		7.60%
Concentration Median Error		5.13%
Load Average Error		-29.96%
Load Median Error		0.82%
Paired t conc		0.98
Paired t load		0.34

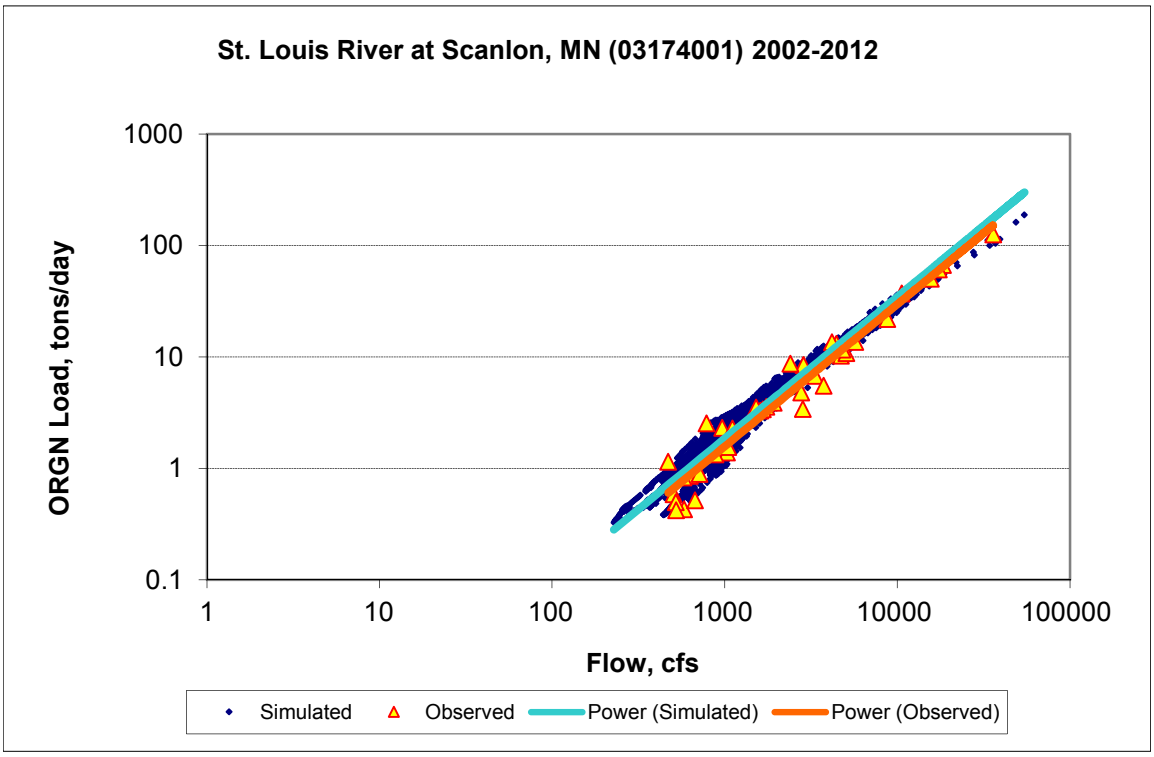

Figure A-124. Power plot of simulated and observed Organic Nitrogen (OrgN) load vs flow at St. Louis River at Scanlon, MN (03174001) (calibration period)

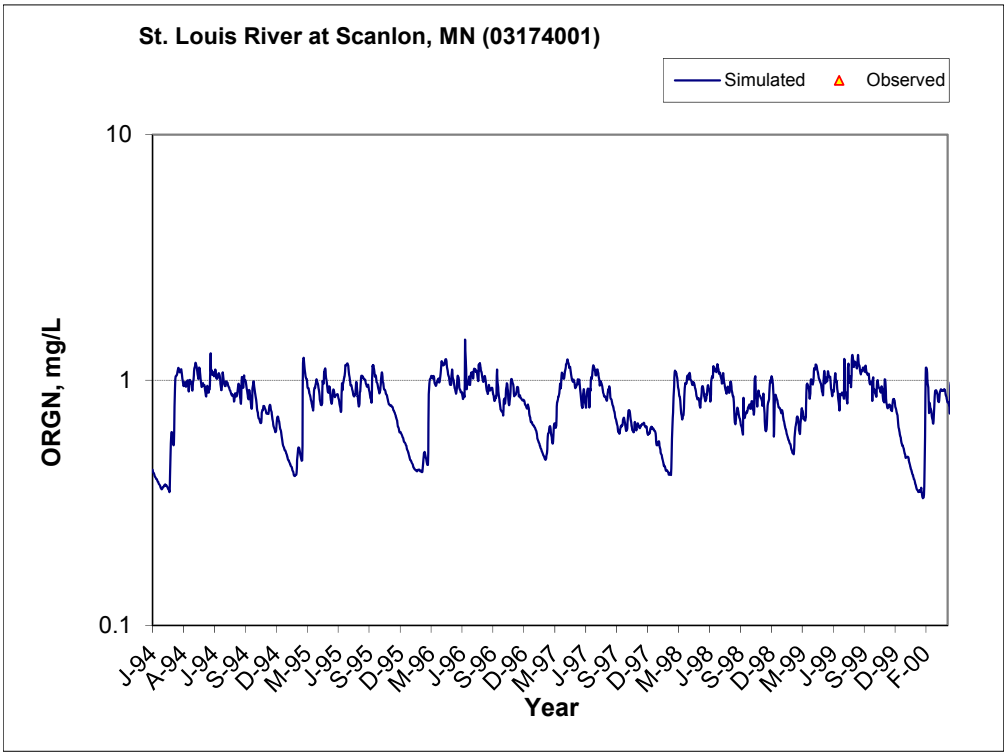

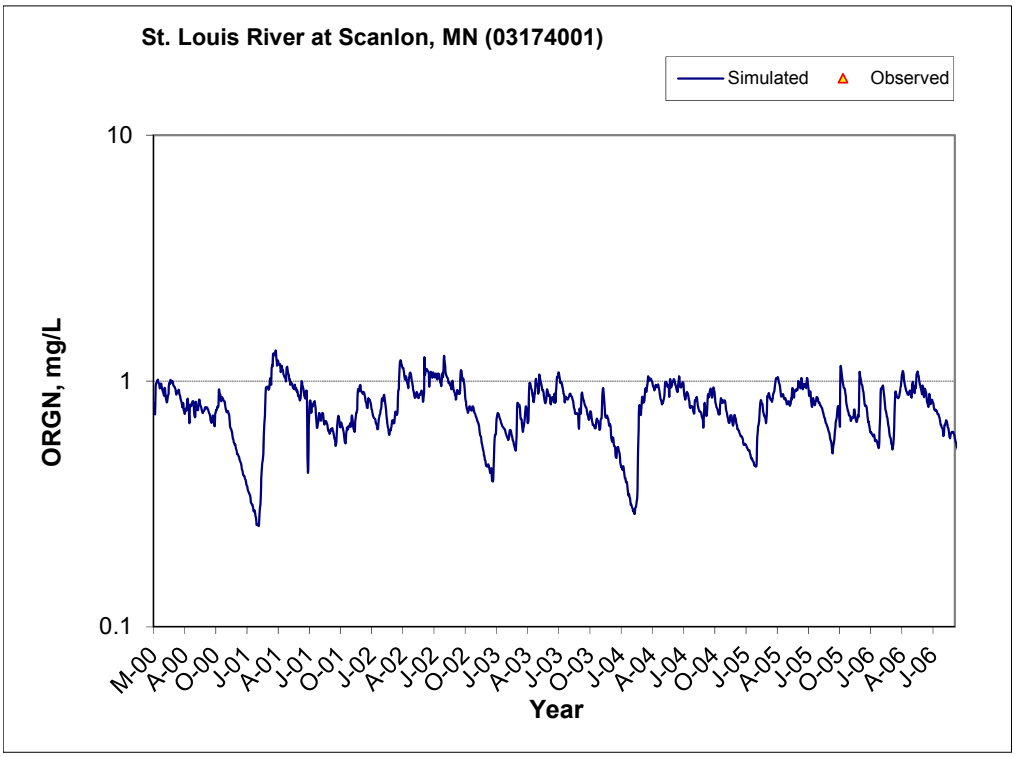

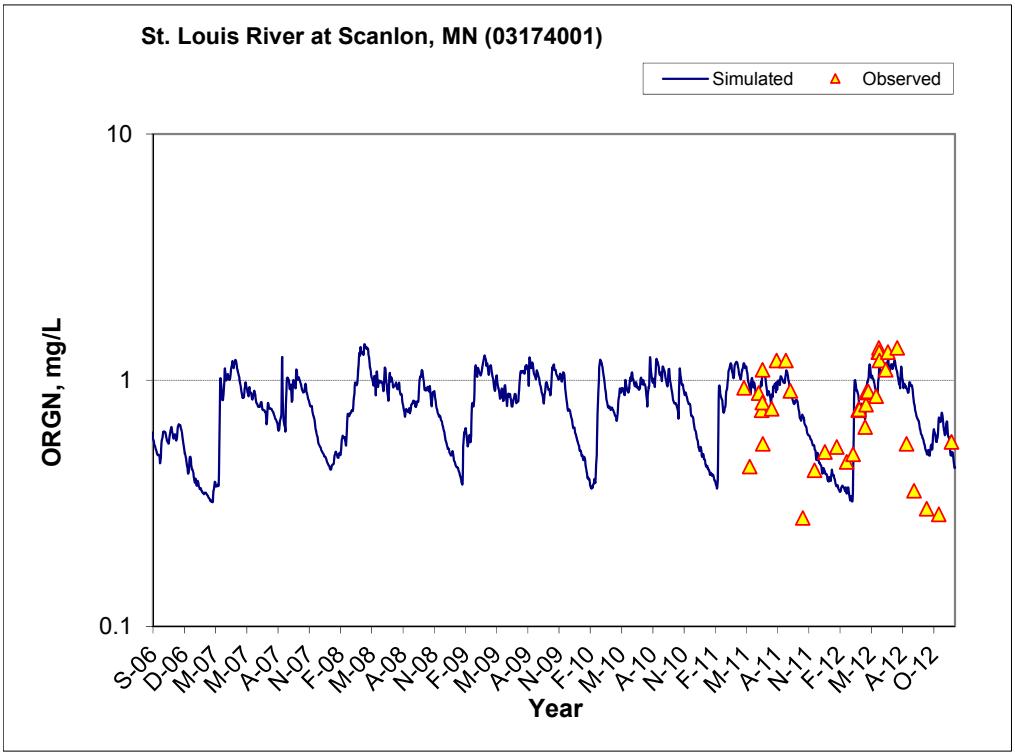

Figure A-125. Time series of observed and simulated Organic Nitrogen (OrgN) concentration at St. Louis River at Scanlon, MN (03174001)

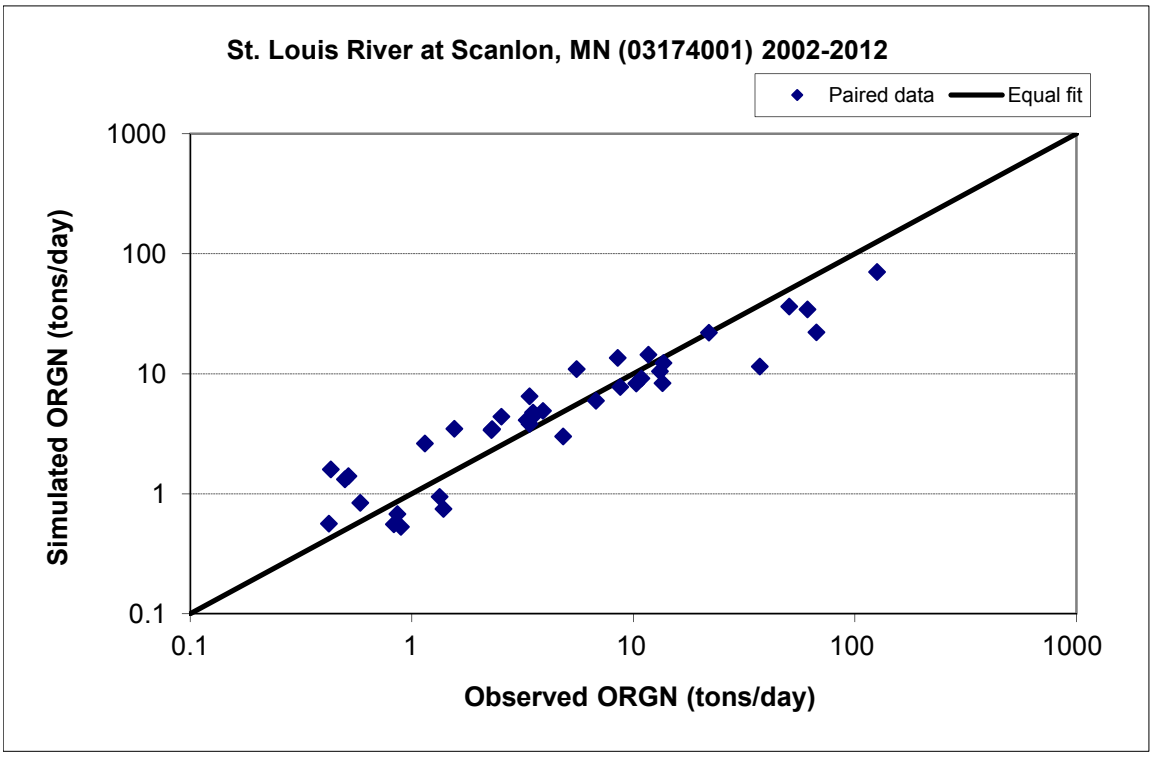

Figure A-126. Paired simulated vs. observed Organic Nitrogen (OrgN) load at St. Louis River at Scanlon, MN (03174001) (calibration period)

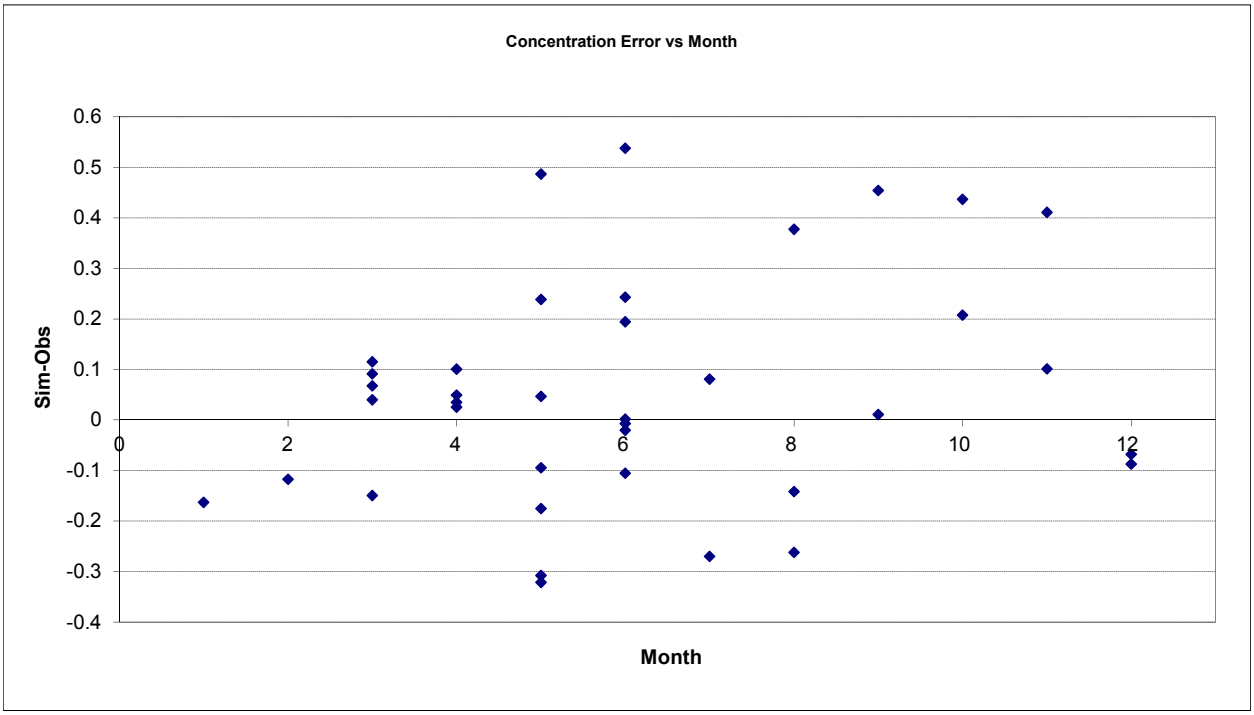

Figure A-127. Residual (Simulated - Observed) vs. Month Organic Nitrogen (OrgN) at St. Louis River at Scanlon, MN (03174001)

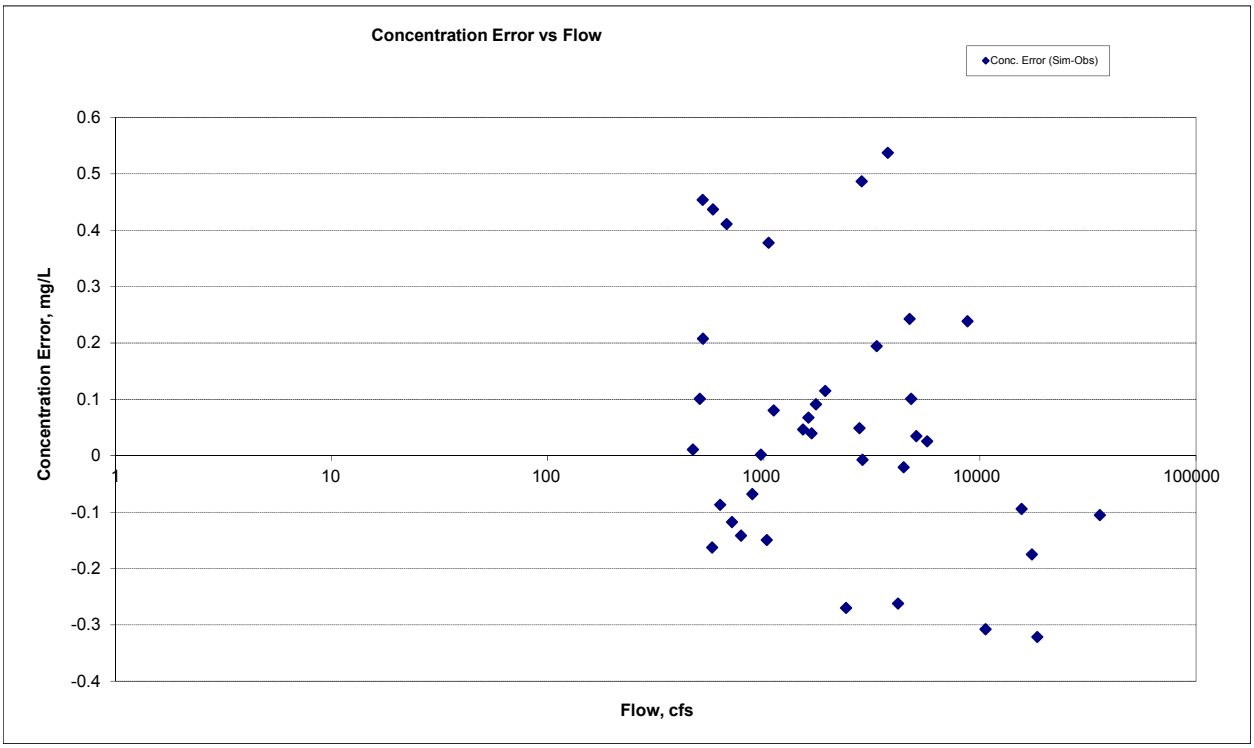

Figure A-128. Residual (Simulated - Observed) vs. Flow Organic Nitrogen (OrgN) at St. Louis River at Scanlon, MN (03174001)

A.5.3 Total Kjeldahl Nitrogen (TKN)

Table A-19. Total Kjeldahl Nitrogen (TKN) statistics

Period	1994-2001	2002-2012
Count	8	95
Concentration Average Error	34.46%	0.32%
Concentration Median Error	37.75%	2.01%
Load Average Error	41.86%	-3.87%
Load Median Error	29.30%	4.56%
Paired t conc	0.06	1.00
Paired t load	0.37	0.79

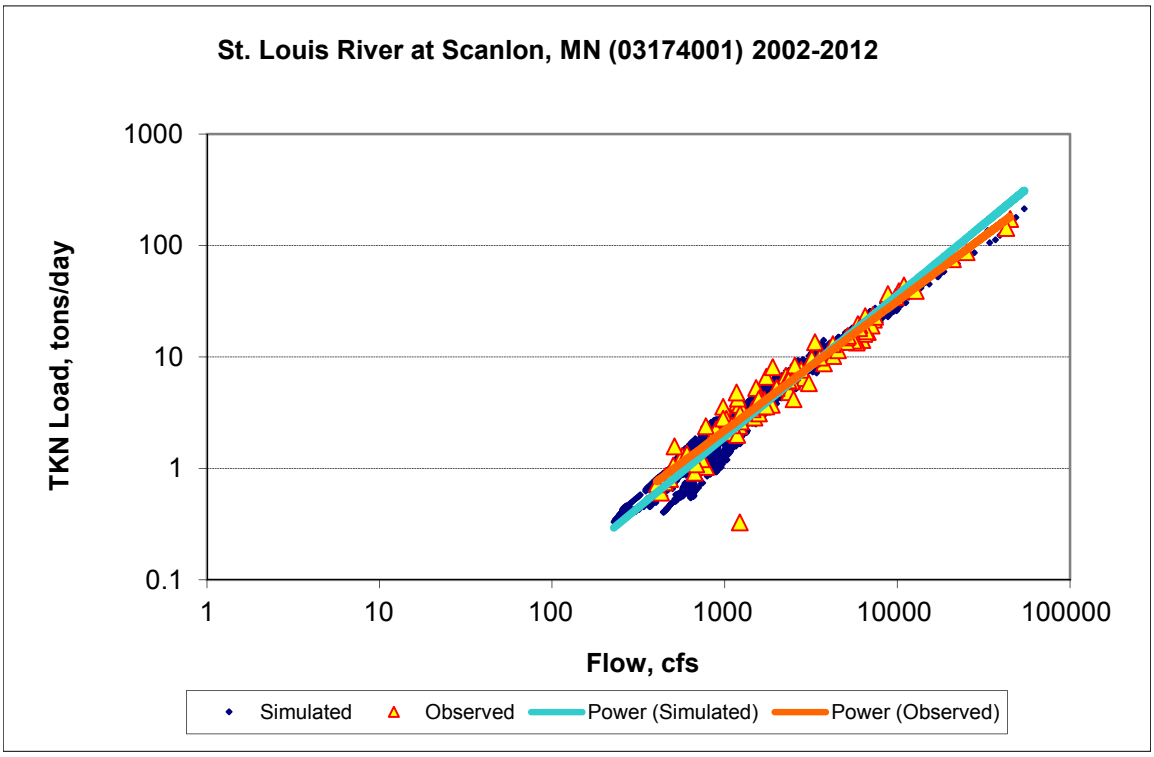

Figure A-129. Power plot of simulated and observed Total Kjeldahl Nitrogen (TKN) load vs flow at St. Louis River at Scanlon, MN (03174001) (calibration period)

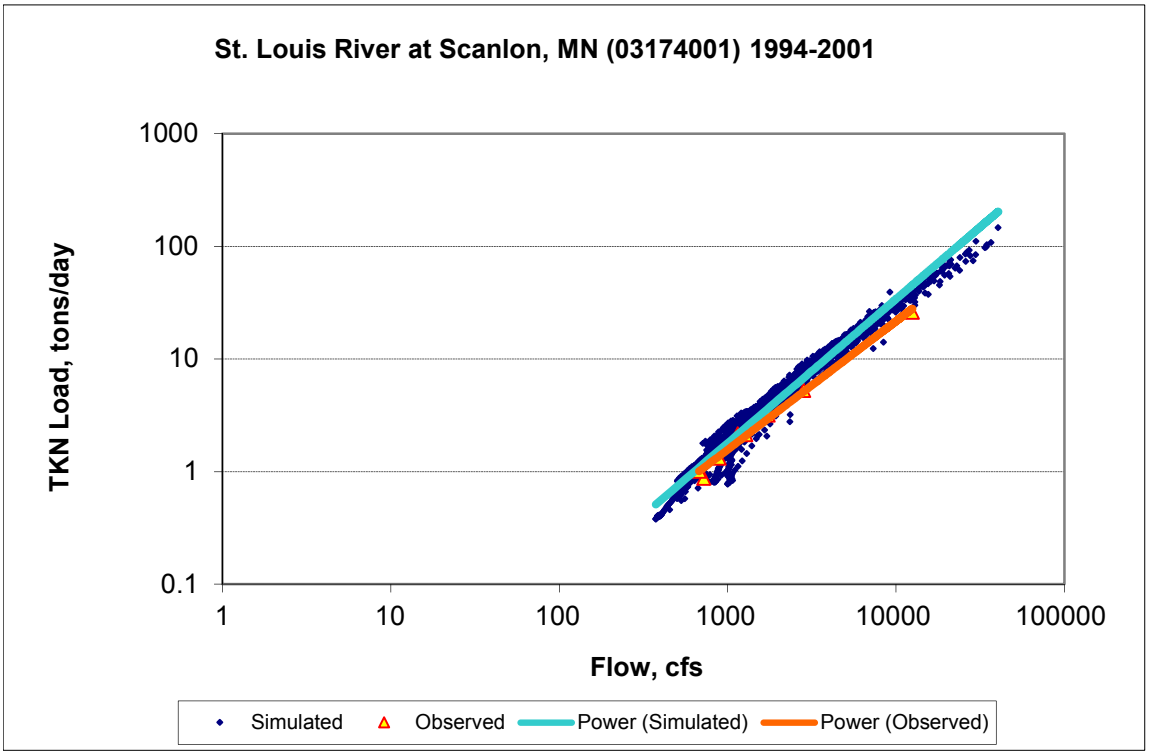

Figure A-130. Power plot of simulated and observed Total Kjeldahl Nitrogen (TKN) load vs flow at St. Louis River at Scanlon, MN (03174001) (validation period)

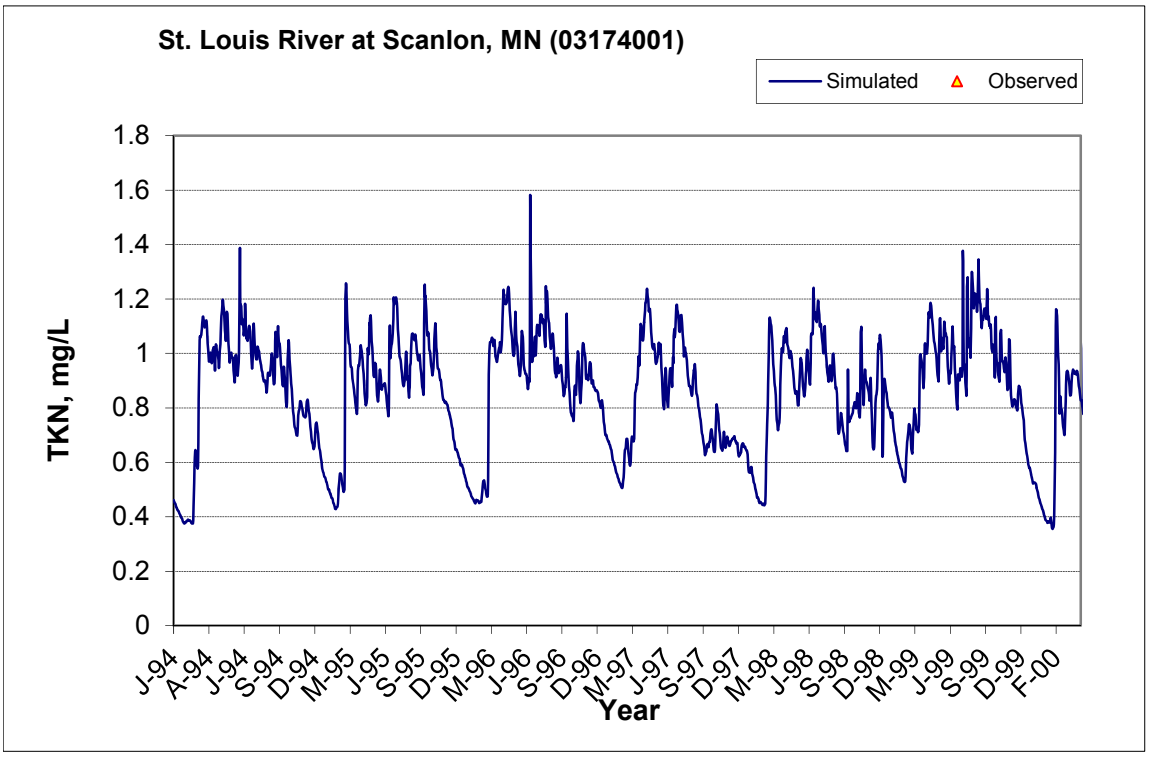
St. Louis River at Scanlon, MN (03174001)
Simulated
Observed
TKN, mg/L
1.8
1.6
1.4
1.2
1
0.8
0.6
0.4
0.2
0
J-94 A-94 J-94 S-94 D-94 M-95 J-95 S-95 D-95 M-96 J-96 S-96 D-96 M-97 J-97 S-97 D-97 M-98 J-98 S-98 D-98 M-99 J-99 S-99 D-99 F-00
Year

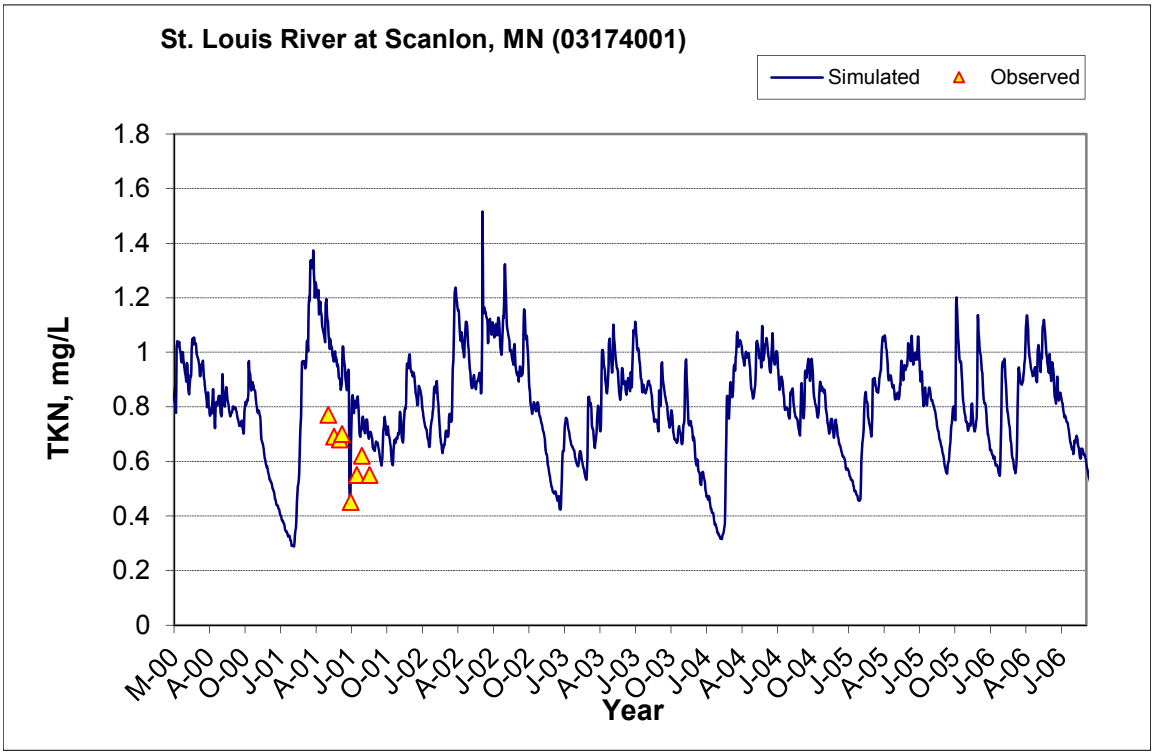
St. Louis River at Scanlon, MN (03174001)
Simulated
Observed
TKN, mg/L
1.8
1.6
1.4
1.2
1
0.8
0.6
0.4
0.2
0
M-00 A-00 O-00 J-01 A-01 J-01 O-01 J-02 A-02 J-02 O-02 J-03 A-03 J-03 O-03 J-04 A-04 J-04 O-04 J-05 A-05 J-05 O-05 J-06 A-06 J-06
Year

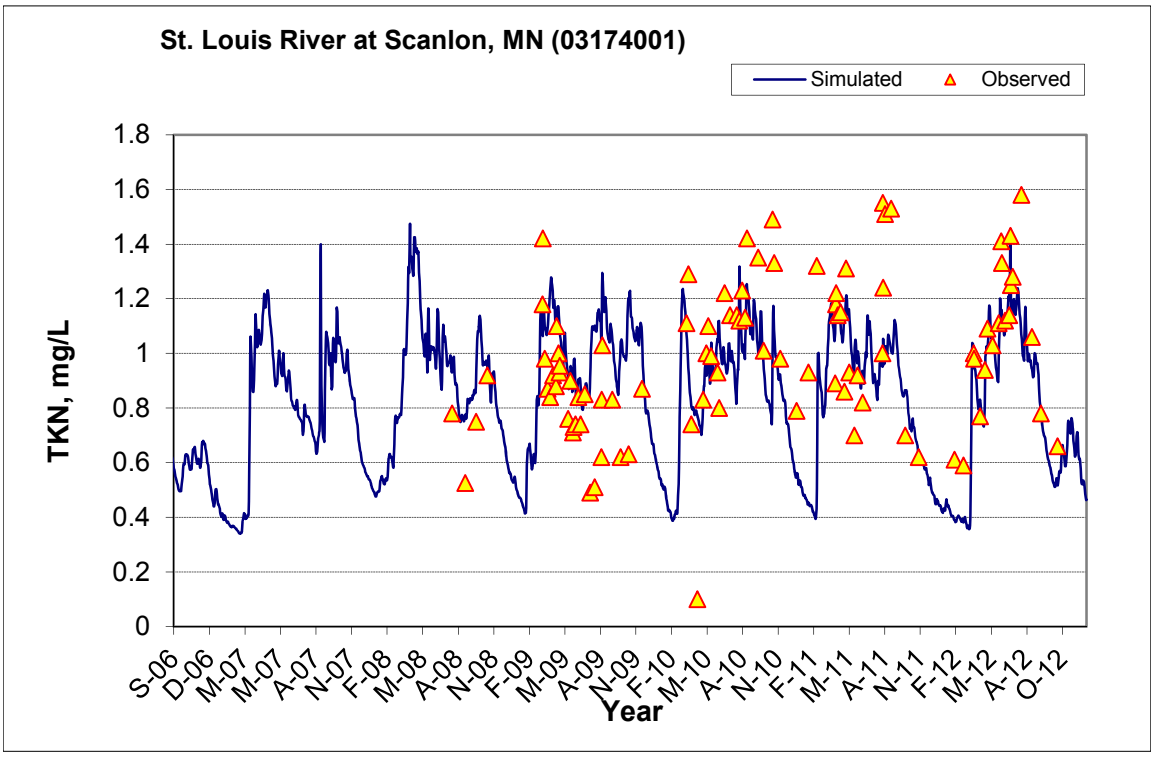

Figure A-131. Time series of observed and simulated Total Kjeldahl Nitrogen (TKN) concentration at St. Louis River at Scanlon, MN (03174001)

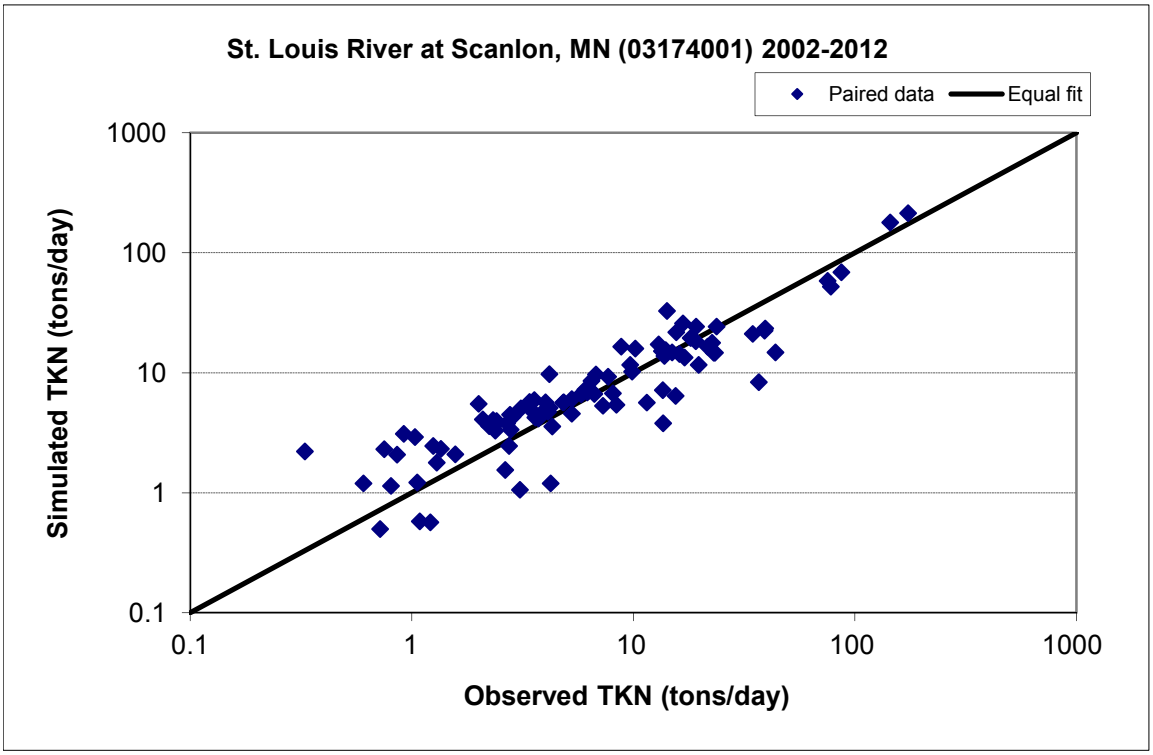

Figure A-132. Paired simulated vs. observed Total Kjeldahl Nitrogen (TKN) load at St. Louis River at Scanlon, MN (03174001) (calibration period)

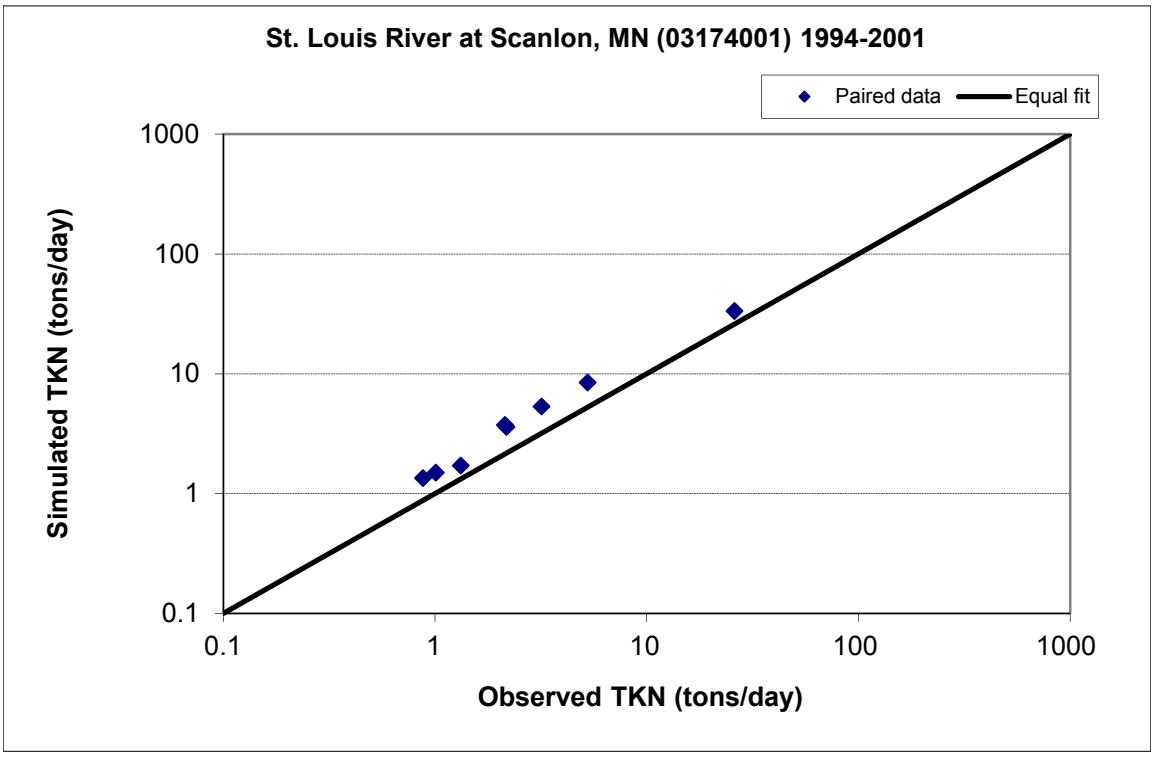

Figure A-133. Paired simulated vs. observed Total Kjeldahl Nitrogen (TKN) load at St. Louis River at Scanlon, MN (03174001) (validation period)

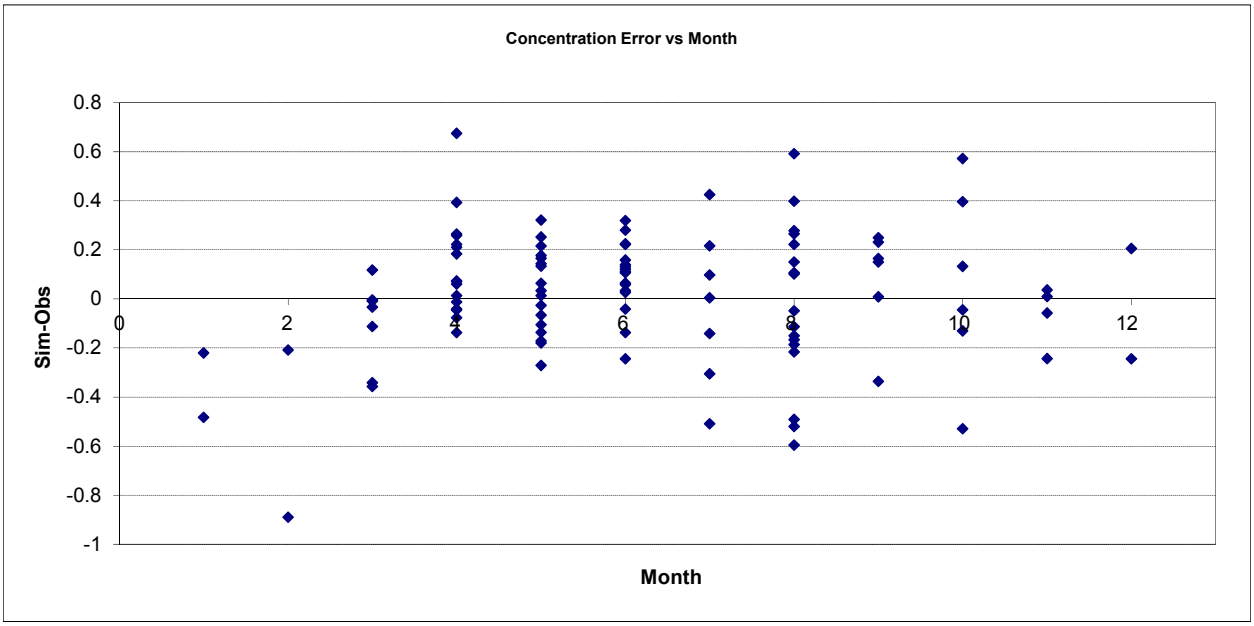

Figure A-134. Residual (Simulated - Observed) vs. Month Total Kjeldahl Nitrogen (TKN) at St. Louis River at Scanlon, MN (03174001)

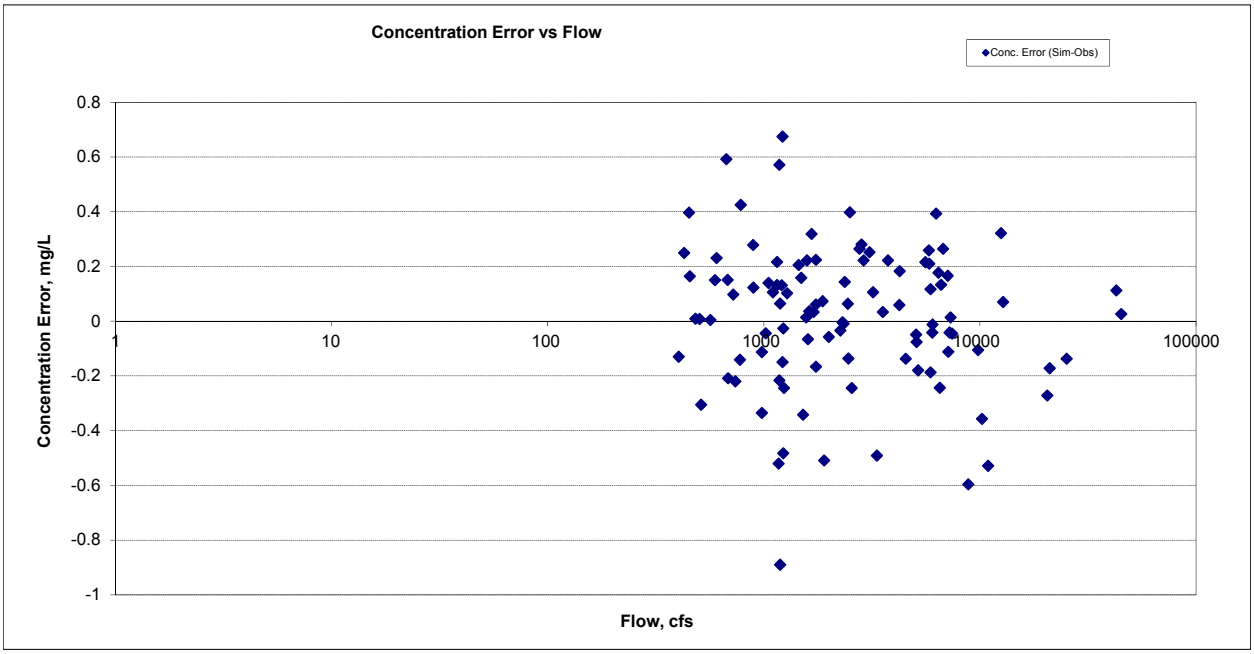

Figure A-135. Residual (Simulated - Observed) vs. Flow Total Kjeldahl Nitrogen (TKN) at St. Louis River at Scanlon, MN (03174001)

A.5.4 Nitrite+ Nitrate Nitrogen (NOx)

Table A-20. Nitrite+ Nitrate Nitrogen (NOx) statistics

Period	1994-2001	2002-2012
Count	8	140
Concentration Average Error	134.96%	-27.60%
Concentration Median Error	119.79%	1.67%
Load Average Error	18.86%	-4.46%
Load Median Error	40.17%	1.01%
Paired t conc	0.00	0.38
Paired t load	0.51	0.84

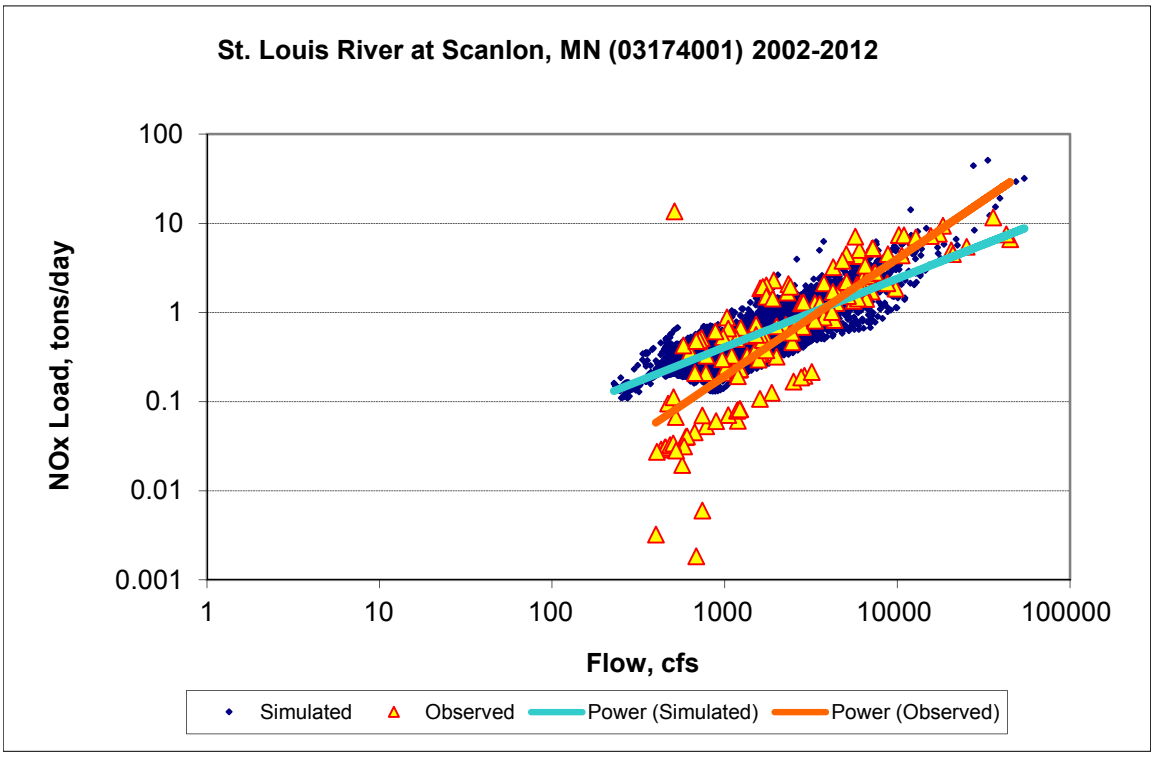

Figure A-136. Power plot of simulated and observed Nitrite+ Nitrate Nitrogen (NOx) load vs flow at St. Louis River at Scanlon, MN (03174001) (calibration period)

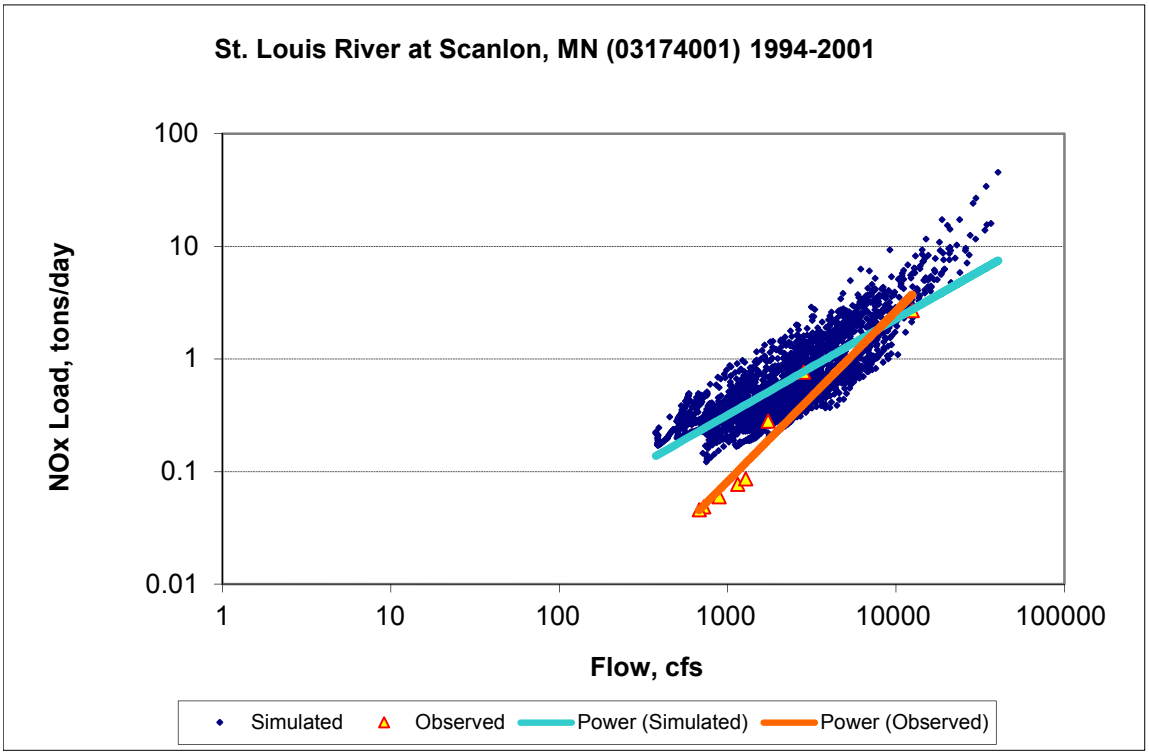

Figure A-137. Power plot of simulated and observed Nitrite+ Nitrate Nitrogen (NOx) load vs flow at St. Louis River at Scanlon, MN (03174001) (validation period)

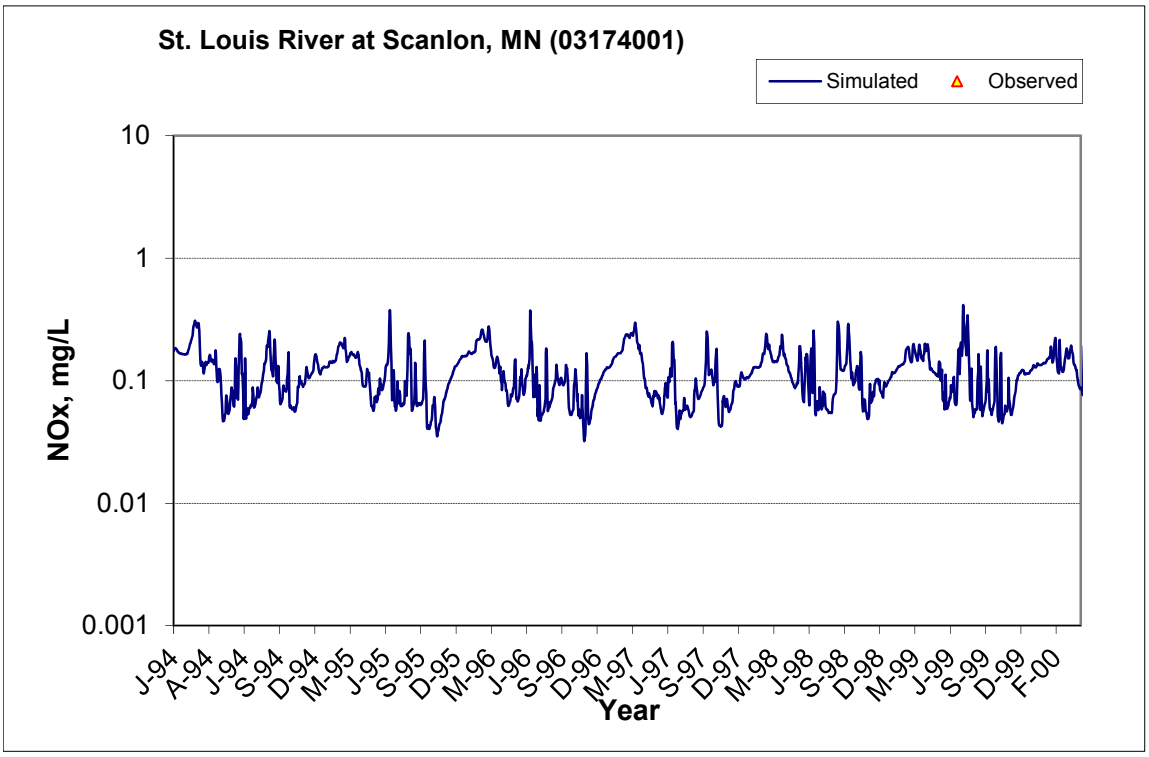
St. Louis River at Scanlon, MN (03174001)
Simulated
Observed
NOx, mg/L
10
1
0.1
0.01
0.001
J-94 A-94 J-94 S-94 D-94 M-95 J-95 S-95 D-95 M-96 J-96 S-96 D-96 M-97 J-97 S-97 D-97 M-98 J-98 S-98 D-98 M-99 J-99 S-99 D-99 F-00
Year

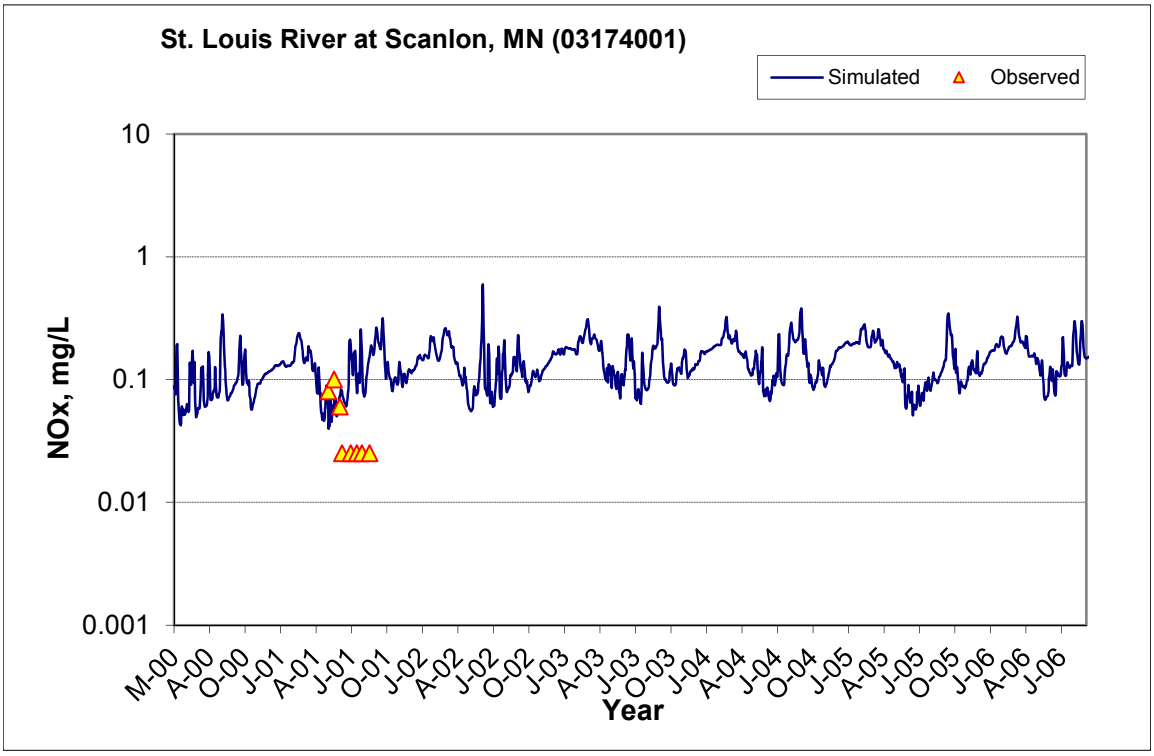
St. Louis River at Scanlon, MN (03174001)
Simulated
Observed
NOx, mg/L
10
1
0.1
0.01
0.001
M-00 A-00 O-00 J-01 A-01 J-01 O-01 J-02 A-02 J-02 O-02 J-03 A-03 J-03 O-03 J-04 A-04 J-04 O-04 J-05 A-05 J-05 O-05 J-06 A-06 J-06
Year

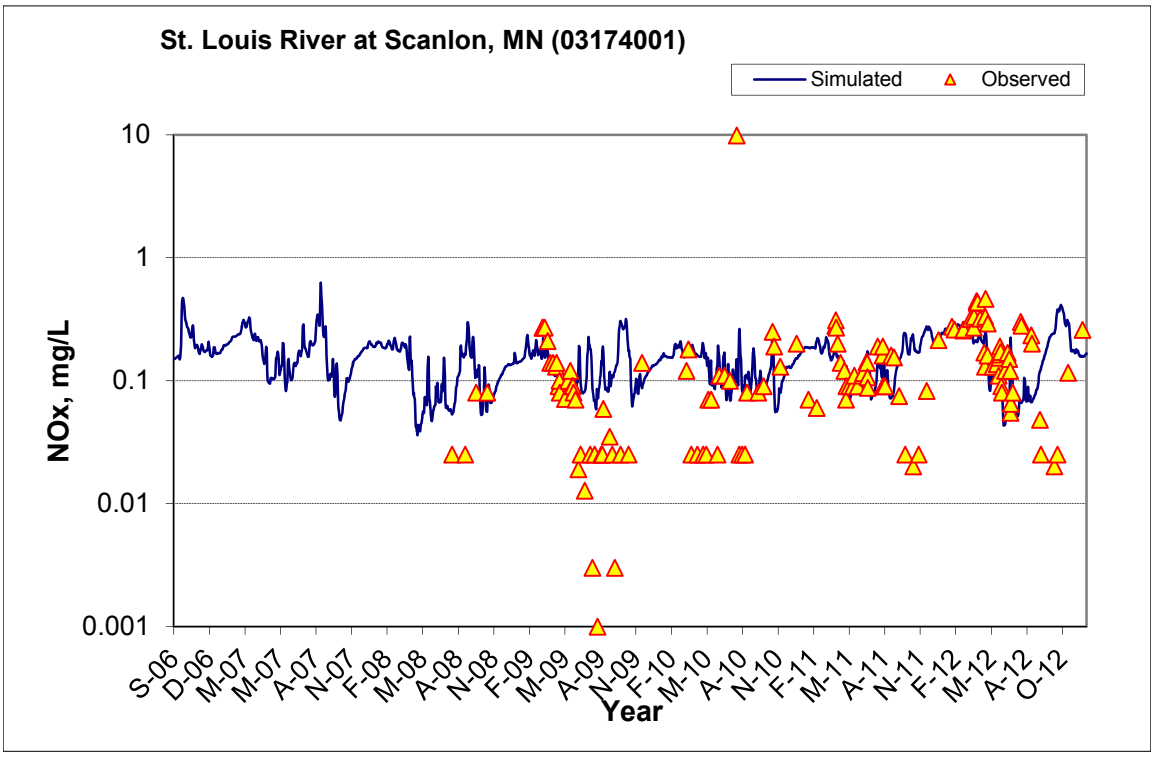

Figure A-138. Time series of observed and simulated Nitrite+ Nitrate Nitrogen (NOx) concentration at St. Louis River at Scanlon, MN (03174001)

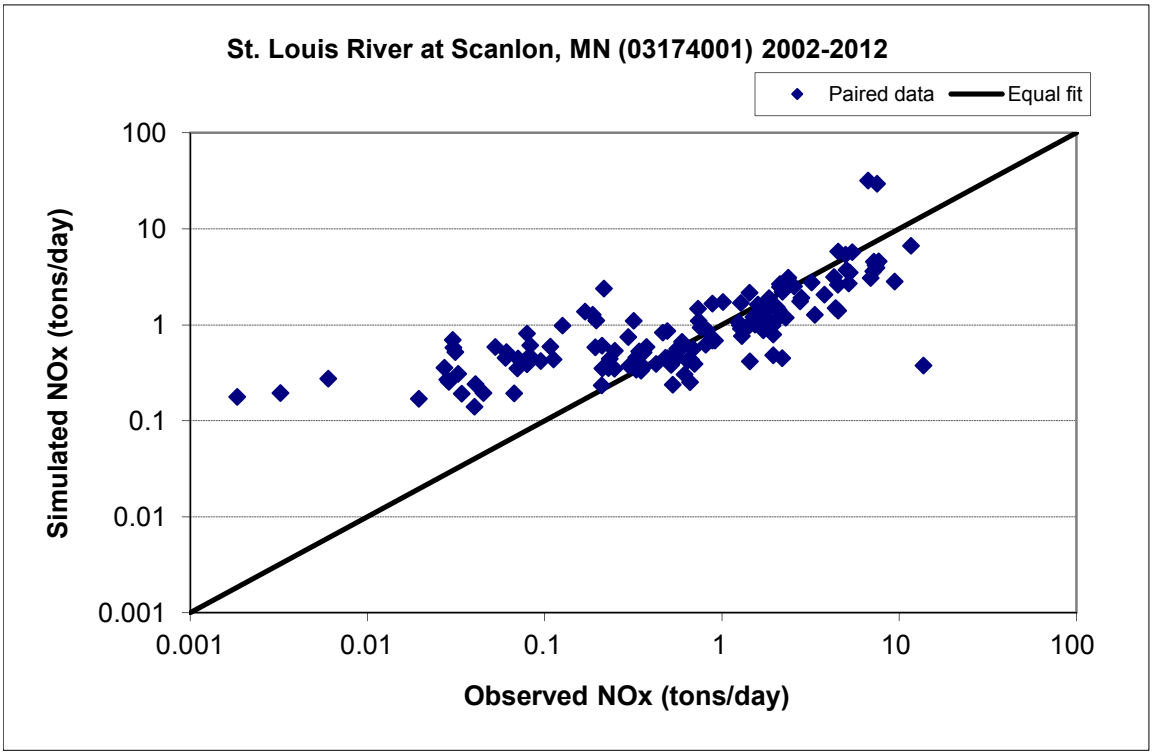

Figure A-139. Paired simulated vs. observed Nitrite+ Nitrate Nitrogen (NOx) load at St. Louis River at Scanlon, MN (03174001) (calibration period)

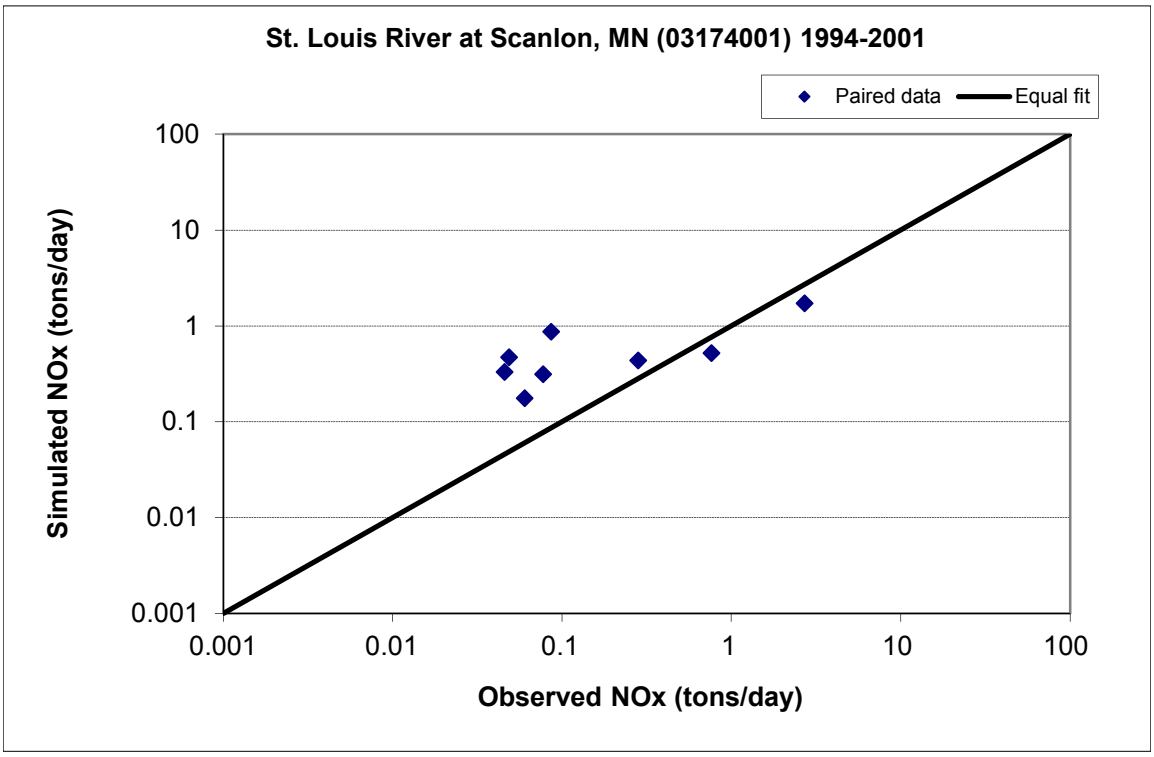

Figure A-140. Paired simulated vs. observed Nitrite+ Nitrate Nitrogen (NOx) load at St. Louis River at Scanlon, MN (03174001) (validation period)

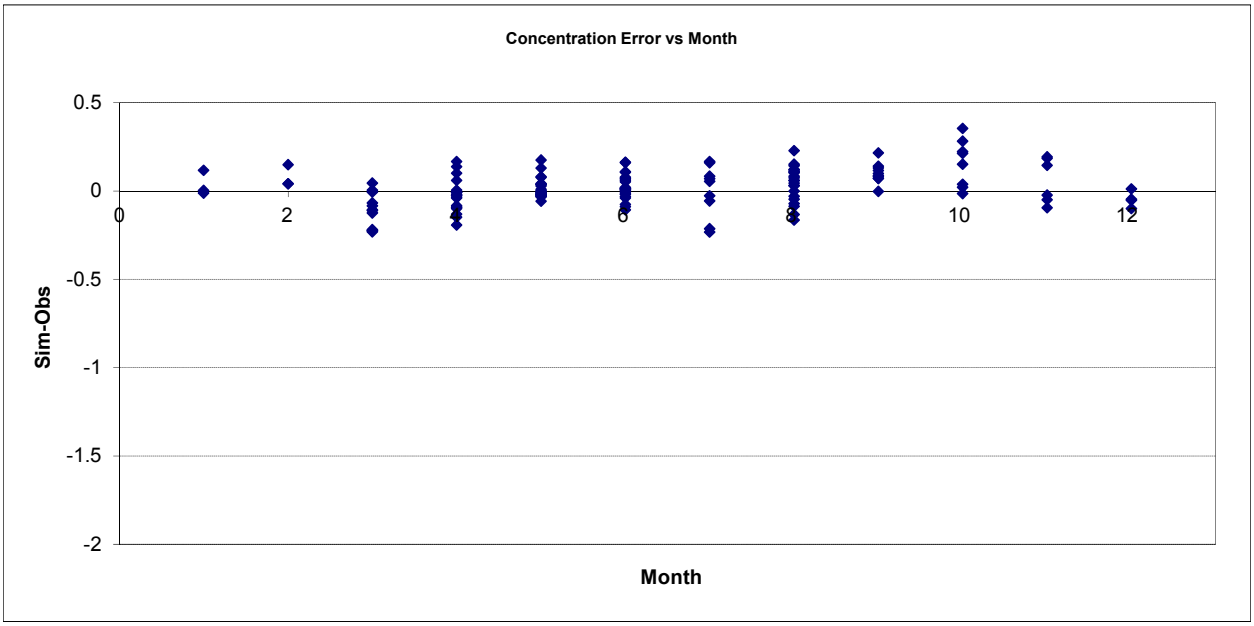

Figure A-141. Residual (Simulated - Observed) vs. Month Nitrite+ Nitrate Nitrogen (NOx) at St. Louis River at Scanlon, MN (03174001)

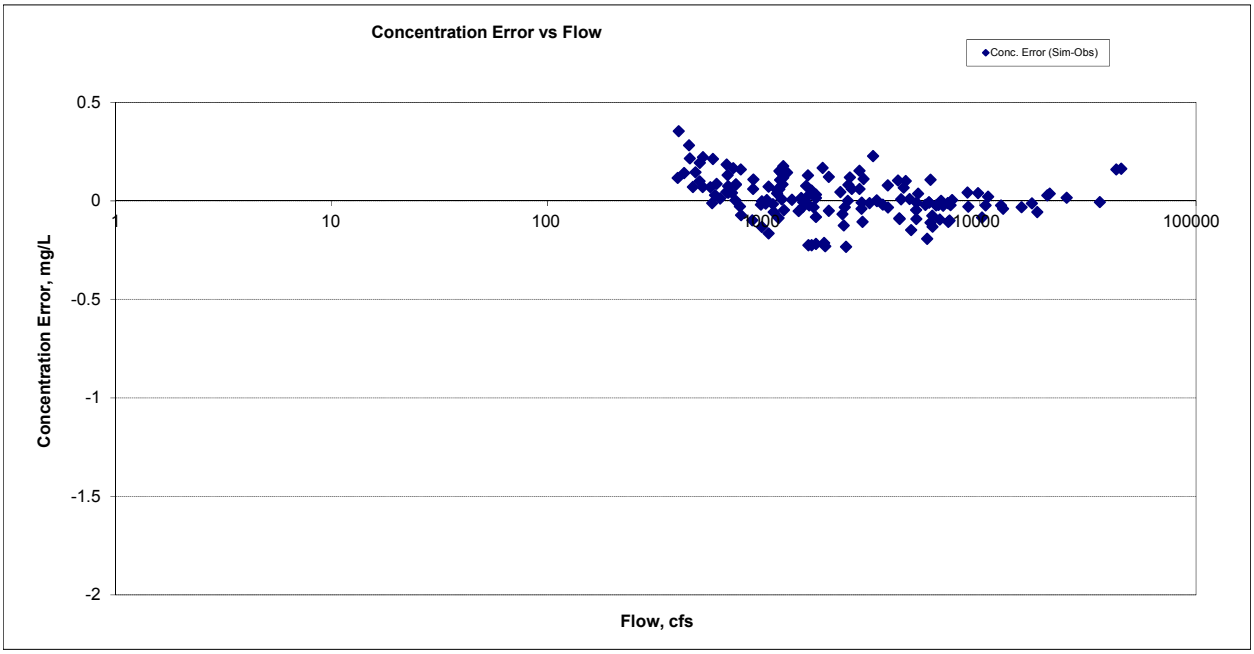

Figure A-142. Residual (Simulated - Observed) vs. Flow Nitrite+ Nitrate Nitrogen (NOx) at St. Louis River at Scanlon, MN (03174001)

A.5.5 Total Nitrogen (TN)

Table A-21. Total Nitrogen (TN) statistics

Period	1994-2001	2002-2012
Count	8	127
Concentration Average Error	38.08%	-6.14%
Concentration Median Error	37.32%	-0.54%
Load Average Error	38.87%	-10.70%
Load Median Error	33.81%	1.69%
Paired t conc	0.01	1.00
Paired t load	0.39	0.73

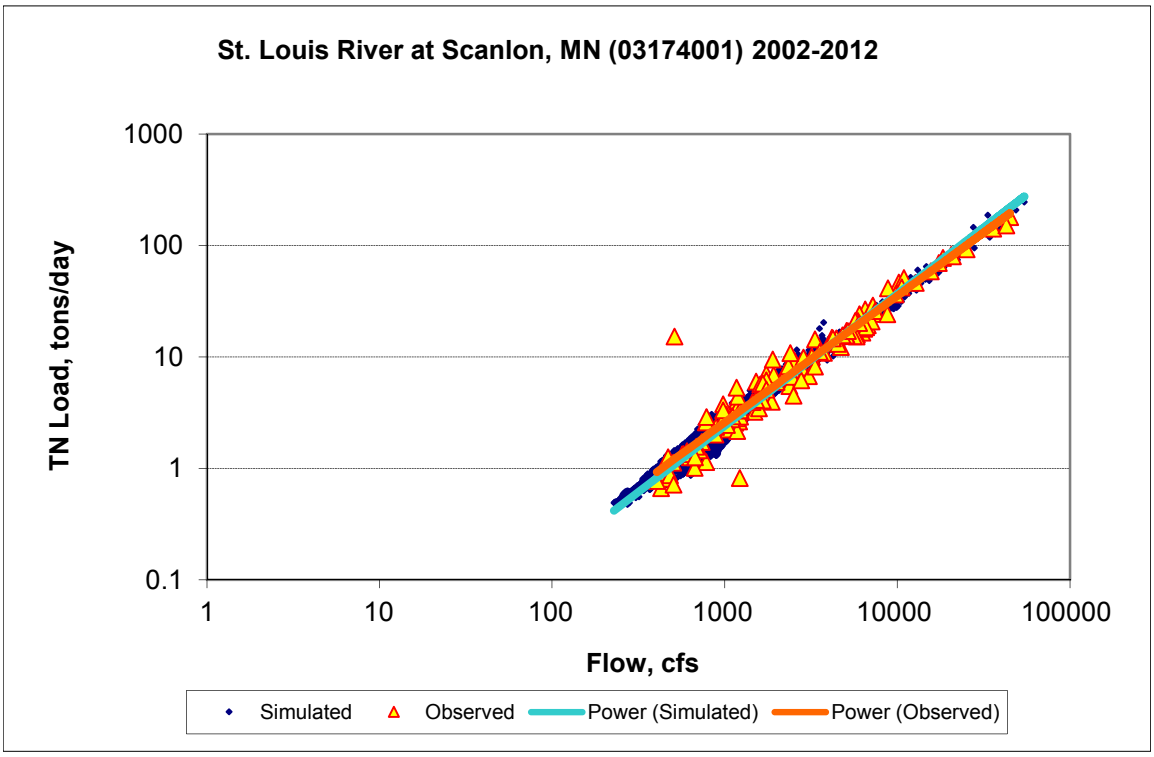

Figure A-143. Power plot of simulated and observed Total Nitrogen (TN) load vs flow at St. Louis River at Scanlon, MN (03174001) (calibration period)

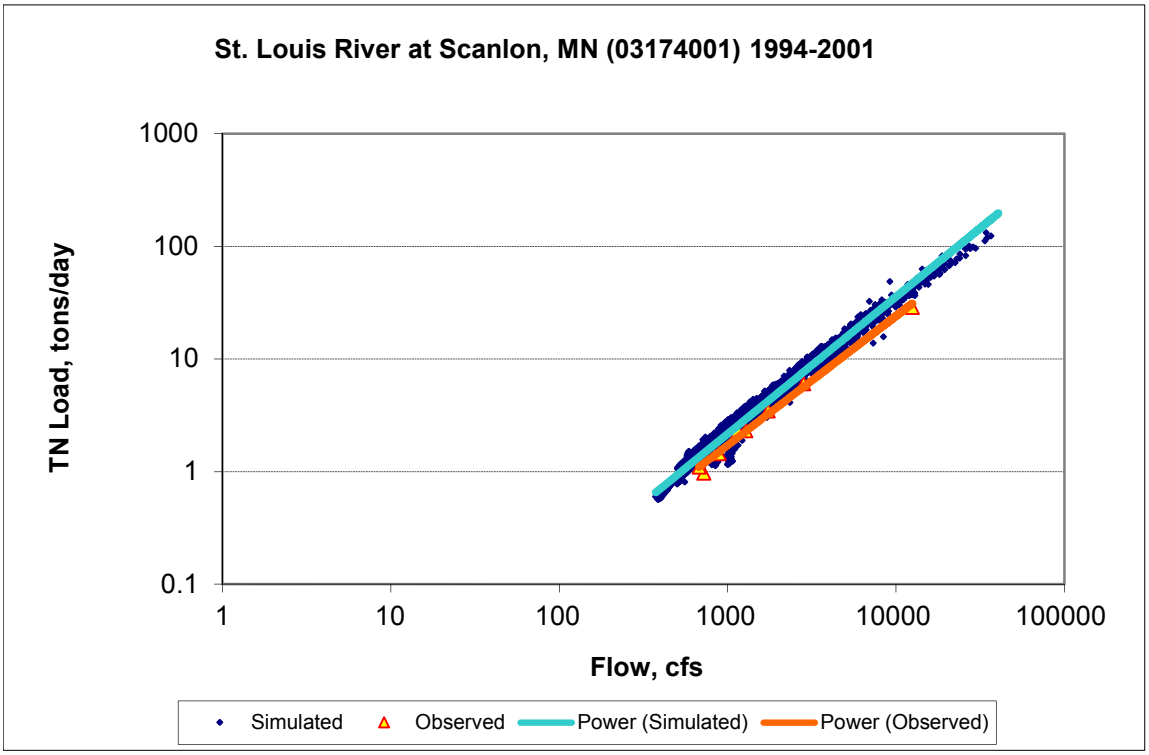

Figure A-144. Power plot of simulated and observed Total Nitrogen (TN) load vs flow at St. Louis River at Scanlon, MN (03174001) (validation period)

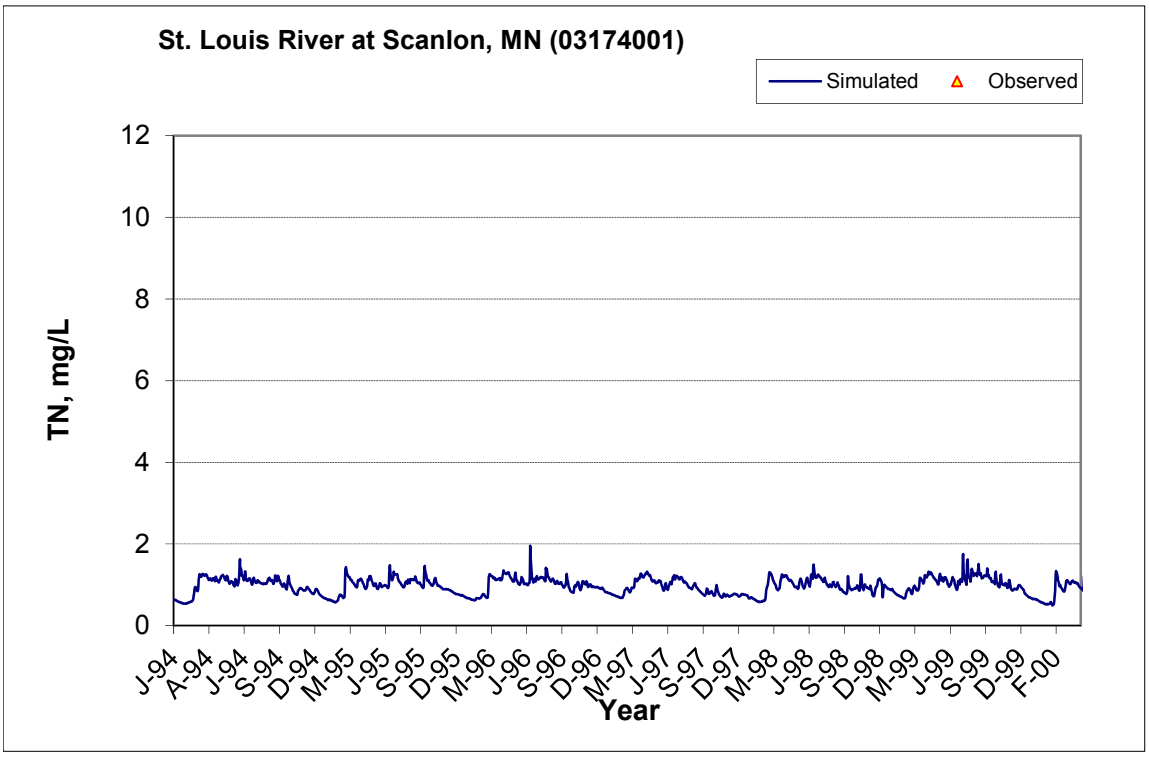
St. Louis River at Scanlon, MN (03174001)
Simulated
Observed
TN, mg/L
0
2
4
6
8
10
12
J-94
A-94
J-94
S-94
D-94
M-95
J-95
S-95
D-95
M-96
J-96
S-96
D-96
M-97
J-97
S-97
D-97
M-98
J-98
S-98
D-98
M-99
J-99
S-99
D-99
F-00
Year

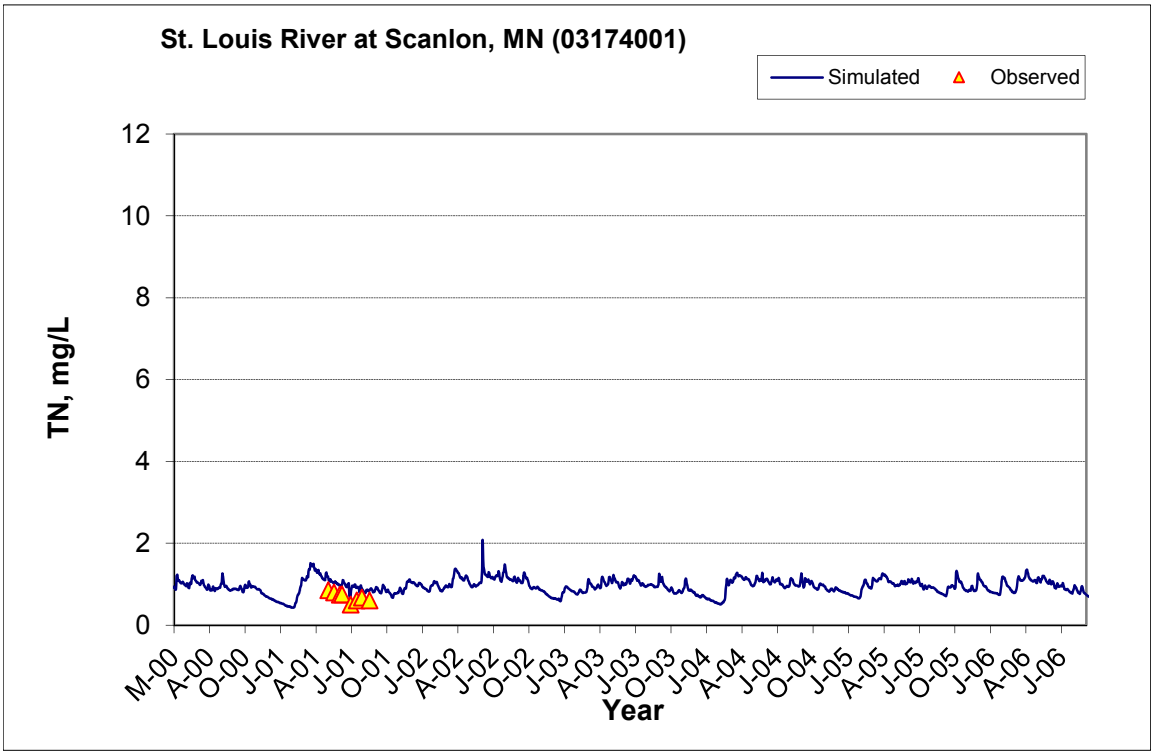
St. Louis River at Scanlon, MN (03174001)
Simulated
Observed
TN, mg/L
0
2
4
6
8
10
12
M-00
A-00
O-00
J-01
A-01
J-01
O-01
J-02
A-02
J-02
O-02
J-03
A-03
J-03
O-03
J-04
A-04
J-04
O-04
J-05
A-05
J-05
O-05
J-06
A-06
J-06
Year

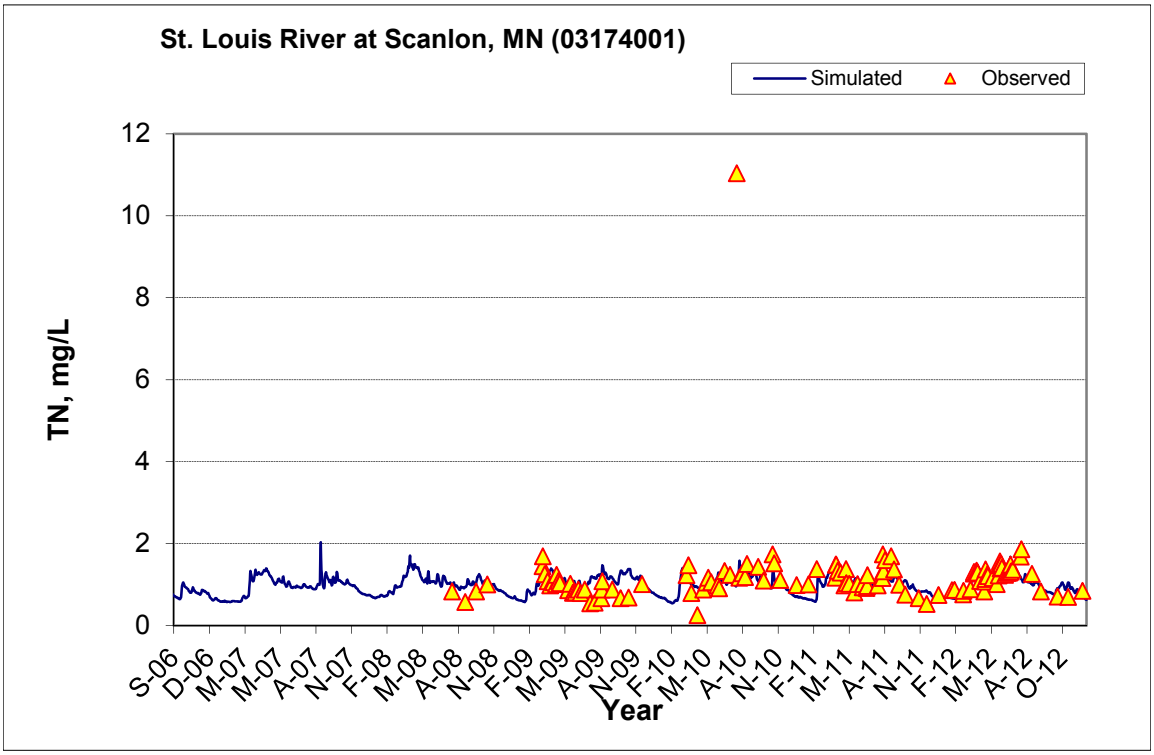

Figure A-145. Time series of observed and simulated Total Nitrogen (TN) concentration at St. Louis River at Scanlon, MN (03174001)

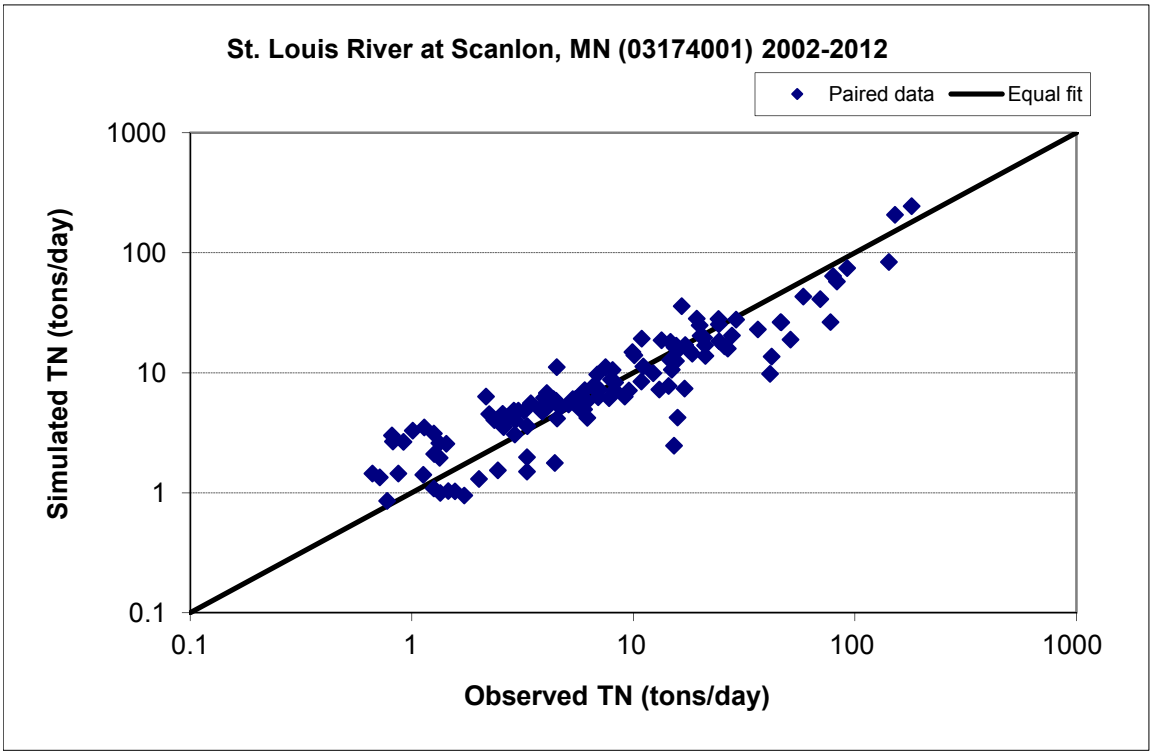

Figure A-146. Paired simulated vs. observed Total Nitrogen (TN) load at St. Louis River at Scanlon, MN (03174001) (calibration period)

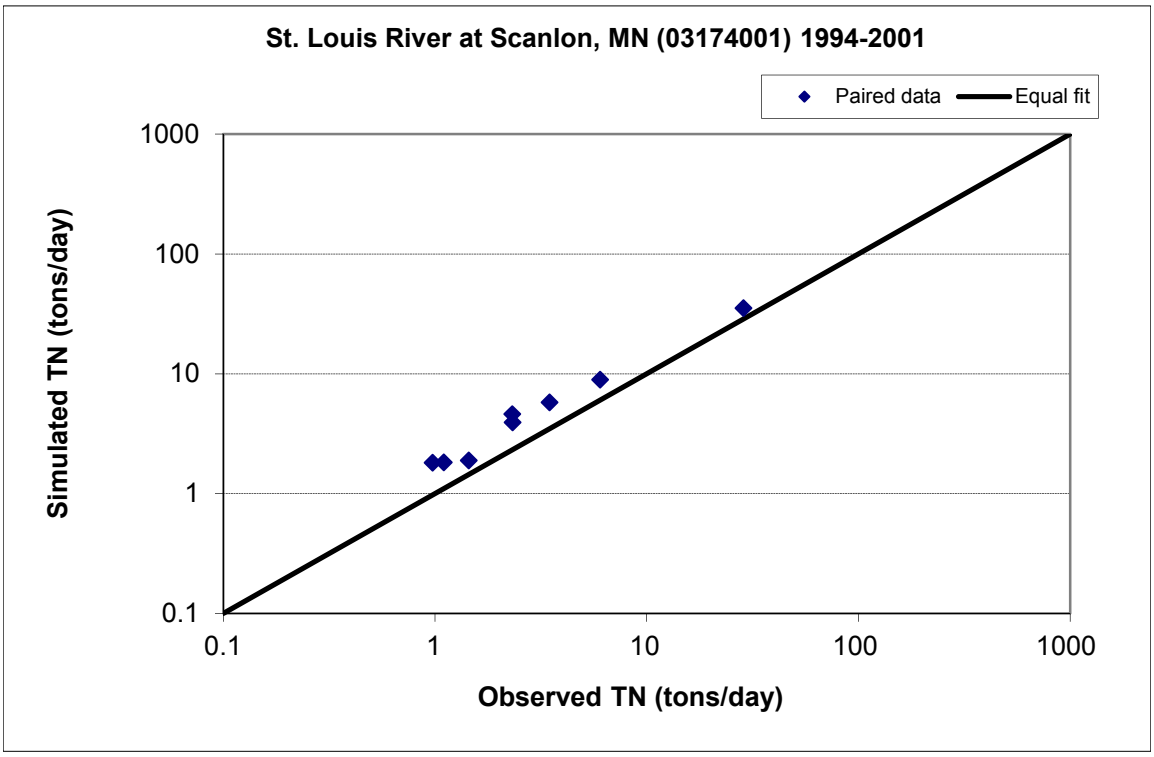

Figure A-147. Paired simulated vs. observed Total Nitrogen (TN) load at St. Louis River at Scanlon, MN (03174001) (validation period)

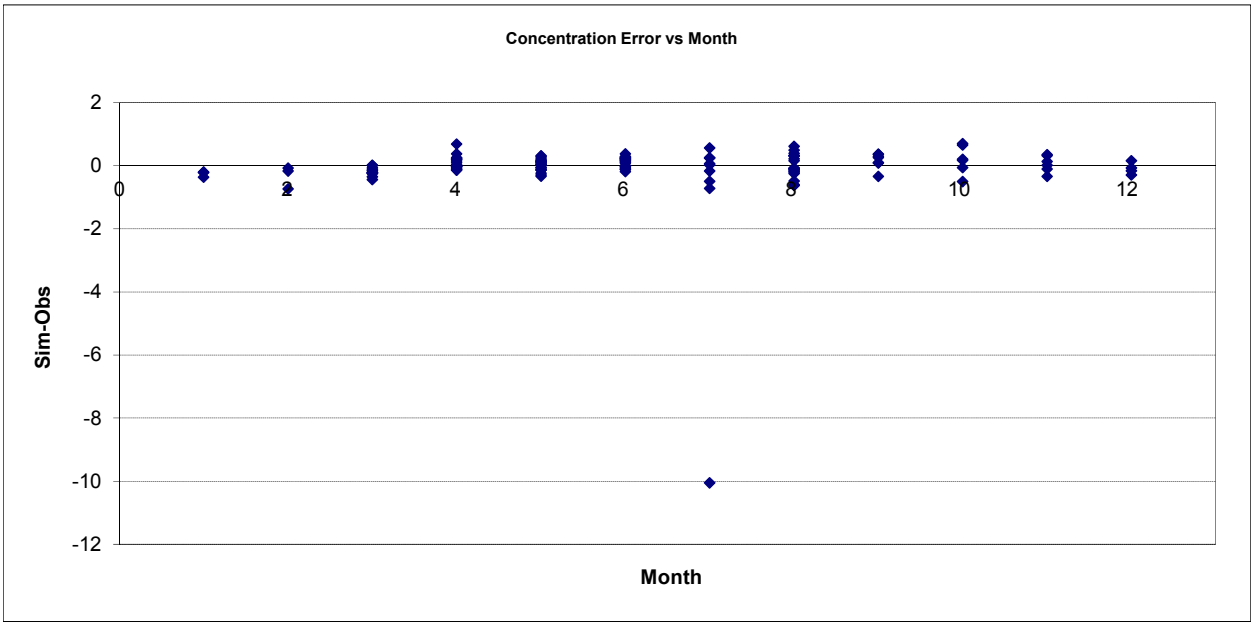

Figure A-148. Residual (Simulated - Observed) vs. Month Total Nitrogen (TN) at St. Louis River at Scanlon, MN (03174001)

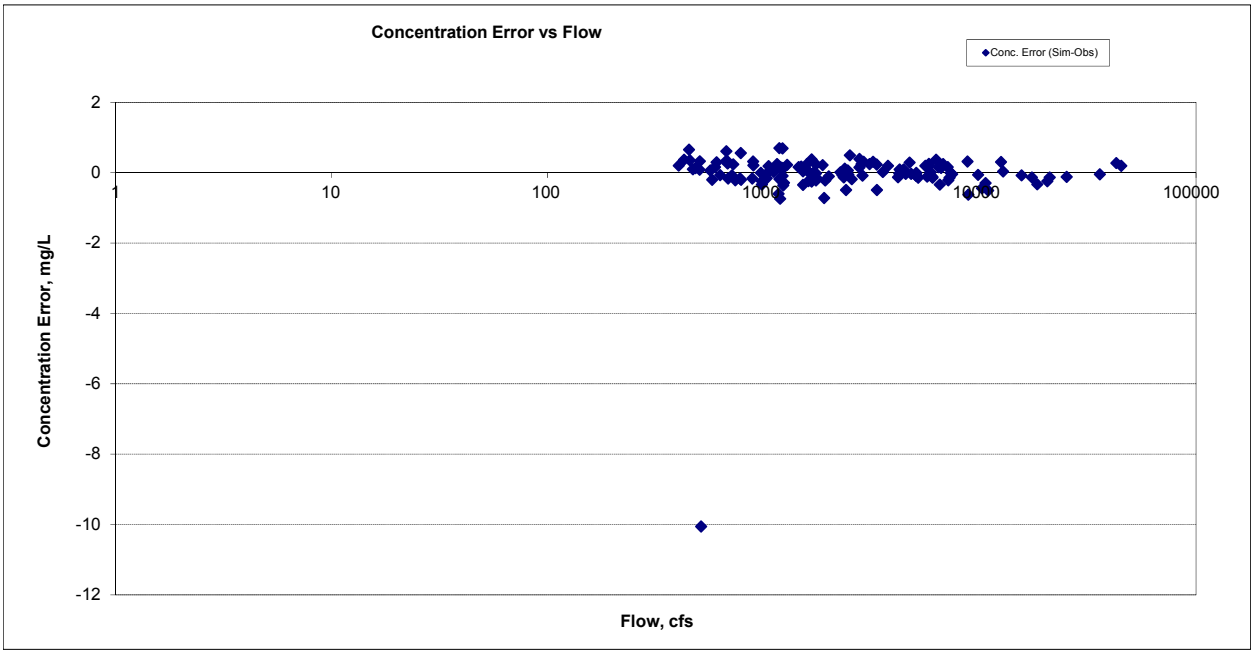

Figure A-149. Residual (Simulated - Observed) vs. Flow Total Nitrogen (TN) at St. Louis River at Scanlon, MN (03174001)

A.5.6 Soluble Reactive Phosphorus (SRP)

Table A-22. Soluble Reactive Phosphorus (SRP) statistics

Period	1994-2001	2002-2012
Count	ND	131
Concentration Average Error		-18.10%
Concentration Median Error		-24.26%
Load Average Error		13.02%
Load Median Error		-3.64%
Paired t conc		0.58
Paired t load		0.58

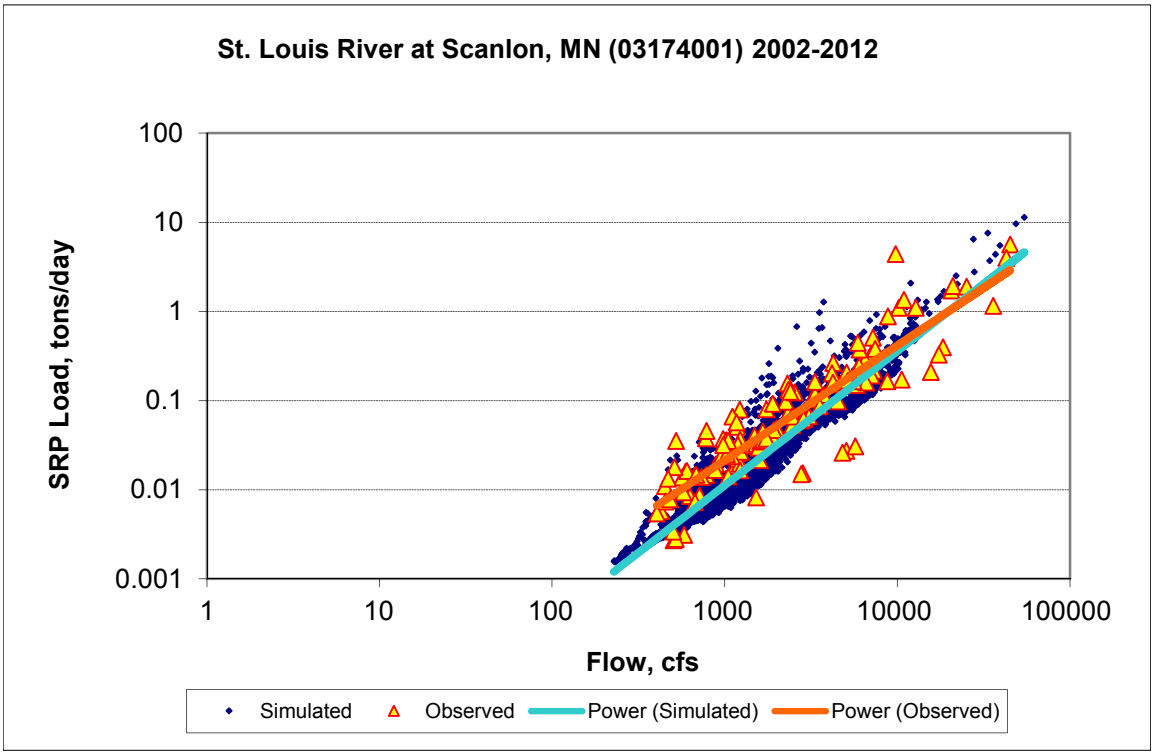

Figure A-150. Power plot of simulated and observed Soluble Reactive Phosphorus (SRP) load vs flow at St. Louis River at Scanlon, MN (03174001) (calibration period)

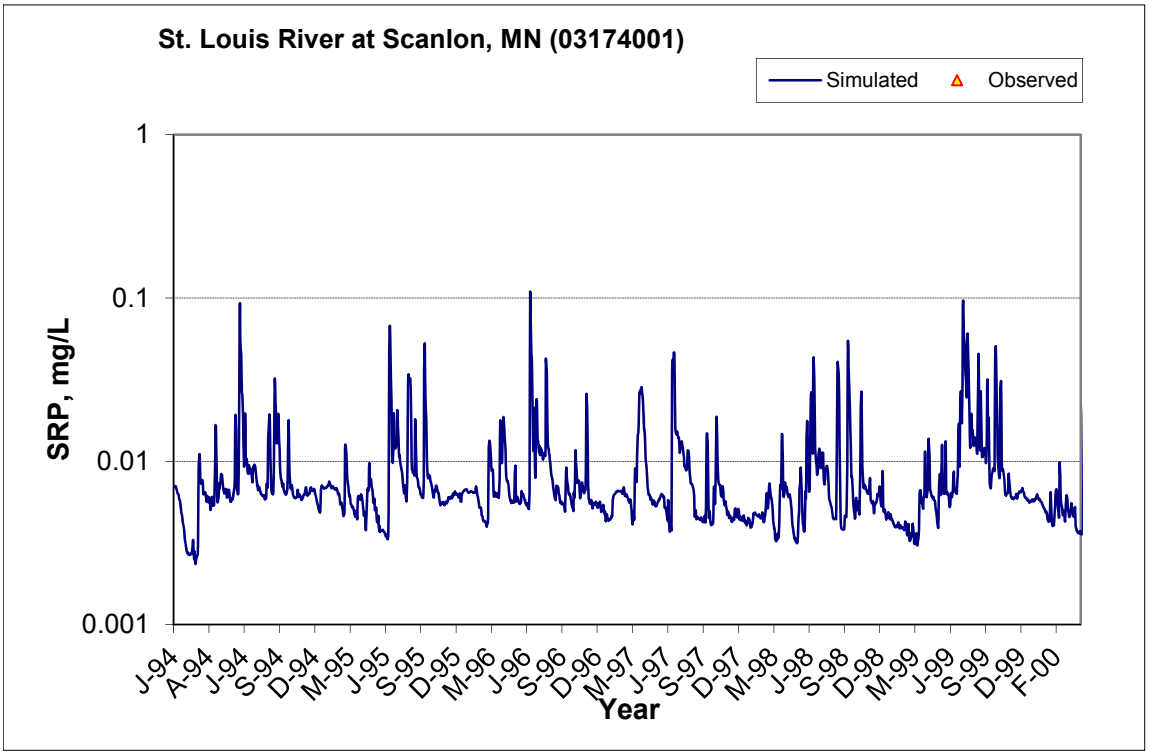

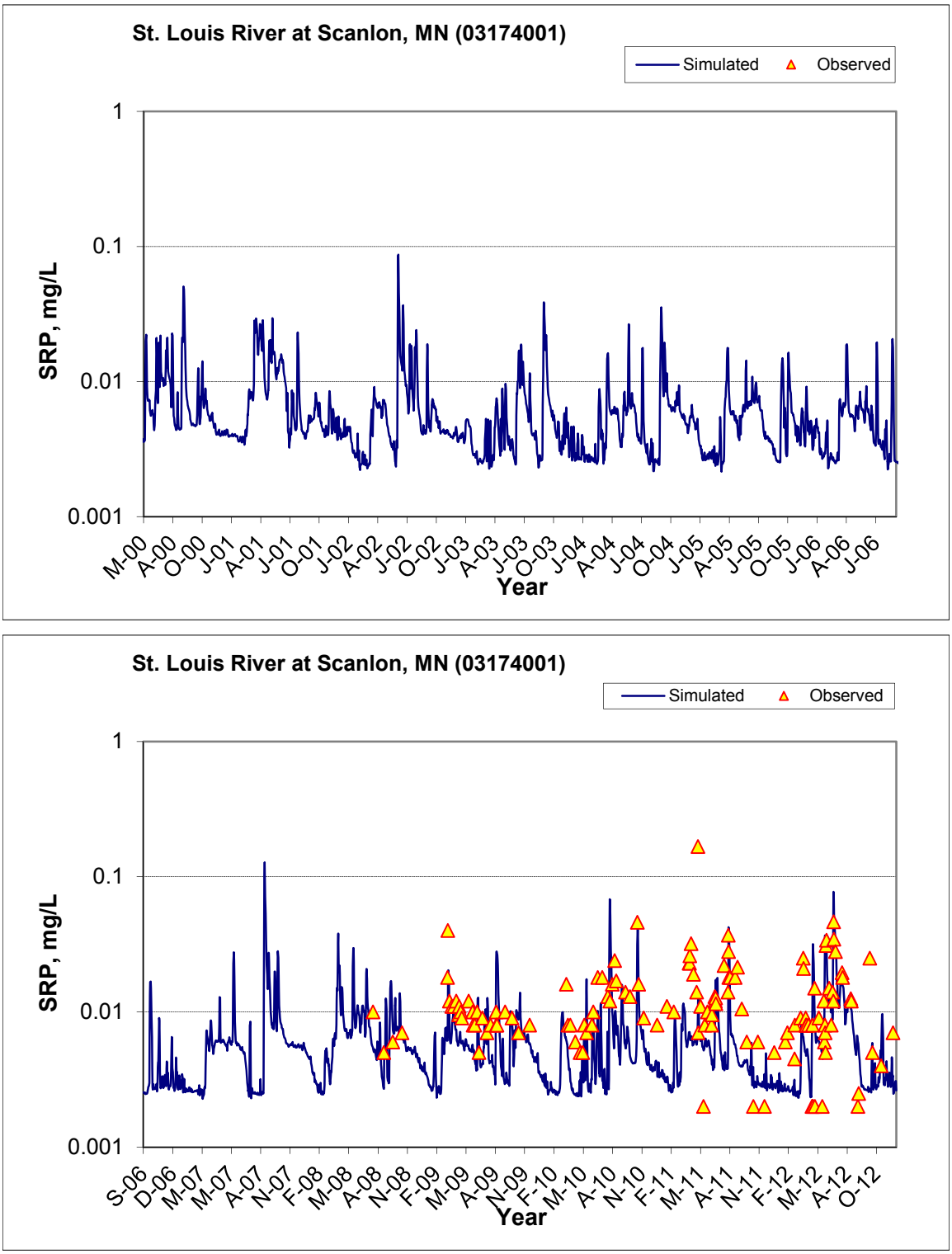

Figure A-151. Time series of observed and simulated Soluble Reactive Phosphorus (SRP) concentration at St. Louis River at Scanlon, MN (03174001)

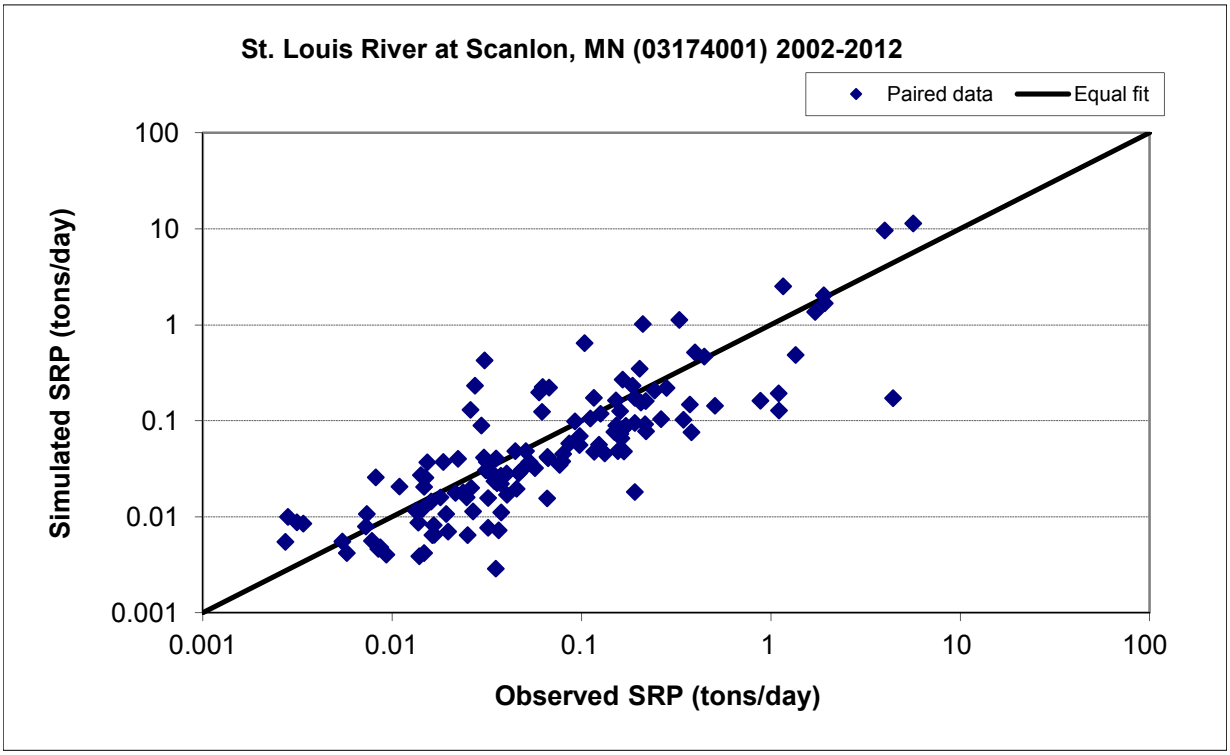

Figure A-152. Paired simulated vs. observed Soluble Reactive Phosphorus (SRP) load at St. Louis River at Scanlon, MN (03174001) (calibration period)

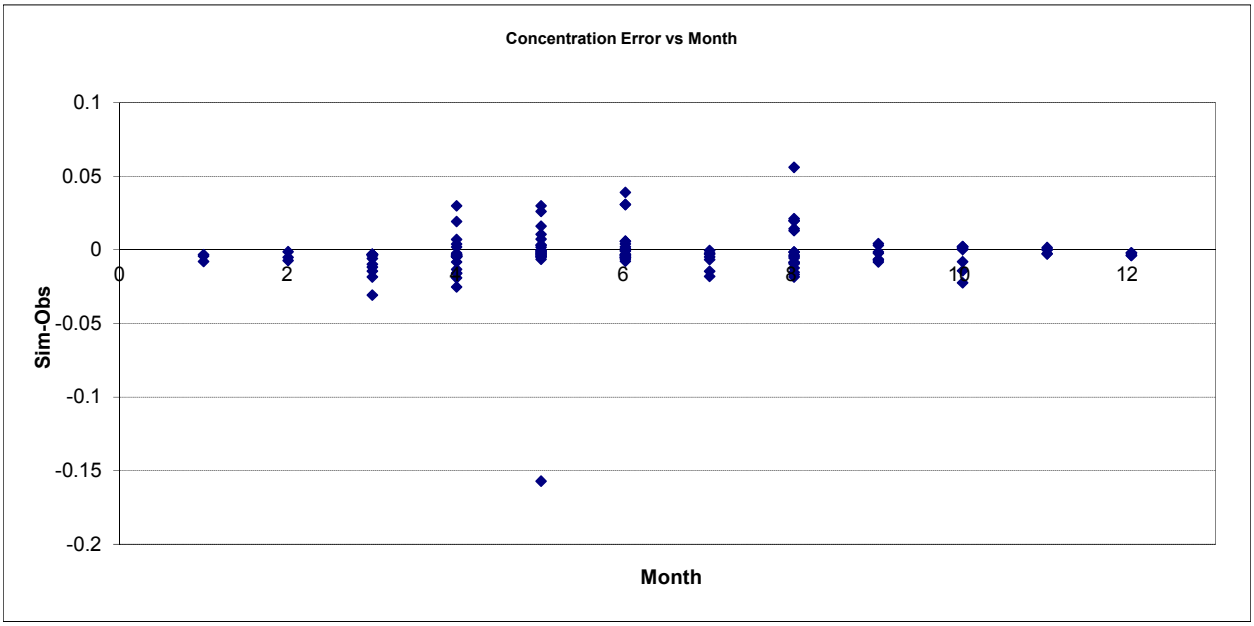

Figure A-153. Residual (Simulated - Observed) vs. Month Soluble Reactive Phosphorus (SRP) at St. Louis River at Scanlon, MN (03174001)

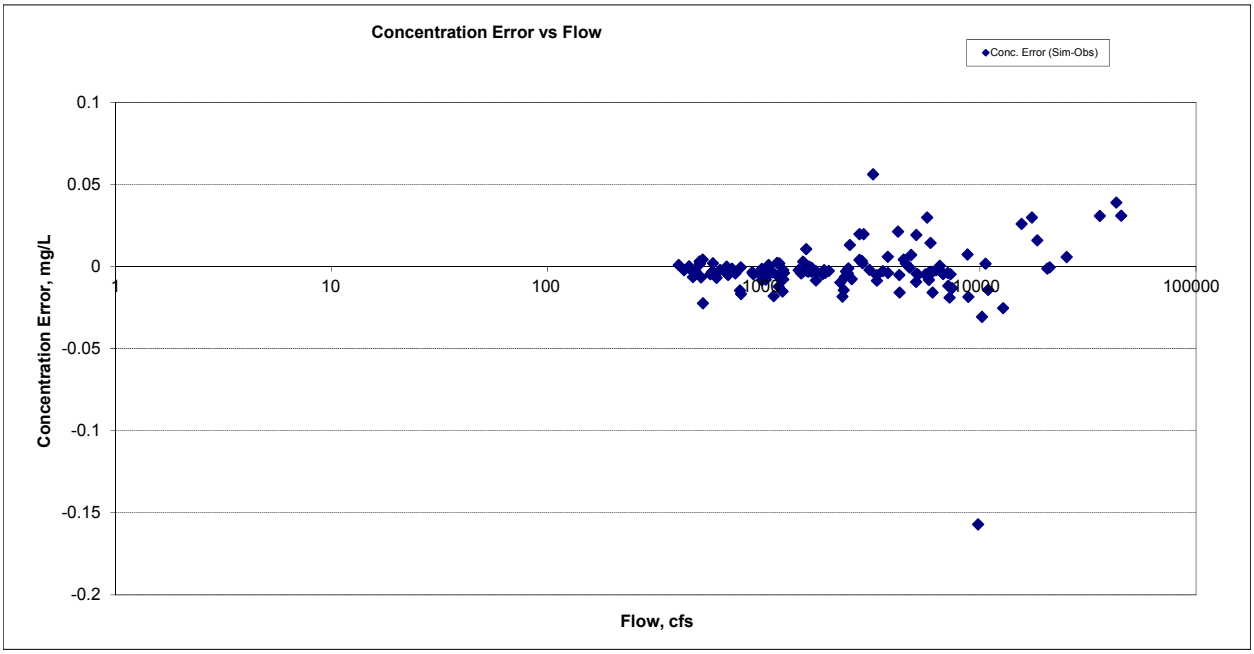

Figure A-154. Residual (Simulated - Observed) vs. Flow Soluble Reactive Phosphorus (SRP) at St. Louis River at Scanlon, MN (03174001)

A.5.7 Organic Phosphorus (OrgP)

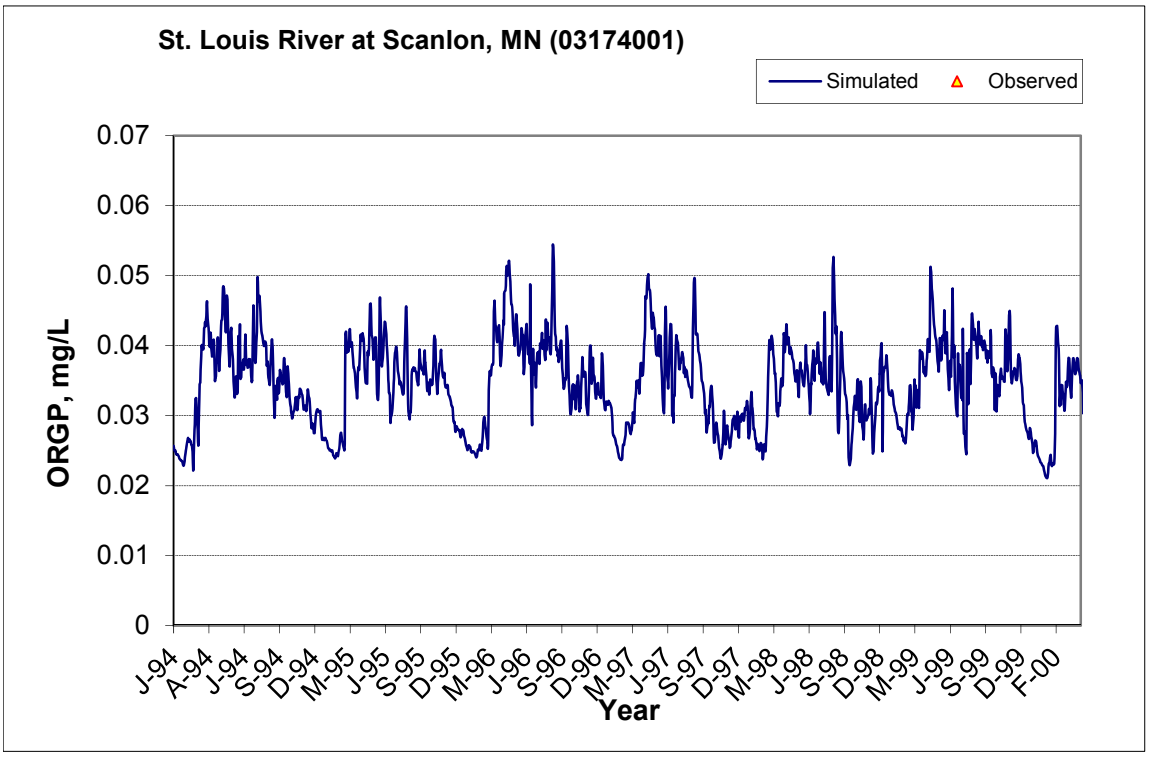

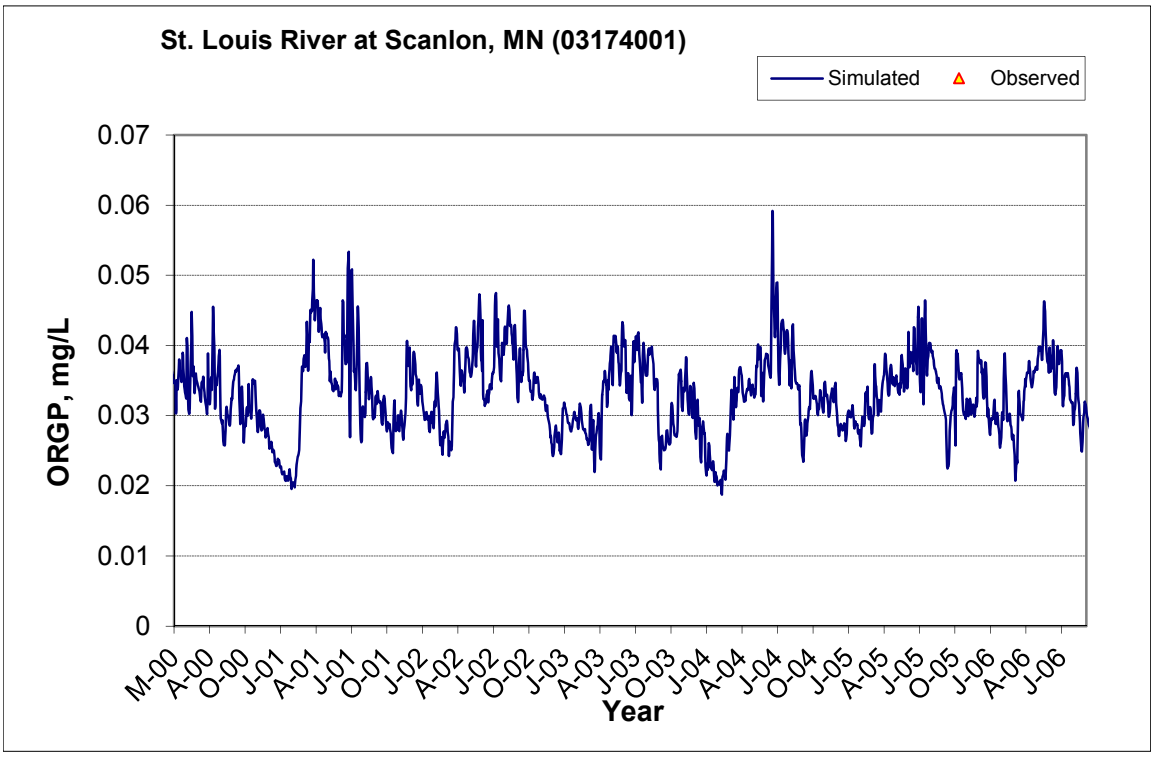

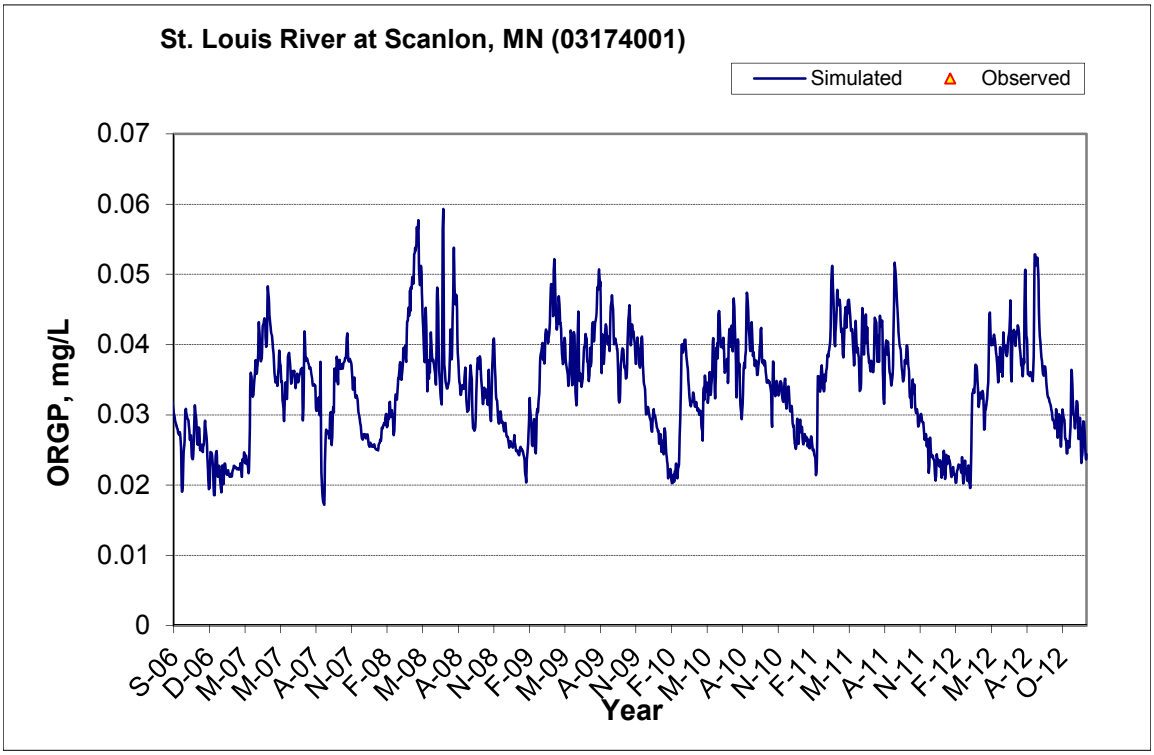

Figure A-155. Time series of observed and simulated Organic Phosphorus (OrgP) concentration at St. Louis River at Scanlon, MN (03174001)

A.5.8 Total Phosphorus (TP)

Table A-23. Total Phosphorus (TP) statistics

Period	1994-2001	2002-2012
Count	41	125
Concentration Average Error	26.65%	-10.36%
Concentration Median Error	21.70%	12.69%
Load Average Error	3.97%	-53.28%
Load Median Error	15.09%	3.26%
Paired t conc	0.10	0.95
Paired t load	0.75	0.07

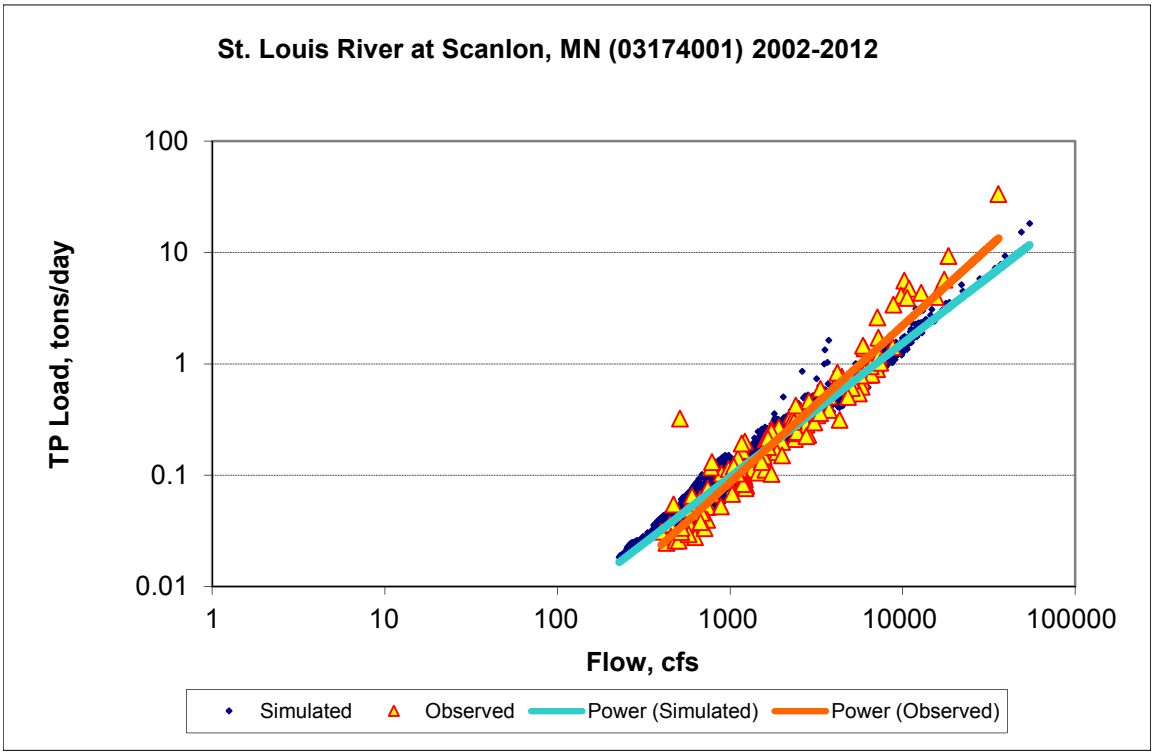

Figure A-156. Power plot of simulated and observed Total Phosphorus (TP) load vs flow at St. Louis River at Scanlon, MN (03174001) (calibration period)

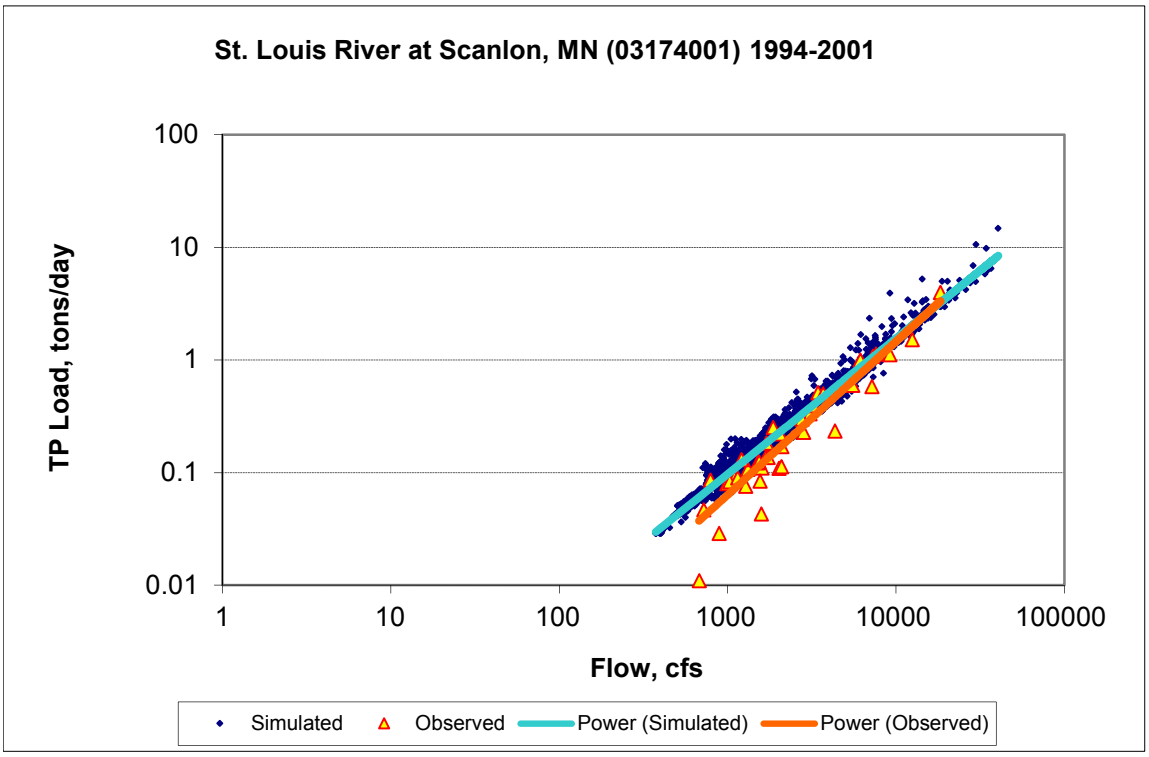

Figure A-157. Power plot of simulated and observed Total Phosphorus (TP) load vs flow at St. Louis River at Scanlon, MN (03174001) (validation period)

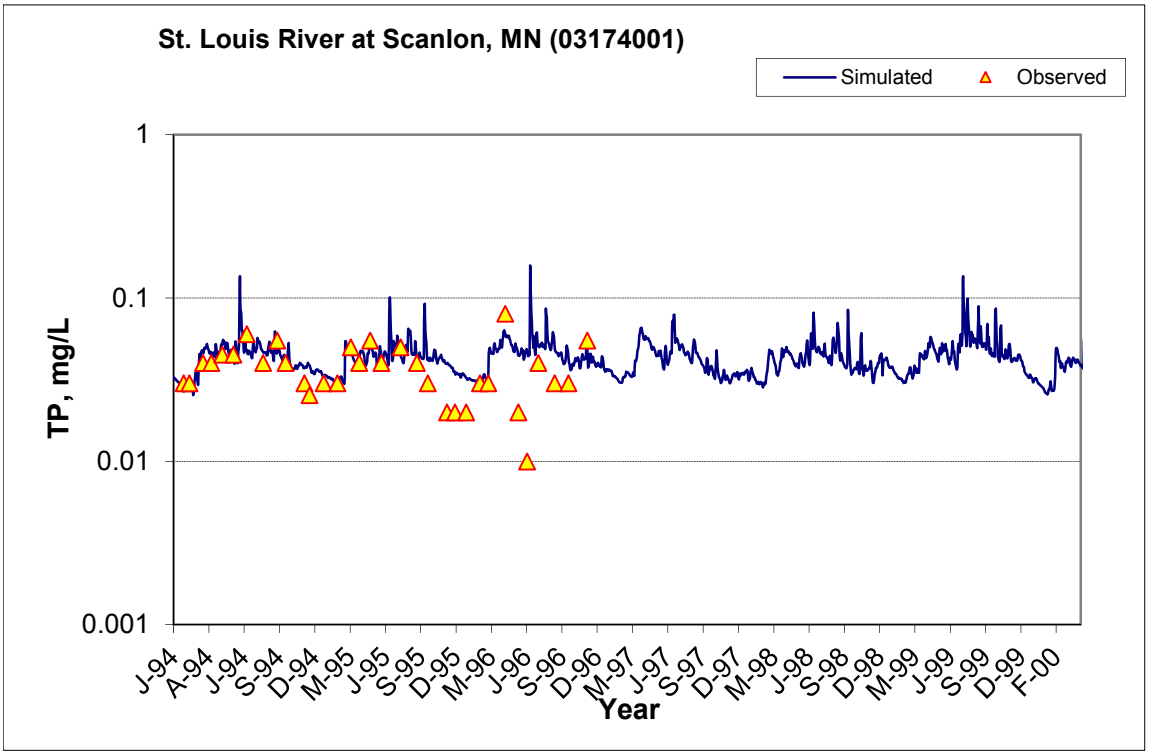

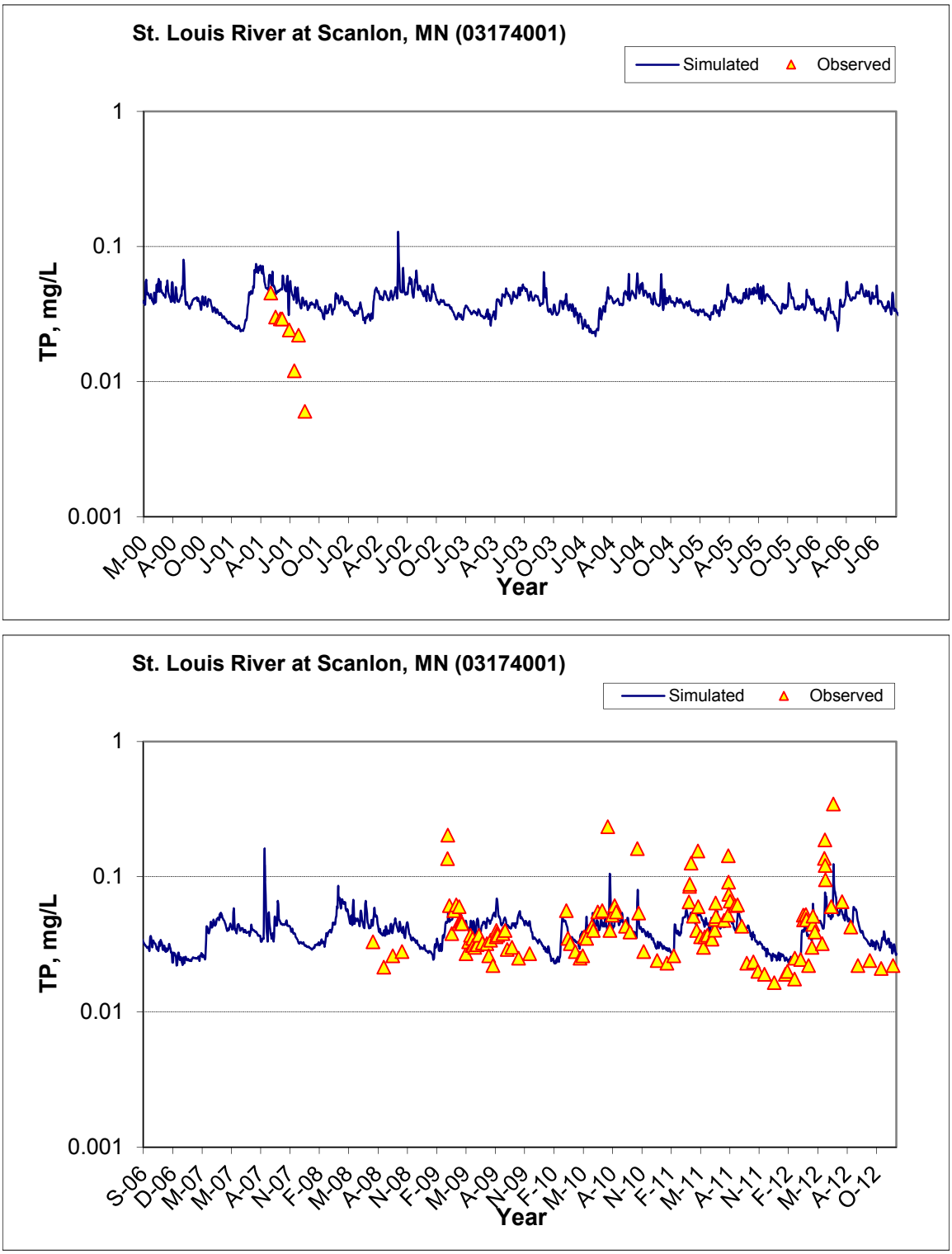

Figure A-158. Time series of observed and simulated Total Phosphorus (TP) concentration at St. Louis River at Scanlon, MN (03174001)

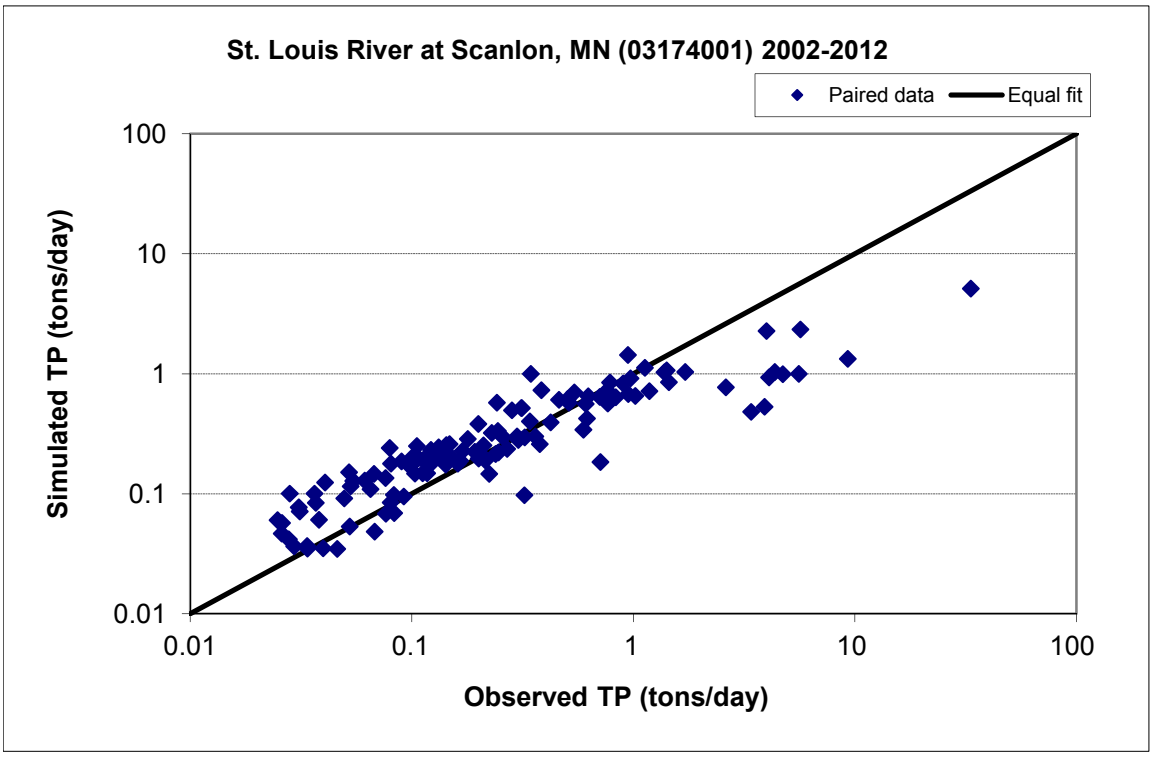

Figure A-159. Paired simulated vs. observed Total Phosphorus (TP) load at St. Louis River at Scanlon, MN (03174001) (calibration period)

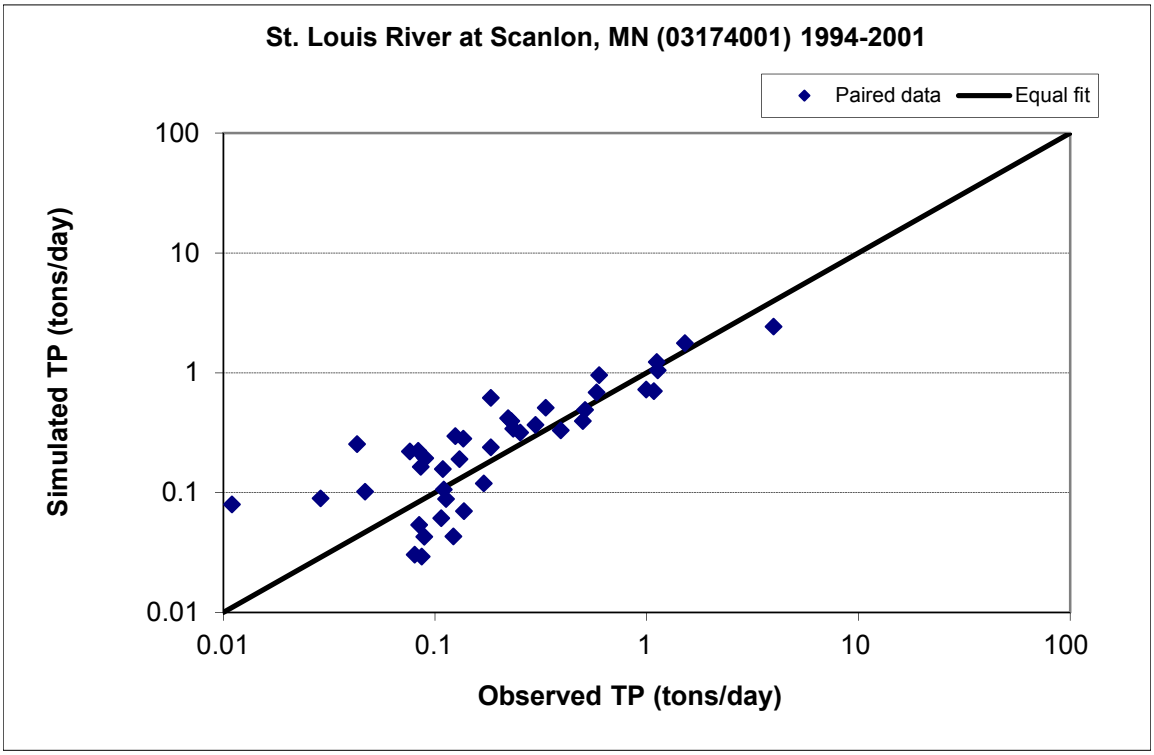

Figure A-160. Paired simulated vs. observed Total Phosphorus (TP) load at St. Louis River at Scanlon, MN (03174001) (validation period)

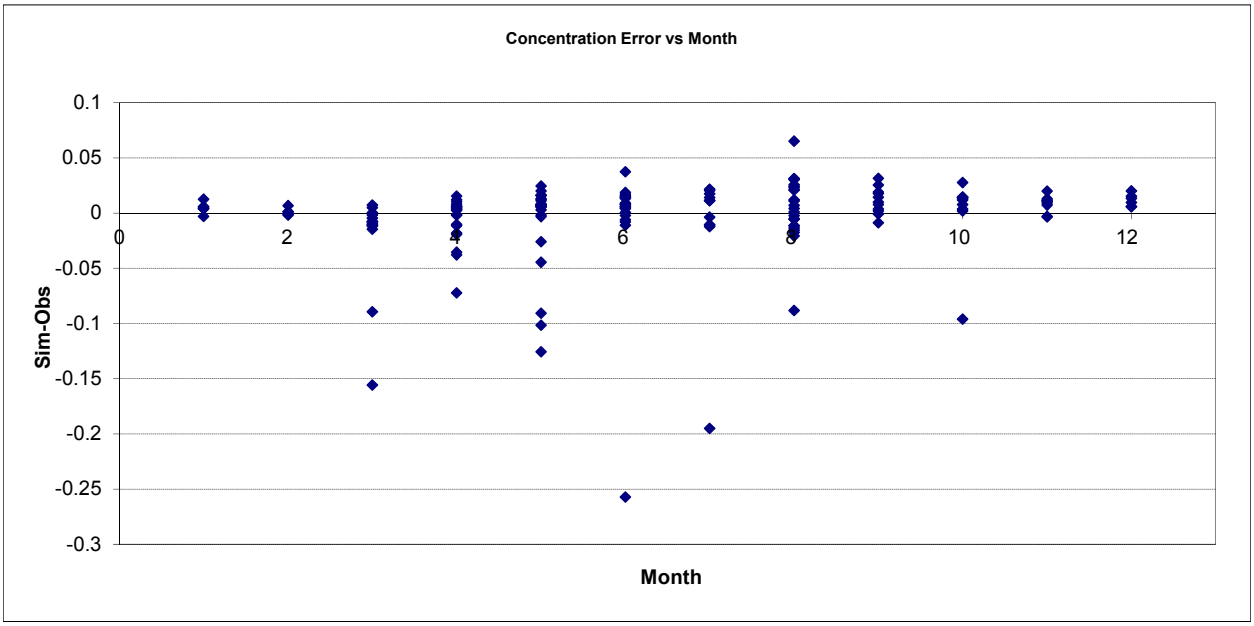

Figure A-161. Residual (Simulated - Observed) vs. Month Total Phosphorus (TP) at St. Louis River at Scanlon, MN (03174001)

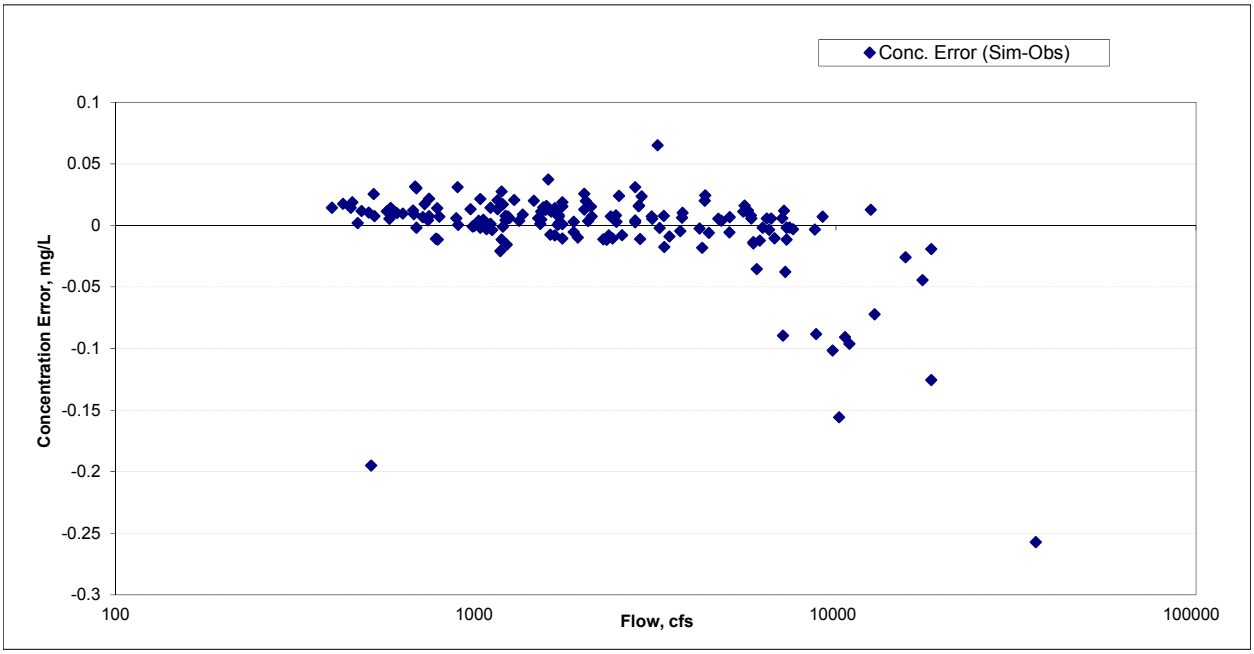

Figure A-162. Residual (Simulated - Observed) vs. Flow Total Phosphorus (TP) at St. Louis River at Scanlon, MN (03174001)

A.6 ST LOUIS RIVER AT BRIDGE ON MN-23 AT FOND DU LAC

A.6.1 Ammonia Nitrogen (NH3)

Table A-24. Ammonia Nitrogen (NH3) statistics

Period	1994-2001	2002-2012
Count	48	49
Concentration Average Error	-33.73%	6.39%
Concentration Median Error	-9.60%	8.61%
Load Average Error	-36.57%	17.11%
Load Median Error	-6.36%	3.84%
Paired t conc	0.06	0.97
Paired t load	0.09	0.55

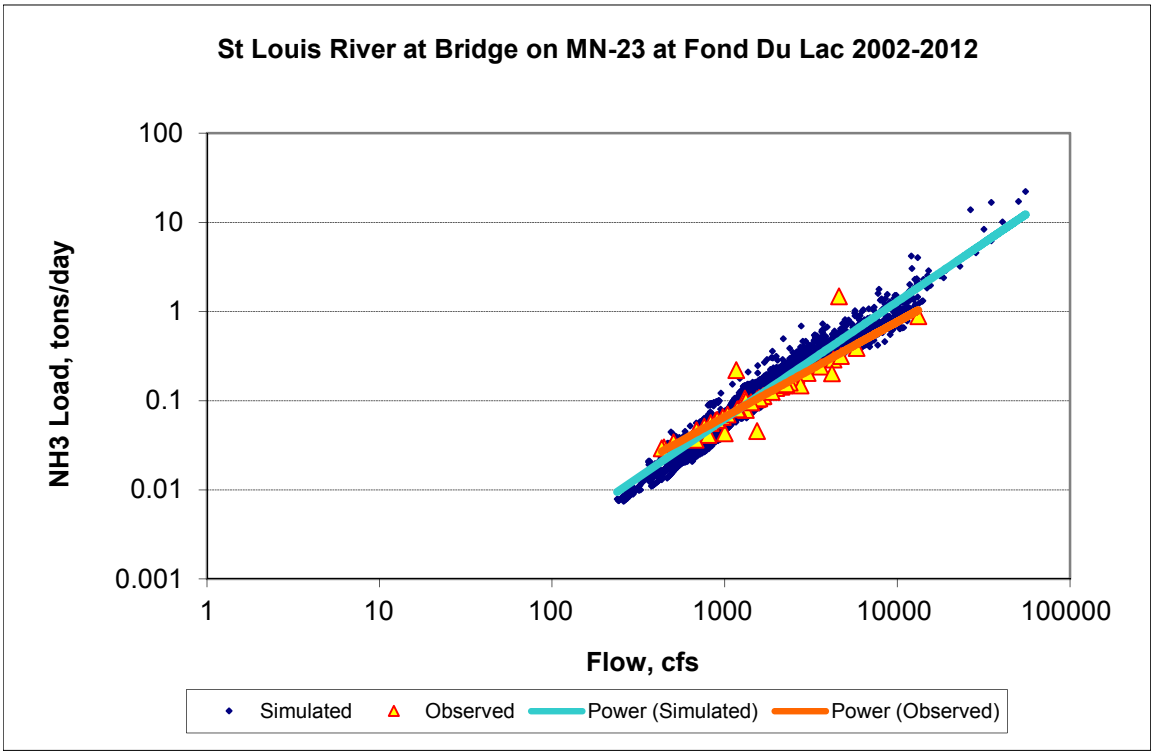

Figure A-163. Power plot of simulated and observed Ammonia Nitrogen (NH3) load vs flow at St Louis River at Bridge on MN-23 at Fond Du Lac (calibration period)

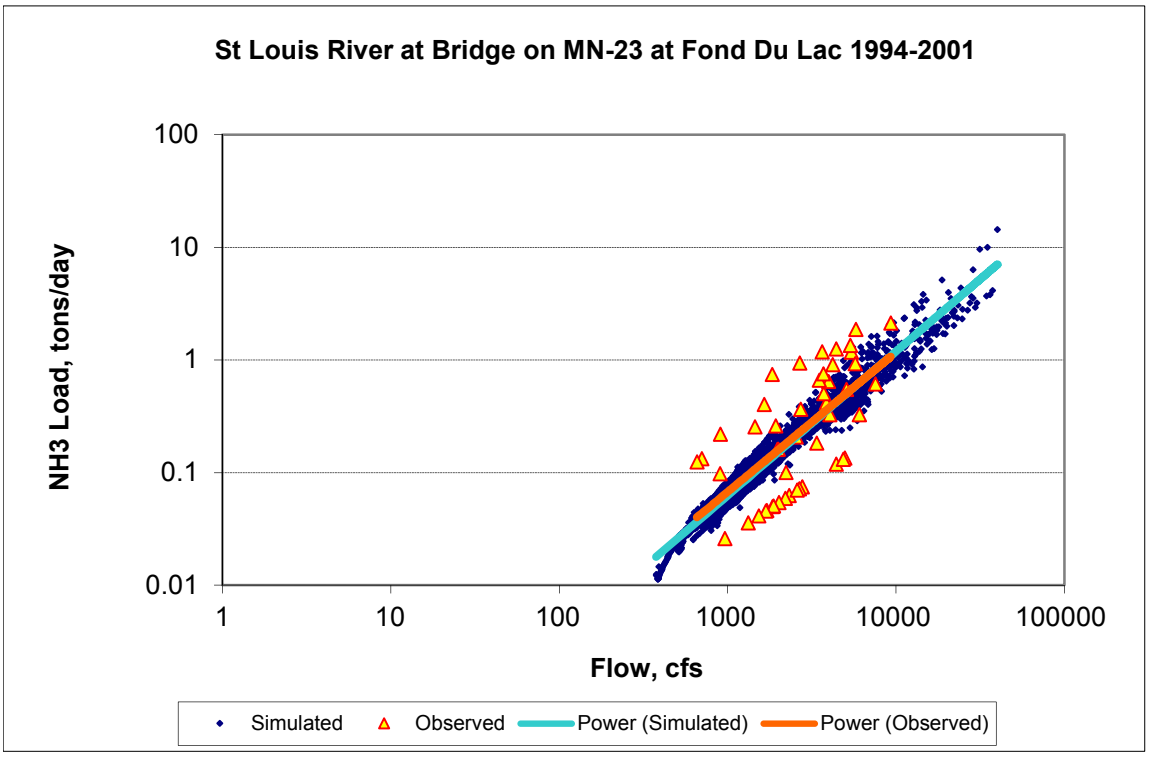

Figure A-164. Power plot of simulated and observed Ammonia Nitrogen (NH3) load vs flow at St Louis River at Bridge on MN-23 at Fond Du Lac (validation period)

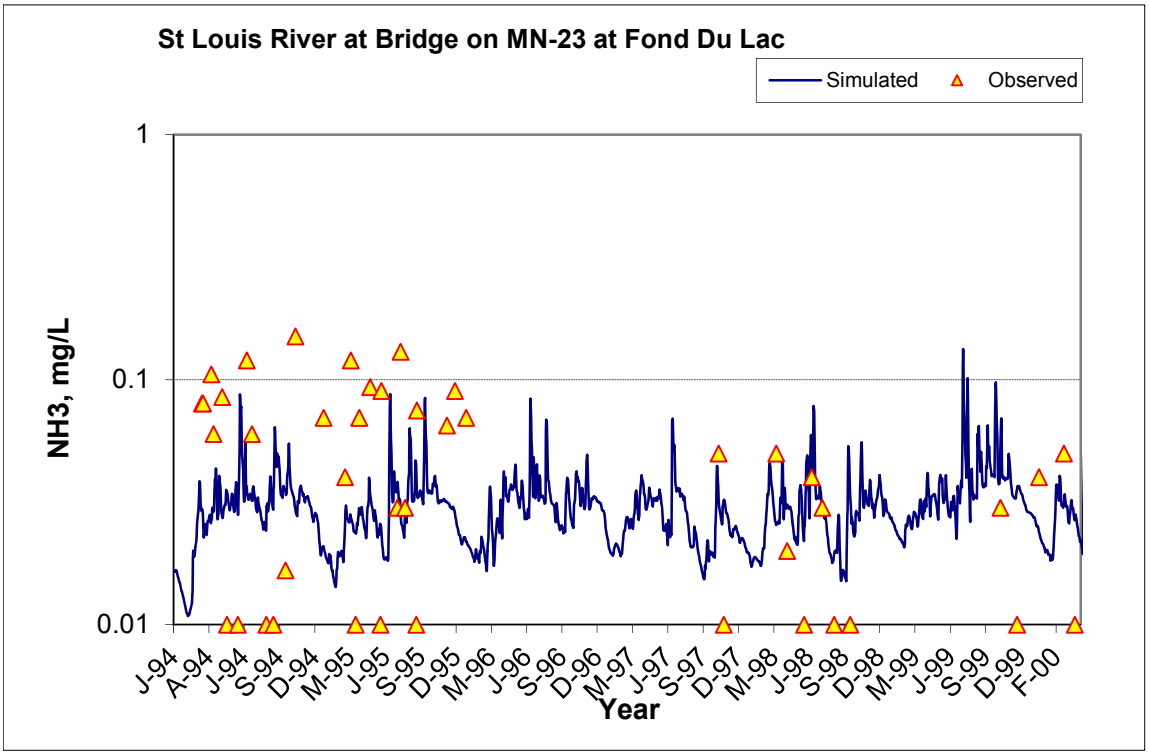

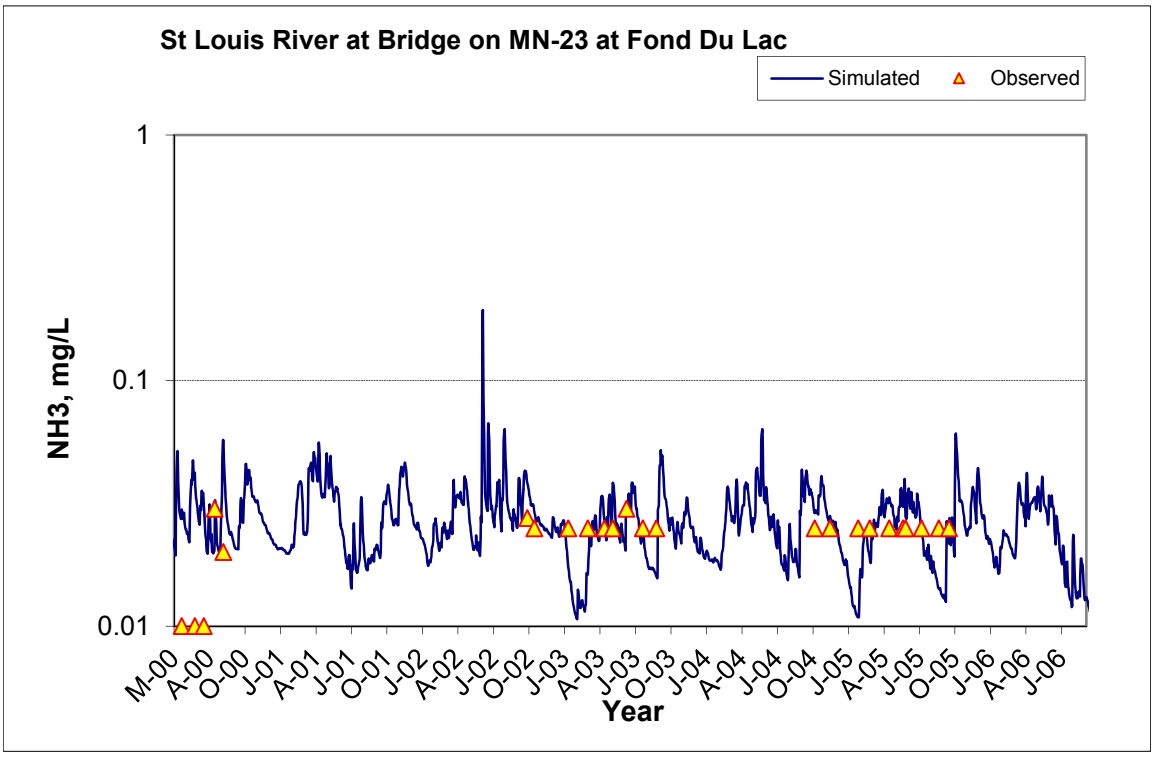

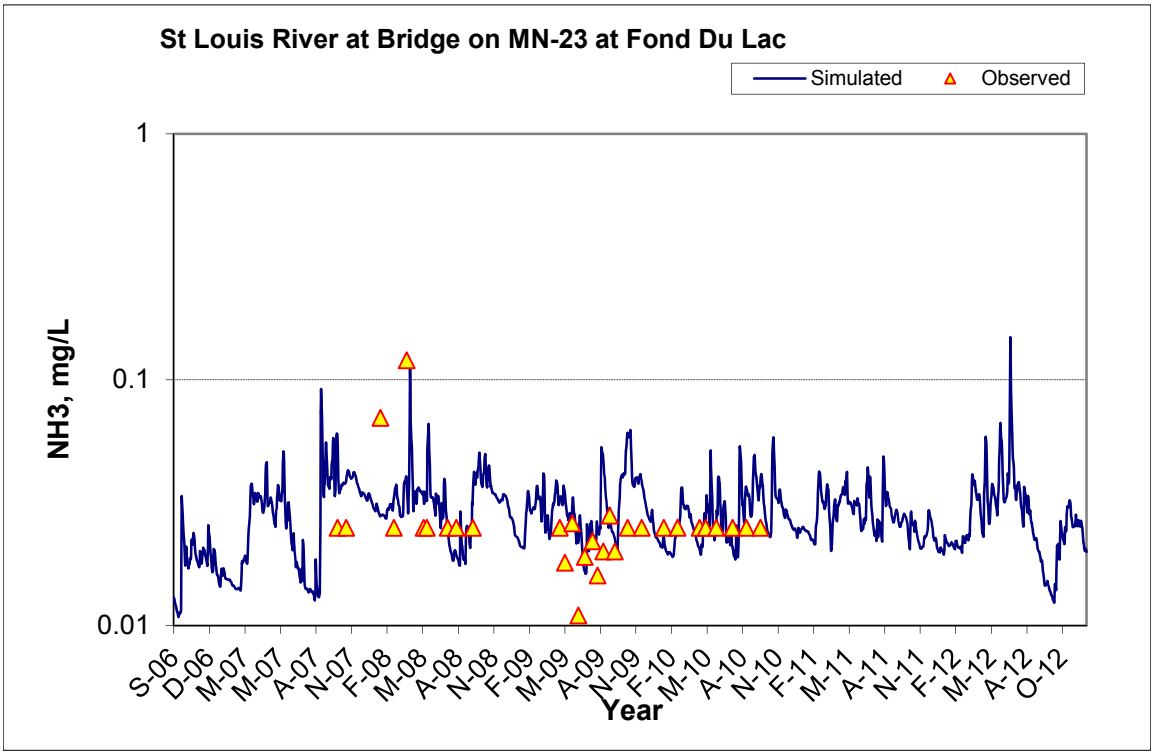

Figure A-165. Time series of observed and simulated Ammonia Nitrogen (NH3) concentration at St Louis River at Bridge on MN-23 at Fond Du Lac

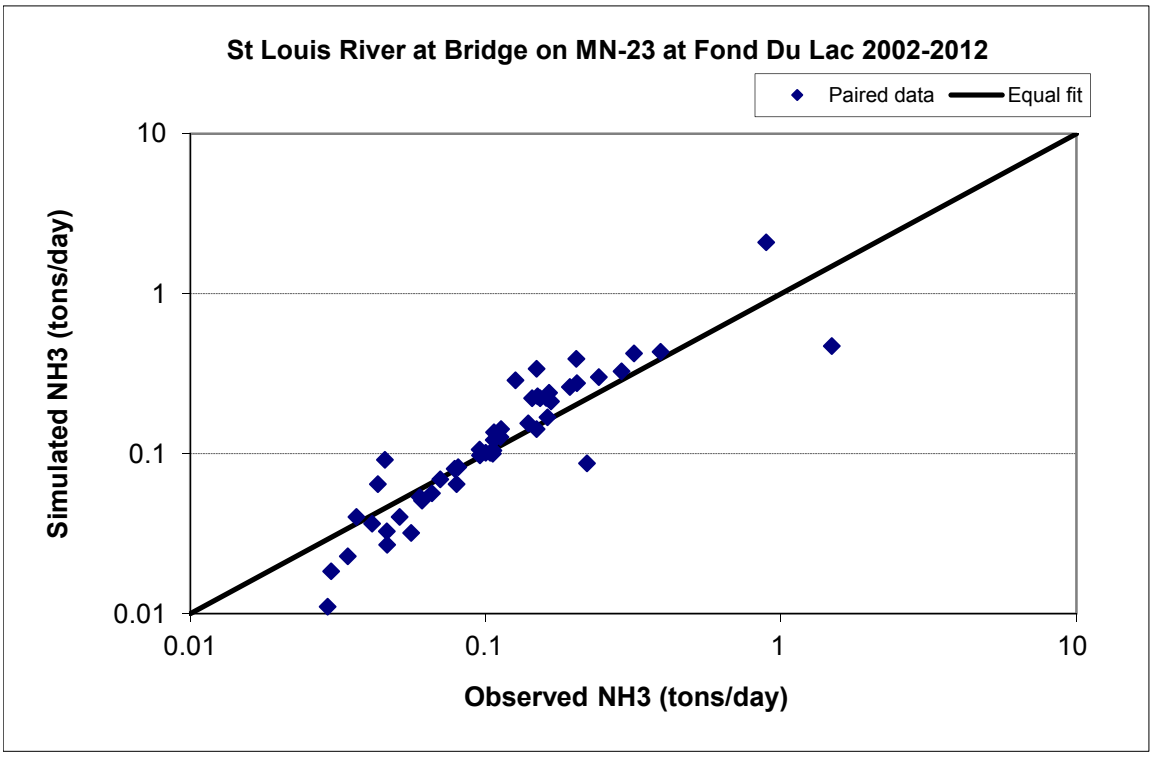

Figure A-166. Paired simulated vs. observed Ammonia Nitrogen (NH3) load at St Louis River at Bridge on MN-23 at Fond Du Lac (calibration period)

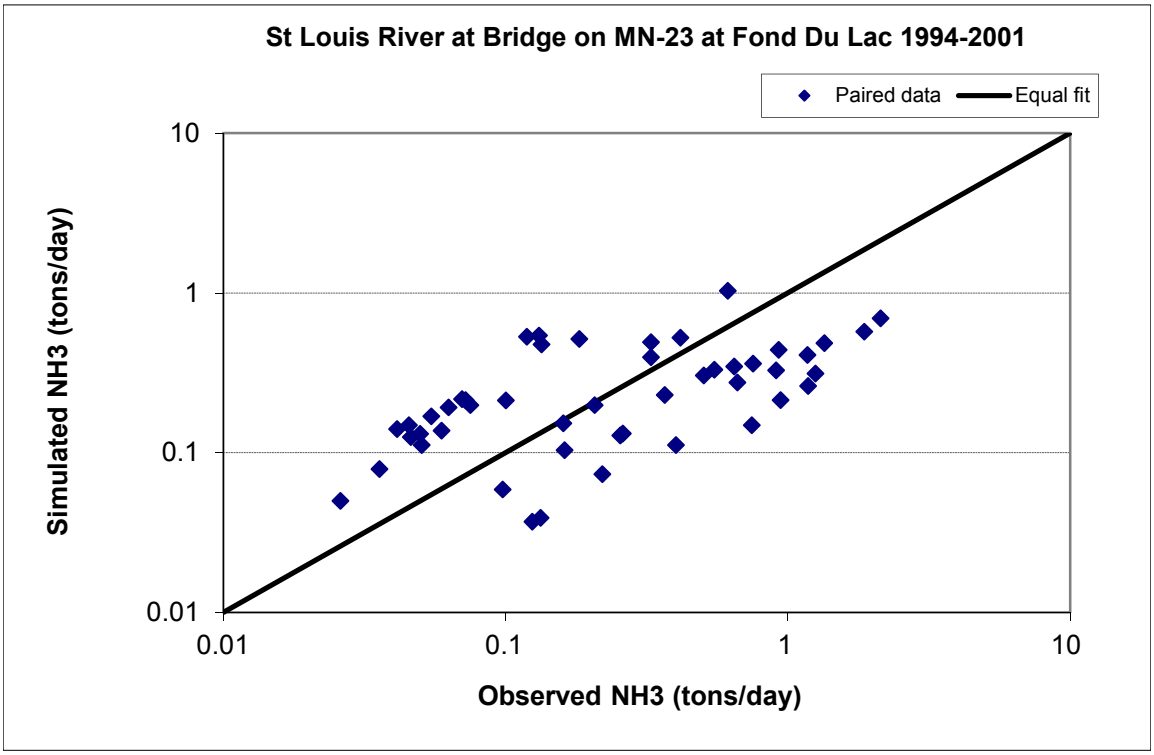

Figure A-167. Paired simulated vs. observed Ammonia Nitrogen (NH3) load at St Louis River at Bridge on MN-23 at Fond Du Lac (validation period)

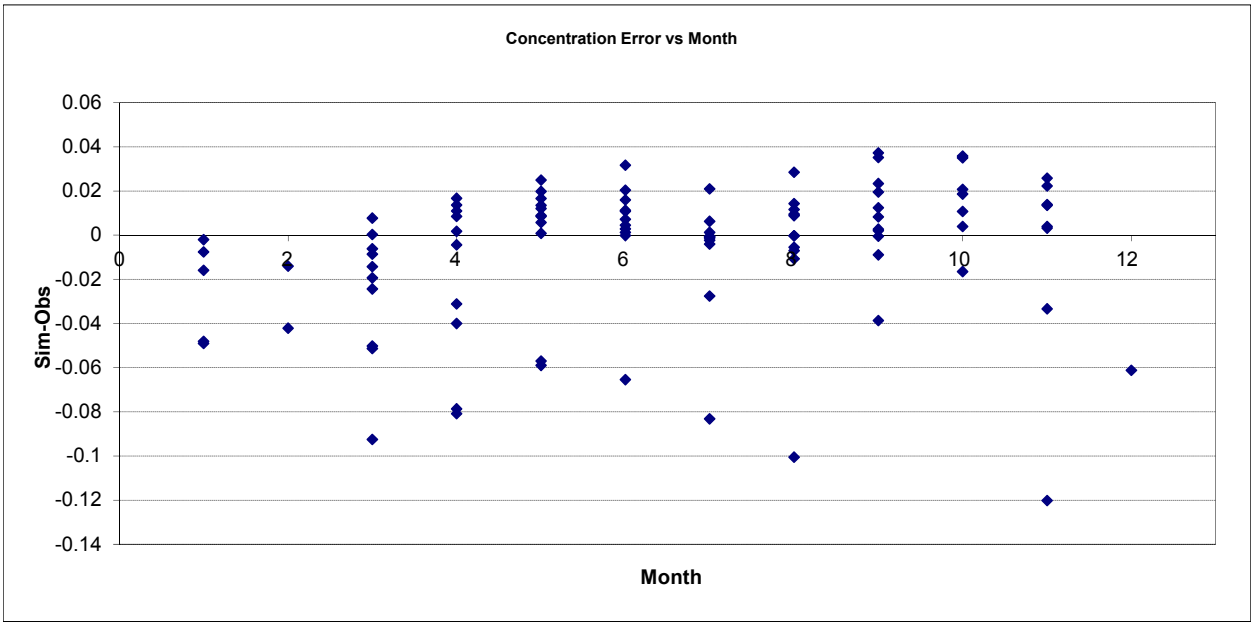

Figure A-168. Residual (Simulated - Observed) vs. Month Ammonia Nitrogen (NH3) at St Louis River at Bridge on MN-23 at Fond Du Lac

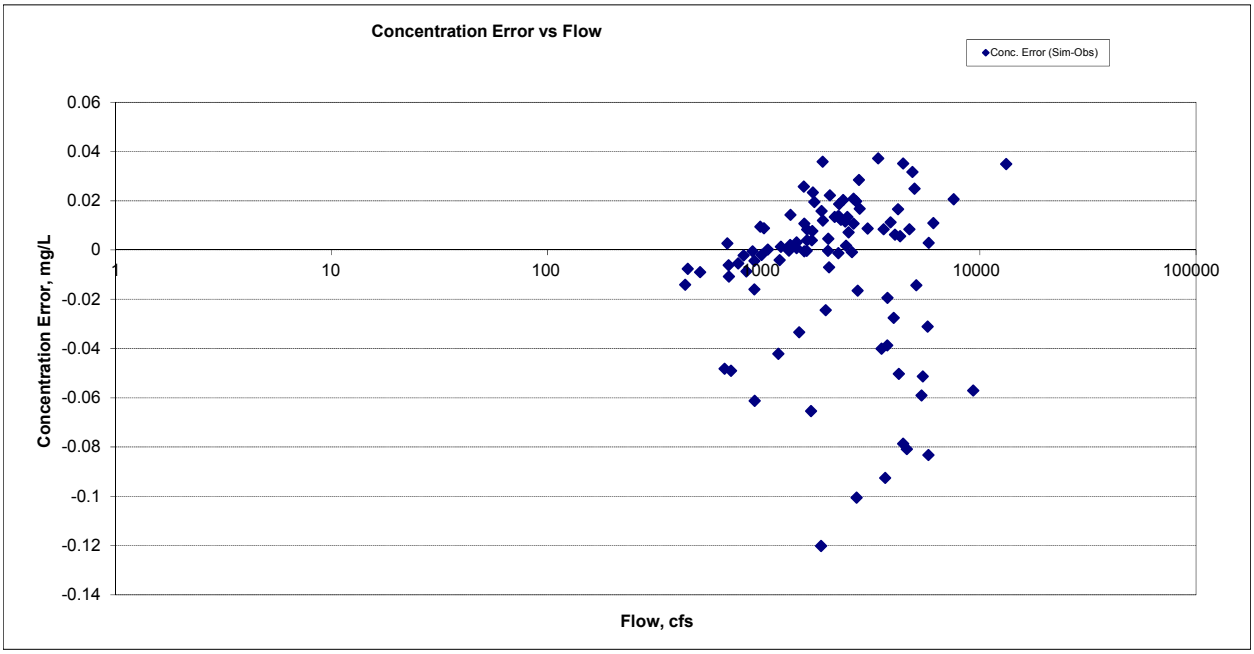

Figure A-169. Residual (Simulated - Observed) vs. Flow Ammonia Nitrogen (NH3) at St Louis River at Bridge on MN-23 at Fond Du Lac

A.6.2 Organic Nitrogen (OrgN)

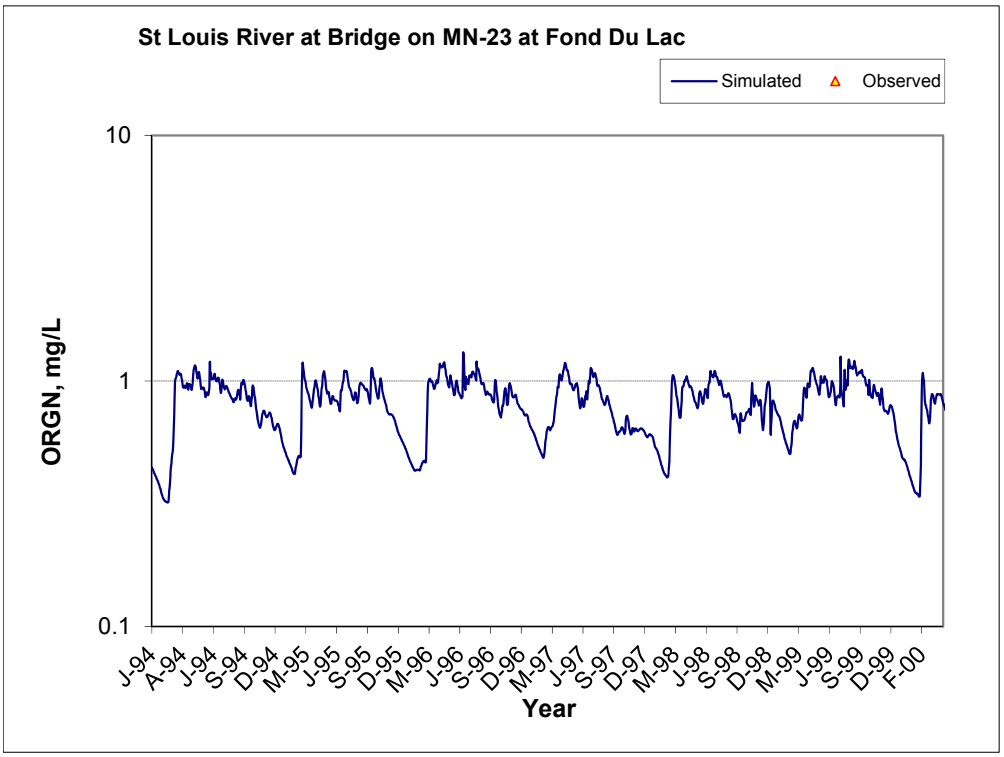

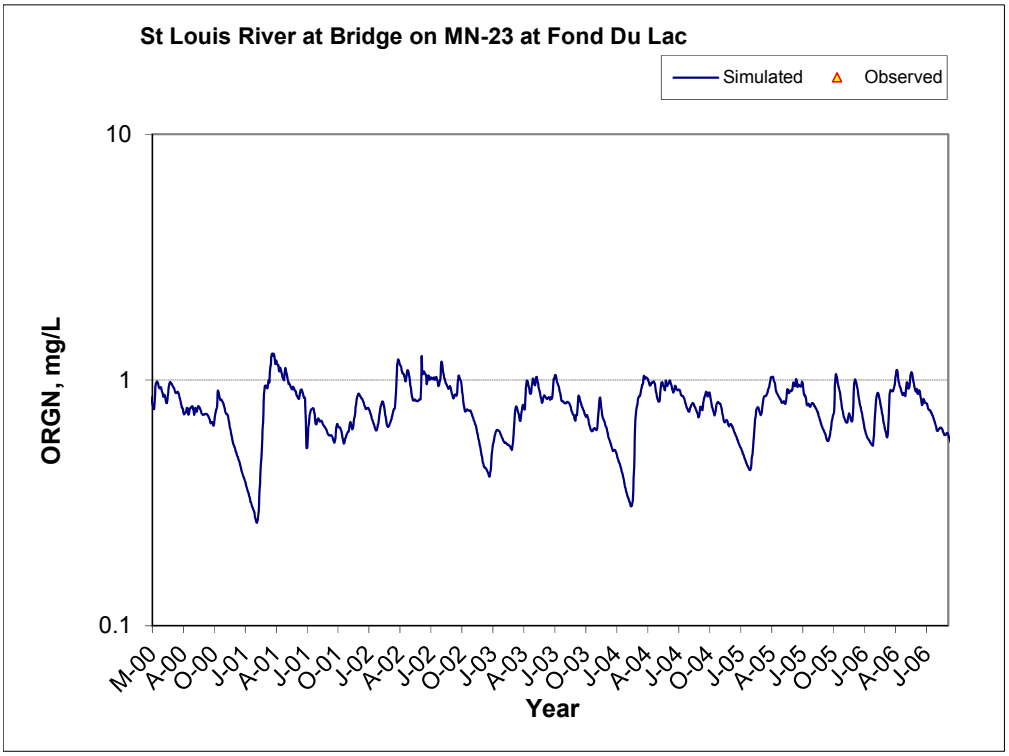

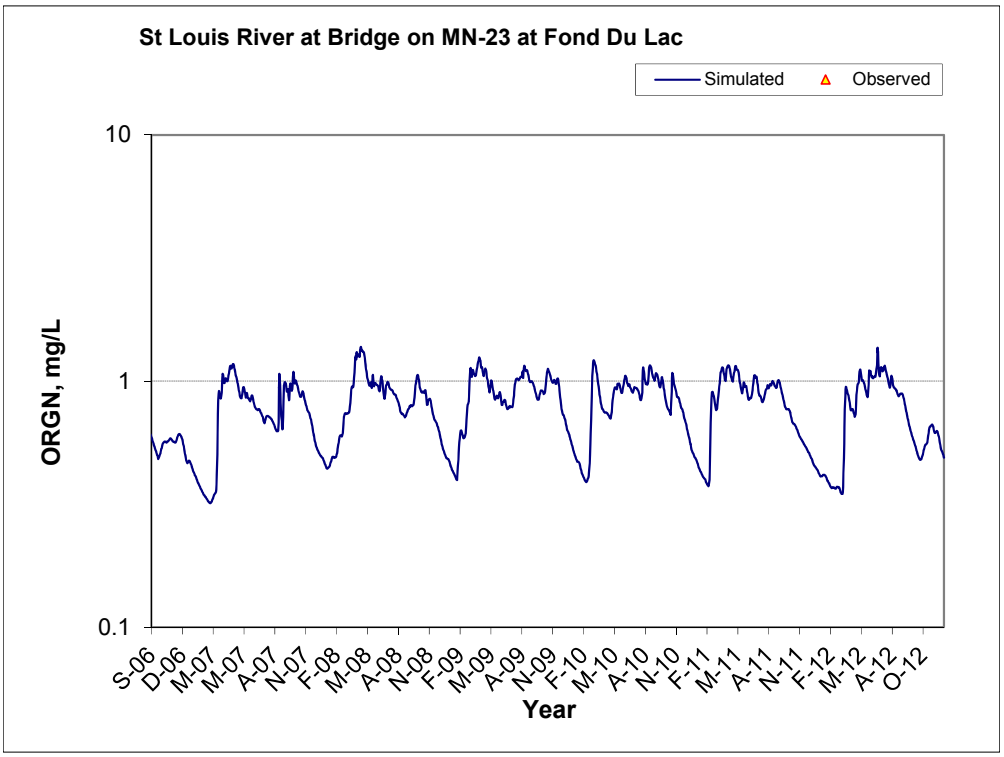

Figure A-170. Time series of observed and simulated Organic Nitrogen (OrgN) concentration at St Louis River at Bridge on MN-23 at Fond Du Lac

A.6.3 Total Kjeldahl Nitrogen (TKN)

Table A-25. Total Kjeldahl Nitrogen (TKN) statistics

Period	1994-2001	2002-2012
Count	7	7
Concentration Average Error	33.33%	-2.98%
Concentration Median Error	40.25%	-2.57%
Load Average Error	36.58%	-3.33%
Load Median Error	14.86%	-2.91%
Paired t conc	0.02	0.99
Paired t load	0.25	0.71

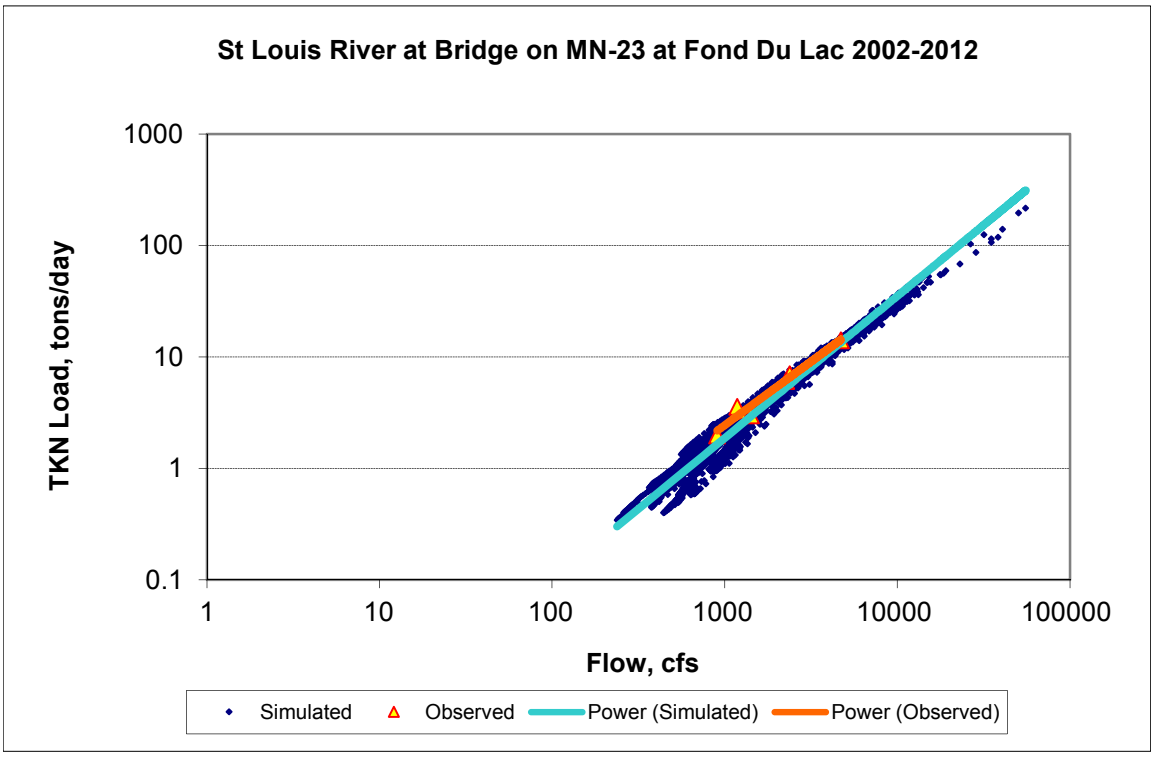

Figure A-171. Power plot of simulated and observed Total Kjeldahl Nitrogen (TKN) load vs flow at St Louis River at Bridge on MN-23 at Fond Du Lac (calibration period)

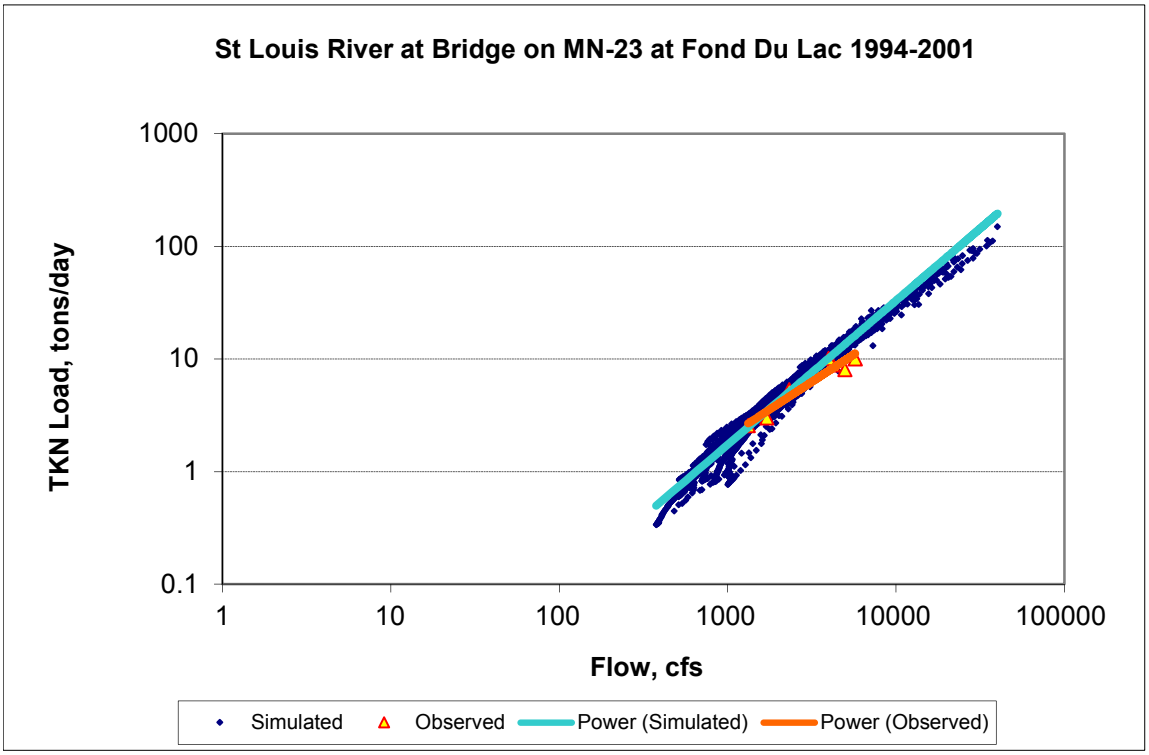

Figure A-172. Power plot of simulated and observed Total Kjeldahl Nitrogen (TKN) load vs flow at St Louis River at Bridge on MN-23 at Fond Du Lac (validation period)

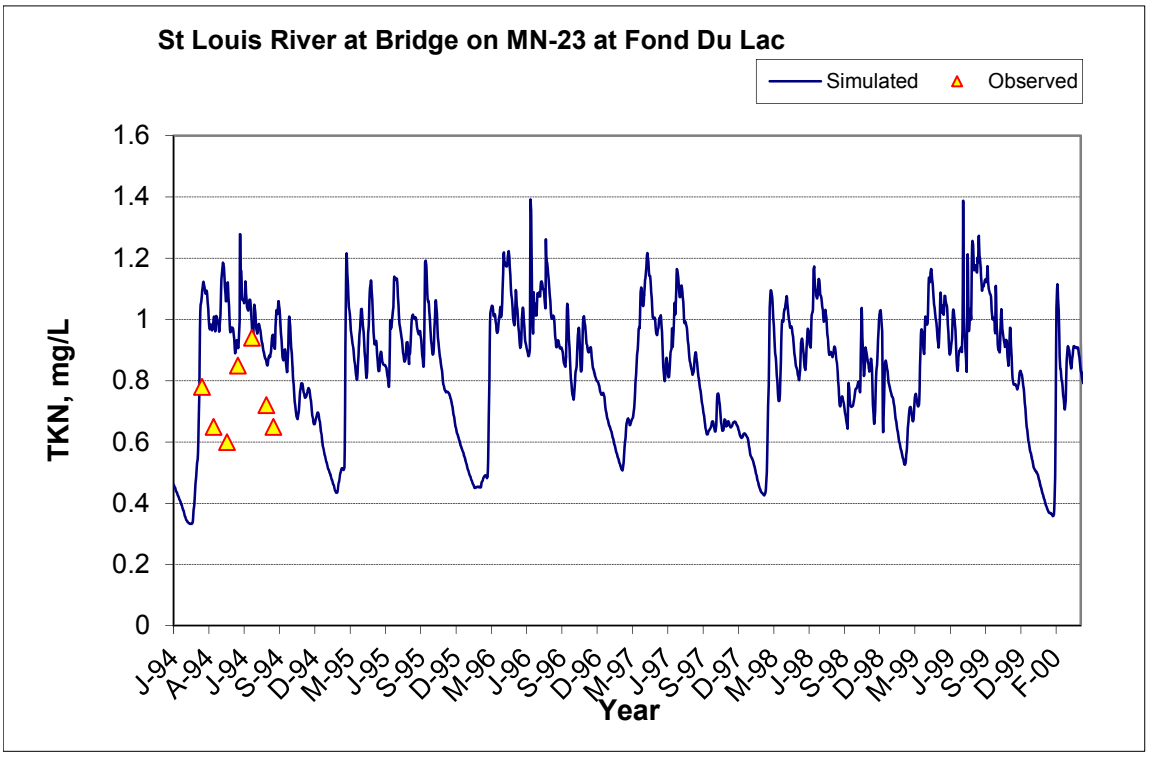
St Louis River at Bridge on MN-23 at Fond Du Lac
Simulated
Observed
TKN, mg/L
1.6
1.4
1.2
1
0.8
0.6
0.4
0.2
0
J-94 A-94 J-94 S-94 D-94 M-95 J-95 S-95 D-95 M-96 J-96 S-96 D-96 M-97 J-97 S-97 D-97 M-98 J-98 S-98 D-98 M-99 J-99 S-99 D-99 F-00
Year

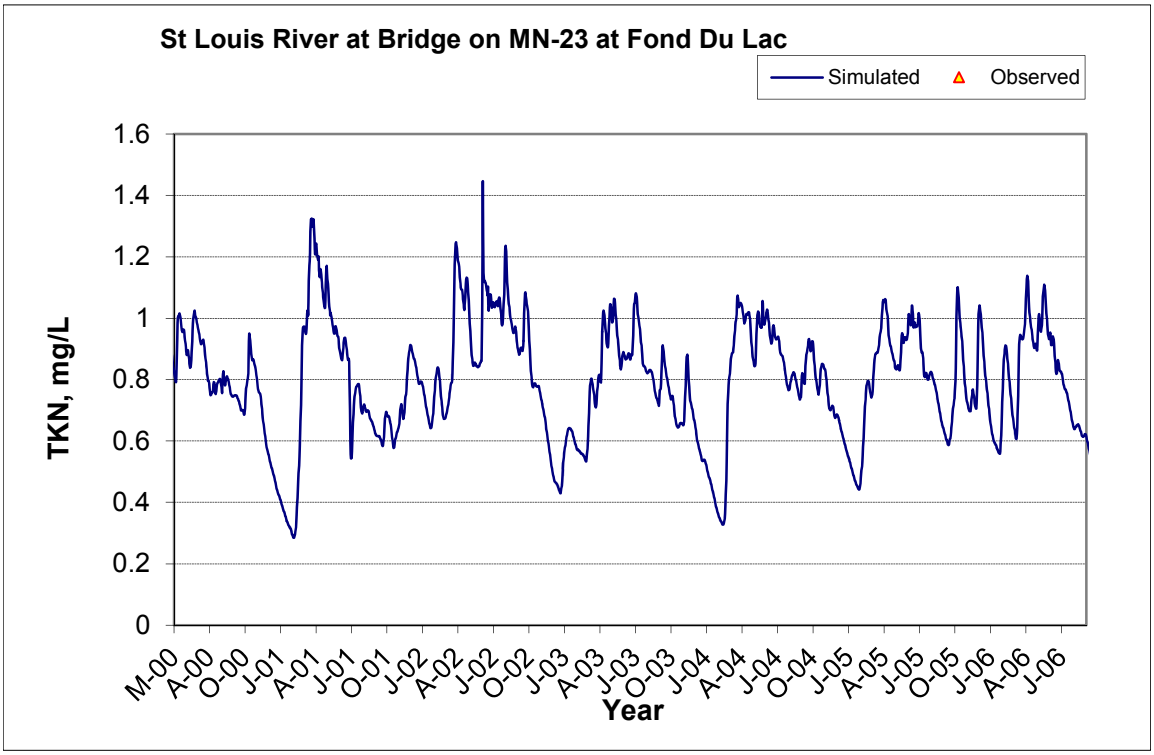
St Louis River at Bridge on MN-23 at Fond Du Lac
Simulated
Observed
TKN, mg/L
1.6
1.4
1.2
1
0.8
0.6
0.4
0.2
0
M-00 A-00 O-00 J-01 A-01 J-01 O-01 J-02 A-02 J-02 O-02 J-03 A-03 J-03 O-03 J-04 A-04 J-04 O-04 J-05 A-05 J-05 O-05 J-06 A-06 J-06
Year

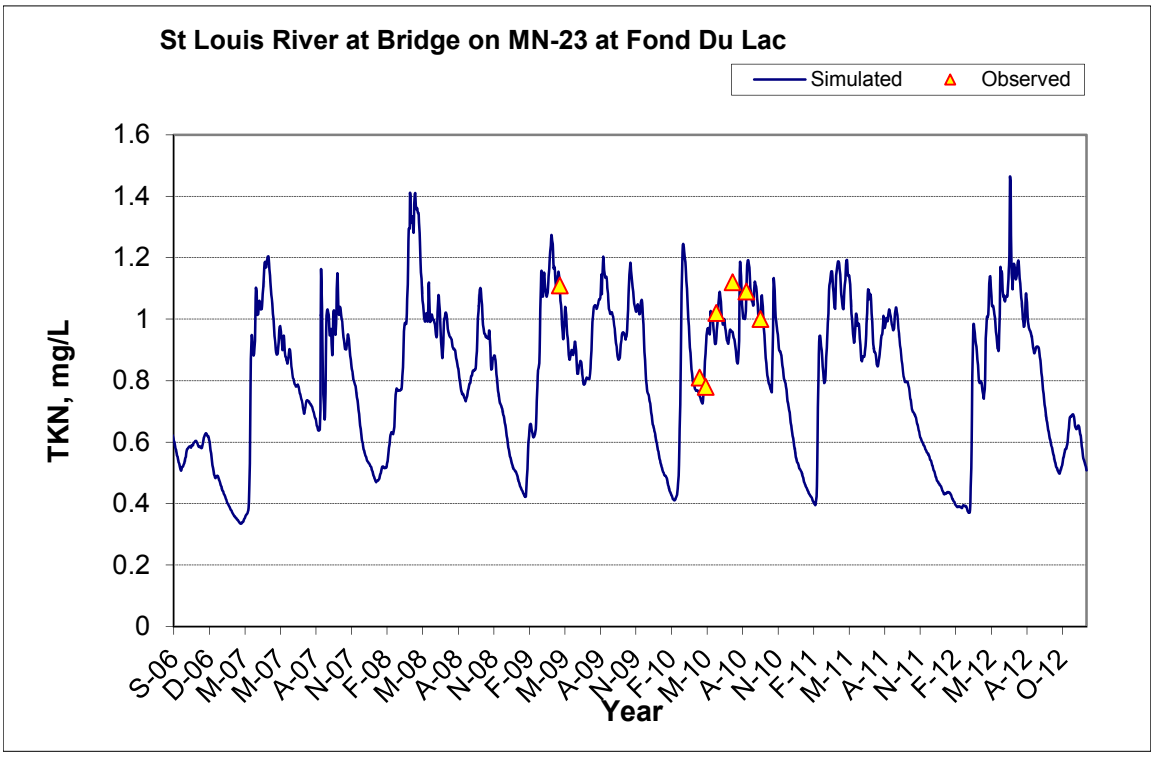

Figure A-173. Time series of observed and simulated Total Kjeldahl Nitrogen (TKN) concentration at St Louis River at Bridge on MN-23 at Fond Du Lac

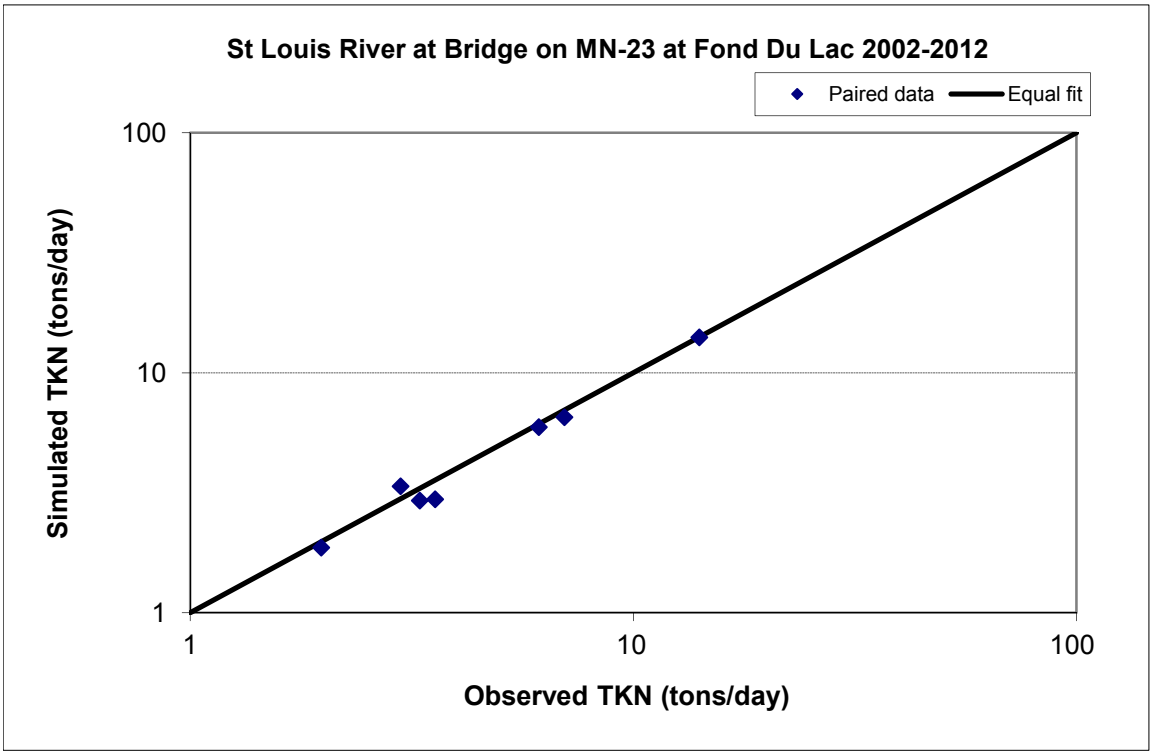

Figure A-174. Paired simulated vs. observed Total Kjeldahl Nitrogen (TKN) load at St Louis River at Bridge on MN-23 at Fond Du Lac (calibration period)

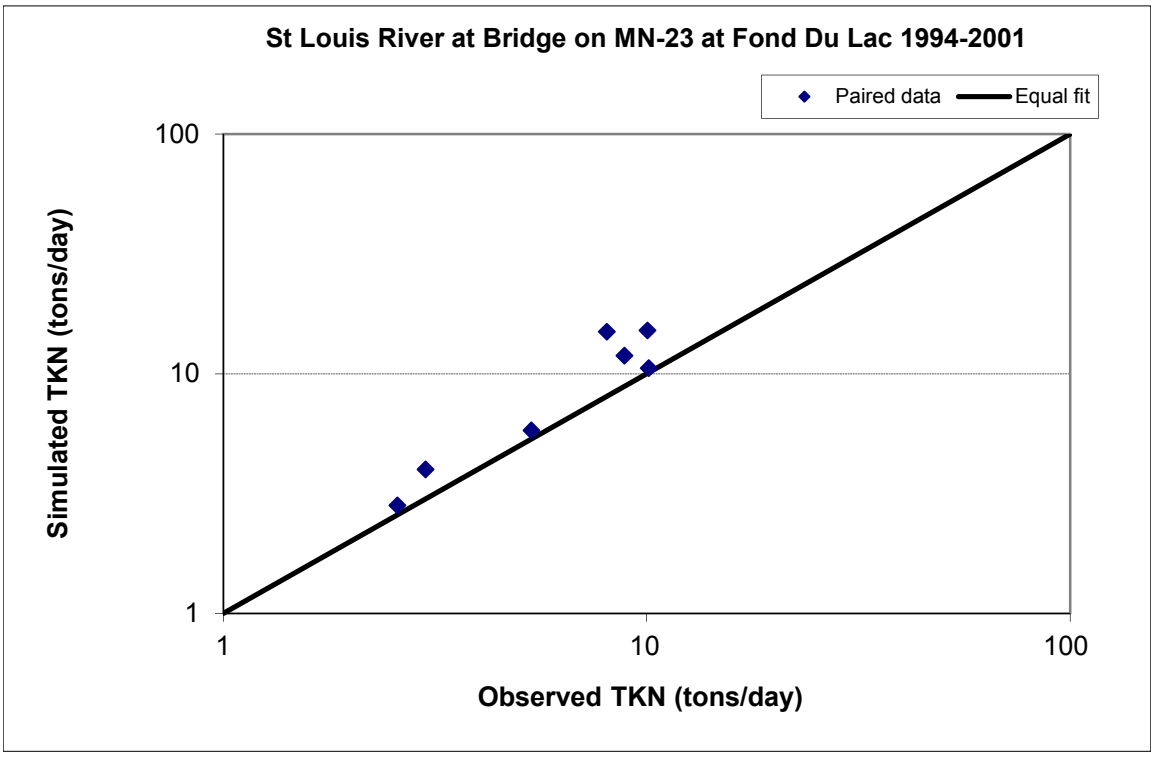

Figure A-175. Paired simulated vs. observed Total Kjeldahl Nitrogen (TKN) load at St Louis River at Bridge on MN-23 at Fond Du Lac (validation period)

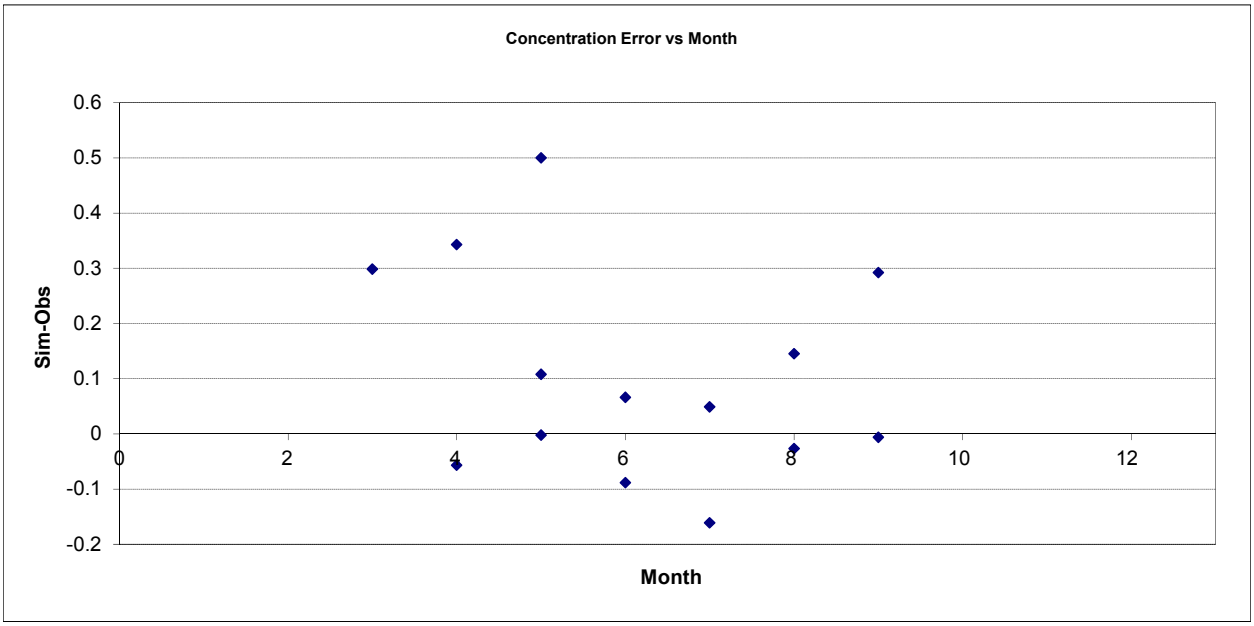

Figure A-176. Residual (Simulated - Observed) vs. Month Total Kjeldahl Nitrogen (TKN) at St Louis River at Bridge on MN-23 at Fond Du Lac

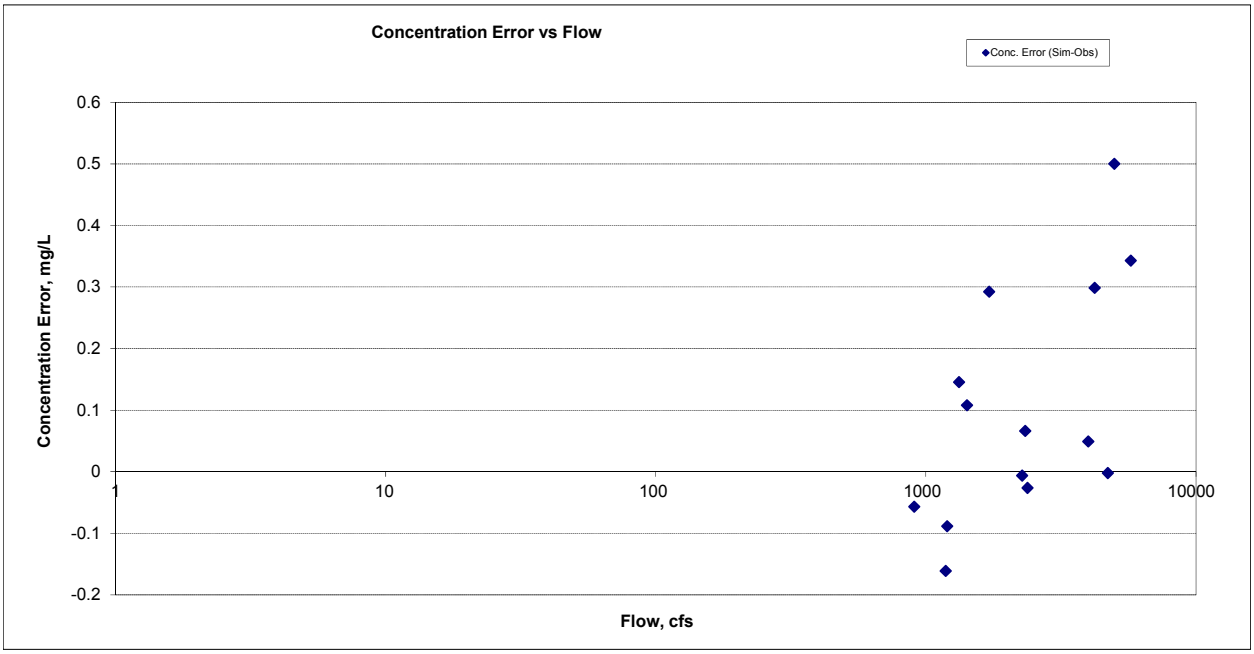

Figure A-177. Residual (Simulated - Observed) vs. Flow Total Kjeldahl Nitrogen (TKN) at St Louis River at Bridge on MN-23 at Fond Du Lac

A.6.4 Nitrite+ Nitrate Nitrogen (NOx)

Table A-26. Nitrite+ Nitrate Nitrogen (NOx) statistics

Period	1994-2001	2002-2012
Count	36	49
Concentration Average Error	0.42%	29.38%
Concentration Median Error	7.07%	23.12%
Load Average Error	-5.12%	4.83%
Load Median Error	5.14%	16.34%
Paired t conc	0.96	0.19
Paired t load	0.84	0.77

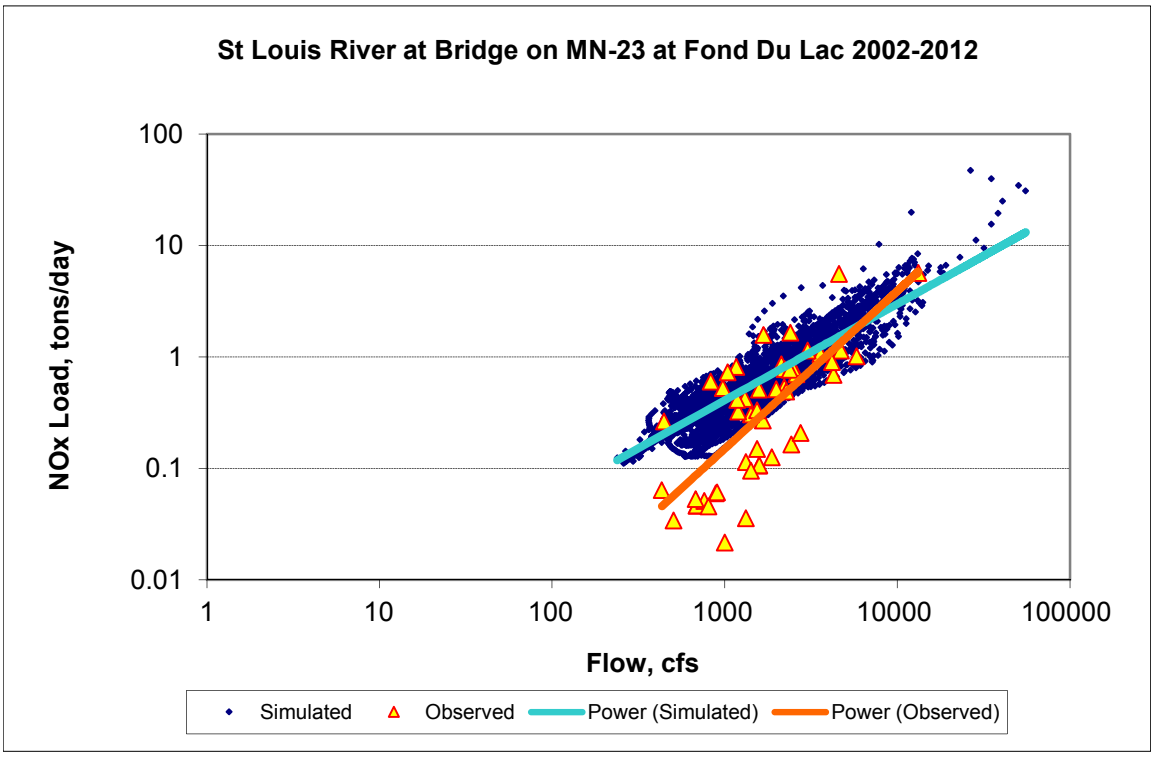

Figure A-178. Power plot of simulated and observed Nitrite+ Nitrate Nitrogen (NOx) load vs flow at St Louis River at Bridge on MN-23 at Fond Du Lac (calibration period)

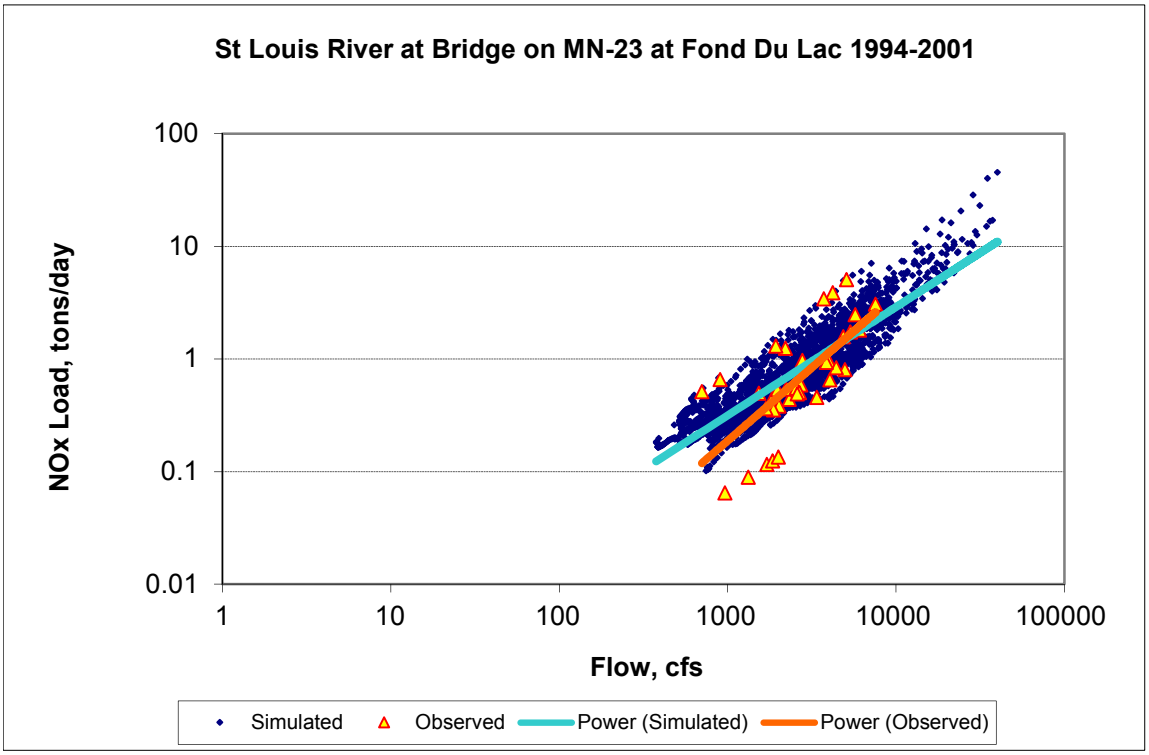

Figure A-179. Power plot of simulated and observed Nitrite+ Nitrate Nitrogen (NOx) load vs flow at St Louis River at Bridge on MN-23 at Fond Du Lac (validation period)

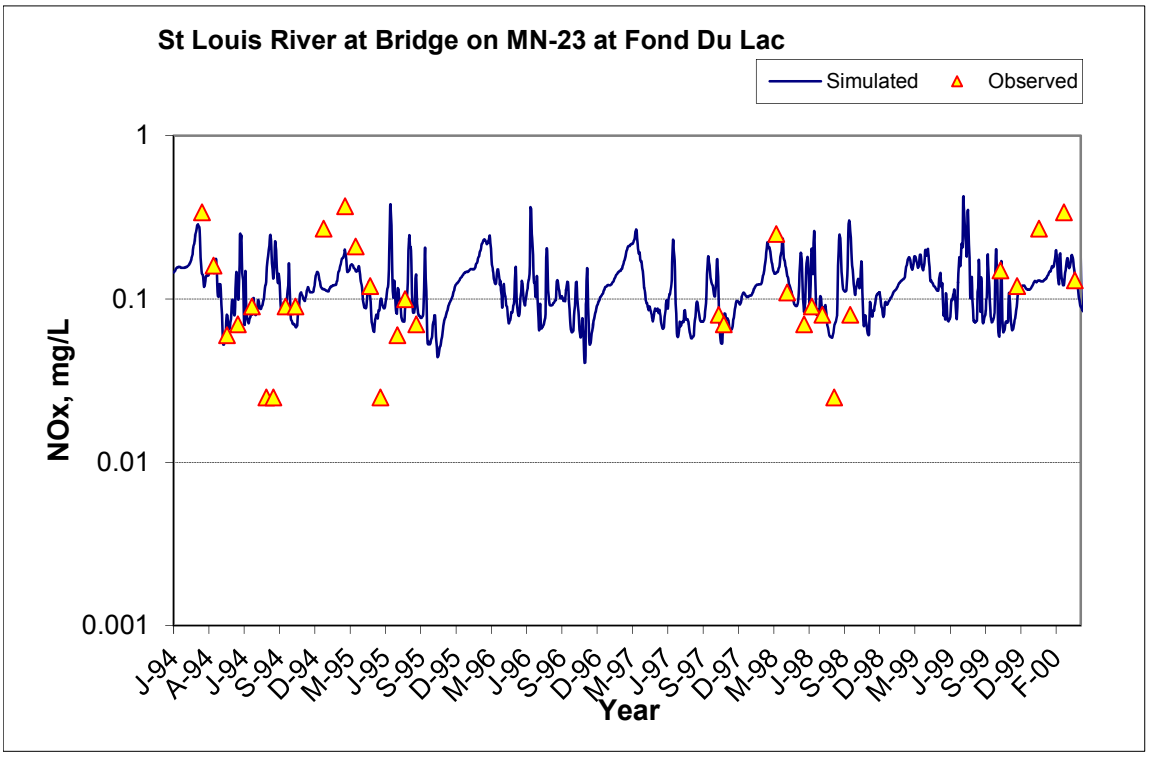
St Louis River at Bridge on MN-23 at Fond Du Lac
Simulated
Observed
NOx, mg/L
1
0.1
0.01
0.001
J-94 A-94 J-94 S-94 D-94 M-95 J-95 S-95 D-95 M-96 J-96 S-96 D-96 M-97 J-97 S-97 D-97 M-98 J-98 S-98 D-98 M-99 J-99 S-99 D-99 F-00
Year

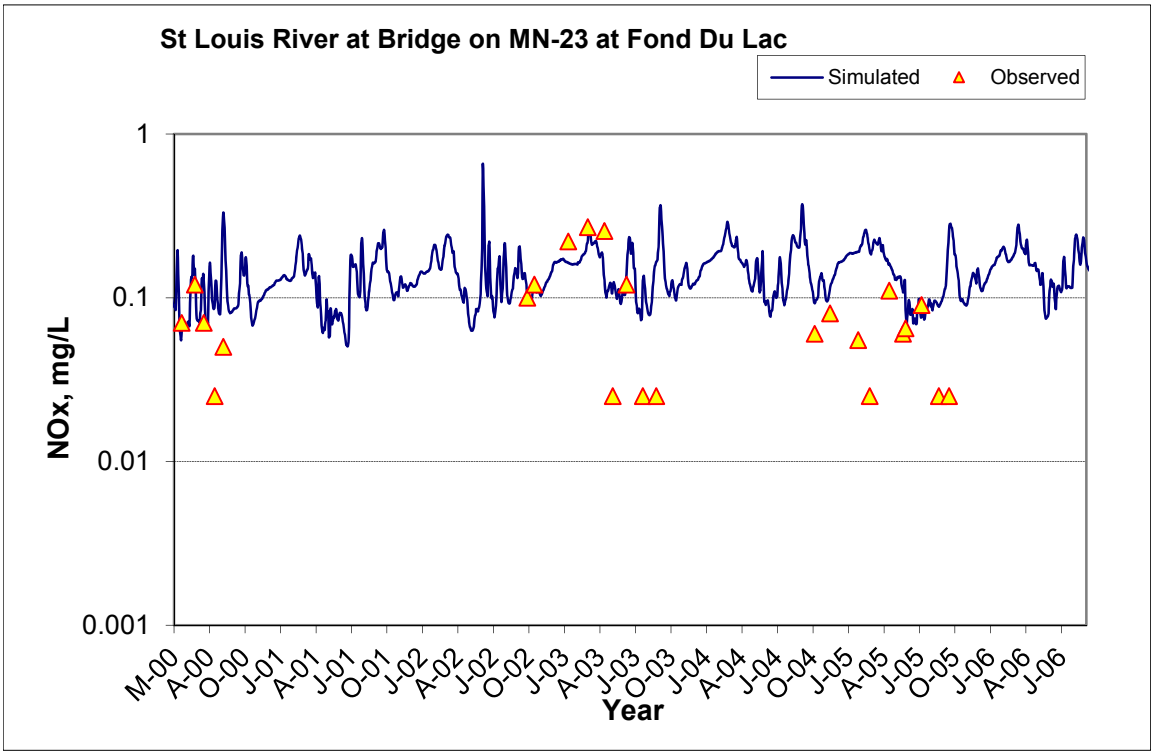
St Louis River at Bridge on MN-23 at Fond Du Lac
Simulated
Observed
NOx, mg/L
1
0.1
0.01
0.001
M-00 A-00 O-00 J-01 A-01 J-01 O-01 J-02 A-02 J-02 O-02 J-03 A-03 J-03 O-03 J-04 A-04 J-04 O-04 J-05 A-05 J-05 O-05 J-06 A-06 J-06
Year

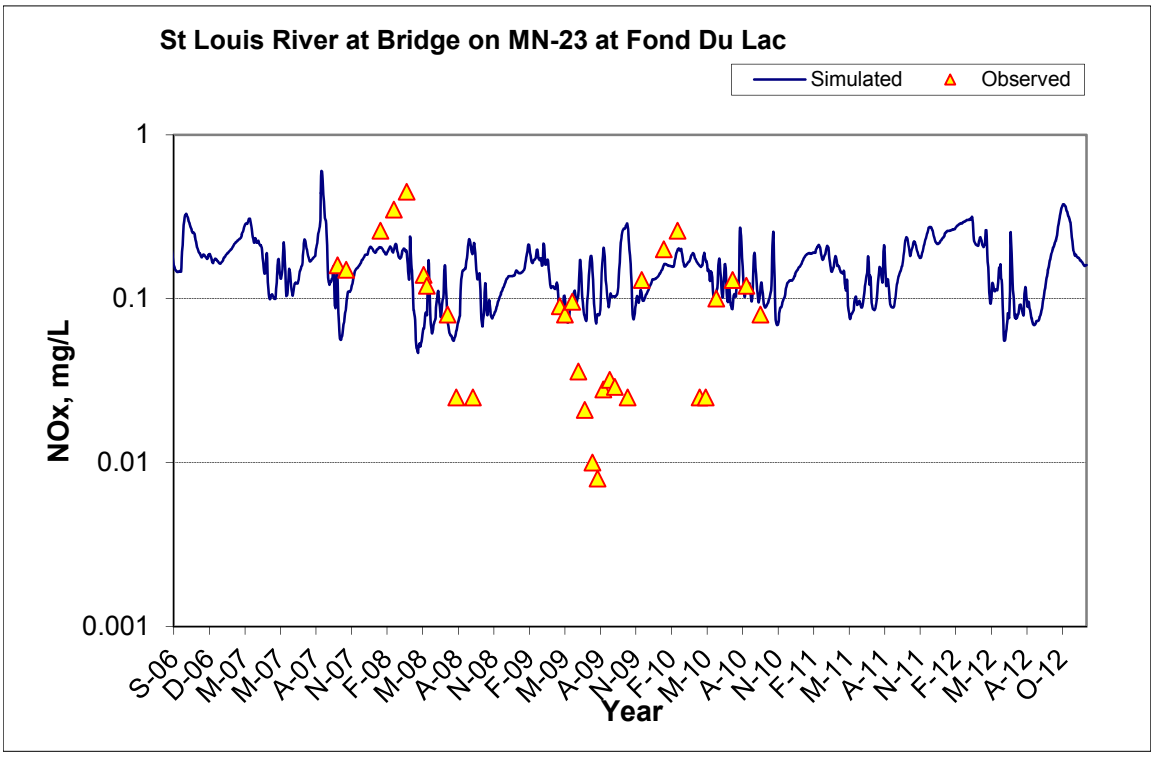

Figure A-180. Time series of observed and simulated Nitrite+ Nitrate Nitrogen (NOx) concentration at St Louis River at Bridge on MN-23 at Fond Du Lac

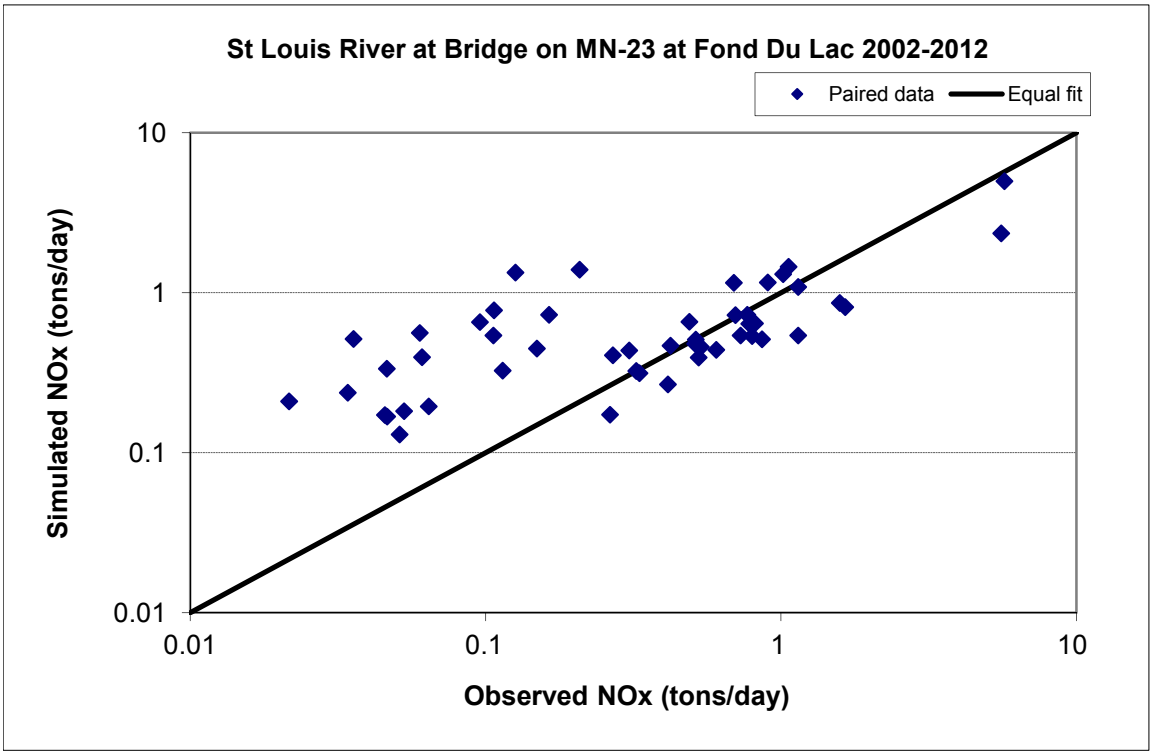

Figure A-181. Paired simulated vs. observed Nitrite+ Nitrate Nitrogen (NOx) load at St Louis River at Bridge on MN-23 at Fond Du Lac (calibration period)

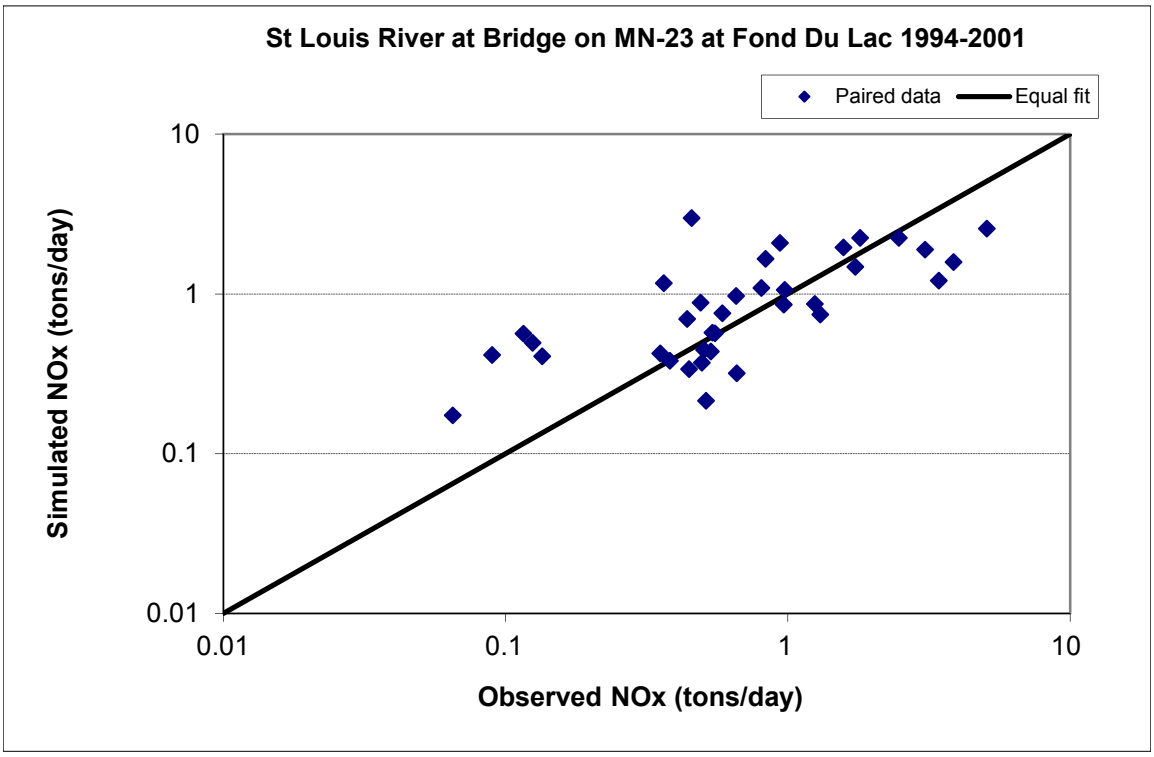

Figure A-182. Paired simulated vs. observed Nitrite+ Nitrate Nitrogen (NOx) load at St Louis River at Bridge on MN-23 at Fond Du Lac (validation period)

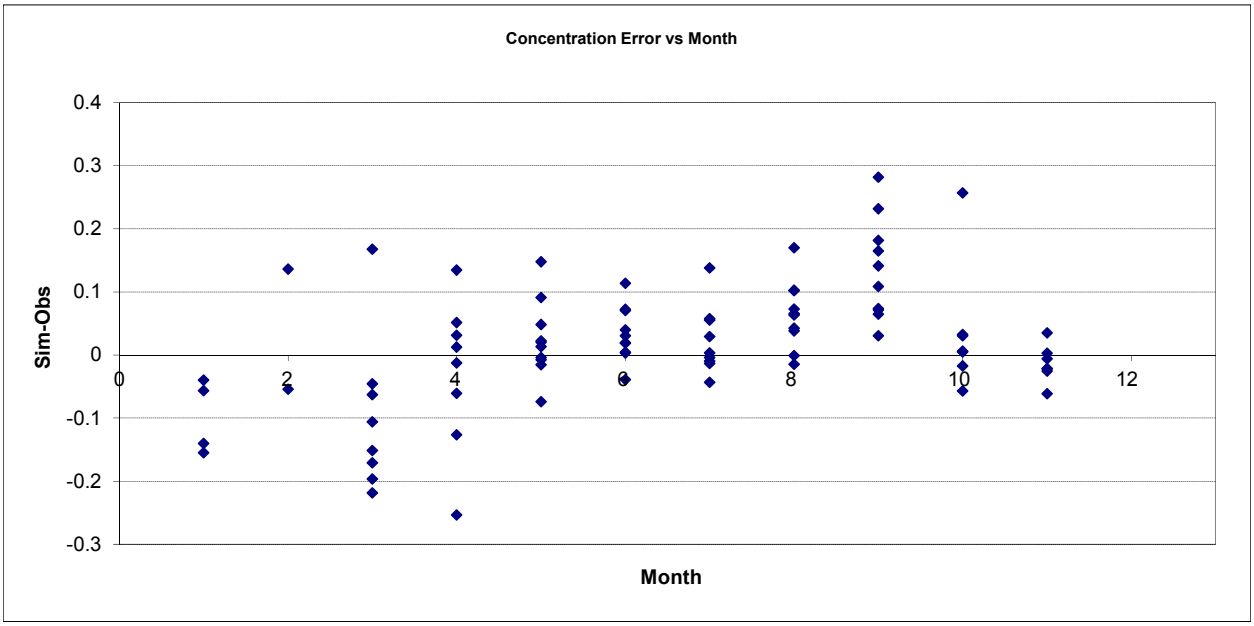

Figure A-183. Residual (Simulated - Observed) vs. Month Nitrite+ Nitrate Nitrogen (NOx) at St Louis River at Bridge on MN-23 at Fond Du Lac

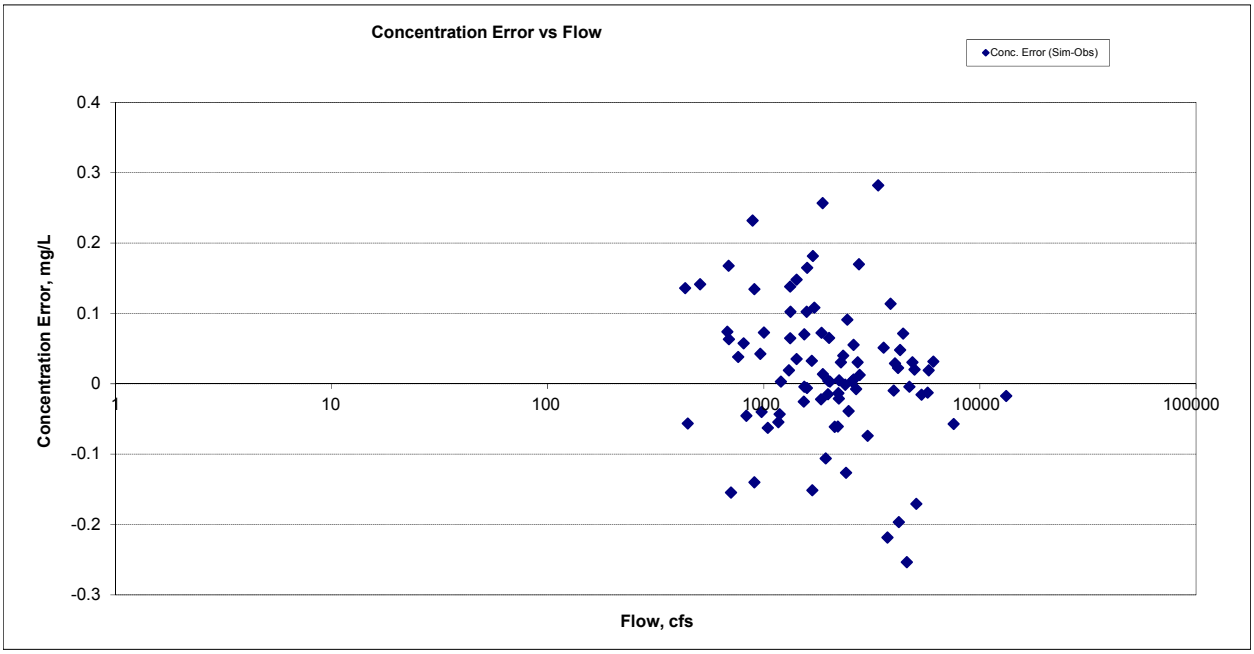

Figure A-184. Residual (Simulated - Observed) vs. Flow Nitrite+ Nitrate Nitrogen (NOx) at St Louis River at Bridge on MN-23 at Fond Du Lac

A.6.5 Total Nitrogen (TN)

Table A-27. Total Nitrogen (TN) statistics

Period	1994-2001	2002-2012
Count	7	7
Concentration Average Error	28.75%	0.22%
Concentration Median Error	27.33%	-0.76%
Load Average Error	28.13%	-1.41%
Load Median Error	9.54%	-2.03%
Paired t conc	0.09	1.00
Paired t load	0.37	0.74

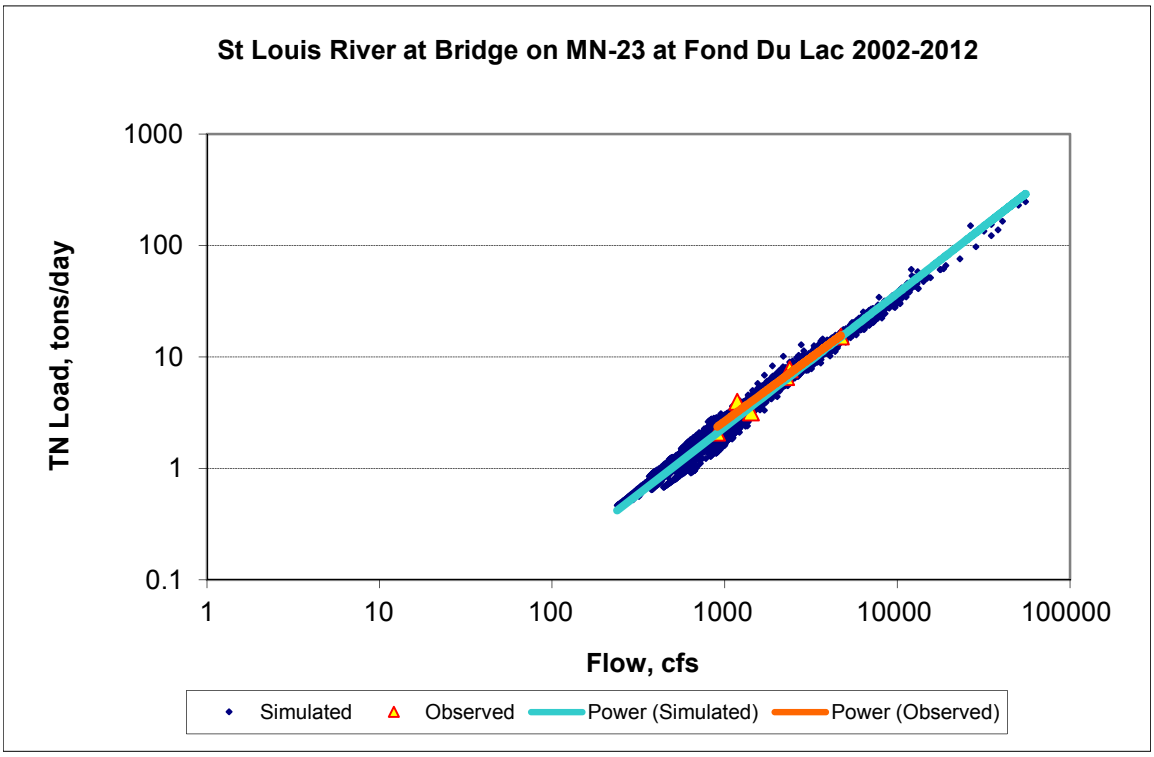

Figure A-185. Power plot of simulated and observed Total Nitrogen (TN) load vs flow at St Louis River at Bridge on MN-23 at Fond Du Lac (calibration period)

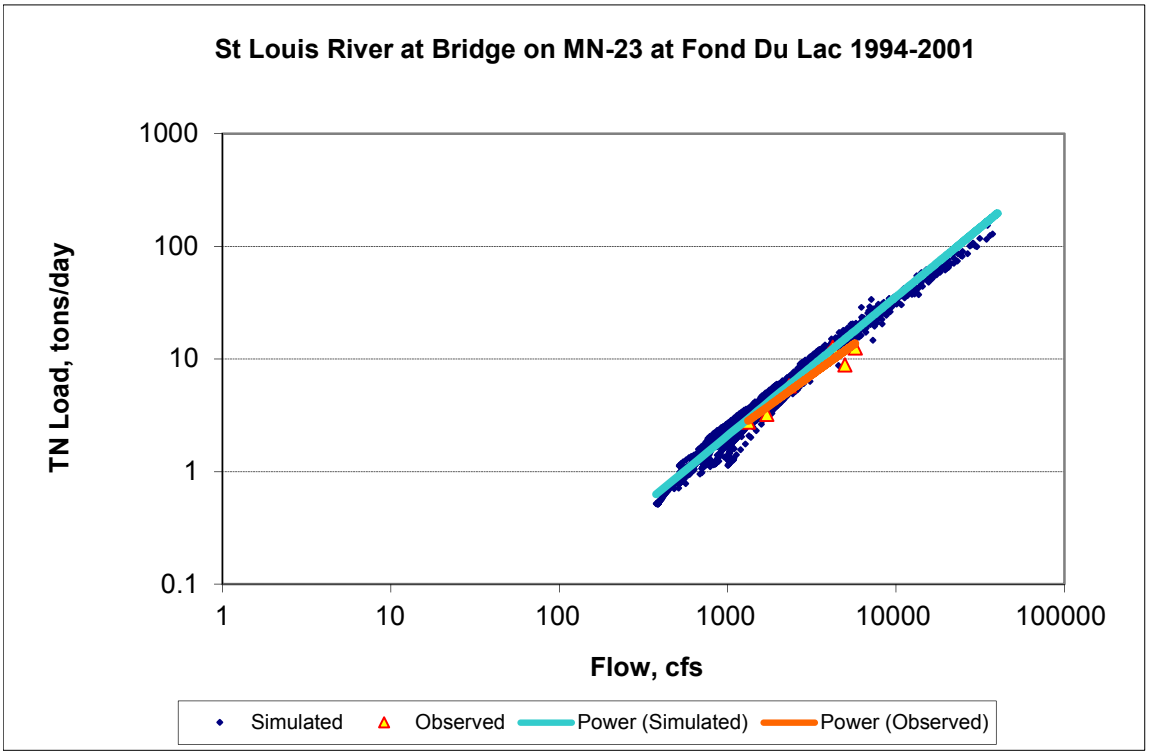

Figure A-186. Power plot of simulated and observed Total Nitrogen (TN) load vs flow at St Louis River at Bridge on MN-23 at Fond Du Lac (validation period)

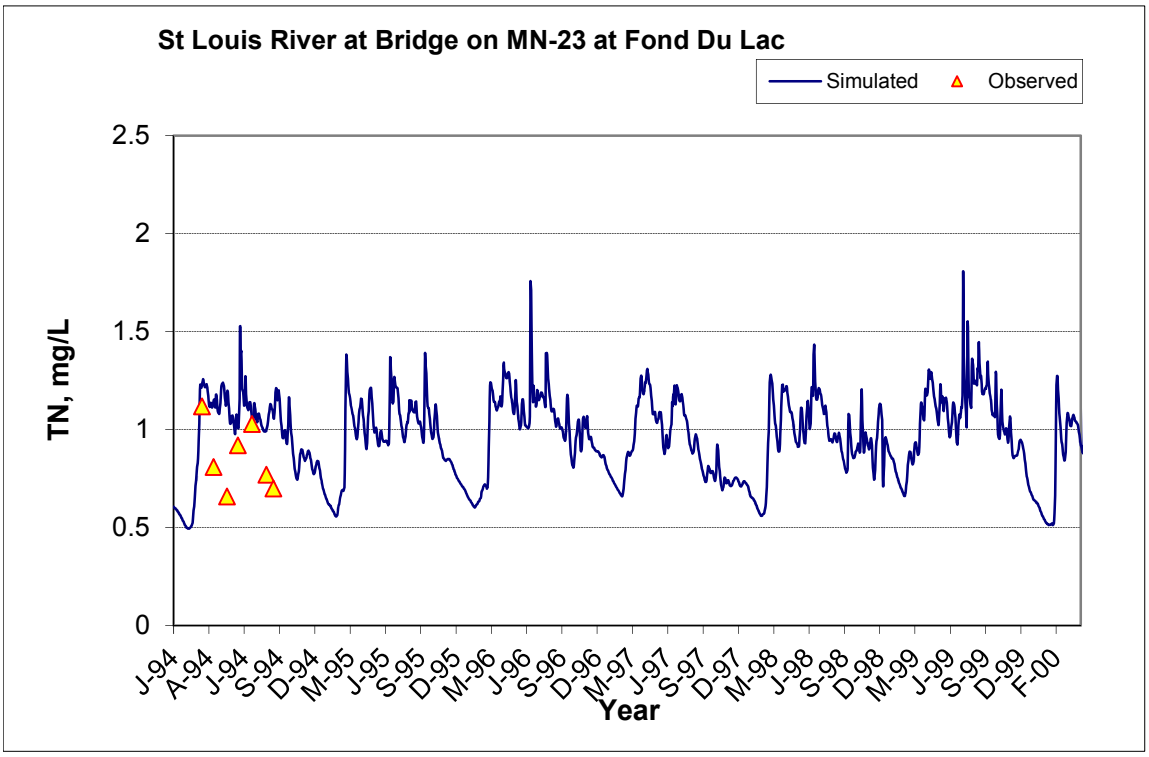
St Louis River at Bridge on MN-23 at Fond Du Lac
Simulated
Observed
TN, mg/L
2.5
2
1.5
1
0.5
0
J-94 A-94 J-94 S-94 D-94 M-95 J-95 S-95 D-95 M-96 J-96 S-96 D-96 M-97 J-97 S-97 D-97 M-98 J-98 S-98 D-98 M-99 J-99 S-99 D-99 F-00
Year

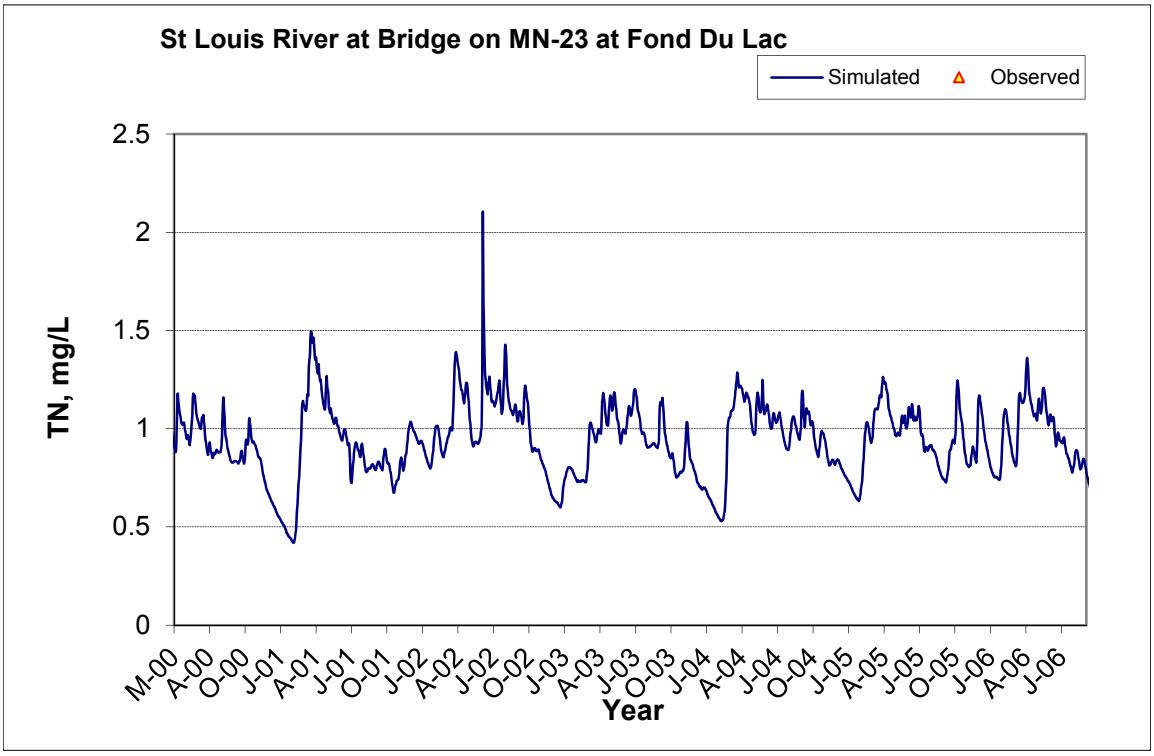
St Louis River at Bridge on MN-23 at Fond Du Lac
Simulated
Observed
TN, mg/L
2.5
2
1.5
1
0.5
0
M-00 A-00 O-00 J-01 A-01 J-01 O-01 J-02 A-02 J-02 O-02 J-03 A-03 J-03 O-03 J-04 A-04 J-04 O-04 J-05 A-05 J-05 O-05 J-06 A-06 J-06
Year

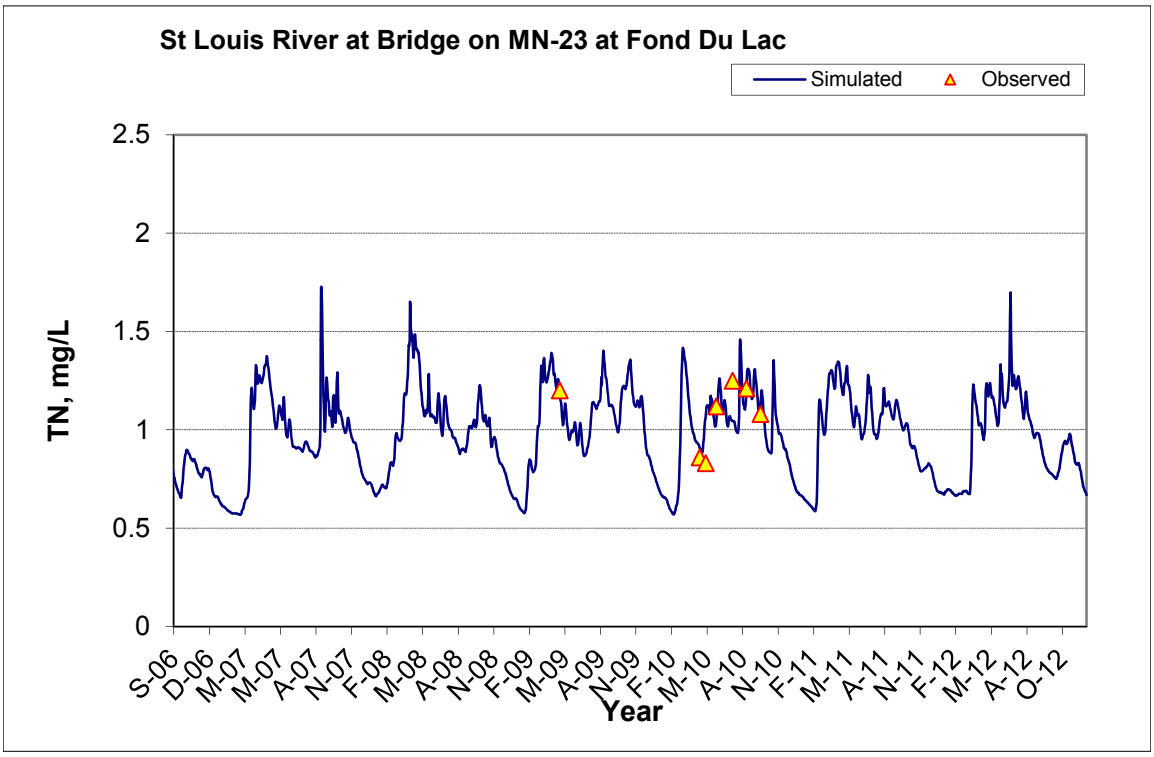

Figure A-187. Time series of observed and simulated Total Nitrogen (TN) concentration at St Louis River at Bridge on MN-23 at Fond Du Lac

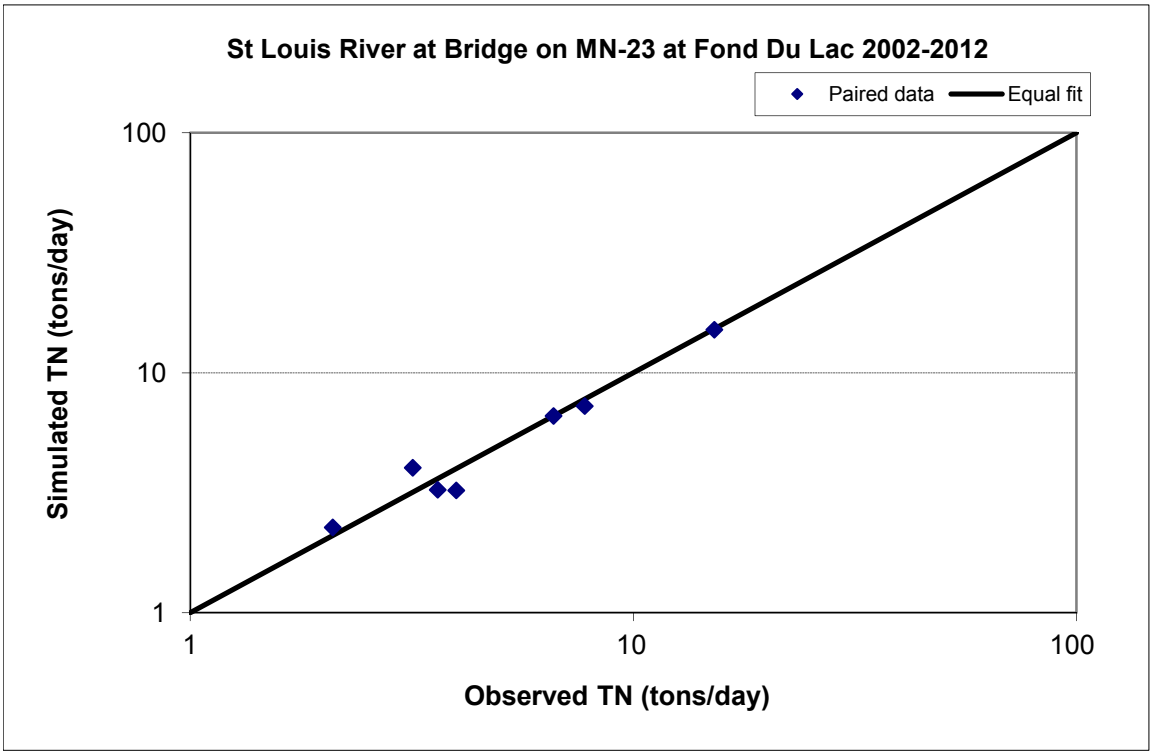

Figure A-188. Paired simulated vs. observed Total Nitrogen (TN) load at St Louis River at Bridge on MN-23 at Fond Du Lac (calibration period)

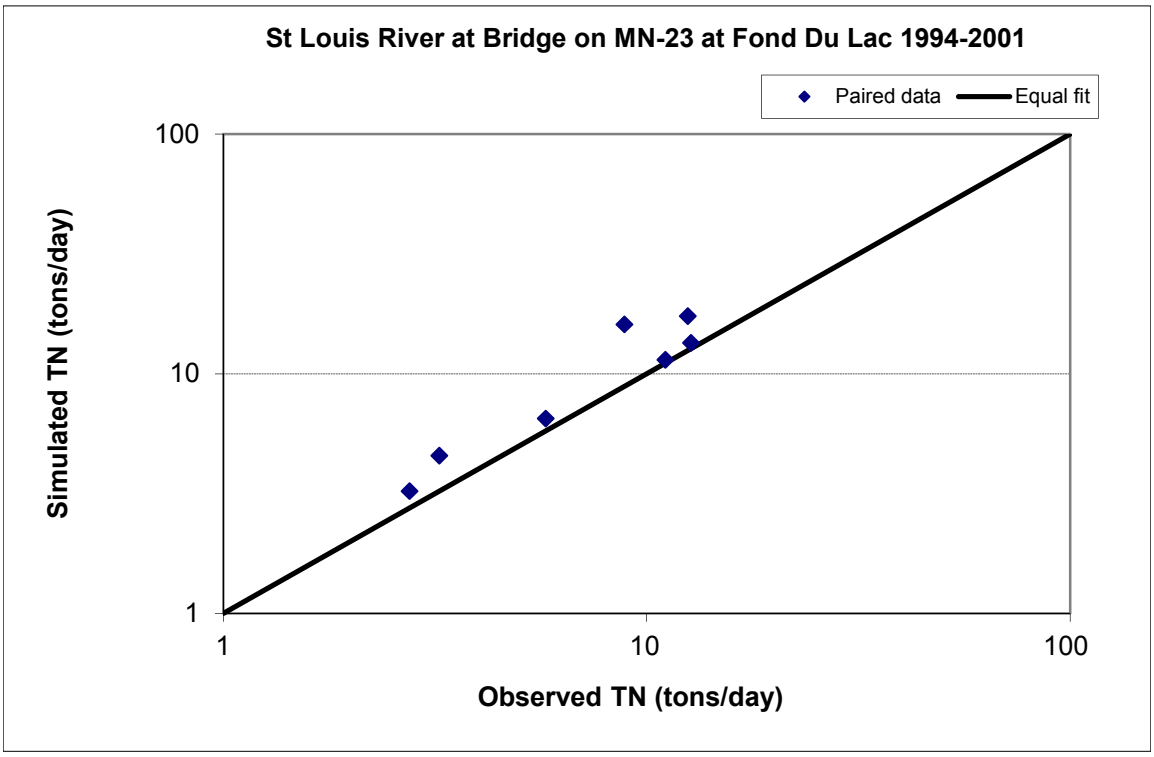

Figure A-189. Paired simulated vs. observed Total Nitrogen (TN) load at St Louis River at Bridge on MN-23 at Fond Du Lac (validation period)

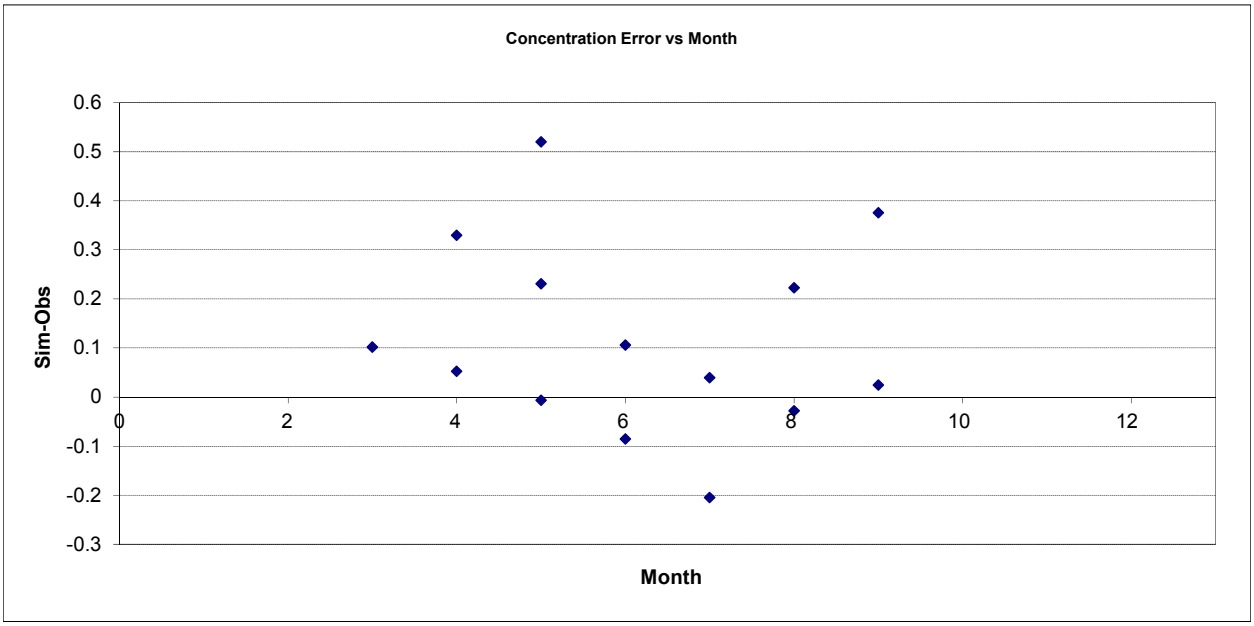

Figure A-190. Residual (Simulated - Observed) vs. Month Total Nitrogen (TN) at St Louis River at Bridge on MN-23 at Fond Du Lac

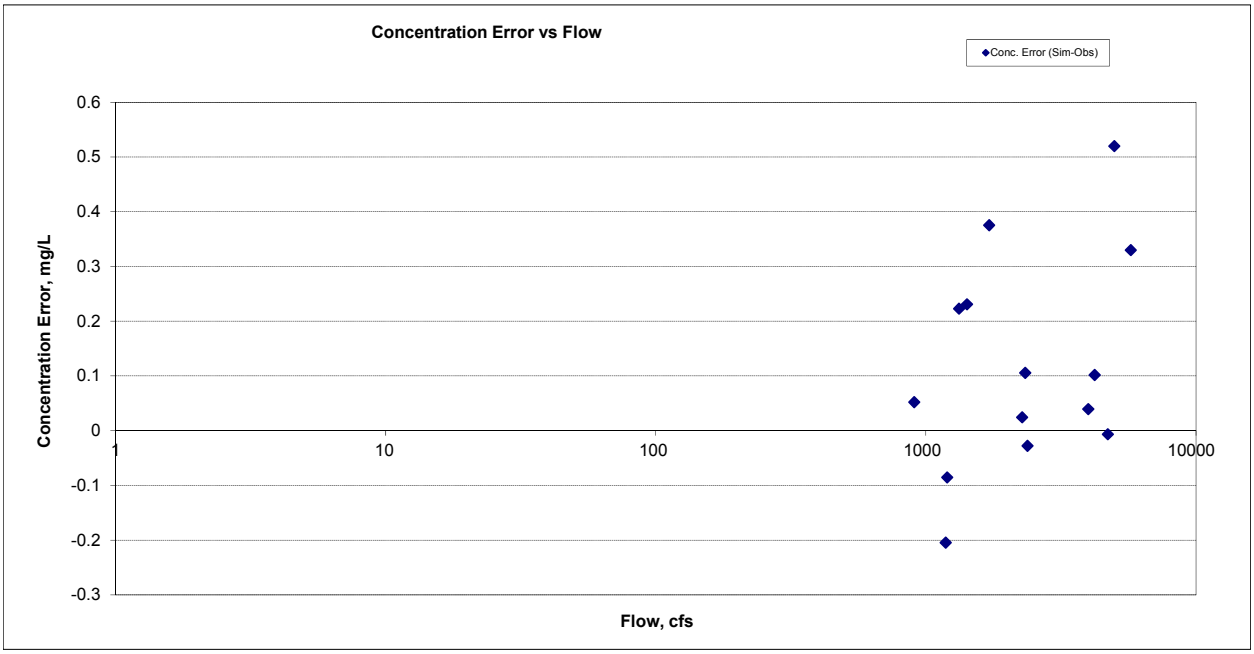

Figure A-191. Residual (Simulated - Observed) vs. Flow Total Nitrogen (TN) at St Louis River at Bridge on MN-23 at Fond Du Lac

A.6.6 Soluble Reactive Phosphorus (SRP)

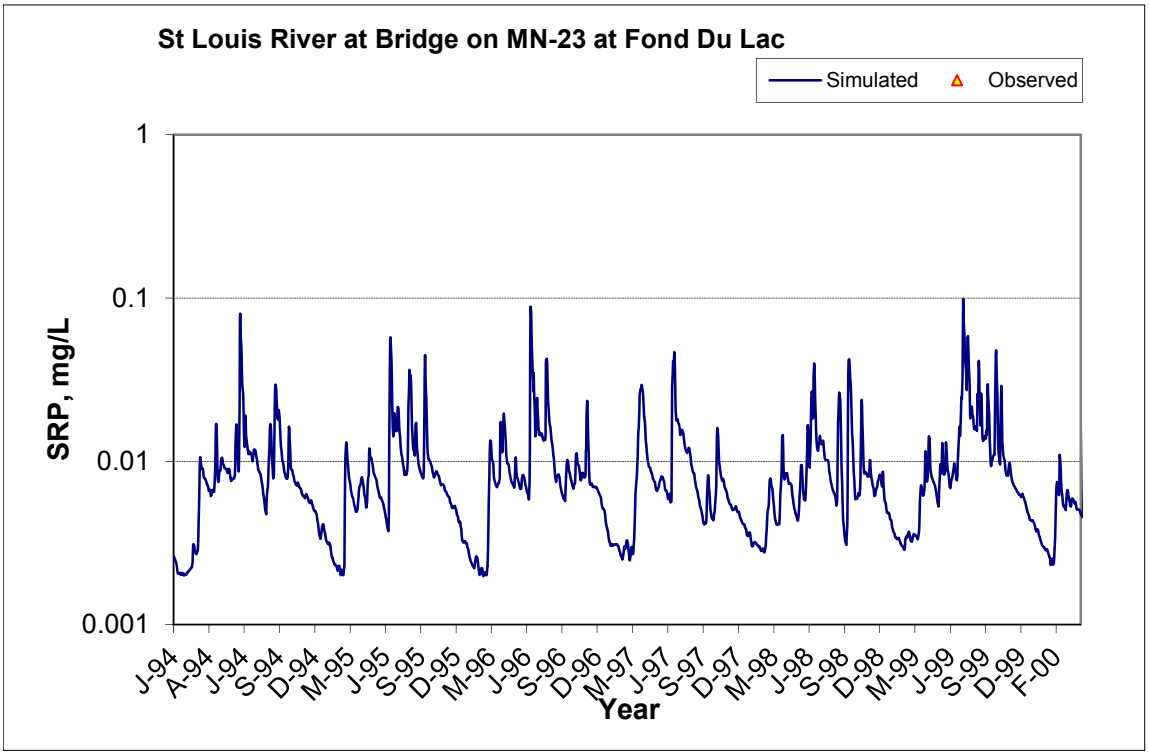

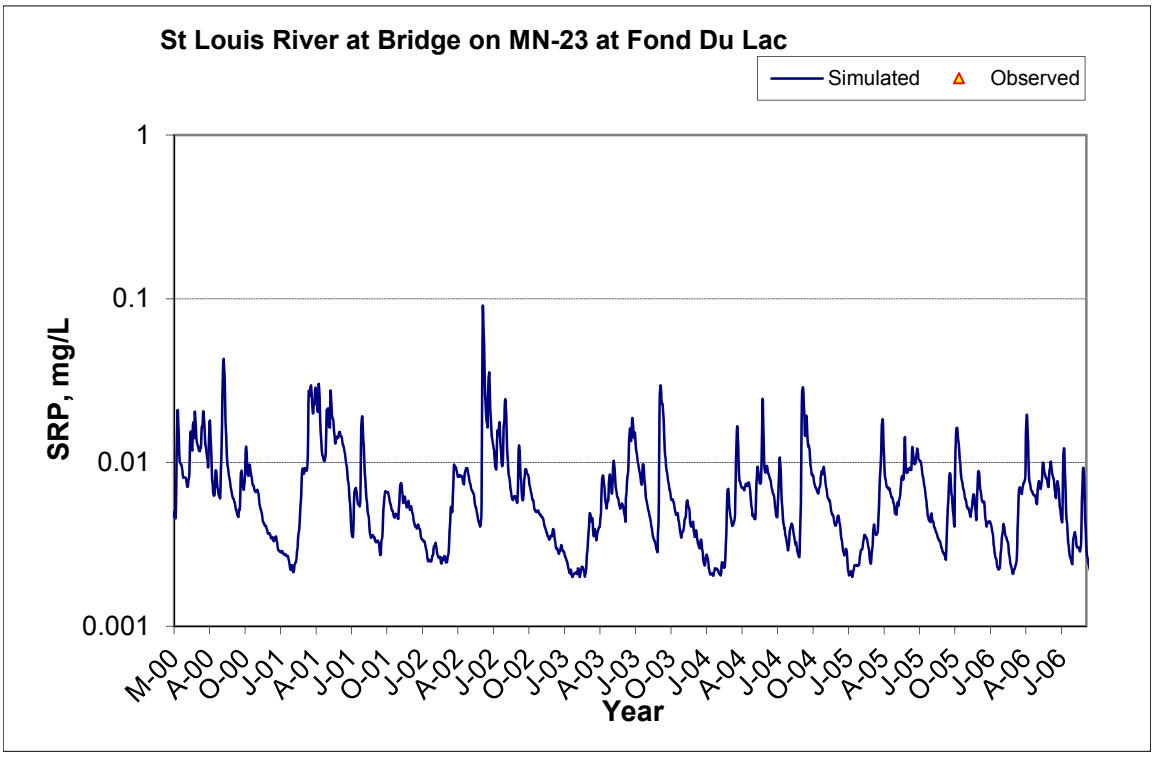

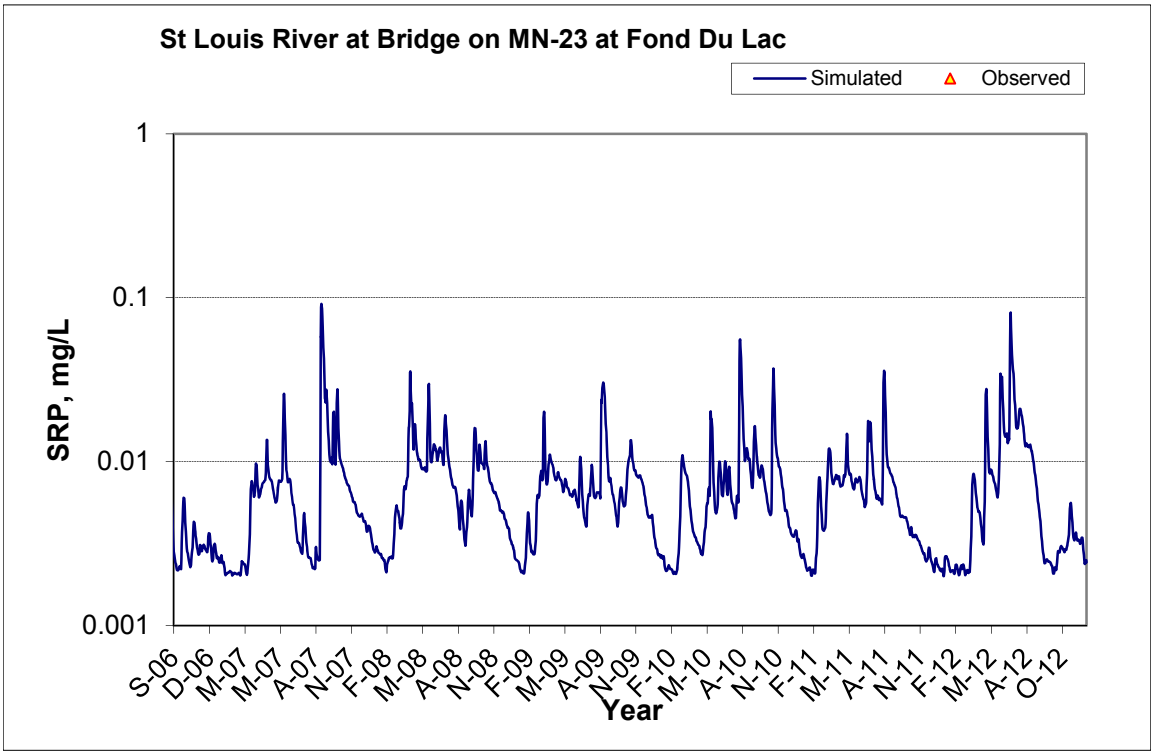

Figure A-192. Time series of observed and simulated Soluble Reactive Phosphorus (SRP) concentration at St Louis River at Bridge on MN-23 at Fond Du Lac

A.6.7 Organic Phosphorus (OrgP)

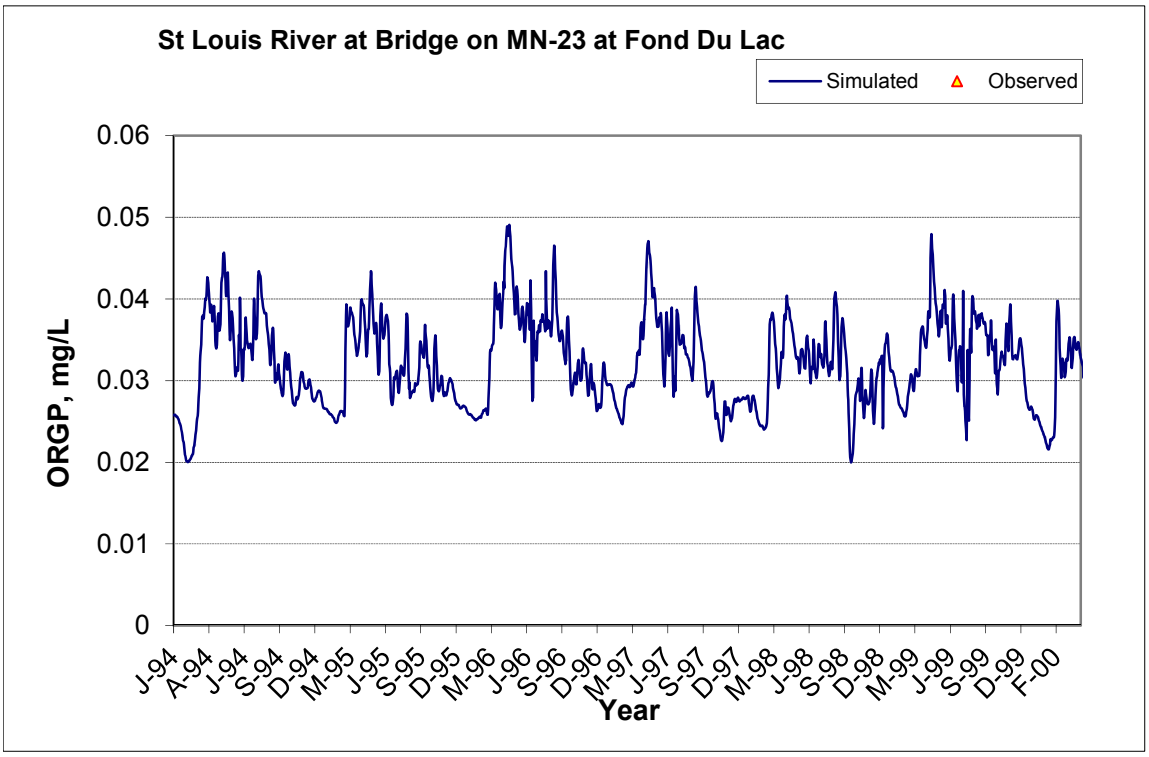

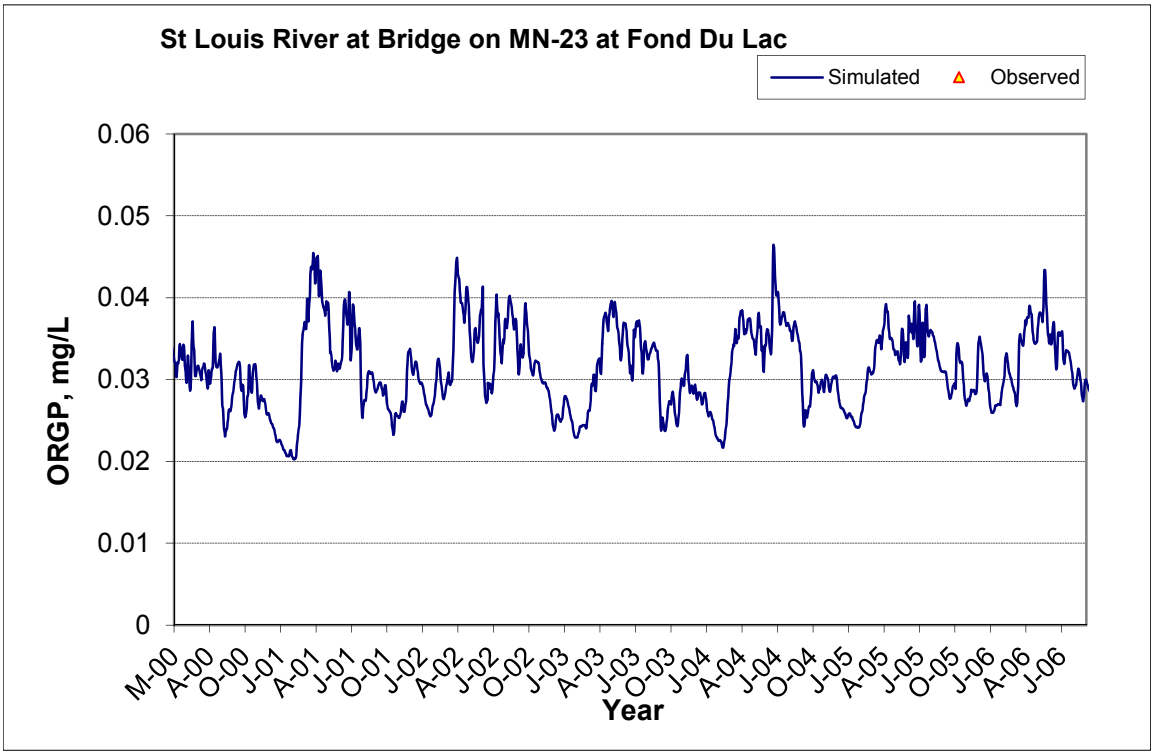

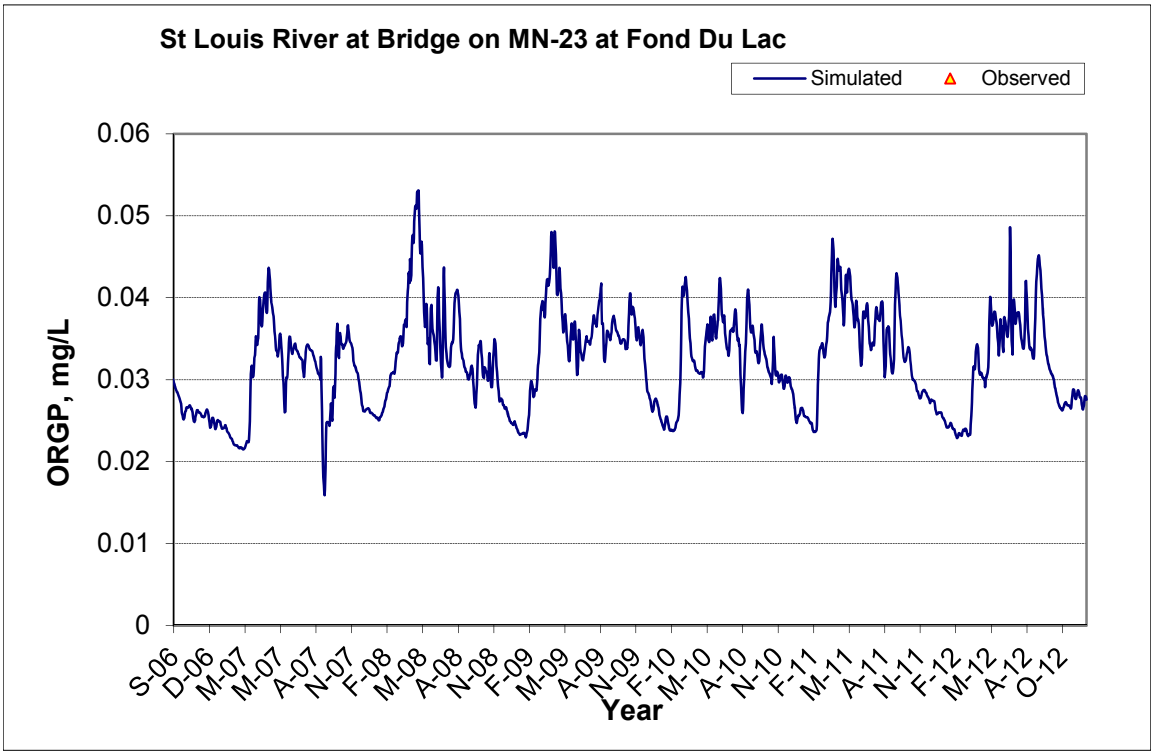

Figure A-193. Time series of observed and simulated Organic Phosphorus (OrgP) concentration at St Louis River at Bridge on MN-23 at Fond Du Lac

A.6.8 Total Phosphorus (TP)

Table A-28. Total Phosphorus (TP) statistics

Period	1994-2001	2002-2012
Count	38	50
Concentration Average Error	12.85%	15.22%
Concentration Median Error	7.03%	22.06%
Load Average Error	4.25%	7.21%
Load Median Error	4.79%	8.07%
Paired t conc	0.93	0.84
Paired t load	0.81	0.72

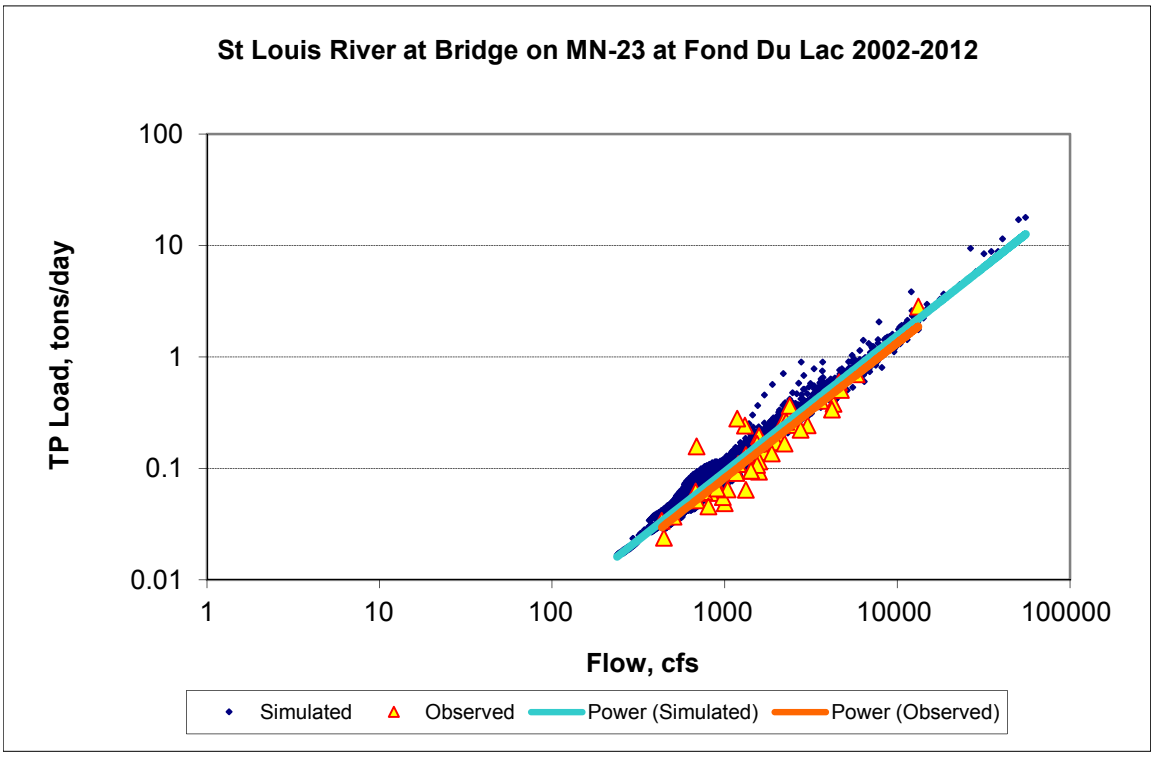

Figure A-194. Power plot of simulated and observed Total Phosphorus (TP) load vs flow at St Louis River at Bridge on MN-23 at Fond Du Lac (calibration period)

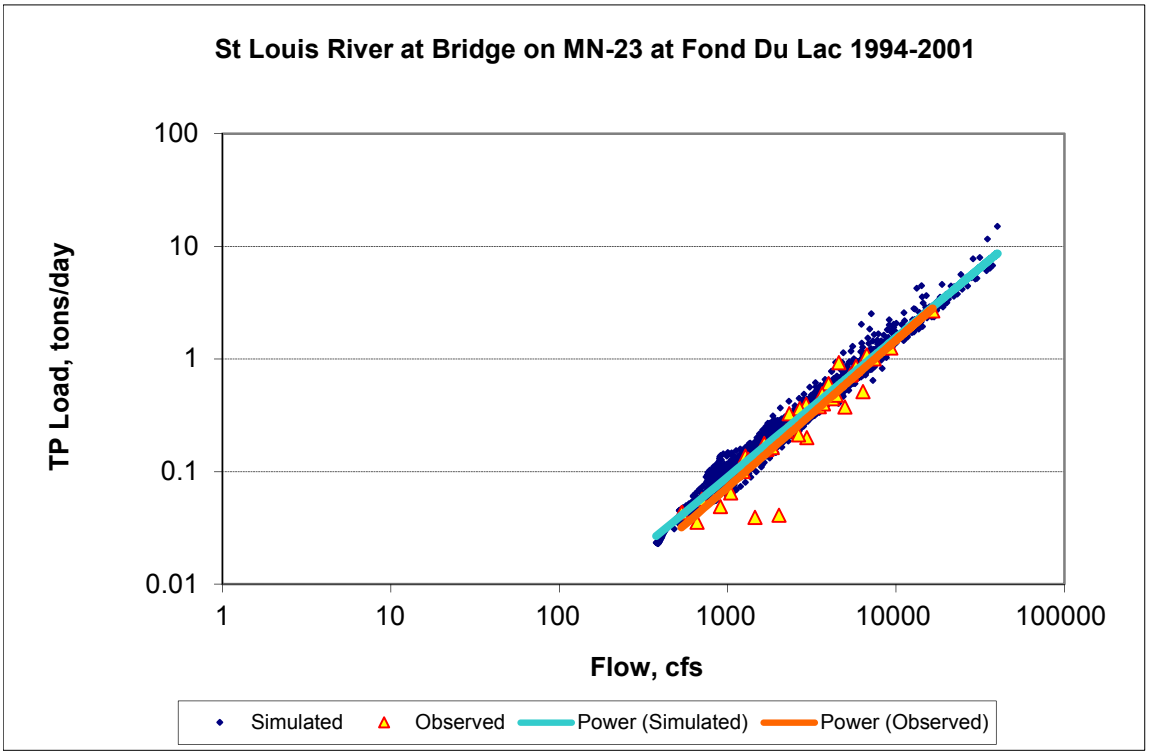

Figure A-195. Power plot of simulated and observed Total Phosphorus (TP) load vs flow at St Louis River at Bridge on MN-23 at Fond Du Lac (validation period)

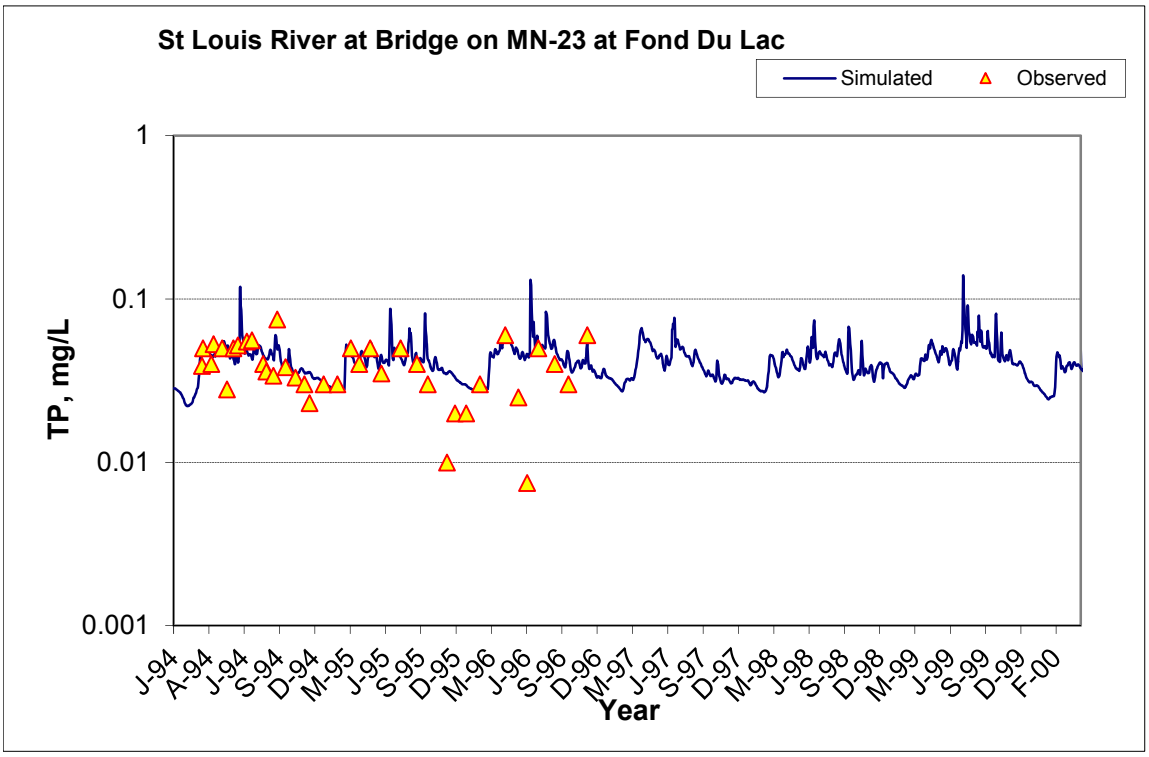
St Louis River at Bridge on MN-23 at Fond Du Lac
Simulated
Observed
TP, mg/L
1
0.1
0.01
0.001
J-94 A-94 J-94 S-94 D-94 M-95 J-95 S-95 D-95 M-96 J-96 S-96 D-96 M-97 J-97 S-97 D-97 M-98 J-98 S-98 D-98 M-99 J-99 S-99 D-99 F-00
Year

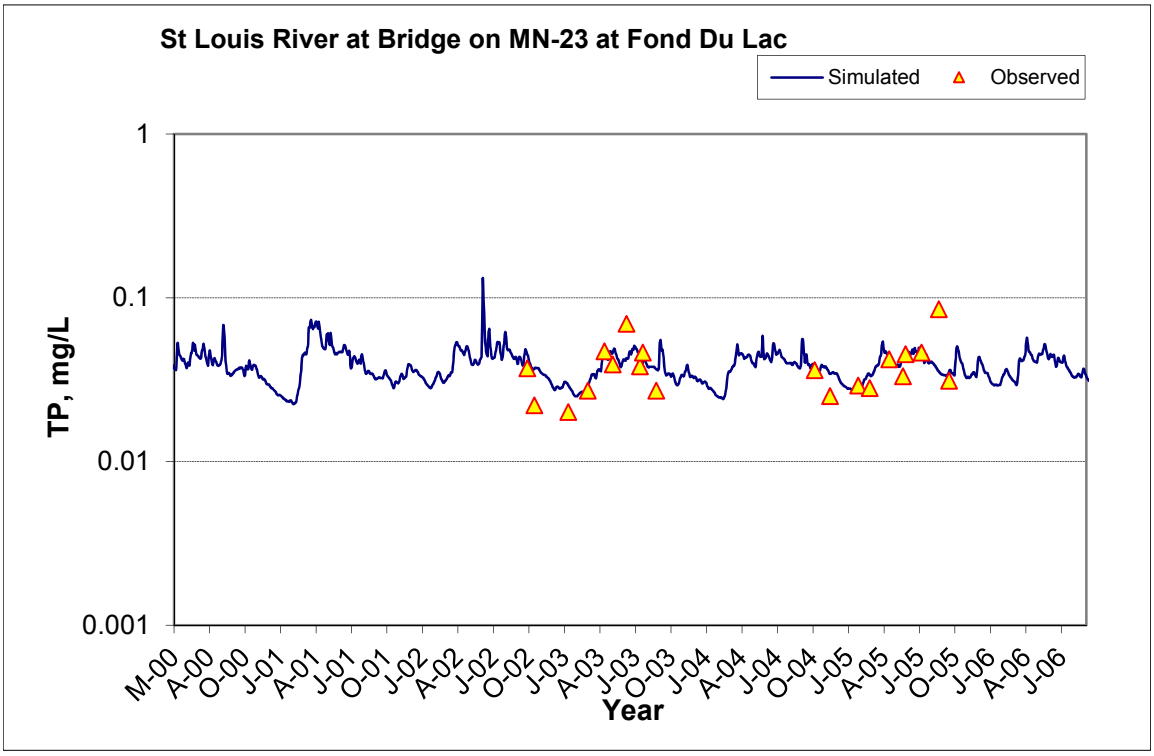
St Louis River at Bridge on MN-23 at Fond Du Lac
Simulated
Observed
TP, mg/L
1
0.1
0.01
0.001
M-00 A-00 O-00 J-01 A-01 J-01 O-01 J-02 A-02 J-02 O-02 J-03 A-03 J-03 O-03 J-04 A-04 J-04 O-04 J-05 A-05 J-05 O-05 J-06 A-06 J-06
Year

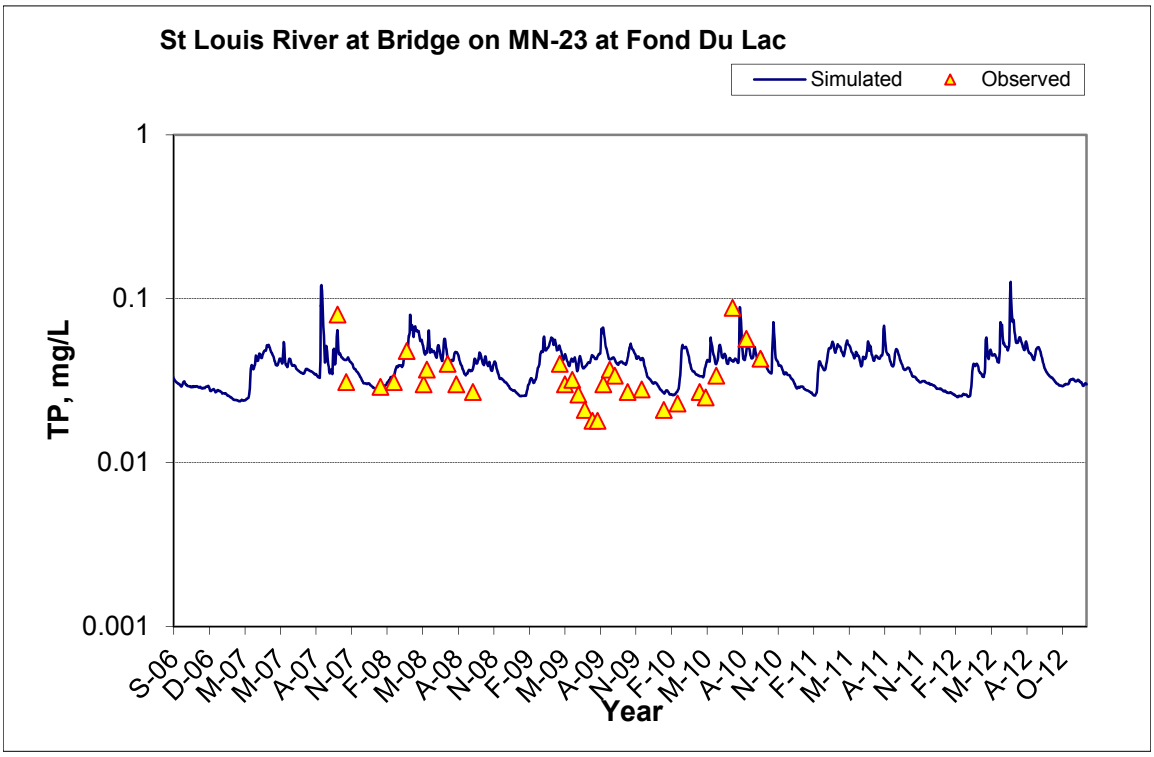

Figure A-196. Time series of observed and simulated Total Phosphorus (TP) concentration at St Louis River at Bridge on MN-23 at Fond Du Lac

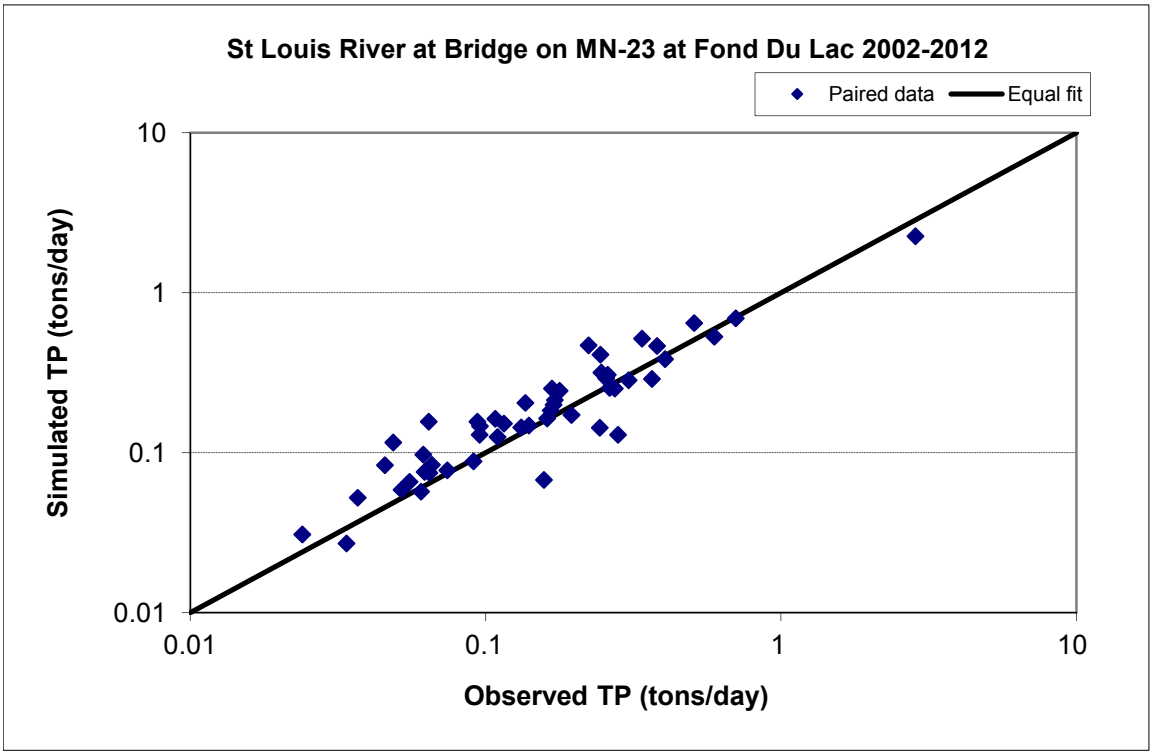

Figure A-197. Paired simulated vs. observed Total Phosphorus (TP) load at St Louis River at Bridge on MN-23 at Fond Du Lac (calibration period)

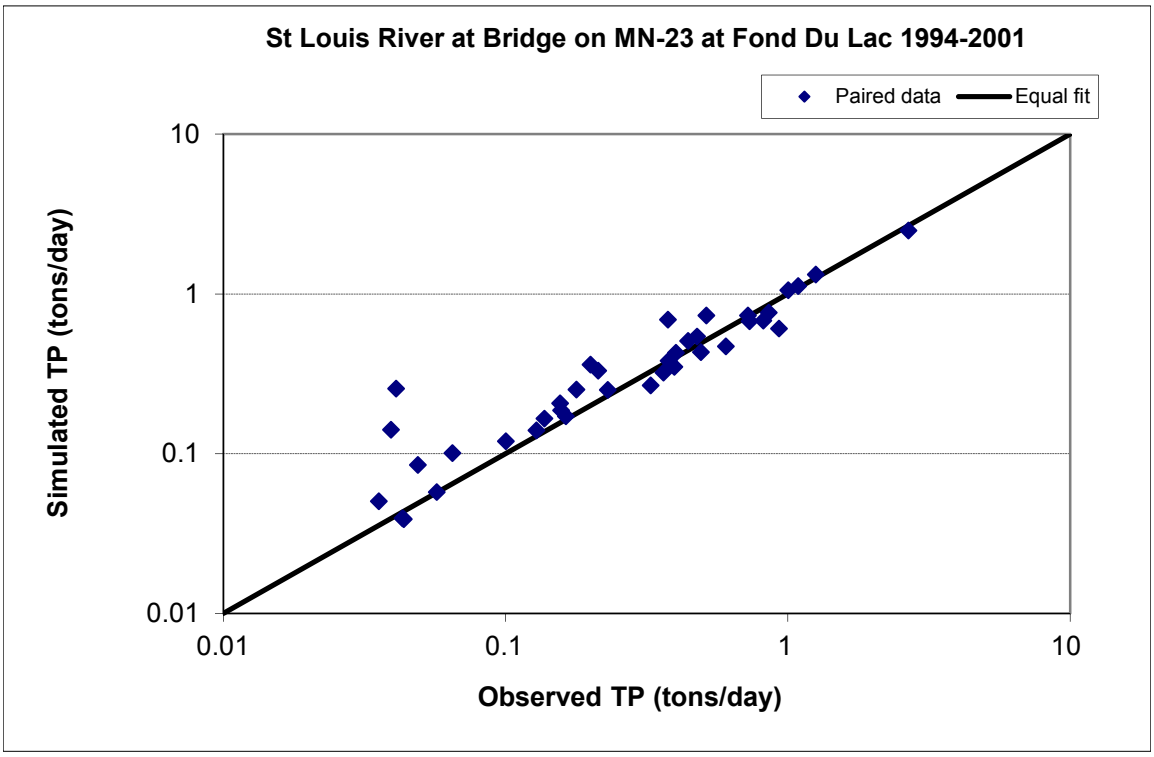

Figure A-198. Paired simulated vs. observed Total Phosphorus (TP) load at St Louis River at Bridge on MN-23 at Fond Du Lac (validation period)

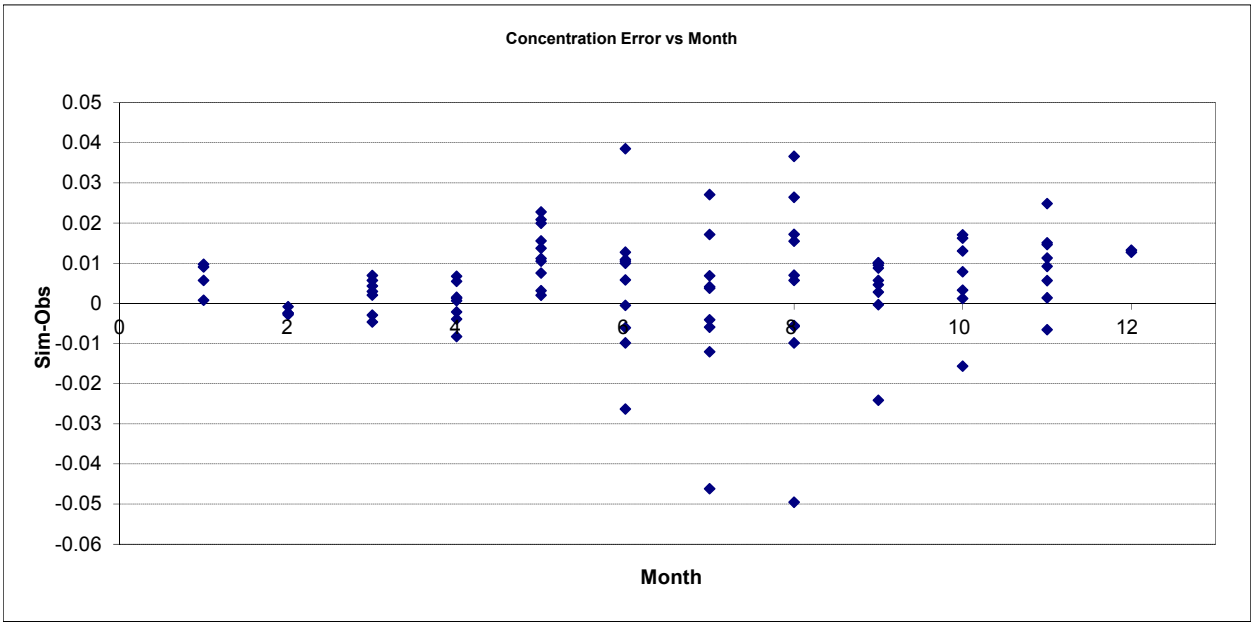

Figure A-199. Residual (Simulated - Observed) vs. Month Total Phosphorus (TP) at St Louis River at Bridge on MN-23 at Fond Du Lac

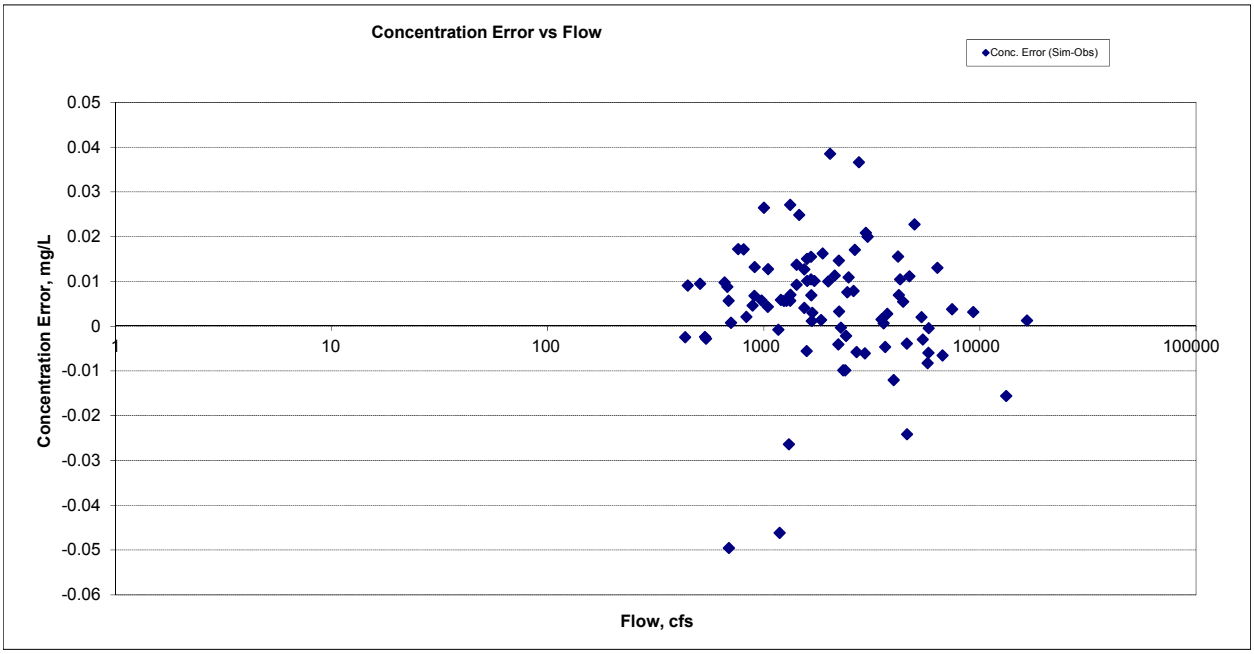

Figure A-200. Residual (Simulated - Observed) vs. Flow Total Phosphorus (TP) at St Louis River at Bridge on MN-23 at Fond Du Lac

A.7 CLOQUET RIVER NR BURNETT (04048001)

A.7.1 Ammonia Nitrogen (NH3)

Table A-29. Ammonia Nitrogen (NH3) statistics

Period	1994-2001	2002-2012
Count	13	18
Concentration Average Error	-58.42%	-17.03%
Concentration Median Error	-50.16%	-2.38%
Load Average Error	-57.17%	-19.43%
Load Median Error	-51.09%	-10.04%
Paired t conc	0.00	0.62
Paired t load	0.01	0.52

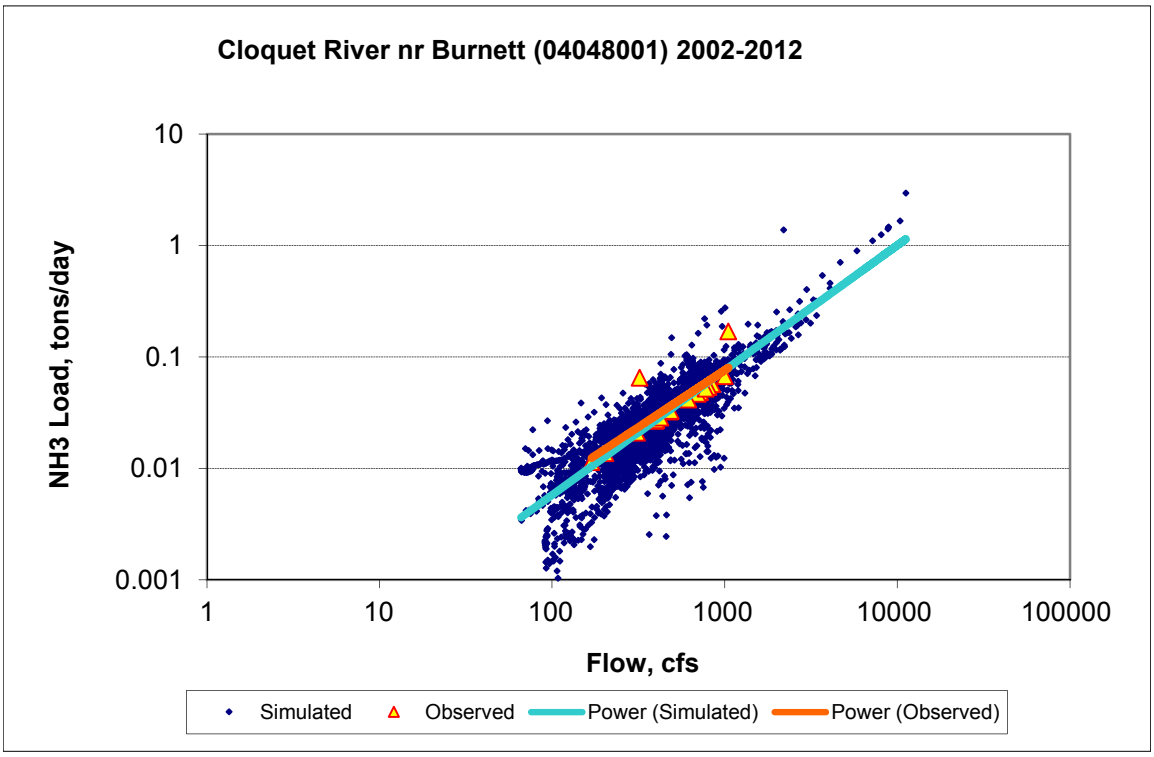

Figure A-201. Power plot of simulated and observed Ammonia Nitrogen (NH3) load vs flow at Cloquet River nr Burnett (04048001) (calibration period)

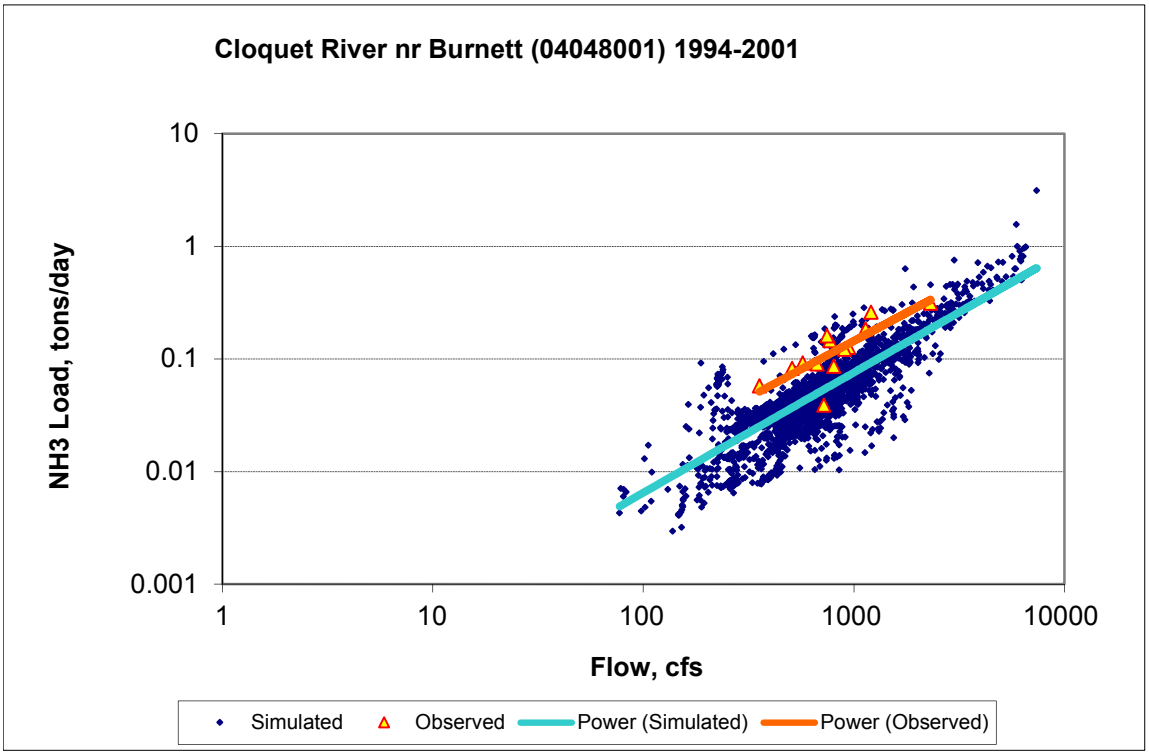

Figure A-202. Power plot of simulated and observed Ammonia Nitrogen (NH3) load vs flow at Cloquet River nr Burnett (04048001) (validation period)

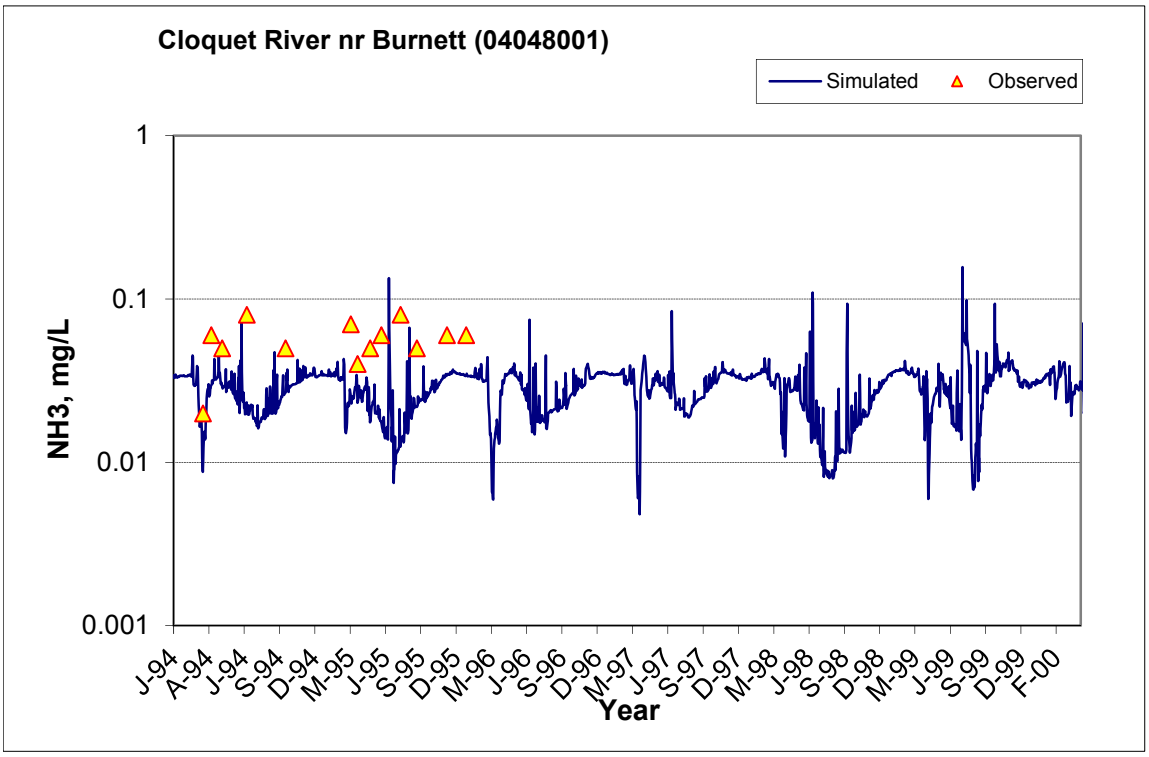
Cloquet River nr Burnett (04048001)
Simulated
Observed
NH3, mg/L
1
0.1
0.01
0.001
J-94 A-94 J-94 S-94 D-94 M-95 J-95 S-95 D-95 M-96 J-96 S-96 D-96 M-97 J-97 S-97 D-97 M-98 J-98 S-98 D-98 M-99 J-99 S-99 D-99 F-00
Year

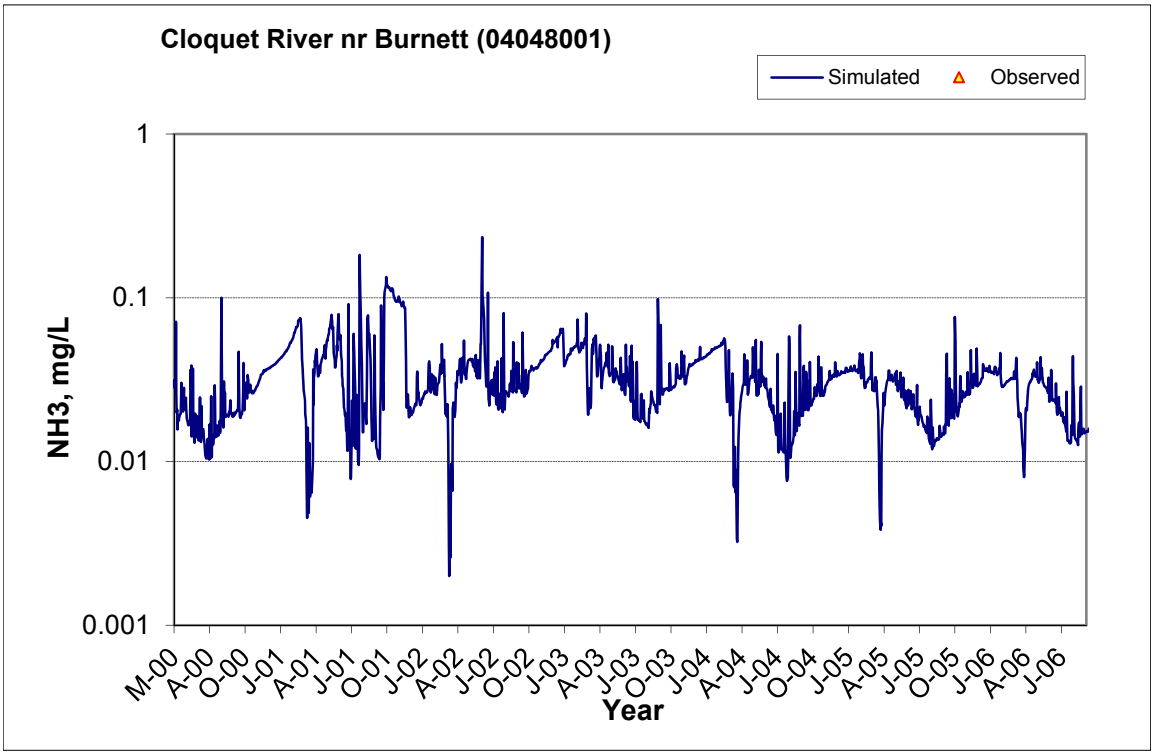
Cloquet River nr Burnett (04048001)
Simulated
Observed
NH3, mg/L
1
0.1
0.01
0.001
M-00 A-00 O-00 J-01 A-01 J-01 O-01 J-02 A-02 J-02 O-02 J-03 A-03 J-03 O-03 J-04 A-04 J-04 O-04 J-05 A-05 J-05 O-05 J-06 A-06 J-06
Year

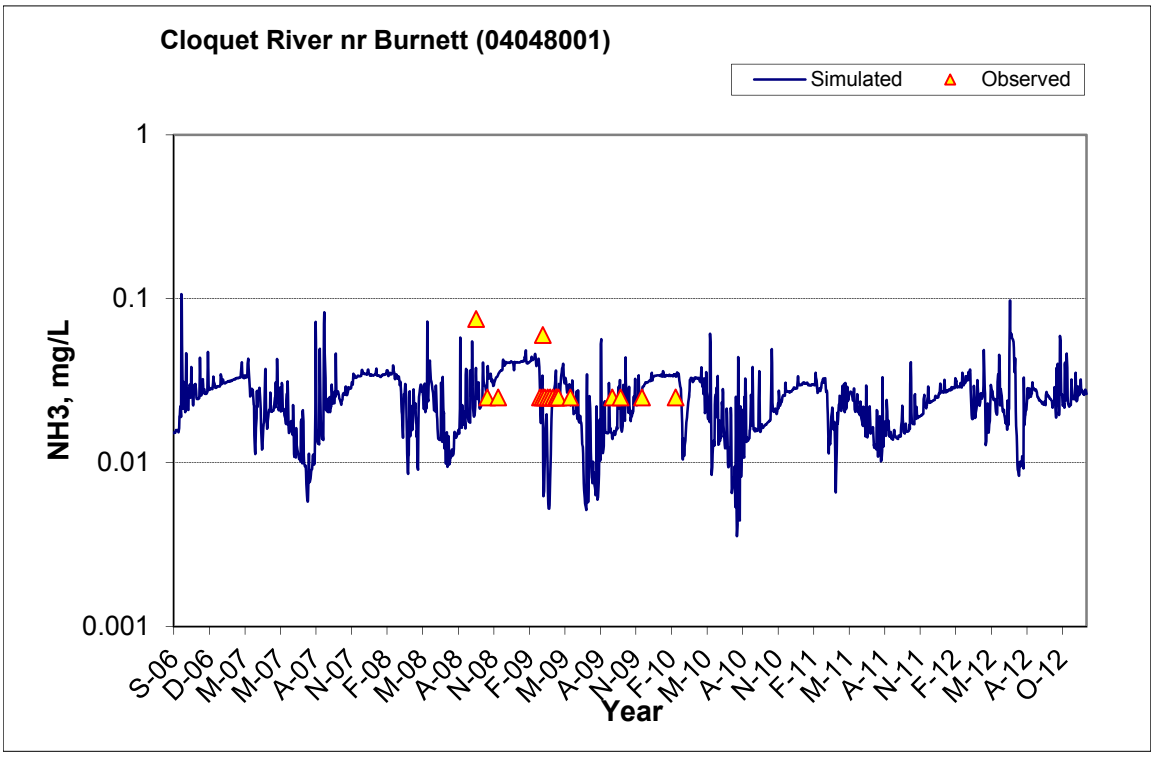

Figure A-203. Time series of observed and simulated Ammonia Nitrogen (NH3) concentration at Cloquet River nr Burnett (04048001)

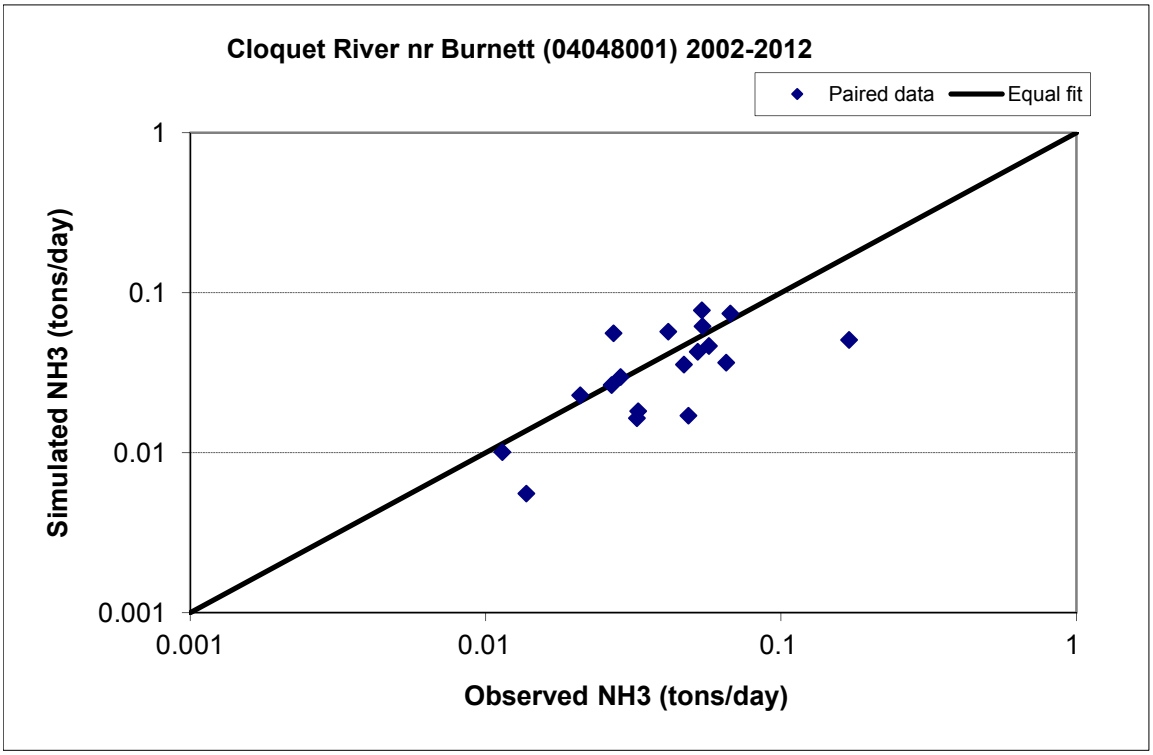

Figure A-204. Paired simulated vs. observed Ammonia Nitrogen (NH3) load at Cloquet River nr Burnett (04048001) (calibration period)

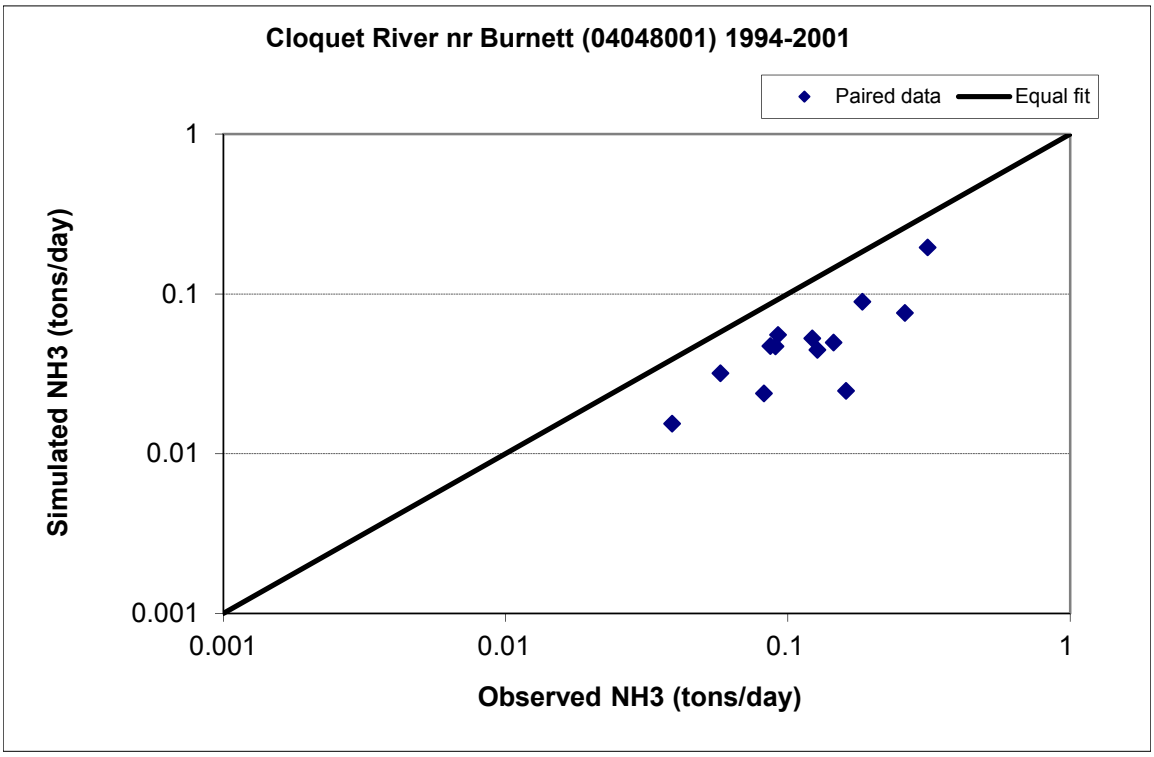

Figure A-205. Paired simulated vs. observed Ammonia Nitrogen (NH3) load at Cloquet River nr Burnett (04048001) (validation period)

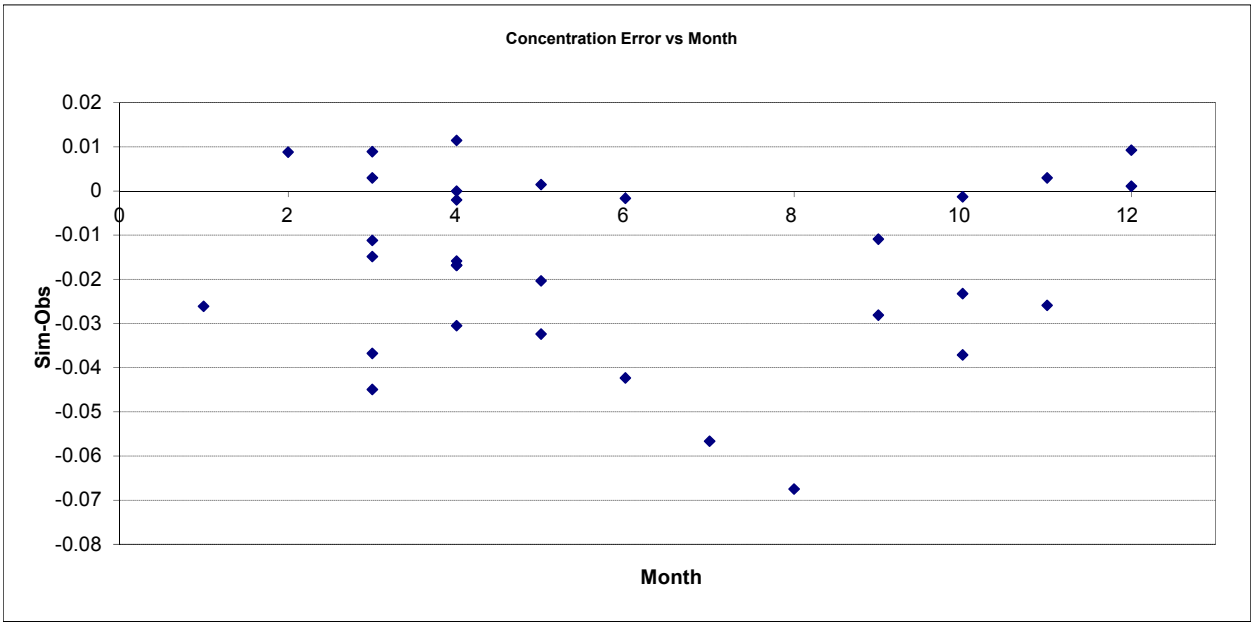

Figure A-206. Residual (Simulated - Observed) vs. Month Ammonia Nitrogen (NH3) at Cloquet River nr Burnett (04048001)

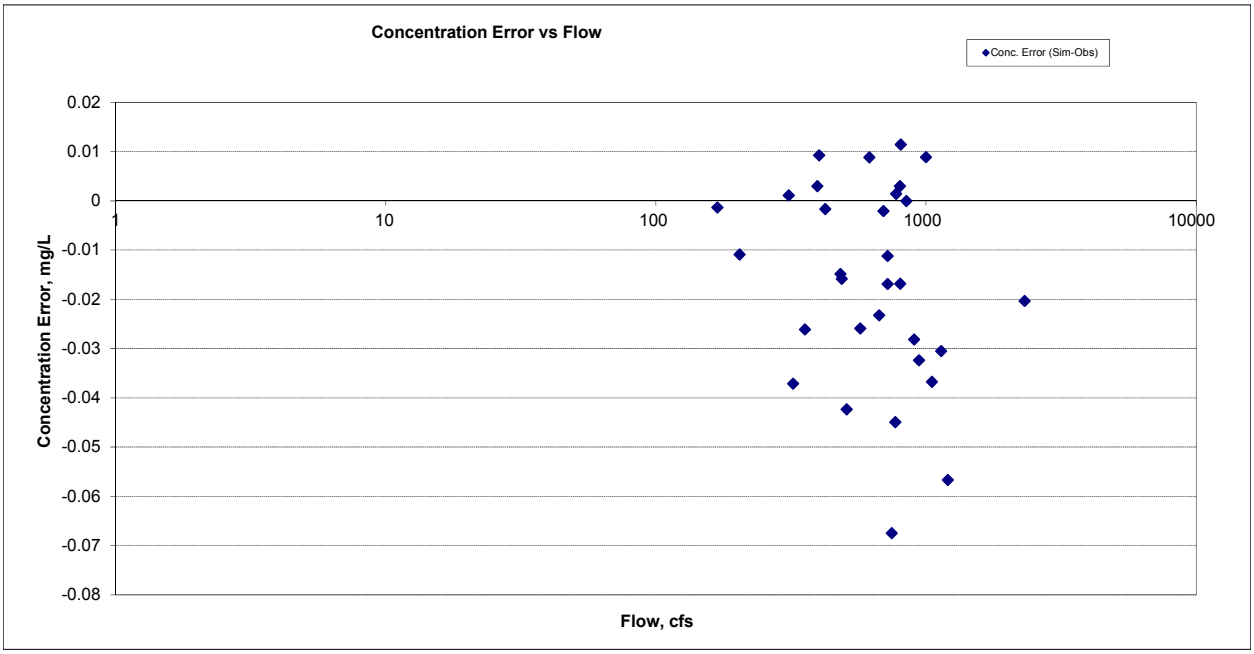

Figure A-207. Residual (Simulated - Observed) vs. Flow Ammonia Nitrogen (NH3) at Cloquet River nr Burnett (04048001)

A.7.2 Organic Nitrogen (OrgN)

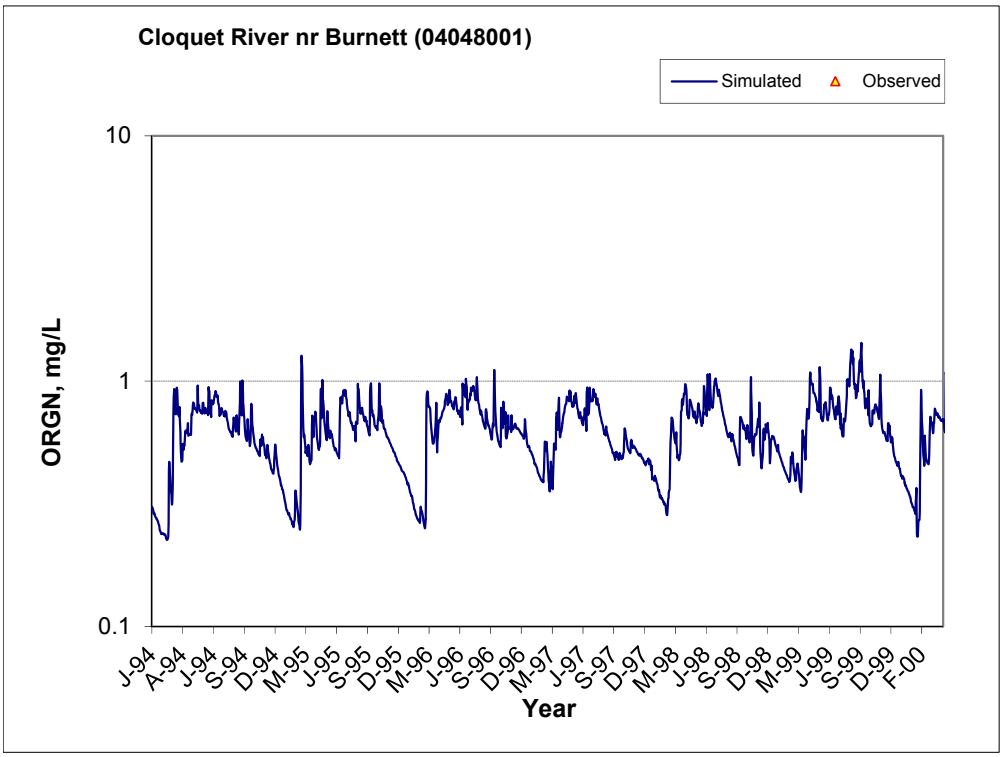

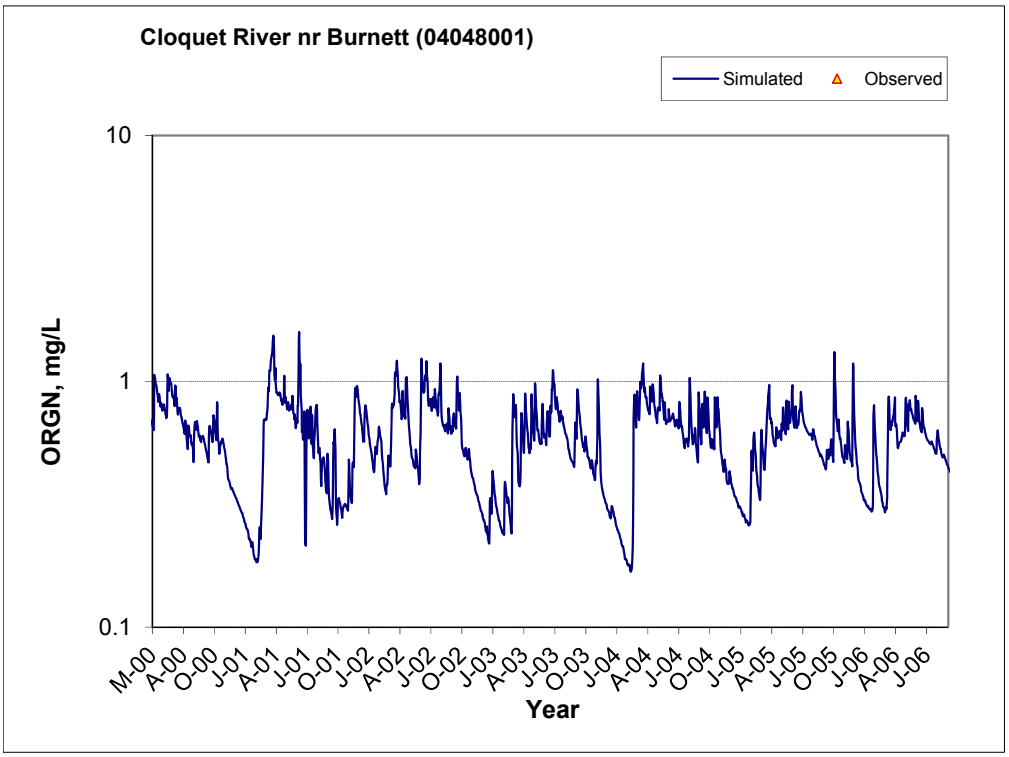

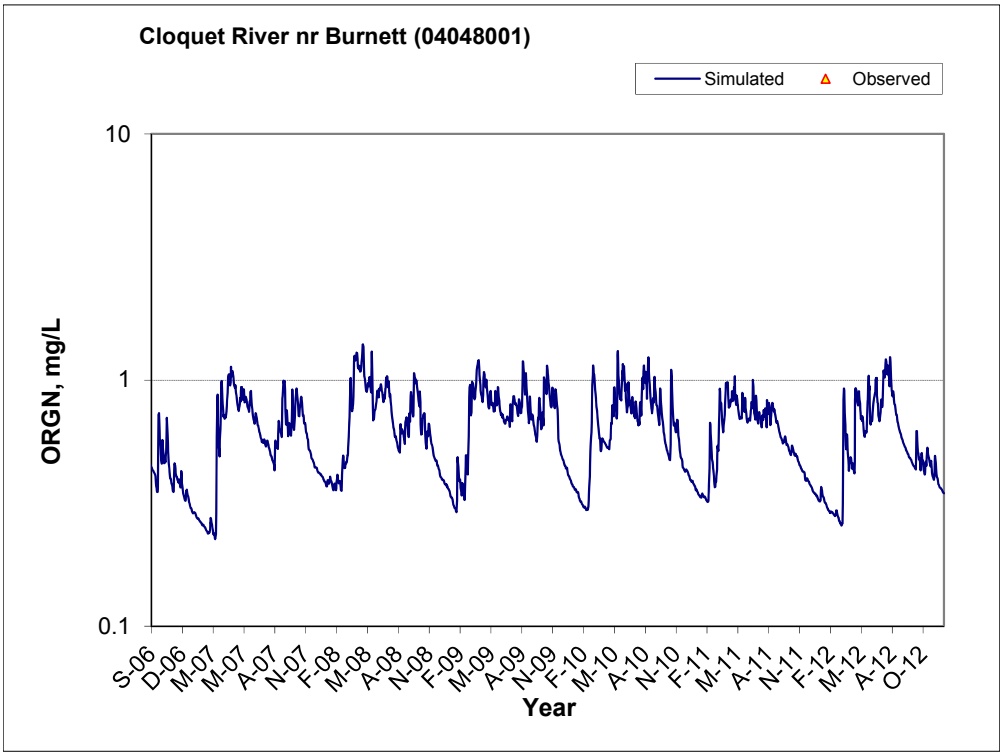

Figure A-208. Time series of observed and simulated Organic Nitrogen (OrgN) concentration at Cloquet River nr Burnett (04048001)

A.7.3 Total Kjeldahl Nitrogen (TKN)

Table A-30. Total Kjeldahl Nitrogen (TKN) statistics

Period	1994-2001	2002-2012
Count	ND	94
Concentration Average Error		10.87%
Concentration Median Error		13.29%
Load Average Error		-10.53%
Load Median Error		3.15%
Paired t conc		1.00
Paired t load		0.72

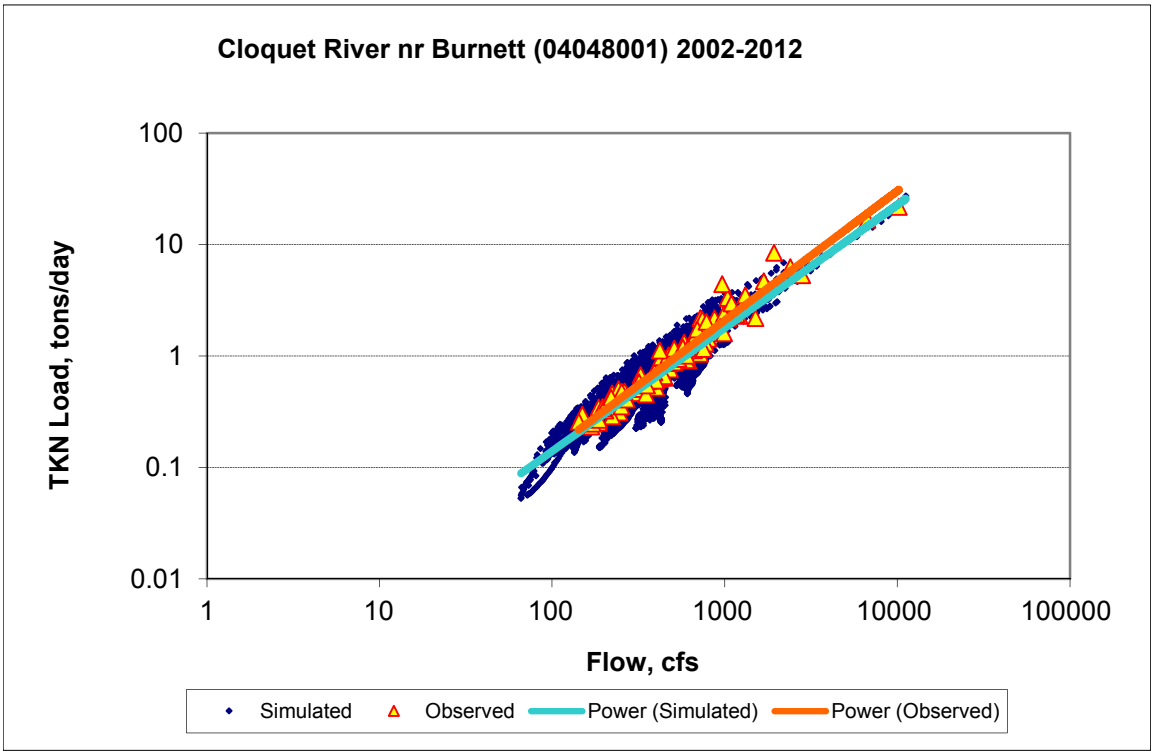

Figure A-209. Power plot of simulated and observed Total Kjeldahl Nitrogen (TKN) load vs flow at Cloquet River nr Burnett (04048001) (calibration period)

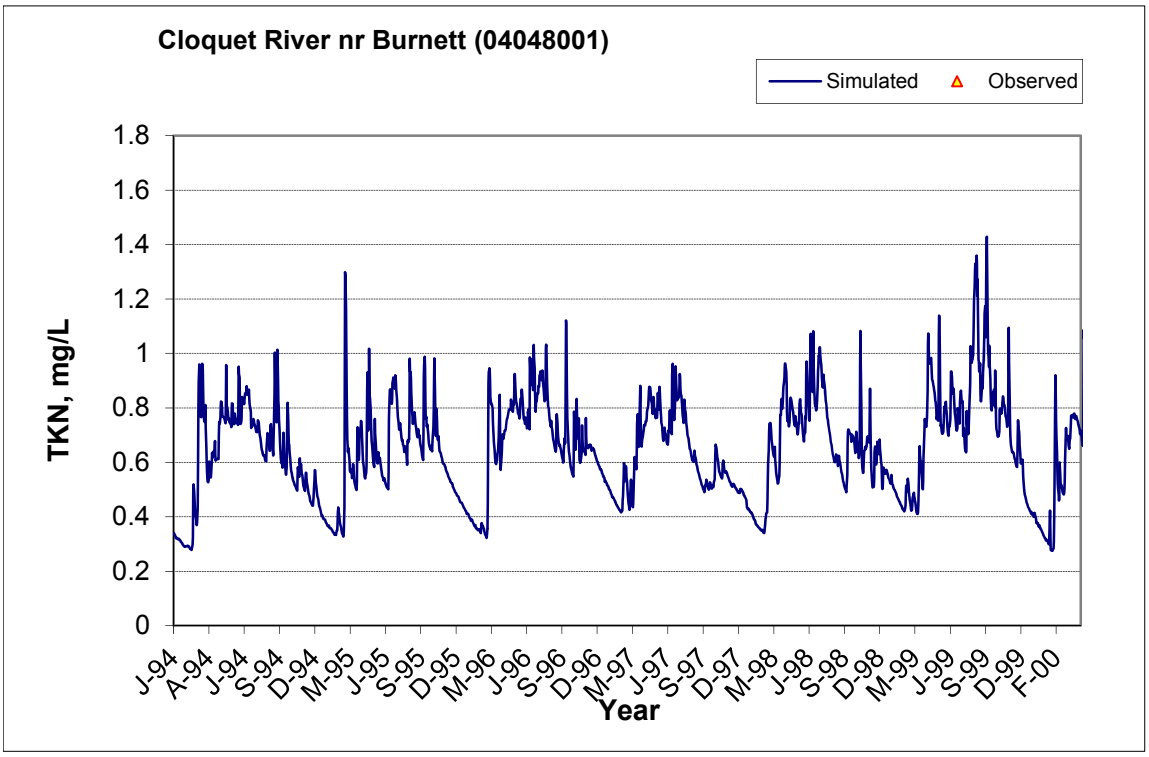
Cloquet River nr Burnett (04048001)
Simulated
Observed
TKN, mg/L
1.8
1.6
1.4
1.2
1
0.8
0.6
0.4
0.2
0
J-94 A-94 J-94 S-94 D-94 M-95 J-95 S-95 D-95 M-96 J-96 S-96 D-96 M-97 J-97 S-97 D-97 M-98 J-98 S-98 D-98 M-99 J-99 S-99 D-99 F-00
Year

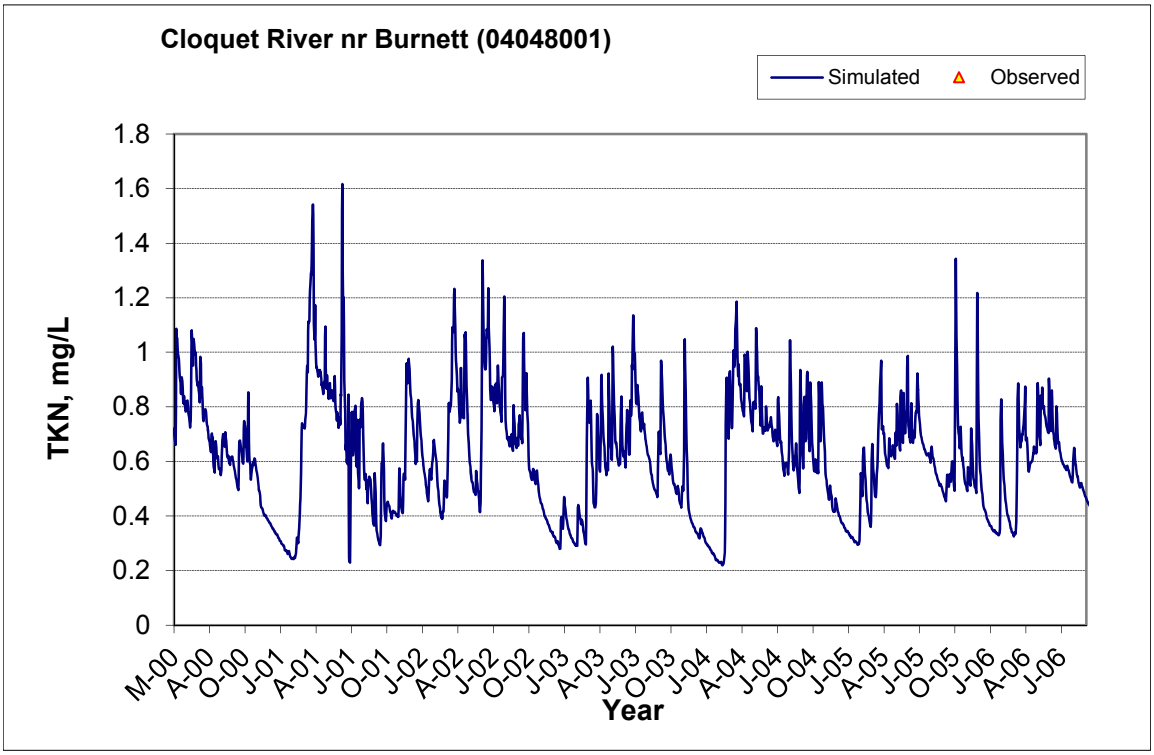
Cloquet River nr Burnett (04048001)
Simulated
Observed
TKN, mg/L
1.8
1.6
1.4
1.2
1
0.8
0.6
0.4
0.2
0
M-00 A-00 O-00 J-01 A-01 J-01 O-01 J-02 A-02 J-02 O-02 J-03 A-03 J-03 O-03 J-04 A-04 J-04 O-04 J-05 A-05 J-05 O-05 J-06 A-06 J-06
Year

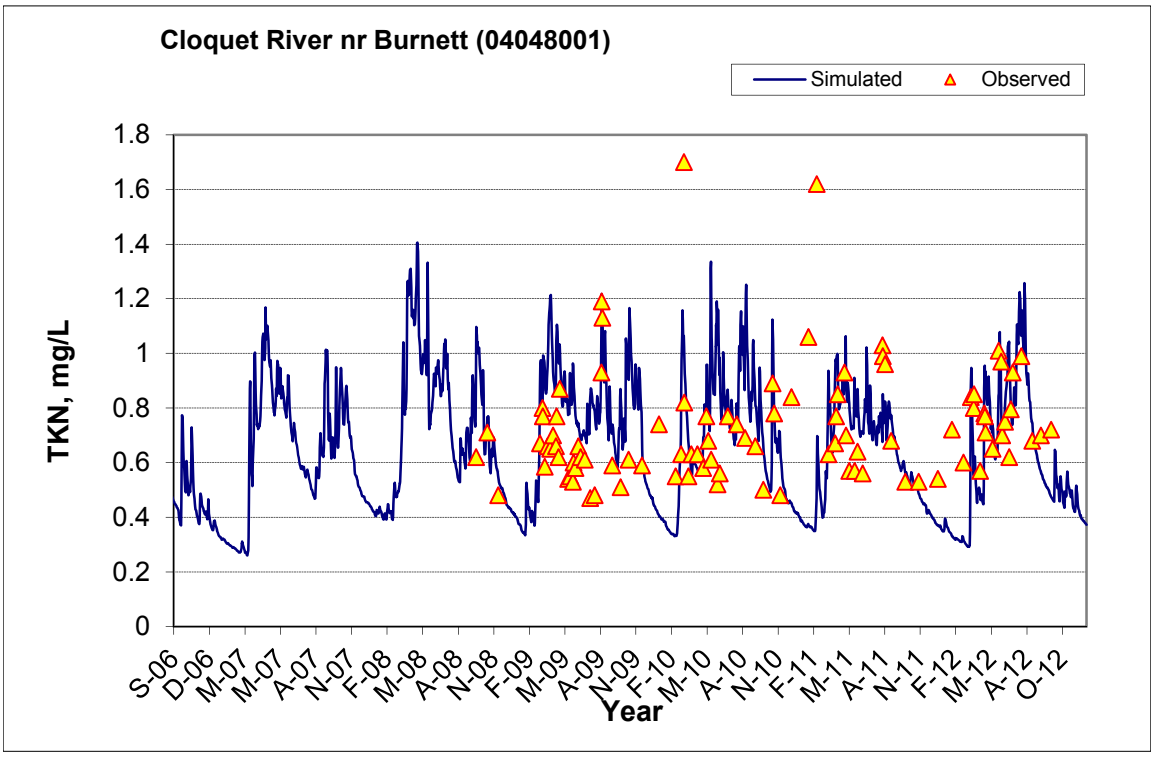

Figure A-210. Time series of observed and simulated Total Kjeldahl Nitrogen (TKN) concentration at Cloquet River nr Burnett (04048001)

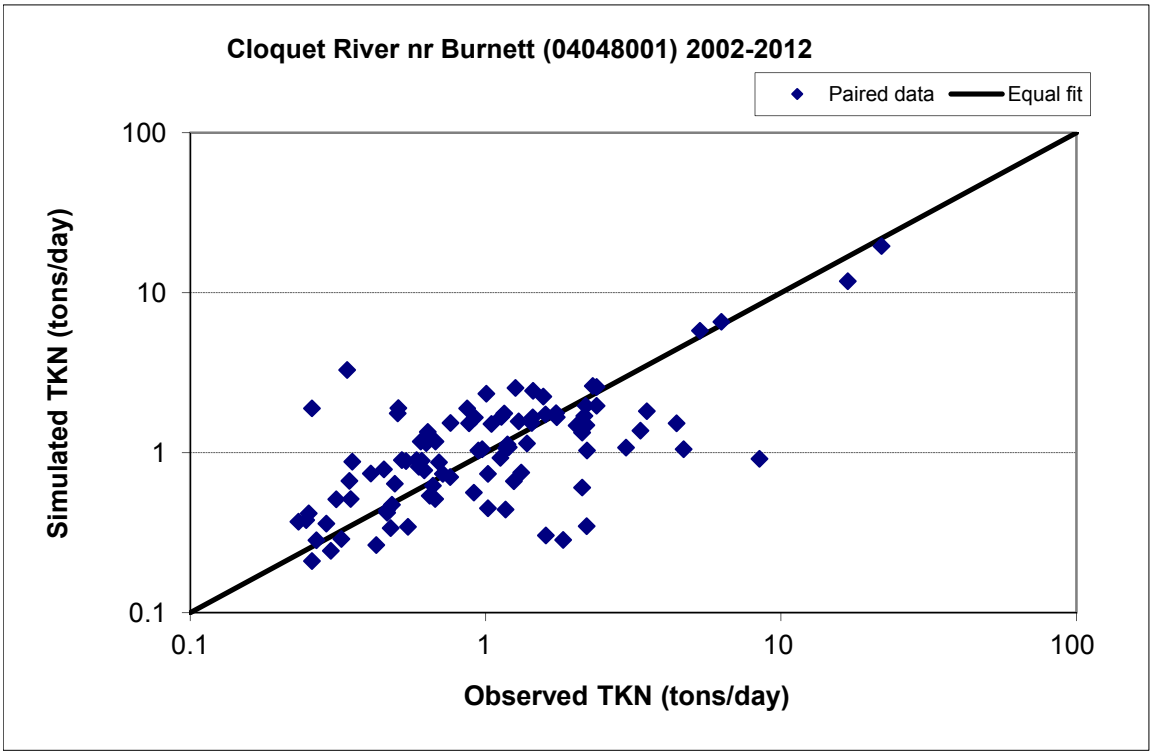

Figure A-211. Paired simulated vs. observed Total Kjeldahl Nitrogen (TKN) load at Cloquet River nr Burnett (04048001) (calibration period)

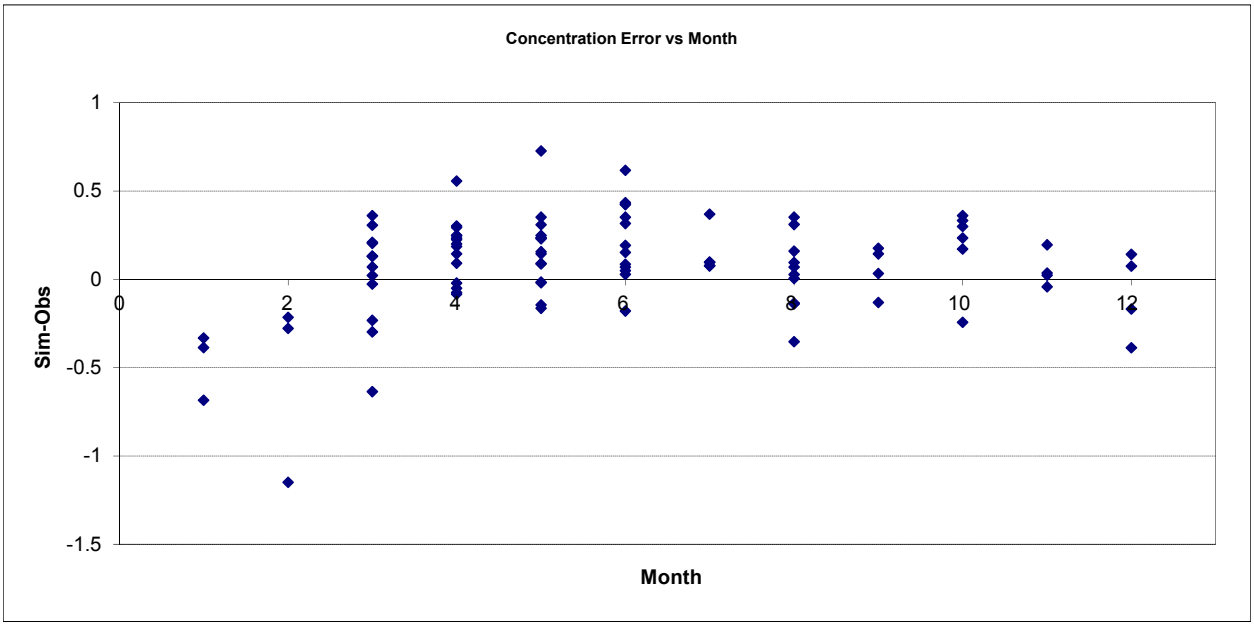

Figure A-212. Residual (Simulated - Observed) vs. Month Total Kjeldahl Nitrogen (TKN) at Cloquet River nr Burnett (04048001)

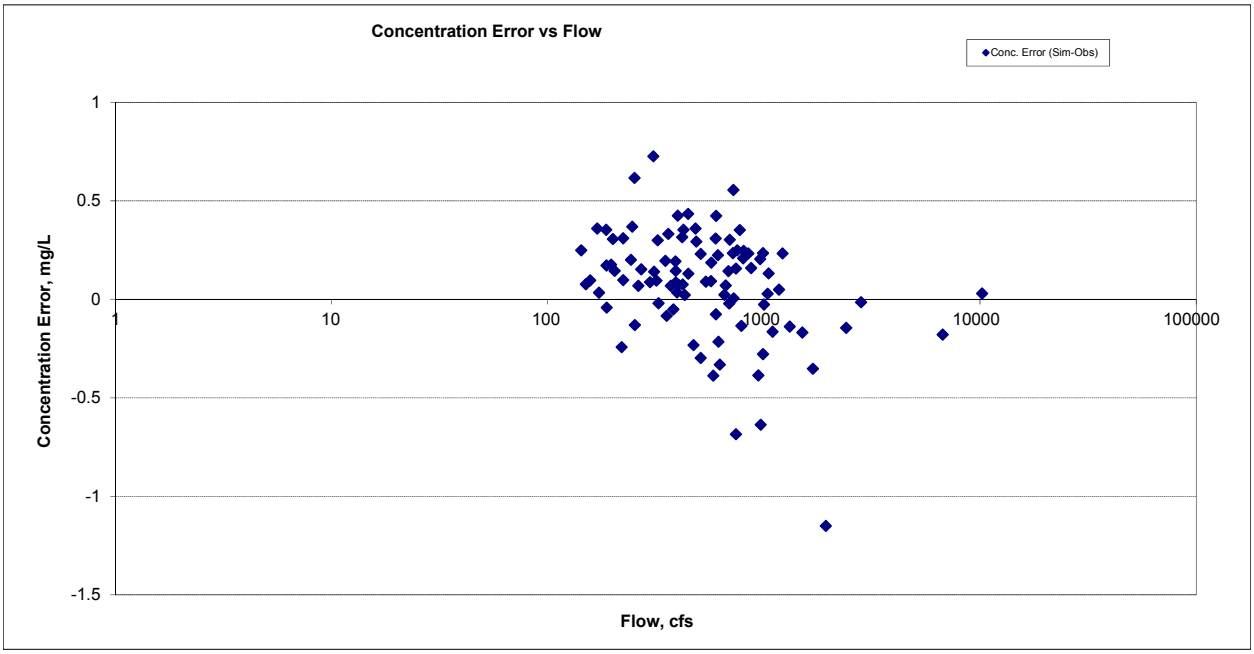

Figure A-213. Residual (Simulated - Observed) vs. Flow Total Kjeldahl Nitrogen (TKN) at Cloquet River nr Burnett (04048001)

A.7.4 Nitrite+ Nitrate Nitrogen (NOx)

Table A-31. Nitrite+ Nitrate Nitrogen (NOx) statistics

Period	1994-2001	2002-2012
Count	ND	94
Concentration Average Error		34.10%
Concentration Median Error		46.16%
Load Average Error		3.29%
Load Median Error		18.11%
Paired t conc		0.01
Paired t load		0.80

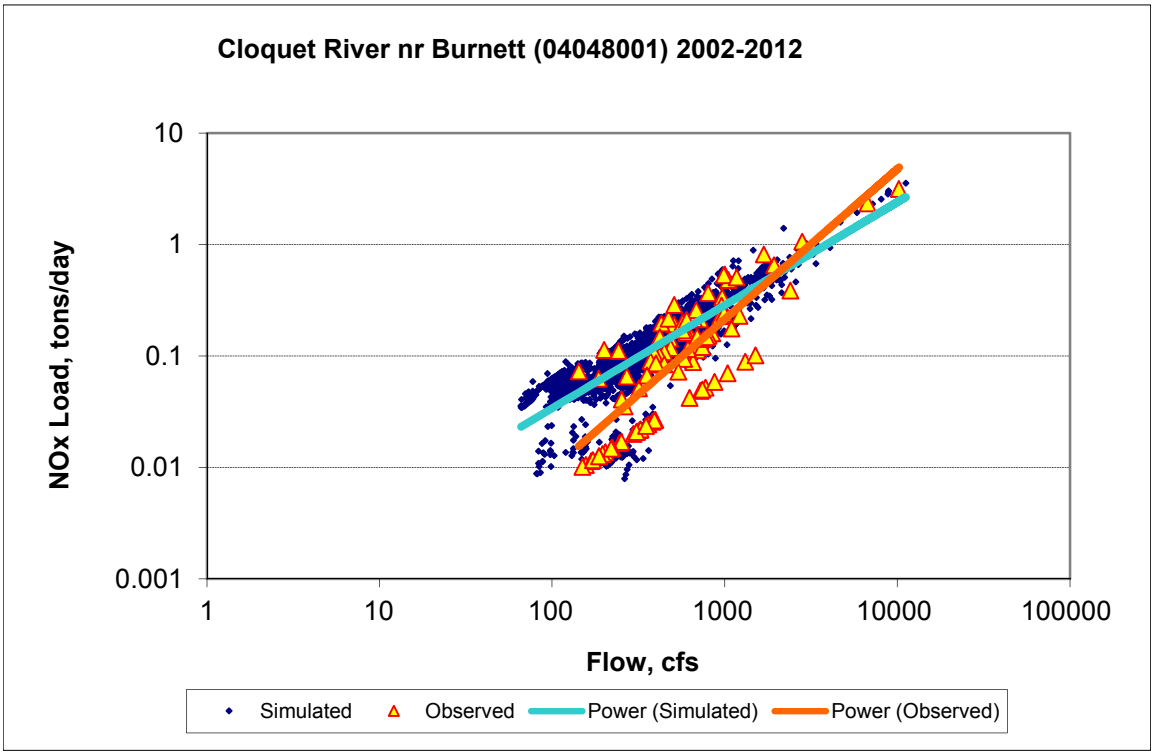

Figure A-214. Power plot of simulated and observed Nitrite+ Nitrate Nitrogen (NOx) load vs flow at Cloquet River nr Burnett (04048001) (calibration period)

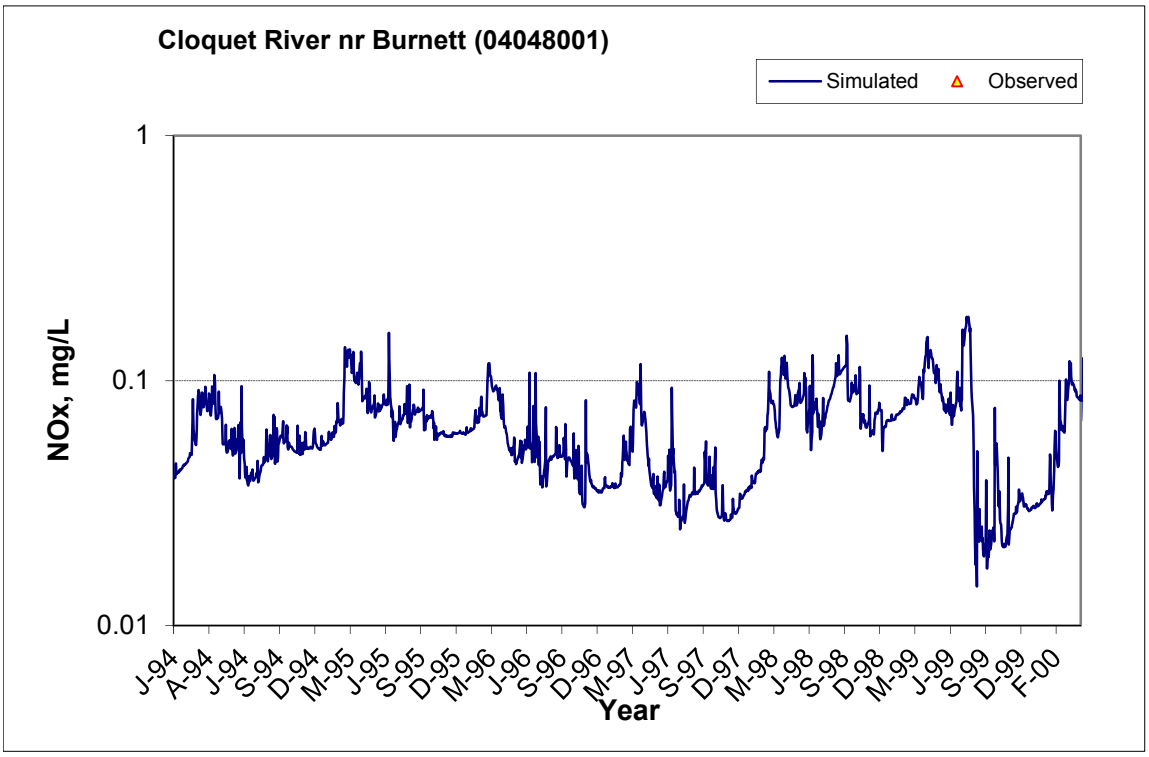
Cloquet River nr Burnett (04048001)
Simulated
Observed
NOx, mg/L
1
0.1
0.01
J-94 A-94 J-94 S-94 D-94 M-95 J-95 S-95 D-95 M-96 J-96 S-96 D-96 M-97 J-97 S-97 D-97 M-98 J-98 S-98 D-98 M-99 J-99 S-99 D-99 F-00
Year

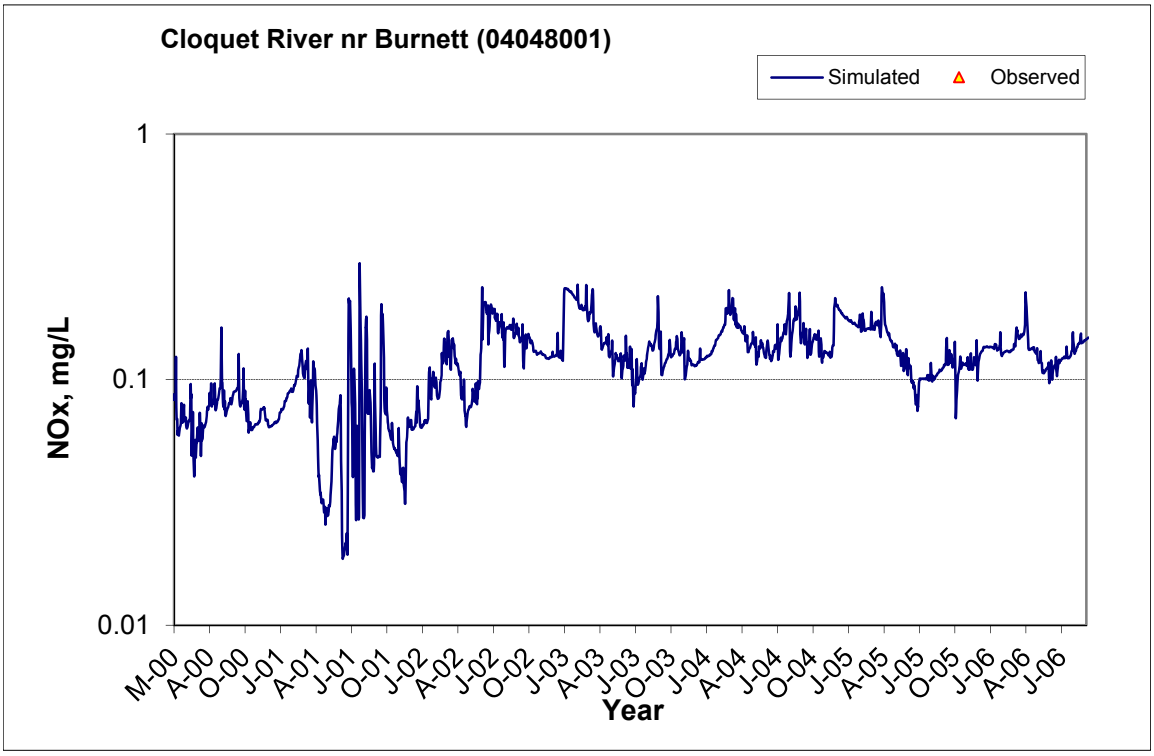
Cloquet River nr Burnett (04048001)
Simulated
Observed
NOx, mg/L
1
0.1
0.01
M-00 A-00 O-00 J-01 A-01 J-01 O-01 J-02 A-02 J-02 O-02 J-03 A-03 J-03 O-03 J-04 A-04 J-04 O-04 J-05 A-05 J-05 O-05 J-06 A-06 J-06
Year

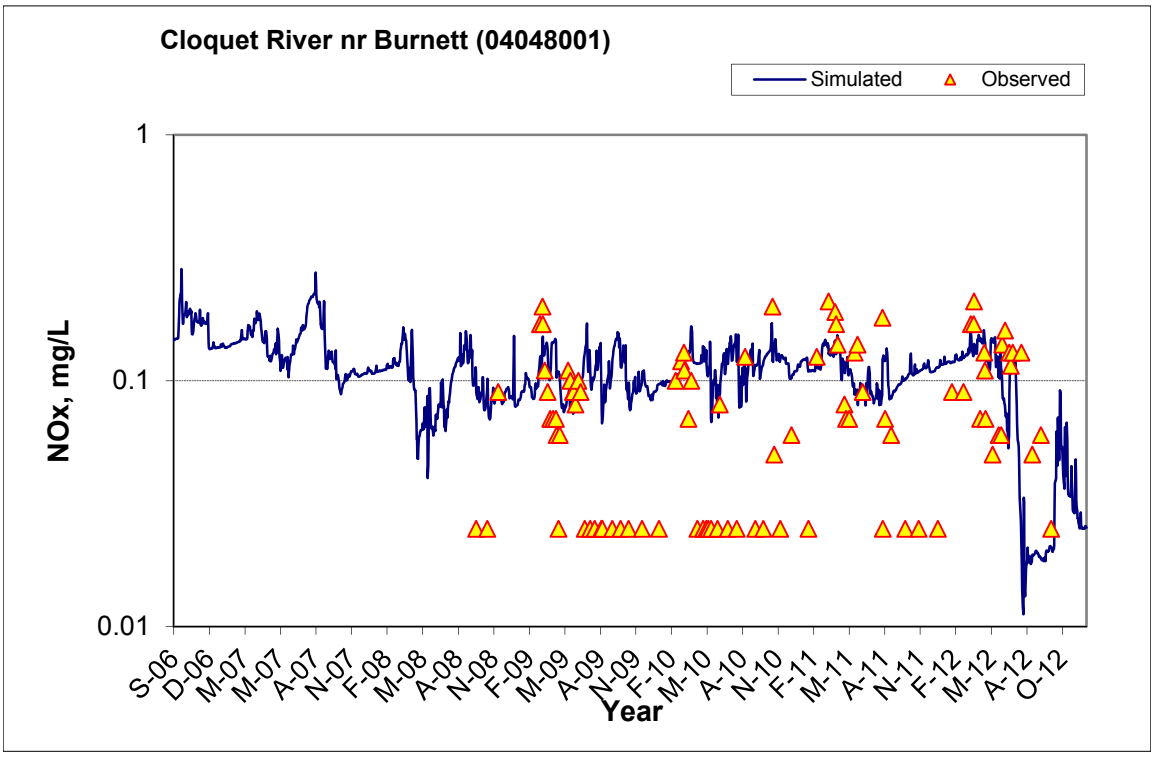

Figure A-215. Time series of observed and simulated Nitrite+ Nitrate Nitrogen (NOx) concentration at Cloquet River nr Burnett (04048001)

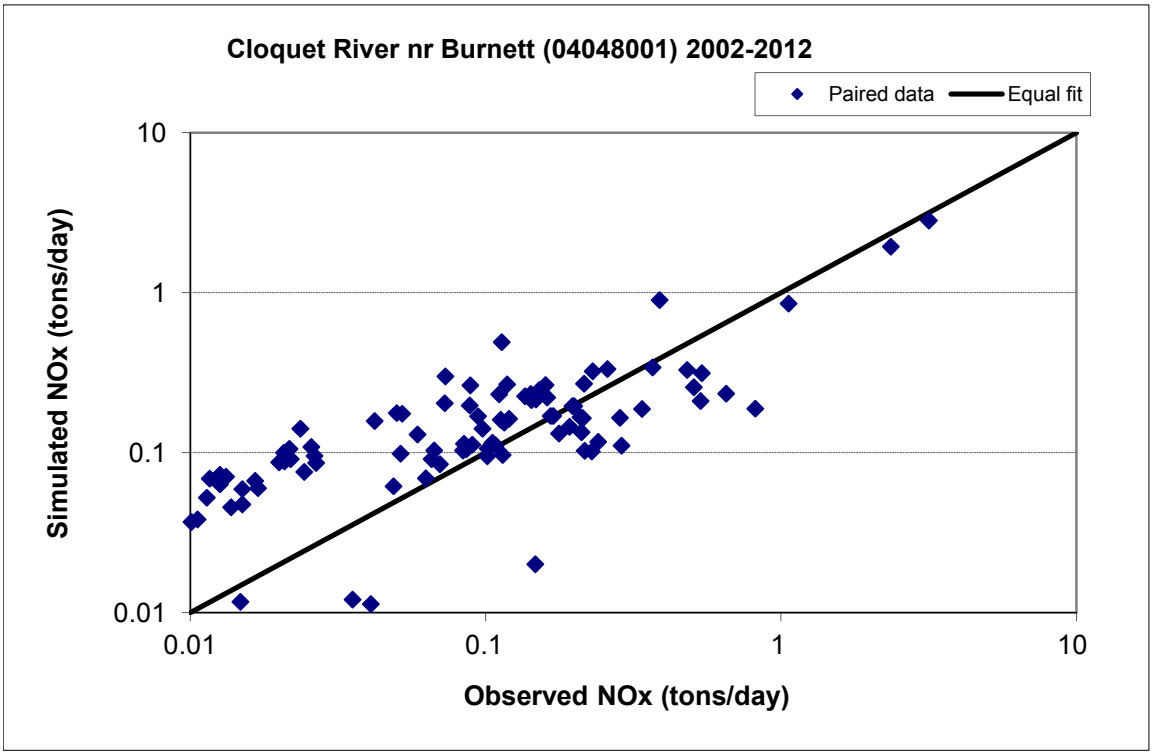

Figure A-216. Paired simulated vs. observed Nitrite+ Nitrate Nitrogen (NOx) load at Cloquet River nr Burnett (04048001) (calibration period)

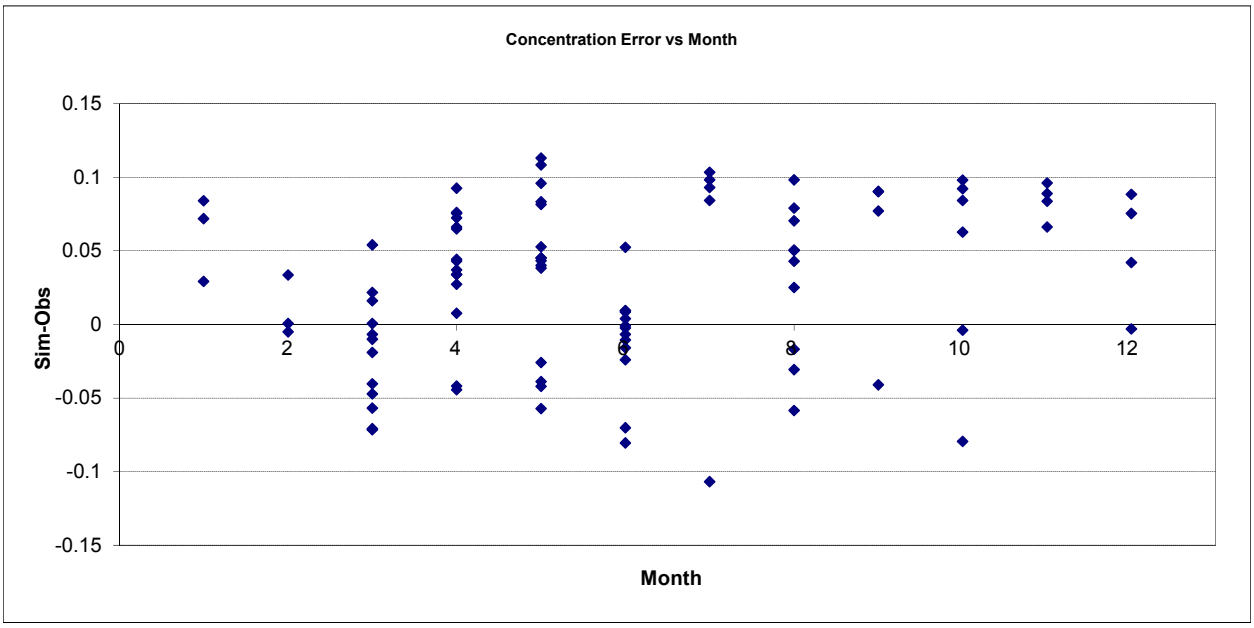

Figure A-217. Residual (Simulated - Observed) vs. Month Nitrite+ Nitrate Nitrogen (NOx) at Cloquet River nr Burnett (04048001)

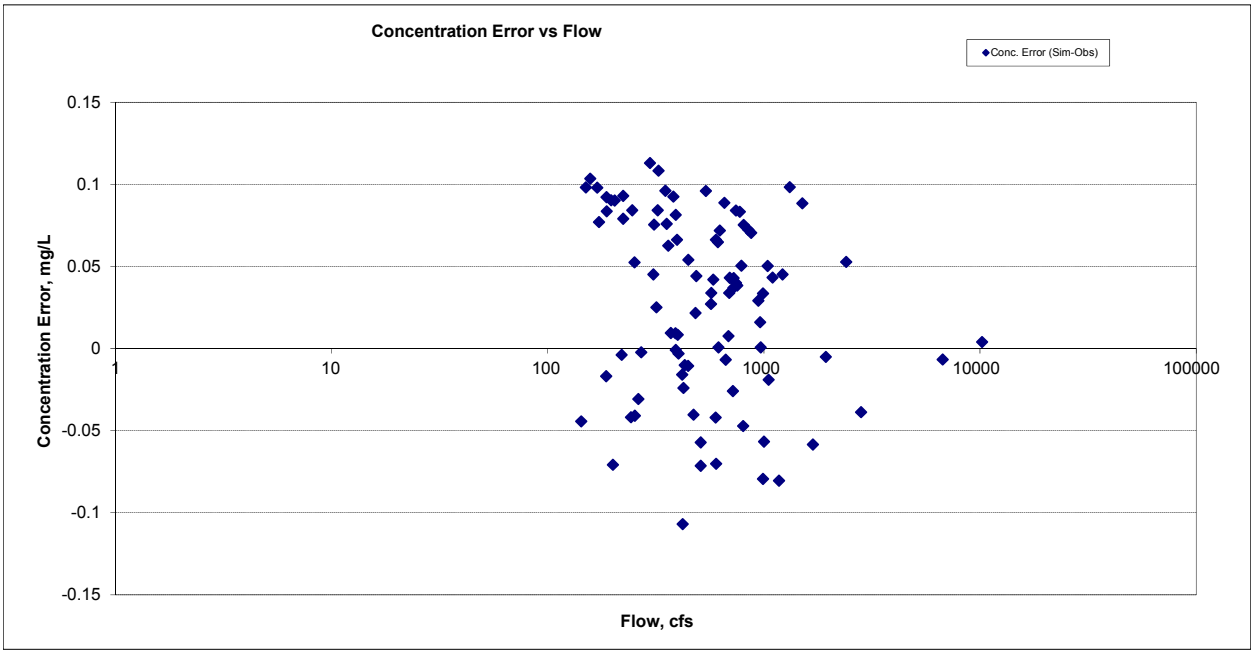

Figure A-218. Residual (Simulated - Observed) vs. Flow Nitrite+ Nitrate Nitrogen (NOx) at Cloquet River nr Burnett (04048001)

A.7.5 Total Nitrogen (TN)

Table A-32. Total Nitrogen (TN) statistics

Period	1994-2001	2002-2012
Count	ND	94
Concentration Average Error		11.71%
Concentration Median Error		18.60%
Load Average Error		-9.86%
Load Median Error		3.74%
Paired t conc		1.00
Paired t load		0.73

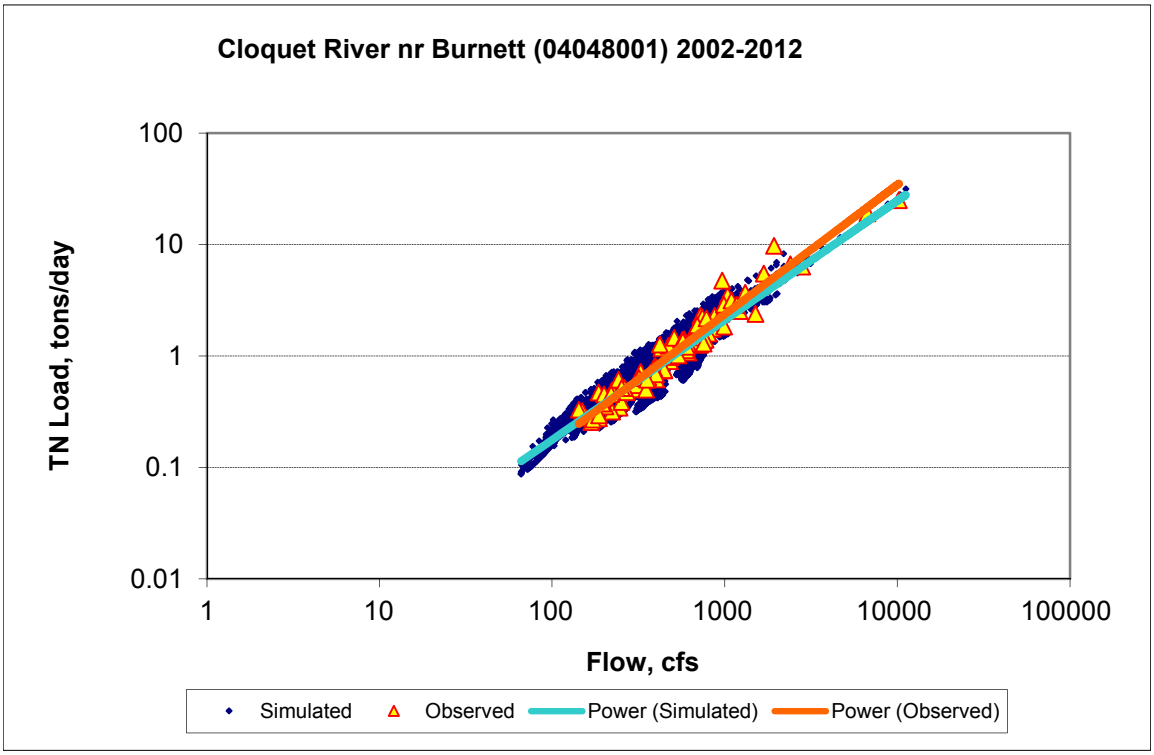

Figure A-219. Power plot of simulated and observed Total Nitrogen (TN) load vs flow at Cloquet River nr Burnett (04048001) (calibration period)

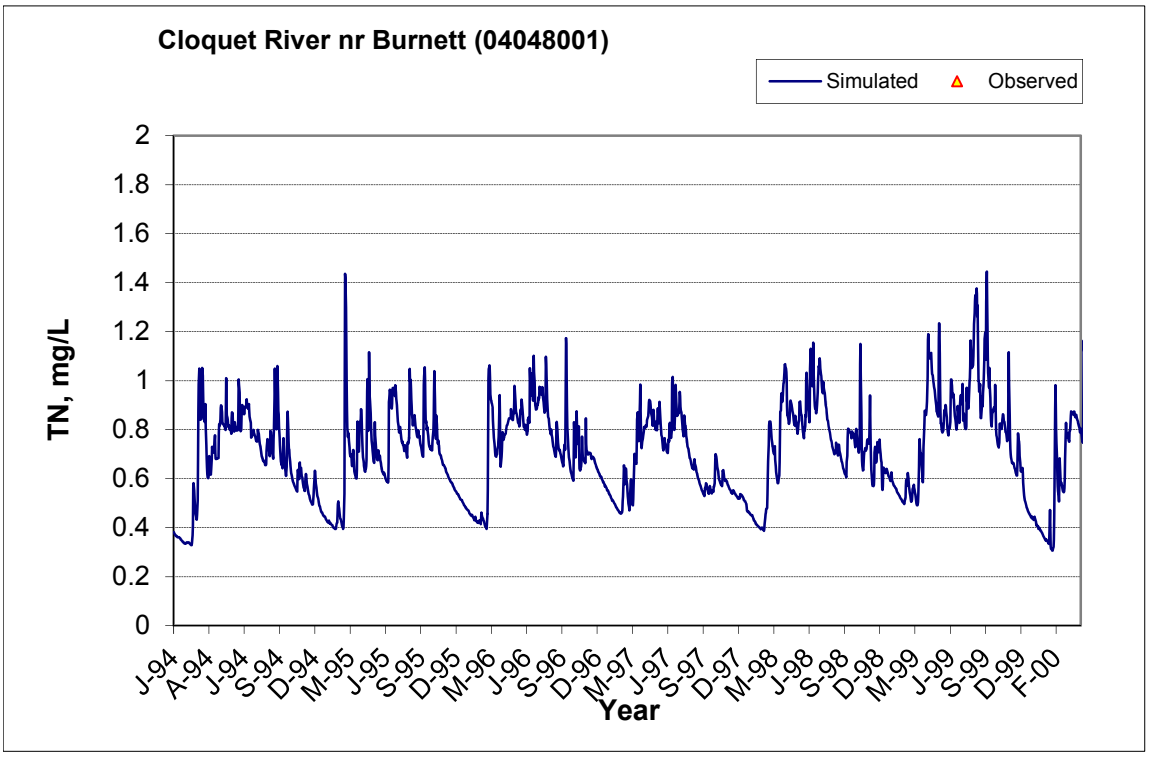
Cloquet River nr Burnett (04048001)
Simulated
Observed
TN, mg/L
2
1.8
1.6
1.4
1.2
1
0.8
0.6
0.4
0.2
0
J-94 A-94 J-94 S-94 D-94 M-95 J-95 S-95 D-95 M-96 J-96 S-96 D-96 M-97 J-97 S-97 D-97 M-98 J-98 S-98 D-98 M-99 J-99 S-99 D-99 F-00
Year

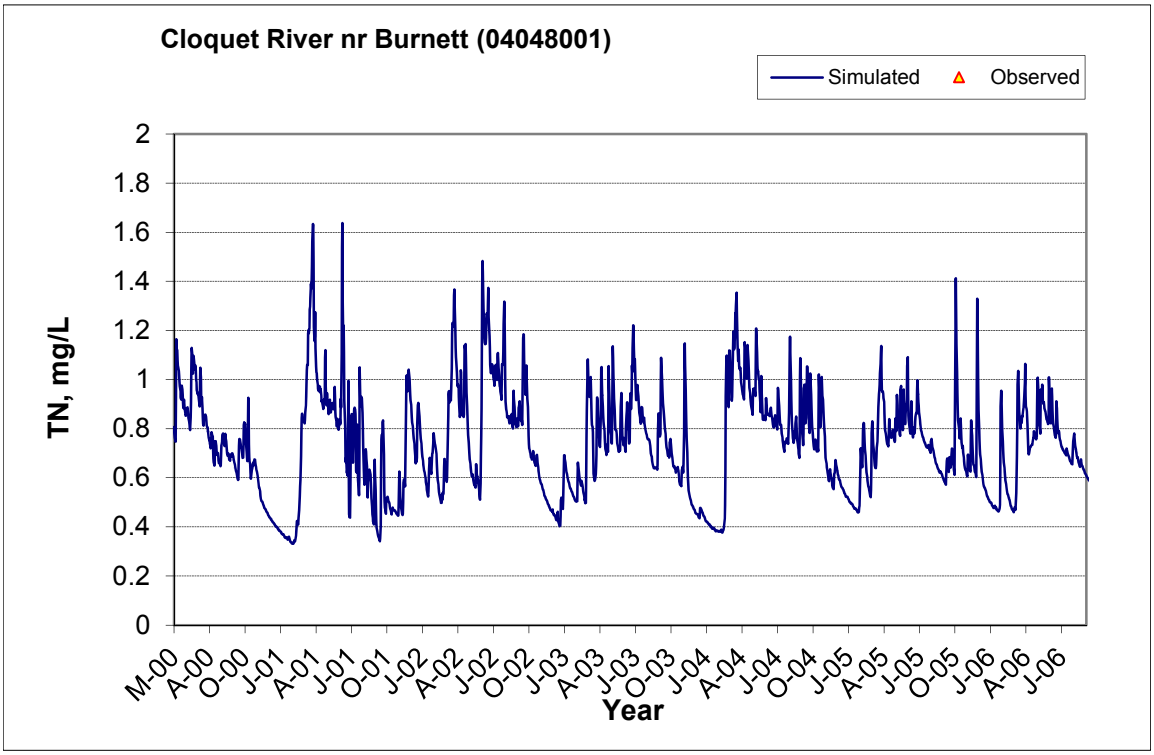
Cloquet River nr Burnett (04048001)
Simulated
Observed
TN, mg/L
2
1.8
1.6
1.4
1.2
1
0.8
0.6
0.4
0.2
0
M-00 A-00 O-00 J-01 A-01 J-01 O-01 J-02 A-02 J-02 O-02 J-03 A-03 J-03 O-03 J-04 A-04 J-04 O-04 J-05 A-05 J-05 O-05 J-06 A-06 J-06
Year

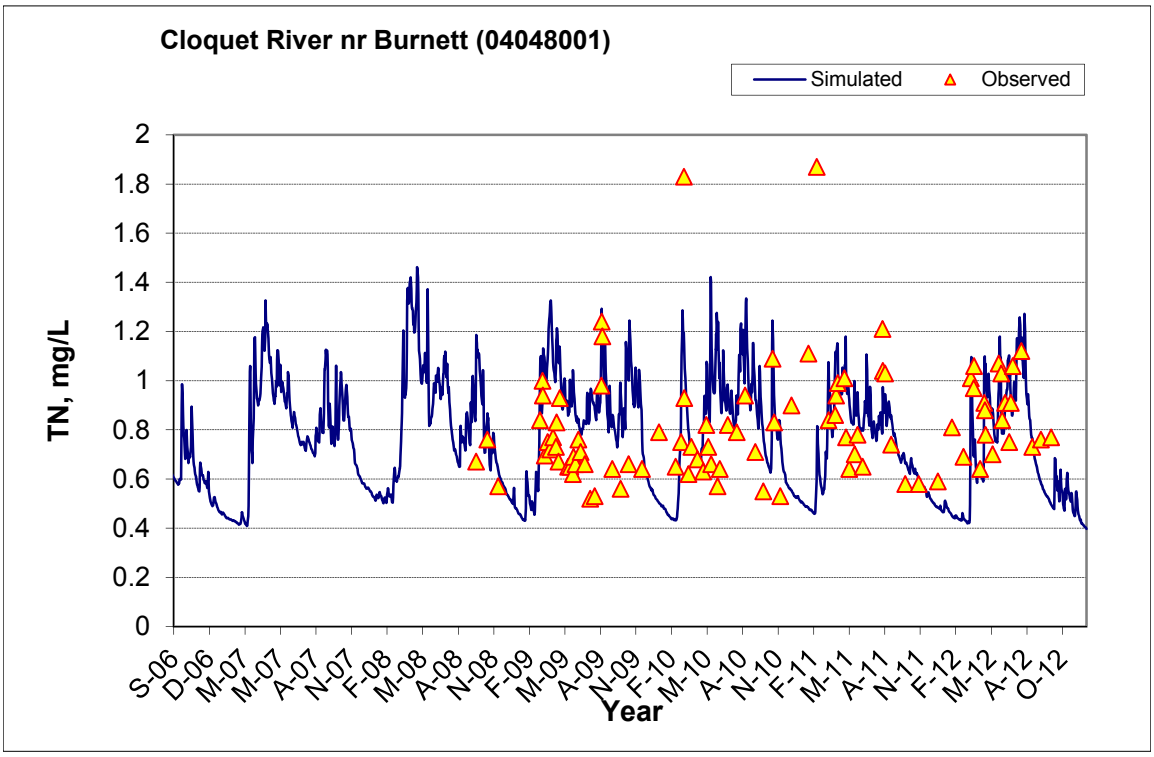

Figure A-220. Time series of observed and simulated Total Nitrogen (TN) concentration at Cloquet River nr Burnett (04048001)

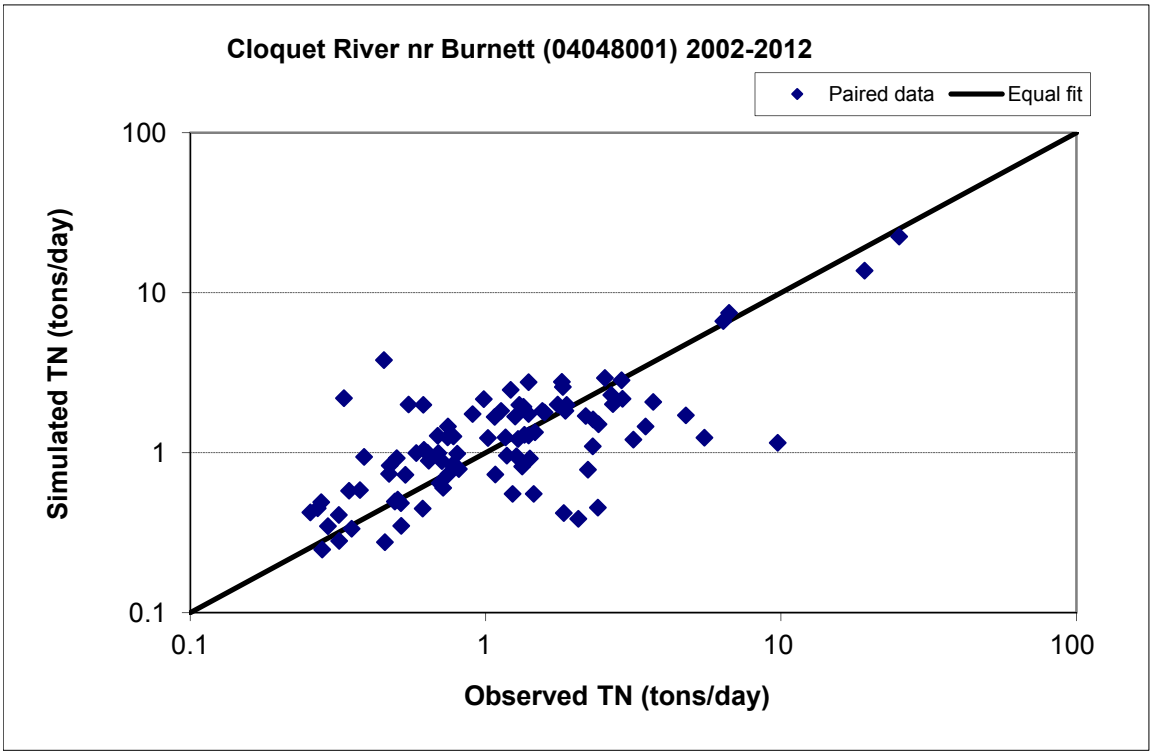

Figure A-221. Paired simulated vs. observed Total Nitrogen (TN) load at Cloquet River nr Burnett (04048001) (calibration period)

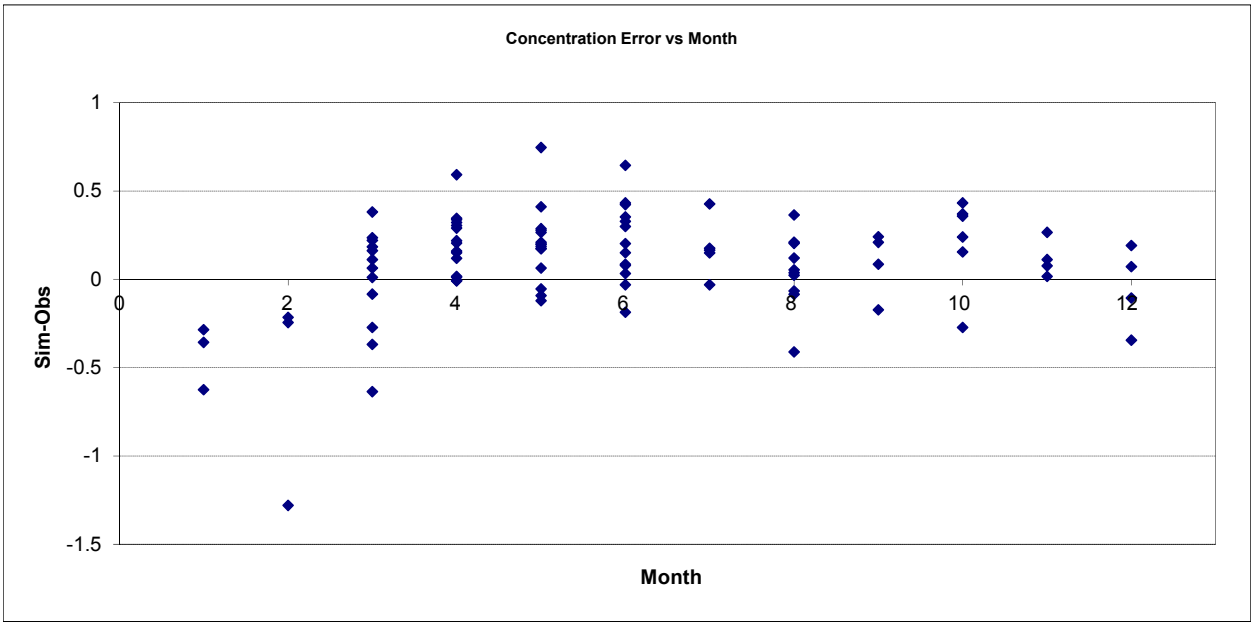

Figure A-222. Residual (Simulated - Observed) vs. Month Total Nitrogen (TN) at Cloquet River nr Burnett (04048001)

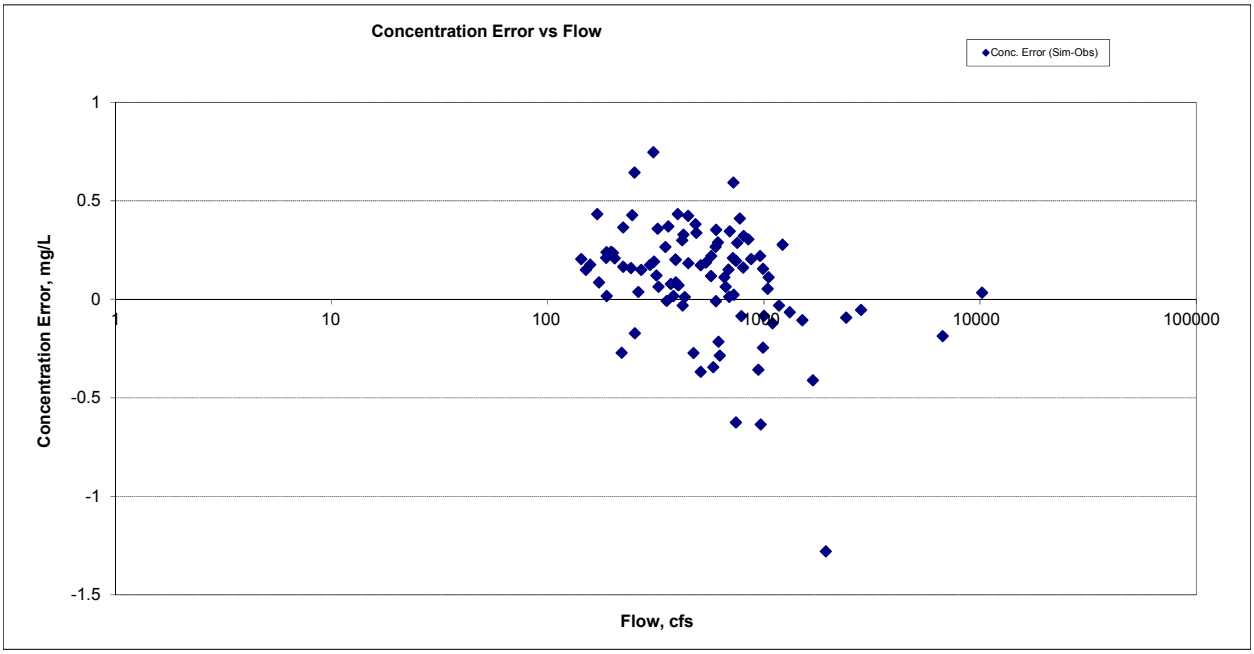

Figure A-223. Residual (Simulated - Observed) vs. Flow Total Nitrogen (TN) at Cloquet River nr Burnett (04048001)

A.7.6 Soluble Reactive Phosphorus (SRP)

Table A-33. Soluble Reactive Phosphorus (SRP) statistics

Period	1994-2001	2002-2012
Count	ND	91
Concentration Average Error		-36.73%
Concentration Median Error		-47.96%
Load Average Error		-16.43%
Load Median Error		-13.91%
Paired t conc		0.00
Paired t load		0.55

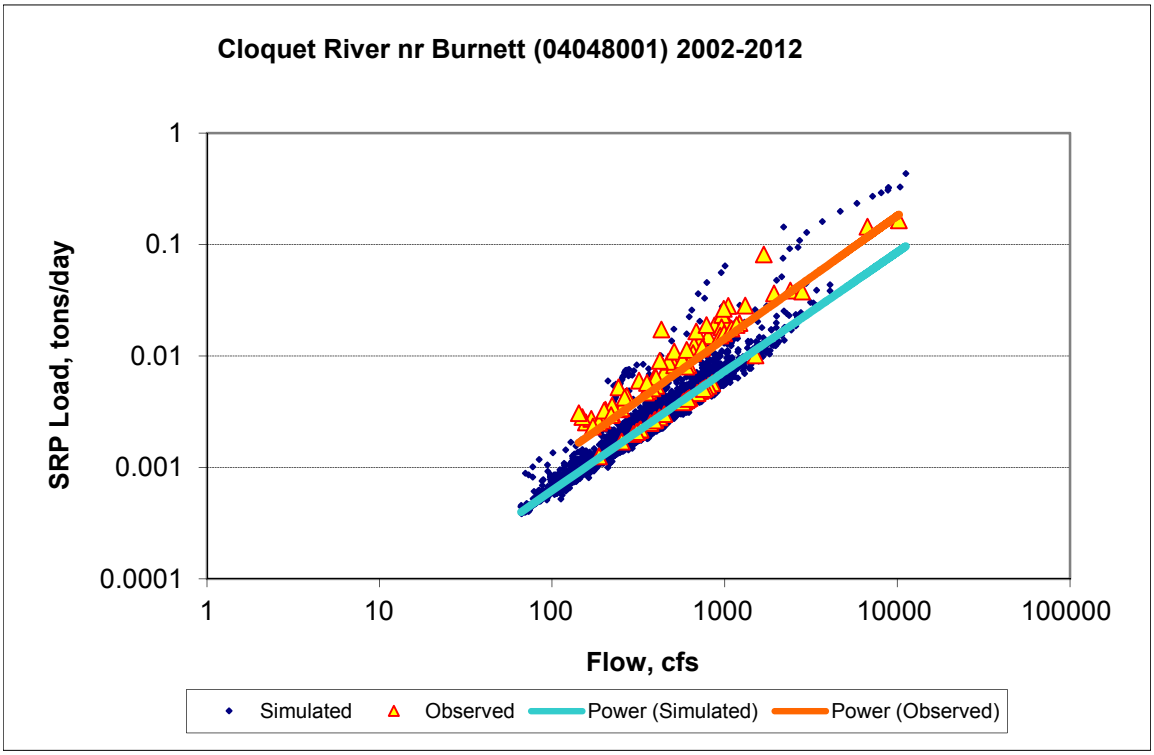

Figure A-224. Power plot of simulated and observed Soluble Reactive Phosphorus (SRP) load vs flow at Cloquet River nr Burnett (04048001) (calibration period)

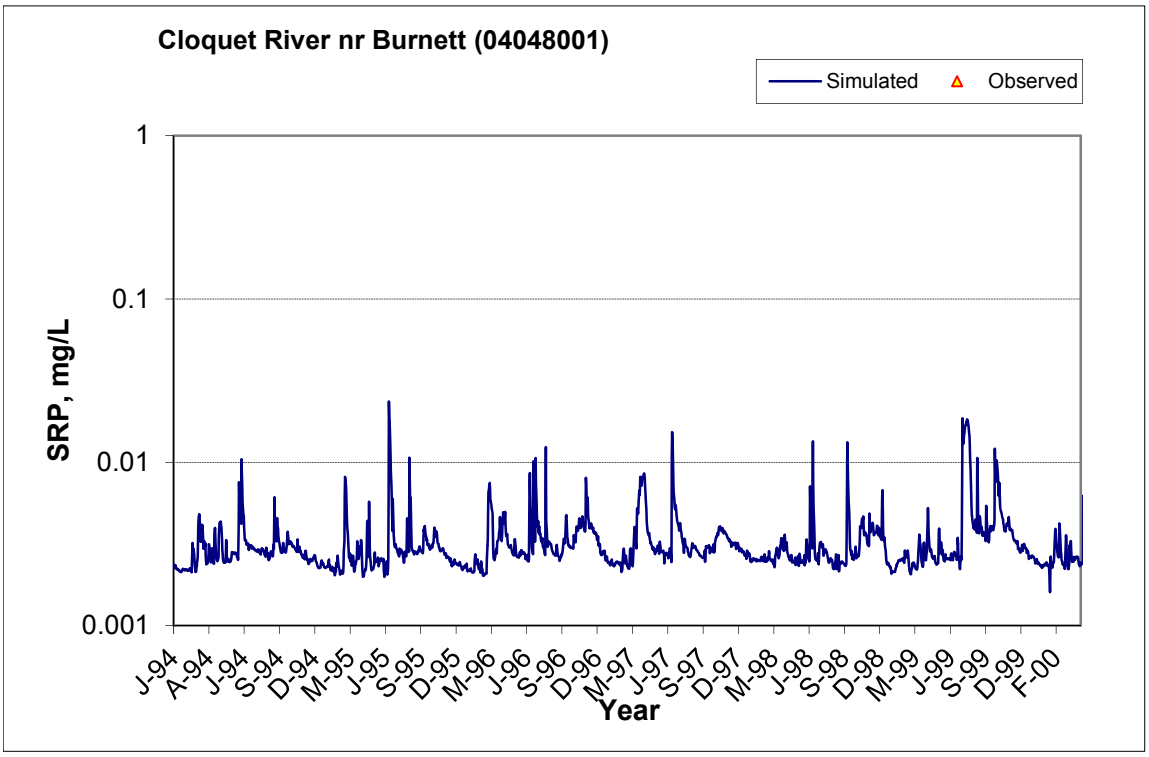
Cloquet River nr Burnett (04048001)
Simulated
Observed
SRP, mg/L
1
0.1
0.01
0.001
J-94 A-94 J-94 S-94 D-94 M-95 J-95 S-95 D-95 M-96 J-96 S-96 D-96 M-97 J-97 S-97 D-97 M-98 J-98 S-98 D-98 M-99 J-99 S-99 D-99 F-00
Year

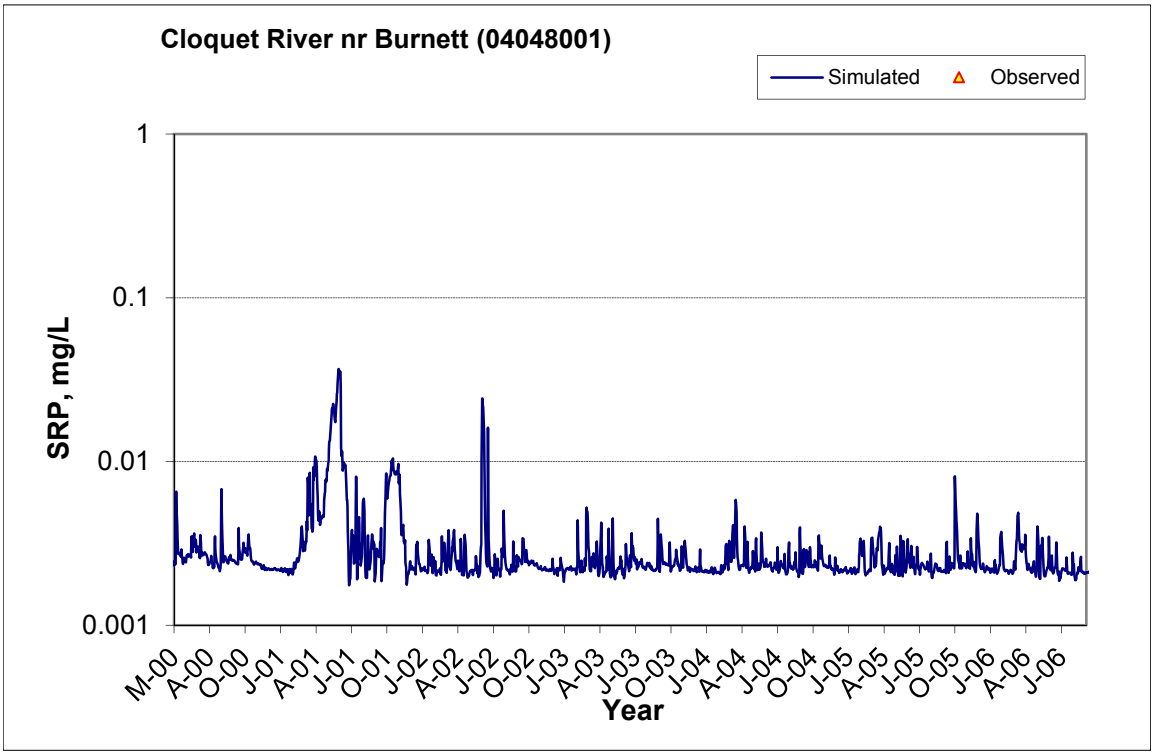
Cloquet River nr Burnett (04048001)
Simulated
Observed
SRP, mg/L
1
0.1
0.01
0.001
M-00 A-00 O-00 J-01 A-01 J-01 O-01 J-02 A-02 J-02 O-02 J-03 A-03 J-03 O-03 J-04 A-04 J-04 O-04 J-05 A-05 J-05 O-05 J-06 A-06 J-06
Year

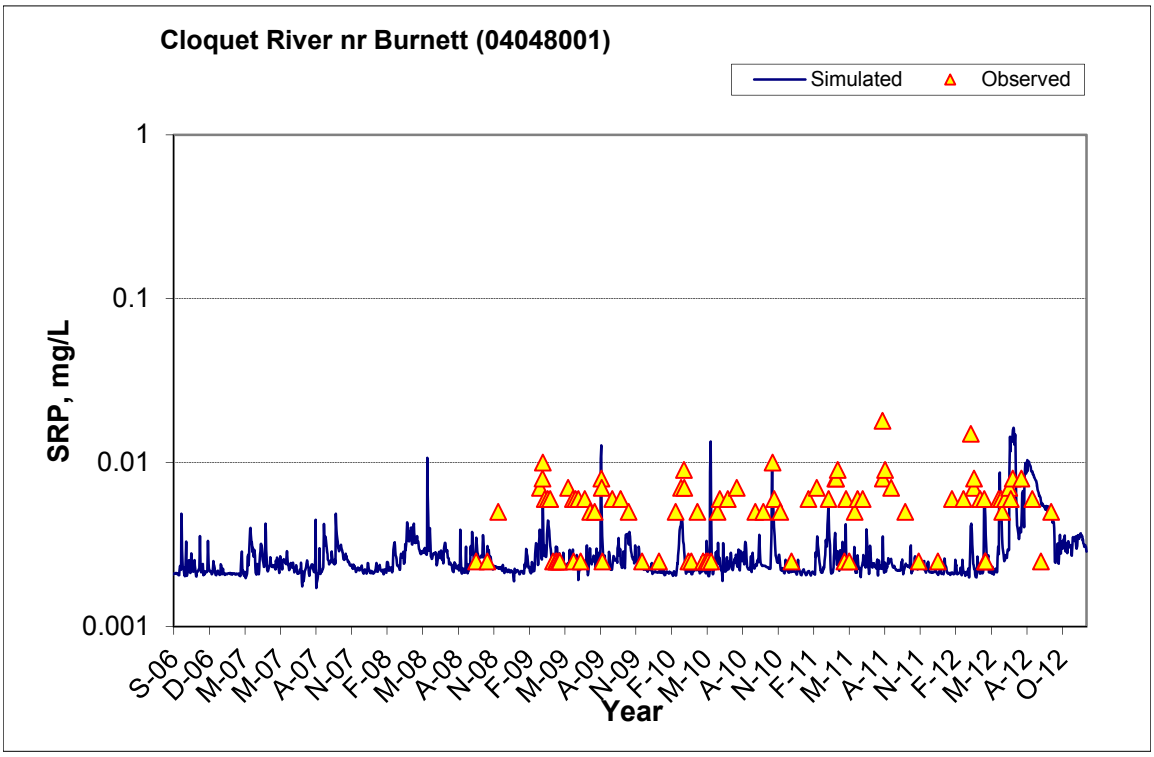

Figure A-225. Time series of observed and simulated Soluble Reactive Phosphorus (SRP) concentration at Cloquet River nr Burnett (04048001)

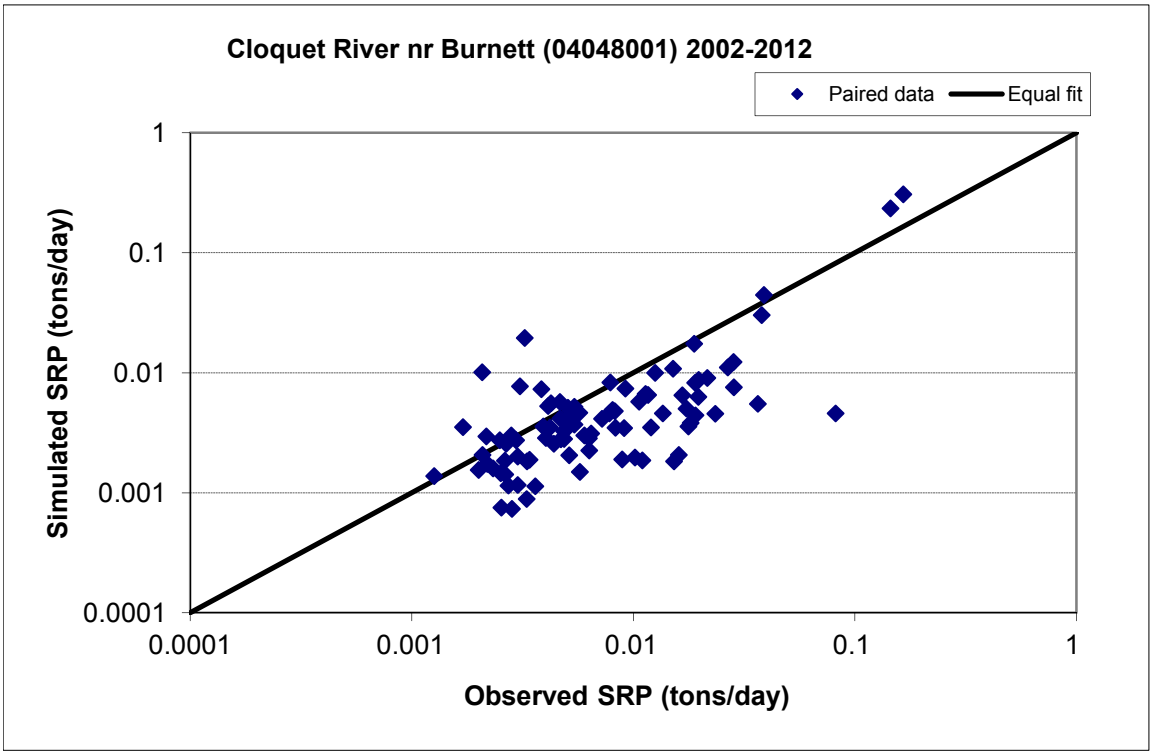

Figure A-226. Paired simulated vs. observed Soluble Reactive Phosphorus (SRP) load at Cloquet River nr Burnett (04048001) (calibration period)

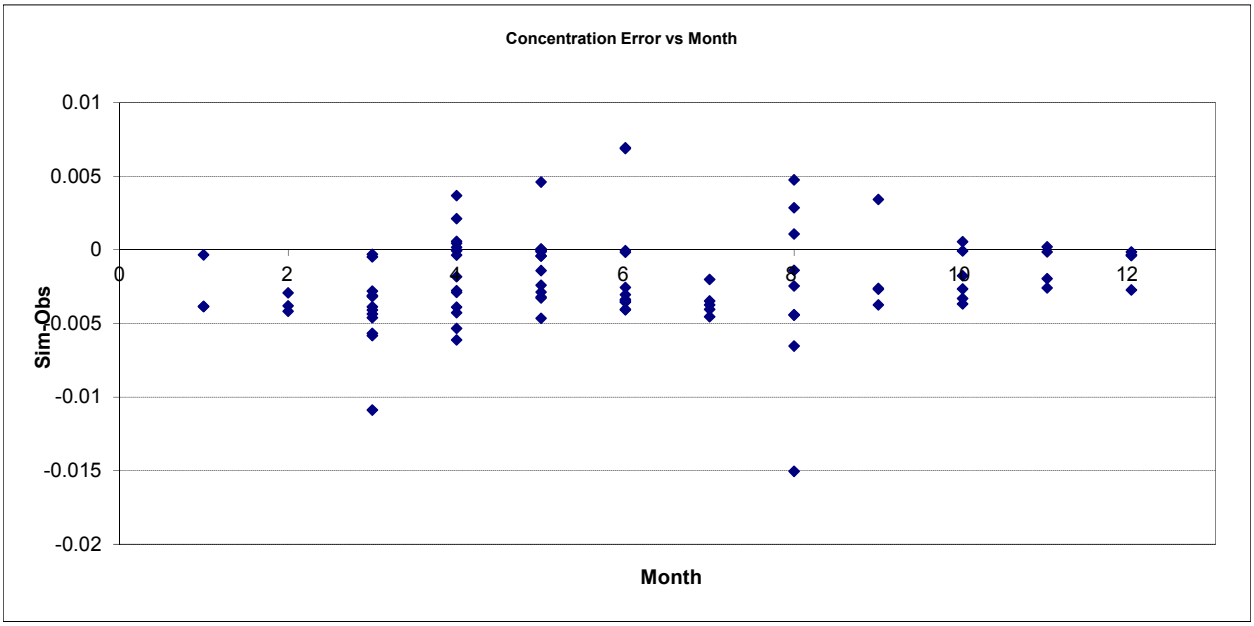

Figure A-227. Residual (Simulated - Observed) vs. Month Soluble Reactive Phosphorus (SRP) at Cloquet River nr Burnett (04048001)

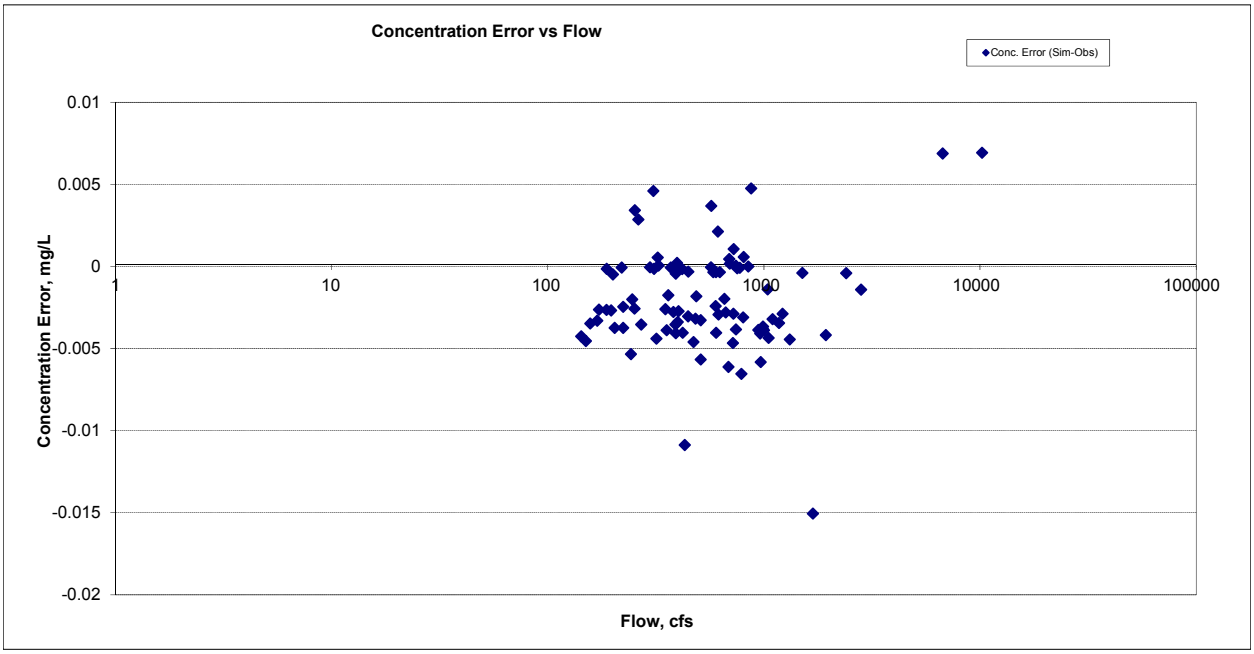

Figure A-228. Residual (Simulated - Observed) vs. Flow Soluble Reactive Phosphorus (SRP) at Cloquet River nr Burnett (04048001)

A.7.7 Organic Phosphorus (OrgP)

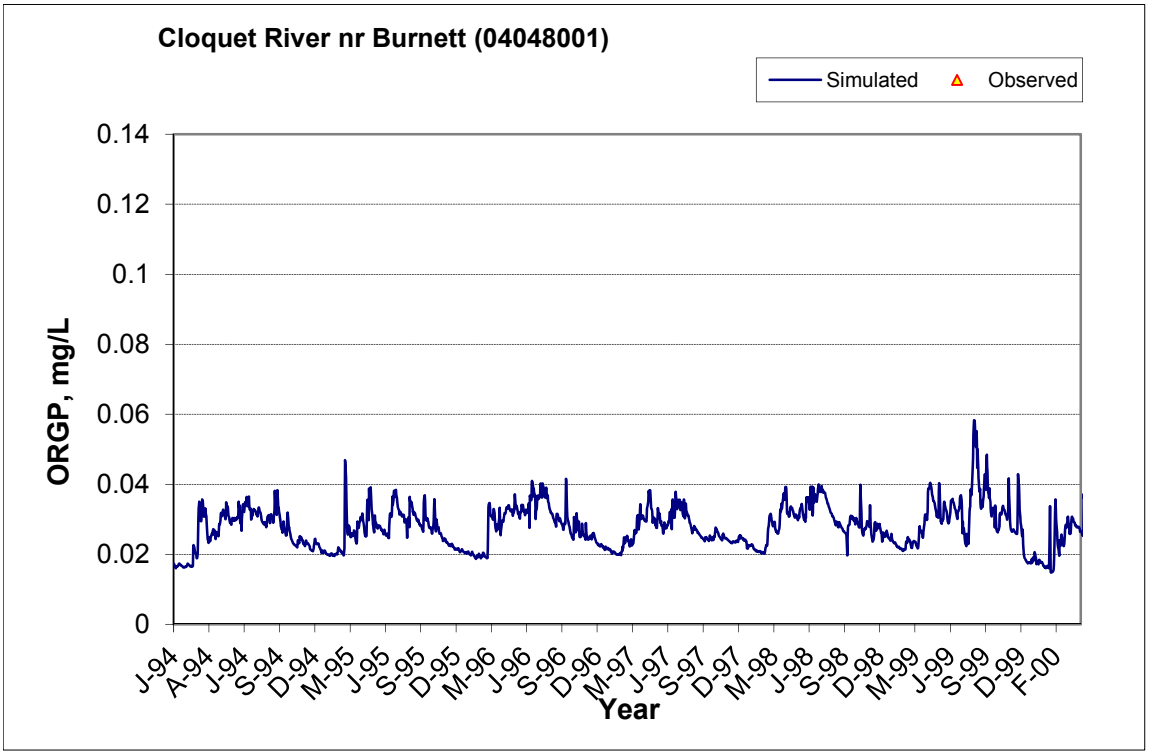

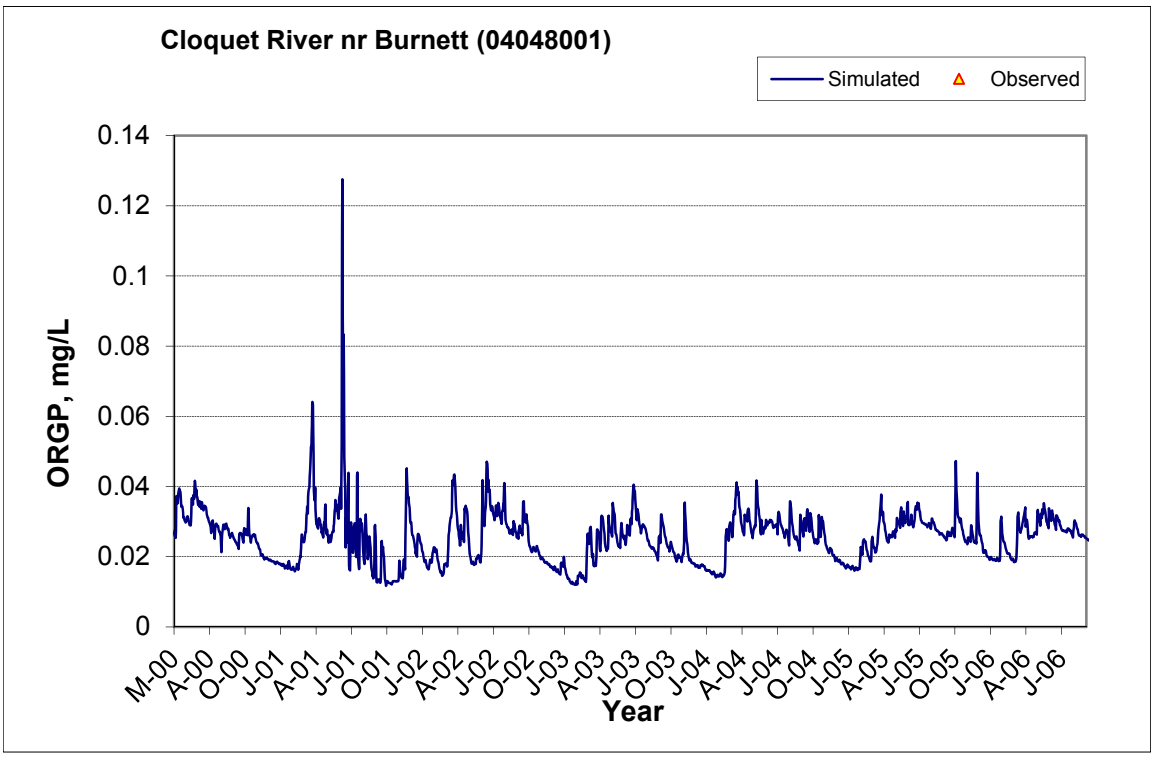

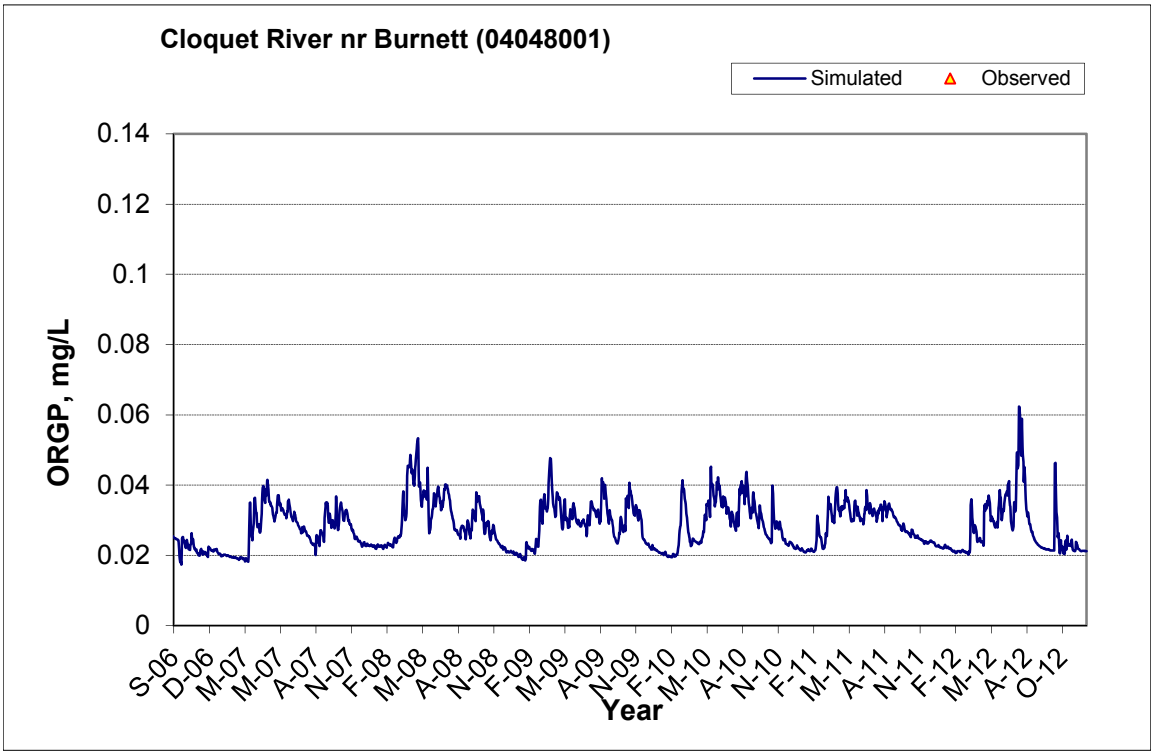

Figure A-229. Time series of observed and simulated Organic Phosphorus (OrgP) concentration at Cloquet River nr Burnett (04048001)

A.7.8 Total Phosphorus (TP)

Table A-34. Total Phosphorus (TP) statistics

Period	1994-2001	2002-2012
Count	29	80
Concentration Average Error	18.98%	6.30%
Concentration Median Error	33.88%	31.57%
Load Average Error	21.40%	-1.04%
Load Median Error	23.59%	17.80%
Paired t conc	0.57	0.82
Paired t load	0.47	0.97

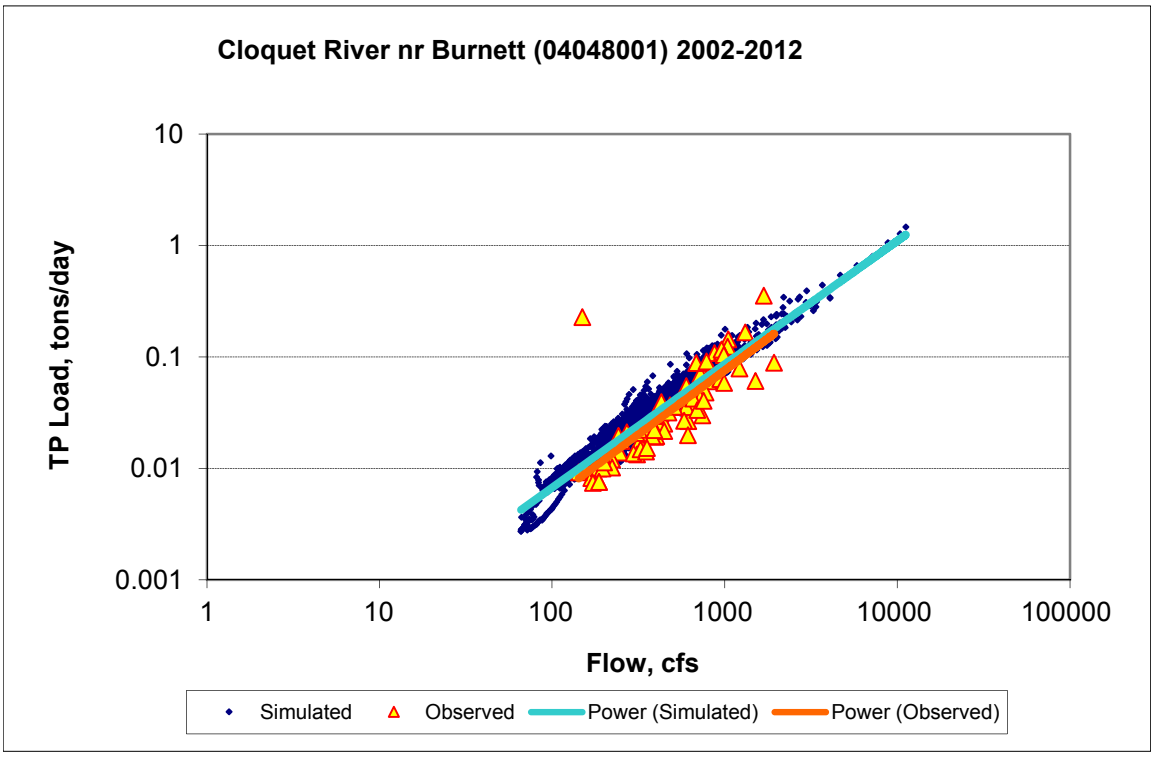

Figure A-230. Power plot of simulated and observed Total Phosphorus (TP) load vs flow at Cloquet River nr Burnett (04048001) (calibration period)

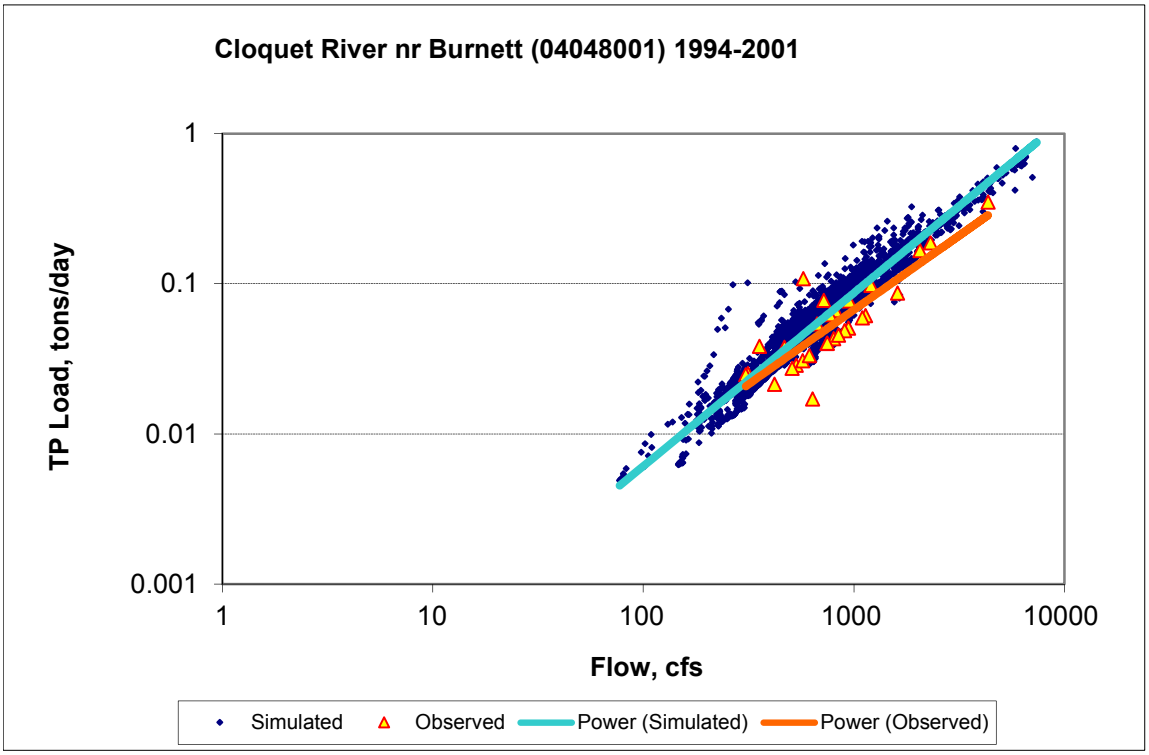

Figure A-231. Power plot of simulated and observed Total Phosphorus (TP) load vs flow at Cloquet River nr Burnett (04048001) (validation period)

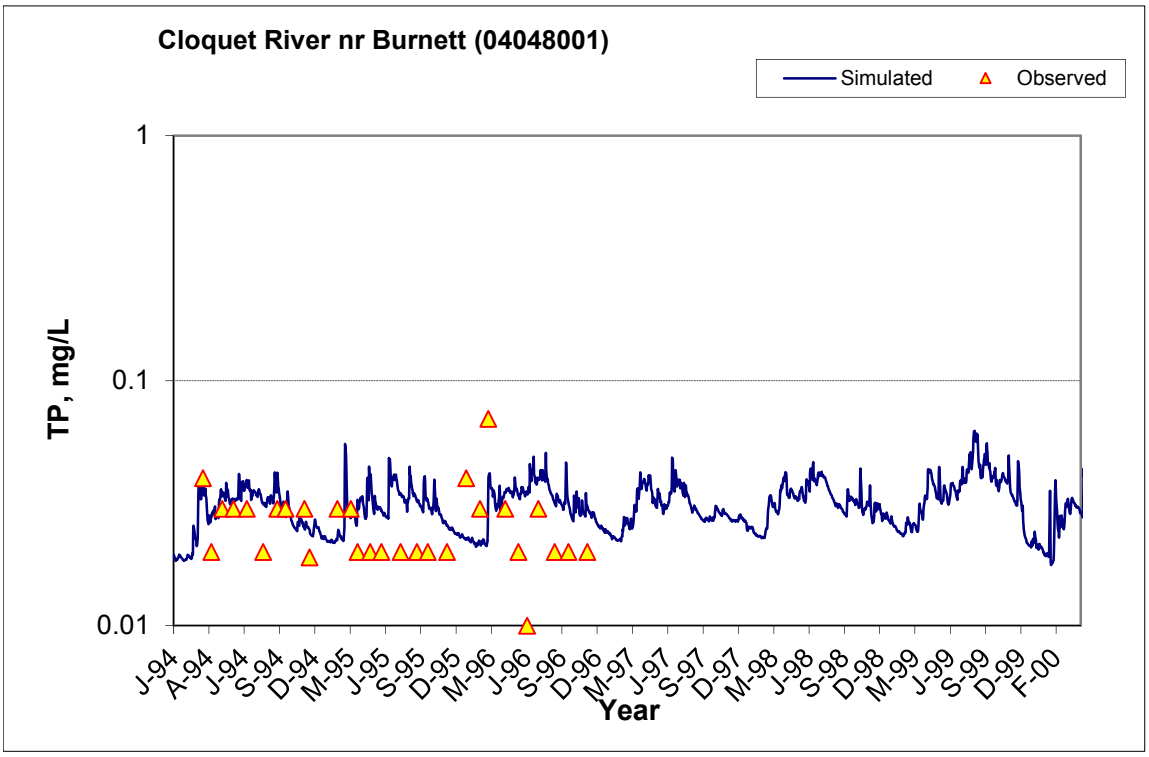
Cloquet River nr Burnett (04048001)
Simulated
Observed
TP, mg/L
1
0.1
0.01
J-94 A-94 J-94 S-94 D-94 M-95 J-95 S-95 D-95 M-96 J-96 S-96 D-96 M-97 J-97 S-97 D-97 M-98 J-98 S-98 D-98 M-99 J-99 S-99 D-99 F-00
Year

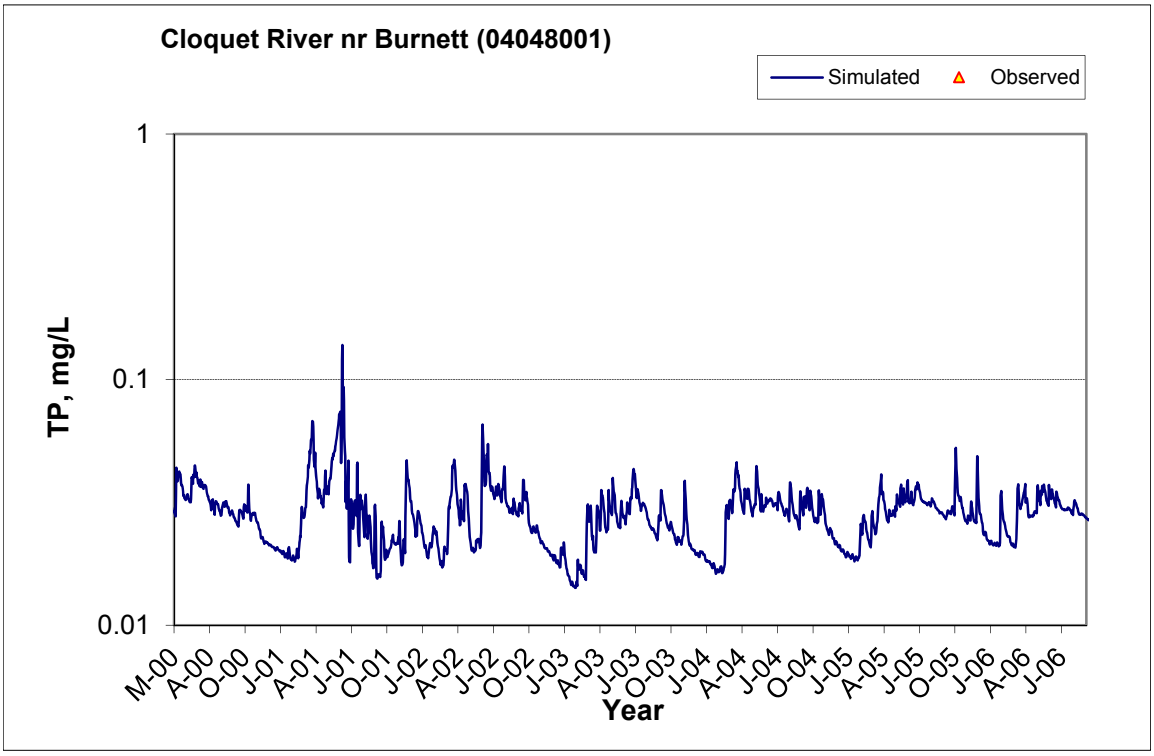
Cloquet River nr Burnett (04048001)
Simulated
Observed
TP, mg/L
1
0.1
0.01
M-00 A-00 O-00 J-01 A-01 J-01 O-01 J-02 A-02 J-02 O-02 J-03 A-03 J-03 O-03 J-04 A-04 J-04 O-04 J-05 A-05 J-05 O-05 J-06 A-06 J-06
Year

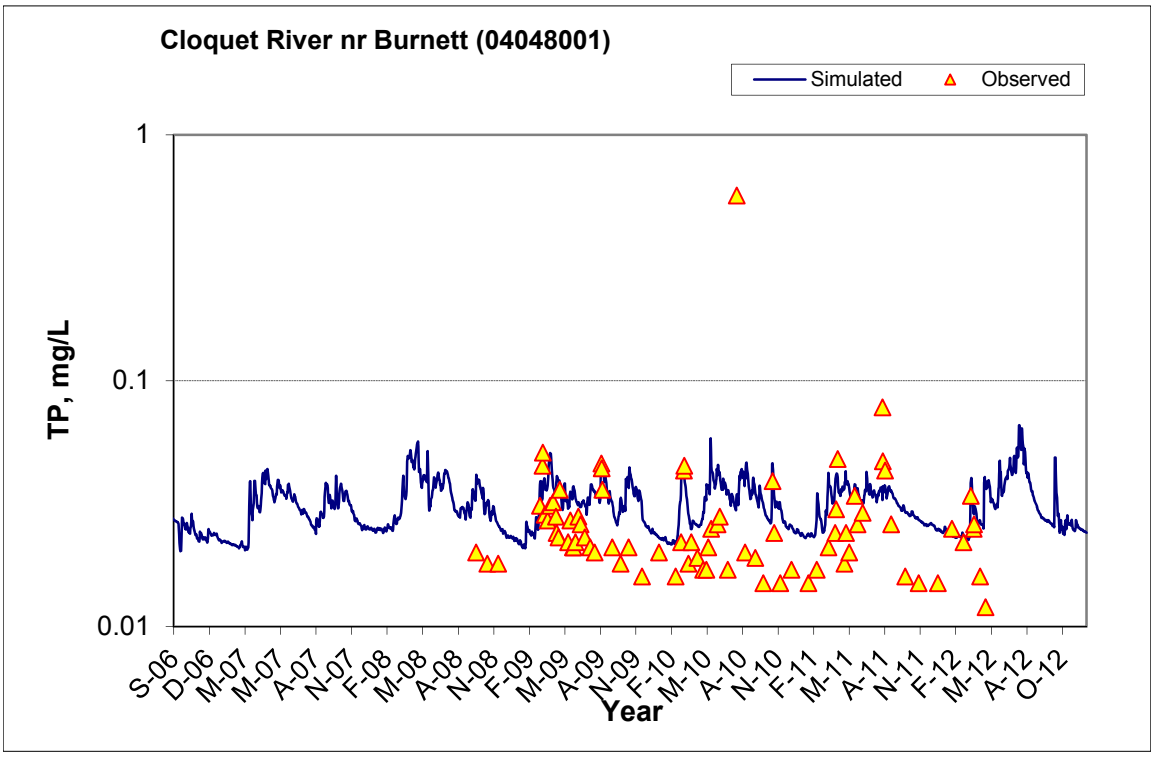

Figure A-232. Time series of observed and simulated Total Phosphorus (TP) concentration at Cloquet River nr Burnett (04048001)

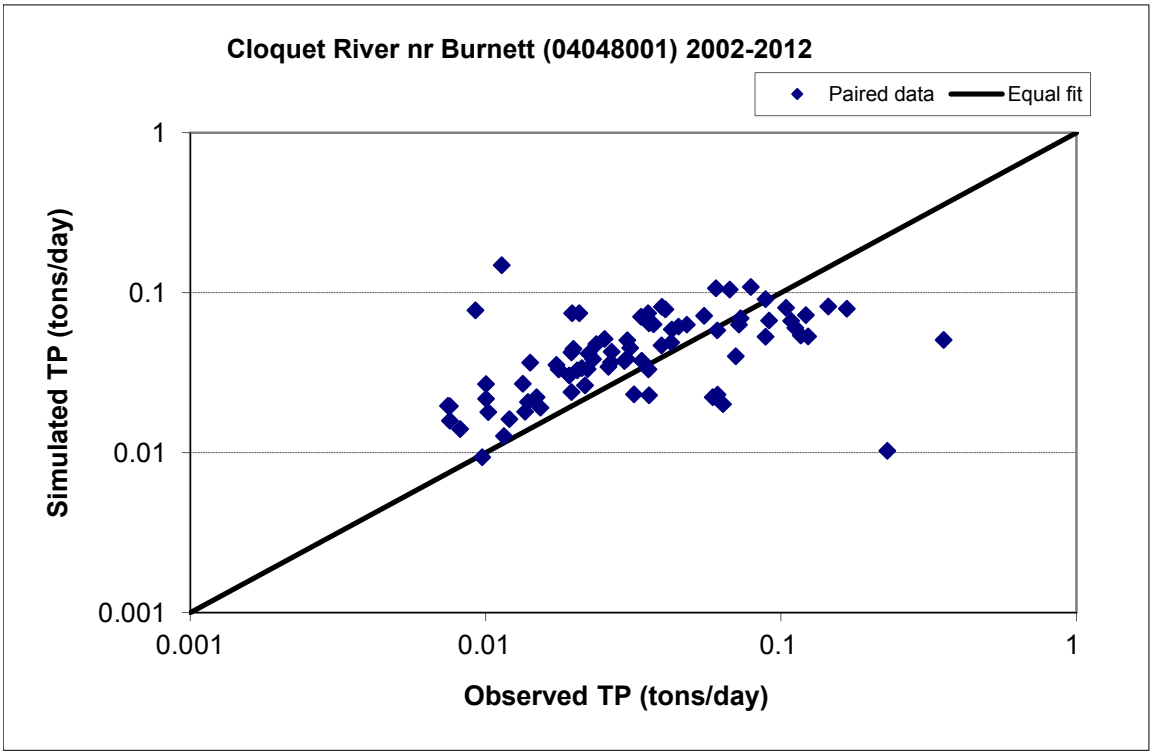

Figure A-233. Paired simulated vs. observed Total Phosphorus (TP) load at Cloquet River nr Burnett (04048001) (calibration period)

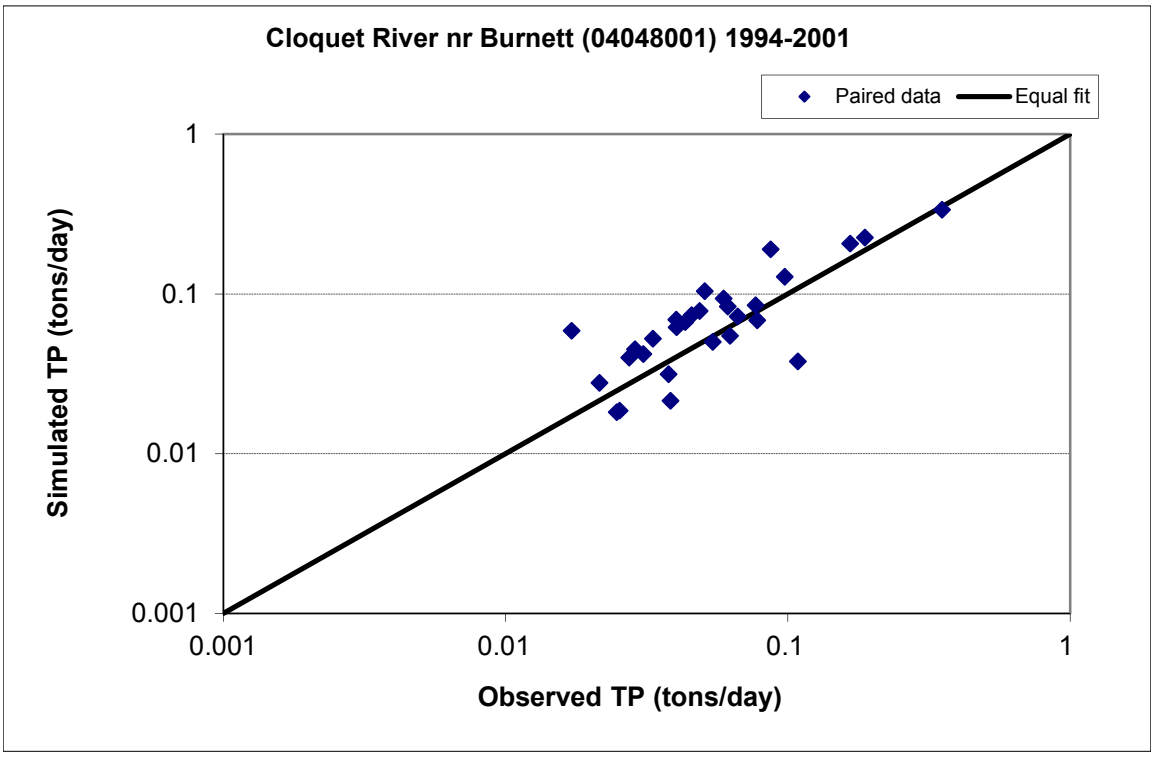

Figure A-234. Paired simulated vs. observed Total Phosphorus (TP) load at Cloquet River nr Burnett (04048001) (validation period)

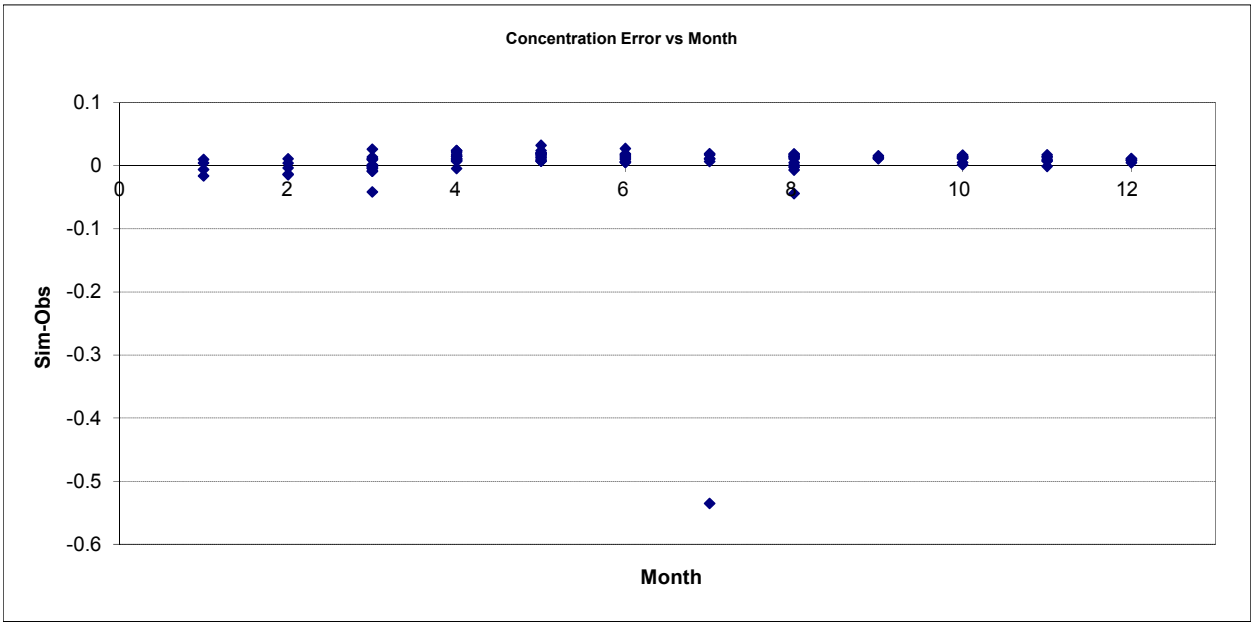

Figure A-235. Residual (Simulated - Observed) vs. Month Total Phosphorus (TP) at Cloquet River nr Burnett (04048001)

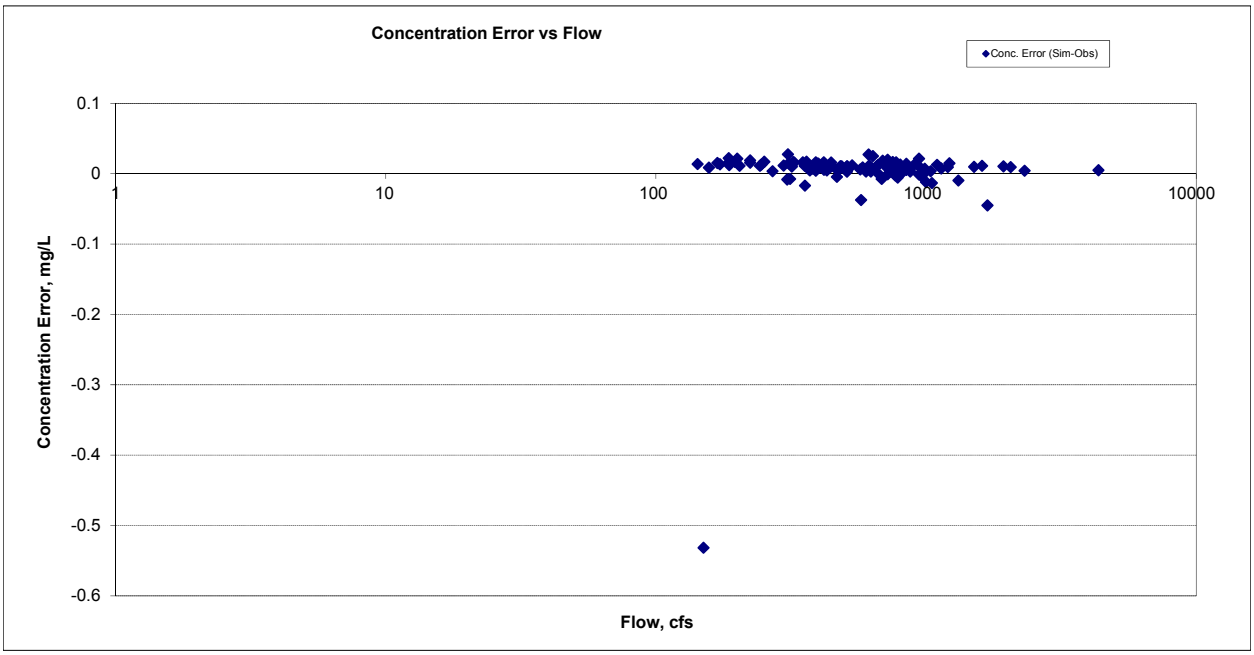

Figure A-236. Residual (Simulated - Observed) vs. Flow Total Phosphorus (TP) at Cloquet River nr Burnett (04048001)

Appendix B. Water Quality Calibration Details for the Nemadji River Watershed

B.1 DEER CREEK NR PLEASANT VALLEY, MN23 (05008001)

B.1.1 Ammonia Nitrogen (NH3)

Table B-1. Ammonia Nitrogen (NH3) statistics

Period	1994-2006	2007-2012
Count	6	18
Concentration Average Error	-44.96%	-75.09%
Concentration Median Error	-22.93%	2.22%
Load Average Error	-50.73%	8.98%
Load Median Error	-28.96%	0.82%
Paired t conc	0.11	0.19
Paired t load	0.13	0.62

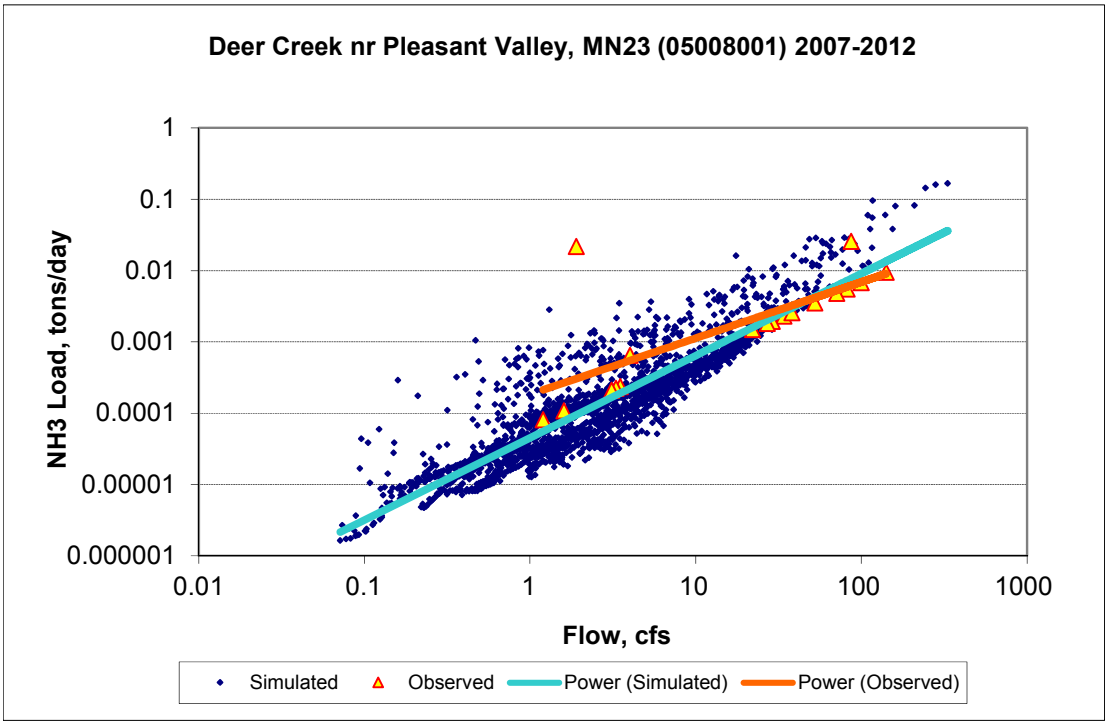

Figure B-1. Power plot of simulated and observed Ammonia Nitrogen (NH3) load vs flow at Deer Creek nr Pleasant Valley, MN23 (05008001) (calibration period)

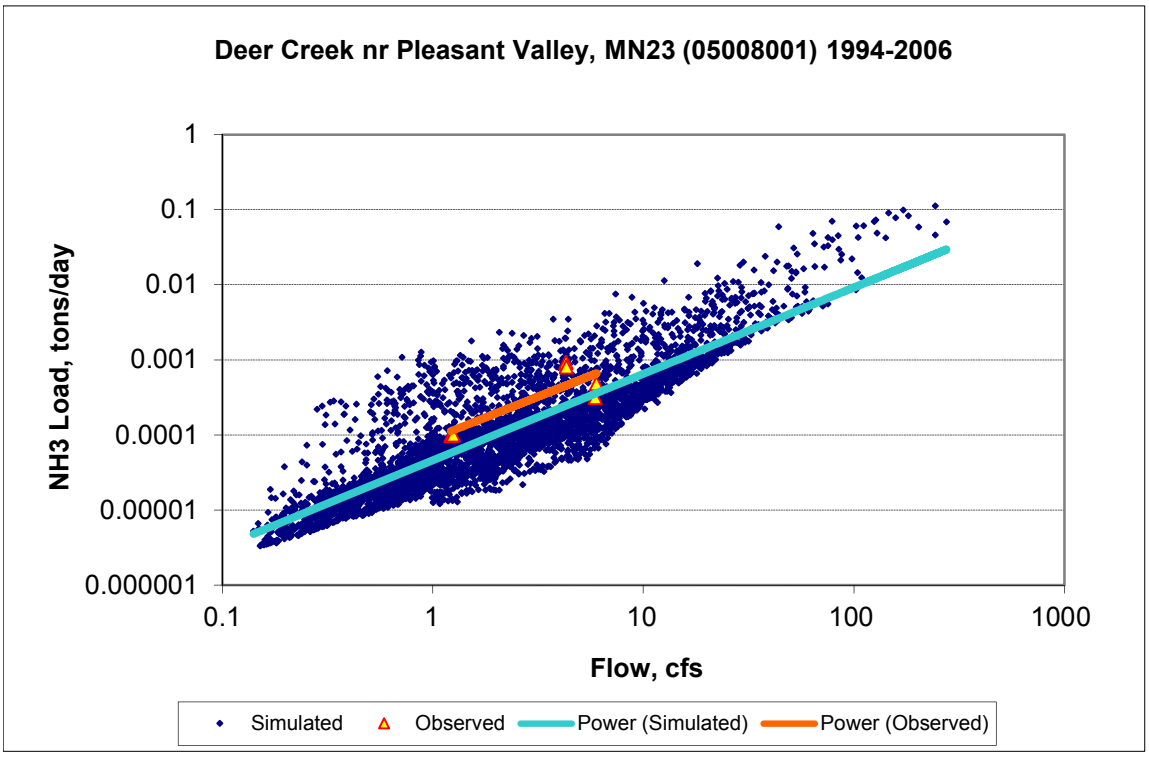

Figure B-2. Power plot of simulated and observed Ammonia Nitrogen (NH3) load vs flow at Deer Creek nr Pleasant Valley, MN23 (05008001) (validation period)

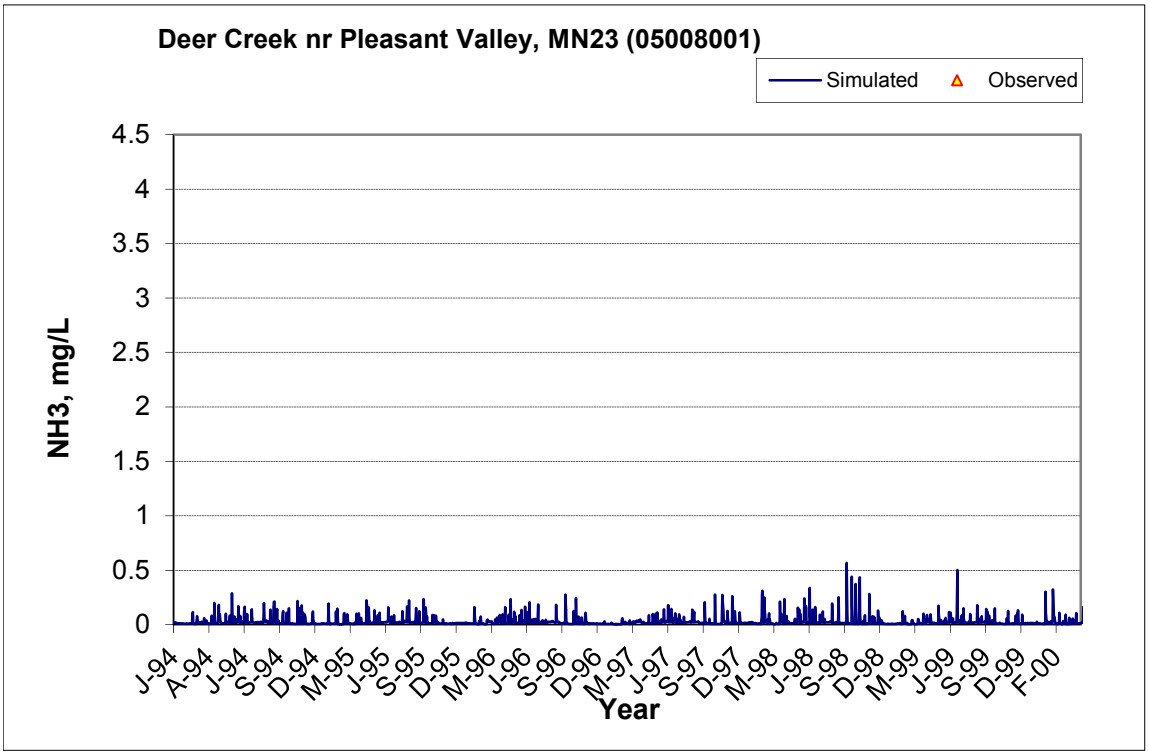

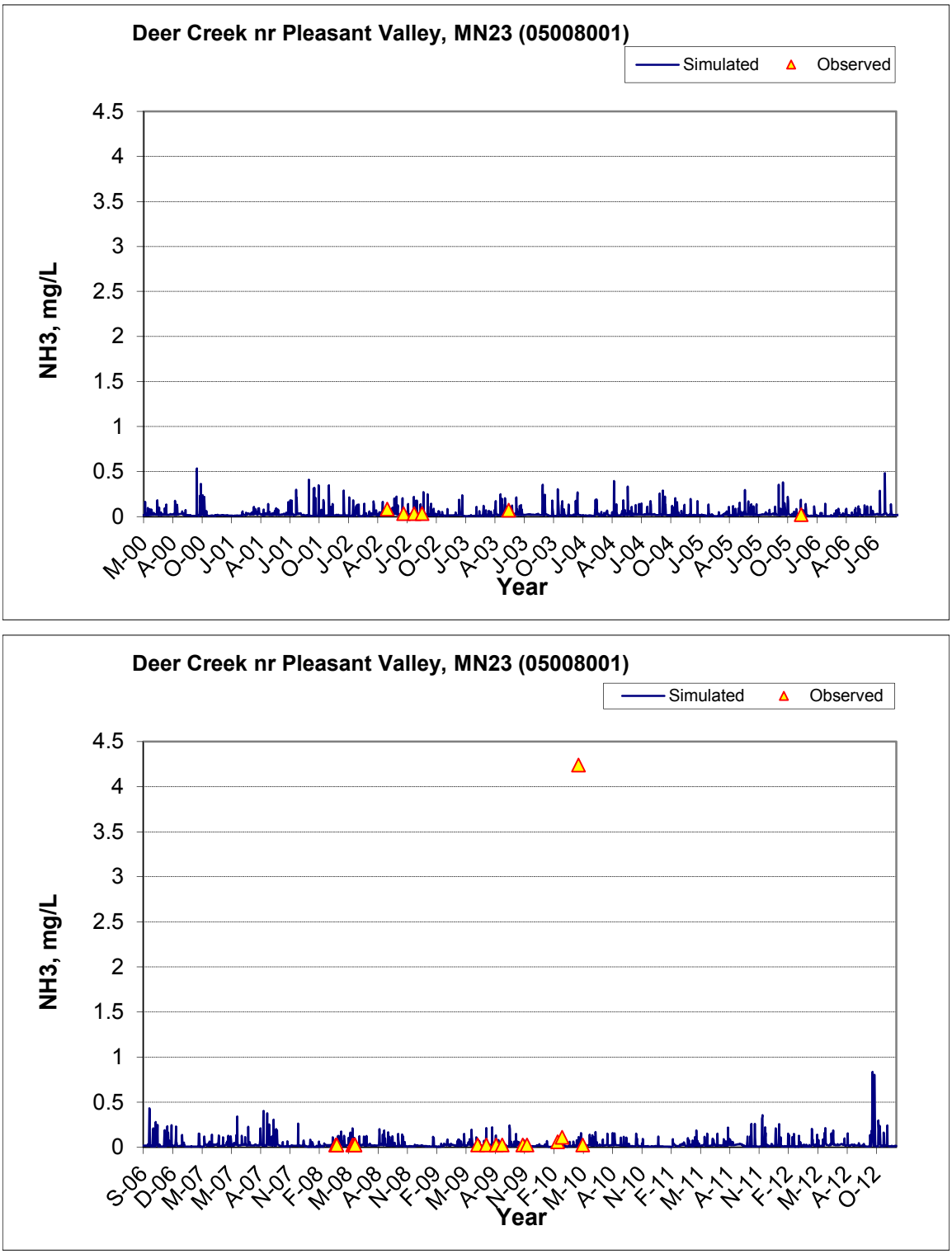

Figure B-3. Time series of observed and simulated Ammonia Nitrogen (NH3) concentration at Deer Creek nr Pleasant Valley, MN23 (05008001)

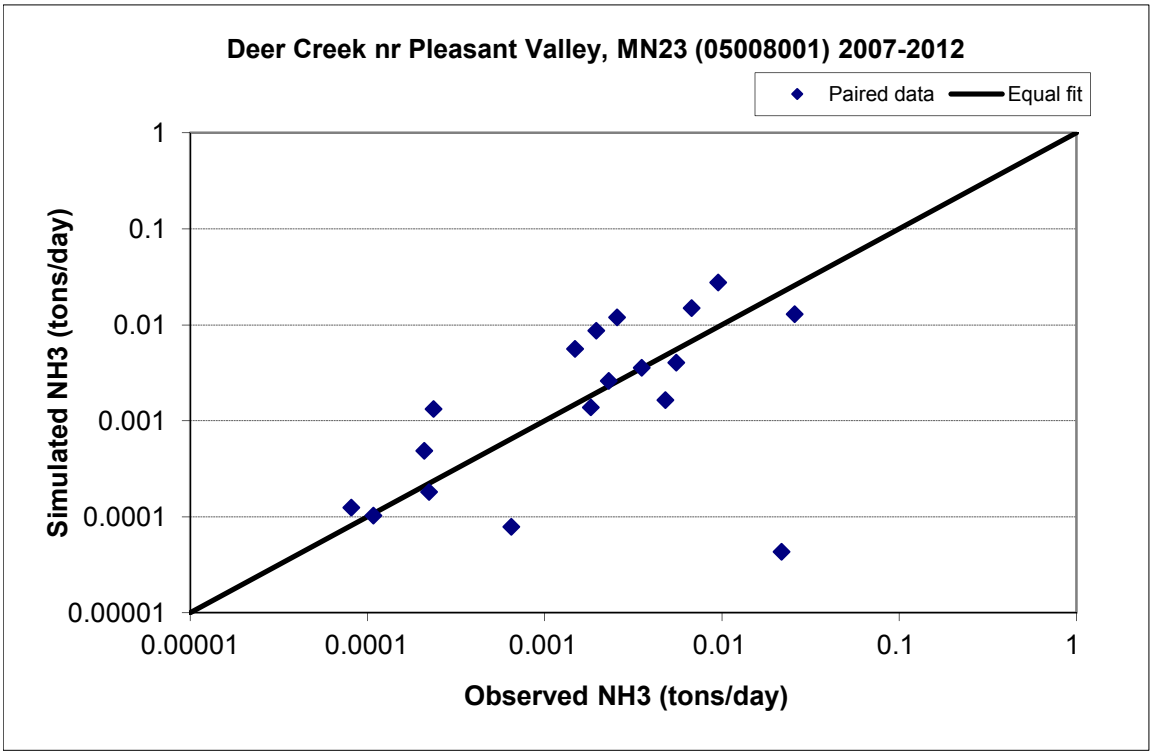

Figure B-4. Paired simulated vs. observed Ammonia Nitrogen (NH3) load at Deer Creek nr Pleasant Valley, MN23 (05008001) (calibration period)

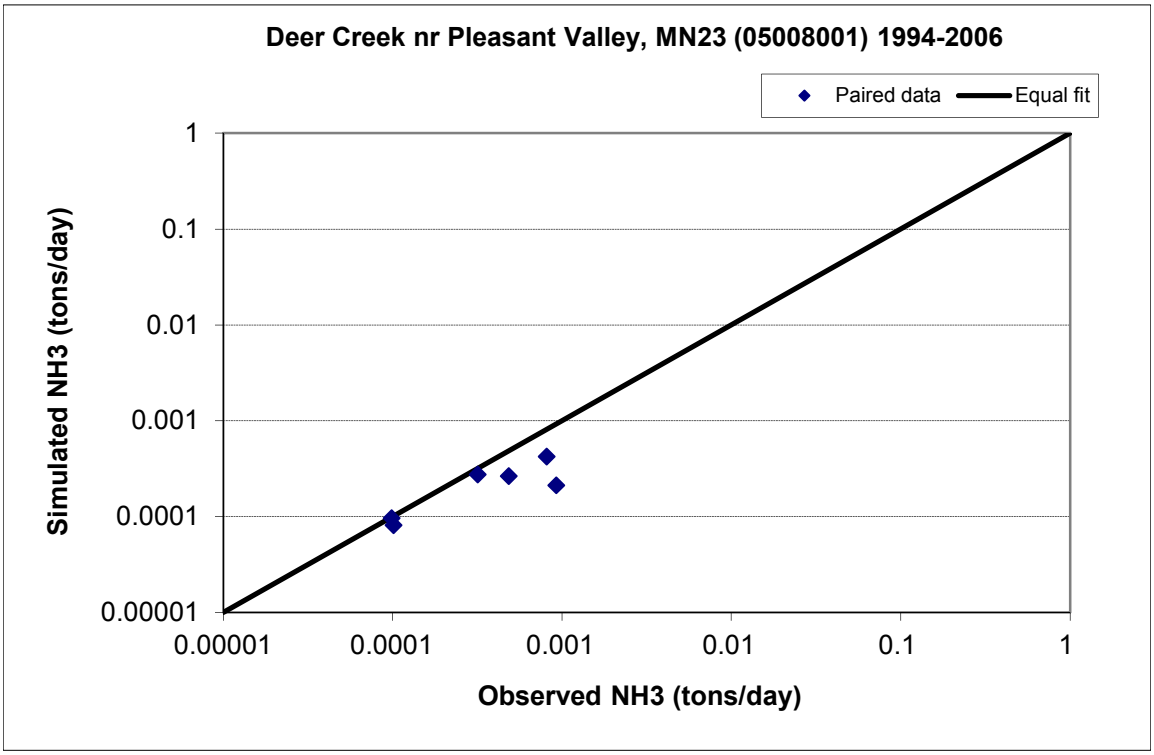

Figure B-5. Paired simulated vs. observed Ammonia Nitrogen (NH3) load at Deer Creek nr Pleasant Valley, MN23 (05008001) (validation period)

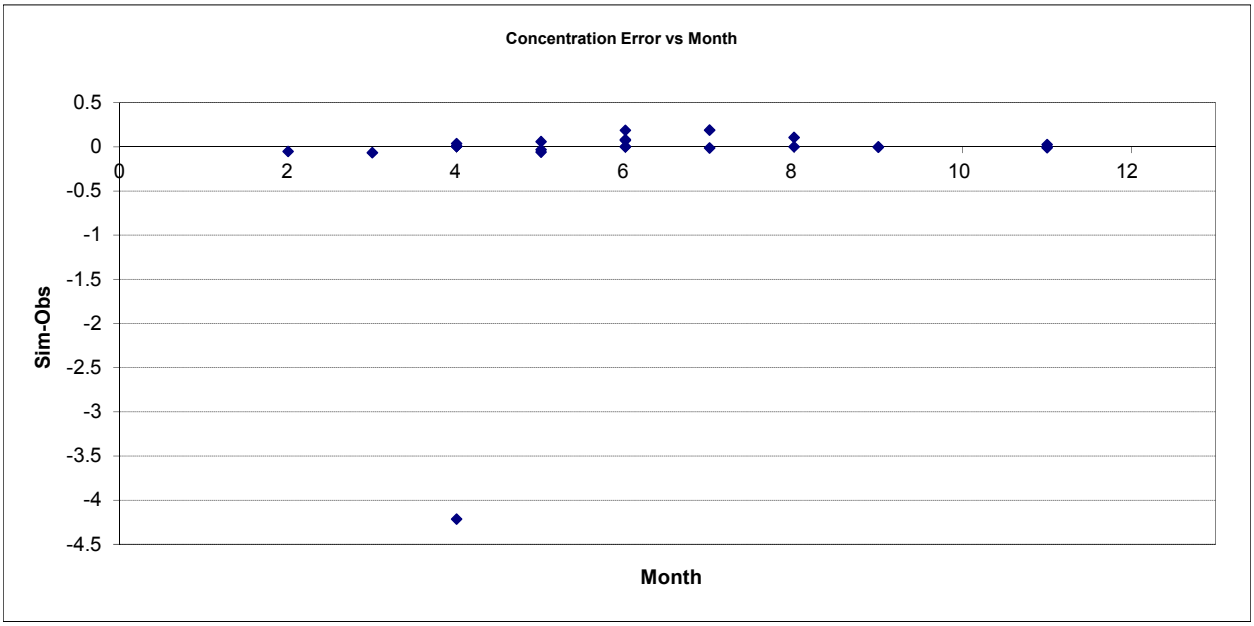

Figure B-6. Residual (Simulated - Observed) vs. Month Ammonia Nitrogen (NH3) at Deer Creek nr Pleasant Valley, MN23 (05008001)

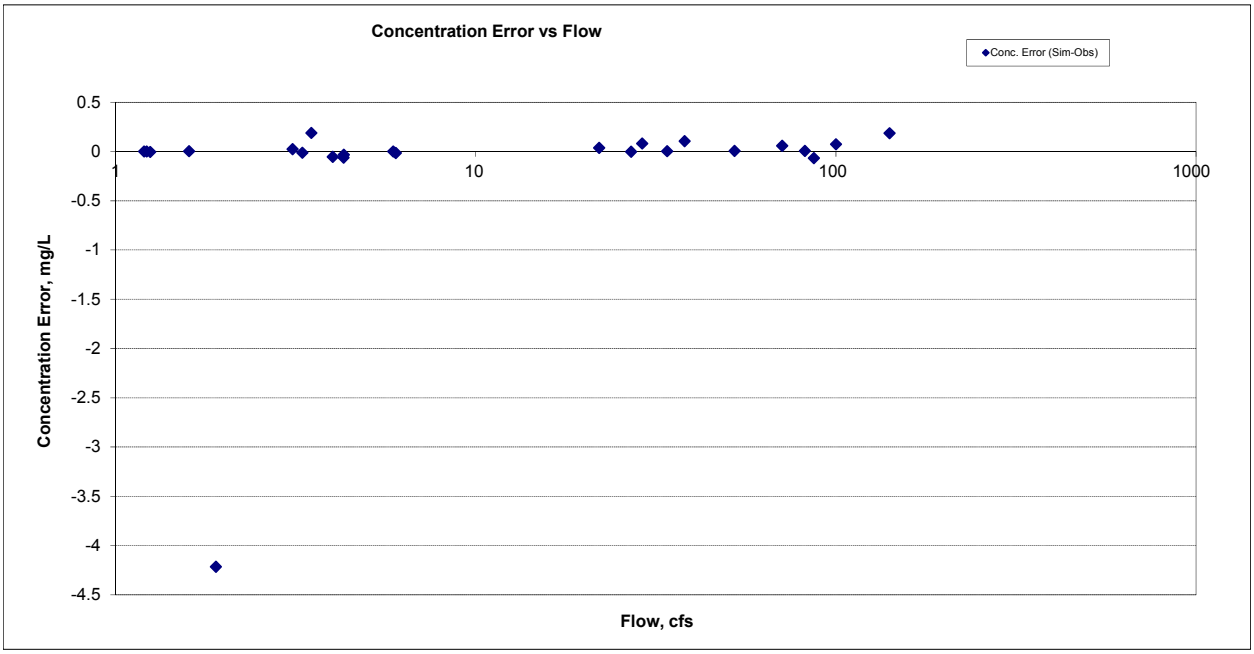

Figure B-7. Residual (Simulated - Observed) vs. Flow Ammonia Nitrogen (NH3) at Deer Creek nr Pleasant Valley, MN23 (05008001)

B.1.2 Organic Nitrogen (OrgN)

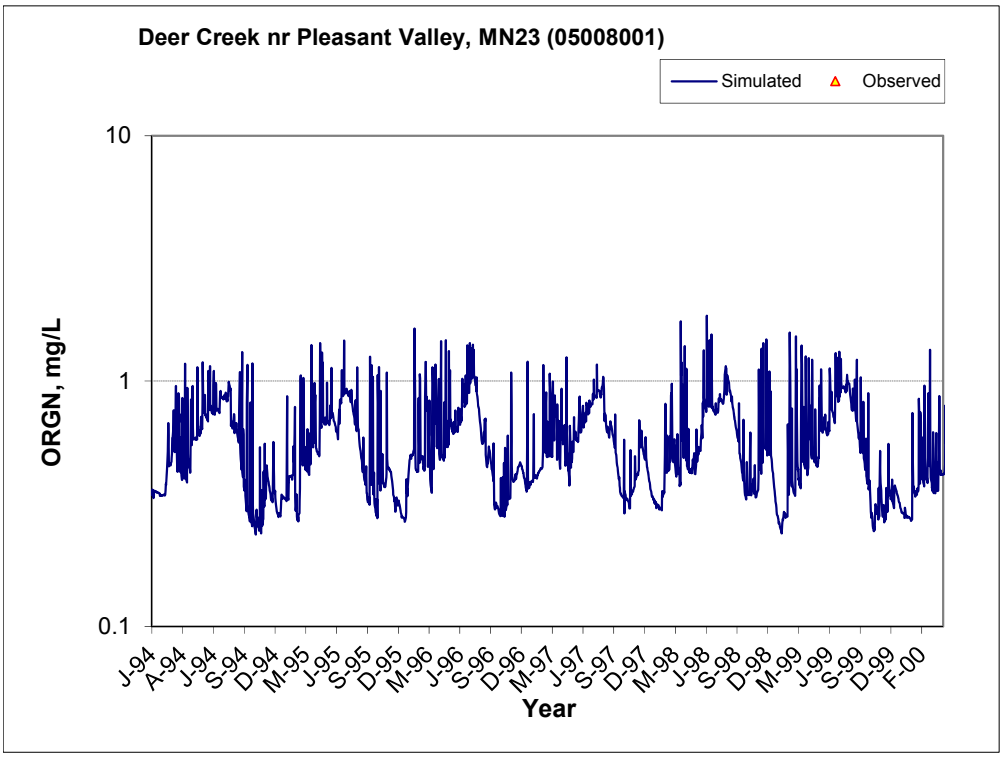

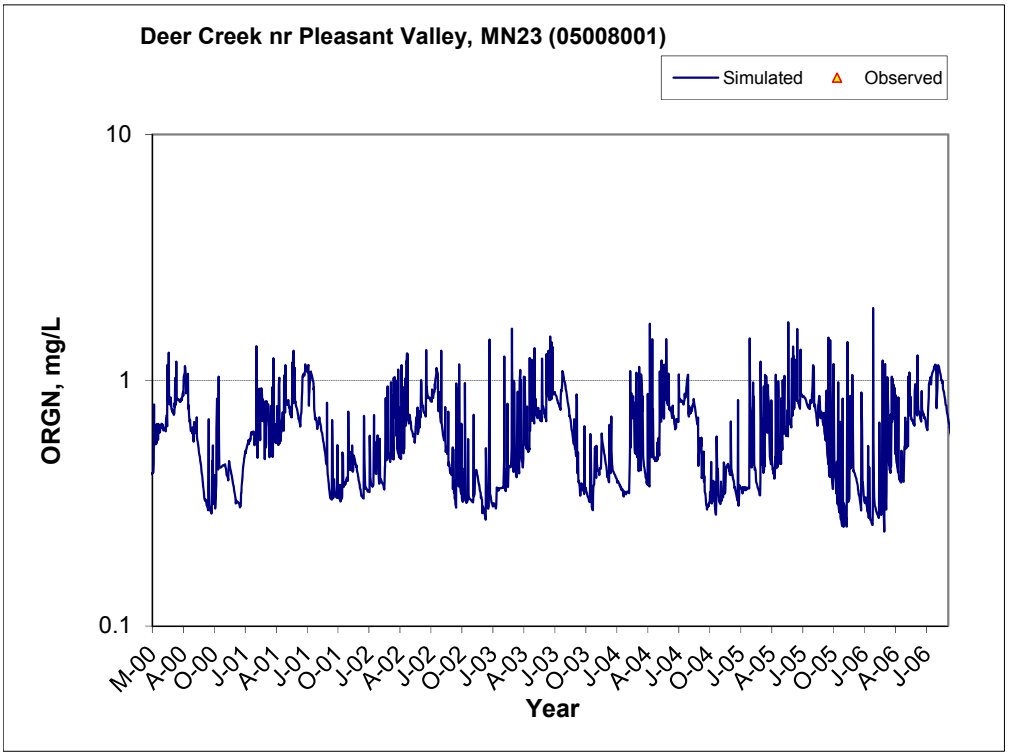

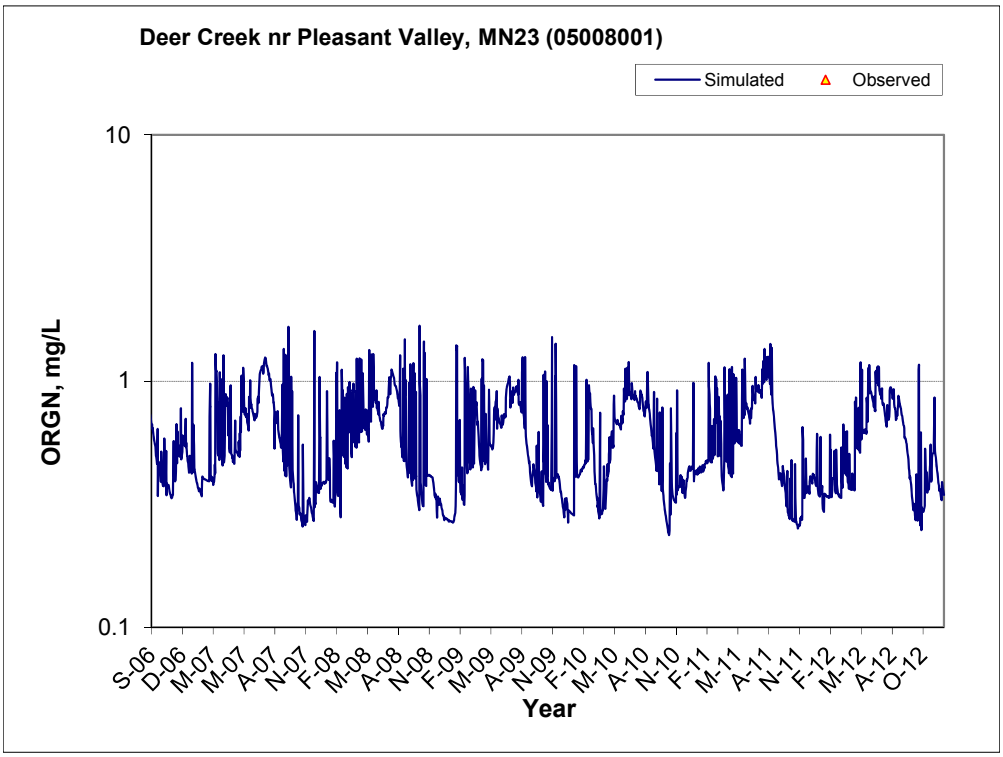

Figure B-8. Time series of observed and simulated Organic Nitrogen (OrgN) concentration at Deer Creek nr Pleasant Valley, MN23 (05008001)

B.1.3 Total Kjeldahl Nitrogen (TKN)

Table B-2. Total Kjeldahl Nitrogen (TKN) statistics

Period	1994-2006	2007-2012
Count	13	17
Concentration Average Error	-12.99%	9.43%
Concentration Median Error	-14.45%	11.94%
Load Average Error	-42.74%	-60.34%
Load Median Error	-5.25%	0.00%
Paired t conc	0.75	0.79
Paired t load	0.30	0.18

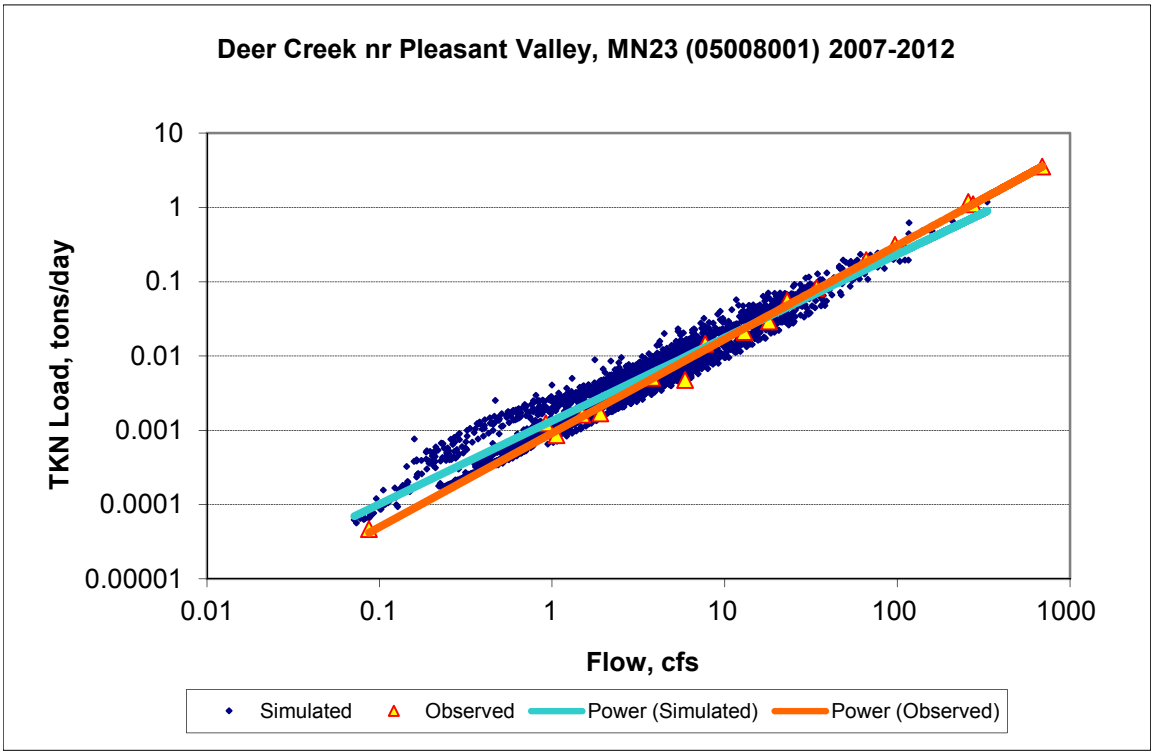

Figure B-9. Power plot of simulated and observed Total Kjeldahl Nitrogen (TKN) load vs flow at Deer Creek nr Pleasant Valley, MN23 (05008001) (calibration period)

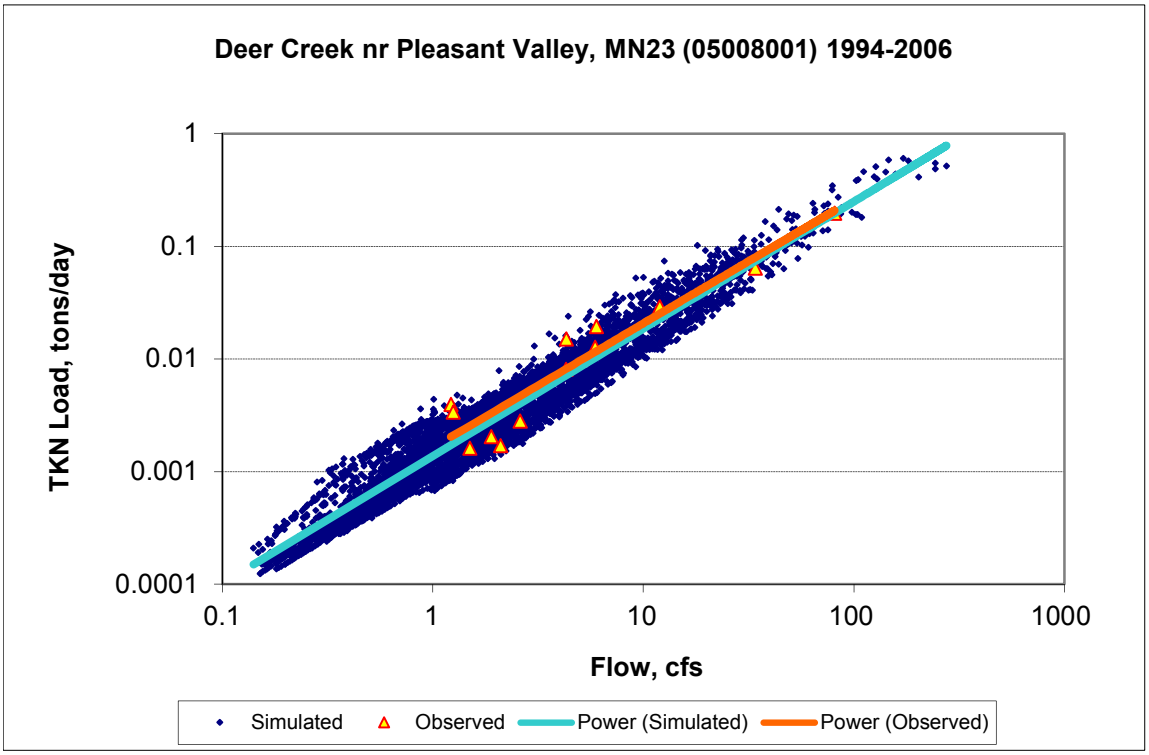

Figure B-10. Power plot of simulated and observed Total Kjeldahl Nitrogen (TKN) load vs flow at Deer Creek nr Pleasant Valley, MN23 (05008001) (validation period)

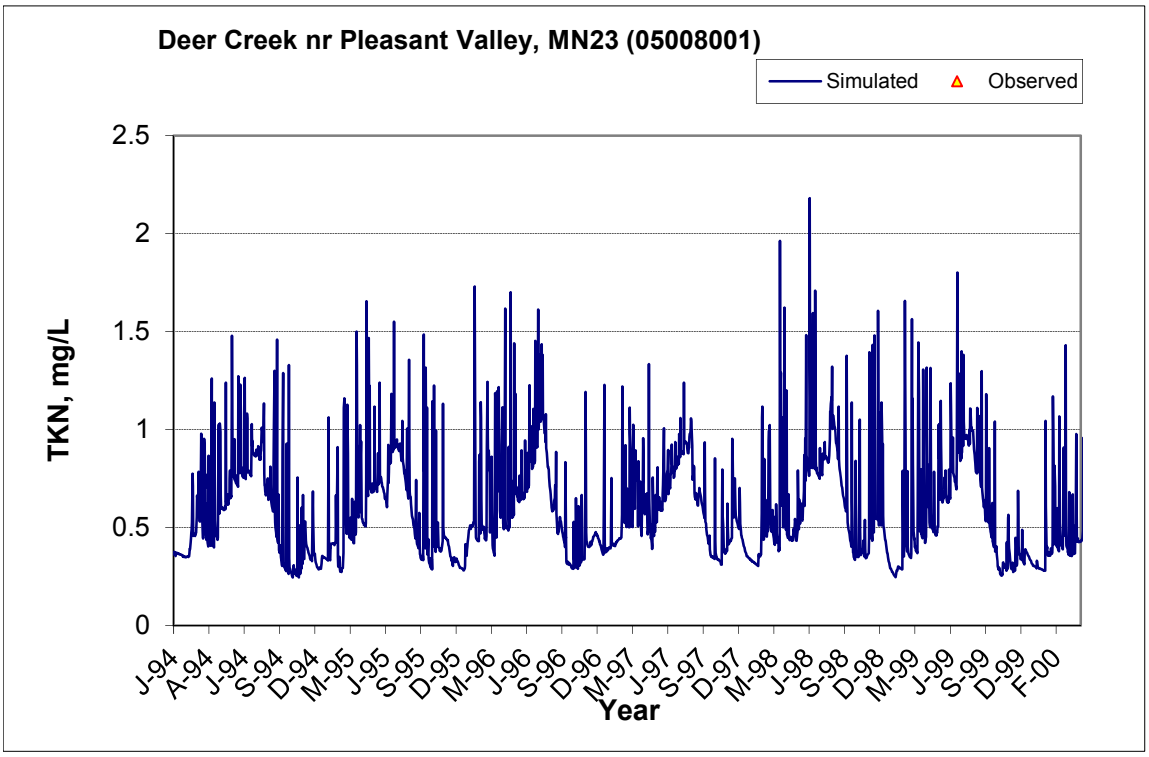
Deer Creek nr Pleasant Valley, MN23 (05008001)
Simulated
Observed
TKN, mg/L
2.5
2
1.5
1
0.5
0
J-94 A-94 J-94 S-94 D-94 M-95 J-95 S-95 D-95 M-96 J-96 S-96 D-96 M-97 J-97 S-97 D-97 M-98 J-98 S-98 D-98 M-99 J-99 S-99 D-99 F-00
Year

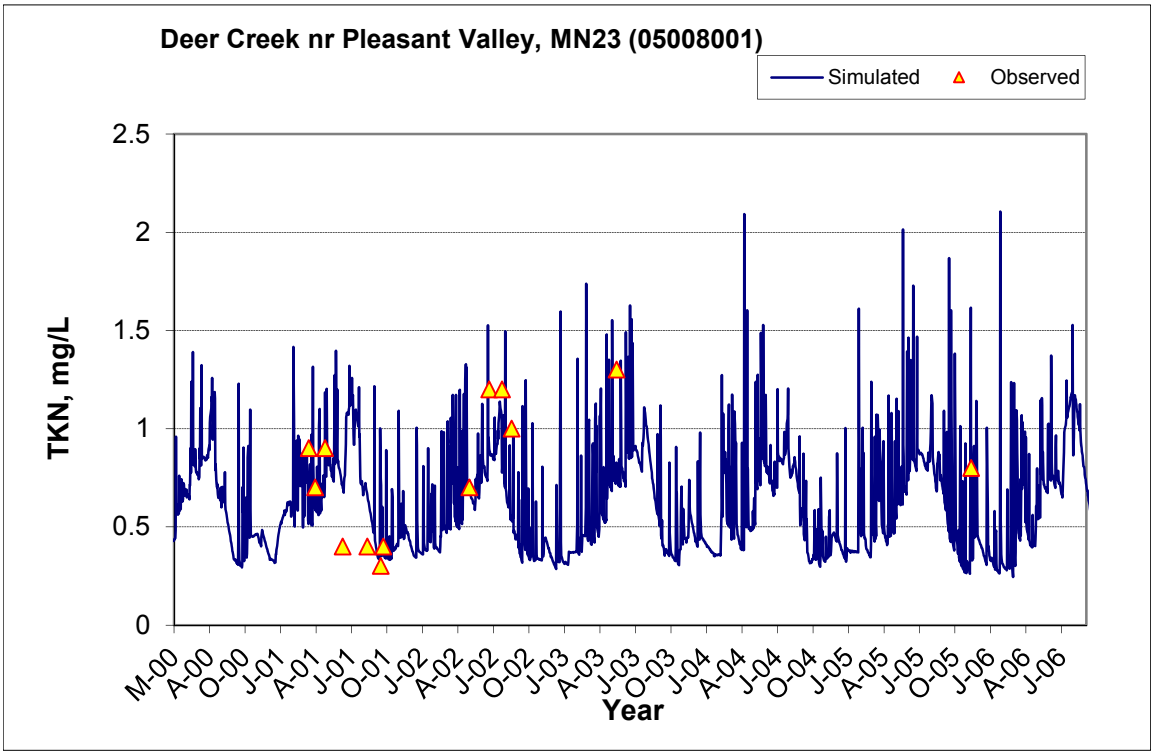
Deer Creek nr Pleasant Valley, MN23 (05008001)
Simulated
Observed
TKN, mg/L
2.5
2
1.5
1
0.5
0
M-00 A-00 O-00 J-01 A-01 J-01 O-01 J-02 A-02 J-02 O-02 J-03 A-03 J-03 O-03 J-04 A-04 J-04 O-04 J-05 A-05 J-05 O-05 J-06 A-06 J-06
Year

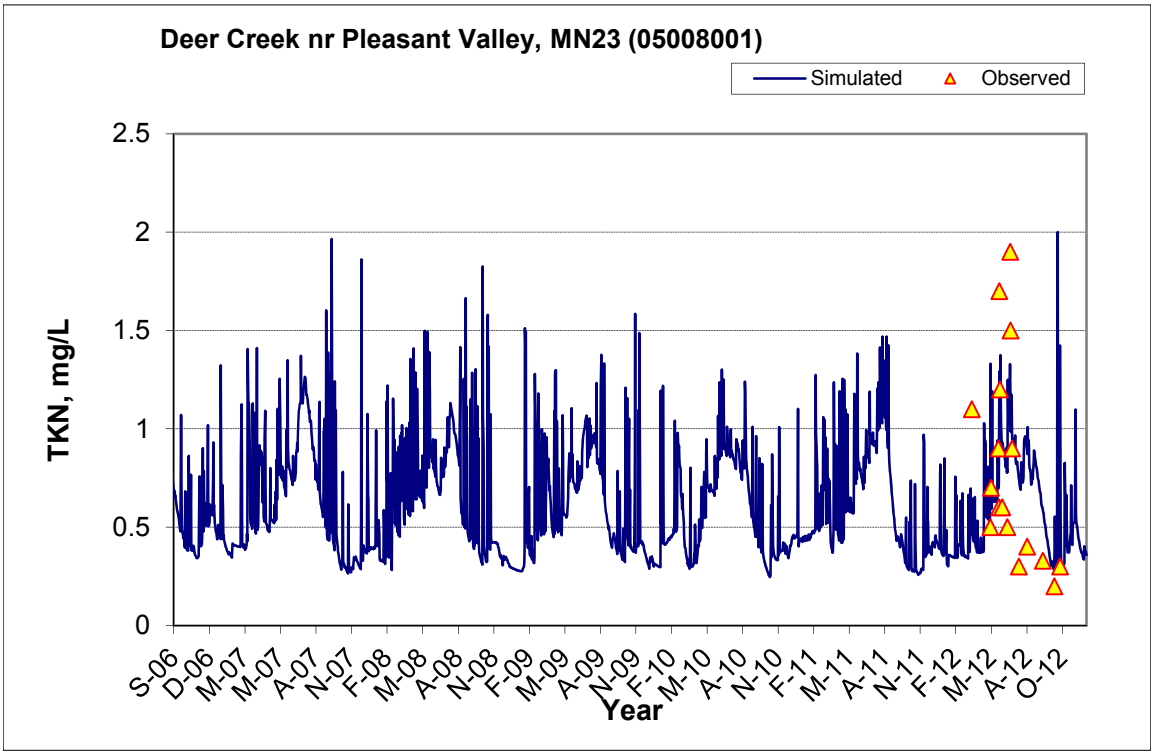

Figure B-11. Time series of observed and simulated Total Kjeldahl Nitrogen (TKN) concentration at Deer Creek nr Pleasant Valley, MN23 (05008001)

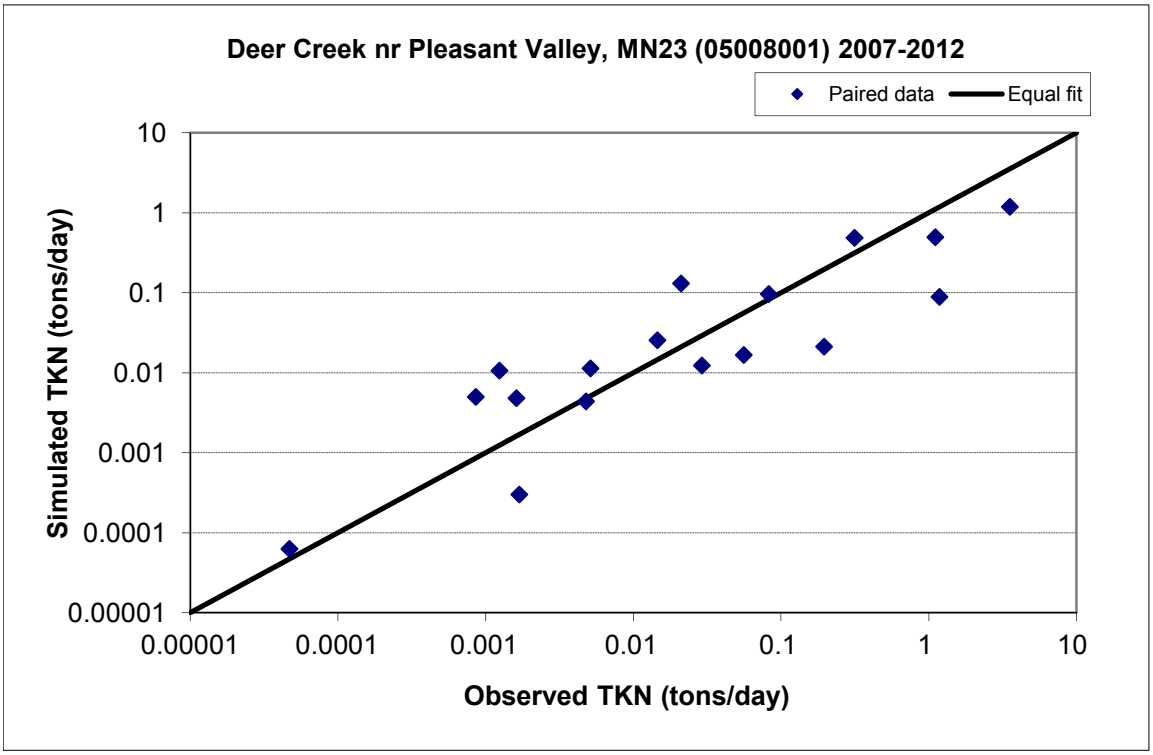

Figure B-12. Paired simulated vs. observed Total Kjeldahl Nitrogen (TKN) load at Deer Creek nr Pleasant Valley, MN23 (05008001) (calibration period)

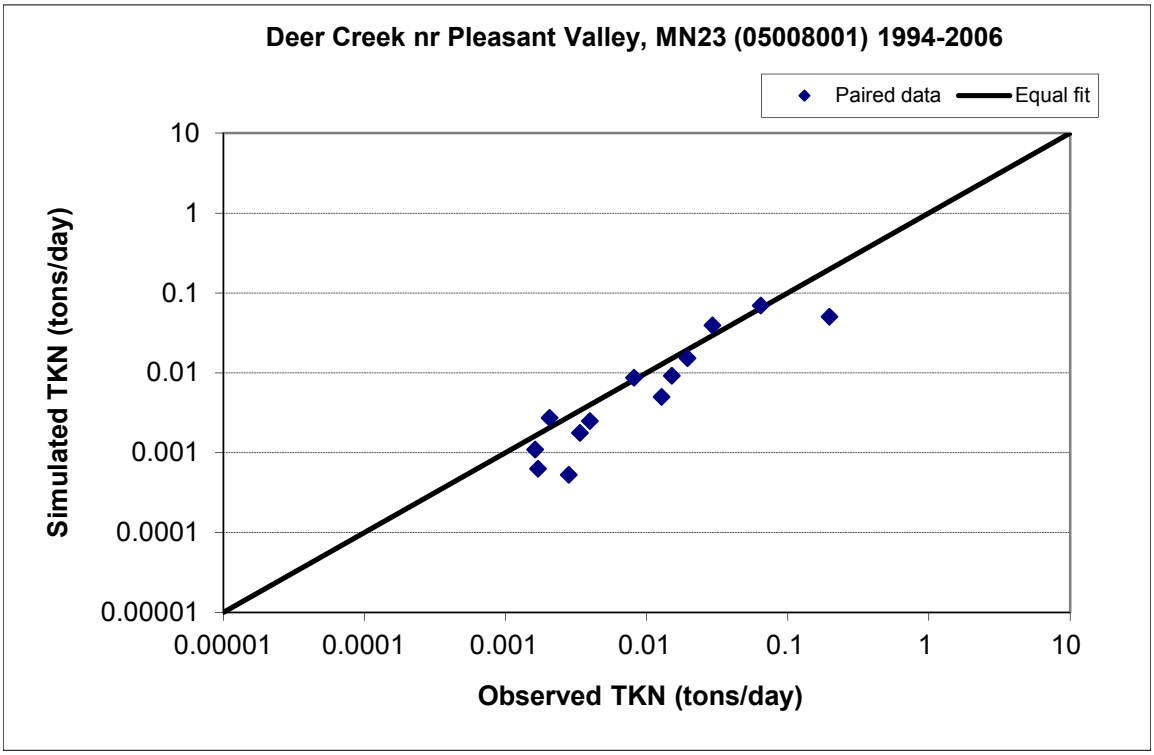

Figure B-13. Paired simulated vs. observed Total Kjeldahl Nitrogen (TKN) load at Deer Creek nr Pleasant Valley, MN23 (05008001) (validation period)

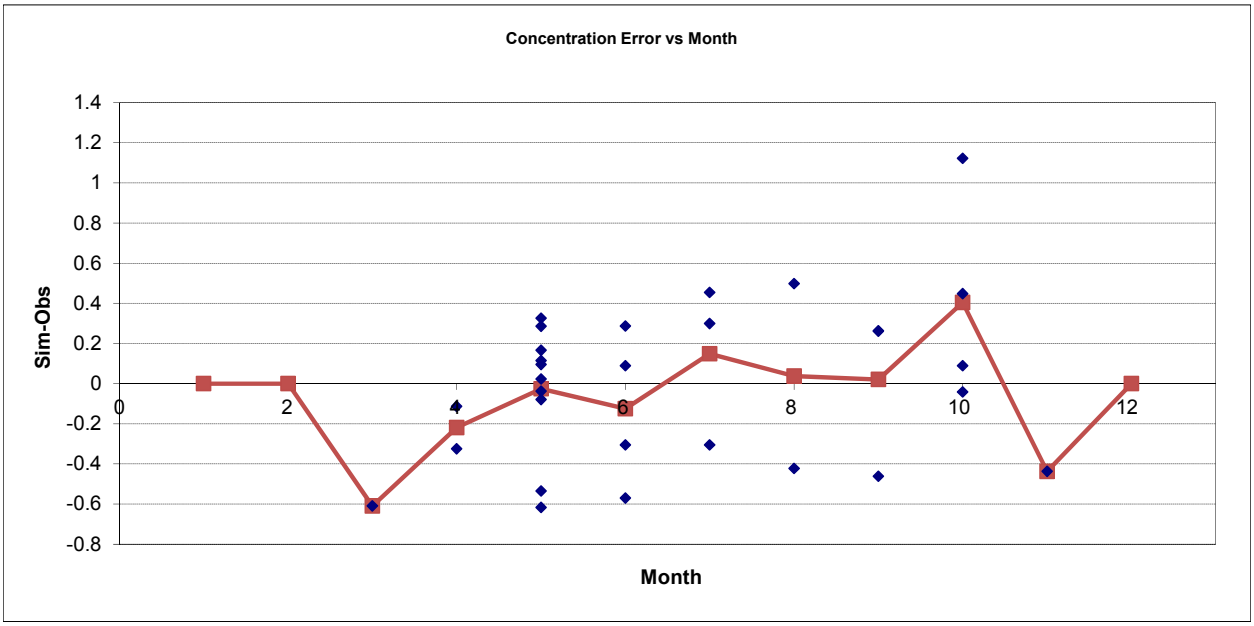

Figure B-14. Residual (Simulated - Observed) vs. Month Total Kjeldahl Nitrogen (TKN) at Deer Creek nr Pleasant Valley, MN23 (05008001)

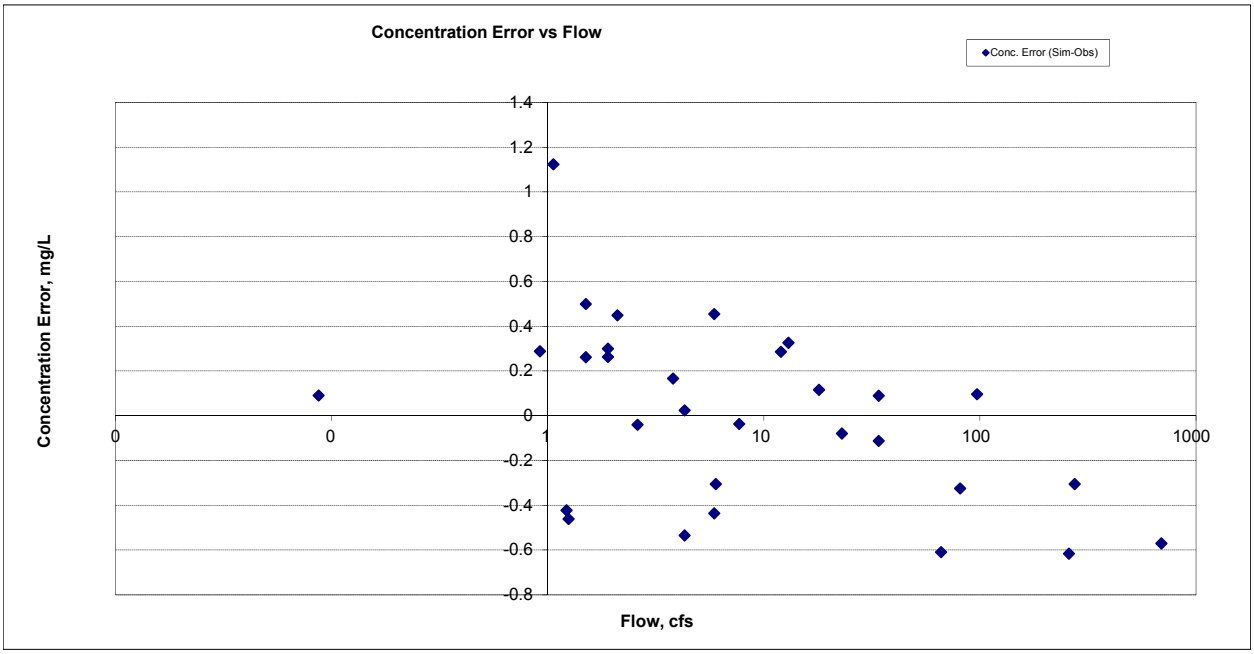

Figure B-15. Residual (Simulated - Observed) vs. Flow Total Kjeldahl Nitrogen (TKN) at Deer Creek nr Pleasant Valley, MN23 (05008001)

B.1.4 Nitrite+ Nitrate Nitrogen (NOx)

Table B-3. Nitrite+ Nitrate Nitrogen (NOx) statistics

Period	1994-2006	2007-2012
Count	5	35
Concentration Average Error	177.51%	-18.95%
Concentration Median Error	62.73%	6.72%
Load Average Error	218.54%	-27.89%
Load Median Error	63.96%	0.04%
Paired t conc	0.05	0.51
Paired t load	0.08	0.38

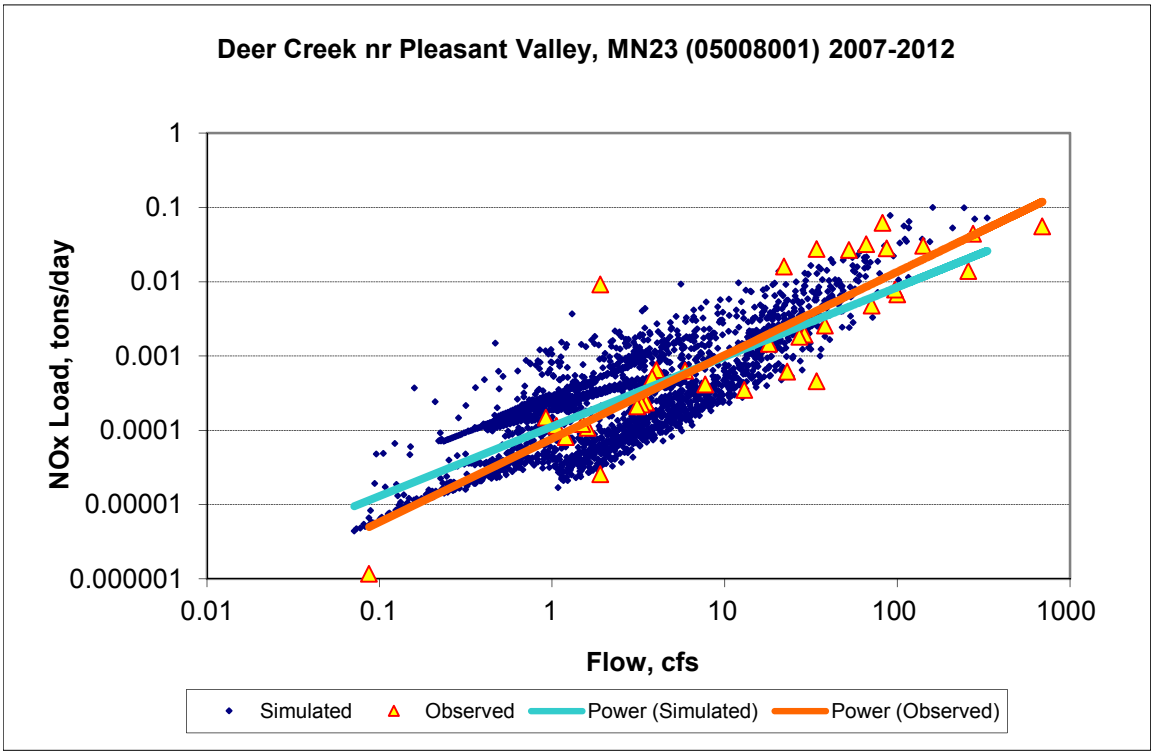

Figure B-16. Power plot of simulated and observed Nitrite+ Nitrate Nitrogen (NOx) load vs flow at Deer Creek nr Pleasant Valley, MN23 (05008001) (calibration period)

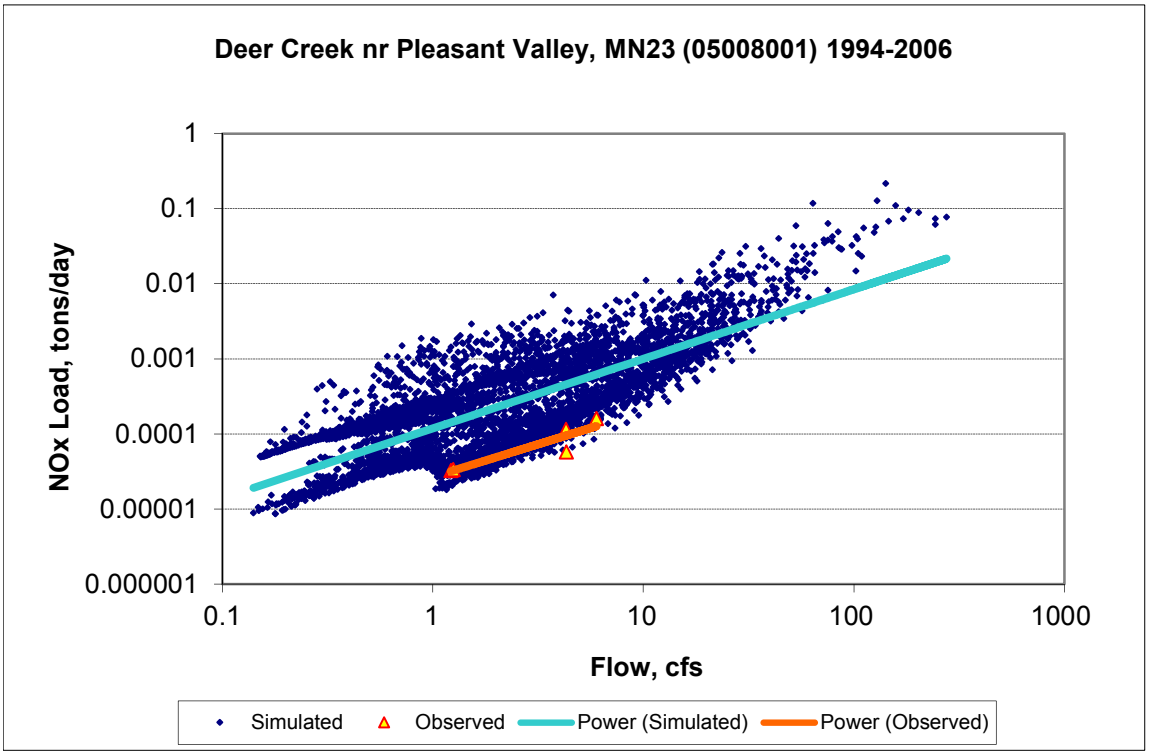

Figure B-17. Power plot of simulated and observed Nitrite+ Nitrate Nitrogen (NOx) load vs flow at Deer Creek nr Pleasant Valley, MN23 (05008001) (validation period)

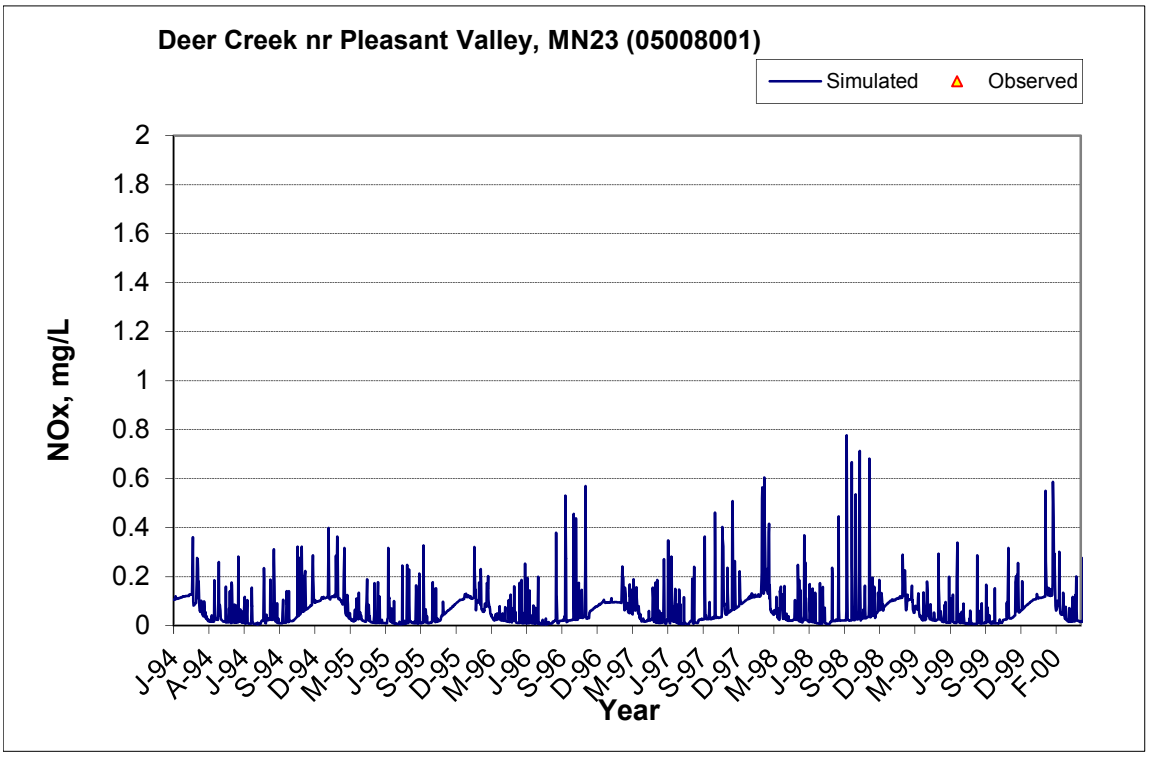
Deer Creek nr Pleasant Valley, MN23 (05008001)
Simulated
Observed
NOx, mg/L
2
1.8
1.6
1.4
1.2
1
0.8
0.6
0.4
0.2
0
J-94 A-94 J-94 S-94 D-94 M-95 J-95 S-95 D-95 M-96 J-96 S-96 D-96 M-97 J-97 S-97 D-97 M-98 J-98 S-98 D-98 M-99 J-99 S-99 D-99 F-00
Year

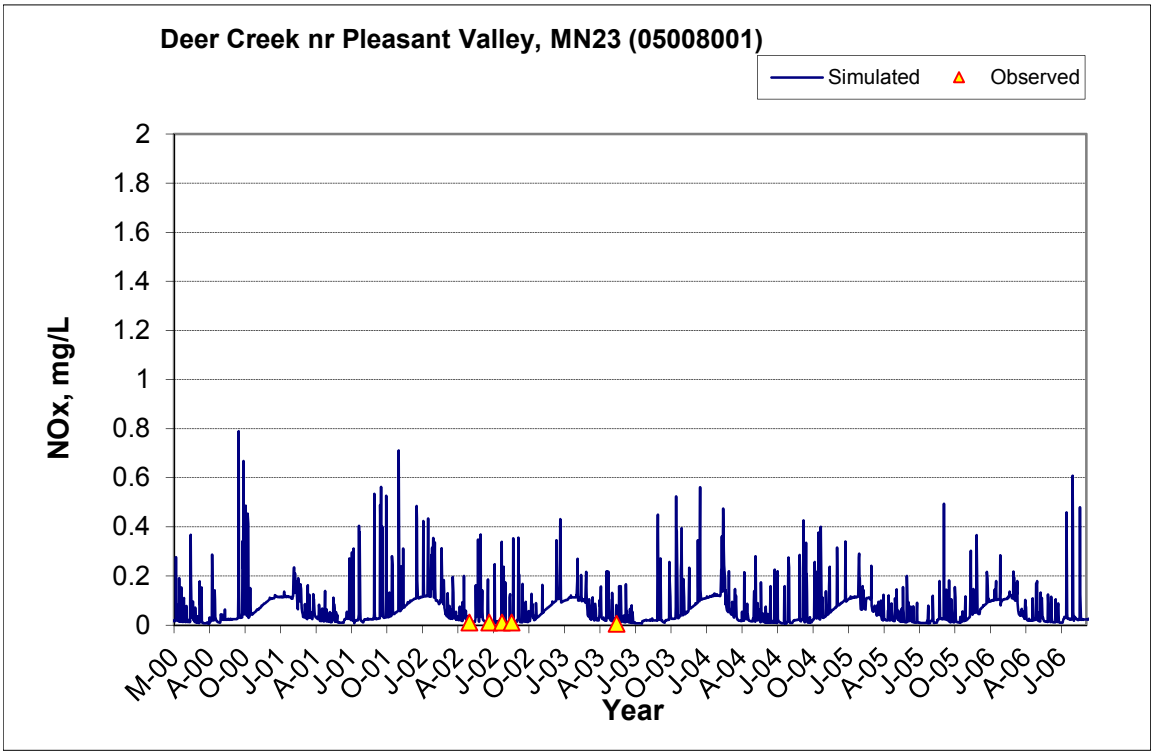
Deer Creek nr Pleasant Valley, MN23 (05008001)
Simulated
Observed
NOx, mg/L
2
1.8
1.6
1.4
1.2
1
0.8
0.6
0.4
0.2
0
M-00 A-00 O-00 J-01 A-01 J-01 O-01 J-02 A-02 J-02 O-02 J-03 A-03 J-03 O-03 J-04 A-04 J-04 O-04 J-05 A-05 J-05 O-05 J-06 A-06 J-06
Year

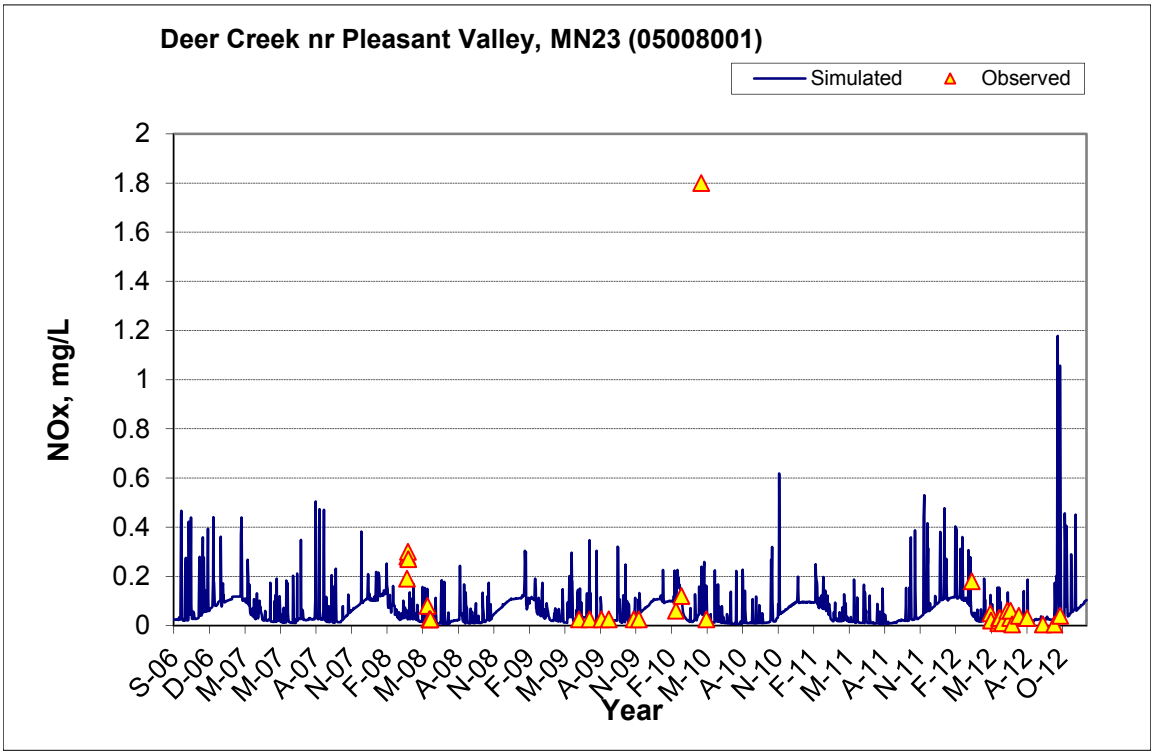

Figure B-18. Time series of observed and simulated Nitrite+ Nitrate Nitrogen (NOx) concentration at Deer Creek nr Pleasant Valley, MN23 (05008001)

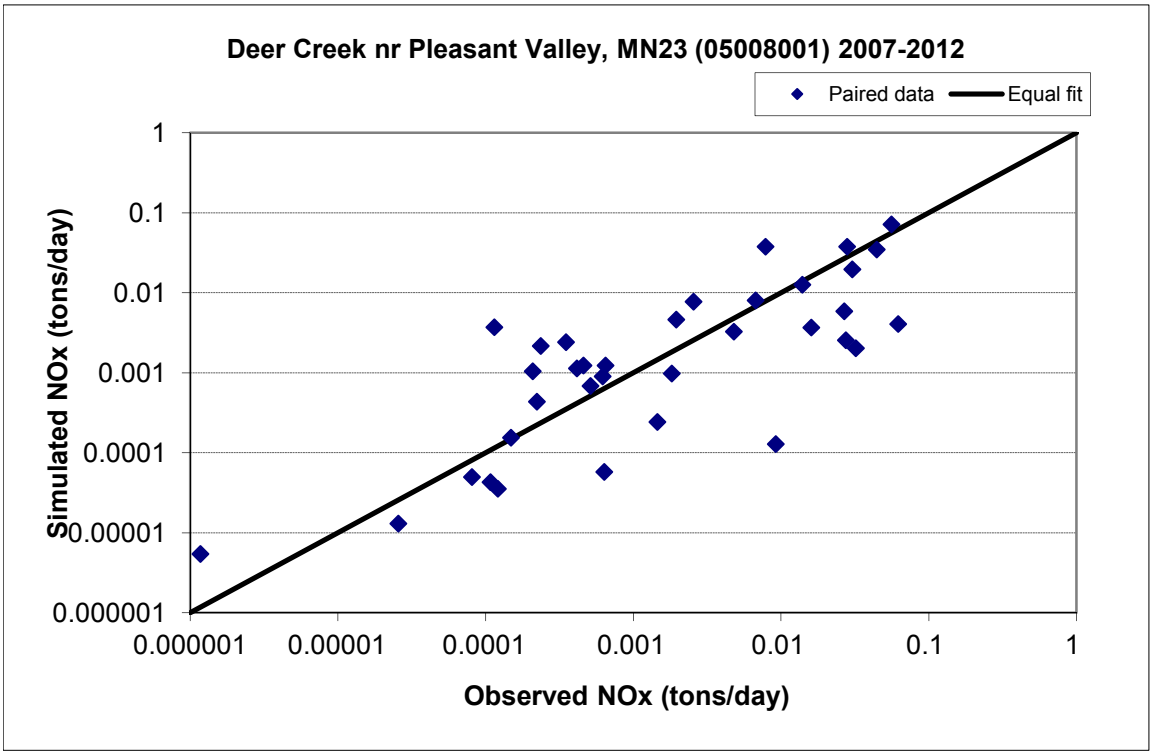

Figure B-19. Paired simulated vs. observed Nitrite+ Nitrate Nitrogen (NOx) load at Deer Creek nr Pleasant Valley, MN23 (05008001) (calibration period)

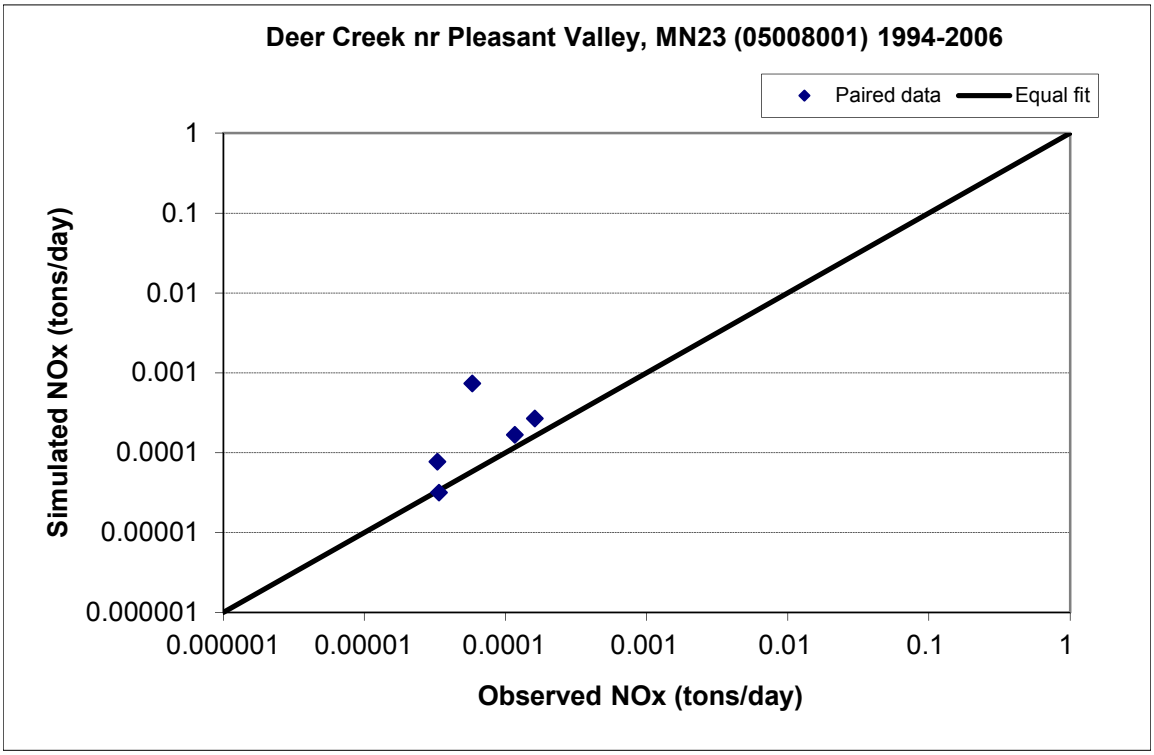

Figure B-20. Paired simulated vs. observed Nitrite+ Nitrate Nitrogen (NOx) load at Deer Creek nr Pleasant Valley, MN23 (05008001) (validation period)

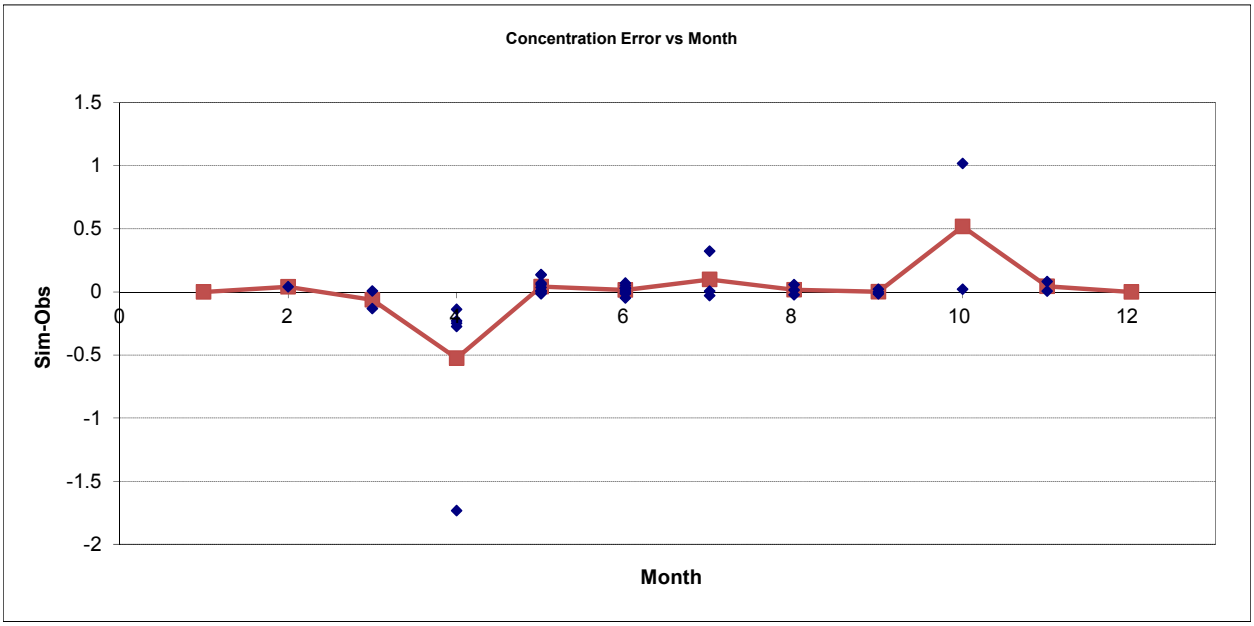

Figure B-21. Residual (Simulated - Observed) vs. Month Nitrite+ Nitrate Nitrogen (NOx) at Deer Creek nr Pleasant Valley, MN23 (05008001)

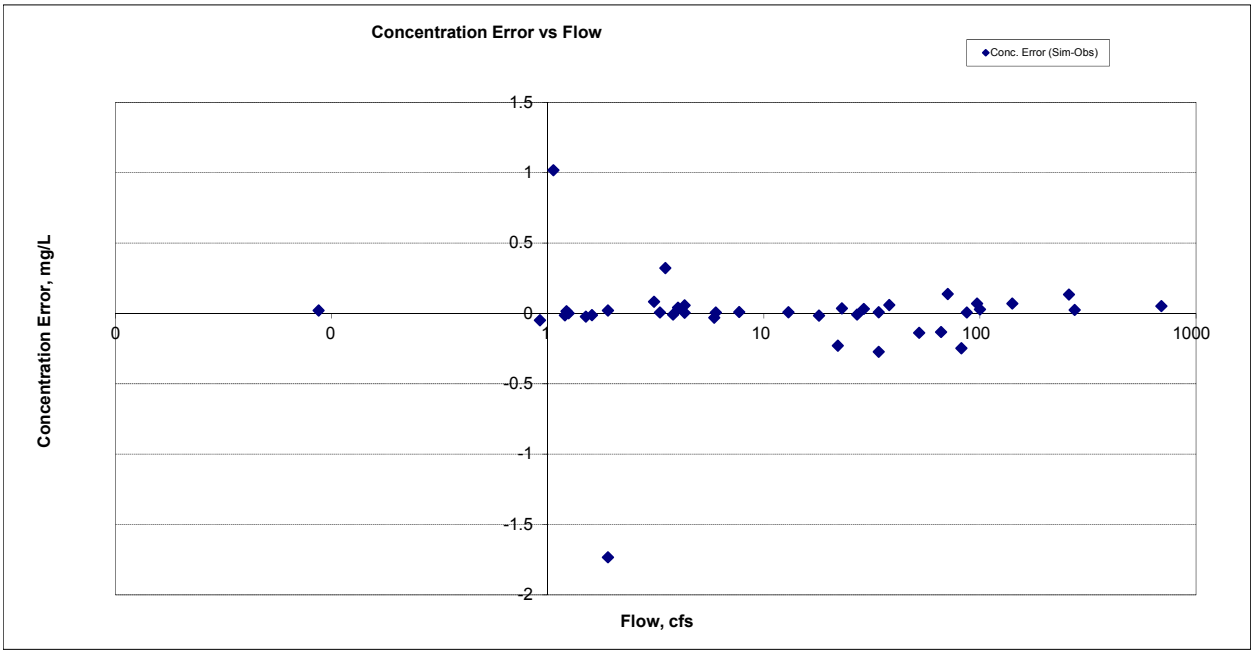

Figure B-22. Residual (Simulated - Observed) vs. Flow Nitrite+ Nitrate Nitrogen (NOx) at Deer Creek nr Pleasant Valley, MN23 (05008001)

B.1.5 Total Nitrogen (TN)

Table B-4. Total Nitrogen (TN) statistics

Period	1994-2006	2007-2012
Count	5	17
Concentration Average Error	-29.85%	16.84%
Concentration Median Error	-37.52%	12.44%
Load Average Error	-23.30%	-58.76%
Load Median Error	-15.87%	0.00%
Paired t conc	0.14	0.58
Paired t load	0.46	0.18

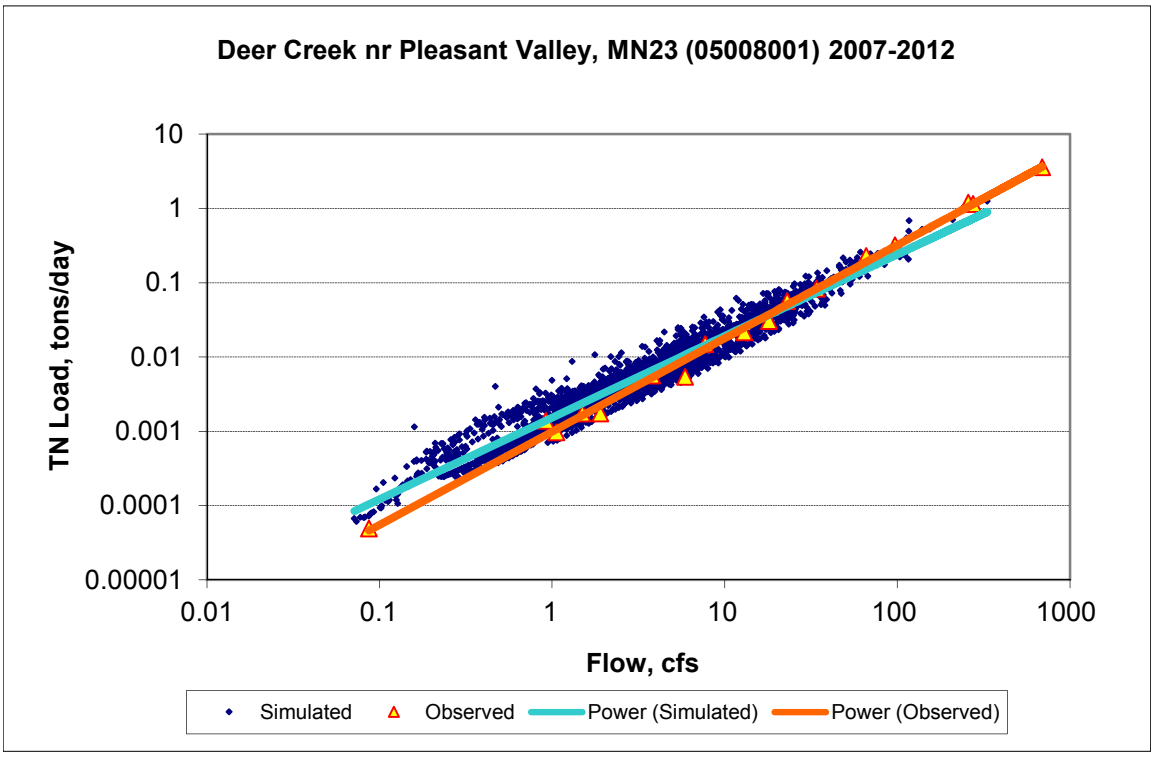

Figure B-23. Power plot of simulated and observed Total Nitrogen (TN) load vs flow at Deer Creek nr Pleasant Valley, MN23 (05008001) (calibration period)

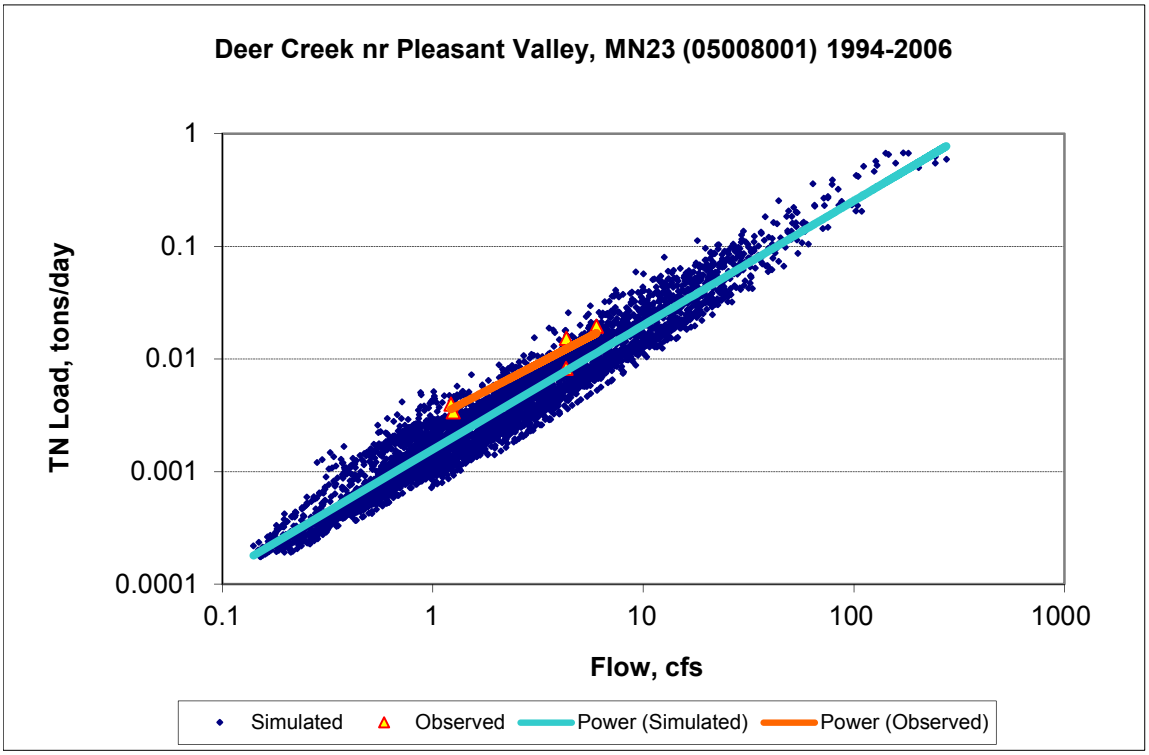

Figure B-24. Power plot of simulated and observed Total Nitrogen (TN) load vs flow at Deer Creek nr Pleasant Valley, MN23 (05008001) (validation period)

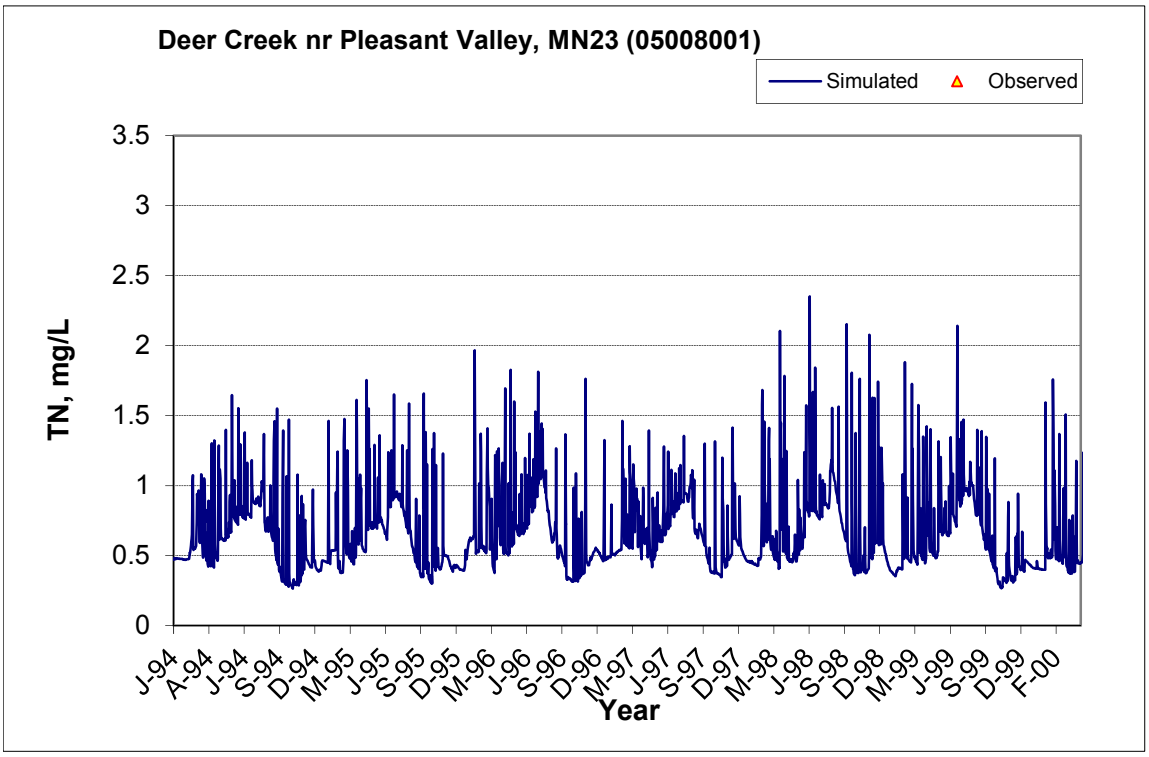
Deer Creek nr Pleasant Valley, MN23 (05008001)
Simulated
Observed
TN, mg/L
3.5
3
2.5
2
1.5
1
0.5
0
J-94 A-94 J-94 S-94 D-94 M-95 J-95 S-95 D-95 M-96 J-96 S-96 D-96 M-97 J-97 S-97 D-97 M-98 J-98 S-98 D-98 M-99 J-99 S-99 D-99 F-00
Year

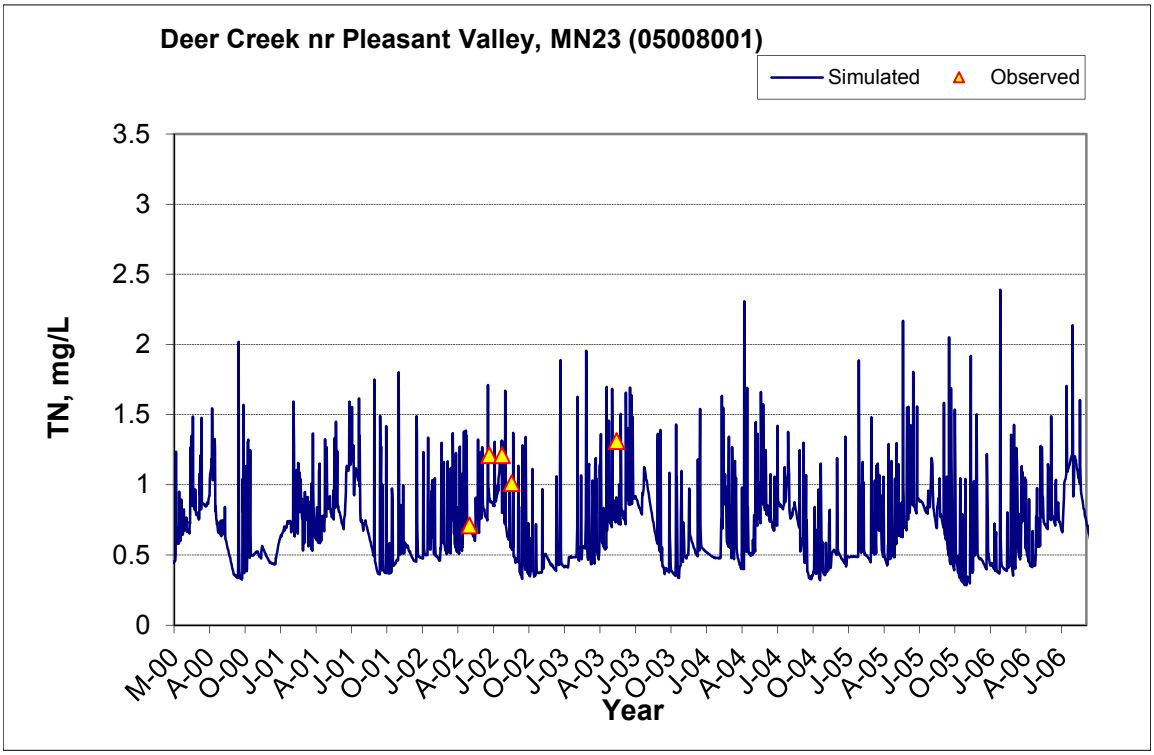
Deer Creek nr Pleasant Valley, MN23 (05008001)
Simulated
Observed
TN, mg/L
3.5
3
2.5
2
1.5
1
0.5
0
M-00 A-00 O-00 J-01 A-01 J-01 O-01 J-02 A-02 J-02 O-02 J-03 A-03 J-03 O-03 J-04 A-04 J-04 O-04 J-05 A-05 J-05 O-05 J-06 A-06 J-06
Year

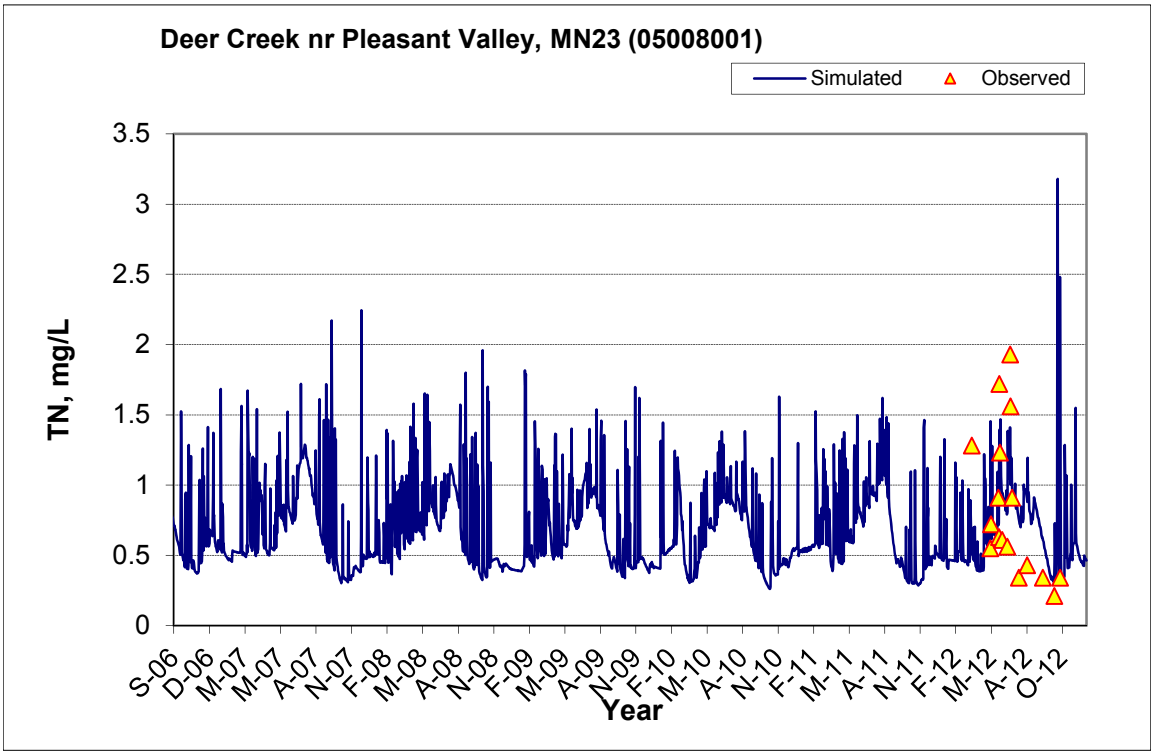

Figure B-25. Time series of observed and simulated Total Nitrogen (TN) concentration at Deer Creek nr Pleasant Valley, MN23 (05008001)

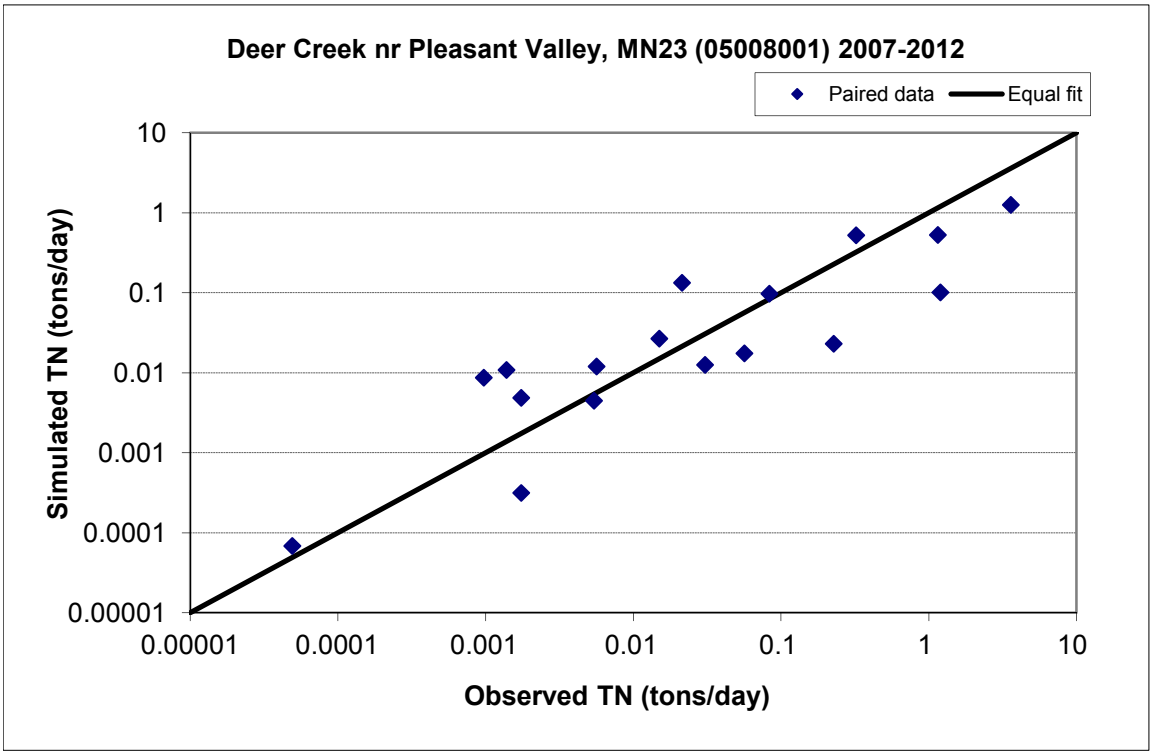

Figure B-26. Paired simulated vs. observed Total Nitrogen (TN) load at Deer Creek nr Pleasant Valley, MN23 (05008001) (calibration period)

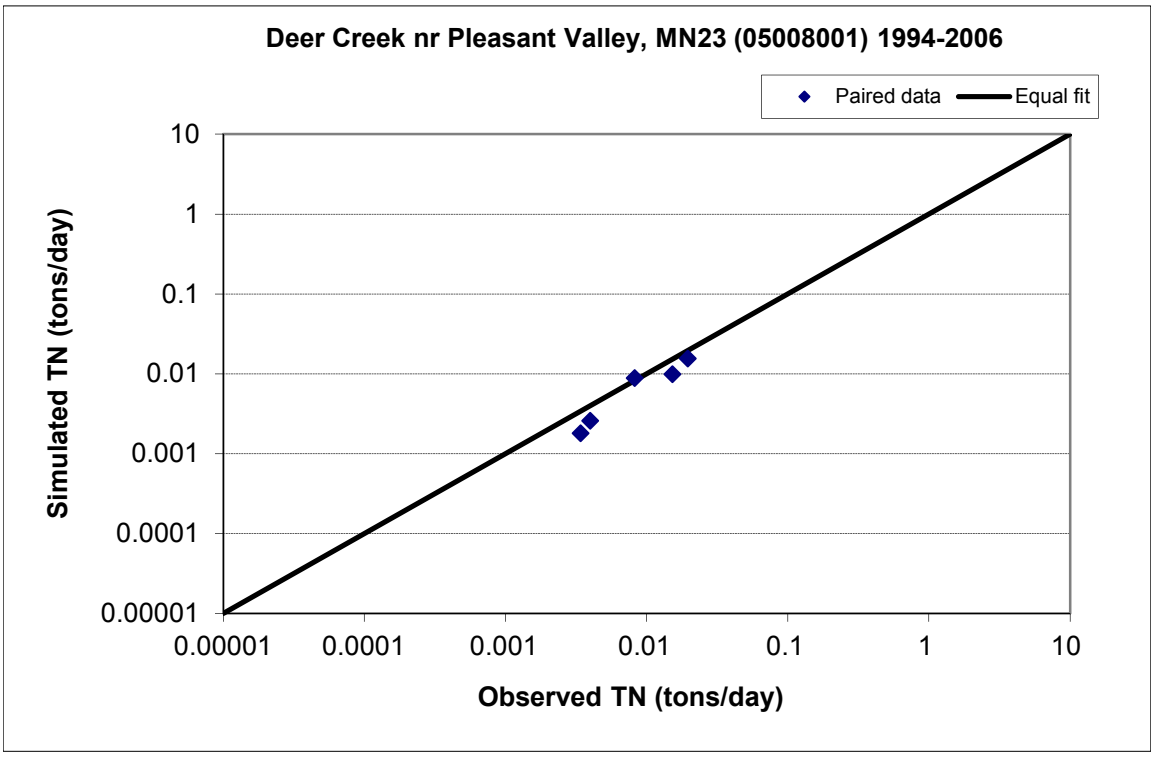

Figure B-27. Paired simulated vs. observed Total Nitrogen (TN) load at Deer Creek nr Pleasant Valley, MN23 (05008001) (validation period)

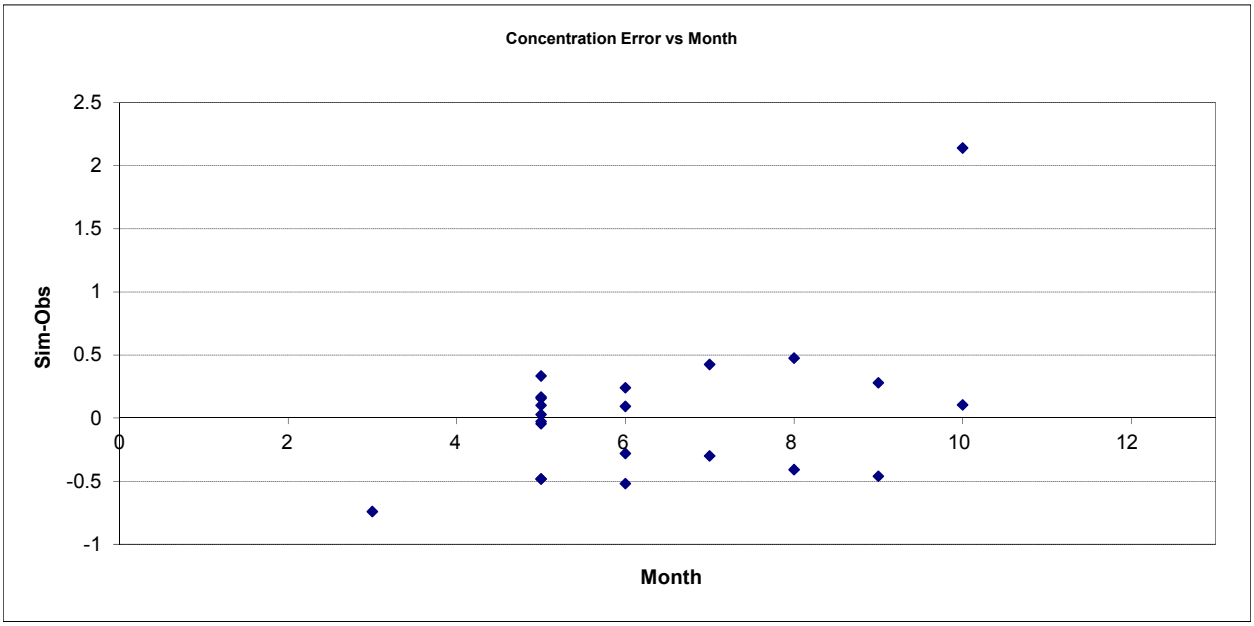

Figure B-28. Residual (Simulated - Observed) vs. Month Total Nitrogen (TN) at Deer Creek nr Pleasant Valley, MN23 (05008001)

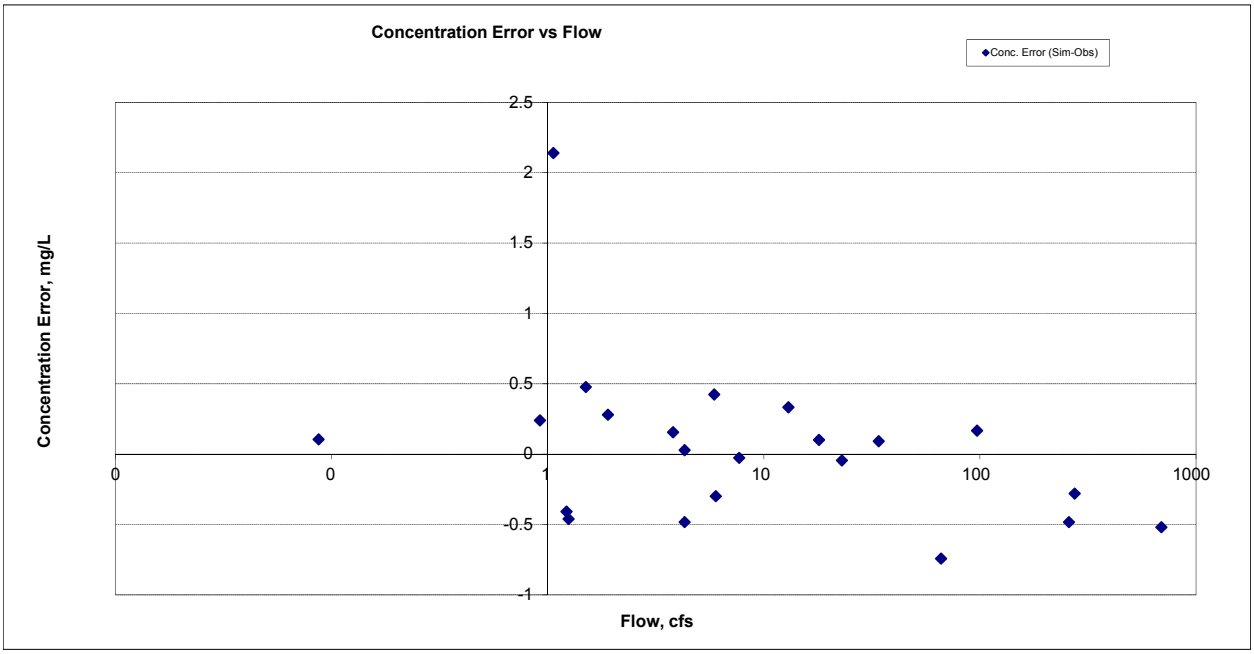

Figure B-29. Residual (Simulated - Observed) vs. Flow Total Nitrogen (TN) at Deer Creek nr Pleasant Valley, MN23 (05008001)

B.1.6 Soluble Reactive Phosphorus (SRP)

Table B-5. Soluble Reactive Phosphorus (SRP) statistics

Period	1994-2006	2007-2012
Count	6	35
Concentration Average Error	-17.99%	53.06%
Concentration Median Error	-41.71%	17.61%
Load Average Error	-19.75%	-1.05%
Load Median Error	-31.95%	0.27%
Paired t conc	0.55	0.12
Paired t load	0.50	0.67

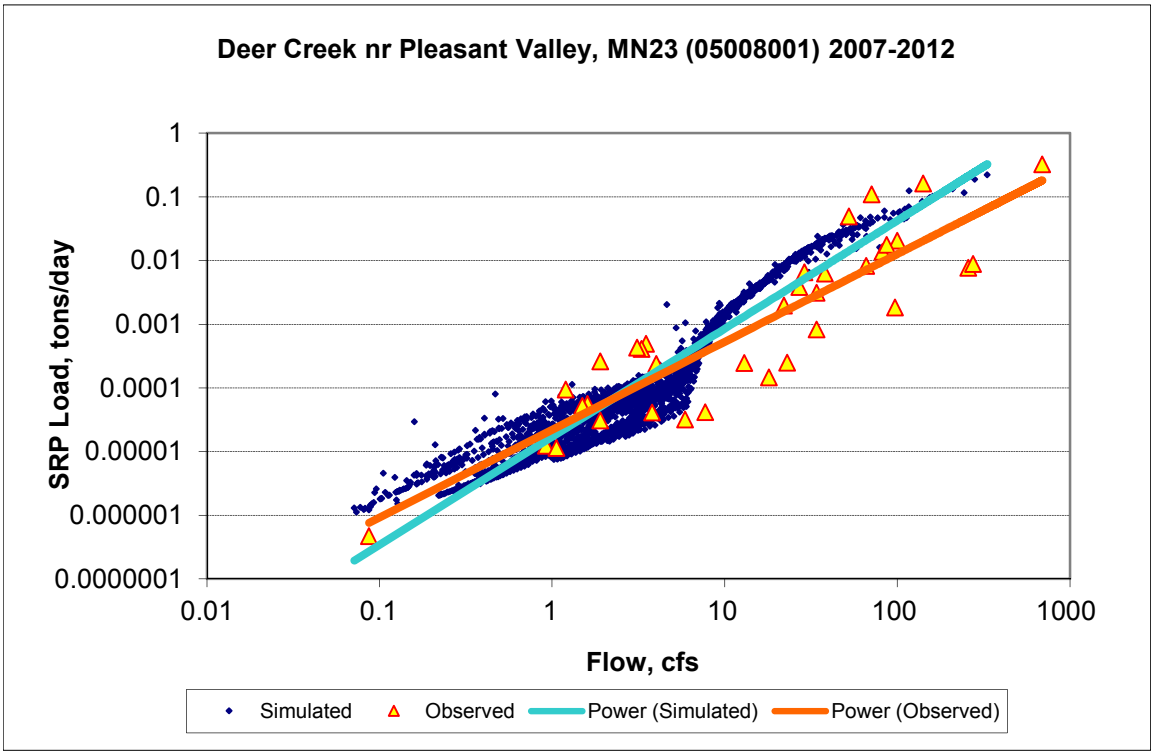

Figure B-30. Power plot of simulated and observed Soluble Reactive Phosphorus (SRP) load vs flow at Deer Creek nr Pleasant Valley, MN23 (05008001) (calibration period)

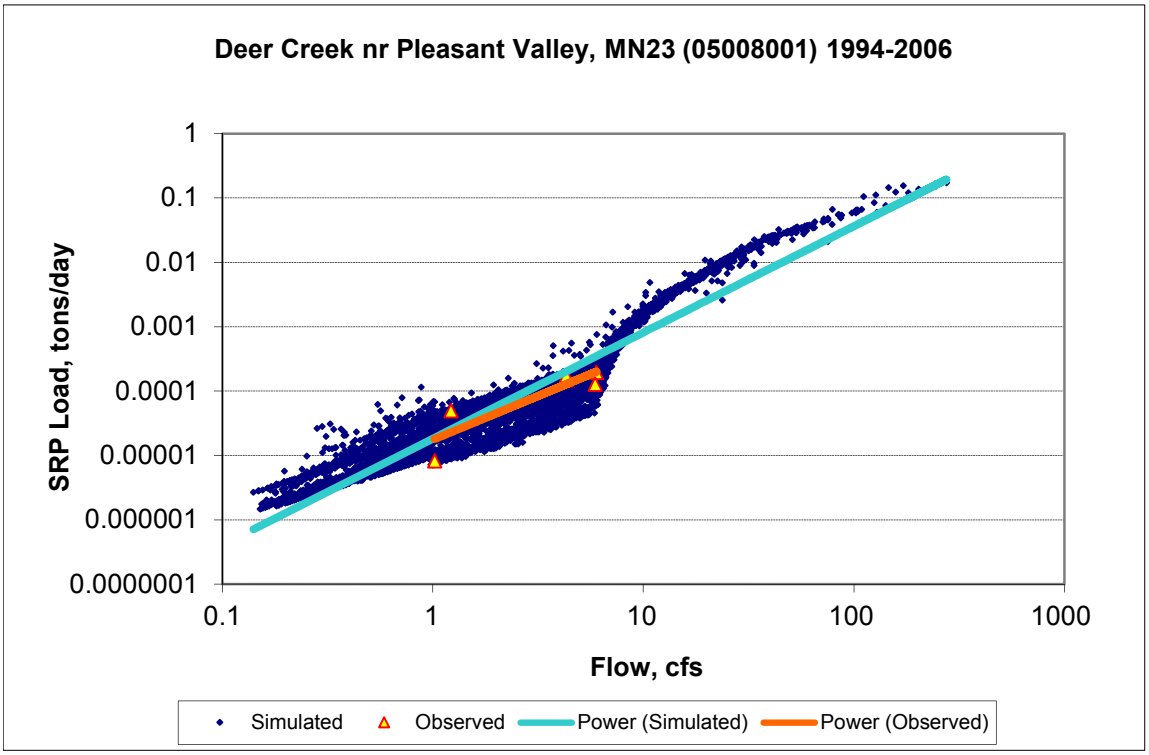

Figure B-31. Power plot of simulated and observed Soluble Reactive Phosphorus (SRP) load vs flow at Deer Creek nr Pleasant Valley, MN23 (05008001) (validation period)

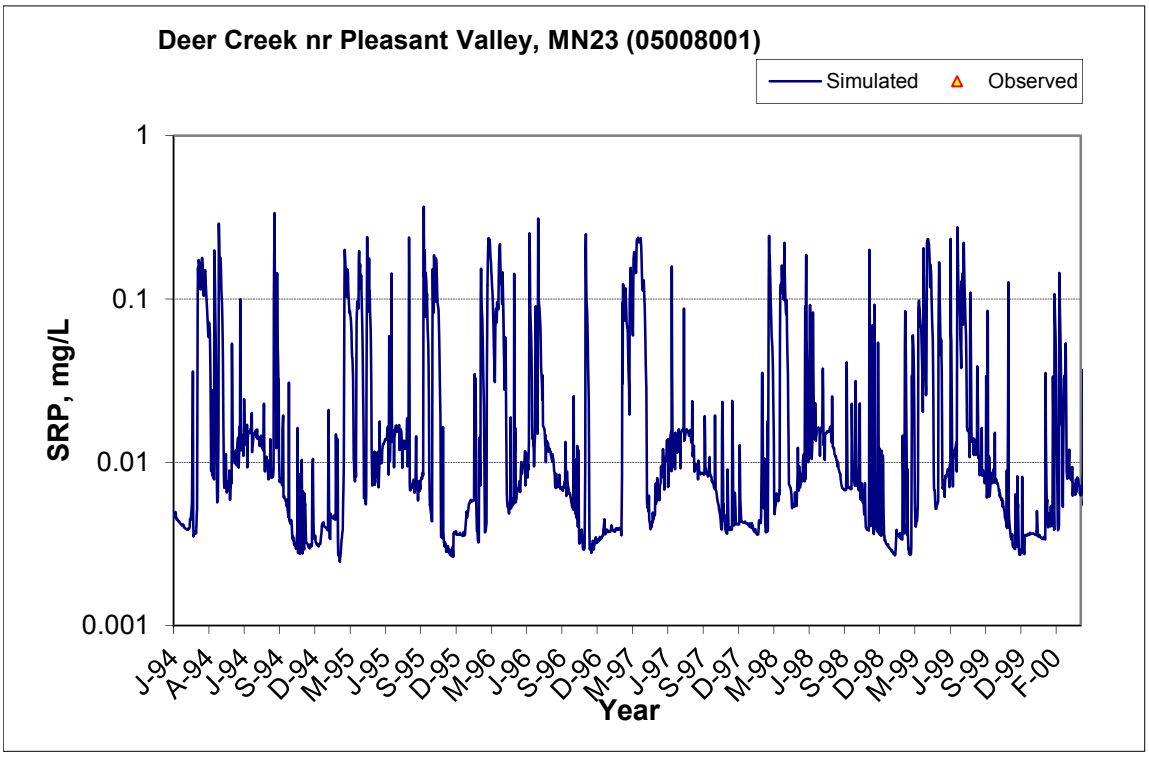
Deer Creek nr Pleasant Valley, MN23 (05008001)
Simulated
Observed
SRP, mg/L
1
0.1
0.01
0.001
J-94 A-94 J-94 S-94 D-94 M-95 J-95 S-95 D-95 M-96 J-96 S-96 D-96 M-97 J-97 S-97 D-97 M-98 J-98 S-98 D-98 M-99 J-99 S-99 D-99 F-00
Year

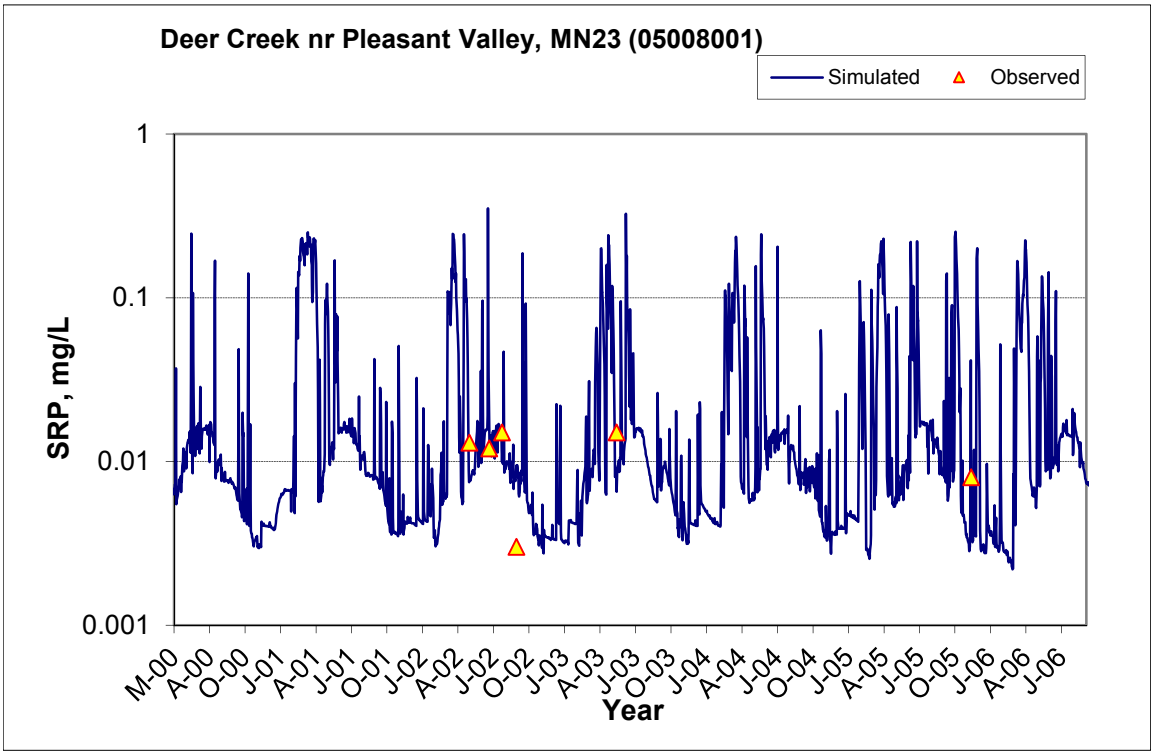
Deer Creek nr Pleasant Valley, MN23 (05008001)
Simulated
Observed
SRP, mg/L
1
0.1
0.01
0.001
M-00 A-00 O-00 J-01 A-01 J-01 O-01 J-02 A-02 J-02 O-02 J-03 A-03 J-03 O-03 J-04 A-04 J-04 O-04 J-05 A-05 J-05 O-05 J-06 A-06 J-06
Year

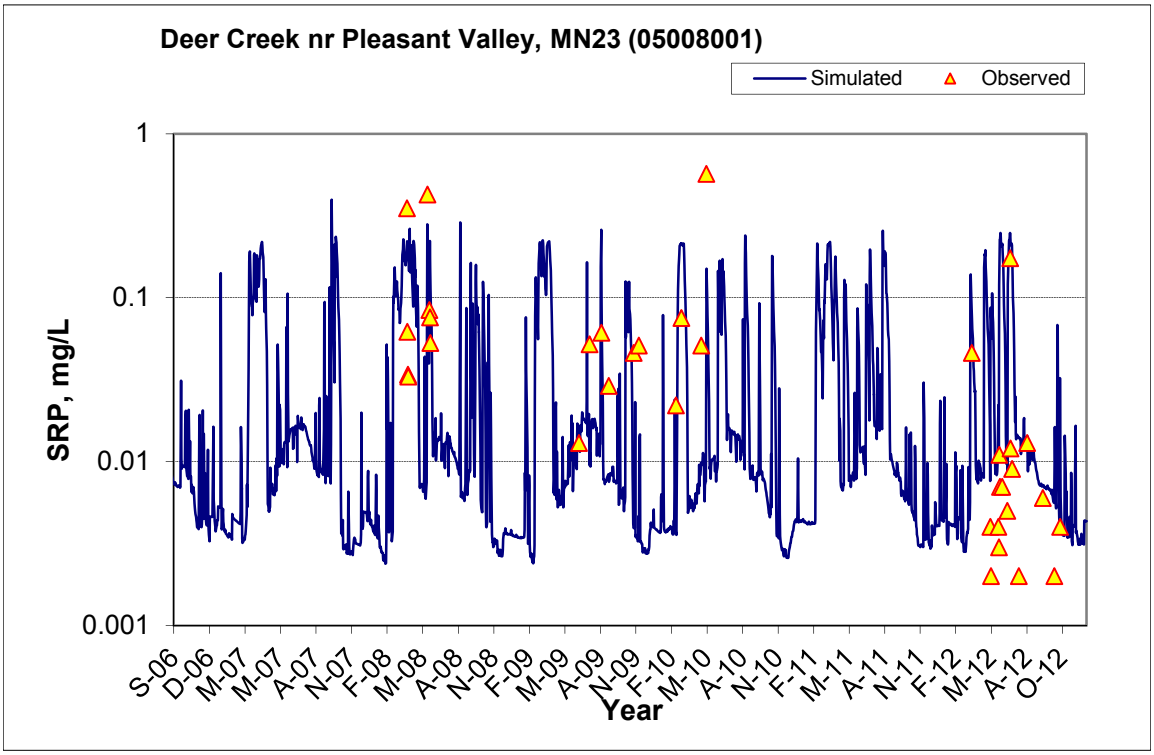

Figure B-32. Time series of observed and simulated Soluble Reactive Phosphorus (SRP) concentration at Deer Creek nr Pleasant Valley, MN23 (05008001)

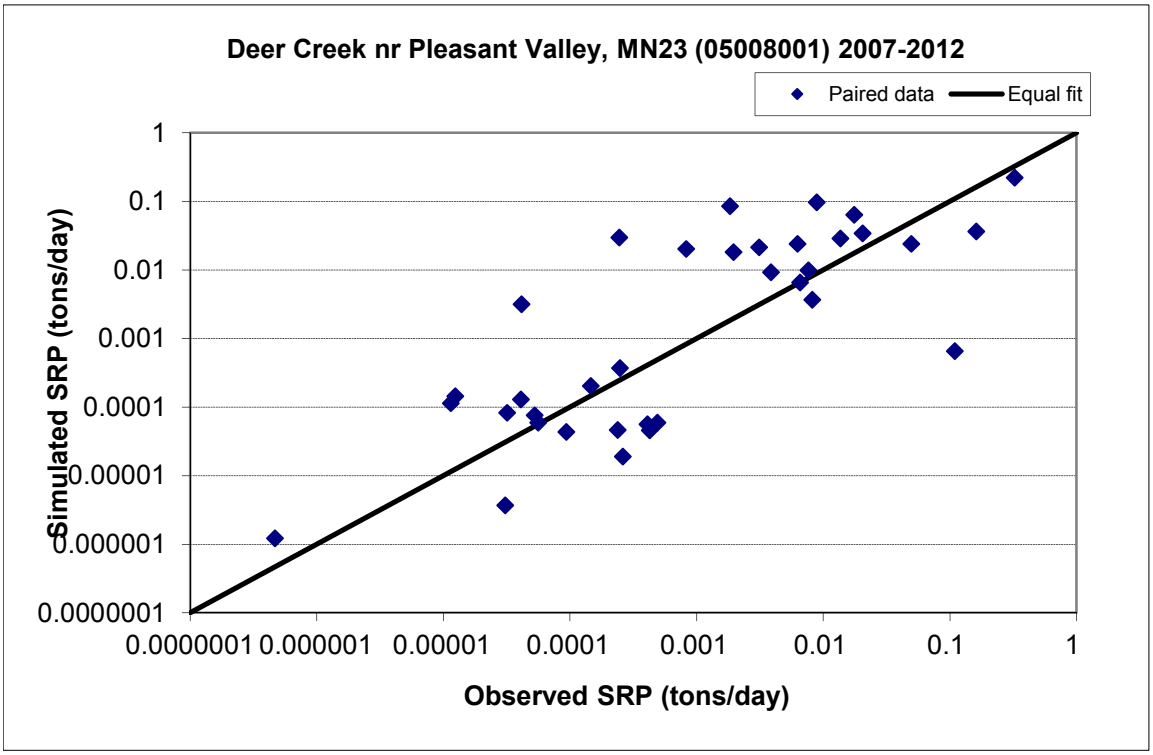

Figure B-33. Paired simulated vs. observed Soluble Reactive Phosphorus (SRP) load at Deer Creek nr Pleasant Valley, MN23 (05008001) (calibration period)

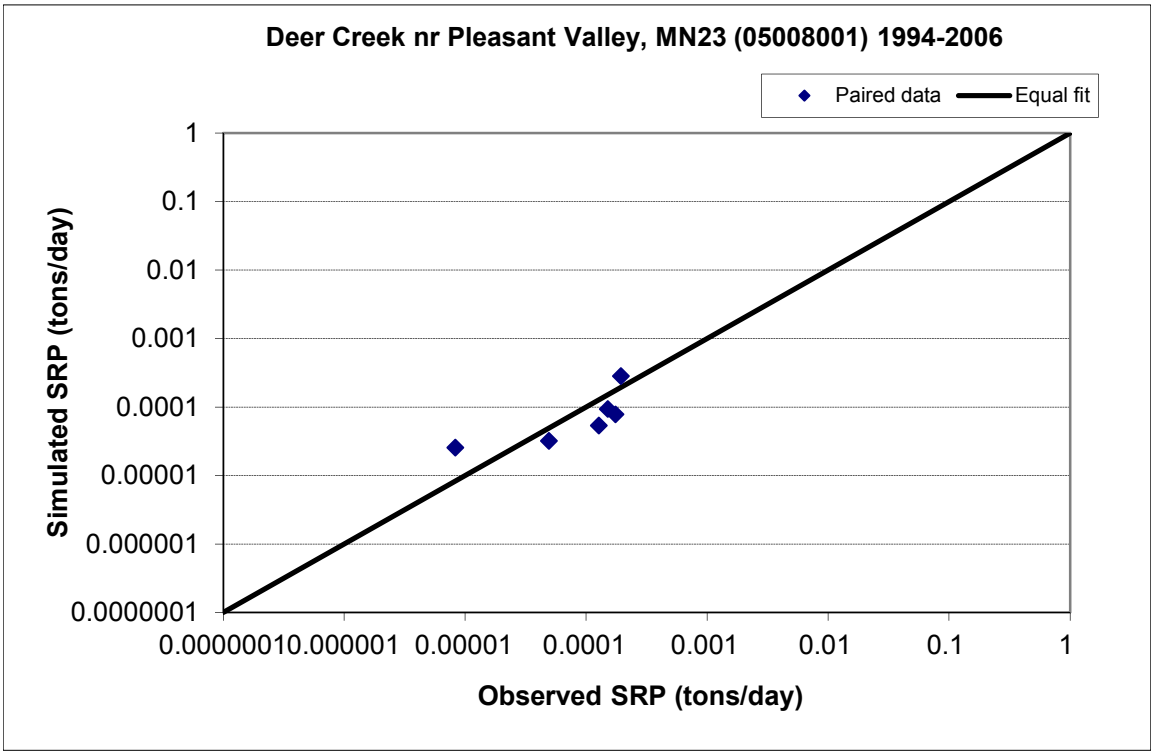

Figure B-34. Paired simulated vs. observed Soluble Reactive Phosphorus (SRP) load at Deer Creek nr Pleasant Valley, MN23 (05008001) (validation period)

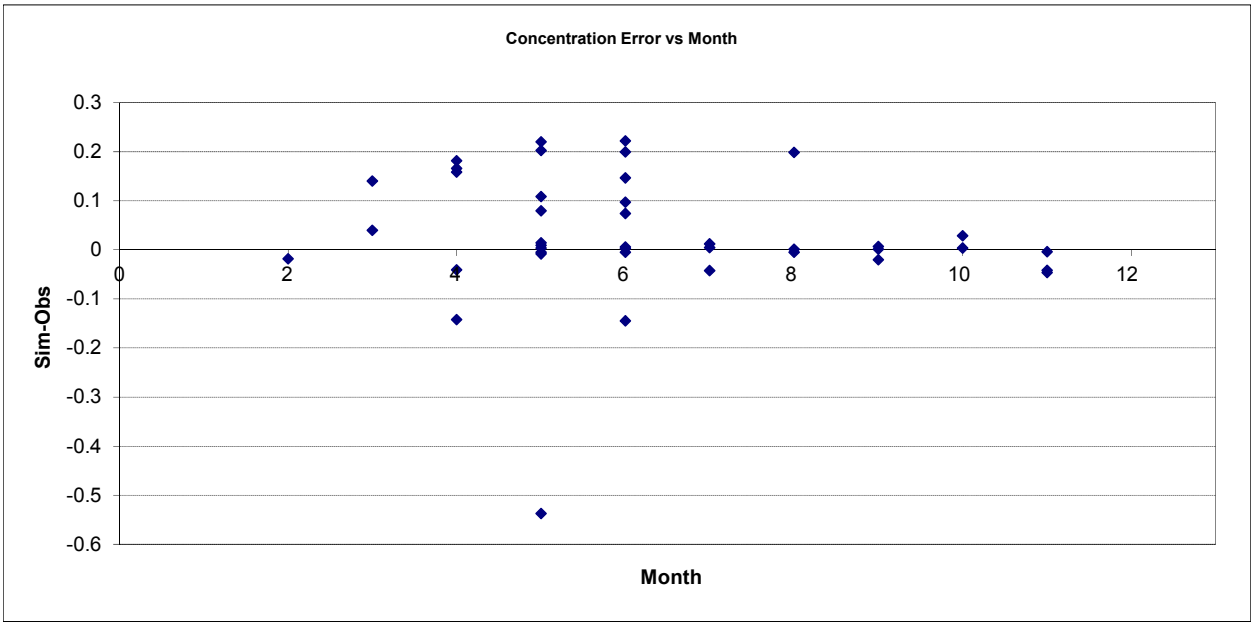

Figure B-35. Residual (Simulated - Observed) vs. Month Soluble Reactive Phosphorus (SRP) at Deer Creek nr Pleasant Valley, MN23 (05008001)

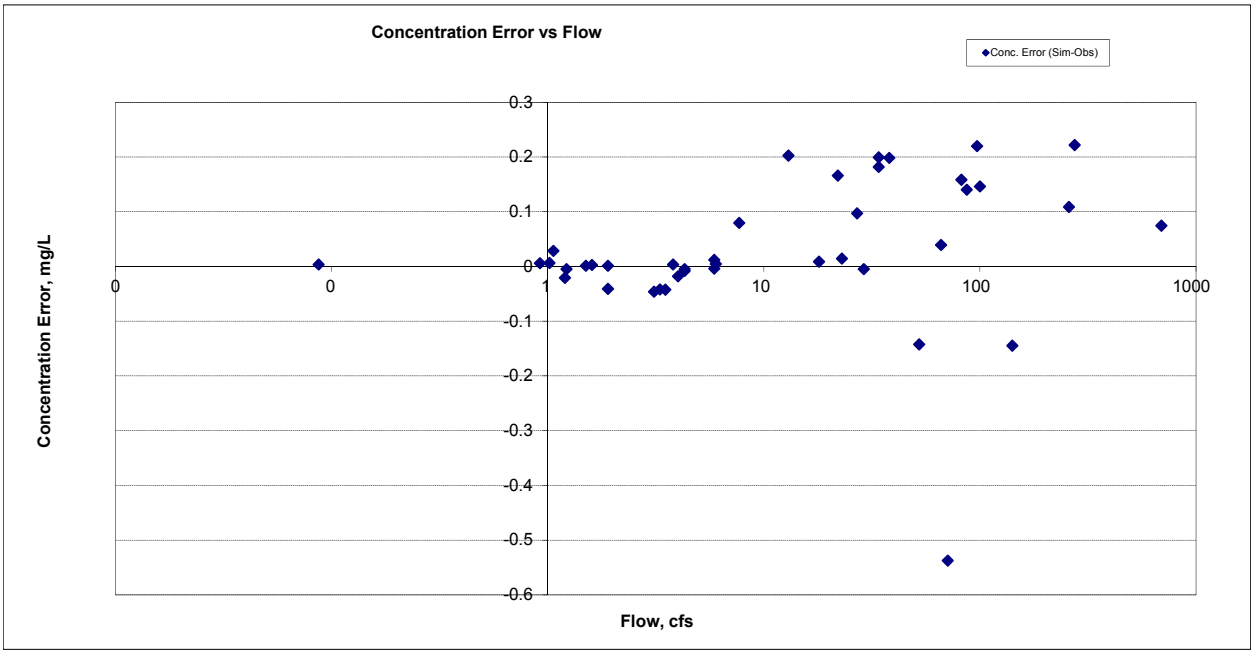

Figure B-36. Residual (Simulated - Observed) vs. Flow Soluble Reactive Phosphorus (SRP) at Deer Creek nr Pleasant Valley, MN23 (05008001)

B.1.7 Organic Phosphorus (OrgP)

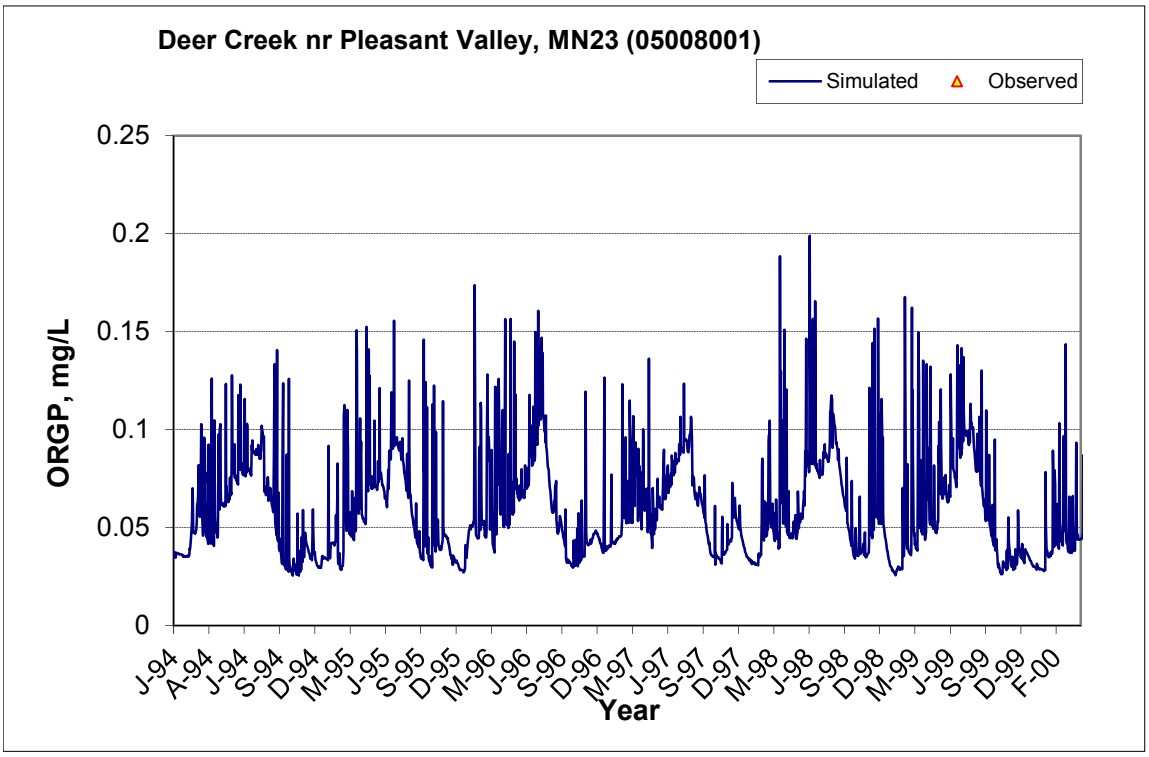

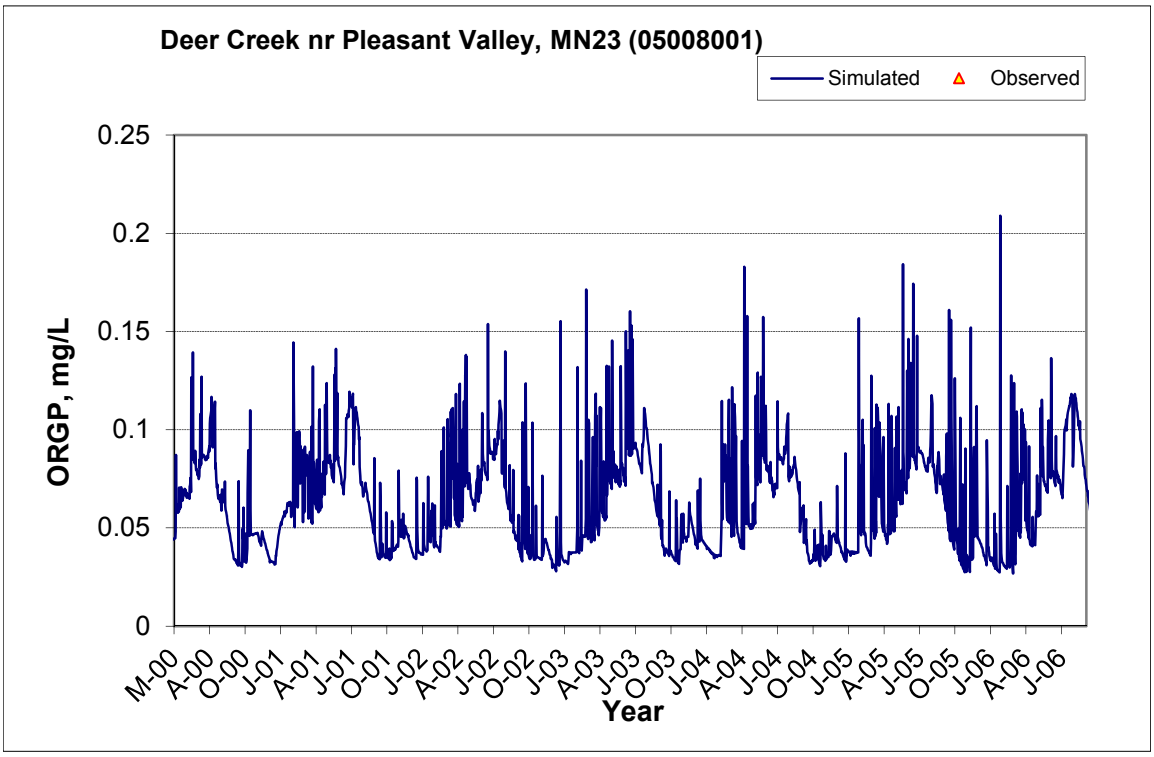

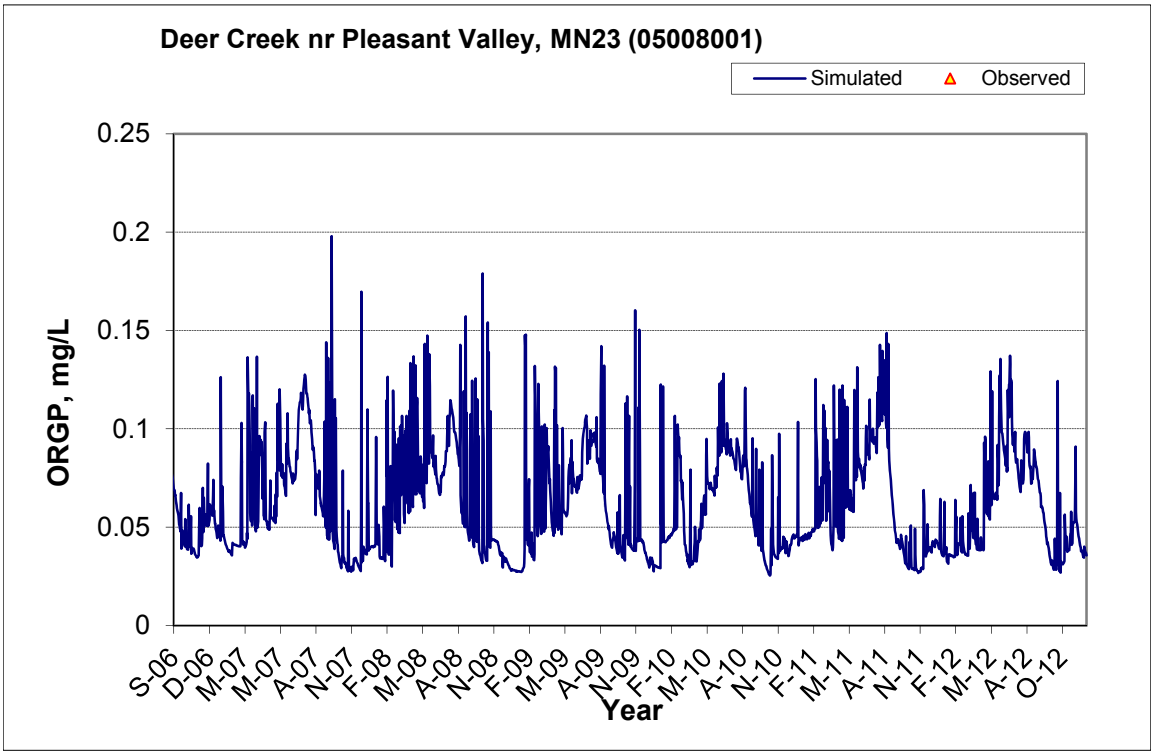

Figure B-37. Time series of observed and simulated Organic Phosphorus (OrgP) concentration at Deer Creek nr Pleasant Valley, MN23 (05008001)

B.1.8 Total Phosphorus (TP)

Table B-6. Total Phosphorus (TP) statistics

Period	1994-2006	2007-2012
Count	79	35
Concentration Average Error	-84.26%	-37.94%
Concentration Median Error	-51.62%	1.03%
Load Average Error	-57.94%	-78.55%
Load Median Error	-12.55%	0.00%
Paired t conc	0.00	0.13
Paired t load	0.06	0.06

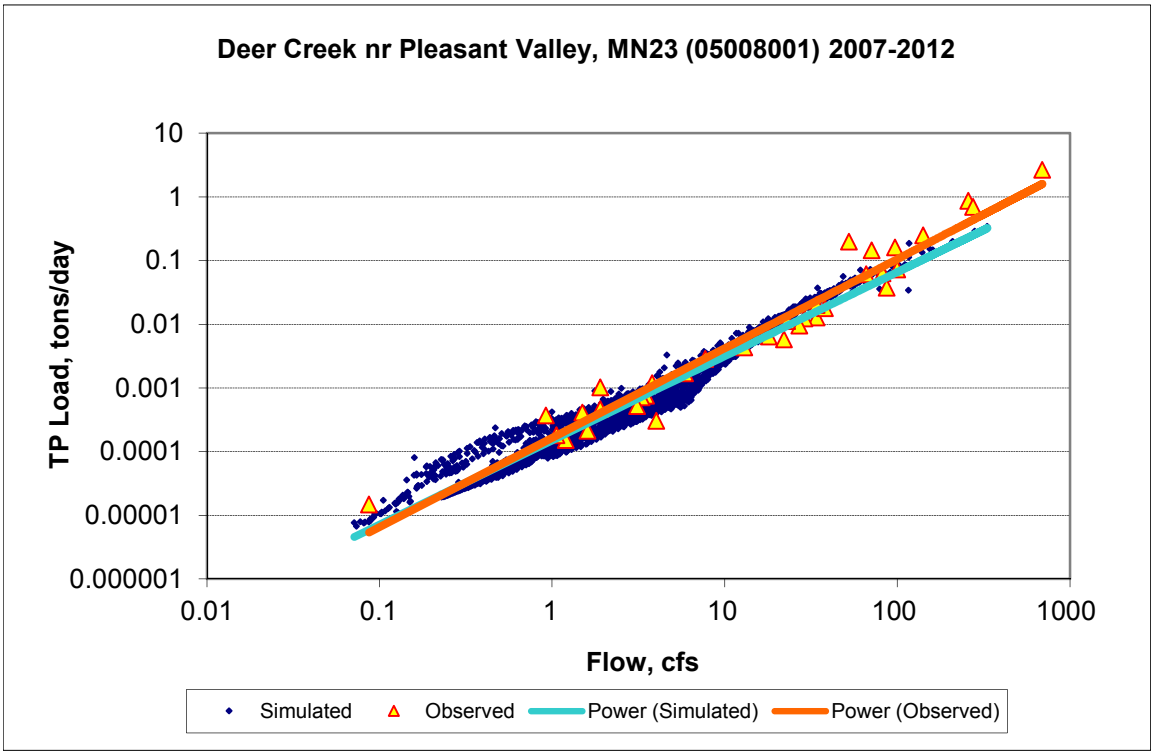

Figure B-38. Power plot of simulated and observed Total Phosphorus (TP) load vs flow at Deer Creek nr Pleasant Valley, MN23 (05008001) (calibration period)

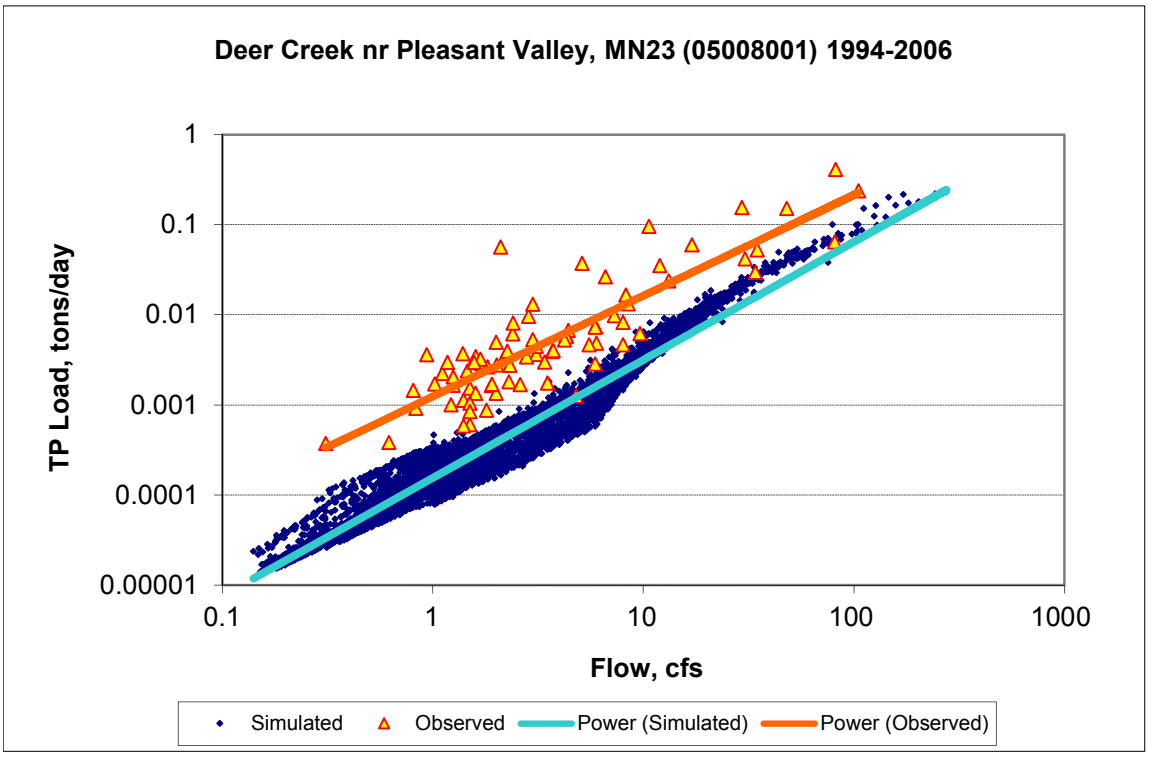

Figure B-39. Power plot of simulated and observed Total Phosphorus (TP) load vs flow at Deer Creek nr Pleasant Valley, MN23 (05008001) (validation period)

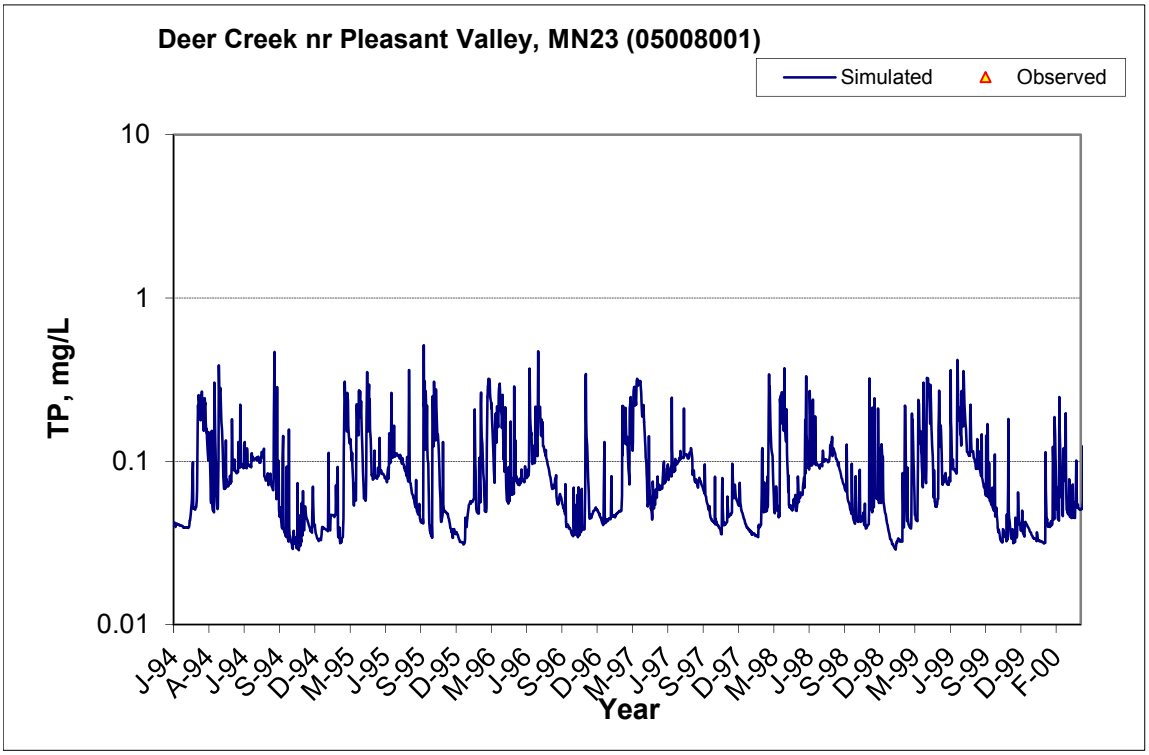

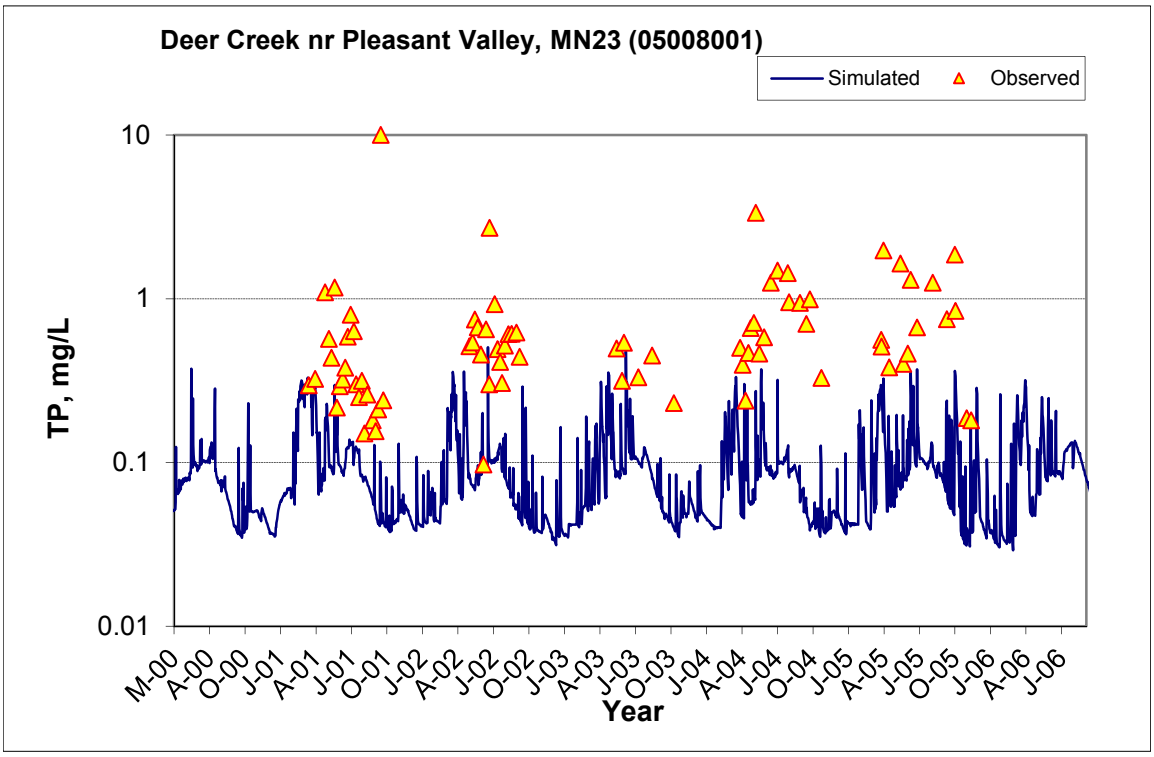

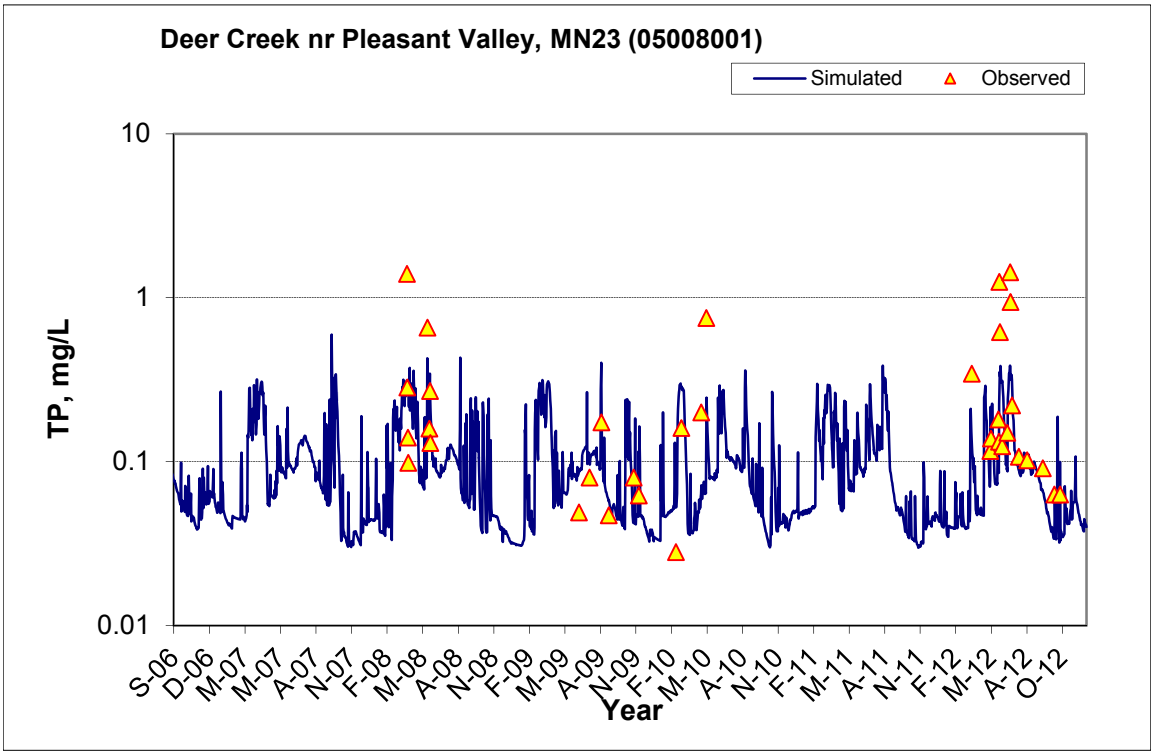

Figure B-40. Time series of observed and simulated Total Phosphorus (TP) concentration at Deer Creek nr Pleasant Valley, MN23 (05008001)

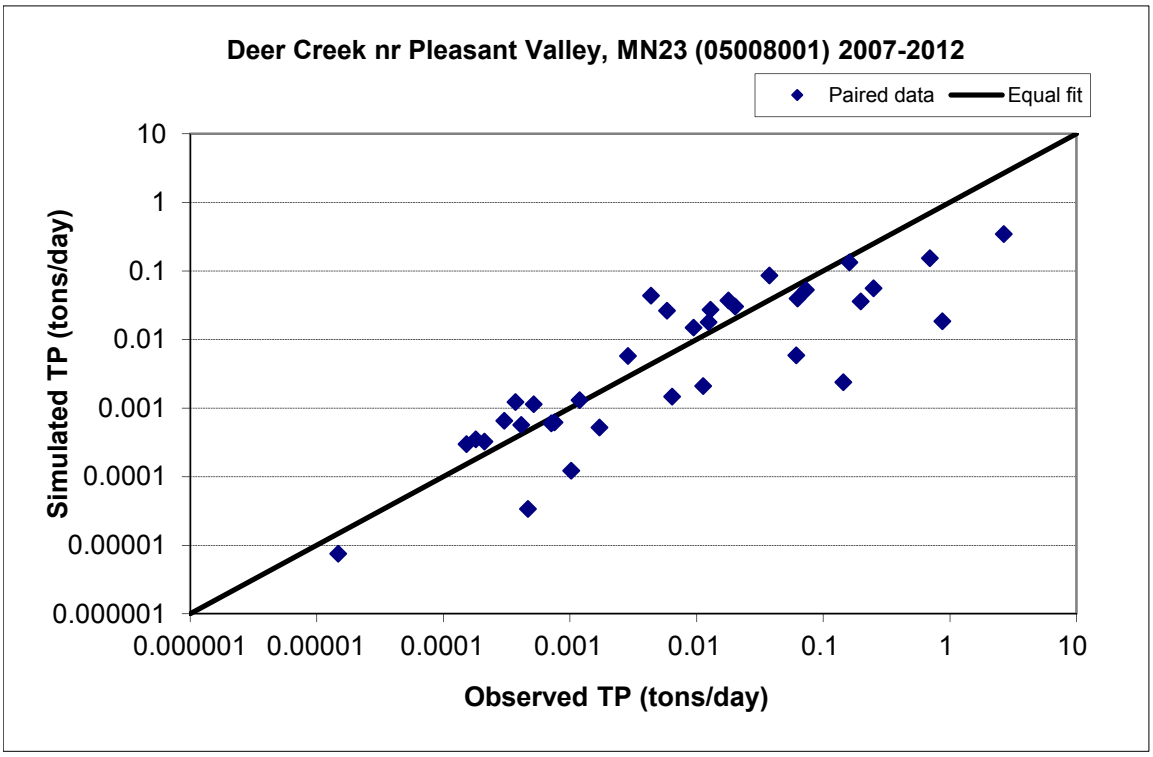

Figure B-41. Paired simulated vs. observed Total Phosphorus (TP) load at Deer Creek nr Pleasant Valley, MN23 (05008001) (calibration period)

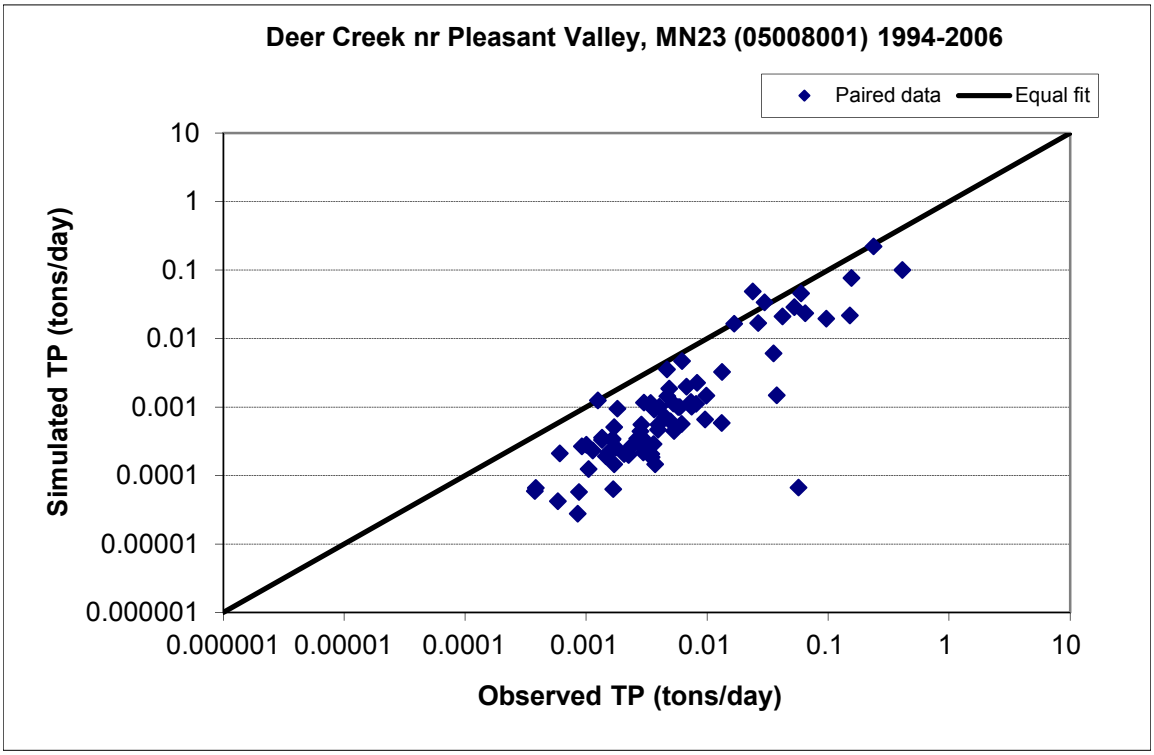

Figure B-42. Paired simulated vs. observed Total Phosphorus (TP) load at Deer Creek nr Pleasant Valley, MN23 (05008001) (validation period)

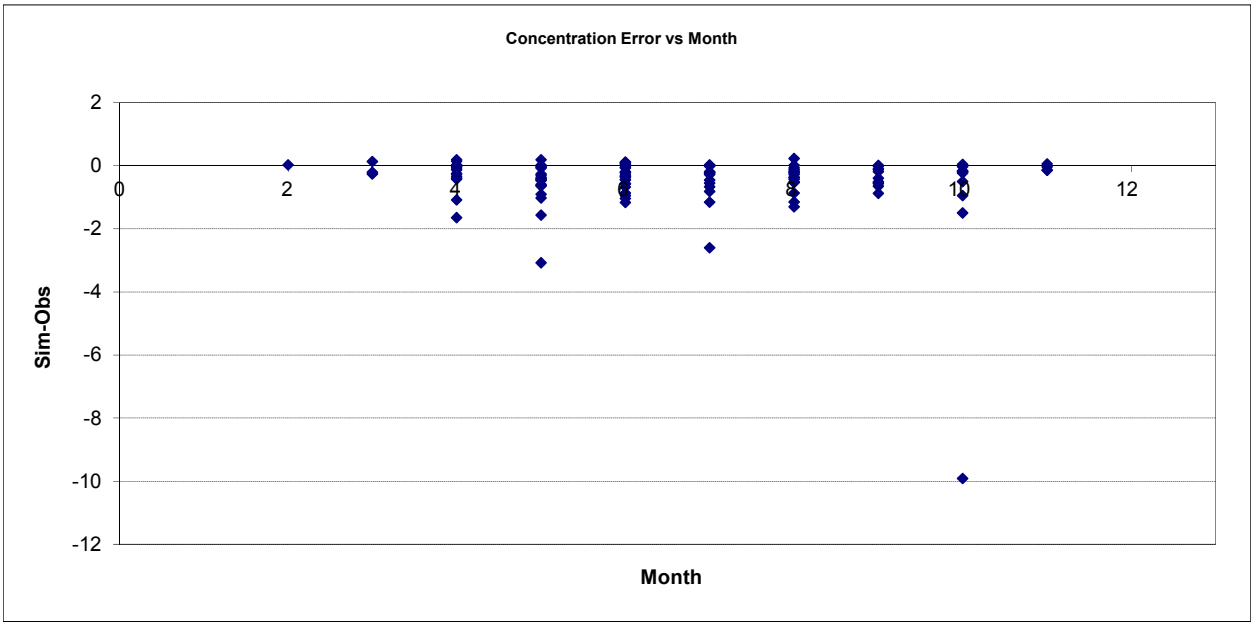

Figure B-43. Residual (Simulated - Observed) vs. Month Total Phosphorus (TP) at Deer Creek nr Pleasant Valley, MN23 (05008001)

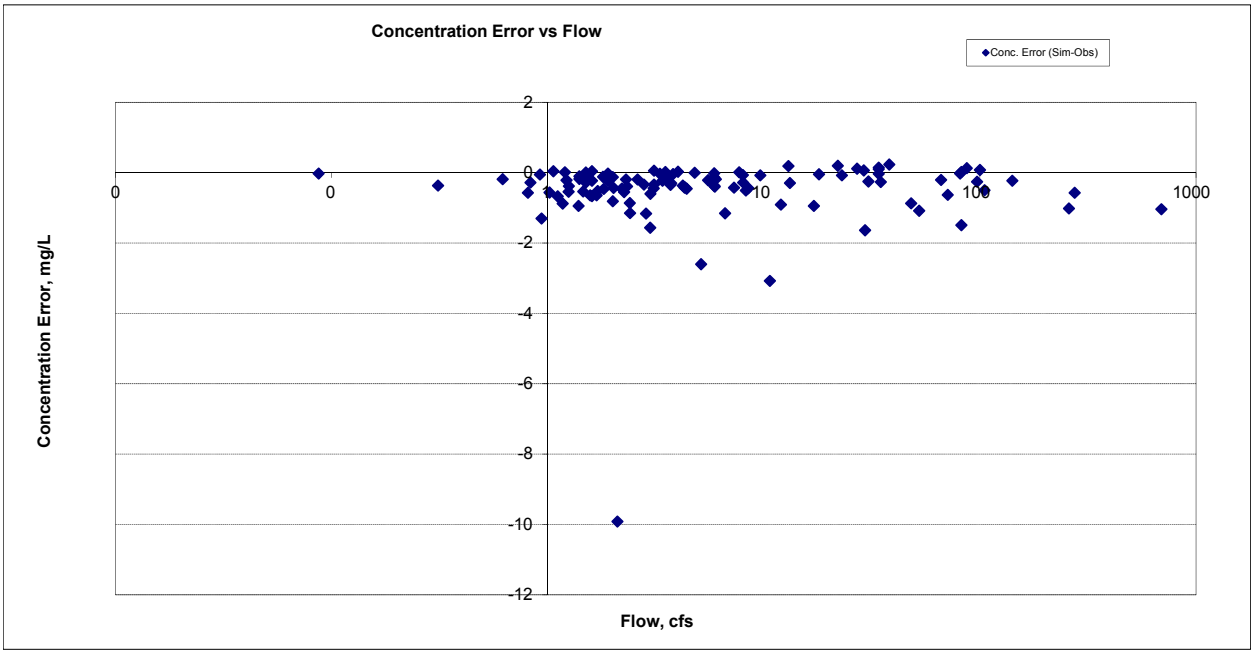

Figure B-44. Residual (Simulated - Observed) vs. Flow Total Phosphorus (TP) at Deer Creek nr Pleasant Valley, MN23 (05008001)

B.2 ROCK CREEK NR PLEASANT VALLEY (05009001)

B.2.1 Ammonia Nitrogen (NH3)

Table B-7. Ammonia Nitrogen (NH3) statistics

Period	1994-2001	2002-2012
Count	ND	15
Concentration Average Error		130.05%
Concentration Median Error		43.19%
Load Average Error		-10.12%
Load Median Error		2.18%
Paired t conc		0.02
Paired t load		0.56

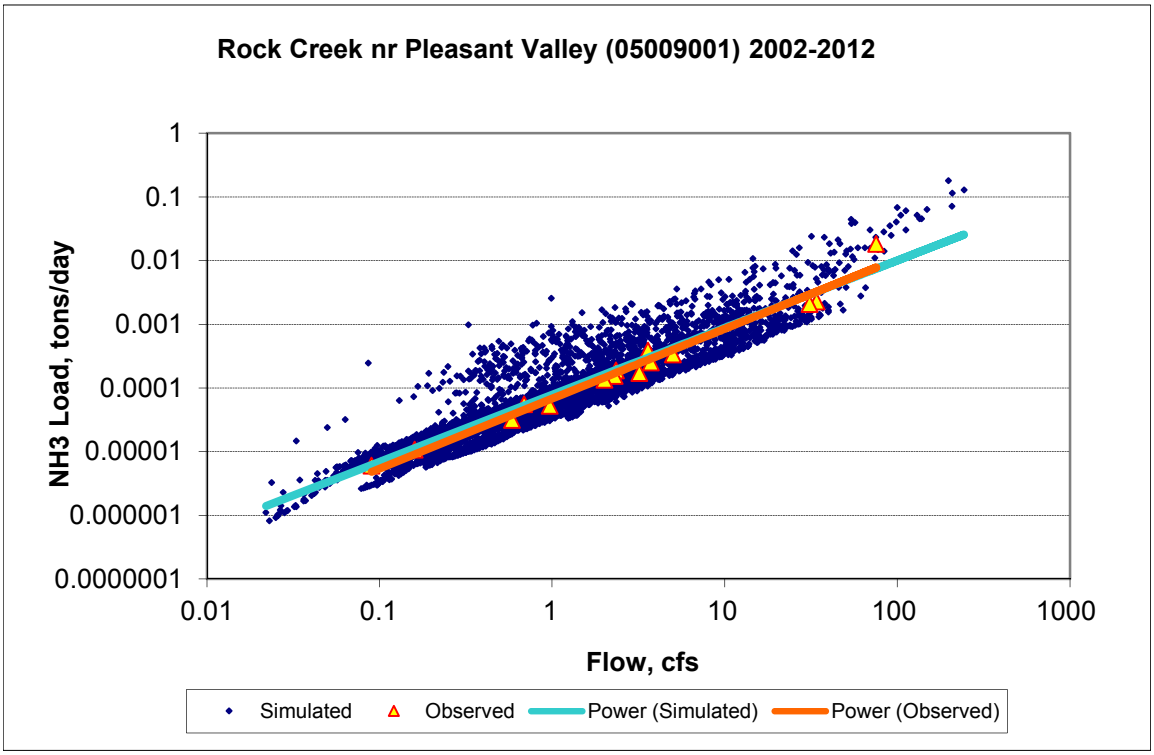

Figure B-45. Power plot of simulated and observed Ammonia Nitrogen (NH3) load vs flow at Rock Creek nr Pleasant Valley (05009001) (calibration period)

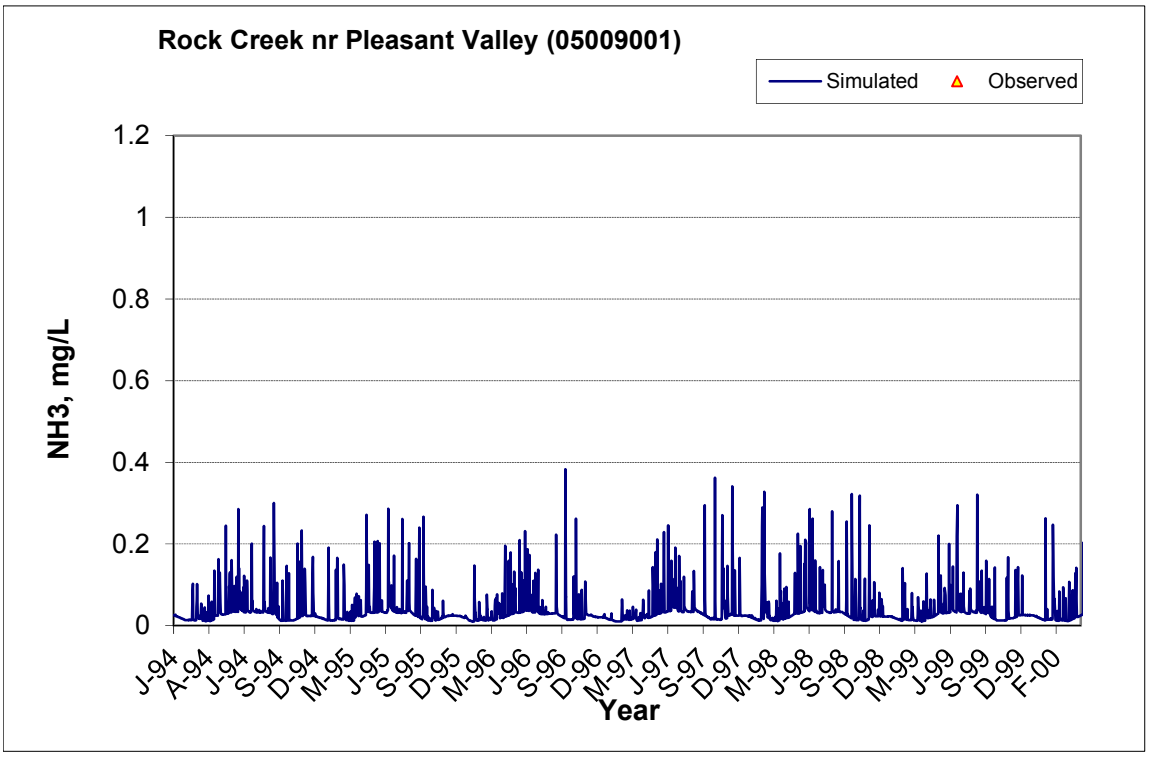
Rock Creek nr Pleasant Valley (05009001)
Simulated
Observed
NH3, mg/L
1.2
1
0.8
0.6
0.4
0.2
0
J-94 A-94 J-94 S-94 D-94 M-95 J-95 S-95 D-95 M-96 J-96 S-96 D-96 M-97 J-97 S-97 D-97 M-98 J-98 S-98 D-98 M-99 J-99 S-99 D-99 F-00
Year

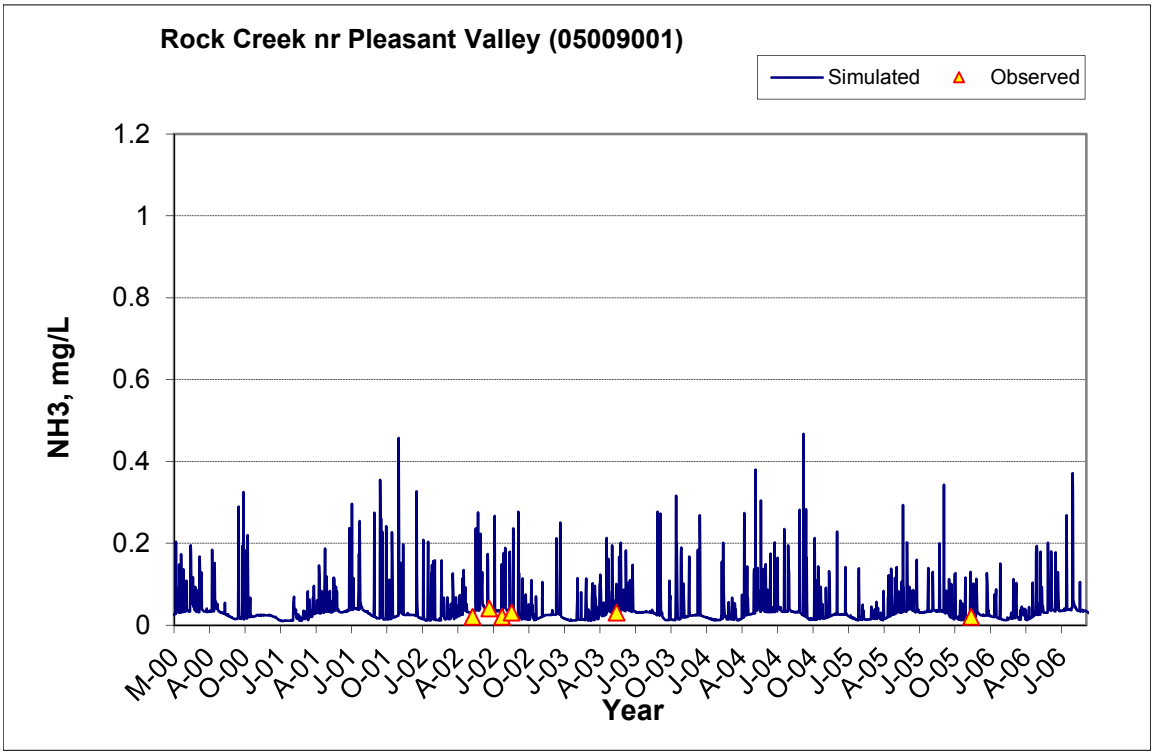
Rock Creek nr Pleasant Valley (05009001)
Simulated
Observed
NH3, mg/L
1.2
1
0.8
0.6
0.4
0.2
0
M-00 A-00 O-00 J-01 A-01 J-01 O-01 J-02 A-02 J-02 O-02 J-03 A-03 J-03 O-03 J-04 A-04 J-04 O-04 J-05 A-05 J-05 O-05 J-06 A-06 J-06
Year

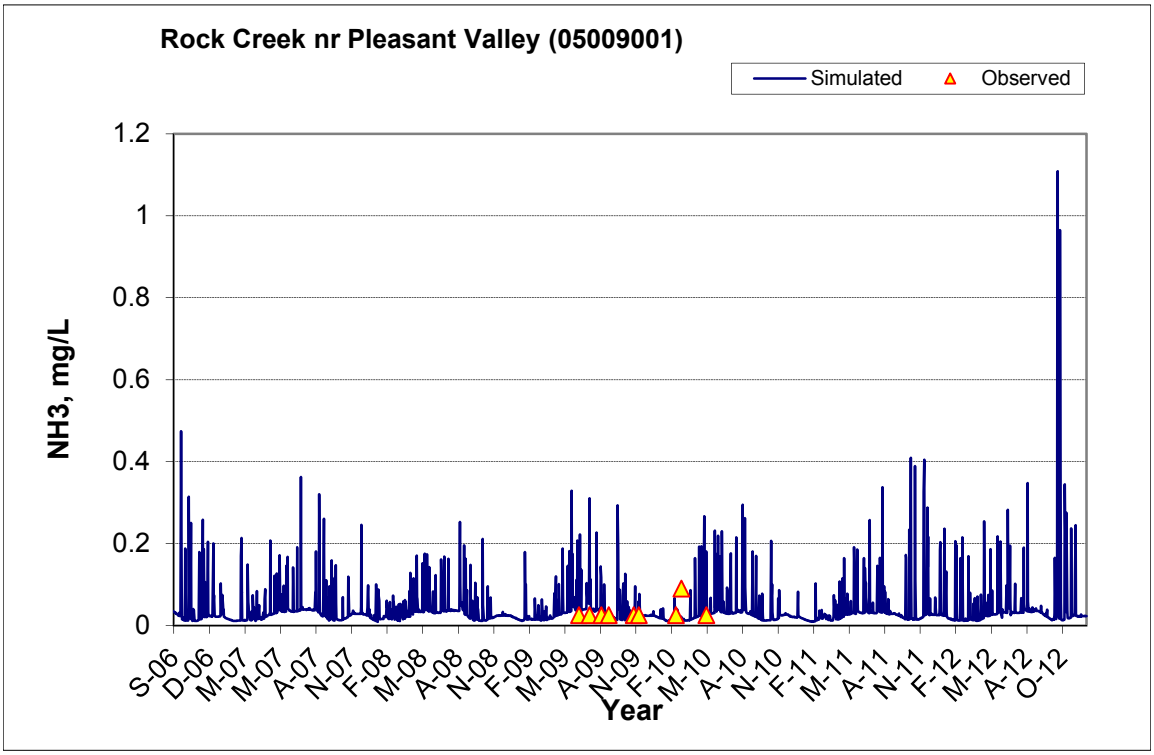

Figure B-46. Time series of observed and simulated Ammonia Nitrogen (NH3) concentration at Rock Creek nr Pleasant Valley (05009001)

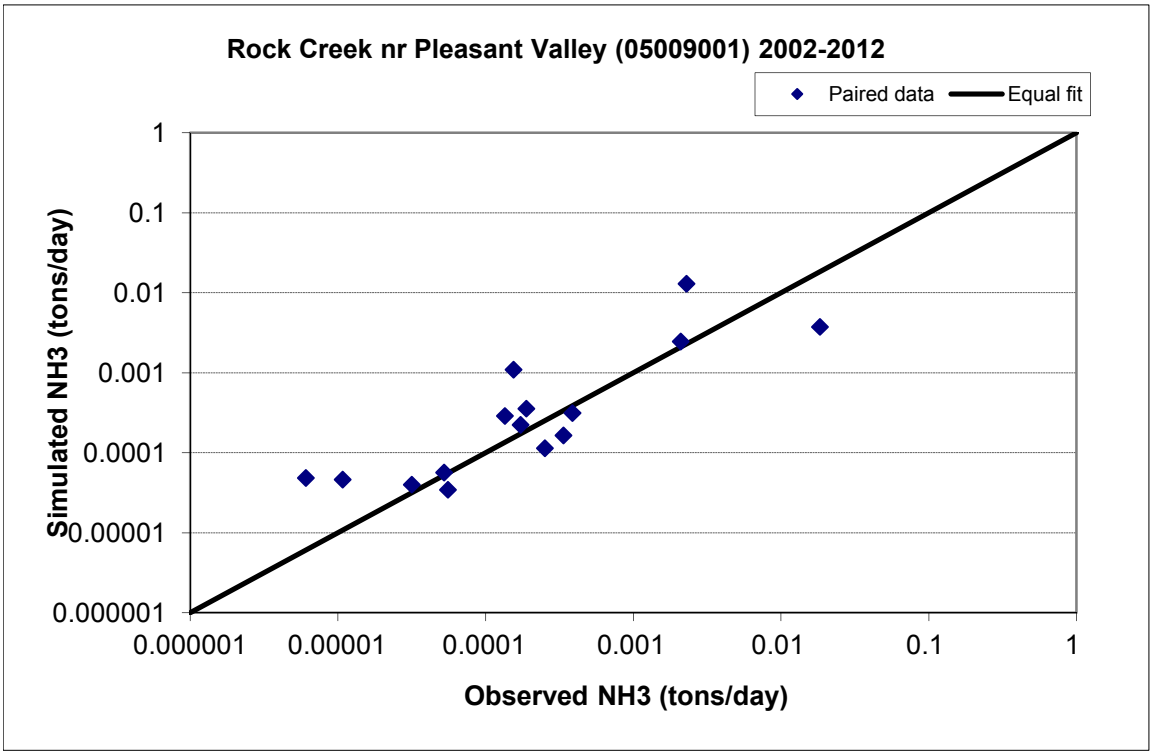

Figure B-47. Paired simulated vs. observed Ammonia Nitrogen (NH3) load at Rock Creek nr Pleasant Valley (05009001) (calibration period)

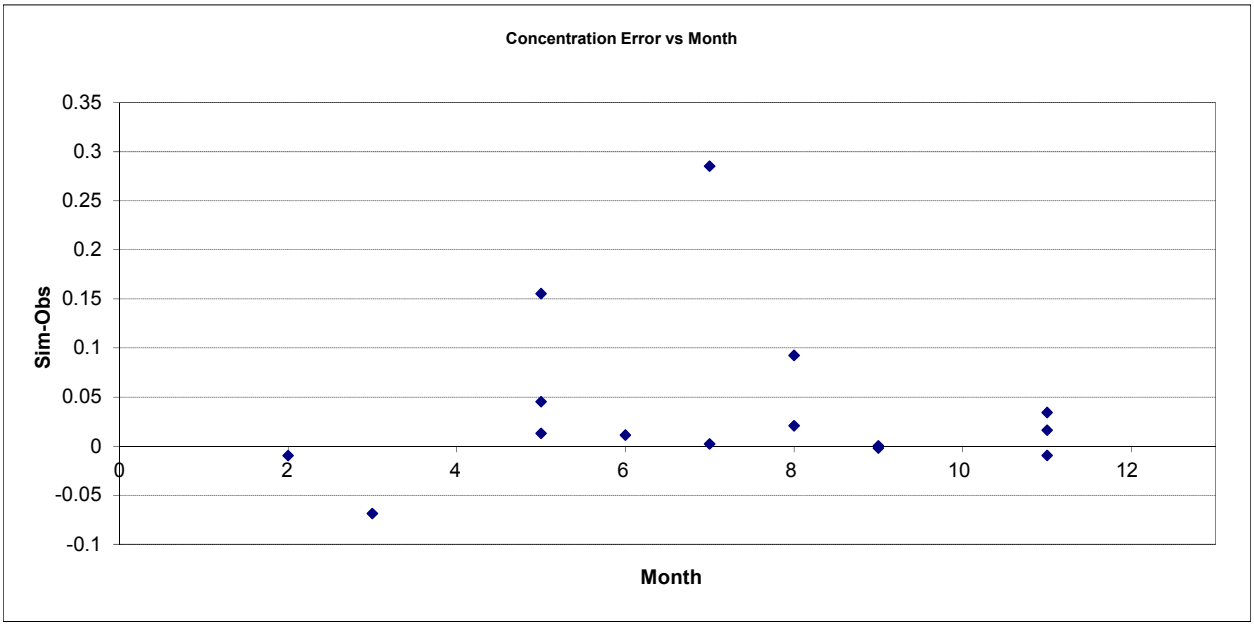

Figure B-48. Residual (Simulated - Observed) vs. Month Ammonia Nitrogen (NH3) at Rock Creek nr Pleasant Valley (05009001)

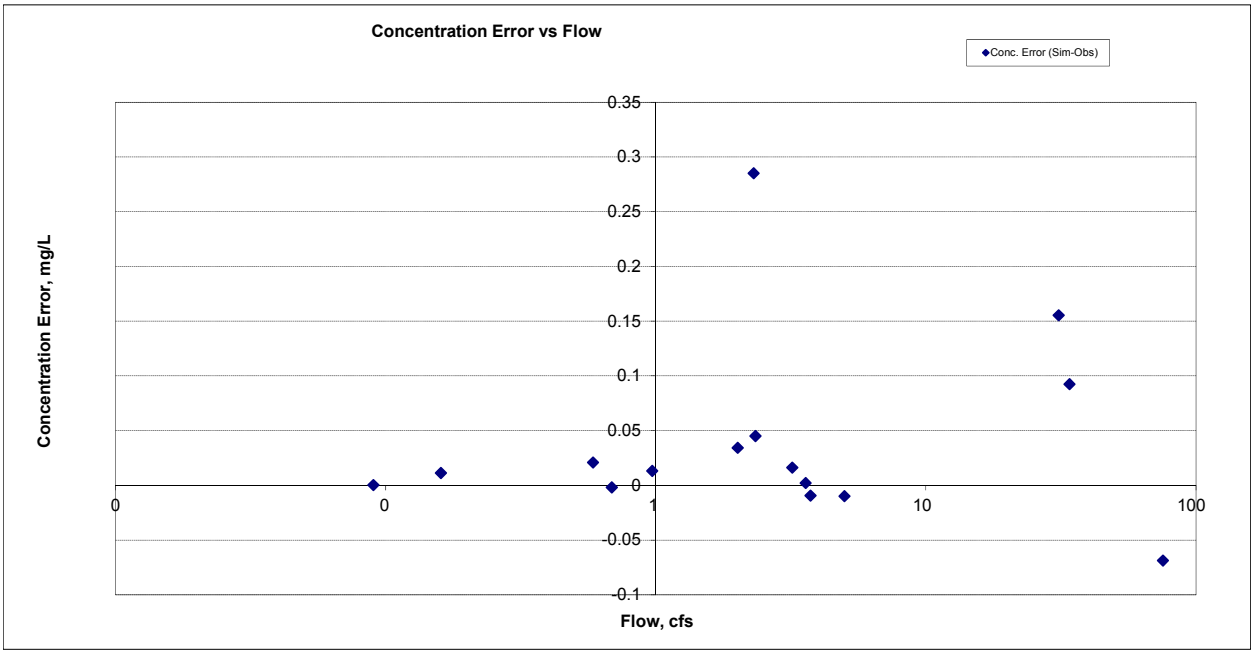

Figure B-49. Residual (Simulated - Observed) vs. Flow Ammonia Nitrogen (NH3) at Rock Creek nr Pleasant Valley (05009001)

B.2.2 Organic Nitrogen (OrgN)

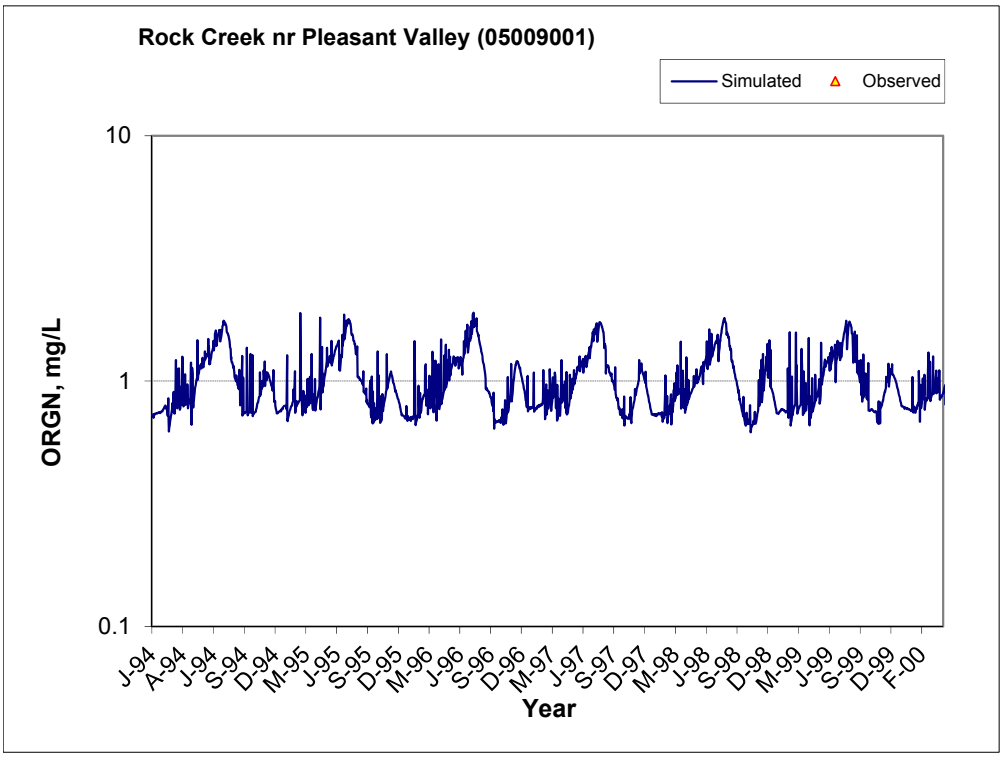

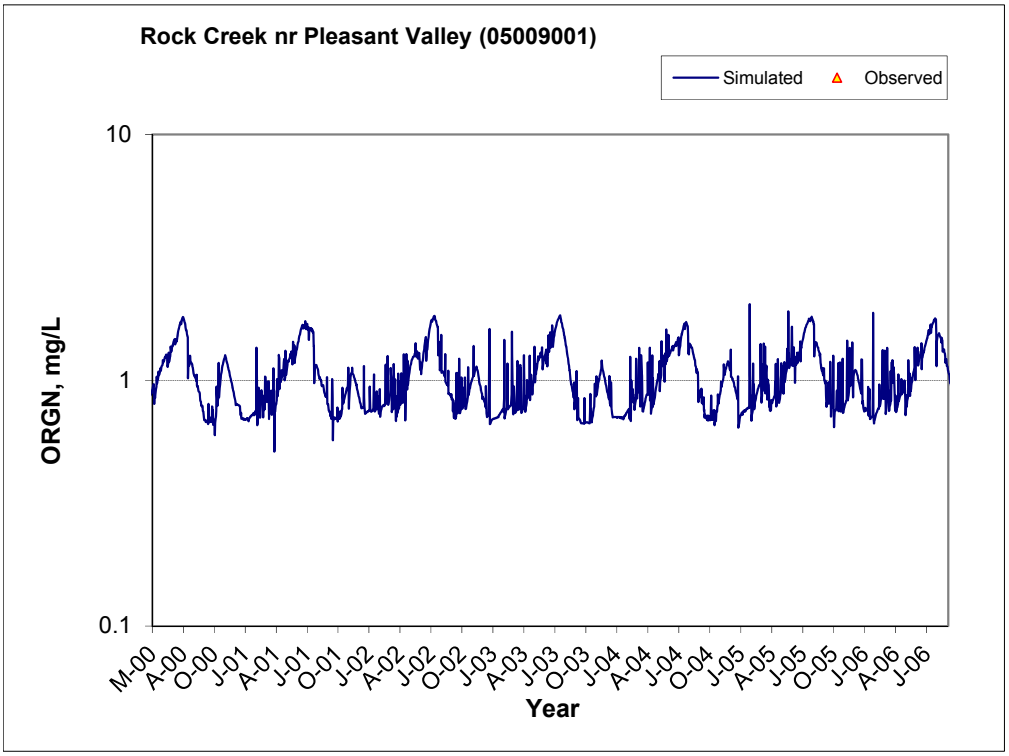

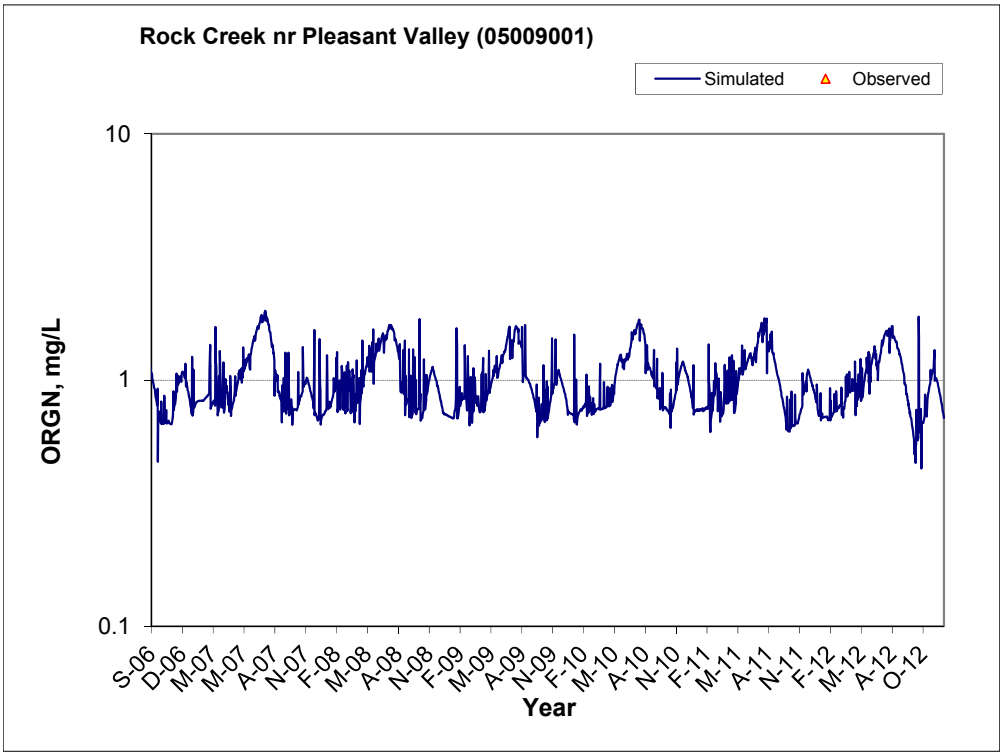

Figure B-50. Time series of observed and simulated Organic Nitrogen (OrgN) concentration at Rock Creek nr Pleasant Valley (05009001)

B.2.3 Total Kjeldahl Nitrogen (TKN)

Table B-8. Total Kjeldahl Nitrogen (TKN) statistics

Period	1994-2001	2002-2012
Count	ND	6
Concentration Average Error		36.66%
Concentration Median Error		37.56%
Load Average Error		0.50%
Load Median Error		-3.85%
Paired t conc		0.16
Paired t load		0.71

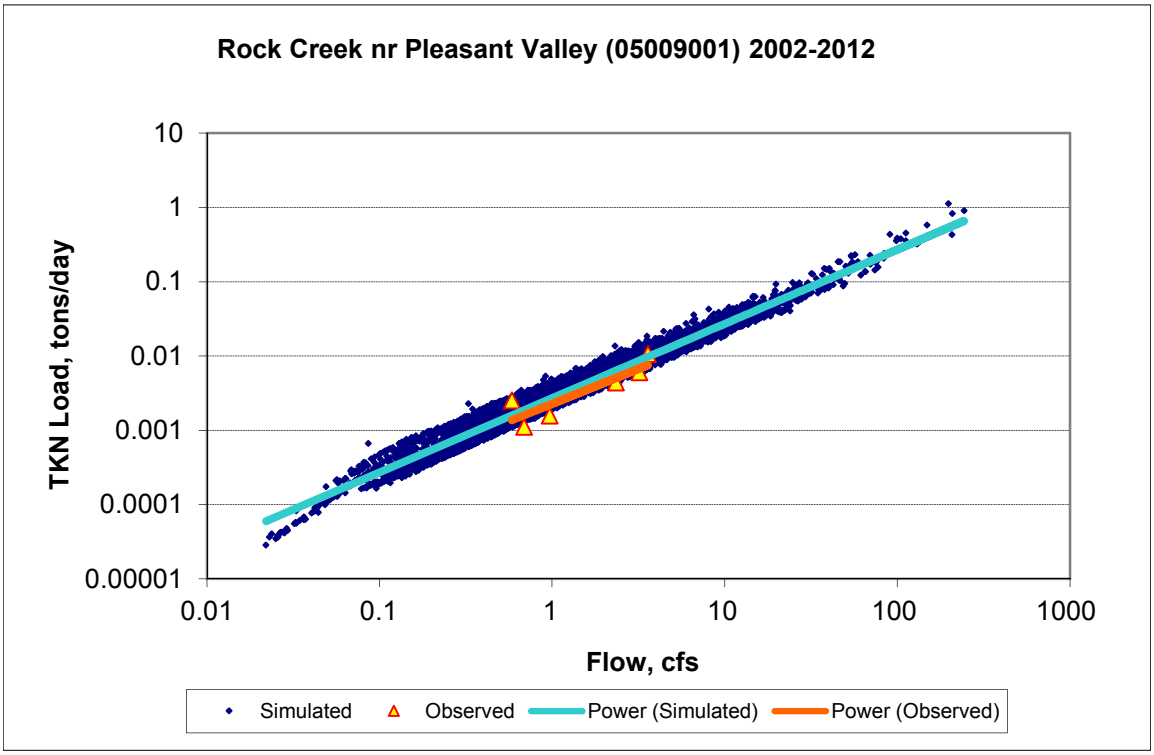

Figure B-51. Power plot of simulated and observed Total Kjeldahl Nitrogen (TKN) load vs flow at Rock Creek nr Pleasant Valley (05009001) (calibration period)

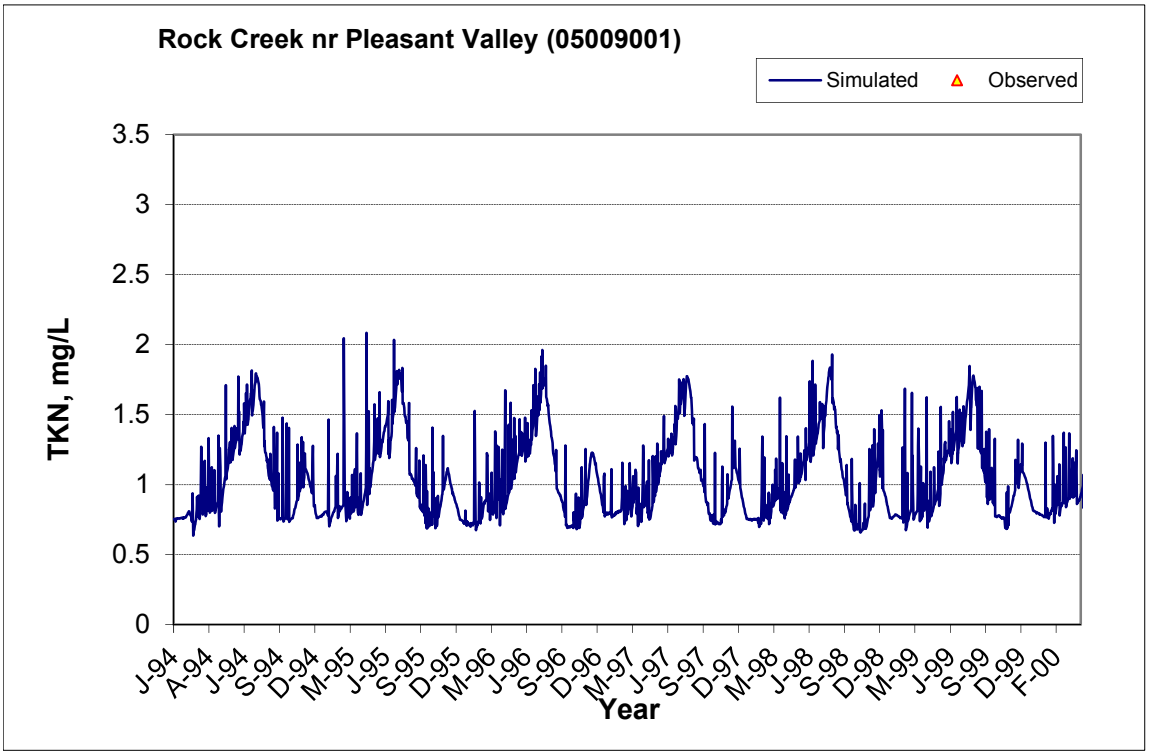

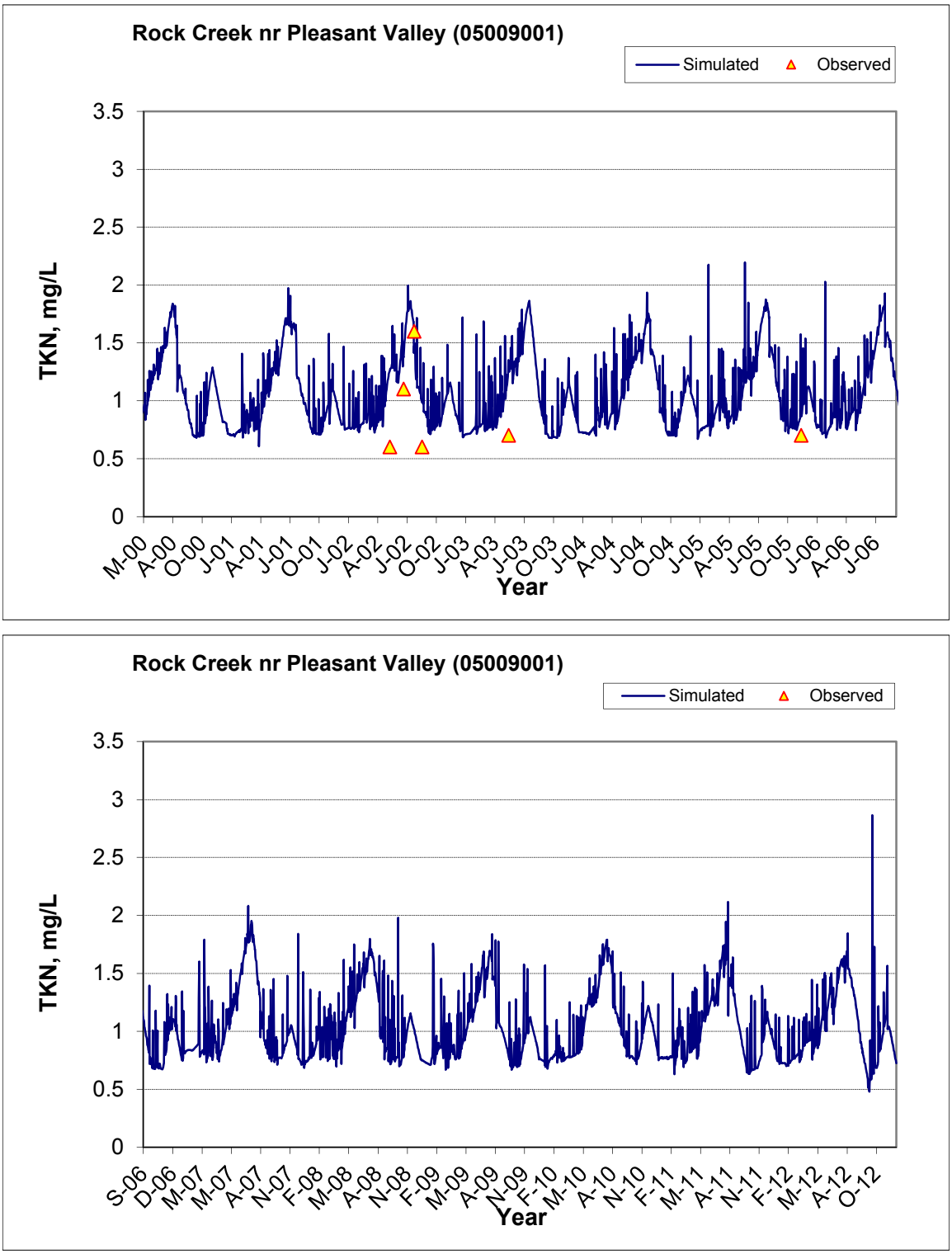

Figure B-52. Time series of observed and simulated Total Kjeldahl Nitrogen (TKN) concentration at Rock Creek nr Pleasant Valley (05009001)

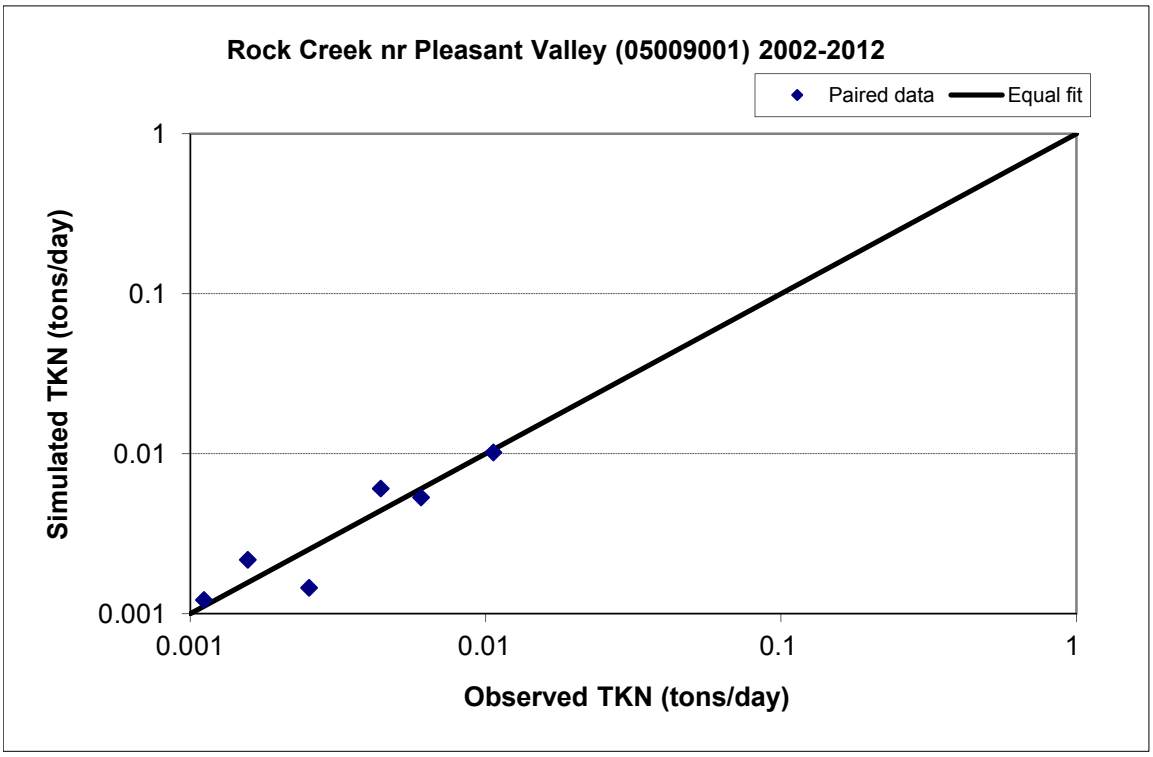

Figure B-53. Paired simulated vs. observed Total Kjeldahl Nitrogen (TKN) load at Rock Creek nr Pleasant Valley (05009001) (calibration period)

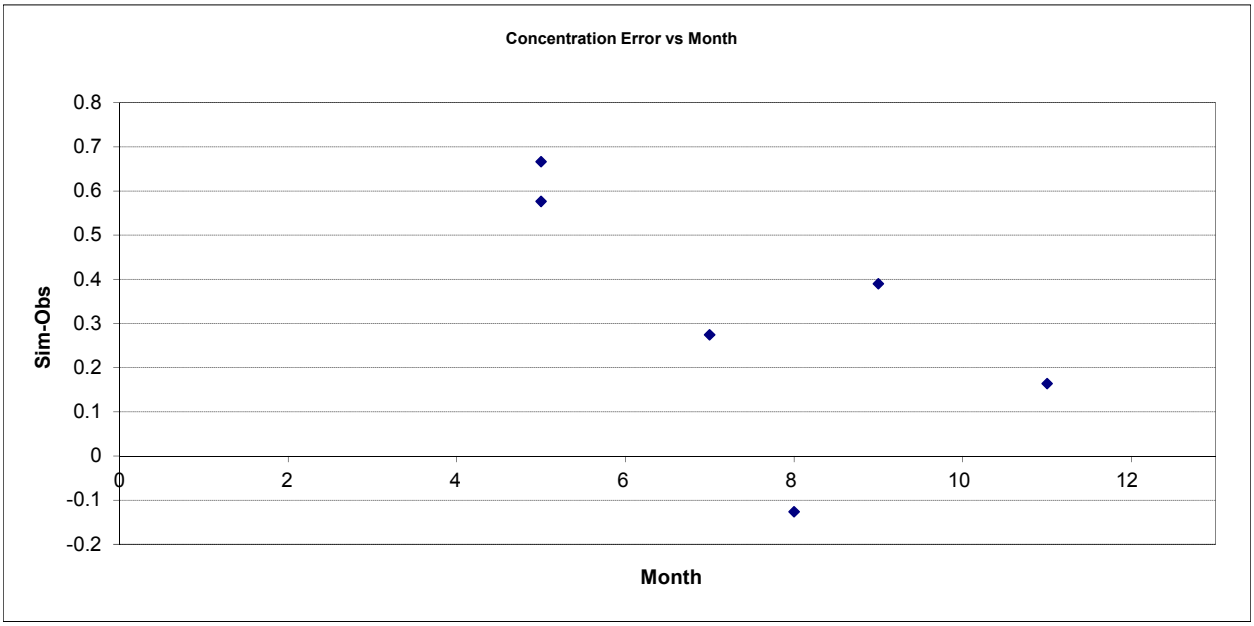

Figure B-54. Residual (Simulated - Observed) vs. Month Total Kjeldahl Nitrogen (TKN) at Rock Creek nr Pleasant Valley (05009001)

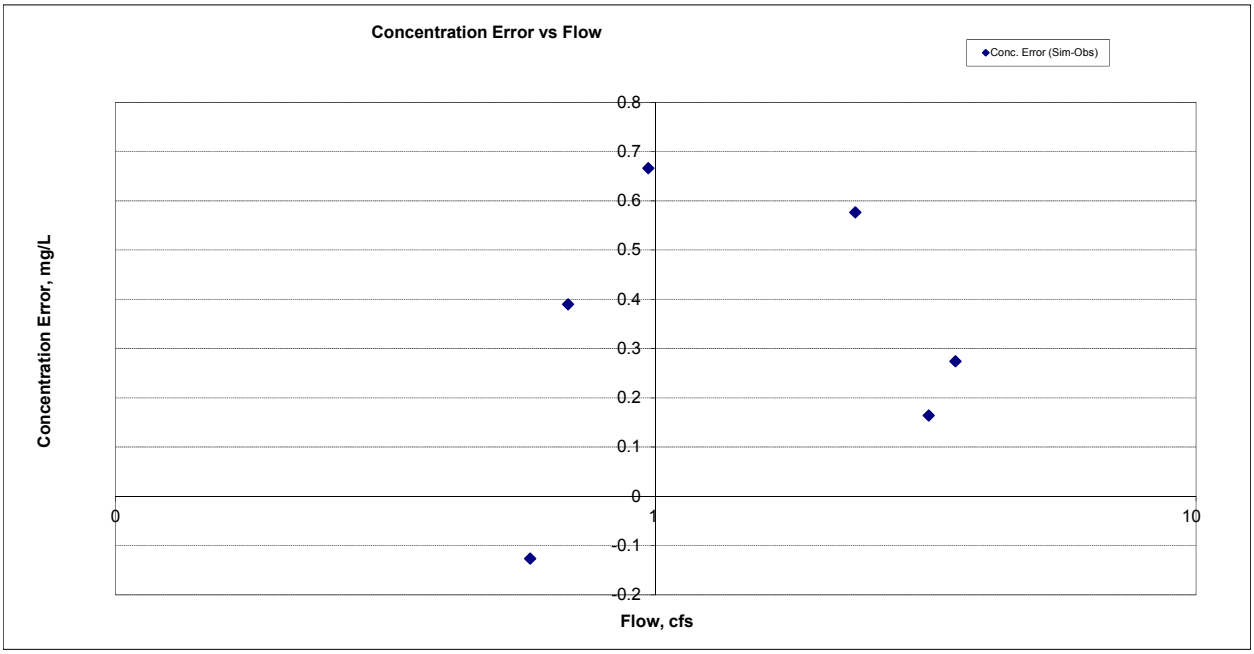

Figure B-55. Residual (Simulated - Observed) vs. Flow Total Kjeldahl Nitrogen (TKN) at Rock Creek nr Pleasant Valley (05009001)

B.2.4 Nitrite+ Nitrate Nitrogen (NOx)

Table B-9. Nitrite+ Nitrate Nitrogen (NOx) statistics

Period	1994-2001	2002-2012
Count	ND	14
Concentration Average Error		361.16%
Concentration Median Error		262.40%
Load Average Error		38.14%
Load Median Error		12.28%
Paired t conc		0.00
Paired t load		0.42

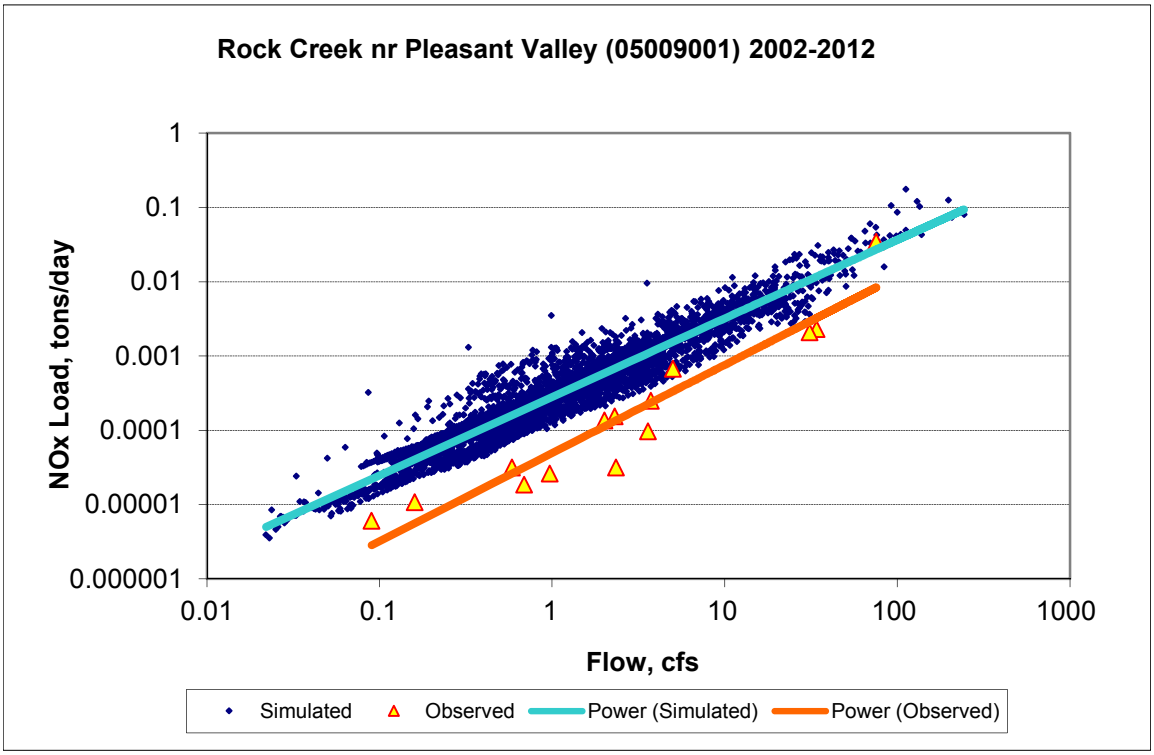

Figure B-56. Power plot of simulated and observed Nitrite+ Nitrate Nitrogen (NOx) load vs flow at Rock Creek nr Pleasant Valley (05009001) (calibration period)

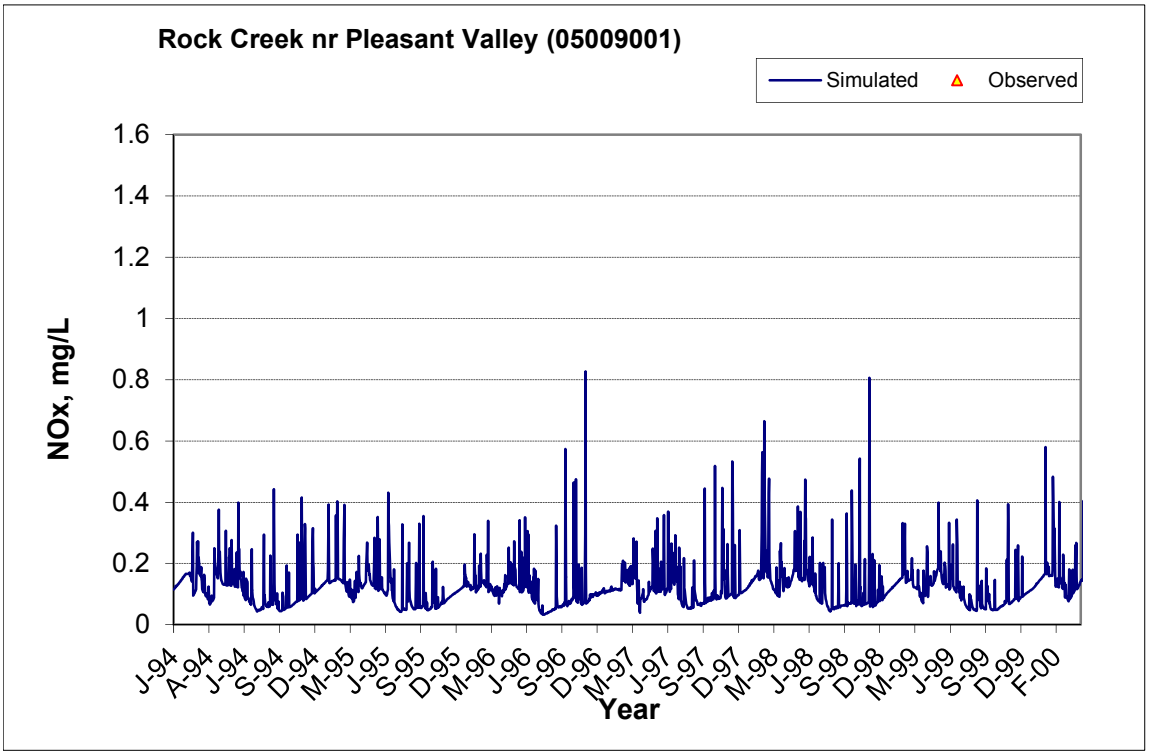

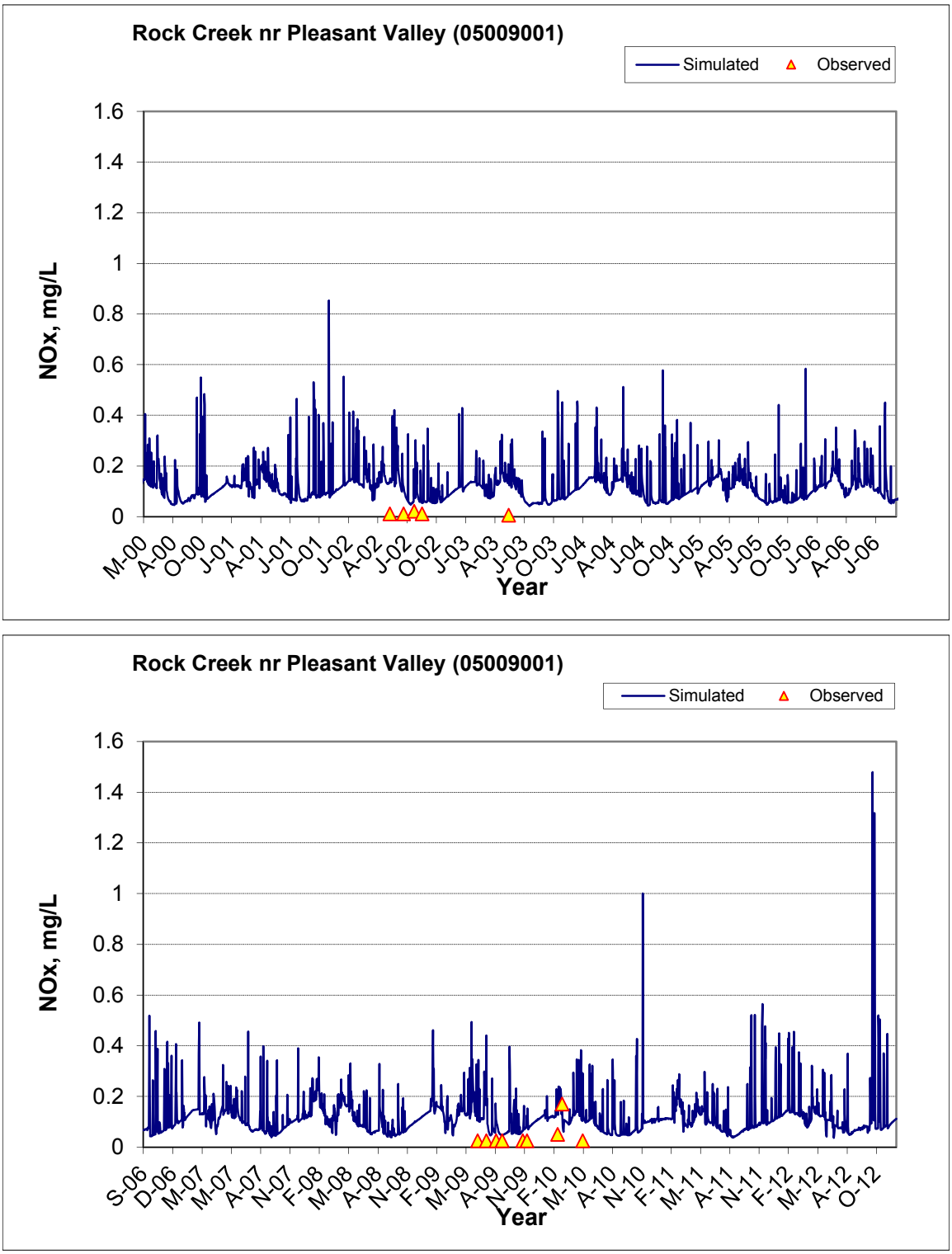

Figure B-57. Time series of observed and simulated Nitrite+ Nitrate Nitrogen (NOx) concentration at Rock Creek nr Pleasant Valley (05009001)

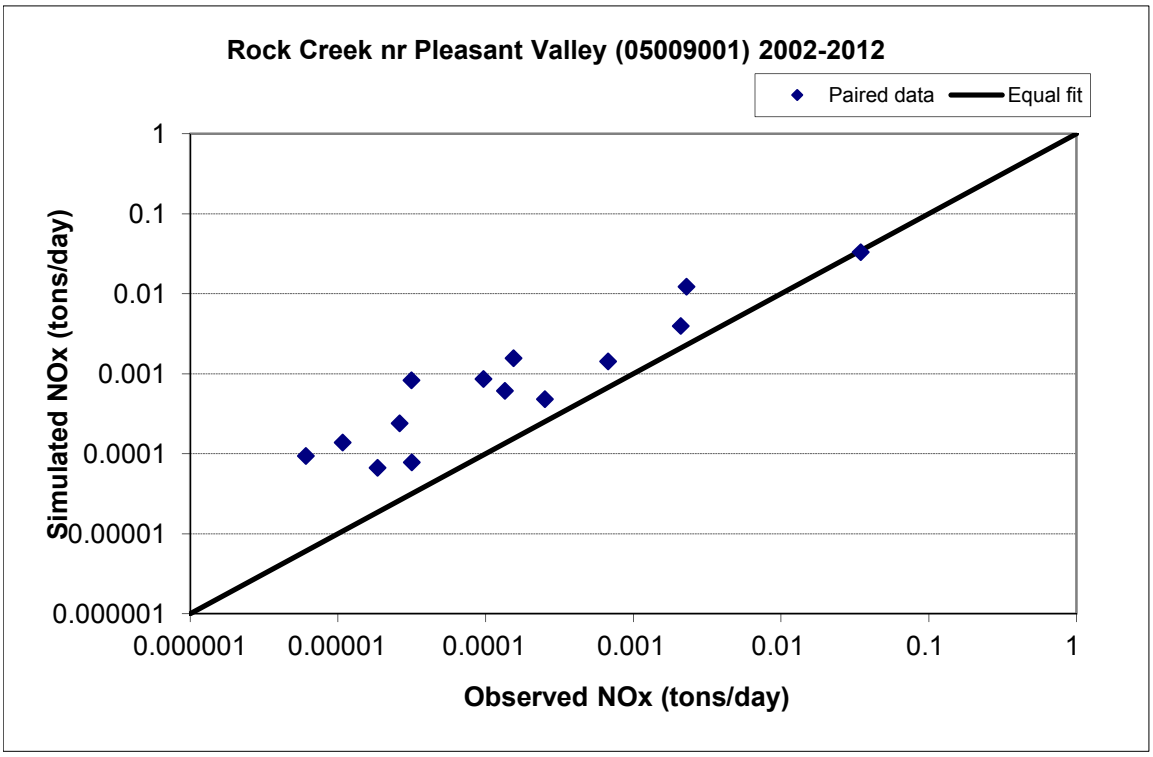

Figure B-58. Paired simulated vs. observed Nitrite+ Nitrate Nitrogen (NOx) load at Rock Creek nr Pleasant Valley (05009001) (calibration period)

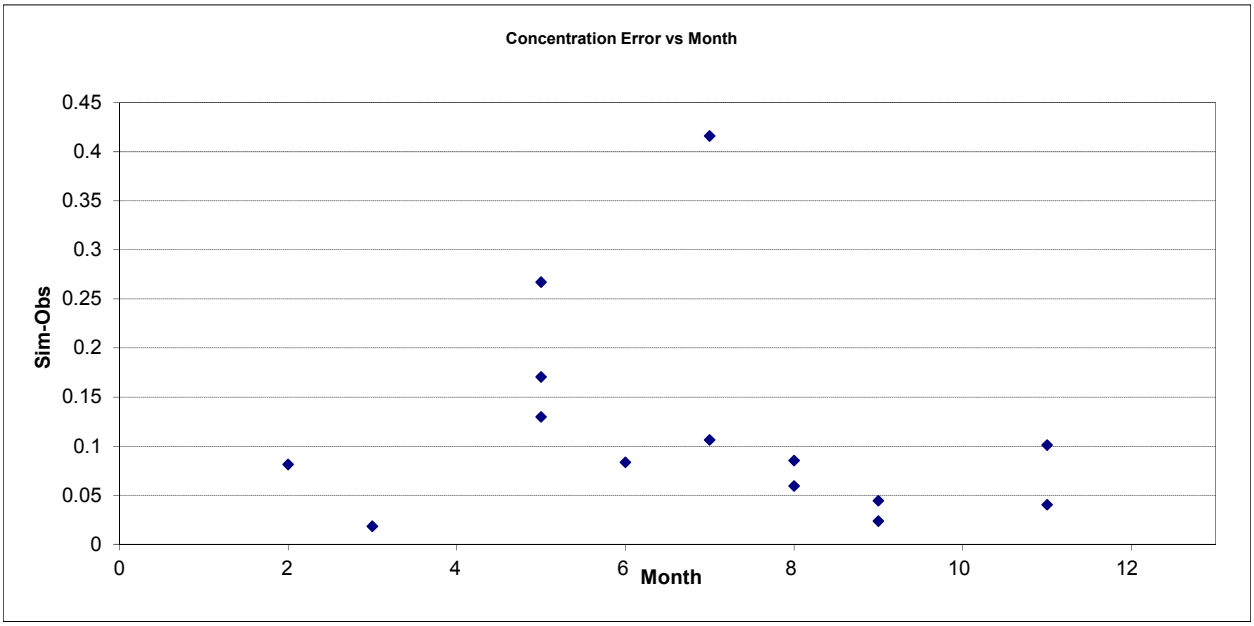

Figure B-59. Residual (Simulated - Observed) vs. Month Nitrite+ Nitrate Nitrogen (NOx) at Rock Creek nr Pleasant Valley (05009001)

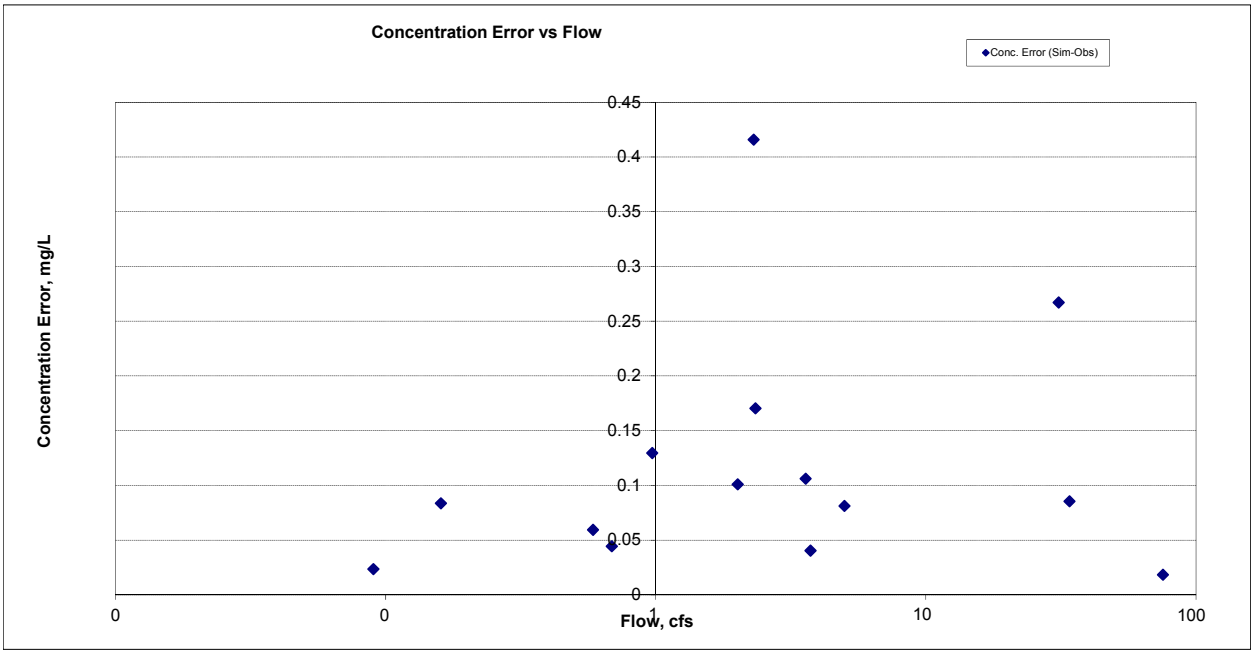

Figure B-60. Residual (Simulated - Observed) vs. Flow Nitrite+ Nitrate Nitrogen (NOx) at Rock Creek nr Pleasant Valley (05009001)

B.2.5 Total Nitrogen (TN)

Table B-10. Total Nitrogen (TN) statistics

Period	1994-2001	2002-2012
Count	ND	5
Concentration Average Error		49.01%
Concentration Median Error		46.54%
Load Average Error		13.08%
Load Median Error		7.85%
Paired t conc		0.07
Paired t load		0.56

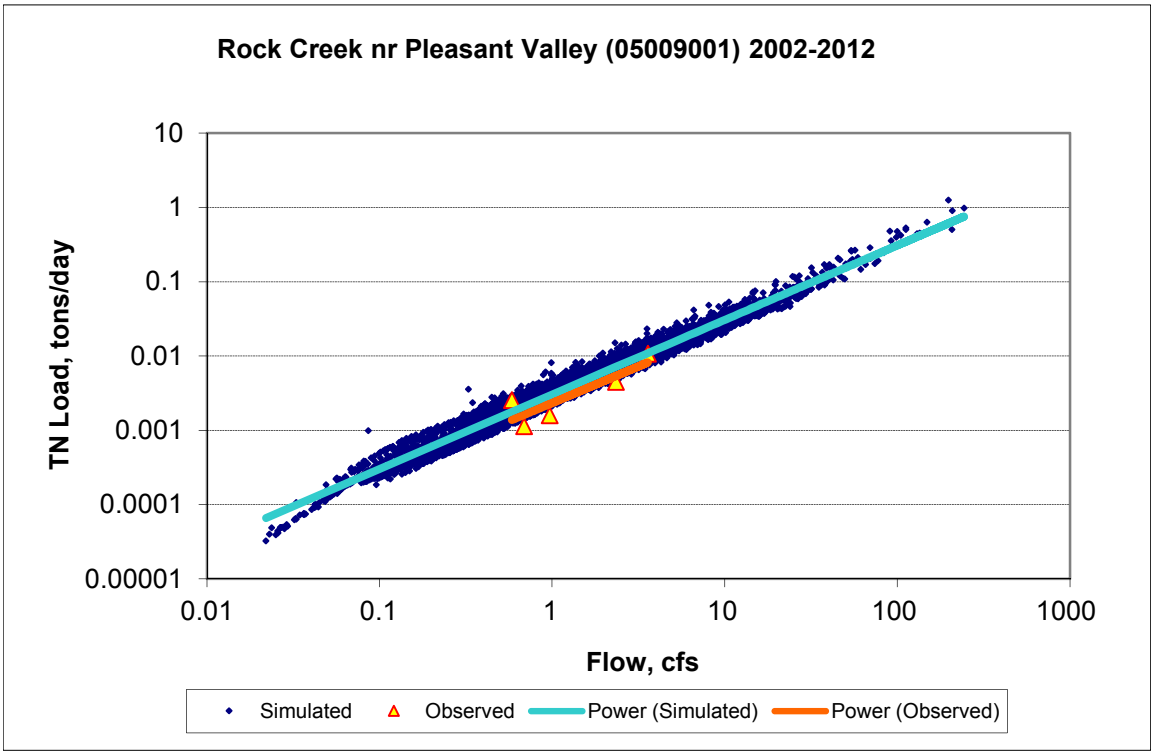

Figure B-61. Power plot of simulated and observed Total Nitrogen (TN) load vs flow at Rock Creek nr Pleasant Valley (05009001) (calibration period)

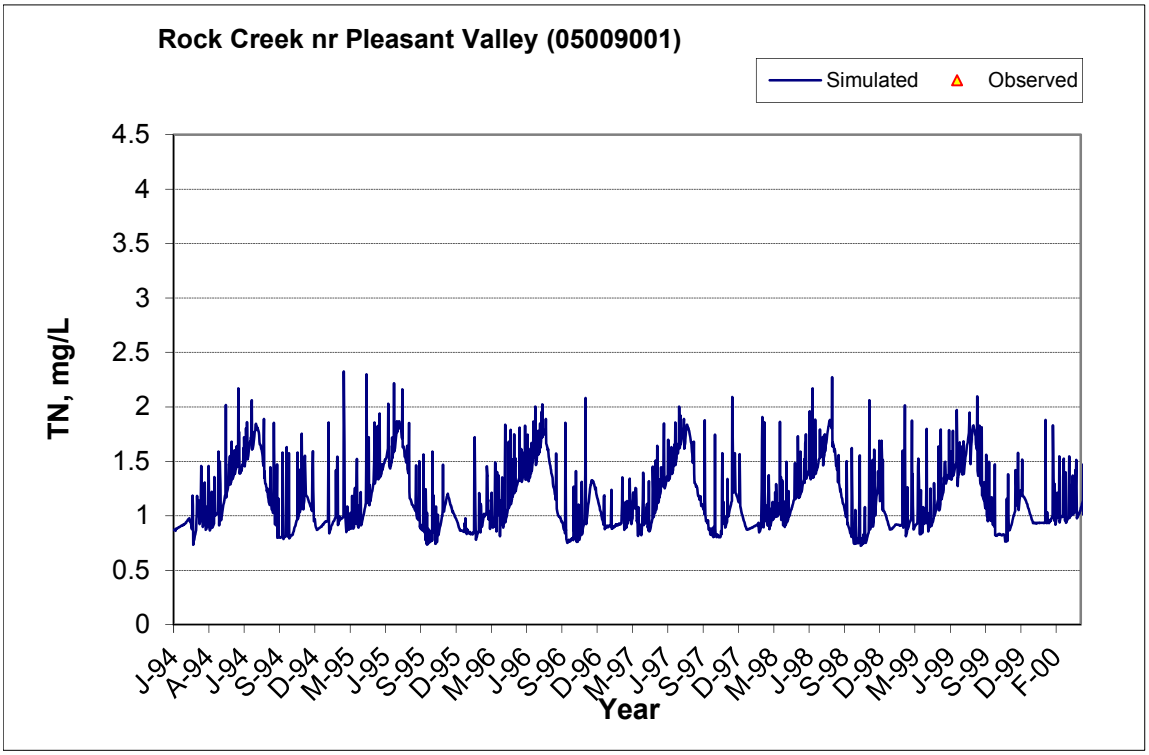

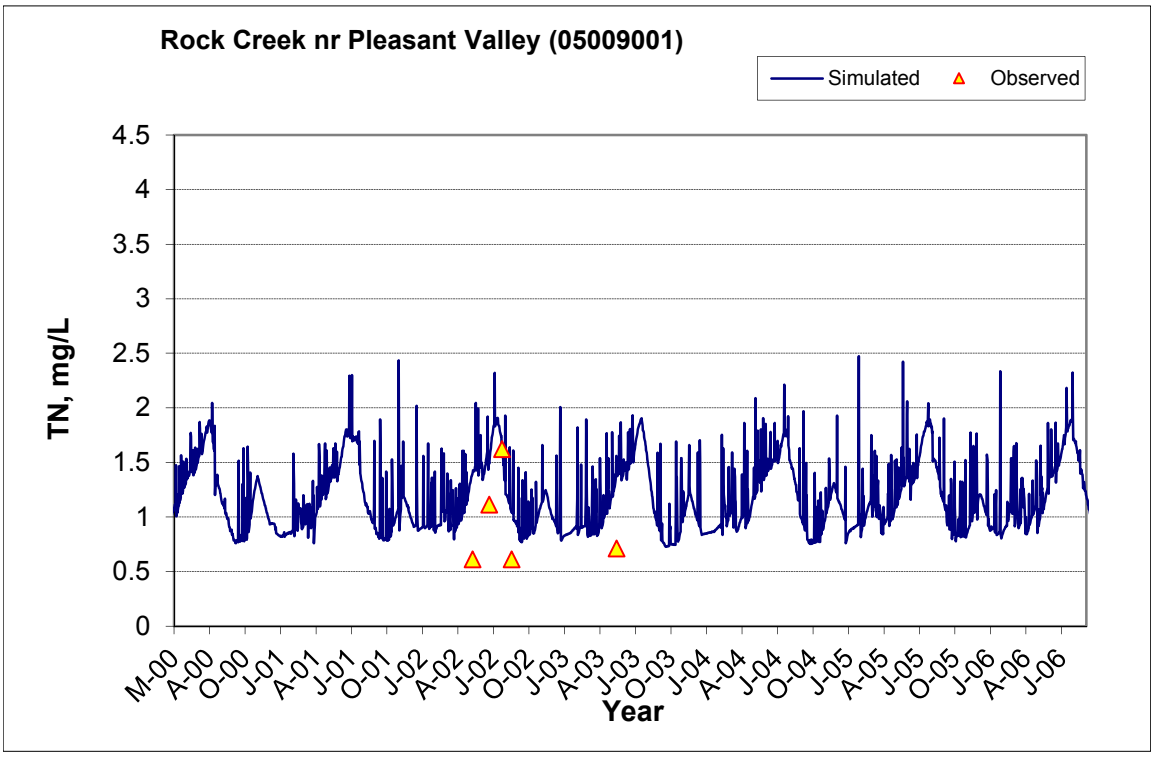

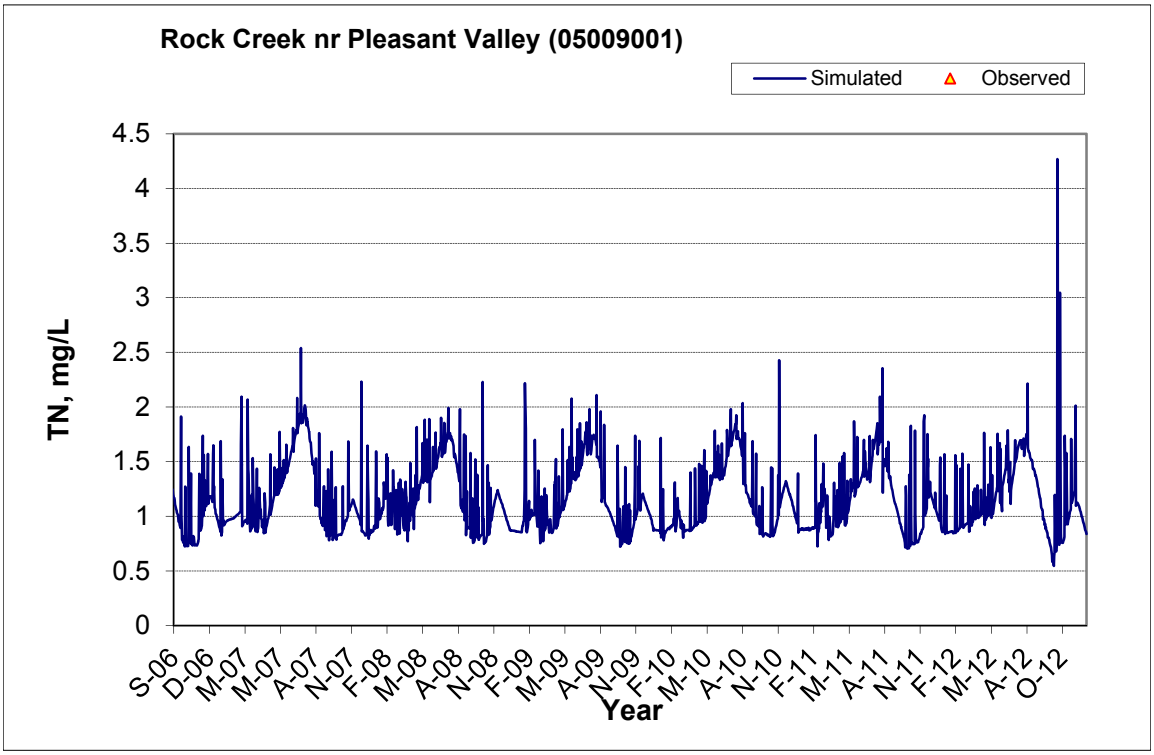

Figure B-62. Time series of observed and simulated Total Nitrogen (TN) concentration at Rock Creek nr Pleasant Valley (05009001)

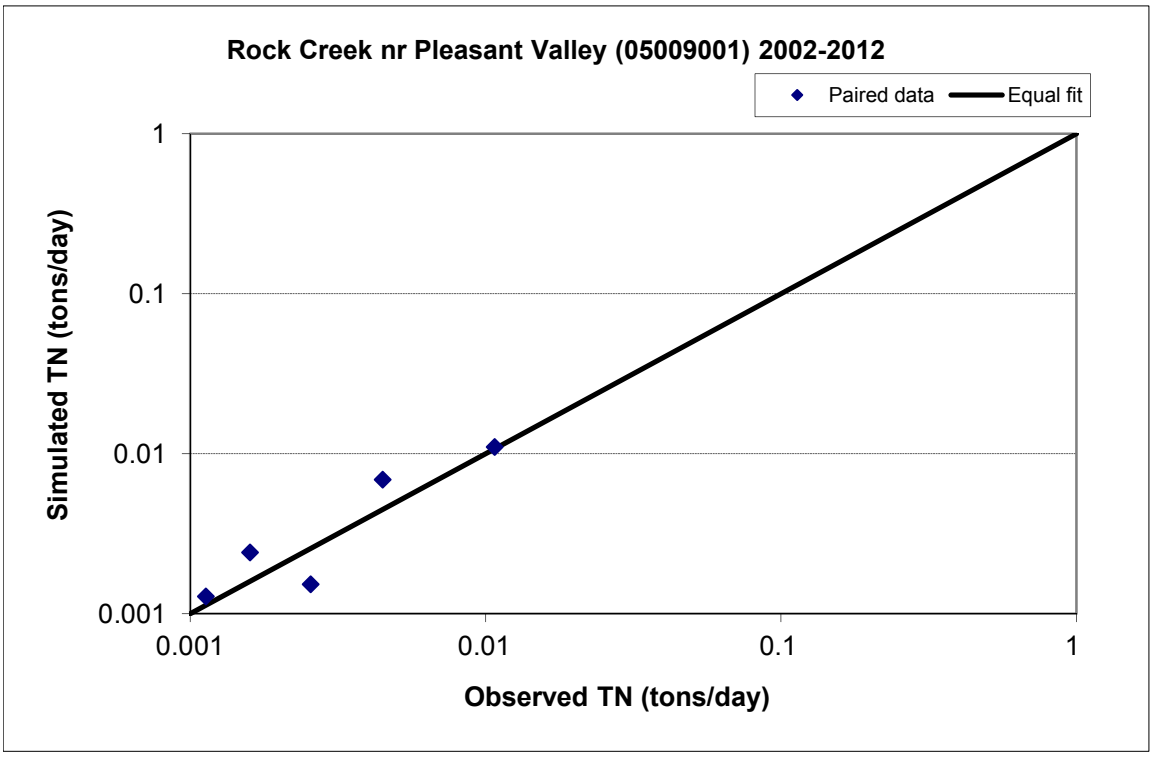

Figure B-63. Paired simulated vs. observed Total Nitrogen (TN) load at Rock Creek nr Pleasant Valley (05009001) (calibration period)

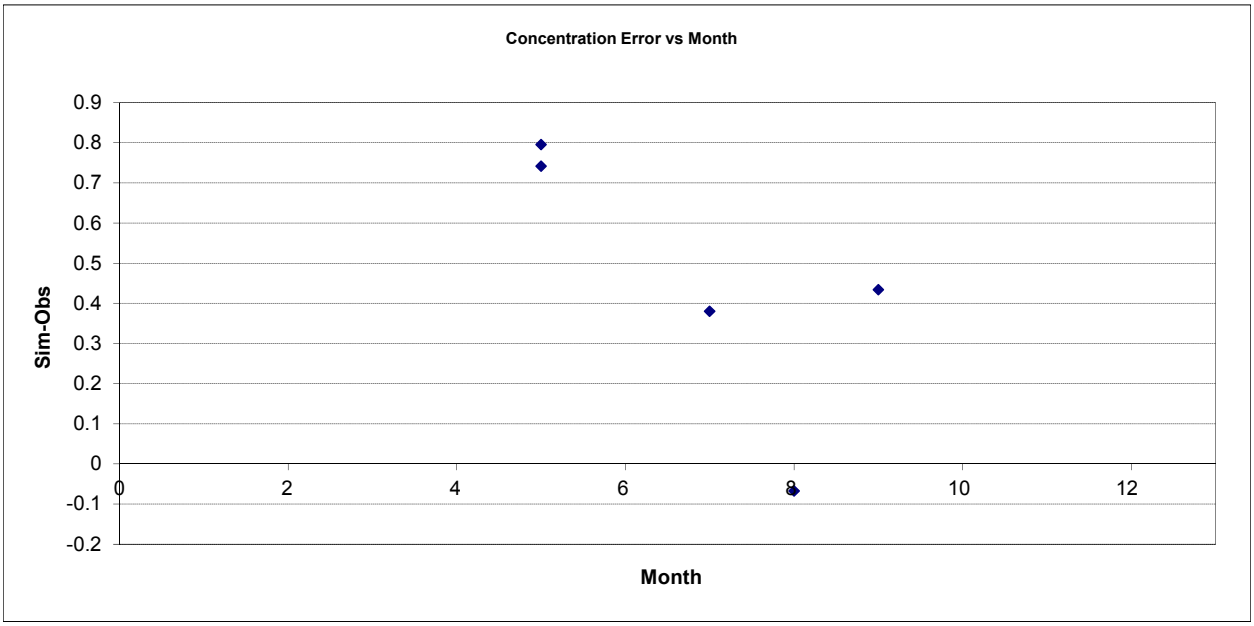

Figure B-64. Residual (Simulated - Observed) vs. Month Total Nitrogen (TN) at Rock Creek nr Pleasant Valley (05009001)

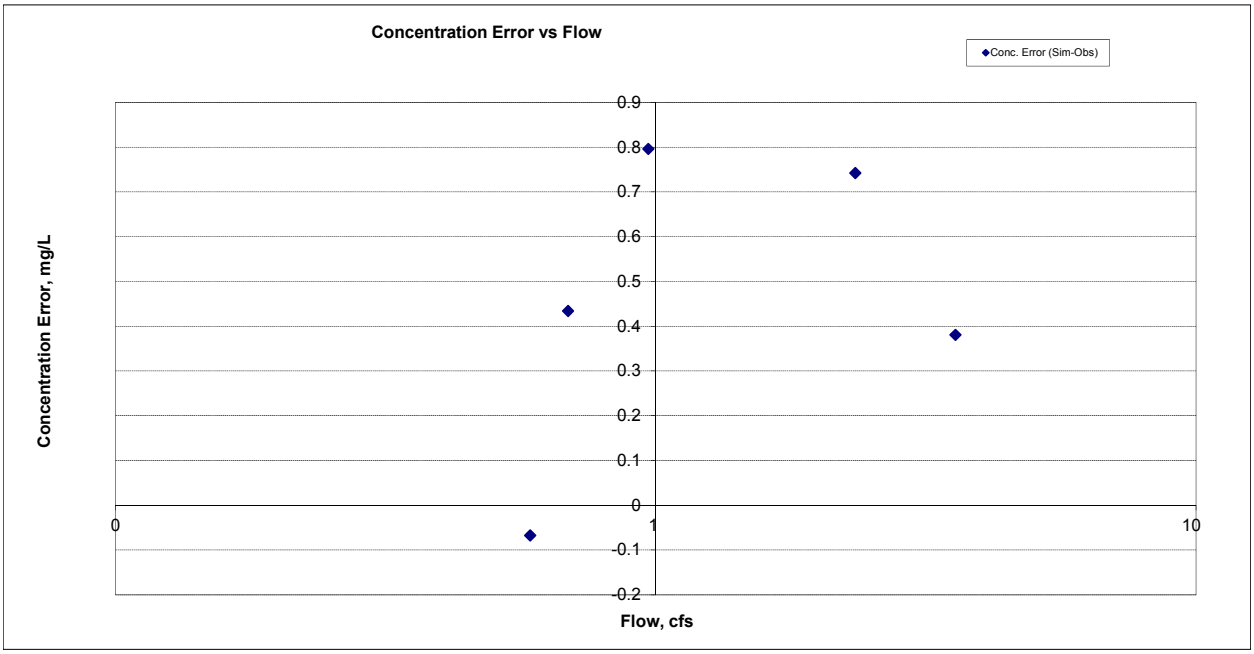

Figure B-65. Residual (Simulated - Observed) vs. Flow Total Nitrogen (TN) at Rock Creek nr Pleasant Valley (05009001)

B.2.6 Soluble Reactive Phosphorus (SRP)

Table B-11. Soluble Reactive Phosphorus (SRP) statistics

Period	1994-2001	2002-2012
Count	ND	15
Concentration Average Error		-5.82%
Concentration Median Error		32.63%
Load Average Error		-19.03%
Load Median Error		0.30%
Paired t conc		0.68
Paired t load		0.51

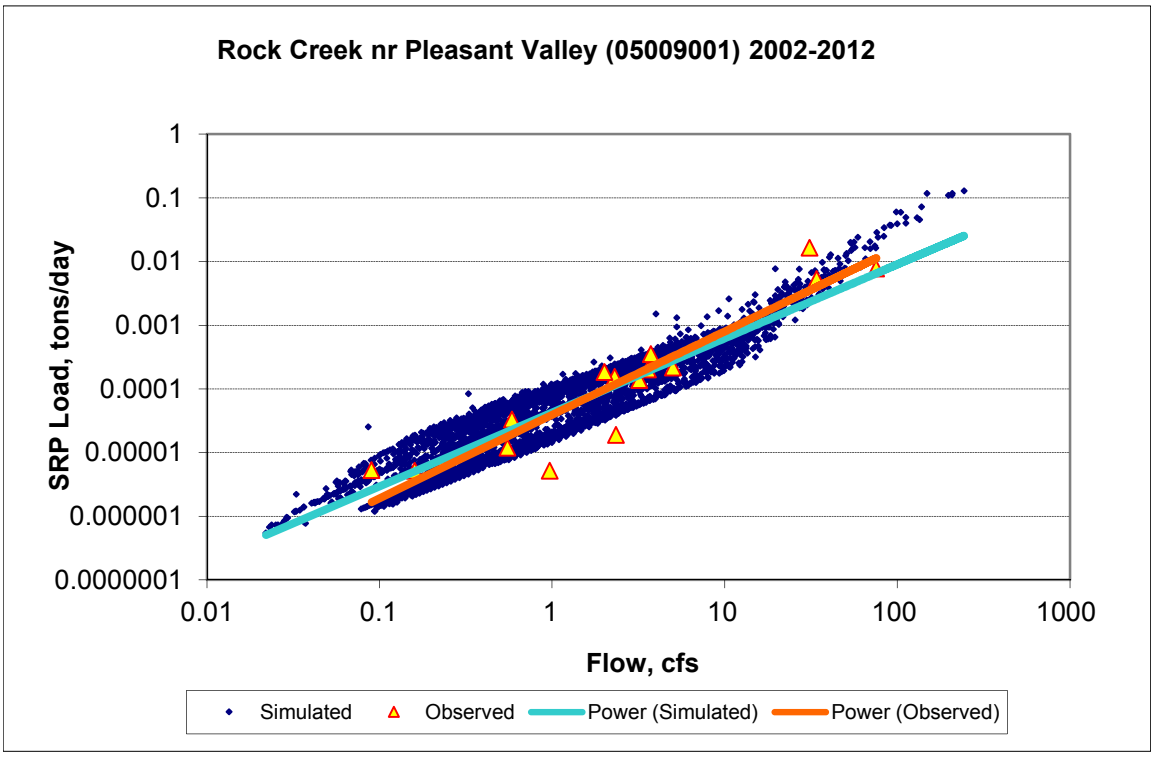

Figure B-66. Power plot of simulated and observed Soluble Reactive Phosphorus (SRP) load vs flow at Rock Creek nr Pleasant Valley (05009001) (calibration period)

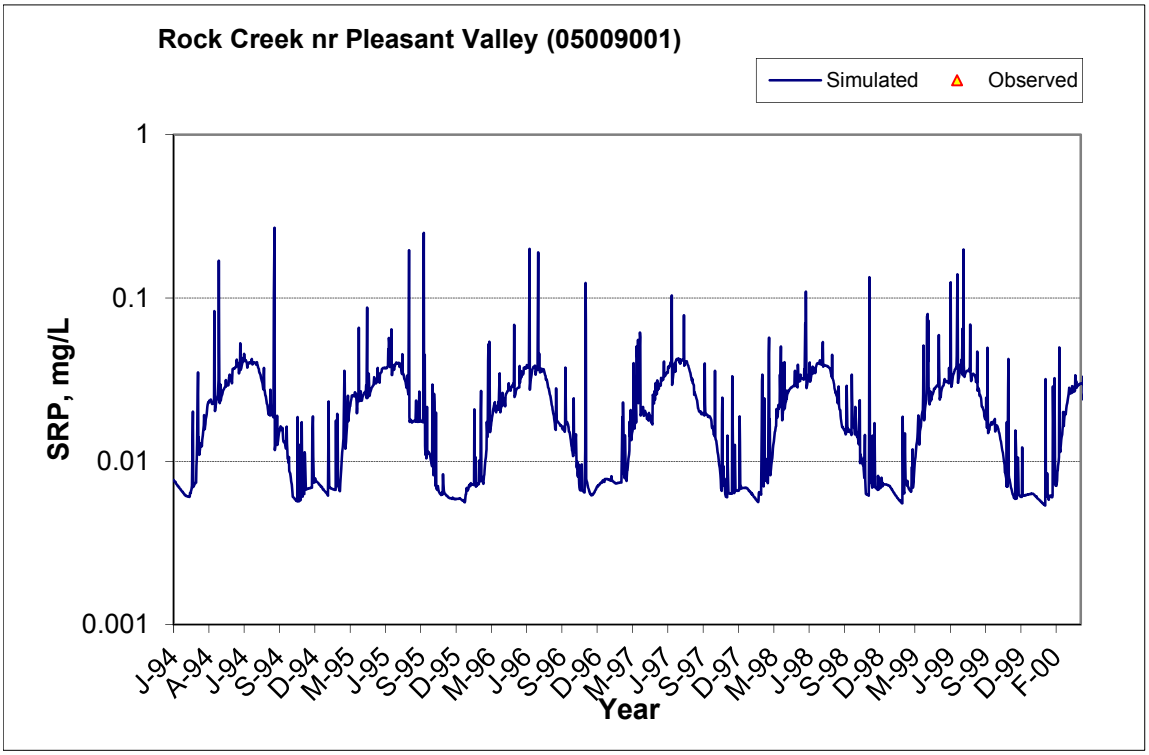

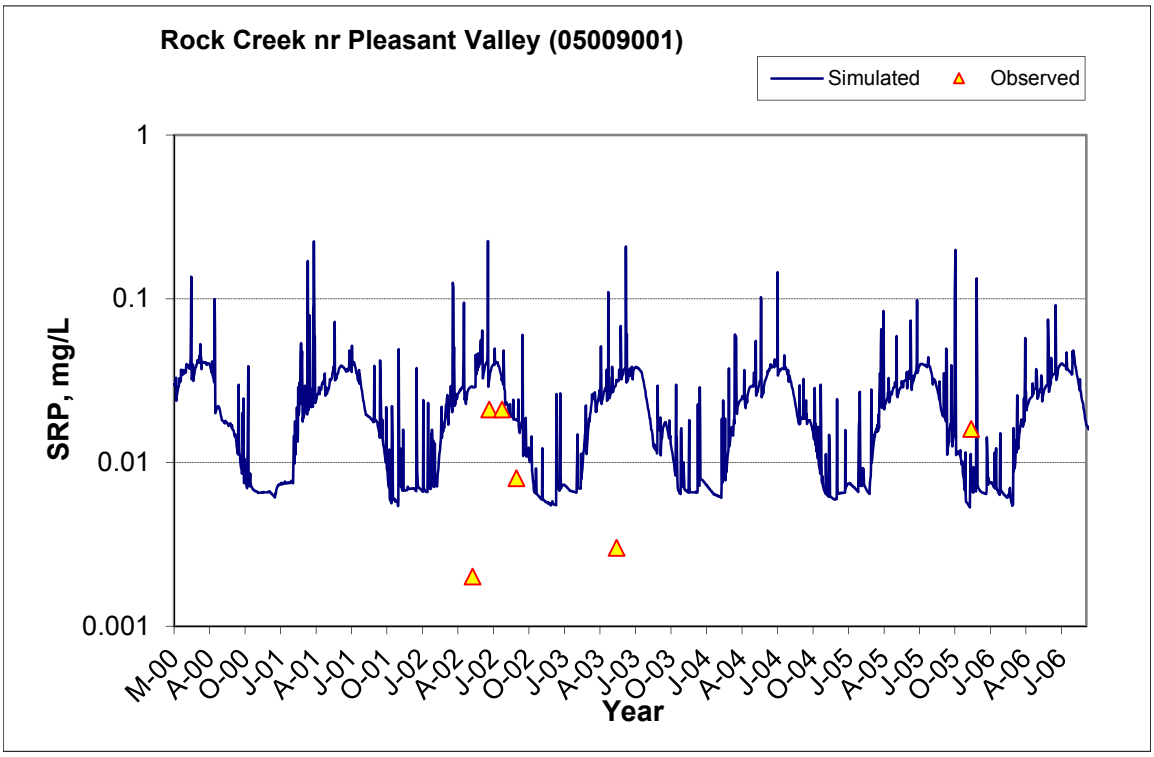

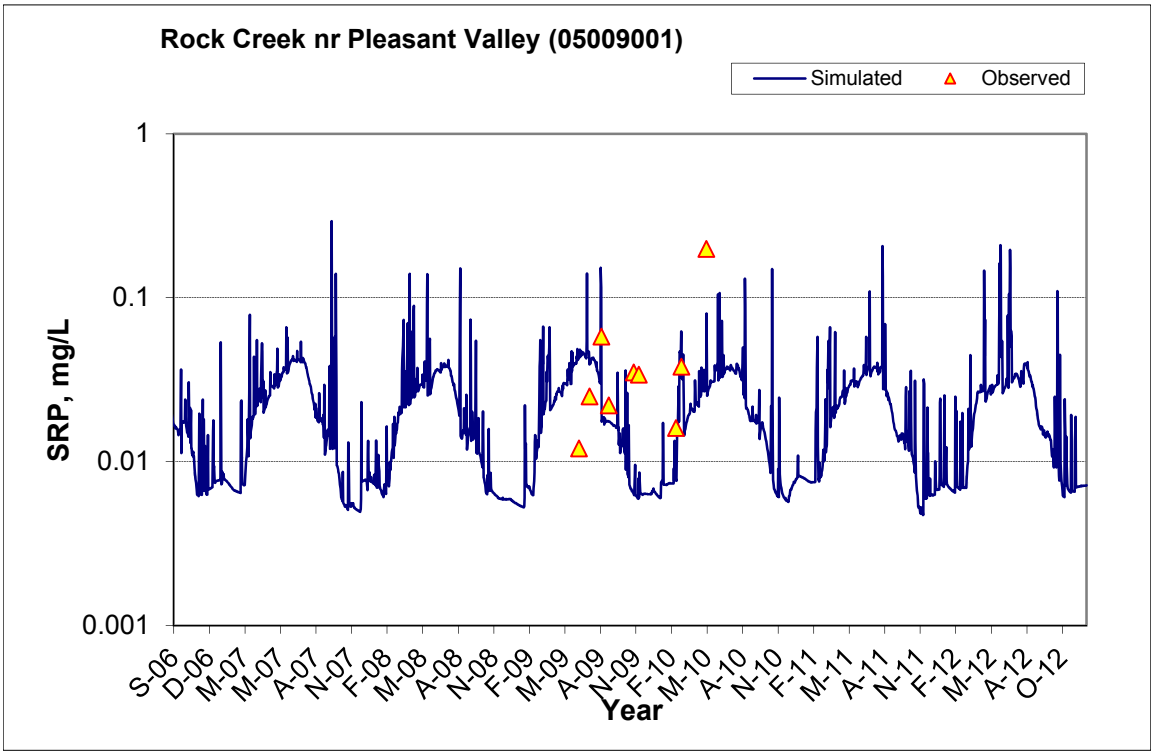

Figure B-67. Time series of observed and simulated Soluble Reactive Phosphorus (SRP) concentration at Rock Creek nr Pleasant Valley (05009001)

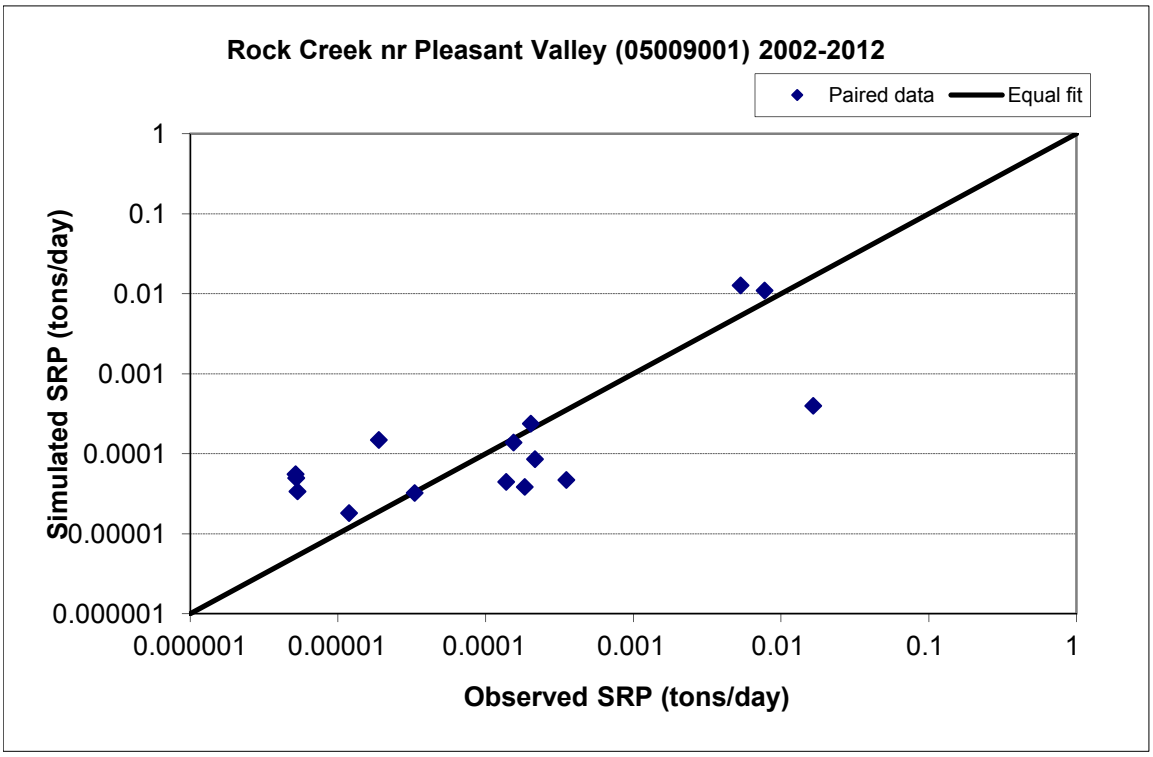

Figure B-68. Paired simulated vs. observed Soluble Reactive Phosphorus (SRP) load at Rock Creek nr Pleasant Valley (05009001) (calibration period)

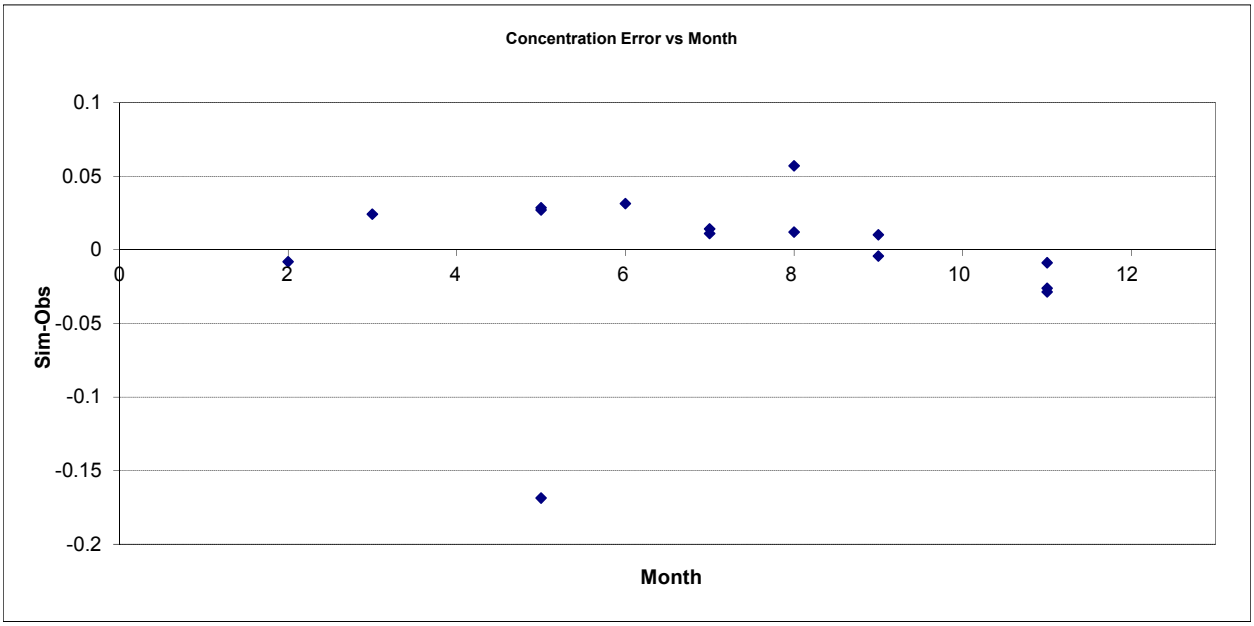

Figure B-69. Residual (Simulated - Observed) vs. Month Soluble Reactive Phosphorus (SRP) at Rock Creek nr Pleasant Valley (05009001)

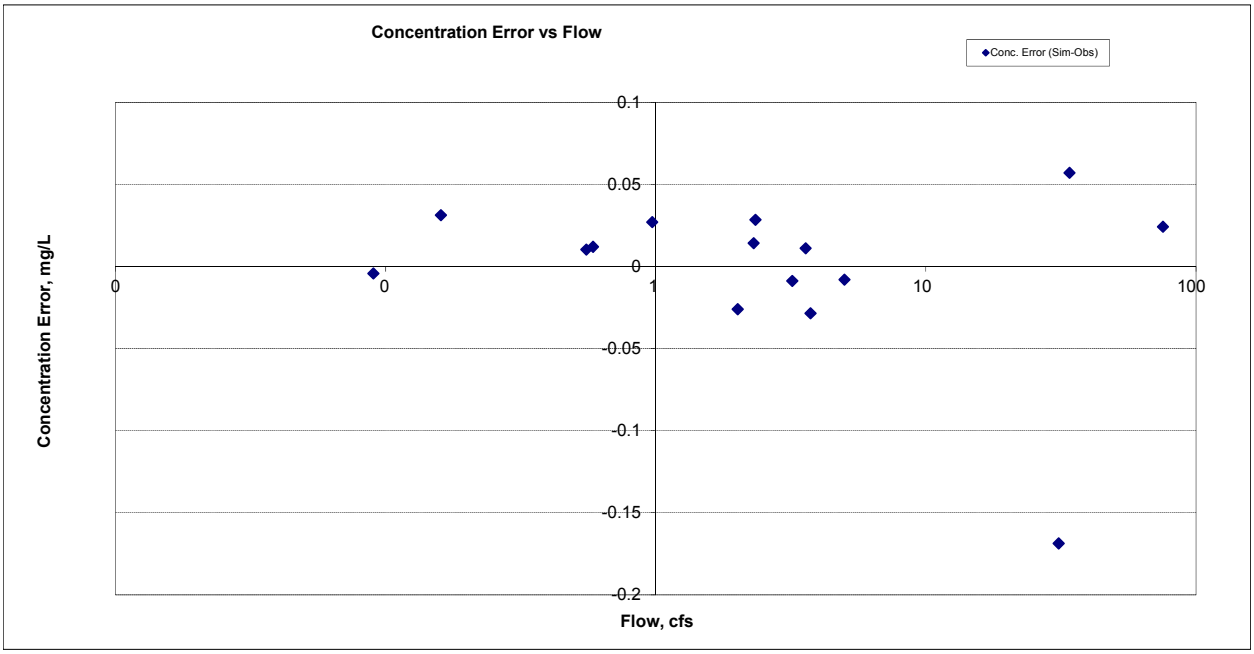

Figure B-70. Residual (Simulated - Observed) vs. Flow Soluble Reactive Phosphorus (SRP) at Rock Creek nr Pleasant Valley (05009001)

B.2.7 Organic Phosphorus (OrgP)

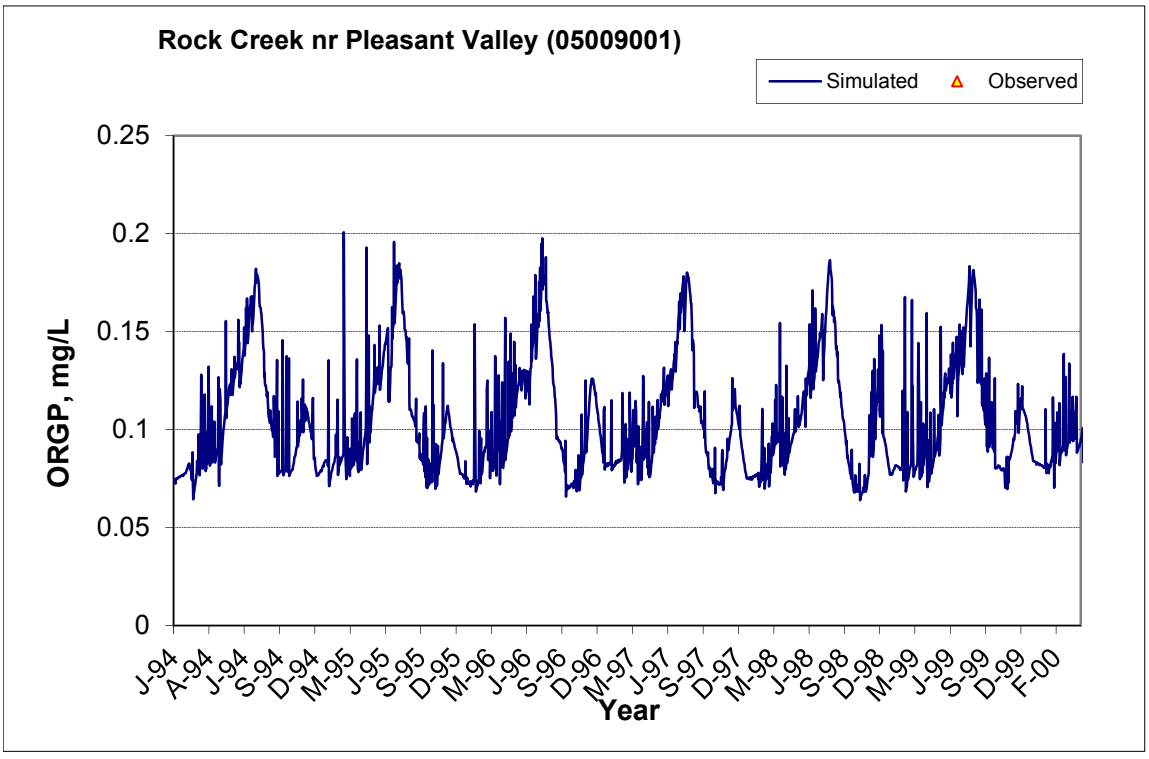

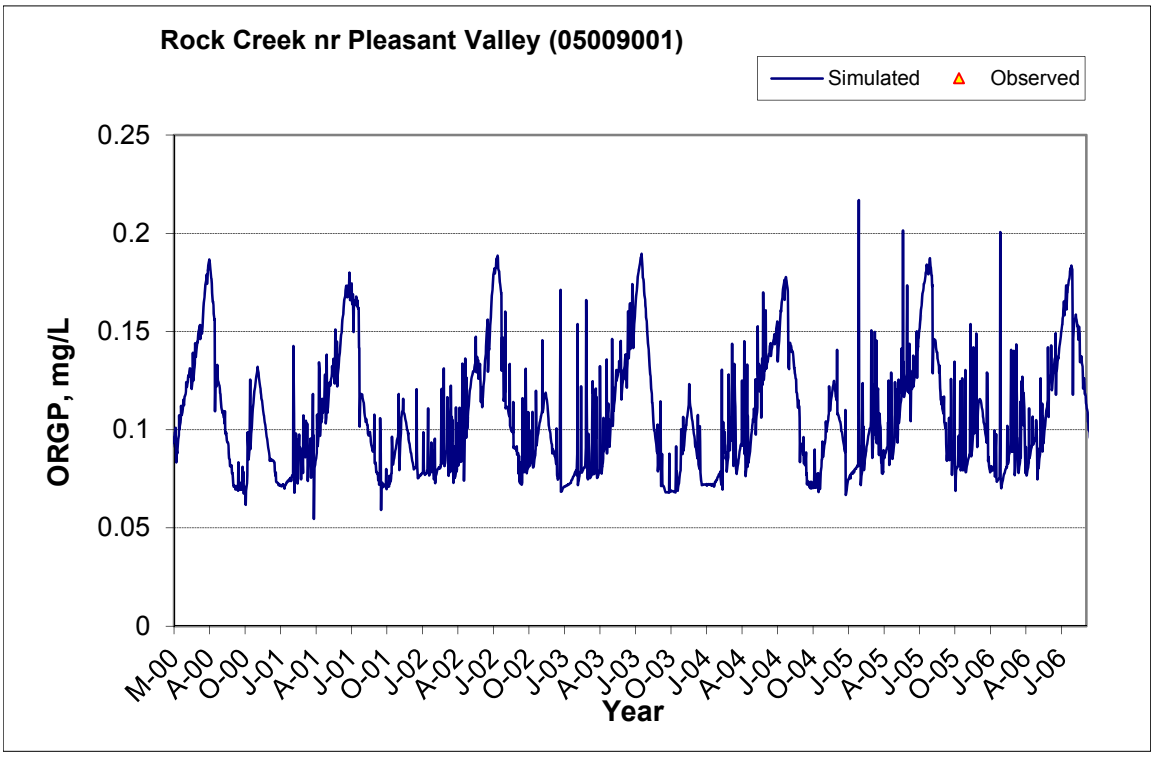

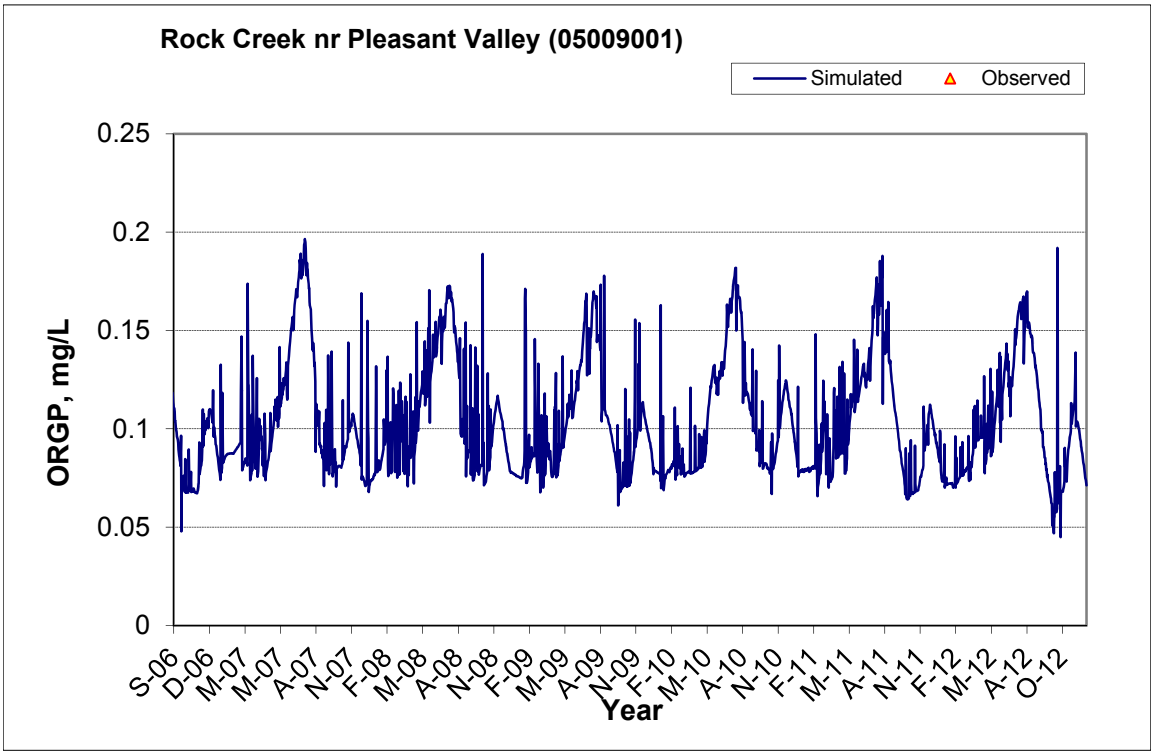

Figure B-71. Time series of observed and simulated Organic Phosphorus (OrgP) concentration at Rock Creek nr Pleasant Valley (05009001)

B.2.8 Total Phosphorus (TP)

Table B-12. Total Phosphorus (TP) statistics

Period	1994-2001	2002-2012
Count	ND	63
Concentration Average Error		27.12%
Concentration Median Error		40.97%
Load Average Error		2.65%
Load Median Error		1.62%
Paired t conc		0.18
Paired t load		0.65

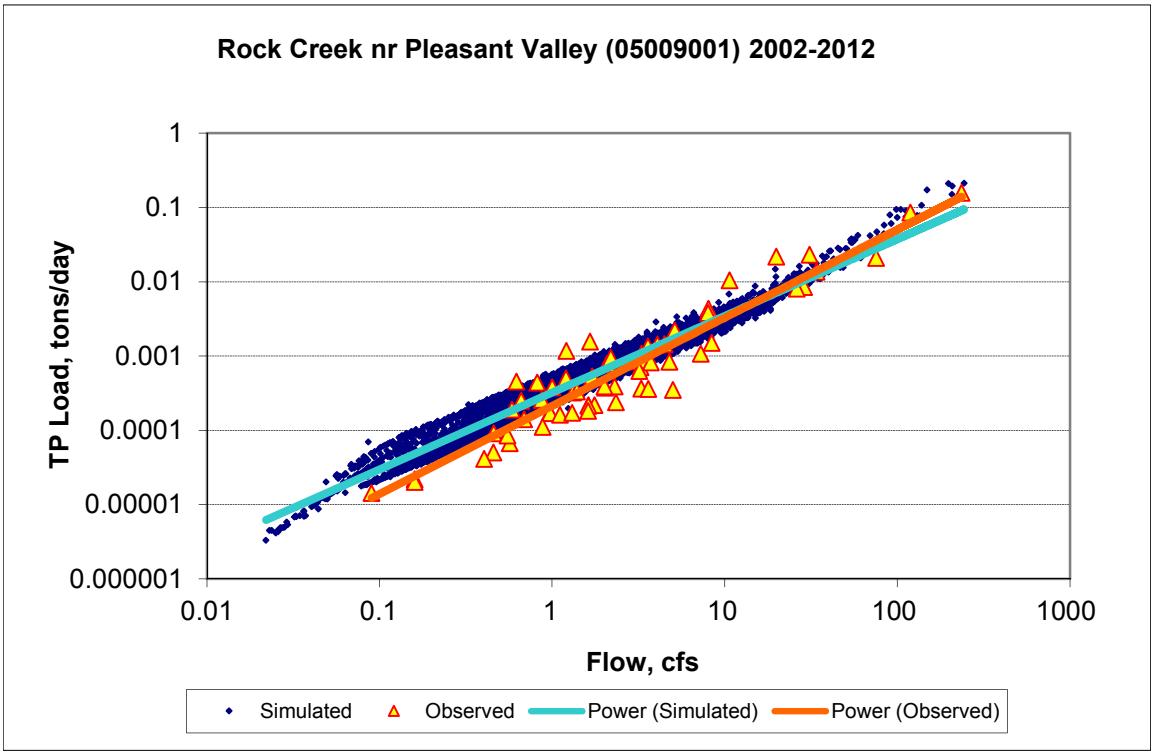

Figure B-72. Power plot of simulated and observed Total Phosphorus (TP) load vs flow at Rock Creek nr Pleasant Valley (05009001) (calibration period)

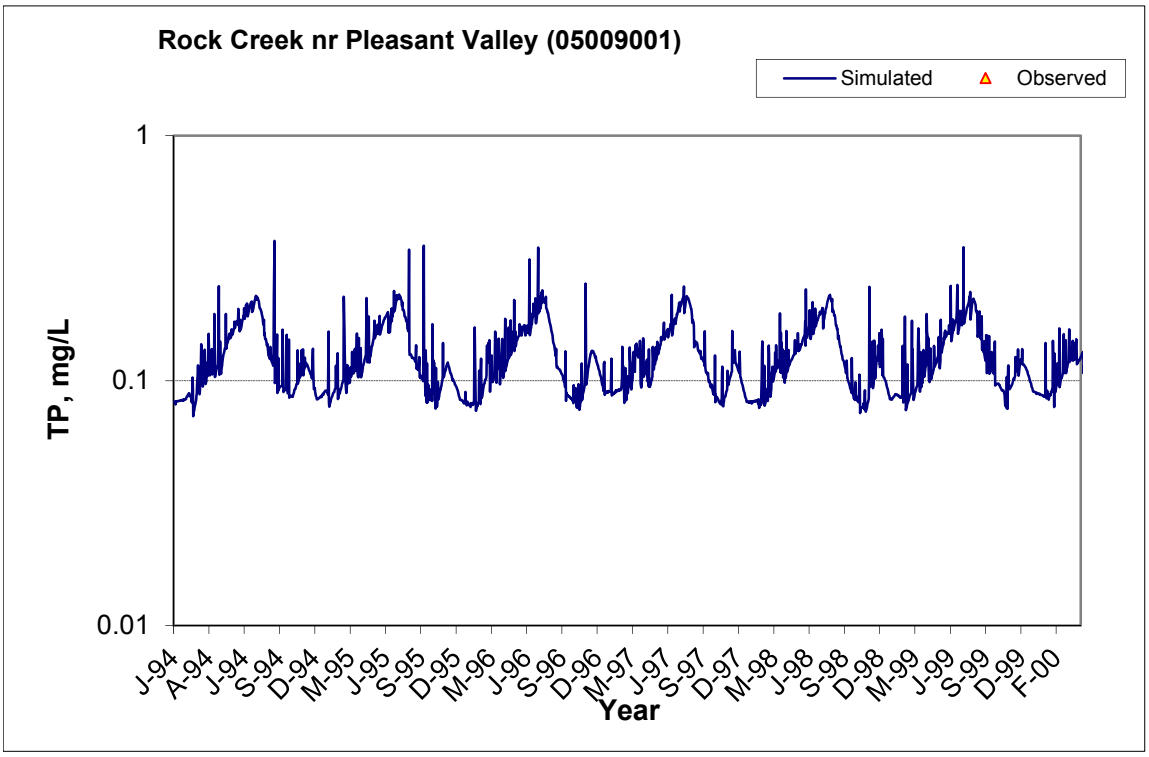
Rock Creek nr Pleasant Valley (05009001)
Simulated
Observed
TP, mg/L
1
0.1
0.01
J-94 A-94 J-94 S-94 D-94 M-95 J-95 S-95 D-95 M-96 J-96 S-96 D-96 M-97 J-97 S-97 D-97 M-98 J-98 S-98 D-98 M-99 J-99 S-99 D-99 F-00
Year

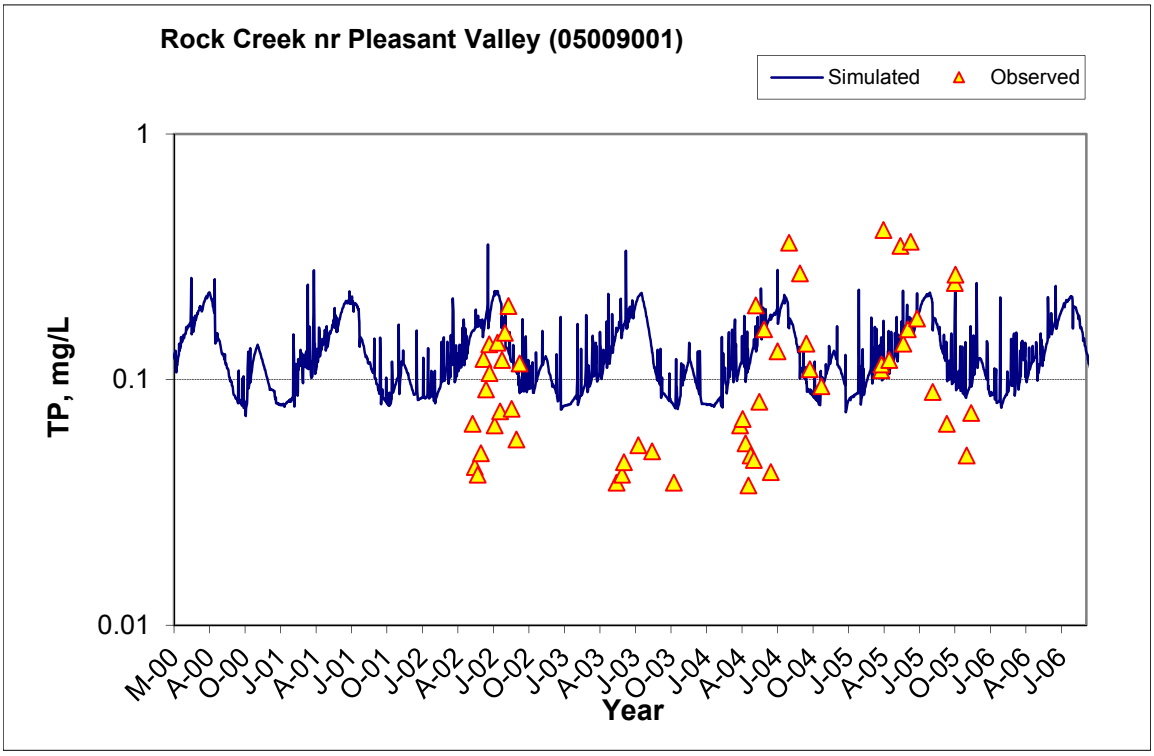
Rock Creek nr Pleasant Valley (05009001)
Simulated
Observed
TP, mg/L
1
0.1
0.01
M-00 A-00 O-00 J-01 A-01 J-01 O-01 J-02 A-02 J-02 O-02 J-03 A-03 J-03 O-03 J-04 A-04 J-04 O-04 J-05 A-05 J-05 O-05 J-06 A-06 J-06
Year

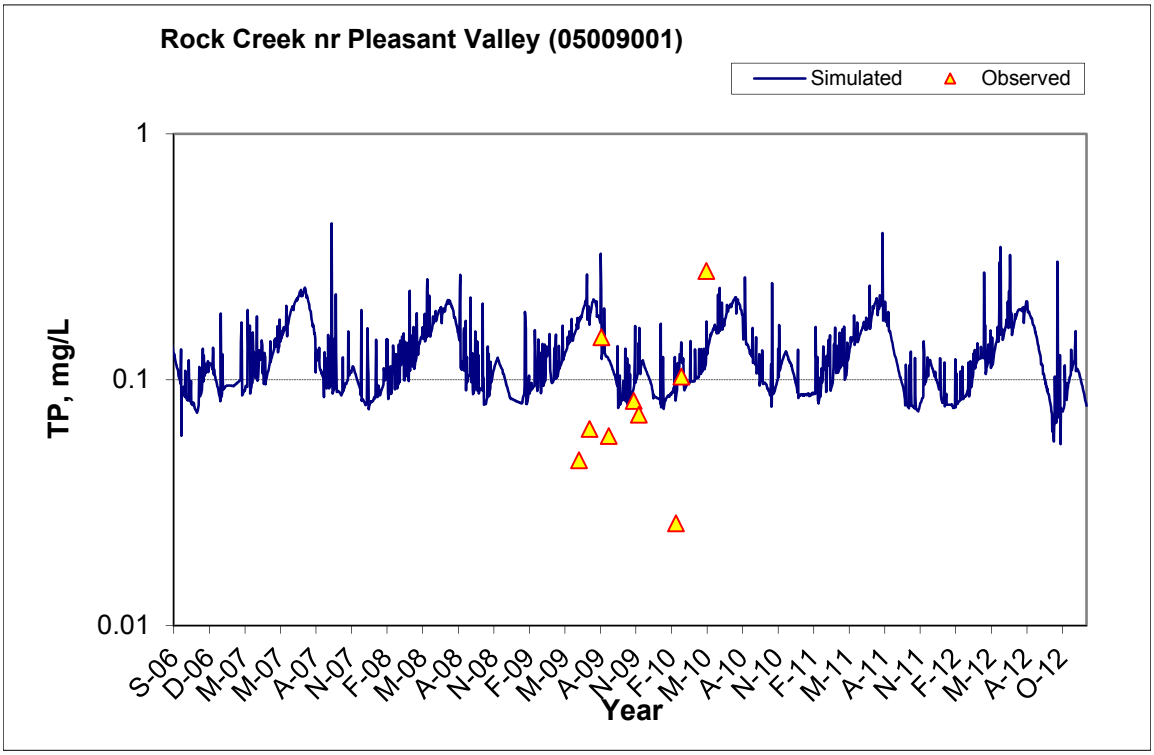

Figure B-73. Time series of observed and simulated Total Phosphorus (TP) concentration at Rock Creek nr Pleasant Valley (05009001)

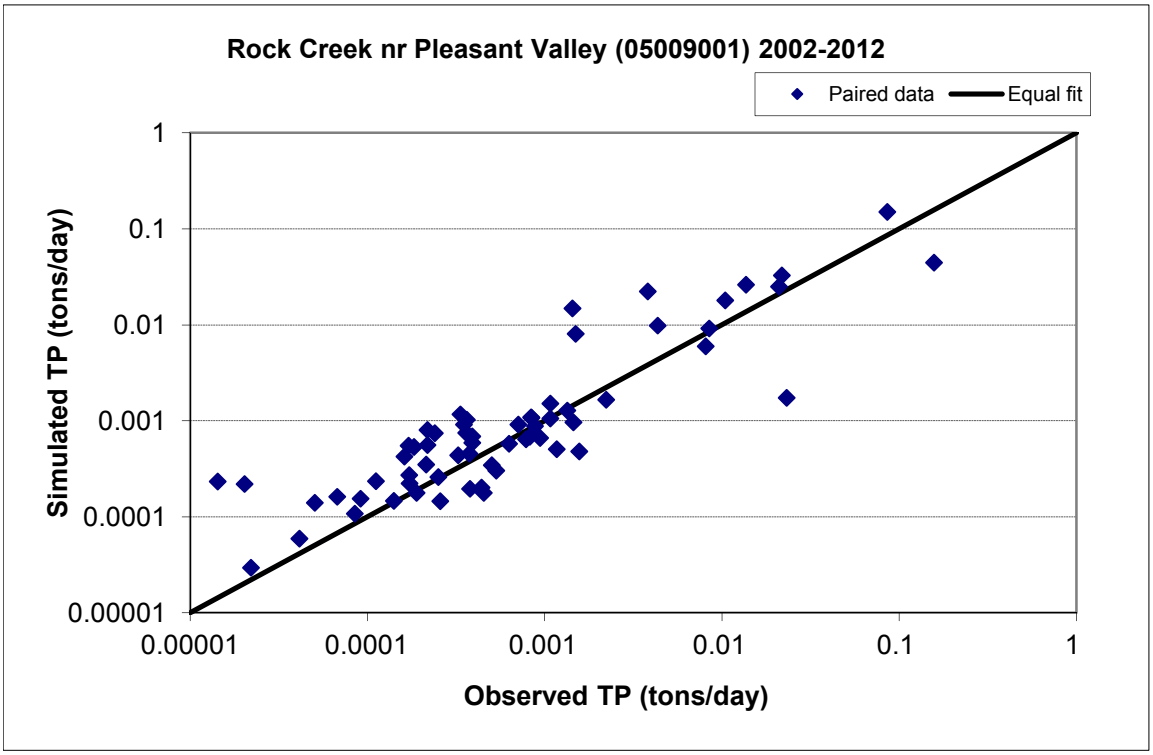

Figure B-74. Paired simulated vs. observed Total Phosphorus (TP) load at Rock Creek nr Pleasant Valley (05009001) (calibration period)

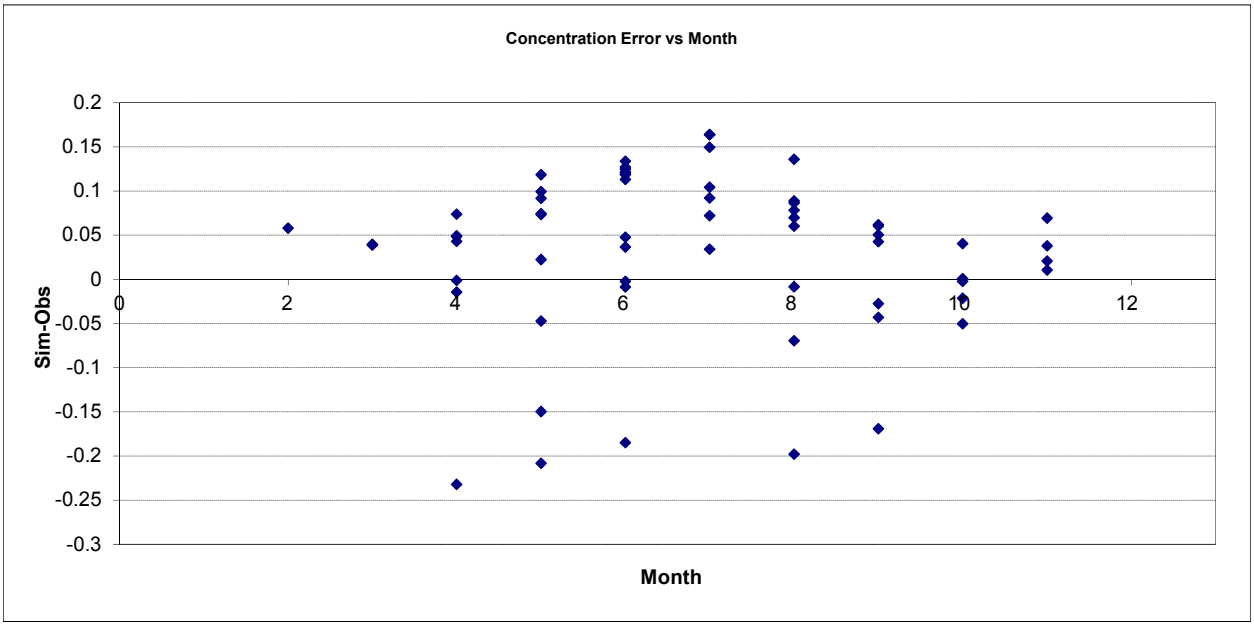

Figure B-75. Residual (Simulated - Observed) vs. Month Total Phosphorus (TP) at Rock Creek nr Pleasant Valley (05009001)

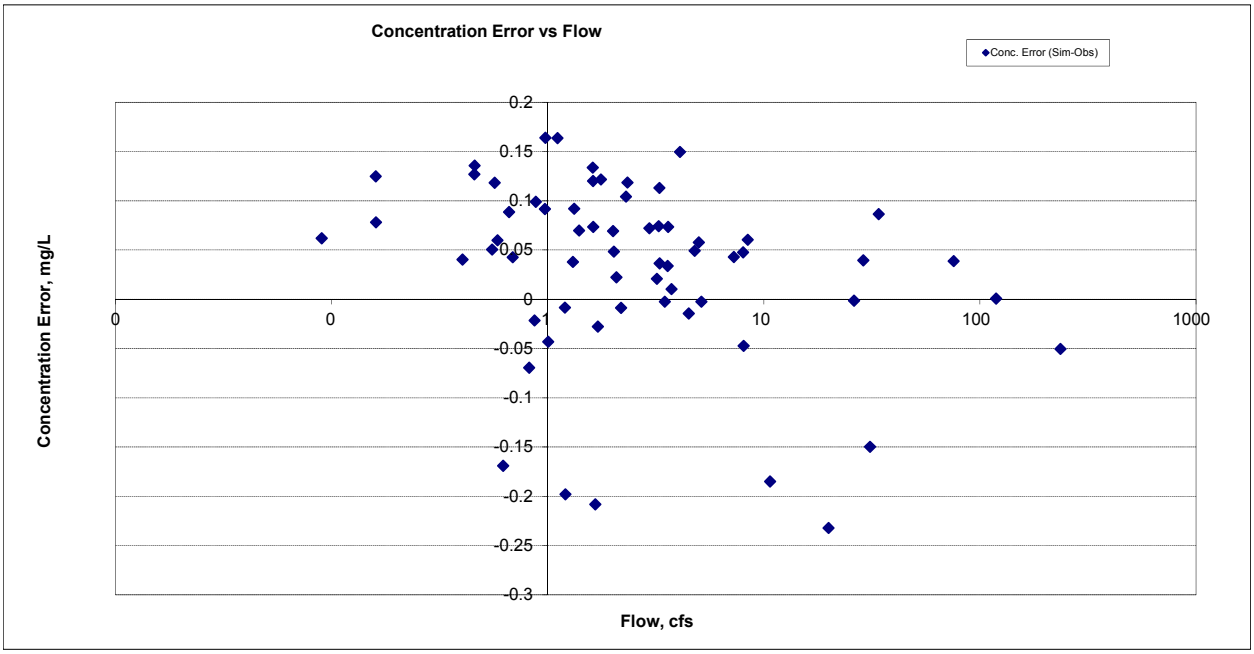

Figure B-76. Residual (Simulated - Observed) vs. Flow Total Phosphorus (TP) at Rock Creek nr Pleasant Valley (05009001)

B.3 BLACKHOOF RIVER NR PLEASANT VALLEY (05006001)

B.3.1 Ammonia Nitrogen (NH3)

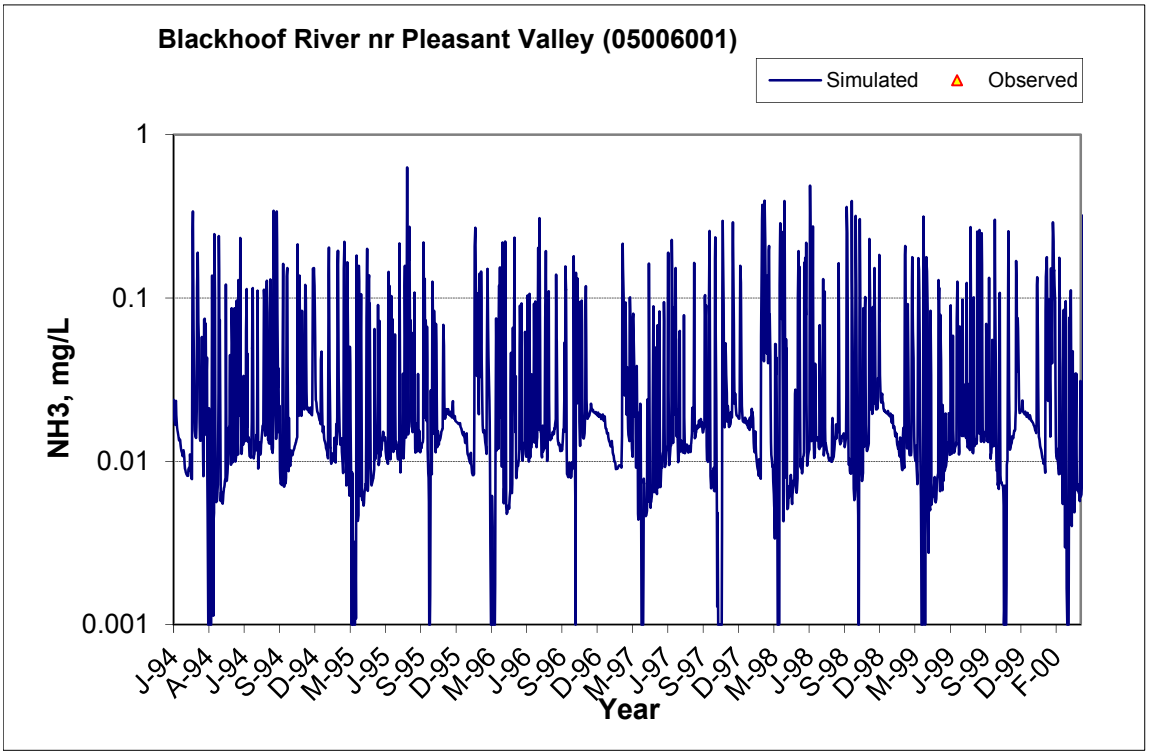

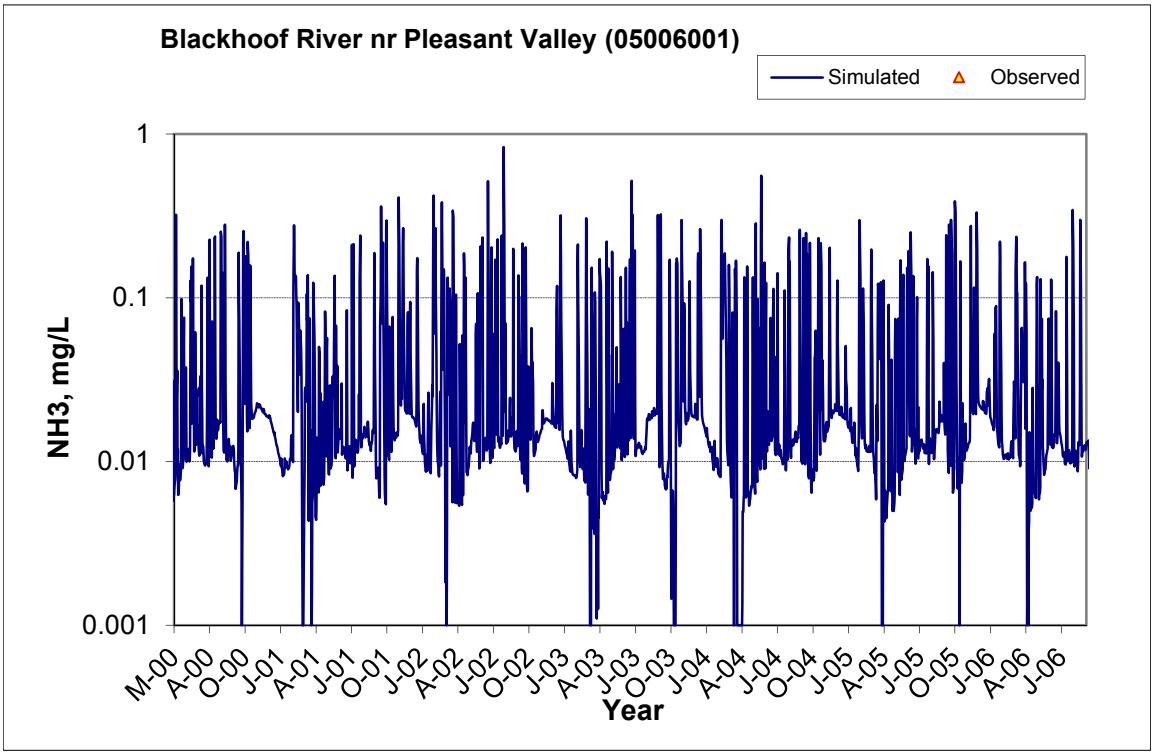

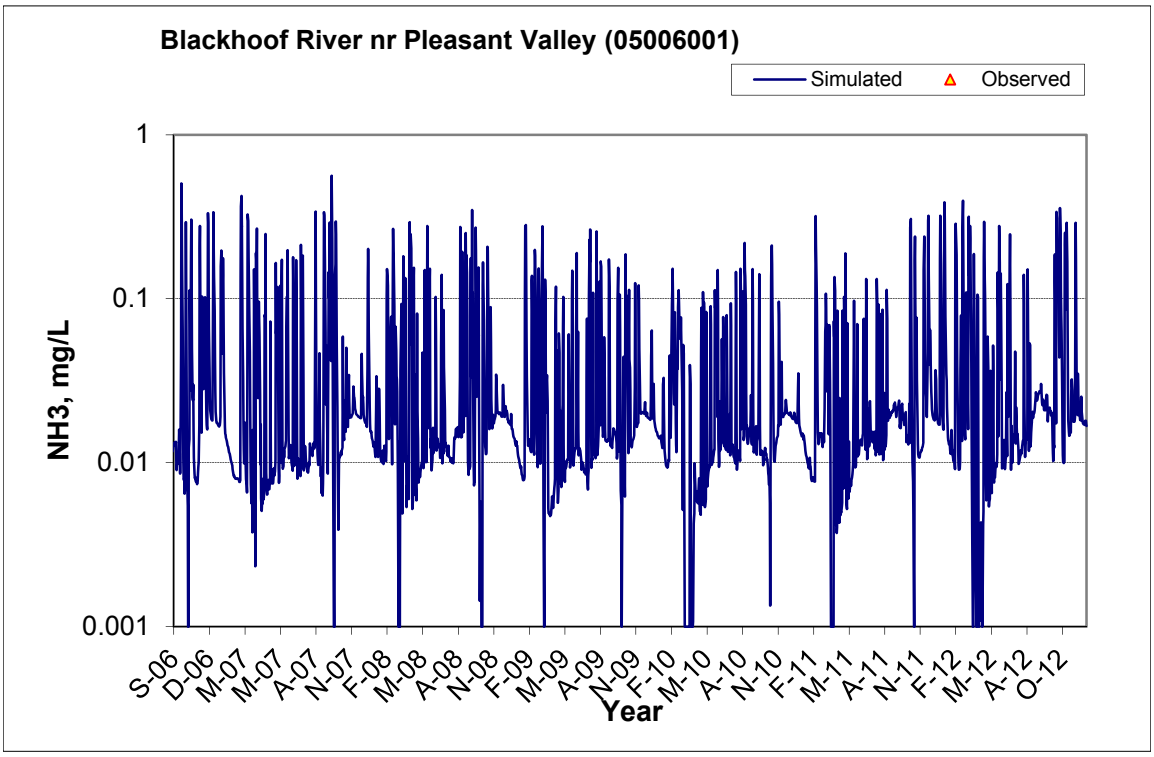

Figure B-77. Time series of observed and simulated Ammonia Nitrogen (NH3) concentration at Blackhoof River nr Pleasant Valley (05006001)

B.3.2 Organic Nitrogen (OrgN)

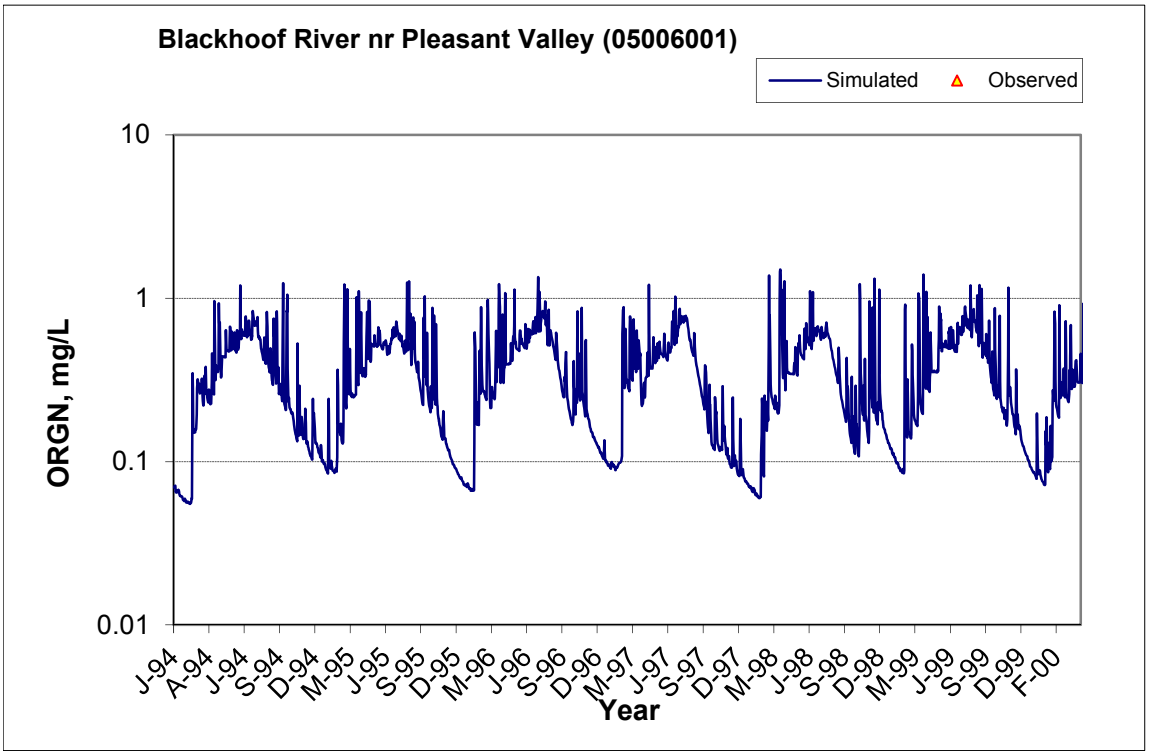

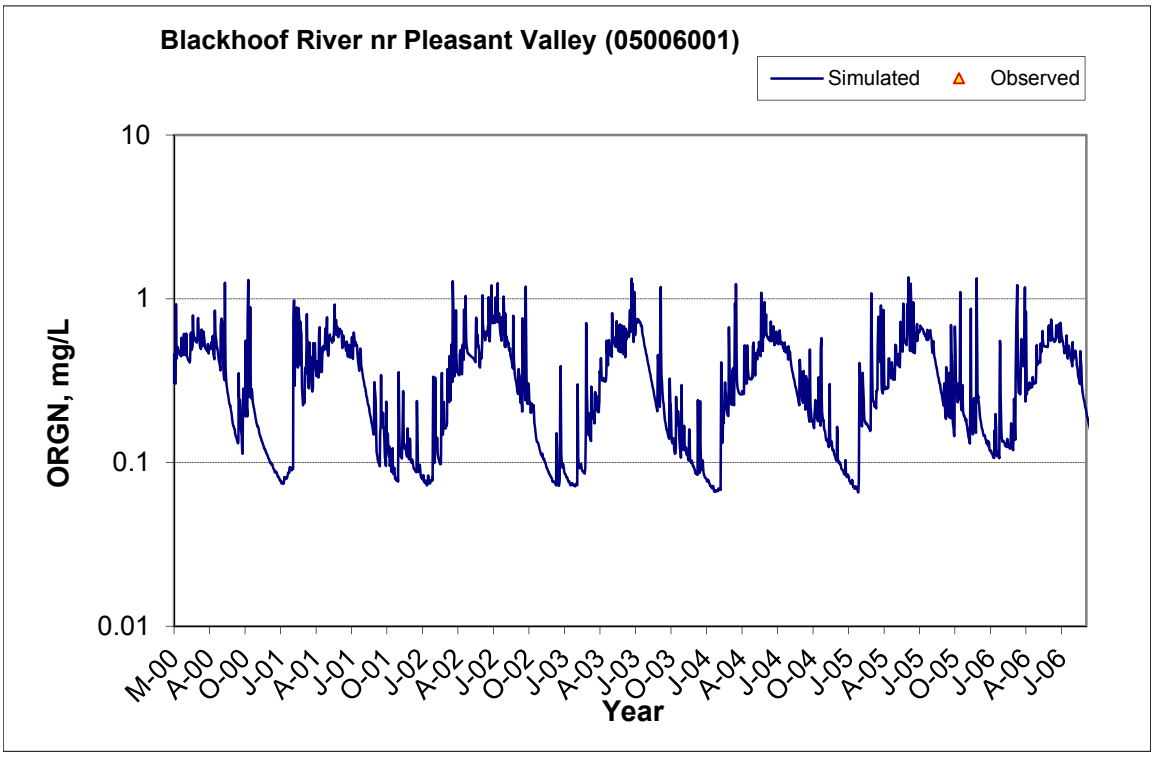

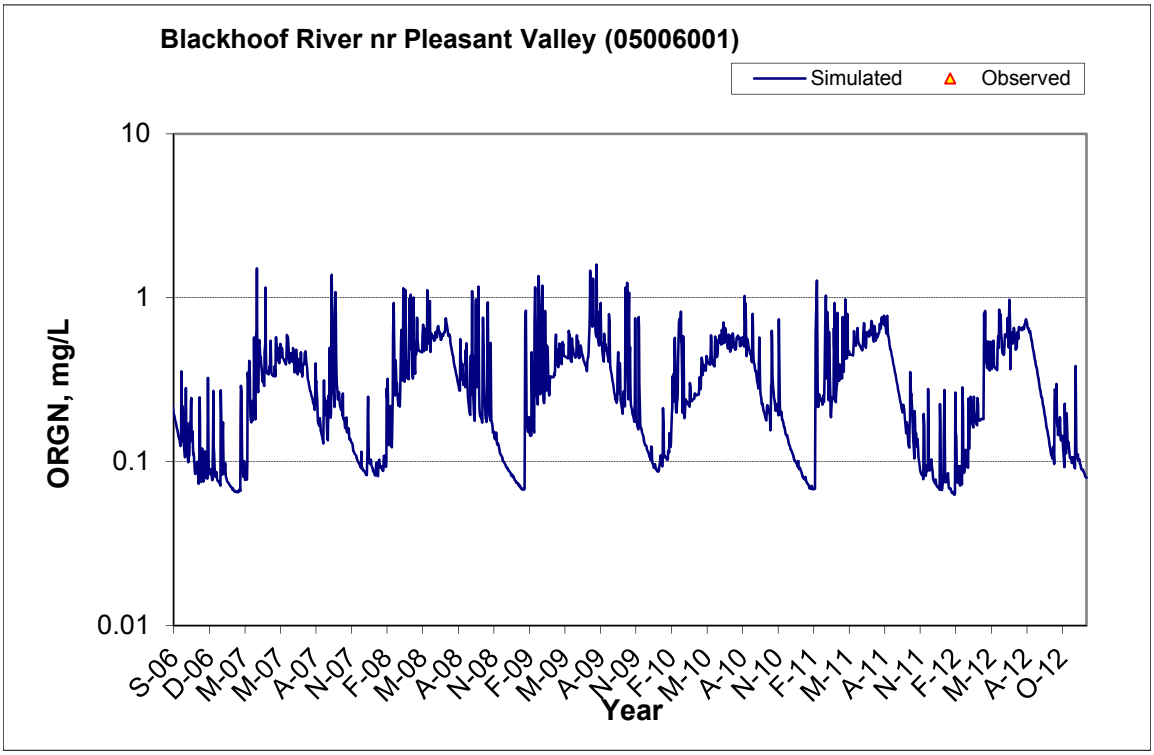

Figure B-78. Time series of observed and simulated Organic Nitrogen (OrgN) concentration at Blackhoof River nr Pleasant Valley (05006001)

B.3.3 Total Kjeldahl Nitrogen (TKN)

Table B-13. Total Kjeldahl Nitrogen (TKN) statistics

Period	1994-2008	2009-2012
Count	ND	17
Concentration Average Error		-19.82%
Concentration Median Error		-16.12%
Load Average Error		9.11%
Load Median Error		-0.40%
Paired t conc		0.51
Paired t load		0.58

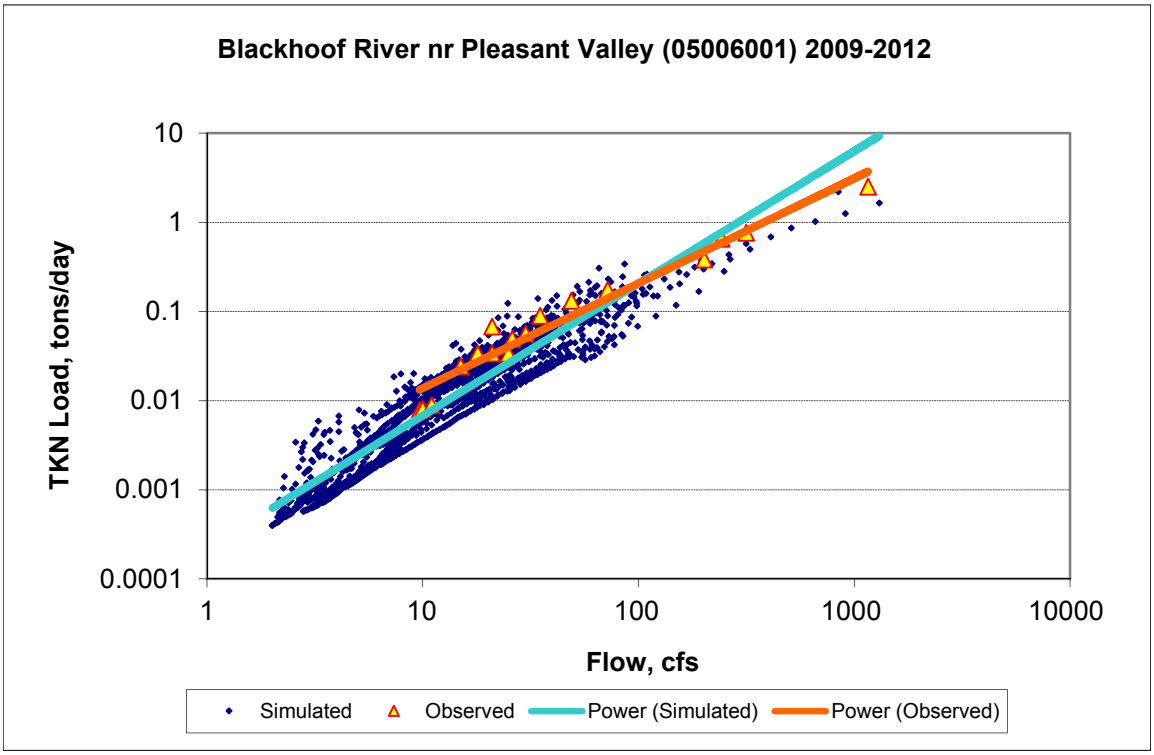

Figure B-79. Power plot of simulated and observed Total Kjeldahl Nitrogen (TKN) load vs flow at Blackhoof River nr Pleasant Valley (05006001) (calibration period)

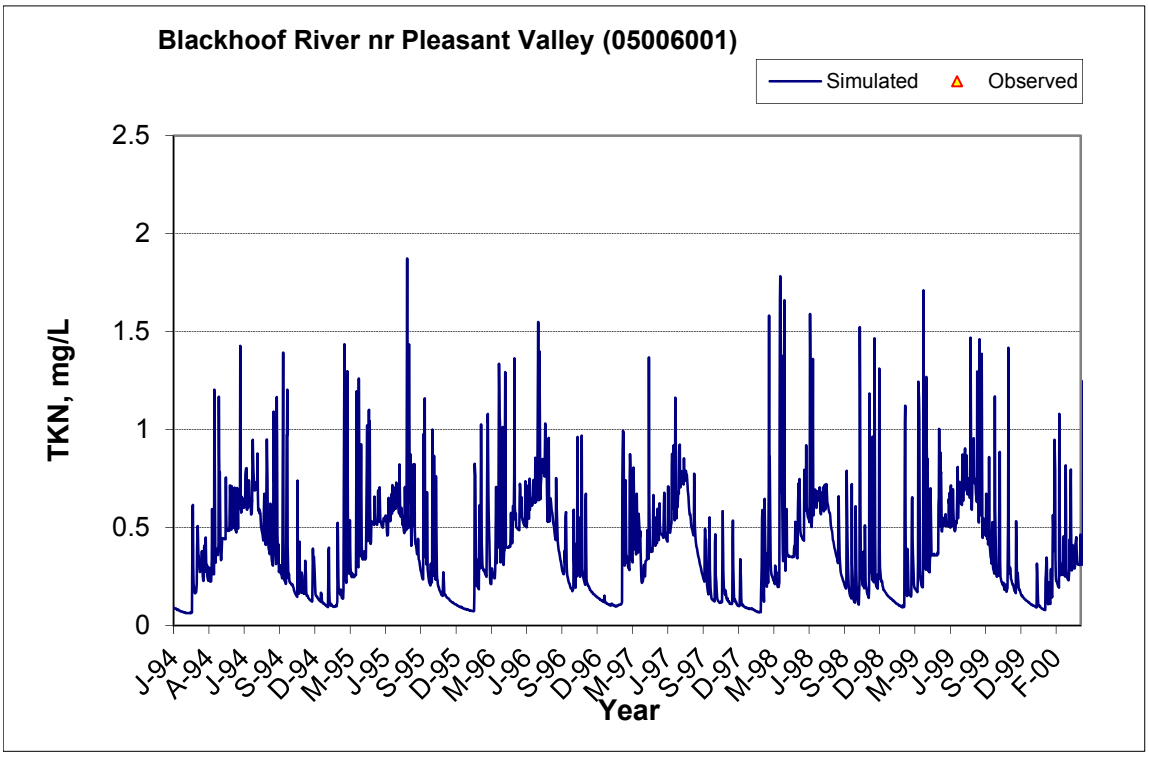
Blackhoof River nr Pleasant Valley (05006001)
Simulated
Observed
TKN, mg/L
2.5
2
1.5
1
0.5
0
J-94 A-94 J-94 S-94 D-94 M-95 J-95 S-95 D-95 M-96 J-96 S-96 D-96 M-97 J-97 S-97 D-97 M-98 J-98 S-98 D-98 M-99 J-99 S-99 D-99 F-00
Year

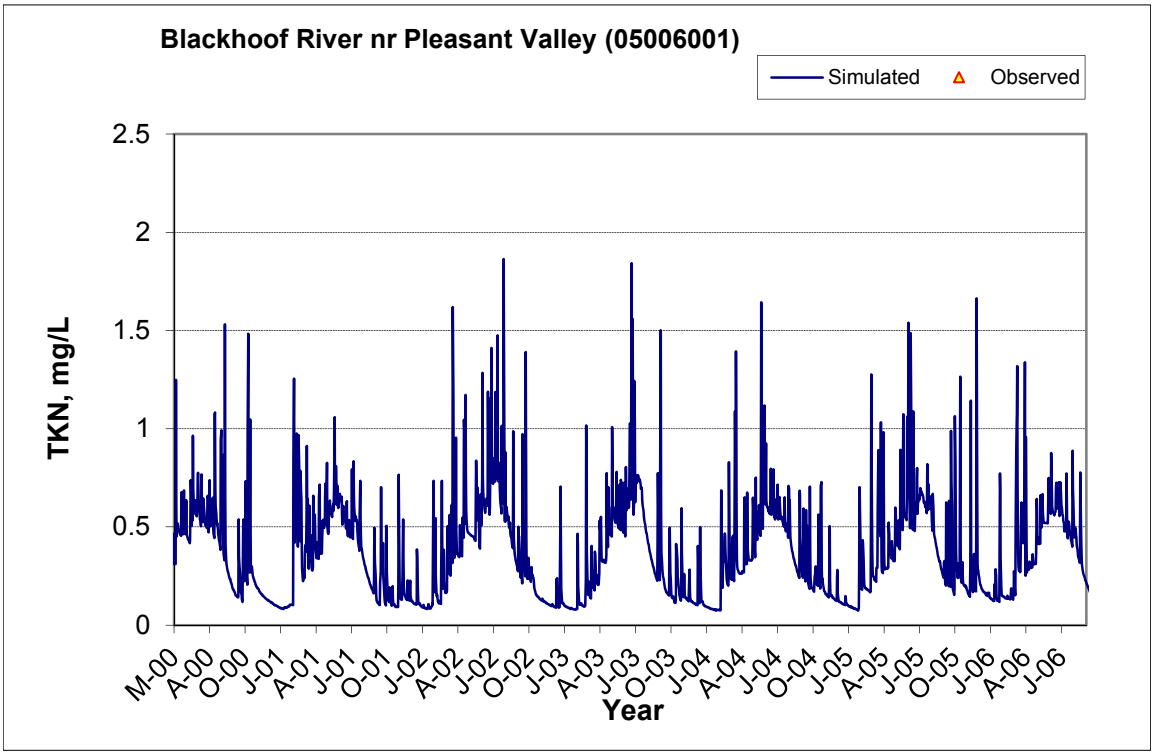
Blackhoof River nr Pleasant Valley (05006001)
Simulated
Observed
TKN, mg/L
2.5
2
1.5
1
0.5
0
M-00 A-00 O-00 J-01 A-01 J-01 O-01 J-02 A-02 J-02 O-02 J-03 A-03 J-03 O-03 J-04 A-04 J-04 O-04 J-05 A-05 J-05 O-05 J-06 A-06 J-06
Year

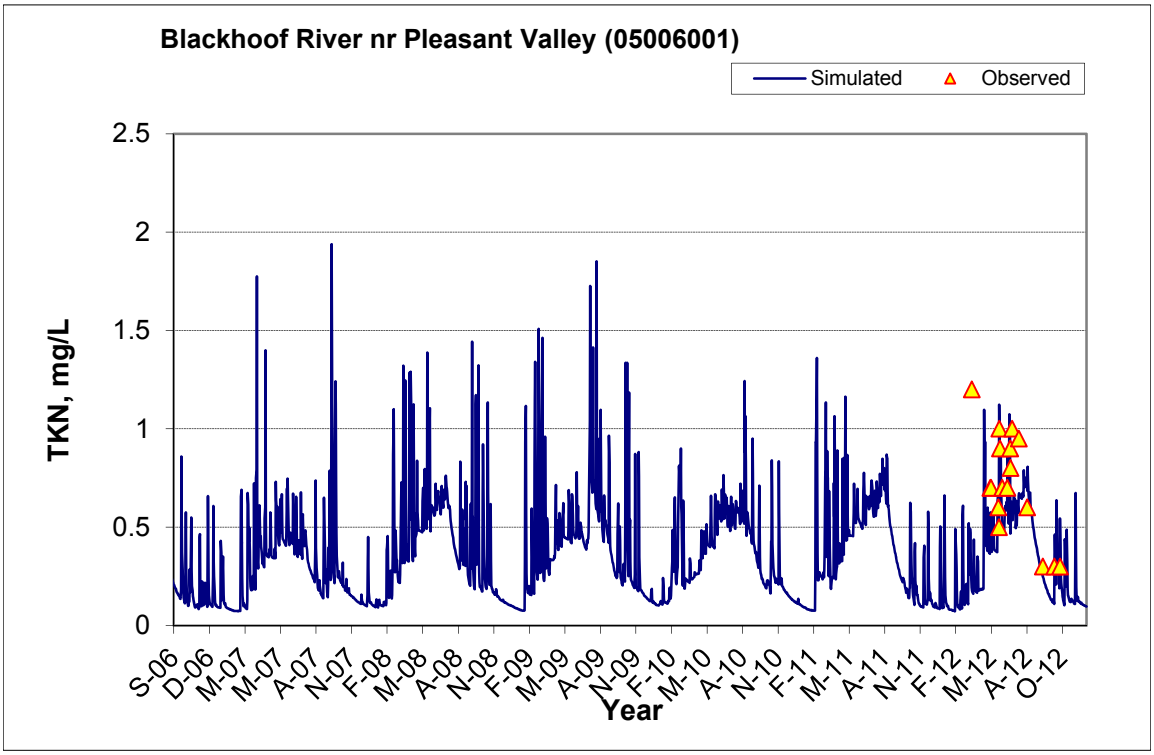

Figure B-80. Time series of observed and simulated Total Kjeldahl Nitrogen (TKN) concentration at Blackhoof River nr Pleasant Valley (05006001)

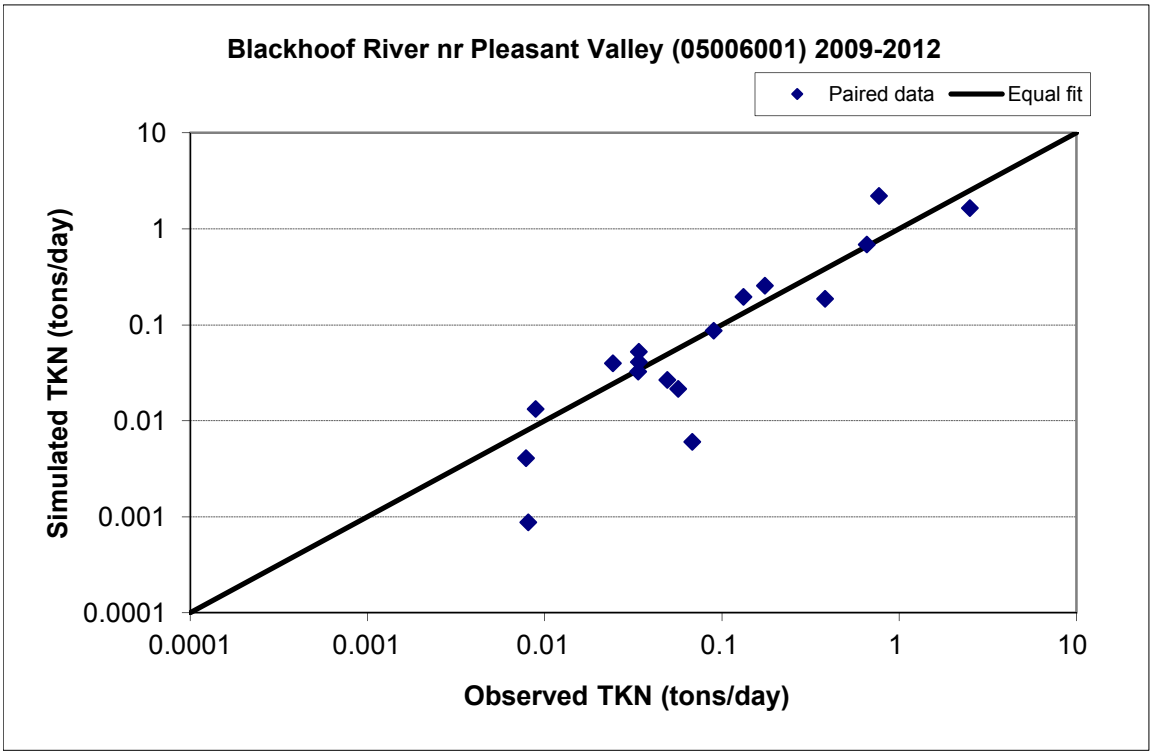

Figure B-81. Paired simulated vs. observed Total Kjeldahl Nitrogen (TKN) load at Blackhoof River nr Pleasant Valley (05006001) (calibration period)

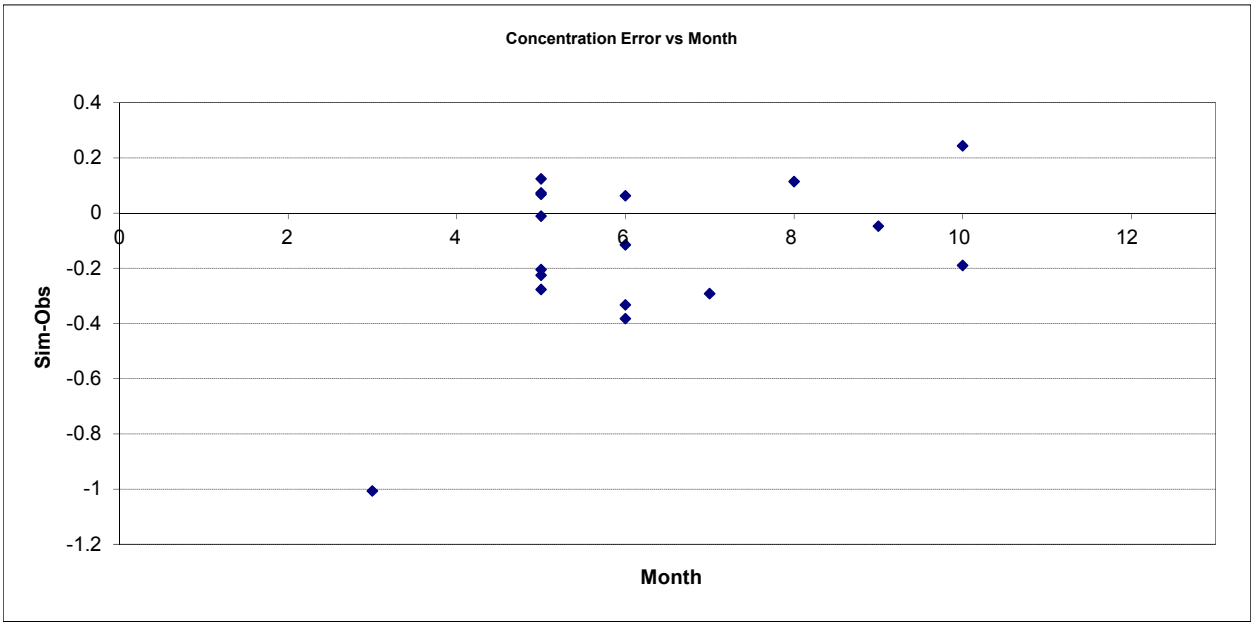

Figure B-82. Residual (Simulated - Observed) vs. Month Total Kjeldahl Nitrogen (TKN) at Blackhoof River nr Pleasant Valley (05006001)

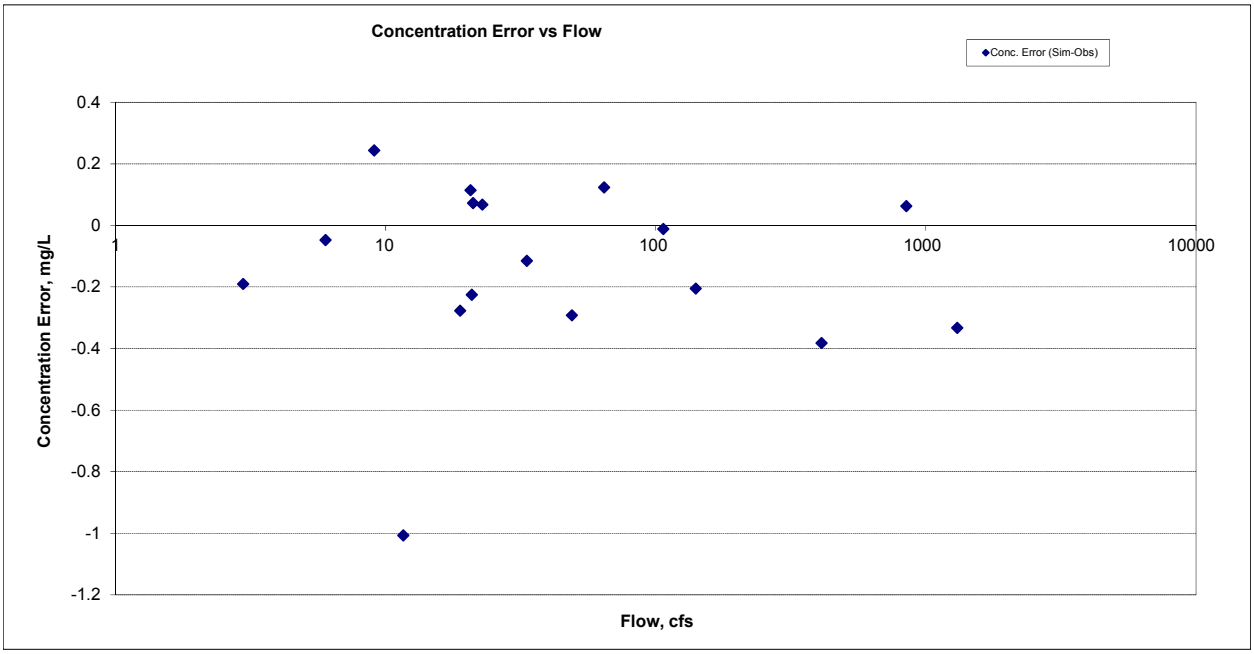

Figure B-83. Residual (Simulated - Observed) vs. Flow Total Kjeldahl Nitrogen (TKN) at Blackhoof River nr Pleasant Valley (05006001)

B.3.4 Nitrite+ Nitrate Nitrogen (NOx)

Table B-14. Nitrite+ Nitrate Nitrogen (NOx) statistics

Period	1994-2008	2009-2012
Count	ND	17
Concentration Average Error		-28.46%
Concentration Median Error		12.34%
Load Average Error		356.44%
Load Median Error		-1.04%
Paired t conc		0.33
Paired t load		0.04

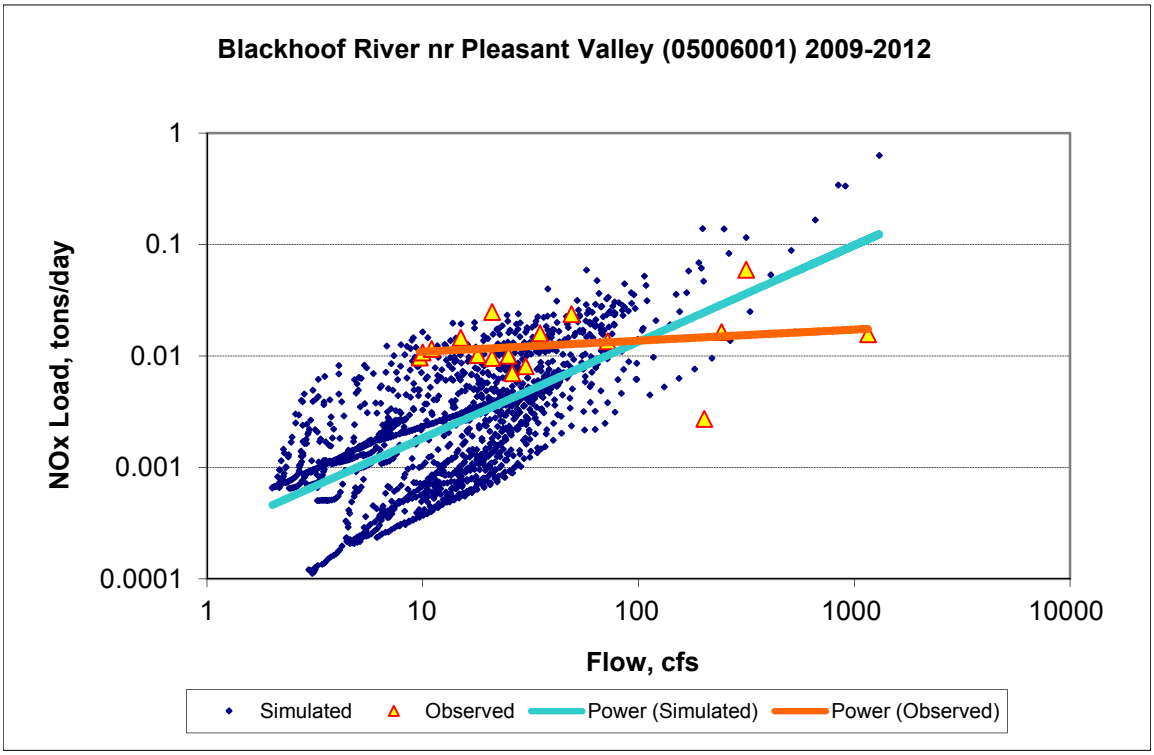

Figure B-84. Power plot of simulated and observed Nitrite+ Nitrate Nitrogen (NOx) load vs flow at Blackhoof River nr Pleasant Valley (05006001) (calibration period)

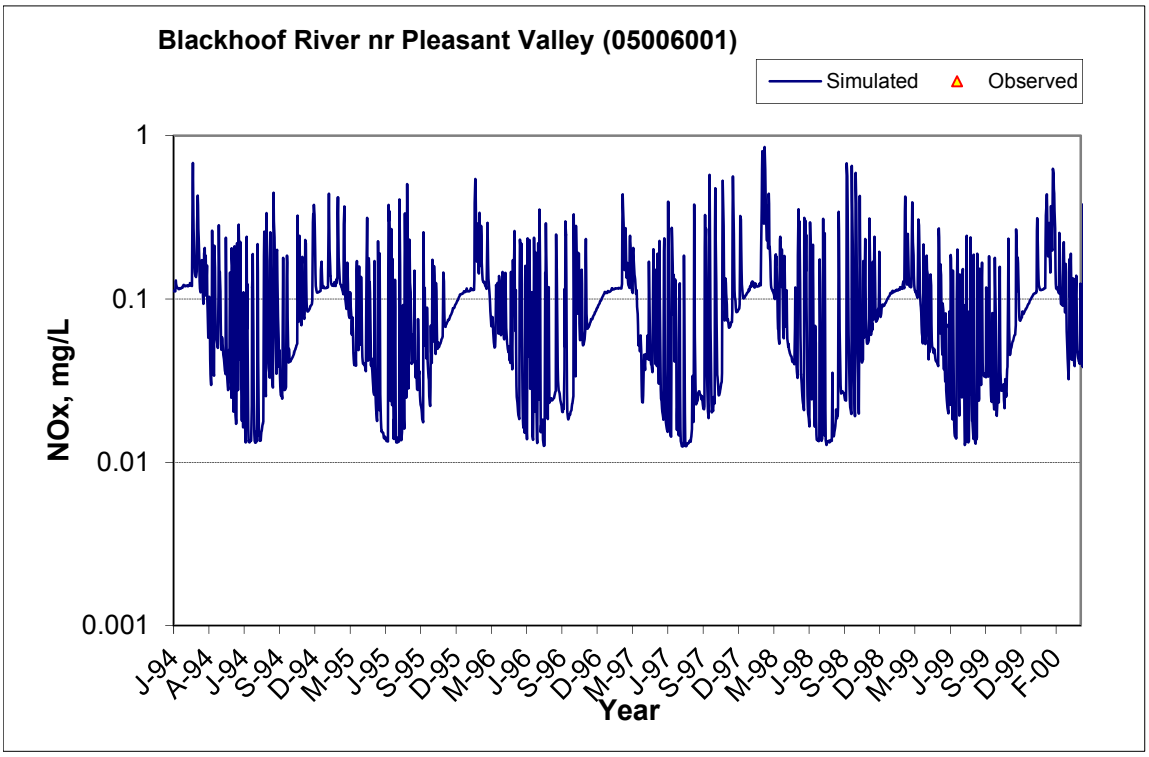
Blackhoof River nr Pleasant Valley (05006001)
Simulated
Observed
NOx, mg/L
1
0.1
0.01
0.001
J-94 A-94 J-94 S-94 D-94 M-95 J-95 S-95 D-95 M-96 J-96 S-96 D-96 M-97 J-97 S-97 D-97 M-98 J-98 S-98 D-98 M-99 J-99 S-99 D-99 F-00
Year

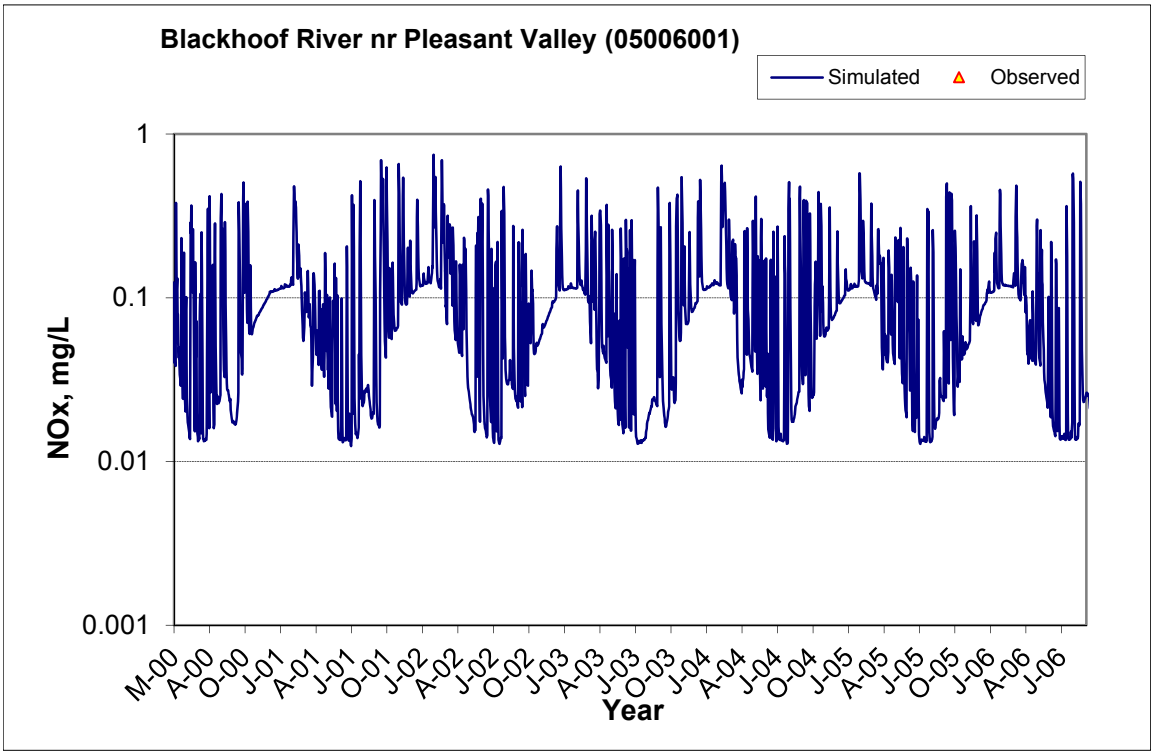
Blackhoof River nr Pleasant Valley (05006001)
Simulated
Observed
NOx, mg/L
1
0.1
0.01
0.001
M-00 A-00 O-00 J-01 A-01 J-01 O-01 J-02 A-02 J-02 O-02 J-03 A-03 J-03 O-03 J-04 A-04 J-04 O-04 J-05 A-05 J-05 O-05 J-06 A-06 J-06
Year

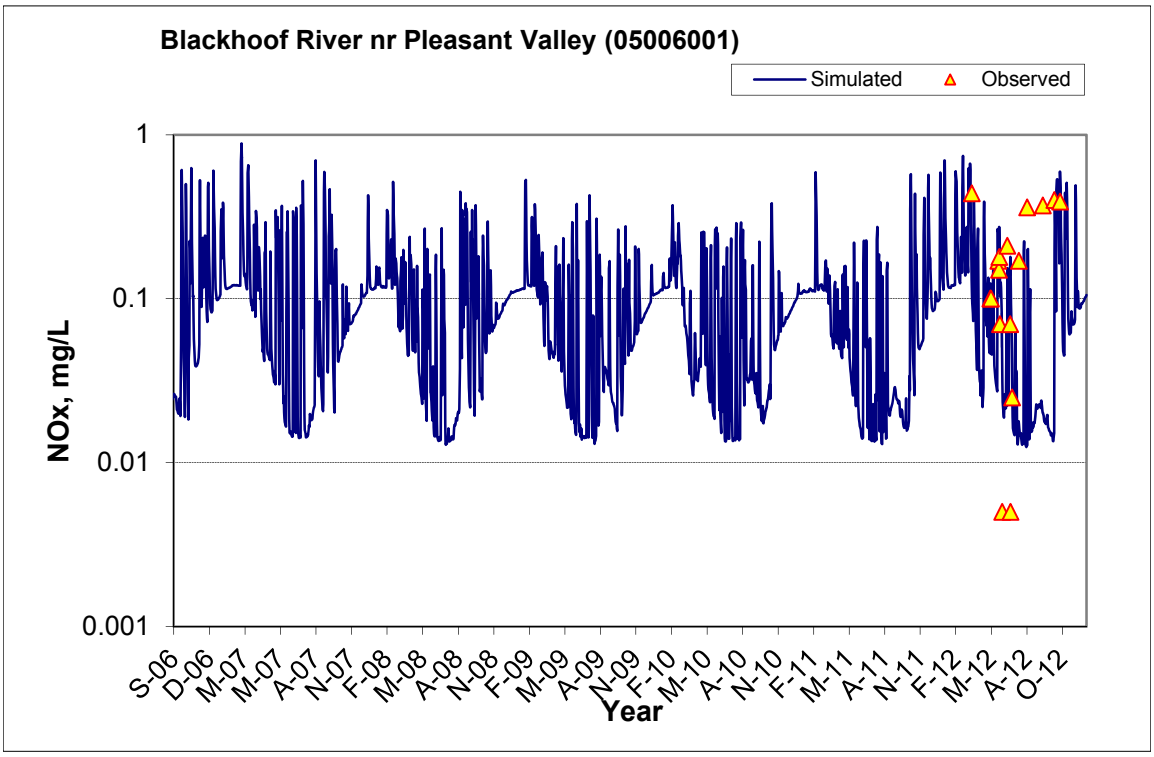

Figure B-85. Time series of observed and simulated Nitrite+ Nitrate Nitrogen (NOx) concentration at Blackhoof River nr Pleasant Valley (05006001)

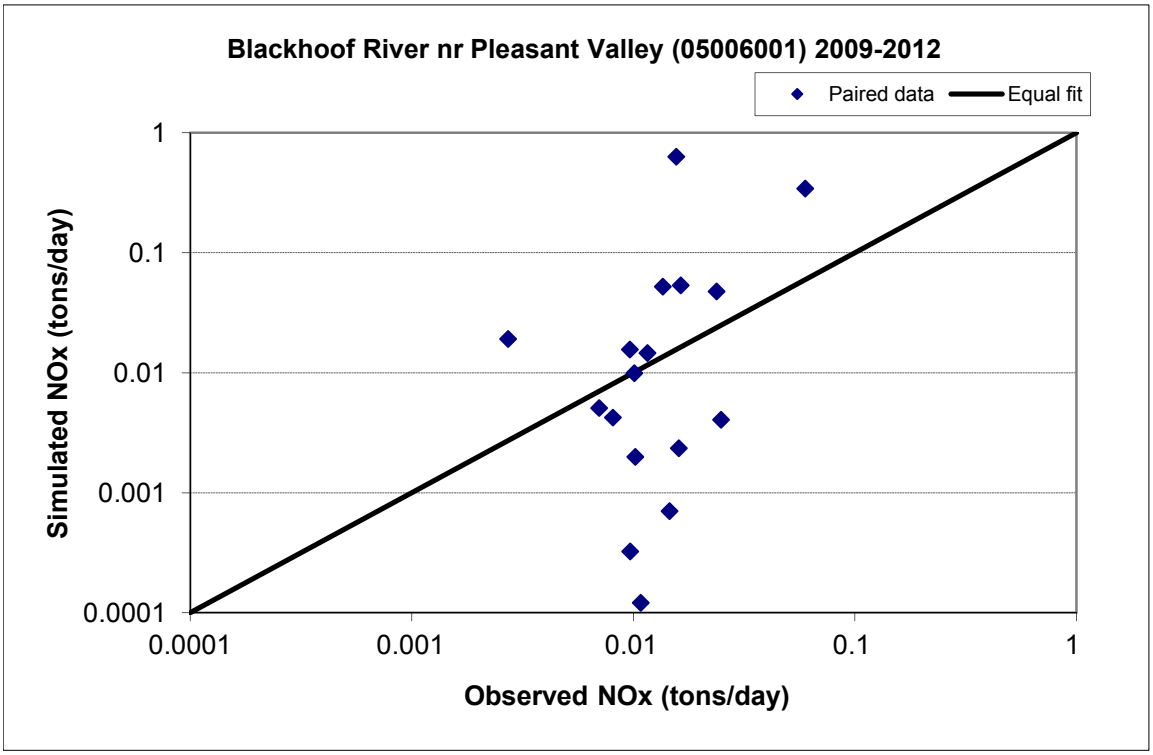

Figure B-86. Paired simulated vs. observed Nitrite+ Nitrate Nitrogen (NOx) load at Blackhoof River nr Pleasant Valley (05006001) (calibration period)

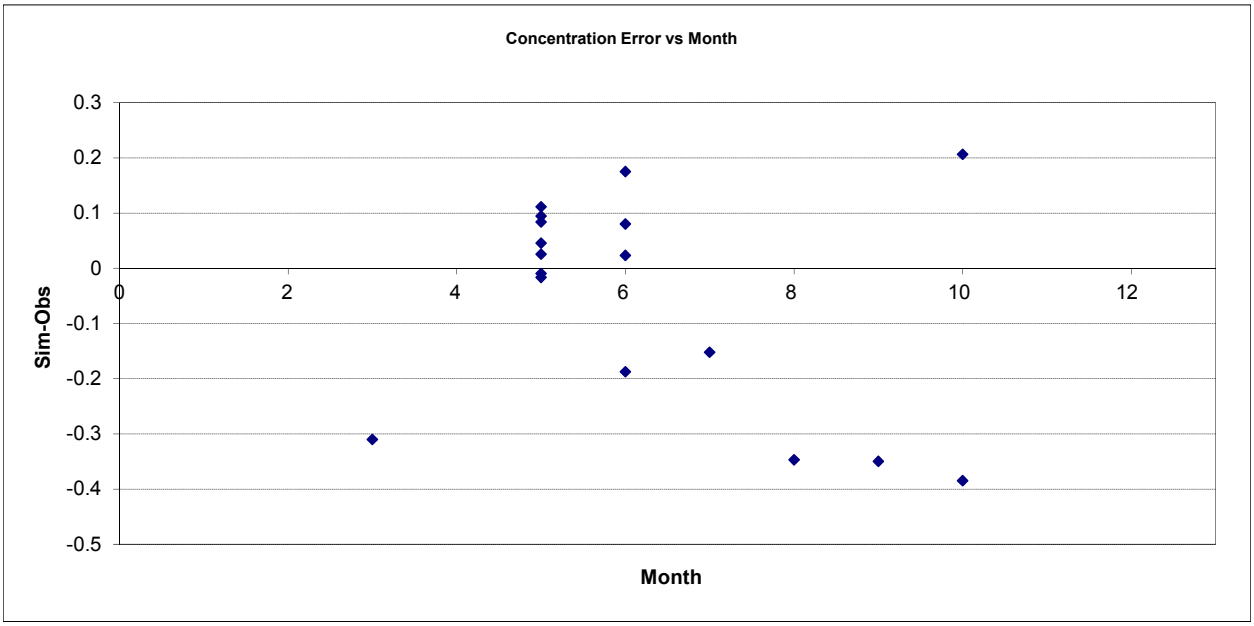

Figure B-87. Residual (Simulated - Observed) vs. Month Nitrite+ Nitrate Nitrogen (NOx) at Blackhoof River nr Pleasant Valley (05006001)

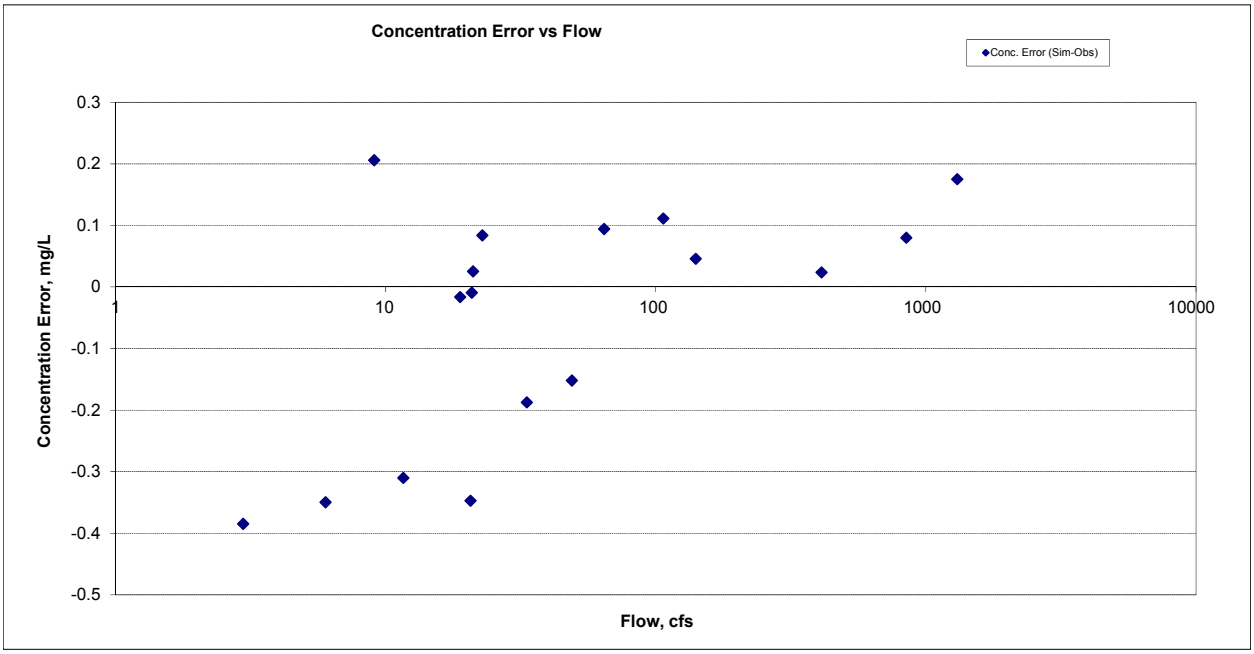

Figure B-88. Residual (Simulated - Observed) vs. Flow Nitrite+ Nitrate Nitrogen (NOx) at Blackhoof River nr Pleasant Valley (05006001)

B.3.5 Total Nitrogen (TN)

Table B-15. Total Nitrogen (TN) statistics

Period	1994-2008	2009-2012
Count	ND	17
Concentration Average Error		-21.80%
Concentration Median Error		-25.79%
Load Average Error		25.63%
Load Median Error		-0.43%
Paired t conc		0.41
Paired t load		0.46

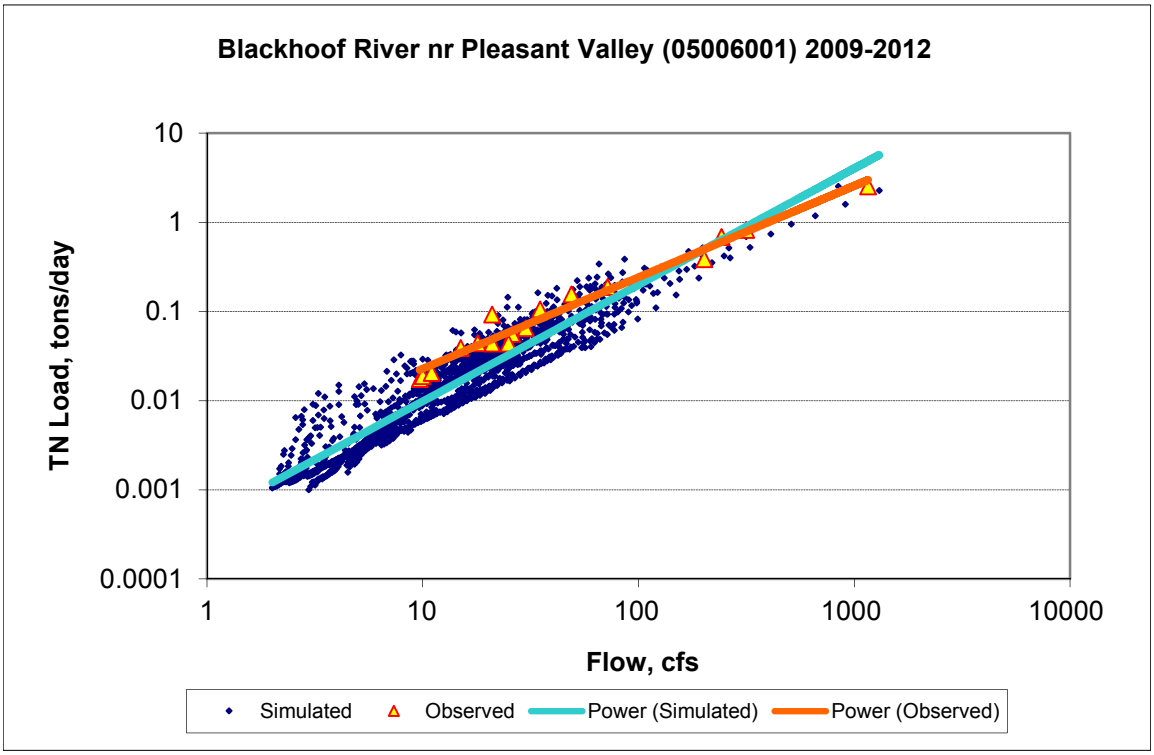

Figure B-89. Power plot of simulated and observed Total Nitrogen (TN) load vs flow at Blackhoof River nr Pleasant Valley (05006001) (calibration period)

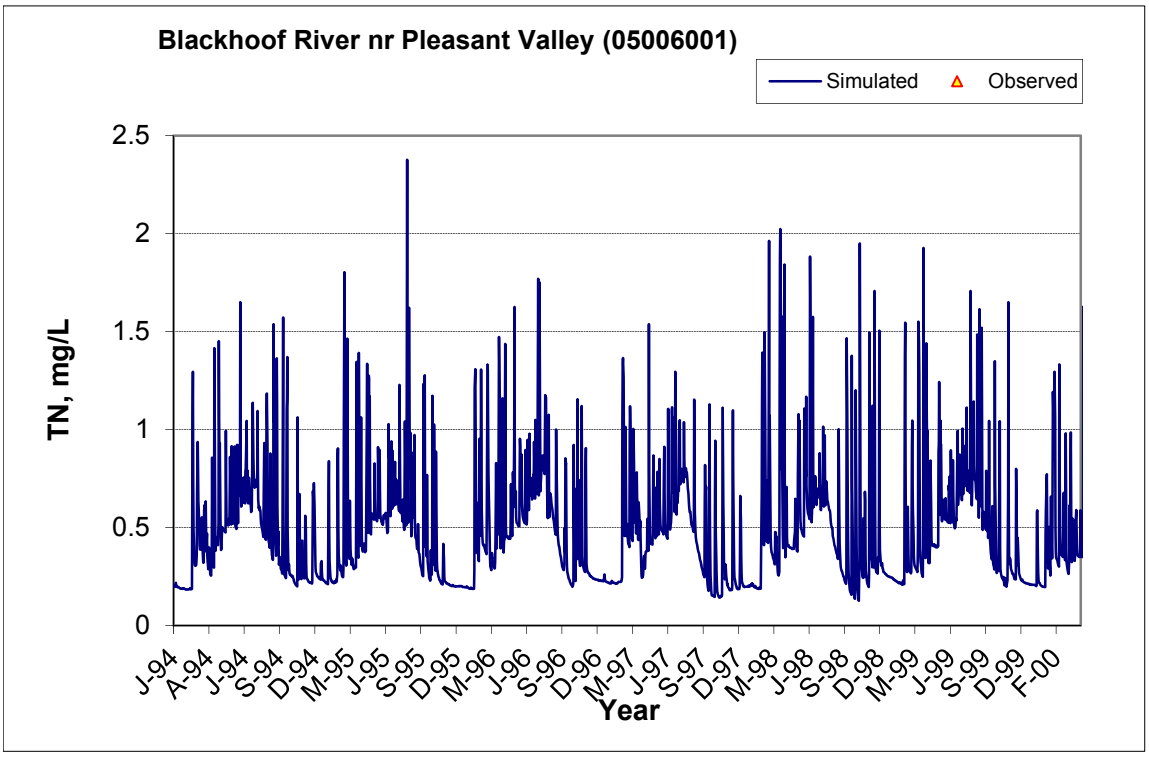
Blackhoof River nr Pleasant Valley (05006001)
Simulated
Observed
TN, mg/L
2.5
2
1.5
1
0.5
0
J-94 A-94 J-94 S-94 D-94 M-95 J-95 S-95 D-95 M-96 J-96 S-96 D-96 M-97 J-97 S-97 D-97 M-98 J-98 S-98 D-98 M-99 J-99 S-99 D-99 F-00
Year

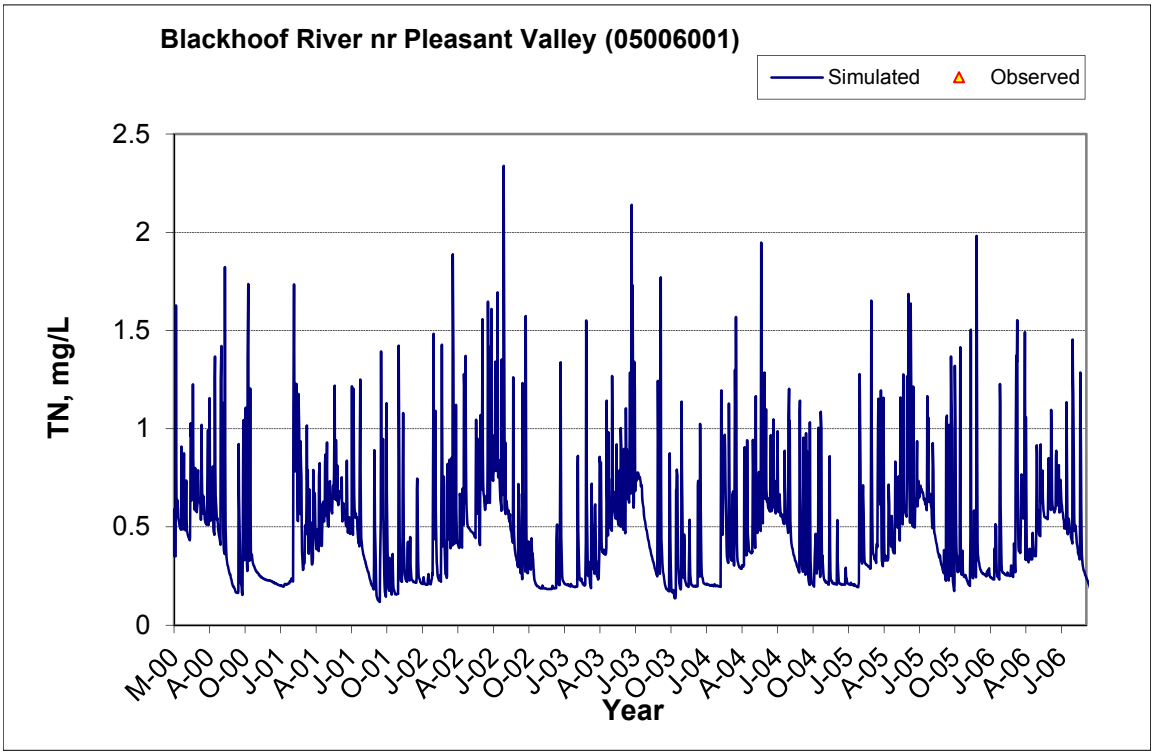
Blackhoof River nr Pleasant Valley (05006001)
Simulated
Observed
TN, mg/L
2.5
2
1.5
1
0.5
0
M-00 A-00 O-00 J-01 A-01 J-01 O-01 J-02 A-02 J-02 O-02 J-03 A-03 J-03 O-03 J-04 A-04 J-04 O-04 J-05 A-05 J-05 O-05 J-06 A-06 J-06
Year

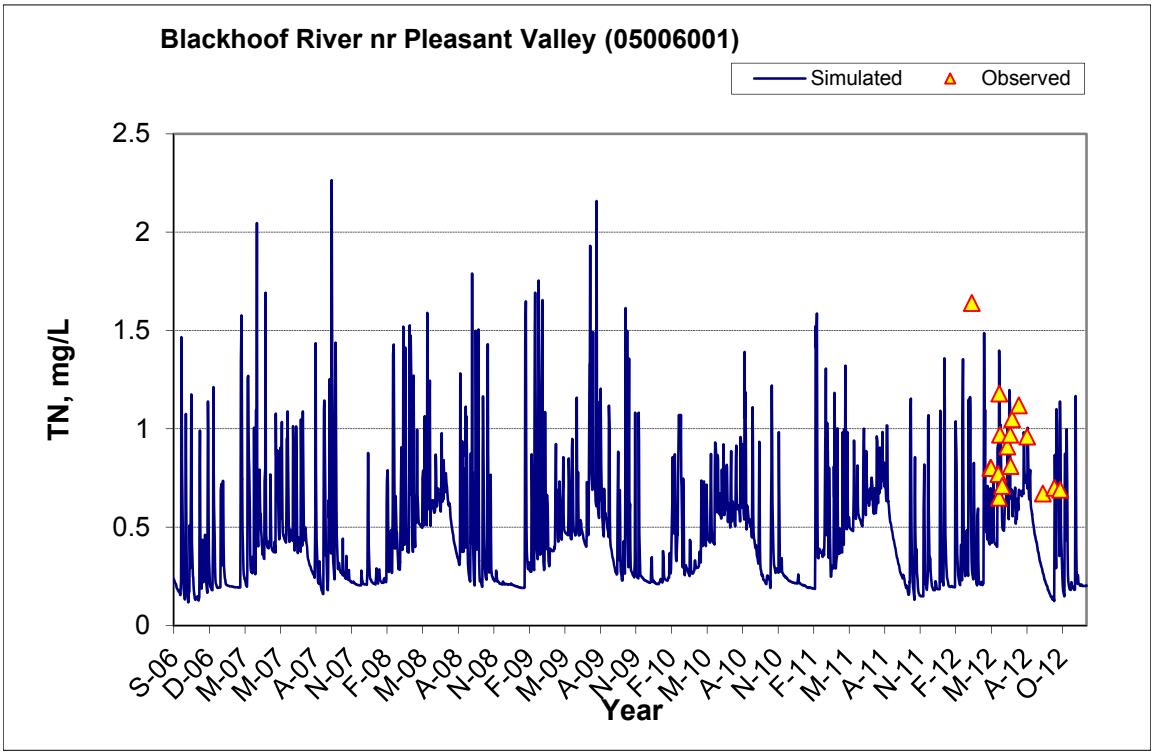

Figure B-90. Time series of observed and simulated Total Nitrogen (TN) concentration at Blackhoof River nr Pleasant Valley (05006001)

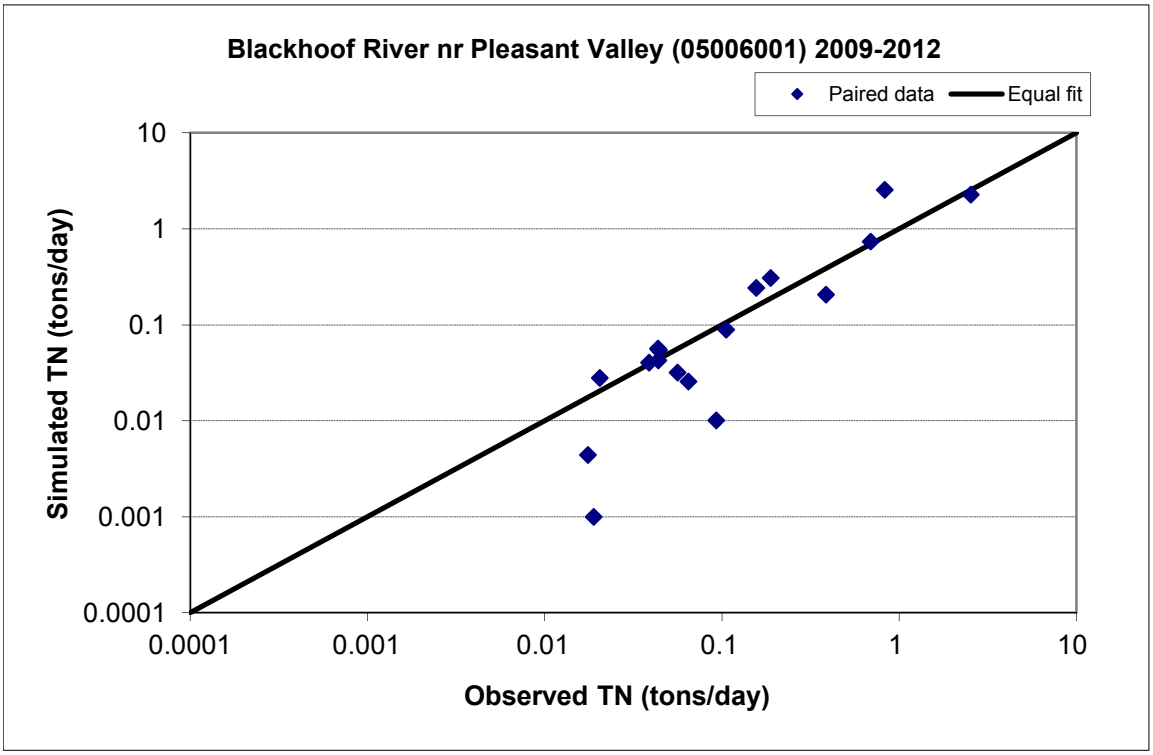

Figure B-91. Paired simulated vs. observed Total Nitrogen (TN) load at Blackhoof River nr Pleasant Valley (05006001) (calibration period)

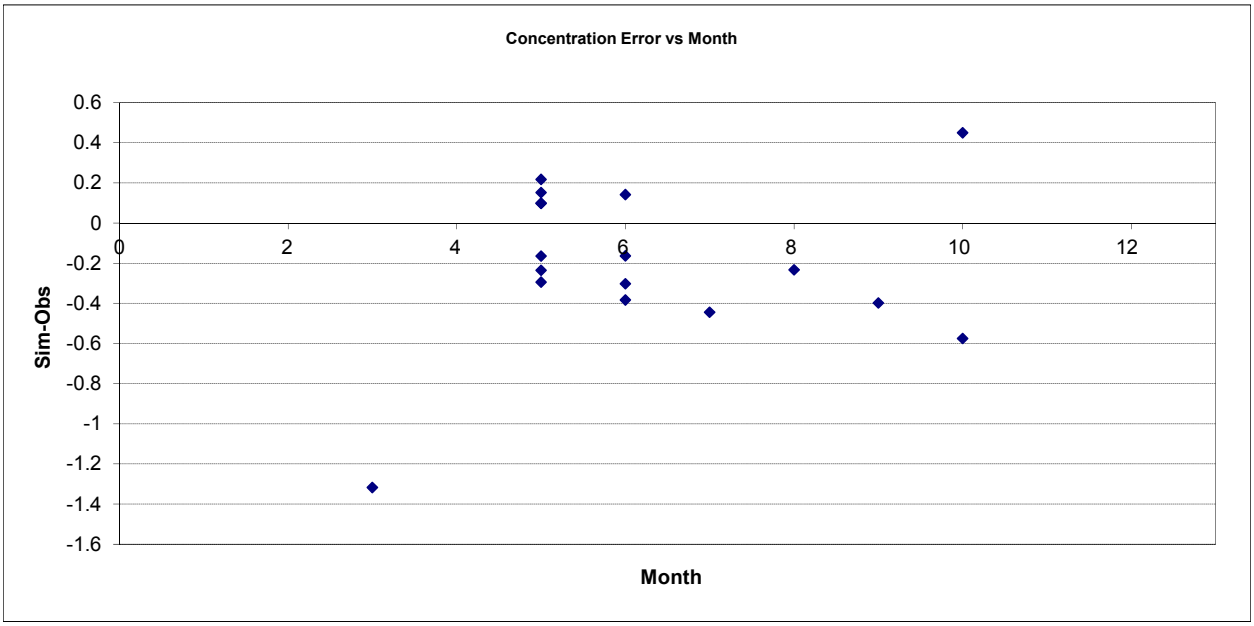

Figure B-92. Residual (Simulated - Observed) vs. Month Total Nitrogen (TN) at Blackhoof River nr Pleasant Valley (05006001)

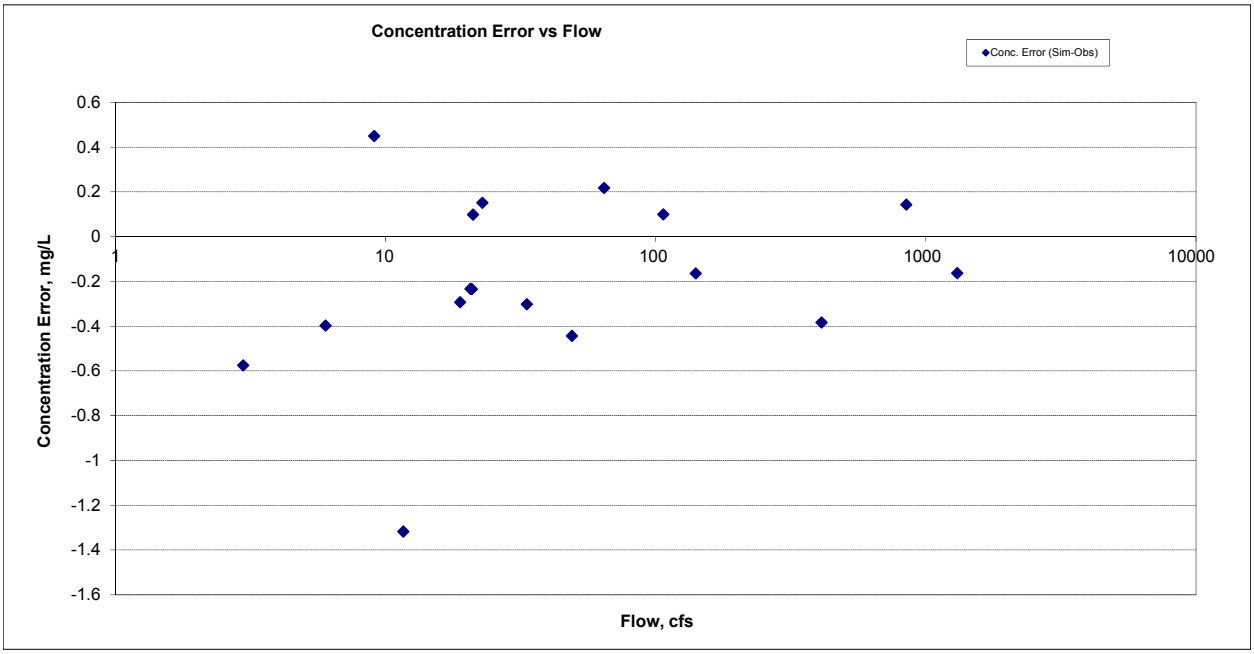

Figure B-93. Residual (Simulated - Observed) vs. Flow Total Nitrogen (TN) at Blackhoof River nr Pleasant Valley (05006001)

B.3.6 Soluble Reactive Phosphorus (SRP)

Table B-16. Soluble Reactive Phosphorus (SRP) statistics

Period	1994-2008	2009-2012
Count	ND	17
Concentration Average Error		-6.87%
Concentration Median Error		7.05%
Load Average Error		72.34%
Load Median Error		0.83%
Paired t conc		0.78
Paired t load		0.25

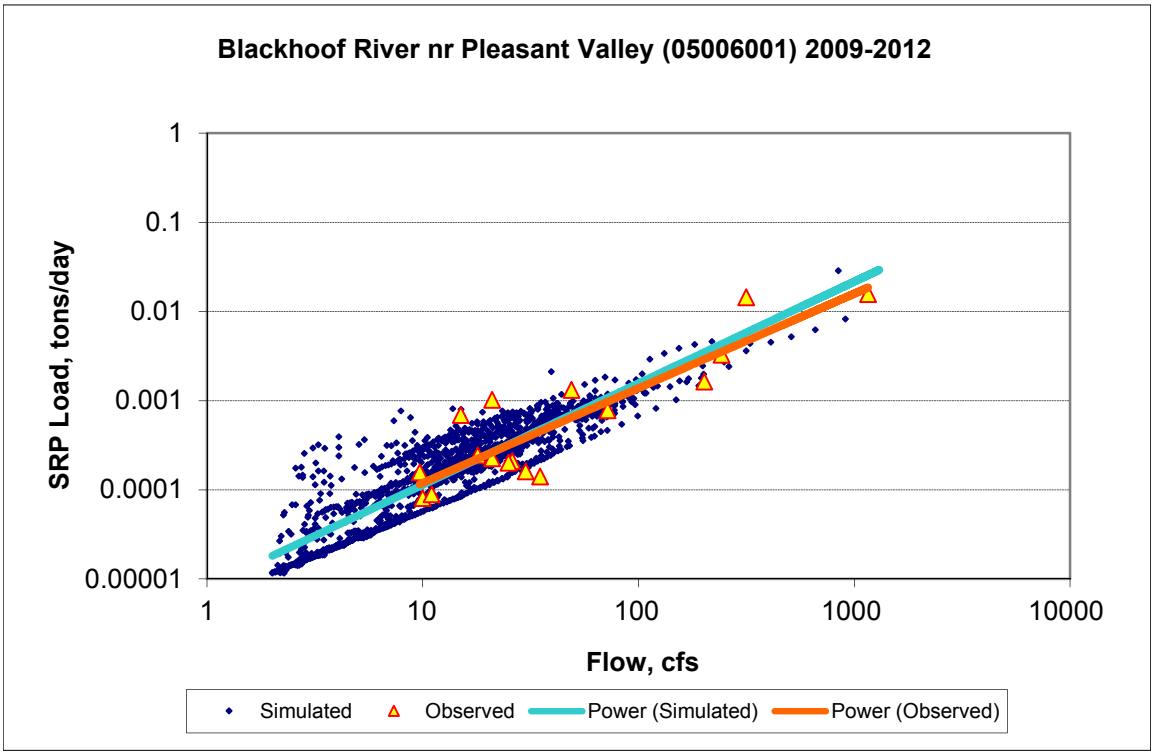

Figure B-94. Power plot of simulated and observed Soluble Reactive Phosphorus (SRP) load vs flow at Blackhoof River nr Pleasant Valley (05006001) (calibration period)

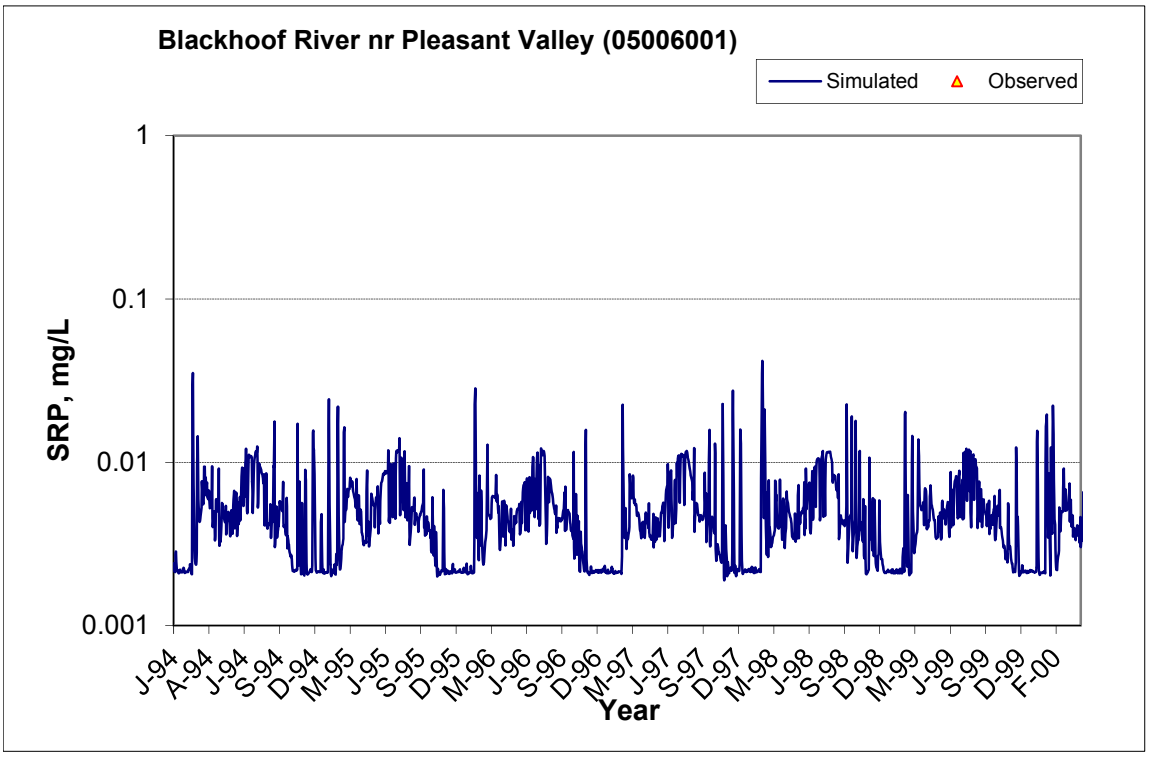
Blackhoof River nr Pleasant Valley (05006001)
Simulated
Observed
SRP, mg/L
1
0.1
0.01
0.001
J-94 A-94 J-94 S-94 D-94 M-95 J-95 S-95 D-95 M-96 J-96 S-96 D-96 M-97 J-97 S-97 D-97 M-98 J-98 S-98 D-98 M-99 J-99 S-99 D-99 F-00
Year

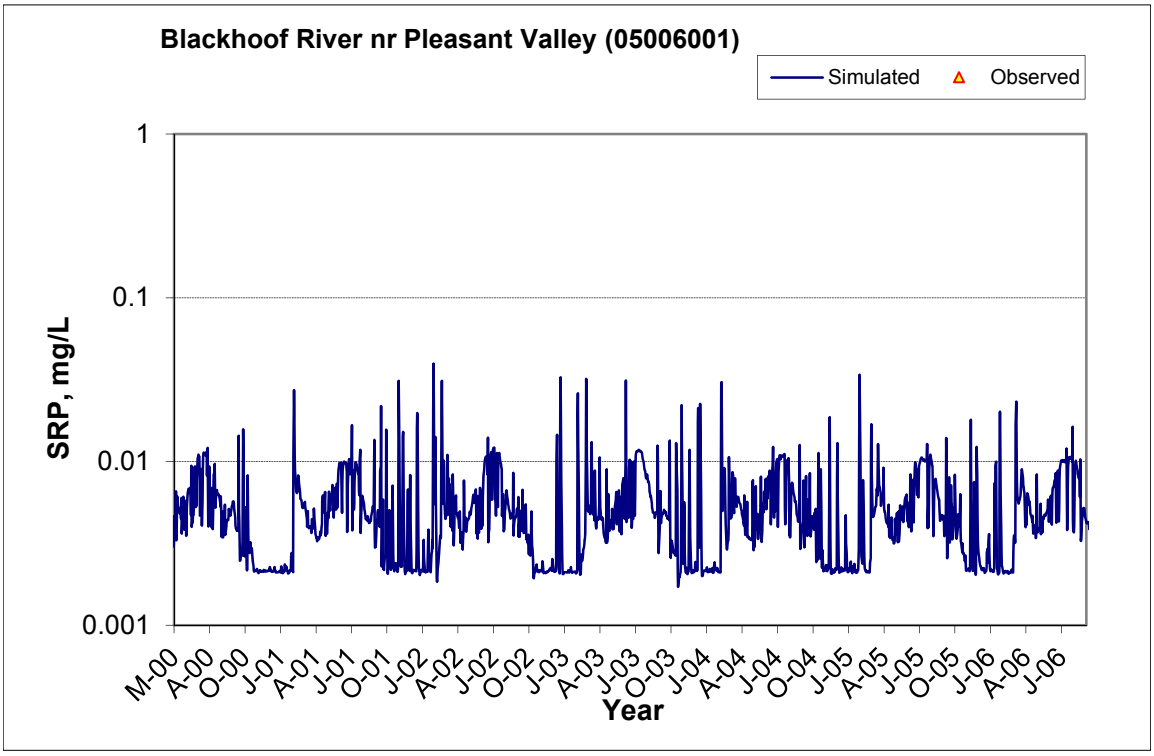
Blackhoof River nr Pleasant Valley (05006001)
Simulated
Observed
SRP, mg/L
1
0.1
0.01
0.001
M-00 A-00 O-00 J-01 A-01 J-01 O-01 J-02 A-02 J-02 O-02 J-03 A-03 J-03 O-03 J-04 A-04 J-04 O-04 J-05 A-05 J-05 O-05 J-06 A-06 J-06
Year

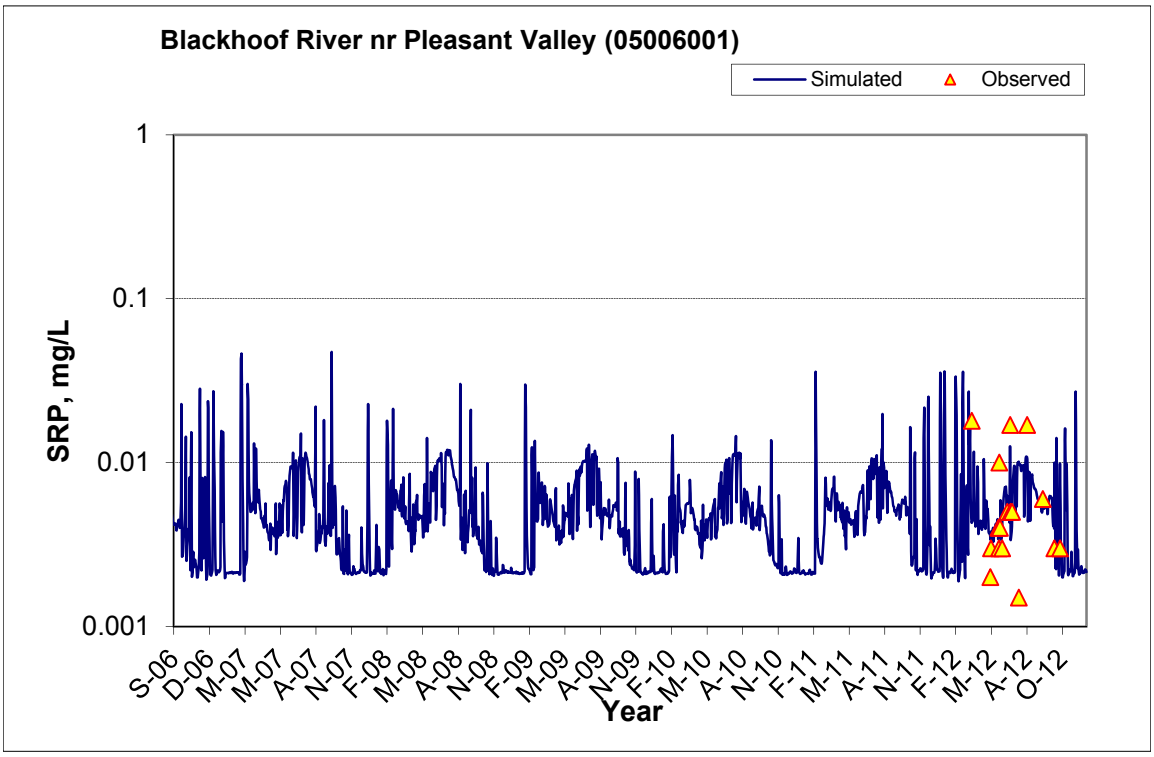

Figure B-95. Time series of observed and simulated Soluble Reactive Phosphorus (SRP) concentration at Blackhoof River nr Pleasant Valley (05006001)

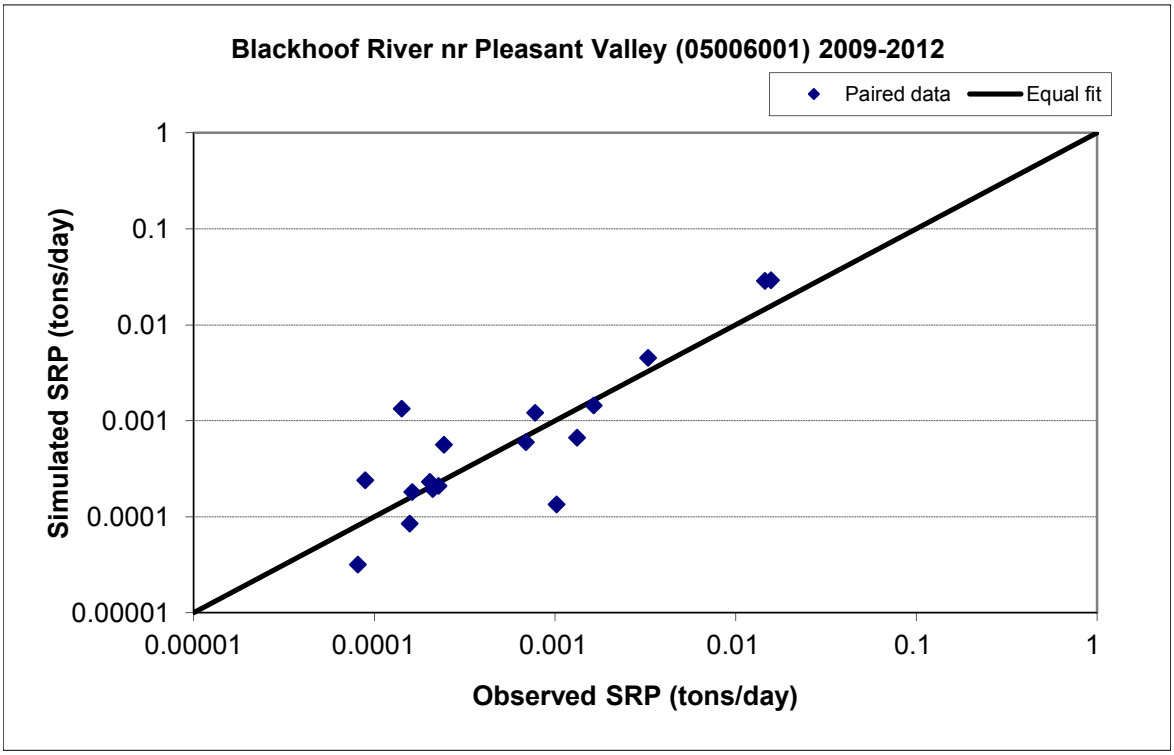

Figure B-96. Paired simulated vs. observed Soluble Reactive Phosphorus (SRP) load at Blackhoof River nr Pleasant Valley (05006001) (calibration period)

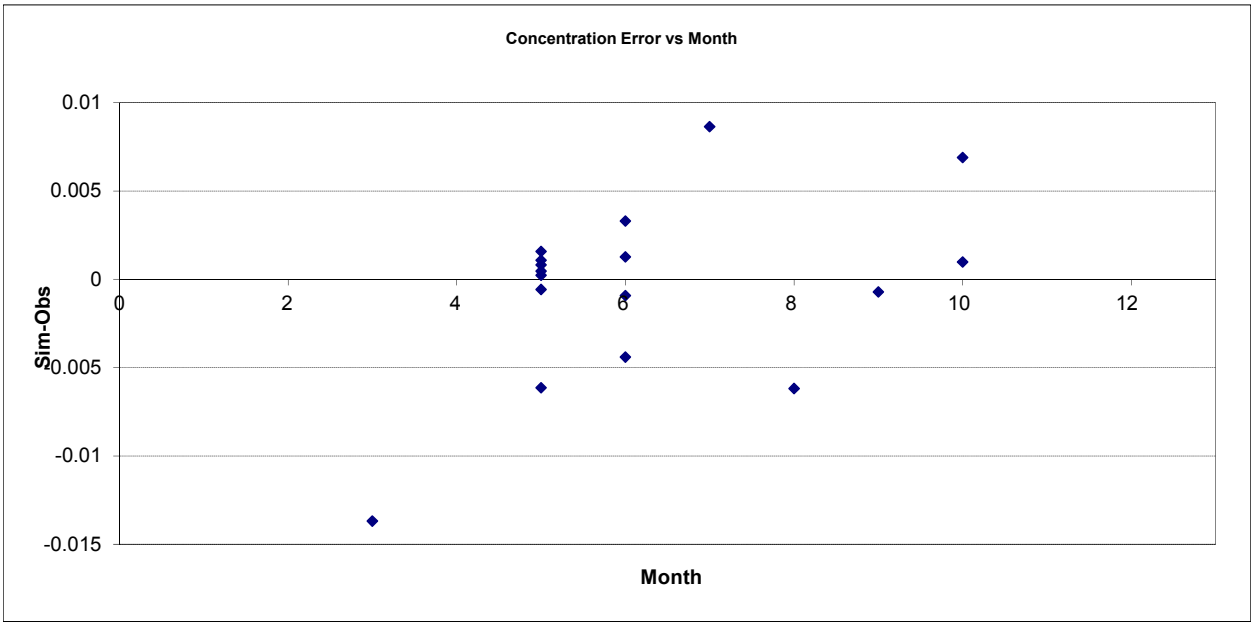

Figure B-97. Residual (Simulated - Observed) vs. Month Soluble Reactive Phosphorus (SRP) at Blackhoof River nr Pleasant Valley (05006001)

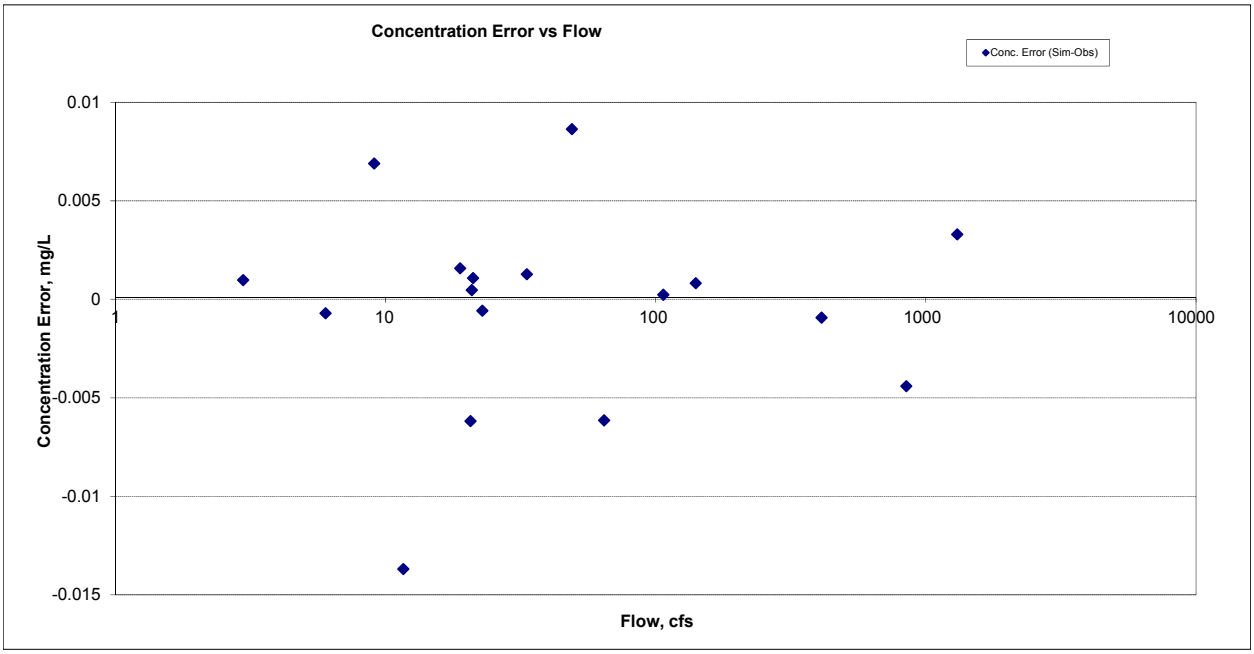

Figure B-98. Residual (Simulated - Observed) vs. Flow Soluble Reactive Phosphorus (SRP) at Blackhoof River nr Pleasant Valley (05006001)

B.3.7 Organic Phosphorus (OrgP)

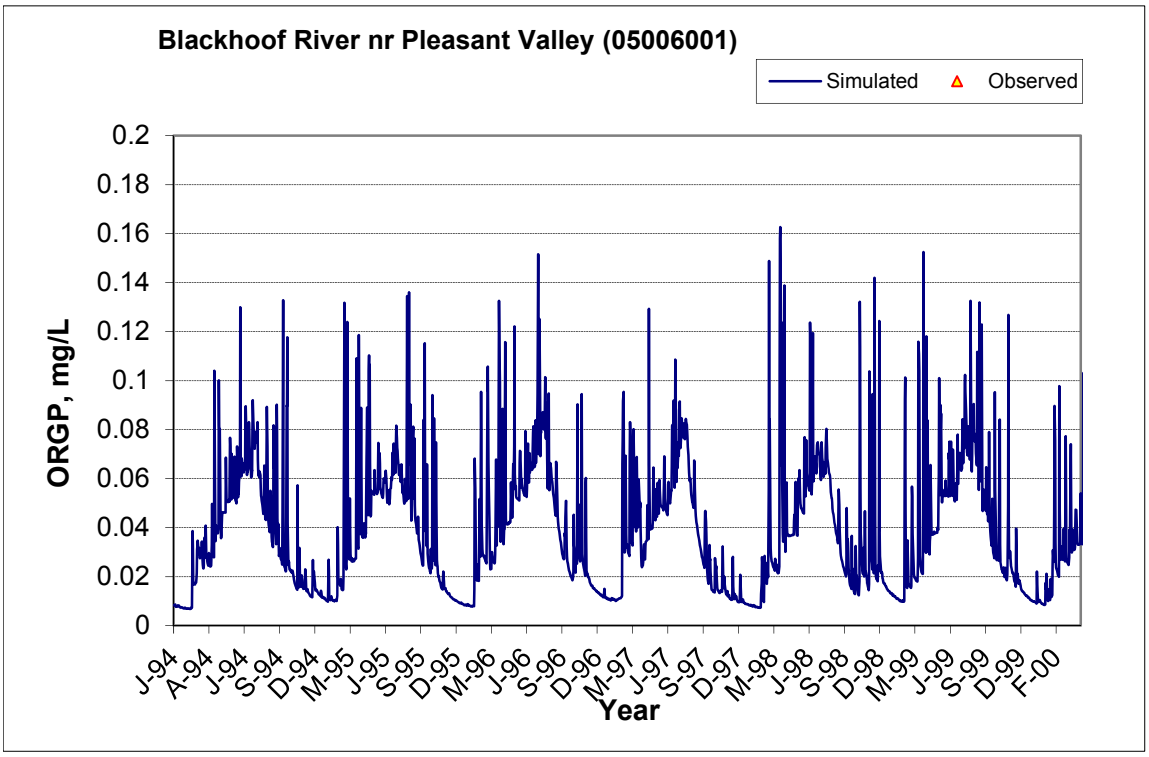

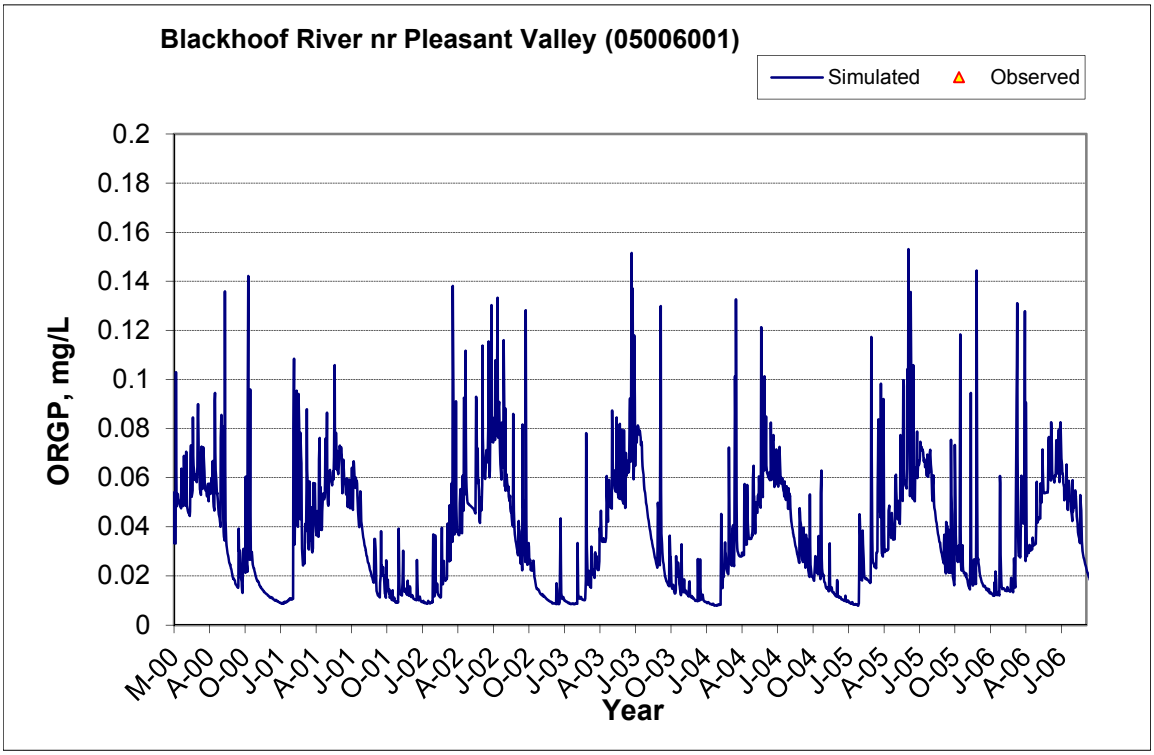

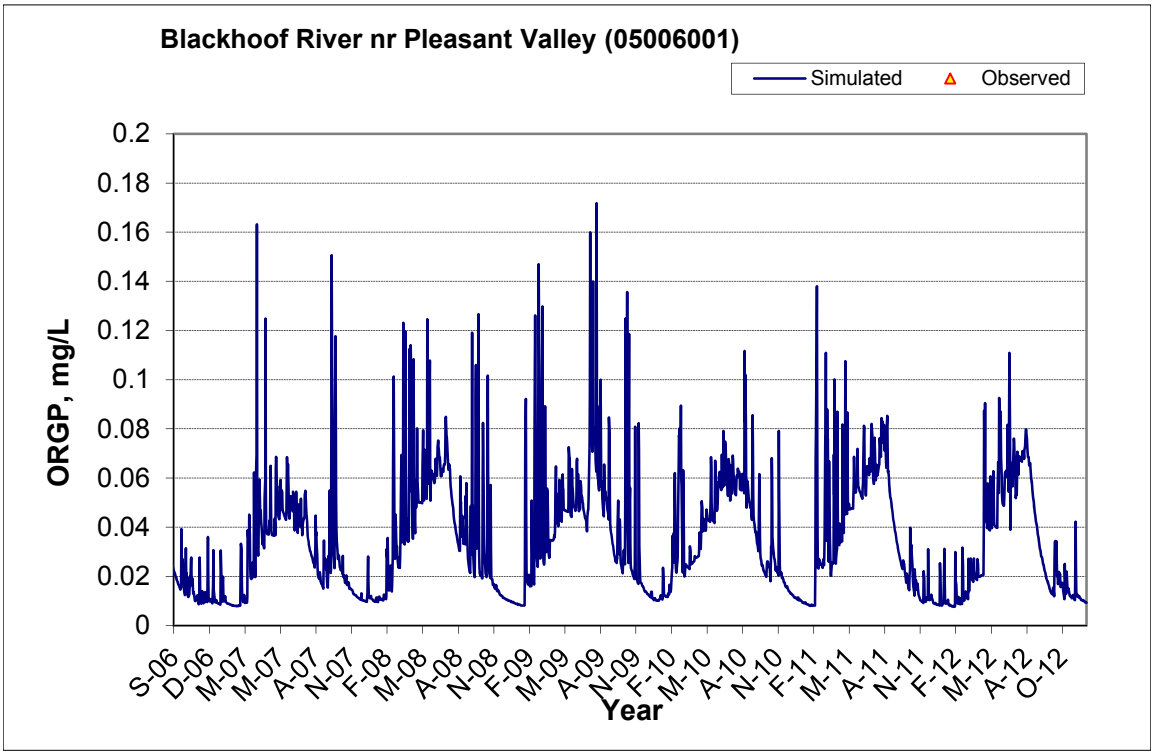

Figure B-99. Time series of observed and simulated Organic Phosphorus (OrgP) concentration at Blackhoof River nr Pleasant Valley (05006001)

B.3.8 Total Phosphorus (TP)

Table B-17. Total Phosphorus (TP) statistics

Period	1994-2008	2009-2012
Count	ND	17
Concentration Average Error		41.06%
Concentration Median Error		53.49%
Load Average Error		85.96%
Load Median Error		19.65%
Paired t conc		0.09
Paired t load		0.18

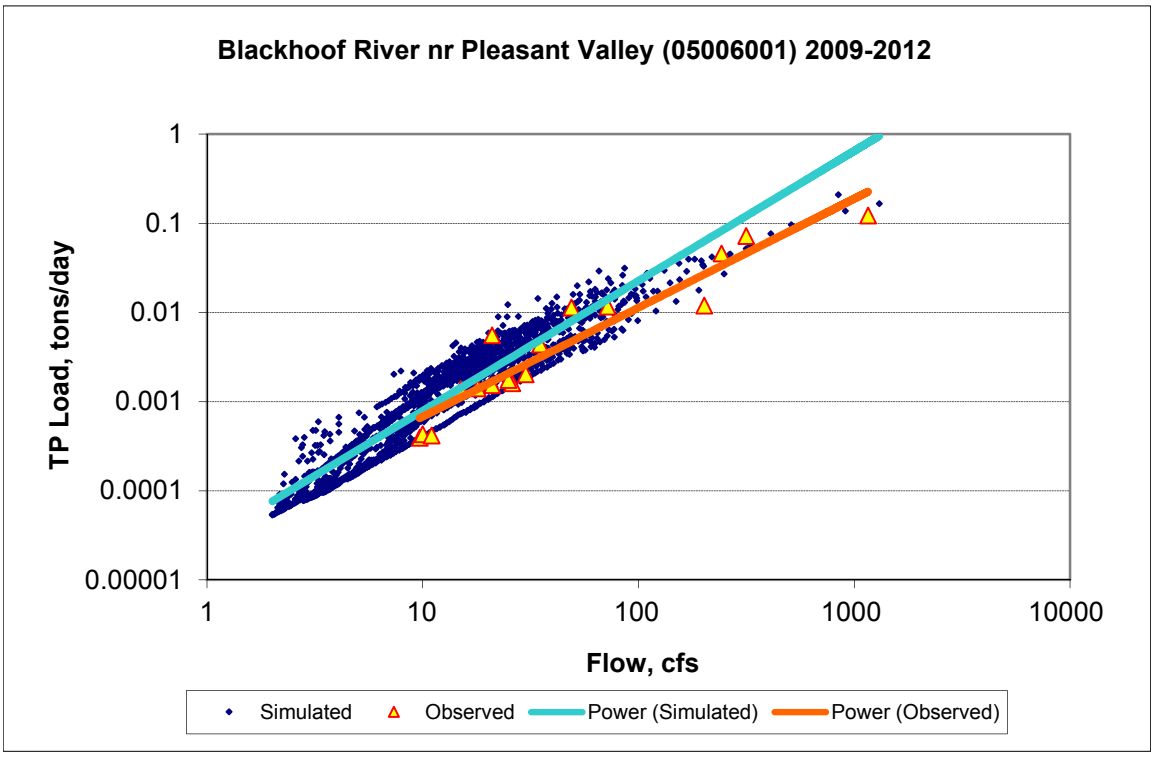

Figure B-100. Power plot of simulated and observed Total Phosphorus (TP) load vs flow at Blackhoof River nr Pleasant Valley (05006001) (calibration period)

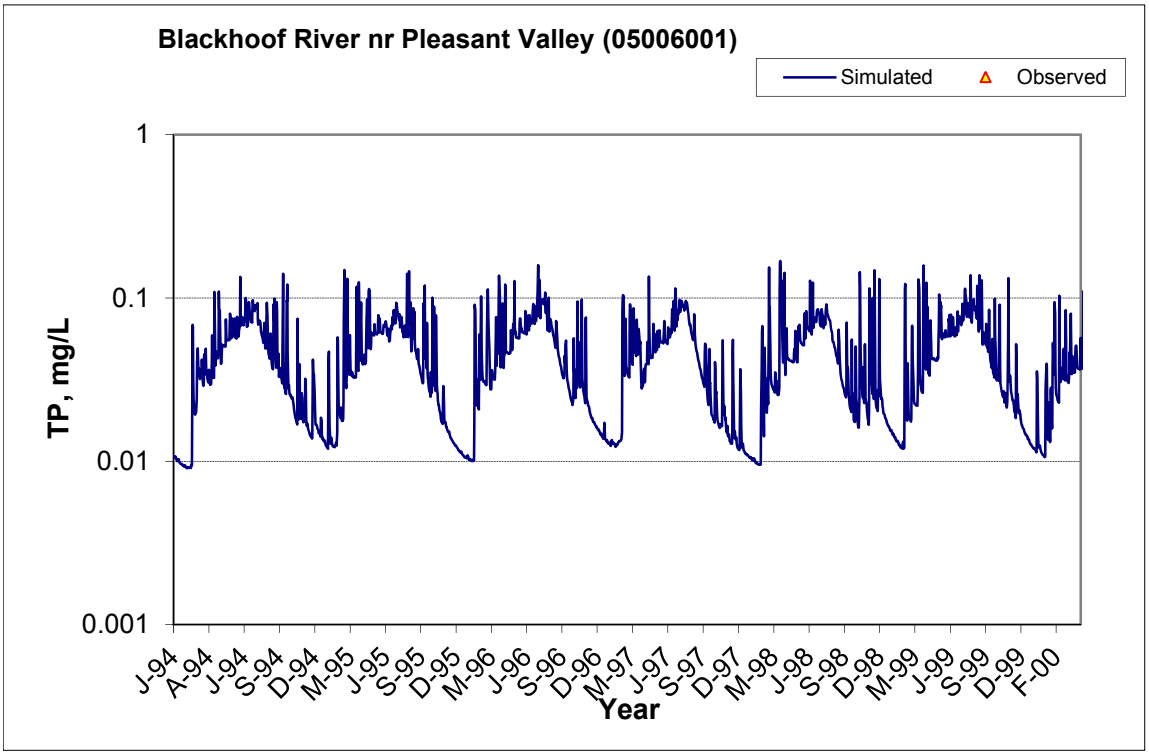

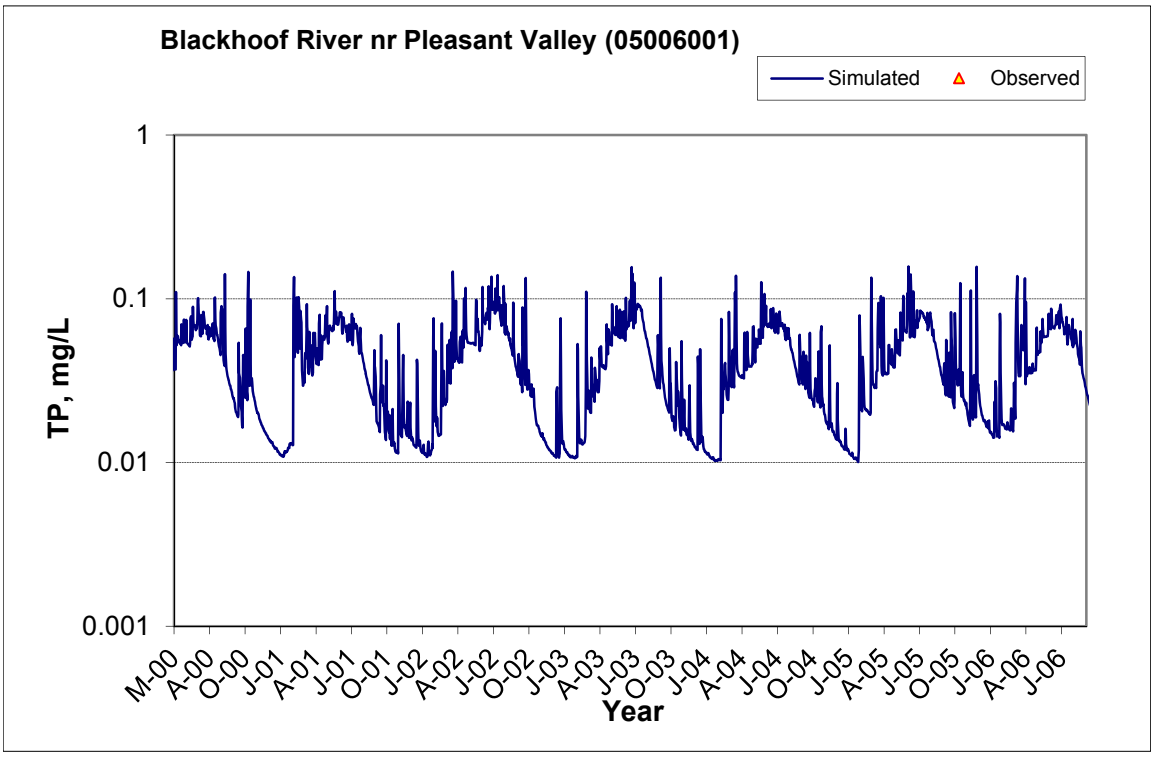

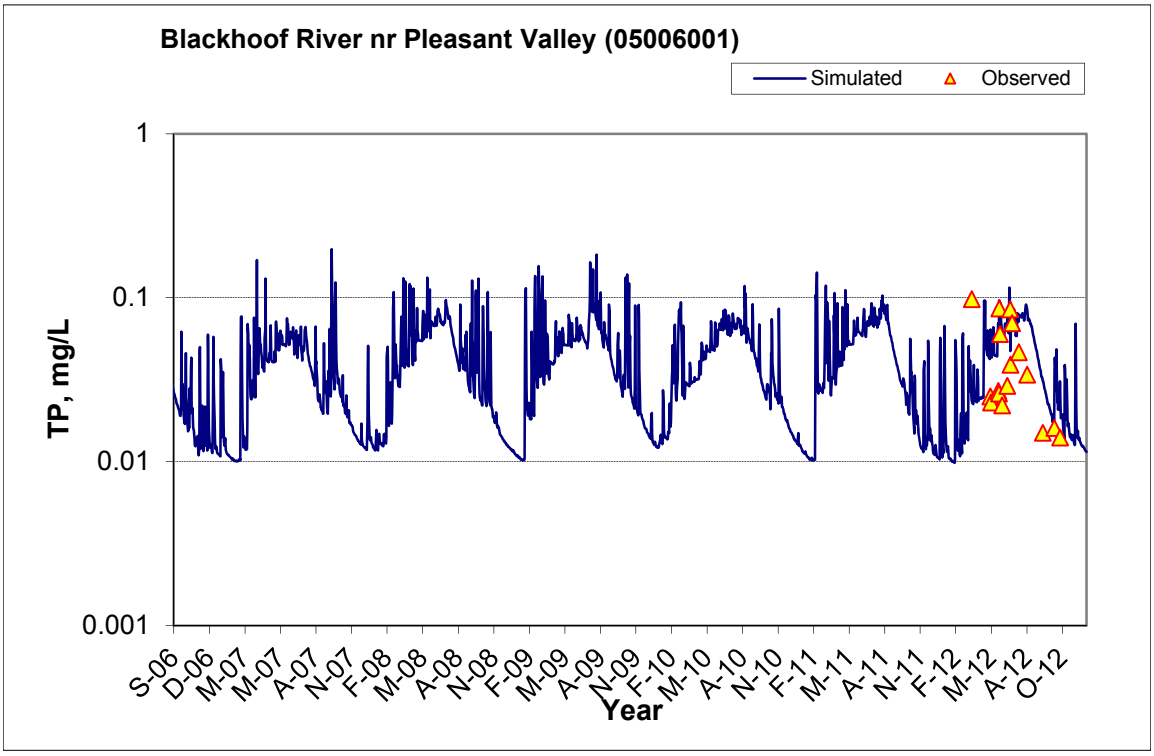

Figure B-101. Time series of observed and simulated Total Phosphorus (TP) concentration at Blackhoof River nr Pleasant Valley (05006001)

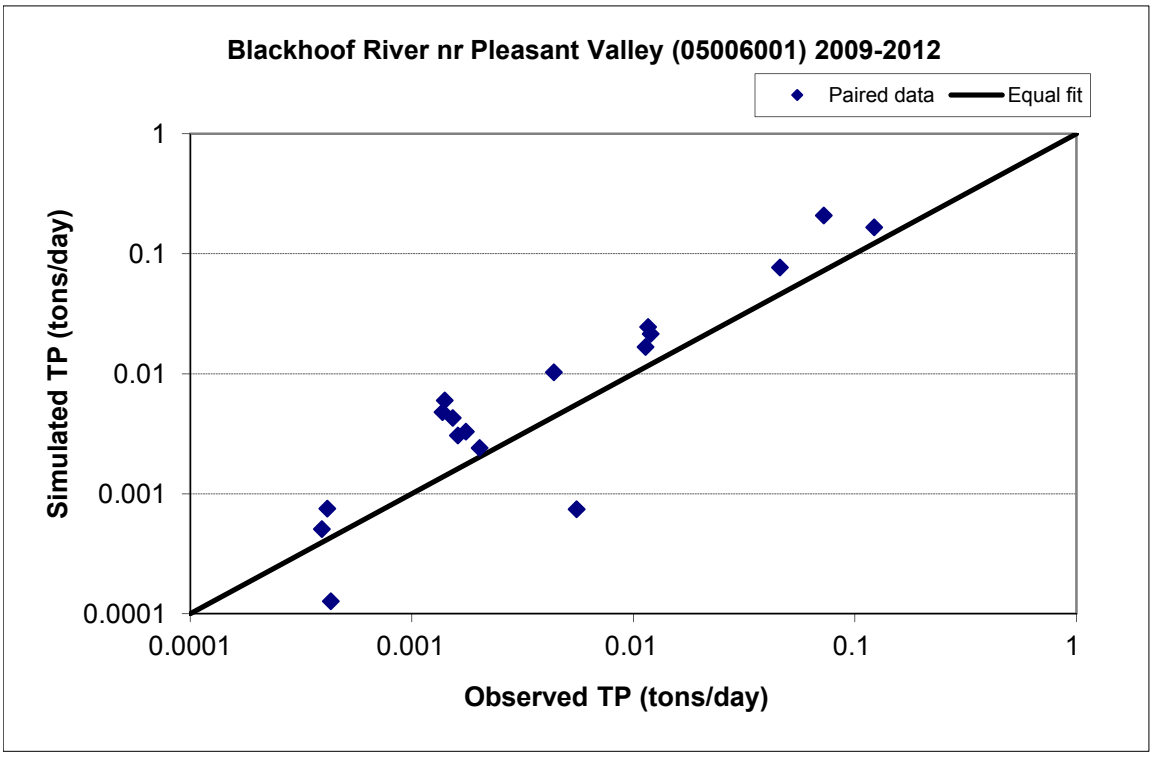

Figure B-102. Paired simulated vs. observed Total Phosphorus (TP) load at Blackhoof River nr Pleasant Valley (05006001) (calibration period)

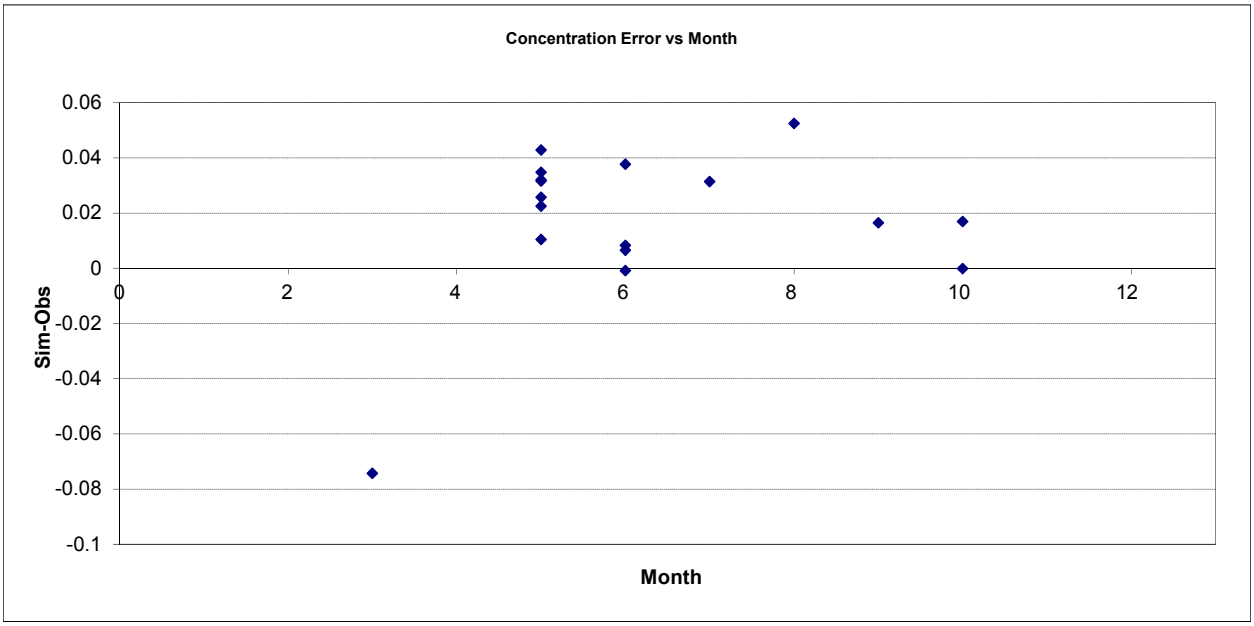

Figure B-103. Residual (Simulated - Observed) vs. Month Total Phosphorus (TP) at Blackhoof River nr Pleasant Valley (05006001)

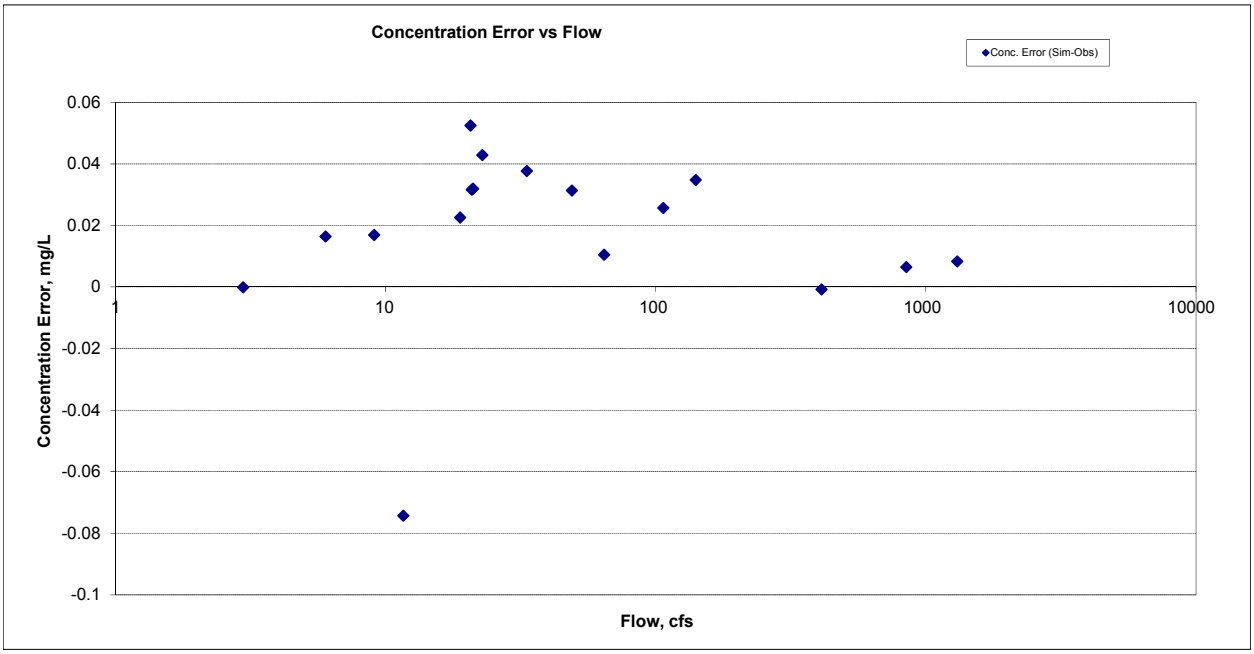

Figure B-104. Residual (Simulated - Observed) vs. Flow Total Phosphorus (TP) at Blackhoof River nr Pleasant Valley (05006001)

B.4 NEMADJI RIVER NR HOLYOKE (05016001)

B.4.1 Ammonia Nitrogen (NH3)

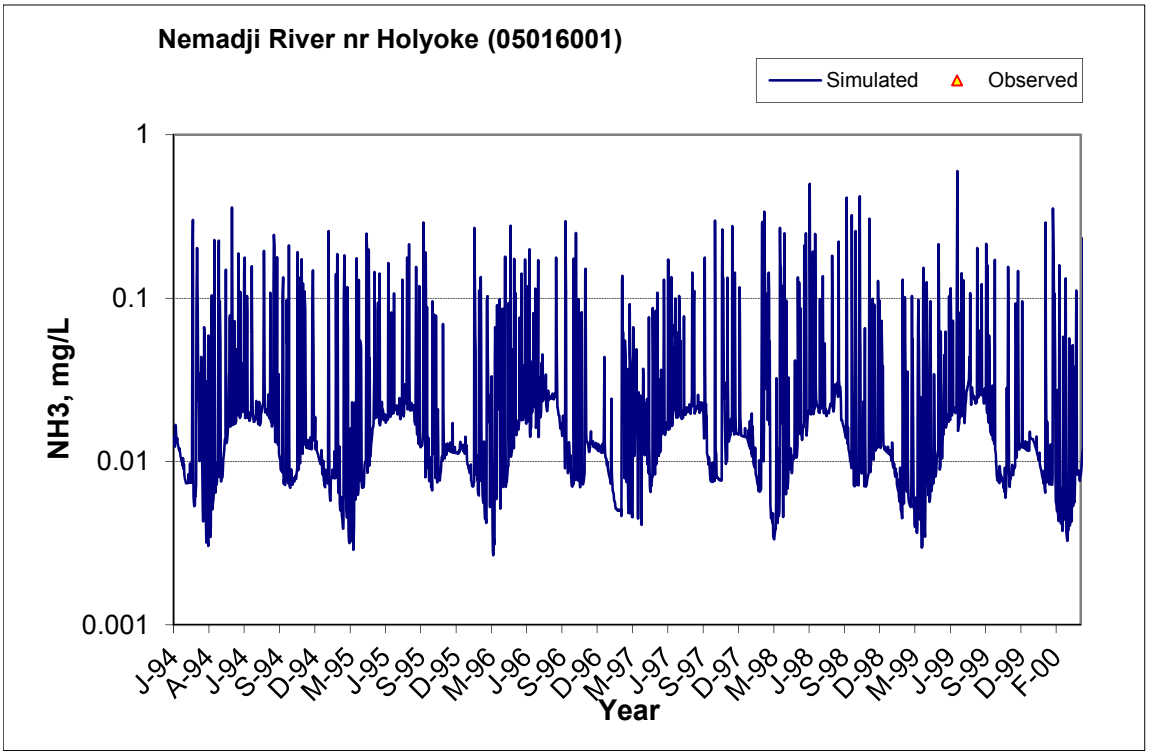

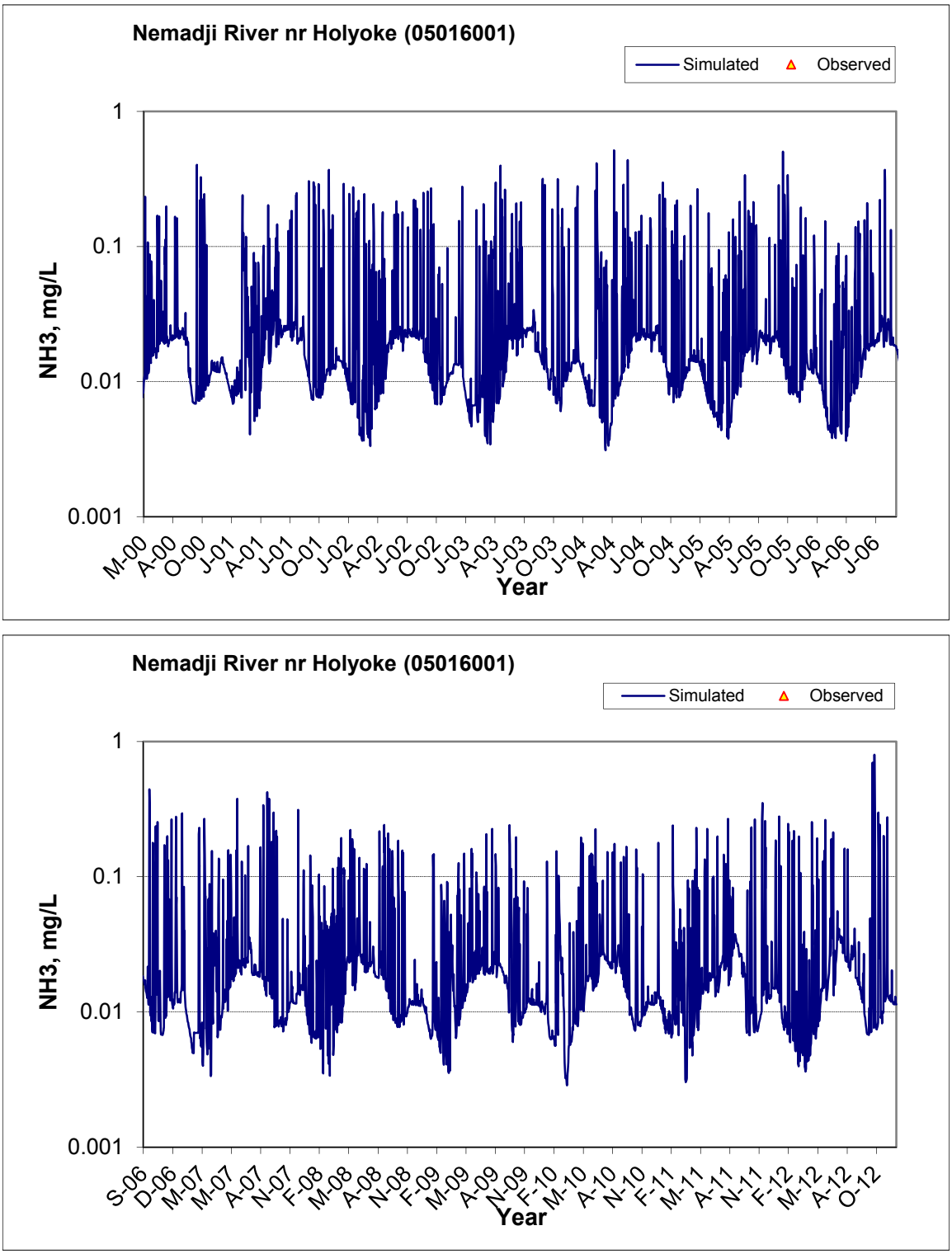

Figure B-105. Time series of observed and simulated Ammonia Nitrogen (NH3) concentration at Nemadji River nr Holyoke (05016001)

B.4.2 Organic Nitrogen (OrgN)

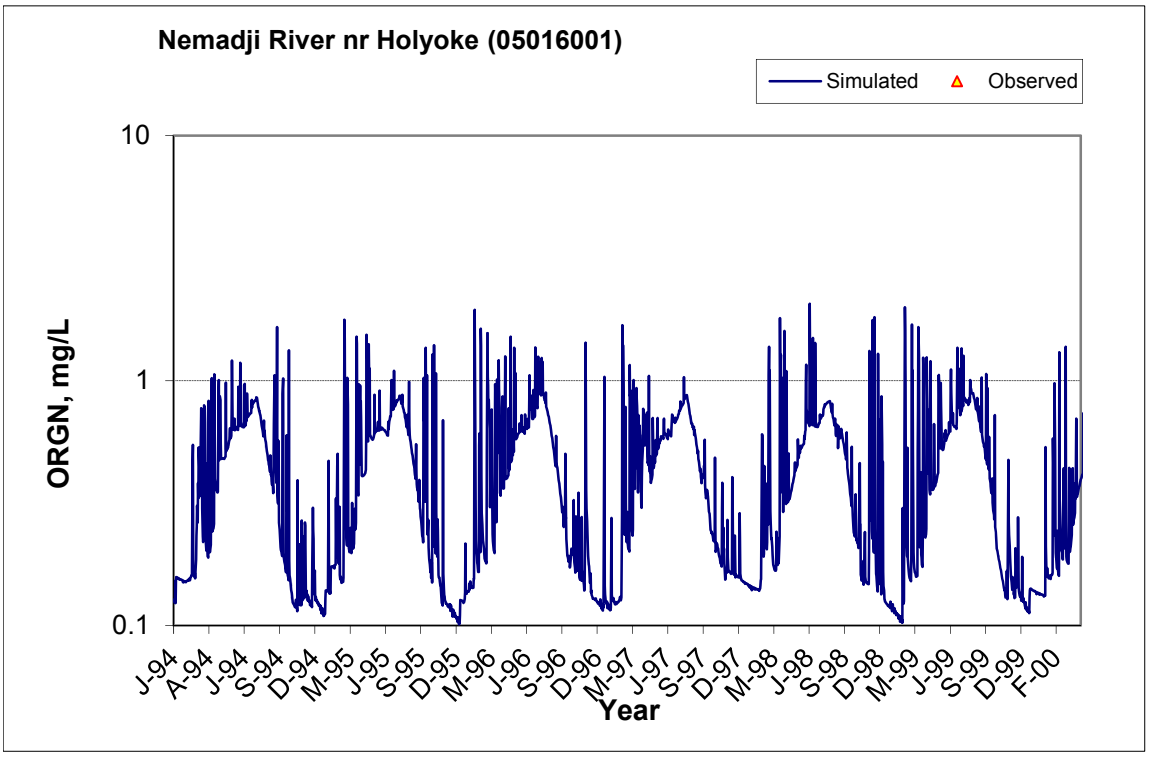

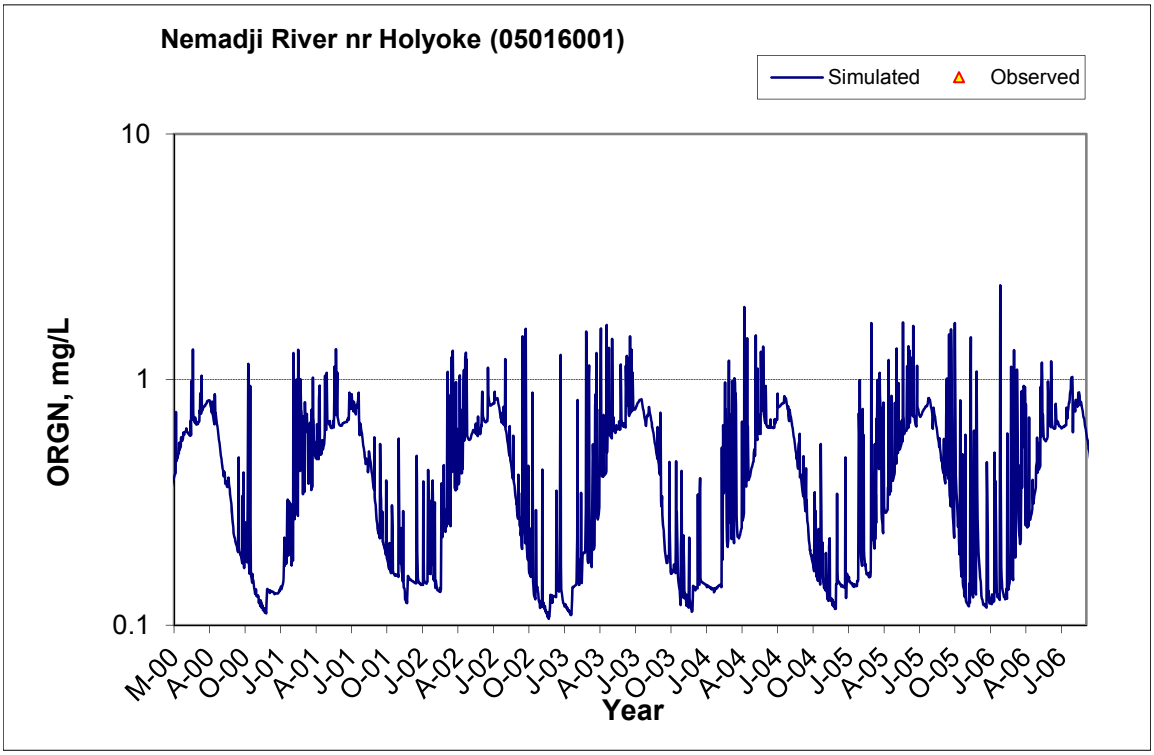

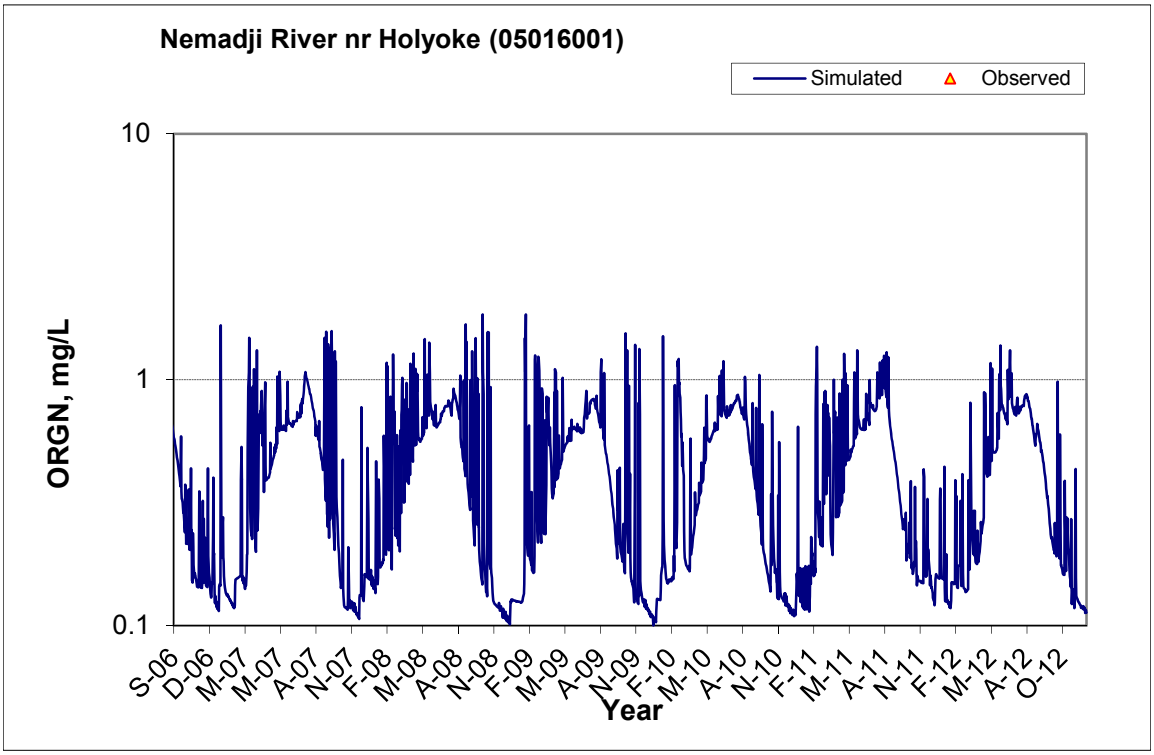

Figure B-106. Time series of observed and simulated Organic Nitrogen (OrgN) concentration at Nemadji River nr Holyoke (05016001)

B.4.3 Total Kjeldahl Nitrogen (TKN)

Table B-18. Total Kjeldahl Nitrogen (TKN) statistics

Period	1994-1993	1994-2012
Count	ND	15
Concentration Average Error		-3.76%
Concentration Median Error		-10.92%
Load Average Error		2.04%
Load Median Error		-6.02%
Paired t conc		0.94
Paired t load		0.64

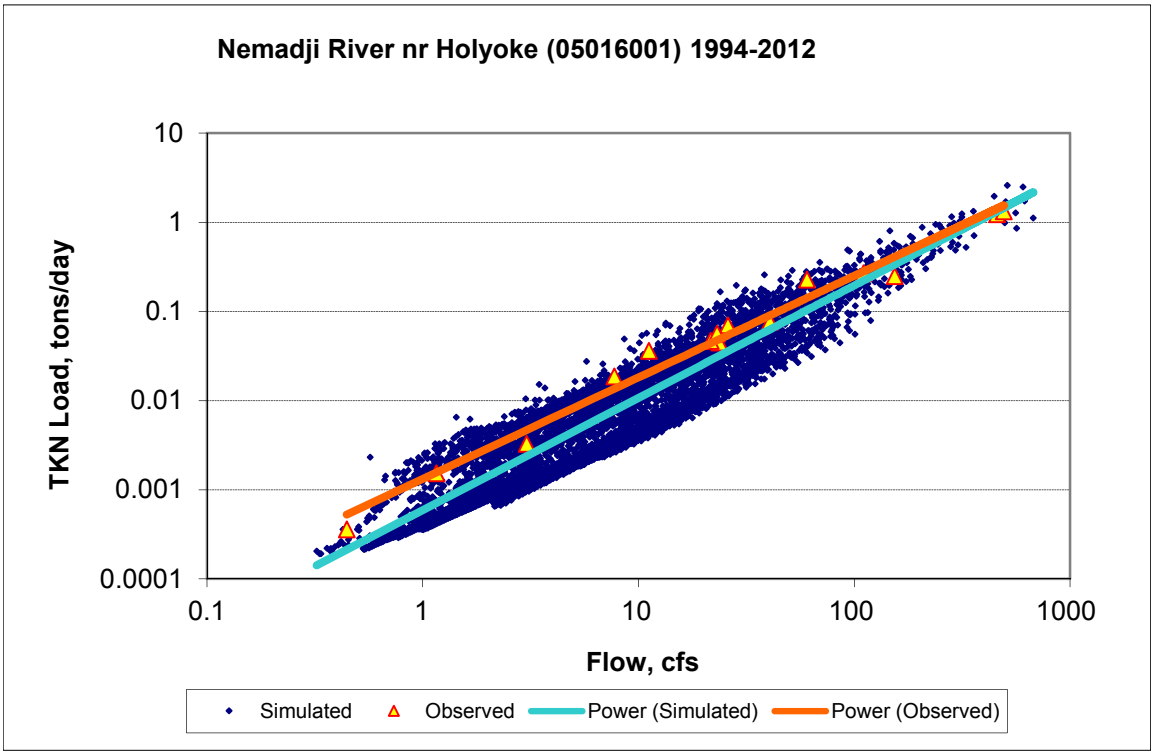

Figure B-107. Power plot of simulated and observed Total Kjeldahl Nitrogen (TKN) load vs flow at Nemadji River nr Holyoke (05016001) (calibration period)

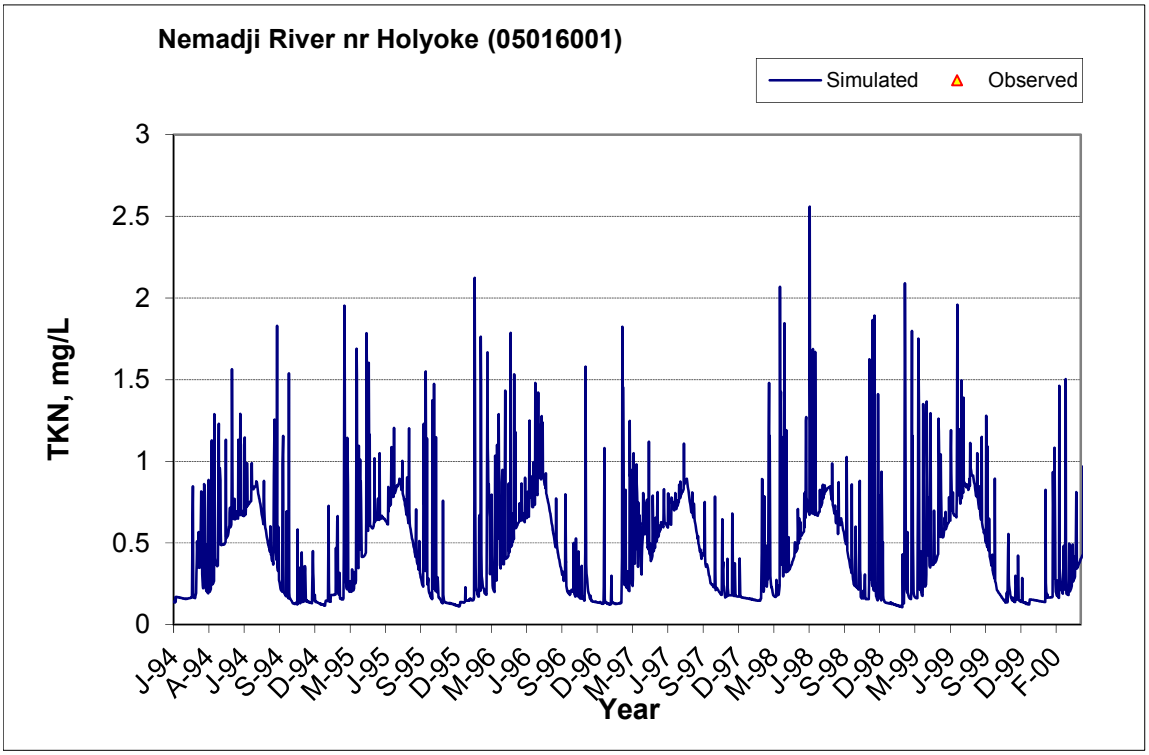

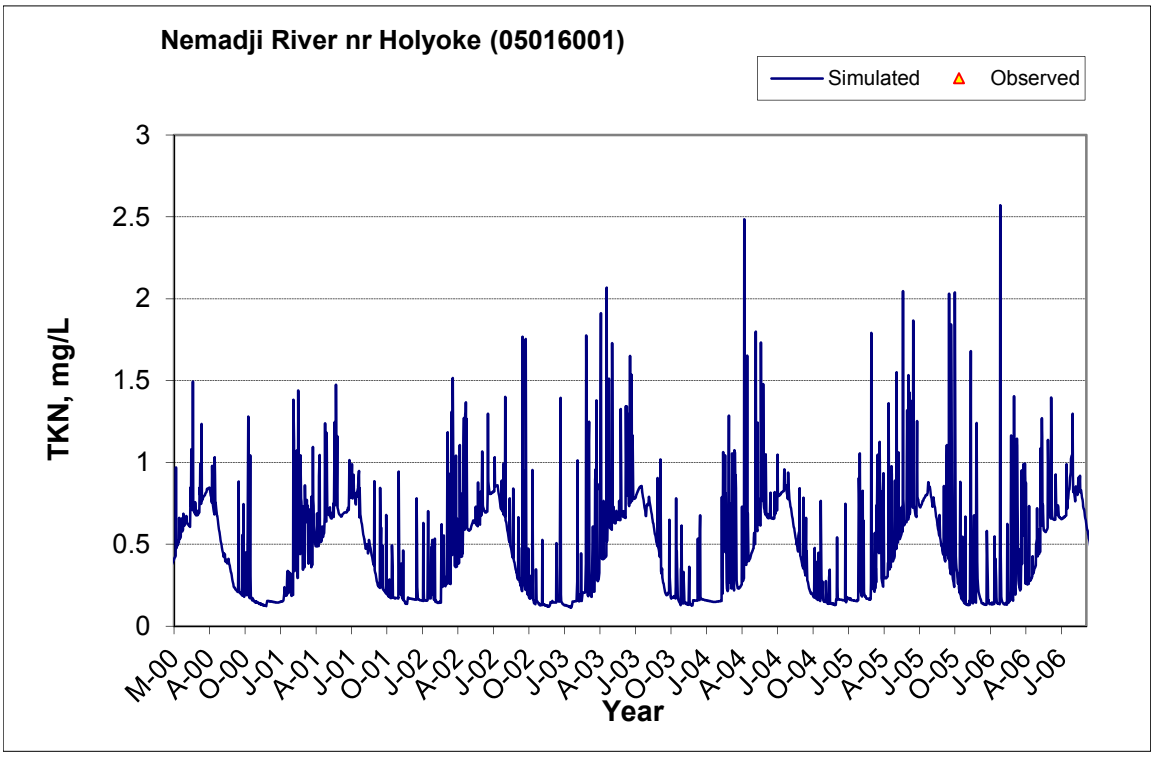

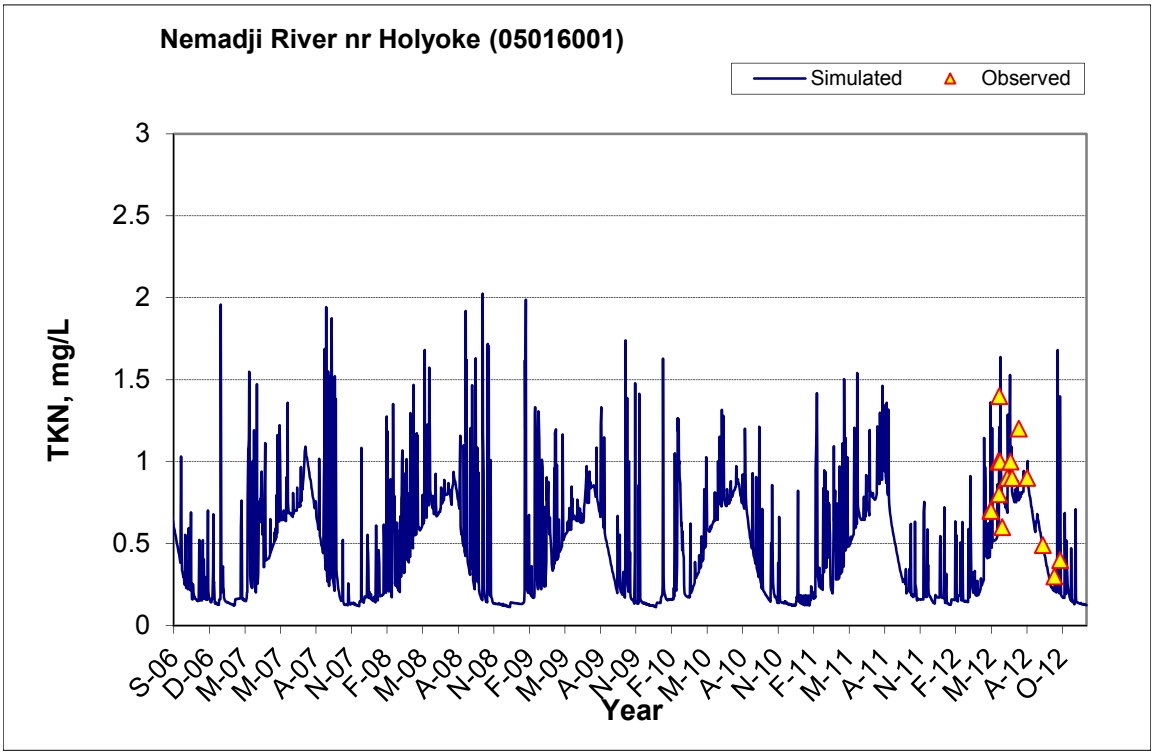

Figure B-108. Time series of observed and simulated Total Kjeldahl Nitrogen (TKN) concentration at Nemadji River nr Holyoke (05016001)

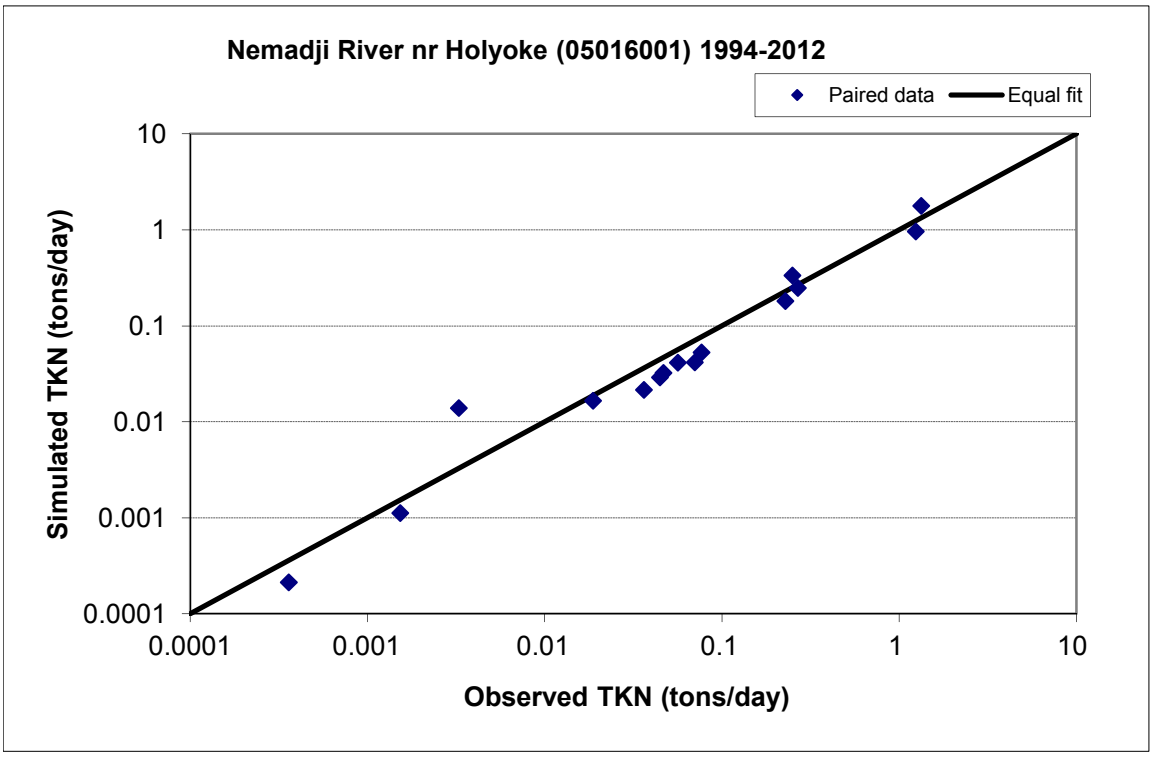

Figure B-109. Paired simulated vs. observed Total Kjeldahl Nitrogen (TKN) load at Nemadji River nr Holyoke (05016001) (calibration period)

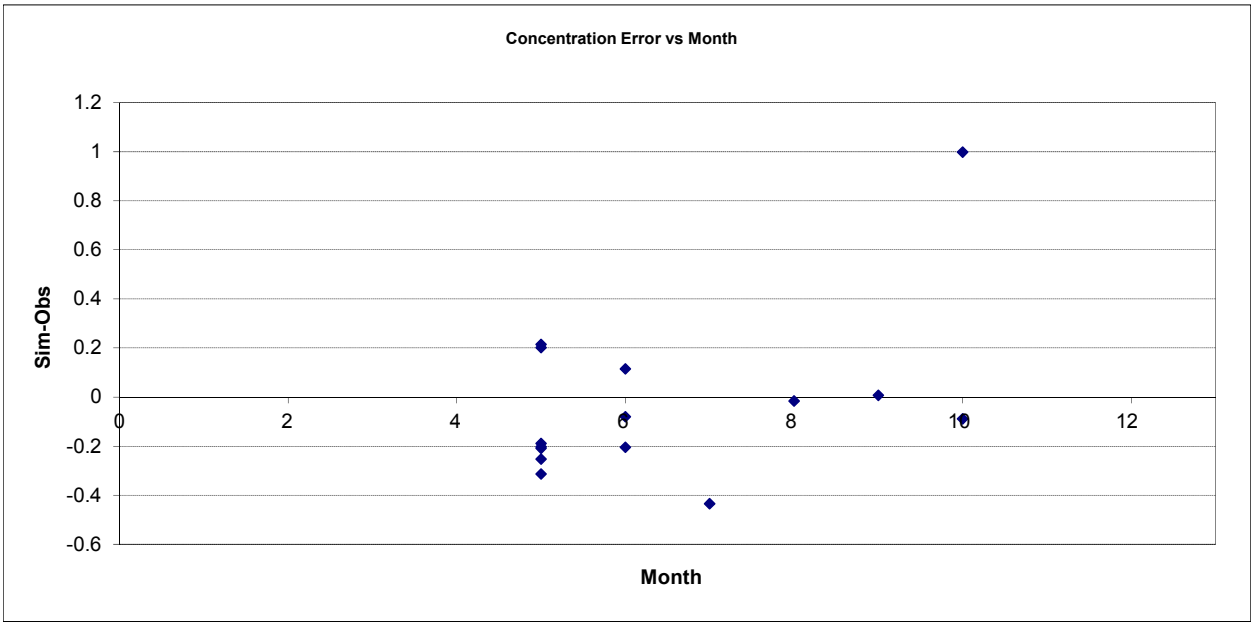

Figure B-110. Residual (Simulated - Observed) vs. Month Total Kjeldahl Nitrogen (TKN) at Nemadji River nr Holyoke (05016001)

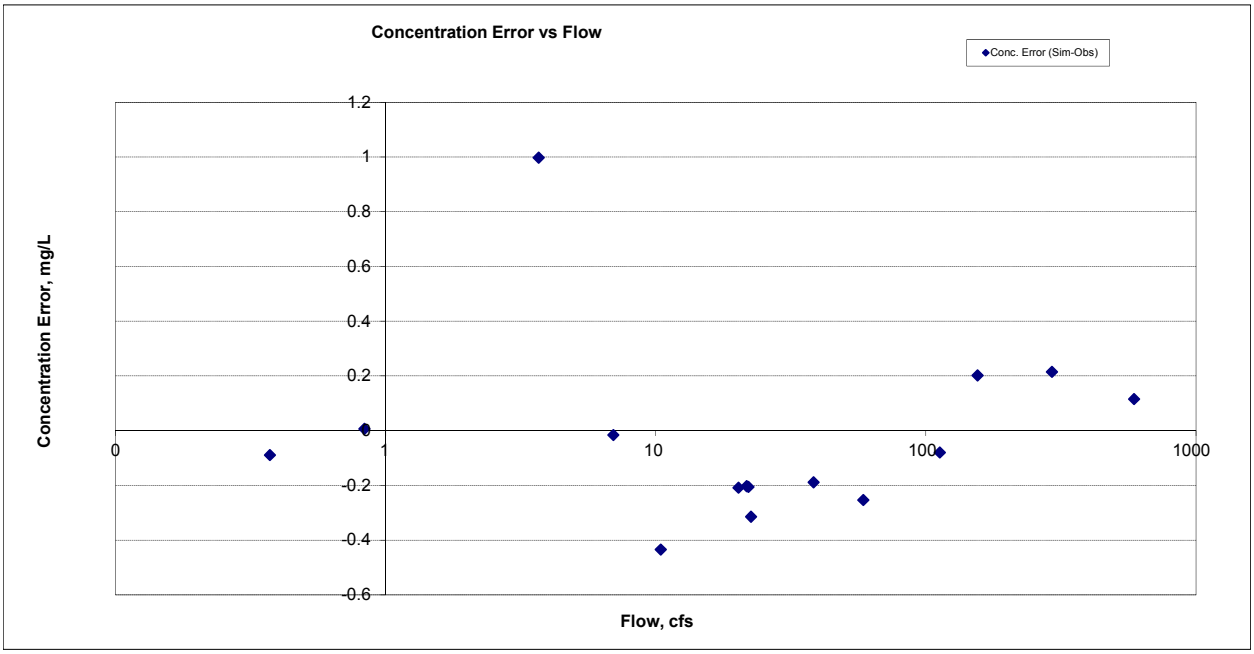

Figure B-111. Residual (Simulated - Observed) vs. Flow Total Kjeldahl Nitrogen (TKN) at Nemadji River nr Holyoke (05016001)

B.4.4 Nitrite+ Nitrate Nitrogen (NOx)

Table B-19. Nitrite+ Nitrate Nitrogen (NOx) statistics

Period	1994-1993	1994-2012
Count	ND	15
Concentration Average Error		437.85%
Concentration Median Error		71.51%
Load Average Error		244.77%
Load Median Error		20.09%
Paired t conc		0.05
Paired t load		0.05

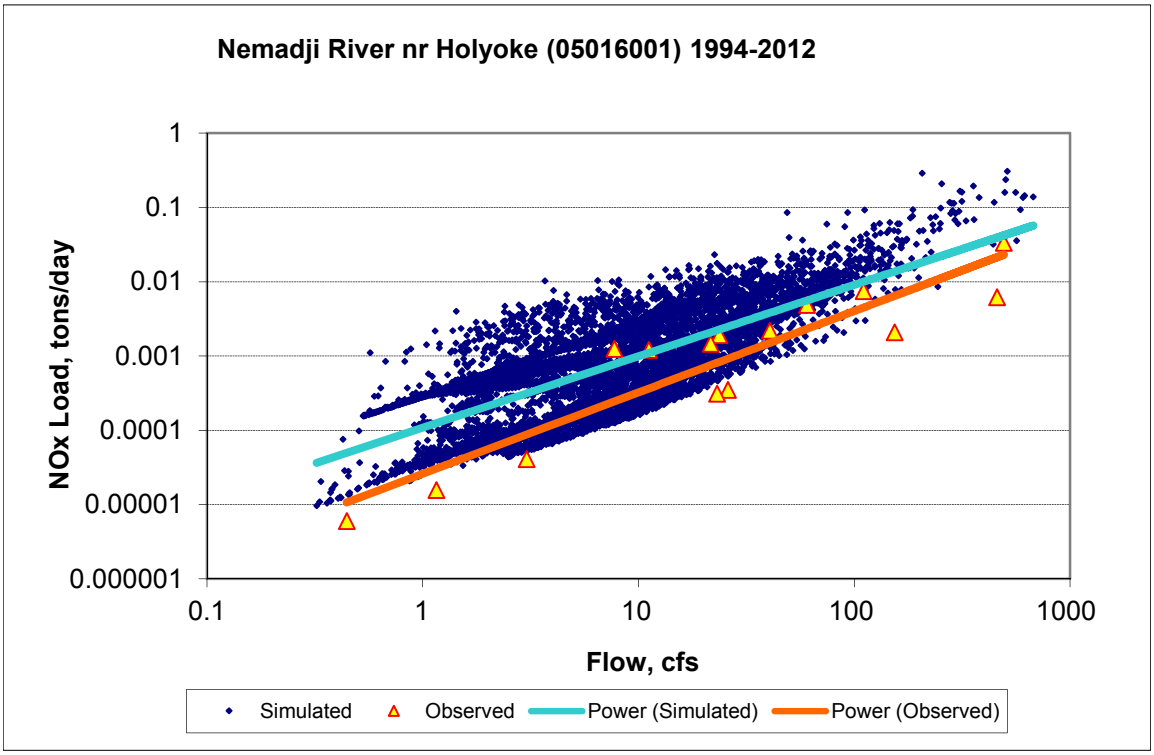

Figure B-112. Power plot of simulated and observed Nitrite+ Nitrate Nitrogen (NOx) load vs flow at Nemadji River nr Holyoke (05016001) (calibration period)

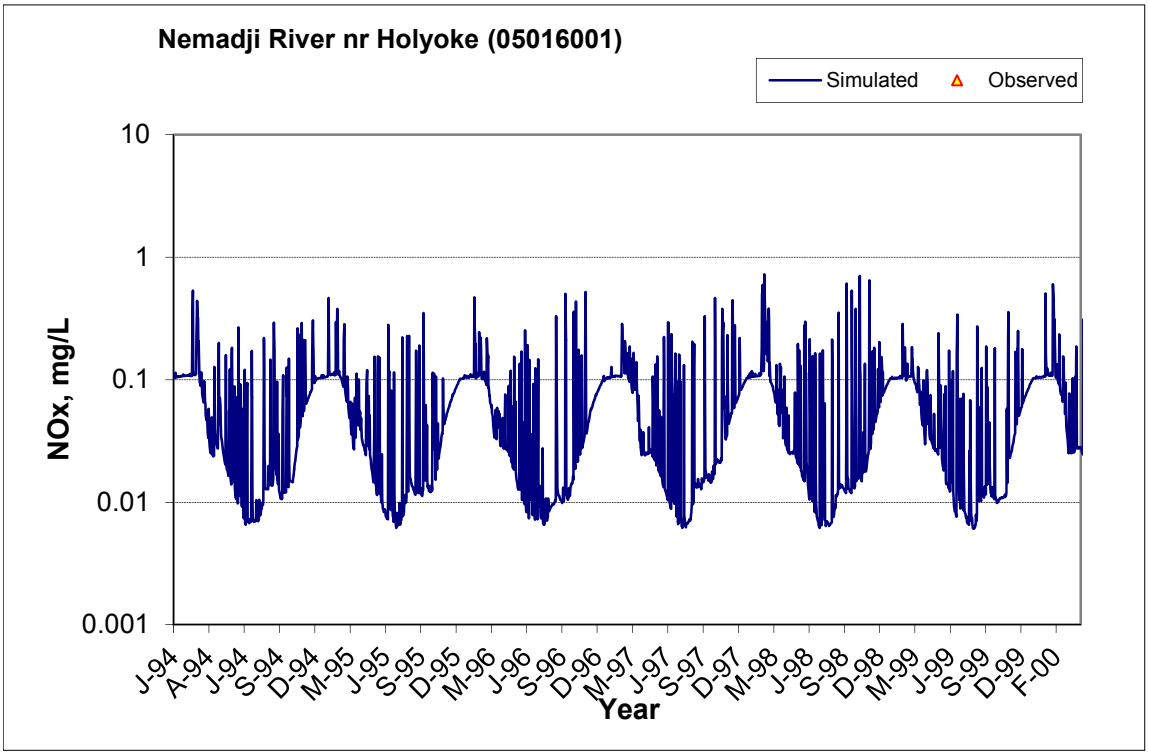

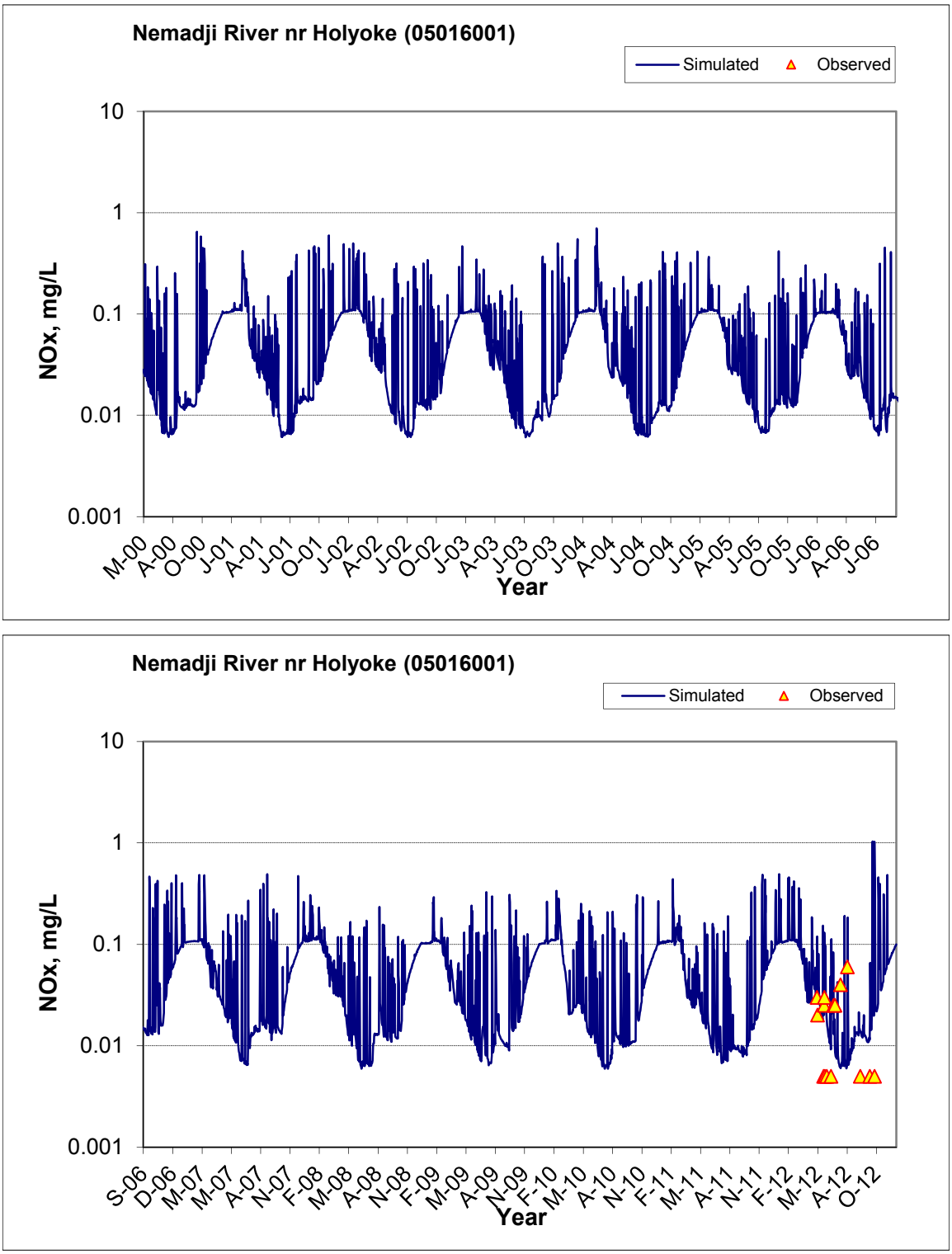

Figure B-113. Time series of observed and simulated Nitrite+ Nitrate Nitrogen (NOx) concentration at Nemadji River nr Holyoke (05016001)

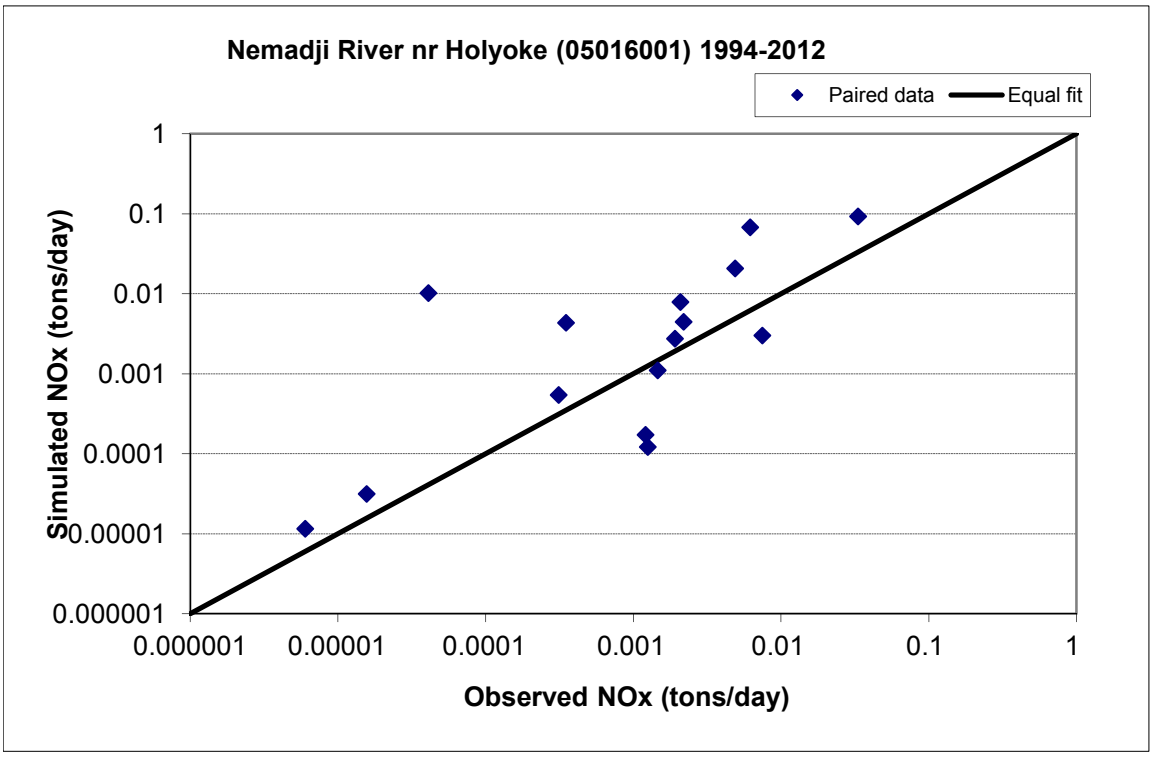

Figure B-114. Paired simulated vs. observed Nitrite+ Nitrate Nitrogen (NOx) load at Nemadji River nr Holyoke (05016001) (calibration period)

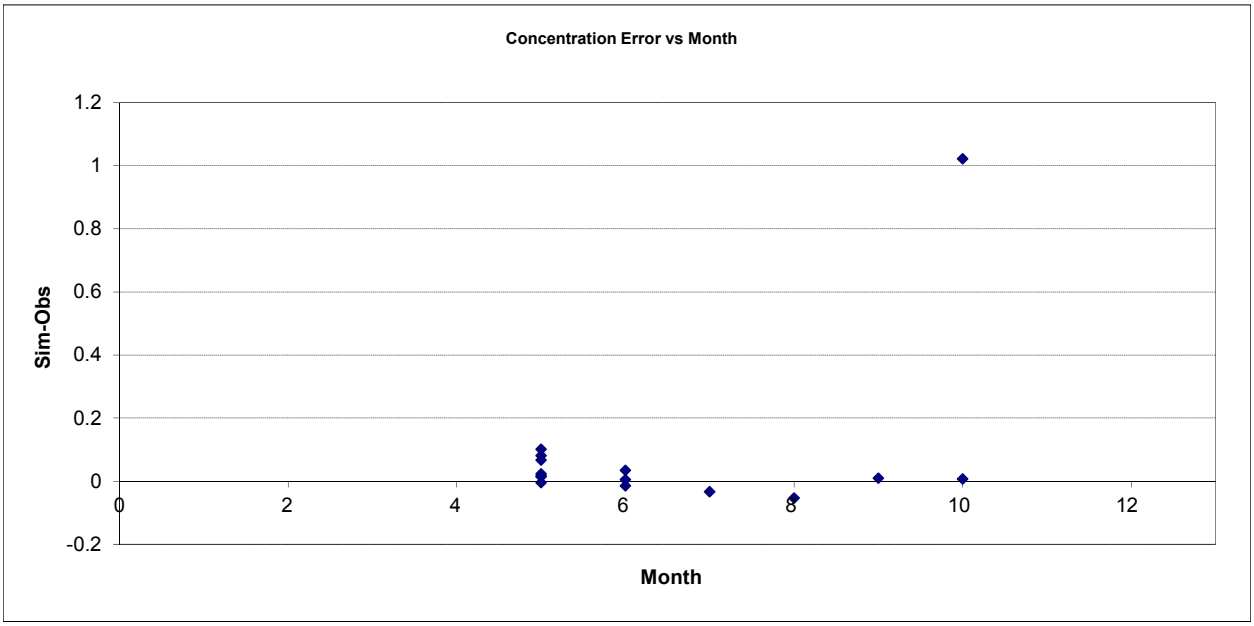

Figure B-115. Residual (Simulated - Observed) vs. Month Nitrite+ Nitrate Nitrogen (NOx) at Nemadji River nr Holyoke (05016001)

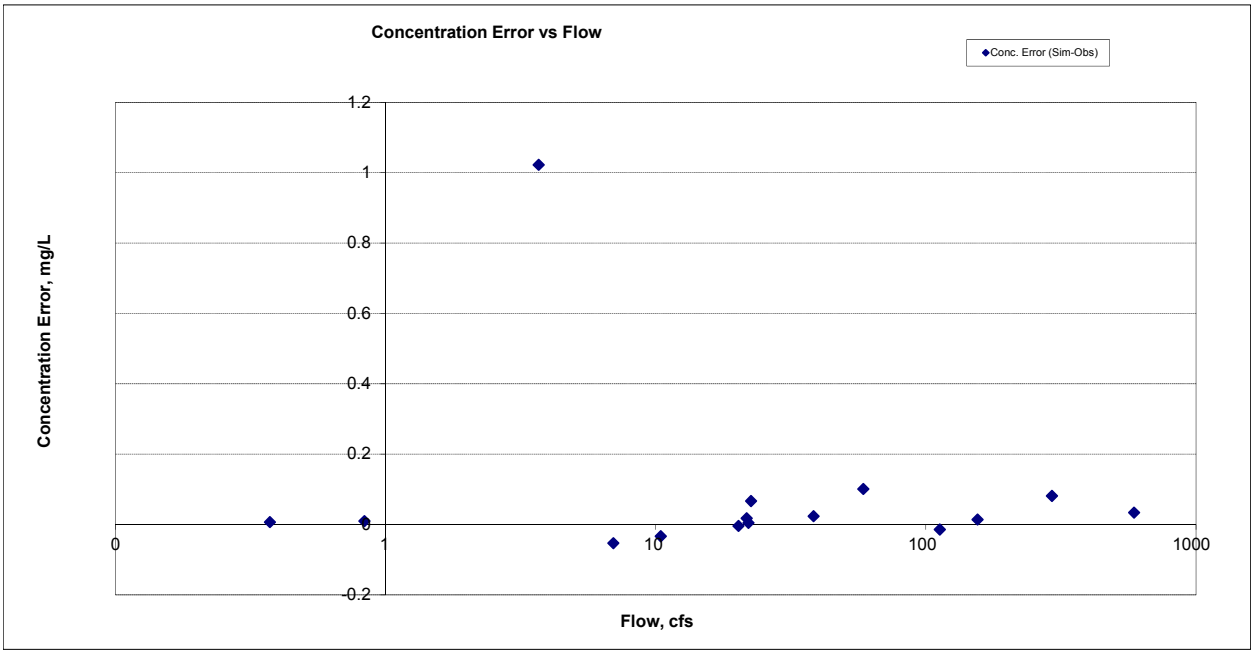

Figure B-116. Residual (Simulated - Observed) vs. Flow Nitrite+ Nitrate Nitrogen (NOx) at Nemadji River nr Holyoke (05016001)

B.4.5 Total Nitrogen (TN)

Table B-20. Total Nitrogen (TN) statistics

Period	1994-1993	1994-2012
Count	ND	15
Concentration Average Error		5.50%
Concentration Median Error		-14.25%
Load Average Error		4.68%
Load Median Error		-5.98%
Paired t conc		0.86
Paired t load		0.62

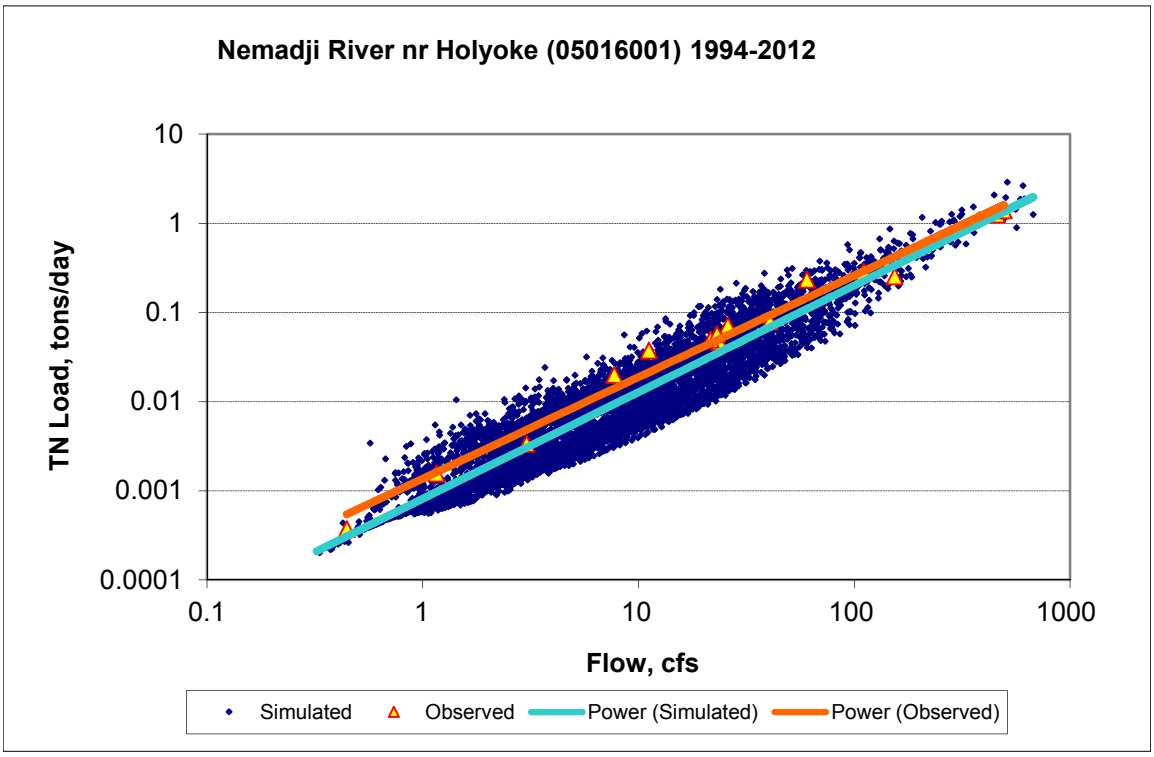

Figure B-117. Power plot of simulated and observed Total Nitrogen (TN) load vs flow at Nemadji River nr Holyoke (05016001) (calibration period)

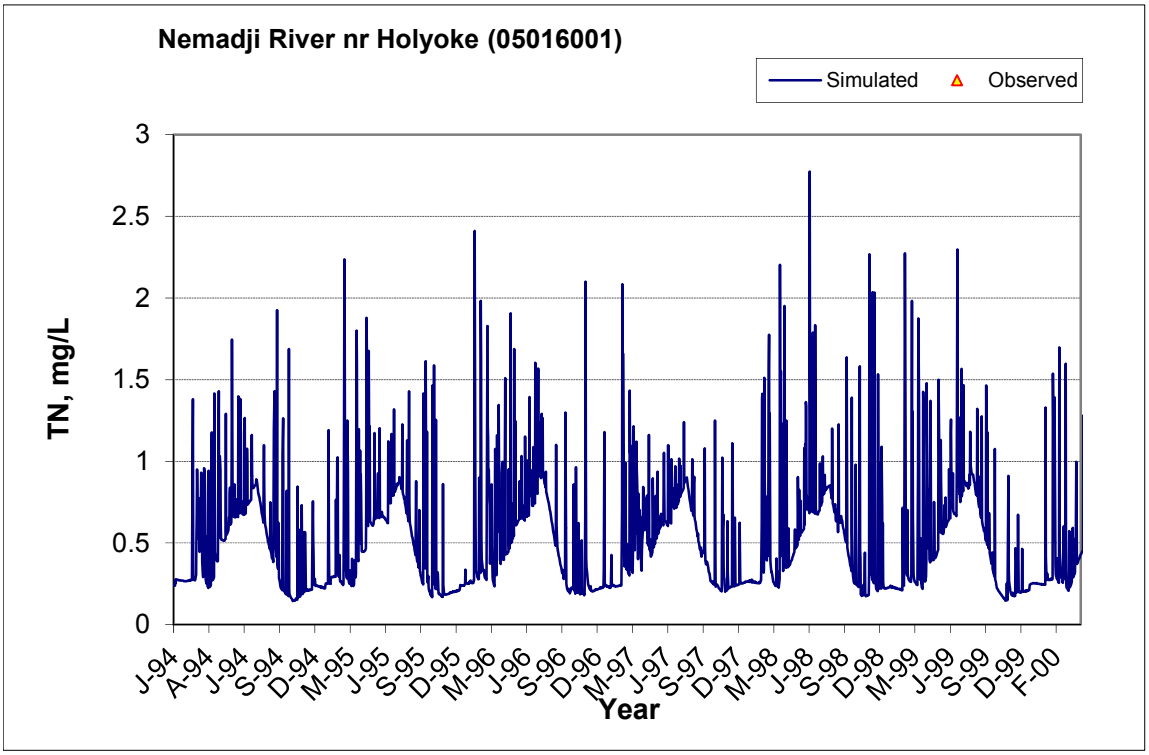

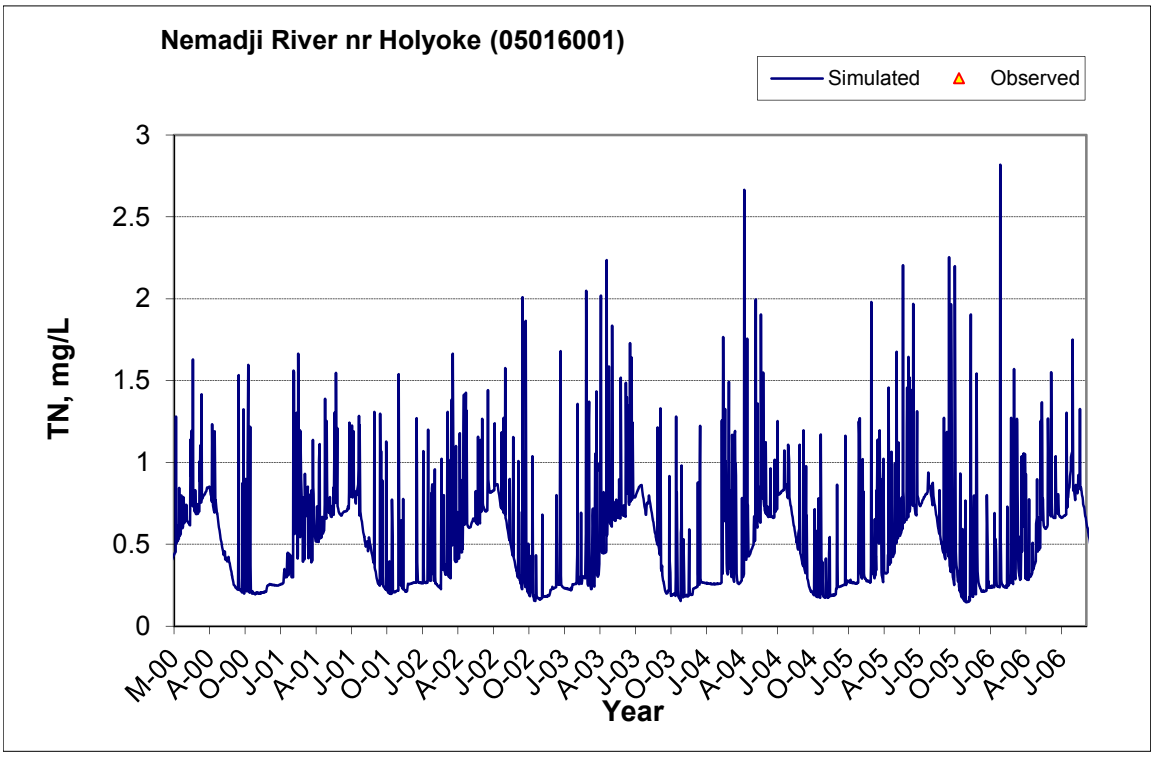

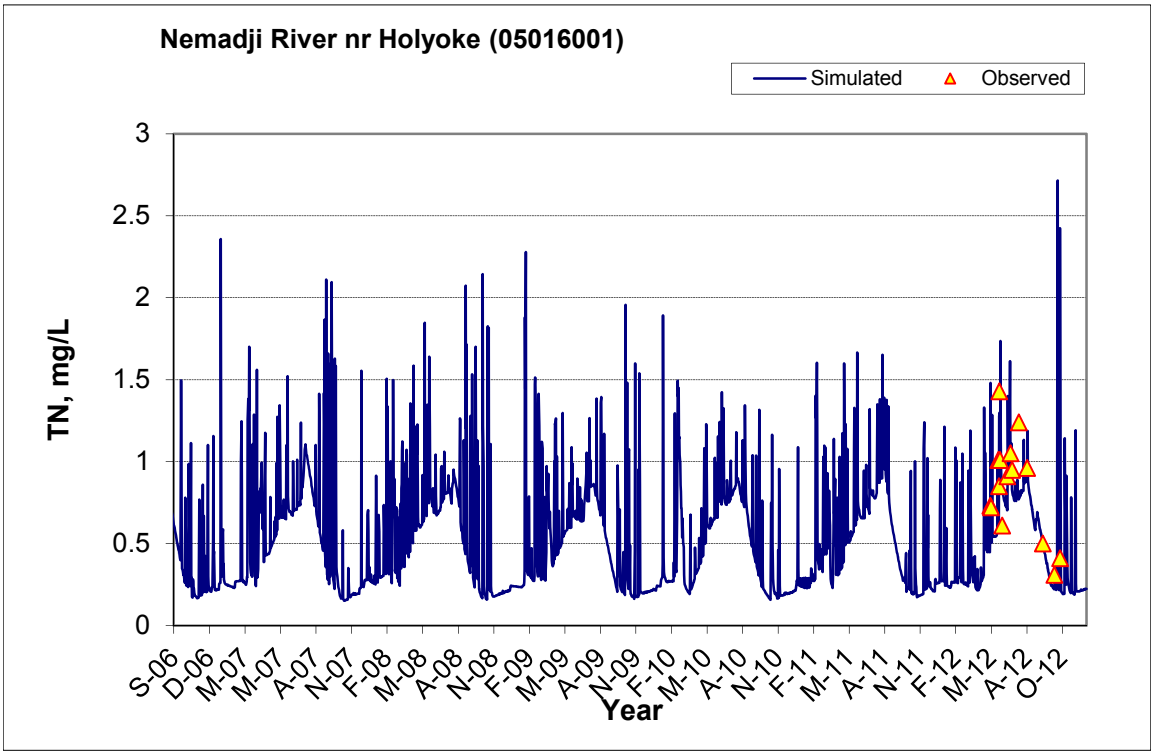

Figure B-118. Time series of observed and simulated Total Nitrogen (TN) concentration at Nemadji River nr Holyoke (05016001)

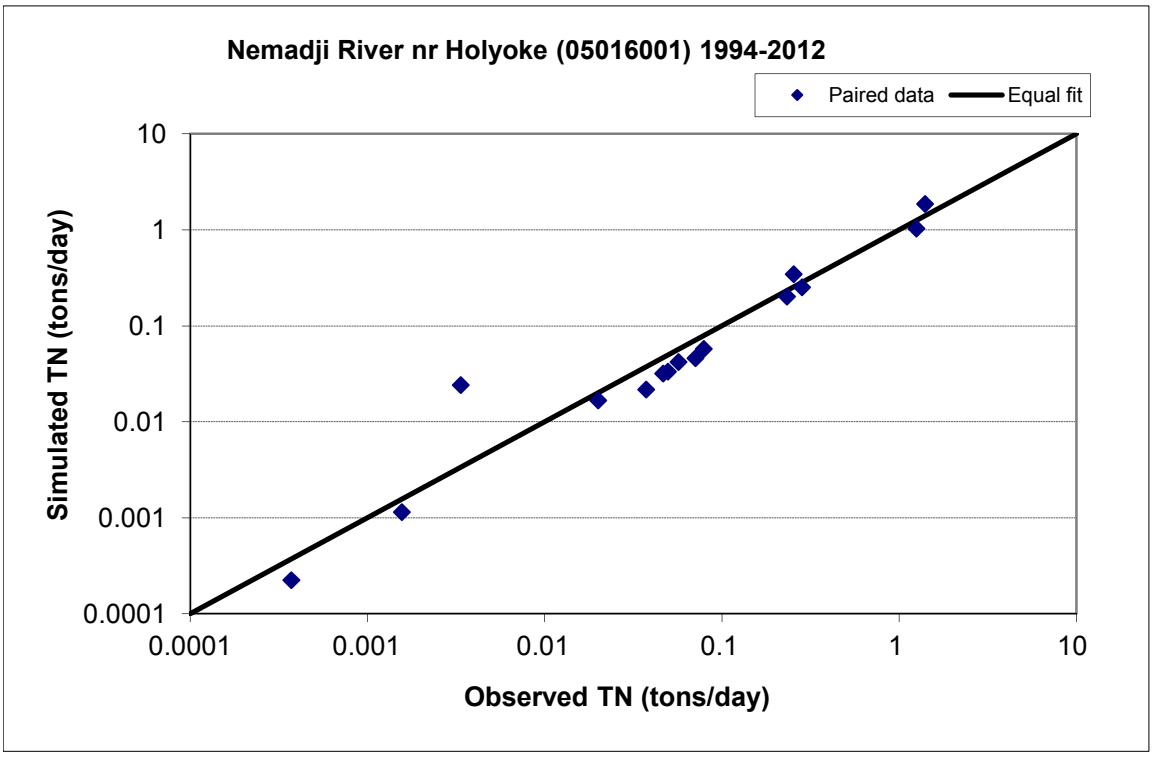

Figure B-119. Paired simulated vs. observed Total Nitrogen (TN) load at Nemadji River nr Holyoke (05016001) (calibration period)

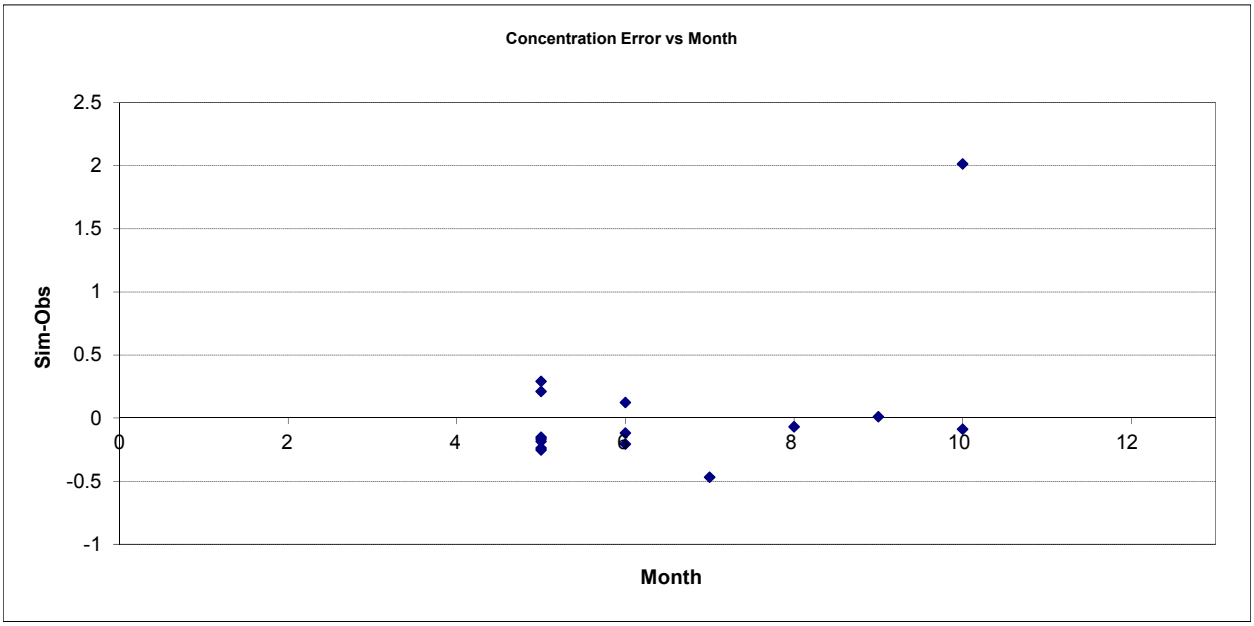

Figure B-120. Residual (Simulated - Observed) vs. Month Total Nitrogen (TN) at Nemadji River nr Holyoke (05016001)

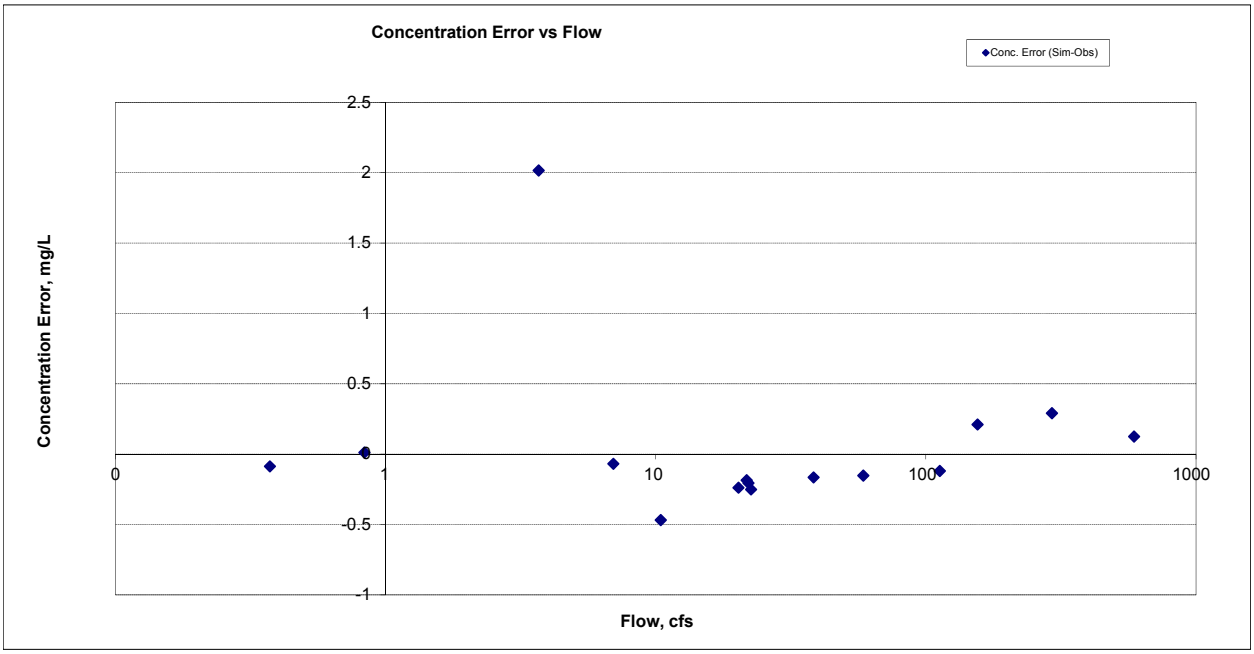

Figure B-121. Residual (Simulated - Observed) vs. Flow Total Nitrogen (TN) at Nemadji River nr Holyoke (05016001)

B.4.6 Soluble Reactive Phosphorus (SRP)

Table B-21. Soluble Reactive Phosphorus (SRP) statistics

Period	1994-1993	1994-2012
Count	ND	15
Concentration Average Error		187.65%
Concentration Median Error		44.52%
Load Average Error		736.70%
Load Median Error		11.52%
Paired t conc		0.01
Paired t load		0.04

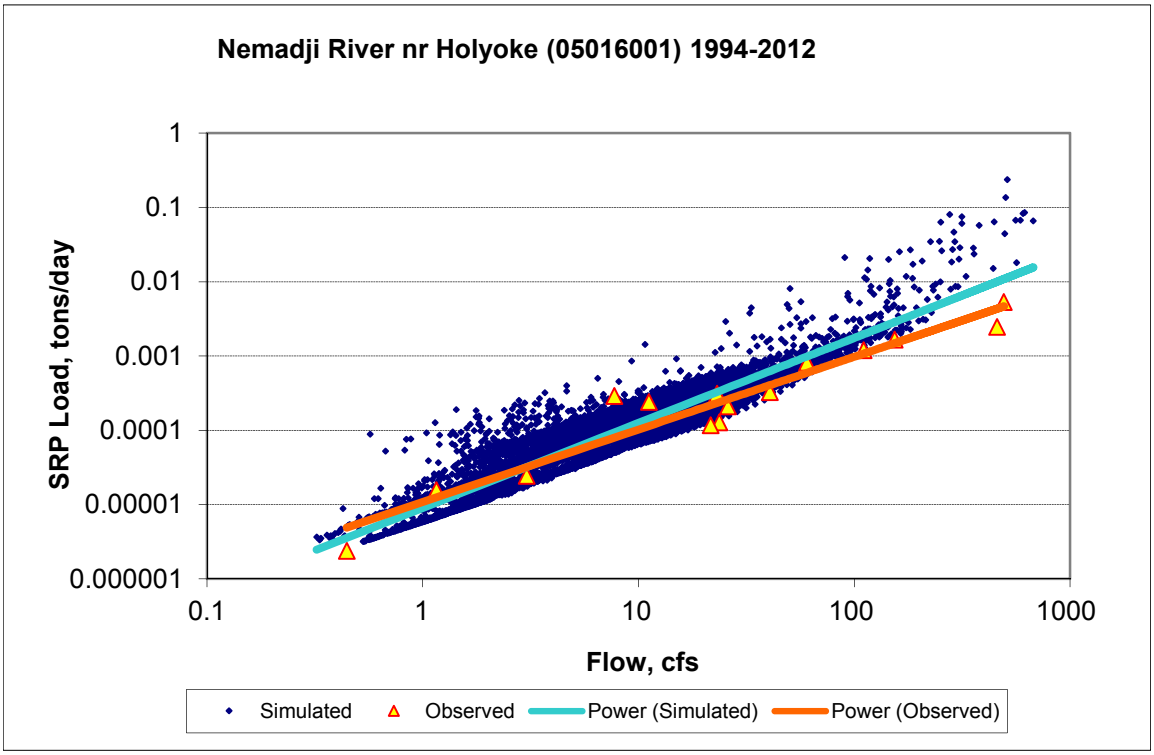

Figure B-122. Power plot of simulated and observed Soluble Reactive Phosphorus (SRP) load vs flow at Nemadji River nr Holyoke (05016001) (calibration period)

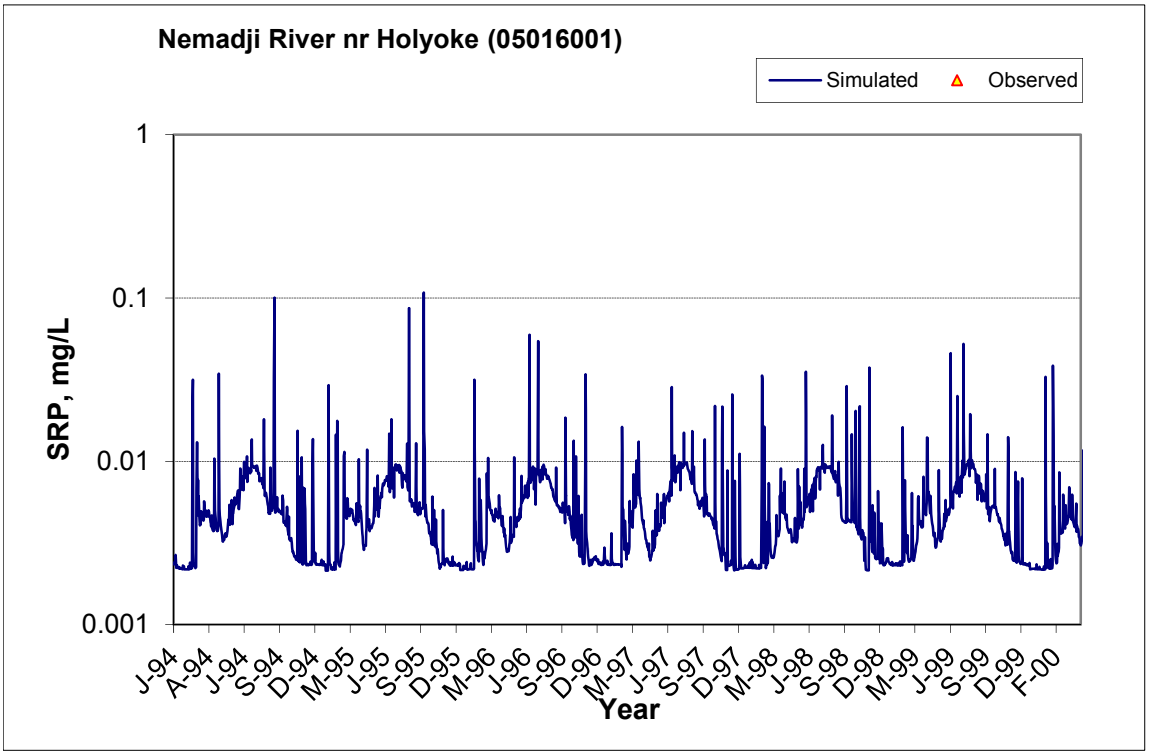

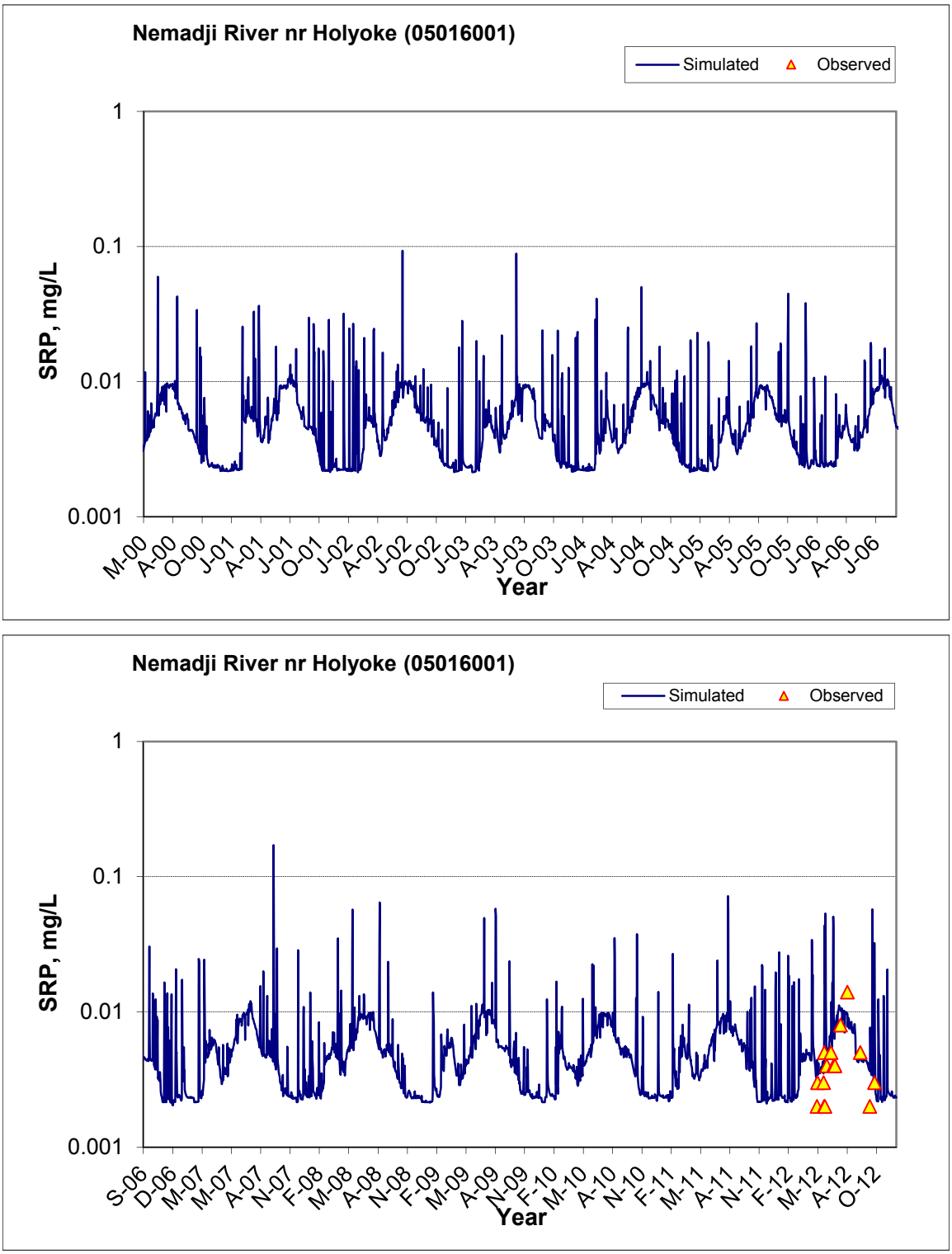

Figure B-123. Time series of observed and simulated Soluble Reactive Phosphorus (SRP) concentration at Nemadji River nr Holyoke (05016001)

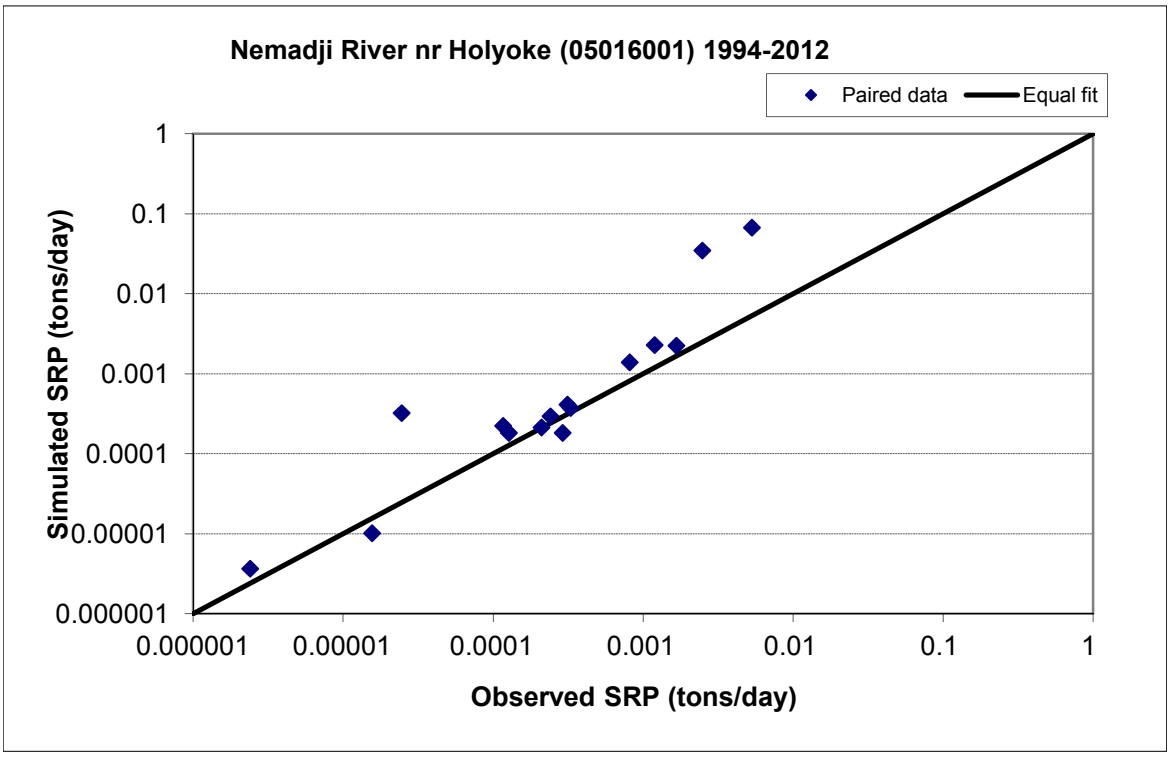

Figure B-124. Paired simulated vs. observed Soluble Reactive Phosphorus (SRP) load at Nemadji River nr Holyoke (05016001) (calibration period)

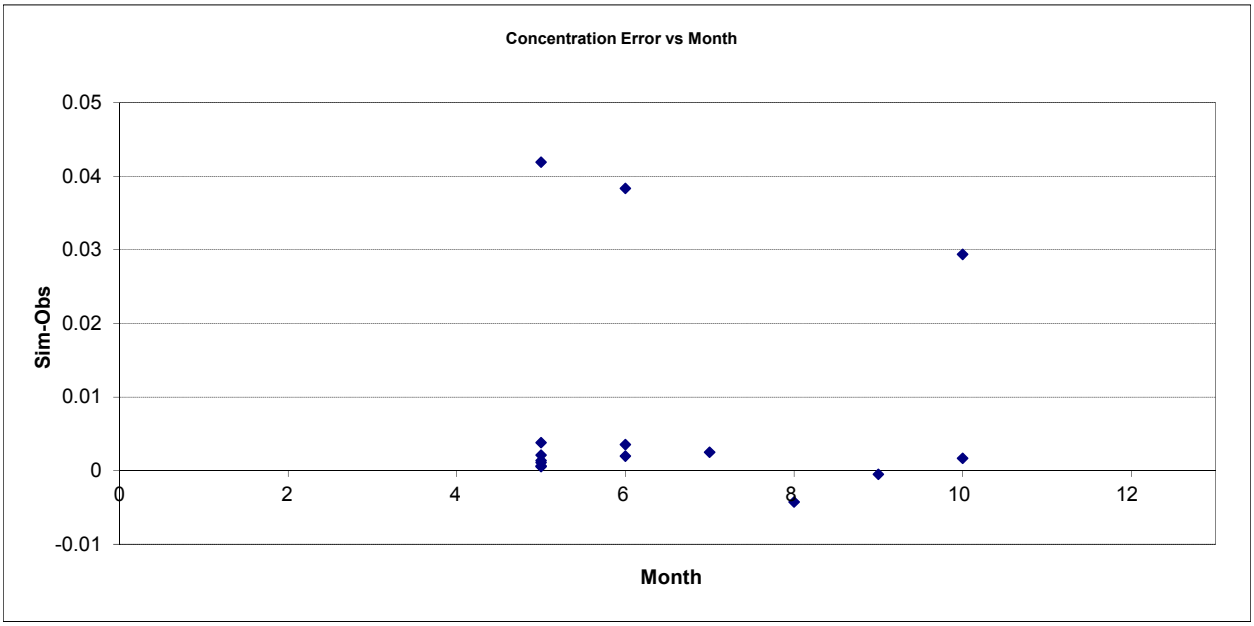

Figure B-125. Residual (Simulated - Observed) vs. Month Soluble Reactive Phosphorus (SRP) at Nemadji River nr Holyoke (05016001)

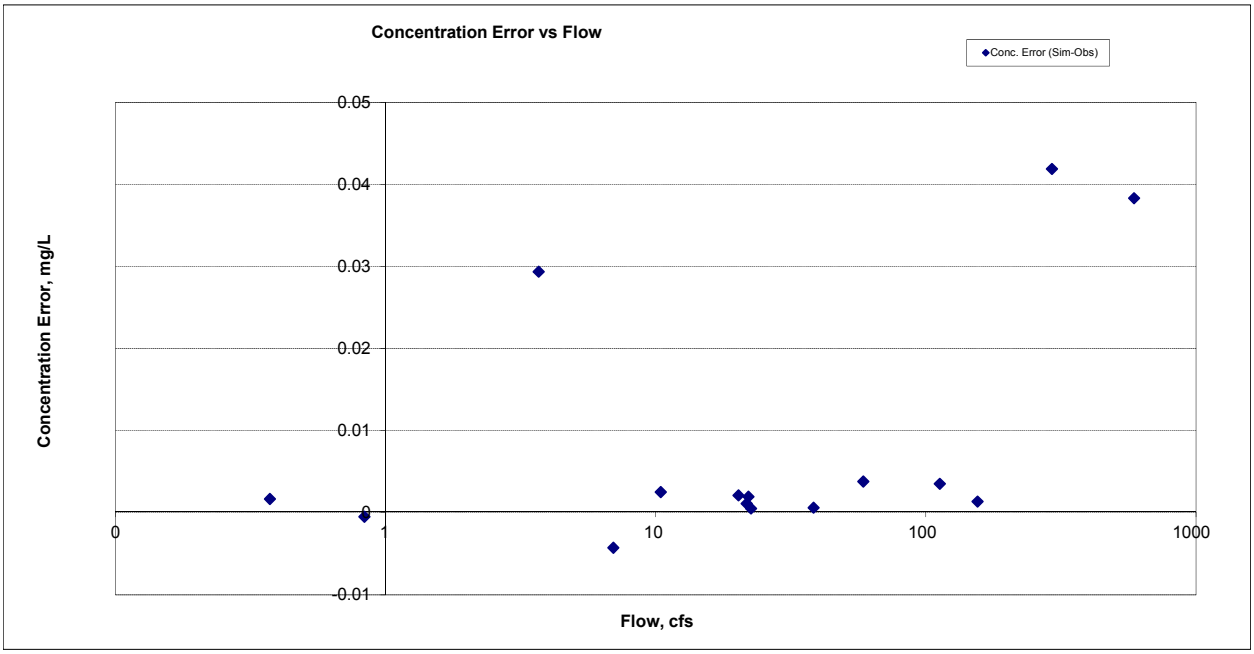

Figure B-126. Residual (Simulated - Observed) vs. Flow Soluble Reactive Phosphorus (SRP) at Nemadji River nr Holyoke (05016001)

B.4.7 Organic Phosphorus (OrgP)

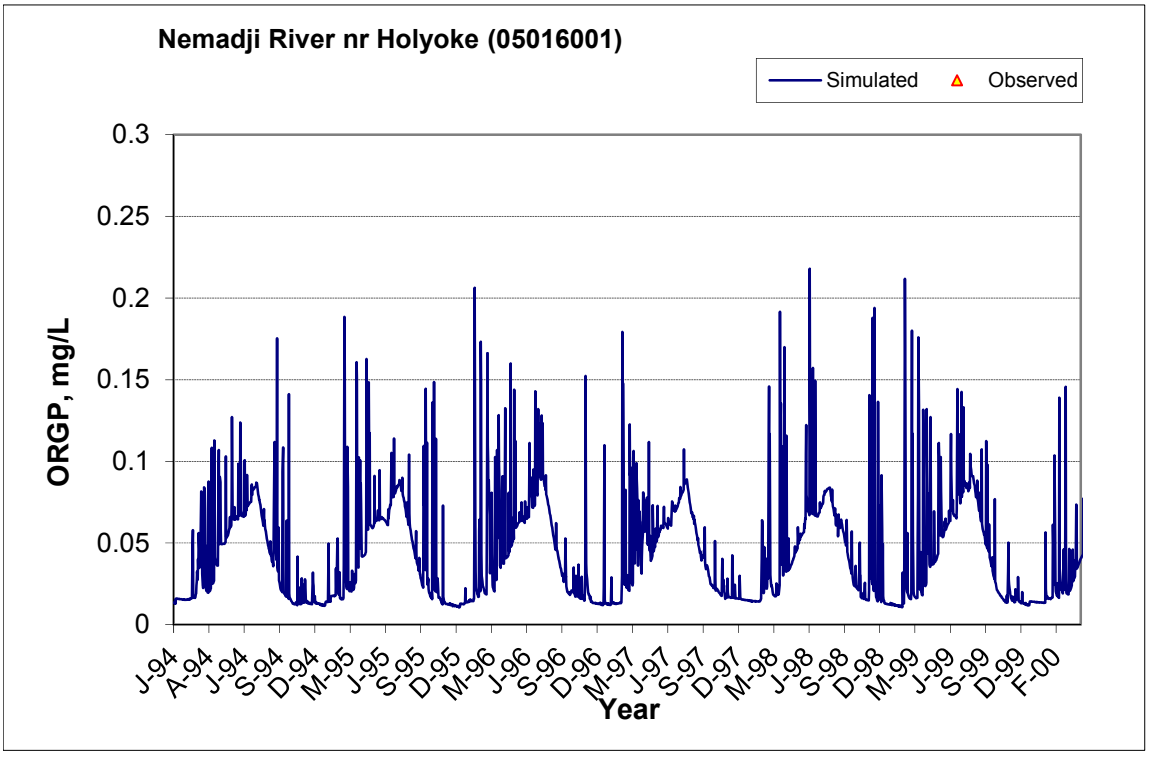

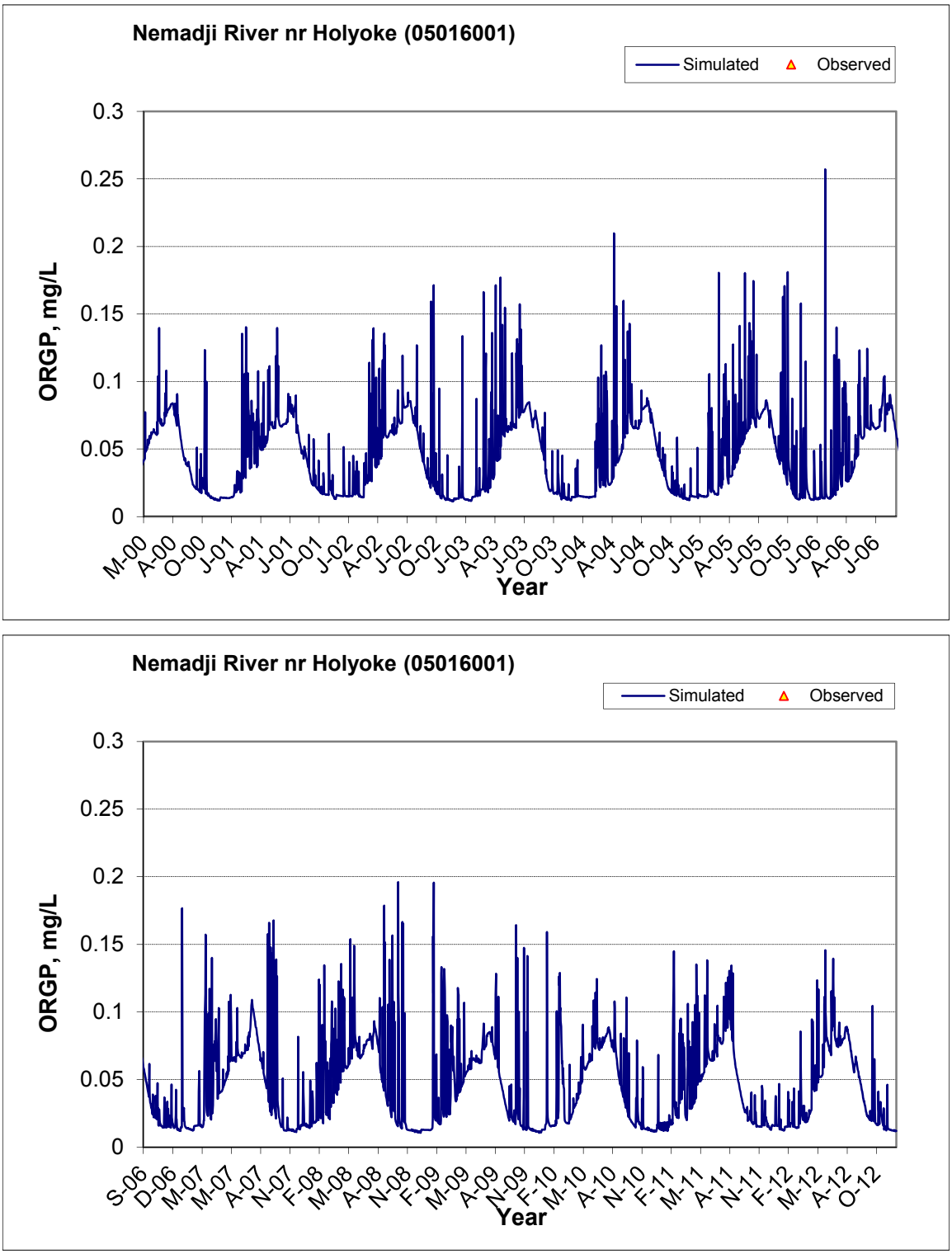

Figure B-127. Time series of observed and simulated Organic Phosphorus (OrgP) concentration at Nemadji River nr Holyoke (05016001)

B.4.8 Total Phosphorus (TP)

Table B-22. Total Phosphorus (TP) statistics

Period	1994-1993	1994-2012
Count	ND	15
Concentration Average Error		6.15%
Concentration Median Error		18.38%
Load Average Error		-1.38%
Load Median Error		0.82%
Paired t conc		0.75
Paired t load		0.64

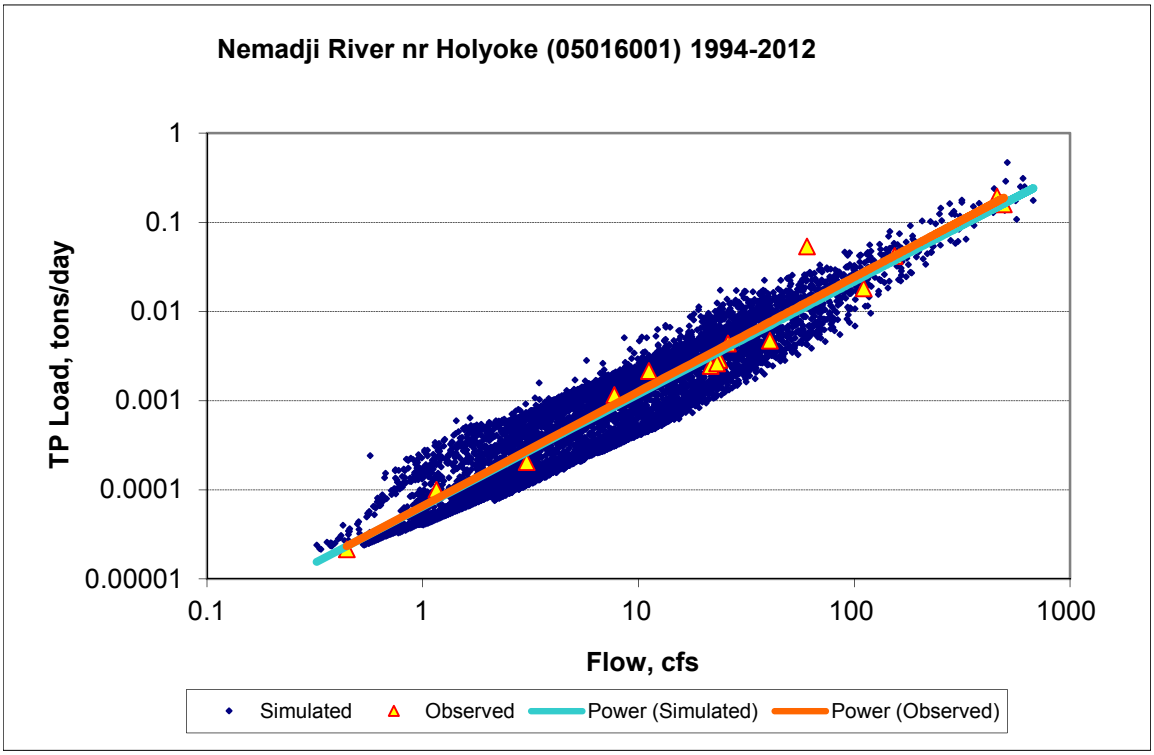

Figure B-128. Power plot of simulated and observed Total Phosphorus (TP) load vs flow at Nemadji River nr Holyoke (05016001) (calibration period)

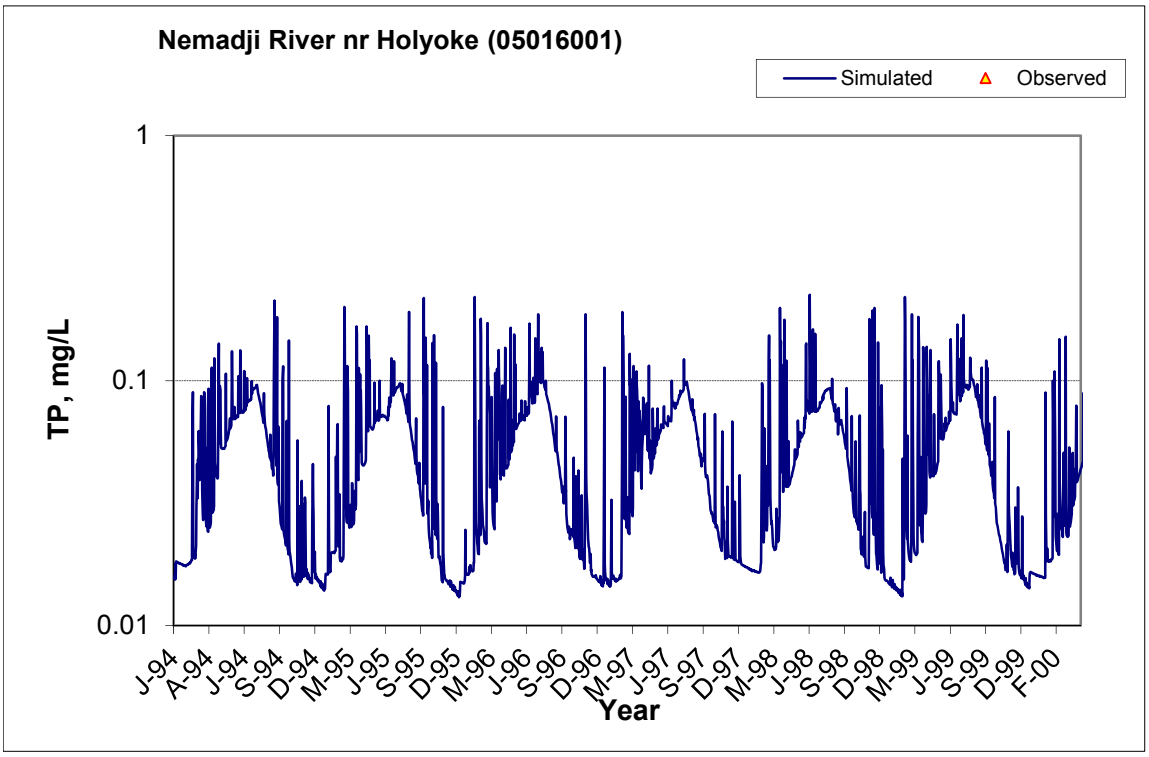
Nemadji River nr Holyoke (05016001)
Simulated
Observed
TP, mg/L
1
0.1
0.01
J-94 A-94 J-94 S-94 D-94 M-95 J-95 S-95 D-95 M-96 J-96 S-96 D-96 M-97 J-97 S-97 D-97 M-98 J-98 S-98 D-98 M-99 J-99 S-99 D-99 F-00
Year

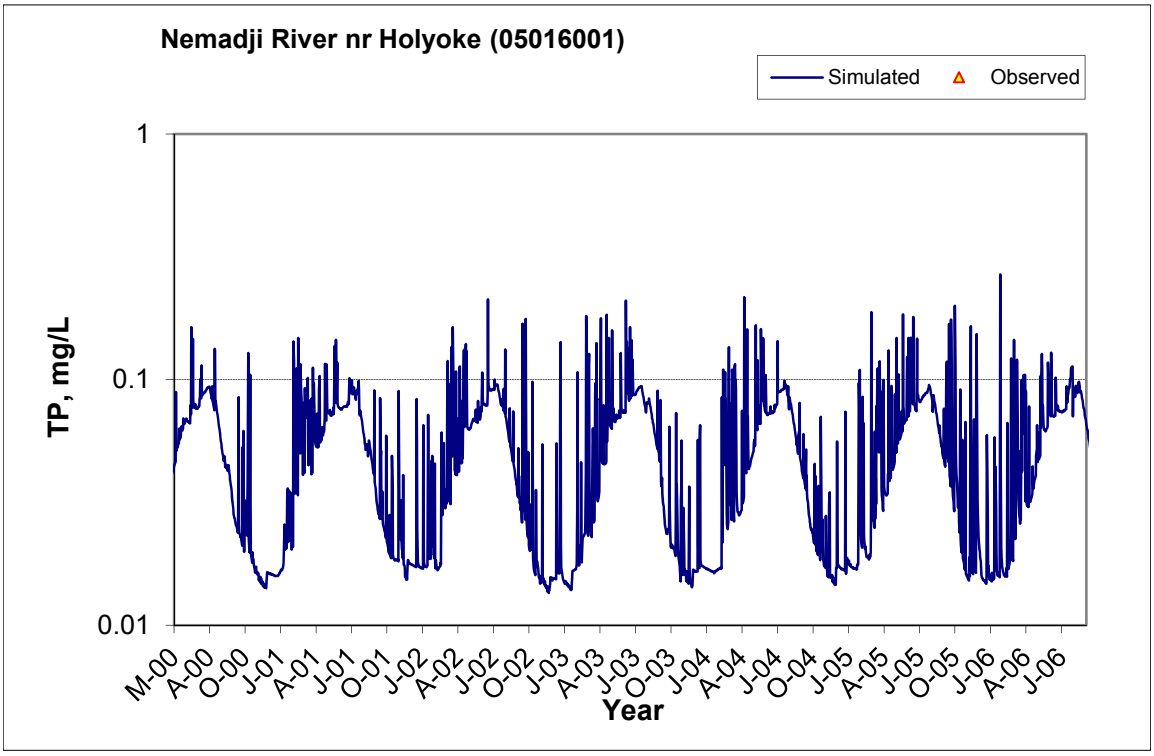
Nemadji River nr Holyoke (05016001)
Simulated
Observed
TP, mg/L
1
0.1
0.01
M-00 A-00 O-00 J-01 A-01 J-01 O-01 J-02 A-02 J-02 O-02 J-03 A-03 J-03 O-03 J-04 A-04 J-04 O-04 J-05 A-05 J-05 O-05 J-06 A-06 J-06
Year

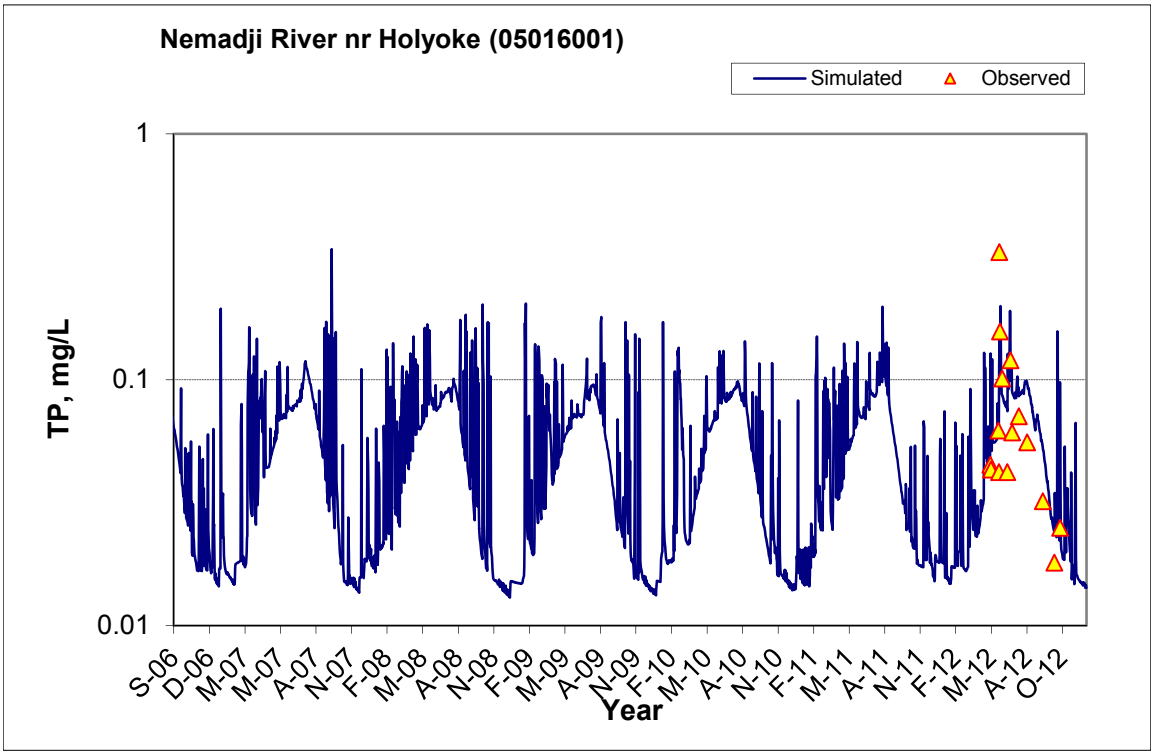

Figure B-129. Time series of observed and simulated Total Phosphorus (TP) concentration at Nemadji River nr Holyoke (05016001)

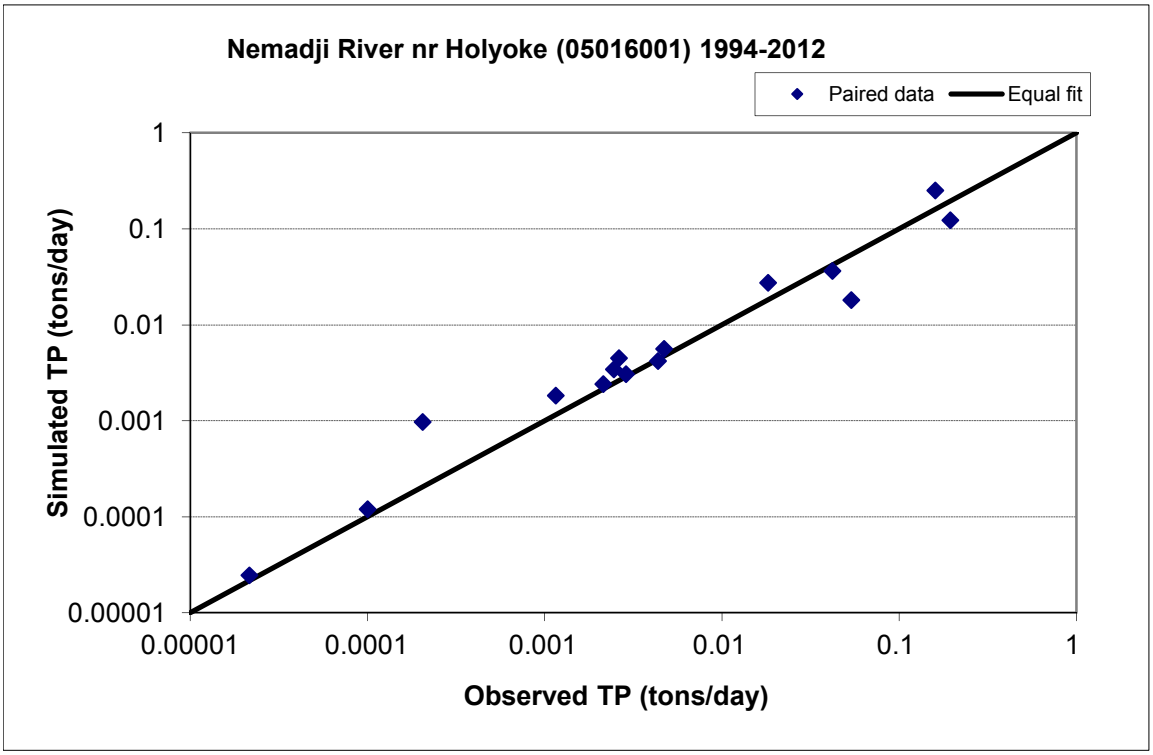

Figure B-130. Paired simulated vs. observed Total Phosphorus (TP) load at Nemadji River nr Holyoke (05016001) (calibration period)

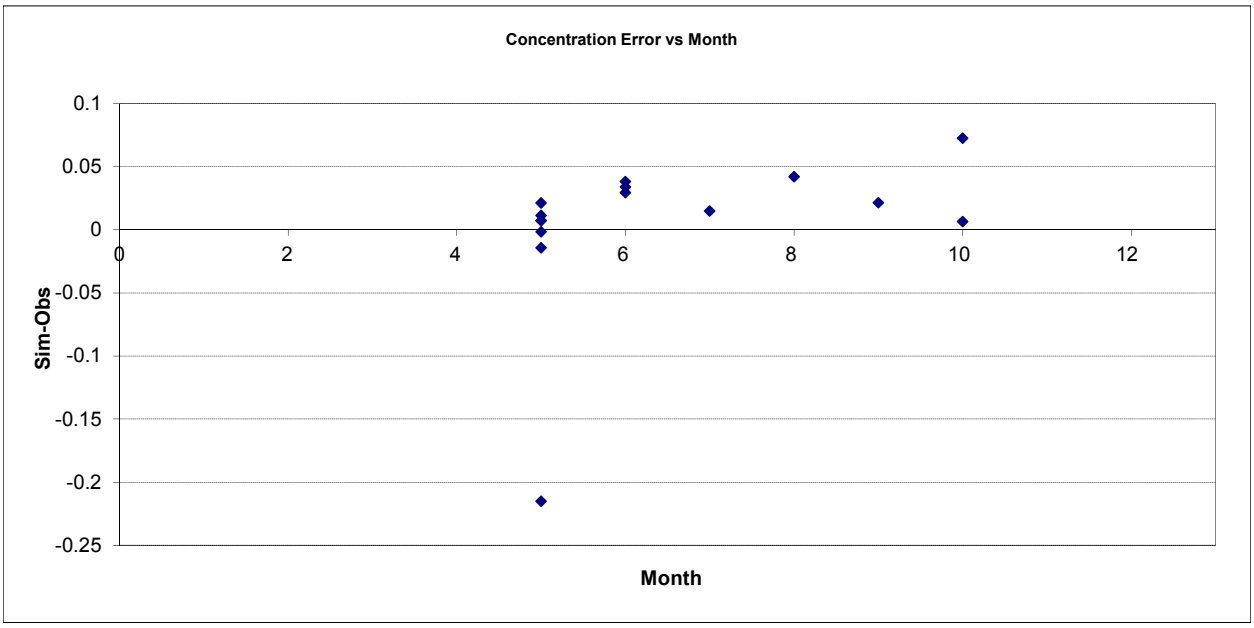

Figure B-131. Residual (Simulated - Observed) vs. Month Total Phosphorus (TP) at Nemadji River nr Holyoke (05016001)

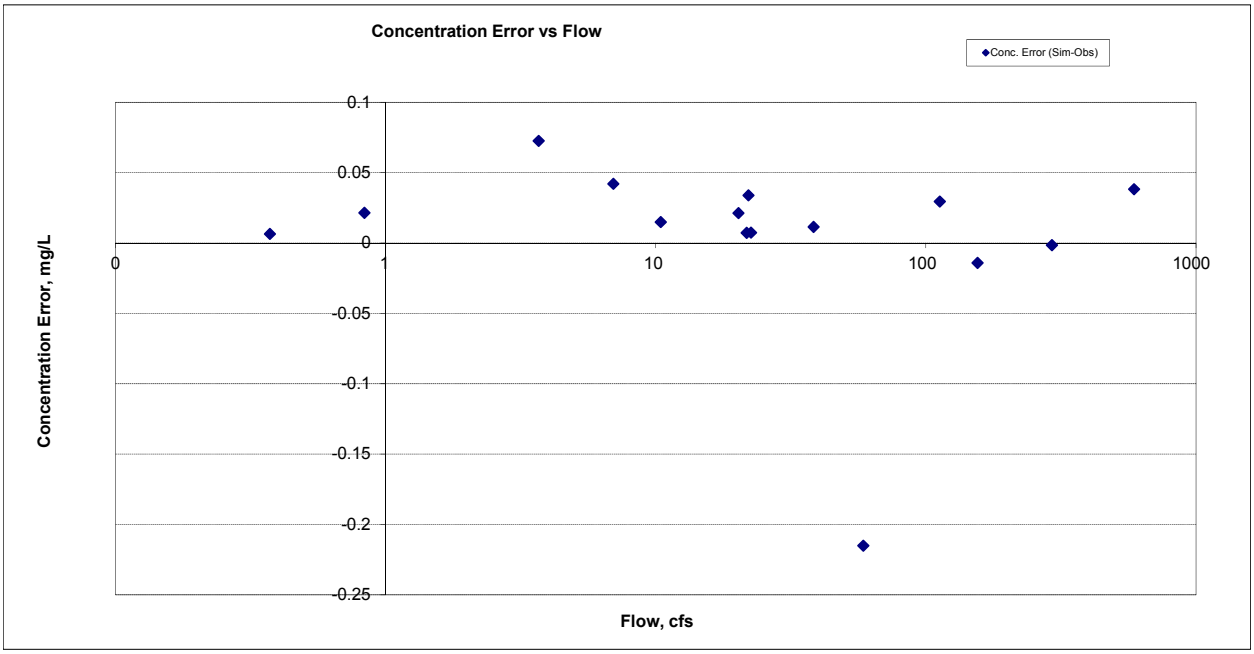

Figure B-132. Residual (Simulated - Observed) vs. Flow Total Phosphorus (TP) at Nemadji River nr Holyoke (05016001)

B.5 NEMADJI RIVER NR PLEASANT VALLEY (05011001)

B.5.1 Ammonia Nitrogen (NH3)

Table B-23. Ammonia Nitrogen (NH3) statistics

Period	1994-2001	2002-2012
Count	ND	31
Concentration Average Error		29.35%
Concentration Median Error		5.20%
Load Average Error		17.49%
Load Median Error		1.40%
Paired t conc		0.36
Paired t load		0.52

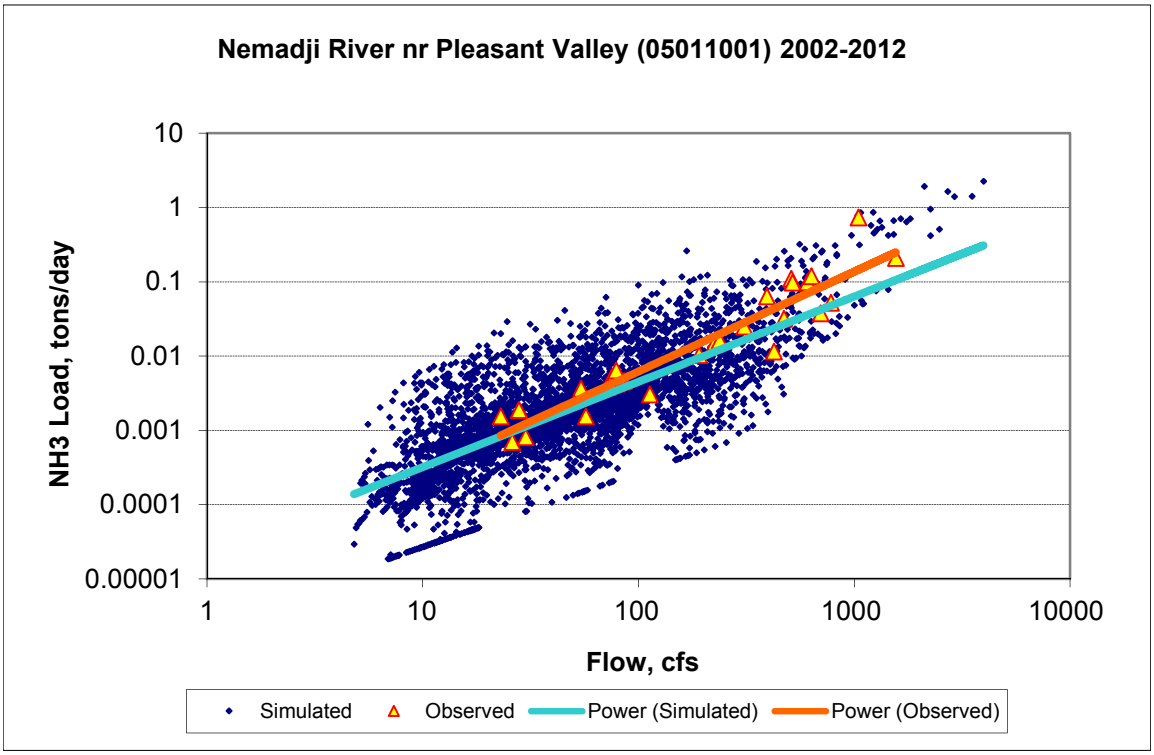

Figure B-133. Power plot of simulated and observed Ammonia Nitrogen (NH3) load vs flow at Nemadji River nr Pleasant Valley (05011001) (calibration period)

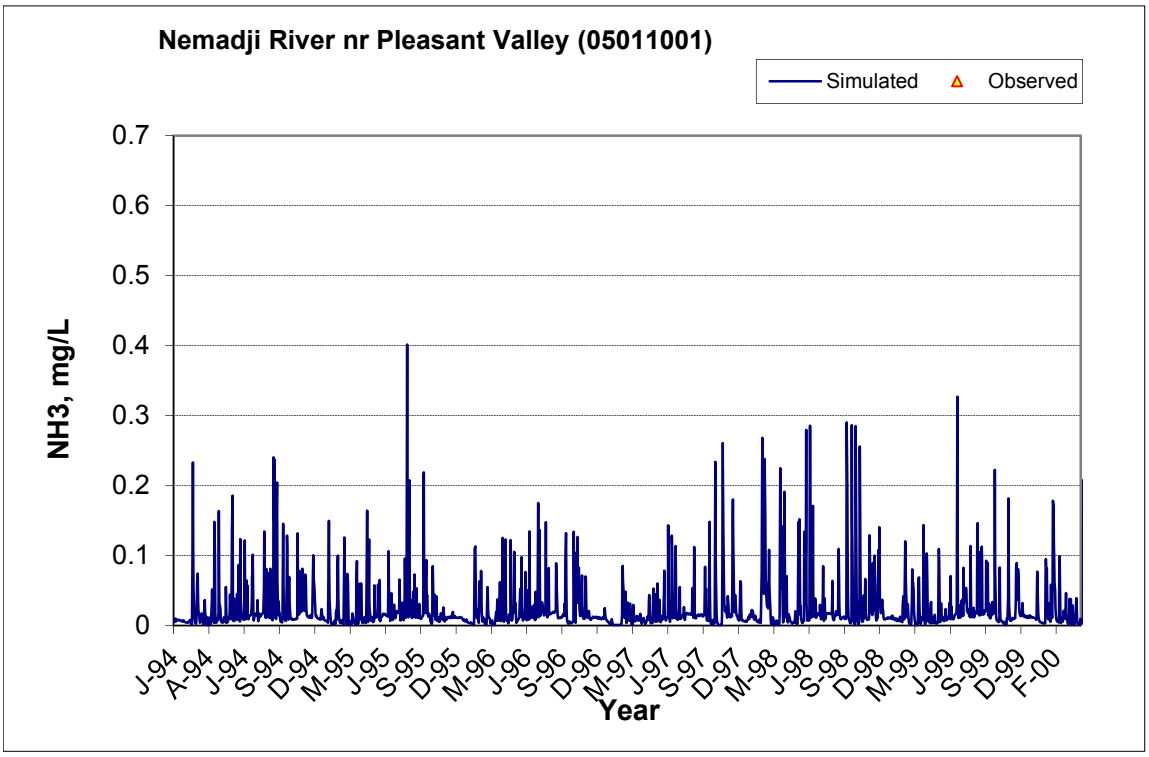
Nemadji River nr Pleasant Valley (05011001)
Simulated
Observed
NH3, mg/L
0.7
0.6
0.5
0.4
0.3
0.2
0.1
0
J-94 A-94 J-94 S-94 D-94 M-95 J-95 S-95 D-95 M-96 J-96 S-96 D-96 M-97 J-97 S-97 D-97 M-98 J-98 S-98 D-98 M-99 J-99 S-99 D-99 F-00
Year

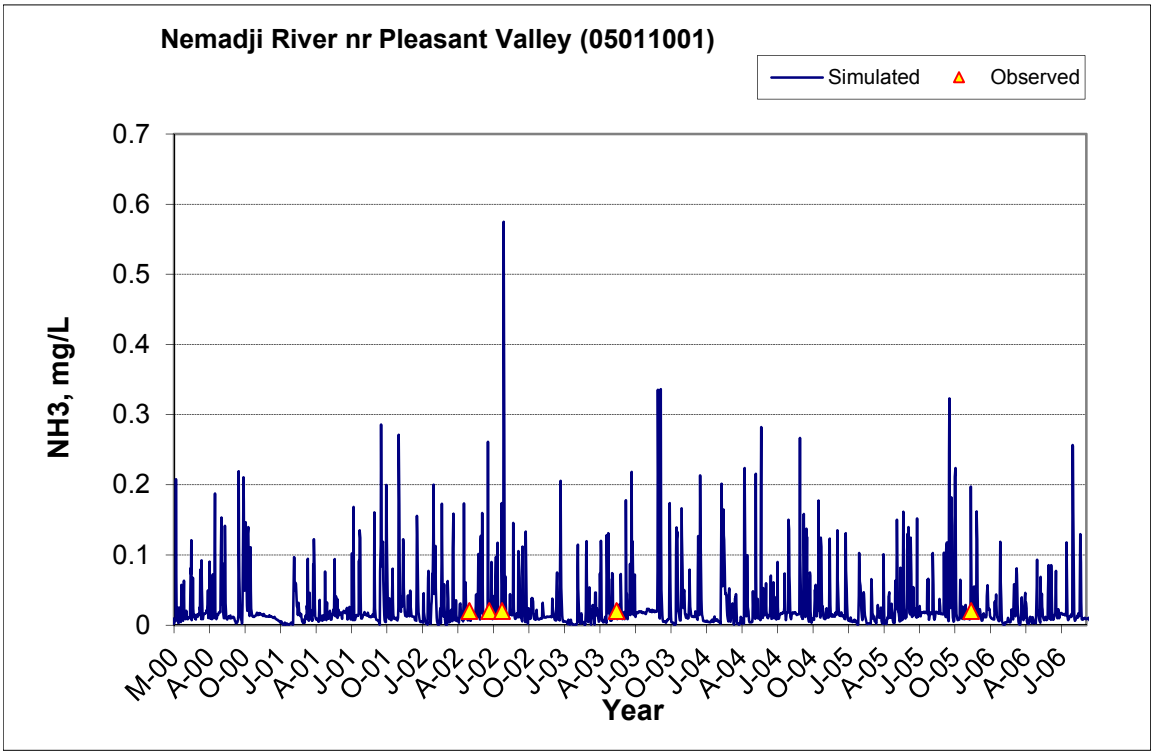
Nemadji River nr Pleasant Valley (05011001)
Simulated
Observed
NH3, mg/L
0.7
0.6
0.5
0.4
0.3
0.2
0.1
0
M-00 A-00 O-00 J-01 A-01 J-01 O-01 J-02 A-02 J-02 O-02 J-03 A-03 J-03 O-03 J-04 A-04 J-04 O-04 J-05 A-05 J-05 O-05 J-06 A-06 J-06
Year

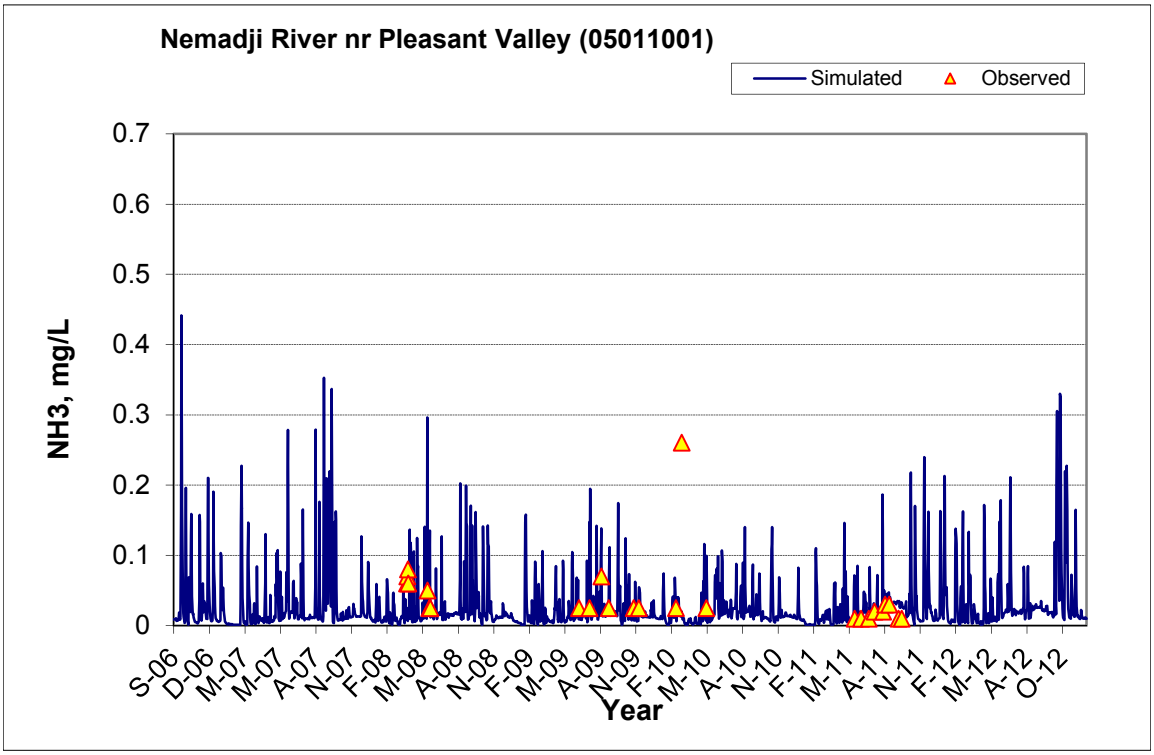

Figure B-134. Time series of observed and simulated Ammonia Nitrogen (NH3) concentration at Nemadji River nr Pleasant Valley (05011001)

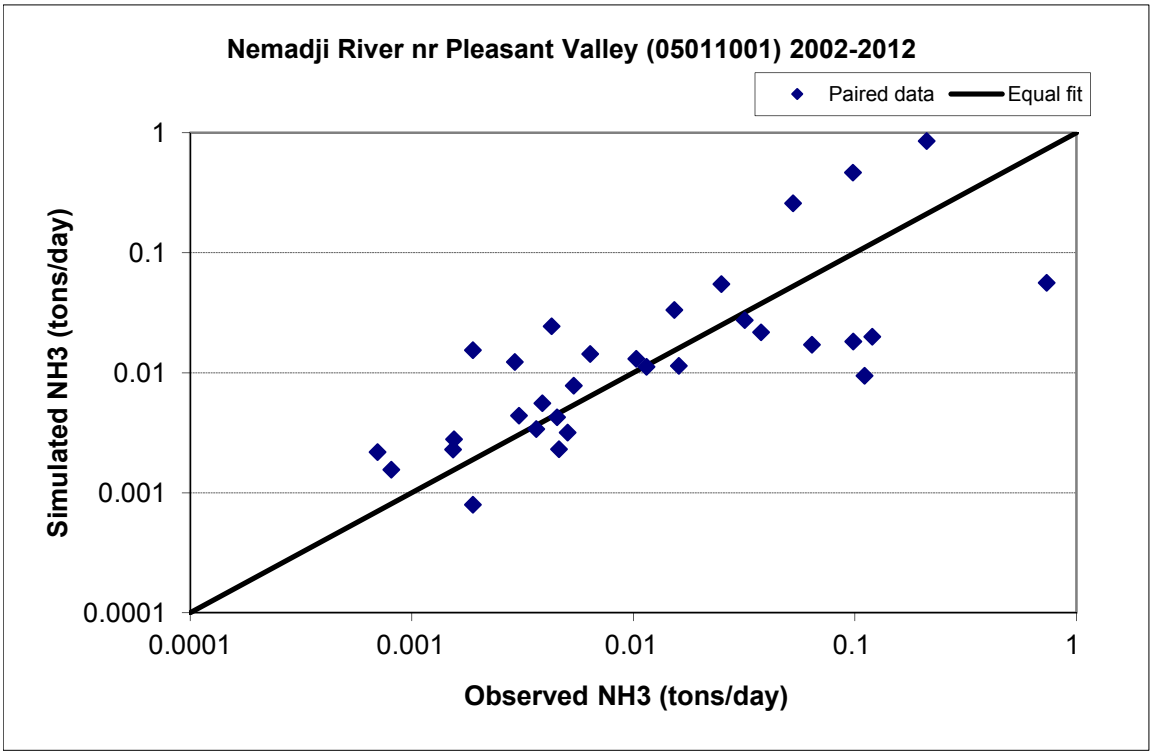

Figure B-135. Paired simulated vs. observed Ammonia Nitrogen (NH3) load at Nemadji River nr Pleasant Valley (05011001) (calibration period)

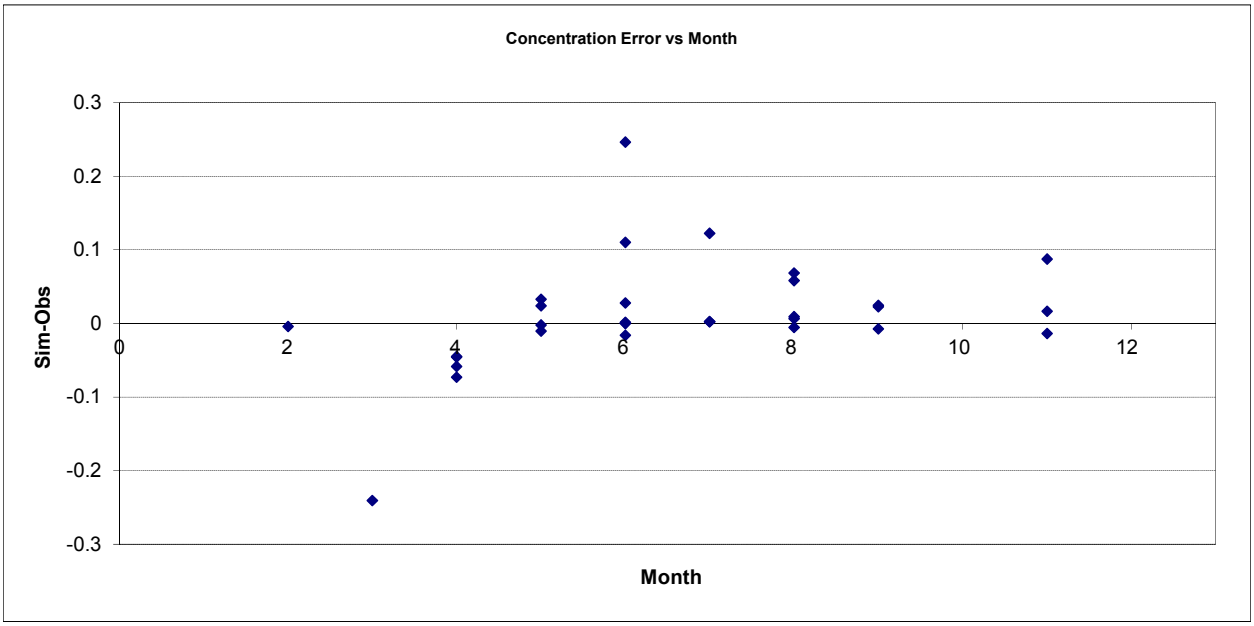

Figure B-136. Residual (Simulated - Observed) vs. Month Ammonia Nitrogen (NH3) at Nemadji River nr Pleasant Valley (05011001)

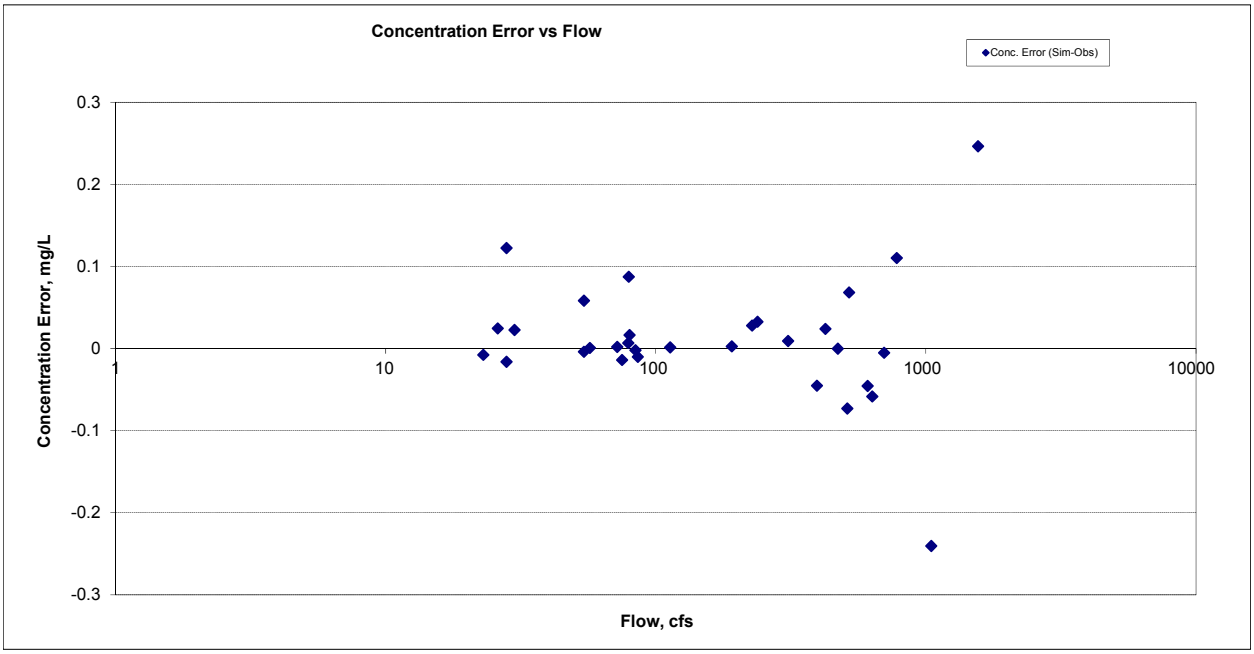

Figure B-137. Residual (Simulated - Observed) vs. Flow Ammonia Nitrogen (NH3) at Nemadji River nr Pleasant Valley (05011001)

B.5.2 Organic Nitrogen (OrgN)

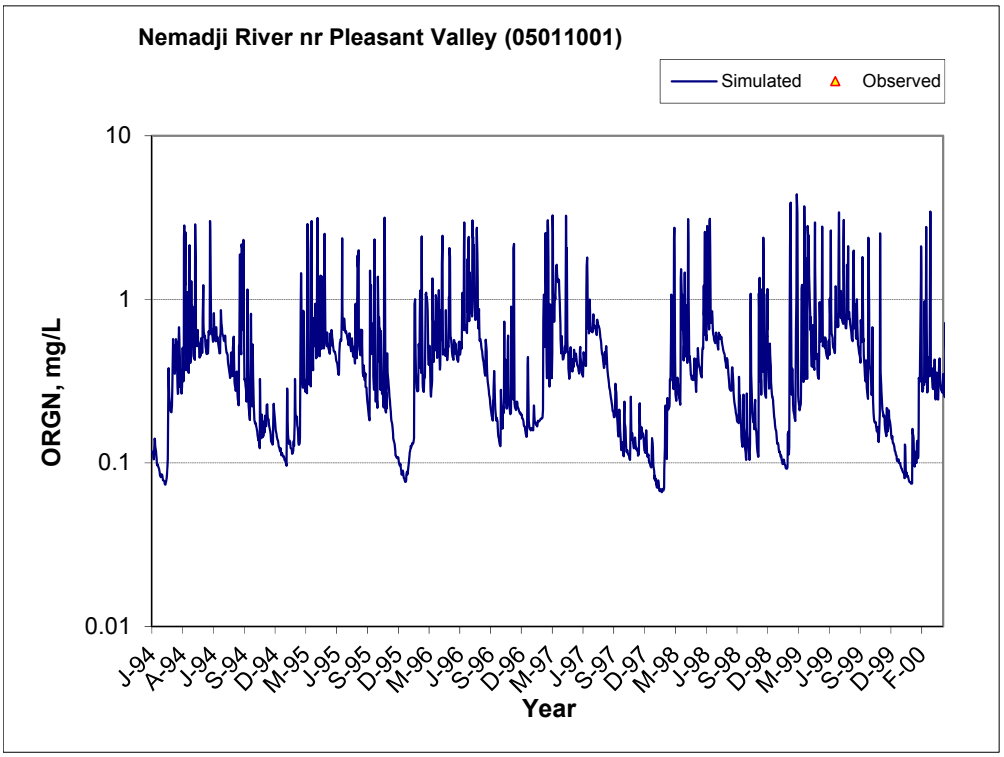

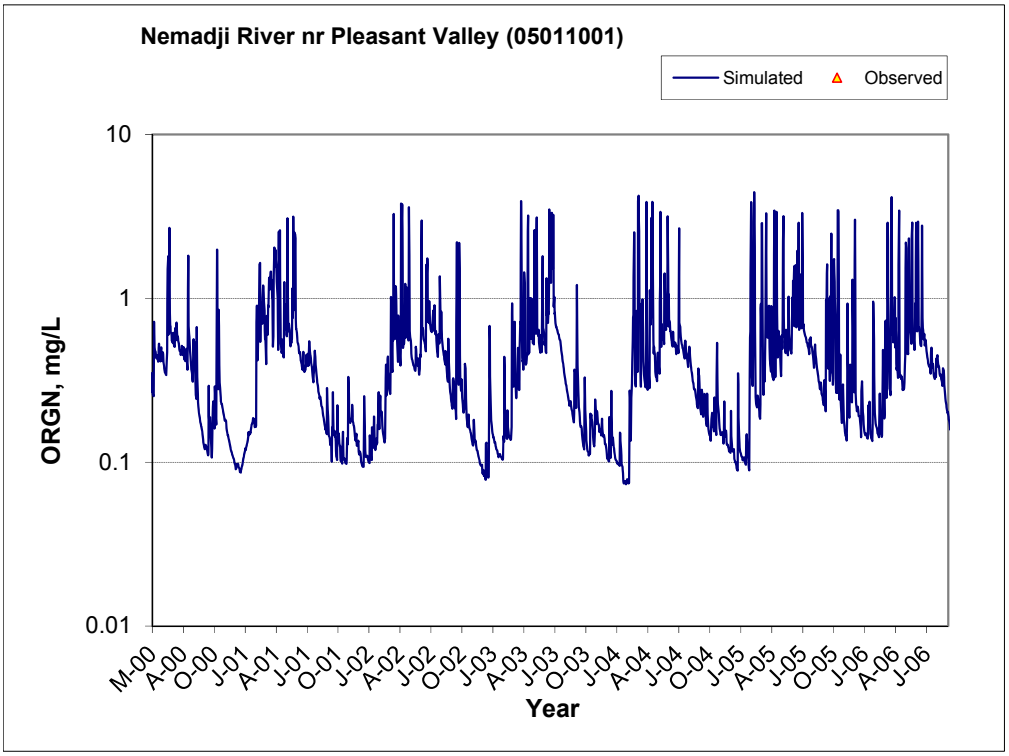

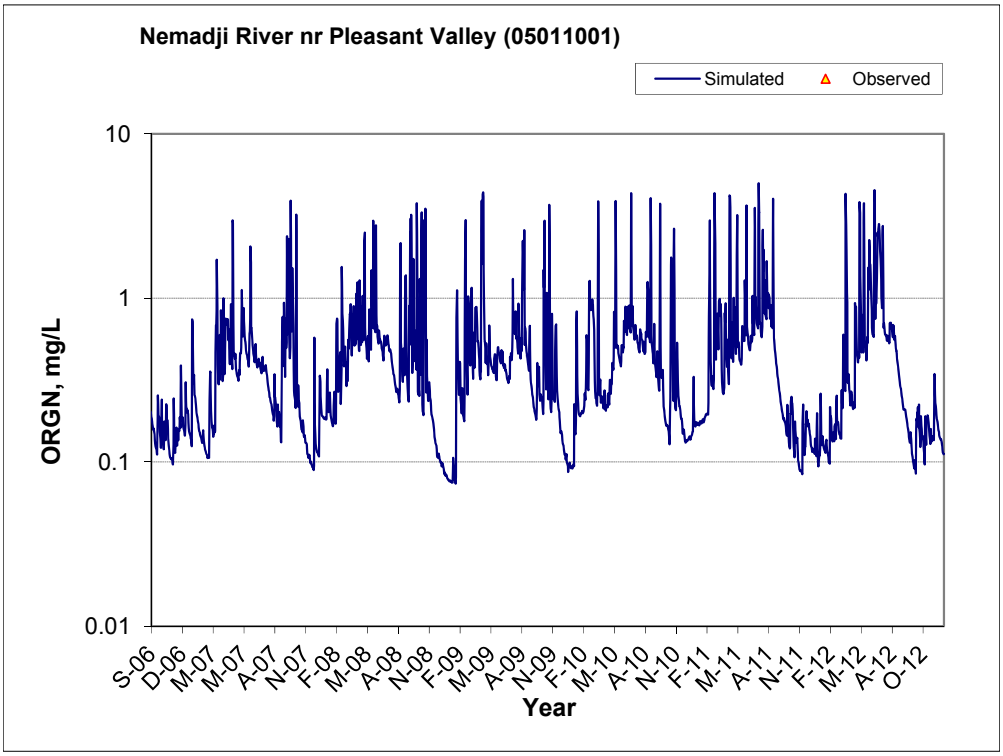

Figure B-138. Time series of observed and simulated Organic Nitrogen (OrgN) concentration at Nemadji River nr Pleasant Valley (05011001)

B.5.3 Total Kjeldahl Nitrogen (TKN)

Table B-24. Total Kjeldahl Nitrogen (TKN) statistics

Period	1994-2001	2002-2012
Count	7	32
Concentration Average Error	36.52%	13.63%
Concentration Median Error	7.09%	-1.52%
Load Average Error	89.06%	-5.58%
Load Median Error	0.21%	0.20%
Paired t conc	0.33	0.68
Paired t load	0.26	0.62

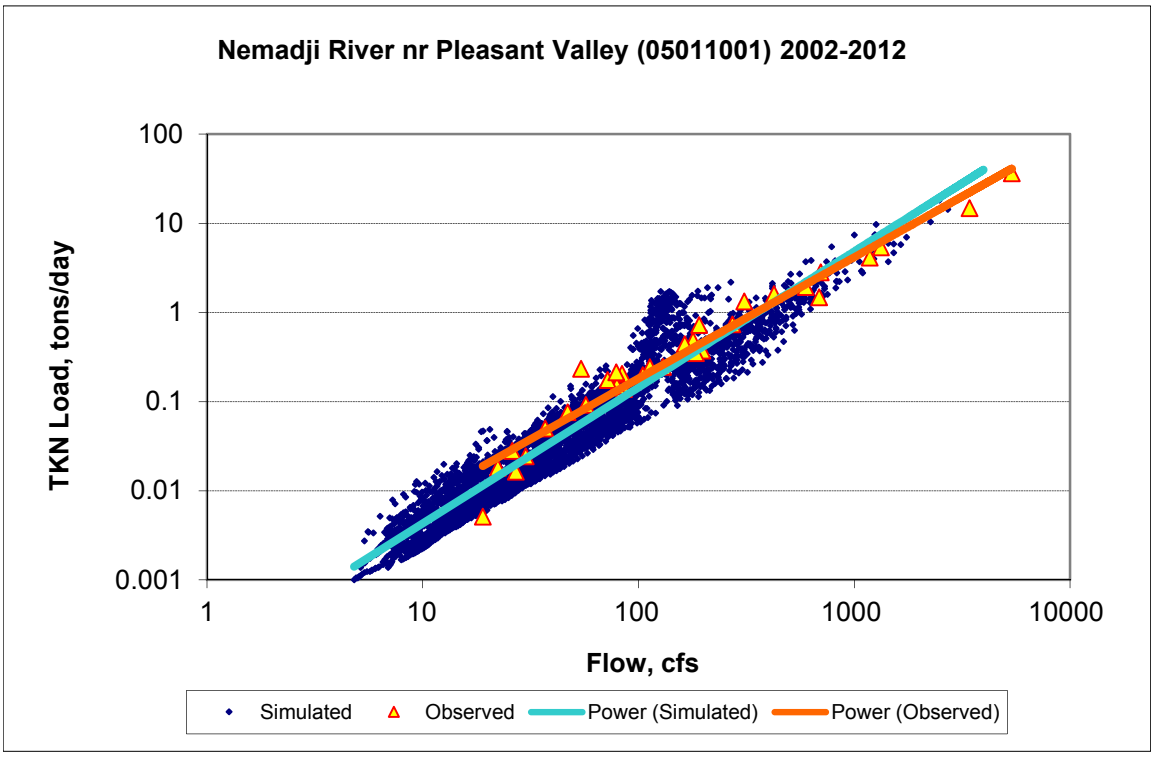

Figure B-139. Power plot of simulated and observed Total Kjeldahl Nitrogen (TKN) load vs flow at Nemadji River nr Pleasant Valley (05011001) (calibration period)

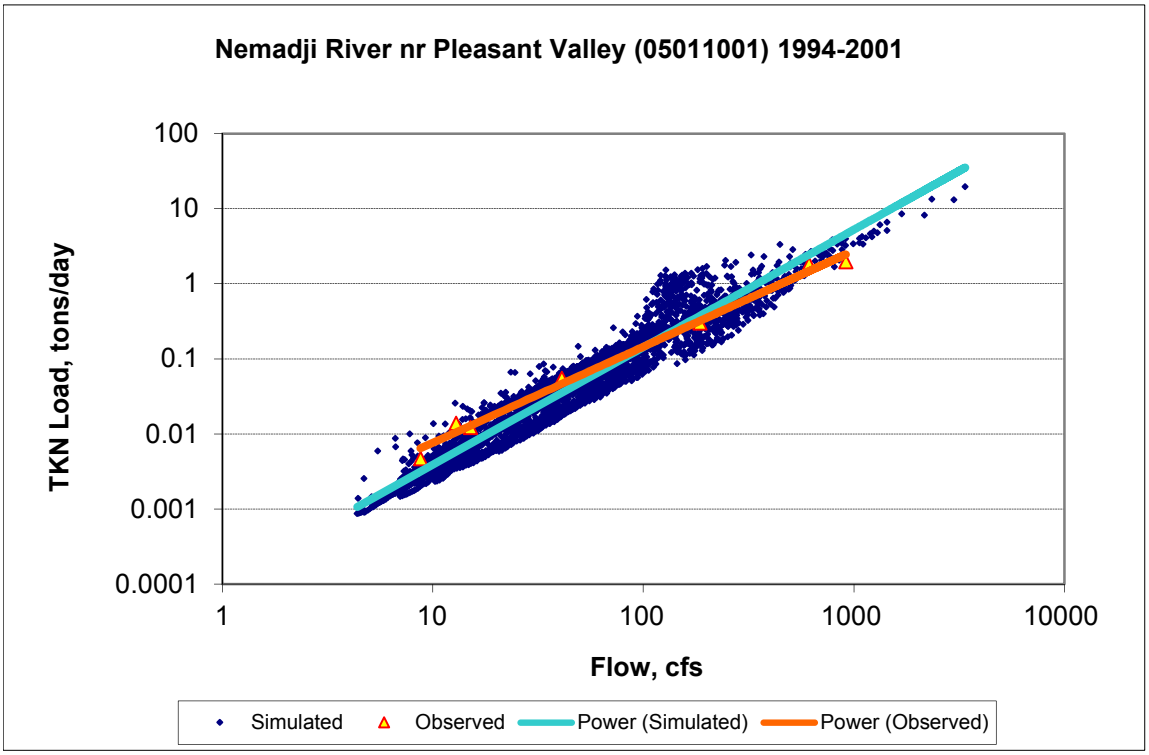

Figure B-140. Power plot of simulated and observed Total Kjeldahl Nitrogen (TKN) load vs flow at Nemadji River nr Pleasant Valley (05011001) (validation period)

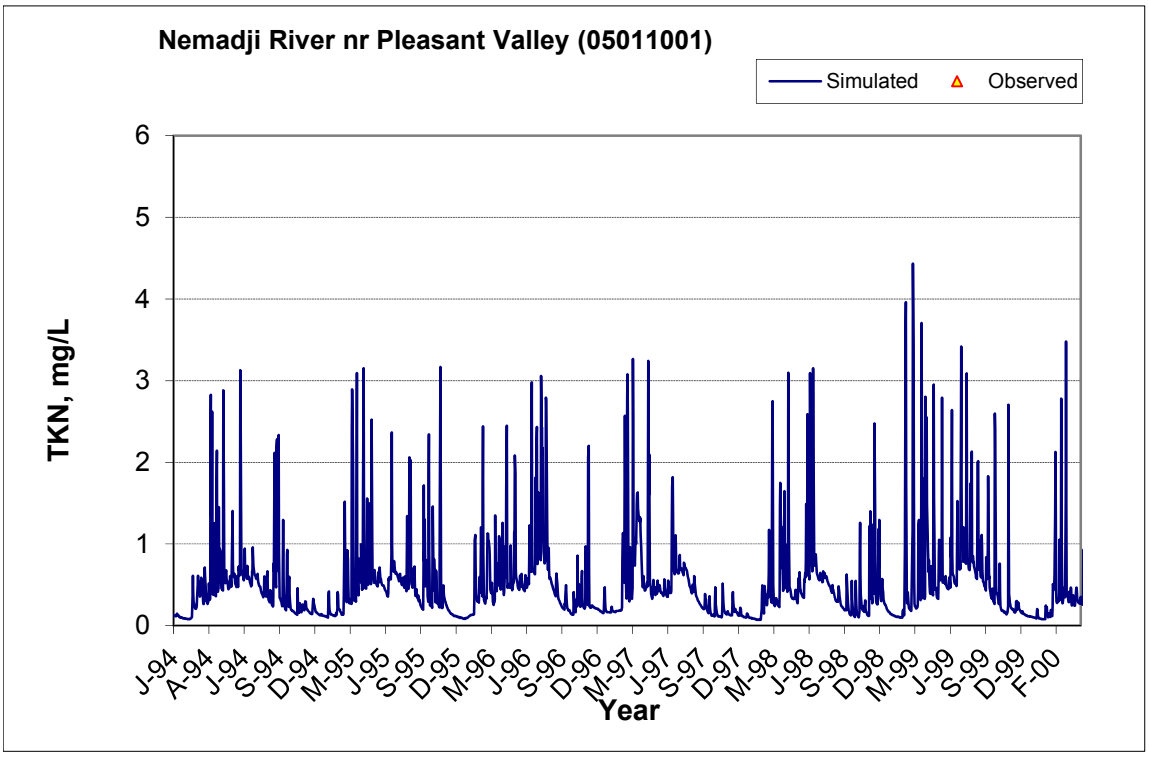
Nemadji River nr Pleasant Valley (05011001)
Simulated
Observed
TKN, mg/L
0
1
2
3
4
5
6
J-94
A-94
J-94
S-94
D-94
M-95
J-95
S-95
D-95
M-96
J-96
S-96
D-96
M-97
J-97
S-97
D-97
M-98
J-98
S-98
D-98
M-99
J-99
S-99
D-99
F-00
Year

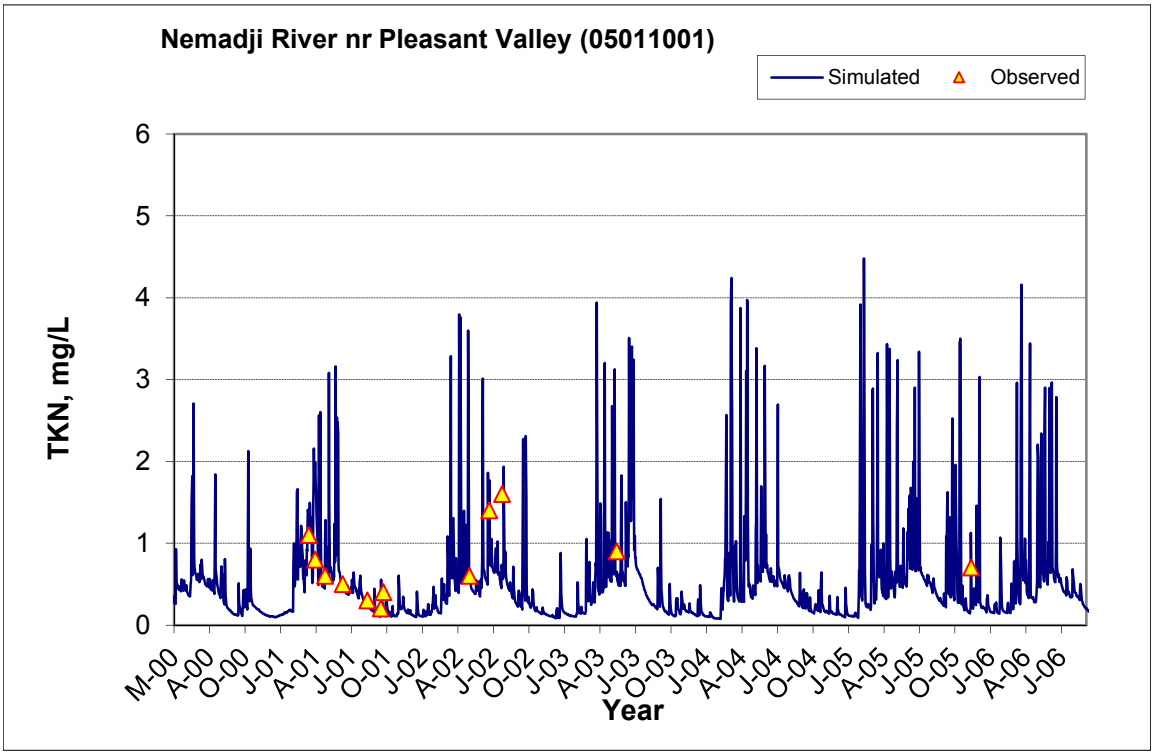
Nemadji River nr Pleasant Valley (05011001)
Simulated
Observed
TKN, mg/L
0
1
2
3
4
5
6
M-00
A-00
O-00
J-01
A-01
J-01
O-01
J-02
A-02
J-02
O-02
J-03
A-03
J-03
O-03
J-04
A-04
J-04
O-04
J-05
A-05
J-05
O-05
J-06
A-06
J-06
Year

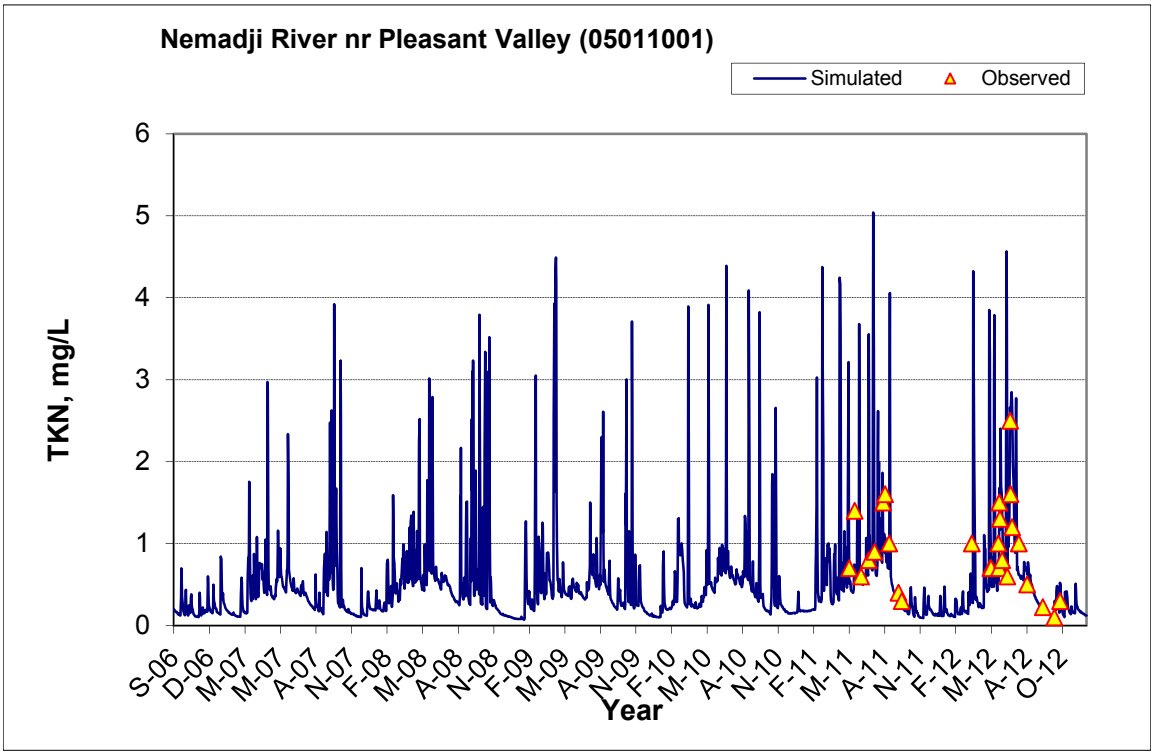

Figure B-141. Time series of observed and simulated Total Kjeldahl Nitrogen (TKN) concentration at Nemadji River nr Pleasant Valley (05011001)

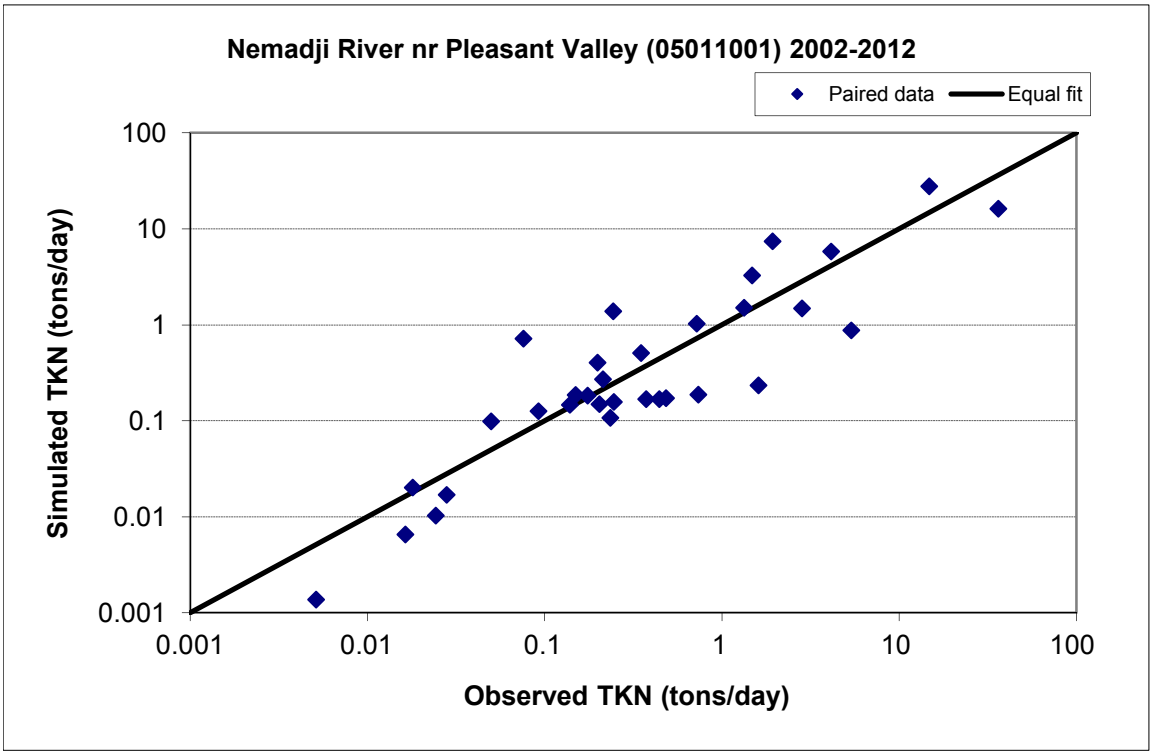

Figure B-142. Paired simulated vs. observed Total Kjeldahl Nitrogen (TKN) load at Nemadji River nr Pleasant Valley (05011001) (calibration period)

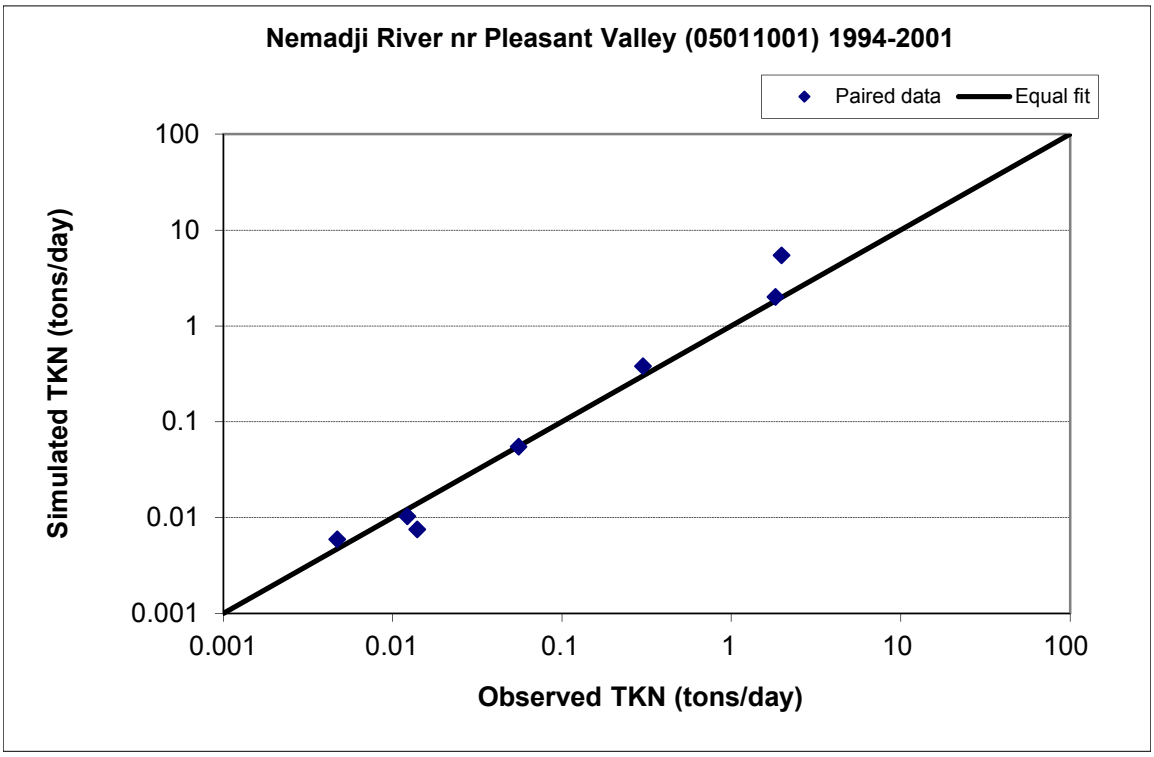

Figure B-143. Paired simulated vs. observed Total Kjeldahl Nitrogen (TKN) load at Nemadji River nr Pleasant Valley (05011001) (validation period)

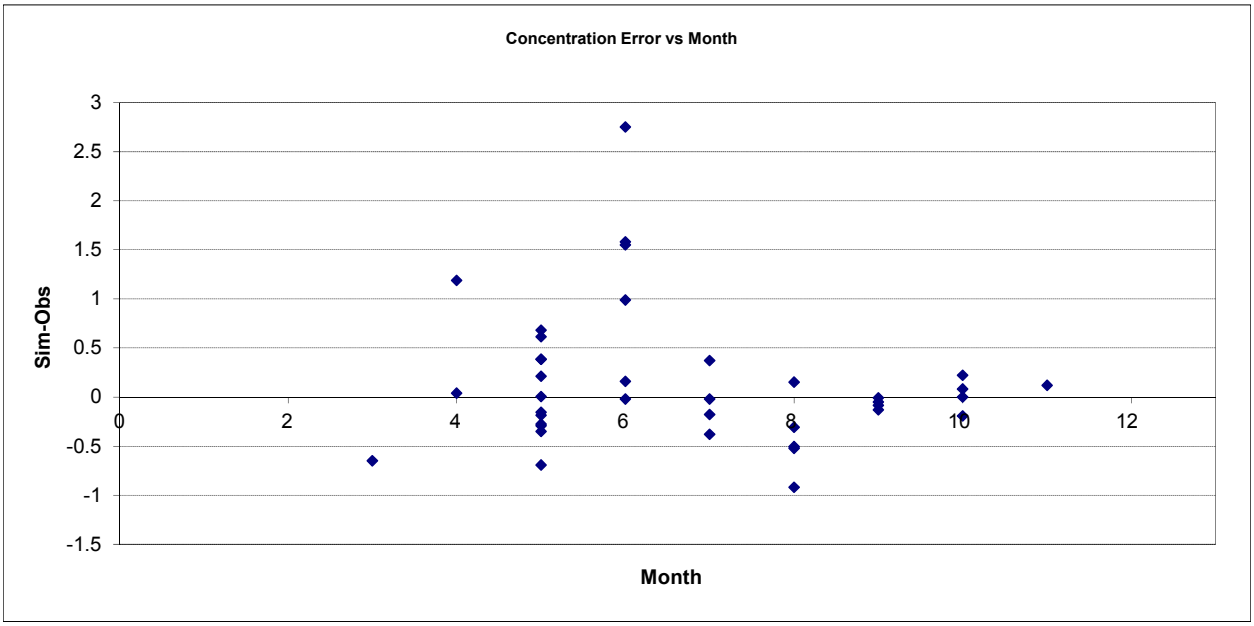

Figure B-144. Residual (Simulated - Observed) vs. Month Total Kjeldahl Nitrogen (TKN) at Nemadji River nr Pleasant Valley (05011001)

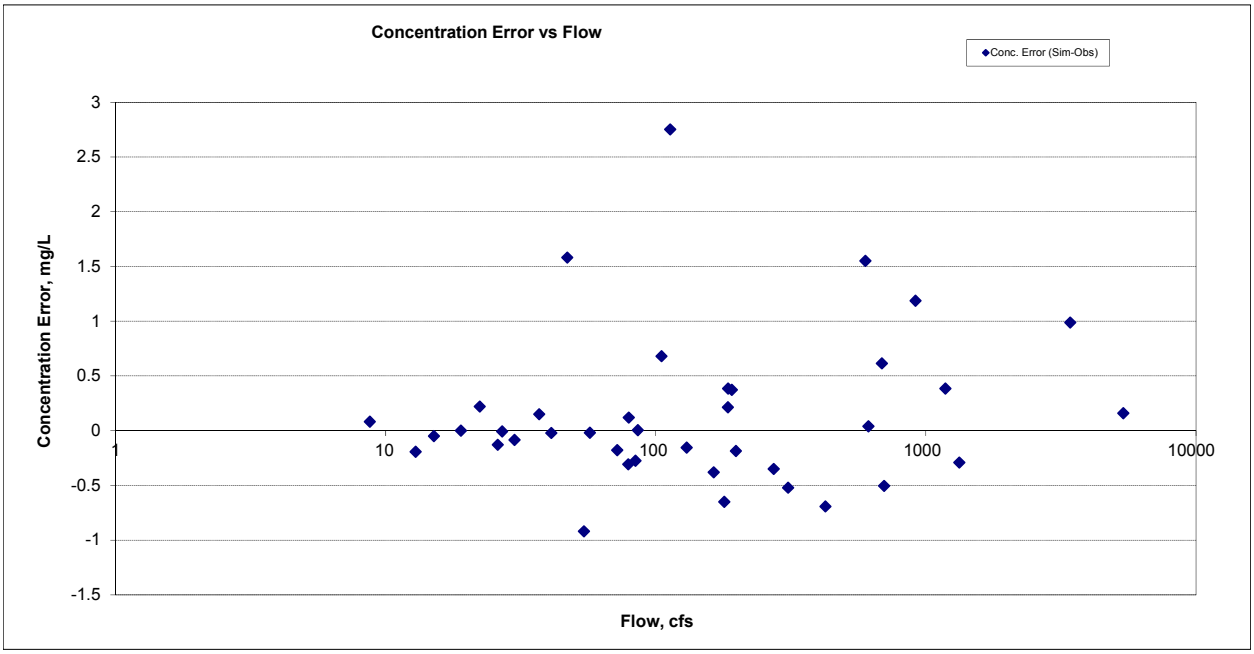

Figure B-145. Residual (Simulated - Observed) vs. Flow Total Kjeldahl Nitrogen (TKN) at Nemadji River nr Pleasant Valley (05011001)

B.5.4 Nitrite+ Nitrate Nitrogen (NOx)

Table B-25. Nitrite+ Nitrate Nitrogen (NOx) statistics

Period	1994-2001	2002-2012
Count	ND	48
Concentration Average Error		-32.35%
Concentration Median Error		-23.60%
Load Average Error		-2.75%
Load Median Error		-5.39%
Paired t conc		0.15
Paired t load		0.70

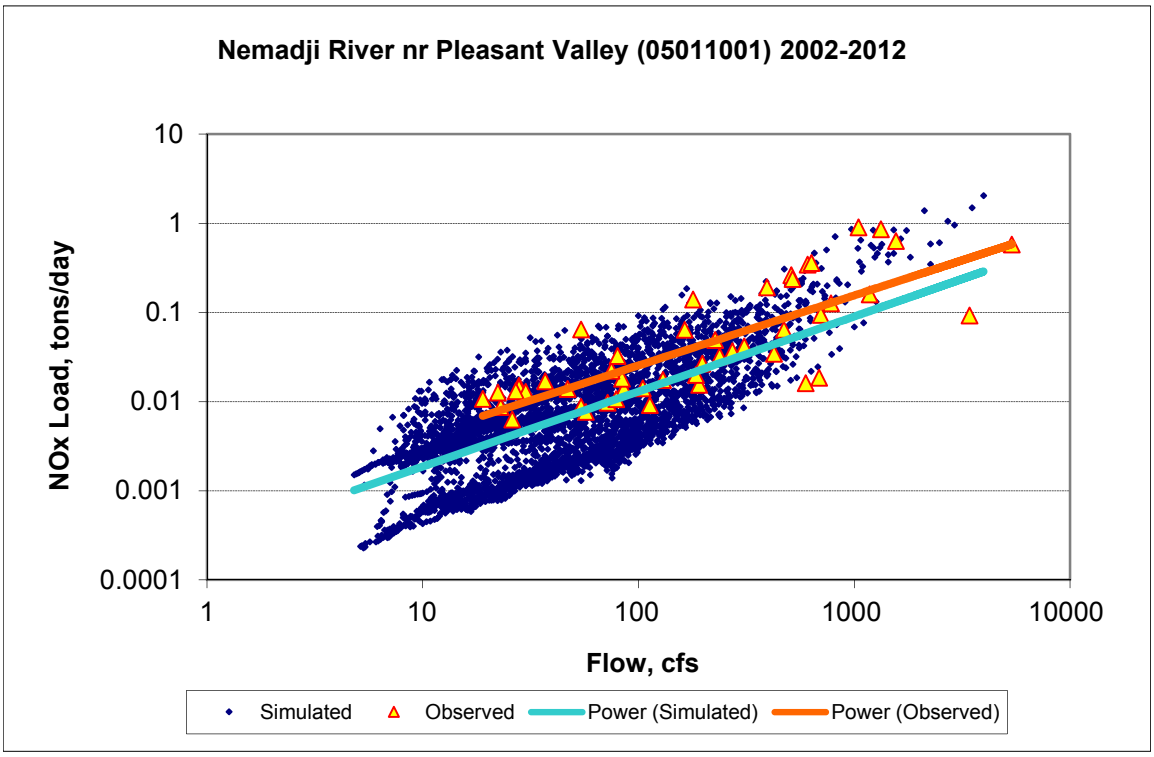

Figure B-146. Power plot of simulated and observed Nitrite+ Nitrate Nitrogen (NOx) load vs flow at Nemadji River nr Pleasant Valley (05011001) (calibration period)

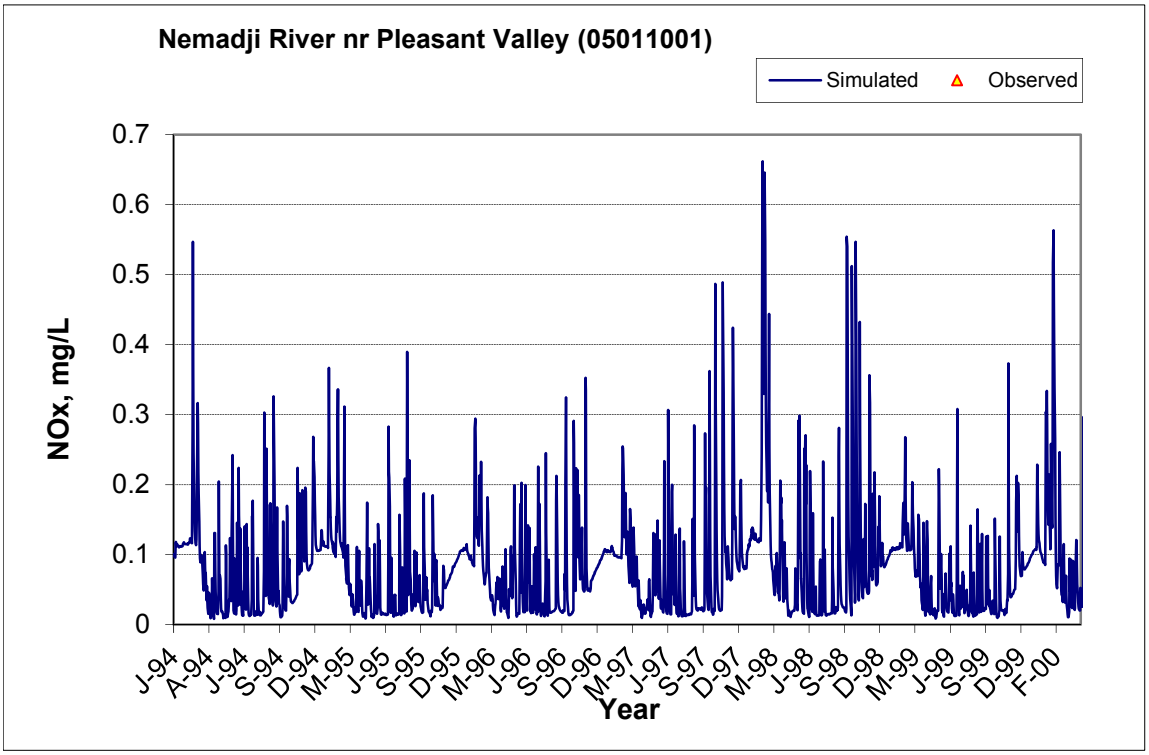

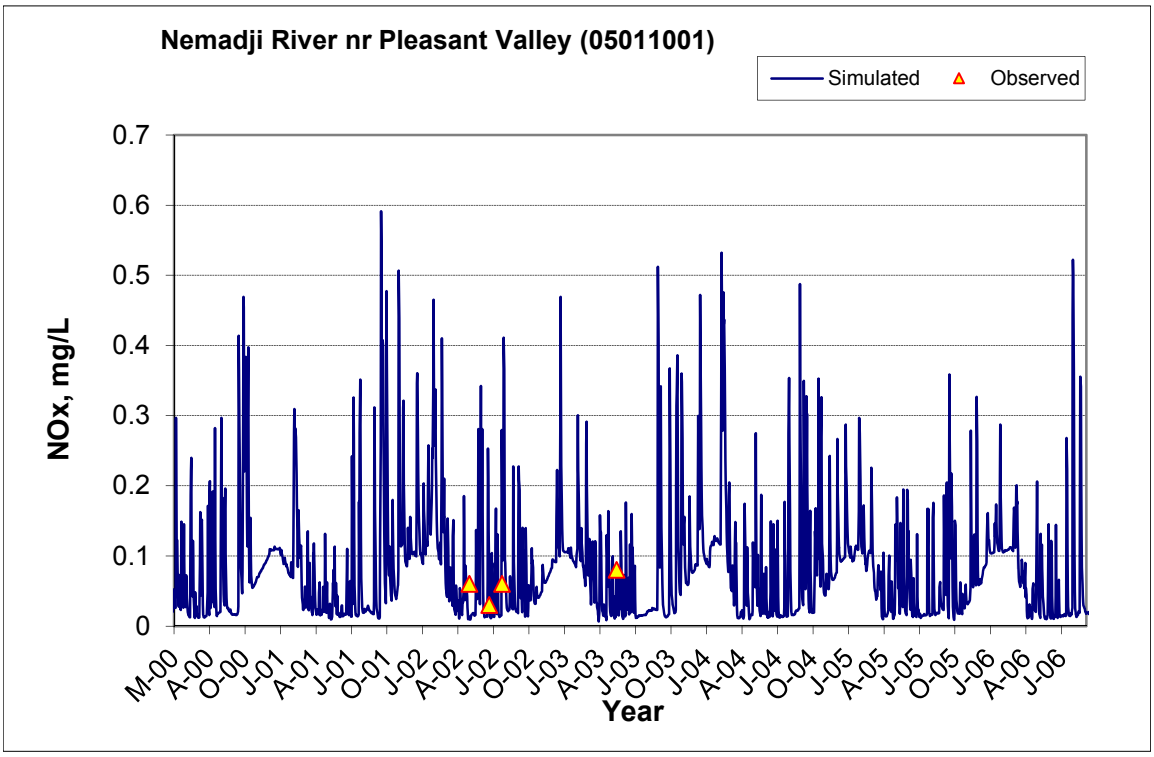

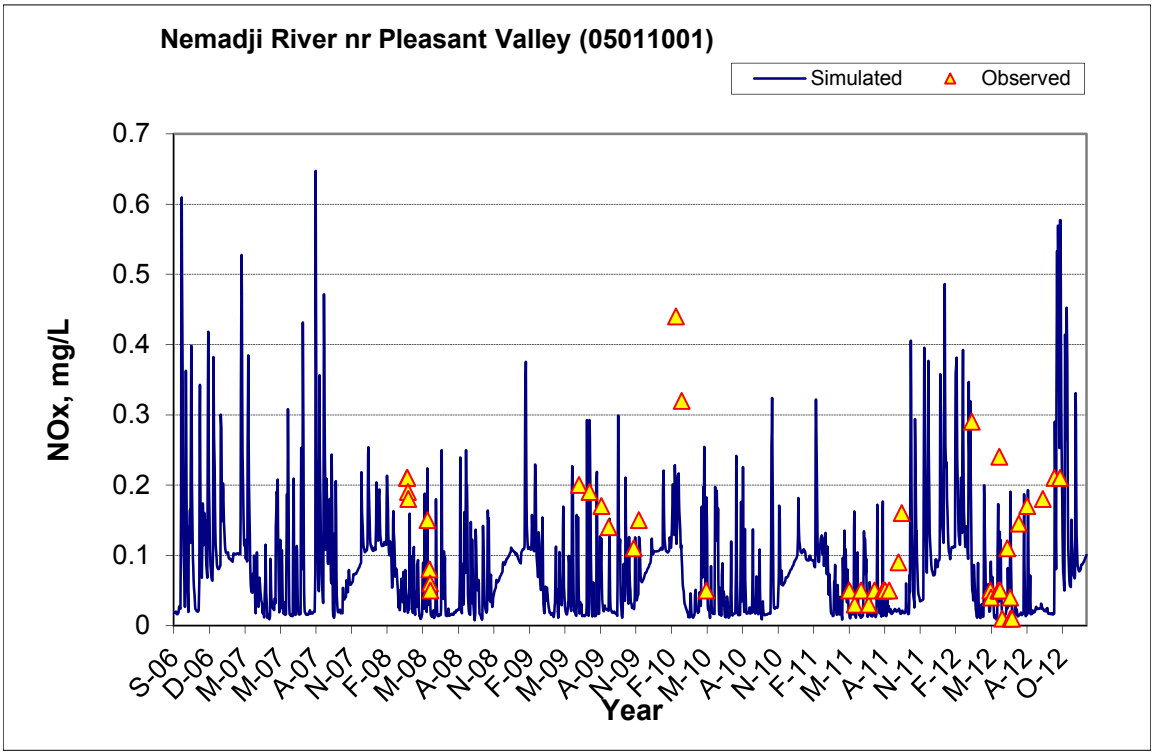

Figure B-147. Time series of observed and simulated Nitrite+ Nitrate Nitrogen (NOx) concentration at Nemadji River nr Pleasant Valley (05011001)

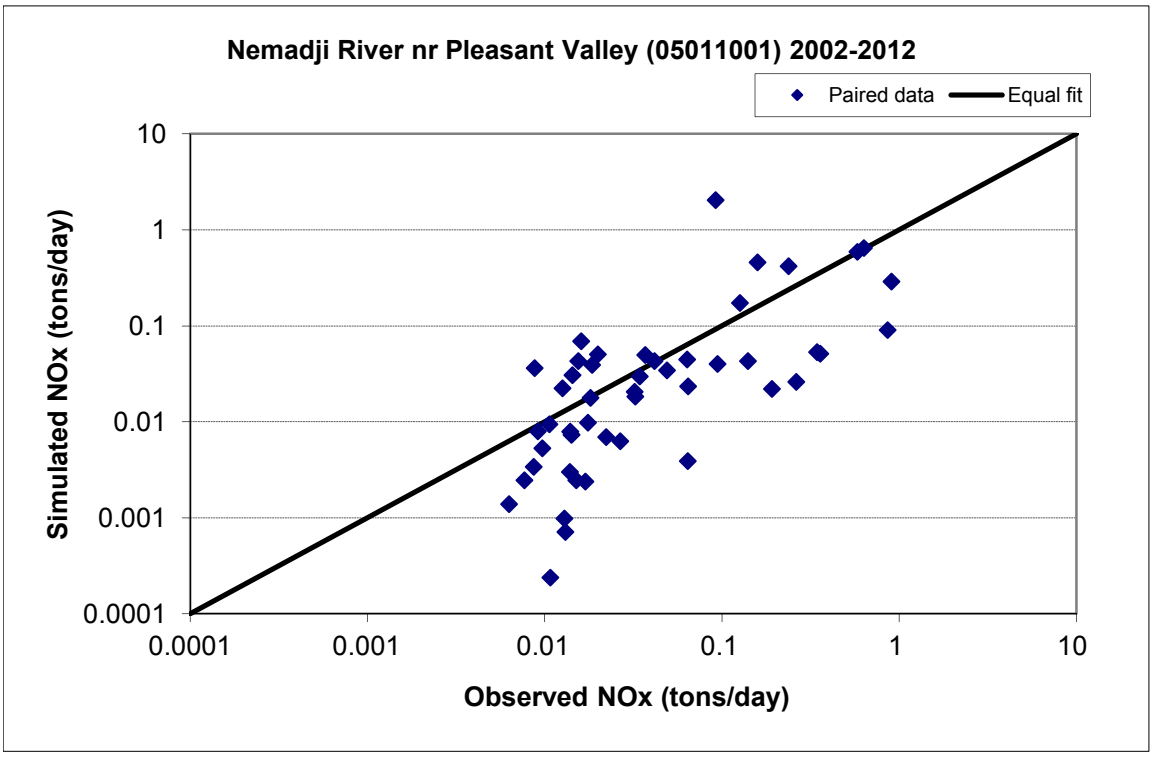

Figure B-148. Paired simulated vs. observed Nitrite+ Nitrate Nitrogen (NOx) load at Nemadji River nr Pleasant Valley (05011001) (calibration period)

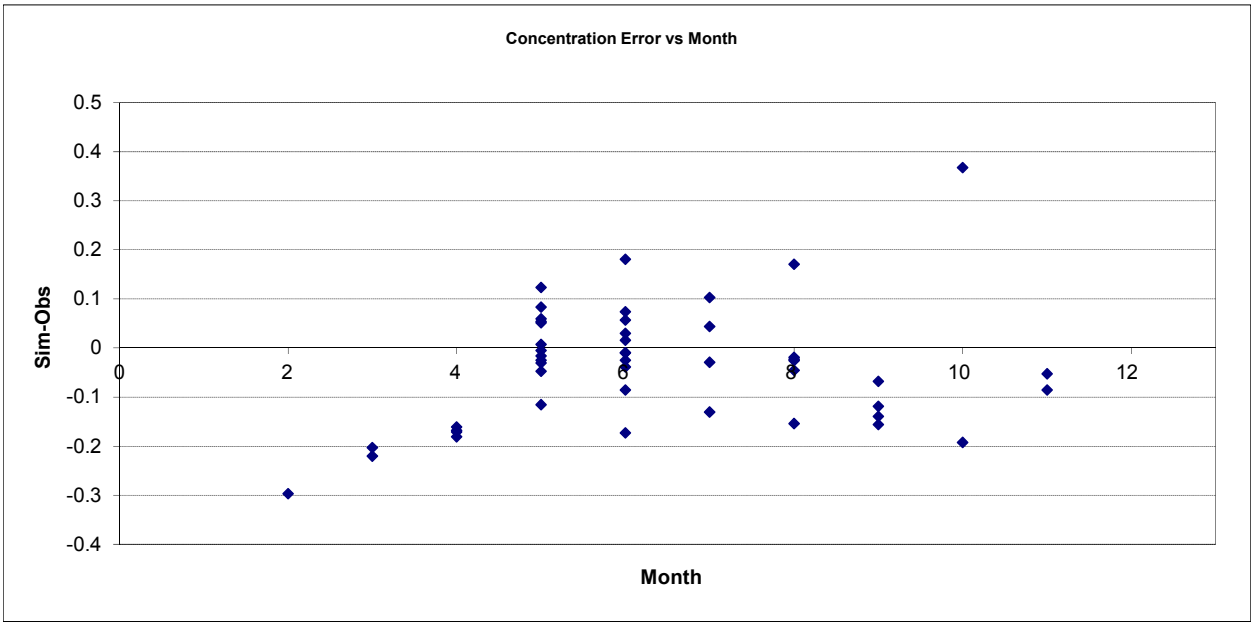

Figure B-149. Residual (Simulated - Observed) vs. Month Nitrite+ Nitrate Nitrogen (NOx) at Nemadji River nr Pleasant Valley (05011001)

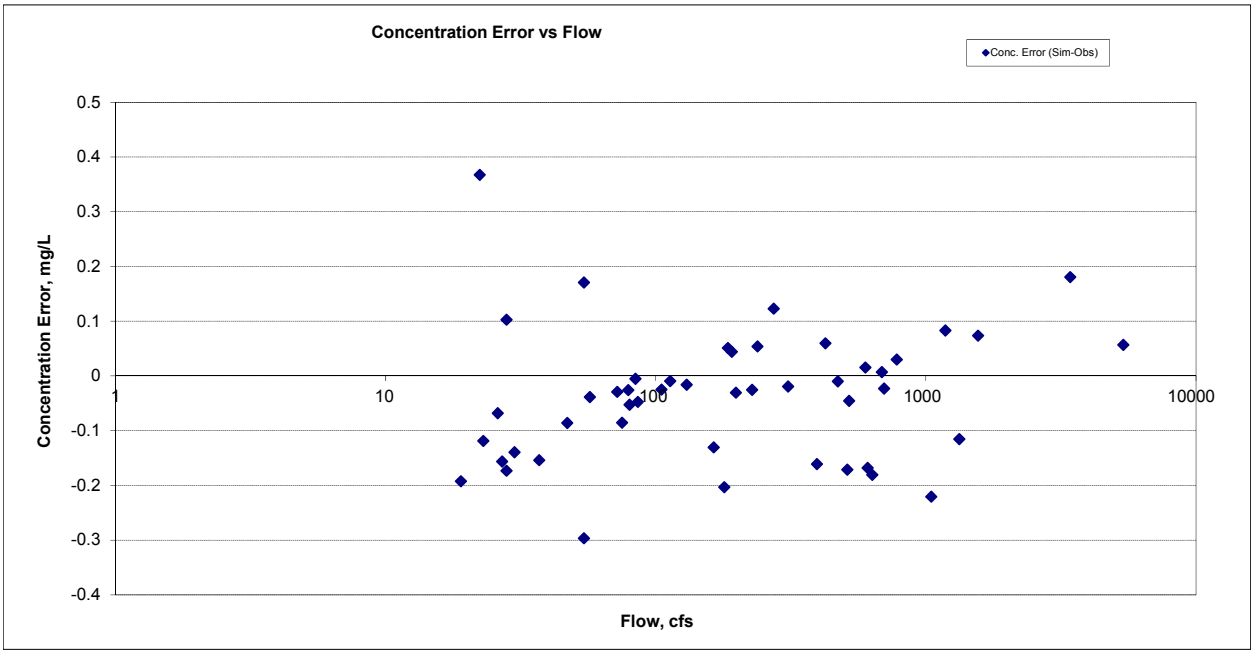

Figure B-150. Residual (Simulated - Observed) vs. Flow Nitrite+ Nitrate Nitrogen (NOx) at Nemadji River nr Pleasant Valley (05011001)

B.5.5 Total Nitrogen (TN)

Table B-26. Total Nitrogen (TN) statistics

Period	1994-2001	2002-2012
Count	ND	31
Concentration Average Error		11.29%
Concentration Median Error		-16.71%
Load Average Error		-3.90%
Load Median Error		-0.12%
Paired t conc		0.76
Paired t load		0.63

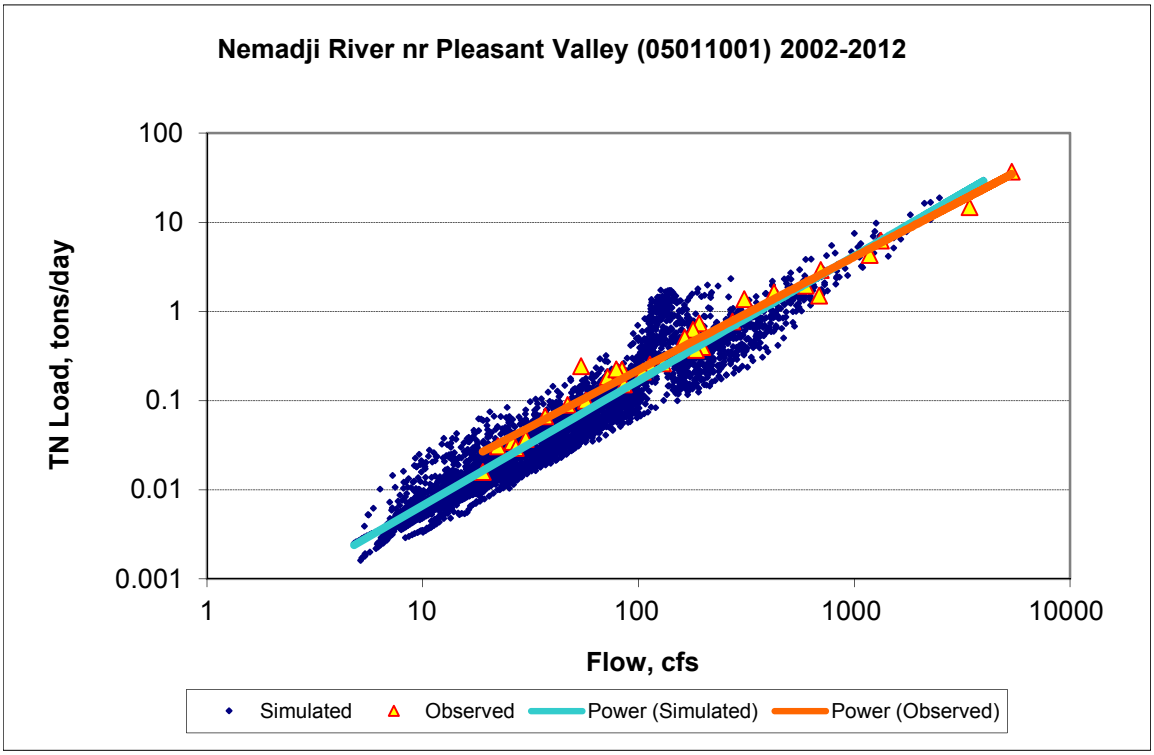

Figure B-151. Power plot of simulated and observed Total Nitrogen (TN) load vs flow at Nemadji River nr Pleasant Valley (05011001) (calibration period)

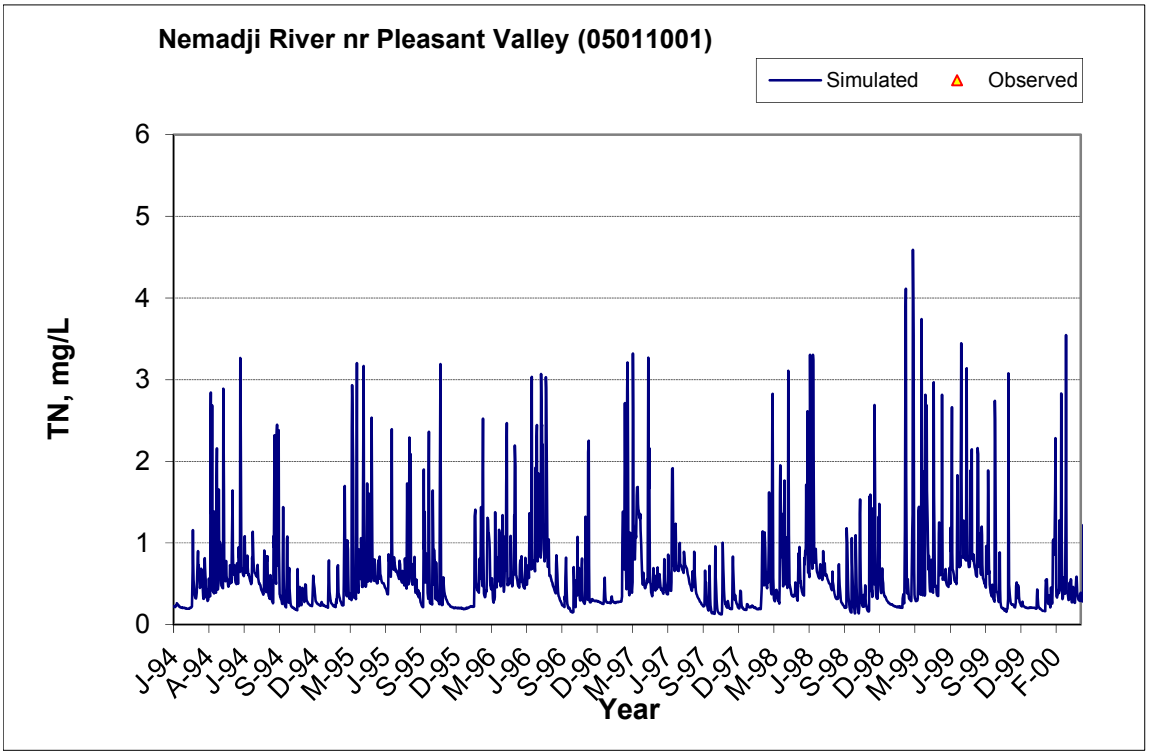

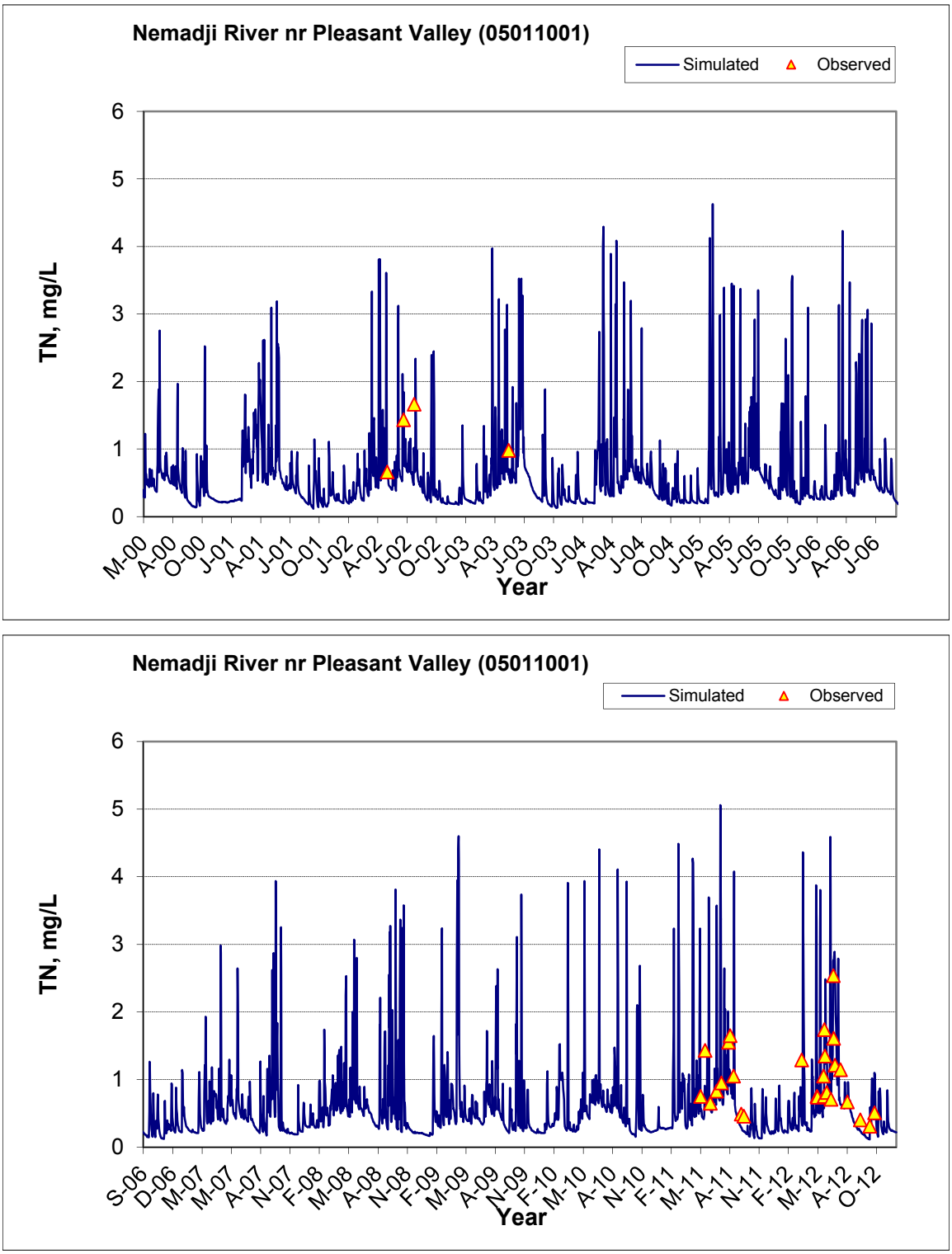

Figure B-152. Time series of observed and simulated Total Nitrogen (TN) concentration at Nemadji River nr Pleasant Valley (05011001)

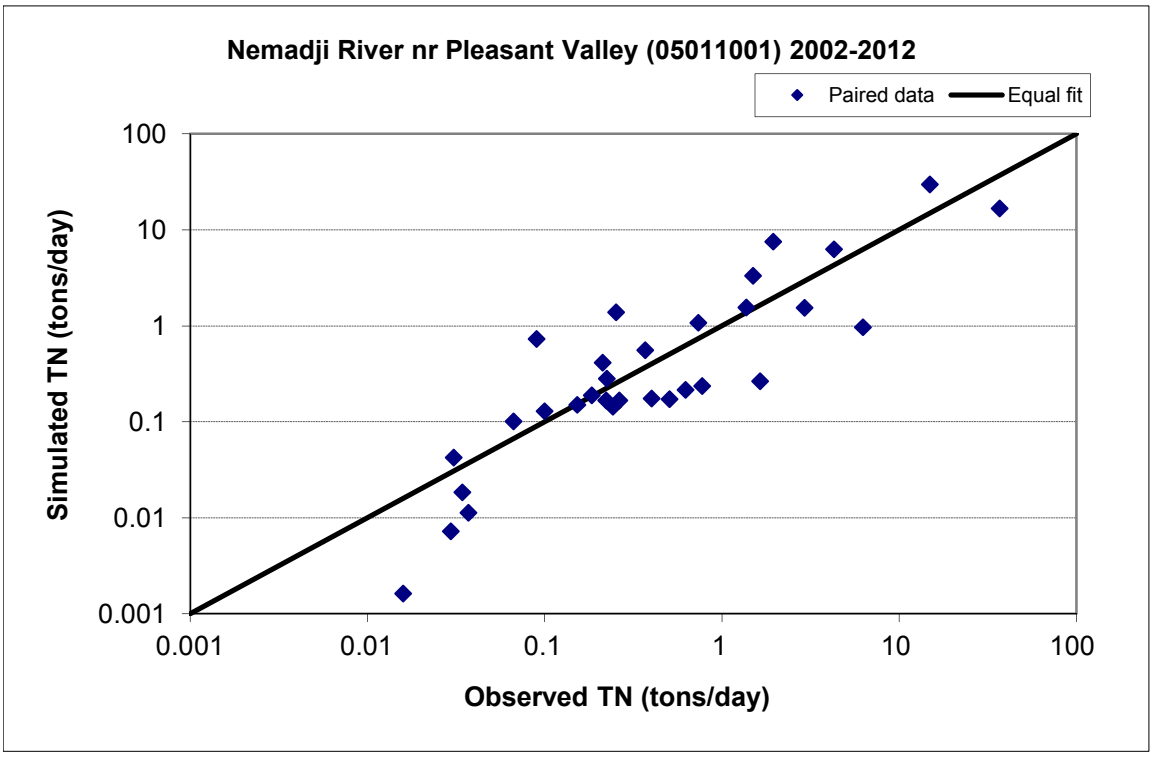

Figure B-153. Paired simulated vs. observed Total Nitrogen (TN) load at Nemadji River nr Pleasant Valley (05011001) (calibration period)

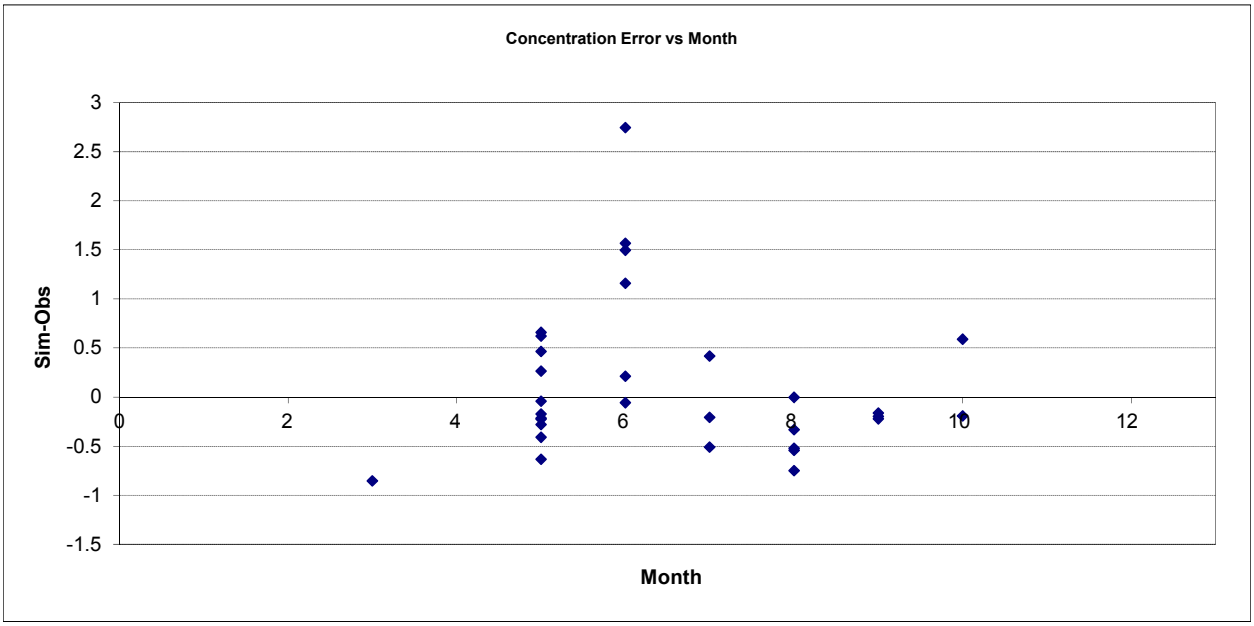

Figure B-154. Residual (Simulated - Observed) vs. Month Total Nitrogen (TN) at Nemadji River nr Pleasant Valley (05011001)

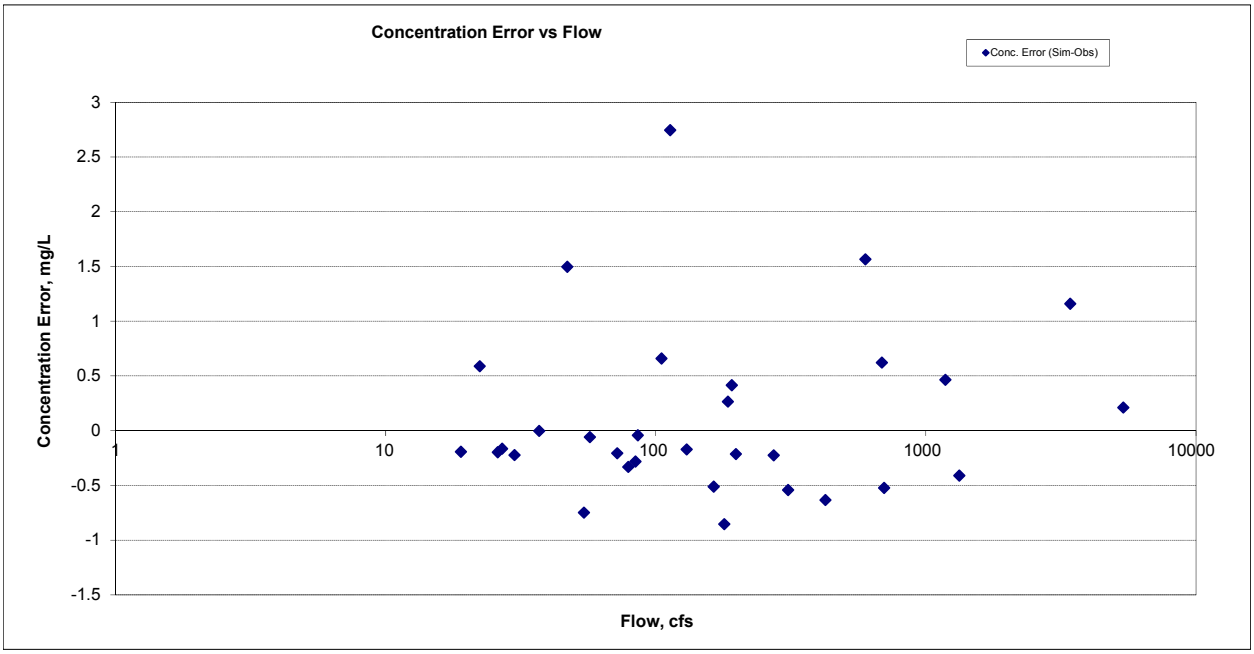

Figure B-155. Residual (Simulated - Observed) vs. Flow Total Nitrogen (TN) at Nemadji River nr Pleasant Valley (05011001)

B.5.6 Soluble Reactive Phosphorus (SRP)

Table B-27. Soluble Reactive Phosphorus (SRP) statistics

Period	1994-2001	2002-2012
Count	ND	39
Concentration Average Error		20.78%
Concentration Median Error		5.59%
Load Average Error		37.02%
Load Median Error		-0.03%
Paired t conc		0.49
Paired t load		0.40

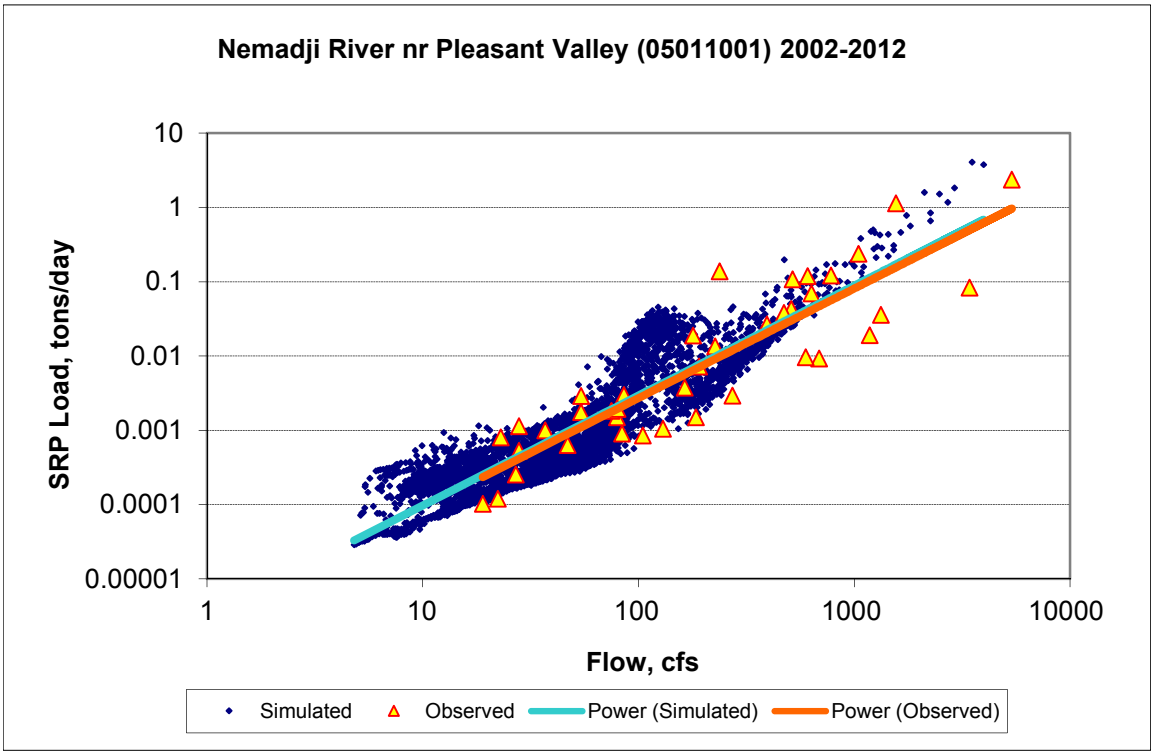

Figure B-156. Power plot of simulated and observed Soluble Reactive Phosphorus (SRP) load vs flow at Nemadji River nr Pleasant Valley (05011001) (calibration period)

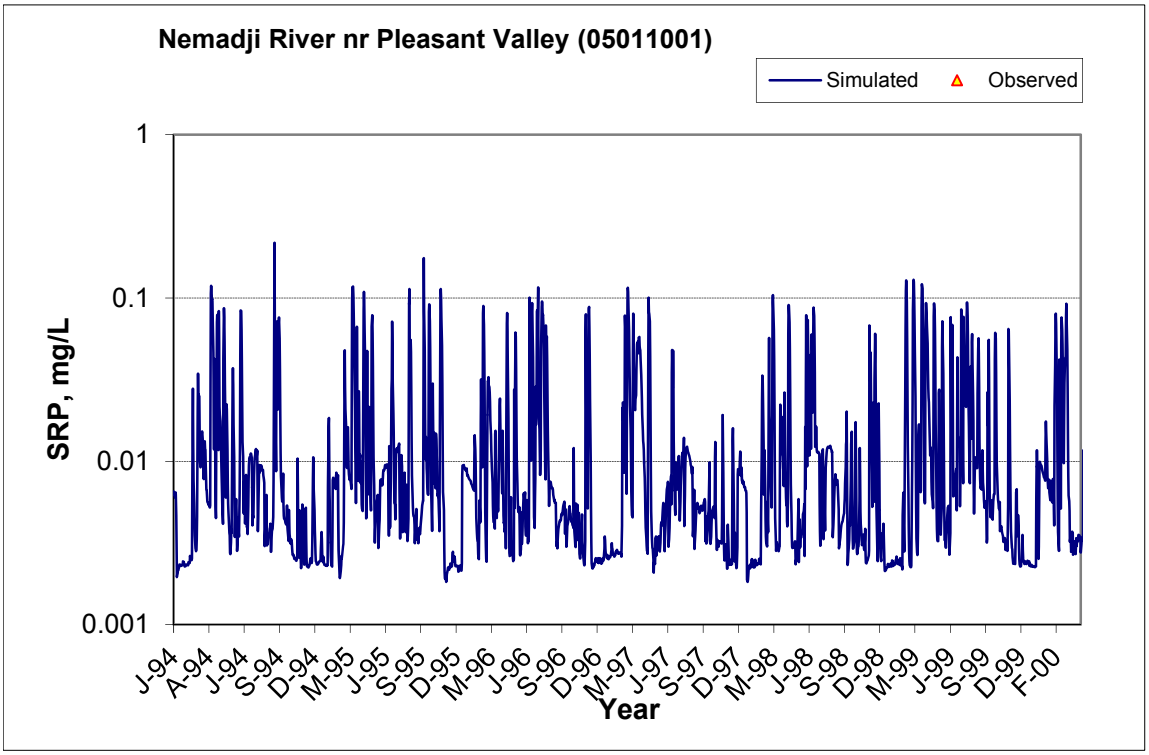

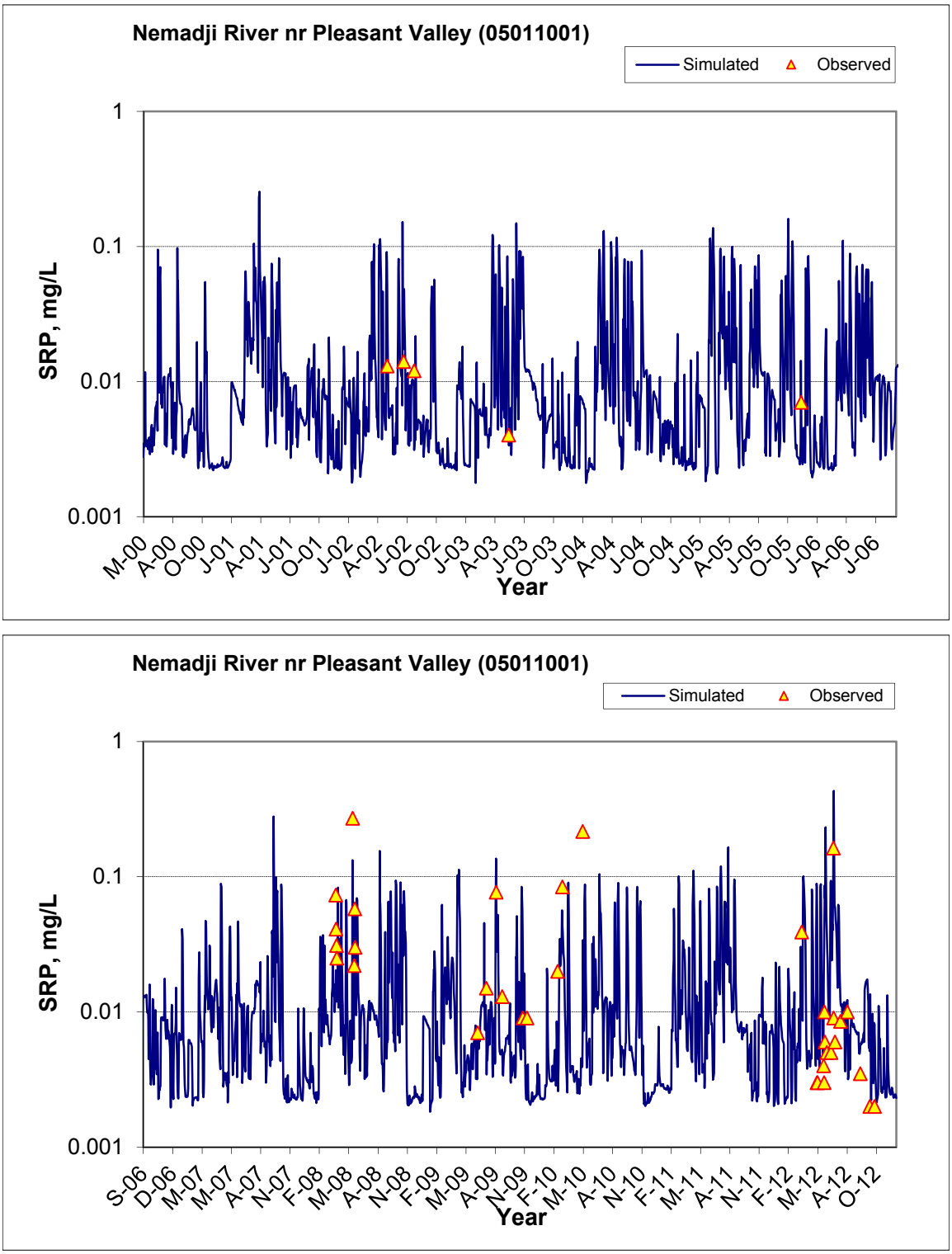

Figure B-157. Time series of observed and simulated Soluble Reactive Phosphorus (SRP) concentration at Nemadji River nr Pleasant Valley (05011001)

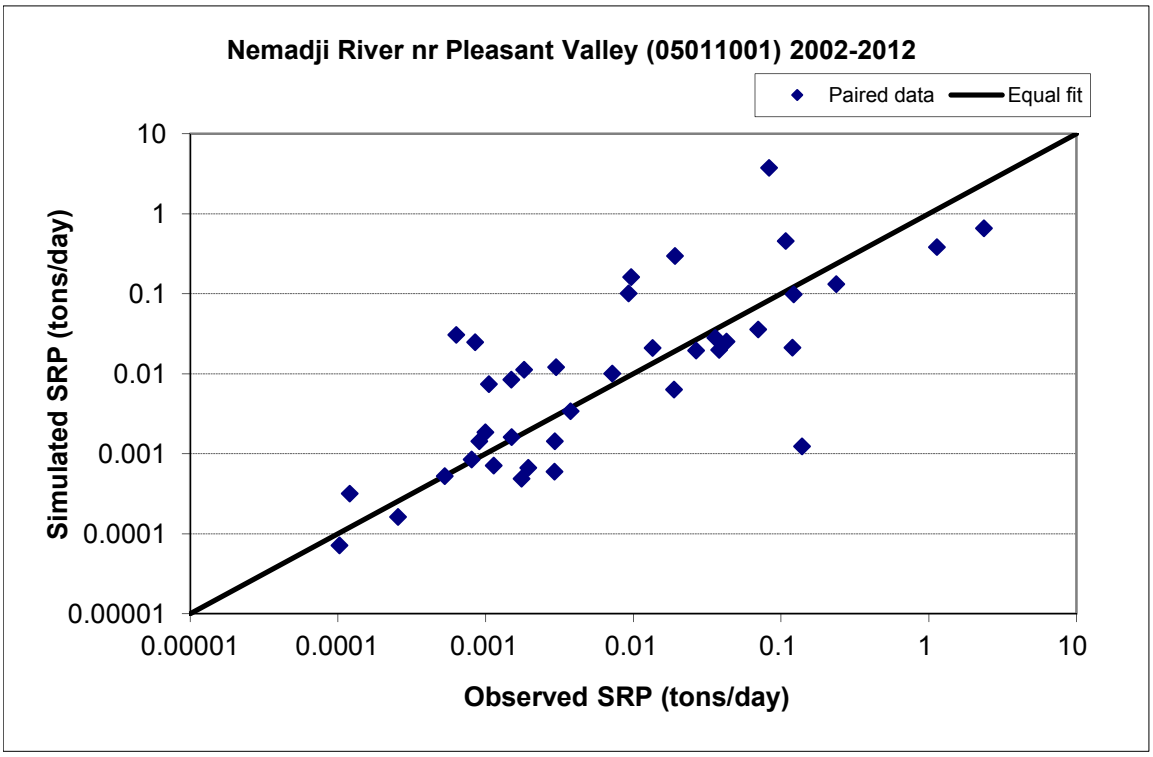

Figure B-158. Paired simulated vs. observed Soluble Reactive Phosphorus (SRP) load at Nemadji River nr Pleasant Valley (05011001) (calibration period)

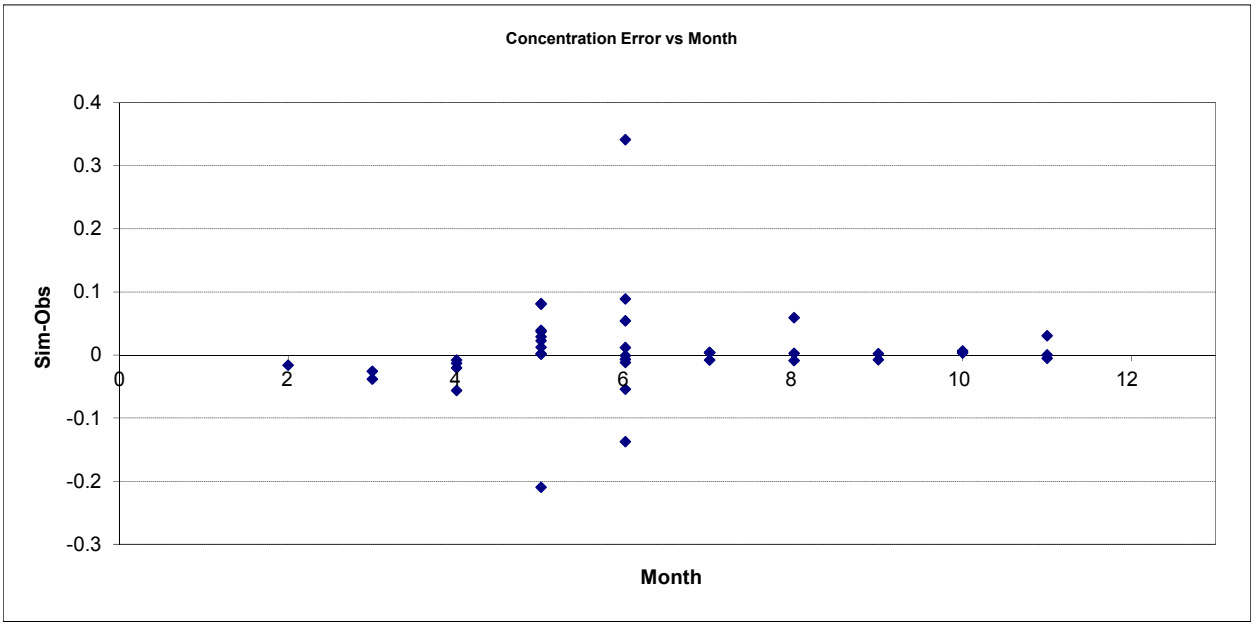

Figure B-159. Residual (Simulated - Observed) vs. Month Soluble Reactive Phosphorus (SRP) at Nemadji River nr Pleasant Valley (05011001)

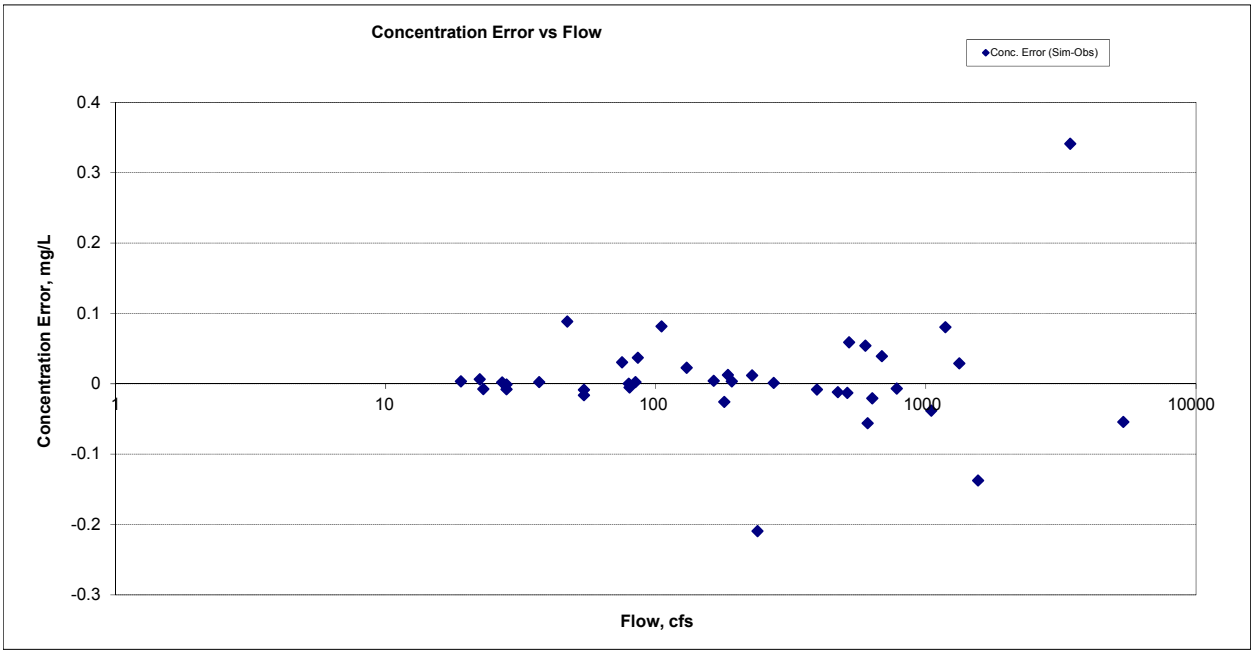

Figure B-160. Residual (Simulated - Observed) vs. Flow Soluble Reactive Phosphorus (SRP) at Nemadji River nr Pleasant Valley (05011001)

B.5.7 Organic Phosphorus (OrgP)

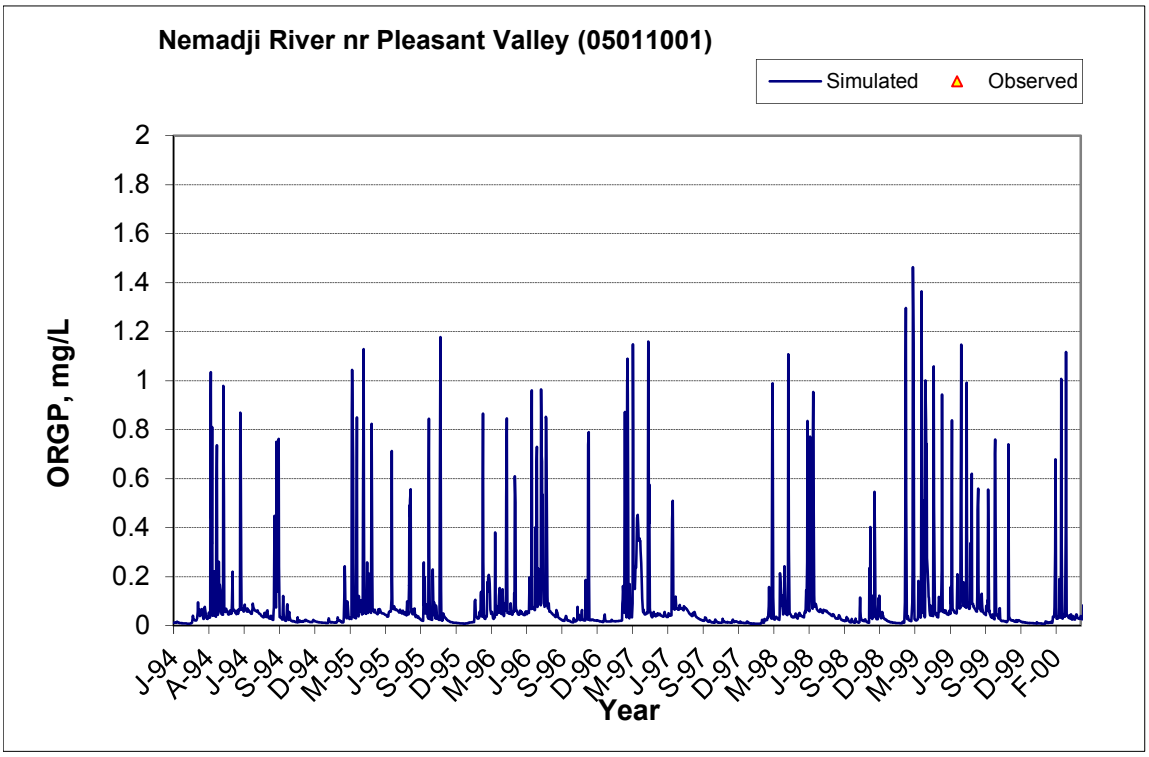

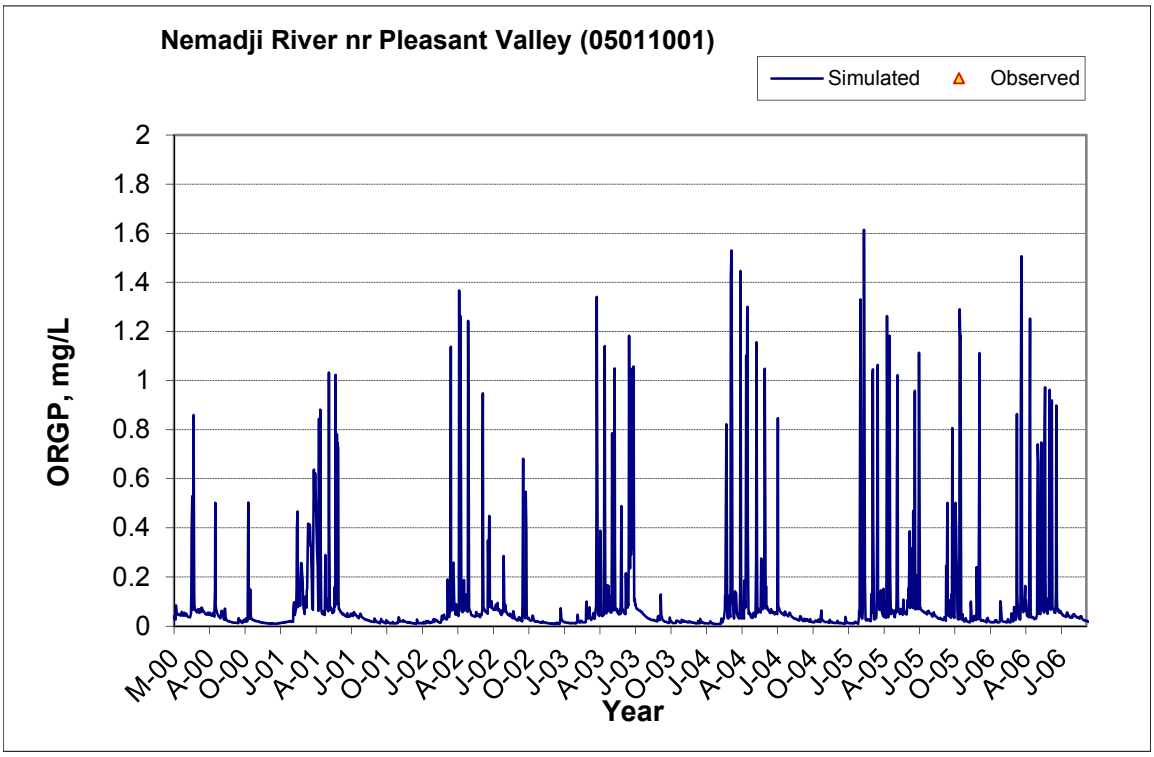

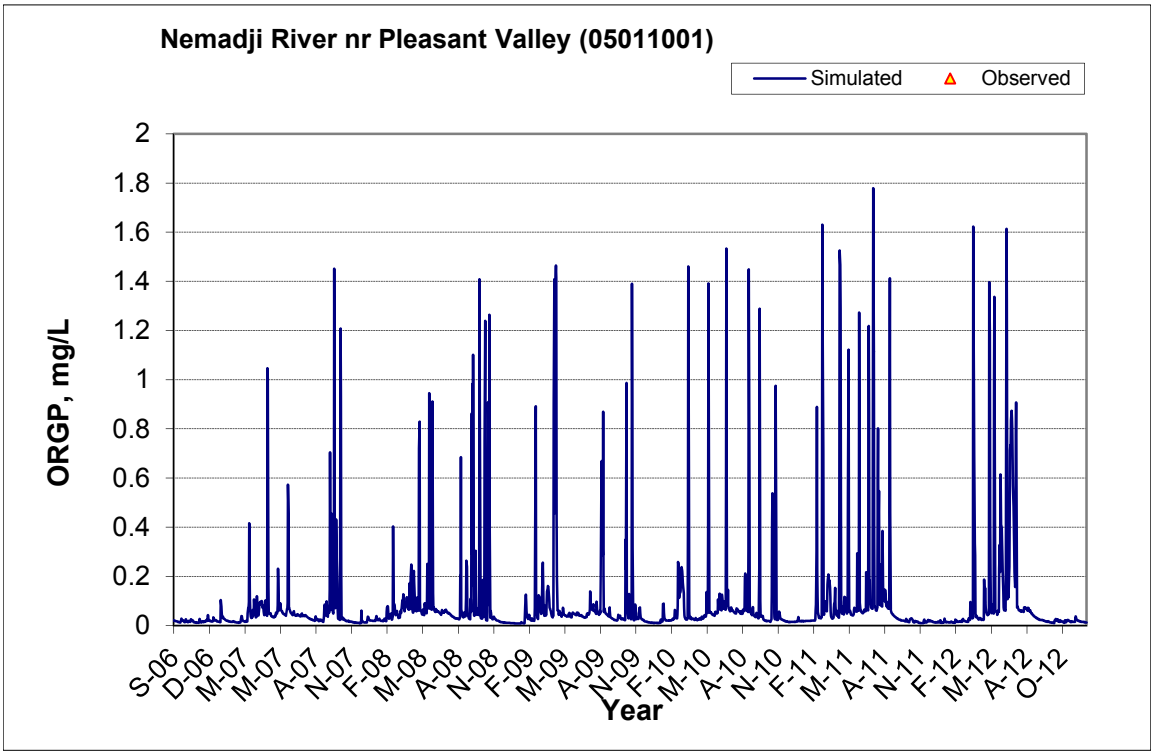

Figure B-161. Time series of observed and simulated Organic Phosphorus (OrgP) concentration at Nemadji River nr Pleasant Valley (05011001)

B.5.8 Total Phosphorus (TP)

Table B-28. Total Phosphorus (TP) statistics

Period	1994-2001	2002-2012
Count	22	100
Concentration Average Error	59.18%	-8.31%
Concentration Median Error	11.38%	0.53%
Load Average Error	35.16%	-35.49%
Load Median Error	0.81%	-0.03%
Paired t conc	0.20	0.82
Paired t load	0.41	0.33

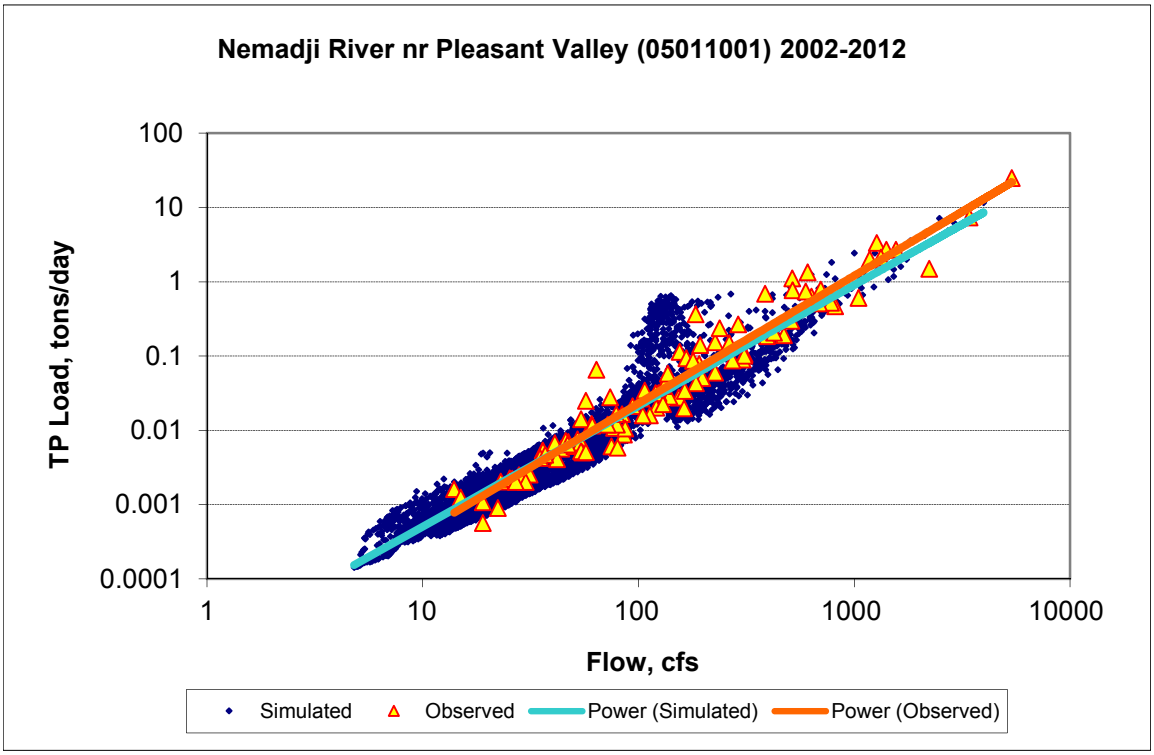

Figure B-162. Power plot of simulated and observed Total Phosphorus (TP) load vs flow at Nemadji River nr Pleasant Valley (05011001) (calibration period)

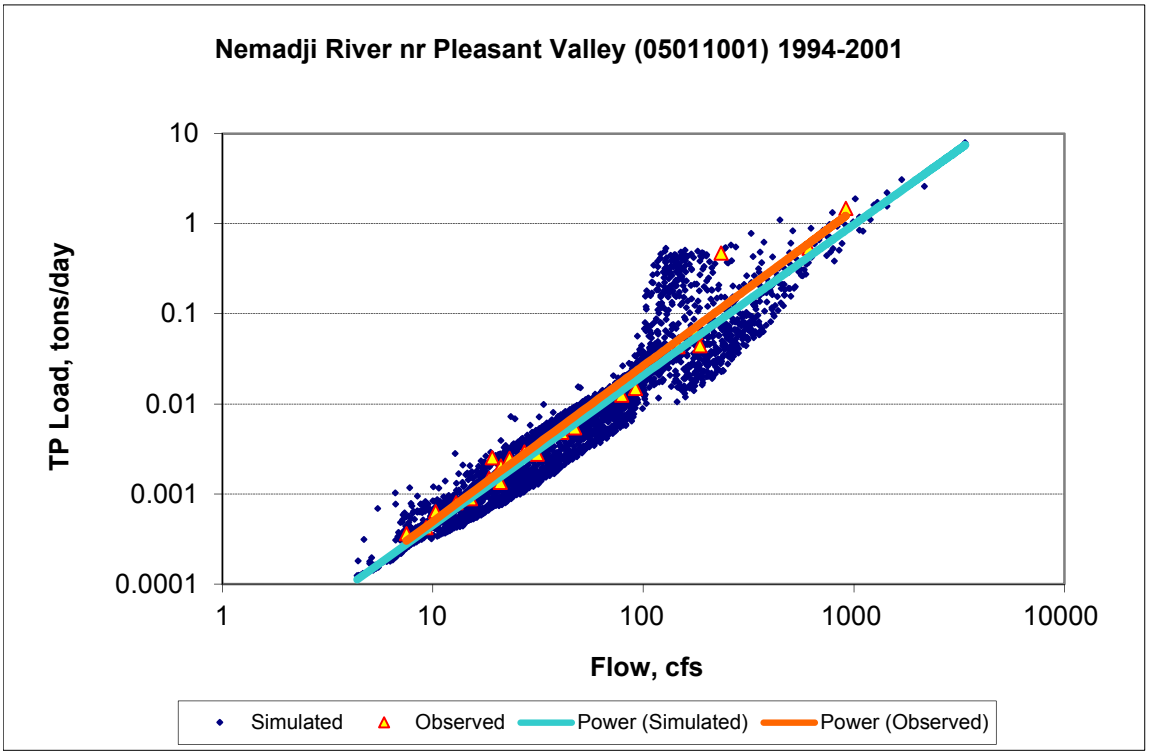

Figure B-163. Power plot of simulated and observed Total Phosphorus (TP) load vs flow at Nemadji River nr Pleasant Valley (05011001) (validation period)

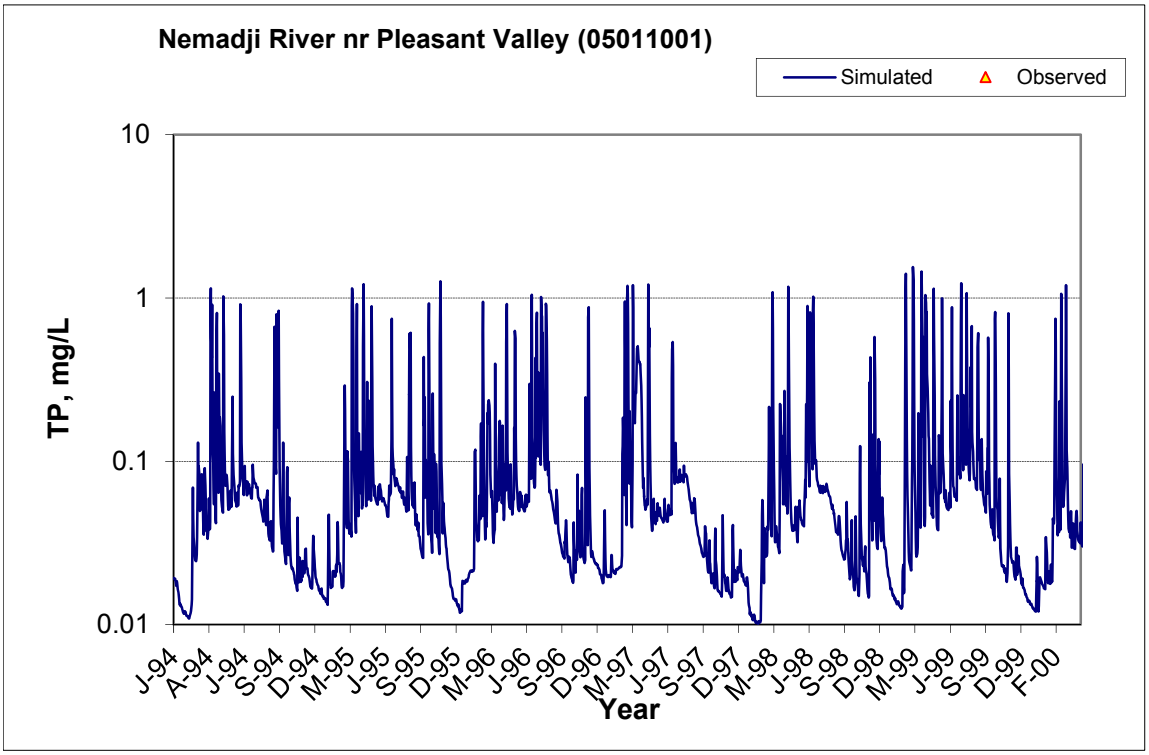

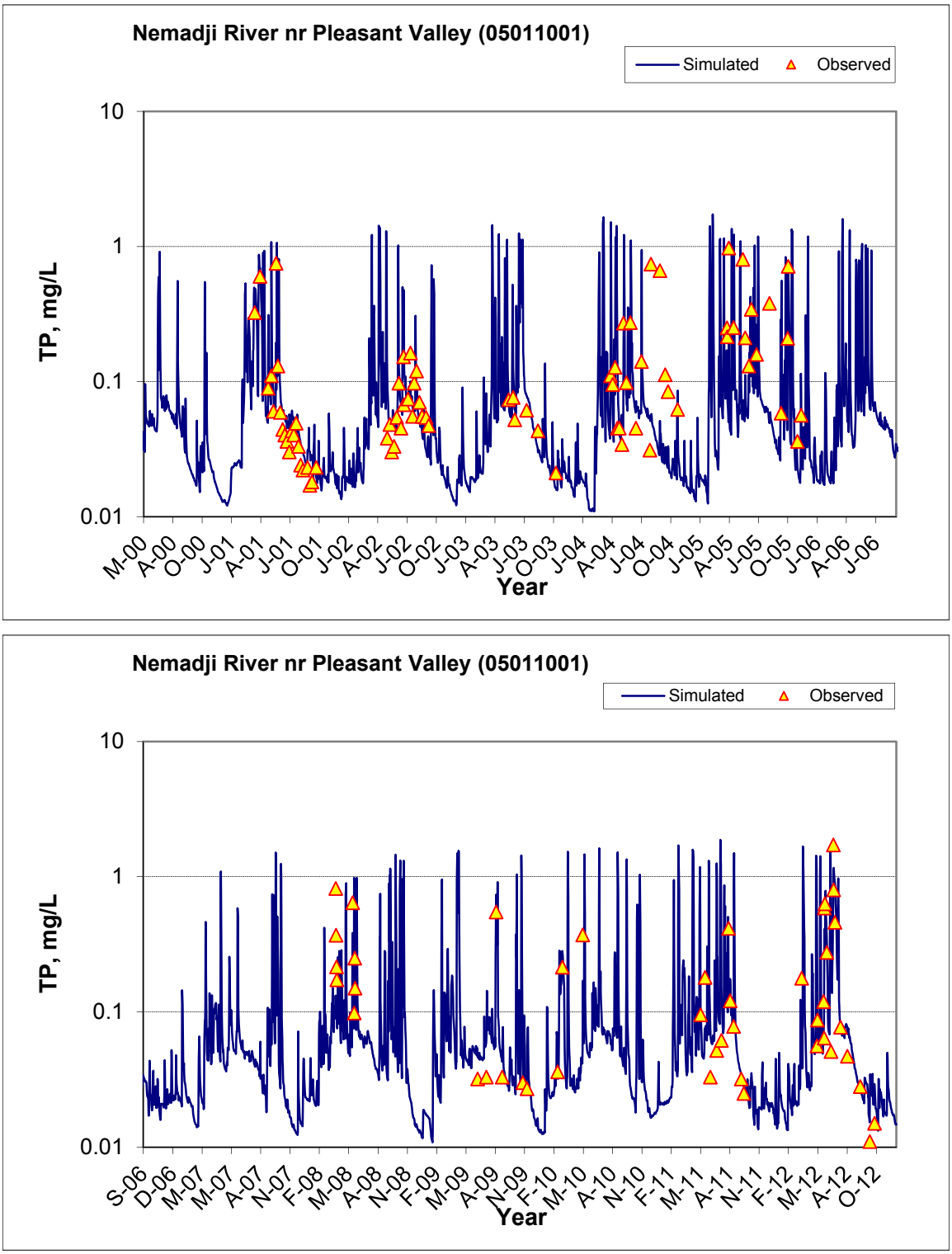

Figure B-164. Time series of observed and simulated Total Phosphorus (TP) concentration at Nemadji River nr Pleasant Valley (05011001)

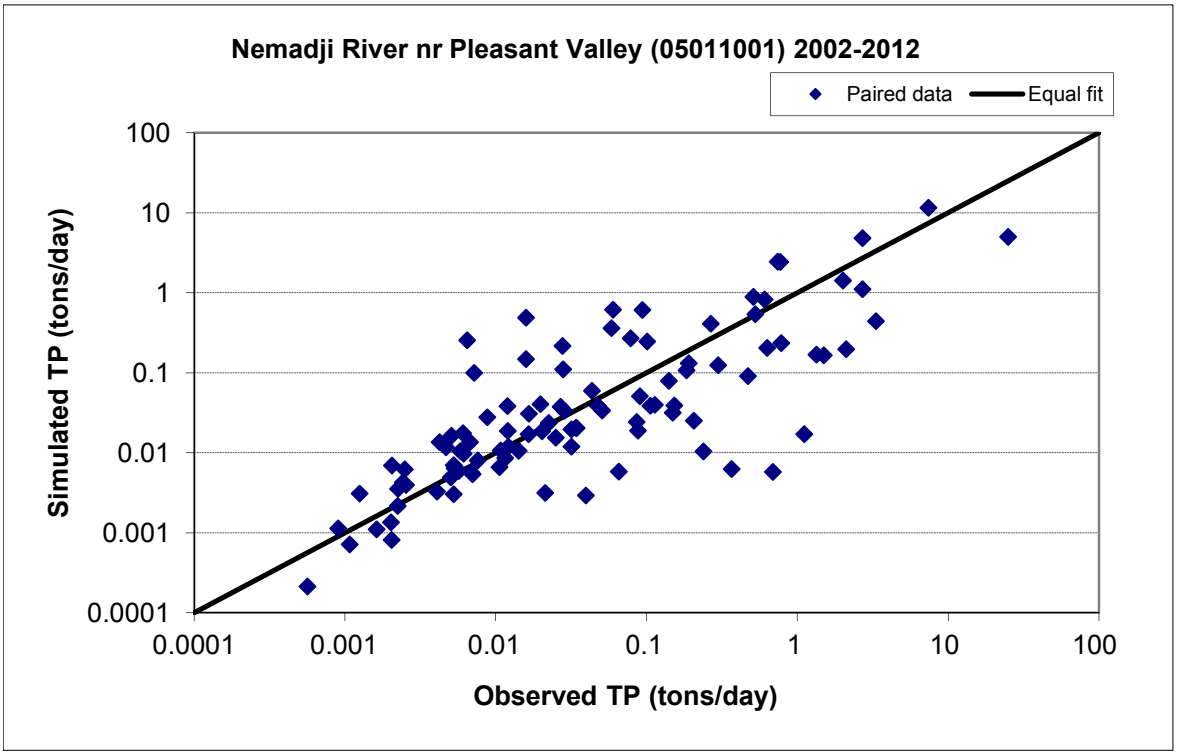

Figure B-165. Paired simulated vs. observed Total Phosphorus (TP) load at Nemadji River nr Pleasant Valley (05011001) (calibration period)

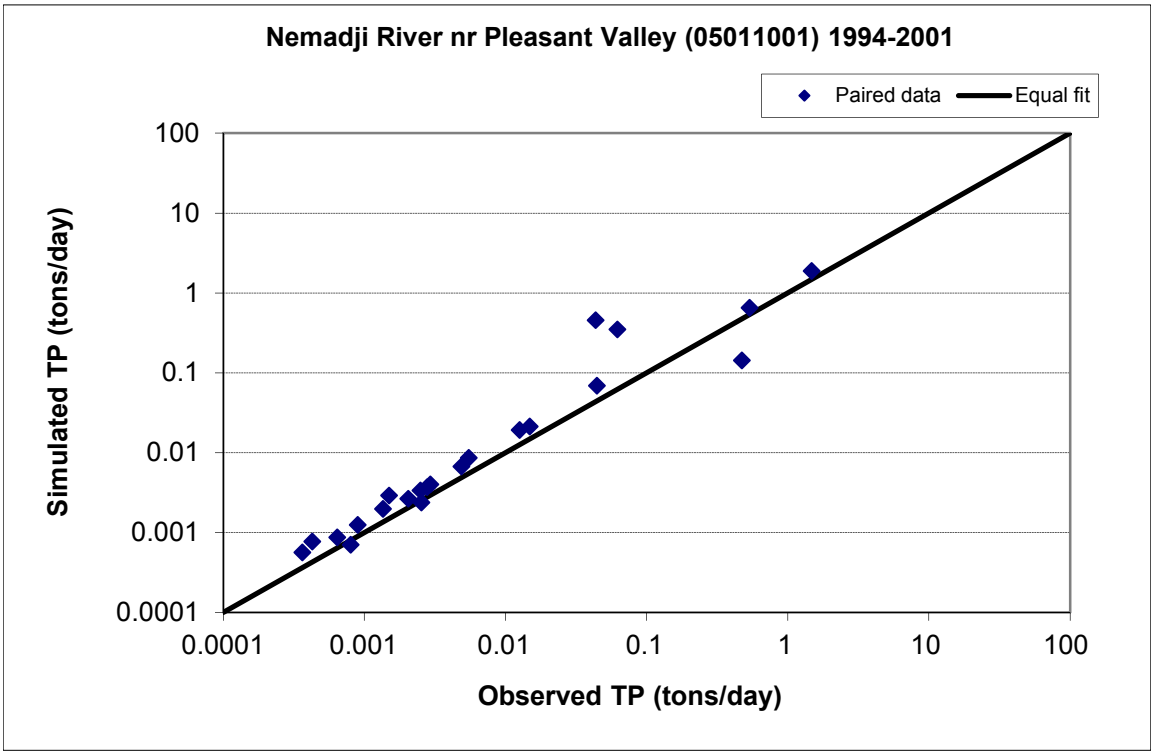

Figure B-166. Paired simulated vs. observed Total Phosphorus (TP) load at Nemadji River nr Pleasant Valley (05011001) (validation period)

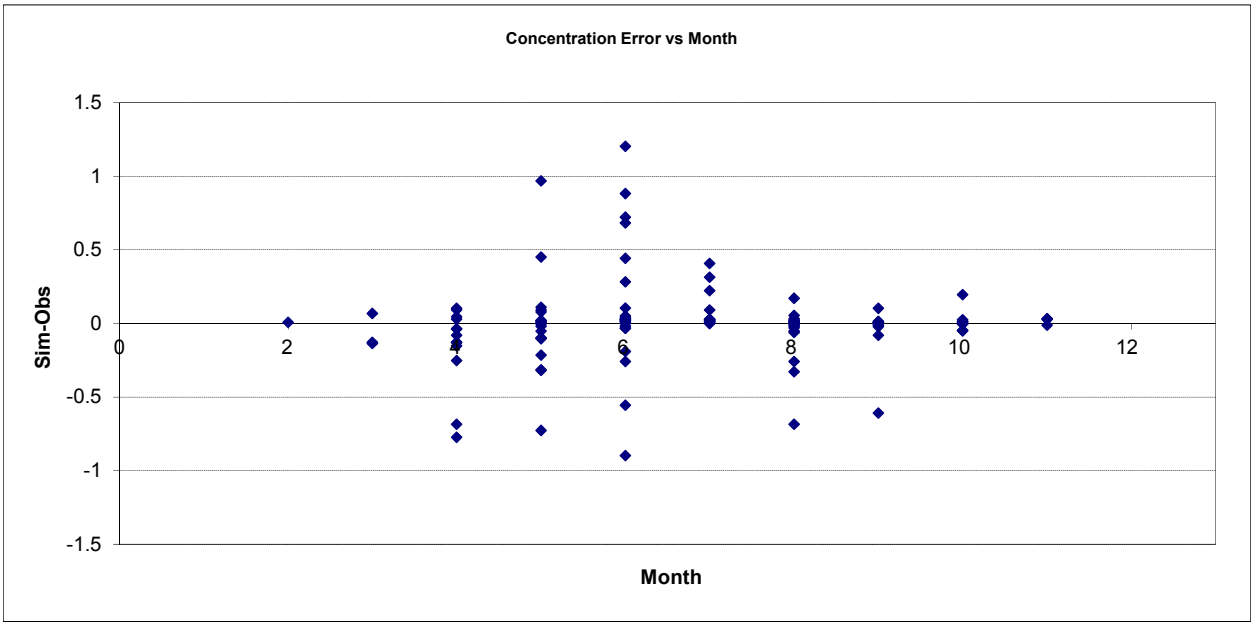

Figure B-167. Residual (Simulated - Observed) vs. Month Total Phosphorus (TP) at Nemadji River nr Pleasant Valley (05011001)

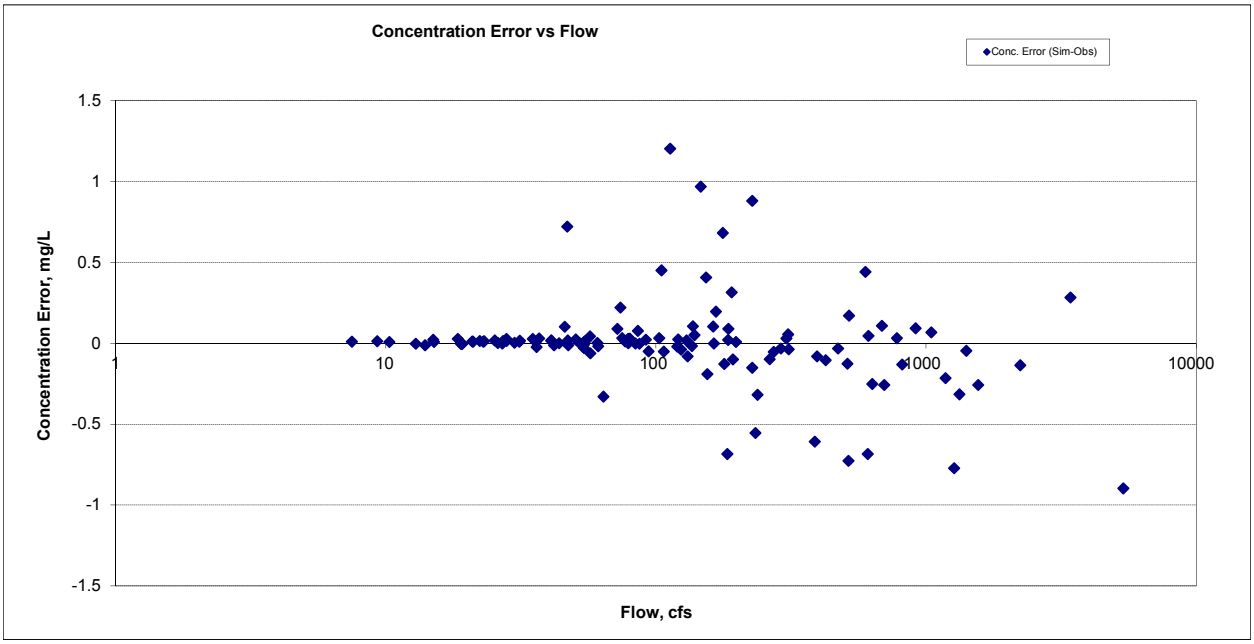

Figure B-168. Residual (Simulated - Observed) vs. Flow Total Phosphorus (TP) at Nemadji River nr Pleasant Valley (05011001)

B.6 NEMADJI RIVER NR SOUTH SUPERIOR, WI (05011002)

B.6.1 Ammonia Nitrogen (NH3)

Table B-29. Ammonia Nitrogen (NH3) statistics

Period	1994-2007	2008-2012
Count	ND	19
Concentration Average Error		23.61%
Concentration Median Error		44.39%
Load Average Error		-43.44%
Load Median Error		11.07%
Paired t conc		0.44
Paired t load		0.24

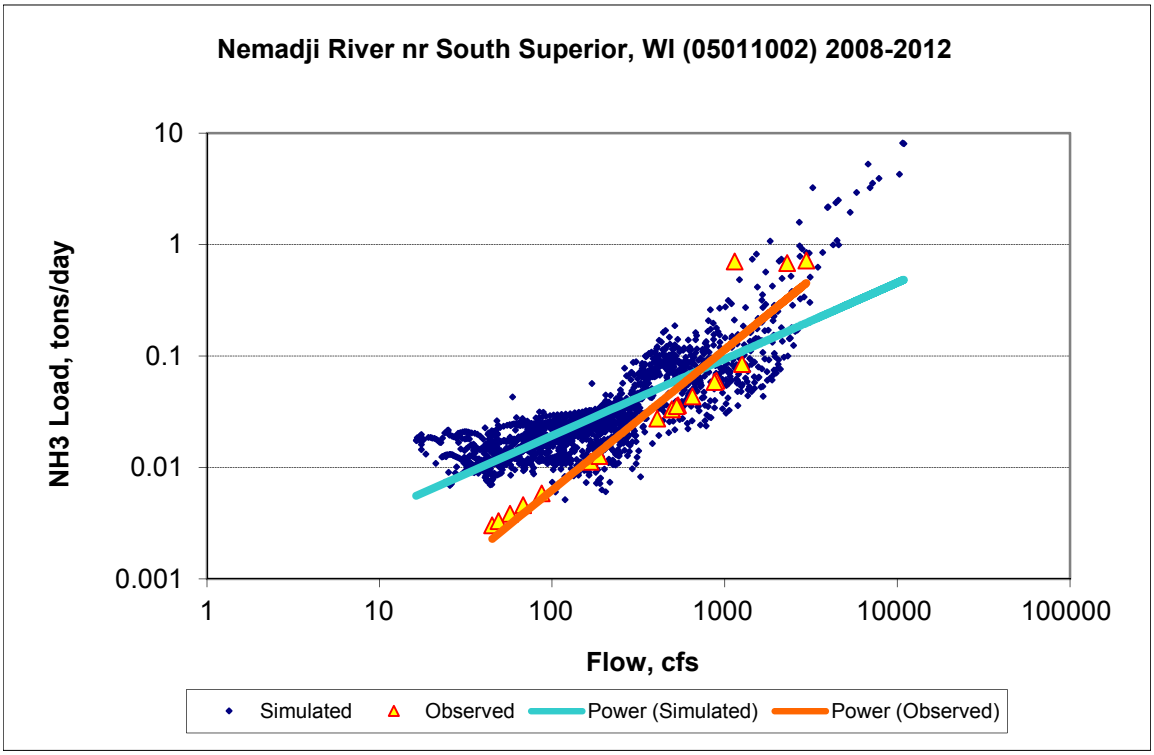

Figure B-169. Power plot of simulated and observed Ammonia Nitrogen (NH3) load vs flow at Nemadji River nr South Superior, WI (05011002) (calibration period)

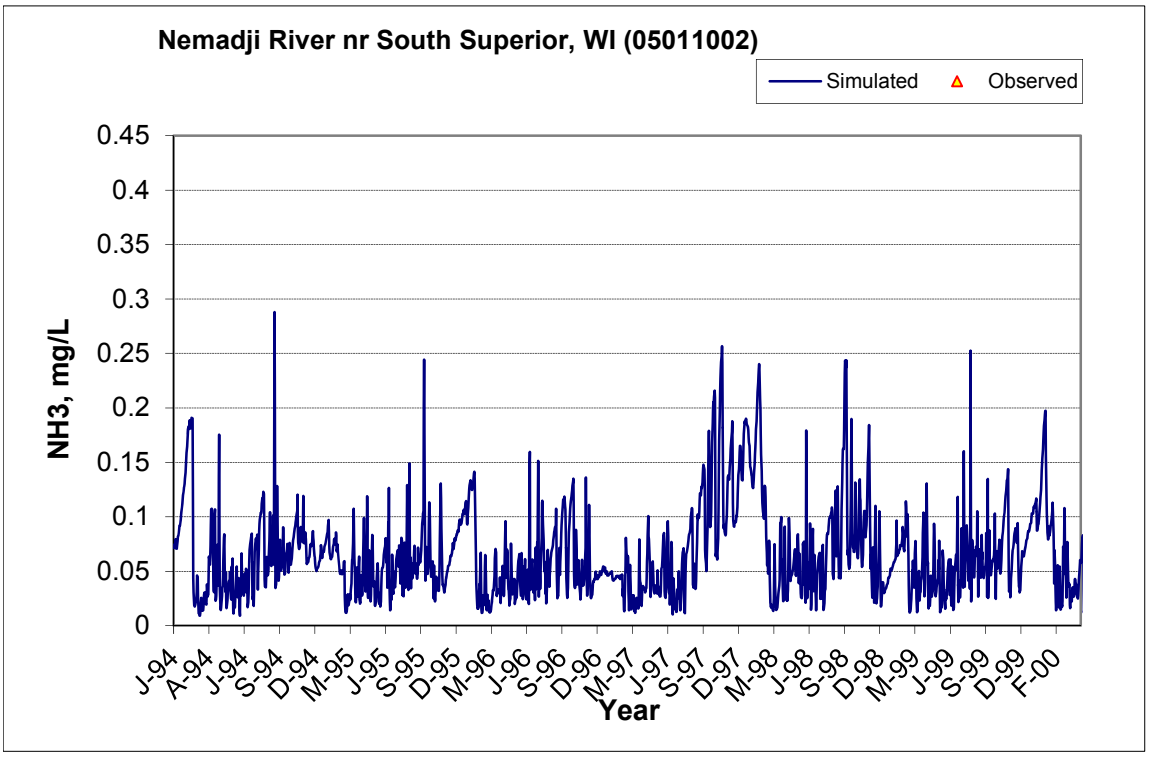
Nemadji River nr South Superior, WI (05011002)
Simulated
Observed
NH3, mg/L
0.45
0.4
0.35
0.3
0.25
0.2
0.15
0.1
0.05
0
J-94 A-94 J-94 S-94 D-94 M-95 J-95 S-95 D-95 M-96 J-96 S-96 D-96 M-97 J-97 S-97 D-97 M-98 J-98 S-98 D-98 M-99 J-99 S-99 D-99 F-00
Year

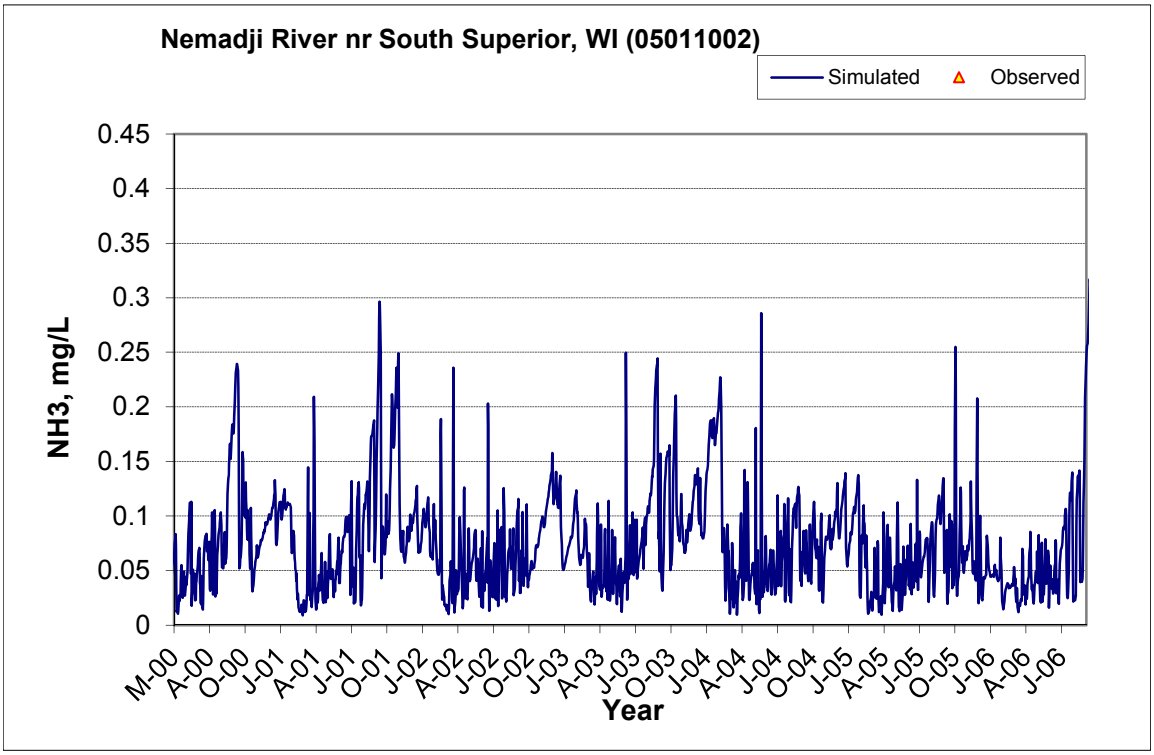
Nemadji River nr South Superior, WI (05011002)
Simulated
Observed
NH3, mg/L
0.45
0.4
0.35
0.3
0.25
0.2
0.15
0.1
0.05
0
M-00 A-00 O-00 J-01 A-01 J-01 O-01 J-02 A-02 J-02 O-02 J-03 A-03 J-03 O-03 J-04 A-04 J-04 O-04 J-05 A-05 J-05 O-05 J-06 A-06 J-06
Year

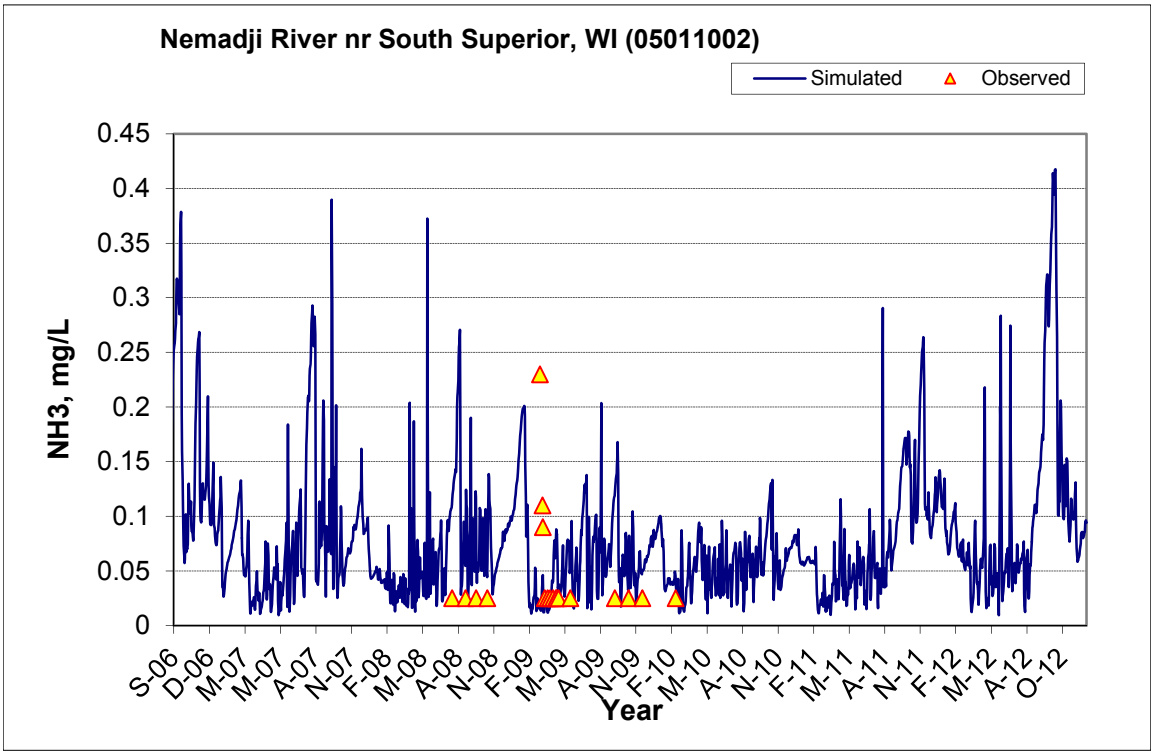

Figure B-170. Time series of observed and simulated Ammonia Nitrogen (NH3) concentration at Nemadji River nr South Superior, WI (05011002)

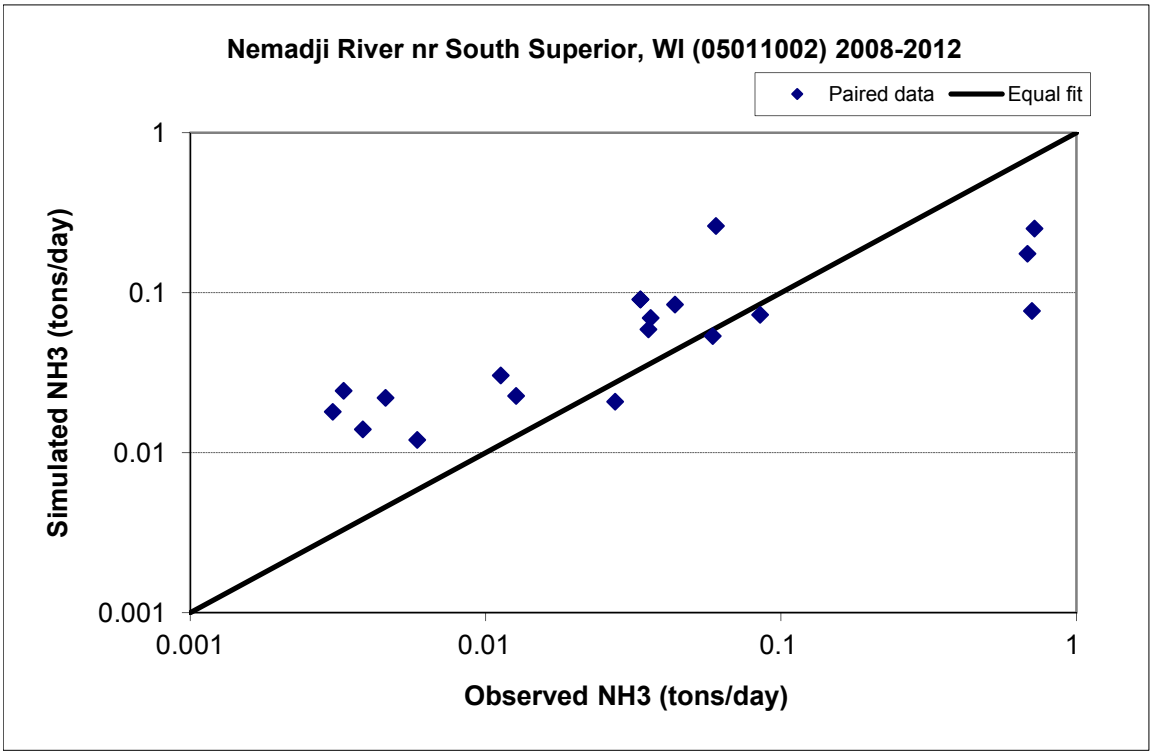

Figure B-171. Paired simulated vs. observed Ammonia Nitrogen (NH3) load at Nemadji River nr South Superior, WI (05011002) (calibration period)

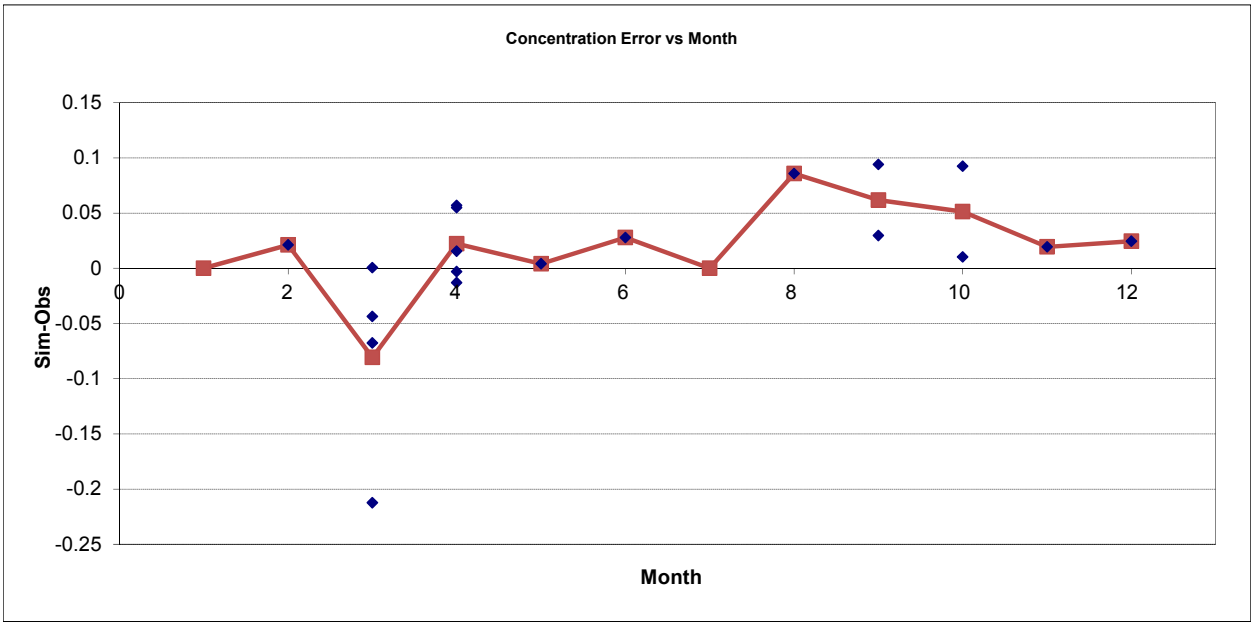

Figure B-172. Residual (Simulated - Observed) vs. Month Ammonia Nitrogen (NH3) at Nemadji River nr South Superior, WI (05011002)

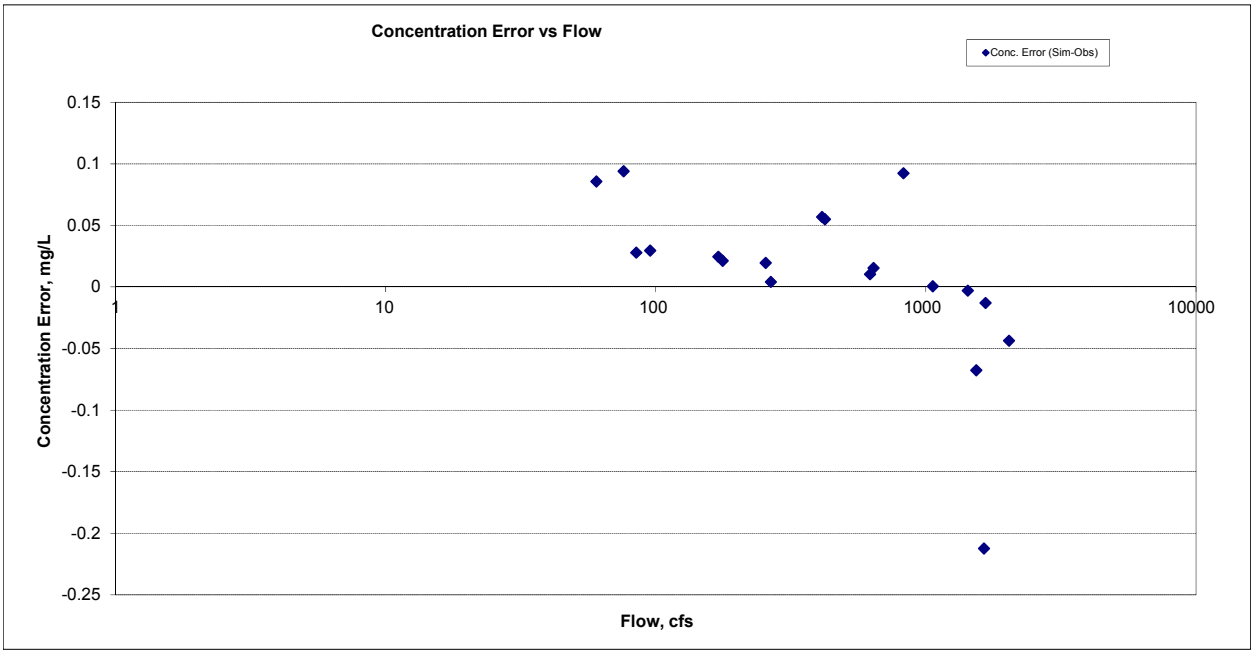

Figure B-173. Residual (Simulated - Observed) vs. Flow Ammonia Nitrogen (NH3) at Nemadji River nr South Superior, WI (05011002)

B.6.2 Organic Nitrogen (OrgN)

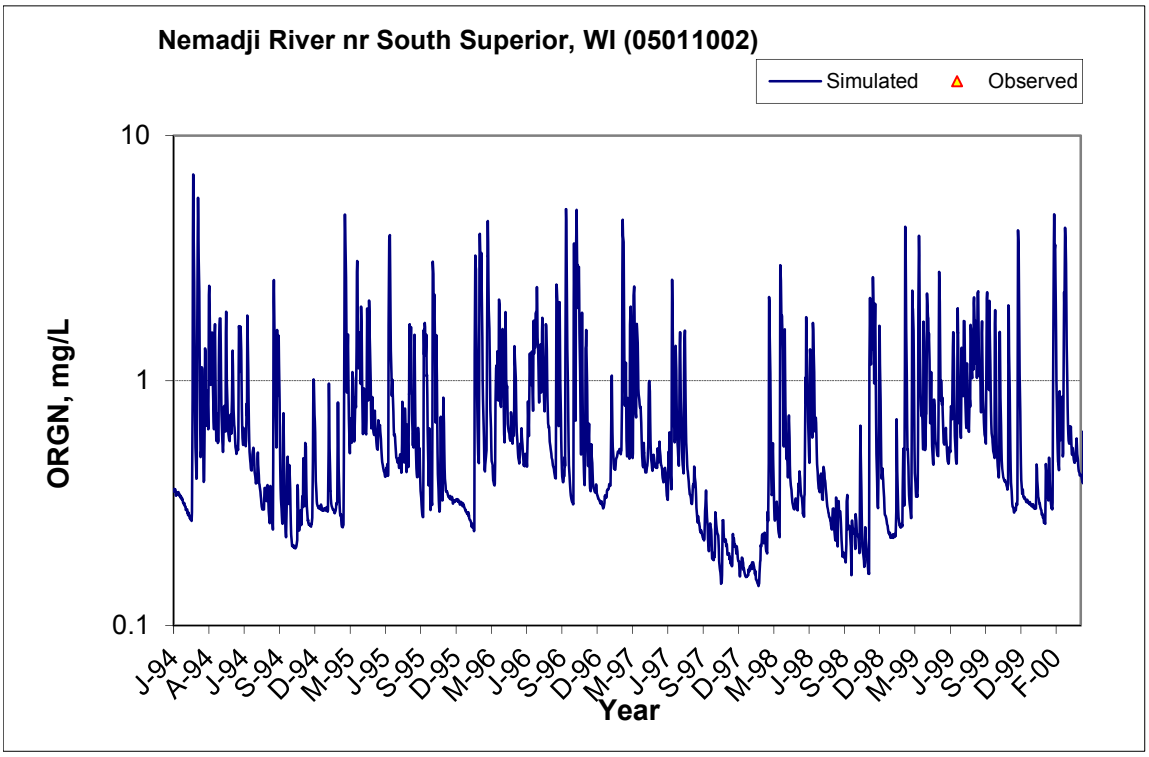

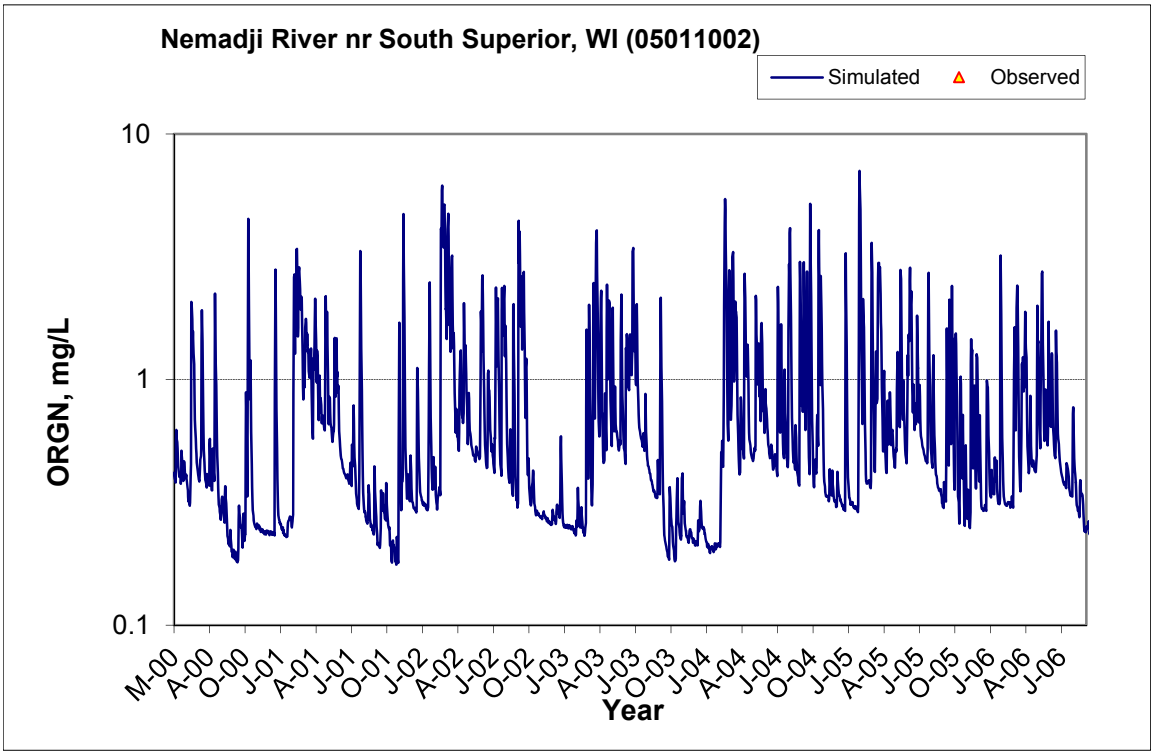

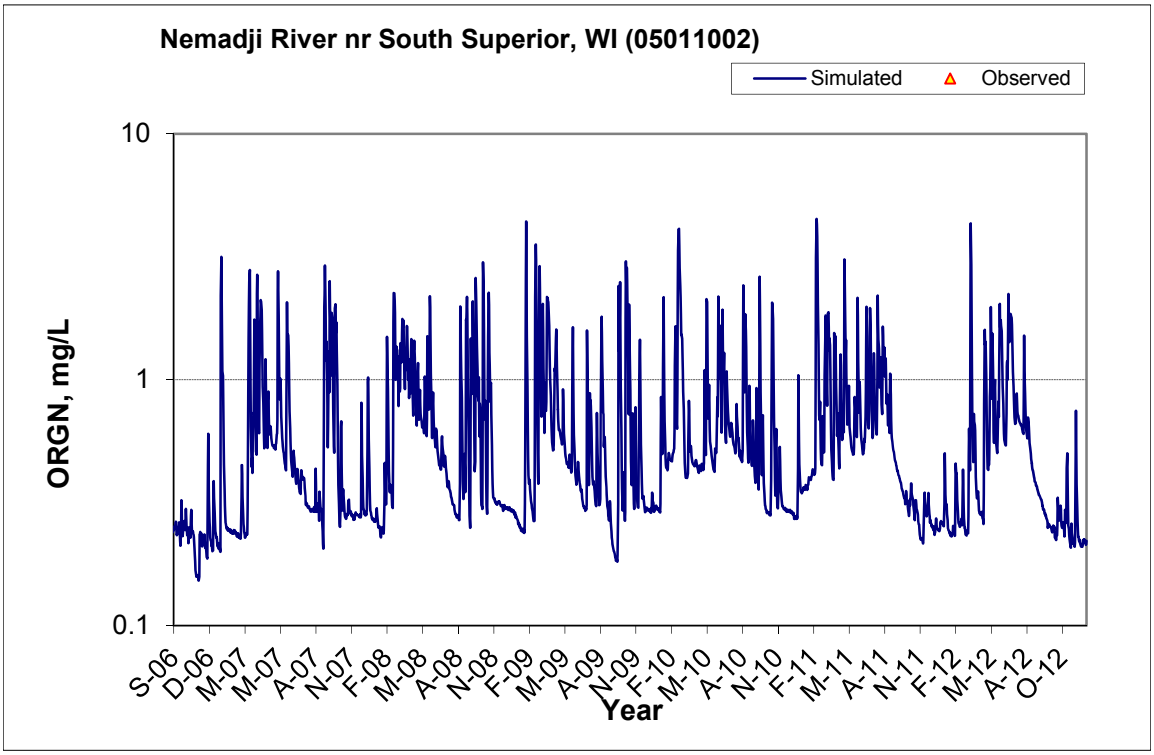

Figure B-174. Time series of observed and simulated Organic Nitrogen (OrgN) concentration at Nemadji River nr South Superior, WI (05011002)

B.6.3 Total Kjeldahl Nitrogen (TKN)

Table B-30. Total Kjeldahl Nitrogen (TKN) statistics

Period	1994-2007	2008-2012
Count	ND	100
Concentration Average Error		0.05%
Concentration Median Error		-3.23%
Load Average Error		-24.43%
Load Median Error		-1.17%
Paired t conc		1.00
Paired t load		0.42

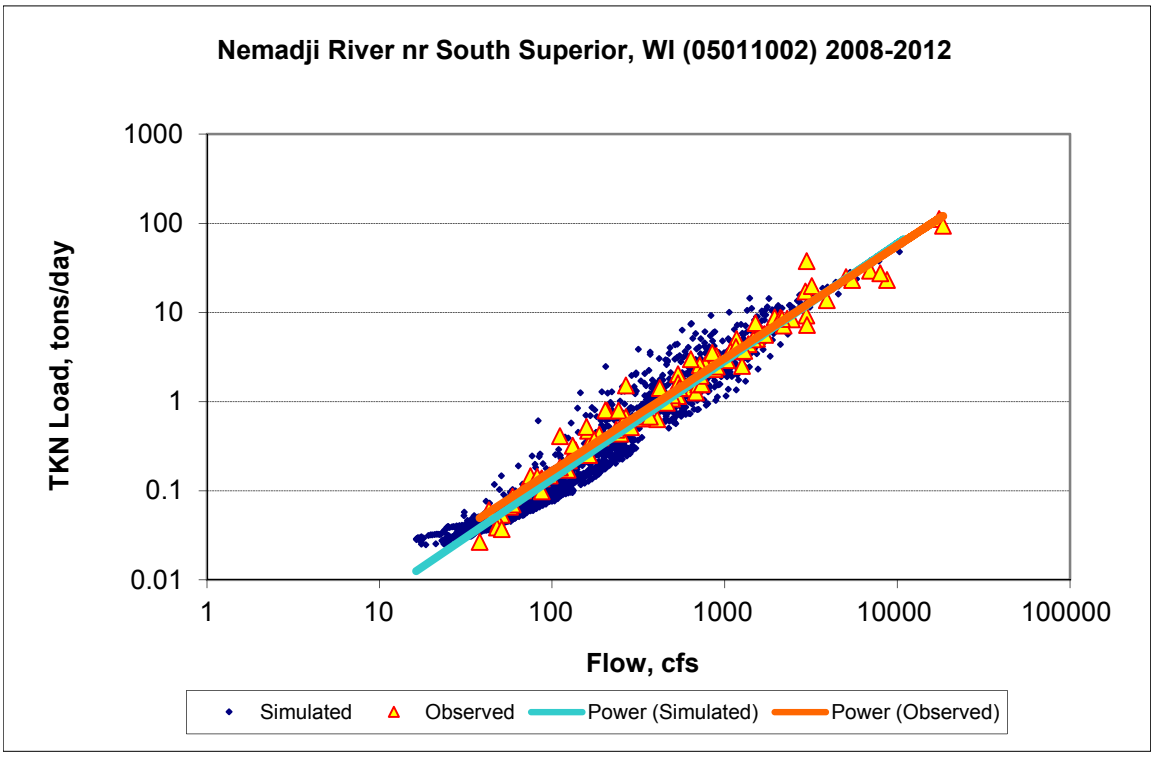

Figure B-175. Power plot of simulated and observed Total Kjeldahl Nitrogen (TKN) load vs flow at Nemadji River nr South Superior, WI (05011002) (calibration period)

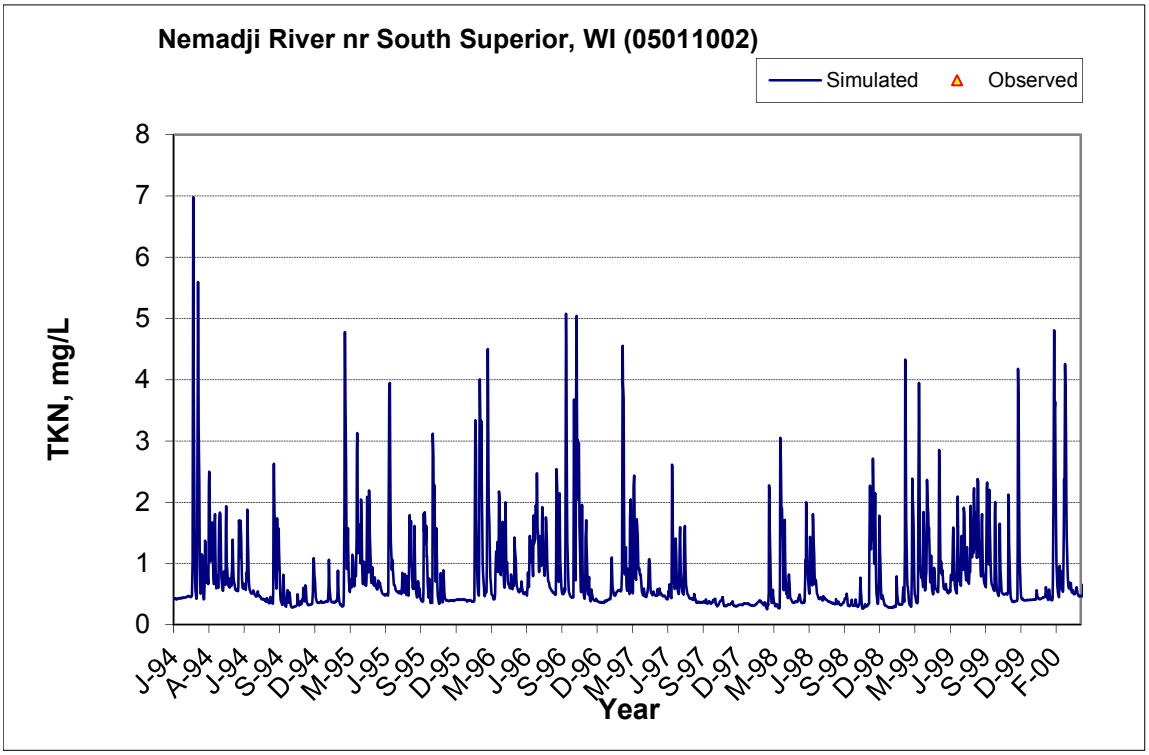

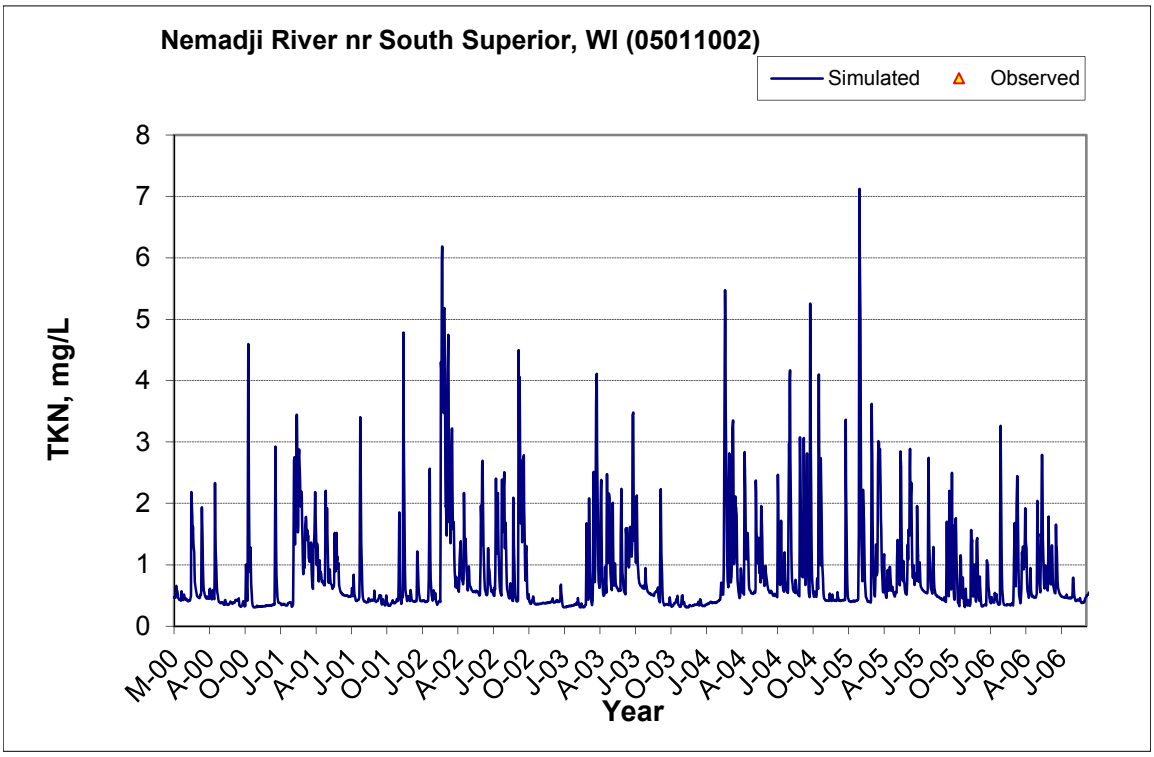

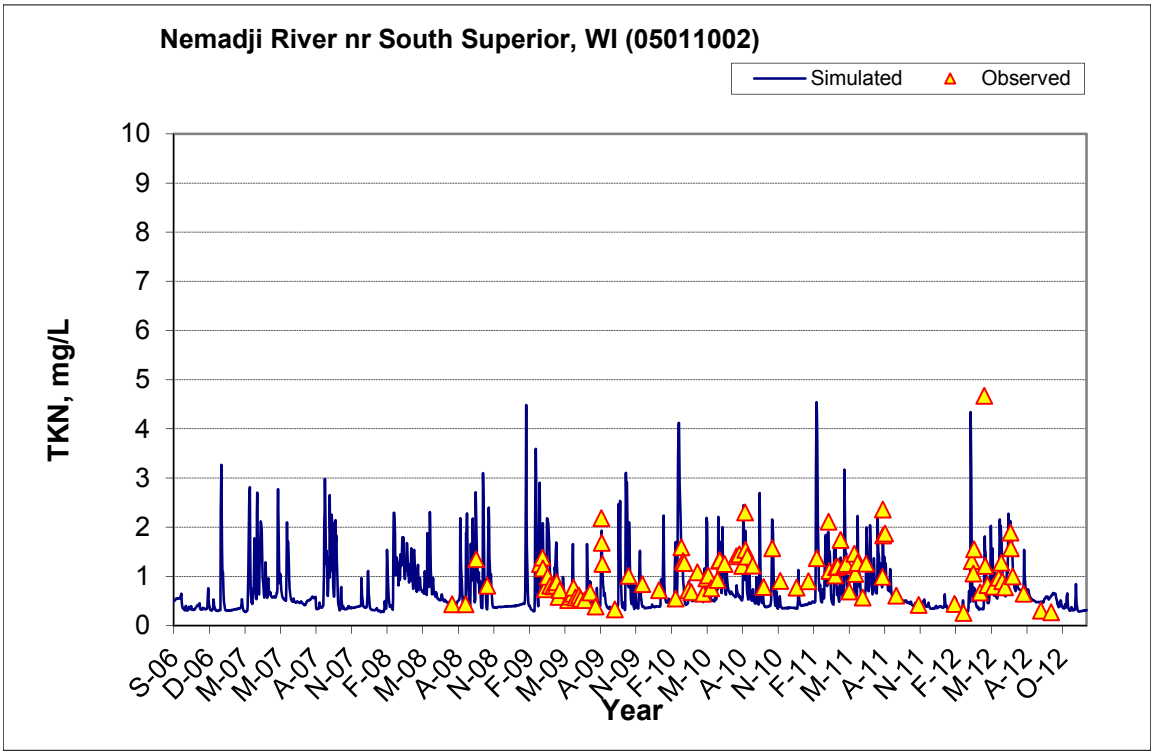

Figure B-176. Time series of observed and simulated Total Kjeldahl Nitrogen (TKN) concentration at Nemadji River nr South Superior, WI (05011002)

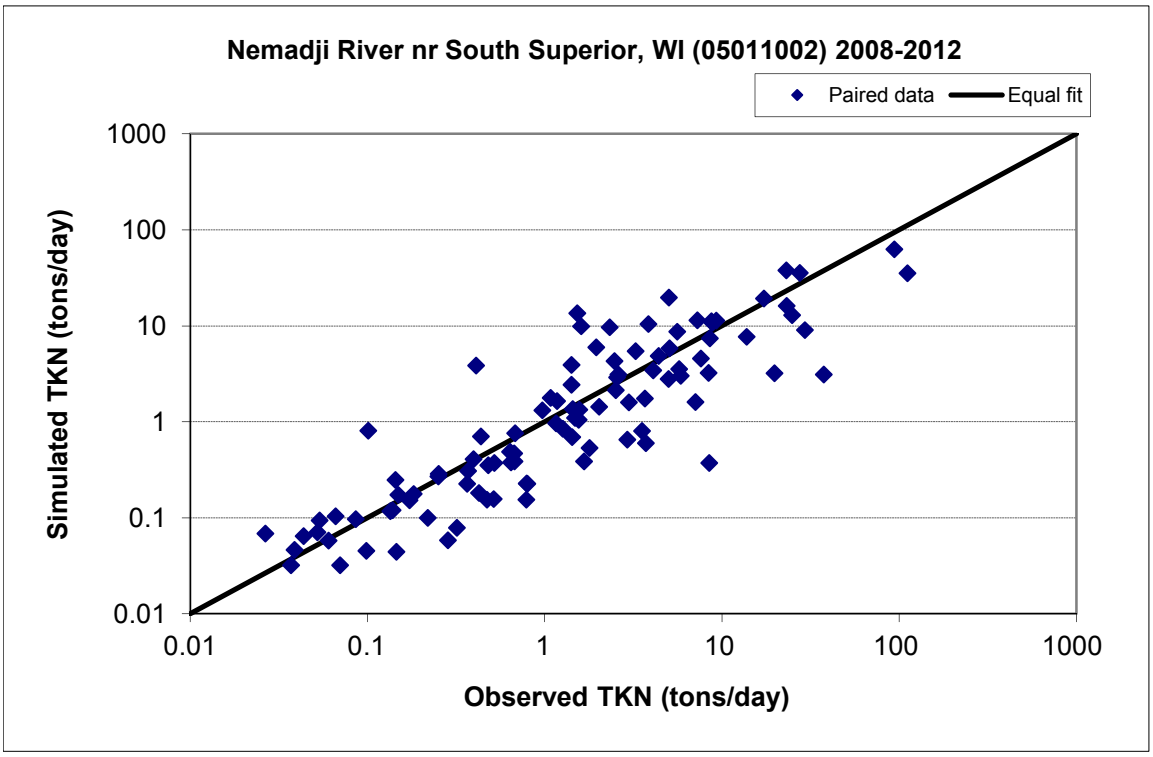

Figure B-177. Paired simulated vs. observed Total Kjeldahl Nitrogen (TKN) load at Nemadji River nr South Superior, WI (05011002) (calibration period)

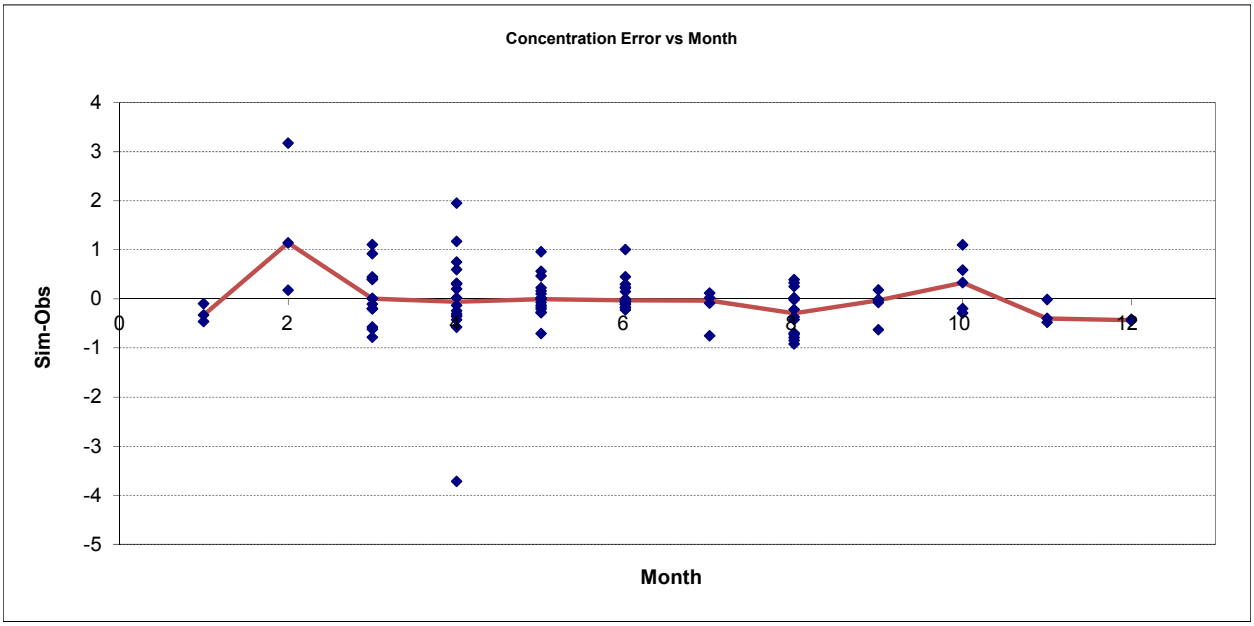

Figure B-178. Residual (Simulated - Observed) vs. Month Total Kjeldahl Nitrogen (TKN) at Nemadji River nr South Superior, WI (05011002)

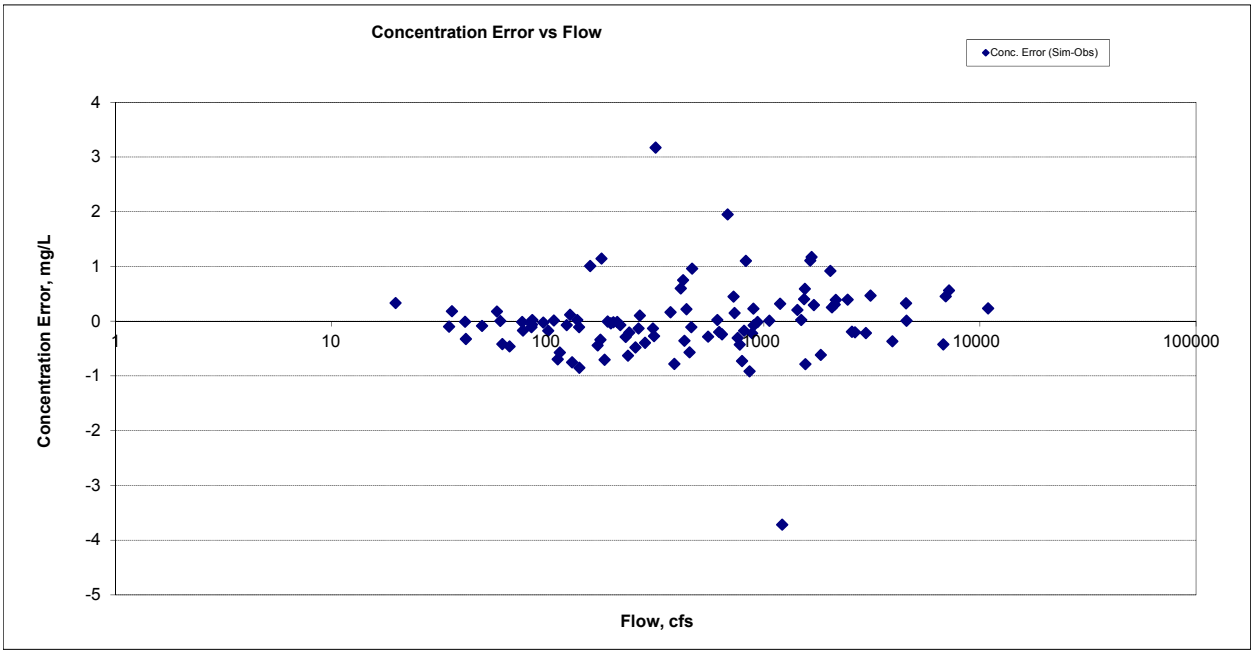

Figure B-179. Residual (Simulated - Observed) vs. Flow Total Kjeldahl Nitrogen (TKN) at Nemadji River nr South Superior, WI (05011002)

B.6.4 Nitrite+ Nitrate Nitrogen (NOx)

Table B-31. Nitrite+ Nitrate Nitrogen (NOx) statistics

Period	1994-2007	2008-2012
Count	ND	100
Concentration Average Error		-6.99%
Concentration Median Error		-9.00%
Load Average Error		30.40%
Load Median Error		-2.57%
Paired t conc		0.94
Paired t load		0.35

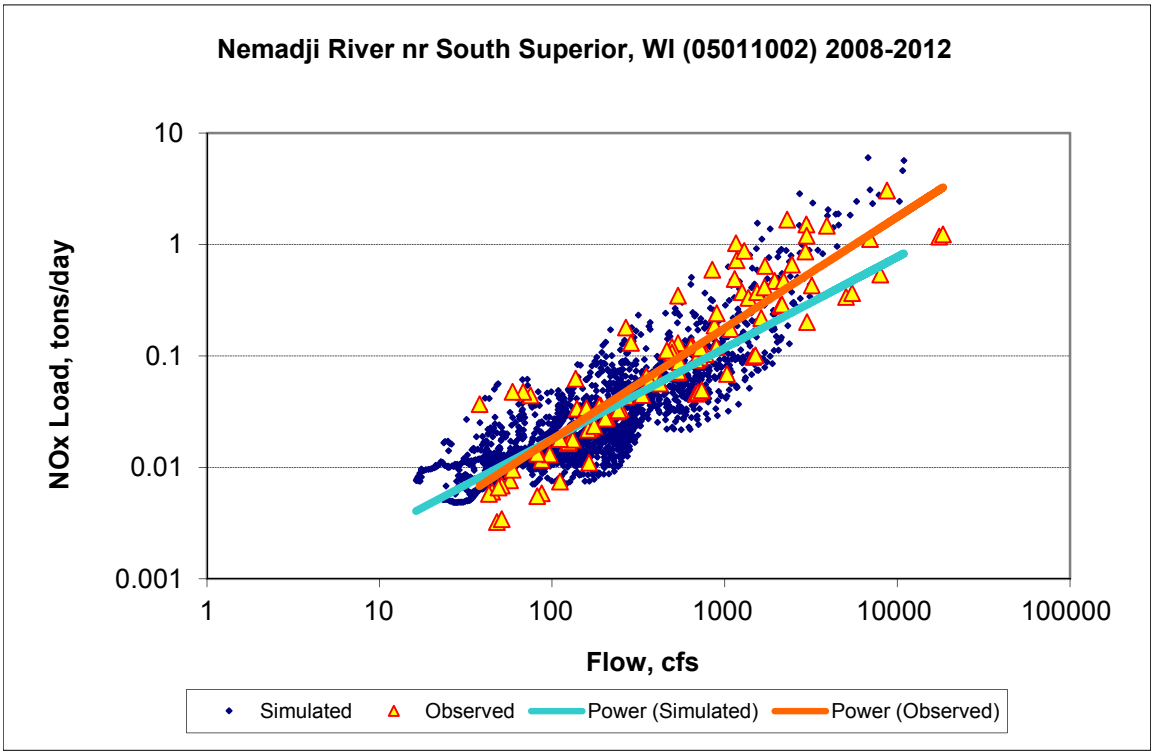

Figure B-180. Power plot of simulated and observed Nitrite+ Nitrate Nitrogen (NOx) load vs flow at Nemadji River nr South Superior, WI (05011002) (calibration period)

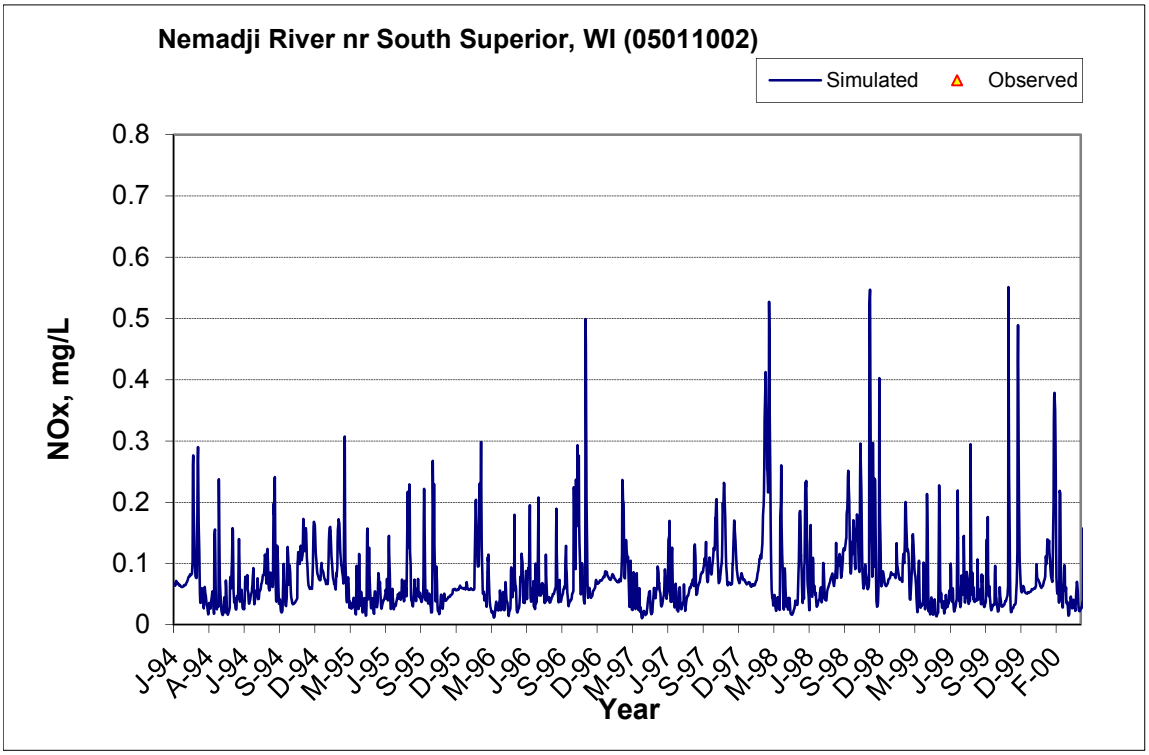

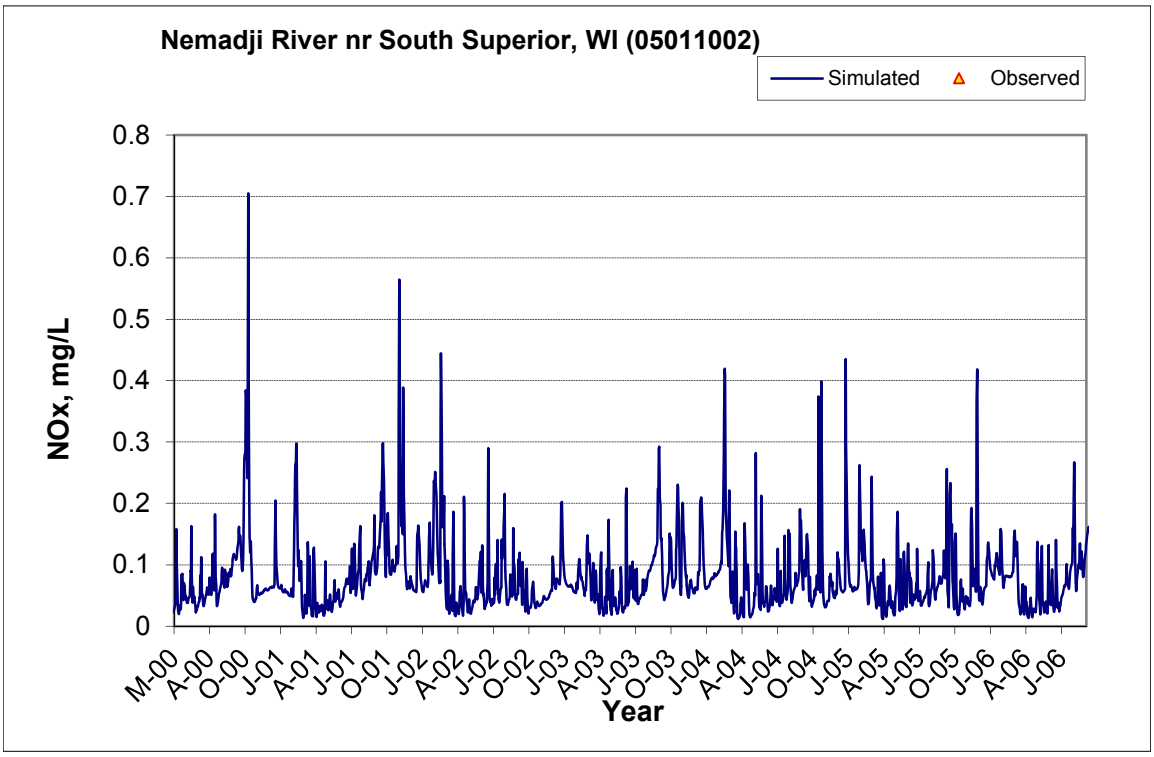

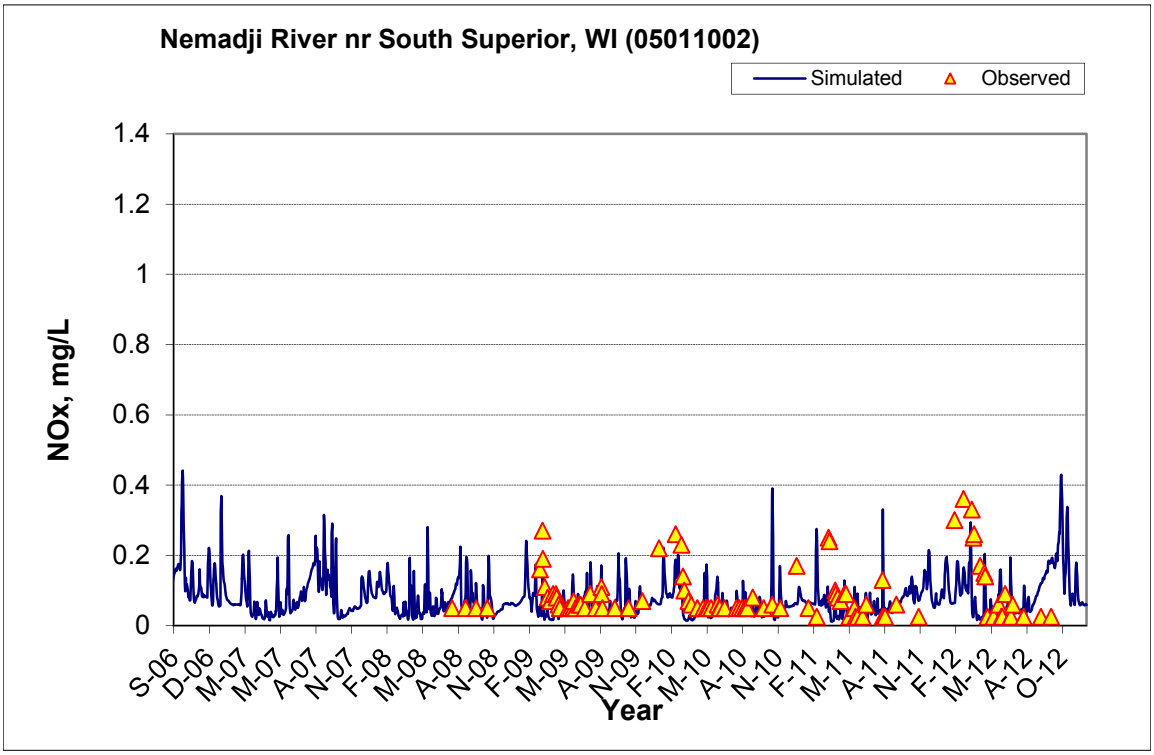

Figure B-181. Time series of observed and simulated Nitrite+ Nitrate Nitrogen (NOx) concentration at Nemadji River nr South Superior, WI (05011002)

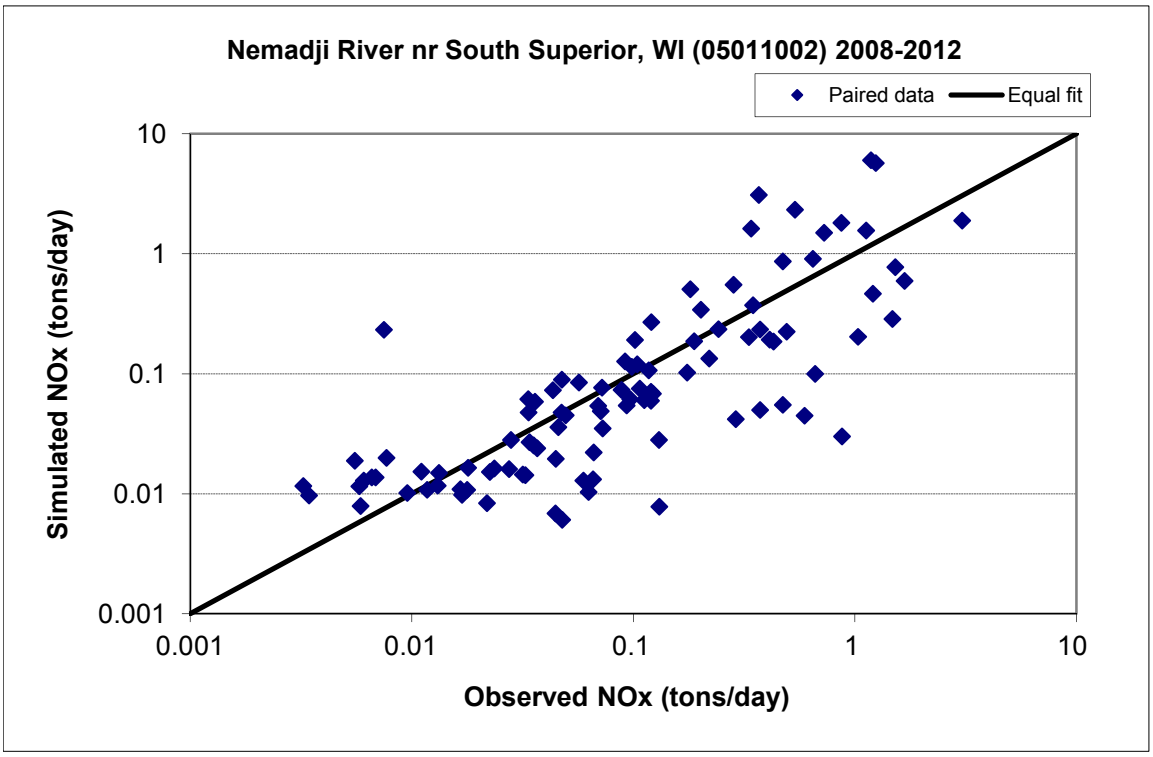

Figure B-182. Paired simulated vs. observed Nitrite+ Nitrate Nitrogen (NOx) load at Nemadji River nr South Superior, WI (05011002) (calibration period)

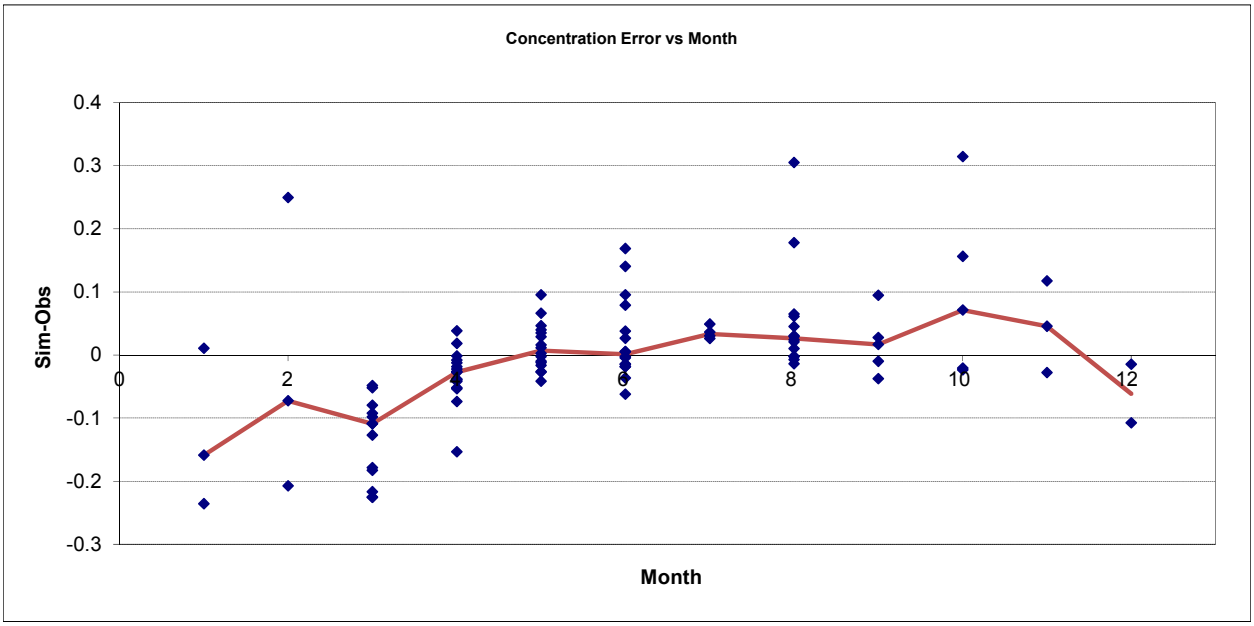

Figure B-183. Residual (Simulated - Observed) vs. Month Nitrite+ Nitrate Nitrogen (NOx) at Nemadji River nr South Superior, WI (05011002)

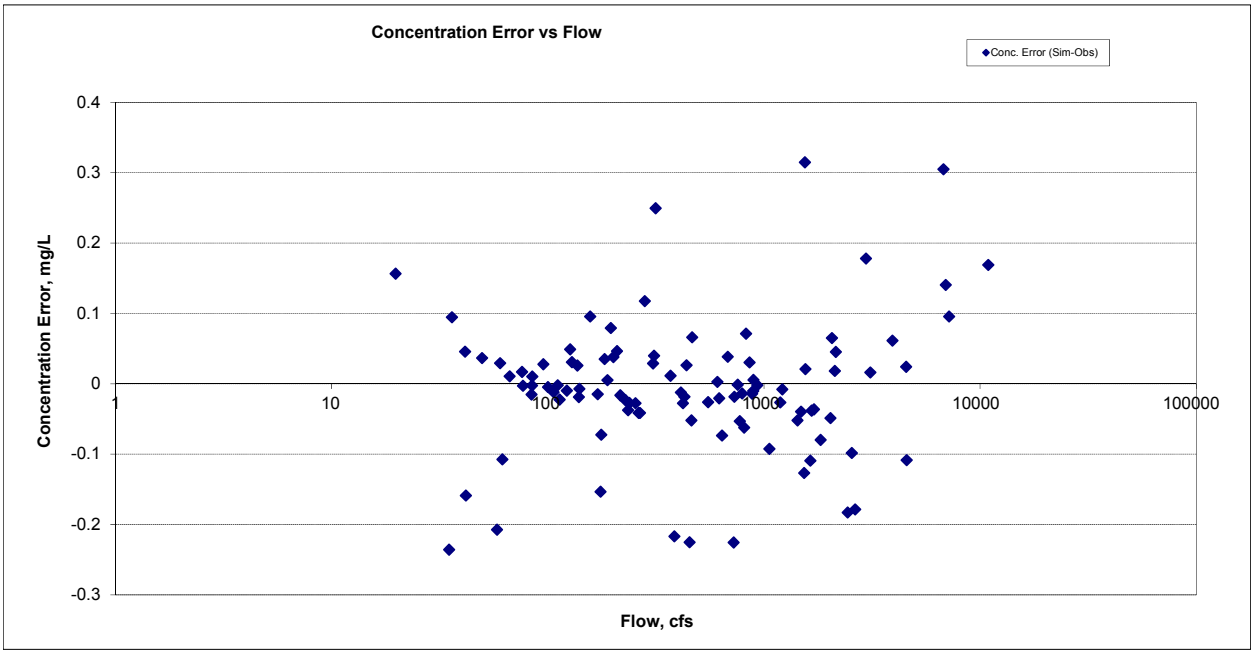

Figure B-184. Residual (Simulated - Observed) vs. Flow Nitrite+ Nitrate Nitrogen (NOx) at Nemadji River nr South Superior, WI (05011002)

B.6.5 Total Nitrogen (TN)

Table B-32. Total Nitrogen (TN) statistics

Period	1994-2007	2008-2012
Count	ND	100
Concentration Average Error		-0.78%
Concentration Median Error		-5.07%
Load Average Error		-22.56%
Load Median Error		-1.42%
Paired t conc		1.00
Paired t load		0.45

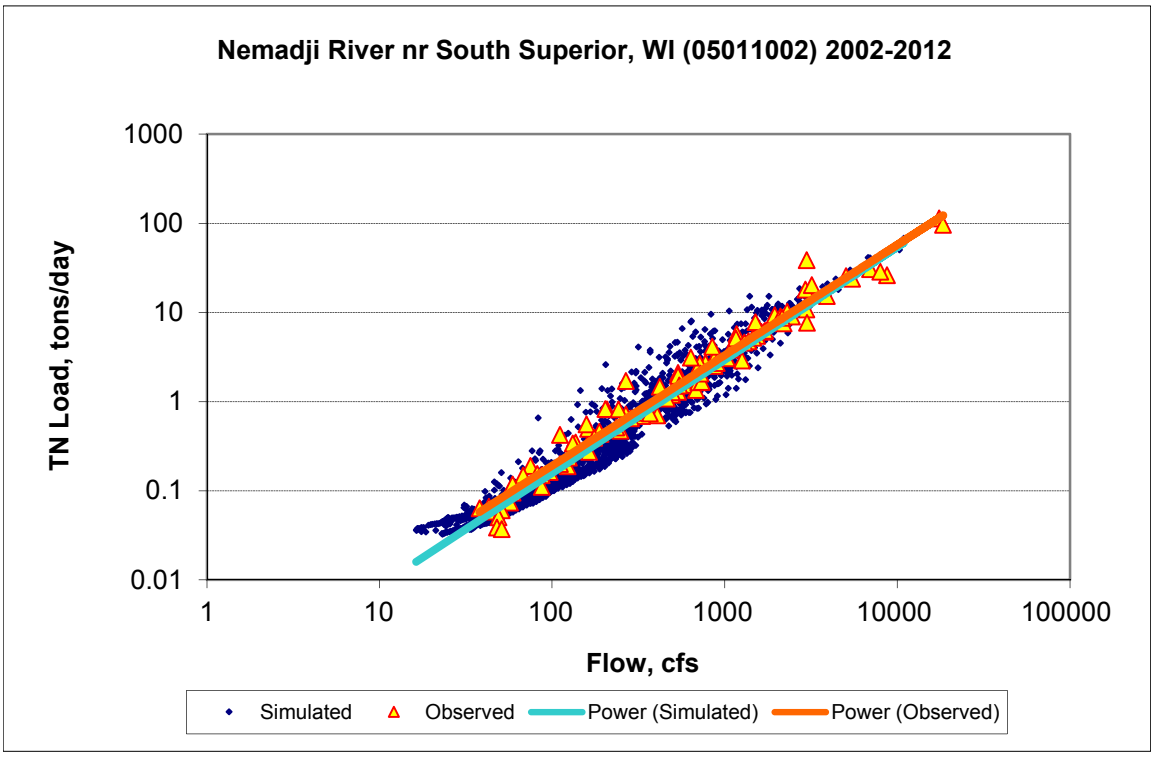

Figure B-185. Power plot of simulated and observed Total Nitrogen (TN) load vs flow at Nemadji River nr South Superior, WI (05011002) (calibration period)

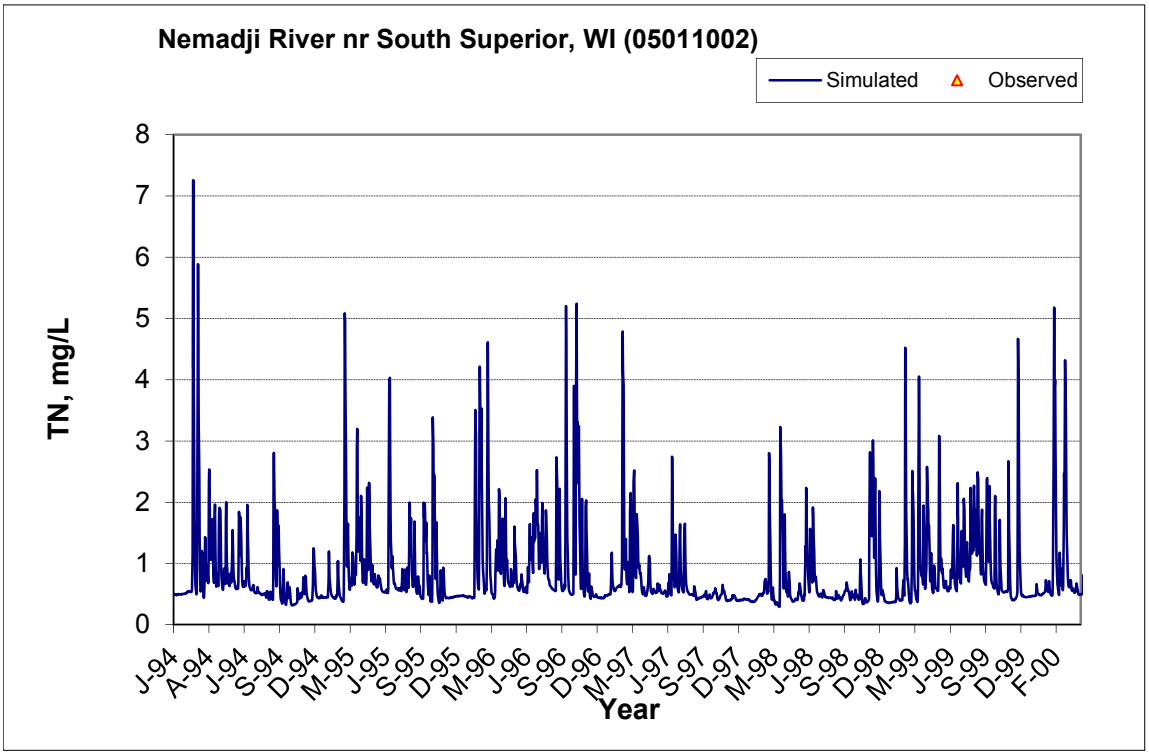

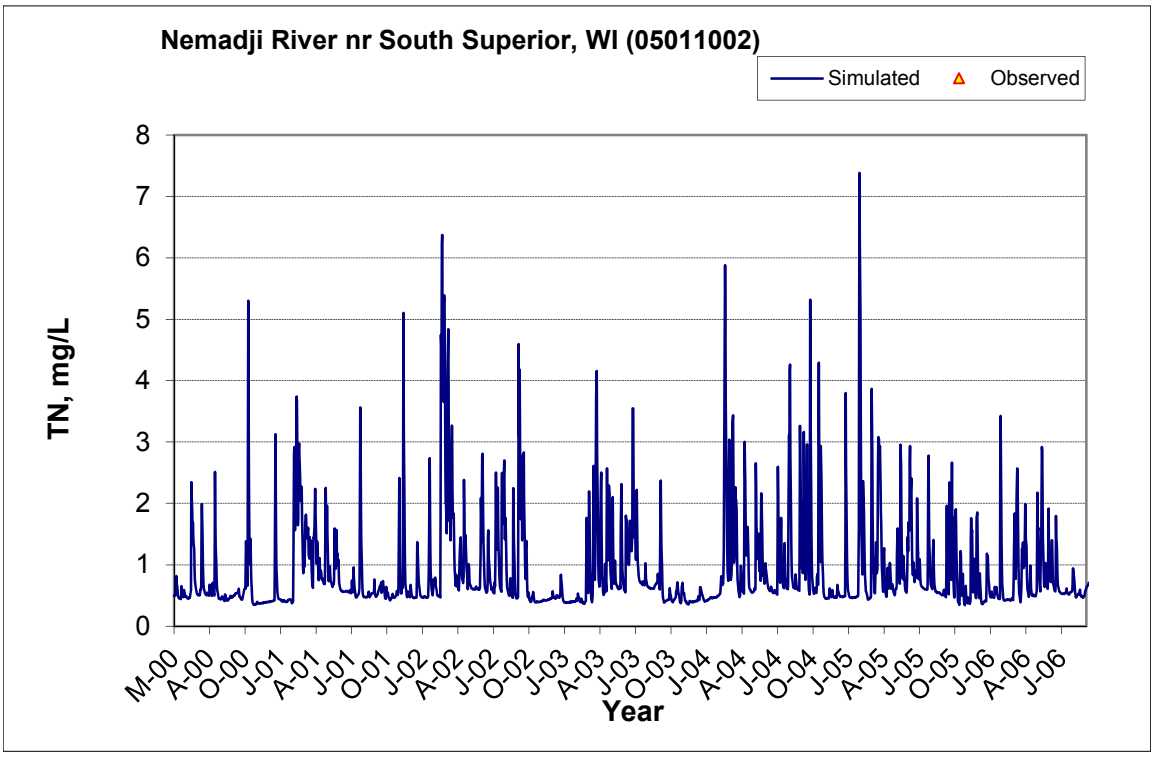

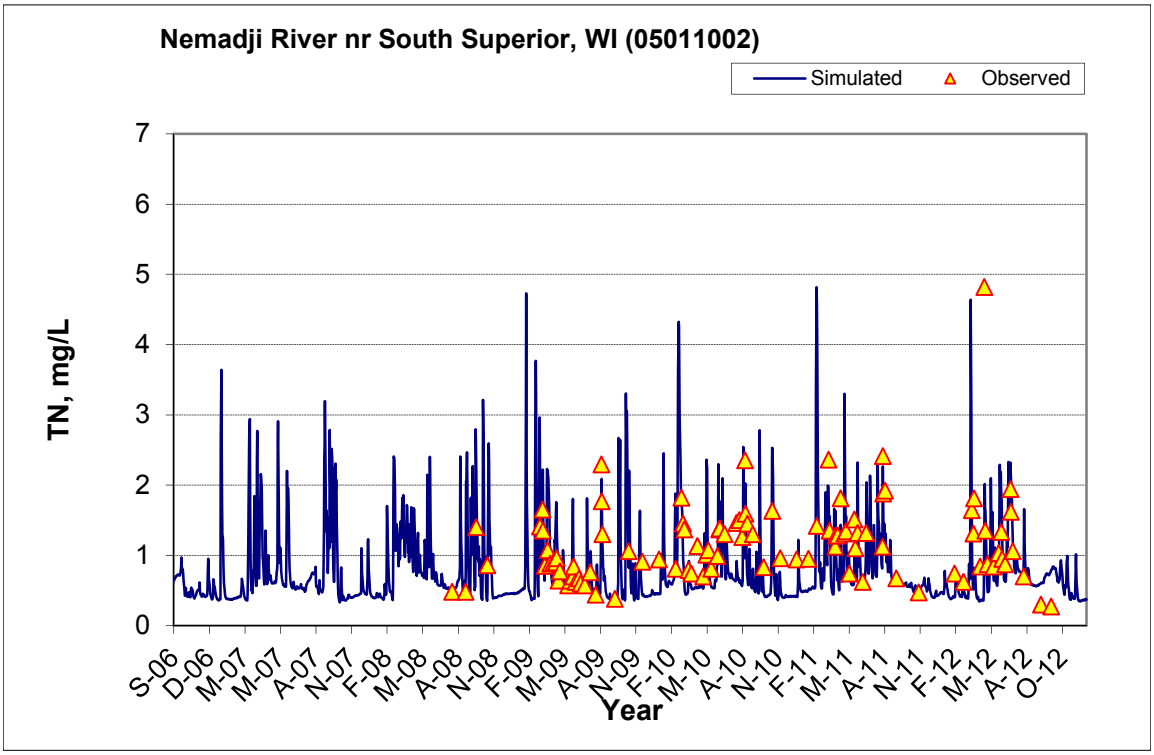

Figure B-186. Time series of observed and simulated Total Nitrogen (TN) concentration at Nemadji River nr South Superior, WI (05011002)

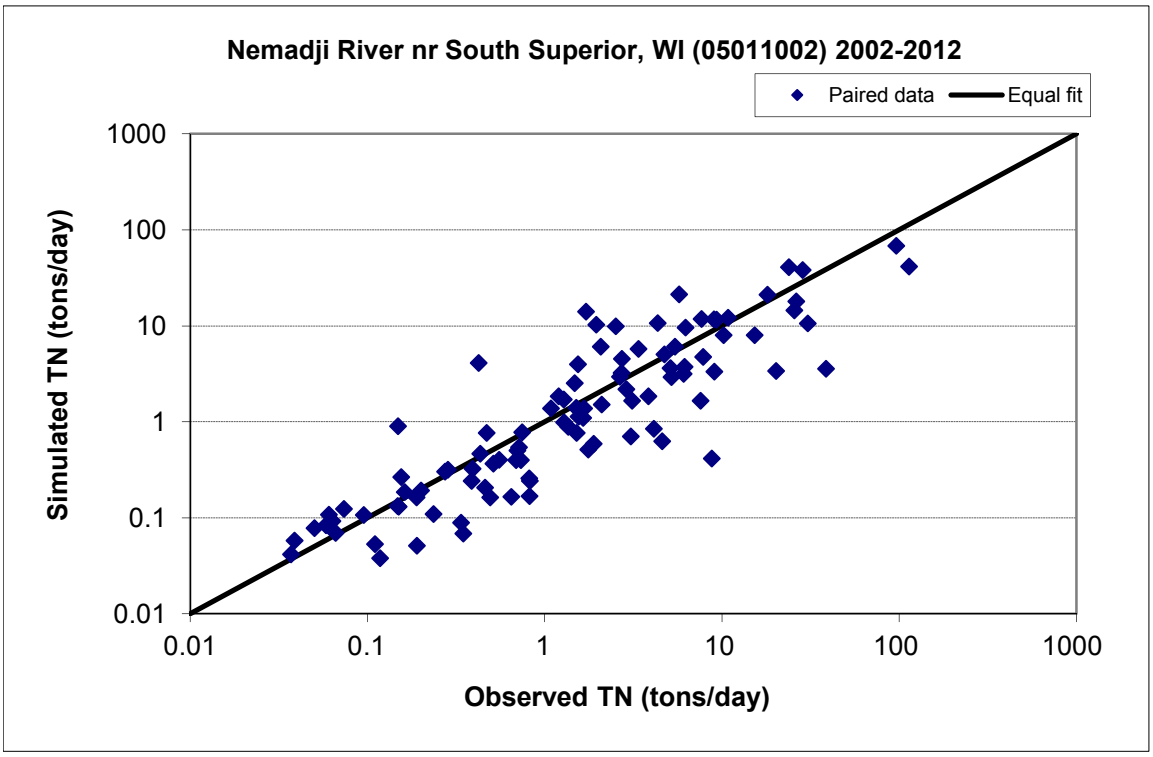

Figure B-187. Paired simulated vs. observed Total Nitrogen (TN) load at Nemadji River nr South Superior, WI (05011002) (calibration period)

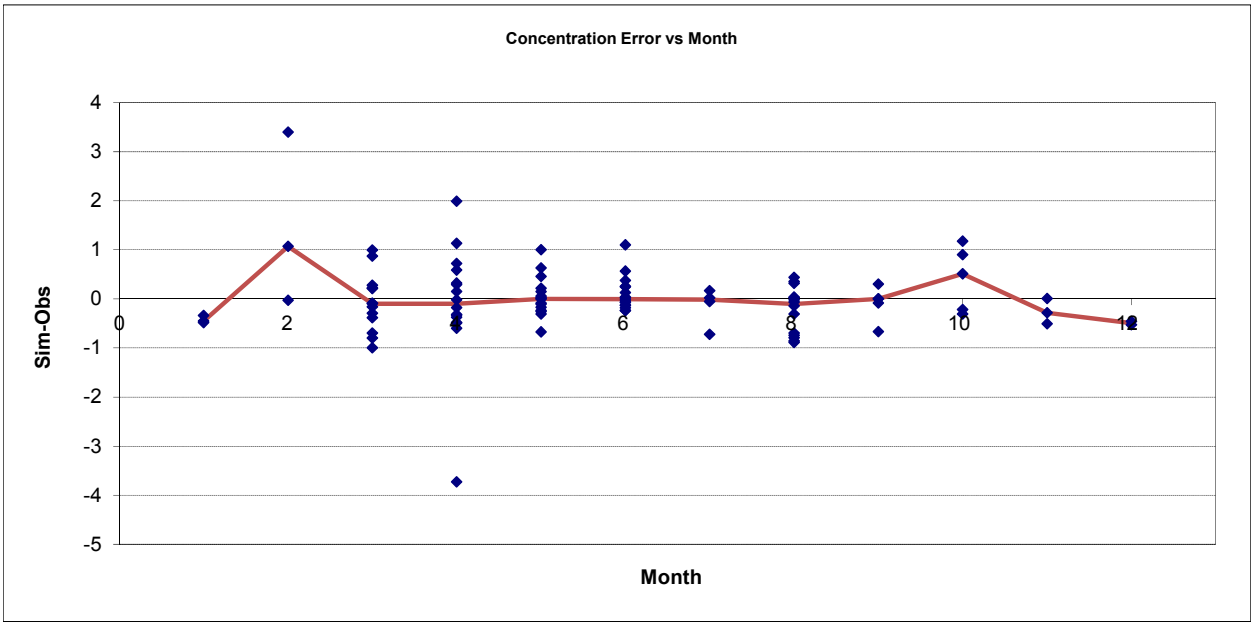

Figure B-188. Residual (Simulated - Observed) vs. Month Total Nitrogen (TN) at Nemadji River nr South Superior, WI (05011002)

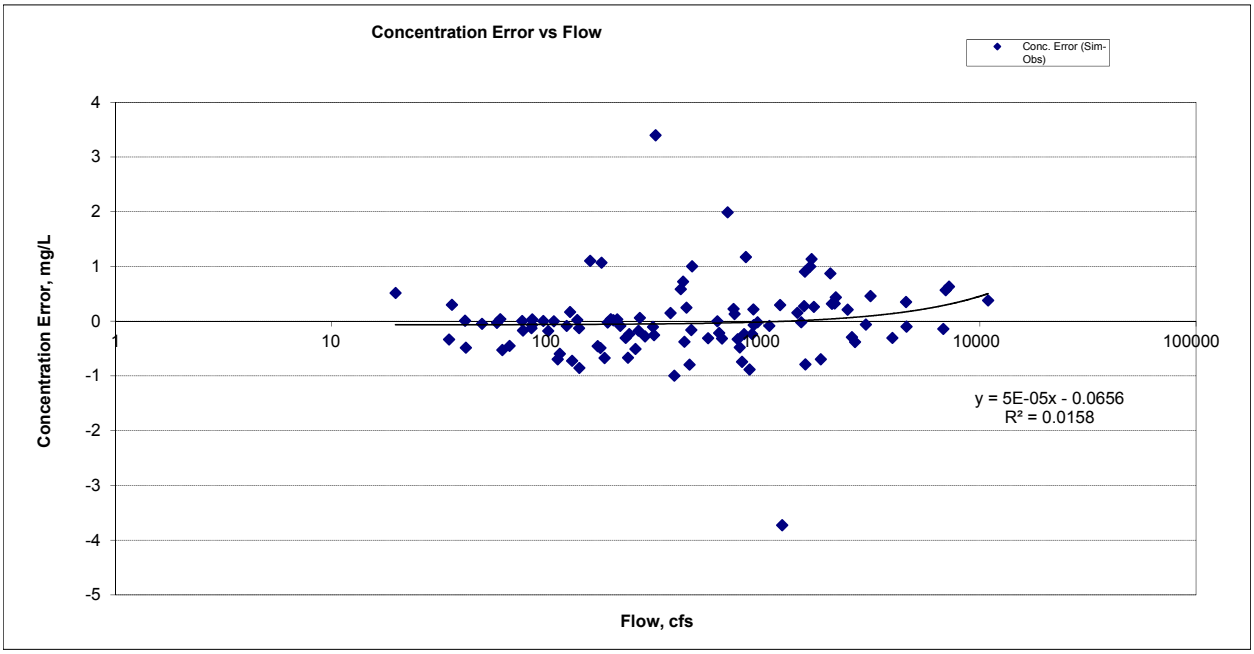

Figure B-189. Residual (Simulated - Observed) vs. Flow Total Nitrogen (TN) at Nemadji River nr South Superior, WI (05011002)

B.6.6 Soluble Reactive Phosphorus (SRP)

Table B-33. Soluble Reactive Phosphorus (SRP) statistics

Period	1994-2007	2008-2012
Count	ND	96
Concentration Average Error		0.10%
Concentration Median Error		1.26%
Load Average Error		-44.48%
Load Median Error		-0.03%
Paired t conc		0.88
Paired t load		0.22

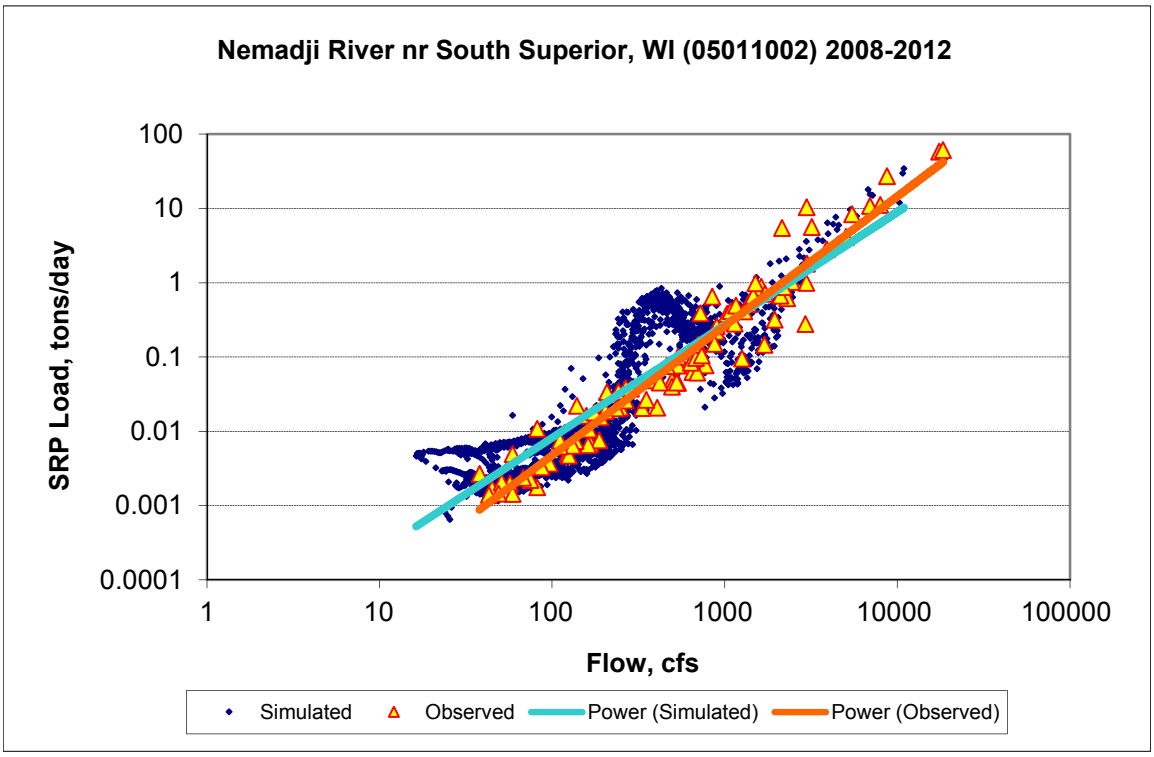

Figure B-190. Power plot of simulated and observed Soluble Reactive Phosphorus (SRP) load vs flow at Nemadji River nr South Superior, WI (05011002) (calibration period)

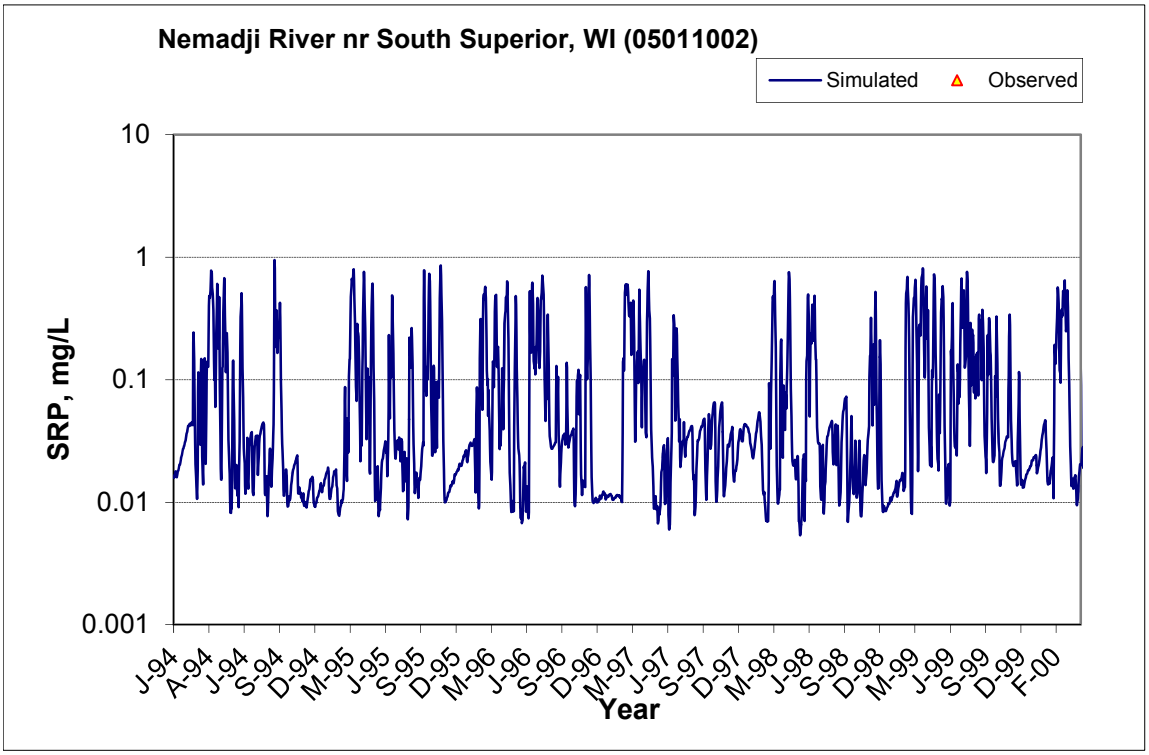

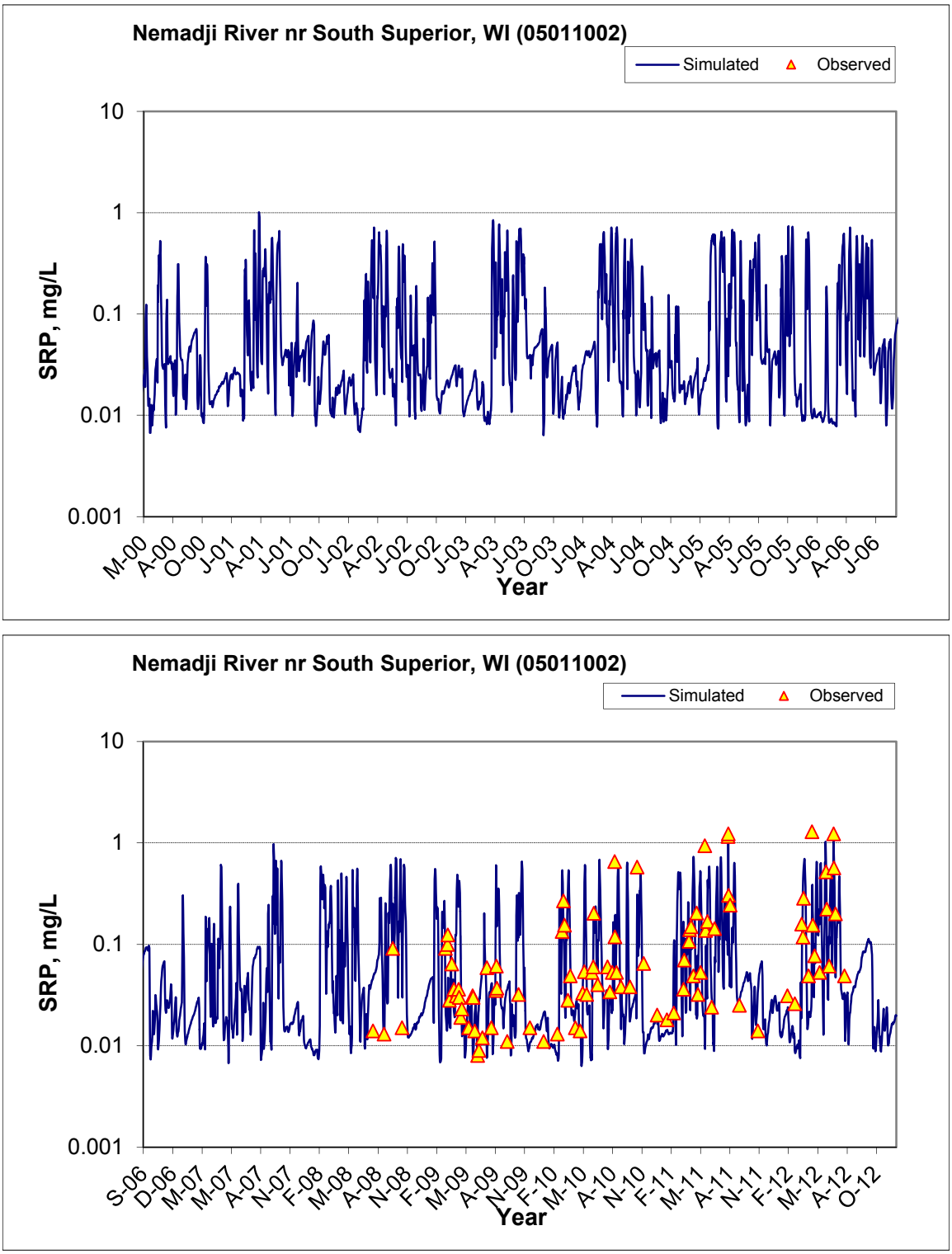

Figure B-191. Time series of observed and simulated Soluble Reactive Phosphorus (SRP) concentration at Nemadji River nr South Superior, WI (05011002)

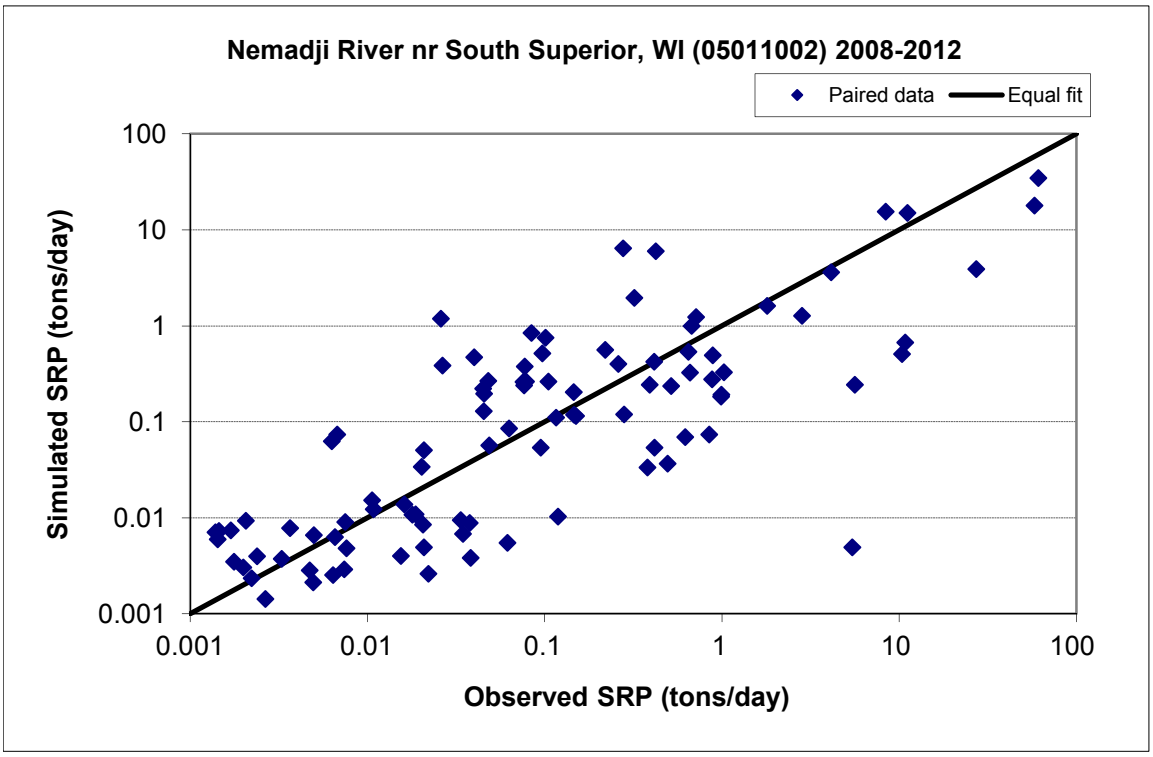

Figure B-192. Paired simulated vs. observed Soluble Reactive Phosphorus (SRP) load at Nemadji River nr South Superior, WI (05011002) (calibration period)

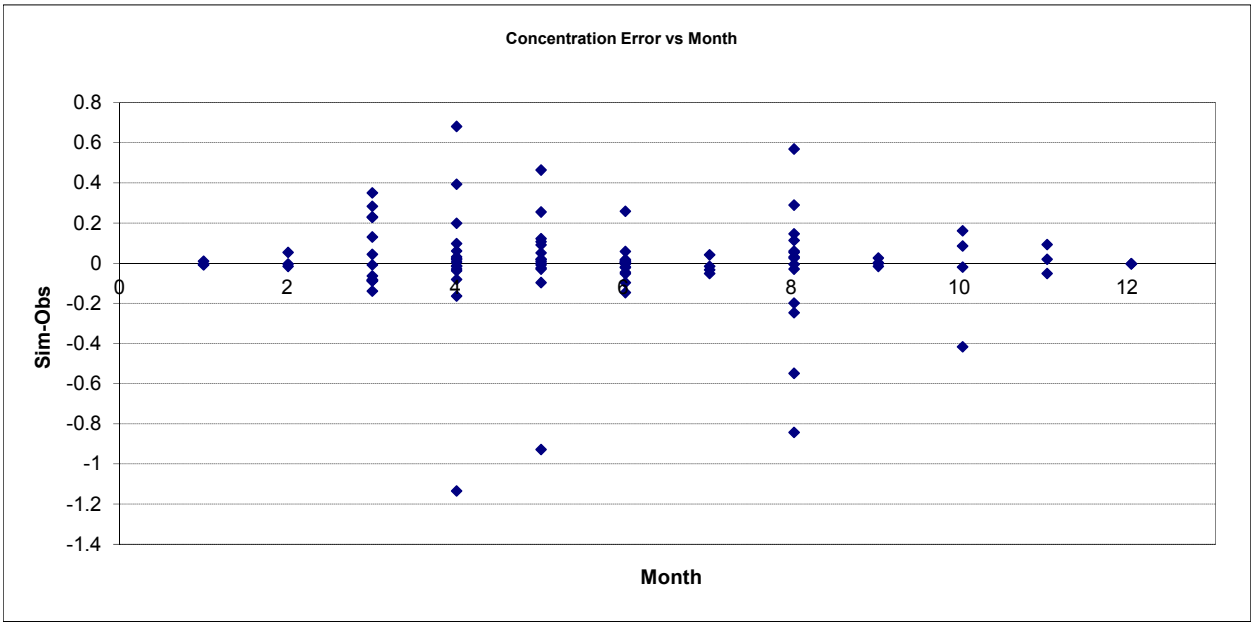

Figure B-193. Residual (Simulated - Observed) vs. Month Soluble Reactive Phosphorus (SRP) at Nemadji River nr South Superior, WI (05011002)

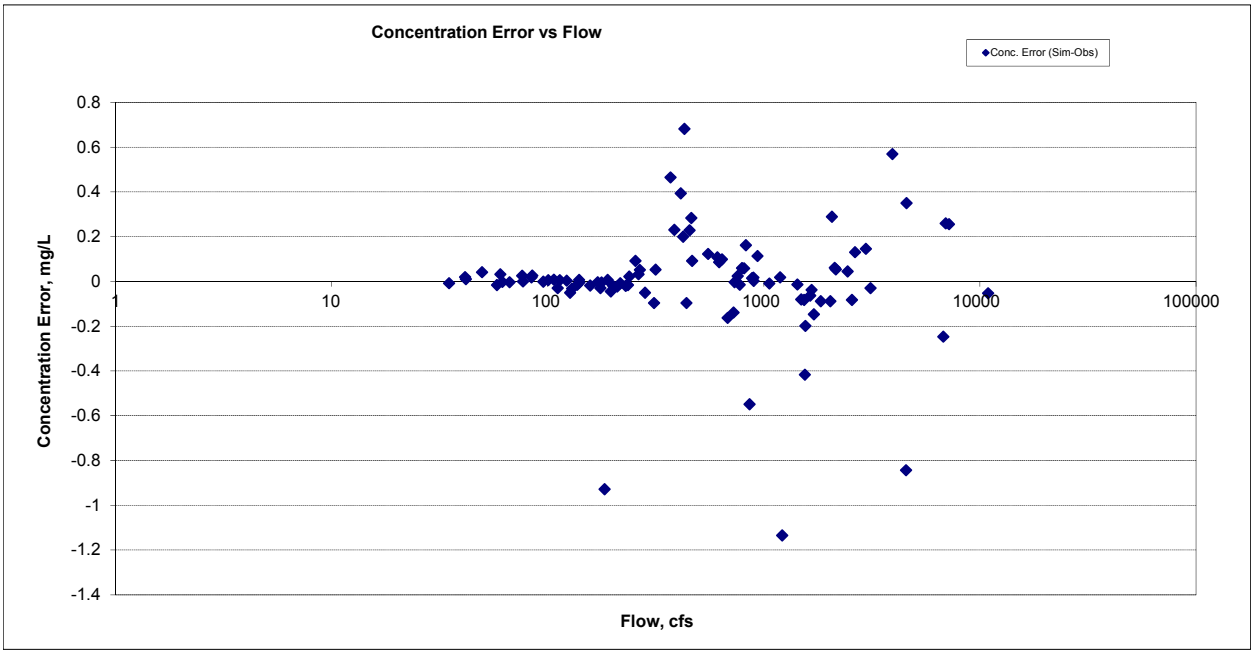

Figure B-194. Residual (Simulated - Observed) vs. Flow Soluble Reactive Phosphorus (SRP) at Nemadji River nr South Superior, WI (05011002)

B.6.7 Organic Phosphorus (OrgP)

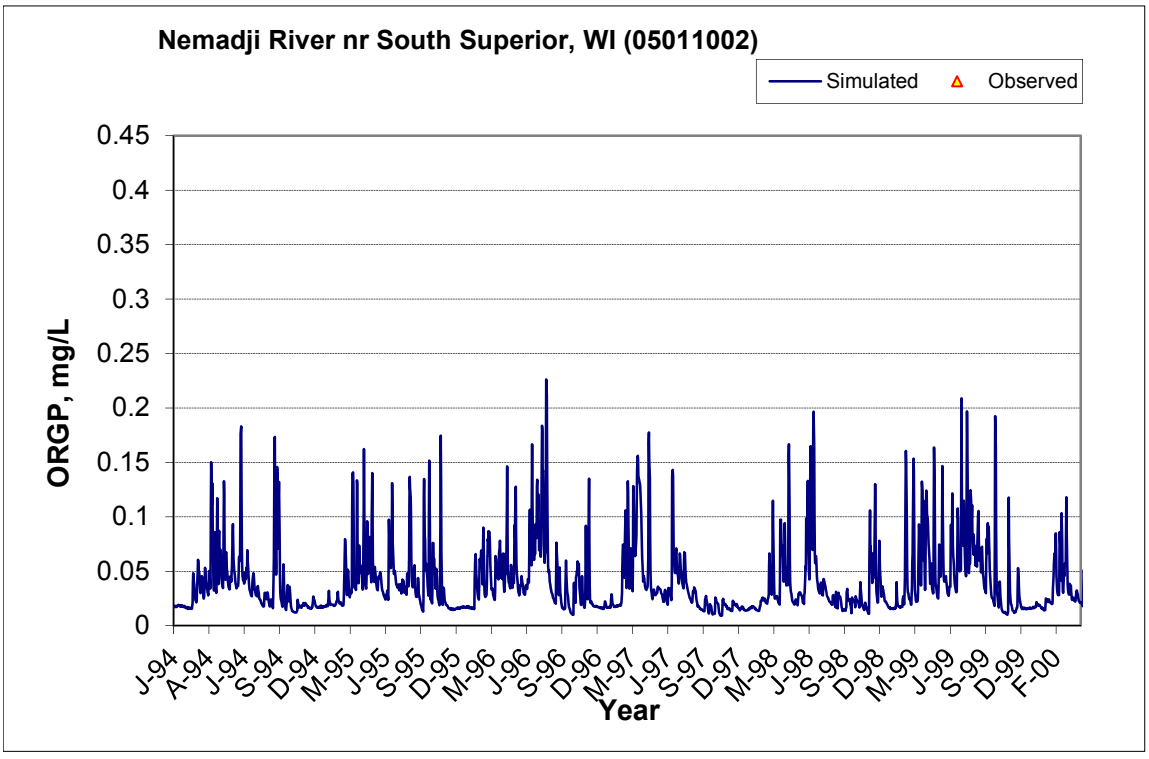

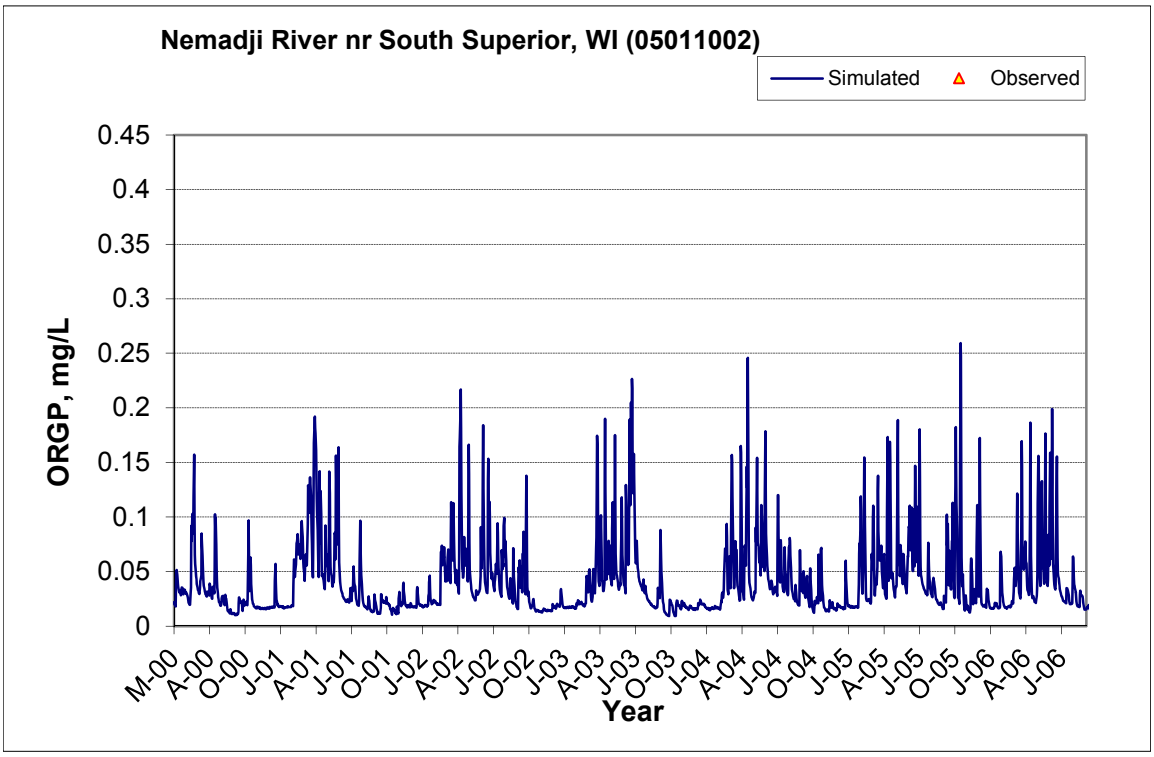

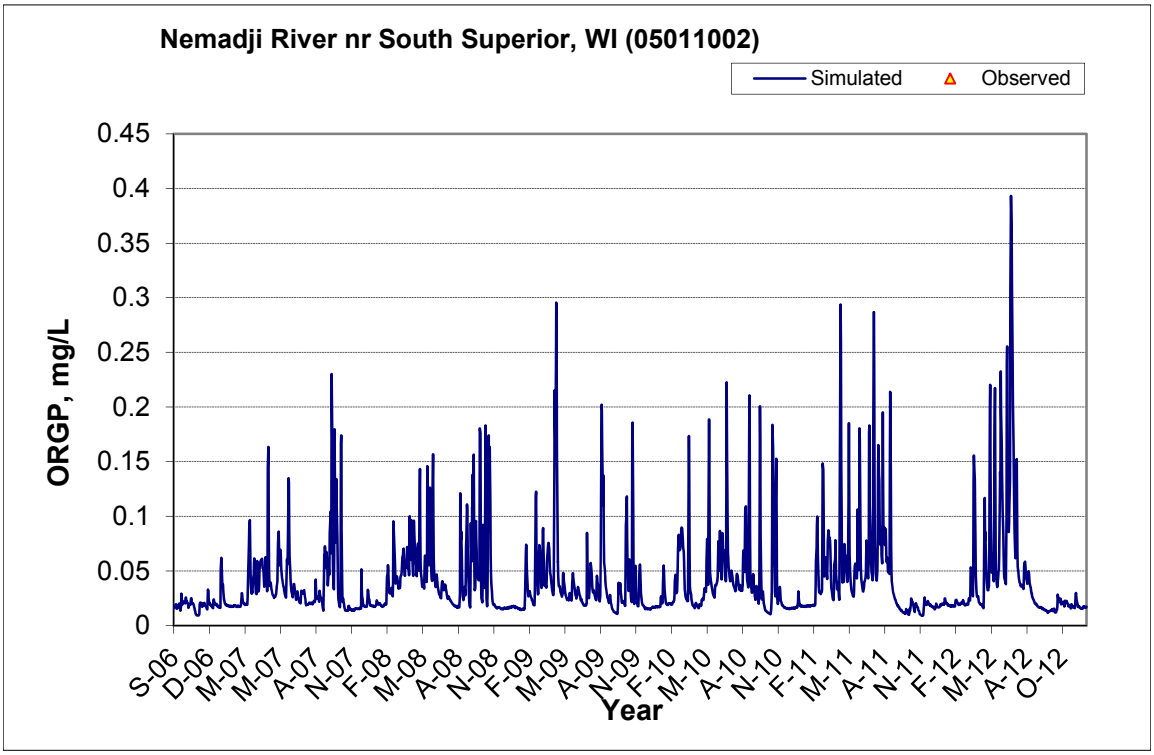

Figure B-195. Time series of observed and simulated Organic Phosphorus (OrgP) concentration at Nemadji River nr South Superior, WI (05011002)

B.6.8 Total Phosphorus (TP)

Table B-34. Total Phosphorus (TP) statistics

Period	1994-2007	2008-2012
Count	ND	97
Concentration Average Error		31.15%
Concentration Median Error		10.75%
Load Average Error		-5.04%
Load Median Error		0.35%
Paired t conc		0.25
Paired t load		0.68

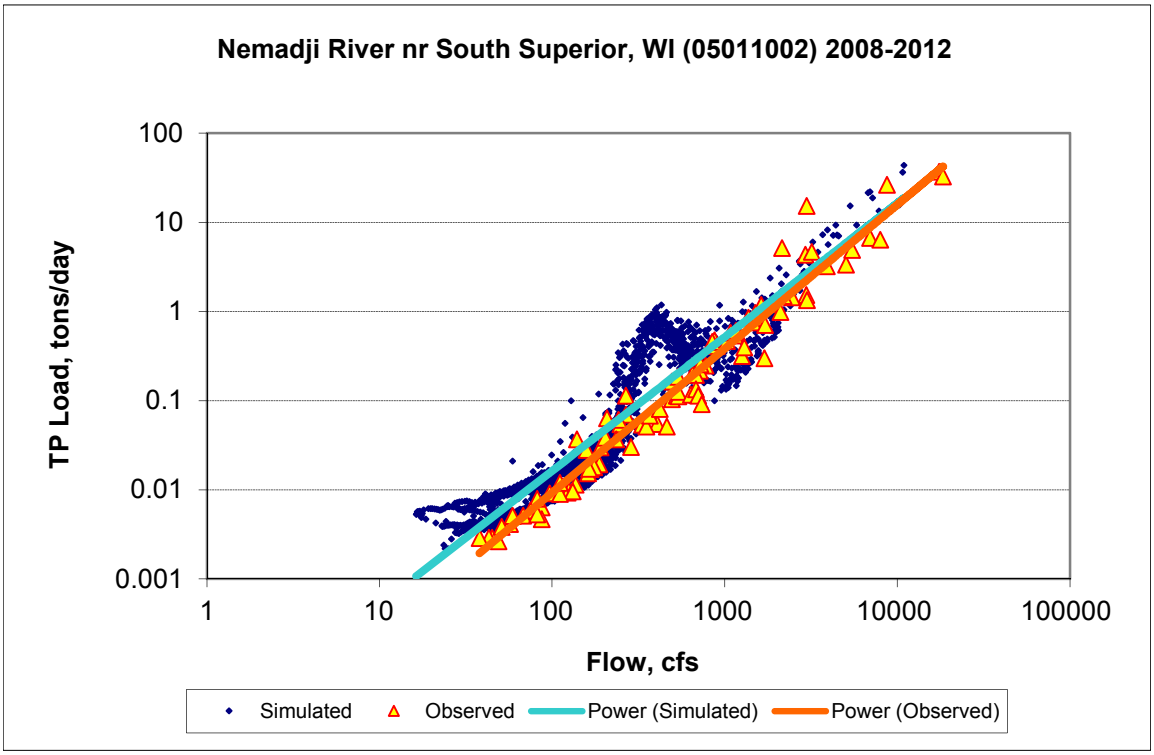

Figure B-196. Power plot of simulated and observed Total Phosphorus (TP) load vs flow at Nemadji River nr South Superior, WI (05011002) (calibration period)

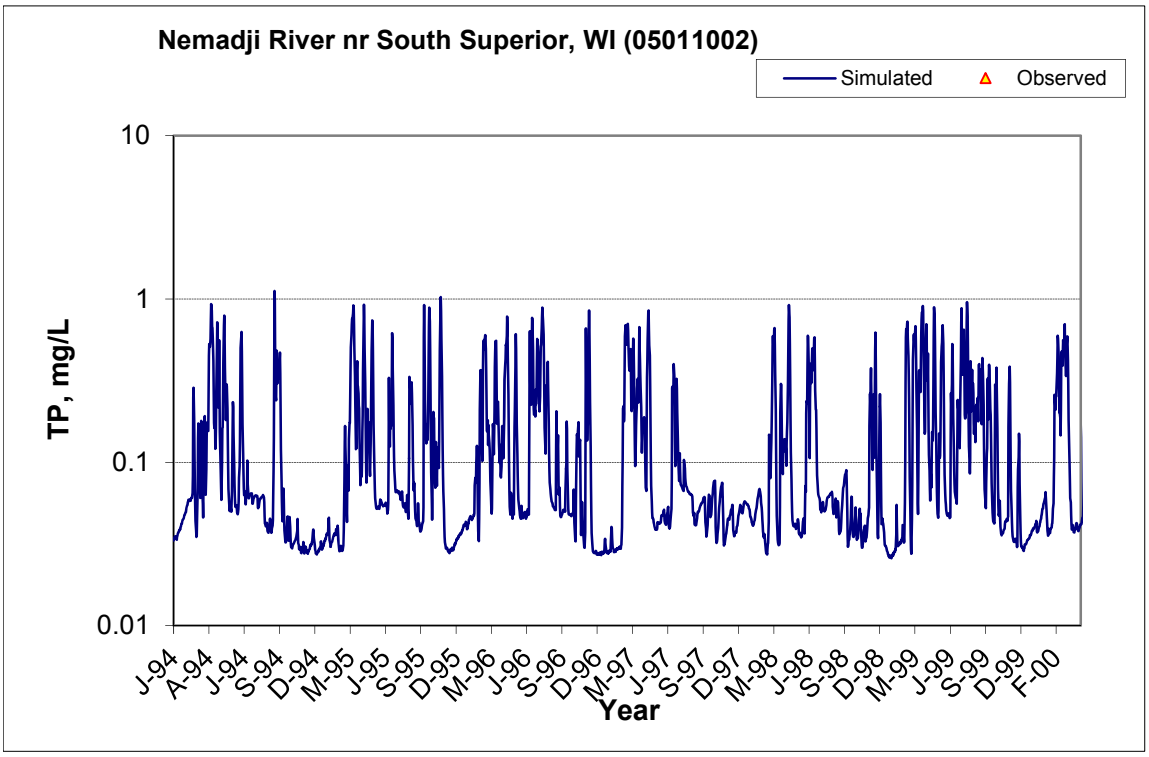
Nemadji River nr South Superior, WI (05011002)
Simulated
Observed
TP, mg/L
10
1
0.1
0.01
J-94 A-94 J-94 S-94 D-94 M-95 J-95 S-95 D-95 M-96 J-96 S-96 D-96 M-97 J-97 S-97 D-97 M-98 J-98 S-98 D-98 M-99 J-99 S-99 D-99 F-00
Year

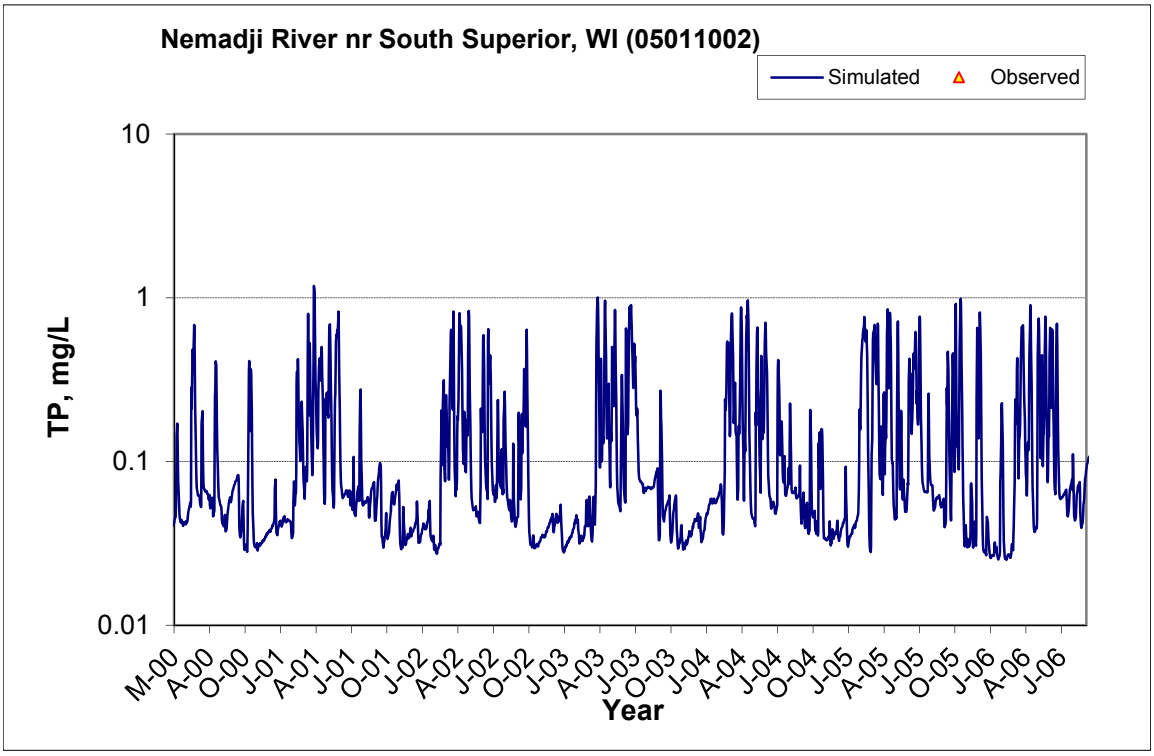
Nemadji River nr South Superior, WI (05011002)
Simulated
Observed
TP, mg/L
10
1
0.1
0.01
M-00 A-00 O-00 J-01 A-01 J-01 O-01 J-02 A-02 J-02 O-02 J-03 A-03 J-03 O-03 J-04 A-04 J-04 O-04 J-05 A-05 J-05 O-05 J-06 A-06 J-06
Year

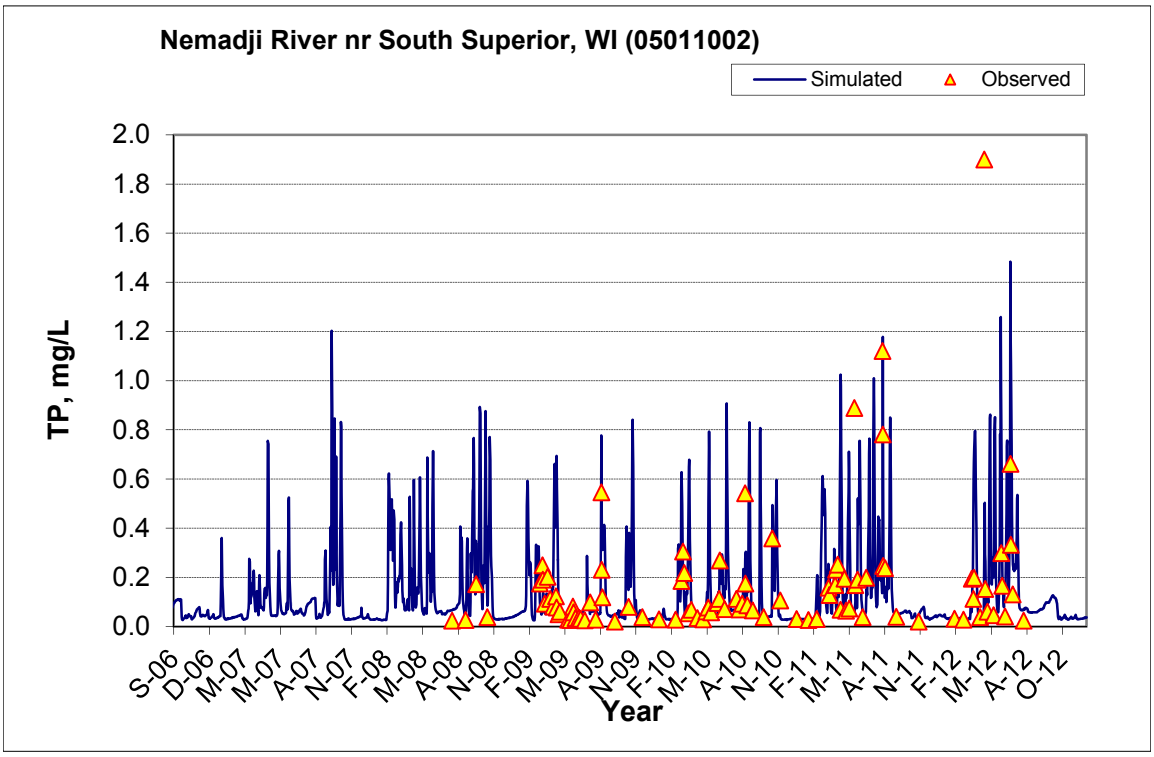

Figure B-197. Time series of observed and simulated Total Phosphorus (TP) concentration at Nemadji River nr South Superior, WI (05011002)

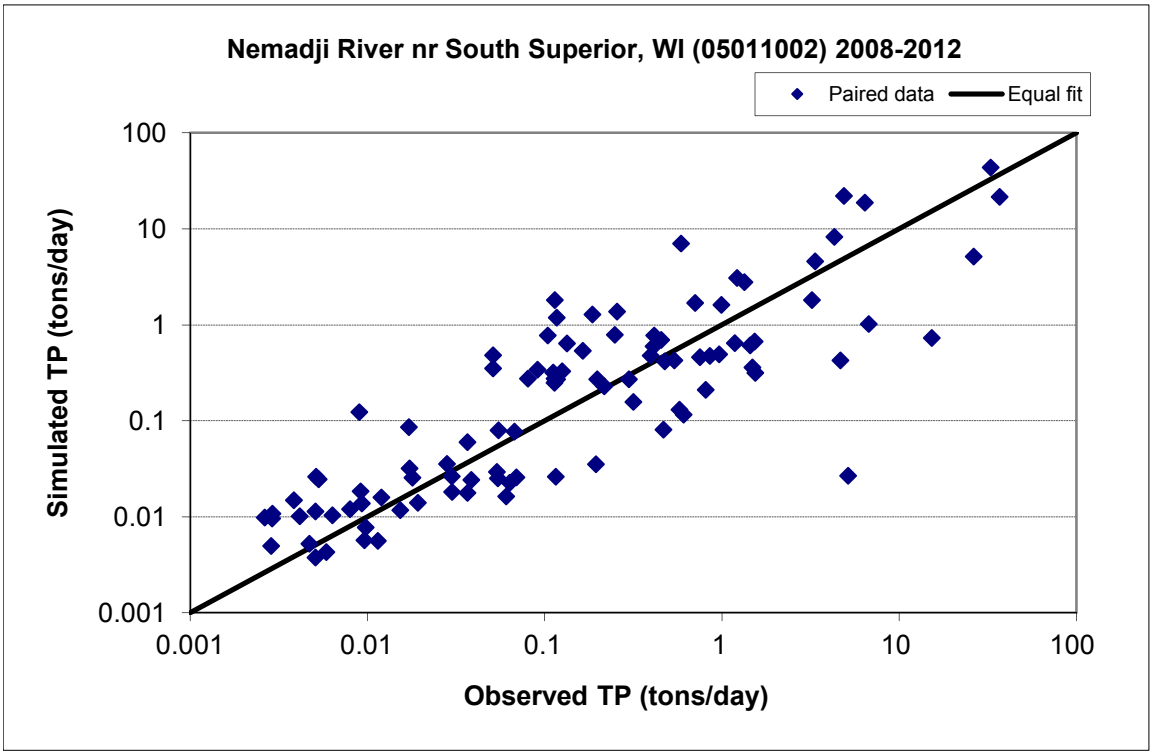

Figure B-198. Paired simulated vs. observed Total Phosphorus (TP) load at Nemadji River nr South Superior, WI (05011002) (calibration period)

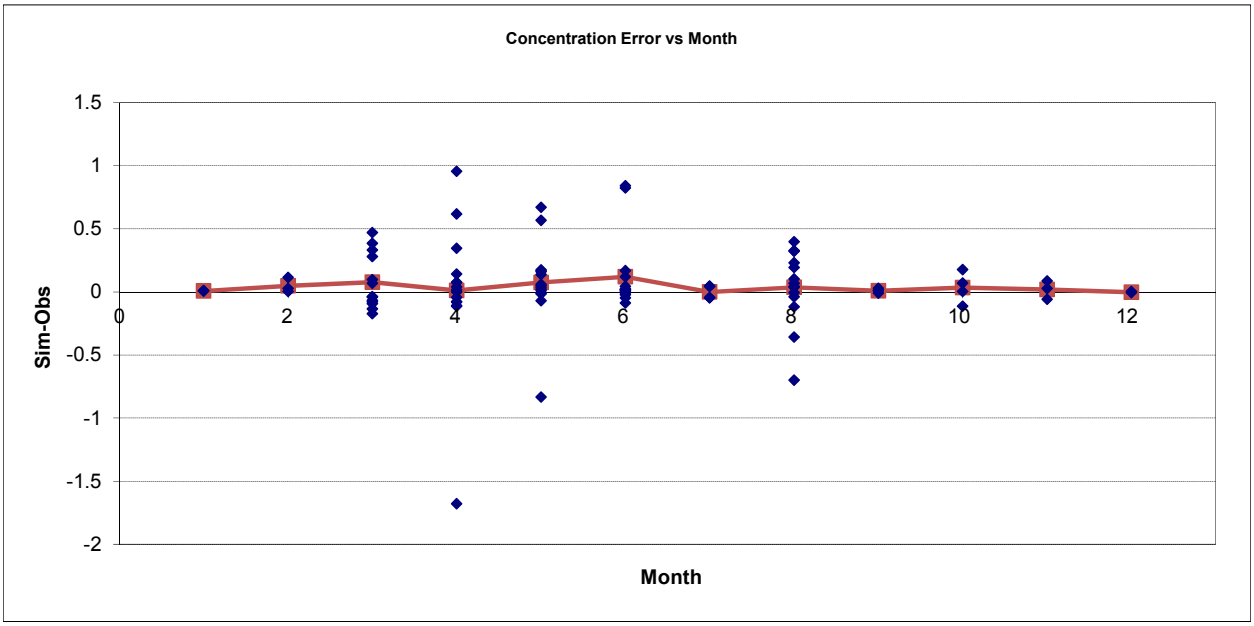

Figure B-199. Residual (Simulated - Observed) vs. Month Total Phosphorus (TP) at Nemadji River nr South Superior, WI (05011002)

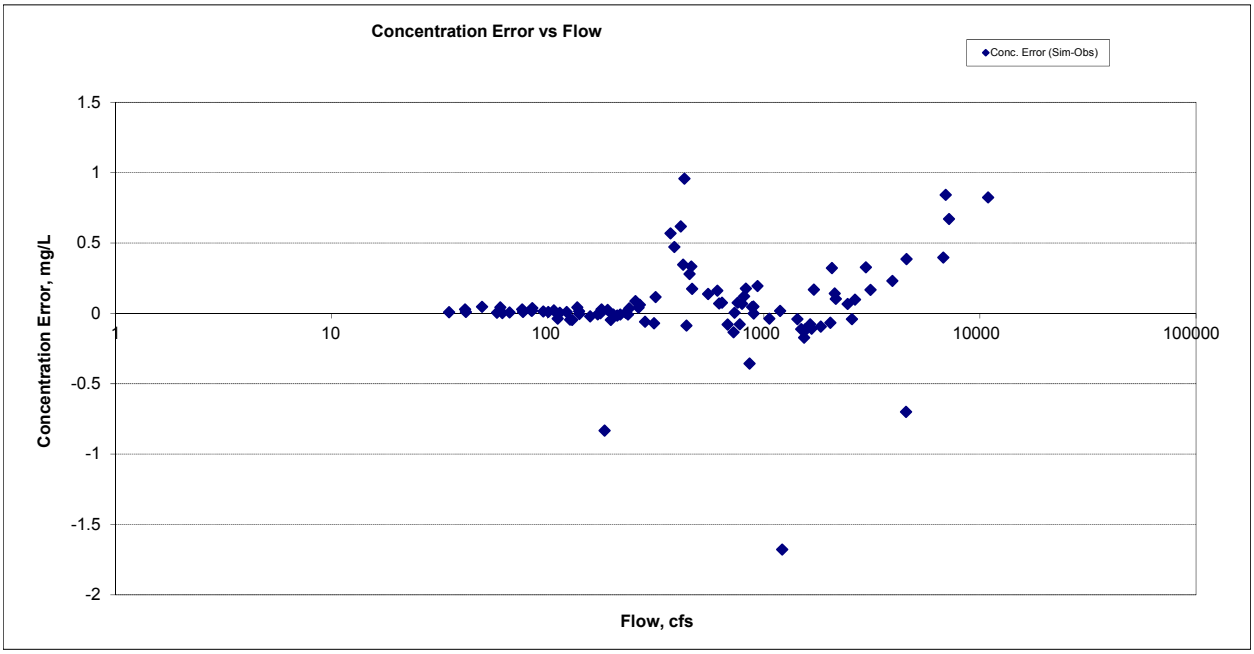

Figure B-200. Residual (Simulated - Observed) vs. Flow Total Phosphorus (TP) at Nemadji River nr South Superior, WI (05011002)